UNIVERSITAT DE
BARCELONA

Biodiversidad, biogeografía y patrones evolutivos en crustáceos (Anomura, Galatheoidea) de zonas tropicales y templadas

Paula Carolina Rodríguez Flores

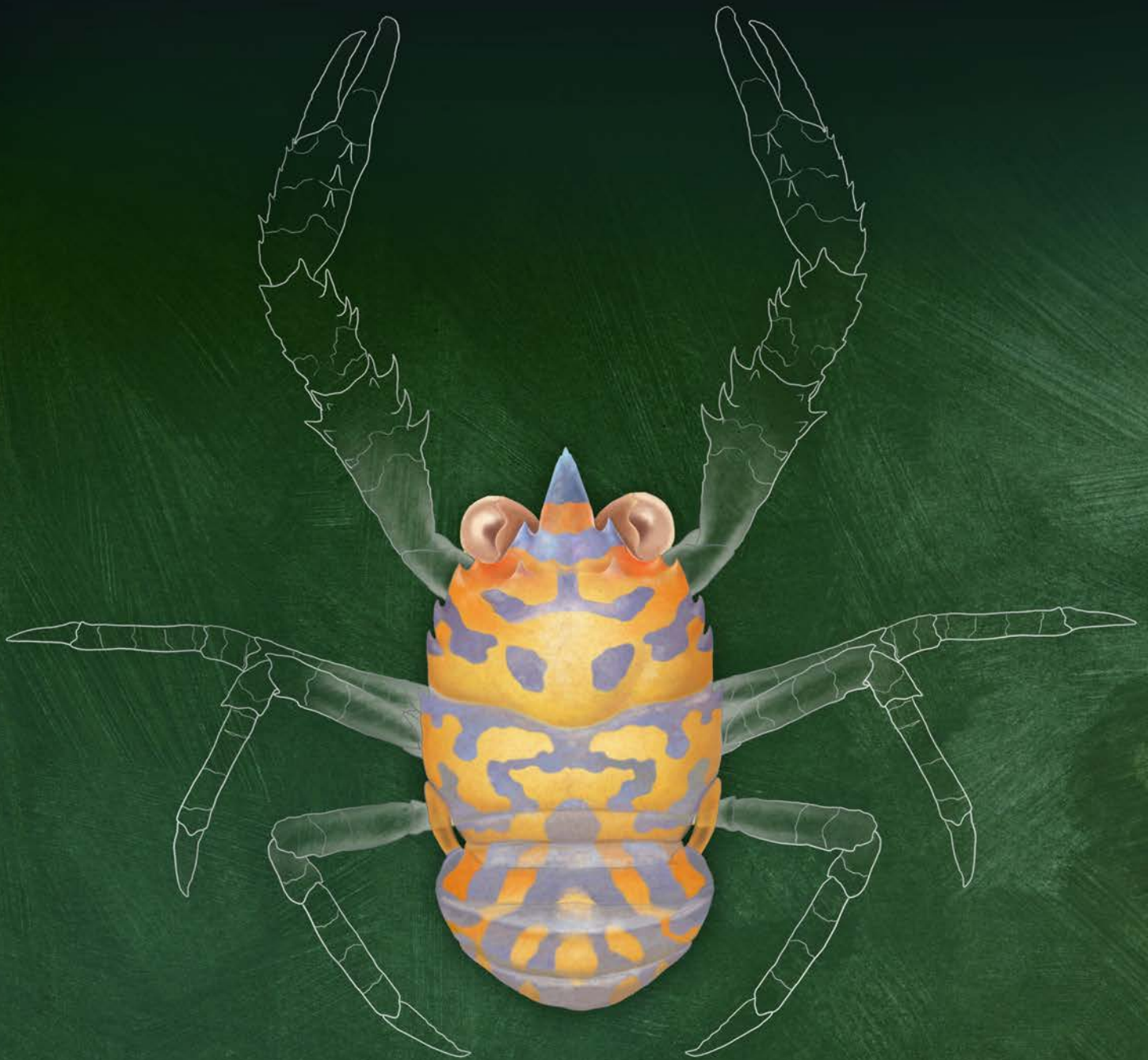# BIODIVERSIDAD, BIOGEOGRAFÍA Y PATRONES EVOLUTIVOS EN CRUSTÁCEOS (ANOMURA, GALATHEOIDEA) DE ZONAS TROPICALES Y TEMPLADAS

Paula Carolina Rodríguez Flores

Tesis Doctoral

UNIVERSITAT DE BARCELONA

BIODIVERSIDAD,

BIOGEOGRAFÍA Y PATRONES EVOLUTIVOS EN

CRUSTÁCEOS (ANOMURA, GALATHEOIDEA) DE ZONAS

TROPICALES Y TEMPLADAS.

Memòria presentada per

Paula Carolina Rodríguez Flores

Per optar al grau de Doctora per la Universitat de Barcelona

Programa de Doctorat en Genètica

Treball realitzat al Museo Nacional de Ciencias Naturales-CSIC i

al Centre d'Estudis Avançats de Blanes-CSIC

Doctoranda
Paula C. Rodríguez Flores

Directora
Annie Machordom

Director
Enrique Macpherson

Tutora
Marta Pascual

Barcelona, novembre de 2020

Rodríguez-Flores PC, 2020. *Biodiversidad, biogeografía y patrones evolutivos en crustáceos (Anomura, Galatheoidea) de zonas tropicales y templadas*. Tesis doctoral, Universidad de Barcelona.

Créditos de las cubiertas: Xavier Macpherson (xavixups@yahoo.es).
Phylladiorhynchus orpheus (portada), *Munidopsis bairdii* (contraportada).

A mis padres y a Ernesto, desde la admiración,

por la imaginación, la libertad y el amor

AGRADECIMIENTOS

Desde que empecé mi recorrido por el mundo científico me han ido llegando titulares de noticias como «La tesis doctoral es perjudicial para la salud mental», o «Depresión: el efecto desconocido del doctorado» y qué alejado me parece todo eso de mi realidad. La Tesis ha permitido que haga justo lo que quiero hacer, ha hecho que cumpla varios de mis sueños como trabajar con invertebrados, investigar, viajar por el mundo y, además, ha traído la felicidad mi vida. Ojalá que esto solo sea el principio.

Así que quiero agradecer a todos los que han hecho posible que el trabajo haya llegado a buen término y que yo haya llegado hasta este punto.

A mis directores Annie Machordom y Enrique Macpherson, muchas gracias por haberme brindado esta gran oportunidad y la financiación para estudiar galateidos. Gracias por la constante ayuda y por el inmenso apoyo que he recibido. Me siento afortunada de haber podido contar con vosotros dos. Gracias por haberme enseñado desde lo más sencillo a lo más complejo, por haberme abierto mil puertas, aconsejado y guiado con paciencia desde el principio de mi carrera investigadora. Esta tesis que tenéis en frente es un mérito compartido por los tres, pues sin vosotros nunca hubiese sido posible.

A Mario García París por ser un pilar en mi carrera científica y en mi vida personal. Gracias por haber apostado siempre todo por mí y por haber estado presente en todo momento, sin excepción, cuando he necesitado algo. Gracias también por ser mi gran amigo en quien confiar y por entenderme tan bien. Qué suerte tengo de que la contingencia haya cruzado nuestros caminos.

A todas las personas que han facilitado que las muestras lleguen a nuestras manos, trabajando en la búsqueda de financiación, recursos, organización de las campañas, recolección de muestras, separación, identificación del material (a veces empleando para ello el tiempo de sus vacaciones o haciéndolo de forma voluntaria) y, en definitiva, a todos y cada uno de los que han contribuido a que esto sea posible: Alain Crosnier, Joseph Poupin, Philippe Bouchet, Bertrand Richer de Forges, Gustav Paulay, Sammy De Grave, Tim-Yan Chan, Chiawei Lin, Kareen Schnabel, Shane Ahyong, Pere Abelló y al personal de museos de todo el mundo, conservadores, técnicos y muchas otras personas que no conozco, pero que gracias a todos ellos se han podido estudiar aquí miles de galateidos. Esta memoria es la punta del iceberg de una enorme cantidad de trabajo previo.

A mi tutora, Marta Pascual de la UB, por su amabilidad y por estar siempre pendiente de todo lo referente a mi tesis doctoral. Muchas gracias. A mi profesor Darío Díaz Cosín de la Universidad Complutense, por enseñar con tanto amor los invertebrados no artrópodos y haber sido mi primera guía.

Cèlia, Leyre y a Héctor, mil gracias por toda tu ayuda y paciencia durante estos años. Una mención especial a Nuria Burgos, pues es de esas personas geniales que te encuentras pocas veces en la vida, gracias por esas dosis de diversión.

A Ferran Palero, gracias por poder contar contigo siempre, por tus consejos, por estar siempre encantado de ayudar y por esa pasión contagiosa por la investigación que es fuente de motivación para cualquiera.

A Xavier Macpherson por su trabajo que tanto admiro y sus maravillosas ilustraciones que adornan las cubiertas de esta tesis.

A todos mis colegas del MNHN, *merci beacoup pour tout*, por hacerme sentir en cada estancia y workshop que el MNHN es mi segunda casa. Gracias a Barbara, Cyril, Manu, PM, PB, Virginie y gracias a todo el equipo de crustáceos; en especial a Paula Rodríguez por todos estos años de compañerismo y por volcarte en absolutamente todo y a Laure Corbari porque tu papel en mi tesis ha sido esencial, gracias por tu inmensa y admirable labor. Gracias a vuestra enorme contribución esta tesis ha podido llevarse a cabo. También quiero mencionar a otros compañeros de workshops en Besse y de la campaña de KOUMAC 2019, que han hecho que sean experiencias inolvidables que espero poder volver a repetir: muchas gracias a Inma, Benoît, Jean Claude, Zdeněk, Anna, Fanny, Christina, Sonia y a todos.

Recuerdo que, en la charla de bienvenida de mi primer día de facultad, nos dijeron que durante los siguientes cinco años haríamos amigos que nos acompañarían para toda la vida y así ha sido. Gracias a mis amigas de la facultad Cris y Ro, gracias por estar siempre ahí para todo, es una suerte teneros en mi vida.

A mi familia, mis padres Mari Carmen y Jorge Enrique, por haberme hecho ser quien soy y por ser las personas más maravillosas del mundo, las que más admiro y admiraré jamás, ¡mucho más que a Sagan, Asimov y a Trevijano! (y a esos los admiro mucho). A Fernando Jiménez, por introducir la naturaleza y las risas en mi vida, muchas gracias. A mi hermano por su alegría y su cariño, y porque espero que esto le motive para perseguir sus sueños como yo hice con los míos.

Y, por último, a la persona más importante sin la cual nunca podría haber hecho nada de esto a tiempo, a Ernesto Recuero por el apoyo incondicional y por esa infinita paciencia; toda la que te sobra es la que a mí me falta. Gracias por ser mi compañero en todo, por ser una persona ejemplar y por ser el mejor regalo de haber hecho esta tesis doctoral.

ABSTRACT

The present dissertation addresses the study of the diversity, systematics, biogeography and evolutionary history of squat lobster superfamily Galatheoidea, founded on integrative taxonomy criteria. Squat lobsters are a highly diverse group of decapods, and every year dozens of new species are described. Galatheoidea includes the families Galatheidae, Munididae and Munidopsidae (squat lobsters), and Porcellanidae (porcellanid crabs), each characterized by their different external morphology, bathymetric distribution and genetic diversity. They have a rich fossil record since the Upper Jurassic and a current peak of maximum global diversity in the Central Indo-Pacific Ocean. Their high diversity, the presence of both cryptic and morphologically variable species, the poorly understood phylogenetic relationships of many lineages at all taxonomic levels, and ecological differences across families make them a challenging group to tackle evolutionary questions. The general aim was to get closer to squat lobster real diversity through the combined analyses of morphological and molecular characters, species delimitation and type specimen revisions. Once having a better taxonomic knowledge, the objective was to solve phylogenetic relationships at supraspecific levels, unveiling their evolutionary and biogeographic history by describing and comparing diversification patterns in different genera from deep-sea and shallow-water. For these purposes, different genera from both deep and shallow environments were studied: *Coralliogalathea*, *Fennerogalathea*, *Phylladiorhynchus* (Galatheidae), Atlantic *Munida* species (Munididae), *Leiogalathea* and *Munidopsis* (Munidopsidae). Several approaches were employed to accomplish the aims: specimen morphological examination, measures and analyses, multilocus and mitogenomic phylogenetic reconstructions, single and multilocus species delimitation, divergence time estimation, ancestral character reconstruction and mapping for geographic distribution and bathymetric patterns. As a result of these approaches, the present dissertation gathers 65 new species formal descriptions: three of *Coralliogalathea*, three of *Fennerogalathea,* three of *Munidopsis,* 15 of *Leiogalathea* and 41 of *Phylladiorhynchus.* Seven synonyms were recovered and one junior synonym proposed. The taxonomic validity and phylogenetic value of morphological characters are discussed, revealing the existence of a high level of homoplasy and the scarcity of synapomorphic characters. Comparison among genetic distances revealed that ranges vary greatly depending on the group. For instance, whereas most *Munidopsis* species present low genetic interspecific distances, some *Phylladiorhynchus* species are highly divergent; this might mean that *Phylladiorhynchus* is constituted by genus-level independent lineages. The evolutionary history reconstruction of *Munidopsis* revealed that the genus is polyphyletic and constituted by more than 20 ancient lineages characterized by different evolutionary histories and trends. Some of these lineages correspond to old genera currently included in the synonymy of

Munidopsis, but others would constitute new genera. These genus-level independent lineages are well differentiated morphologically on the basis of the number of telson plates, the type of rostrum and the presence and position of ocular spines, among other characters. A new phylogenetic hypothesis for Galatheoidea was proposed with mitogenomic data; Porcellanidae was recovered as the earliest offshoot within Galatheoidea, supporting an earlier acquisition of the crab morphology than previously thought. A biogeographic origin in the Tethys Sea during the Upper Oligocene was recovered for *Leiogalathea*; its current pattern of diversity (low diversity in the Atlantic and high diversity in the Central Indo-Pacific) is explained by Tethyan vicariance and posterior dispersal and high diversification towards the East. Several species of squat lobsters from both shallow and deep-waters share patterns of diversification and centers of diversity but have slight differences likely because the bathymetric ranges might influence their evolutionary history. A pattern from shallow-waters to deep-sea colonization was found for *Phylladiorhynchus*, which occurred at least twice in the evolutionary history of the genus. The taxonomic effort made along these years has allowed inferring all these evolutionary processes, highlighting taxonomy as an essential part in the study of biodiversity evolution.

ÍNDICE

Lista de abreviaturas

ESS = Tamaño de muestra efectivo

F = Hembra

G1 = Primer gonópodo

G2 = Segundo gonópodo

IB = Inferencia bayesiana

ICZN = Comisión Internacional de Nomenclatura Zoológica

Juv = Juvenil

LTT = Linajes a través del tiempo

M = Macho

ML = Máxima verosimilitud

MP = Máxima parsimonia

MRCA = Ancestro común más reciente

Mxp1 = Primer maxilípedo

Mxp3 = Tercer maxilípedo

My = Millón de años

ov. = Ovígera

P1 = Primer pereiópodo (quelípedo)

P2–4 = Segundo a cuarto pereiópodos (primera a tercera pata ambulatoria)

PNG = Papúa Nueva Guinea

s. str. = sensu stricto

Stn = Estación

TMRCA = Tiempo hasta el ancestro común más reciente

vs. = versus

INTRODUCCIÓN GENERAL
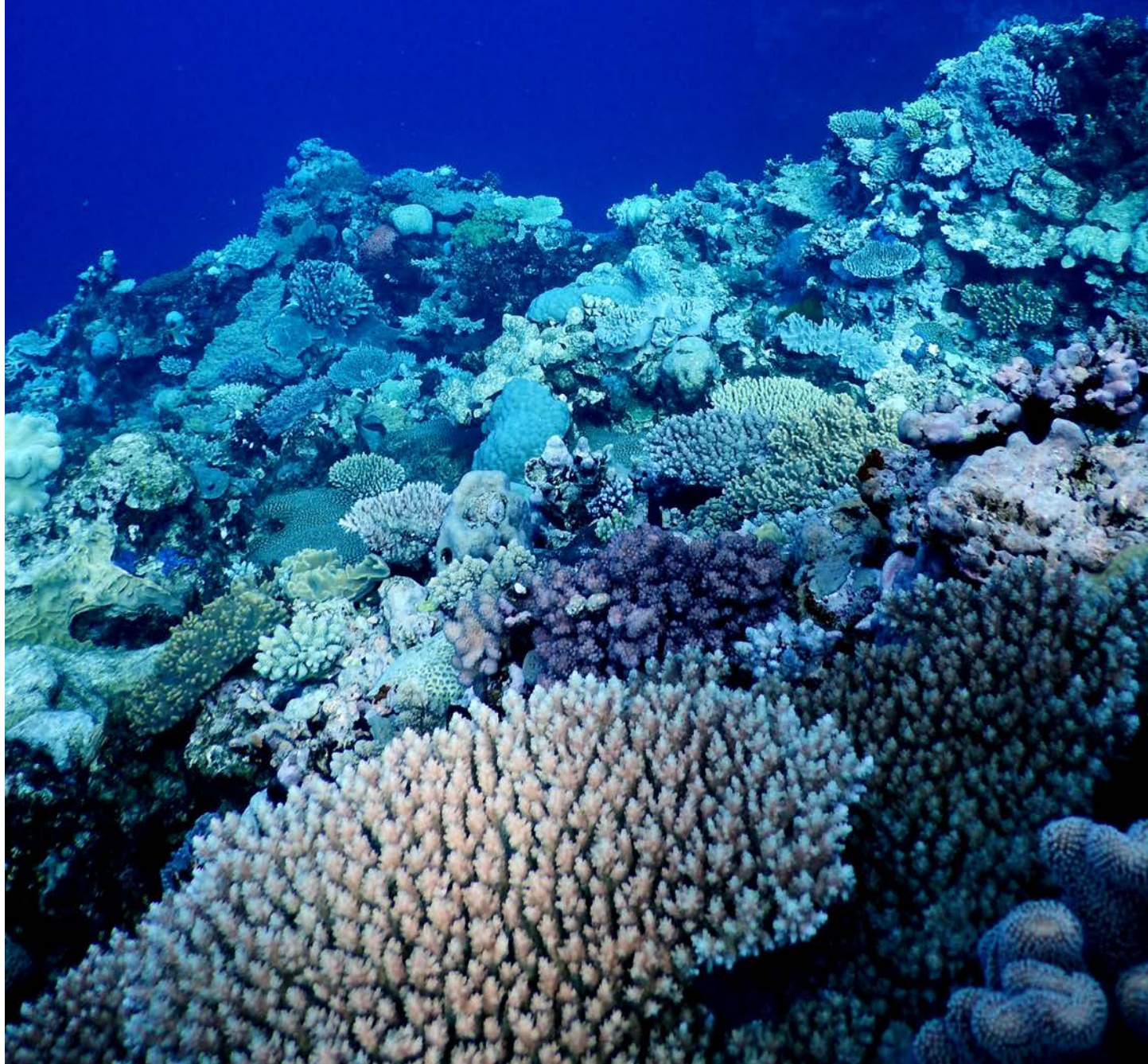
1. La taxonomía y su papel en el estudio de la diversidad

Para un mejor entendimiento del fenómeno que supone la diversificación de la vida, ésta debe contemplarse con un prisma tridimensional de forma, espacio y tiempo, entendiéndose como «forma» el conjunto de caracteres intrínsecos a los organismos. Así, todo estudio holístico que pretenda abarcar los procesos que generan la diversidad, debe recurrir a la biología comparada en el marco de la evolución y lidiar con tres aspectos: (1) diferencias y similitudes entre los atributos de los organismos (forma), (2) historia de los organismos en el tiempo (tiempo) y (3) historia de los organismos en el espacio (biogeografía) (Croizat 1964).

La especie es considerada como unidad básica del estudio de la diversidad y su definición un problema central en biología. Después de décadas de discusión, existen unas 24 definiciones del concepto de especie (Hennig 1966, Simpson 1951, 1961, Mayden 1997, de Queiroz 1998, 2005, 2007). Los autores proponen por un lado los distintos conceptos de especie (ecológico, filogenético, morfológico) en un sentido epistemológico/ontológico, mientras que su asunción establece criterios con objetivos prácticos, como una manera de establecer los límites entre especies (de Queiroz 2005, Freudenstein et al. 2017, Fišer et al. 2018). Por lo tanto, asumiendo el concepto de especie probablemente más aceptado actualmente, el concepto evolutivo (Mayden, 1997, Freudenstein et al. 2017), el papel de la taxonomía en el estudio de la diversidad comienza identificando linajes (ancestro y sus descendientes) que comparten una identidad particular y una trayectoria y destino común (Wiley 1981). Así, la disciplina taxonómica tiene por objeto el reconocimiento de dichas unidades evolutivas, su definición, descripción (Padial et al. 2010) y su propuesta como hipótesis (Fitzhugh 2009, Pante et al. 2015), incluyendo la asignación de nombres siguiendo criterios universales de nomenclatura (ICZN para animales). Lo que se conoce como taxonomía integradora propone, además, un enfoque multidisciplinar para delimitar, describir y nombrar especies basándose en diversas fuentes de evidencias, sean genéticas, morfológicas o ecológicas, entre otras (Dayrat 2005, Padial et al. 2010, Fišer et al. 2018).

Lamentablemente, existe en la actualidad un conjunto de problemas conocidos como «impedimento taxonómico» (Dayrat 2005, Meier 2008, Valdecasas et al. 2008, Padial et al. 2010, Pearson et al. 2011): faltan especialistas y estudiantes en formación, hay escasez de medios y poca o nula financiación para taxónomos, porque no cumplen las expectativas de producción científica actual (Coleman 2015). Es un hecho que cada vez menos científicos serán capaces de identificar especies (Margalef 1968). El propio sistema científico es responsable de esta problemática, pues la valoración de la producción científica está sujeta a modas (Wei et al. 2013), reflejándose también una

tendencia a sobrevalorar las novedades metodológicas y cierta infravaloración por parte de la comunidad científica de las ciencias históricas como la sistemática o la paleontología (véase la discusión sobre «ciencias A *vs.* ciencias B» en Gould 1990). Esto se debe, entre otros factores, a que las ciencias históricas no emplean un razonamiento científico «hipotético-deductivo» (verificación de hipótesis propuestas a priori), sino otro tipo de razonamiento científico no-deductivo, la «abducción» (Fitzhugh, 2006). La abducción implica un razonamiento que empieza observando los efectos o patrones (ejemplo: caracteres diferenciales entre los organismos) de los que se infieren causas (relaciones causales que han producido esos efectos) adoptando hipótesis explicativas (Lipton 1991, Niiniluoto 1999).

2. Diversidad de galateidos, biología y riqueza de especies

Esta tesis aborda el estudio de la diversidad e historia evolutiva de los crustáceos de la superfamilia Galatheoidea Samouelle, 1819 con los criterios previamente mencionados. Son un grupo de decápodos marinos que viven desde el litoral hasta los fondos abisales, en todas las latitudes y continentes a excepción de la Antártida (Baba et al. 2008). Es unos de los grupos de decápodos marinos más diverso, que también presenta una considerable riqueza de formas y taxones en el registro fósil, desde el Jurásico Medio-Superior hasta el Plioceno (Feldmann y Schweitzer 2006, Robins et al. 2013, Hyžný et al. 2014, Feldmann et al. 2015). Estos animales han colonizado múltiples ambientes, desarrollando una gran variedad de estrategias ecológicas, disparidad de formas, tamaños y colores, así como diversos ciclos biológicos (Baba et al. 2008). Desde la descripción de *Galathea strigosa* como *Cancer strigosus* Linnaeus, 1761, hasta el presente se han descrito cerca de un millar especies. Actualmente se describen docenas de especies cada año. Por ejemplo, en 2007 se describieron más de 25 especies, alrededor de 20 en 2010 y más de 90 en 2015. Durante la última década (2007–2017) se han descrito más de 250 nuevas especies. De este modo, después del infraorden Brachyura (con unas 7000 especies), los galateidos son el grupo de crustáceos decápodos que acumula un mayor número de nuevas descripciones (ver estadísticas en WoRMS: http://www.marinespecies.org/index.php). Estos datos ponen de manifiesto que la diversidad real de galateidos podría estar claramente infraestimada y que falta mucho esfuerzo taxonómico antes de tener una imagen más exacta de sus pautas evolutivas y filogenéticas (Appeltans et al. 2012).

Los galateidos pueden ser animales muy conspicuos, de aspecto muy llamativo, con coloraciones intensas. Por otro lado, también pueden exhibir formas y coloraciones crípticas para camuflarse en su entorno, ausencia de pigmentación en el caparazón y otras adaptaciones en función de su modo de vida, como en el caso la reducción de los ojos en especies abisales (Fig. 1). Muestran un rango de tamaño que va desde el milímetro, como

es el caso de *Nanogalathea raymondi* Tirmizi & Javed, 1980, hasta casos de gigantismo como el de la especie abisal *Munidopsis aries* (A. Milne Edwards, 1880), que puede alcanzar tallas de más de 10 cm de caparazón. Presentan varias estrategias para consumir recursos alimenticios: ingieren materia en suspensión o que se deposita en el fondo, son depredadores, carroñeros, omnívoros, herbívoros o incluso caníbales, micófagos o bacterióvoros, por lo que son relevantes en el reciclaje de materia orgánica que se procesa en zonas frías y profundas del océano (Lovrich y Thiel 2011, Hoyoux et al. 2009, 2012).

Muchas especies exhiben asociaciones comensales o simbióticas con otros invertebrados marinos como, por ejemplo, equinodermos crinoideos de arrecifes o de la plataforma continental (Fig. 1). Algunos son comensales de esponjas, a veces en asociaciones específicas como es el caso de *Lauriea sagiani* Baba, 1994 que vive sobre *Xestospongia testudinaria* (Lamarck, 1815). Existe una gran diversidad de especies asociadas a arrecifes de coral de zonas tropicales, ligadas a algas o que viven entre grietas de hábitats rocosos en ambientes litorales o sublitorales, como es el caso de algunas especies europeas. Especies de aguas profundas suelen estar asociadas a corales de aguas frías, siendo el caso de algunas especies de *Munidopsis* Whiteaves, 1874, que se encuentran en asociaciones con alcionarios, antipatarios y gorgonias (Fig. 1) (Fujita y Baba 1999, Lin et al. 2007, Baeza 2011, Macpherson et al. 2016).

Asimismo, hay una gran diversidad de especies asociada a hábitats quimioautótrofos del océano profundo, en chimeneas hidrotermales, emanaciones frías o en esqueletos de ballena, mostrando incluso en algunos casos especializaciones para la xilofagia (Sahling et al. 2003, Baeza 2011, Hoyoux et al. 2009, 2012). Algunas de estas especies, como *Shinkaia crosnieri* Baba & Williams, 1998, presentan bacterias ectosimbiontes en las sedas de los quelípedos implicadas en la fijación de carbono en estos ambientes quimioautótrofos (Goffredi et al. 2008). Las especies del océano profundo se encuentran formando parte de las comunidades bentónicas de montañas submarinas y periferias, crestas, cañones submarinos y también a lo largo de las llanuras abisales (Fig. 1) (Tsuchida et al. 2003, Samadi et al. 2006, Cubelio et al. 2007, Rowden et al. 2010, Dong y Li 2015). La dificultad de acceso a este tipo de ambientes constituye el motivo principal por el que los datos básicos sobre distribución geográfica y biología de galateidos de profundidad están más incompletos que en otros grupos (Baba et al. 2009, 2011a, Kilgour y Shirley 2014).

En general, se desconocen muchos datos sobre la biología de estos crustáceos. En las especies estudiadas la reproducción es comúnmente estacional, pudiendo las hembras producir más de una puesta durante el periodo reproductor y comenzando el periodo de muda después de este periodo. Además, suele existir dimorfismo sexual en el tamaño del P1, lo que sugiere una fuerte selección sexual (Thiel y Lovrich 2011).

Figura 1. Diversidad de colores, formas y hábitats en galateidos. De izquierda a derecha y de arriba abajo: *Galathea inflata* Potts, 1915, *Allogalathea babai* Cabezas, Macpherson & Machordom, 2011 y *Munida intermedia* Milne-Edwards & Bouvier, 1899 en asociación a crinoideos. *Lauriea siagiani* sobre esponja*, Galathea tanegashimae* Baba, 1969; *Galathea mauritiana* Bouvier, 1914 y *Galathea celiae* Macpherson & Robainas-Barcia, 2015 sobre corales; *Galathea strigosa* (Linnaeus, 1761) en grietas rocosas, *Raymunida* Macpherson & Machordom, 2000**;** *Munidopsis tuerkayi* Macpherson, Beuck & Freiwald, 2016. *Eumunida* Smith, 1883 y *Munidopsis* Whiteaves, 1874 asociados a corales de aguas frías. *Galacantha rostrata* A. Milne Edwards, 1880 sobre llanuras abisales; *Munidopsis* sp. y *Shinkia cronieri* Baba & Williams, 1998 en chimeneas hidrotermales.

En galateidos se conocen tanto especies con huevos grandes y poco numerosos como especies con huevos pequeños y cuantiosos (Boyd 1960, Boyd y Johnson 1963, Gore 1979, Wenner 1982; Van Dover y Williams 1991, Baba et al. 2011a, Kilgour y Shirley 2014). Los huevos pequeños suelen experimentar un desarrollo con varios estados larvarios y con las larvas de las primeras etapas planctotróficas (alimentación de plancton). En cambio, los huevos grandes pueden indicar un desarrollo abreviado y larvas lecitotróficas (alimentación de yema) o con piezas bucales no funcionales (Van Dover et al. 1985, Baba et al. 2011a). Se ha comentado que estas estrategias pueden ser diferentes en los distintos grupos taxonómicos de Galatheoidea (Baba et al. 2011a). Algunos grupos de especies tienden a presentar un gran número de huevos de pequeño diámetro, 4–6 zoeas y larvas planctotróficas (Adams & White, 1848, Fujita et al. 2001, 2003, Fujita 2007), mientras que otros tienden a mostrar un menor número de huevos y de mayor tamaño, con 2–3 zoeas (larvas lecitotróficas, por ejemplo, especies abisales del género *Munidopsis*). Este tipo de desarrollo podría estar íntimamente ligado con los procesos de dispersión en las profundidades abisales (Nakamura et al. 2015). Sin embargo, faltan datos para la mayoría de especies de galateidos, por lo que no puede deducirse si esto constituye un carácter adaptativo o una tendencia evolutiva, ya que los datos actuales apuntan a que hay múltiples excepciones y variabilidad de estrategias de reproducción en especies de una misma familia (Kilgour y Shirley 2014).

Desde un punto de vista taxonómico, la superfamilia Galatheoidea actualmente engloba cuatro familias definidas en base a rasgos morfológicos, ecológicos y genéticos (Ahyong et al. 2010) (Fig. 2).

(1) Galatheidae Samouelle, 1819 (≈200 especies, 16 géneros) muestra un rostro triangular o subtriangular y ancho en la base e incluye taxones principalmente sublitorales, que se extienden desde la zona intermareal hasta la plataforma continental, con unas pocas especies de profundidades batiales (>200 m) (Schnabel et al. 2011a).

(2) Munididae Ahyong et al., 2010 (≈380 especies, 22 géneros) presenta un rostro generalmente en forma de tridente (con una espina rostral y sendas espinas supraorbitales) y comprende especies de plataforma y talud continental (generalmente > 200 m < 2000 m) (Baba et al. 2008, Schnabel et al. 2011a).

(3) Munidopsidae Ortmann, 1898 (≈225 especies, 4 géneros) incluye especies que viven a las mayores profundidades de todo Galatheoidea, comprendiendo especies de plataforma y talud continentales y también abisales, que pueden superar los 5400 m (Baba 2005, Macpherson 2007). Estas especies muestran ciertas adaptaciones a la vida en profundidad, como la pérdida de la pigmentación y la reducción de los ojos, además de

presentar un caparazón con menor estriación y mayor tuberculación (Ahyong et al. 2010, 2011b).

(4) Porcellanidae Haworth, 1825 (≈350 especies, 30 géneros), está representada por especies intermareales y sublitorales, a menudo asociadas a corales y esponjas, con morfología convergente a la de cangrejos braquiuros y subsecuente reducción de un pleon musculado y prolongado, lo que constituye una característica diferencial del resto de Galatheoidea.
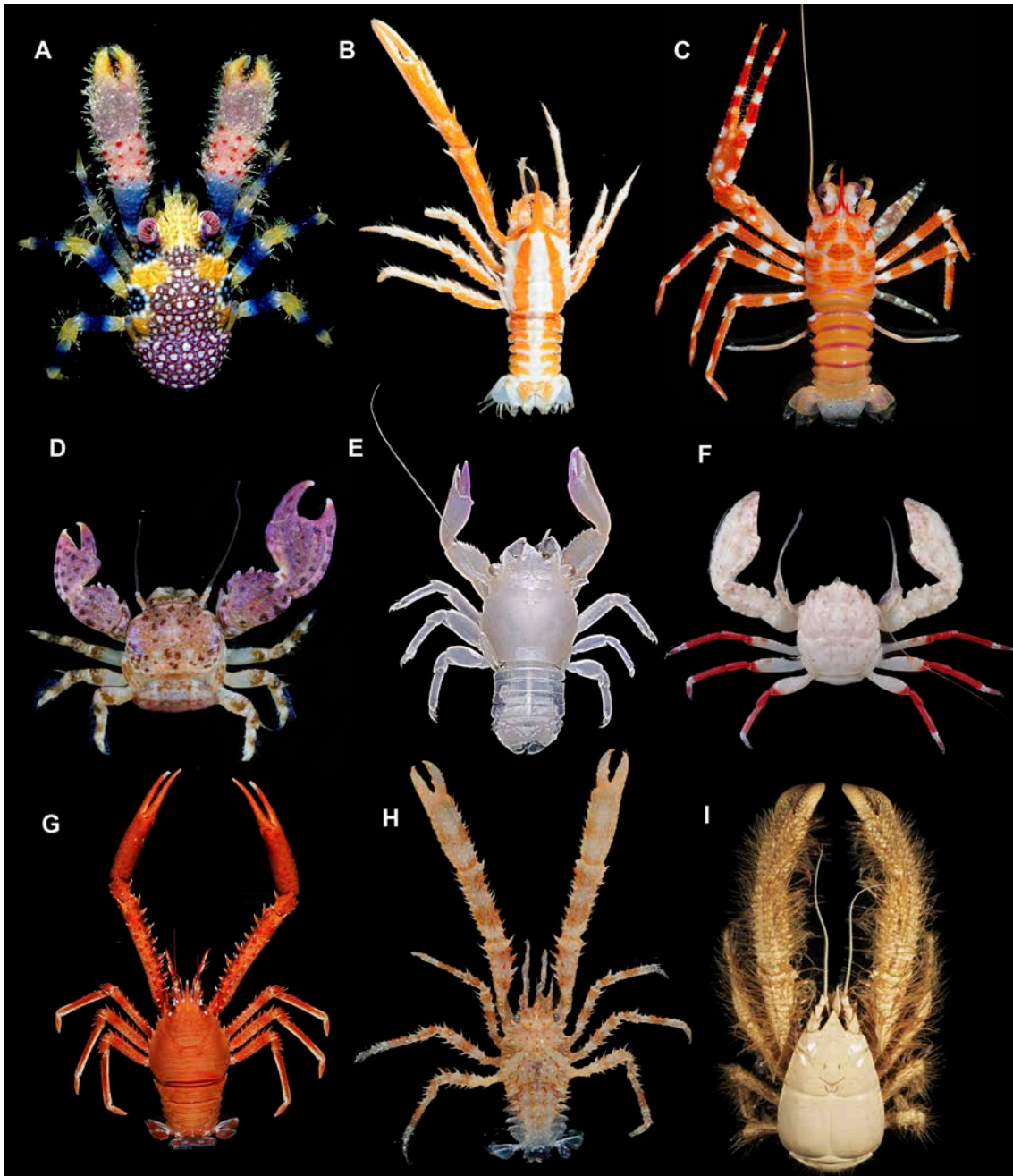
Figura 2. Representación de las distintas familias de Anomura con morfología externa de langosta (a excepción de Aeglidae) y Porcellanidae (Galatheoidea). A-F Galatheoidea, G-I Chirostyloidea. A, Galatheidae, B, Munidopsidae, C, Munididae, D-F Porcellanidae, G, Eumunididae, H, Chirostylidae, I, Kiwaidae.
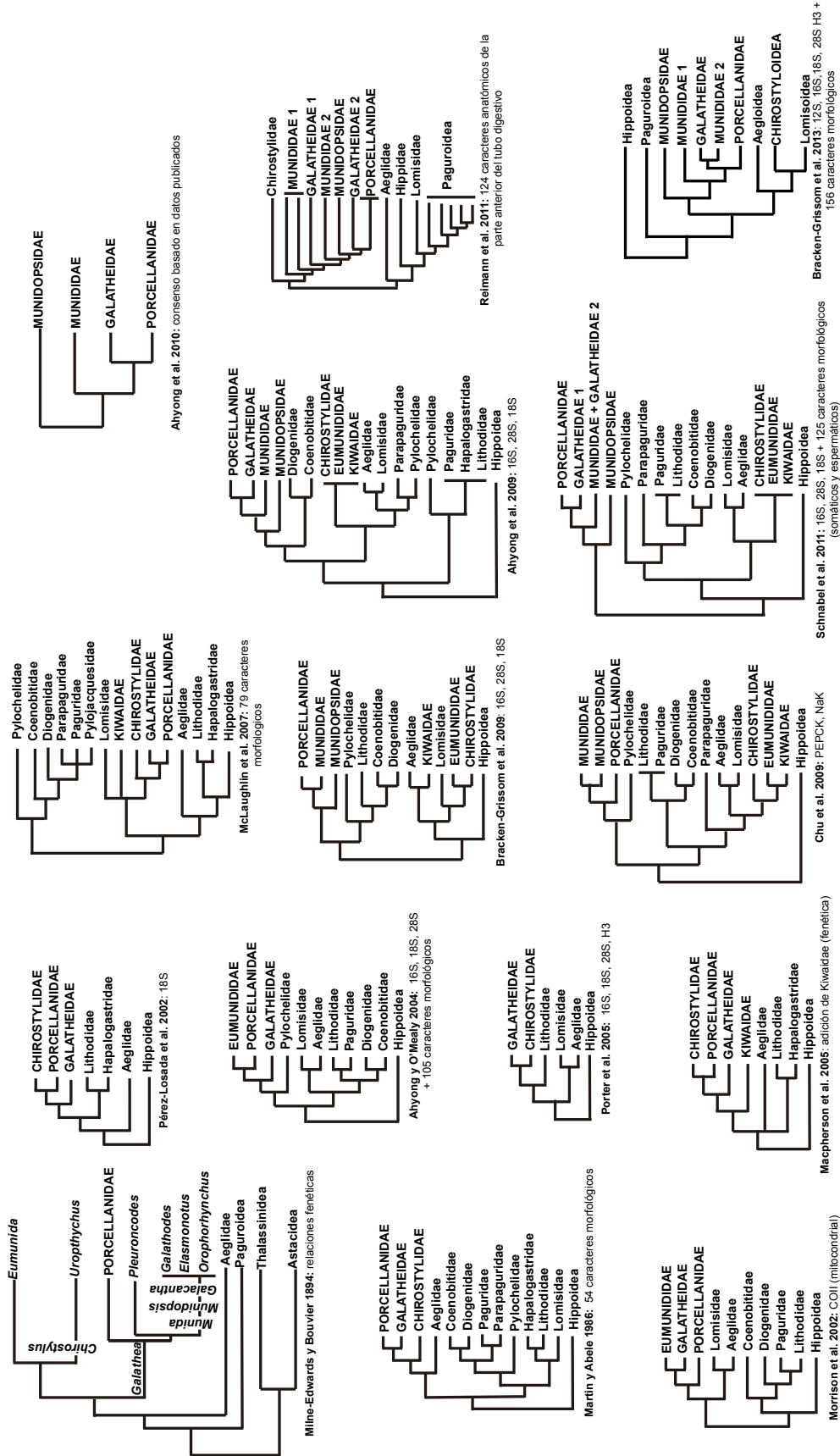
Figura 3. Resumen de las propuestas filogenéticas de las relaciones de Galatheoidea con Anomura, indicando la fuente de datos en la que se apoyan. Modificado de Ahyong et al. (2011a).
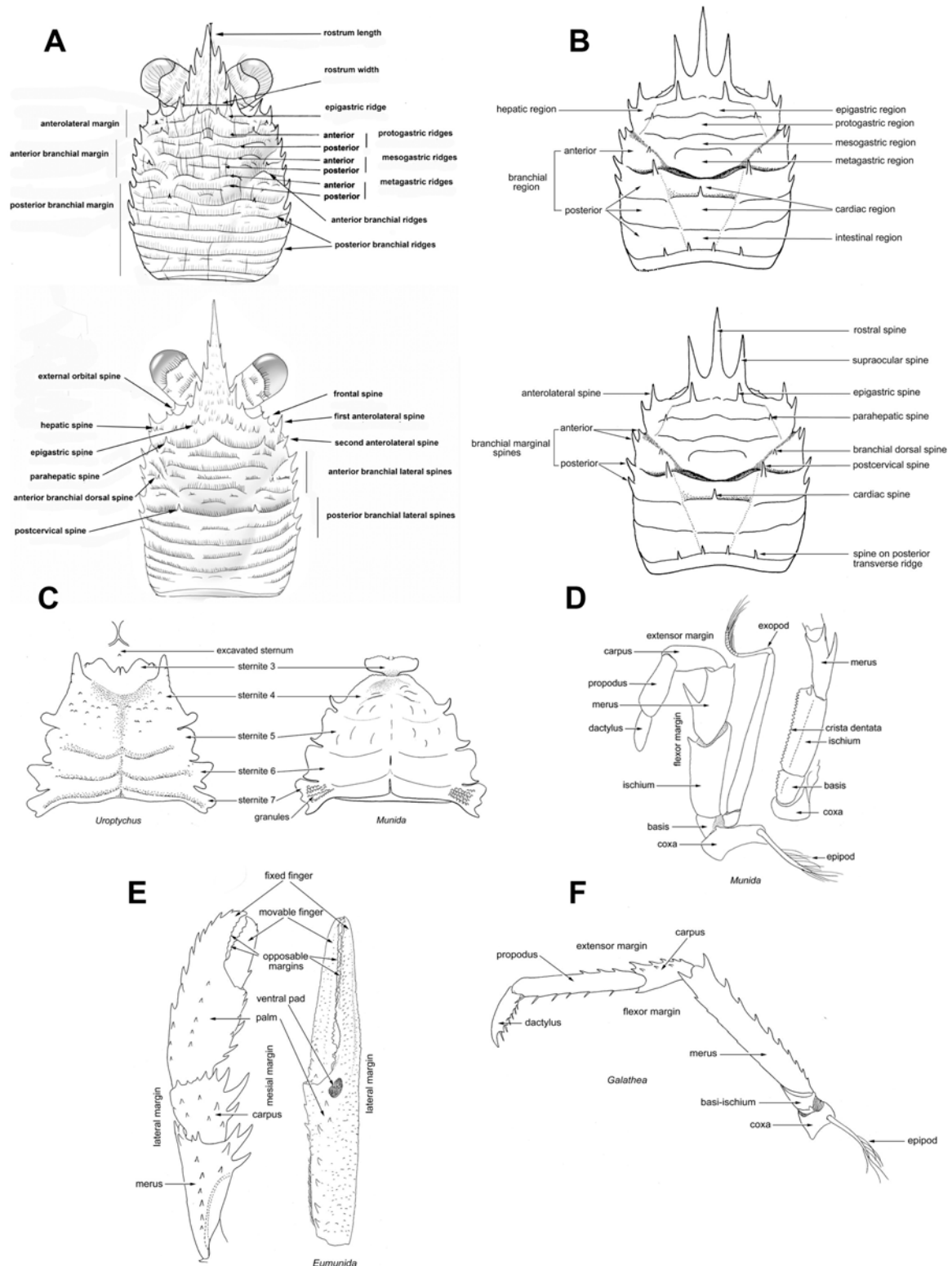
Figura 4. Caracteres morfológicos empleados en la taxonomía de «squat lobsters». A caparazón de *Galathea* y B de *Munida,* vista dorsal. C, Plastrón, vista ventral. D, Mxp3 vista lateral (izquierda) y vista ventral (derecha). E, P1 de *Galathea,* vista dorsal (izquierda), y de *Eumunida*, vista ventral (derecha). F, P2 de *Galathea*, vista lateral. Modificado de Baba et al. (2009) y Macpherson y Robainas-Barcia (2015).

En inglés el término «squat lobster» se refiere a los crustáceos anomuros en los que centramos esta memoria, incluidos en Galatheoidea excluyendo Porcellanidae, que exhiben una morfología externa característica de langosta. Esta morfología se caracteriza

por presentar los últimos segmentos del pleon, telson y urópodos «en abanico», el cuerpo aplanado dorso-ventralmente y el pleon típicamente plegado hacia el cefalotórax de forma que en posición dorsal son visibles solamente tres segmentos del pleon (Baba et al. 2011b, Ahyong et al. 2011a). Sin embargo, este *habitus* anatómico general constituye una convergencia morfológica, adoptada de forma independiente en la evolución de los crustáceos anomuros varias veces.

3. Sistemática y propuestas filogenéticas en Galatheoidea.

En esta memoria se utilizarán indistintamente taxonomía y sistemática como sinónimos (ver: Small 1989, Wheeler 2008) (etimologías: taxonomía —griego—taxis: organizar + nomia: método, esto es método de ordenar; sistemática —griego— sustēmatikós: procedimiento ordenado o método regular y organizado, relacionado con la clasificación taxonómica), para evitar confusión y con el fin de evitar acepciones que se acogen al uso de distintas metodologías para usar un término (sistemática) en detrimento del otro (taxonomía). La definición aceptada de sistemática es el estudio de la clasificación de las especies con arreglo a su historia evolutiva o filogenia. Pero, en definitiva, la taxonomía como parte de cualquier estudio biológico (Dobzhansky 1973) debe siempre realizarse en un contexto evolutivo, considerando las relaciones ancestrales y de parentesco entre los organismos.

Los «squat lobsters» pertenecen al infraorden Anomura MacLeay, 1838, considerado el grupo de crustáceos con mayor disparidad fenotípica (Ahyong et al. 2011a, Reiman et al. 2011, Tsang et al. 2011). Tradicionalmente, la superfamilia Galatheoidea (*sensu* Martin y Davis 2001) se consideraba como un grupo monofilético que englobaba las familias Aeglidae Dana, 1852 (grupo restringido a Chile, Brasil y Argentina y el único de agua dulce), Chirostylidae Ortmann, 1892, Galatheidae Samouelle, 1819 y Porcellanidae Haworth, 1825. Estas familias comparten, a excepción de los porcelánidos, una anatomía externa similar a langosta (A. Milne-Edwards y Bouvier 1894, Martin y Davis 2001) (Fig. 2). Con el descubrimiento del emblemático taxón *Kiwa hirsuta* Macpherson, Jones & Segonzac, 2005*,* popularmente conocido como el «yeti-crab» (Macpherson et al. 2005), la familia monotípica Kiwaidae Macpherson, Jones & Segonzac, 2005 se incluyó en Galatheoidea (Fig. 2). Sin embargo, esta clasificación no reflejaba las relaciones evolutivas del grupo, por lo que no se mantiene actualmente. Pero para comprender la sistemática de Galatheoidea es necesario explorar: (1) su posición filogenética respecto a sus parientes más cercanos dentro de Anomura, (2) las relaciones filogenéticas entre las familias del linaje principal y (3) las relaciones a nivel inter e intra-género y entre especies.

(1) Las distintas propuestas sistemáticas e hipótesis filogenéticas en Anomura varían según los datos utilizados (caracteres somáticos, anatómicos, de desarrollo, espermáticos, ADN, proteínas, etc.) y según el tipo de marcadores moleculares. También dependen del tamaño del muestreo taxonómico utilizado, ya que algunos estudios solo usan una especie por familia, lo que obviamente puede sesgar el análisis. No obstante, las distintas propuestas parecen demostrar que la carcinización (adquisición de forma de cangrejo) y la aparición de linajes con forma de langosta («squat lobster») ha ocurrido varias veces de forma independiente en la historia evolutiva de anomuros (Fig. 3) (Martin y Abele 1986, Morrison et al. 2002, Pérez-Losada et al. 2002, Ahyong y O'Meally 2004, Porter et al. 2005, McLaughlin et al. 2007, Ahyong et al. 2009, Bracken-Grissom et al. 2009, Chu et al. 2009, Schnabel et al. 2011b).

Actualmente hay un consenso respecto a que lo conocido tradicionalmente como Galatheoidea *sensu* Martin y Davis (2001) no constituye un grupo natural (McLaughin et al. 2007, Ahyong et al. 2009, Schnabel et al. 2011b) y que en realidad son tres clados que no comparten ancestro común reciente, aunque sí patrones básicos en sus planes anatómicos corporales (Baba et al. 2011b). Actualmente se aceptan como grupos naturales los siguientes taxones: Aegloidea Dana, 1852 (familia Aeglidae), Chirostyloidea Ortmann, 1892 (familias Kiwaidae, Eumunididae y Chirostylidae), más estrechamente emparentados con Paguroidea que con los linajes «squat lobster», y Galatheoidea *s. str.* (familias Porcellanidae, Munididae, Munidopsidae y Galatheidae) (Ahyong et al. 2010, Schnabel y Ahyong 2010). Estas superfamilias presentan orígenes evolutivos independientes, lo que correspondería a la adquisición de una morfología de langosta de forma paralela/convergente durante la evolución de Anomura (Fig. 3) (Chu et al. 2009, Ahyong et al. 2009, Schnabel et al. 2011b, Ahyong et al. 2010, 2011b, Bracken-Grissom et al. 2013). Los linajes de Galatheoidea *s. str.* compartirían entre otras sinapomorfías el pedúnculo antenal constituido por cuatro artejos y la división del telson en múltiples placas.

(2) Las relaciones filogenéticas dentro de Galatheoidea no se han investigado en profundidad. Existe un consenso general que considera grupos hermanos Porcellanidae y Galatheidae (Ahyong et al. 2009, 2010, Schnabel et al. 2011b), cuya sinapomorfía principal sería la existencia de un rostro ancho en la base. Este clado sería el grupo hermano de la familia Munididae, linaje que compartiría con las familias mencionadas la presencia de flagelo en el exópodo del Mxp1 (ver Fig. 4 para caracteres morfológicos y Baba et al. 2009). A su vez, Munidopsidae, que carece de dicho flagelo, resultaría el grupo hermano del linaje conformado por las tres familias anteriores (Ahyong et al. 2010, Baba et al. 2011b, Ahyong et al. 2011a). Este consenso está basado exclusivamente en filogenias moleculares, pues ni la anatomía interna, espermática, o los caracteres

morfológicos apoyan el clado conformado por Porcellanidae + Galatheidae (Martin y Abele 1986, Reimann et al. 2011), o cuando se consideran estos datos junto a los moleculares de forma conjunta, el apoyo de este clado es dudoso (Schnabel et al. 2011b). Alternativamente, existen indicios de que algunas de las familias pudiesen no ser grupos naturales, sino definidos por caracteres morfológicos o genéticos resultantes de convergencias/paralelismos u homoplasias. Esto podría deberse al predominio del uso de genes ribosomales en las reconstrucciones filogenéticas de Anomura (ver detalles en Fig. 3), cuyo alineamiento de estructuras secundarias-terciarias podría ensombrecer el análisis de zonas homólogas. Además, el empleo de caracteres morfológicos somáticos de los adultos que pudieran ser homoplásicos (por ejemplo, la forma del rostro) también podría dar como resultado la recuperación de grupos no naturales. Esto último también se puede inferir a partir del registro fósil. Por ejemplo, durante el Mesozoico la disparidad fenotípica era muy elevada y se observa un elevado solapamiento de los caracteres diagnósticos entre géneros (ver Robins 2012, Robins et al. 2013, entre otros). Por otro lado, los estudios filogenéticos con un mayor muestreo taxonómico de Galatheoidea han revelado que Munididae constituye una familia para- o polifilética, tanto estudiándose caracteres anatómicos (Reiman et al. 2011) como en filogenias moleculares y morfológicas (Schnabel et al. 2011b, Bracken-Grissom et al. 2013). Sin embargo, la familia Galatheidae está infra-representada en estos estudios (Schnabel et al. 2011b: 3 especies, Reiman et al. 2011: 3 especies, Bracken-Grissom et al. 2013: 3 especies), por lo que un incremento de taxones a nivel de género podría esclarecer mejor las relaciones entre las familias de Galatheoidea.

(3) Paralelamente, el estudio de las relaciones filogenéticas y taxonómicas en Galatheoidea ha aumentado en las últimas décadas. Se han realizado múltiples reasignaciones en ciertos géneros de las familias Galatheidae, Munididae y Munidopsidae. Como consecuencia, varios taxones inicialmente asignados a los géneros *Galathea, Munida* y *Munidopsis* se han incluido en otros géneros e incluso en otras familias (Baba 1991, Macpherson y Machordom 2000, Macpherson 2007, Cabezas et al. 2008, Ahyong et al. 2011b, Bracken-Grissom et al. 2013, Cabezas y Macpherson 2014) (Tabla 1).

Sin embargo, se sospecha que los grupos con una mayor diversidad de especies de Galatheoidea (*Munidopsis, Munida* y *Galathea*) podrían ser polifiléticos y estar conformados por linajes independientes. Machordom y Macpherson (2004) ya indicaron la existencia en Munididae de géneros para – o polifiléticos a partir de datos morfológicos y mitocondriales, resultados que se han visto corroborados por trabajos posteriores (Cabezas et al. 2011). Por otro lado, Ahyong et al. (2011b) a partir del análisis de los fragmentos mitocondriales citocromo oxidasa subunidad I (COI) y ARNr 16S de

Familia	Género actual	Género original
Galatheidae	*Alainius* Baba, 1991	
	Allogalathea Baba, 1969	*Galathea* Fabricius, 1793
	Allomunida Baba, 1988	
	Coralliogalathea Baba & Javed, 1974	*Galathea* Fabricius, 1793
	Fennerogalathea Baba, 1988	
	Galathea Fabricius, 1793	
	Janetogalathea Baba & Wicksten, 1997	*Galathea* Fabricius, 1793
	Lauriea Baba, 1971	*Galathea* Fabricius, 1793
	Macrothea Macpherson & Cleva, 2010	
	Nanogalathea Tirmizi & Javed, 1980	
	Phylladiorhynchus Baba, 1969	*Galathea* Fabricius, 1793
	Triodonthea Macpherson & Robainas-Barcia, 2013	
Munididae	*Agononida* Baba & de Saint Laurent, 1996	*Munida* Leach, 1820
	Anomoeomunida Baba, 1993	*Phylladiorhynchus* Baba, 1969
	Anoplonida Baba & de Saint Laurent, 1996	*Bathymunida* Balss, 1914
	Babamunida Cabezas, Macpherson & Machordom, 2008	*Munida* Leach, 1820
	Bathymunida Balss, 1914	
	Cervimunida Benedict, 1902	
	Crosnierita Macpherson, 1998	*Munida* Leach, 1820
	Enriquea Baba, 2005	*Munida* Leach, 1820
	Hendersonida Cabezas & Macpherson, 2014	*Paramunida* Baba, 1988
	Heteronida Baba & de Saint Laurent, 1996	*Bathymunida* Balss, 1914
	Munida Leach, 1820	
	Neonida Baba & de Saint Laurent, 1996	
	Onconida Baba & de Saint Laurent, 1996	
	Paramunida Baba, 1988	*Munida* Leach, 1820
	Plesionida Baba & de Saint Laurent, 1996	
	Pleuroncodes Stimpson, 1860	*Galathea* Fabricius, 1793
	Raymunida Macpherson & Machordom, 2000	*Munida* Leach, 1820
	Sadayoshia Baba, 1969	
	Setanida Macpherson, 2006	
	Tasmanida Ahyong, 2007	
	Torbenella Baba, 2008	
Munidopsidae	*Galacantha* A. Milne Edwards, 1880	
	Leiogalathea Baba, 1969	*Galathea* Fabricius, 1793
	Munidopsis Whiteaves, 1874	
	Shinkaia Baba & Williams, 1998	

Tabla 1. Géneros incluidos en la superfamilia Galatheoidea (excluyendo Porcellanidae) y reorganizaciones taxonómicas de los mismos.

varias especies del clado Munidopsidae, indicaron la necesidad de una revisión exhaustiva del grupo, ya que se demostró la polifilia de *Munidopsis,* además de la posible existencia de múltiples linajes independientes a nivel de género que podrían compartir similitudes morfológicas. Hasta el momento, la mayor parte de estudios filogenéticos se han realizado con pequeños grupos de especies de *Munidopsis*, a nivel local o poblacional (Creasey et al. 2000, Cubelio et al. 2007, Jones y Macpherson 2007, Ahyong et al. 2011b, Thaler et al. 2014). Por lo tanto, es necesario realizar un estudio más completo, incluyendo más caracteres, más taxones y, en general, más datos sobre este grupo tan diverso.

4. Procesos evolutivos en Galatheoidea y los retos que supone su estudio

El estudio de la historia evolutiva de los galateidos engloba varios retos o preguntas que están aún por resolver. Estos retos implican la investigación sobre los procesos que han generado la gran diversidad de especies, la complejidad en su evolución morfológica y molecular, además de los distintos patrones evolutivos y biogeográficos complejos que se han revelado durante su estudio (Machordom y Macpherson 2004, Schnabel et al. 2011a, Cabezas et al. 2012).

Reto 1: Estudiar los patrones de cambio morfológico en las distintas unidades evolutivas. Este reto se debe a (i) una frecuente estasis morfológica en algunos clados (conservación extrema de la morfología externa en varios linajes) y, como consecuencia, existencia de complejos de especies y especies crípticas; y (ii), en contraste con lo anterior, una alta variabilidad morfológica y plasticidad fenotípica, más acusada en taxones de profundidades abisales que a su vez exhiben una baja variabilidad genética intra- e interespecífica.

Reto 2: Analizar la heterogeneidad en la diversidad de cada linaje. Algunos linajes reflejan radiaciones adaptativas (o no adaptativas) explosivas. A estos se le contraponen otros linajes poco diversos, que han podido sufrir una mayor extinción o alternativamente una especiación más lenta.

Reto 3: Los patrones de distribución geográfica han ido variando durante los periodos geológicos desde la aparición de los galateidos. Se observan cambios sustanciales en la distribución geográfica de la diversidad a lo largo del tiempo. El estudio de la historia evolutiva y biogeográfica del grupo debe ser datada, analizada y discutida a la luz de dichos patrones.

Reto 4: El estudio de procesos macroevolutivos, como, por ejemplo, radiaciones adaptativas debido a la colonización de diferentes nichos ecológicos o a cualquier otro proceso implicado.
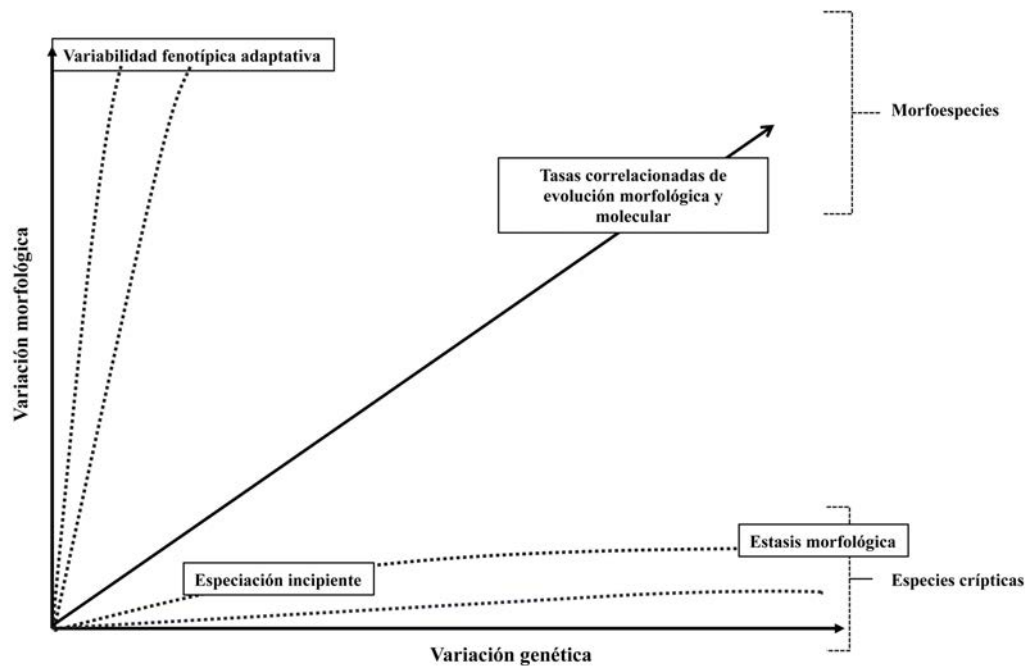
Figura 5. Posibles escenarios de correlación de las tasas de cambio morfológico y molecular que generarían, por un lado, una elevada variabilidad fenotípica como respuesta a radiación adaptativa y baja tasa de cambio molecular, mientras que en el otro extremo que generarían especies de morfología altamente conservada, que acumularían una gran variabilidad genética.

4.1. Reto 1: Cambio morfológico entre los taxones

La identificación de galateidos mediante el uso de caracteres morfológicos externos se basa fundamentalmente en los caracteres del caparazón, rostro, esternitos torácicos, quelípedos, pereiópodos, maxilípedos y las estructuras de la antena y anténula (Fig. 4). En muchos casos es complejo encontrar congruencias en los caracteres morfológicos con respecto a los datos moleculares debido a una mala interpretación al desconocer los patrones de desarrollo o al elevado grado de homoplasia. Esto se debe a que existe un desacoplamiento de las tasas de cambio morfológico y molecular (Fig. 5) en varios linajes de Galatheoidea. De modo que la presencia de múltiples grupos de especies crípticas que divergen genéticamente de forma notable se ha detectado gracias a la integración de caracteres moleculares en el estudio taxonómico. Por ejemplo, se ha puesto en evidencia diversidad críptica en *Raymunida*, *Munida*, *Paramunida*, *Allogalathea*, *Agononida*, *Sadayoshia* y *Lauriea* (Macpherson y Machordom 2001, 2005, Machordom y Macpherson 2004, Cabezas et al. 2008, 2010; Poore & Andreakis 2012, 2014, McCallum et al. 2016). Sin embargo, existen todavía casos de grupos cuya variabilidad morfológica es difícilmente delimitable o asignable a unidades evolutivas,

como ya se ha observado en animales de pequeño tamaño y supuestamente poco diversos, por ejemplo, en *Phylladiorhynchus*, *Coralliogalathea* o *Leiogalathea* (Baba 1969, 1991).

Por el contrario, las especies abisales de la familia Munidopsidae presentan una extraordinaria variabilidad de morfologías, tamaños, ornamentaciones y, en general, tal disparidad morfológica, que durante la historia de la taxonomía de galateidos se han reconocido varios géneros y subgéneros ahora incluidos dentro de *Munidopsis* (Milne Edwards 1880, Smith 1883, Henderson 1885, Chace 1942, Mayo 1974, Macpherson 2007). Además, es patente que las propias especies presentan una elevada variabilidad fenotípica, como se ya se ha constatado en *Munidopsis antonii* (Filhol, 1884) (Baba 2005), *M. serricornis* (Lovén, 1852) (Baba y Poore 2002, Fig. 6) o *M. polymorpha* Koelbel, 1892 (Macpherson 2011 Figs. 2 y 3). Asimismo, se observa una baja variabilidad genética entre distintas poblaciones, a veces muy distantes entre sí (Samadi et al. 2006, Thaler et al. 2014). También se ha destacado la baja diferenciación genética interespecífica presente entre pares de especies que, a su vez, difieren morfológicamente de forma notable, como *M. recta* Baba, 2005/*M. bracteosa* Jones & Macpherson, 2007/*M. exuta* Macpherson & Segonzac, 2005/*M. scotti* Jones & Macpherson, 2007 (Jones y Macpherson 2007). Esta baja diferenciación molecular asociada a una elevada diferenciación morfológica podría deberse a una desaceleración/ralentización de la velocidad de evolución molecular (Fig. 5) como un efecto de la profundidad abisal, en contraste con una mayor tasa de evolución molecular en otros taxones no abisales y que presentan diversidad críptica.

4.2 Reto 2: Patrón variable de diversidad de especies

Se han observado patrones de radiación explosiva en grupos relativamente diversos de la familia Munididae (Machordom y Macpherson 2004, Cabezas et al. 2012). Estos episodios se caracterizan en el tiempo por una rápida cladogénesis inicial, coincidente en el límite Oligoceno-Mioceno en *Munida* y *Paramunida*, en las que los nodos basales suelen aparecer rápidamente, carecer de apoyos estadísticos y presentar múltiples politomías. Estas fases de alta especiación suelen estar seguidas por periodos de especiación más lenta o incluso de estasis. Otro linaje de Munididae, *Agononida*, ha debido tener una radiación explosiva similar, aunque más reciente considerando la divergencia genética entre los grupos morfológicos (Poore y Andreakis 2012, 2014).

Paralelamente, Munididae y Galatheidae incluyen también grupos poco diversos ligados a arrecifes sublitorales y con pocas especies actuales, cuya diversificación se remonta al Paleógeno, como es el caso de *Sadayoshia* o *Lauriea*, o quizá algo más recientes, como en el caso de *Allogalathea* (Cabezas et al. 2009, Palero et al. 2017). Estos clados podrían haber sufrido una extinción mayor o alternativamente una menor

especiación que los inicialmente mencionados. Estos procesos de radiación/estasis, especiación/extinción promotores de patrones diversidad diferenciales podrían estar relacionados con factores extrínsecos e intrínsecos de estos organismos: el desafío impuesto por la selección ambiental y la propia capacidad evolutiva (Kirschner y Gerhart 1998). Sin embargo, antes de abordar el estudio evolutivo comparado de linajes muy diversificados *vs*. poco diversificados es necesario tener una idea aproximada de la diversidad real del grupo de estudio, por eso es fundamental incrementar su conocimiento taxonómico.
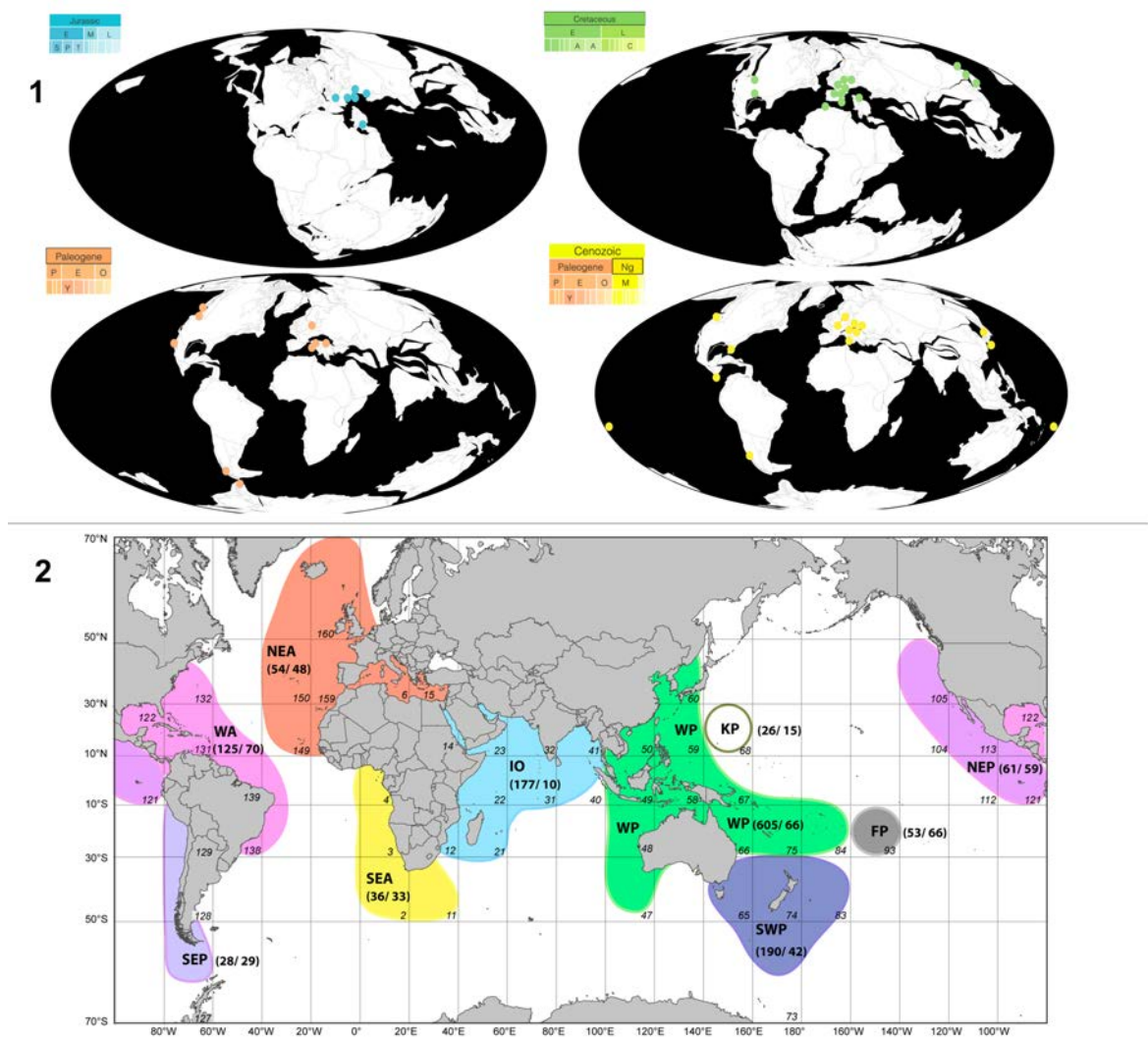
Figura 6. 1. Patrones de distribución geográfica de Galatheoidea desde su aparición en el registro fósil con respecto a la disposición de las placas continentales en el Jurásico, Cretácico, Paleógeno y Neógeno. (Datos de https://paleobiodb.org). **2**. Distribución de taxones (diversidad/endemismos) actuales en correspondientes áreas biogeográficas (SEP: Pacífico Sureste, NEP: Pacífico Noreste, WA: Atlántico Oeste, SEA: Atlántico Sureste, NEA: Atlántico Noreste, IO: Océano Índico, WP: Pacífico Oeste, SWP: Pacífico Suroeste, FP: Polinesia Francesa, KP: Kyushu-Palau/Bonin), tomado de Schnabel et al. (2011a).

4.3 Retos 3 y 4: Biogeografía y patrones macroevolutivos

El fósil más antiguo de un galateido aparece en el margen oriental del Mar de Tetis, en el Jurásico Medio-Superior y está representado por un taxón afín a Munidopsidae (*Palaeomunidopsis* Van Straelen, 1924) (Robins 2012, Robins et al. 2013). Los fósiles asignados a esta familia aparecen de forma abundante en yacimientos del Jurásico Superior y del Cretácico, con algunas apariciones en el Terciario (Schweitzer y Feldmann 2000, Klompmaker et al. 2012, Robins et al. 2013, Beschin et al. 2016).

Los taxones fósiles relacionados con Galatheidae empiezan a aparecer en el registro fósil también a partir del Jurásico Superior. Sin embargo, estas formas extintas presentan similitudes evidentes con taxones de Munidopsidae, por lo que es posible que esta diversidad forme parte del grupo basal («stem-group») de Galatheoidea. De este modo, Galatheidae *s. str.* empezaría a diversificarse durante el Cretácico, también en los márgenes del Tetis (Schweitzer y Feldmann 2000), posteriormente ampliaría su distribución en el hemisferio norte a lo largo de estos márgenes, desplazándose hacia el hemisferio sur durante el Mesozoico Tardío y el Eoceno (Feldmann et al. 1993, Schweitzer y Feldmann 2000, Casadío et al. 2004) (Fig. 6).

Paradójicamente, Munididae, el grupo moderno más diverso, tiene la representación fósil más pobre de todos los galateidos (Ahyong et al. 2011a). Además, los taxones fósiles de Munididae *s. str.* (es decir, taxones morfológicamente similares a Munididae actuales, con la espina rostral en forma de aguja) son más modernos que los de los grupos antes citados, surgiendo en el Eoceno (Schweitzer y Feldmann 2000, Casadío et al. 2004, Hyžný & Schlögl 2011, Nyborg y Garassino 2015). La familia se caracteriza por la presencia de un rostro tridentiforme con una espina dorsal en forma de aguja (Ahyong et al. 2010, Baba et al. 2011b), carácter que suele perderse durante la fosilización por rotura o compresión. La estriación del caparazón, que permanece en el proceso de fosilización, suele ser similar en Galatheidae y Munididae, por lo que la asignación a una familia u otra en ausencia de caracteres rostrales resulta complicada (Robins et al. 2013). De este modo, existen varios taxones cuya identificación como Munididae podría ser dudosa (ejemplo: Beschin et al. 2016). Los fósiles de este grupo aparecen por primera vez en Atlántico noroeste, desde donde pudieron dispersarse hacia el sur y, a través del istmo de Panamá, o hacia el este, a través del Tetis, colonizar el Pacífico Central donde alcanzan su punto máximo de diversidad actual (Schweitzer y Feldmann 2000) (Fig. 6).

Además, los paleoambientes ocupados por la mayoría de los Galatheoidea extintos suelen ser, salvo algunas excepciones, similares a los que ocupan los taxones actuales. Por ejemplo:

- *Munidopsis lieskovensis* Hyžný & Schlögl, 2011 (Mioceno Inferior de Eslovaquia) se ha recuperado de facies de aguas profundas (300 m) (Hyžný y Schlögl 2011).

- Especies de *Galathea* se obtienen con frecuencia en depósitos asociados a arrecifes fósiles de aguas someras del Mioceno-Pleistoceno de Japón (Karasawa 1993, 2000), del Oligoceno de Italia (De Angeli et al. 2010) y del Mioceno Superior de Malta (Gatt y De Angeli 2010).

- *Sadayoshia pentacantha* Müller & Collins, 1991, de forma análoga a sus parientes modernos, se encontró en estratos que corresponden a arrecifes de coral.

- Ejemplares de la especie *Shinkaia katapsyxis* Schweitzer & Feldmann, 2008 fueron descubiertos en abundancia en rocas eocénicas procedentes de un hábitat quimiosintético muy similar al que ocupa la única especie actual del género.

Actualmente se observa un patrón de máxima riqueza de especies, tanto en especies de arrecife como de profundidades batiales en Galatheidae, Munididae y Munidopsidae, en el Pacífico Occidental (o Indo-Pacífico Central *sensu* Spalding et al. 2007), donde se encuentra el 80% de los taxones. Le sigue un 23% en el Océano Índico y un 15% en el Atlántico (Fig. 6) (Schnabel et al. 2011a).

Estudios enfocados en la distribución geográfica exclusivamente de las especies de plataforma y talud demuestran que existe una clara separación entre las faunas del Pacífico Occidental y Central, rica y diversa, y la del Pacífico Oriental, moderadamente pobre (Macpherson et al. 2010). Este patrón se solapa con el de otros organismos como peces, equinodermos y corales, tanto de aguas frías como de arrecife, en los que el centro de máxima diversidad está localizado en el archipiélago Indo-Malayo-Filipino (Cairns 2007, Bowen et al. 2013, Cowman y Bellwood 2013). Este punto caliente de diversidad marina mundial se ha mantenido así durante los últimos millones de años, desde el Mioceno temprano hasta la actualidad, en un patrón concéntrico en el que la diversidad disminuye con el aumento progresivo de distancia desde el centro de diversidad (Bowen et al. 2013). Sin embargo, este punto máximo de diversidad actual ha cambiado a lo largo de la historia. Las zonas de máxima diversidad marina, se localizaban en el Tetis occidental durante el Paleógeno y en el Tetis oriental durante el Neógeno, de forma que los puntos calientes de diversidad marina han ido desplazándose a lo largo de los periodos geológicos (Renema et al. 2008).

A escala local, la mayor diversidad de especies y endemismos de galateidos parece encontrarse en el área de las islas Solomon-Vanuatu-Nueva Caledonia (Macpherson et al. 2010, Schnabel et al. 2011a). Por lo tanto, las áreas con mayor diversidad de galateidos serían con diversidad decreciente: Solomon-Vanuatu-Nueva Caledonia, Archipiélago Indo-Malayo-Filipino y Polinesia Francesa (Fig. 6). A grandes rasgos, estas áreas

geográficas de mayor diversidad son comunes tanto para taxones someros como de plataforma y talud, aunque existe una ligera diferencia respecto a la predominancia de especies de plataforma y talud en el Pacífico occidental meridional con respecto a las especies someras (Schnabel et al. 2011a).

A este patrón de distribución geográfica hay que añadirle los patrones de diversidad vertical. En este sentido Galatheidae, Munididae y Munidopsidae, como se ha comentado previamente, presentan diferencias respecto a sus rangos batimétricos, presentando las especies de Galatheidae preferencia por arrecifes, Munididae por plataforma y talud continental y Munidpsidae por talud y zonas abisales. Además, existen especies con rangos batimétricos muy amplios (Schnabel et al. 2011a), lo que podría deberse a la presencia de complejos de especies crípticas sin resolver. Además, si especies hermanas con estrechos rangos batimétricos coexisten en simpatría (lo que se infiere por los patrones generales de distribución geográfica) nos conduce a preguntarnos qué mecanismos de especiación pueden estar actuando. Por ejemplo, sería interesante averiguar si existen factores de especiación asociados a la batimetría, además de factores de especiación a causa del aislamiento geográfico (dispersión), como ya se ha visto en otras especies de crustáceos (Malay y Paulay 2010).

Para abordar todos estos retos sobre la diversidad, evolución e historia biogeográfica de galateidos, se hace necesario contar con un muestreo global. La mayor parte del material de galateidos estudiado se ha obtenido por las expediciones IRD-MNHN con objeto de explorar los fondos del Pacífico Sur. Lo que solía ser «MUSORSTOM», expediciones centradas en Nueva Caledonia, se convirtió más tarde en el programa «Tropical Deep-Sea Benthos», expandiéndose a las islas Salomón, Vanuatu, Fiji, Tonga y a la Polinesia Francesa, así como a los mares del Índico sudeste. Estas exploraciones a lo largo de más de 40 años han generado descubrimientos científicos de una magnitud e intensidad que solo se pueden comparar con las famosas «expediciones históricas» como las del Challenger, el Albatros o el Siboga. La serie *Tropical Deep-Sea Benthos*, que lleva el nombre del programa, representa solo la punta de un iceberg de literalmente cientos de artículos científicos resultantes, que reflejan diferencias claras entre zonas (Nueva Caledonia y Filipinas) no solo en patrones biogeográficos sino en intensidad de muestreo (Heros et al. 2008, Bouchet et al. 2008, Richer de Forges et al. 2013). Este valioso material, junto a material adicional procedente de colecciones biológicas de todo el mundo (por ejemplo, Western Australian Museum, Smithsonian National Museum of Natural History, Florida Museum of Natural History, y Naturmuseum Senckenberg, entre otros) ha sido la fuente principal de datos de la presente disertación.

De este modo, los distintos capítulos abordados en esta memoria se han basado en las siguientes hipótesis, que pretenden abordar los retos anteriormente propuestos del estudio de Galatheoidea y proponer un marco estructural para el estudio de la Diversidad (Capítulo I), Relaciones Filogenéticas (Capítulo II) y Patrones biogeográficos y evolutivos (Capítulo III):

Hipótesis I. La diversidad real está infraestimada. Esta subestimación no está relacionada exclusivamente con la limitación del muestreo geográfico o la falta de estudio de determinados taxones, sino con procesos de miniaturización, la existencia de homoplasias y el solapamiento de caracteres morfológicos que dificultan la delimitación de las unidades evolutivas. Se esperaría un incremento de nuevos taxones para la ciencia, sobre todo en grupos miniaturizados.

Hipótesis II. La reconstrucción de las relaciones filogenéticas dentro y entre los linajes de Galatheoidea puede variar en función del muestreo taxonómico y de los caracteres empleados. Existen grupos a nivel de género cuya monofilia es dudosa, por lo que es posible que constituyan complejos de linajes con historias evolutivas y biogeográficas independientes. Se esperan cambios sustanciales en la sistemática de los grupos mediante un muestreo taxonómico más exhaustivo y un análisis con mayor número de caracteres.

Hipótesis III: La estasis morfológica *vs*. elevada variabilidad morfológica observada en distintos linajes se debe a procesos asociados al ambiente. Se esperaría que (1) linajes adaptados a aguas profundas presenten una variabilidad morfológica distinta a la de linajes que viven en ambientes someros y (2) una aceleración y/o deceleración de las tasas de substitución molecular en función del ambiente.

Hipótesis IV. Los grupos objeto de estudio que comparten áreas geográficas y que son filogenéticamente cercanos presentarán una historia evolutiva común y, por lo tanto, patrones de biogeografía histórica similares. Se podría predecir la existencia de: (1) eventos similares en la diversificación, (2) solapamiento de áreas ancestrales y centros de especiación, y (3) tendencias paralelas en diversificación neta (extinción + especiación).

OBJETIVOS

Objetivo general: Aproximación a la diversidad real en Galatheoidea (Galatheidae, Munididae y Munidopsidae) mediante el análisis combinado de caracteres morfológicos y moleculares, delimitación de especies y el estudio de material tipo procedente de colecciones científicas. A partir de este mejor conocimiento taxonómico, abordar las relaciones filogenéticas a niveles supraespecíficos y su historia evolutiva y biogeográfica mediante la descripción/comparación de los patrones de diversificación en distintos géneros, tanto de aguas profundas como de arrecifes.

Para abordar este objetivo general se partirán de una serie de objetivos parciales, que consistirán en:

1. Realizar una revisión exhaustiva, mediante el análisis de caracteres morfológicos y moleculares, y de delimitación de especies de los géneros *Fennerogalathea*, *Phylladiorhynchus* y *Coralliogalathea* (Galatheidae), *Munidopsis*, *Leiogalathea* (Munidopsidae) y *Munida* en el Atlántico (Munididae).
2. Reconstruir las relaciones filogenéticas de los linajes a nivel de familia en Galatheoidea mediante diferentes aproximaciones (filogenia multilocus y mitogenómica).
3. Reconstruir las relaciones filogenéticas de los linajes a nivel de género en Munidopsidae, mediante análisis multilocus, estimas de tiempos de divergencia, y el estudio de caracteres morfológicos diagnósticos de linajes.
4. Reconstruir la historia evolutiva y biogeográfica de especies de arrecife y de plataforma continental (*Coralliogalathea*, *Leiogalathea* y *Phylladiorhynchus*).
5. Realizar una aproximación al estudio de la evolución de la ocupación de hábitat en distintos linajes de Galatheoidea (somero *vs*. profundo). El caso de *Phylladiorhynchus*.
6. Comparar y evaluar las tendencias de diversificación, historia biogeográfica y evolutiva entre linajes de profundidad y linajes someros.

INFORME DEL IMPACTO Y PARTICIPACIÓN DE **PAULA CAROLINA RODRÍGUEZ FLORES** EN LOS ARTÍCULOS PRESENTADOS EN LA TESIS DOCTORAL

La doctoranda, Paula Carolina Rodríguez Flores, presenta en el cuerpo de su tesis doctoral 10 artículos, siete ya publicados, uno enviado y dos en preparación.

CAPÍTULO I: Delimitación de especies mediante taxonomía integradora en Galatheoidea

Rodríguez-Flores PC, Machordom A, & Macpherson E. 2017. Three new species of squat lobsters of the genus *Fennerogalathea* Baba, 1988 (Decapoda: Galatheidae) from the Pacific Ocean. *Zootaxa*, 4276, 46–60

Factor de impacto: 0.955 (2019) (Q3, ZOOLOGY)

URL: http://dx.doi.org/10.11646/zootaxa.4276.1.2

Contribución: Recolección o selección en colecciones científicas de los ejemplares, toma de datos (morfológicos y moleculares) y análisis de los mismos, y redacción del manuscrito.

Rodríguez-Flores PC, Macpherson E, & Machordom, A. 2018. Three new species of squat lobsters of the genus *Munidopsis* Whiteaves, 1874, from Guadeloupe Island, Caribbean Sea (Crustacea, Decapoda, Munidopsidae). *Zootaxa,* 4422(4), 569–580

Factor de impacto: 0.955 (2019) (Q3, ZOOLOGY)

URL: https://doi.org/10.11646/zootaxa.4422.4.7

Contribución: Estudio de los ejemplares en el Muséum national d'Histoire naturelle de París. Descripción y redacción del manuscrito.

Rodríguez-Flores PC, Macpherson E, & Machordom A. 2019. Revision of the squat lobsters of the genus *Leiogalathea* Baba, 1969 (Crustacea, Decapoda, Munidopsidae) with the description of 15 new species. *Zootaxa*, 4560, 201–256

Factor de impacto: 0.955 (2019) (Q3, ZOOLOGY)

URL: http://dx.doi.org/10.11646/zootaxa.4560.2.1

Contribución: Separación de las muestras procedentes de las diferentes campañas. Estudio de los ejemplares en el Muséum national d'Histoire naturelle de París. Descripción y redacción del manuscrito.

Rodríguez-Flores PC, Macpherson E, & Machordom A. Revision of the squat lobsters of the genus *Phylladiorhynchus* Baba, 1969 (Crustacea, Decapoda, Galatheidae) with the description of 41 new species (Enviado)

Contribución: Separación de las muestras procedentes de las diferentes campañas. Estudio de los ejemplares en el Muséum national d'Histoire naturelle de París y del material adicional procedente de otros Museos. Descripción y redacción del manuscrito.

Rodríguez-Flores PC, Machordom A, Abello P, Cuesta J, & Macpherson E. 2019. Species delimitation and multi-locus species tree solve an old taxonomic problem for European squat lobsters of the genus *Munida* Leach, 1820. *Marine Biodiversity,* 49, 1751–1773

Factor de impacto: 1.487 (2019) (Q2 MARINE & FRESH WATER BIOLOGY)

URL: https://doi.org/10.1007/s12526-019-00941-3

Contribución: Separación de las muestras procedentes de las diferentes colecciones. Estudio de los ejemplares en el Instituto de Ciencias del Mar (ICM-CSIC) y del Centro de Estudios Avanzados de Blanes (CEAB-CSIC). Descripción, análisis y redacción del manuscrito.

CAPÍTULO II. Relaciones filogenéticas en Galatheoidea

Palero F, **Rodríguez-Flores PC**, Cabezas P, Machordom A, Macpherson E, & Corbari L. 2019. Evolution of squat lobsters (Crustacea, Galatheoidea): mitogenomic data suggest an early divergent Porcellanidae. *Hydrobiologia,* 833(1), 173–184

Factor de impacto: 2.385 (Q1 MARINE & FRESH WATER BIOLOGY)

URL: https://doi.org/10.1007/s10750-019-3898-7

Contribución: discusión de los datos y contribución en la redacción del manuscrito.

Rodríguez-Flores PC, Macpherson E, Baba K, Ahyong ST, Chan T-Y, Lin C-W, & Machordom A. Moving forward by moving back: integrative systematics supports revival of old, and creation of new genera in the composite taxon, *Munidopsis* Whiteaves, 1874. *The Crustacean Society Mid-Year Meeting* 2019, Hong Kong, May 2019 (manuscrito en preparación)

Contribución: Estudio de los ejemplares en el Muséum national d'Histoire naturelle de París y CEAB. Descripción, análisis y redacción del manuscrito.

Rodríguez-Flores PC, Macpherson E, Buckley D, & Machordom, A. 2019. High morphological similarity coupled with high genetic differentiation in new sympatric species of coral-reef squat lobsters (Crustacea: Decapoda: Galatheidae). *Zoological Journal of the Linnean Society,* 185: 984–1017

Factor de impacto: 2.824 (2019) (Q1, ZOOLOGY)

URL: https://doi.org/10.1093/zoolinnean/zly074

Contribución: Separación de las muestras. Identificación y análisis de los ejemplares. Análisis filogenéticos y redacción del manuscrito.

CAPÍTULO III. Biogeografía y patrones evolutivos

Rodríguez-Flores PC, Buckley D, Macpherson E, Corbari L, & Machordom A. 2020. Deep-sea squat lobster biogeography (Munidopsidae: *Leiogalathea*) unveils Tethyan vicariance and evolutionary patterns shared by shallow-water relatives. *Zoologica Scripta*, 49(3), 340–356

Factor de impacto: 2.603 (2019) (Q1, ZOOLOGY)

URL: https://onlinelibrary.wiley.com/doi/abs/10.1111/zsc.12414

Contribución: Análisis de las muestras genéticas. Elaboración de modelos biogeográficos y filogenéticos. Redacción del artículo.

Rodríguez-Flores PC, Macpherson E, Schnabel K, Ahyong ST, Corbari L & Machordom A. Phylogenetic relationships and evolutionary patterns of *Phylladiorhynchus* Baba, 1969 (Crustacea, Decapoda, Galatheidae). *The Crustacean Society Mid-Year Meeting 2019, Hong Kong, May 2019* (manuscrito en preparación)

Contribución: Comparación con material de Australia y Nueva Zelanda. Análisis global de los datos genéticos y obtención de los modelos filogenéticos. Redacción del artículo.

Para que así conste firmamos la presente a seis de noviembre de dos mil veinte:

Annie Machordom   Enrique Macpherson

Capítulo I
Delimitación de especies mediante taxonomía integradora en Galatheoidea

DELIMITACIÓN DE ESPECIES MEDIANTE TAXONOMÍA INTEGRADORA EN
GALATHEOIDEA

Artículos incluidos:

Rodríguez-Flores PC, Machordom A, & Macpherson E. 2017. Three new species of squat lobsters of the genus *Fennerogalathea* Baba, 1988 (Decapoda: Galatheidae) from the Pacific Ocean. *Zootaxa*, 4276, 46–60

Rodríguez-Flores PC, Macpherson E, & Machordom, A. 2018. Three new species of squat lobsters of the genus *Munidopsis* Whiteaves, 1874, from Guadeloupe Island, Caribbean Sea (Crustacea, Decapoda, Munidopsidae). *Zootaxa*, 4422(4), 569–580

Rodríguez-Flores PC, Macpherson E, & Machordom A. 2019. Revision of the squat lobsters of the genus *Leiogalathea* Baba, 1969 (Crustacea, Decapoda, Munidopsidae) with the description of 15 new species. *Zootaxa*, 4560, 201–256

Rodríguez-Flores PC, Macpherson E, & Machordom A. Revision of the squat lobsters of the genus *Phylladiorhynchus* Baba, 1969 (Crustacea, Decapoda, Galatheidae) with the description of 41 new species. (**Enviado**)

Rodríguez-Flores PC, Machordom A, Abello P, Cuesta J, & Macpherson E. 2019. Species delimitation and multi-locus species tree solve an old taxonomic problem for European squat lobsters of the genus *Munida* Leach, 1820. *Marine Biodiversity*, 49, 1751–1773

Article

Three new species of squat lobsters of the genus *Fennerogalathea* Baba, 1988 (Decapoda: Galatheidae) from the Pacific Ocean

PAULA C. RODRIGUEZ-FLORES[1,3], ANNIE MACHORDOM[1] & ENRIQUE MACPHERSON[2]

[1]*Museo Nacional de Ciencias Naturales (MNCN-CSIC), José Gutiérrez Abascal 2, 28006 Madrid, Spain.*
E-mail: paulacrf@mncn.csic.es; annie@mncn.csic.es
[2]*Centre d'Estudis Avançats de Blanes (CEAB-CSIC), C. acc. Cala Sant Francesc 14, 17300 Blanes, Girona, Spain.*
E-mail: macpherson@ceab.csic.es
[3]*Corresponding author*

Abstract

The genus *Fennerogalathea* Baba, 1988 was known to contain two species: *F. chacei* Baba, 1988, the type species, from the Philippines, Taiwan and Indonesia and *F. chirostyloides* Tirmizi & Javed, 1993 from the Bay of Bengal. In the present study, three new species of the genus are described and illustrated: *F. chani* **n. sp.** from Papua New Guinea, *F. cultrata* **n. sp.** from New Caledonia and Vanuatu and *F. ensifera* **n. sp.** from Fiji. The new species are morphologically distinguishable on the basis of the shape and spination of the rostrum and the presence/absence of a small spine on the frontal margin of the carapace. The species also show clear genetic differences (COI and 16S rDNA) among them.

Key words: Crustacea, Anomura, morphology, mitochondrial genes, West Pacific

Introduction

The combined analysis of molecular and morphological characters in the last decade has accelerated recognition of the number of species of squat lobster (e.g. Poore & Andreakis 2011, 2012, 2014). In the family Galatheidae Samouelle, 1819, a recent revision of the more speciose genus *Galathea* Fabricius, 1793 has revealed the existence of species complexes and cryptic diversity (Macpherson & Robainas-Barcia 2015). Additionally, some genera that were known as monospecific, e.g. *Allogalathea* Baba, 1969, or containing few species, e.g. *Lauriea* Baba, 1971, have increased in size well beyond what was previously thought (Cabezas *et al*. 2011; Macpherson & Robainas-Barcia 2013). The existence of this cryptic diversity in the squat lobsters, therefore, recommends a revision of the different genera, including those thought to contain a small number of species (Palero *et al.* 2017).

The genus *Fennerogalathea* Baba, 1988 contains, at present, two species. The genus was described by Baba (1988) on the basis of the type species *F. chacei* Baba, 1988, collected on the continental shelf (152–165 m) of the southwestern Luzon, Philippines, during the "Albatross" expedition in 1907–1910. The species has been also cited in Taiwan (Baba *et al*. 2009) and Bali (Baba 2005). *Fennerogalathea* belongs to the family Galatheidae Samouelle, 1819 (Ahyong *et al.* 2010), and can be differentiated from other genera of the family by a carapace with weak rugosity, lacking setiferous striae and having small scattered spines on the dorsal surface. Furthermore, the rostrum is elongate, triangular, and the eyestalks are narrow (Macpherson & Baba 2011). The other known species, *F. chirostyloides* Tirmizi & Javed, 1993 was described from three males, without pereopods, collected in the deep waters (2417 m) of the Bay of Bengal (Tirmizi & Javed 1993).

In the last decades numerous French expeditions have been carried out in the coastal, continental shelf and slope waters of the Pacific Ocean (Richer de Forges *et al*. 2013). As result of this sampling effort, a considerable number of *Fennerogalathea* specimens from Suva (Fiji), Vanuatu, New Caledonia and Papua New Guinea are held in the collections in the Muséum national d'Histoire naturelle, Paris (MNHN).

Here, we examined all this material analyzing both morphological and molecular characters, which include partial sequences from two mitochondrial genes (cytochrome c oxidase subunit I and 16S rRNA) frequently used in molecular studies of squat lobsters (Machordom & Macpherson 2004; Ahyong *et al.* 2011; Cabezas *et al.* 2011).

Material and methods

Sampling and identification. Specimens were collected using beam trawls or Waren dredges in expeditions to central and western Pacific biogeographic areas (Spalding 2007) in 1993 (New Caledonia, BATHUS 1), 1994 (New Caledonia, HALIPRO 1; Vanuatu, MUSORSTOM 8), 1998 (Fiji, MUSORSTOM 10), 1999 (Fiji, BORDAU 1), 2006 (Vanuatu, SANTO), 2012 (Papua New Guinea, PAPUA NIUGINI) and 2014 (Papua New Guinea, KAVIENG). The types and other specimens of the new species are deposited in the collections of the Muséum national d'Histoire naturelle, Paris (MNHN). The material of *Fennerogalathea chacei* is deposited in the National Taiwan Ocean University, Keelung (NTOU). The general terminology employed in the descriptions largely follows Baba *et al.* (2009) and Macpherson & Baba (2011). The size of the carapace indicates the postorbital carapace length measured along the dorsal midline from the posterior margin of the orbit to the posterior margin of the carapace. The length of the rostrum is measured from the tip to between the basal spine incisions, the breadth is between left and right basal spine incisions. The length of each pereopod article is measured in lateral view along its extensor margin (excluding distal spine), the breadth is measured at its widest portion. Abbreviations used are: Mxp3 = maxilliped 3; P1, pereopod 1; P2–4, pereopods 2–4; M = male; F = female; ovig. = ovigerous.

Molecular analysis. DNA was isolated from the muscle of the pereopods. The tissues of each specimen were homogenized overnight with 20 ml proteinase K in 180 ml of buffer ATL (QIAGEN). The extraction was performed using DNeasy Blood and Tissue Kit following manufacturer instructions (QIAGEN). Two molecular markers were amplified: a partial gene from the mitochondrial cytochrome c oxidase subunit I (COI) using primers LCO1490 (Folmer *et al.* 1994) and COI-H (Machordom *et al.* 2003), and a partial gene from 16S rRNA (16S) using 16SAR-16SBR from Palumbi *et al.* (2002) pair of primers.

The pre-mixing of the PCR reagents was yielded in a total volume of 50 μl which included 2 μl of DNA extracted, 0.2 mM of each deoxyribonucleotide triphosphate (dNTP), 0.2 μM of each primer forward and reverse, 2U of Taq polymerase (Biotools), 5 μl of 10 × buffer solution with $MgCl_2$ and sterilized H_2O. Also MyTaq polymerase 2U (Bioline) was used instead Taq polymerase (Biotools) in a solution with MyTaq Buffer 5 × when the previous premix did not work.

PCR amplification was performed with a thermal cycle including an initial denaturation of 94–95°C for 1–4 min and 40 cycles with 95°C for 1 min, annealing in 42–45°C for 1 min followed by an extension set on 72ºC for 1 min. A final extension cycle at 72°C was set for 10 min. The PCR products were visualized in agarose 0.8% gels and purified with β-Agarase following protocol digestion (BioLabs) before sequencing. The purification products were sent to Secugen S.L. for DNA Sanger sequencing.

The nucleotide sequences were assembled with Sequencher 4.10.1 software package (Gene Codes Corp.). The primer regions were removed before forward and reverse DNA strands were compared. Manual alignment was carried out in Se-Al v2.0a11 (Rambaut 1996) preceded by using MAFFT (Katoh *et al.* 2002) for the 16S genes alignment. Uncorrected-p pairwise distances were calculated in PAUP (Swofford 2002). All the obtained sequences were deposited in GenBank (Table 1).

TABLE 1. Species of *Fennerogalathea* included in the study for mitochondrial DNA analyses (COI and 16S), including sampling localities-expedition, station, and voucher and GenBank codes.

Voucher Code	Species	COI	16S	Locality-Expedition	Station
MNHN-IU-2013-17411	*F. cultrata* **n. sp.**	KY230476	KY230486	Vanuatu-MUSORSTOM 8	Stn CP1120
MNHN-IU-2013-17412	*F. cultrata* **n. sp.**	KY230477	KY230487	Vanuatu-SANTO	Stn AT69
MNHN-IU-2013-17399	*F. ensifera* **n. sp.**	KY230478	KY230488	Fiji-MUSORSTOM 10	Stn CP1351
MNHN-IU-2013-17396	*F. ensifera* **n. sp.**	KY230479	KY230489	Fiji-MUSORSTOM 10	Stn CP1322
MNHN-IU-2013-17410	*F. ensifera* **n. sp.**	KY230480	–	Fiji-BORDAU 1	Stn CP1404
MNHN-IU-2014-13380	*F. chani* **n. sp.**	KY230481	–	Papua-Kavieng 2014	CP4457
MNHN-IU-2013-503	*F. chani* **n. sp.**	KY230482	–	Papua-PAPUA NIUGINI	Stn PP3
NTOU-55	*F. chacei*	KY230483	KY230490	Taiwan	Dongkong
NTOU-96	*F. chacei*	KY230484	KY230491	Philippines-PANGLAO	T10
NTOU-97	*F. chacei*	KY230485	KY230492	Philippines-PANGLAO	T10

Bayesian phylogenetic analysis was performed in MrBayes v3. 2. 1 (Huelsenbeck & Ronquist 2001) using only the COI sequences because 16S sequencing was not successful for all species. *Allogalathea elegans* (Adams & White, 1848) was selected as the outgroup (GenBank accession: GU392168). To estimate the posterior probabilities, four Markov Chains Monte Carlo (MCMC) were run for 5×10^6 generations, sampling trees and parameters every 1000 generations. Twenty five per cent of the initial trees were discarded as burn-in. The maximum credibility tree was visualized and edited in FigTree v1. 4. 2 (Rambaut 2014).

Results

Our results demonstrate the existence of three new species of *Fennerogalathea* supported both by molecular and morphological characters, all well differentiated from the type species, *F. chacei*. We provide COI and 16S data from each taxon, except for *F. chani* **n. sp.**, where only COI was successfully sequenced (Table 1).

Molecular analysis. The ingroup molecular dataset comprised 10 sequences of 658 bp (COI) each and seven sequences of 529 bp (16S) (after alignment). Three specimens represented *Fennerogalathea ensifera* **n. sp.**, two specimens *F. cultrata* **n. sp.**, and two specimens of *F. chani* **n. sp.** Additionally, T.-Y. Chan (National Taiwan Ocean University, Keelung, Taiwan) provided us sequences of *F. chacei* from Taiwan and Philippines for both markers. No specimens of *F. chirostyloides* were available for molecular analysis. Moreover, one of the analyzed specimens of *F. ensifera* **n. sp.** was unable to be sequenced for the 16S and we faced the same problem with *F. chani* **n. sp.** from Papua New Guinea for this marker.

The divergences between the four species of *Fennerogalathea* ranged from 7.60% to 10.69% for COI. We found smaller divergences for the 16S, ranging from 0.70% to 1.69%. The intraspecific COI divergence was normally under 0.61%, except for *F. chani* **n. sp.**, where this value rose up 1.67%, being the values for 16S always under 0.21% (Table 2).

The genetic divergence between *F. chacei* and *F. ensifera* **n. sp.** was 10.69% (COI) and 1.69% (16S), between *F. chacei* and *F. cultrata* **n. sp.** 9.68% (COI) and 1.64% (16S) and between *F. chacei* and *F. chani* **n. sp.**, 7.60% (COI). *Fennerogalathea ensifera* **n. sp.** and *F. cultrata* **n. sp.** were 9.43% divergent in COI and 0.70% in 16S, and *F. ensifera* **n. sp.** and *F. chani* **n. sp.** 10.41% divergent in COI. The genetic divergence between *F. cultrata* **n. sp.** and *F. chani* **n. sp.** was 10.57% (COI) (Table 2). Such divergence values are estimated to be in the upper range of molecular interspecific divergences so far found for squat lobsters, normally beyond 3% among COI sequences and higher than 0.7% among 16S sequences (Cabezas *et al*. 2008, 2011; Poore & Andreakis 2012, 2014; Macpherson & Robainas-Barcia 2013, 2015).

The mitochondrial COI phylogeny indicated two major divergent clades: *F. cultrata* **n. sp.**+ *F. ensifera* **n. sp.** and *F. chacei* + *F. chani* **n. sp.**, having the first clade a low support (Fig. 1). Molecular divergence between these clades was 10.36 % for this marker, almost the same divergence found between *F. cultrata* **n. sp.** and *F. ensifera* **n. sp.** (Table 2). *Fennerogalathea chacei* + *F. chani* **n. sp.** seem to be geographically distributed in Taiwan, the Philippines and Papua New Guinea, whereas the clade *F. cultrata* **n. sp.** + *F. ensifera* **n. sp.** was found in New Caledonia, Vanuatu and Fiji. Morphologically the two clades can be differentiated by the presence or absence of a small frontal spine and the shape of the rostrum (see below). Unfortunately, we failed to sequence the 16S for *F. chani* **n. sp.**, and the two main clades were not supported in the 16S phylogeny. The *F. chacei* + *F. ensifera* **n. sp.** clade received low support and the position of *F. cultrata* **n. sp.** remained unresolved.

TABLE 2. Uncorrected pairwise genetic distances (%) for the analyzed markers. Under diagonal are represented the divergences among COI sequences, up to the diagonal are represented the 16S distances. Numbers on diagonal (bold) show the intraspecific genetic distances, left for COI, right for 16S.

	F. chacei	*F. ensifera* **n. sp.**	*F. cultrata* **n. sp.**	*F. chani* **n. sp.**
F. chacei	**0.61, 0.13**	1.69	1.64	–
F. ensifera **n. sp.**	10.69	**0.51, 0.00**	0.70	–
F. cultrata **n. sp.**	9.68	9.43	**0.00, 0.21**	–
F. chani **n. sp.**	7.60	10.41	10.57	**1.67, –**
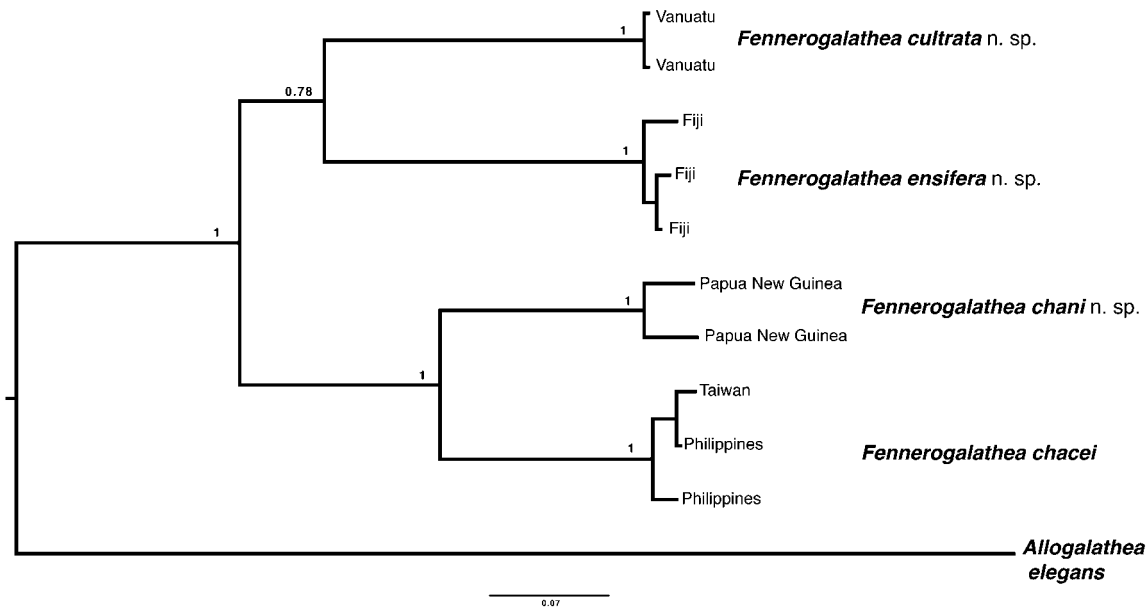
FIGURE 1. Bayesian phylogeny of *Fennerogalathea* based on the COI data. Numbers above branches indicate Bayesian posterior probabilities (BPPs).

Systematic account

Superfamily Galatheoidea Samouelle, 1819

Family Galatheidae Samouelle, 1819

Fennerogalathea Baba, 1988

Fennerogalathea Baba 1988: 60 (gender: feminine).—Baba 2005: 68 (key).—Baba *et al*. 2008: 60 (list of species and synonymies).—Baba *et al*. 2009: 98.—Macpherson & Baba 2011: 53.

Remarks. Prior to the present study, the genus *Fennerogalathea* Baba, 1988 contained two species: *F. chacei* Baba, 1988 (type species of the genus) from the Bali Sea, off south-west Luzon, and Taiwan, at 100–165 m (Baba 1988; Baba *et al*. 2009), and *F. chirostyloides* Tirmizi & Javed, 1993, from the Bay of Bengal, at 2417 m. Unfortunately, the type material of *F. chirostyloides* (three males, with P1–4 missing in all specimens) is probably lost (Baba *et al*. 2008). Nevertheless, the depth of occurrence of this species, clearly deeper than in all other species of the genus (100–321 m, see below), recommends a further study with topotypic material. Tirmizi & Javed (1993) did not provide any difference between the two species, although Baba (2005) indicated that the two species could be separated by the presence in *F. chacei* instead of absence in *F. chirostyloides* of a tuft of setae on the median part of anterior transverse ridge of abdominal somites 2–4. This tuft of setae is always present in the three new species described in the present study.

Key to species of *Fennerogalathea*

1. Rostrum narrow and elongate, more than twice longer than broad, clearly exceeding end of corneae. Spines along carapace margin small . . . . *F. ensifera* **n. sp.**
-   Rostrum moderately long, at most twice longer than broad, not reaching or slightly exceeding end of corneae. Spines along carapace margin well developed 2
2. Absence of tuft of setae on median part of anterior transverse ridge of abdominal somites 2–4 . . . . *F. chirostyloides* Tirmizi & Javed, 1993

-       Presence of tuft of setae on median part of anterior transverse ridge of abdominal somites 2–4 3
3.   Front margin with one spine between lateral orbital spine and first anterolateral spine of carapace . . . . *F. cultrata* **n. sp.**
-       Front margin between lateral orbital spine and first anterolateral spine of carapace unarmed. 4
4.   Lateral margin of rostrum with 2 basal spines at each side. . . . . *F. chacei* Baba, 1988
-       Lateral margin of rostrum with 3 spines at each side . . . . *F. chani* **n. sp.**

Fennerogalathea chani n. sp.
(Figs 2, 3, 6A, B)

Material examined. *Holotype*: Papua New Guinea, New Ireland, KAVIENG CP4457, 2°33'S, 150°41'E, 133–178 m, 2 September 2014, M 3.6 mm (MNHN-IU-2014-13380).
Paratype: Papua New Guinea, PAPUA NIUGINI Stn PP3, 0.5°14'S, 145°49'E, 120–180 m, 30 December 2012 (in gorgonians): 1 M 3.4 mm (MNHN-IU-2013-503).
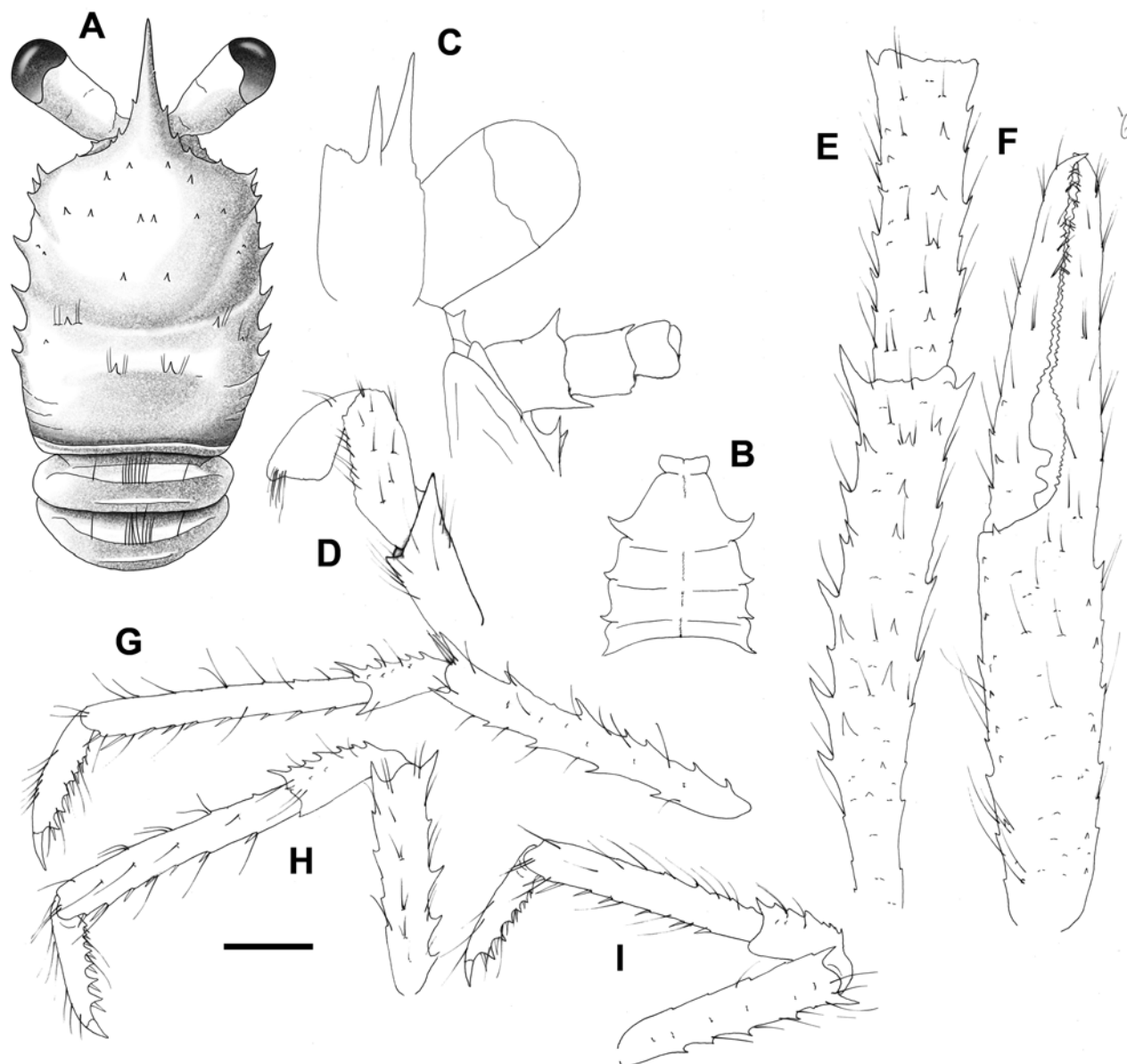
FIGURE 2. *Fennerogalathea chani* **n. sp.**, holotype, male 3.6 mm (MNHN IU-2014-13380), Papua New Guinea. A, carapace and abdomen, dorsal view. B, sternal plastron. C, cephalic region, showing antennular and antennal peduncles, ventral view. D, right Mxp3, lateral view. E, right P1, merus and carpus, dorsal view. F, palm of right P1, dorsal view. G, left P2, lateral view. H, left P3, lateral view. I, left P4, lateral view. Scale: A, B, E–H, I = 1 mm; C, D = 2 mm.

FIGURE 3. *Fennerogalathea chani* **n. sp.**, paratype, male 3.4 mm (MNHN-IU-2013-503), Papua New Guinea. Dorsal view.

Etymology. Name for our colleague and friend Tin-Yam Chan, for his contribution of the knowledge of crustacean biology.

Description. *Carapace*: 1.3 times longer than broad, dorsally armed with scattered spines and setae and some short transverse ridges; cervical groove distinct. Gastric region indistinctly defined and armed with 3 transverse rows of small spines: anterior row epigastric composed of 4 spines; median row protogastric composed of 6 spines, and posterior row mesogastric composed of 2 spines on a medially interrupted ridge. Cardiac region with 2 spines distinctly defined. Anterior branchial regions each armed with 1 or 2 small spines; 1 or 2 postcervical spines on each side. Front margin moderately oblique; limit of orbit ending in minute spine, margin between orbit spine and first anterolateral spine unarmed; 1 or 2 spines on ventral orbital margin. Lateral margins of carapace nearly parallel medially and slightly convex; carapace margin armed with 6 or 7 well-developed spines: 2 spines in front

and 4 or 5 spines behind anterior cervical groove; first spine anterolateral, subequal to second spine, at level of epigastric spines; 1 or 2 spines on anterior branchial margin and 3 spines on posterior branchial margin; posterior transverse ridge spineless. Rostrum triangular, flattish dorsally, narrow and elongate, 1.6–2.0 times longer than broad, 0.4 times of as long as remaining carapace; each lateral margin armed with 3 basal and 1–2 distal tiny distal spines; distance between distalmost lateral incisions 0.3 distance between proximalmost lateral incisions.

Sternum: Plastron longer than broad, lateral limits divergent anteriorly. Third thoracic sternite nearly quadrangular, sternite 4 contiguous to entire posterior margin of sternite 3, and wider than sternite 5.

Abdomen: Somites 2–3 with 2 uninterrupted transverse ridges on tergite, somite 4 smooth, with anterior uninterrupted ridge with median tuft of setae; somites 5 and 6 smooth; posteromedian margin on somite 6 straight. Males with G1 and G2.

Eyes: Eyes stalk subcylindrical, narrow and elongate, 0.7 times shorter than rostrum. Ocular peduncles 1.7–2.0 times longer than broad, maximum corneal diameter 0.8 rostrum width.

Antennule: Article 1 with well-developed distolateral and distodorsal spines, distodorsal slightly overreaching distolateral, distomesial margin with 1 or 2 minute spines.

Antenna: Article 1 hardly visible from dorsal view, without distinct distomesial spine. Article 2 slightly wider and longer than article 3, with short distolateral and distomesial spines subequal in size. Article 3 with 1 small distomesial and minute distolateral spine. Article 4 unarmed.

Mxp3: Ischium with well-developed distal spine on flexor margin; extensor margin unarmed; crista dentata with 25 or 26 denticles. Merus subequal in length to ischium, with 3 or 4 acute granules (holotype) or spines (paratype) on flexor margin, proximal longer than others; extensor margin unarmed. Carpus spineless along extensor margin.

P1: 5.0 times postorbital carapace length, with some scattered short and long setae on dorsal surface and along lateral and mesial margins of all articles. Merus 2.1 longer than carapace, 1.9 times as long as carpus, with numerous spines, stronger spines along mesial and dorsodistal margins. Carpus 0.8 times as long as palm, 4.1 times longer than broad, lateral and mesial margins subparallel, dorsal surface with small spines; mesial surface with some strong spines; row of spines along lateral margin. Palm 3.2 times longer than broad, lateral and mesial margins subparallel; spines arranged in dorsolateral and dorsomesial rows. Fingers as long as palm, each finger with a few minute proximal spines, distally with 2 rows of teeth, spooned.

P2–4: Slender, moderately setose, sparsely with long plumose setae on all articles. P2 2.9 times carapace length. Meri successively shorter posteriorly (P3 merus 0.7 length of P2 merus, P4 merus 0.9 length of P3 merus); P2 merus 1.1 of carapace length, 8.0–8.5 times as long as broad, 1.2 times longer than P2 propodus; P3 merus 4.5 times as long as broad, as long as P3 propodus; P4 merus 5.0 times as long as broad, as long as P4 propodus; extensor margins each with row of 5–7 spines in P2–4; lateral surfaces unarmed in P2–3, 2–3 minute spines in P4; flexor margins each with strong terminal spine in P2–4, 3–5 additional spines in P2–3, unarmed in P4; ventromesial margins each with terminal spine in P2–4. Carpi each with 6 or 7 spines on extensor margin of P2–4; lateral surfaces each all with row of 2 or 3 small acute granules paralleling extensor row; flexor margins unarmed or with minute spine. P2–4 propodi 7.5 (P4)–9.5 (P2) times as long as broad; extensor margins each with 2–3 small proximal spines in P2–4; flexor margins nearly straight, each with 2 pair of terminal spines preceded by 8–9 slender movable spines. Dactyli subequal in length, 0.5 length of propodi, ending in incurved, strong, sharp spine; flexor margins each with prominent triangular terminal tooth preceded by row of 6 teeth.

Distribution. Papua New Guinea, at 120–180 m.

Coloration. Base color translucent whitish with scattered red spots on carapace and abdomen; spines on rostrum and carapace whitish; epigastric and cardiac regions pale orange; abdominal somites 2–5 each with median orange stripe, median long setae reddish. Ocular peduncles with lateral margin orange, some scattered minute red spots. P1 with orange and whitish bands, with numerous scattered red spots. P2–4 translucent whitish, with some scattered minute red spots.

Remarks. The new species is closely related to *Fennerogalathea chacei* Baba, 1988, from the Philippines, Taiwan and Bali Sea (Baba 1988, 2005; Baba *et al.* 2009). Both species have the frontal margin between the lateral orbital spine and the first anterolateral spine of carapace unarmed. However, morphologically they can be easily distinguished by the number of spines along the lateral margins of the rostrum, two in *F. chacei* and three in *F. chani* **n. sp.** The molecular divergence between these species is 7.60% (COI).

38

Fennerogalathea cultrata **n. sp.**
(Figs 4, 6C, D)

Material examined. *Holotype*: Vanuatu, MUSORSTOM 8, Stn CP1120, 15°07'S, 166°53'E, 282–321 m, 9 October 1994, M 5.8 mm (MNHN-IU-2013-17411).

Paratypes: New Caledonia. East Coast, BATHUS 1. Stn CP712, 21°43' S, 166°35' E, 210 m, 19 March 1993: 1 F 4.8 mm (MNHN-IU-2013-17418).

New Caledonia. HALIPRO 1. Stn CP863, 21°31'S, 166°20'E, 190–227 m, 22 March 1994: 1 M 4.6 mm (MNHN-IU-2013-17416).

Vanuatu. MUSORSTOM 8. Stn CP1077, 16°04'S, 167°06'E, 180–210 m, 5 October 1994: 1 ov F 4.0 mm (MNHN-IU-2013-17419).—Stn CP1086, 15°36'S, 167°16'E, 185–215 m, 5 October 1994: 1 M 4.2 mm (MNHN-IU-2013-17415).—Stn CP1103, 15°03'S, 167°07'E, 163–165 m, 7 October 1994: 1 M 5.5 mm (MNHN-IU-2013-17417).

Vanuatu. SANTO.— Stn AT22, 15°32.3'S, 167°16.0'E, 180–227 m, 22 September 2006: 1 M 4.1 mm, 1 ov. F 3.7 mm (MNHN-IU-2013-17413).—Stn AT24, 15°27.5'S, 167°16.2'E, 190–210 m, 23 September 2006: 1 F 4.8 mm (MNHN-IU-2013-17414).—Stn AT69, 15°40.4'S, 167°17.3'E, 207–229 m, 5 October 2006: 1 M 3.2 mm (MNHN-IU-2013-17412).

Etymology. From the Latin *cultratus*, knife-shaped, in reference to the shape of the rostrum.

Description. *Carapace*: 1.3 times longer than broad, dorsally armed with scattered spines and setae and some short transverse ridges; cervical groove distinct. Gastric region indistinctly defined and armed with 3 transverse rows of small spines: anterior row epigastric composed of 4 spines; median row protogastric composed of 6 spines, and posterior row mesogastric composed of 2 spines on a medially interrupted ridge; one additional spine between protogastric and mesogastric rows on each side. Cardiac region with 2 spines distinctly defined. Anterior branchial regions each armed with 1 or 2 spines; 2 postcervical spines on each side. Front margin distinctly oblique; limit of orbit ending in small spine, one small spine between orbit spine and first anterolateral spine; 1 spine on ventral orbital margin. Lateral margins of carapace nearly parallel medially and slightly convex; carapace margin armed with 7 well-developed spines: 2 spines in front and 5 spines behind anterior cervical groove; first spine anterolateral, stronger than second spine, at level of epigastric row of spines; 2 spines on anterior branchial margin and 3 spines on posterior branchial margin; posterior transverse ridge spineless. Rostrum triangular, flattish dorsally, narrow and elongate, 1.6–1.9 longer than broad, 0.4 times of as long as remaining carapace; lateral margin armed with 3 incised teeth; distance between distalmost lateral incisions 0.4 distance between proximalmost lateral incisions.

Sternum: Plastron longer than broad, lateral limits divergent anteriorly. Third thoracic sternite nearly quadrangular, sternite 4 contiguous to entire posterior margin of sternite 3, and wider than sternite 5.

Abdomen: Somite 2 with anterior uninterrupted transverse ridge only on tergite, somites 3 or 4 smooth, with anterior uninterrupted ridge with median tuft of setae; somites 5 and 6 smooth; posteromedian margin on somite 6 straight. Males with G1 and G2.

Eyes: Eyes stalk subcylindrical, narrow and elongate, 0.7 times shorter than rostrum. Ocular peduncles 1.7–2.0 times longer than broad, maximum corneal diameter 0.8 rostrum width.

Antennule: Article 1 with well-developed distolateral and distodorsal spines on, distodorsal slightly overreaching distolateral, distomesial margin with 0–2 minute spines.

Antenna: Article 1 hardly visible from dorsal view, without distinct distomesial spine. Article 2 slightly wider and longer than article 3, with short distolateral and distomesial spines subequal in size. Article 3 with 1 small distomesial and distolateral spine. Article 4 unarmed.

Mxp3: Ischium with well-developed distal spine on flexor margin; extensor margin unarmed; crista dentata with 25 or 26 denticles. Merus subequal in length to ischium, with 3 or 4 spines on flexor margin, proximal longer than others; extensor margin unarmed. Carpus spineless, or with rugosities along extensor margin.

P1: 5.3–5.5 (males), 6.2–6.7 (females) times postorbital carapace length, with some scattered short and long setae on dorsal surface and along lateral and mesial margins of all articles. Merus 2.3–2.5 longer than carapace, 1.8–2.0 times as long as carpus, with numerous spines, stronger spines along mesial and dorsodistal margins. Carpus 0.8–1.0 times as long as palm, 3.6–3.8 (males), 5.2–6.6 times longer than broad, lateral and mesial margins subparallel, dorsal surface with small spines; mesial surface with some strong spines; row of spines along lateral

margin. Palm 2.7–3.2 (males), 5.4–6.0 times longer than broad, lateral and mesial margins subparallel; spines arranged in longitudinal dorsolateral and dorsomesial rows. Fingers 0.8–1.0 times palm length, each finger with minute proximal spines, distally with 2 rows of teeth, spooned.
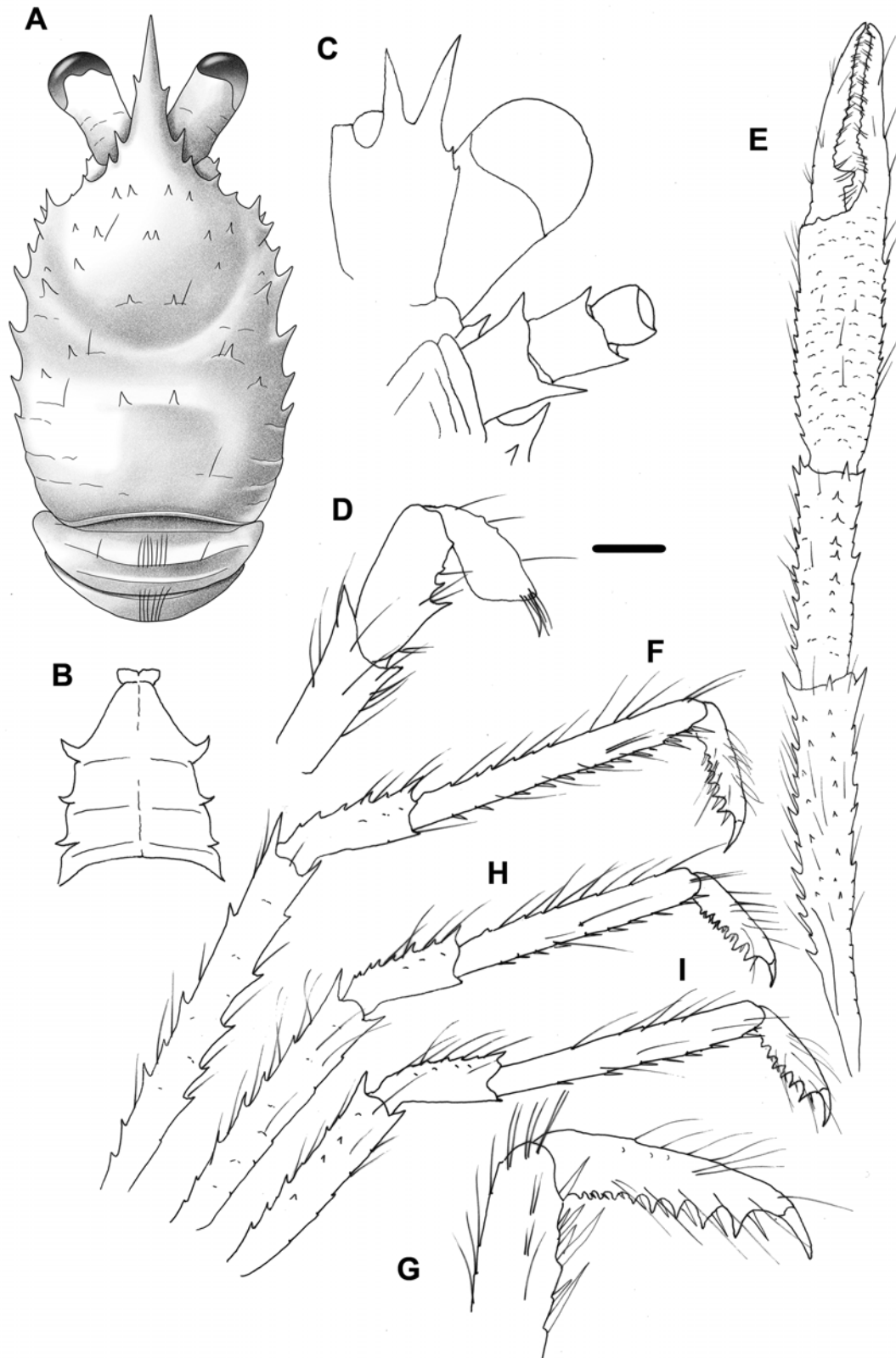
FIGURE 4. *Fennerogalathea cultrata* **n. sp.**, holotype, male 5.8 mm (MNHN- IU-2013-17411), Vanuatu. A, carapace and abdomen, dorsal view. B, sternal plastron. C, cephalic region, showing antennular and antennal peduncles, ventral view. D, right Mxp3, lateral view. E, right P1, dorsal view. F, right P2, lateral view. G, dactylus of right P2, lateral view. H, right P3, lateral view. I, right P4, lateral view. Scale: A, B, E, F, H, I = 1 mm; C, D, G = 2 mm.

P2–4: Slender, moderately setose, sparsely with long plumose setae on all articles. P2 2.7–2.8 times carapace length. Meri successively shorter posteriorly (P3 merus 0.7–0.8 length of P2 merus, P4 merus 0.8 length of P3 merus); P2 merus 1.1 of carapace length, 10 times as long as broad, 1.3 times longer than P2 propodus; P3 merus 6 times as long as broad, 1.1–1.2 times length of P3 propodus; P4 merus 2.5 times as long as broad, 0.4 length of P4 propodus; extensor margins each with row of 6 or 7 spines in P2–4; lateral surfaces unarmed in P2–3, 2 or 3 minute spines in P4; flexor margins each with strong terminal spine in P2–4, 3–5 additional spines in P2–3, unarmed in P4; ventromesial margins each with 1 or 2 spines in P2. Carpi each with 6–8 spines on extensor margin of P2–4; lateral surfaces each all with row of 2 or 3 small spines paralleling extensor row; flexor margins unarmed or with minute spine. P2–4 propodi 7.5 (P4)–10.5 (P2) times as long as broad; extensor margins each with 5 or 6 small proximal spines in P2–3, unarmed in P4; flexor margins nearly straight, each with 3 pair of terminal spines preceded by 8 or 9 slender movable spines. Dactyli subequal in length, 0.4–0.5 length of propodi, ending in incurved, strong, sharp spine; flexor margins each with prominent triangular terminal tooth preceded by row of 8 or 9 teeth.

Distribution. Vanuatu and New Caledonia, at 163–321 m.

Remarks. *Fennerogalathea cultrata* **n. sp.** is closely related to *F. ensifera* **n. sp.** from Fiji (see below). Both species have one small spine on the frontal margin between the lateral orbital spine and the first anterolateral spine of the carapace. However, they can be differentiated by the length and shape of the rostrum (see below). Molecular divergence between *F. cultrata* **n. sp.** and *F. ensifera* **n. sp.** is 9.43% (COI) and 0.70 % (16S).

Fennerogalathea ensifera **n. sp.**
(Figs 5, 6E, F)

Material examined. *Holotype*: Fiji, MUSORSTORM 10, Stn CP1323, 17°16.10'S, 177°45.75'E, 143–173 m, 7 August 1998, M 6.1 mm (MNHN-IU-2013-17407).

Paratypes: Fiji. MUSORSTOM 10: Stn CP1320, 17°16.78'S, 177°53.57'E, 290–300 m, 6 August 1998: 4 M 6.3–8.8 mm, 1 ov. F 7.2 mm (MNHN-IU-2013-17397).—Stn CP1323, 17°16.10'S, 177°45.75'E, 143–173 m, 7 August 1998: 3 M 4.1–7.1 mm, 3 F 4.8–5.6 mm (MNHN-IU-2013-17409).—Stn CP1322, 17°17.10'S, 177°47.92'E, 210–282 m 7 August 1998: 2 M 5.2–6.8 mm (MNHN-IU-2013-17408).—Stn CP1322, 17°17.10'S, 177°47.92'E, 210–282 m, 7 August 1998: 1 ov F 4.9 mm (MNHN-IU-2013-17396).—Stn DW1329, 17°19.33'S, 177°47.36'E, 102–106 m, 8 August 1998: 1 ov F 4.8 mm (MNHN-IU-2013-17405).—Stn CP1351, 17°31.14'S, 178°39.96'E, 292–311 m, 11 August 1998: 1 M 4.7 mm (MNHN-IU-2013-17398).—Stn CP1351, 17°31.14'S, 178°39.96'E, 292–311 m, 11 August 1998: 1 ov F 4.6 mm (MNHN-IU-2013-17399).—Stn CP1349, 17°31.07'S, 178°38.79'E, 244–252 m, 11 August 1998: 1 F 5.1 mm (MNHN-IU-2013-17406).—Stn CP1364, 18°11.9'S, 178°34.5'E, 80–86 m, 15 August 1998: 1 ov F 5.5 mm (in gorgonians) (MNHN-IU-2013-13919).

Fiji. BORDAU 1. Stn CP1402, 16°38.33'S, 179°36.40'E, 260–279 m, 25 February 1999: 1 F, 3.9 mm (MNHN-IU-2013-17401).—Stn CP1404, 16°39.87'S, 179°35.70'E, 180 m, 25 February 1999: 1 F 5.3 mm (MNHN-IU-2013-17410).—Stn CP1404, 16°39.87'S, 179°35.70'E, 180 m, 25 February 1999: 1 F 3.7 mm (MNHN-IU-2013-17400).

Etymology. From de Latin *ensis*, sword in reference to the long rostrum.

Description. *Carapace*: 1.3 times longer than broad, dorsally armed with scattered spines and setae and some short transverse ridges; cervical groove distinct. Gastric region indistinctly defined and armed with 3 transverse rows of small spines: anterior row epigastric composed of 4 or 5 spines; median row protogastric composed of 7 or 8 spines, and posterior row mesogastric composed of 2 spines on a medially interrupted ridge. Cardiac region with 2 spines distinctly defined. Anterior branchial regions each armed with 2 small spines; one postcervical spine on each side. Front margin oblique; limit of orbit ending in small spine, one small spine between orbit spine and first anterolateral spine; one spine on the ventral orbital margin. Lateral margins of carapace nearly parallel medially and slightly convex; carapace margin armed with 6 or 7 small spines: 2 spines in front and 4–5 spines behind anterior cervical groove; first spine anterolateral, small, poorly-developed at level of epigastric row of spines; 2 spines on anterior branchial margin and 2–3 spines on posterior branchial margin; posterior transverse ridge straight and spineless. Rostrum triangular, flattish dorsally, narrow and elongate, 2.2–2.5 times longer than broad, 0.5 times of as long as remaining carapace; lateral margin armed with 4–5 incised teeth; distance between distalmost lateral incisions 0.25 distance between proximalmost lateral incisions.
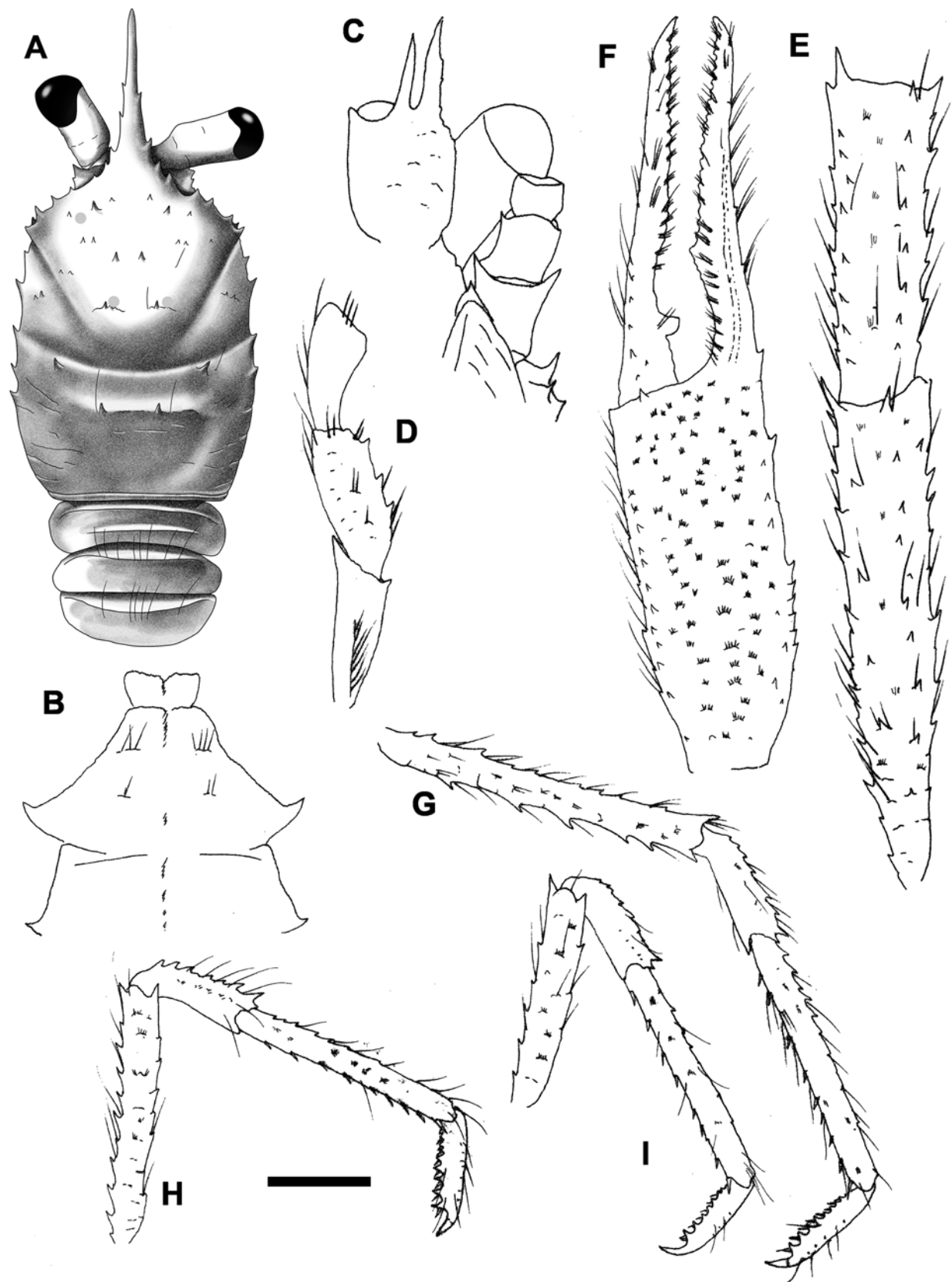
FIGURE 5. *Fennerogalathea ensifera* **n. sp.**, holotype, male 6.1 mm (MNHN- IU-2013-17407), Fiji. A, carapace and abdomen, dorsal view. B, sternal plastron. C, cephalic region, showing antennular and antennal peduncles, ventral view. D, right Mxp3, lateral view. E, right P1, merus and carpus, dorsal view. F, palm of right P1, dorsal view. G, right P2, lateral view. H, right P3, lateral view. I, right P4, lateral view. Scale: A, E–I = 1 mm; B–D = 2 mm.
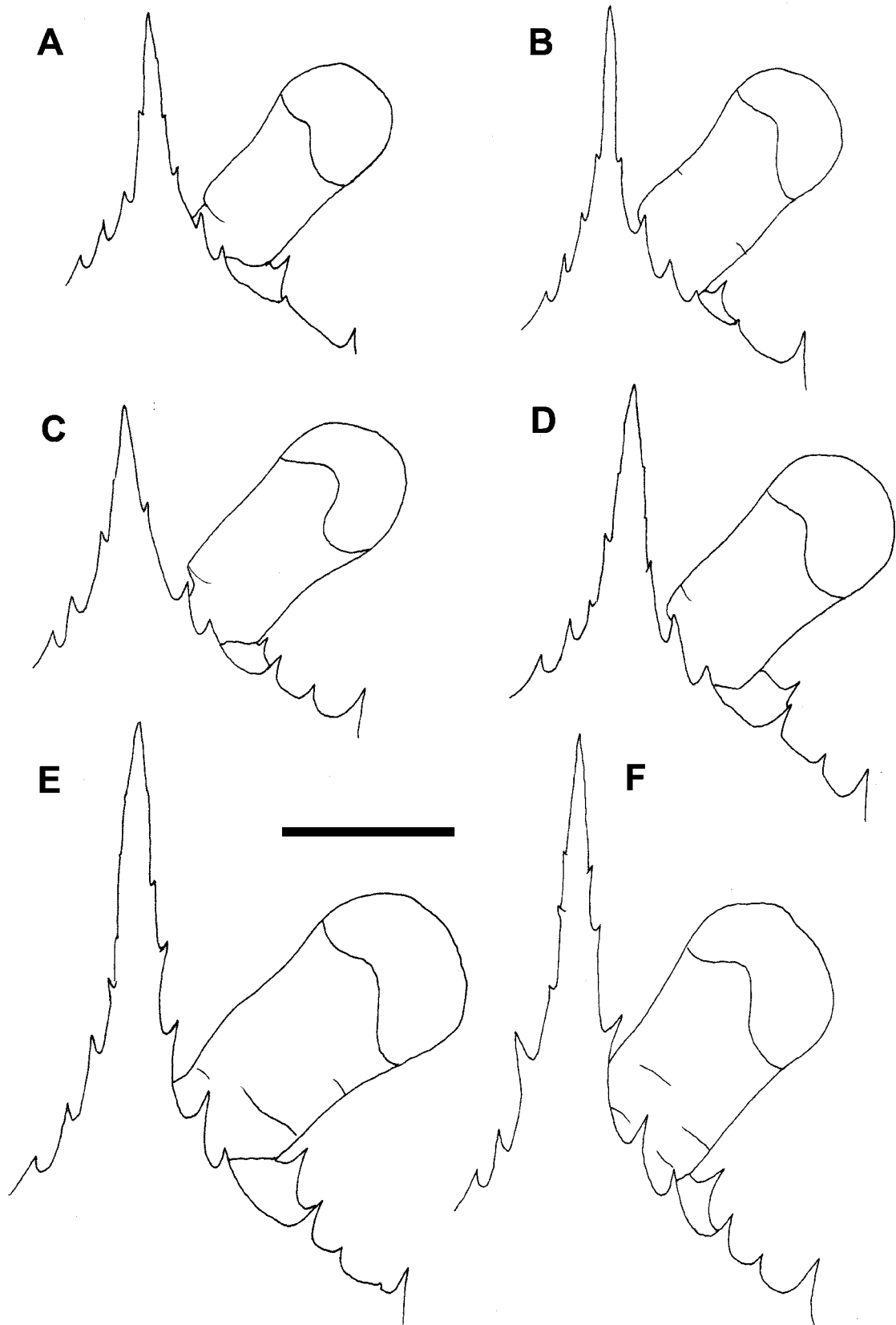
FIGURE 6. Rostrum and right anterior part of cephalothorax, dorsal view, showing eyes and orbit. *Fennerogalathea chani* **n. sp.**: A, male 3.4 mm (MNHN-IU-2013-503); B, male 3.6 mm (MNHN IU-2014-13380). *Fennerogalathea cultrata* **n. sp.**: C, ovigerous female 4.0 mm (MNHN-IU-2013-17419); D, male 3.2 mm (MNHN-IU-2013-17412). *Fennerogalathea ensifera* **n. sp.**: E, ovigerous female 4.9 mm (MNHN-IU-2013-17396); F, male 4.7 mm (MNHN-IU-2013-17398). Scale = 1 mm.

Sternum: Plastron longer than broad, lateral limits divergent anteriorly. Third thoracic sternite nearly quadrangular, sternite 4 contiguous to entire posterior margin of sternite 3, and wider than sternite 5.

Abdomen: Somite 2 with 2 uninterrupted transverse ridges on tergite, somites 3–4 smooth, with anterior uninterrupted ridge without tuft of setae; somites 5 and 6 smooth; posteromedian margin on somite 6 straight. Males with G1 and G2.

Eyes: Eyes stalk subcylindrical, narrow and elongate, 0.6–0.7 times shorter than rostrum. Ocular peduncles 1.7–2.1 times longer than broad, maximum corneal diameter 0.8 rostrum width.

Antennule: Article 1 with well-developed distolateral and distodorsal spines on, distodorsal overreaching distolateral, distomesial margin usually unarmed or with one minute spine.

Antenna: Article 1 hardly visible from dorsal view, with 1 small, distinct distomesial spine. Article 2 slightly wider and longer than article 3 with distolateral and distomesial spines subequal in size. Article 3 with 1 small distomesial spine. Article 4 unarmed.

Mxp3: Ischium with well-developed distal spine on flexor margin; extensor margin unarmed; crista dentata with 25 or 26 denticles. Merus subequal in length to ischium, with 3 subequal spines on flexor margin; extensor margin unarmed. Carpus spineless.

P1: 4.3–4.4 (males), 5.7–6.0 (females) times postorbital carapace length, with some scattered short and long setae on dorsal surface and along lateral and mesial margins of all articles. Merus 1.6 longer than carapace, 1.5–1.6 times as long as carpus, with numerous spines, stronger spines along mesial and dorsodistal margins. Carpus 0.9–1.0 times as long as palm, 3.4–3.6 times longer than broad, lateral and mesial margins subparallel, dorsal surface with small spines; mesial surface with some strong spines; row of spines along lateral margin. Palm 2.4–2.5 (males), 4.5–4.8 (females) times longer than broad, lateral and mesial margins subparallel; spines arranged in longitudinal rows; dorsolateral row continued onto whole lateral margin of fixed finger. Fingers as long as or slightly longer than palm, each finger distally with 2 rows of teeth, spooned; movable finger with row of some spines in proximal half of mesial margin, otherwise unarmed.

P2–4: Slender, moderately setose, sparsely with long plumose setae on all articles. P2 2.7 times carapace length. Meri successively shorter posteriorly (P3 merus 0.8 length of P2 merus, P4 merus 0.8 length of P3 merus); P2 merus 1.1 of carapace length, 10 times as long as broad, 1.3 times longer than P2 propodus; P3 merus 7.5 times as long as broad, 1.2 times length of P3 propodus; P4 merus 6.0 times as long as broad, 0.9 length of P4 propodus; extensor margins each with row of 10–12 spines in P2–3, and with 6 small spines in P4; lateral surfaces unarmed in P2–3, 1 or 2 minute spines in P4; flexor margins each with strong terminal spine in P2–4, 5 or 6 additional spines in P2–3, 1 or 2 in P4; ventromesial margins with 1 or 2 spines in P2. Carpi each with 6 or 7 spines on extensor margin of P2–4; lateral surfaces each all with row of 2 or 3 small spines paralleling extensor row; flexor margins unarmed or with minute spine. P2–4 propodi 8.5–9.5 times as long as broad; extensor margins each with 5–7 small proximal spines in P2–4; flexor margins nearly straight, each with 2 pairs of terminal spines preceded by 7 or 8 slender movable spines. Dactyli subequal in length, 0.4–0.5 length of propodi, ending in incurved, strong, sharp spine; flexor margins each with prominent triangular terminal tooth preceded by row of 8 or 9 teeth.

Distribution. Fiji, between 102 and 311 m.

Remarks. *Fennerogalathea ensifera* **n. sp.** is clearly differentiated from its congeners by the shape of the rostrum, which is narrower and more elongate than in the other species. The differences are as follows.

The rostrum is more than twice longer than broad, and clearly exceeding the corneae in *F. ensifera* **n. sp.**, whereas it is at most twice longer than broad, not reaching or slightly exceeding the corneae in the other species.

The distance between the distalmost lateral incisions of the rostrum is 0.25 the distance between the proximalmost lateral incisions in *F. ensifera* **n. sp.**, whereas this ratio is 0.4 in the other species.

The lateral spines of the carapace are small in *F. ensifera* **n. sp.**, whereas these spines are always well developed in the other species.

The minimum molecular divergence observed between *F. ensifera* **n. sp.** and *F. cultrata* **n. sp.** was 9.43% and 0.70% for the COI and 16S, respectively.

References

Adams, A. & White, A. (1848) Crustacea. *In*: Adams, A. (Ed.), *The Zoology of the voyage of the HMS "Samarang" under the command of Captain Sir Edward Belcher, C.B., F.R.A.S., F.G.S., during the years 1843–1846*. Benham and Leeve, London, pp. 1–66, 13 pls.

Ahyong, S.T., Baba, K., Macpherson, E. & Poore, G.C.B. (2010) A new classification of the Galatheoidea (Crustacea: Decapoda: Anomura). *Zootaxa*, 2676, 57–68.

Ahyong, S.T., Andreakis, N. & Taylor, J. (2011) Mitochondrial phylogeny of the deep-sea squat lobsters, Munidopsidae (Galatheoidea). *Zoologischer Anzeiger*, 250, 367–377.
https://doi.org/10.1016/j.jcz.2011.06.005

Baba, K. (1969) Four new genera with their representatives and six new species of the Galatheidae in the collection of the Zoological Laboratory, Kyushu University, with redefinition of the genus *Galathea. Ohmu*, 2, 1–32.

Baba, K. (1971) *Lauriea*, a new genus proposed for *Galathea gardineri* Laurie (Crustacea, Anomura, Galatheidae). *Memoirs of the Faculty of Education, Kumamoto University, Section 1 (Natural Science)*, 19, 51–53.

Baba, K. (1988) Chirostylid and galatheid crustaceans (Decapoda: Anomura) of the "Albatross" Philippine Expedition, 1907–1910. *Researches on Crustacea*, Special Number, 2, 1–203.

Baba, K. (2005) Deep-sea chirostylid and galatheid crustaceans (Decapoda: Anomura) from the Indo-West Pacific, with a list of species. *Galathea Reports*, 20, 1–317.

Baba, K., Macpherson, E., Poore, G.C.B., Ahyong, S.T., Bermudez, A., Cabezas, P., Lin, C.-W., Nizinski, M., Rodrigues, C. & Schnabel, K. (2008) Catalogue of squat lobsters of the world (Crustacea: Decapoda: Anomura—families Chirostylidae, Galatheidae and Kiwaidae). *Zootaxa*, 1905, 1–220.

Baba, K., Macpherson, E. & Chan, T.Y. (2009) *Crustacean Fauna of Taiwan. Squat lobsters (Chirostylidae and Galatheidae)*. National Taiwan Ocean University, Keelung, 311 pp.

Cabezas, P., Macpherson, E. & Machordom, A. (2008) A new genus of squat lobster (Decapoda: Anomura: Galatheidae) from the South West Pacific and Indian Ocean inferred from morphological and molecular evidence. *Journal of Crustacean Biology*, 28 (1), 68–75.
https://doi.org/10.1651/07-2823R.1

Cabezas, P., Macpherson, E. & Machordom, A. (2011) *Allogalathea* (Decapoda: Galatheidae): a monospecific genus of squat lobster? *Zoological Journal of the Linnean Society*, 162, 245–270.
https://doi.org/10.1111/j.1096-3642.2010.00681.x

Fabricius, J.C. (1793) *Entomologia systematica emendata et aucta. Secundum classes, ordines, genera, species adjectis synonymis, locis; observatiosnibus, descriptionibus*. Hafniae, 519 pp.

Folmer, O., Black, M., Hoeh, W., Lutz, R. & Vrijenhoek, R. (1994) DNA primers for amplification of mitochondrial cytochrome c oxidase subunit I from diverse metazoan invertebrates. *Molecular Marine Biology and Biotechnology*, 3, 294–299.

Huelsenbeck, J.P. & Ronquist, F. (2001) MrBayes: Bayesian inference of phylogeny. *Bioinformatics*, 17, 754–755.
https://doi.org/10.1093/bioinformatics/17.8.754

Katoh, K., Misawa, K., Kuma, K. & Miyata, T. (2002) MAFFT: a novel method for rapid multiple sequence alignment based on fast Fourier transform. *Nucleic Acids Research*, 30, 3059–3066.
https://doi.org/10.1093/nar/gkf436

Machordom, A. & Macpherson, E. (2004) Rapid radiation and cryptic speciation in squat lobsters of the genus *Munida* (Crustacea, Decapoda) and related genera in the South West Pacific: molecular and morphological evidence. *Molecular Phylogenetics and Evolution*, 33, 259–279.
https://doi.org/10.1016/j.ympev.2004.06.001

Machordom, A., Araujo, R., Erpenbeck, D. & Ramos, M.A. (2003) Phylogeography and conservation genetics of endangered European Margaritiferidae (Bivalvia: Unionoidea). *Biological Journal of the Linnean Society*, 78, 235–252.
https://doi.org/10.1046/j.1095-8312.2003.00158.x

Macpherson, E. & Baba, K. (2011) Chapter 2. Taxonomy of squat lobsters. *In*: Poore, G.C.B., Ahyong, S.T. & Taylor, J. (Eds.), *The biology of squat lobsters*. CSIRO Publishing, Melbourne, pp. 39–71. [also published as Crustacean Issues Vol. 20 by CRC Press: Baton Roca]

Macpherson, E. & Robainas-Barcia, A. (2013) A new genus and some new species of the genus *Lauriea* Baba, 1971 (Crustacea, Decapoda, Galatheidae) from the Pacific and Indian Oceans, using molecular and morphological characters.

Zootaxa, 3599 (2), 136–160.
https://doi.org/10.11646/zootaxa.3599.2.2.

Macpherson, E. & Robainas-Barcia, A. (2015) Species of the genus *Galathea* Fabricius, 1793 (Crustacea, Decapoda, Galatheidae) from the Indian and Pacific Oceans, with descriptions of 92 species. *Zootaxa*, 3913 (1), 1–335.
https://doi.org/10.11646/zootaxa.3913.1.1

Palero, F., Robainas-Barcia, A., Corbari, L. & Macpherson, E. (2017) Phylogeny and evolution of shallow-water squat lobsters (Decapoda, Galatheoidea) from the Indo-Pacific. *Zoologia Scripta*. [in press]
https://doi.org/10.1111/zsc.12230

Palumbi, S., Martin, A., Romano, S., McMillan, W.O., Stice, L. & Grabowski, G. (2002) *The simple fool's guide to PCR. Version 2.0.* Department of Zoology and Kewalo Marine Laboratory, University of Hawaii, Honolulu, 45 pp.

Poore, G.C.B. & Andreakis, N. (2011) Morphological, molecular and biogeographic evidence support two new species in the *Uroptychus naso* complex (Crustacea: Decapoda: Chirostylidae). *Molecular Phylogenetics and Evolution*, 60, 152–169.
https://doi.org/10.1016/j.ympev.2011.03.032

Poore, G.C.B. & Andreakis, N. (2012) The *Agononida incerta* species complex unravelled (Crustacea: Decapoda: Anomura: Munididae). *Zootaxa*, 3429, 1–29.

Poore, G.C.B. & Andreakis, N. (2014) More species of the *Agononida incerta* complex revealed by molecules and morphology (Crustacea: Decapoda: Anomura: Munididae). *Zootaxa*, 3860 (3), 201–225.
https://doi.org/10.11646/zootaxa.3860.3.1

Rambaut, A. (1996) Se-Al v2.0a11. University of Oxford, Oxford. [software]

Rambaut, A. (2014) Figtree v.1.4.2. Available from: http://tree.bio.ed.ac.uk/software/figtree/ (accessed 16 May 2017)

Richer de Forges, B., Chan, T.-Y., Corbari, L., Lemaitre, R., Macpherson, E., Ahyong, S.T. & Ng, P.K.L. (2013) The MUSORSTOM-TDSB deep-sea benthos exploration program (1976–2012): An overview of crustacean discoveries and new perspectives on deep-sea zoology and biogeography. *In*: Ahyong, S.T., Chan, T.-Y., Corbari, L. & Ng, P.K.L. (Eds.), *Tropical Deep-Sea Benthos. Vol. 27. Mémoires du Muséum national d'Histoire naturelle, Paris*, 204, pp. 13–66.

Samouelle, G. (1819) *The entomologists' useful compendium; or an introduction to the knowledge of British Insects, comprising the best means of obtaining and preserving them, and a description of the apparatus generally used; together with the genera of Linné, and modern methods of arranging the Classes Crustacea, Myriapoda, spiders, mites and insects, from their affinities and structure, according to the views of Dr. Leach. Also an explanation of the terms used in entomology; a calendar of the times of appearance and usual situations of near 3,000 species of British Insects; with instructions for collecting and fitting up objects for the microscope.* Thomas Boys, London, 496 pp., 412 pls.

Spalding, M.D., Fox, H.E., Allen, G.R., Davidson, N., Ferdaña, Z.A., Finlayson, M., Halpern, B.S., Jorge, M.A., Lombana, A., Lourie, S.A., Martin, K.D., McManus, E., Molnar, J., Recchia, C.A. & Robertson, J. (2007) Marine ecoregions of the world: a bioregionalization of coastal and shelf areas. *Bioscience*, 57, 573–583.
https://doi.org/10.1641/B570707

Swofford, D.L. (2002) PAUP*: Phylogeny Analysis Using Parsimony (*and other methods). Version 4.0a147. Sinauer Associates Inc., Sunderland, Massachusetts.

Tirmizi, N.M. & Javed, W. (1993) *Indian Ocean galatheids (Crustacea: Anomura)*. Marine Reference Collection and Resource Centre, University of Karachi, Karachi, 147 pp.

RODRIGUEZ-FLORES *ET AL.*

Article

Three new species of squat lobsters of the genus *Munidopsis* Whiteaves, 1874, from Guadeloupe Island, Caribbean Sea (Crustacea, Decapoda, Munidopsidae)

PAULA C. RODRÍGUEZ-FLORES[1,2,3], ENRIQUE MACPHERSON[2] & ANNIE MACHORDOM[1]

[1]*Museo Nacional de Ciencias Naturales (MNCN-CSIC), José Gutiérrez Abascal, 2, 28006 Madrid, Spain.*
E-mails: paulacrf@mncn.csic.es; annie@mncn.csic.es
[2]*Centre d'Estudis Avançats de Blanes (CEAB-CSIC), C. d'Accés Cala Sant Francesc 14, 17300 Blanes, Spain.*
E-mail: macpherson@ceab.csic.es
[3]*Corresponding author*

Abstract

The genus *Munidopsis* is one of the most diverse genera within squat lobsters. Here, three new species of *Munidopsis*, *M. cornuata* **n. sp.**, *M. senticosa* **n. sp.**, and *M. turgida* **n. sp.**, from <500 m off Guadeloupe Island (Caribbean Sea), are fully described and illustrated. Among the Atlantic species of the genus, *M. cornuata* **n. sp.** belongs to the group of species having the dorsal surface of the carapace with spines and is most similar to *M. robusta* (A. Milne-Edwards, 1880), from the Gulf of Mexico and Caribbean Sea. *Munidopsis senticosa* **n. sp.** resembles *M. barbarae* (Boone, 1927) from the Bahamas and the Gulf of Mexico and *M. penescabra* Pequegnat & Williams 1995, from off Georgia and Gulf of Mexico; the three species belong to the group having the carapace covered with sharp spines. Finally, *M. turgida* **n. sp.** is characterized by having the dorsal surface of the carapace, abdomen and pereiopods covered by granules; and resembles *M. granulens* Mayo, 1972, from NW Caribbean Sea. Apart from the morphological evidence, the analysis of mitochondrial genes (COI and 16S) supports establishing these new species, showing very high genetic divergences compared to their congeners (from 14.5 to 17% for COI, and 7.7 to 12.8% for 16S data).

Key words: Anomura, Galatheoidea, mitochondrial genes, Caribbean Sea, Atlantic Ocean

Introduction

The works on the genus *Munidopsis* Whiteaves, 1874 from the Caribbean Sea and Gulf of Mexico are numerous, revealing the existence of a rich fauna (Wicksten & Packard 2005; Baba *et al.* 2008; Coykendall *et al.* 2017). The genus is the most diverse within the family Munidopsidae Ortmann, 1898 (Ahyong *et al.* 2010). This high diversity was firstly mentioned by A. Milne-Edwards (1880), albeit briefly, in his preliminary report on the crustaceans collected by the "Blake" during the trawling expedition into the Caribbean Sea and Gulf of Mexico, which contains descriptions of 22 species of *Munidopsis*. The formal report of the "Blake" was published some years later (A. Milne-Edwards & Bouvier 1897). Subsequently, Benedict (1902), Boone (1927), and Chace (1942) reported numerous species including new species. The studies on this genus continued with the collections made by the "Alaminos" and other expeditions in the Gulf of Mexico and the Caribbean Sea (Pequegnat & Pequegnat 1970, 1971; Mayo 1972, 1974; Gore 1983; Baba & Camp 1988). More recently, some studies have improved our knowledge on the distribution of the species (Navas *et al.* 2003; Campos *et al.* 2005; Herrera-Medina *et al.* 2014; Vazquez-Bader & Gracia 2016), including the description of some new species (Pequegnat & Williams 1995; Vazquez-Bader *et al.* 2014; Macpherson *et al.* 2016). Thus, 56 species of the genus *Munidopsis* are currently known in the Western Atlantic.

During 2015, the cruise KARUBENTHOS sampled around the Guadeloupe Island (Caribbean Sea) and collected numerous decapod crustaceans. These authors cited 17 species of *Munidopsis*, some of which, however, were left as uncertain in the systematic status, pending extensive studies (Poupin & Corbari 2016). Here, we use morphological and molecular characters to reveal that these uncertain species can be considered as new to science.

Material and methods

Sampling and identification. The samples were collected by the R/V Antea in July 2015, using a Warén dredge and a benthic beam trawl. The expedition was organized jointly by the Muséum national d'Histoire naturelle, Paris (MNHN), the National Park of Guadeloupe, and the Université des Antilles et de la Guyane, with the support by GENAVIR and IRD (Poupin & Corbari 2016).

The terminology used for the descriptions follows Baba *et al.* (2009, 2011). The size of the specimens is indicated by the postorbital carapace length. Measurements of appendages are taken on dorsal (pereiopod 1), lateral (antennule, pereiopods 2–4) and ventral (antenna) midlines. Ranges of morphological and meristic variations are included in the description. Abbreviations used are: Mxp = maxilliped; P1 = pereiopod 1 (cheliped); P2–4 = pereiopods 2–4 (walking legs 1–3); M = male; F = female; ovig. = ovigerous. The material is deposited at the Muséum national d'Histoire naturelle, Paris (MNHN).

Molecular analysis. The methodology for molecular analyses largely follows previous studies (Rodríguez-Flores *et al.* 2017; Macpherson *et al.* 2017). The tissue was isolated from the fifth pereiopods. DNA extraction was carried out with the DNeasy kit (Qiagen) following manufacturer's protocol. A digestion of the samples during 18–24 hours was performed and RNase added at later stage. Partial sequences of the mitochondrial cytochrome oxidase subunit I (COI) and 16S rRNA (16S) genes were amplified by polymerase chain reaction (PCR) using the following primers: LCO1490/HCOI2198 (Folmer *et al.* 1994), COI-H (Machordom *et al.* 2003), and 16SAR and 16SBR (Palumbi *et al.* 1991), respectively. Specimens extracted, sequenced genes and sequences extracted from GenBank for comparison are listed in Table 1. The amplified fragments were purified using ExoSAP-IT (Affymetrix). A BigDye Terminator in an ABI 3730 genetic analyzer was used for sequencing of both strands using the SECUGEN service. Forward and reverse DNA sequences obtained for each specimen and partial genes were checked and assembled using the program Sequencher 4.8 (Gene Code Corporation) and aligned using MAFFT (Katoh *et al.* 2002) with a posterior correction in Se-Al alignment editor (http://tree.bio.ed.ac.uk/software/seal/).

Uncorrected divergences (p) between pair of species were calculated using MEGA 7.0.26 (Kumar *et al.* 2016).

TABLE 1. Species of *Munidopsis* included in the study for mitochondrial DNA analyses (COI and 16S), including sampling localities: expedition, station, codes and GenBank accession numbers.

Species	Code	Locality-Cruise	Station	16S rRNA	COI
M. barbarae	MNHN-IU-2014-13823	Guadeloupe-KARUBENTHOS	DW4604	MG979471	MG979478
M. barbarae	MNHN-IU-2014-13822	Guadeloupe-KARUBENTHOS	DW4604	MG979472	MG979479
M. cornuata **n. sp.**	MNHN-IU-2013-19128	Guadeloupe-KARUBENTHOS	DW4630	MG979474	MG979481
M. cornuata **n. sp.**	MNHN-IU-2016-2560	Guadeloupe-KARUBENTHOS	DW4630	MG979473	MG979480
M. penescabra	-	Gulf of Mexico	-	-	KX016547–8
M. granulens	MNHN-IU-2016-6103	Guadeloupe-KARUBENTHOS	DW4604	-	MG979486
M. robusta	MNHN-IU-2013-2550	French Guiana-GUYANE	CP4367	MG979477	MG979484
M. robusta	MNHN-IU-2013-3367	French Guiana-GUYANE	CP4367	-	MG979485
M. senticosa **n. sp.**	MNHN-IU-2013-18962	Guadeloupe-KARUBENTHOS	DW4573	MG979475	MG979482
M. senticosa **n. sp.**	MNHN-IU-2013-18964	Guadeloupe-KARUBENTHOS	DW4573	MG979476	MG979483
M. turgida **n. sp.**	MNHN-IU-2016-2873	Guadeloupe-KARUBENTHOS	DW4606	-	MG979487

Results

Our results demonstrate the clear genetic divergences between each new species and their closest relative. We provide COI and 16S data from the following species: *Munidopsis barbarae* (Boone, 1927)*, M. cornuata* **n. sp.**, *M. penescabra* Pequegnat & Williams, 1995 (obtained from the GenBank), *M. granulens* Mayo, 1972, *M. robusta* (A. Milne-Edwards, 1880)*, M. senticosa* **n. sp.** and *M. turgida* **n. sp.** (Table 1). The divergences are indicated in the Remarks of each new species.

Systematic account

Family Munidopsidae Ortmann, 1898

Munidopsis **Whiteaves, 1874**

Munidopsis cornuata **n. sp.**
(Fig. 1)

Munidopsis robusta.—Poupin & Corbari, 2016: 49, figs 11m–n (Guadeloupe, 379–428 m).

Material examined. *Holotype*: KARUBENTHOS 2015, Stn DW4630, 1548'N, 6129'W, 27 June 2015, 379–428 m: M 4.8 mm (MNHN-IU-2013-19128).

Paratypes: KARUBENTHOS 2015, Stn DW4630, same as holotype: M 4.4 mm (MNHN-IU-2016-2560). Stn DW4633, 1548'N, 6129'W, 27 June 2015, 378–432 m: M 3.9 mm (MNHN-IU-2016-2907).

Etymology. From the Latin, *cornuatus*, hornlike, in reference to the strong median gastric and cardiac spines.

Description. *Carapace*: As long as broad; quadrangular, dorsal surface granulated, moderately convex from side to side. Two thick epigastric spines, one large median mesogastric spine and one large median cardiac spine. Regions well delineated by deep furrows including distinct anterior and posterior cervical grooves. Posterior cardiac region weakly triangular, preceded by deep transverse depression. Posterior margin unarmed. Rostrum narrowly triangular, spine-like, directed slightly upwards, dorsally carinate, lateral margins straight; 0.5 × carapace length. Frontal margin transverse behind ocular peduncle, then slightly oblique toward anterolateral spine of carapace; antennal spine at level of lateral margin of antenna and near anterolateral spine. Lateral margins straight and subparallel; anterolateral spine broad; short spine at each end of anterior and posterior branches of cervical groove. Pterygostomian flap with minute granules, anteriorly acute.

Sternum: As long as broad, maximum width at sternite 7. Sternite 3 moderately broad, 2.5 times wider than long, anterolaterally angular, anterior margin with rounded median process flanked by 2 lobes. Sternite 4 narrowly elongate anteriorly; surface depressed in midline, with some granules; greatest width 3 times that of sternite 3, and twice wider than long.

Abdomen: Somites 2–4 each with elevated transverse ridge and thick median spine, much smaller on somite 4; somites 5–6 lacking such spines; somite 6 with weakly produced posterolateral lobes and slightly convex posteromedian margin. Telson composed of 8 plates; posterior plates combined, 1.8 times as wide as long.

Eye: Ocular peduncle fused; cornea subglobular, unarmed.

Antennule: Article 1 of peduncle granulate, with strong distolateral and distodorsal spiniform projections; distomesial angle unarmed, minutely serrated; lateral margin swollen, unarmed.

Antenna: Peduncle not reaching end of rostrum; article 1 with strong distolateral spine, reaching midlength of article 2, distomesial angle rounded; article 2 with well-developed distomesial and distolateral spines, latter larger; article 3 with 3 small spines (distomesial, distolateral and distodorsal); article 4 with small distomesial and distolateral spines.

Mxp3: Surface granulate. Ischium as long as merus measured on extensor margin; extensor and flexor margins unarmed; crista dentata finely denticulate; merus having flexor margin with 2 distinct thick spines, and 1 or 2 small additional spines, extensor margin with distal spine; carpus, propodus and dactylus unarmed.

P1: Twice as long as carapace, granulate. Merus twice carpus length, with several thick distal spines. Carpus 1.5 times longer than wide, with 1 or 2 thick mesial spines and lateral distal spine. Palm 1.3 times as long as carpus, 1.5 times longer than wide, and as long as fingers, unarmed. Fingers not gaping; prehensile edges each with row of very small subtriangular teeth; fixed finger without denticulate carina on distolateral margin.

P2–4: Surface of articles granulate. P2 longer than P3 and P4, nearly reaching end of P1. P2 merus moderately elongate, 0.9 times carapace length, 3.0 times longer than high and 1.2 times length of P2 propodus. P2–4 meri with row of spines along extensor margin; carpi with one thick distal spine on extensor margin; P2–4 propodi 4.8–5.0 times as long as high, one distal spine on extensor margin; 0–1 distal spinules on flexor margin; dactylus 0.6 × length of propodus; distal claw short, moderately curved; flexor margin distally curved, with 6 or 7 minute teeth decreasing in size proximally, each with slender corneous spine, ultimate tooth closer to penultimate tooth than to dactylar tip.
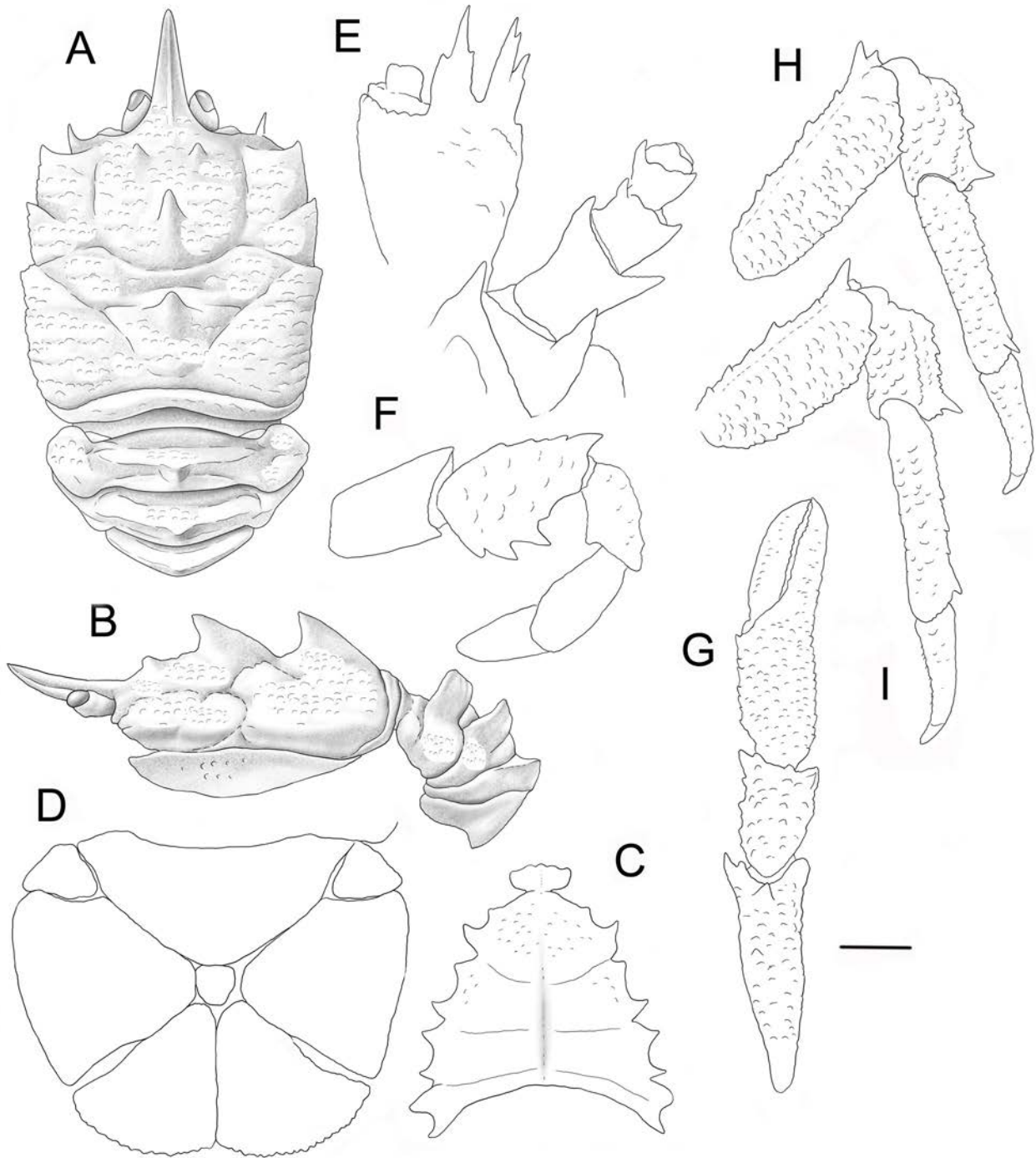
FIGURE 1. *Munidopsis cornuata* **n. sp.**, holotype, male 4.8 mm (MNHN-IU-2013-19128), Guadeloupe. A, carapace and abdomen, dorsal view. B, carapace and abdomen, lateral view. C, sternal plastron. D, telson. E, cephalic region, showing antennular and antennal peduncles, ventral view. F, right Mxp3, lateral view. G, right P1, dorsal view. H, right P2, lateral view. I, right P3, lateral view. Scales: A–C, G–I = 1.0 mm; D–F = 0.5 mm.

Epipods absent from pereiopods.

Colour: Ground colour of carapace, abdomen and pereiopods orange. Tip of rostrum whitish. P2–4 with some whitish bands; dactyli distally whitish (see Poupin & Corbari 2016).

Distribution. Guadeloupe, between 378 and 432 m.

Remarks. *Munidopsis cornuata* **n. sp.** resembles *M. robusta* (A. Milne-Edwards 1880) from the Gulf of Mexico and Caribbean Sea (Baba *et al*. 2008). Both species belong to the group of species having the dorsal

surface of the carapace with spines, the abdominal somites 2–4 armed with one spine, and the rostrum unarmed laterally. The new species can be easily distinguished from *M. robusta* by the following features:

•	The gastric region has a large central protuberance and five small epigastric protuberances in *M. robusta;* whereas there are two epigastric spines and a large mesogastric spine in *M. cornuata.* The cardiac region presents a small median spine in *M. robusta*, whereas this spine is very strong in the new species. Furthermore, the posterior margin of the carapace is unarmed in the new species, whereas this margin has a median spine in *M. robusta.*
•	The spines on the abdominal somites are acute in *M. robusta*, whereas they are blunt and thick in *M. cornuata.*
•	The P2 nearly reaches the end of P1 in the new species, whereas it is clearly shorter in *M. robusta.*
•	Molecular divergence between *Munidopsis cornuata* and *M. robusta* (recently collected from French Guiana, Table 1) is very high, presenting 17% of divergence for the COI and 12.8% for the 16S.

Munidopsis senticosa n. sp.
(Figs 2, 3B)

Munidopsis aff. *barbarae.*—Poupin & Corbari, 2016: 46, fig. 11c (Guadeloupe, 389–542 m) (in part, Stn DW4604 = *M. barbarae,* see below).

Material examined. *Holotype*. KARUBENTHOS 2015, Stn DW4573, 1620'N, 6055'W, 17 June 2015, 389–413 m: M 4.2 mm (MNHN-IU-2013-18964).
	Paratype. KARUBENTHOS, Stn DW4573, same as holotype: F 3.8 mm (MNHN-IU-2013-18962).
	Etymology. From the Latin, *senticosus*, thorny, rough, in reference to the spiny surface of the carapace.
	Description. *Carapace*: Slightly longer than broad; dorsal surface moderately convex from side to side, covered with regularly arranged sharp spines; each spine with some long plumose setae. Regions well delineated by furrows including distinct anterior and posterior cervical grooves. Posterior cardiac region weakly triangular, preceded by deep transverse depression. Posterior margin preceded by elevated ridge with 10 spines. Rostrum narrow, spiniform and horizontal, 0.4 carapace length; unarmed and with numerous long plumose setae; dorsally carinate; lateral margin slightly concave. Frontal margin oblique behind ocular peduncle, leading to 2 small antennal (outer orbital) spines (mesial longer than lateral), then transverse toward anterolateral spine of carapace, 1 or 2 spines between antennal and anterolateral spines; distinct spine ventral to front margin between ocular and antennal peduncles. Lateral margins weakly convex and subparallel; anterolateral spine well developed, as long as mesial antennal spine; lateral end of anterior branch of cervical groove with distinct notch followed by 2 distinct spines; lateral end of posterior cervical groove with notch, followed by 3 distinct spines. Pterygostomian flap with minute spines, anteriorly acute, overreaching anterolateral spine.
	Sternum: As long as broad, maximum width at sternites 6 and 7. Sternite 3 moderately broad, 3 times wider than long, anterior margin with shallow median notch flanked by 2 low denticulate lobes, lateral margin rounded. Sternite 4 narrowly elongate anteriorly; surface depressed in midline, smooth; greatest width 2.5 times that of sternite 3, and twice wider than long.
	Abdomen: Somites unarmed; somites 2–3 each with 2 elevated transverse ridges, furnished with plumose setae; somite 4 with one ridge only, with some plumose setae; somites 5–6 lacking such ridges; somite 6 with weakly produced posterolateral lobes and nearly transverse posteromedian margin. Telson composed of 7 plates; posterior plates combined, 1.5 times as wide as long.
	*Eye*: Ocular peduncle fused; cornea subglobular, slightly narrower than eyestalk, with long median eyespine arising from centre of dorsal surface.
	Antennule: Article 1 with strong distolateral and 2 distodorsal spines, distomesial angle unarmed, minutely serrated; lateral margin swollen, unarmed.
	Antenna: Peduncle not reaching end of rostrum; article 1 with small distomesial and distolateral spines, latter larger, clearly not reaching end of article 2; article 2 with strong distomesial and distolateral spines; article 3 with 3 strong distal spines (lateral, ventral and dorsal); article 4 unarmed.
	Mxp3: Ischium as long as merus measured on extensor margin; extensor and flexor margins terminating in spine; crista dentata finely denticulate; merus having flexor margin with 3 well-developed spines, median spine much larger, extensor margin with distal spine; carpus with row of small spines along extensor margin, propodus and dactylus unarmed.
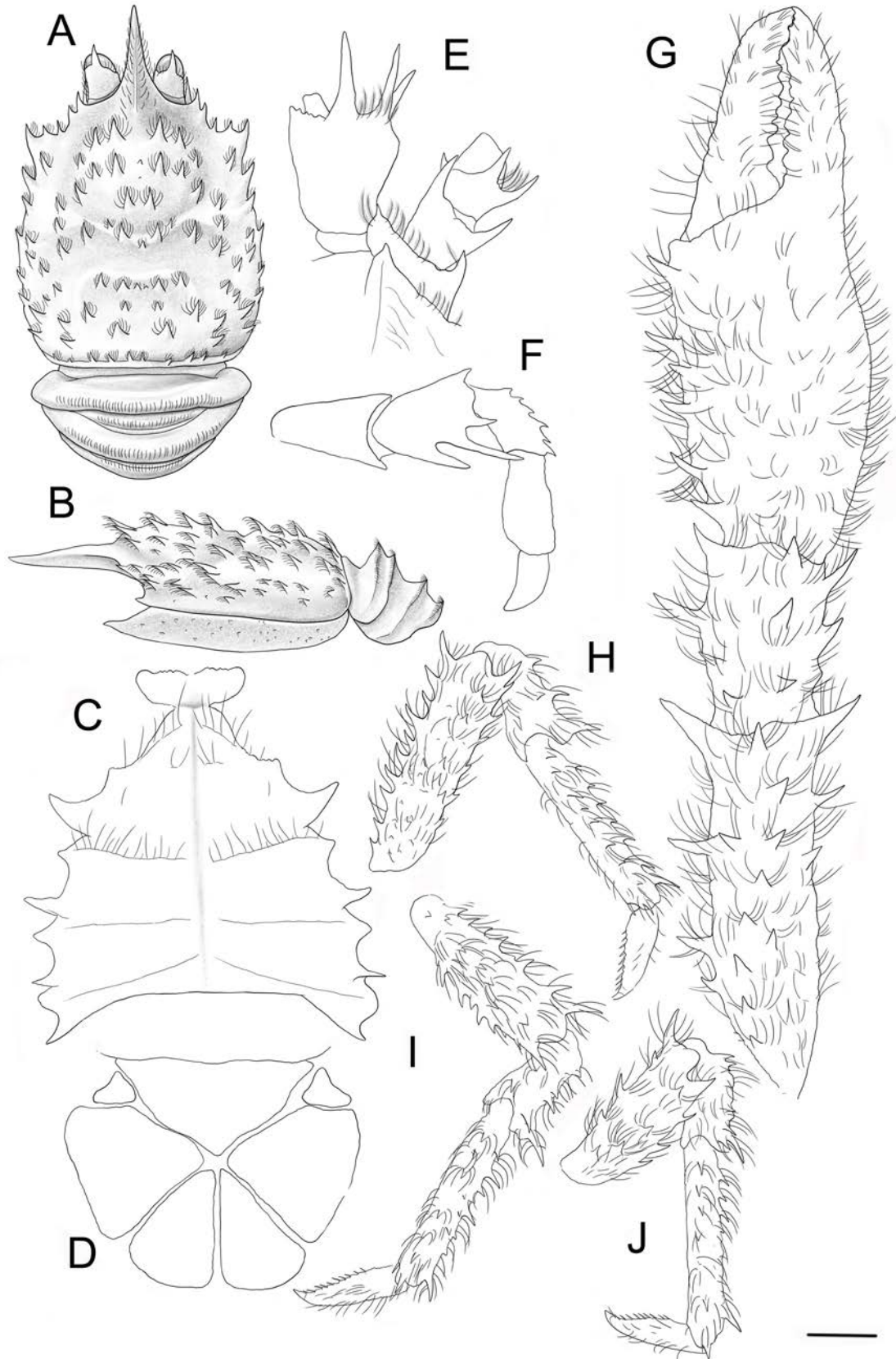
FIGURE 2. *Munidopsis senticosa* **n. sp.**, holotype, male 4.2 mm (MNHN-IU-2013-18964), Guadeloupe. A, carapace and abdomen, dorsal view. B, carapace and abdomen, lateral view. C, sternal plastron. D, telson. E, cephalic region, showing antennular and antennal peduncles, ventral view. F, right Mxp3, lateral view. G, right P1, dorsal view. H, right P2, lateral view. I, right P3, lateral view. J, right P4, lateral view. Scales: A, B, G–J = 1.0 mm; C–F = 0.5 mm.

P1: 4.3 times longer than carapace, covered with numerous long plumose setae on merus to dactylus. Merus, twice longer than carpus, with rows of spines (mesial, lateral and dorsal), distal ones stronger than others. Carpus 1.4 times longer than wide, with some spines along mesial, lateral and dorsal sides. Palm nearly twice longer than carpus, 1.6 times as long as wide, and 1.4 times as long as fingers, row of spines along mesial margin. Fingers not gaping; prehensile edges each with row of blunt teeth; fixed finger without denticulate carina on distolateral margin.

P2–4: moderately slender, with dense plumose setae. P2 longer than P3 and P4, clearly not exceeding end of P1. P2 merus elongate, 0.9 times carapace length, 3.8 times longer than high and 1.1 times length of P2 propodus. P2–4 meri with row of spines along extensor and flexor margins; carpi with spines along extensor margin, 1 or 2 spines on lateral side; P2–4 propodi 5 times as long as high, with row of spines along extensor margin and dorsal side; a few distal spinules along flexor margin; dactylus 0.5 length of propodus; distal claw short, moderately curved; flexor margin nearly straight, with 8 or 9 small teeth decreasing in size proximally, each with slender corneous spine, ultimate tooth closer to penultimate tooth than to dactylar tip.

Epipods absent from pereiopods.

Colour: Entire body reddish orange; P1 pale.

Distribution. Guadeloupe, between 389 and 413 m.
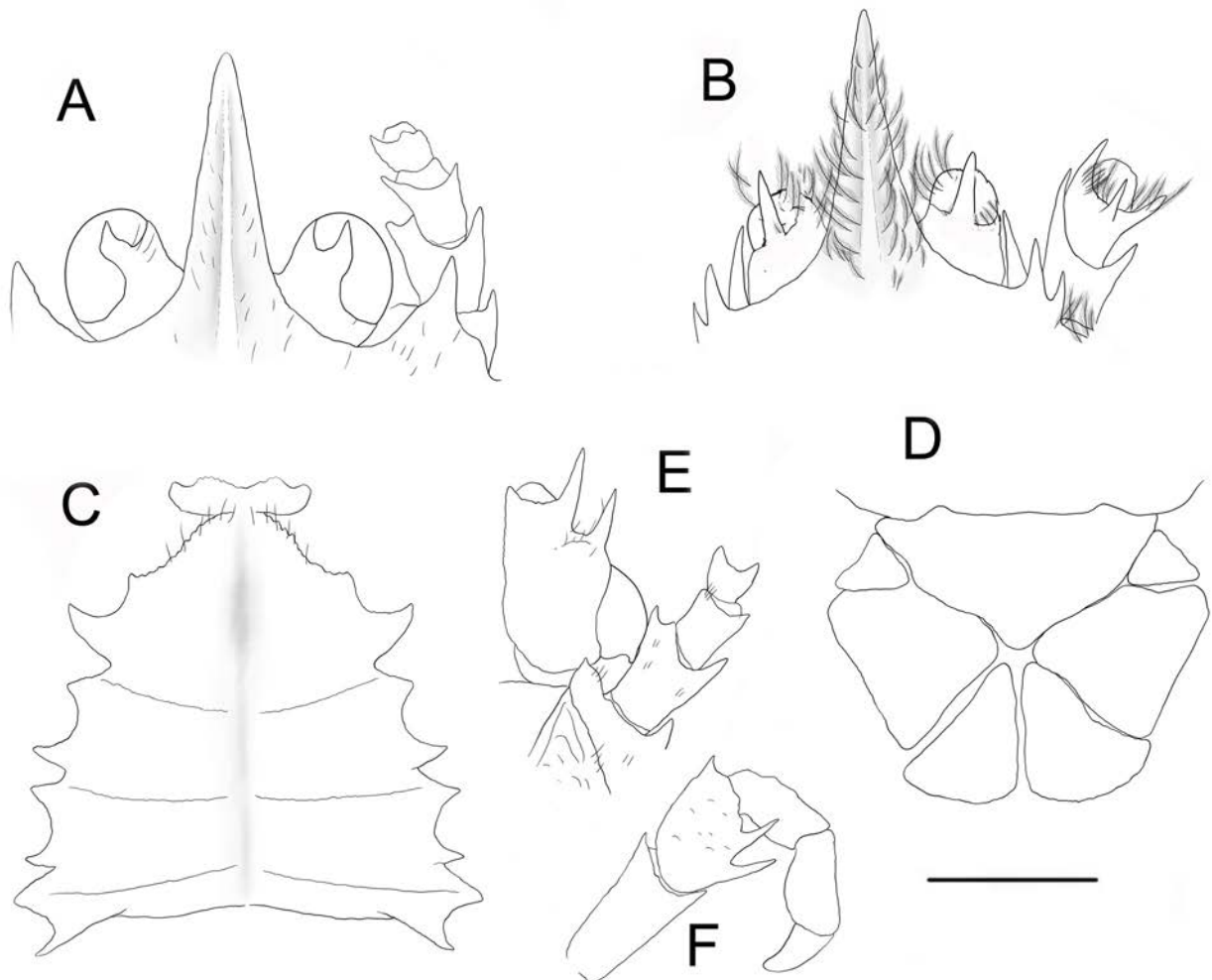
FIGURE 3. A, C–F. *Munidopsis barbarae*, male 4.7 mm (MNHN-IU-2016-2645), Guadeloupe. B, *Munidopsis senticosa* **n. sp.**, holotype, male 4.2 mm (MNHN-IU-2013-18964), Guadeloupe. A–B, anterior part of carapace, showing rostrum eyes and right antenna, dorsal view. C, sternal plastron. D, telson. E, cephalic region, showing antennular and antennal peduncles, ventral view. F, right Mxp3, lateral view. Scale = 1.0 mm.

Remarks. *Munidopsis senticosa* **n. sp.** belongs to the group of species with the dorsal surface of the carapace covered with sharp spines, the posterior margin of the carapace preceded by a row of spines, the abdominal somites

unarmed, and the eyestalk with median spine projecting from upper surface. This group of species contains two other western Atlantic species: *M. barbarae* (Boone, 1927) from the Bahamas and the Gulf of Mexico (Boone 1927; Chace 1942) and *M. penescabra* Pequegnat & Williams 1995, from off Georgia and Gulf of Mexico (Pequegnat & Williams 1995; Macpherson *et al*. 2016). *Munidopsis barbarae* was described by a single specimen collected in Green Cay, Bahamas, at 885 m, and the type could not be located at the Bingham Oceanographic collection. Another juvenile specimen was collected by the "Blake" from the Gulf of Mexico, at 185 m, although its identification does not fully agree with Boone's description (Chace 1942). The description and illustration of *M. barbarae* suggest that it is very similar to *M. penescabra*. However, their taxonomic status needs further study with additional topotypic material. During the cruise KARUBENTHOS 2015, several specimens were collected from two stations, and identified as *M.* aff. *barbarae* (see Poupin & Corbari 2016). However, the specimens from Stn DW4604 agree quite well with the original description and illustration of *M. barbarae* (Figs 3A, C–F, see also Macpherson *et al*. 2016), whereas the specimens collected at Stn DW4573 belongs to the new species. *Munidopsis senticosa* can be easily distinguished from *M. barbarae* and *M. penescabra* by the following features:

• The spines of the carapace and pereiopods are covered by long plumose setae in the new species, whereas these setae are absent or they are short and uniramous in *M. barbarae* and *M. penescabra*.
• The frontal margins of the carapace have more spines in the new species than in the other two species.
• The ridges on abdominal somites 2–4 are more elevated in the new species than in the other two species.
• The eyespine clearly exceeding the cornea in *M. senticosa* whereas this spine is clearly shorter in the other two species. Furthermore, the spines of the antennular and antennal peduncles are longer in *M. senticosa* than in the other species.
• Molecular divergence between *Munidopsis senticosa* and *M. barbarae* are very large: 14.5% for the COI and 7.7% for the 16S; *M. senticosa* and *M. penescabra* collected from the Gulf of Mexico (Coykendall *et al*. 2017) (Table 1) diverge on 15.1% for the COI (no data for the 16S).

Munidopsis turgida **n. sp.**
(Fig 4)

Material examined. *Holotype*: KARUBENTHOS 2015, Stn DW4606, 1611'N, 6052'W, 24 June 2015, 457–484 m: M 4.0 mm (MNHN-IU-2016-2873).

Etymology. From the Latin, *turgidus*, inflated, swollen, in reference to the processes and grooves on the carapace surface.

Description. *Carapace*: Slightly longer than broad; rather rectangular, dorsal surface granulated, moderately convex from side to side. Two thick epigastric processes. Regions well delineated by deep furrows including distinct posterior cervical grooves. Posterior cardiac region weakly triangular, preceded by deep transverse depression; deep depression on each branchial region and transverse depression near posterior margin, medially interrupted in intestinal region. No spine along posterior margin. Rostrum spade-shaped, lateral margins concave in proximal half between eyes, tapering to tip from widest point at distal margin of cornea, distolateral margins straight; 0.3 × carapace length; flattish, not carinate dorsally. Frontal margin transverse behind ocular peduncle, then transverse toward anterolateral angle of carapace. Lateral margins straight and subparallel; anterolateral angle nearly rounded; concave around end of anterior and posterior branches of cervical groove. Pterygostomian flap with minute granules, anteriorly acute.

Sternum: As long as broad, maximum width at sternites 6 and 7. Sternite 3 moderately broad, 2.5 times wider than long, anterolaterally angular, anterior margin with shallow median notch flanked by 2 denticulate lobes. Sternite 4 narrowly elongate anteriorly; surface depressed in midline, with some granules; greatest width 2.5 times that of sternite 3, and 3 times wider than long.

Abdomen: Somites unarmed, minutely granulated; somites 2–4 each with elevated transverse ridge, each with 3 low processes, somites 5–6 lacking such ridges; somite 6 with weakly produced posterolateral lobes and slightly concave posteromedian margin. Telson composed of 8 plates; posterior plates combined, 1.8 times as wide as long.

Eye: Ocular peduncle fused to granular overgrowths covering mesial part of cornea.

Antennule: Basal article granulate, with strong distolateral and distodorsal projections, distally serrated; distomesial angle unarmed, minutely serrated; lateral margin swollen, unarmed.
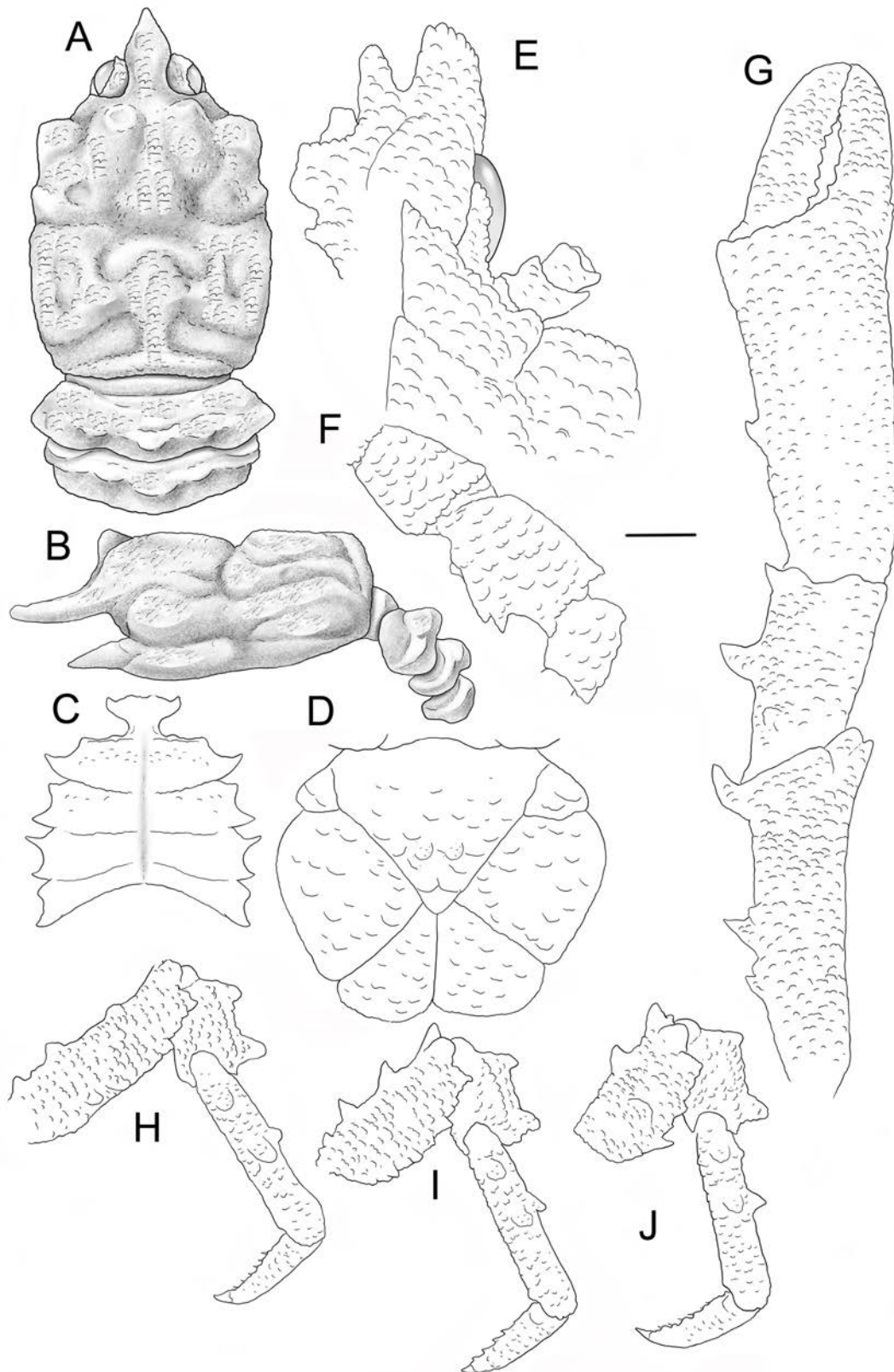
FIGURE 4. *Munidopsis turgida* **n. sp.**, holotype, male 4.0 mm (MNHN-IU-2016-2873), Guadeloupe. A, carapace and abdomen, dorsal view. B, carapace and abdomen, lateral view. C, sternal plastron. D, telson. E, cephalic region, showing antennular, antennal and ocular peduncles, ventral view. F, right Mxp3 ischium, merus and carpus, lateral view. G, right P1, dorsal view. H, right P2, lateral view. I, right P3, lateral view. J, right P4, lateral view. Scales: A–C, G–J = 1.0 mm; D–F = 0.5 mm.

Antenna: Peduncle granulate, not reaching end of rostrum; article 1 with strong distomesial projection, distolateral angle rounded; articles 2–3 unarmed distomesially, each with small distolateral projection.

Mxp3: Surface granulate. Ischium as long as merus measured on extensor margin; extensor and flexor margins unarmed; crista dentata finely denticulate; merus having flexor margin with 3 distinct thick spines, median spine larger than others, extensor margin with distal spine; carpus, propodus and dactylus unarmed.

P1: 3.8 times longer than carapace, granulate. Merus 1.6 times carpus length, with 3 thick mesial spines. Carpus twice longer than wide, with 2 thick mesial spines. Palm 1.9 times longer than carpus, twice longer than wide, and twice longer than fingers, with 1 or 2 thick spines along mesial margin. Fingers slightly gaping in proximal half; prehensile edges each with row of subtriangular teeth; fixed finger without denticulate carina on distolateral margin.

P2–4: Surface of articles granulate. P2 longer than P3 and P4, clearly not exceeding end of P1. P2 merus moderately elongate, 0.8 times carapace length, 3.2 times longer than high and 1.1 times length of P2 propodus. P2–4 meri with row of thick spines along extensor margin, lateral sides with a few large granules; carpi with 2 thick and rounded processes along extensor margin; P2–4 propodi 4–5 times as long as high, one thick median process along extensor margin; dorsal side with 2 protuberances; 0–1 minute distal spinules on flexor margin (not figured); dactylus 0.5 length of propodus; distal claw short, moderately curved; flexor margin nearly straight, with 6 or 7 small teeth decreasing in size proximally, each with slender corneous spine, ultimate tooth closer to penultimate tooth than to dactylar tip.

Epipods on P1.

Distribution. Guadeloupe, between 457–484 m.

Remarks. *Munidopsis turgida* **n. sp.** belongs to the group of species having the dorsal surface of the carapace, abdomen and pereiopods covered by granules, the rostrum spade-shaped, epigastric region with two large prominences and the ocular peduncle fused to granular overgrowths covering mesial part of cornea. The closest relative is *M. granulens* Mayo, 1972, from NW Caribbean Sea (Mayo 1972).

The two species can be easily distinguished by the following features:

• The armature of the carapace is very different in both species. The new species has very deep furrows, whereas these furrows are very shallow in *M. granulens*.
• The abdominal somites 2–4 have 3 protuberances in the new species, whereas these protuberances are absent in *M. granulens*.
• The P1–4 have some protuberances in *M. turgida*, whereas these protuberances are absent in *M. granulens*.
• The epipods are present on P1–2 in *M. granulens*, whereas there are only present on P1 in the new species.
• *Munidopsis turgida* and *M. granulens* diverge 16.3% for the COI (no data for the 16S).

References

Ahyong, S.T., Baba, K., Macpherson, E. & Poore, G.C.B. (2010) A new classification of the Galatheoidea (Crustacea: Decapoda: Anomura). *Zootaxa*, 2676, 57–68.
Baba, K., Ahyong, S.T. & Macpherson, E. (2011) Chapter 1. Morphology of the marine squat lobsters. *In*: Poore GCB, Ahyong ST & Taylor J. (Eds.), *The biology of squat lobsters*. CSIRO Publishing, Melbourne, pp. 1–37. [also published as

Crustacean Issues. Vol. 20. CRC Press, Baton Roca]

Baba, K. & Camp, D.K. (1988) Two species of galatheid crustaceans (Decapoda: Anomura) new to Florida, *Munida spinifrons* Henderson, and *Munidopsis kucki*, new species. *Proceedings of the Biological Society of Washington*, 101, 414–422.

Baba, K., Macpherson, E, Poore, G.C.B., Ahyong, S.T., Bermudez, A., Cabezas, P., Lin, C.W., Nizinski, M., Rodrigues, C. & Schnabel, K.E. (2008) Catalogue of squat lobsters of the world (Crustacea: Decapoda: Anomura - families Chirostylidae, Galatheidae and Kiwaidae). *Zootaxa*, 1905, 1–220.

Baba, K., Macpherson, E., Lin, C.W., & Chan, T.Y. (2009) *Crustacean Fauna of Taiwan. Squat lobsters (Chirostylidae and Galatheidae)*. National Taiwan Ocean University, Keelung, ix + 311 pp.

Benedict, J.E. (1902) Description of a new genus and forty-six new species of crustaceans of the family Galatheidae with a list of the known marine species. *Proceedings of the Biological Society of Washington*, 26, 243–334.
https://doi.org/10.5479/si.00963801.26-1311.243

Boone, L. (1927) Scientific results of the first oceanographic expedition of the "Pawnee", 1925. Crustacea from the tropical east American Seas. *Bulletin of the Bingham Oceanographic Collection*, 1, 1–147.

Campos, N.H., Navas, G.R., Bermúdez, A. & Cruz, N. (2005) *Los crustáceos decápodos de la franja superior del talud continental (300–500 m) del mar Caribe colombiano (Monografía 2 de la Fauna de Colombia)*. Instituto Nacional de Ciencias Naturales. Universidad Nacional de Colombia, Bogotá, 272 pp.

Chace, F.A. (1942) The Anomura Crustacea. I. Galatheidea. Reports of the scientific results of the Atlantis Expeditions to the West Indies, under the joint auspices of the University of Havana and Havard University. *Torreia*, 11, 1–106.

Coykendall, D.K., Nizinski, M.S. & Morrison, C.L. (2017) A phylogenetic perspective on diversity of Galatheoidea (*Munida*, *Munidopsis*) from cold-water coral and cold seep communities in the western North Atlantic Ocean. *Deep-Sea Research II*, 137, 258–272.
https://doi.org/10.1016/j.dsr2.2016.08.014

Folmer, O., Black, M., Hoeh, W., Lutz, R. & Vrijenhoek, R. (1994) DNA primers for amplification of mitochondrial cytochrome c oxidase subunit I from diverse metazoan invertebrates. *Molecular Marine Biology and Biotechnology*, 3, 294–299.
https://doi.org/10.1371/journal.pone.0013102

Gore, R.H. (1983) Notes on rare species of *Munidopsis* (Anomura: Galatheidae) and *Ethusina* (Brachyura: Dorippidae) collected by the USNS Barlett in the Venezuela Basin, Caribbean Sea. *Proceedings of the Academy of Natural Sciences of Philadelphia*, 135, 200–217. [http://www.jstor.org/stable/4064804]

Herrera-Medina, Y., Bermudez-Tobon, A. & Navas-Suarez, G.R. (2014) Primer registro de *Munidopsis cubensis* Chace, 1942 (Crustacea: Anomura: Munidopsidae) para el mar Caribe sur, Colombia. *Revista de la Academia Colombiana de Ciencias*, 38, 88–92.
https://doi.org/10.18257/raccefyn.42

Katoh, K., Misawa, K., Kuma, K. & Miyata, T. (2002) MAFFT: a novel method for rapid multiple sequence alignment based on fast Fourier transform. *Nucleic Acids Research*, 30, 3059–3066.
https://doi.org/10.1093/nar/gkf436

Kumar, S., Stecher, G. & Tamura, K. (2016) MEGA7: Molecular Evolutionary Genetics Analysis version 7.0 for bigger datasets. *Molecular Biology and Evolution*, 33, 1870–1874.
https://doi.org/10.1093/molbev/msw054

Machordom, A., Araujo, R., Erpenbeck, D. & Ramos, M.A. (2003) Phylogeography and conservation genetics of endangered European Margaritiferidae (Bivalvia: Unionoidea). *Biological Journal of the Linnean Society*, 78, 235–252.
https://doi.org/10.1046/j.1095-8312.2003.00158.x

Macpherson, E., Beuck, L. & Freiwald, A. (2016) Some species of *Munidopsis* from the Gulf of Mexico, Florida Straits and Caribbean Sea (Decapoda: Munidopsidae), with the description of two new species. *Zootaxa*, 4137 (3), 405–416.
https://doi.org/10.11646/zootaxa.4137.3.7

Macpherson, E., Rodríguez-Flores, P.C. & Machordom, A. (2017) New sibling species and new occurrences of squat lobsters (Crustacea, Decapoda) from the western Indian Ocean. *European Journal of Taxonomy*, 343, 1–61.
https://doi.org/10.11646/zootaxa.4137.3.7

Mayo, B.S. (1972) Three new species of the family Galatheidae (Crustacea, Anomura) from the western Atlantic. *Bulletin of Marine Science*, 22, 522–535.

Mayo, B.S. (1974) *The systematics and distribution of the deep-sea genus Munidopsis (Crustacea, Galatheidae) in the western Atlantic Ocean*. Ph. D. Thesis, University of Miami, Coral Gables, FL, 432 pp.

Milne-Edwards, A. (1880) Reports on the results of dredging under the supervision of Alexander Agassiz, in the Gulf of Mexico and in the Caribbean Sea, etc. VIII. Études préliminaires sur les Crustacés. *Bulletin of the Museum of Comparative Zoology at Harvard College*, 8, 1–168.

Milne-Edwards, A. & Bouvier, E.L. (1897) Reports on the results of dredging, under the supervision of Alexander Agassiz, in the Gulf of Mexico (1877–78), in the Caribbean Sea (1878–79), and along the Atlantic coast of the United States (1880), by the U. S. Coast Survey steamer "Blake," Lieut.-Com. C.D. Sigsbee, U.S.N., and Commander J.R. Bartlett, U.S.N., commanding. XXXV: Description des Crustacés de la Famille des Galathéidés recueillis pendant l'expédition. *Memoirs of the Museum of Comparative Zoology at Harvard College*, 19, 5–141.

Navas, G.R., Bermúdez, A., Cruz, N. & Campos, N.H. (2003) Galatéideos (Decapoda, Anomura, Galatheidae) del Caribe

colombiano, incluyendo doce primeros registros. *Boletín Investigaciones Marinas y Costeras*, 32, 183–218.

Palumbi, S.R., Martin, A.P., Romano, S., McMillan, W.O., Stice, L. & Grabowski, G. (1991) *The simple fool's guide to PCR.* Special Publishing Department of Zoology, University of Hawaii, Honolulu, 47 pp.

Pequegnat, L.H. & Pequegnat, W.E. (1970) Deep-sea anomurans of superfamily Galatheoidea with description of three new species. *In*: Pequegnat, W.E. & Chace, F.A. (Eds.), *Contributions on the Biology of the Gulf of Mexico.* Texas A & M University, College Station, Texas, pp. 125–170.

Pequegnat, W.E. & Pequegnat, L.H. (1971) *New species and new records of* Munidopsis *(Decapoda: Galatheidae) from the Gulf of Mexico and Caribbean Sea (Supplement to Texas A & M University Oceanographic Studies. Vol. 1).* Gulf Publishing Co, Houston, 25 pp.

Pequegnat, L.H. & Williams, A.B. (1995) Two new species of *Munidopsis* (Decapoda, Anomura, Galatheidae) from the Western Atlantic Ocean. *Journal of Crustacean Biology*, 15, 786–792.
https://doi.org/10.1163/193724095X00181

Poupin, J. & Corbari, L. (2016) A preliminary assessment of the deep-sea Decapoda collected during the KARUBENTHOS 2015 Expedition to Guadeloupe Island. *Zootaxa*, 4190 (1), 1–107.
https://doi.org/10.11646/zootaxa.4190.1.1

Rodríguez-Flores, P.C., Machordom, A. & Macpherson, E. (2017) Three new species of squat lobsters of the genus *Fennerogalathea* Baba, 1988 (Decapoda: Galatheidae) from the Pacific Ocean. *Zootaxa*, 4276 (1), 46–60.
https://doi.org/10.11646/zootaxa.4276.1.2

Vazquez-Bader, A.R. & Gracia, A. (2016) Diversity and distribution of Chirostyloidea and Galatheoidea (Decapoda, Anomura) in the Southern Gulf of Mexico. *Zookeys*, 612, 1–30.
https://doi.org/10.3897/zookeys.612.9492

Vazquez-Bader, A.R., Gracia, A., & Lemaitre, R. (2014) A new species of *Munidopsis* Whiteaves, 1874 (Crustacea: Anomura: Galatheoidea: Munidopsidae) from the Gulf of Mexico and Caribbean Sea. *Zootaxa*, 3821 (3), 354–362.
https://doi.org/10.11646/zootaxa.3821.3.4

Wicksten, M.K. & Packard, J.M. (2005) A qualitative zoogeographic analysis of decapod crustaceans of the continental slopes and abyssal plain of the Gulf of Mexico. *Deep-Sea Research I*, 52, 1745–1765.
https://doi.org/10.1016/j.dsr.2005.04.006

Whiteaves, J.F. (1874) On the recent deep-sea dredging operations in the Gulf of St. Lawrence. *American Journal of Science*, Series III, 7, 210–219.
https://doi.org/10.2475/ajs.s3-7.39.210

Article

Revision of the squat lobsters of the genus *Leiogalathea* Baba, 1969 (Crustacea, Decapoda, Munidopsidae) with the description of 15 new species

PAULA C. RODRÍGUEZ-FLORES[1,2,3], ENRIQUE MACPHERSON[2] & ANNIE MACHORDOM[1]

[1]*Museo Nacional de Ciencias Naturales (MNCN-CSIC), José Gutiérrez Abascal, 2, 28006 Madrid, Spain.*
E-mail: paulacrf@mncn.csic.es; annie@mncn.csic.es
[2]*Centre d'Estudis Avançats de Blanes (CEAB-CSIC), C. d'Accés Cala Sant Francesc, 14, 17300 Blanes, Spain.*
E-mail: macpherson@ceab.csic.es
[3]*Corresponding author*

Table of contents

Abstract

The genus *Leiogalathea* Baba, 1969 currently contains only two benthic species both occurring on the continental shelves and slope: *L. laevirostris* (Balss, 1913), widely reported in the Indo-Pacific region, and *L. agassizii* (A. Milne Edwards, 1880), from both sides of the Central Atlantic. A certain degree of morphological variability linked to their geographic distributions was previously noticed, mostly in *L. laevirostris*. In the present study, we revise numerous specimens collected from the Atlantic, Indian and Pacific Oceans, analysing morphological and molecular characters (COI and 16S rRNA). We found 15 new species; all of them are distinguished from *L. laevirostris* and *L. agassizii* by subtle but constant morphological differences and show clear genetic separation. Furthermore, *L. imperialis* (Miyake & Baba, 1967), previously

201

synonymized with *L. laevirostris*, was found to be a valid species. All species are described and illustrated. Species of the genus *Leiogalathea* are morphologically distinguishable on the basis of the spinulation of the carapace, the shape and the armature of the rostrum, the shape of the propodi of the walking legs, and the pattern of the setae covering on rostrum, carapace and chelae. Some species are barely discernible on the basis of these characters but are highly divergent genetically.

Key words: Anomura, Atlantic Ocean, cryptic species, Galatheoidea, Indian Ocean, mitochondrial genes, morphology, Pacific Ocean

Introduction

Prior to the present study, the genus *Leiogalathea* Baba, 1969 contained only two species (Baba *et al.* 2008; Macpherson & Baba 2011). The genus was established by Baba (1969) to include *Galathea imperialis* Miyake & Baba, 1967 collected off Sagami Bay, Japan (Miyake & Baba 1967; Baba 1969). Miyake & Baba (1967) noticed that this species was morphologically related to *Galathea laevirostris* Balss, 1913 described from the Nicobar Islands (Andaman Sea) during the Valdivia Expedition (Balss 1913). Later, Baba (1990) considered only one single and valid species to occur in the Indo-Pacific (*Leiogalathea laevirostris*). Recently, Baba *et al.* (2008) transferred *Galathea agassizii* A. Milne Edwards, 1880 to *Leiogalathea*. This species, described from St. Lucia and Barbados (Caribbean Sea), was also recorded from Cape Verde Canary Islands and the coast of Morocco (A. Milne Edwards 1880; A. Milne Edwards & Bouvier 1897; Bouvier 1922; Chace 1942; d'Udekem d'Acoz 1999). A complete list of citations and synonymies of *Leiogalathea* is provided in Baba *et al.* (2008).

The genus was originally considered as belonging to the family Galatheidae Samouelle, 1819 because its general *Galathea*-like habitus. However, it has recently been transferred to the family Munidopsidae Ortmann, 1898 (Ahyong *et al.* 2010) after molecular phylogenetic studies (Ahyong *et al.* 2009, 2011; Schnabel *et al.* 2011). The family Munidopsidae differs from Galatheidae in the reduction of the eyes and the lack of a flagellum on the exopod of the first maxilliped. Distinctively, *Leiogalathea* presents an intermediate state of this character between both families, bearing a reduced flagellum on the exopod (Miyake & Baba 1967; Macpherson & Baba 2011). In fact, Miyake & Baba (1967) had already proposed that the genus presented intermediate characters between the genera *Galathea* and *Munidopsis* Whiteaves, 1874.

Leiogalathea laevirostris and *L. agassizii* occur primarily in corals, sponges, sand and mud on the continental shelf and slope (d'Udekem d'Acoz 1999; Baba *et al.* 2008). Baba (1990) observed high variability in the spinulation of the carapace and the rostrum of *Leiogalathea laevirostris*, which led to the question of whether it could represent a species complex. Also, the species was widely reported throughout the Indo-Pacific, from Madagascar and the western Indian Ocean to Indonesia, New Caledonia, Japan, Norfolk Island, eastern Australia and French Polynesia (Ahyong 2007; Baba *et al.* 2008). Additional specimens have been recorded from the Philippines and southeast Taiwan (Baba *et al.* 2009).

In the last decade, numerous expeditions have been carried out on the continental shelf and slope of the Atlantic (Caribbean Sea and Sahara coasts), Indian and Pacific Oceans (from Madagascar to French Polynesia) under the Program Tropical Deep-Sea Benthos (Richer de Forges *et al.* 2013). As result of this sampling effort, a considerable number of specimens belonging to the genus *Leiogalathea* available in the collections of the Muséum national d'Histoire naturelle, Paris (MNHN), are studied herein. We have also revised the material collected on both sides of the Atlantic Ocean and deposited in the Forschungsinstitut und Natur-Museum Senckenberg, Frankfurt (SMF). The types of *L. laevirostris*, deposited in the Zoologisches Museum, Berlin (ZMB), *L. agassizii,* deposited in the Museum of Comparative Zoology, Harvard (MCZ), *L. imperialis* deposited in the Kitakyushu Museum of Natural History, Japan (BLIH) and topotypic material of *L. agassizii* were also examined. To clarify the boundaries of the morphological variability shown by these species and their taxonomic position, we have included molecular data (cytochrome c oxidase subunit I and 16S rRNA). DNA samples from Taiwan and the Philippines were also provided from the National Taiwan Ocean University (NTOU), Keelung. Overall, the study demonstrates the existence of 15 new species and the validity of *L. imperialis*.

Material and methods

Sampling and identification. Specimens were collected using beam trawls or Warén dredges in numerous deep-sea cruises along the Atlantic, the Indian and the Pacific Oceans: 1985 (New Caledonia, MUSORSTOM 4), 1986 (Norfolk Ridge, New Caledonia, CHALCAL 2), 1987 (Lifou and New Caledonia, BIOGEOCAL), 1987 (New Caledonia, SMIB 3), 1989 (New Caledonia, SMIB 4), 1989 (New Caledonia, VOLSMAR), 1991 (Indonesia, KARUBAR), 1992 (New Caledonia, BERYX 11), 1992 (Wallis and Futuna, MUSORSTOM 7), 1993 (Loyalty Islands Ridge, New Caledonia, BATHUS 3), 1994 (Vanuatu economic zone, MUSORSTOM 8), 1996 (Norfolk Ridge, New Caledonia, HALIPRO 2), 1997 (Marquesas Archipelago, MUSORSTOM 9), 2000 (Fiji Islands, BORDAU 2), 2001 (Norfolk Ridge, New Caledonia, NORFOLK 1), 2001 (Solomon Sea, Solomon Island, SALOMON 1), 2005 (Chesterfield Islands, New Caledonia, EBISCO), 2003 (Norfolk Ridge, New Caledonia, NORFOLK 2), 2005 (North Vanuatu, BOA1), 2006 (Vanuatu, SANTO 2006), 2009 (Society Islands, French Polynesia, TARASOC), 2010 (Bismarck Sea and west Salomon Sea, Papua New Guinea, BIOPAPUA), 2012 (Papua New Guinea, PAPUA NIUGINI), 2014 (Bismarck Sea, Papua New Guinea, KAVIENG 2014), 2014 (Salomon Sea and Woodlark Islands, Papua New Guinea, MADEEP), 2015 (Guadeloupe Island, KARUBENTHOS 2015), 2016 (New Caledonia, KANACONO), 2017 (Channel of Mozambique, Mayotte-Glorieuses Islands, BIOMAGLO; New Caledonia, KANADEEP) (MNHN). Other cruises also provided additional specimens: 1883 (Northwest Africa, TALISMAN), 1963 (Congo, GERONIMO), 1975 (Sahara, RV Meteor), 1983 (West Indian, P.P. Shirshov Institute of Oceanology of Russian Academy of Sciences), 2012 (Caribbean Sea, MSM 20/4).

The general terminology employed for morphological descriptions largely follows Baba *et al.* (2009, 2011) and Macpherson & Robainas-Barcia (2015). The size of the carapace is indicated by the postorbital carapace length measured along the dorsal midline from the posterior margin of the orbit to the posterior margin of the carapace. The rostrum length is measured from the tip of the rostrum to between the lateral basal incisions; rostrum breadth is measured as the distance between the left and right lateral basal incisions. The ridges on the posterior branchial region are always counted along the lateral margins, excluding the mid-transverse ridge and the posterior-most ridge anterior to the posterior margin of the carapace. The length of the eye peduncle is measured along the lateral margin of the ocular peduncle; the width is measured at the midlength of the ocular peduncle and the orbit. The length of each pereiopod article is measured along its extensor margin (excluding distal spine), and the breadth is measured at its widest portion. The ranges of meristic and morphological variations are included in the descriptions. Abbreviations: Mxp3 = third maxilliped, P1 = first pereiopod (cheliped), P2–4 = second to fourth pereiopods (first to third walking legs), M = males, F = females, ov = ovigerous. A total of 436 specimens were examined morphologically and 70 were selected for extraction, amplification and sequencing of DNA.

Molecular analysis. The methodology implemented for the molecular analyses follows recent studies (Rodríguez-Flores *et al.* 2017; Macpherson *et al.* 2017a). Tissue was isolated from second–fifth pereiopods. DNA extraction was carried out employing the DNeasy (Qiagen) kit and following manufacturer's protocol. RNase was added, with a previous digestion of the sample during 18–24 hours including proteinase in a buffer ATL. Partial sequences of the mitochondrial cytochrome c oxidase subunit I (COI) and 16S rRNA (16S) genes were amplified by polymerase chain reaction (PCR) using the following primers: LCO1490/HCOI2198 (Folmer *et al.* 1994), COI-H (Machordom *et al.* 2003), 16SAR/16SBR (Palumbi *et al.* 1991), and 16S1471/16SR1472 (Crandall & Fitzpatrick 1996) respectively. PCR amplifications were carried out in 25 μl final volume containing distilled H_2O, 5 μl of 5× buffer solution with $MgCl_2$ (Bioline) and 0.2 mM of each deoxyribonucleotide triphosphate (dNTP), 0.2 μM of forward and reverse primers, 2–5 U of MyTaq polymerase (Bioline) and 2–5 μl of DNA template (2–20 ng/μl). The thermal cycling conditions involved an initial denaturation at 95°C for 3 minutes before 40 cycles of denaturation at 95°C for 45–60s, annealing at 42–50°C for 1 min and extension at 72°C for 45–60s, and finally a last extension at 72°C for 10 min. We failed to amplify DNA of some of the specimens because the material was previously preserved in formalin. The amplified fragments were purified using ExoSAP-IT (Affymetrix). A BigDye Terminator in an ABI 3730 genetic analyser was used for sequencing of both strands in the SECUGEN (Madrid, Spain) service. Forward and reverse DNA sequences obtained for each specimen were checked and assembled using the program Sequencher 4.8 (Gene Code Corporation) and aligned using MAFFT (Katoh *et al.* 2002) with a posterior correction in Se-Al alignment editor (http://tree.bio.ed.ac.uk/software/seal/). Uncorrected divergences (p) between pair of species were calculated using MEGA 7.0.26 (Kumar *et al.* 2016).

TABLE 1. Material employed for DNA sequencing including voucher codes, taxonomy, cruise, geographic area, and GenBank accession numbers.

Voucher Code	DNA Code	Species	Cruise	Geographic area	COI	16S
MNHN-IU-2016-7125	G487	*L. achates* **n. sp.**	BIOMAGLO	Channel of Mozambique	MK140857	MK140893
MNHN-IU-2016-3203	G488	*L. achates* **n. sp.**	BIOMAGLO	Channel of Mozambique	MK140858	MK140894
MNHN-IU-2016-3207	G491	*L. achates* **n. sp.**	BIOMAGLO	Channel of Mozambique	MK140859	MK140895
SMF 51247	G415	*L. agassizii*	SAM-ID	Caribbean Sea	MK140828	MK140862
MNHN-IU-2013-18858	G465	*L. agassizii*	KARUBENTHOS	Caribbean Sea	MK140854	MK140890
MNHN-IU-2013-18894	G466	*L. agassizii*	KARUBENTHOS	Caribbean Sea	MK140855	MK140891
MNHN-IU-2014-13779	G420	*L. amata* **n. sp.**	MUSORSTOM 7	Wallis and Futuna	MK140833	MK140867
MNHN-IU-2014-13780	G424	*L. amata* **n. sp.**	BATHUS 3	New Caledonia		MK140871
MNHN-IU-2014-13786	G418	*L. anchises* **n. sp.**	SALOMON	Solomon	MK140831	MK140865
MNHN-IU-2015-350	G435	*L. anchises* **n. sp.**	MADEEP	Papua New Guinea	MK140839	MK140874
MNHN-IU-2013-17425	G425	*L. ascanius* **n. sp.**	NORFOLK 2	New Caledonia	MK140837	MK140872
MNHN-IU-2014-13706	G443	*L. ascanius* **n. sp.**	BATHUS 3	New Caledonia		MK140878
MNHN-IU-2014-13725	G451	*L. ascanius* **n. sp.**	HALIPRO 2	New Caledonia	MK140848	MK140884
MNHN-IU-2014-13772	G452	*L. ascanius* **n. sp.**	EXBODI	New Caledonia	MK140849	MK140885
MNHN-IU-2014-13728	G444	*L. camilla* **n. sp.**	BATHUS 3	New Caledonia	MK140843	MK140879
MNHN-IU-2014-13788	G454	*L. camilla* **n. sp.**	NORFOLK 1	New Caledonia	MK140850	MK140886
MNHN-IU-2014-13716	G441	*L. creusa* **n. sp.**	TARASOC	French Polynesia	MK140842	
MNHN-IU-2013-17431	G422	*L. dido* **n. sp.**	HALIPRO 2	New Caledonia	MK140835	MK140869
MNHN-IU-2013-17430	G423	*L. dido* **n. sp.**	HALIPRO 2	New Caledonia	MK140836	MK140870
-	170	*L. evander* **n. sp.**	NTOU	Philippines	MK140826	MK140860

62

TABLE 1. (Continued)

Voucher Code	DNA Code	Species	Cruise	Geographic area	COI	16S
MNHN-IU-2013-17429	G417	*L. evander* **n. sp.**	MUSORSTOM 9	Marquesas Islands	MK140830	MK140864
MNHN-IU-2015-820	G457	*L. evander* **n. sp.**	MADEEP	Papua New Guinea	MK140851	MK140887
MNHN-IU-2013-17421	G481	*L. evander* **n. sp.**	MUSORSTOM 9	Marquesas Islands	MK140856	MK140892
-	65	*L. juturna* **n. sp.**	NTOU	Taiwan	MK140827	MK140861
MNHN-IU-2013-17404	G416	*L. juturna* **n. sp.**	KARUBAR	Indonesia	MK140829	MK140863
MNHN-IU-2014-13764	G447	*L. pallas* **n. sp.**	MUSORSTOM 8	Vanuatu	MK140845	MK140881
MNHN-IU-2014-13775	G448	*L. pallas* **n. sp.**	SANTO	Vanuatu	MK140846	MK140882
MNHN-IU-2014-13395	G458	*L. pallas* **n. sp.**	KAVIENG	Papua New Guinea	MK140852	MK140888
MNHN-IU-2014-13785	G459	*L. pallas* **n. sp.**	EBISCO	Chesterfield Islands	MK140853	MK140889
MNHN-IU-2014-13720	G419	*L. paris* **n. sp.**	TARASOC	French Polynesia	MK140832	MK140866
MNHN-IU-2015-296	G434	*L. paris* **n. sp.**	MADEEP	Papua New Guinea	MK140838	MK140873
MNHN-IU-2011-4471	G450	*L. paris* **n. sp.**	TARASOC	French Polynesia	MK140847	MK140883
MNHN-IU-2014-13697	G436	*L. priam* **n. sp.**	MADEEP	Papua New Guinea	MK140840	MK140875
MNHN-IU-2014-13696	G440	*L. priam* **n. sp.**	MADEEP	Papua New Guinea	MK140841	MK140876
MNHN-IU-2014-13711	G421	*L. sinon* **n. sp.**	BORDAU 2	Tonga	MK140834	MK140868
MNHN-IU-2014-13719	G442	*L. sinon* **n. sp.**	TARASOC	French Polynesia		MK140877
MNHN-IU-2014-13744	G445	*L. turnus* **n. sp.**	NORFOLK 2	New Caledonia	MK140844	MK140880

63

Results

Our results demonstrate the existence of 15 new species of *Leiogalathea* supported both by molecular and very subtle morphological characters. These new species can consistently be differentiated from the type species, *L. imperialis,* from Sagami Bay (species previously synonymized with *L. laevirostris*), differing also from *L. laevirostris* from off Sombrero Channel and the other currently considered species, *L. agassizii,* from tropical west Atlantic.

The majority of the species can be identified on the basis of subtle but constant morphological differences. In some cases, we found morphological overlap in some features between some species, but significant genetic distances between them, indicating that the incidence of pseudocryptic species seems to be common within the genus. We separated the species into two main groups based on the most conspicuous character (see key to species). We provide COI and 16S data from the majority of the taxa (15 of the 18 species considered in this study). Unfortunately, amplification of *Leiogalathea aeneas* **n. sp.** from the tropical eastern Atlantic Ocean was unsuccessful for both markers. We also were unable to obtain sequences of the type material of *L. laevirostris* and *L. imperialis* but some morphological differences were found to consider each of them independent taxonomic units.

The divergences between species-pairs were relatively high for the markers analysed for almost all taxa (Table 2). These distances ranged from 3.5 to 16.0% for the COI and from 0.3 to 8.9% for the 16S. The lowest genetic distances were found between pairs of related species that are easily distinguished by constant morphological characters. In some cases, we have found intraspecific morphological variability in several of the characters analysed, sometimes higher than morphological variability among species (cryptic species) which was not reflected in the genetic distances, making species delimitation difficult to determine. We have also illustrated this variability.

Systematic account

Family Munidopsidae Ortmann, 1898

Genus *Leiogalathea* Baba, 1969

Leiogalathea Baba, 1969: 2 (gender: feminine).—Baba 2005: 88.—Baba *et al*. 2008: 83 (compilation).—Baba *et al.* 2009: 133.—Macpherson & Baba 2011: 63.
Liogalathea Baba, 1990: 962 (misspelling).

Type species. *Galathea imperialis* Miyake & Baba, 1967, by original designation.

Diagnosis. (Modified from Baba *et al*. 2009; Macpherson & Baba 2011). Carapace dorsally unarmed, surface transversely convex, with few uninterrupted transverse striae and numerous short and scale-like ridges of different length, usually with numerous short setae and scattered stiff long setae, laterally with a few spines; anterior cervical groove barely discernible. Rostrum triangular, dorsally flat or concave, with 0–9 lateral teeth, usually obsolescent. Lateral limit of orbit rounded. Sternum broader than long, maximum width at sternites 6 and 7; sternite 3 relatively short, anterolaterally produced; anterior margin of sternite 4 broad, often contiguous to entire posterior margin of preceding sternite. Abdomen unarmed, smooth, with sparse long and thick uniramous setae; telson subdivision nearly complete. Ocular peduncles short relative to breadth, cornea not dilated. Antennular article 1 with strong distolateral spine, strong distodorsal spine and with or without small or minute distomesial spine. Antennal peduncle not reaching end of rostrum. Antennal article 1 armed with distomesial spine only, article 2 with distomesial and distolateral spines. Short flagellum on Mxp1. Mxp3 merus with strong median spine and with or without minute distal spine on flexor median margin, distinct spine on extensor distal margin, carpus, propodus and dactylus unarmed. P1–4 with stiff long setae. P1 spinose, triangular in cross section. P2–4 dactyli distally ending in a strong claw, with row of distinct flexor teeth. Gonopods 1 and 2 in males present.

Remarks. Baba (1969) designated *Galathea imperialis* Miyake & Baba, 1967 as the type species of the genus *Leiogalathea*, but later considered *L. imperialis* as a junior synonym of *L. laevirostris* (Balss, 1913) (Baba, 1990). Therefore, *L. laevirostris* has been inadvertently listed as the type species of the genus in more recent studies (e.g.

Baba 2005; Baba *et al*. 2008; Macpherson & Baba 2011) although the type species of *Leiogalathea* remained *Galathea imperialis*. Here, we resurrected *Leiogalathea imperialis* from synonymy as a valid species.

Key to species of the genus *Leiogalathea*

Leiogalathea achates n. sp.
(Figs. 1, 10A, 21A)

Liogalathea laevirostris.—Baba, 1990: 962 (misspelling).

Type material. *Holotype:* Mayotte-Glorieuses islands. BIOMAGLO Stn DW4853, 13°00'S, 44°56'E, 665–669 m, 3 February 2017: ov. F 3.6 mm (MNHN-IU-2016-7125).

Paratypes: Madagascar. "Vauban" CREVETTIERE 1972 Stn CH37, 12°51'S, 48°06.3'E, 675–705 m, 14 September 1972: 1 ov. F 7.1 mm (MNHN-IU-2016-423).

Seychelles W Indian, R/V Akademik Karchatov, P.P. Shirshov Institute of Oceanology of Russian Academy of Sciences, Stn 36 (3731), 06°11.5'S, 54°21.3'E, 560–640 m, 28 March 1983: 1 ov. F 4.5 mm (MNHN-IU-2014-13705).

Mayotte-Glorieuses islands. BIOMAGLO Stn DW4842, 12°23'S, 43°33'E, 420–388m, 29 January 2017: 1 M

4.2 mm, 1 F 3.9 mm (MNHN-IU-2016-3213).—Stn DW4851, 3°01'S, 44°57'E, 660–664 m, 3 February 2017: 1 F 5–5.2 mm, 3 ov. F 4.9–5.2 mm, 2 F 4.0–4.9 mm (MNHN-IU-2016-8833).—Stn DW4863, 12°30'S, 44°56'E, 606–610 m, 6 February 2017: 2 M 5–6.5 mm (MNHN-IU-2016-8832).—Stn DW4864, 12°56'S, 45°15'E, 455–487 m, 7 February 2017: 1 ov. F 5.8 mm (MNHN-IU-2016-3203), 1 F 3.9 mm (MNHN-IU-2016-3204).—Stn DW4866, 12°58'S, 45°15'E, 687–712 m, 7 February 2017: 1 F 4.8 mm (MNHN-IU-2016-3205).—Stn DW4872, 12°44'S, 45°19'E, 502–568 m, 8 February 2017: 1 M 3.8 mm, 1 ov. F 4.9 mm, 1 F 4.2 mm (MNHN-IU-2016-8831).—Stn DW4873, 12°42'S, 45°22'E, 795–1033 m, 8 February 2017: 1 M 6.0 mm (MNHN-IU-2016-2201), 1 M 7 mm (MNHN-IU-2016-8834), 1 M 7.2 mm (MNHN-IU-2016-3207), 2 ov. F 4.8–4.9 mm (MNHN-IU-2016-3208).—Stn DW4874, 12°42'S, 45°19'E, 706–887 m, 9 February 2017: 1 M 6.1 mm (MNHN-IU-2016-3206).—Stn DW4875, 12°44'S, 45°20'E, 617–664 m, 9 February 2017: 1 F 3.9 mm (MNHN-IU-2016-3508).—Stn CP4876, 12°43'S, 45°18'E, 452–462 m, 9 February 2017: 1 M 5.2 mm (MNHN-IU-2016-3202).

Etymology. From the name *Achates*, a Trojan and a personal friend of *Aeneas* in the *Aeneid*. The name is considered a substantive in apposition.

Description. *Carapace*: 1.2–1.3 × as long as broad. Mid-transverse ridge usually interrupted, preceded by shallow cervical groove, followed by 5 interrupted transverse ridges. Lateral margins slightly convex, with 2 or 3 spines: first spine anterolateral, well-developed; hepatic margin unarmed; 1 well-developed spine on anterior branchial margin, 0–1 spine on posterior branchial margin. Rostrum horizontal, dorsally slightly concave, 1.4–1.5 × as long as broad, length 0.4 × and breadth 0.2–0.3 × that of carapace; lateral margin armed with 2 or 3 well-developed proximal teeth and 1 or 2 minute distal teeth.

Sternum: Sternite 3 acutely broad, 4.0–4.5 × as wide as long, anterolaterally produced, anterior margin with a median shallow notch flanked by 2 shallow lobes. Sternite 4 narrowly contiguous to sternite 3; surface depressed in midline, smooth; greatest width 2.4 × as wide as long, 4.7 × that of sternite 3.

Abdomen: Tergite 2 with 2 elevated transverse ridges, tergites 3–4 each with transverse ridge, tergites 5–6 smooth; tergite 6 with transverse posteromedian margin.

Eye: Ocular peduncle slightly longer than wide; cornea subglobular, maximum corneal diameter 0.8 × rostrum width, as wide as eyestalk.

Antennule: Article 1 with distomesial angle unarmed; lateral margin smooth.

Antenna: Article 1 with distomesial spine not reaching end of article 2; article 2 with distomesial spine longer than distolateral spine and nearly reaching end of article 3; articles 3 and 4 unarmed.

Mxp3: Ischium as long as merus measured along extensor margin; flexor margin sharply ridged, terminating in small spine; extensor margin unarmed; crista dentata finely denticulate; merus having flexor margin with 1 strong median spine, extensor margin with 1 distal spine.

P1: 2.4–2.6 (males), 2.1 (females) × carapace length, with numerous short striae, and covered by uniramous long setae on merus to dactylus. Merus 0.9 length of carapace, twice as long as carpus, with strong mesial and distal spines, and scattered dorsal spines. Carpus 0.8 × shorter than palm, 1.6 × as long as broad, dorsal surface with scattered spines, mesial and lateral margins with 1 or 2 strong spines. Palm 1.6 × as long as broad, mesial and lateral margins with spines in irregular longitudinal rows, dorsal surface unarmed. Fingers 1.1 × as long as palm; fixed finger with several proximal lateral spines; movable finger with proximal mesial spine.

P2–4: Moderately slender, somewhat compressed laterally, with sparse short setiferous striae on dorsal surface, and sparse long thick setae on ischium to dactylus. Meri successively shorter posteriorly (P3 merus 0.8 × length of P2 merus, P4 merus 0.9 × length of P3 merus). P2 merus 0.6 × carapace length, 4.6 × as long as broad, 1.1 × as long as P2 propodus; P3 merus 3.9 × as long as broad, 1.1 × as long as P3 propodus; P4 merus 3.6 × as long as broad, as long as P4 propodus; extensor margins with row of 7 or 8 proximally diminishing spines distinct on P2; unarmed or obsolescent on P3, absent on P4; lateral surface unarmed; flexor margin with well-developed distal spine proximally followed by several scattered projecting scales. Carpi with 2 or 3 spines on extensor margin on P2–3, unarmed on P4, lateral side smooth; flexor margin with small distal spine. Propodi 6.0–6.5 × as long as broad on P2–4, flexor margin with 4–6 movable spinules. Dactyli 0.7–0.8 length of propodi; distal claw short, moderately curved; flexor margin nearly straight, with 7 or 8 small teeth along entire margin decreasing in size proximally, each with slender movable spinule, ultimate tooth equidistant between base of distal claw and penultimate tooth.

Colour in life. Ground colour pale yellow, orange or whitish. Carapace and abdominal somites 2–3 pale orange, posterior part of abdomen translucent. Ocular peduncles covered by small brown spots. P1 totally orange with some white bands. P2–4 whitish with orange or pale orange bands, white to translucent at tips.

TABLE 2. Average percentage genetic distances between species of *Leiogalathea*. Numbers in bold indicate intraspecific distances for COI and 16S, respectively. Molecular divergences for COI sequences are indicated beneath the bold numbers; numbers above those in bold show distances for 16S.

	L. achates n. sp.	*L. agassizii*	*L. amata* n. sp.	*L. anchises* n. sp.	*L. ascanius* n. sp.	*L. camilla* n. sp.	*L. creusa* n. sp.	*L. dido* n. sp.	*L. evander* n. sp.	*L. juturna* n. sp.	*L. pallas* n. sp.	*L. paris* n. sp.	*L. priam* n. sp.	*L. sinon* n. sp.	*L. turnus* n. sp.
L. achates **n. sp.**	**0.4, 0.3**	5.4	6.7	5.9	3.4	6.6	-	5.9	0.8	5.5	6.9	6.2	7.2	5.0	5.7
L. agassizii	12.7	**0.9, 0.0**	6.0	5.5	5.5	7.7	-	6.0	5.5	6.9	6.2	7.6	8.4	6.8	5.7
L. amata **n. sp.**	11.6	12.0	**-, 0.0**	6.0	6.3	6.9	-	7.3	6.8	5.4	1.4	5.7	6.5	6.4	7.1
L. anchises **n. sp.**	13.3	13.7	14.3	**0.2, 0.0**	5.7	7.4	-	5.0	6.0	6.4	6.7	6.8	6.8	6.0	4.7
L. ascanius **n. sp.**	11.9	13.1	15.9	15.4	**0.7, 0.0**	6.9	-	6.8	3.4	5.6	6.0	5.7	7.3	6.0	6.5
L. camilla **n. sp.**	13.6	12.6	13.5	15.6	15.4	**0.0, 0.3**	-	7.4	6.7	3.4	7.1	4.0	5.6	6.7	7.4
L. creusa **n. sp.**	13.7	12.8	13.1	7.1	15.0	15.9	**-, -**	-	-	-	-	-	-	-	-
L. dido **n. sp.**	14.9	11.7	12.6	14.3	15.8	12.9	12.6	**0.0, 0.0**	6.0	6.9	7.5	7.6	8.9	6.5	0.3
L. evander **n. sp.**	4.4	11.3	12.1	13.3	11.3	13.6	13.1	14.2	**0.5, 0.0**	5.6	7.0	6.3	7.3	5.2	5.7
L. juturna **n. sp.**	13.3	14.1	15.0	16.0	15.0	11.9	15.5	14.9	13.0	**1.1, 0.3**	5.5	1.4	4.0	5.1	6.7
L. pallas **n. sp.**	11.9	12.0	4.1	14.2	14.8	13.3	13.8	12.9	12.0	14.6	**0.4, 0.1**	6.2	6.7	6.9	7.2
L. paris **n. sp.**	12.9	11.1	12.3	15.5	14.0	11.3	13.8	14.0	12.2	7.2	13.2	**0.1, 0.0**	4.7	5.7	7.3
L. priam **n. sp.**	12.1	12.5	12.9	15.4	14.4	12.0	15.5	13.9	11.9	10.3	13.4	9.0	**0.0, 0.0**	6.1	8.6
L. sinon **n. sp.**	10.7	11.8	12.9	13.8	11.7	13.1	14.2	13.3	10.8	12.7	13.0	11.9	11.5	**-, 0.5**	6.3
L. turnus **n. sp.**	14.9	12.8	14.2	13.6	15.4	12.6	13.1	3.5	13.9	14.5	14.1	12.9	15.3	13.5	**-, -**
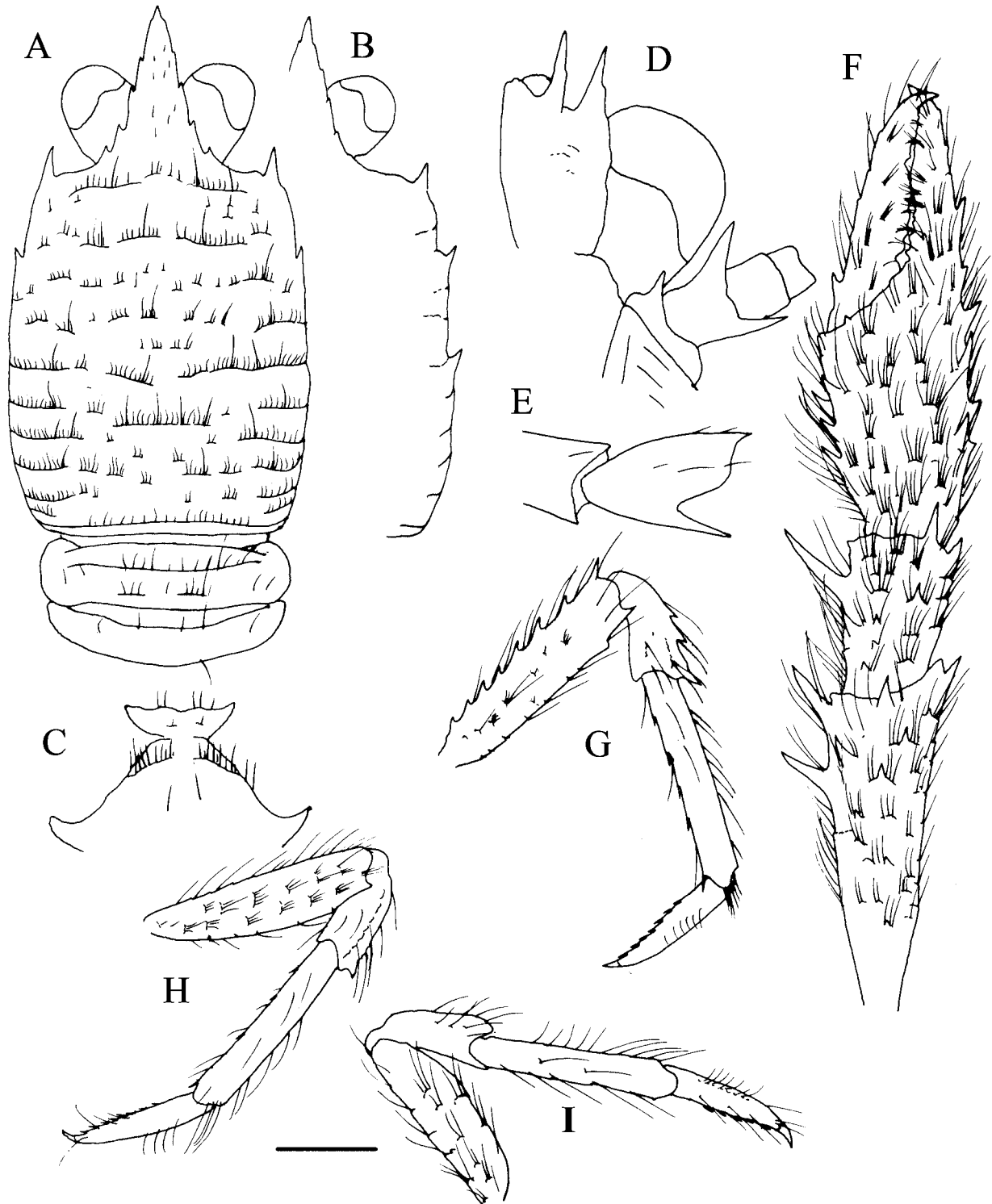
FIGURE 1. *Leiogalathea achates* **n. sp.**, A, C–I, holotype, ov. F 3.6 mm, Mayotte-Glorieuses Islands (MNHN-IU-2016-7125); B, paratype, M 7.0 mm, Mayotte-Glorieuses Islands (MNHN-IU-2016-8834). A, carapace and abdomen, dorsal view. B, carapace, right side, dorsal view. C, Sternites 3–4. D, cephalic region, showing antennular and antennal peduncles, ventral view. E, right Mxp3 ischium and merus, lateral view. F, right P1, dorsal view. G, right P2, lateral view. H, right P3, lateral view. I. right P4, lateral view. Scales: A, B, F–I = 1.0 mm; C–E = 0.5 mm.

Genetic data. COI and 16S (Table 2).

Distribution. Madagascar, Channel of Mozambique (Mayotte-Glorieuses islands) and Seychelles, on quartz-calcareous sand, from 388 to 1033 m.

Remarks. *Leiogalathea achates* belongs to the group of species having the hepatic margin of the carapace unarmed and the branchial margin of the carapace armed with 1 or 2 spines. The closest relative is *L. evander* from French Polynesia, Philippines and Papua New Guinea (see below, under the Remarks of that species). The specimen examined from the Seychelles shows some morphological inconsistences in the pattern of striae of the carapace, shape and armature of the rostrum, with most of the pereiopods lost. Additional material from this area would be desirable in order to confirm its taxonomic status.

***Leiogalathea aeneas* n. sp.**
(Figs. 2, 10B)

Galathea agassizii.—A. Milne Edwards & Bouvier 1900: 282 (part), pl. 6, fig. 7.—Bouvier 1922: 43.—d'Udekem d'Acoz 1999: 160 (compilation).

Type material. *Holotype:* NW Africa. M36-98 AT149, 25°31.5'N, 16°02.2'W, 658–888 m, 24 February 1975: F 7.6 mm (SMF51246).

Paratypes: Morocco. OTSB 14 Stn 8966, 31°35'N, 10°07'W, 686–742 m, 2 August 1976: 1 M 8 mm (CEAB.CRU.241 I).

NW Africa. TALISMAN Stn 34, 32°27'N, 12°19'W, 836–868 m, 13 June 1883: 1 F 9.3 mm (MNHN-IU-2019-2004).—Stn 37, 31°34'N, 12°43'W, 1050 m, 21 June 1883: 2 M 3.8–6.7 mm, 1 ov. F 5.3 mm (MNHN-IU-2019-2005).—Stn 63, 26°18'N, 17°12'W, 640 m, 8 July 1883: 1 M 5.0 mm (MNHN-IU-2019-2002).—Stn 71, 25°39'N, 18°18'W, 640 m, 9 July 1883: 1 ov. F 5.2 mm (MNHN-IU-2019-2001).—Stn 73, 640 m, 9 July 1883: 7 M 5.2–7.3 mm, 10 F 4.5–6.4 mm (MNHN-IU-2019-2003).—Stn 72, 25°39'N, 18°22'W, 882 m, 9 July 1883: 1 M 9.8 mm, 1 ov. F 6.4 mm (MNHN-IU-2019-2006).—Stn 72, 25°39'N, 18°22'W, 882 m, 9 July 1883: 1 M 6.7 mm, 1 ov. F 7.0 mm (MNHN-IU-2019-2007).

NW Africa. M36–98 AT149, 25°31.5'N, 16°02.2'W, 658–888 m, 24 February 1975: 8 M 6.0–8.5 mm, 4 F 4.4–6.5 mm (SMF39233).

Congo. GERONIMO Stn 2–221, 3°02'S, 09°16'E, 348 m, 6 September 1963: 1 M 7.3 mm (MNHN-IU-2016-422).

Etymology. From the name *Aeneas*, the protagonist of the *Aeneid*. The name is considered a substantive in apposition.

Description. *Carapace*: 1.3 × as long as broad. Mid-transverse ridge interrupted (holotype) or uninterrupted, preceded by deep cervical groove, followed by 4 medially interrupted transverse ridges. Lateral margins convex, with 6 spines: first spine anterolateral, well-developed; spine on hepatic margin smaller than first spine, 2 well-developed spines on anterior branchial margin, posterior spine smaller, and 2 spines on posterior branchial margin, last spine small. Rostrum horizontal, dorsally flattish, 1.6–1.8 × as long as broad, length 0.4 × and breadth 0.2 × that of carapace; lateral margin with 1–5 spines, 1 or 2 proximal teeth well-developed, the others rudimentary and decreasing in size distally.

Sternum: Sternite 3 moderately broad, 2.5–2.7 × as wide as long, anterolaterally obtuse, not strongly produced, anterior margin with a median shallow notch flanked by denticulate low lobes. Sternite 4 broadly contiguous to sternite 3, denticulate on anterolateral angles; surface depressed in midline, smooth; greatest width 2.4 × that of sternite 3, 2 × as wide as long.

Abdomen: Tergites 2–3 each with 2 elevated transverse ridges, tergite 4 with transverse ridge, tergites 5–6 smooth; tergite 6 with transverse posteromedian margin.

Eye: Ocular peduncle slightly longer than broad, cornea subglobular, maximum corneal diameter 0.7 × rostrum width, cornea as broad as eyestalk.

Antennule: Article 1 with distomesial angle granulated; lateral margin smooth along distal part.

Antenna: Article 1 with strong distomesial spine overreaching end of article 2; article 2 with strong distomesial spine longer than distolateral spine and reaching end of article 3; articles 3 and 4 unarmed.

Mxp3: Ischium as long as merus measured along extensor margin; flexor margin sharply ridged, terminating in small spine; extensor margin unarmed; crista dentata finely denticulate; merus having flexor margin with strong median spine and distally serrated, extensor margin with distal spine.
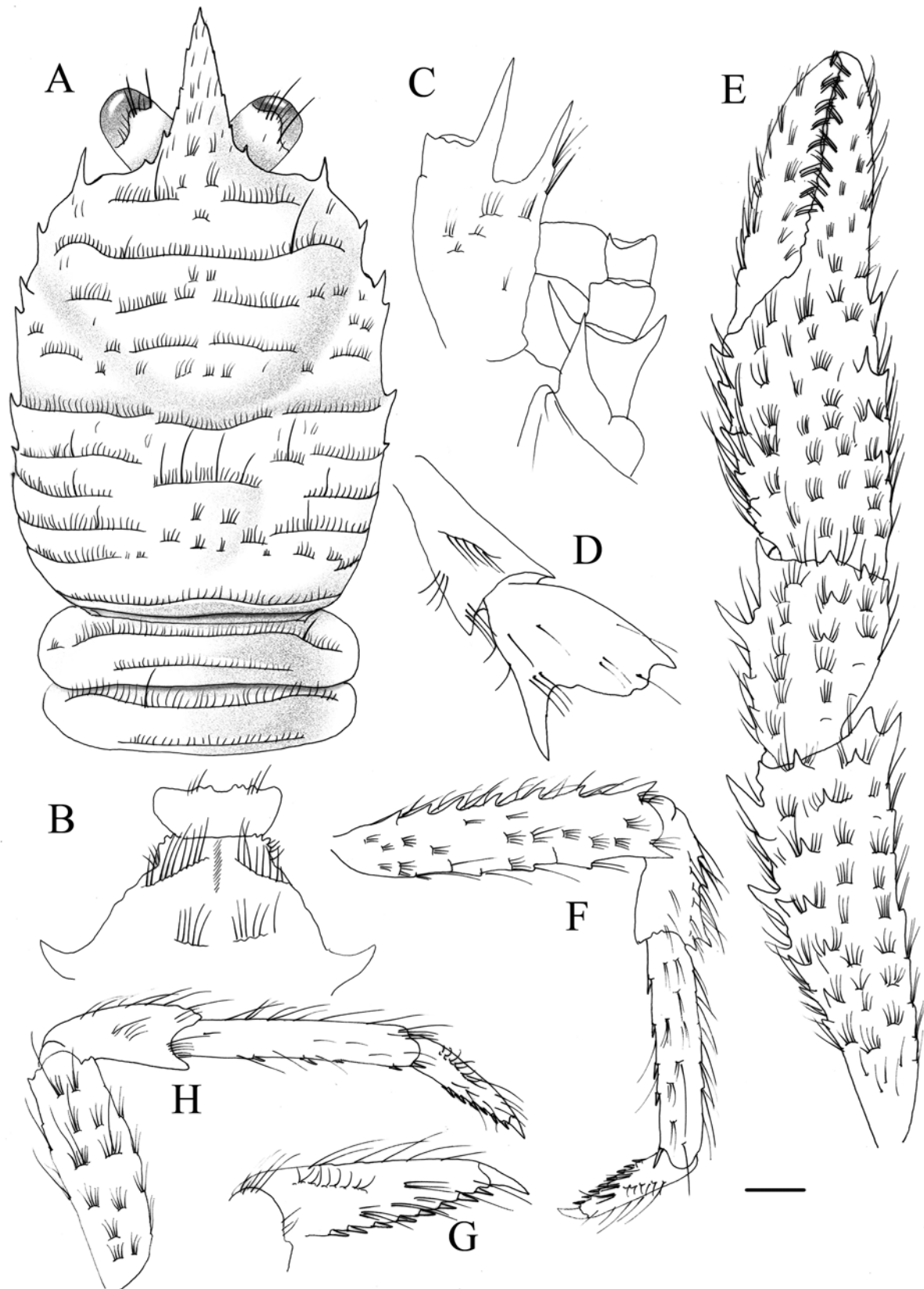
FIGURE 2. *Leiogalathea aeneas* **n. sp.**, holotype, F 7.6 mm, NW Africa (SMF51246). A, carapace and abdomen, dorsal view. B, sternites 3–4. C, cephalic region, showing antennular and antennal peduncles, ventral view. D, right Mxp3 ischium and merus, lateral view. E, right P1, dorsal view. F, right P2, lateral view. G, dactylus of right P2, lateral view. H, right P4, lateral view. Scales: A, E, F, H = 1.0 mm; B–D, G = 0.5 mm.

P1: 2.8–3.3 (males), 2.2–2.5 (females) × carapace length, with numerous short striae, and uniramous setae scattered on merus to dactylus. Merus 0.9 length of carapace, 2.2 × as long as carpus, with strong mesial and distal spines, and some scattered dorsal spines. Carpus 0.8 × as long as palm, 1.5 × as long as broad, dorsal surface with scattered small spines, mesial margin with 4 or 5 strong spines, lateral margin unarmed. Palm 1.6 × as long as broad, armed with small spines in irregular longitudinal rows on mesial and lateral margins, dorsal surface unarmed. Fingers as long as or slightly longer than palm; fixed finger unarmed; movable finger occasionally with proximal mesial spine.

P2–4: Moderately stout, somewhat compressed laterally, with short striae on dorsal surface; with sparse long and thick setae on ischium to dactylus. Meri successively shorter posteriorly (P3 merus 0.9 × length of P2, P4 merus 0.9 × length of P3 merus). P2 merus 0.7 × carapace length, 4.8 × as long as broad, 1.4 × as long as P2 propodus; P3 merus 0.7 × carapace length, 4.2 × as long as broad, P4 merus 0.5 × carapace length, 3.2 × as long as broad, as long as P4 propodus; extensor margin with a row of 7 or 8 proximally diminishing spines in P2–P3, unarmed on P4; lateral surface unarmed; flexor distal margin with well-developed distal spine and sparse projecting scales. Carpi with 3 or 4 spines on extensor margin on P2–3, unarmed on P4, lateral side smooth; flexor margin with small distal spine. Propodi 5.2–6.4 × as long as broad in P2–4, flexor margin with 4 or 5 movable spinules. Dactyli 0.6 length of propodi; distal claw strong, moderately curved; flexor margin nearly straight, with 8 small teeth along entire margin decreasing in size proximally, each with slender movable spinule, ultimate tooth equidistant between base of distal claw and penultimate tooth.

Colour in life. Ground colour pale rose to bright rose, pereiopods whitish, P1 coloured at tips (Bouvier 1922).

Genetic data. No data.

Distribution. Coast of Morocco, Canary Islands, Cape Verde Islands, coast of Sahara, in corals, from 640 to 1642 m.

Remarks. *Leiogalathea aeneas* belongs to the group of species having a spine on the hepatic margin of the carapace. The closest relatives are *L. agassizii* from the Caribbean Sea and *L. ascanius* from tropical west Africa (see below, under the Remarks of these species).

Leiogalathea agassizii (A. Milne Edwards, 1880)
(Figs. 3, 10C, 21B)

Galathea agassizii —A. Milne Edwards 1880: 47.—A. Milne Edwards & Bouvier 1894: 252 (key).—A. Milne Edwards & Bouvier 1897: 17, pl. 1, figs 6–15.—Chace, 1942: 30.
Leiogalathea agassizii—Baba *et al.* 2008: 83 (compilation, in part).—Poupin & Corbari 2016: 44, fig. 10i.

Type material. *Syntypes:* Barbados. USCSS Blake Expeditions Stn 283, 13°05'05"N, 59°40'50"W, 432 m, 07 March 1879: 4 ov. F 4.6–6.8 mm (MCZ-CRU-4708).

Other material examined. Florida. MSM 20/4, Cruise SAM ID 2627 Stn163 34–1, 26°20.198'N, 84°45.672'W, 522 m, 27 March 2012, on live *Enallopsammia* sp.: 2 F 6.9–5.4 mm (SMF51247).

Guadeloupe Island. KARUBENTHOS 2015 Stn DW4510, 16°15'N, 61°51'W, 660–690 m, 07 June 2015: 1 M 6.7 mm (MNHN-IU-2013-18858).—Stn DW4511, 16°14'N, 61°52'W, 660–630 m, 08 June 2015: 1 F 4.1 mm (MNHN-IU-2013-18894).

Description. *Carapace*: 1.2 × as long as broad. Mid-transverse ridge usually interrupted, preceded by shallow cervical groove, followed by 4 interrupted transverse ridges. Lateral margins slightly convex, with 5 or 6 spines: first spine anterolateral, well-developed; spine on hepatic margin smaller than first spine; 2 well-developed spines on anterior branchial margin usually decreasing in size posteriorly; 1 or 2 small spines on posterior branchial margin. Rostrum horizontal, slightly concave dorsally, 1.3–1.4 × as long as broad, length 0.4 × and breadth 0.3 × that of carapace; lateral margin with 2 well-developed proximal teeth, distal margin serrated.

Sternum: Sternite 3 acutely broad, 3.7–4.0 × as wide as long, anterolaterally somewhat produced, anterior margin serrated, straight, with a median shallow notch. Sternite 4 broadly contiguous to sternite 3; surface depressed in midline, smooth; greatest width 2.4 × that of sternite 3, 2 × as wide as long.

Abdomen: Tergites 2–3 each with 1 or 2 elevated transverse ridges, tergite 4 with or without transverse ridge, tergites 5–6 smooth; tergite 6 with transverse posteromedian margin.
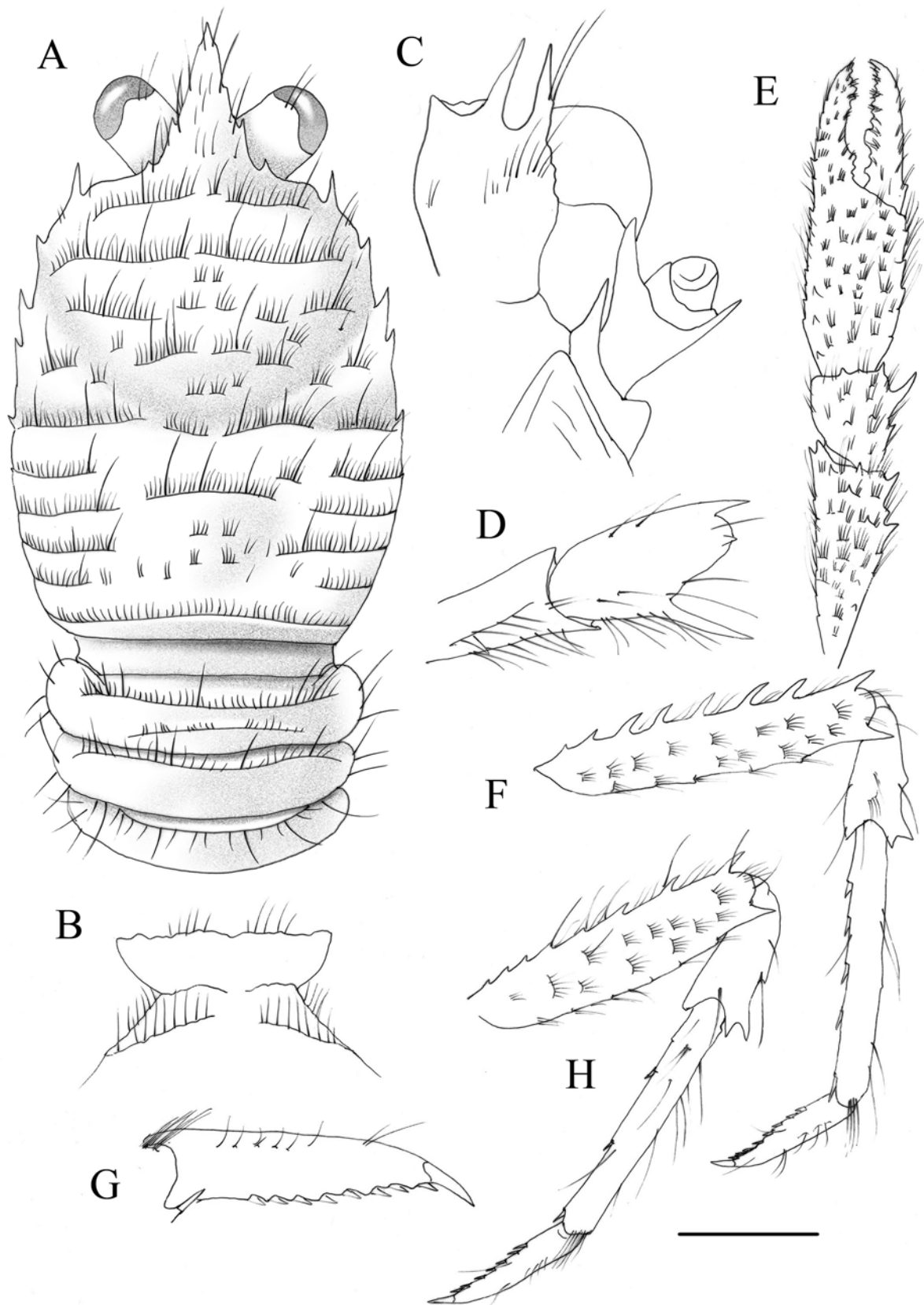
FIGURE 3. *Leiogalathea agassizii* (A. Milne Edwards, 1880), A–D, F–H, F 6.9 mm, Florida (SMF51247); E, M 6.7 mm, Guadeloupe (MNHN-IU-2013-18858). A, carapace and abdomen, dorsal view. B, sternites 3–4. C, cephalic region, showing antennular and antennal peduncles, ventral view. D, right Mxp3 ischium and merus, lateral view. E, left P1, dorsal view. F, right P2, lateral view. G, dactylus of right P2, lateral view. H, right P3, lateral view. Scales: A, F, H = 1.0 mm; E = 2 mm; B–D, G = 0.5 mm.

Eye: Ocular peduncle slightly longer than broad, cornea subglobular, maximum corneal diameter 0.7 × rostrum width, cornea as wide as eyestalk.

Antennule: Article 1 with distomesial angle unarmed; lateral margin serrated along distal part.

Antenna: Article 1 with strong distomesial spine nearly reaching end of article 2; article 2 with strong distomesial spine, longer than distolateral spine and reaching end of peduncle, distolateral spine overreaching article 3; articles 3 and 4 unarmed.

Mxp3: Ischium as long as merus measured along extensor margin; flexor margin sharply ridged, terminating in well-developed spine; extensor margin unarmed; crista dentata finely denticulate; merus having flexor margin with 1 strong median spine and with or without minute distal spine, extensor margin with distal spine.

P1: 2.8 (males), 2.4–2.5 (females) × carapace length, with numerous short striae, and uniramous setae scattered on merus to dactylus. Merus 0.5–0.6 length of carapace, 2.3 × as long as carpus, with strong mesial spines, sparse small distal spines, and scattered dorsal spines. Carpus 0.7 × as long as palm, 1.3 × as long as broad, dorsal surface with several scattered spines, mesial margin with strong spine and several small spines, lateral margin unarmed. Palm 1.6 × as long as broad, armed with small spines in irregular longitudinal rows on mesial and lateral margins, dorsal surface unarmed. Fingers as long as or slightly shorter than palm; fixed finger with 2 lateral small proximal spines; movable finger with small mesial proximal spine.

P2–4: Moderately slender, somewhat compressed laterally, with short striae on dorsal surface, ischium to dactylus sparsely with long and thick setae. Meri successively shorter posteriorly (P2 merus as long as P3 merus, P4 merus 0.9 × length of P3). P2 merus 0.6 × carapace length, 5.6–5.8 × as long as broad, 1.2 × as long as P2 propodus; P3 merus 5.5 × as long as broad, 1.2 × as long as P3 propodus, P4 merus 5 × as long as broad, as long as P4 propodus; extensor margins with row of 7 or 8 proximally diminishing spines on P2–3, extensor margin unarmed on P4; lateral surface unarmed; flexor distal margin with well-developed distal spine and several additional projecting scales. Carpi with 2 or 3 spines on extensor margin on P2–3, unarmed on P4, lateral side smooth; flexor margin with small distal spine. Propodi 8.0–9.0 × as long as broad on P2–4, flexor margin with 4 or 5 movable spinules. Dactyli 0.5–0.6 × length of propodi; distal claw strong, moderately curved; flexor margin nearly straight, with 8–10 small teeth along entire margin decreasing in size proximally, each with slender movable spinule, ultimate tooth closer to base of distal claw than to penultimate tooth.

Colour. Ground colour pale yellow, orange or whitish. Carapace and anterior half of abdomen pale orange, posterior part of abdomen translucent; posterior half of carapace covered with reddish orange small spots. P1 totally orange, white at tip of fingers. P2–4 pale orange, white at tips (propodi and dactyli).

Genetic data. COI and 16S (Table 2).

Distribution. Caribbean Sea: St Lucia and Barbados and north coast of Cuba at depths of 300–897 m. The present material was collected in Florida and Guadeloupe Island, between 519 and 690 m.

Remarks. *Leiogalathea agassizii* belongs to the group of species having the hepatic margin of the carapace armed with a spine. The closest relative is *L. aeneas* from Northwest Africa and both species can be differentiated by the following characters:

The rostrum is slender in *L. aeneas* (1.6–1.8 × as long as wide), whereas it is 1.3–1.4 as long as wide in *L. agassizii*.

L. agassizii has usually three spines on branchial margin whereas this margin has usually four spines in *L. aeneas*.

Anterolateral angle of sternite 4 is denticulate in *L. aeneas*, whereas this angle is smooth in *L. agassizii*.

The P1 fixed finger is unarmed in *L. aeneas*, whereas there are several proximal spines in *L. agassizii*.

The P2–4 propodi in *L. agassizii* are moderately slender (more than 8 × as long as broad), whereas the propodi are moderately stout (less than 6 × longer than broad) in *L. aeneas*.

Leiogalathea agassizii also resembles *L. ascanius* from New Caledonia and Hunter and Mathew Islands (see below under the Remarks of that species).

Leiogalathea amata **n. sp.**
(Figs. 4, 10D)

Type material. *Holotype:* Wallis and Futuna. MUSORSTOM 7 Stn DW556, 11°48.7'S, 178°18.0'W, 440 m, 19 May 1992: F 3.6 mm (MNHN-IU-2014-13779).

Paratypes: Wallis and Futuna. MUSORSTOM 7 Stn DW542, 12°26.4'S, 177°28.2'W, 370 m, 17 May 1992: 1 M 3.8 mm (MNHN-IU-2014-13778).

New Caledonia. BATHUS 3 Stn DW807, 23°40'S, 167°59'E, 420–438 m, 27 November 1993: 1 M 5.2 mm (MNHN-IU-2014-13780).

Etymology. From the name *Amata*, queen of *Laurentum* and wife of *Latinus* in the *Aeneid*. The name is considered a substantive in apposition.

Description. *Carapace*: 1.2–1.3 × as long as broad. Mid-transverse ridge usually interrupted, preceded by shallow cervical groove, followed by 5 or 6 interrupted or scale-like transverse ridges. Lateral margins slightly convex, with 2 spines: first spine anterolateral, well-developed; second small spine on anterior branchial margin, hepatic margin and posterior branchial margin unarmed. Rostrum horizontal, dorsally flattish or slightly concave and slightly inclined downwards, 1.3–1.7 × as long as broad, length 0.4 × and breadth 0.3 × that of carapace; lateral margin unarmed, smooth.

Sternum: Sternite 3 broad, 3.5 × as wide as long, anterolaterally produced, anterior margin slightly sinuous, straight, with a median wide shallow notch. Sternite 4 narrowly contiguous to sternite 3; surface depressed in midline, smooth; greatest width 3.6 × that of sternite 3, 2.6 × as wide as long.

Abdomen: Tergite 2 with 2 elevated transverse ridges, tergites 3–4 each with transverse ridge, tergites 5–6 smooth; tergite 6 with transverse posteromedian margin.

Eye: Ocular peduncle slightly longer than wide; cornea subglobular, maximum corneal diameter 0.7 × rostrum width, as wide as eyestalk.

Antennule: Article 1 with distomesial angle minutely serrated; lateral margin smooth.

Antenna: Article 1 with distomesial spine reaching midlength of article 2; article 2 with strong distomesial spine, longer than distolateral spine, and nearly reaching end of article 3; articles 3 and 4 unarmed.

Mxp3: Ischium as long as merus measured along extensor margin; flexor margin sharply ridged, terminating in small spine; extensor margin unarmed; crista dentata finely denticulate; merus having flexor margin with 1 strong median spine, extensor margin with distal spine.

P1: 2.2–2.4 × carapace length, with scattered short striae, and densely covered by uniramous long setae on merus to dactylus. Merus 0.8 length of carapace, twice as long as carpus, with strong mesial and distal spines, and scattered dorsal spines. Carpus 0.8 as long as palm, 1.8 × as long as broad, dorsal surface with several spines, mesial margin with 2 or 3 spines. Palm 1.7 × as long as broad, armed with spines in irregular longitudinal rows along mesial and lateral margins, dorsal surface unarmed. Fingers 1.4 × as long as palm; fixed finger with row of well-developed spines; movable finger with well-developed proximal spine.

P2–4: Slender, somewhat compressed laterally, with short setiferous striae on dorsal surface, with short setae and sparsely with some long and thick setae on ischium to dactylus. Meri successively shorter posteriorly (P3 merus 0.9 × length of P2 merus, P4 merus 0.9 × length of P3 merus). P2 merus as long as or slightly shorter than carapace, 5.3–6.9 × as long as broad, 1.1 × as long as P2 propodus; P3 merus 0.7 × as long as carapace, 4.2 × as long as broad, 1.1 × as long as P2 propodus. P4 merus 4.7 × as long as broad, 1.1 × as long as P4 propodus; extensor margins with row of 6 or 7 proximally diminishing spines on P2–3; unarmed on P4; lateral surface unarmed; flexor margin with well-developed distal spine and several additional projecting scales. Carpi with 1–3 spines on extensor margin on P2–3, unarmed on P4, lateral side smooth; flexor margin with small distal spine. Propodi 7.7–8.3 × as long as broad in P2–4, flexor margin with 4–6 movable spinules. Dactyli 0.6 × length of propodi; distal claw short, moderately curved; flexor margin nearly straight, with 6 or 7 small teeth decreasing in size proximally, each with slender movable spinule, ultimate tooth equidistant between base of distal claw and penultimate tooth.

Colour in life. Unknown.

Genetic data. COI and 16S (Table 2).

Distribution. New Caledonia and Wallis & Futuna, from 370 to 440 m.

Remarks. *Leiogalathea amata* belongs to the group of species having the hepatic margin of the carapace unarmed and the margin of the rostrum smooth. The species is easily differentiated from the others by the rostrum lacking lateral teeth and the branchial margin of the carapace being armed with one spine. The closest relative is *L. imperialis* from Sagami Bay (see below under the Remarks of that species).
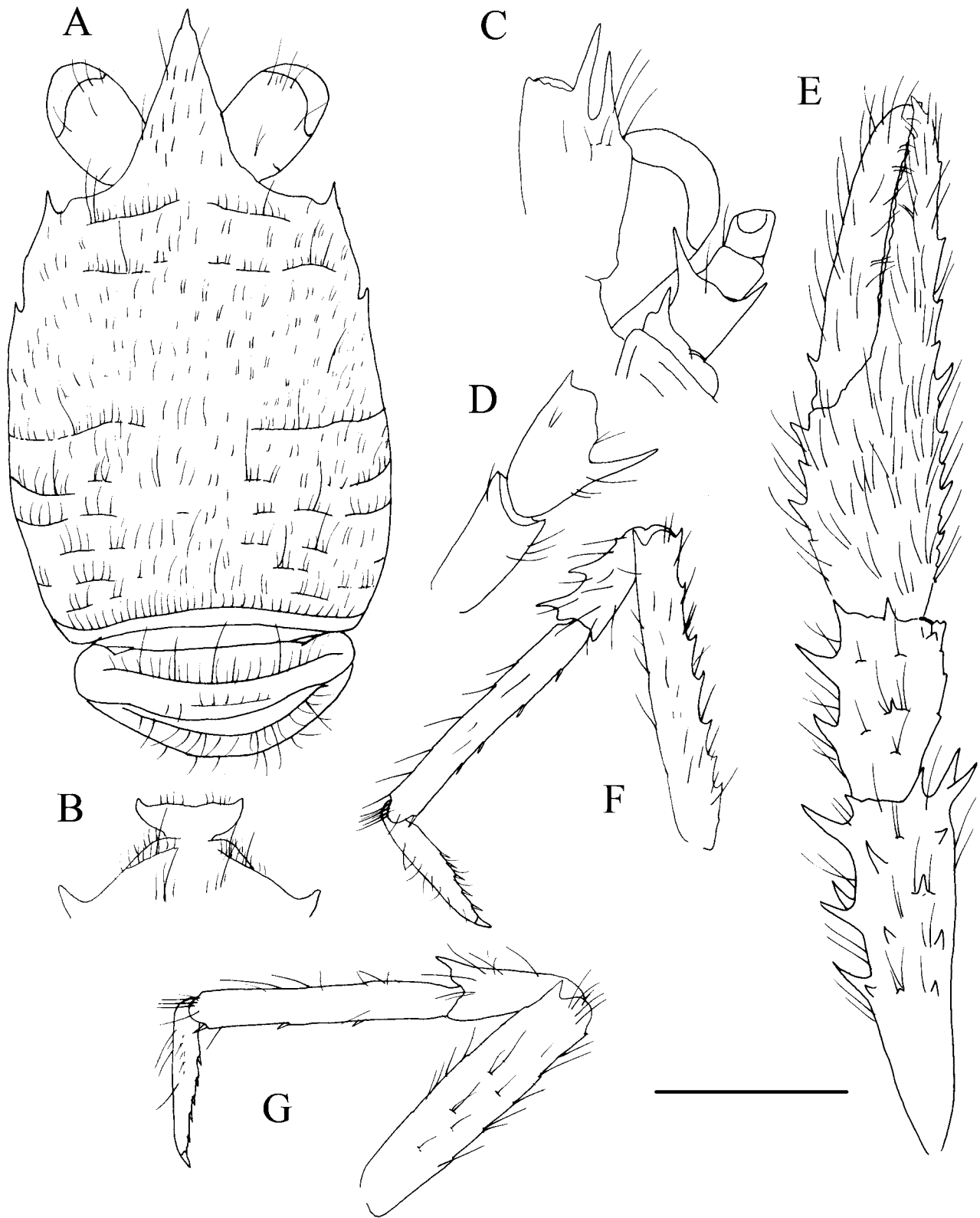
FIGURE 4. *Leiogalathea amata* **n. sp.**, A–D, F–G, holotype, F 3.6 mm, Wallis and Futuna (MNHN-IU-2014-13779); E, paratype, M 3.8 mm, Wallis and Futuna (MNHN-IU-2014-13778). A, carapace and abdomen, dorsal view. B, sternites 3–4. C, cephalic region, showing antennular and antennal peduncles, ventral view. D, right Mxp3 ischium and merus, lateral view. E, right P1, dorsal view. F, left P2, lateral view. G, left P3, lateral view. Scales: A, E–G = 1.6 mm; B–D = 1.0 mm.

Leiogalathea anchises **n. sp.**
(Figs. 5, 10E)

Type material. *Holotype*: Solomon Islands. SALOMON 1 Stn CP1833, 10°12'S, 161°19'E, 367–533 m, 05 October 2001: F 6.4 mm (MNHN-IU-2014-13786).

Paratypes: Solomon Islands. SALOMON 1 Stn CP1833, 10°12'S, 161°19'E, 367–533 m, 5 October 2001: 1 ov. F, 7.2 mm (MNHN-IU-2014-13767).

Papua New Guinea. MADEEP Stn DW4287, 09°12'S, 153°56'E, 340–375 m, 30 April 2014: 1 F 4.3 mm (MNHN-IU-2014-13791).—Stn DW4290, 09°13'S, 153°54'E, 593–593 m, 30 April 2014: 1 M 3.3 mm, 1 ov. F 6.0 mm (MNHN-IU-2016-5798).—Stn DW4292, 09°14'S, 153°52'E, 530–530 m, 30 April 2014: 1 M 7.4 mm (MNHN-IU-2015-350).—Stn DW4293, 09°12'S, 153°57'E, 630–670 m, 30 April 2014: 1 M 5.3 mm, 1 ov. F 7.8 mm, 1 F 4.3 mm (MNHN-IU-2015-496).

Etymology. From the name *Anchises*, *Aeneas*'s father, and a symbol of *Aeneas*'s Trojan heritage in the *Aeneid*. The name is considered a substantive in apposition.

Description. *Carapace*: 1.3 × as long as broad. Mid-transverse ridge usually interrupted, preceded by discernible cervical groove, followed by 6 medially interrupted transverse ridges. Lateral margins slightly convex, with 5 spines: first spine anterolateral, well-developed; spine on hepatic margin, smaller than first spine; 2 spines on anterior branchial margin; and 1 small spine on posterior branchial margin. Rostrum horizontal, dorsally flattish or slightly concave, 1.2–1.3 × as long as broad, length and breadth 0.3 × that of carapace; lateral margin with 5–8 small teeth decreasing in size distally.

Sternum: Sternite 3 somewhat quadrangular, 1.8–2.0 × as wide as long, anterior margin anterolaterally produced, with minute shallow median notch flanked by 2 low lobes. Sternite 4 broadly contiguous to sternite 3; surface depressed in midline, smooth; greatest width 3.1 × that of sternite 3, almost twice as wide as long.

Abdomen: Tergites 2–3 each with 2 elevated transverse ridges, tergites 4–5 with 1 transverse ridge, terguite 6 smooth; tergite 6 with transverse posteromedian margin.

Eye: Ocular peduncle as broad as long or slightly longer than broad; cornea subglobular, maximum corneal diameter 0.7 × rostrum width, as wide as eyestalk.

Antennule: Article 1 with distomesial angle minutely serrated; lateral margin smooth.

Antenna: Article 1 with strong distomesial spine nearly reaching end of article 2; article 2 with strong distomesial spine, longer than distolateral spine and reaching end of article 3; articles 3 and 4 unarmed.

Mxp3: Ischium as long as merus measured along extensor margin; flexor margin sharply ridged, terminating in well-developed spine; extensor margin unarmed; crista dentata finely denticulate; merus having flexor margin with strong median spine, extensor margin with strong distal spine.

P1: 2.4 (males), 1.4–1.8 (females) × carapace length, with numerous short scale-like striae, densely covered by uniramous stiff long setae on merus to dactylus. Merus 0.5 × shorter than carapace, 1.6 × as long as carpus, with strong mesial and distal spines, and scattered dorsal spines. Carpus 0.8 as long as palm, 1.5 × as long as broad, dorsal surface with scattered spines, mesial margin with 1 strong spine, lateral margin with 2 small spines. Palm 1.6 × as long as broad, armed with spines in irregular longitudinal rows along mesial and lateral margins, dorsal surface unarmed. Fingers as long as palm; fixed finger with some proximal lateral spines; movable finger with 1 well-developed proximal spine mesially.

P2–4: Stout, somewhat compressed laterally, with short setiferous striae on dorsal surface, sparsely with long and thick setae on ischium to dactylus. Meri successively shorter posteriorly (P3 merus 0.9 × length of P2 merus, P4 merus 0.9 × length of P3 merus). P2 merus 0.5 × carapace length, 3.8 × as long as broad, 1.2 × as long as P2 propodus; P3 merus 3.2 × as long as broad, 1.1 × as long as P3 propodus; P4 merus 3.1 × as long as broad, as long as P4 propodus; extensor margins with a row of 7–9 proximally diminishing spines on P2–3; unarmed on P4; lateral surface unarmed; flexor margin with well-developed distal spine and several additional projecting scales. Carpi with 3 or 4 spines on extensor margin on P2, 2 spines on P3, unarmed on P4; lateral side smooth; flexor margin unarmed. Propodi 4.5–5 × as long as broad on P2–4, flexor margin with 4 or 5 movable spinules. Dactyli 0.6–0.7 × length of propodi; distal claw short, moderately curved; flexor margin nearly straight, with 6 or 7 small teeth along entire margin decreasing in size proximally, each with slender movable spinule, ultimate tooth equidistant between base of distal claw and penultimate tooth.

Colour in life. Unknown.
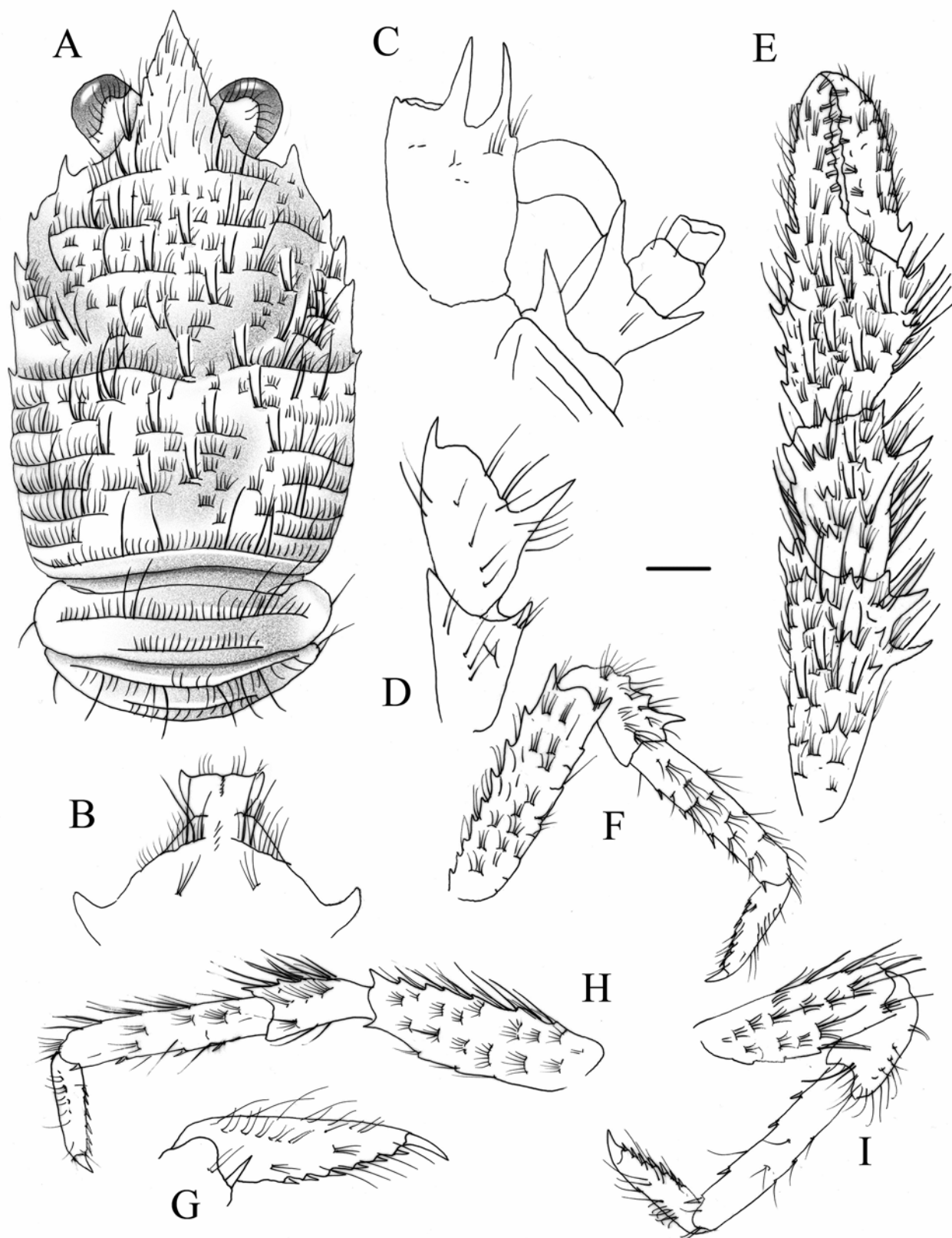
FIGURE 5. *Leiogalathea anchises* **n. sp.**, holotype, F 6.4 mm, Solomon Islands (MNHN-IU-2014-13786). A, carapace and abdomen, dorsal view. B, sternites 3–4. C, cephalic region, showing antennular and antennal peduncles, ventral view. D, right Mxp3 ischium and merus, lateral view. E, left P1, dorsal view. F. right P2, lateral view. G, dactylus of right P2, lateral view. H, left P3, lateral view. I, right P4, lateral view. Scales: A, E, F, H, I = 1.0 mm; B–D, G = 0.5 mm.

Genetic data. COI and 16S (Table 2).

Distribution. Solomon Islands and Papua New Guinea, from 340 to 670 m.

Remarks. *Leiogalathea anchises* belongs to the group of species having a hepatic marginal spine. The closest relative is *L. creusa* from French Polynesia (see below under the Remarks of that species).

Leiogalathea ascanius n. sp.
(Figs. 6, 10F)

Leiogalathea laevirostris.—Baba 1991: 487 (in part, only specimens from CHALCAL 2, SMIB 3, SMIB 4, and VOSLMAR).

Type material. *Holotype*: New Caledonia. NORFOLK 2 Stn DW2027, 23°26.34'S, 167°51.38'E, 465–650 m, 21 October 2003: M 5.9 mm (MNHN-IU-2013-17425).

Paratypes: New Caledonia. CHALCAL 2 Stn DW73, 24°40'S, 168°38'E, 573 m, 29 October 1986: 1 M 4.2 mm (MNHN-IU-2014-13770), 1 M 4.2 mm, 3 F 3.6–4.9 mm (MNHN-IU-2016-421).—Stn DW74, 24º40.36'S, 168º38.38'E, 650 m, 29 October 1986: 3 M, 3.1–3.9 mm, 1 F 3.8 mm (MNHN-IU-2016-420).—Stn DW75, 24°39.31'S, 168°39.67'E, 600 m, 29 October 1986: 2 M 4.5–4.6 mm (MNHN-IU-2016-419).

New Caledonia. SMIB 3 Stn DW1, 24°55.7'S, 168°21.8'E, 520 m, 6 May 1987: 1 ov. F, 4.1 mm (MNHN-IU-2016-414).—Stn DW2, 24°53.4'S, 168°21.7'E, 530–537 m, 26 May 1987: 1 M 3.6 mm, 1 ov. F 3.7 mm (MNHN-IU-2016-415).

New Caledonia. SMIB 4 no station data, 1 F 4.0 mm (MNHN-IU-2016-413).

Hunter and Mathew Islands. VOLSMAR Stn DW5, 22°25.9'S, 171°46.5'E, 700 m, 1 June 1989: 3 M 3.4–5.2 mm (MNHN-IU-2016-417).

New Caledonia. BERYX 11 Stn DW9, 24°52.10'S, 168°21.95'E, 635–680 m, 15 October 1992: 1 ov. F 3.9 mm (MNHN-IU-2014-13790).—Stn DW10, 24°52.85'S, 168°21.40'E, 565–600 m, 15 October 1992: 3 M 3.4–3.9 mm, (MNHN-IU-2014-13782).

New Caledonia. BATHUS 3 Stn DW776, 24°44' S, 170°08' E, 770–830 m, 24 November 1993: 1 M 5.9 mm (MNHN-IU-2014-13713).—Stn DW778, 24°43' S, 170°07' E, 750–760 m, 24 November 1993: 5 M 3.0–4.3 mm, 2 F 3.4–4.5 mm (MNHN-IU-2014-13707), 1 F 3.2 mm (MNHN-IU-2014-13706).—Stn DW794, 23°48' S, 169°49' E, 751–755 m, 26 November 1993: 1 M 6.0 mm (MNHN-IU-2014-13721).—Stn DW798, 23°34' S, 169°36' E, 657–660 m, 26 November 1993: 1 F 4.7 mm (MNHN-IU-2014-13710).—Stn DW809, 23°39' S, 167°58' E, 650–730 m, 28 November 1993: 1 M 6 mm, 2 F 4.9–5 mm (MNHN-IU-2014-13709).

New Caledonia. HALIPRO 2 Stn BT04, 23°31'S, 169°34'E, 790–845 m, 6 November 1996: 1 F 4.9 mm (MNHN-IU-2014-13726).—Stn BT45, 25°45'S, 167°15'E, 680–780 m, 15 November 1996: 1 F 4.6 mm (MNHN-IU-2014-13725).

New Caledonia. NORFOLK 1 Stn DW1666, 23°42'S, 167°43'E, 469–860 m, 20 June 2001: 1 ov. F 4.7 mm, 1 F 4.5 mm (MNHN-IU-2014-13776).—Stn DW1699, 24°40'S, 168°39'E, 581–600 m, 24 June 2001: 1 M 4.3 mm, 3 ov. F 3.4–3.7 mm (MNHN-IU-2014-13789).

New Caledonia. NORFOLK 2 Stn DW2027, 23°26.34'S, 167°51.38'E, 465–650 m, 21 October 2003: 2 M 5.1–5.5 mm (MNHN-IU-2013-17423), 1 F 4.9 mm (MNHN-IU-2013-17424).—Stn DW2046, 23°43.87'S, 168°01.03'E, 333–375 m, 23 October 2003: 1 ov. F 5.8 mm (MNHN-IU-2014-13743).—Stn DW2053, 23°39.64'S, 168°15.60'E, 670–708 m, 24 October 2003: 2 M 4.5–5-9 mm (MNHN-IU-2014-13756), 1 F 6.6 mm (MNHN-IU-2014-13755).—Stn DW2057, 24°40.10'S, 168°39.34'E, 555–565 m, 25 October 2003: 2 M 4.2–4.6 mm (MNHN-IU-2014-13760).—Stn DW2058, 24°39.76'S, 168°40.43'E, 591–1032 m, 25 October 2003: 3 M 2.5–3.9 mm, 5 F 2.4–4.0 mm (MNHN-IU-2014-13753).—Stn DW2056, 24°40'S, 168°39'E, 573–600 m, 25 October 2003: 1 M 4.3 mm (MNHN-IU-2014-13757).—Stn DW2064, 25°17'S, 168°56'E, 609–691 m, 26 October 2003: 1 M 3.1 mm, 3 F 4.0–4.6 mm (MNHN-IU-2014-13759).—Stn DW2069, 25°20.07'S, 168°57.60'E, 795–852 m, 26 October 2003: 2 M 4.8–5.0 mm (MNHN-IU-2014-13750).—Stn DW2070, 25°22.97'S, 168°57.12'E, 630–1150 m, 26 October 2003: 1 F 4.3 mm (MNHN-IU-2014-13758).—Stn DW2075, 25°23.12'S, 168°20.07'E, 650–1000 m, 27 October 2003: 1 ov. F 3.7 mm (MNHN-IU-2014-13751).—Stn DW2084, 24°52.00'S, 168°22.00'E, 586–730 m, 28 October 2003: 12 M 2.8–4.7 mm, 1 ov. F 4.3 mm, 7 F 3.0–5.1 mm (MNHN-IU-2014-13741).—Stn DW2087, 24°56.22'S, 168°21.66'E, 518–586 m, 28 October 2003: 1 M 4.5 mm, 1 ov. F 3.9 mm (MNHN-IU-2014-13754).—Stn DW2110, 23°48.34'S, 168°16.81'E, 493–850 m, 31 October 2003: 3 M 3.7–4.1 mm, 6 ov. F 3.9–4.5 mm (MNHN-

IU-2014-13729).—Stn CP2111, 23°49'S, 168°17'E, 500–1074 m, 31 October 2003: 1 M 4.9 mm, 2 F 3.9–5.6 mm (MNHN-IU-2010-5412).—Stn DW2112, 23°44.44'S, 168°18.40'E, 640–1434 m, 31 October 2003: 13 M 2.5–6.2 mm, 5 F 4.2–5.2mm (MNHN-IU-2014-13752).—Stn DW2113, 23°45.17'S, 168°17.99'E, 888–966 m, 31 October 2003: 1 M 5.2 mm, 1 ov. F 3.3 mm (MNHN-IU-2014-13742).

New Caledonia. EXBODI Stn CP3893, 22°24'S, 171°47'E, 786–814 m, 19 September 2011: 1 m 7.1 mm (MNHN-IU-2014-13772).

New Caledonia. KANACONO Stn CP4667, 22°54'S, 167°17'E, 550–529 m, 12 August 2016: 1 ov. F 6.0 mm, 1 F 4.5 mm (MNHN-IU-2017-3847).—Stn CP4692, 23°01'S, 167°33'E, 802–800 m, 15 August 2016: 3 M 6.8–8.7 mm, 1 F 7.5 mm (MNHN-IU-2017-11507).—Stn DR4771, 23°03'S, 168°20'E, 900–220 m, 28 August 2016: 1 M 2.3 mm (MNHN-IU-2017-3970).

New Caledonia. KANADEEP Stn CP4963, 21°21'S, 158°00'E, 1000–978 m, 7 September 2017: 1 M 4.5 mm (MNHN-IU-2017-3627).

Etymology. From the name *Ascanius*, *Aeneas*'s young son by his first wife *Creusa,* in the *Aeneid*. The name is considered a substantive in apposition.

Description. *Carapace*: 1.2 × as long as broad. Mid-transverse ridge usually uninterrupted, preceded by cervical groove, followed by 4 or 5 interrupted transverse ridges. Lateral margins slightly convex, with 3–6 spines: first spine anterolateral, well-developed; small spine on hepatic margin; 1 or 2 spines on anterior branchial margin, and 0–2 spines on posterior branchial margin, last spine, if present, very small. Rostrum horizontal, dorsally concave, 1.4–1.5 × as long as broad, length 0.4 × and breadth 0.3 × that of carapace; lateral margin with 4 or 5 teeth, 1 or 2 proximal spines well-developed, others rudimentary and decreasing in size distally.

Sternum: Sternite 3 broad, 3.4–3.5 × as wide as long, anterolaterally produced, anterior margin with shallow minute median notch flanked by 2 low and smooth lobes. Sternite 4 narrowly contiguous to sternite 3; surface depressed in midline, smooth; greatest width 2.5 × that of sternite 3, twice as wide as long.

Abdomen: Tergites 2–3 each with 2 elevated transverse ridges, tergite 4 with transverse ridge, tergites 5–6 smooth; tergite 6 with transverse posteromedian margin.

Eye: Ocular peduncle slightly longer than wide; cornea subglobular, maximum corneal diameter 0.6 × rostrum width, as wide as eyestalk.

Antennule: Article 1 with distomesial angle unarmed or with minute spine; lateral margin smooth along distal part.

Antenna: Article 1 with strong distomesial spine nearly reaching end of article 2; article 2 with strong distomesial spine, longer than distolateral and overreaching article 3; articles 3 and 4 unarmed.

Mxp3: Ischium as long as merus measured along extensor margin; flexor margin sharply ridged, terminating in well-developed spine; extensor margin unarmed; crista dentata finely denticulate; merus having flexor margin with strong median spine, extensor margin with well-developed distal spine.

P1: 2.8–3.4 (males), 2.3–2.4 (females) × carapace length, with numerous short setose striae, and uniramous setae scattered on merus to dactylus. Merus slightly longer than carapace, 1.8 × as long as carpus, with strong mesial and distal spines, and some scattered dorsal spines. Carpus 0.7 as long as palm, 1.8 × as long as broad, dorsal surface with scattered spines, mesial margins with 3 strong spines, lateral margin unarmed. Palm, 1.8 × as long as broad, mesial and lateral margins with spines in irregular longitudinal rows, dorsal surface unarmed. Fingers as long as or slightly shorter than palm; fixed finger with 2 proximal lateral spines; movable finger with proximal mesial spine.

P2–4: Slender, somewhat compressed laterally, with short setiferous striae on dorsal surface, with sparse long and thick setae on ischium to dactylus. Meri successively shorter posteriorly (P3 merus 0.6 × length of P2 merus, P4 merus 0.8 × length of P3 merus). P2 merus 0.8 × carapace length, 5.6 × as long as broad, as long as P2 propodus; P3 merus 4.6 × as long as broad, as long as P3 propodus, P4 merus 3.7 × as long as broad, as long as P3 propodus; extensor margins with row of 7 or 8 proximally diminishing spines on P2–3, 4 or 5 minute spines on P4; lateral surface unarmed; flexor margin with 1 well-developed distal spine proximally followed by several additional projecting scales. Carpi with 4 or 5 spines on extensor margin on P2–3, unarmed on P4, flexor margin with small distal spine. Propodi 7.6–9.6 × as long as broad on P2–4, flexor margin with 5 movable spinules. Dactyli 0.4–0.5 × length of propodi; distal claw short, moderately curved; flexor margin nearly straight, with 8–10 small teeth along entire margin decreasing in size proximally, each with slender movable spinule, ultimate tooth equidistant between base of distal claw and penultimate tooth.
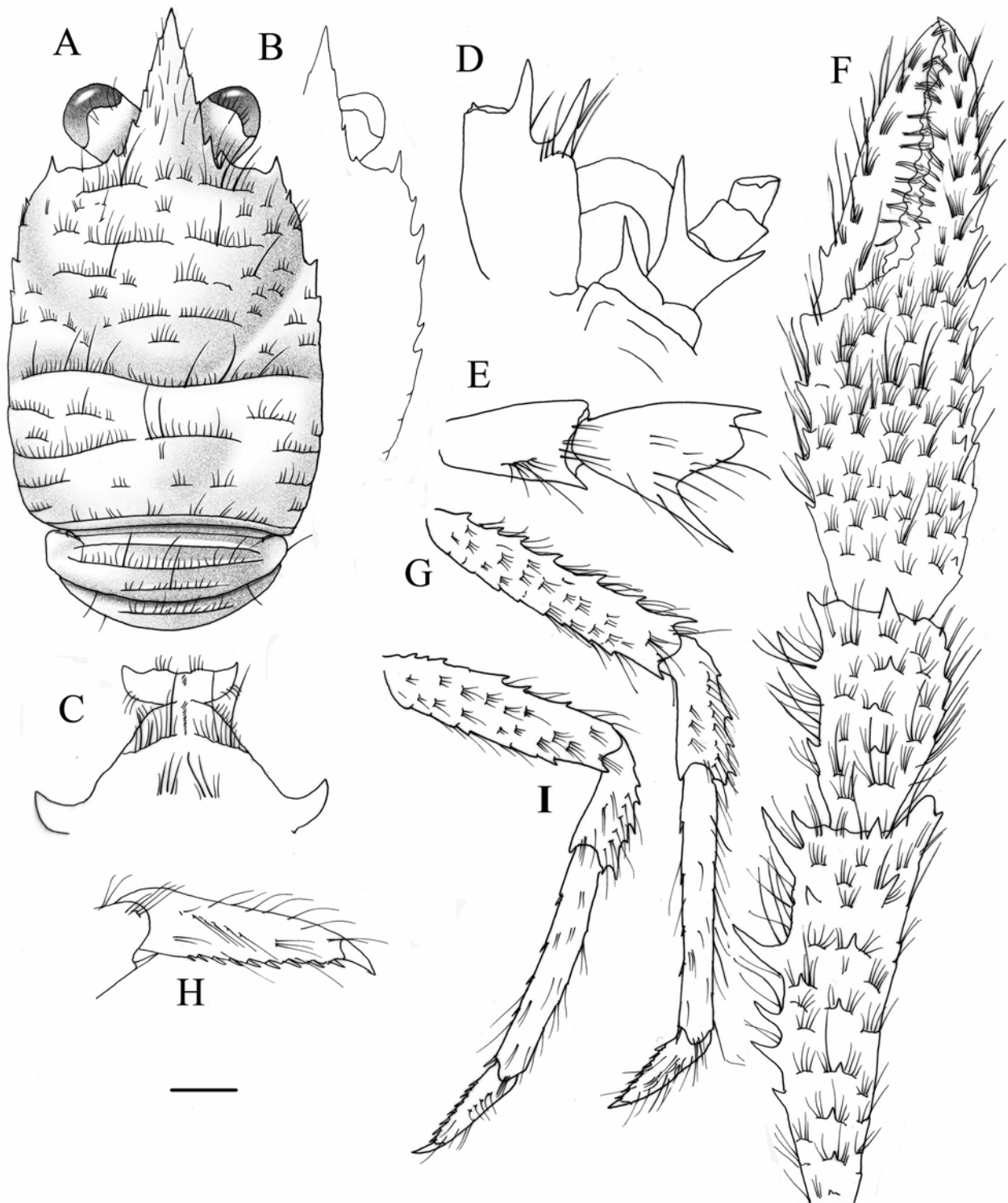
FIGURE 6. *Leiogalathea ascanius* **n. sp.**, A, C–I, holotype, M 5.9 mm, New Caledonia (MNHN-IU-2013-17425); B, paratype, M 7.1 mm, New Caledonia (MNHN-IU-2014-13772). A, carapace and abdomen, dorsal view. B, carapace, right profile, dorsal view. C, sternites 3–4. D, cephalic region, showing antennular and antennal peduncles, ventral view. E, right Mxp3 ischium and merus, lateral view. F, right P1, dorsal view. G, right P2, lateral view. H, dactylus of right P2, lateral view. I, right P3, lateral view. Scales: A, B, F, G, I = 1.0 mm; C–E, H = 0.5 mm.

Colour in life. Unknown.
Genetic data. COI and 16S (Table 2).

Distribution. New Zealand (K. Schnabel, personal communication), New Caledonia, and Hunter and Mathew Islands on bank of sponges from 220 to 1434 m.

Remarks. *Leiogalathea ascanius* belongs to the group of species having the hepatic margin of the carapace armed with one spine. The closest relatives are *L. agassizii* from the Caribbean Sea and *L. aeneas* from eastern Atlantic. These species differ only in the number of spines along the flexor margin of the P2–4 dactyli (7 or 8 in *L. agassizii* and 8 in *L. aeneas*, 9 or 10 in *L. ascanius*). Furthermore the P2 dactylus is 0.5–0.6 × the length of the P2 propodus in *L. agassizii,* whereas the P2 dactylus is ≤ than half (0.4–0.5) length of the P2 propodus in *L. ascanius*. The P2–4 propodi are slender (8–10 × as long as broad) in *L. ascanius*, whereas are stout in *L. aeneas* (less than 6 × as long as broad). *Leiogalathea ascanius* and *L. agassizii* are very different genetically, with divergences of 13.1% in COI and 5.5% in 16S.

Leiogalathea camilla n. sp.
(Figs. 7, 10G)

Type material. *Holotype*: New Caledonia, BATHUS 3 Stn DW817, 23°42'S, 168°15'E, 405–410 m, 29 November 1993: M 3.0 mm (MNHN-IU-2014-13728).

Paratypes: New Caledonia. BERYX 11 Stn CP51, 23°45'S, 168°17'E, 390–400 m, 21 October 1992: 1 ov. F 3.0 mm (MNHN-IU-2014-13781).

New Caledonia. BATHUS 3 Stn DW807, 23°40'S, 167°59'E, 420–438 m, 27 November 1993: 1 M 5.1 mm (MNHN-IU-2014-13727).—Stn CP815, 23°47'S, 168°17'E, 460–470 m, 28 November 1993: 1 M 3.4 mm (MNHN-IU-2014-13722).—Stn DW817, 23°42'S, 168°15'E, 405–410 m, 28 November 1993: 1 M 3.0 mm, 1 ov. F 2.2 mm (MNHN-IU-2014-13724).

New Caledonia. NORFOLK 1 Stn DW1704, 23°47'S, 168°17'E, 400–420 m 25 June 2001: 1 ov. F, 3.0 mm (MNHN-IU-2014-13788), 2 ov. F, 2.7–3.2 mm (MNHN-IU-2014-13787).—Stn CP1706, 23°43'S, 168°16'E, 383–394 m, 25 June 2001: 1 ov. F 3.0 mm (MNHN-IU-2014-13777).

New Caledonia. NORFOLK 2 Stn CP2048, 23°43.82'S, 168°16.24'E, 380–389 m, 24 October 2003: 1 ov. F 2.3 mm (MNHN-IU-2014-13747).—Stn DW2109, 23°47.46'S, 168°17.04'E, 422–495 m, 31 October 2003: 3 M 2–3.3 mm, 3 ov. F 2.1–3.0 mm, 1 F 2.3 mm (MNHN-IU-2014-13749).

New Caledonia. KANACONO Stn DW4783, 22°56'S, 167°48'E, 385–395 m, 29 August 2016: 1 ov. 2.8 mm (MNHN-IU-2017-3949).

Etymology. From the name *Camilla*, the leader of the *Volscians*, a race of warrior maidens in the *Aeneid*. The name is considered a substantive in apposition.

Description. *Carapace*: 1.1–1.3 × as long as broad. Mid-transverse ridge usually medially interrupted, preceded by shallow cervical groove, followed by 3–5 laterally interrupted transverse ridges. Lateral margins slightly convex and subparallel, with 2 spines: first spine anterolateral, usually well-developed; second spine small, located on anterior branchial margin, hepatic margin and posterior branchial margins unarmed. Rostrum horizontal, slightly concave dorsally, 1.3–1.5 × as long as broad, length 0.3 × and breadth 0.2–0.3 × that of carapace; lateral margin with 4 or 5 distinct teeth.

Sternum: Sternite 3 moderately broad, 2.8–3.0 × as wide as long, anterolaterally produced, anterior margin straight and serrated. Sternite 4 anteriorly contiguous to sternite 3; surface depressed in midline, smooth; greatest width 3 × that of sternite 3, and 2.5 × as wide as long.

Abdomen: Tergite 2 with 2 elevated transverse ridges, tergites 3–4 each with transverse ridge, tergites 5–6 smooth; tergite 6 with transverse posteromedian margin.

Eye: Ocular peduncle short, longer than wide; cornea subglobular, maximum corneal diameter 0.8 × rostrum width, as wide as eyestalk.

Antennule: Article 1 with distomesial angle minutely serrated; lateral margin smooth.

Antenna: Article 1 with strong distomesial spine reaching end of article 2; article 2 with relatively short distolateral and distomesial spines, distomesial spine not reaching end of article 3; articles 3 and 4 unarmed.

Mxp3: Ischium as long as merus measured along extensor margin; flexor margin sharply ridged, terminating in small spine; extensor margin unarmed; crista dentata finely denticulate; merus having flexor margin with strong median spine, extensor margin with distal spine.

FIGURE 7. *Leiogalathea camilla* **n. sp.**, holotype, M 3.0 mm, New Caledonia (MNHN-IU-2014-13728). A, carapace and abdomen, dorsal view. B, sternites 3–4. C, cephalic region, showing antennular and antennal peduncles, ventral view. D, right Mxp3 ischium and merus, lateral view. E, left P1, dorsal view. F, right P2, lateral view. G, dactylus of right P2, lateral view. H, right P3, lateral view. I, right P4, lateral view. Scales: A, E, F, H, I = 1.0 mm; B–D, G = 0.5 mm.

P1: 2.6–2.9 (males), 1.8–2.0 (females) × carapace length, with numerous short striae, and covered by uniramous long setae on merus to dactylus. Merus 0.7 length of carapace, 2.1 × as long as carpus, with strong

mesial and distal spines, and several scattered dorsal spines. Carpus slightly shorter than palm, 1.6 × as long as broad, dorsal surface with scattered spines, mesial margin with strong spines, lateral margin unarmed. Palm 2.1 × as long as broad, armed with spines in irregular longitudinal rows along mesial and lateral margins, dorsal surface unarmed. Fingers 1.3 × as long as palm; fixed finger with 1 or 2 proximal spines along lateral margin; movable finger with well-developed proximal mesial spine.

P2–4: Stout, somewhat compressed laterally, with short setiferous striae on dorsal surface, with sparse long and thick setae on ischium to dactylus. Meri successively shorter posteriorly (P3 merus 0.9 × length of P2 merus, P4 merus 0.8 × length of P3 merus). P2 merus 0.6 × carapace length, 4.4 × as long as broad, 1.2 × as long as P2 propodus; P3 merus 4.2 × as long as broad, 1.2 × as long as P3 propodus; P4 merus 3.7 × as long as broad, as long as P4 propodus; extensor margins with row of 8 or 9 proximally diminishing spines on P2, with minute spines on P3, unarmed on P4; lateral surface unarmed; flexor margin with well-developed distal spine and several additional projecting scales. Carpi with 3 or 4 spines on extensor margin on P2–3, unarmed on P4, lateral side smooth; flexor margin with small distal spine. Propodi 5.9–6.1 × as long as broad on P2–4, flexor margin with 3–5 movable spinules. Dactyli 0.6–0.7 × length of propodi; distal claw short, moderately curved; flexor margin nearly straight, with 5 or 6 small teeth decreasing in size proximally, each with slender movable spinule, ultimate tooth equidistant between base of distal claw and penultimate tooth.

Colour in life. Unknown.

Genetic data. COI and 16S (Table 2).

Distribution. New Caledonia, and adjacent waters, from 383 to 495 m.

Remarks. *Leiogalathea camilla* belongs to the group of species having the hepatic margin unarmed and is characterized by its small size and the strongly dentate rostrum margin. The closest relative is *L. evander* from French Polynesia, Philippines and Papua New Guinea (see below under the Remarks of that species).

Leiogalathea creusa n. sp.
(Figs. 8, 10H)

Type material. *Holotype*: French Polynesia. TARASOC Stn CP3376, 15°41'S, 146°54'W, 646–737 m, 04 October 2009: 1 F 5.0 mm (MNHN-IU-2014-13716).

Etymology. From the name *Creusa*, *Aeneas*'s wife at Troy, and the mother of *Ascanius* in the *Aeneid*. The name is considered a substantive in apposition.

Description. *Carapace*: 1.3 × as long as broad. Mid-transverse ridge uninterrupted, preceded by shallow cervical groove, followed by 5 medially interrupted transverse ridges. Lateral margins straight and subparallel, with 5 strong spines: first spine anterolateral, well-developed, small spine on hepatic margin, spine on anterior branchial margin, and 2 spines on posterior branchial margin. Rostrum horizontal, dorsally flattish, 1.6 × as long as broad, length and breadth 0.3 × that of carapace; lateral margin with 4 or 5 teeth, decreasing in size distally.

Sternum: Sternite 3 subquadrangular, 2.5–3.0 × as wide as long, anterolaterally produced, anterior margin serrated, straight, with a median very shallow notch. Sternite 4 broadly contiguous to sternite 3; surface depressed in midline, smooth; greatest width 3.1 × that of sternite 3, 2.5 × as wide as long.

Abdomen: Tergites 2–3 each with 2 elevated transverse ridges, tergites 4–5 with 1 transverse ridge, tergite 6 smooth; tergite 6 with transverse posteromedian margin.

Eye: Ocular peduncle slightly longer than wide; cornea subglobular, maximum corneal diameter 0.8 × rostrum width, as wide as eyestalk.

Antennule: Article 1 with distomesial angle armed with 1 small spine; lateral margin smooth.

Antenna: Article 1 with distomesial spine not reaching end of article 2; article 2 with strong distomesial spine larger than distolateral, nearly reaching end of article 3; articles 3 and 4 unarmed.

Mxp3: Ischium as long as merus measured along extensor margin; flexor margin sharply ridged, terminating in small spine; extensor margin unarmed; crista dentata finely denticulate; merus having flexor margin with strong median spine, extensor margin with distal spine.

P1: 2.2 × carapace length, with numerous short scale-like striae, and uniramous setae scattered on merus to dactylus without stiff long setae. Merus 0.7 × as long as carapace, 1.9 × as long as carpus, with strong mesial and distal spines, and scattered dorsal spines. Carpus 0.8 as long as palm, 1.5 × as long as broad, dorsal surface with

scattered spines, mesial and lateral margins with 2–3 spines. Palm, 1.5 × as long as broad, armed with spines in irregular longitudinal rows on mesial and lateral margins, dorsal surface unarmed. Fingers as long as or slightly longer than palm; fixed finger with a row of spines along lateral margin; movable finger with proximal mesial spine.
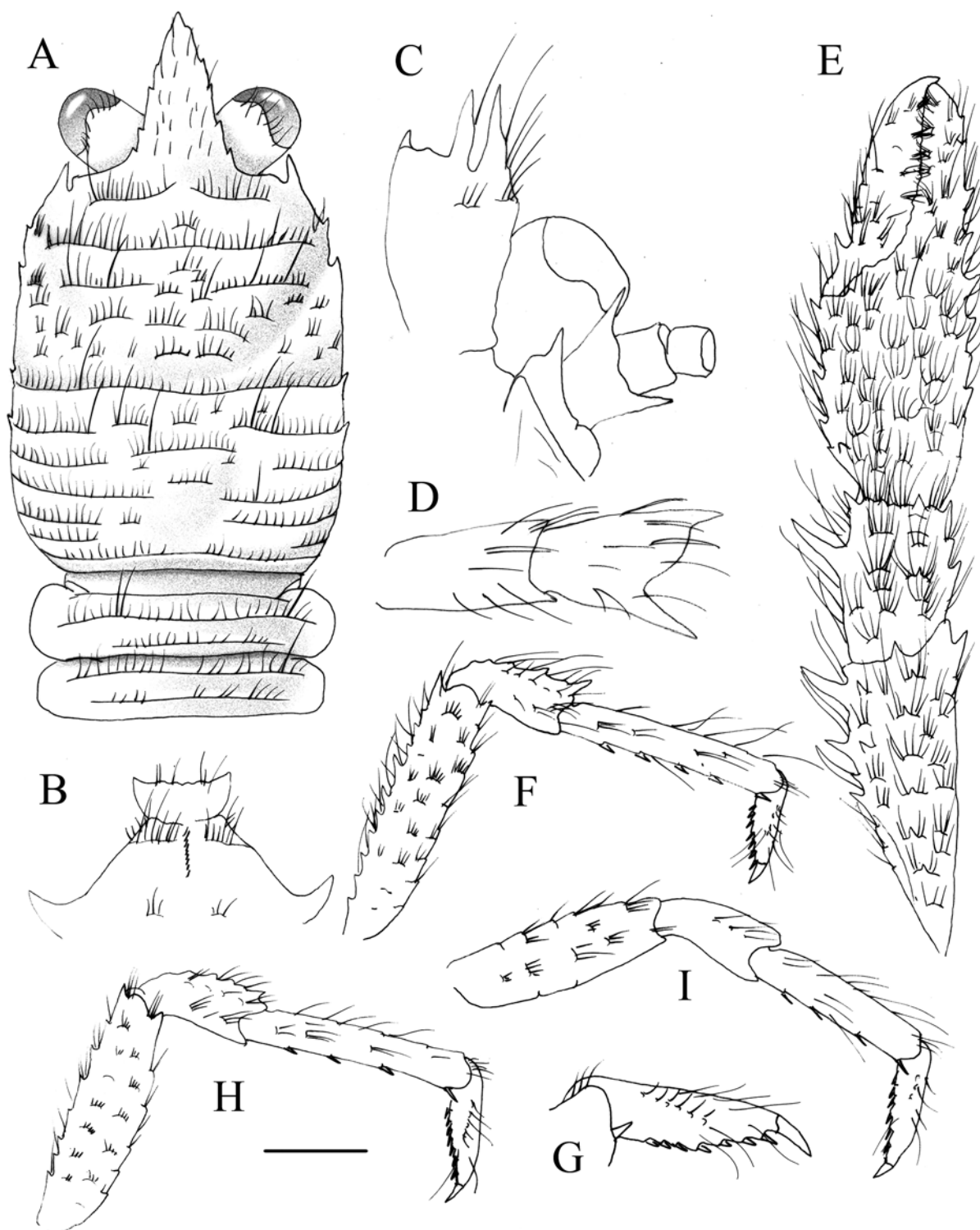
FIGURE 8. *Leiogalathea creusa* **n. sp.**, holotype, F 5.0 mm, French Polynesia (MNHN-IU-2014-13716). A, carapace and abdomen, dorsal view. B, sternites 3–4. C, cephalic region, showing antennular and antennal peduncles, ventral view. D, right Mxp3 ischium and merus, lateral view. E, right P1, dorsal view. F, right P2, lateral view. G, dactylus of right P2, lateral view. H, right P3, lateral view. I, right P4, lateral view. Scales: A, E, F, H, I = 1.0 mm; B–D, G = 0.5 mm.

P2–4: Stout, somewhat compressed laterally, with short setiferous striae on dorsal surface, with sparse long and thick setae on ischium to dactylus. Meri successively shorter posteriorly (P3 merus 0.8 × length of P2 merus, P4 merus 0.9 × length of P3 merus). P2 merus 0.7 × carapace length, 4.8 × as long as broad, 1.2 × as long as P2 propodus; P3 merus 3.7 × as long as broad, 1.1 × as long as P3 propodus; P4 merus 3.4 × as long as broad, 1.2 × as long as P4 propodus; extensor margins with row of 8–11 proximally diminishing spines on P2–3; extensor margin unarmed on P4; lateral surface unarmed; flexor margin with well-developed distal spine and several additional projecting scales. Carpi with 4 or 5 spines on extensor margin on P2–3, unarmed on P4, lateral side smooth; flexor margin with small dorsal spine. Propodi 5.0–6.7 × as long as broad on P2–4, flexor margin with 4 or 5 movable spinules along. Dactyli 0.6 × length of propodi; distal claw short, moderately curved; flexor margin often oblique, with 7 small teeth along the entire margin decreasing in size proximally, each with slender movable spinule, ultimate tooth equidistant between base of distal claw and penultimate tooth.

Colour in life. Unknown.

Genetic data. COI (no data for 16S) (Table 2).

Distribution. French Polynesia, from 646 to 737 m.

Remarks. *Leiogalathea creusa* belongs to the group of species having the hepatic margin of the carapace armed with one spine. This species is morphologically related to *L. anchises* from Papua New Guinea and the Solomon Islands. They can be distinguished on the basis of the following traits:

The P1 is densely covered with long setae in *L. anchises* rather than minimally setose in *L. creusa*.

L. creusa has slender rostrum (1.6 × as long as broad) whereas the rostrum is 1.2–1.3 × as long as broad in *L. anchises*.

The genetic distance between these two species is 7.1% in COI (no data for 16S).

Leiogalathea dido n. sp.
(Figs. 9, 10I)

Type material. *Holotype:* New Caledonia. HALIPRO 2 Stn BT55, 25°04'S, 168°44'E, 1098–1480 m, 17 November 1996: ov. F 9.8 mm (MNHN-IU-2013-17431).

Paratypes: New Caledonia. BATHUS 3 Stn CP823, 23°22'S, 167°51'E, 980–1000 m, 29 November 1993: 4 M 5.9–8.5 mm, 1 ov. F 6.9 mm (MNHN-IU-2014-13708).

New Caledonia. HALIPRO 2 Stn BT25, 25°17'S, 170°24'E, 1100–1348 m, 11 November 96: 1 F 3.6 mm (MNHN-IU-2013-17403).—Stn BT55, 25°04'S, 168°44'E, 1098–1480 m, 17 November 1996: 1 M 10.2 mm (MNHN-IU-2013-17432), 12 M 3.9–11.2 mm, 5 ov F 6.0–8.5 mm, 4 F 5.0–5.9 mm (MNHN-IU-2013-17402), 1 ov. F 6.0 mm (MNHN-IU-2013-17430), 10 M 2.8–10.8 mm, 8 ov. F 2.7–4.1 mm (MNHN-IU-2013-17433).—Stn BT58, 25°05'S, 168°45'E, 1303–1500 m, 17 November 96: 7 M 4.3–7.1 mm, 2 ov. F 7.1–9.2 mm (MNHN-IU-2014-13712).

New Caledonia. NORFOLK 2 Stn DW2055, 23°39.23'S, 168°16.43'E, 900–950 m, 24 October 2003: 1 F 5.0 mm (MNHN-IU-2014-13745).

New Caledonia. EBISCO Stn DW2488, 23°50'S, 161°42'E, 932–996 m, 05 October 2005: 1 F 4.6 mm (MNHN-IU-2014-13783).

Etymology. From the name *Dido*, the queen of Carthage in the *Aeneid*. The name is considered a substantive in apposition.

Description. *Carapace*: 1.1–1.3 × as long as broad. Mid-transverse ridge usually uninterrupted, preceded by deep cervical groove, followed by 5 or 6 interrupted or scale-like transverse ridges. Lateral margins convex, with 7 spines: first spine anterolateral, well-developed; strong spine on hepatic margin, smaller than first spine; 3 well-developed spines on anterior branchial margin, decreasing in size posteriorly, and 2 spines on posterior branchial margin, last spine small. Rostrum horizontal or directed slightly downwards, dorsally flattish or slightly concave, 1.1–1.2 × as long as broad, length 0.2–0.3 × and breadth 0.2–0.3 × that of carapace; lateral margin with 3–6 spines decreasing in size distally.

Sternum: Sternite 3 moderately broad, 2.5–2.8 × as wide as long, anterior margin with median notch flanked by 2 lobes, moderately produced anterolaterally. Sternite 4 narrowly contiguous to sternite 3; surface depressed in midline, smooth; greatest width 2.6 × that of sternite 3, 2.1 × as wide as long.
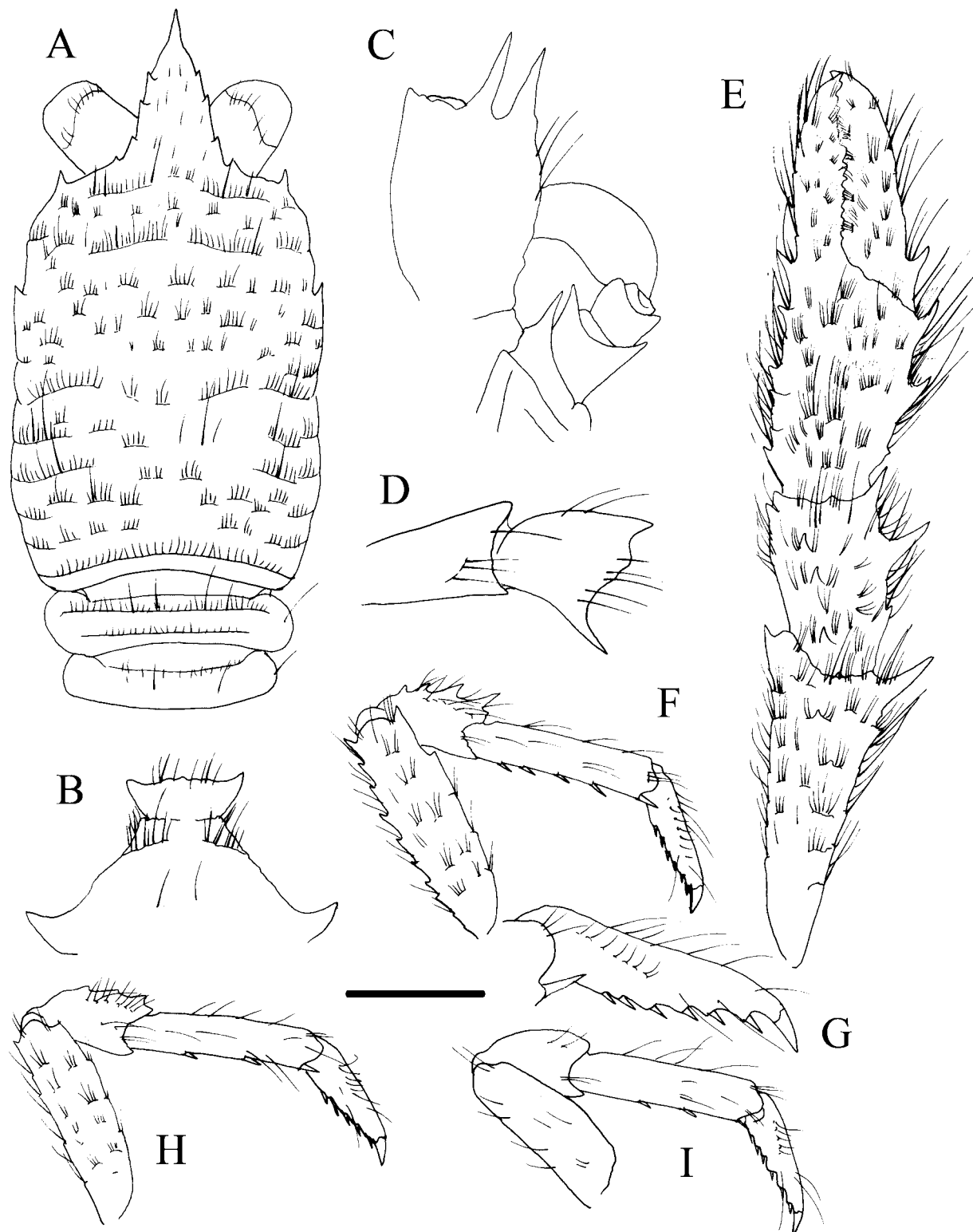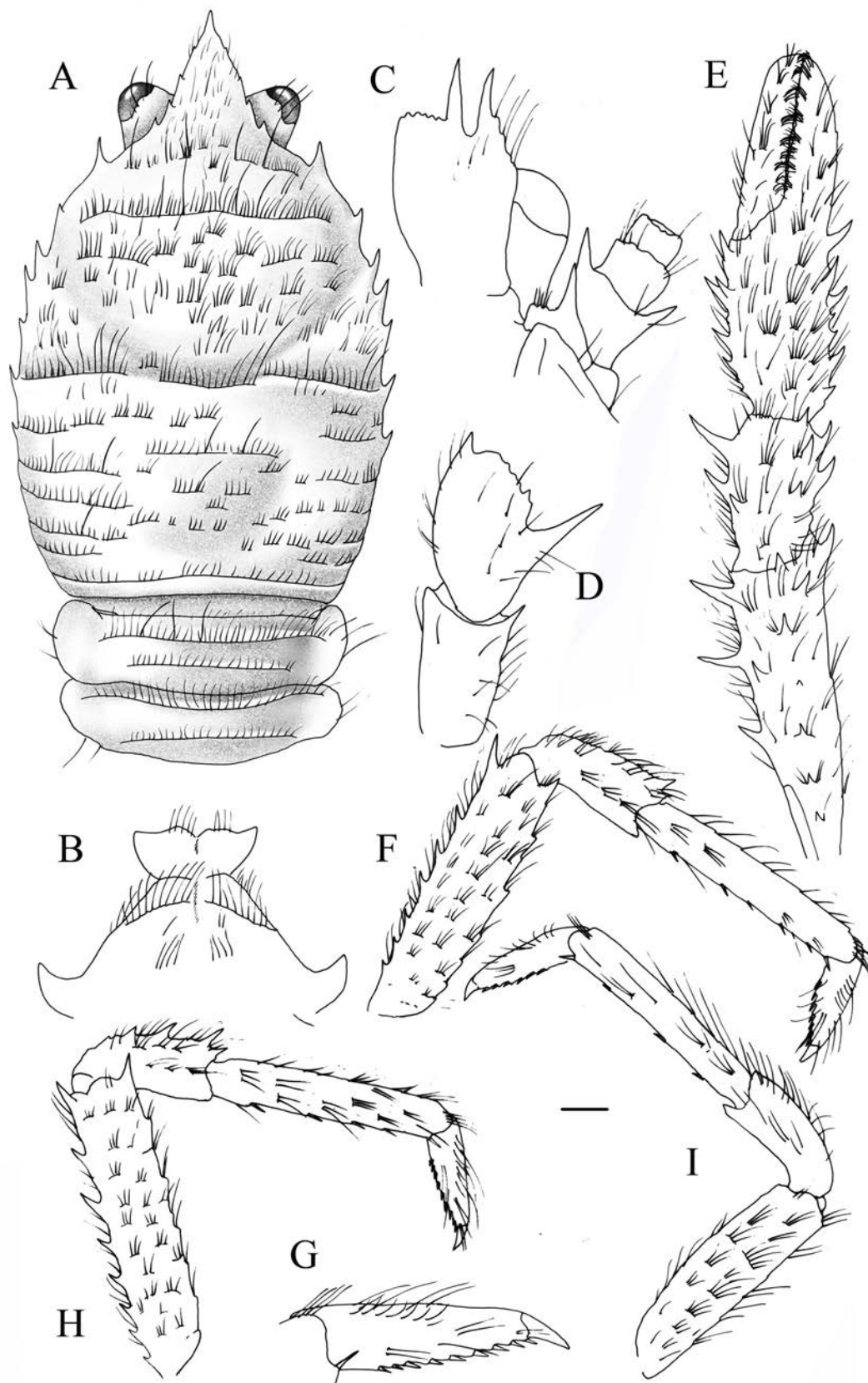
FIGURE 9. *Leiogalathea dido* **n. sp.**, holotype, ov. F 9.8 mm, New Caledonia (MNHN-IU-2013-17431). A, carapace and abdomen, dorsal view. B, sternites 3–4. C, cephalic region, showing antennular and antennal peduncles, ventral view. D, right Mxp3 ischium and merus, lateral view. E, right P1, dorsal view. F, right P2, lateral view. G, dactylus of right P2, lateral view. H, right P3, lateral view. I, left P4, lateral view. Scales: A, E, F, H, I = 1.0 mm; B–D, G = 0.5 mm.
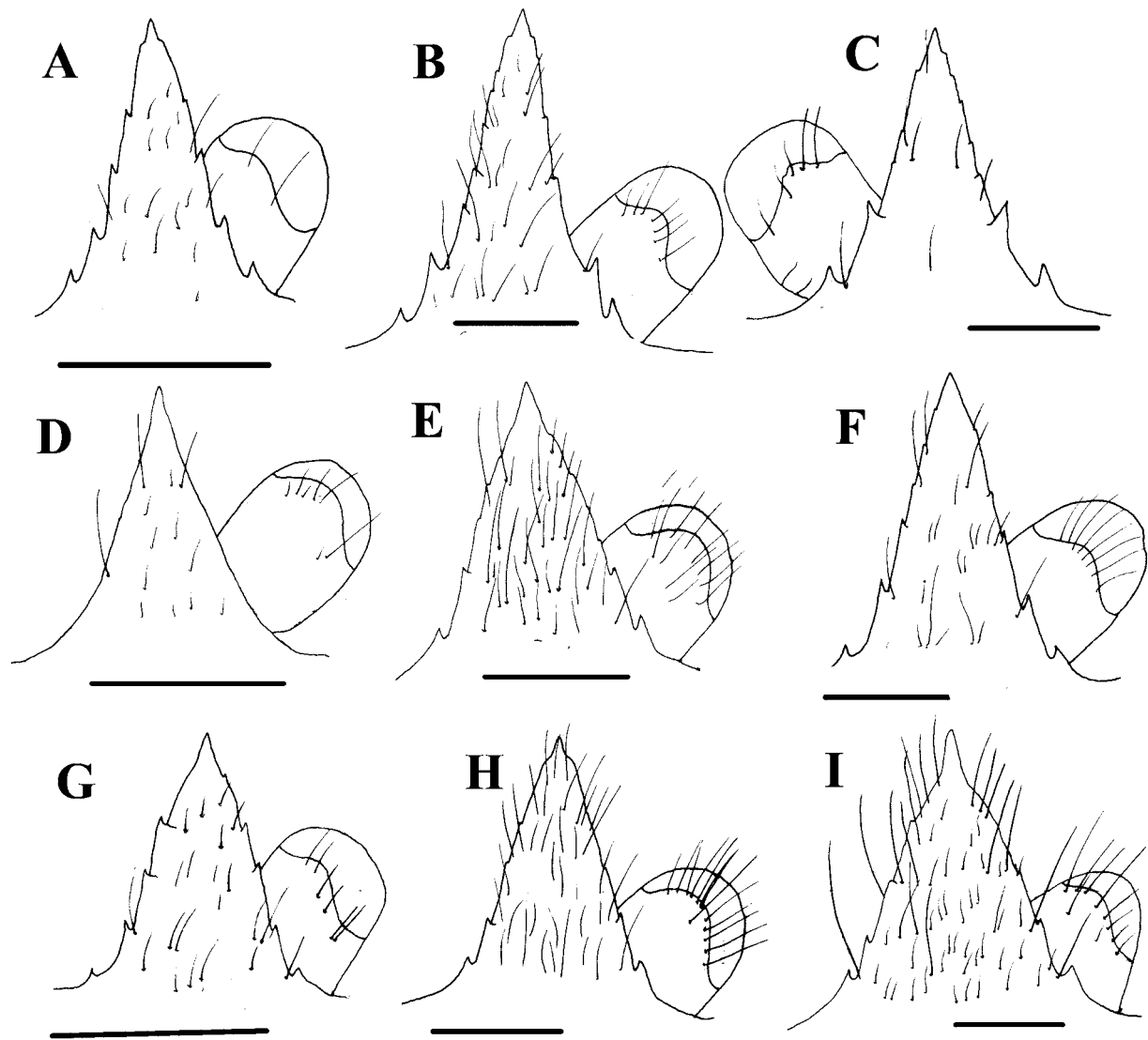
FIGURE 10. Rostrum, and ocular peduncle, dorsal view. A, *Leiogalathea achates* **n. sp.**, holotype, ov. F 3.6 mm (MNHN-IU-2016-7125). B, *L. aeneas* **n. sp.**, holotype, F 7.6 mm (SMF51246). C, *L. agassizii* (A. Milne Edwards, 1880), F 6.9 mm (SMF51247), Florida. D, *L. amata* **n. sp.**, holotype, F 3.6 mm (MNHN-IU-2014-13779). E, *L. anchises* **n. sp.**, holotype, F 6.4 mm (MNHN-IU-2014-13786). F, *L. ascanius* **n. sp.**, holotype, M 5.9 mm (MNHN-IU-2013-17425). G, *L. camilla* **n. sp.**, holotype, M 3.0 mm, (MNHN-IU-2014-13728). H, *L. creusa* **n. sp.**, holotype, F 5.0 mm (MNHN-IU-2014-13716). I, *L. dido* **n. sp.**, holotype, ov. F 9.8 mm (MNHN-IU-2013-17431). Scale = 1 mm.

Abdomen: Tergites 2–3 each with 2 elevated transverse ridges, tergite 4 with transverse ridge, tergites 5–6 with scale-like ridges or smooth; tergite 6 with transverse posteromedian margin.

Eye: Ocular peduncle slightly broader than long, cornea subglobular, maximum corneal diameter 0.4–0.5 × rostrum width, clearly narrower than eyestalk, 0.7 × maximum peduncle width.

Antennule: Article 1 with distomesial angle minutely serrated; lateral margin serrated along distal part.

Antenna: Article 1 with strong distomesial spine nearly reaching end of article 2; article 2 with distolateral and distomesial spines of subequal size, not reaching end of article 3; articles 3 and 4 unarmed.

Mxp3: Ischium as long as merus measured along extensor margin; flexor margin sharply ridged, terminating in well-developed spine; extensor margin unarmed; crista dentata finely denticulate; merus having flexor margin with strong median spine and with or without minute distal spine, extensor margin with distal spine.

P1: 2.3–3.1 (males), 1.8–2.3 (females) × carapace length, with numerous short striae, and densely covered by uniramous short setae on merus to dactylus. Merus 0.6–0.7 length of carapace, 2 × as long as carpus, with strong

mesial and distal spines, and some scattered dorsal spines. Carpus slightly shorter than palm, 1.7 × as long as broad, dorsal surface with scattered spines, mesial and lateral margins each with 2 strong spines. Palm, 1.8 × as long as broad, armed with spines in irregular longitudinal rows on mesial and lateral margins, dorsal surface unarmed. Fingers unarmed, as long as or slightly longer than palm.

P2–4: Moderately slender, somewhat compressed laterally, with short setiferous striae on dorsal surface, with some long and thick setae on ischium to dactylus, meri successively shorter posteriorly (P3 merus 0.9 × of length P2 merus, P4 merus 0.8 × of length P3 merus). P2 merus 0.7 × carapace length, 4.5 × as long as broad, 1.2 × as long as P2 propodus; P3 merus 4.2 × as long as broad, 1.2 × as long as P3 propodus; P4 merus 3.5–3.6 × as long as broad, as long as P4 propodus; extensor margins with row of 7 or 8 proximally diminishing spines on P2–3; unarmed on P4; lateral surface unarmed; flexor margin with well-developed distal spine and several additional projecting scales. Carpi with 2–4 spines on extensor margin on P2–3, unarmed on P4, lateral side smooth; flexor margin with small distal spine. Propodi 5.5–6.5 × as long as broad in P2–4, flexor margin with 4–6 movable spinules. Dactyli 0.5–0.6 × length of propodi; distal claw short, moderately curved; flexor margin nearly straight, with 8–10 small teeth along entire margin decreasing in size proximally, each with slender movable spinule, ultimate tooth most nearly always contiguous to base of distal claw than to penultimate tooth.

Colour in life. Unknown.

Genetic data. COI and 16S (Table 2).

Distribution. New Caledonia and Norfolk Ridge, in sponges, from 670 to 1480 m.

Remarks. *Leiogalathea dido* belongs to the group of species having the hepatic margin of the carapace armed with one spine. The new species is easily differentiated from the other species of the genus by the reduced cornea, being clearly narrower than the ocular peduncle. This species is morphologically related to *L. turnus* from New Caledonia and adjacent waters, having a low genetic distances between them (see below under the Remarks of *L. turnus*).

Leiogalathea evander n. sp.
(Figs. 11A, 12, 21C)

Type material. *Holotype*: Papua New Guinea. MADEEP Stn DW4288, 09°12'S, 153°54'E, 504 m, 30 April 2014: 1 M 3.9 mm (MNHN-IU-2015-820).

Paratypes: Marquesas Islands, Polynesia. MUSORSTOM 9 Stn DR1253, 9°47.9'S, 139°38.1'W, 360–405 m, 2 September 1997: 1 M 4.8 mm (MNHN-IU-2013-17420).—Stn DR1255, 9°38.5'S, 139°48.4'W, 416–440 m, 2 September 1997: 1 ov. F 4.0 mm (MNHN-IU-2013-17429).—Stn CP1282, 7°51.7'S, 140°30.6'W, 416–460 m, 7 September 1997: M 4.9 mm (MNHN-IU-2013-17421).—Stn CP1306, 8°55.2'S, 140°14.8'W, 283–448 m, 10 September 1997: 1 M 3.7 mm (MNHN-IU-2013-17422).

Papua New Guinea. MADEEP Stn DW4286, 09°12'S, 153°55'E, 306–365 m, 30 April 2014: 2 M 4.8–5.9 mm, 1 ov. F 3.8 mm (MNHN-IU-2015-146, MNHN-IU-2016-9657)**.**

Etymology. From the name *Evander*, king of *Pallanteum* and father of *Pallas* in the *Aeneid*. The name is considered a substantive in apposition.

Description. *Carapace*: 1.1–1.3 × as long as broad. Mid-transverse ridge usually medially interrupted or scale-like, preceded by shallow cervical groove, followed by 4 or 5 laterally interrupted transverse ridges. Lateral margins slightly convex, with 2 spines: first spine anterolateral, well-developed; second spine well-developed located on anterior branchial margin, hepatic and posterior branchial margin unarmed. Rostrum slender, dorsally slightly concave and usually directed downwards, 1.6 × as long as broad, length 0.4 × and breadth 0.2–0.3 × that of carapace; lateral margin armed with 4–6 rudimentary teeth along entire margin.

Sternum: Sternite 3 moderately broad, 2.6–2.8 × as wide as long, anterolaterally produced, anterior margin minutely serrated with median notch flanked by 2 shallow lobes. Sternite 4 broadly contiguous to sternite 3; surface depressed in midline, smooth; greatest width 3 × that of sternite 3, 2.5 × as wide as long.

Abdomen: Tergites 2–3 with 2 elevated transverse ridges, tergite 4 with 1 transverse ridge, tergites 5–6 smooth; tergite 6 with transverse posteromedian margin.

Eye: Ocular peduncle slightly longer than wide; cornea subglobular, maximum corneal diameter 0.7 × rostrum width, as wide as eyestalk.
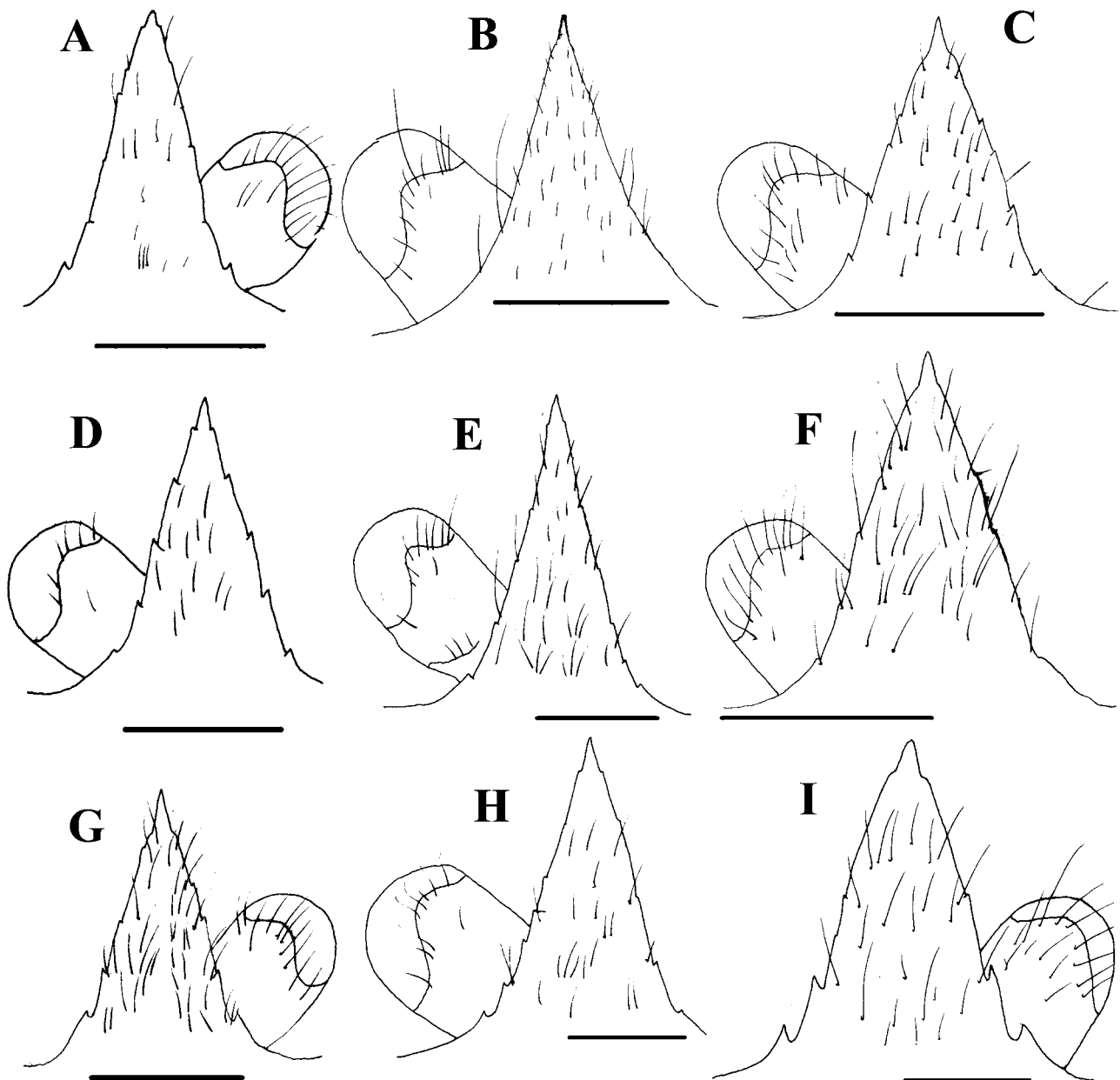
FIGURE 11. Rostrum, and ocular peduncle, dorsal view. A, *Leiogalathea evander* **n. sp.**, holotype, M 3.9 mm (MNHN-IU-2015-820). B, *L. imperialis* (Miyake & Baba, 1967), holotype, ov. F 5.2 mm (BLIH 205a). C, *L. juturna* **n. sp.**, holotype, F 4.2 mm (MNHN-IU-2013-17404). D, *L. laevirostris* (Balss, 1913), syntype, F 4.9 mm (ZMB17488). E, *L. pallas* **n. sp.**, holotype, F 6.9 mm (MNHN-IU-2014-13395). F, *L. paris* **n. sp.**, holotype, ov. F 4.0 mm (MNHN-IU-2011-4471). G, *L. priam* **n. sp.**, holotype, M 5.0 mm (MNHN-IU-2014-13697). H, *L. sinon* **n. sp.**, holotype, F 8.3 mm (MNHN-IU-2014-13711). I, *L. turnus* **n. sp.**, holotype, M 8.0 mm (MNHN-IU-2014-13744). Scale = 1 mm.

Antennule: Article 1 with distomesial angle unarmed; lateral margin smooth.

Antenna: Article 1 with short, stout distomesial spine not reaching mid-length of article 2; article 2 with distomesial spine longer than distolateral spine, not reaching end of article 3; articles 3 and 4 unarmed.

Mxp3: Ischium as long as merus measured along extensor margin; flexor margin sharply ridged, terminating in small spine; extensor margin unarmed; crista dentata finely denticulate; merus having flexor margin with 1 strong median spine, extensor margin with distal spine.
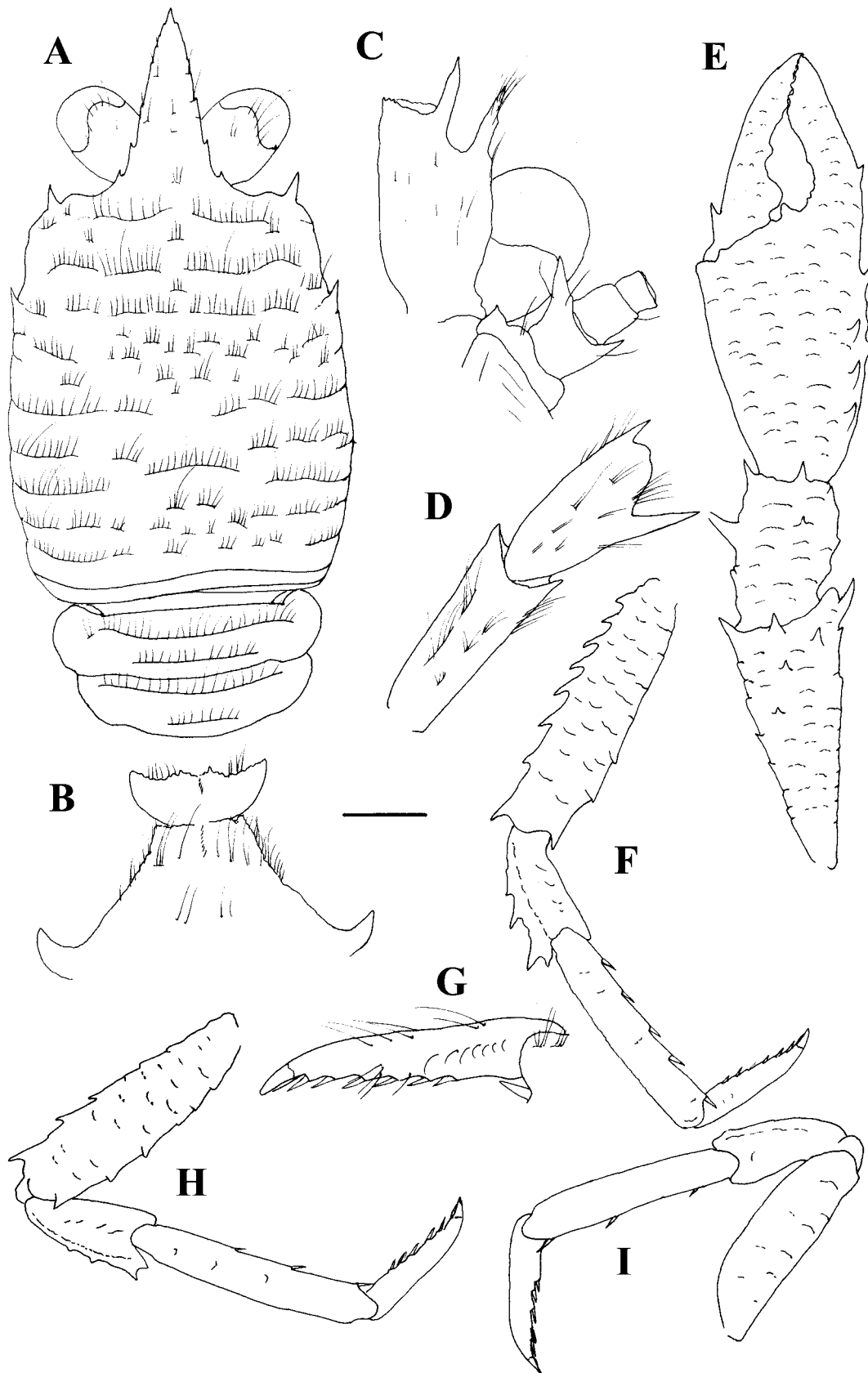
FIGURE 12. *Leiogalathea evander* **n. sp.**, holotype, M 3.9 mm, Papua New Guinea (MNHN-IU-2015-820). A, carapace and abdomen, dorsal view. B, sternites 3–4. C, cephalic region, showing antennular and antennal peduncles, ventral view. D, right Mxp3 ischium and merus, lateral view. E, right P1, dorsal view. F, left P2, lateral view. G, dactylus of left P2, lateral view. H, left P3, lateral view. I, left P4, lateral view. Scales: A, E, F, H, I = 1.0 mm; B–D, G = 0.5 mm. Setae omitted on P1–4.

P1: 2.4–2.9 (males), 1.8–2.3 (females) × carapace length, with numerous short striae, and covered by uniramous short setae on merus to dactylus, long stiff setae absent. Merus 0.7 length of carapace, 2.1 × as long as carpus, with strong mesial and distal spines, and scattered dorsal spines. Carpus slightly shorter than palm, 1.6 × as long as broad, dorsal surface with scattered spines, mesial margins with 1 or 2 strong spines, lateral margin unarmed. Palm 2.1 × as long as broad, armed with spines in irregular longitudinal rows along mesial and lateral margins, dorsal surface unarmed. Fingers 1.3 × as long as palm; fixed finger with one or several proximal spines along lateral margin; movable finger usually with 1 well-developed proximal mesial spine.

P2–4: stout, somewhat compressed laterally, with short setiferous striae on dorsal surface, with some long and thick setae on ischium to dactylus, meri successively shorter posteriorly (P3 merus 0.9 × length of P2 merus, P4 merus 0.8 × length of P3 merus). P2 merus, 0.6 × carapace length, 4.4 × as long as broad, 1.2 × as long as P2 propodus; P3 merus 4.2 × as long as broad, 1.2 × as long as P3 propodus; P4 merus 3.7 × as long as broad, as long as P4 propodus; extensor margins with row of 7 or 8 proximally diminishing spines on P2–3; extensor margin unarmed on P4; lateral surface unarmed; flexor distal margin with well-developed distal spine and several additional projecting scales. Carpi with 2–4 spines on extensor margin on P2–3, unarmed on P4, lateral side smooth; flexor margin with small distal spine. Propodi 5.9–6.1 × as long as broad on P2–4, flexor margin with 3–5 movable spinules. Dactyli 0.6–0.7 × length of propodi; distal claw short, moderately curved; flexor margin nearly straight, with 6–8 small teeth along entire margin decreasing in size proximally, each with slender movable spinule, ultimate tooth closer to base of distal claw than to penultimate tooth.

Colour in life. Unknown.

Genetic data. COI and 16S (Table 2).

Distribution. Marquesas Island, Polynesia, Philippines and Papua New Guinea, from 283 to 504 m.

Remarks. *Leiogalathea evander* belongs to the group of species having the hepatic margin unarmed and is easily distinguished from all the other species by having the rostrum slender and usually inclined downwards. Male P1 fingers clearly gap in specimens reaching big sizes, although this is a character highly variable not considered in the diagnosis of the species. This species is morphologically related to *L. achates* from Mayotte-Glorieuses islands and Madagascar in the Western Indian Ocean. Genetic distances between these species for the molecular markers analysed are 4.4% for COI and 0.8% for 16S. However, *L. evander* is easily distinguished from *L. achates* by the following morphological characters: the rostrum is usually deflected ventrally rather than horizontal and proportionally narrower (1.6 versus 1.4–1.5 × as long as broad).

Leiogalathea evander also resembles *L. camilla* from New Caledonia and adjacent waters, from which it can be differentiated by the rostrum usually deflected ventrally instead of straight horizontal or directed slightly downwards, and its lateral margin with rudimentary or obsolete instead of sharp teeth. Their genetic distance is high: 13.6% for COI and 6.7% for 16S.

Leiogalathea imperialis (Miyake & Baba, 1967)
(Figs. 11B, 13)

Galathea imperialis Miyake & Baba, 1967: 213, figs 1, 2.
Leiogalathea imperialis.—Baba 1969: 3.

Type material. *Holotype*: WSW of Joga-shima Islet, Sagami Bay, 160–230 m, 19 March 1958: ov. F 5.2 mm (BLIH 205a).

Paratype: Collected with holotype: ov. F 4.2 mm (BLIH 205b).

Description. *Carapace*: 1.3 × as long as broad. Mid-transverse ridge interrupted, preceded by shallow cervical groove, followed by 8–11 interrupted or scale-like transverse ridges. Lateral margins slightly convex, with 2 or 3 spines: first spine anterolateral, well-developed; hepatic margin unarmed; small spine on anterior branchial margin, with or without small spine on posterior branchial margin. Rostrum horizontal, dorsally flattish and slightly directed downwards, 1.5 × as long as broad, length 0.4 × and breadth 0.3 × that of carapace; lateral margin unarmed, smooth.

Sternum: Sternite 3 acutely broad, 3.9 × as wide as long, anterolaterally produced, anterior margin smooth, straight, with a median minute shallow notch. Sternite 4 narrowly contiguous to sternite 3; surface depressed in midline, smooth; greatest width 3.6 × that of sternite 3, 2.6 × as wide as long.
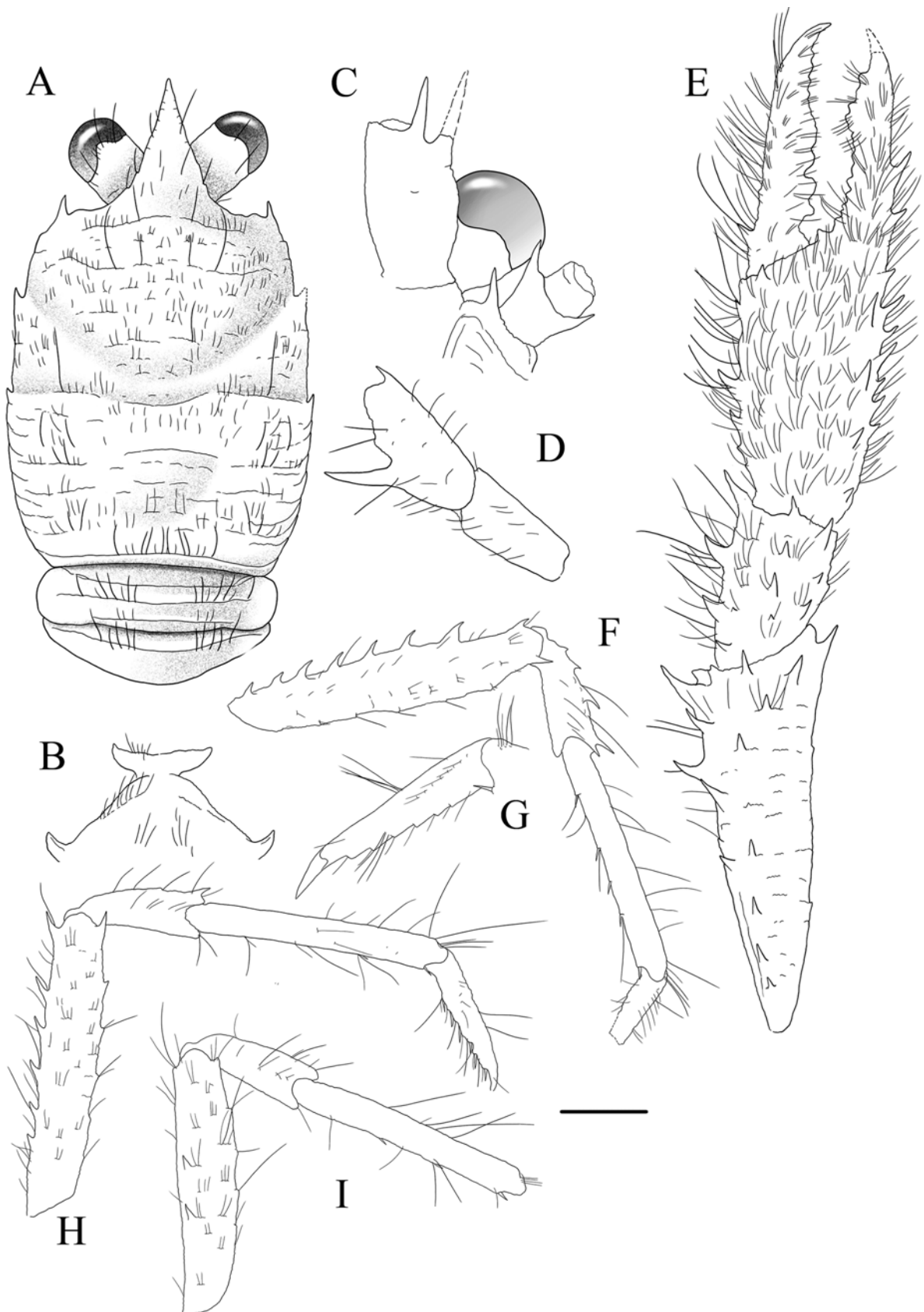
FIGURE 13. *Leiogalathea imperialis* (Miyake & Baba, 1967), holotype, ov. F 5.2 mm, Sagami Bay, Japan (BLIH 205a). A, carapace and abdomen, dorsal view. B, sternites 3–4. C, cephalic region, showing antennular and antennal peduncles, ventral view. D, left Mxp3 ischium and merus, ateral view. E, right P1, dorsal view. F, right P2, lateral view. G, dactylus of left P2, lateral view. H, right P3, lateral view. I, right P4, lateral view. Scales: A, E, F, H, I = 1.0 mm; B–D, G = 0.5 mm.

Abdomen: Tergite 2 with 2 elevated transverse ridges, tergite 3–4 each with transverse ridge, tergites 5–6 smooth; tergite 6 with transverse posteromedian margin.

Eye: Ocular peduncle slightly longer than wide; cornea subglobular, maximum corneal diameter 0.7 × rostrum width, as wide as eyestalk.

Antennule: Article 1 with distomesial angle minutely serrated; lateral margin smooth.

Antenna: Article 1 with distomesial spine nearly reaching end of article 2; article 2 with strong distomesial spine, longer than distolateral spine, and reaching end of article 3; articles 3 and 4 unarmed.

Mxp3: Ischium as long as merus measured along extensor margin; flexor margin sharply ridged, terminating in small spine; extensor margin unarmed; crista dentata finely denticulate; merus having flexor margin with strong median spine, extensor margin with distal spine.

P1: 2.4 × carapace length, with scattered short striae, and densely covered by uniramous long setae on merus to dactylus. Merus 0.8 length of carapace, twice as long as carpus, with strong mesial and distal spines, and scattered dorsal spines. Carpus 0.8 × shorter than palm, 1.8 × as long as broad, dorsal surface with sparse spines, mesial and lateral margins with several spines. Palm 1.7 × as long as broad, armed with spines in irregular longitudinal rows on mesial and lateral margins, dorsal surface unarmed. Fingers 1.4 × as long as palm; fixed finger with 2 well-developed lateral proximal spines; movable finger with 1 well-developed proximal spine on mesial margin.

P2–4: slender, somewhat compressed laterally, with short setiferous striae on dorsal surface; with sparse long and thick setae on ischium to dactylus. Meri successively shorter posteriorly (P3 merus 0.8 × length of P2 merus, P4 merus 0.9 × length of P3 merus). P2 merus as long as carapace, 6.9 × as long as broad, 1.1 × as long as P2 propodus; P4 merus 4.7 × as long as broad, 1.1 × as long as P4 propodus; extensor margins with a row of 6 or 7 proximally diminishing spines on P2–3; 2 distal spines on P4; lateral surface unarmed; flexor margin with 1 well-developed distal spine and several additional projecting scales. Carpi with 1–3 spines on extensor margin on P2–3, unarmed on P4, lateral side smooth; flexor margin with small distal spine. Propodi 7.5–8.5 × as long as broad on P2–4, flexor margin with 3–5 movable spinules. Dactyli 0.6 × length of propodi; distal claw short, moderately curved; flexor margin nearly straight, with 5 or 6 small teeth decreasing in size proximally, each with slender movable spinule, ultimate tooth equidistant between base of distal claw and penultimate tooth.

Colour in life. Unknown.

Genetic data. No data.

Distribution. Japan, Sagami Bay, between 160 and 230 m.

Remarks. *Leiogalathea imperialis* belongs to the group of species having the hepatic margin of the carapace unarmed and the margin of the rostrum smooth. *Leiogalathea imperialis* morphologically resembles *L. amata* from Wallis and Futuna and New Caledonia. However, they can be differentiated by the presence or absence of 1 small spine on the posterior branchial margin of the carapace (present in *L. imperialis*, absent in *L. amata*).

Leiogalathea juturna **n. sp.**
(Figs. 11C, 14)

Leiogalathea laevirostris.—Baba *et al*. 2009: 134, figs. 112–114.

Dubious identification: *Leiogalathea laevirostris.*—Baba 2005: 88, 246.

Type material. *Holotype*: Kei Islands, Indonesia, KARUBAR Stn DW18, 05°18'S, 133°01'E, 205–212 m, 24 October 1991: 1 F 4.2 mm (MNHN-IU-2013-17404).

Paratypes: Kei Islands, Indonesia. KARUBAR Stn DW18, 05°18'S, 133°01'E, 205–212 m, 24 October 1991: 1 F 3.3 mm (MNHN-IU-2016-2996), 3 F 3.3–4.0 mm (MNHN-IU-2013-17428), 2 M 4.2–4.4 mm (MNHN-IU-2013-17427).—Stn CP25, 05°30'S, 132°52'E, 336–346 m, 26 October 1991: 1, M, 5.4 mm (MNHN-IU-2013-17426).

Etymology. From the name *Juturna*, *Turnus*'s sister in the *Aeneid*. The name is considered a substantive in apposition.

Description. *Carapace*: 1.1–1.3 × as long as broad. Mid-transverse ridge usually medially interrupted or scale-like, preceded by shallow cervical groove, followed by 5 or 6 interrupted or scale-like transverse ridges. Lateral margins slightly convex and subparallel, with 2 small spines: first spine anterolateral; second spine on anterior branchial margin; hepatic and posterior branchial margin unarmed. Rostrum horizontal, dorsally flattish or slightly

concave, 1.2–1.4 × as long as broad, length 0.3 × and breadth 0.2–0.3 × that of carapace; lateral margin with 4 or 5 rudimentary teeth.

Sternum: Sternite 3 moderately broad, 3.3–4.0 × as wide as long, anterolaterally produced, anterior margin serrated, straight, with a median minute shallow notch. Sternite 4 narrowly contiguous to sternite 3; surface depressed in midline, smooth; greatest width 3 × that of sternite 3, 2.5 × as wide as long.
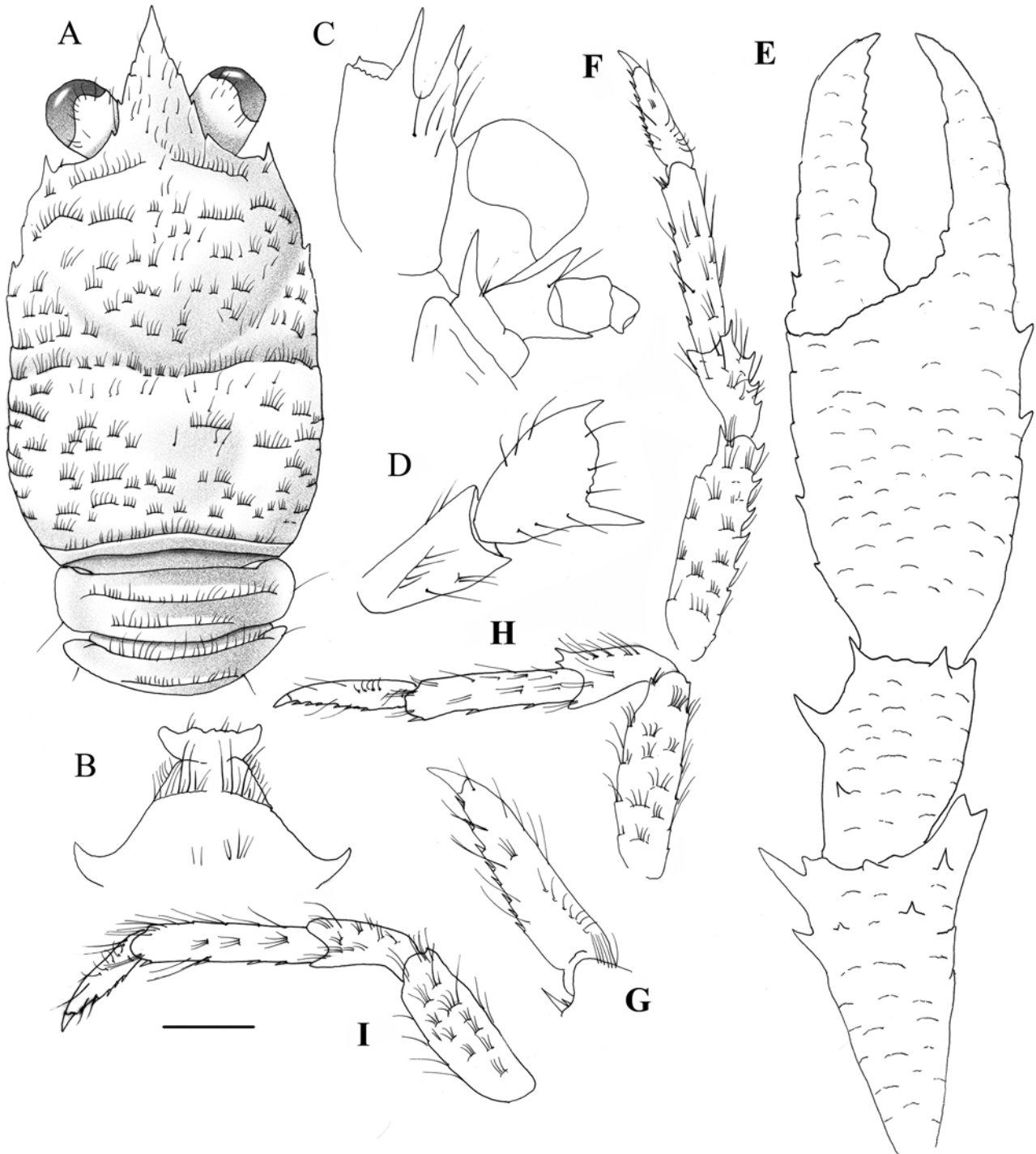
FIGURE 14. *Leiogalathea juturna* **n. sp.**, A–D, F–I, holotype, F 4.3 mm, Kei Islands (MNHN-IU-2013-17404). E, paratype, M 4.4 mm, Kei Islands (MNHN-IU-2013-17427). A, carapace and abdomen, dorsal view. B, sternites 3–4. C, cephalic region, showing antennular and antennal peduncles, ventral view. D, right Mxp3 ischium and merus, lateral view. E, right P1, dorsal view. F, left P2, lateral view. G, dactylus of left P2, lateral view. H, left P3, lateral view. I, left P4, lateral view. Scales: A, E, G, H, I = 1.0 mm; B–D, F = 0.5 mm. Setae omitted on P1.

Abdomen: Tergites 2–3 each with 2 elevated transverse ridges, tergite 4 with transverse ridge, tergites 5–6 smooth; tergite 6 with transverse posteromedian margin.

Eye: Ocular peduncle slightly longer than wide; cornea subglobular, maximum corneal diameter 0.7 × rostrum width, as wide as eyestalk.

Antennule: Article 1 with distomesial angle serrated; lateral margin smooth.

Antenna: Article 1 with strong distomesial spine reaching end of article 2; article 2 with strong distomesial spine larger than distolateral, not reaching end of article 3; articles 3 and 4 unarmed.

Mxp3: Ischium as long as merus measured along extensor margin; flexor margin sharply ridged, terminating in small spine; extensor margin unarmed; crista dentata finely denticulate; merus having flexor margin with 1 strong median spine, extensor margin with distal spine.

P1: 2.5–2.7 (males), 2.0 (females) × carapace length, with numerous short striae, and covered by uniramous long setae on merus to dactylus. Merus 0.7 length of carapace, 2.1 × as long as carpus, with strong mesial and distal spines, and scattered dorsal spines. Carpus slightly shorter than palm, 1.6 × as long as broad, dorsal surface with a few scattered spines, mesial and lateral margins with several spines. Palm 2.1 × as long as broad, armed with spines in irregular longitudinal rows along mesial and lateral margins, dorsal surface unarmed. Fingers 1.3 × as long as palm; fixed finger unarmed; movable finger with 1 proximal mesial spine.

P2–4: Stout, with setiferous setose striae on dorsal surface, somewhat compressed laterally, with sparse long and thick setae on ischium to dactylus. Meri successively shorter posteriorly (P3 merus 0.9 × length of P2 merus, P4 merus 0.9 × length of P3 merus). P2 merus 0.6 × carapace length, 6 × as long as broad, 1.4 × as long as P2 propodus; P3 merus 4.8 × as long as broad, 1.5 × as long as P3 propodus; P4 merus 3.3 × as long as broad, 1.3 × as long as P4 propodus; extensor margins with row of 7–8 proximally diminishing spines on P2, unarmed on P3–4; lateral surface unarmed; flexor margin with well-developed distal spine and several additional projecting scales on. Carpi with 2–4 spines on extensor margin on P2–3, unarmed on P4, lateral side smooth; flexor margin with small distal spine. Propodi 4.0–5.0 × as long as broad on P2–4, flexor margin with 4–6 movable spinules. Dactyli 0.5 × length of propodi; distal claw short, moderately curved; flexor margin nearly straight, with 7 or 8 small teeth along the entire margin decreasing in size proximally, each with slender movable spinule, ultimate tooth closer to base of distal claw than to penultimate tooth.

Colour in life. Ground colour reddish, orange to pale. Carapace and anterior half of abdomen pale orange. P1 occasionally totally orange with orange red bands, tips of fingers whitish; P2–4 with orange or reddish bands (from Baba *et al.* 2009).

Genetic data. COI and 16S (Table 2).

Distribution. Indonesia and Taiwan, from 205 to 356 m.

Remarks. *Leiogalathea juturna* belongs to the group of species having the hepatic margin of the carapace unarmed, the branchial margin with or without a spine, and the rostral lateral margin armed with 4 or 5 rudimentary teeth. The closest relatives are *L. paris* from French Polynesia, Papua New Guinea and New Caledonia, *L. laevirostris* from Andaman Sea and *L. priam* from Papua New Guinea (see below, under the Remarks of *L. priam*).

Leiogalathea laevirostris (Balss, 1913)
(Figs. 11D; 15)

Galathea laevirostris Balss, 1913: 221.—Doflein & Balss 1913: 140, fig. 7, pl. 12, fig. 1.

Dubious identifications: *Galathea laevirostris.*—Laurie 1926: 135.
Leiogalathea laevirostris.—Baba 2005: 88, 246.—Ahyong 2007: 14, fig. 8.—Rowden *et al.* 2010: tab. 3, 4.—Yaldwyn & Webber 2011: 213.

Type material. *Lectotype*: Sombrero Channel, Nicobar Islands. VALDIVIA Stn 211, 805 m, 8 February 1899: 1F 4.9 mm (ZMB 17488).

Paralectotype: Sombrero Channel, Nicobar Islands. VALDIVIA Stn 211, 805 m, 8 February 1899: 1 M 4.8 (ZMB 17488B).

Description. *Carapace*: 1.3 × as long as broad. Mid-transverse ridge interrupted, followed by 5 interrupted transverse ridges. Lateral margins straight and subparallel, with 2 spines: first spine anterolateral well-developed;

second small spine on anterior branchial margin; hepatic and posterior branchial margin unarmed. Rostrum horizontal, dorsally flattish or slightly concave, 1.5 × as long as broad, length 0.3 × and breadth 0.2–0.3 × that of carapace; lateral margin serrated, with 4 or 5 small teeth decreasing in size distally.

Sternum: Sternite 3 moderately broad, 3.0 × as wide as long, somewhat produced anterolaterally, anterior margin serrated, straight, with a median shallow notch. Sternite 4 narrowly contiguous to sternite 3; surface depressed in midline, smooth; greatest width 3.3 × that of sternite 3, 2.2 × as wide as long.
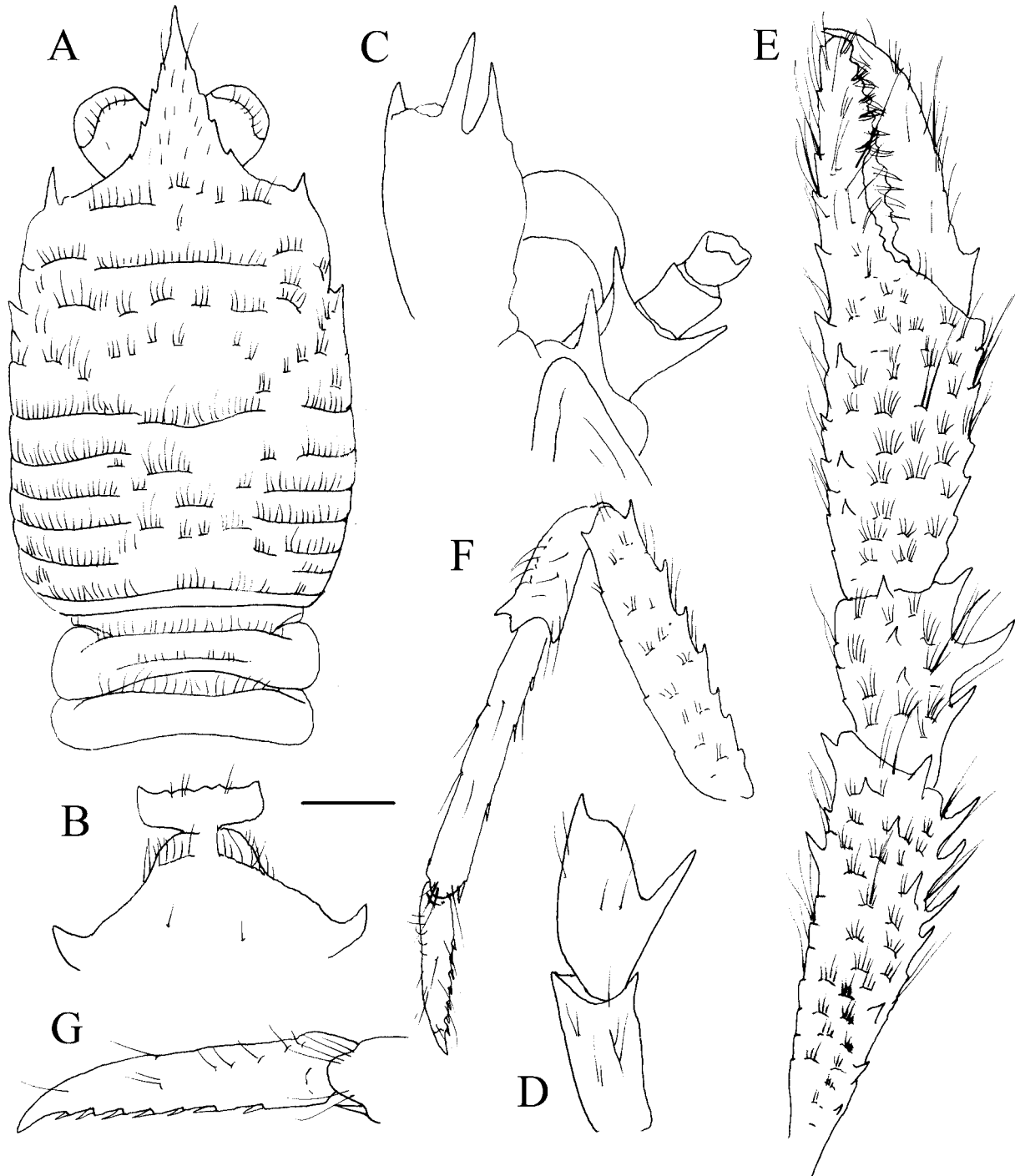
FIGURE 15. *Leiogalathea laevirostris* (Balss, 1913), lectotype, F 4.9 mm (ZMB17488). A, carapace and abdomen, dorsal view. B, sternites 3–4. C, cephalic region, showing antennular and antennal peduncles, ventral view. D, right Mxp3 ischium and merus, lateral view. E, left P1, dorsal view. F, detached left pereiopod, probably P3, lateral view. G, dactylus of the same pereiopod, lateral view. Scales: A, E, F = 1.0 mm; B–D, G = 0.5 mm.

Abdomen: Tergite 2 with 2 elevated transverse ridges, tergites 3–4 with transverse ridge, tergites 5–6 smooth; tergite 6 with transverse posteromedian margin.

Eye: Ocular peduncle slightly longer than wide; cornea subglobular, maximum corneal diameter 0.7 × rostrum width, as wide as eyestalk.

Antennule: Article 1 with a spine on distomesial angle; lateral margin smooth.

Antenna: Article 1 with strong distomesial spine nearly reaching end of article 2; article 2 with subequal distolateral and distomesial spines, not reaching end of article 3; articles 3 and 4 unarmed.

Mxp3: Ischium as long as merus measured along extensor margin; flexor margin sharply ridged, terminating in small spine; extensor margin unarmed; crista dentata finely denticulate; merus having flexor margin with strong median spine, extensor margin with distal spine.

P1: 2.7 (female, lost in male) × carapace length, with numerous short striae, and uniramous long setae scattered on merus to dactylus. Merus 0.9 length of carapace, 2.4 × as long as carpus, with strong mesial and distal spines, some scattered dorsal spines. Carpus slightly shorter than palm, 1.6 × as long as broad, dorsal surface with scattered spines, mesial margin with 3 strong spines, lateral margin unarmed. Palm, 1.9 × as long as broad, armed with spines in irregular longitudinal rows on mesial and lateral margins, dorsal surface unarmed. Fingers as long as palm; fixed finger with a row of spines along lateral border; movable finger with well-developed proximal mesial spine.

P3 (*other pereiopods lost*): Slender, somewhat compressed laterally, with short setiferous striae on dorsal surface, with sparse long and thick setae on ischium to dactylus. Merus, 0.7 × carapace length, 5 × as long as broad, 1.2 × as long as propodus; P3 merus 4.2 × as long as broad, 1.2 × as long as P3 propodus; extensor margins with a row of 7 proximally diminishing spines; flexor margin with 1 well-developed distal spine and several projecting scales. Carpi with 2 distal spines on extensor margin; flexor margin with small distal spine. Propodi 9 × as long as broad, flexor margin with 4 movable spinules. Dactyli 0.6 × length of propodi; distal claw short, moderately curved; flexor margin nearly straight, with 7 small teeth along entire margin decreasing in size proximally, each with slender movable spinule, ultimate tooth closer to base of distal claw than to penultimate tooth.

Colour in life. Unknown.

Genetic data. No data.

Distribution. Andaman Sea, 805 m.

Remarks. *Leiogalathea laevirostris* belongs to the group of species having the hepatic margin of the carapace unarmed, the branchial margin with or without a spine, and the margin of the rostrum armed with 4 or 5 small teeth. The closest relatives are *L. juturna* from Indonesia and Taiwan, *L. paris* from Polynesia, Papua New-Guinea and New Caledonia, and *L. priam* from Papua New-Guinea. *Leiogalathea laevirostris* can be differentiated from these congeners by the more slender P2–4 propodi (9 versus 5–6 × as long as broad) and the distomesial margin of the antennule being armed with a small spine instead of being unarmed.

Unfortunately, we were not able to obtain molecular data for *L. laevirostris*.

Leiogalathea pallas **n. sp.**
(Figs. 11E, 16, 21D)

Leiogalathea laevirostris.—Baba 1991: 487–488 (in part, only specimens from MUSORSTOM 4 and BIOGEOCAL).

Type material. *Holotype:* Papua New Guinea. KAVIENG 2014 Stn DW4470, 02°45'S, 150°37'E, 163–358 m, 3 September 2014: F 6.9 mm (MNHN-IU-2014-13395).

Paratypes: New Caledonia. R/v Vauban Stn 475, 10°35.7'S, 163°11.2'E, 415–460 m, 2 March 1985: 1 M 5.3 mm (MNHN-IU-2014-13766).

New Caledonia. MUSORSTOM 4 Stn 165, 18°30'S, 163°14.5'E, 440 m, 16 September 1985: 1 F 4.7 mm (MNHN-IU-2016-418).

New Caledonia. BIOGEOCAL. Stn DW307, 20°35.38'S, 166°55.25'E, 470–480 m, 1 may 1987: 1 M 4.4 mm (MNHN-IU-2016-416).

Vanuatu. MUSORSTOM 8 Stn DW1009, 17°46'S, 168°13'E, 430–460 m, 27 September 1994: 1 M 7.1 mm, 3 ov. F 4.7–6.0 mm, 1 F 2.8 mm (MNHN-IU-2014-13761).—Stn DW1015, 17°54'S, 168°22'E, 420–375 m, 27

September 1994: 1 ov. F 4.7 mm (MNHN-IU-2014-13764).—Stn CP1049, 16°39'S, 168°03'E, 469–525 m, 1 October 1994: 1 ov. F 4.6 mm, 1 F 3.6 mm (MNHN-IU-2014-13762).—Stn DW1060, 16°14'S, 167°21'E, 394–375 m, 2 October 1994: 1 F 5.3 mm (MNHN-IU-2014-13763).—Stn DW1061, 16°15'S, 167°20'E, 458–512 m, 2 October 1994: 1 F 4.8 mm (MNHN-IU-2014-13765).

Vanuatu. SANTO Stn AT10, 15°41'S, 167°01'E, 509–659 m, 17 September 2006: 1 M 8.3 mm (MNHN-IU-2014-13775).

Solomon Islands. SALOMON 2 Stn DW2303, 09°07.55'S, 158°22.23'E, 402–413 m, 7 October 2004: 1 F 4.7 mm (MNHN-IU-2014-13768), 1 M 5.0 mm (MNHN-IU-2014-13769).

Solomon Islands. BOA 1 Stn CP2415, 15°44'S, 167°03'E, 420–670 m, 5 September 2005: 1 ov. F 6.3 mm (MNHN-IU-2014-13771).

Chesterfield Islands. EBISCO StnDW2629, 21°06'S, 160°46'E, 569–583 m, 21 October 2005: 1 M 6.0 mm (MNHN-IU-2014-13785).

Papua New Guinea. BIOPAPUA Stn DW3696, 01°54'S, 147°12'E, 326–355 m, 30 September 2010: 1 ov. F 4.1 mm (MNHN-IU-2011-3411).

Papua New Guinea. MADEEP Stn DW4268, 05°33'S, 153°59'E, 383–720 m, 27 April 2014: 1 specimen broken (MNHN-IU-2015-921).—Stn DW4274, 05°38'S, 153°56'E, 435–442 m, 27 April 2014: 1 M 7.8 mm (MNHN-IU-2015-912).

New Caledonia. KANADEEP Stn DW4989, 24°15'S, 166°58'E, 420–600 m, 13 September 2017: 1 M 6.9 mm (MNHN-IU-2017-2485).

Etymology. From the name *Pallas*, son of the King *Evander* in the *Aeneid*. The name is considered a substantive in apposition.

Description. *Carapace*: 1.2–1.3 × as long as broad. Mid-transverse ridge usually interrupted, preceded by deep cervical groove, followed by 6 or 7 interrupted transverse ridges. Lateral margins convex, with 4 spines: first spine anterolateral, well-developed; hepatic margin unarmed; 2 spines on anterior branchial margin variable in size (posterior spine smaller, rarely obsolescent), and spine on posterior branchial margin. Rostrum horizontal, dorsally flattish or slightly concave, 1.7–1.9 × as long as broad, length 0.3 × and breadth 0.2–0.3 × that of carapace; lateral margin minutely serrated.

Sternum: Sternite 3 moderately broad, 3.2–3.7 × as wide as long, anterolaterally strongly produced, anterior margin with shallow median notch flanked by 2 lobes. Sternite 4 narrowly contiguous to sternite 3; surface depressed in midline, smooth; greatest width 4.4 × that of sternite 3, and twice as wide as long.

Abdomen: Tergites 2–3 each with 2 elevated transverse ridges, tergite 4 with transverse ridge, tergites 5–6 smooth; tergite 6 with transverse posteromedian margin.

Eye: Ocular peduncle slightly longer than wide; cornea subglobular, maximum corneal diameter 0.8 × rostrum width, as wide as eyestalk.

Antennule: Article 1 with distomesial angle serrated; lateral margin serrated.

Antenna: Article 1 with strong distomesial spine overreaching end of article 2; article 2 with strong distomesial spine larger than distolateral spine and reaching or overreaching end of article 3; articles 3 and 4 unarmed.

Mxp3: Ischium as long as merus measured along extensor margin; flexor margin sharply ridged, terminating in well-developed spine; extensor margin unarmed; crista dentata finely denticulate; merus having flexor margin with strong median spine, extensor margin with well-developed distal spine.

P1: 2.5–3.5 (male), 2.2–2.7 (female) × carapace length, with numerous short striae, and covered by scales with uniramous long and short setae on merus to dactylus. Merus as long as carapace, 2.5 × as long as carpus, with strong mesial and distal spines, and scattered dorsal spines. Carpus 0.6 shorter than palm, 1.4 × as long as broad, dorsal surface with scattered spines, mesial and lateral margins with 2–4 strong spines. Palm, 1.7 × as long as broad, armed with spines in irregular longitudinal rows on mesial and lateral margins, dorsal surface unarmed. Fingers as long as palm; fixed finger with row of spines along lateral margin; movable finger with well-developed proximal mesial spine.

P2–4: Slender, somewhat compressed laterally, with short setiferous striae on dorsal surface, with numerous long and thick setae on ischium to dactylus. Meri successively shorter posteriorly (P3 merus 0.9 × length of P2 merus, P4 merus 0.7–0.8 × length of P3 merus). P2 merus 0.9 × carapace length, 8 × as long as broad, 1.2 × as long as P2 propodus; P3 merus 5.3 × as long as broad, 1.2 × as long as P3 propodus, P4 merus 4.2 × as long as broad, 1.3 × as long as P3 propodus; extensor margins with a row of 8–11 proximally diminishing spines on P2–4; lateral
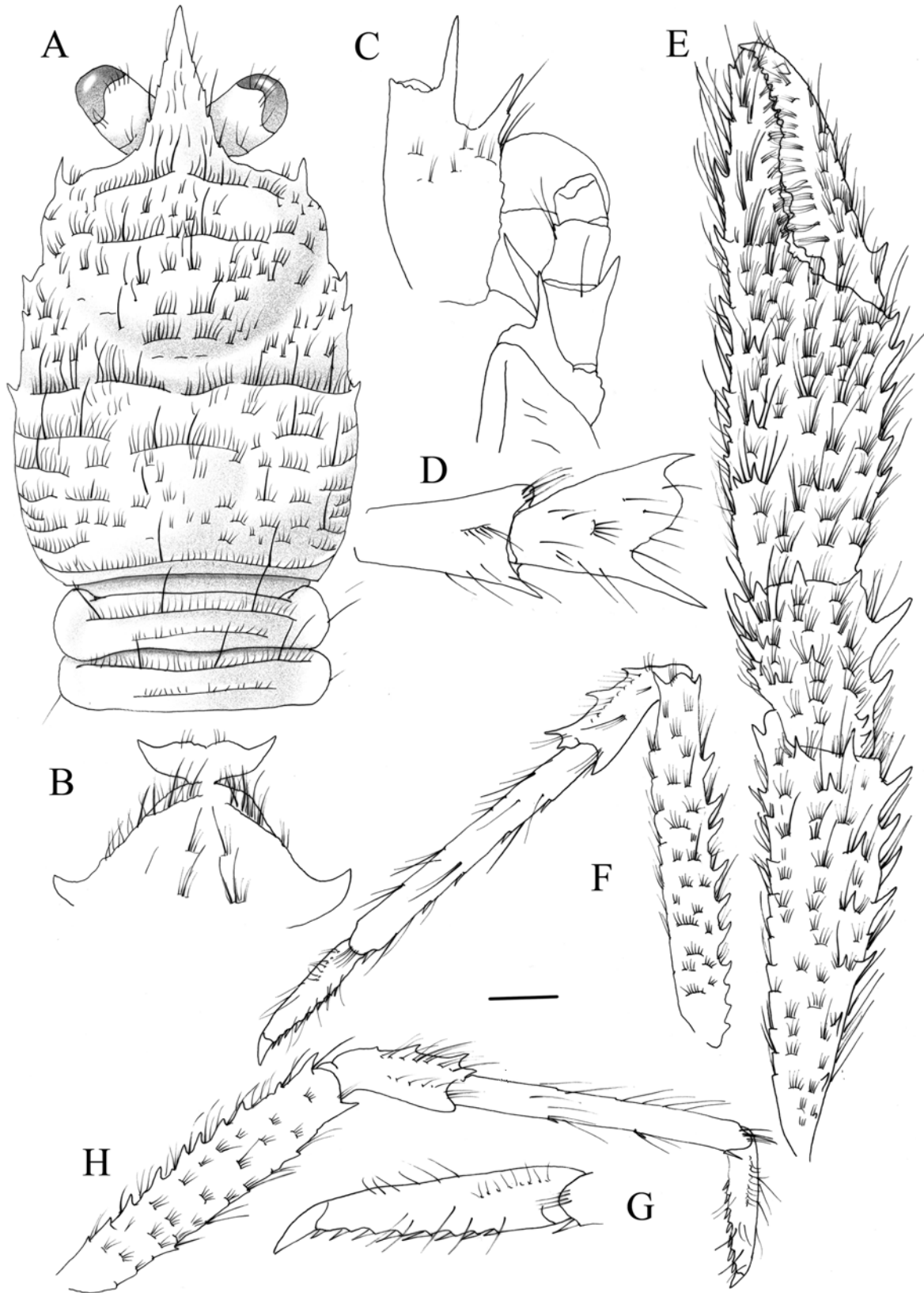
FIGURE 16. *Leiogalathea pallas* **n. sp.**, holotype, F 6.9 mm, Papua New Guinea (MNHN-IU-2014-13395). A, carapace and abdomen, dorsal view. B, sternites 3–4. C, cephalic region, showing antennular and antennal peduncles, ventral view. D, right Mxp3 ischium and merus, lateral view. E, left P1, dorsal view. F, left P2, lateral view. G, dactylus of left P2, lateral view. H, right P3, lateral view. Scales: A, E, F, H = 1.0 mm; B–D, G = 0.5 mm.

surface unarmed; flexor distal margin with well-developed distal spine and several additional projecting scales. Carpi with 2–4 spines on extensor margin on P2–4, smooth lateral side; flexor margin with small distal spine. Propodi 11.0–11.6 × as long as broad on P2–3, 8 × as long as broad on P4, flexor margin with 3–5 movable spinules. Dactyli slender, 0.5 × length of propodi; distal claw short, moderately curved; flexor margin nearly straight, with 7 or 8 small teeth along entire margin decreasing in size proximally, each with slender movable spinule, ultimate tooth closer to penultimate tooth than to base of distal claw.

Colour in life. Base colour reddish, orange to pale orange. Carapace and anterior half of abdomen reddish orange, posterior part of abdomen pale orange, occasionally translucent. P1 totally reddish orange, tip of spines on mesial margin white. P2–4 reddish orange, white at basis and at tips of dactyli.

Genetic data. COI and 16S (Table 2).

Distribution. New Caledonia, Vanuatu, Chesterfield Islands, Papua New Guinea, and Solomon Islands, from 163 to 720 m.

Remarks. *Leiogalathea pallas* belongs to the group of species having the hepatic margin of the carapace unarmed and the anterior branchial margin with 2 spines at most. This species is morphologically very similar to *L. sinon* from Tonga and Polynesia (see below, under the Remarks of that species).

Genetically, the closest species is *L. amata* from Wallis and Futuna and New Caledonia (genetic distance for COI and 16S: 4.1 and 1.4%, respectively) (Table 2). However, *L. pallas* is clearly distinguished from *L. amata* by the following characters: the rostral lateral margin is serrated instead of smooth and entire; the branchial margin of the carapace has 2 or 3 instead of 1 spine; the mesial spine on the antennal article 1 clearly overreaches instead of falling short of article 2; and the flexor margin of the P2–4 dactyli has 8 instead of 5 or 6 teeth.

Leiogalathea paris **n. sp.**
(Figs. 11F, 17, 21E)

Leiogalathea laevirostris.—Baba 1991: 487 (in part, specimens from French Polynesia only).—Poupin 1996: 20, 21 (fig. h).

Type material. *Holotype*: French Polynesia. TARASOC Stn DW3441, 16°43'S, 151°26'W, 350–360 m, 16 October 2009: ov. F 4.0 mm (MNHN-IU-2011-4471).

Paratypes: French Polynesia. MARARA Stn D25, 16°07'S, 145°49'W, 398 m, 7 June 1990: 1 M 4.7 mm (MNHN-IU-2014-13773); 1 M 5.1 mm (MNHN-IU-2014-13774).

Wallis and Futuna. MUSORSTOM 7 Stn DW582, 13°10.5'S, 176°14.1' W, 360 m, 22 May 1992: 1 M 4.6 mm (MNHN-IU-2014-13715).

New Caledonia. NORFOLK 2 Stn DW2024, 23°27.92'S, 167°50.90'E, 370–371 m, 21 October 2003: 1 M 2.6 mm (MNHN-IU-2014-13748).

Tonga. BORDAU 2 Stn DW1616, 23°04.22'S, 175°54.09'W, 664–781 m, 17 June 2000: 1 F 4.5 mm (MNHN-IU-2014-13714).

French Polynesia. TARASOC Stn DW3356, 15°57'S, 147°08'W, 490 m, 1 October 2009: 1 F 4.0 mm (MNHN-IU-2011-3926).—Stn DW3357, 15°57'S, 147°08'W, 480 m, 10 October 2009: 1 F 4.5 mm (MNHN-IU-2014-13718).—Stn DW3359, 15°57'S, 147°08'W, 462–980 m, 1 October 2009: 1 ov. F 4.3 mm (MNHN-IU-2011-4333).—Stn DW3367, 16°07'S, 146°22'W, 396–501 m, 3 October 2009: 1 M 5.0 mm (MNHN-IU-2014-13717).—Stn DW3369, 16°08'S, 146°24'W, 412–520 m, 3 October 2009: 1 M 4.3 mm (MNHN-IU-2014-13704).—Stn DW3484, 17°47'S, 149°23'W, 300–650 m, 23 October 2009: 1 M 5.2 mm (MNHN-IU-2014-13720).

Chesterfield Islands. EBISCO Stn DW2537, 22°18'S, 159°29'E, 990–990 m, 10 October 2005: 1 ov. F 4.2 mm (MNHN-IU-2014-13784).

New Caledonia. EXBODI Stn DW3922, 18°33'S, 164°21'E, 525–560 m, 26 September 2011: 1 F 5.4 mm (MNHN-IU-2013-1727).

Papua New Guinea. MADEEP Stn DW4314, 09°48'S, 151°33'E, 278–420 m, 3 May 2014: 1 M 2.0 mm (MNHN-IU-2015-296).

New Caledonia. KANADEEP Stn DW4921, 21°39'S, 162°42'E, 800–800 m, 1 September 2017: 1 F 2.7 mm (MNHN-IU-2017-3535).—Stn DW4962, 23°02'S, 159°28'E, 315–1260 m, 6 September 2017: 1 F 2.6 mm (MNHN-IU-2017-3834), 1 ov. F 3.4 mm, 1 F 3.3 mm (MNHN-IU-2017-2732).

Etymology. From the name *Paris,* a Trojan prince, son of *Priam* The name is considered a substantive in apposition.

Description. *Carapace*: 1.1–1.3 × as long as broad. Mid-transverse ridge usually medially interrupted, followed by rows of setae usually not situated on marked discernible ridges. Lateral margins straight and subparallel, with 1 anterolateral spine only; hepatic and branchial margins unarmed (rarely with a obsolescent spine on anterior branchial margin). Rostrum horizontal, dorsally flattish or slightly concave, 1.3–1.4 × as long as broad, length 0.3 × and breadth 0.2–0.3 × that of carapace; lateral margin with 4 or 5 rudimentary teeth, dorsal surface densely covered by long setae.

Sternum: Sternite 3 moderately broad, 2.8–3.0 × as wide as long, anterolaterally strongly produced, anterior margin serrated, straight, with a median shallow minute notch. Sternite 4 broadly contiguous to sternite 3; surface depressed in midline, smooth; greatest width 3 × that of sternite 3, 2.5 × as wide as long.

Abdomen: Tergites 2–3 each with 2 elevated transverse ridges, tergite 4 with transverse ridge, tergites 5–6 smooth; tergite 6 with transverse posteromedian margin.

Eye: Ocular peduncle as long as broad; cornea subglobular, maximum corneal diameter 0.7 × rostrum width, as wide as eyestalk.

Antennule: Article 1 with distomesial angle usually armed with 1 small spine; lateral margin smooth.

Antenna: Article 1 with distomesial spine overreaching end of article 2; article 2 with distomesial and distolateral spines, distolateral stouter, both not reaching end of article 3; articles 3 and 4 unarmed.

Mxp3: Ischium as long as merus measured along extensor margin; flexor margin sharply ridged, terminating in well-developed spine; extensor margin unarmed; crista dentata finely denticulate; merus flexor margin with strong median spine and with or without distal spine, extensor margin with distal spine.

P1: 2.5–3.2 (males), 1.8–2.5 (females) × carapace length, with numerous short striae, and densely covered by uniramous short and long setae on merus to dactylus. Merus 0.7 length of carapace, 2.1 × as long as carpus, with strong mesial and distal spines, and scattered dorsal spines. Carpus slightly shorter than palm, 1.6 × as long as broad, dorsal surface with scattered spines, mesial margin with 2 strong spines (distal smaller). Palm 2.1 × as long as broad, armed with spines in irregular longitudinal rows on mesial and lateral margins, dorsal surface unarmed. Fingers 1.3 × as long as palm; fixed finger unarmed; movable finger with proximal mesial spine.

P2–4: Stout, somewhat compressed laterally, with short setiferous striae on dorsal surface; with numerous long and thick setae on ischium to dactylus. Meri successively shorter posteriorly (P3 merus 0.8 × length of P2 merus, P4 merus 0.9 × length of P3 merus). P2 merus 0.7 × carapace length, 4.1 × as long as broad, 1.6 × as long as P2 propodus; P3 merus 4 × as long as broad, 1.5 × as long as P3 propodus; P4 merus 4 × as long as broad, 1.2 × as long as P4 propodus; extensor margins with row of 7–8 proximally diminishing spines on P2–3; unarmed on P4; lateral surface unarmed; flexor margin with well-developed distal spine and several additional projecting scales. Carpi with 2–4 spines on extensor margin on P2–3, unarmed on P4, lateral side smooth; flexor margin with small distal spine. Propodi 4.0–4.8 × as long as broad on P2–4, flexor margin with 4 or 5 movable spinules. Dactyli 0.5–0.6 × length of propodi; distal claw short, moderately curved; flexor margin nearly straight, with 6 or 7 small teeth along the entire margin decreasing in size proximally, each with slender movable spinule, ultimate tooth equidistant between base of distal claw and penultimate tooth.

Colour in life. Ground colour reddish, orange to pale. Carapace and anterior half of abdomen pale orange. P1 occasionally totally orange with orange red bands, tips of fingers whitish; P2–4 with orange or reddish bands.

Genetic data. COI and 16S (Table 2).

Distribution. Polynesia, Papua New Guinea, Wallis and Futuna, New Caledonia and Chesterfield Island, from 396 to 1260 m.

Remarks. *Leiogalathea paris* belongs to the group of species having the hepatic margin of the carapace unarmed, the branchial margin with or without a spine, and the lateral margin of the rostrum armed with 4 or 5 rudimentary teeth. This species is morphologically very similar to *L. juturna* from Indonesia and Taiwan, from which it is differentiated by the absence of marked discernible ridges on branchial regions and the anterior branchial margin unarmed instead of bearing a distinct spine. Furthermore, the flexor margin of Mxp3 merus occasionally has a small distal spine in *L. paris,* instead of being consistently unarmed. The genetic divergences between them are on average 7.2% (COI) and 1.4% (16S) (see also below, under the Remarks of *L. priam*).
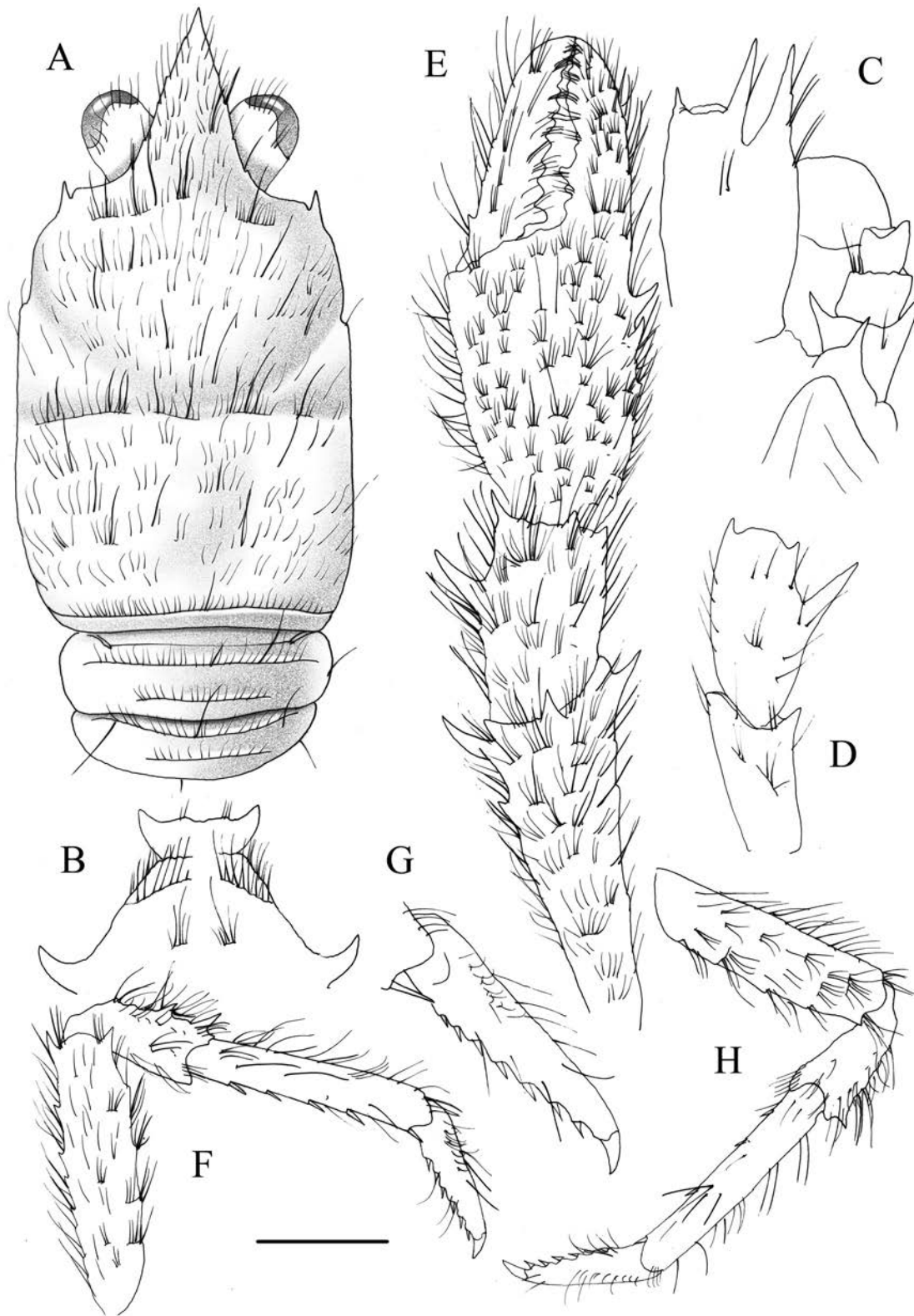
FIGURE 17. *Leiogalathea paris* **n. sp.**, holotype, ov. F 4.0 mm, French Polynesia (MNHN-IU-2011-4471). A, carapace and abdomen, dorsal view. B, sternites 3–4. C, cephalic region, showing antennular and antennal peduncles, ventral view. D, right Mxp3 ischium and merus, lateral view. E, right P1, dorsal view. F, right P2, lateral view. G, dactylus of right P2, lateral view. H, right P3, lateral view. Scales: A, E, F, H = 1.0 mm; B–D, G = 0.5 mm.

***Leiogalathea priam* n. sp.**
(Figs. 11G, 18, 21F)

Type material. *Holotype*: Papua New Guinea. MADEEP Stn DW4287, 09°12'S, 153°56'E, 340–375 m, 30 April 2014: M 5.0 mm (MNHN-IU-2014-13697).

Paratypes: Papua New Guinea. PAPUA NIUGINI DW3973, 04°34'S, 146°17'E, 411–430 m, 5 December 2012: 1 F 3.1 mm (MNHN-IU-2014-13793).—Stn DW3992, 06°03'S, 147°36'E, 450–480 m, 9 December 2012: 6 M 2.9–5.6 mm, 1 ov. F 3.6 mm, 2 F 3.9–4.2 mm (MNHN-IU-2017-2391).

Papua New Guinea. MADEEP Stn DW4285, 09°11'S, 153°55'E, 380–411 m, 30 April 2014: 1 M 5.2 mm (MNHN-IU-2015-212), 3 M 5.2–5.6 mm, 2 ov. F 4.8–5.2 mm, 2 F 3.4–3.8 mm (MNHN-IU-2014-9706), 1 ov. F 3.7 mm (MNHN-IU-2016-5797).—Stn DW4286, 09°12'S, 153°55'E, 306–365 m, 30 April 2014: 4 M 4.6–5.1 mm, 2 ov. F 5.1–6.6 mm (MNHN-IU-2014-18341), 9 M 3.4–5.3 mm, 12 ov. F 3.0–6.2 mm, 3 F 2.8–4.2 mm (MNHN-IU-2014-18573).—Stn DW4287, 09°12'S, 153°56'E, 340–375 m, 30 April 2014: 13 M 3.4–7.2 mm, 18 ov. F 3.2–6.1 mm, 1 F 4.3 mm (MNHN-IU-2014-9570), 1 M 4.5 mm, 1 ov. F 6.1 mm, 3 F 2.9–3.9 mm (MNHN-IU-2017-2396).—Stn DW4288, 09°12'S, 153°54'E, 504 m, 30 April 2014: 1 F 5.1 mm (MNHN-IU-2016-522), 1 ov. F 4.8 mm (MNHN-IU-2014-13792).—Stn DW4314, 09°48'S, 151°33'E, 278–420 m, 3 May 2014: 1 F 3.1 mm (MNHN-IU-2014-13696).

Etymology. From the name *Priam*, the king of Troy in the *Iliad*. The name is considered a substantive in apposition.

Description. *Carapace*: 1.1–1.3 × as long as broad. Mid-transverse ridge uninterrupted or medially interrupted, followed by 5 interrupted or scale-like transverse ridges. Lateral margins straight and subparallel, with 2 small spines: first spine anterolateral; second small spine on anterior branchial margin (sometimes obsolescent), hepatic and posterior branchial margin unarmed. Rostrum moderately slender, horizontal, dorsally flattish or slightly concave, 1.5 × as long as broad, length 0.3 × and breadth 0.2–0.3 × that of carapace; lateral margin serrated with 4 or 5 minute teeth.

Sternum: Sternite 3 moderately broad, 2.0–2.5 × as wide as long, anterolaterally produced, anterior margin serrated, straight, with a minute median shallow notch. Sternite 4 narrowly contiguous to sternite 3; surface depressed in midline, smooth; greatest width 3 × that of sternite 3, and 2.5 × as wide as long.

Abdomen: Tergites 2–3 each with 2 elevated transverse ridges, tergite 4 with transverse ridge, tergites 5–6 smooth; tergite 6 with transverse posteromedian margin.

Eye: Ocular peduncle slightly longer than wide; cornea subglobular, maximum corneal diameter 0.4 × rostrum width, as wide as eyestalk.

Antennule: Article 1 with distomesial angle serrated; lateral margin smooth.

Antenna: Article 1 with strong distomesial spine nearly reaching end of article 2; article 2 with strong distomesial spine much larger than distolateral, nearly reaching end of article 3; articles 3 and 4 unarmed.

Mxp3: Ischium as long as merus measured along extensor margin; flexor margin sharply ridged, terminating in small spine; extensor margin unarmed; crista dentata finely denticulate; merus having flexor margin with strong median spine, extensor margin with distal spine.

P1: 2.2–2.8 (males), 2.0–2.1 (females) × carapace length, densely covered with setiferous scales on merus to dactylus. Merus 0.7 length of carapace, 2.1 × as long as carpus, with strong mesial and distal spines, and scattered dorsal spines. Carpus slightly shorter than palm, 1.6 × as long as broad, dorsal surface with scattered spines, mesial margin with 2 spines (distal small), lateral margin with distal spine. Palm 2.1 × as long as broad, armed with spines in irregular longitudinal rows on mesial and lateral margins, dorsal surface unarmed. Fingers 1.3 × as long as palm; fixed finger usually unarmed or with several proximal spines along lateral margin; movable finger with well-developed proximal mesial spine.

P2–4: Stout, somewhat compressed laterally, with setiferous striae on dorsal surface, sparsely with long and thick setae on ischium to dactylus. Meri successively shorter posteriorly (P3 merus 0.9 × length of P2 merus, P4 merus 0.8 × length of P3 merus). P2 merus 0.6 × carapace length, 4.4 × as long as broad, 1.2 × as long as P2 propodus; P3 merus 4.2 × as long as broad, 1.2 × as long as P3 propodus; P4 merus 3.7 × as long as broad, as long as P4 propodus; extensor margins with row of 7 or 8 proximally diminishing spines on P2–3, unarmed on P4; lateral surface unarmed; flexor distal margin with well-developed distal spine and several additional projecting scales. Carpi with 2–4 spines on extensor margin on P2–3, unarmed on P4, lateral side smooth; flexor margin with

small dorsal spine. Propodi 5.0–5.8 × as long as broad on P2–4, flexor margin with 4–6 movable spinules. Dactyli 0.6–0.7 × length of propodi; distal claw short, moderately curved; flexor margin nearly straight, with 6 or 7 small teeth along the entire margin decreasing in size proximally, each with slender movable spinule, ultimate tooth closer to penultimate tooth than to base of distal claw.
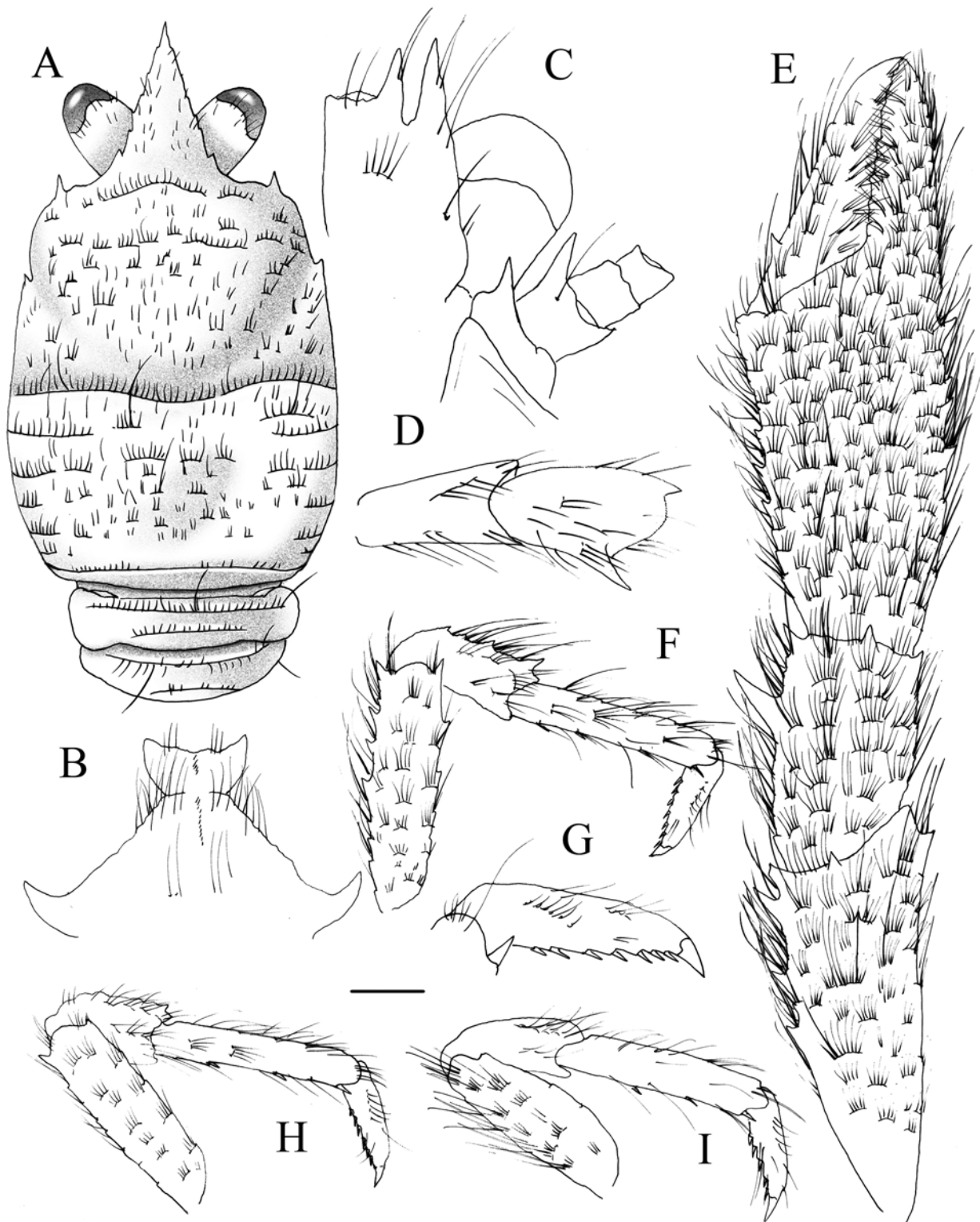
FIGURE 18. *Leiogalathea priam* **n. sp.**, holotype, M 5.0 mm, Papua New Guinea (MNHN-IU-2014-13697). A, carapace and abdomen, dorsal view. B, sternites 3–4. C, cephalic region, showing antennular and antennal peduncles, ventral view. D, right Mxp3 ischium and merus, lateral view. E, right P1, dorsal view. F, right P2, lateral view. G, dactylus of right P2, lateral view. H, right P3, lateral view. I, right P4, lateral view. Scales: A, E, F, H, I = 1.0 mm; B–D, G = 0.5 mm.

Colour in life. Ground colour reddish orange to pale yellow orange. Carapace and abdominal somites 2–3 orange, sparsely with whitish ridges, posterior part of abdomen translucent. P1 totally orange. P2–4 orange with whitish or pale orange bands, white to translucent at tips.

Distribution. Papua New Guinea, from 278 to 504 m.

Genetic data. COI and 16S (Table 2).

Remarks. *Leiogalathea priam* belongs to the group of species having the hepatic margin of the carapace unarmed, the branchial margin armed with at most one spine, and the margin of the rostrum armed with 4 or 5 minute teeth. This species is morphologically very close to *L. juturna* from Indonesia and Taiwan and *L. paris* from French Polynesia, Papua New Guinea and New Caledonia. However, these species can be distinguished by the following differences:

The dorsal surface of the branchial regions has rows of setae not situated on marked discernible ridges in *L. paris,* whereas these setose ridges are clearly marked in *L. juturna* and *L. priam*.

In *L. juturna* and *L. priam*, a spine on the anterior branchial margin of the carapace is consistently present, whereas this spine is usually absent in *L. paris*.

The sternite 3 is 3.3–4.0 × as wide as long in *L. juturna,* whereas this sternite is 2.0–2.5 × in *L. priam.*.

The species are clearly divergent genetically: *L. juturna* and *L. paris* diverge on average 7.2% for COI and 1.4 % for the 16S. *Leigalathea juturna* and *L. priam* present higher genetic differences: 10.3% for COI and 4.0% for 16S. *Leigalathea paris* and *L. priam* are also highly divergent for COI (9%) and 16S (4.7 %).

Leiogalathea sinon **n. sp.**
(Figs. 11H, 19)

Type material. *Holotype*: Tonga. BORDAU 2 Stn CP1539, 21°36.75'S, 175°19.37'W, 558–586 m, 5 June 2000: F 8.3 mm (MNHN-IU-2014-13711).

Paratype: French Polynesia. TARASOC Stn DW3435, 16°41'S, 151°02'W, 500–612 m, 15 October 2009: 1 M 3.2 mm (MNHN-IU-2014-13719).

Etymology. From the name *Sinon*, the Greek youth who persuades the Trojans to take in the wooden horse. The name is considered a substantive in apposition.

Description. Carapace: 1.2–1.3 × as long as broad. Mid-transverse ridge usually interrupted, preceded by deep cervical groove, followed by 6 or 7 laterally interrupted transverse ridges. Lateral margins slightly convex, with 4 distinct spines: first spine anterolateral, well-developed; hepatic margin unarmed; second and third spines on anterior branchial margin, and fourth spine on posterior branchial margin. Rostrum horizontal, dorsally flattish or slightly concave, 1.4–1.6 × as long as broad, length 0.3 × and breadth 0.2–0.3 × that of carapace; lateral margin with 6–8 rudimentary teeth.

Sternum: Sternite 3 broad, 3.0–3.5 × as wide as long, anterolaterally produced, anterior margin with shallow median notch flanked by 2 shallow denticulate lobes. Sternite 4 broadly contiguous to sternite 3; surface depressed in midline, smooth; greatest width 2.2 × that of sternite 3, 2.8 × as wide as long.

Abdomen: Tergite 2 with 2 elevated transverse ridges, tergites 3–4 each with transverse ridge, tergites 5–6 smooth; tergite 6 with transverse posteromedian margin.

Eye: Ocular peduncle, slightly longer than wide; cornea subglobular, maximum corneal diameter 0.8 × rostrum width, as wide as eyestalk.

Antennule: Article 1 with distomesial angle minutely serrated; lateral margin serrated.

Antenna: Article 1 with strong distomesial spine not reaching mid-length of article 2; article 2 with strong distomesial spine larger than distolateral and overreaching end of article 3; articles 3 and 4 unarmed.

Mxp3: Ischium as long as merus measured along extensor margin; flexor margin sharply ridged, terminating in well-developed spine; extensor margin unarmed; crista dentata finely denticulate; merus flexor margin with strong median spine and with or without distal spine, extensor margin with distal spine.

P1: 2.8 (male), 2.5 (female) × carapace length, with numerous short striae, and scattered uniramous long setae on merus to dactylus. Merus 0.7 length of carapace, 2.1 × as long as carpus, with strong mesial and distal spines, and scattered dorsal spines. Carpus slightly shorter than palm, 1.6 × as long as broad, dorsal surface with scattered spines, mesial margins with 3 or 4 strong spines (distal second strongest), lateral margin unarmed. Palm, 2.1 × as
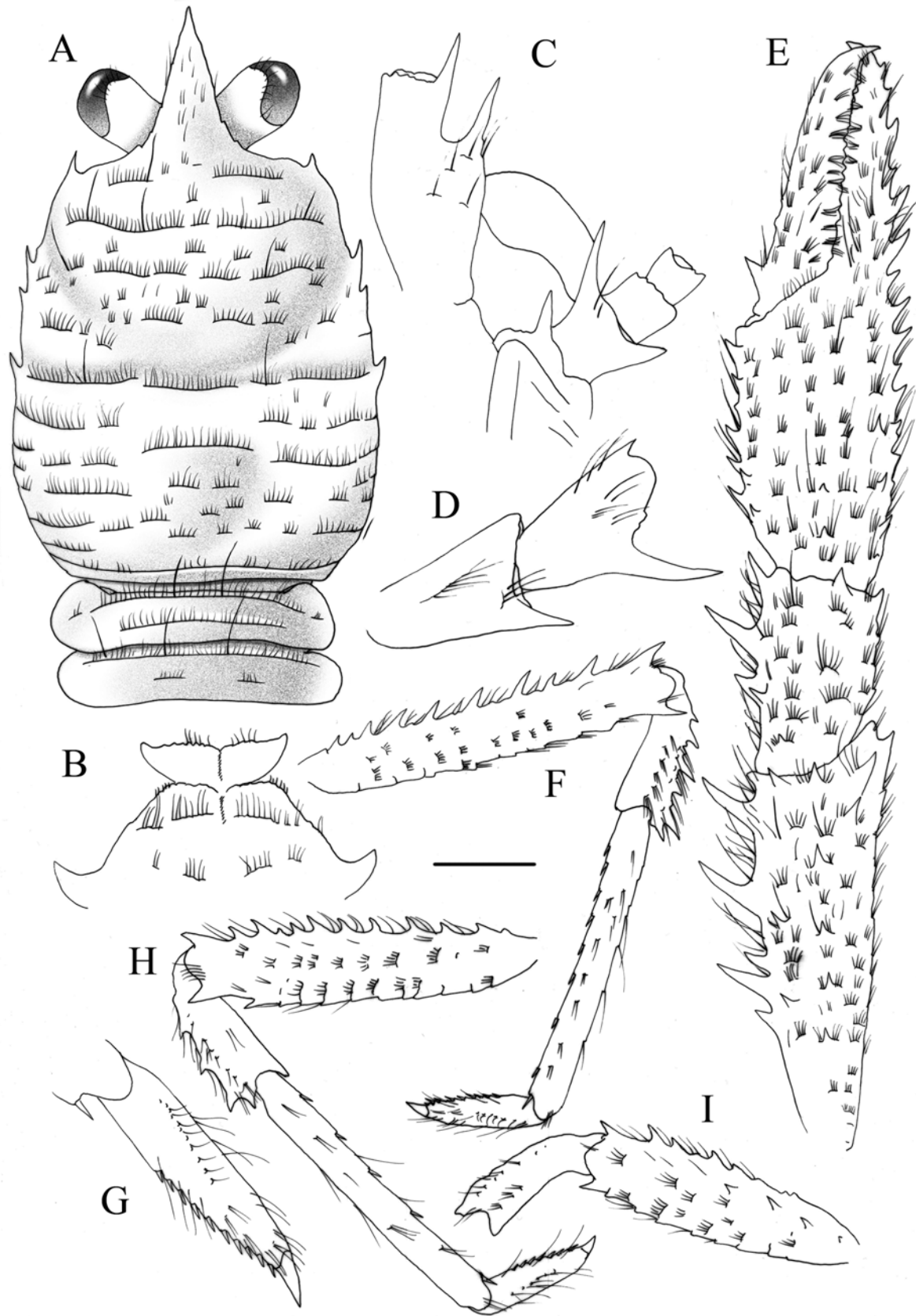
FIGURE 19. *Leiogalathea sinon* **n. sp.**, holotype, F 8.3 mm, Tonga (MNHN-IU-2014-13711). A, carapace and abdomen, dorsal view. B, sternites 3–4. C, cephalic region, showing antennular and antennal peduncles, ventral view. D, right Mxp3 ischium and merus, lateral view. E, right P1, dorsal view. F, right P2, lateral view. G, dactylus of right P2, lateral view. H, left P3, lateral view. I, left P4, lateral view. Scales: A, E, F, H, I = 2.0 mm; B–D, G = 1.0 mm.

long as broad, armed with spines in irregular longitudinal rows on mesial and lateral margins, dorsal surface unarmed. Fingers 1.3 × as long as palm; fixed finger with row of spines along lateral margin; movable finger with well-developed proximal mesial spine.

P2–4: Slender, somewhat compressed laterally, with short setiferous striae on dorsal surface; with sparse long and thick setae on ischium to dactylus. Meri successively shorter posteriorly (P3 merus 0.9 × length of P2 merus, P4 merus 0.9 × length of P3 merus). P2 merus 0.6 × carapace length, 7.2 × as long as broad, 1.2 × as long as P2 propodus; P3 merus 5.7 × as long as broad, 1.2 × as long as P3 propodus; P4 merus 5.6 × as long as broad, 1.3 × as long as P4 propodus; extensor margins with row of 9–12 proximally diminishing spines on P2–4; lateral surface unarmed on P2–3, with several dorso-extensor spines in P4; flexor margin with well-developed distal spine and several additional projecting scales. Carpi with 4–6 spines on extensor margin on P2–3, unarmed on P4, lateral side smooth; flexor margin with small distal spine. Propodi 9.4–11 × as long as broad on P2–4, flexor margin with 6–9 movable spinules on. Dactyli slender, 0.6–0.7 × length of propodi; distal claw short, moderately curved; flexor margin nearly straight, with 8–10 small teeth decreasing in size proximally, each with slender movable spinule, ultimate tooth closer to penultimate tooth than to base of distal claw.

Colour in life. Unknown

Genetic data. COI and 16S (Table 2).

Distribution. Tonga and Polynesia, from 500 to 612 m.

Remarks. *Leiogalathea sinon* belongs to the group of species having the hepatic margin of the carapace unarmed and the branchial margin armed with 3 spines. The species is morphologically very similar to *L. pallas* from New Caledonia, Papua New Guinea, Vanuatu, Chesterfield Islands and Solomon Islands. However, *L. sinon* can be distinguished from that species by following differences: *Leiogalathea pallas* has the lateral margin of the rostrum serrated, whereas this margin has 6–8 rudimentary teeth in *L. sinon*; the distomesial spine on the antennal article 1 overreaches the article 2 in *L. pallas,* whereas this spine barely reaches the article 2 in *L. sinon*; the anterior margin of sternite 4 is broadly contiguous with sternite 3 in *L. sinon,* and narrowly contiguous in *L. pallas*.

The two species are clearly different genetically, with the average divergence of 6.9% and 13% for 16S and COI respectively.

Leiogalathea turnus n. sp.
(Figs. 11I, 20)

Type material. *Holotype*: New Caledonia. NORFOLK 2 Stn DW2046, 23°43.87'S, 168°01.03'E, 333–375 m, 23 October 2003: M 8.0 mm (MNHN-IU-2014-13744).

Etymology. From the name *Turnus*, *Aeneas*'s major antagonist among mortals in the *Aeneid*. The name is considered a substantive in apposition.

Description. *Carapace*: 1.2 × as long as broad. Mid-transverse ridge interrupted, preceded by cervical groove, followed by 5 or 6 interrupted transverse ridges. Lateral margins convex, with 7 or 8 spines: first spine anterolateral, well-developed; spine on hepatic margin; 3 well-developed spines on anterior branchial margin decreasing in size posteriorly; and 2 or 3 spines on posterior branchial margin. Rostrum horizontal, dorsally flattish or slightly concave, 1.3–1.5 × as long as broad, length and breadth 0.3 × that of carapace; lateral margin with 3 teeth, decreasing in size distally, proximal tooth well-developed.

Sternum: Sternite 3 broad, 3.5 × as wide as long, anterolaterally produced, anterior margin minutely serrated, straight. Sternite 4 broadly contiguous to sternite 3; surface depressed in midline, smooth; greatest width 2.2 × that of sternite 3, twice as wide as long.

Abdomen: Tergites 2–3 each with 2 elevated transverse ridges, tergite 4 with 1 transverse ridge, tergites 5–6 smooth; tergite 6 with transverse posteromedian margin.

Eye: Ocular peduncle slightly longer than wide; cornea subglobular, maximum corneal diameter 0.4 × rostrum width, cornea as broad as eyestalk.

Antennule: Article 1 with distomesial angle minutely serrated; lateral margin smooth.

Antenna: Article 1 with small distomesial spine not reaching end of article 2; article 2 with strong distomesial spine, longer than distolateral spine and reaching end of article 3; articles 3 and 4 unarmed.

FIGURE 20. *Leiogalathea turnus* **n. sp.**, holotype, M 8.0 mm, New Caledonia (MNHN-IU-2014-13744). A, carapace and abdomen, dorsal view. B, Sternites 3–4. C, cephalic region, showing antennular and antennal peduncles, ventral view. D, right Mxp3 ischium and merus, lateral view. E, right P1, dorsal view. F, right P2, lateral view. G, dactylus of right P2, lateral view. H, left P3, lateral view. I, right P4, lateral view. Scales: A, E, F, H, I = 1.0 mm; B–D, G = 0.5 mm.
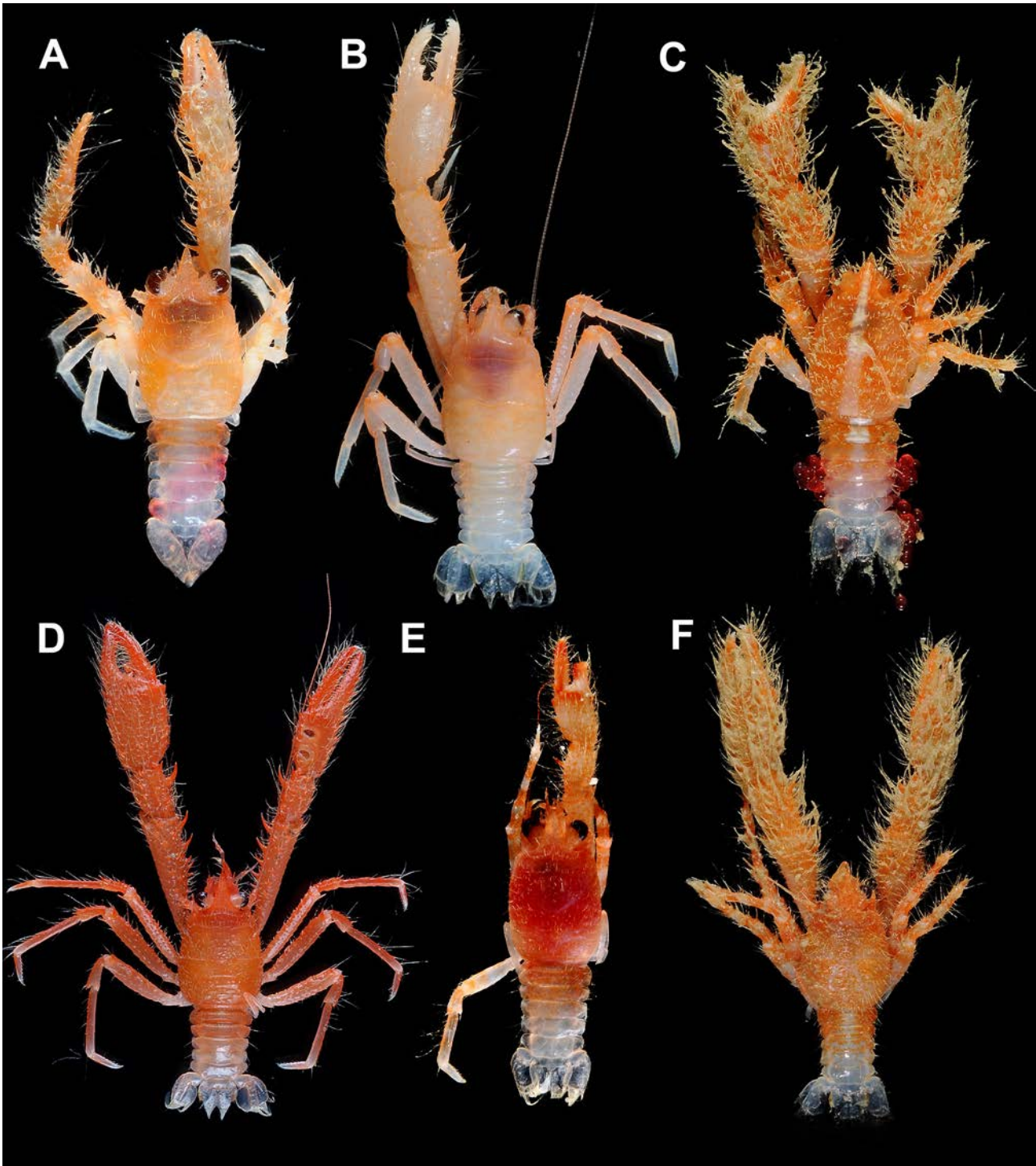
FIGURE 21. A, *Leiogalathea achates* **n. sp.**, holotype, ovigerous female 3.6 mm (MNHN-IU-2016-7125), Mayotte-Glorieuses islands. B, *Leiogalathea agassizii*, male 6.7 mm (MNHN-IU-2013-18858), Guadeloupe Island. C, *Leiogalathea evander* **n. sp.***,* male 5.9 mm (MNHN-IU-2015-146), Papua New Guinea. D, *Leiogalathea pallas* **n. sp.**, male 8.3 mm (MNHN-IU-2014-13775), Vanuatu. E, *Leiogalathea paris* **n. sp.**, female 5.4 mm (MNHN-IU-2013-1727), New Caledonia. F, *Leiogalathea priam* **n. sp.**, male 5.2 mm (MNHN-IU-2015-212), Papua New Guinea. Dorsal view.

Mxp3: Ischium as long as merus measured along extensor margin; flexor margin sharply ridged, terminating in well-developed spine; extensor margin unarmed; crista dentata finely denticulate; merus having flexor margin with strong median spine and with or without minute distal spine, extensor margin with strong distal spine.

P1: 2.5 × carapace length, with numerous short striae, and uniramous setae scattered on merus to dactylus. Merus slightly shorter than carapace, 2.2 × as long as carpus, with strong mesial and distal spines, and scattered

dorsal spines. Carpus 0.8 as long as palm, 1.8 × as long as broad, dorsal surface with scattered spines, mesial and lateral margins with 2 or 3 spines. Palm, 1.8 × as long as broad, armed with spines in irregular longitudinal rows on mesial and lateral margins, dorsal surface unarmed. Fingers 1.3 × as long as palm; fixed finger with row of spines along lateral margin; movable finger with proximal mesial spine.

P2–4: Slender, somewhat compressed laterally, with short setiferous striae on dorsal surface; ischium to dactylus sparsely with long and thick setae. Meri successively shorter posteriorly (P3 merus as long as P2 merus, P4 merus 0.9 × length of P3 merus). P2 merus 0.8 × carapace length, 5.1 × as long as broad, 1.1 × as long as P2 propodus; P3 merus 5.3 × as long as broad, 1.1 × as long as P3 propodus; P4 merus 7 × as long as broad, 1.2 × as long as P4 propodus; extensor margins with row of 8 or 9 proximally diminishing spines on P2–4; lateral surface unarmed; flexor margin with well-developed distal spine and several additional spines or projecting scales. Carpi with 2–4 well-developed spines on extensor margin on P2–4, lateral side smooth; flexor margin with small distal spine. Propodi 7.9–9.6 × as long as broad on P2–4, flexor margin with 3–5 movable spinules. Dactyli 0.4–0.5 × length of propodi; distal claw short, strongly curved; flexor margin nearly straight, with 7 or 8 small teeth decreasing in size proximally, each with slender movable spinule, ultimate tooth closer to distal claw than to penultimate tooth.

Colour in life. Unknown.

Genetic data. COI and 16S (Table 2).

Distribution. New Caledonia, from 333 to 375 m.

Remarks. *Leiogalathea turnus* belongs to the group of the species having the hepatic margin of the carapace armed with one spine. This species is morphologically related to *L. dido* also from New Caledonia and adjacent waters, with a relatively small genetic divergence, 3.5% and 0.3% for COI and 16S, respectively. However, the two species are morphologically different, largely in the following particulars: in *L. dido*, the cornea is clearly narrower than the peduncle rather than being as equally wide, the P1 fingers are unarmed instead of bearing spines along their lateral and mesial margins, the P2–4 propodi are broader (the length-breadth ratio, 5.5–6.5 versus 7.6–9.6), the P4 merus is unarmed instead of bearing spines along extensor and flexor margins, and the rostrum is proportionally narrower (the length-breadth ratio, 1.1–1.2 versus 1.5).

Conclusions

The results confirm the validity of subtle morphological characters to distinguish species of the genus *Leiogalathea*, as observed in other genera of squat lobsters, e.g. *Raymunida* (Macpherson & Machordom 2001; Lin *et al.* 2004), *Munida* (Macpherson *et al.* 2017a,b), *Allogalathea* (Cabezas *et al.* 2011), *Paramunida* (Cabezas *et al.* 2010; McCallum *et al.* 2016), *Fennerogalathea* (Rodríguez-Flores *et al.* 2017) and *Galathea* (Macpherson & Robainas-Barcia 2015). The present study illustrates the need to combine different sources of information when morphological characters are not clear. Molecular data provide a complementary approach to discriminate species separated by subtle morphological characters (Mathews *et al.* 2002; Goetze 2003).

We have been very cautious dealing with the assignment of species within the genus *Leiogalathea*. These species are morphologically conservative, without a great amount of morphological variation among them, which made delimitation and diagnosis of each species difficult. We also found intraspecific variability for some species in the number and size of the spines on the anterior (*L. paris*, *L. ascanius*) and posterior branchial margin (*L. achates* and *L. imperialis*).

In addition, some previous identifications, e.g. those from the Lord Howe Rise and New Zealand (Ahyong 2007; Yaldwyn & Webber 2011) require confirmation because they do not appear to match any species analysed in the present study and might belong to new species. Similarly, *Galathea paucilineata* Benedict, 1902, from the Galapagos Islands could belong to *Leiogalathea* based on the type description and illustration. More material from the area would be necessary to solve the taxonomic status of this species.

The molecular divergence ranges between closely related species are similar or even larger to those observed for other species of squat lobsters (Machordom & Macpherson 2004; Macpherson & Machordom 2005) and for other decapod taxa (e.g., Tong *et al.* 2000; Puillandre *et al.* 2011). Most species pairs have divergences larger than 6% for 16S rRNA and 11% for COI, with a very low intraspecific divergence in all species, even in those with a wide distribution (see Table 2). For instance, *L. juturna* from Taiwan and Kei Islands diverge only 1.1 % for the

COI gene; *L. paris* from French Polynesia, New Caledonia and Papua New Guinea and *L. evander* from the Marquesas Islands, Papua New Guinea and Philippines diverge only 0.3–0.5% for the same marker (Table 2). The smallest interspecific genetic divergences were observed between *L. dido* and *L. turnus* (0.3% for 16S rRNA and 3.5% for COI) and between *L. evander* and *L. achates* (0.8% for 16S rRNA and 4.4% for COI). However, these two pairs of species can be clearly differentiated from each other by several constant morphological characters. Therefore, we have considered all of them as distinct species.

Our results highlight the importance of the subtle morphological differences mentioned by Baba (1991) for this genus. Characters describing the spinulation of the rostrum, the number of spines along the lateral margins of the carapace, and relative length of P2–4 have greatly helped to resolve to the taxonomy of *Leiogalathea*. The morphological differences detected here among the different species are subtle, but constant in all the specimens examined. On the other hand, the genetic divergences are, in general, very large in the two genes here analysed. Including the descriptions given above, the genus *Leiogalathea* now contains 18 species. The existence of more species is likely and a more detailed study designed to fill in distribution range gaps, and including more specimens, is recommended.

References

Ahyong, S.T. (2007) Decapod Crustacea collected by the NORFANZ expedition: Galatheidae and Polychelidae. *Zootaxa*, 1593, 1–54.

Ahyong, S.T., Schnabel, K.E. & Maas, E. (2009) Anomuran phylogeny: new insights from molecular data. *In*: Martin, J.W., Crandall, K.A. & Felder, D.L. (Eds.), *Decapod Crustacean Phylogenetics. Crustacean Issues. Vol. 18*. CRC Press, Boca Raton, Florida, pp. 399–414.
https://doi.org/10.1201/9781420092592-c20

Ahyong, S.T., Baba, K., Macpherson, E. & Poore, G.C.B. (2010) A new classification of the Galatheoidea (Crustacea: Decapoda: Anomura). *Zootaxa*, 2676 (1), 57–68.
https://doi.org/10.11646/zootaxa.2676.1.4

Ahyong, S.T., Andreakis, N. & Taylor, J. (2011) Mitochondrial phylogeny of the deep-sea squat lobsters, Munidopsidae (Galatheoidea). *Zoologischer Anzeiger-A Journal of Comparative Zoology*, 250, 367–377.
https://doi.org/10.1016/j.jcz.2011.06.005

Balss, H. (1913) Neue Galatheiden aus der Ausbeute der deutschen Tiefsee-Expedition. 'Valdivia'. *Zoologischer Anzeiger*, 41, 221–226.

Baba, K. (1969) Four new genera with their representatives and six new species of the Galatheidae in the collection of the Zoological Laboratory, Kyushu University, with redefinition of the genus *Galathea*, *Ohmu*, 2, 1–32.

Baba, K. (1990) Chirostylid and galatheid crustaceans of Madagascar (Decapoda, Anomura). *Bulletin du Muséum National d'Histoire Naturelle, Paris*, 4e Série, Section A, 11, 921–975.

Baba, K. (1991) Crustacea Decapoda: *Alainius* gen. nov., *Leiogalathea* Baba, 1969, and *Phylladiorhynchus* Baba, 1969 (Galatheidae) from New Caledonia. *In*: Crosnier, A. (Ed.), Résultats des Campagnes MUSORSTOM. Vol. 9. *Mémoires du*

Muséum National d'Histoire Naturelle, Paris, (A), pp. 152, 479–491.

Baba, K. (2005) Deep-sea chirostylid and galatheid crustaceans (Decapoda: Anomura) from the Indo-West Pacific, with a list of species. *Galathea Reports*, 20, 1–317.

Baba, K., Macpherson, E., Poore, G.C.B., Ahyong, S.T., Bermudez, A., Cabezas, P., Lin, C.W., Nizinski, M., Rodrigues, C. & Schnabel, K.E. (2008) Catalogue of squat lobsters of the world (Crustacea: Decapoda: Anomura—families Chirostylidae, Galatheidae and Kiwaidae). *Zootaxa*, 1905, 1–220.

Baba, K., Macpherson, E., Lin, C.W. & Chan, T.-Y. (2009) *Crustacean Fauna of Taiwan: squat lobsters (Chirostylidae and Galatheidae)*. National Science Council, Taipei, ix + 312 pp

Baba, K, Ahyong, S.T. & Macpherson, E. (2011) Chapter 1. Morphology of the marine squat lobsters. *In*: Poore, G.C.B., Ahyong, S.T. & Taylor, J. (Eds.), *The biology of squat lobsters*. CSIRO Publishing, Melbourne, pp. 1–37. [also published as *Crustacean Issues. Vol. 20*. CRC Press, Boca Raton]

Benedict, J.E. (1902) Description of a new genus and forty-six new species of crustaceans of the family Galatheidae with a list of the known marine species. *Proceedings of the Biological Society of Washington*, 26, 243–334.

Bouvier, E.L. (1922) Observations complémentaires sur les crustacés décapodes (Abstraction faite des Caridés) provenant des Campagnes de S.A.S. le Prince de Monaco. *Résultats des Campagnes Scientifiques accomplis sur son Yacht par Albert Ier Prince Souverain de Monaco*, 62, 1–106, pls. 1–6.

Cabezas, P., Macpherson, E. & Machordom, A. (2010) Taxonomic revision of the genus *Paramunida* Baba, 1988 (Crustacea: Decapoda: Galatheidae): a morphological and molecular approach. *Zootaxa*, 2712 (1), 1–60.
https://doi.org/10.11646/zootaxa.2712.1.1

Cabezas, P., Macpherson, E. & Machordom, A. (2011) *Allogalathea* (Decapoda: Galatheidae): a monospecific genus of squat lobster? *Zoological Journal of the Linnean Society*, 162, 245–270.
https://doi.org/10.1111/j.1096-3642.2010.00681.x

Chace, F.A. (1942) The Anomura Crustacea. I. Galatheidea. Reports of the scientific results of the Atlantis Expeditions to the West Indies, under the joint auspices of the University of Havana and Harvard University. *Torreia*, 11, 1–106.

Crandall, K.A. & Fitzpatrick, J.F. Jr. (1996) Crayfish molecular systematics: using a combination of procedures to estimate phylogeny. *Systematic Biology*, 45, 1–26.
https://doi.org/10.1093/sysbio/45.1.1

d'Udekem d'Acoz, C.D. (1999) *Inventaire et distribution des crustacés décapodes de l'Atlantique nord-oriental, de la Méditerranée et des eaux continentales adjacentes au nord de 25°N. Patrimoines naturels (M.N.H.N./S.P.N.)*, 40, 1–383.

Doflein, F. & Balss, H. (1913) Die Galatheiden der Deutschen Tiefsee-Expedition. *Wissenschaftliche Ergebnisse der Deutschen Tiefsee-Expedition auf dem Dampfer "Valdivia" 1898–1899*, 20, 125–184, pls 12–17.

Folmer, O., Black, M., Hoeh, W., Lutz, R., Vrijenhoek, R. (1994) DNA primers for amplification of mitochondrial cytochrome c oxidase subunit I from diverse metazoan invertebrates. *Molecular Marine Biology and Biotechnology*, 3, 294–299.

Goetze, E. (2003) Cryptic speciation on the high seas; global phylogenetics of the copepod family Eucalanidae. *Proceedings of the Royal Society of London*, Serie A, 370, 2321–2331.
https://doi.org/10.1098/rspb.2003.2505

Katoh, K., Misawa, K., Kuma, K.I. & Miyata, T. (2002) MAFFT: a novel method for rapid multiple sequence alignment based on fast Fourier transform. *Nucleic acids research*, 30 (14), 3059–3066.
https://doi.org/10.1093/nar/gkf436

Kumar, S., Stecher, G. & Tamura, K. (2016) MEGA7: Molecular Evolutionary Genetics Analysis version 7.0 for bigger datasets. *Molecular Biology and Evolution*, 33, 1870–1874.
https://doi.org/10.1093/molbev/msw054

Laurie, R.D. (1926) Reports of the Percy Sladen Trust Expedition to the Indian Ocean in 1905, under the leadership of Mr. J. Stanley Gardiner, M.A. Vol. 8. No. VI. Anomura collected by Mr. J. Stanley Gardiner in the western Indian Ocean in H.M.S. Sealark. *Transactions of the Zoological Society of London*, Series 2 (Zoology), 19, 121–167, pls 8, 9.

Lin, C.W., Chan, T.Y. & Chu, K.H. (2004) A new squat lobster of the genus *Raymunida* (Decapoda: Galatheidae) from Taiwan. *Journal of Crustacean Biology*, 24, 149–156.
https://doi.org/10.1651/C-2432

Machordom, A., Araujo, R., Erpenbeck, D., Ramos, M.Á. (2003) Phylogeography and conservation genetics of endangered European Margaritiferidae (Bivalvia: Unionoidea). *Biological Journal of the Linnean Society*, 78, 235–252.
https://doi.org/10.1046/j.1095-8312.2003.00158.x

Machordom, A. & Macpherson, E. (2004) Rapid radiation and cryptic speciation in galatheid crabs of the genus *Munida* and related genera in the South West Pacific: molecular and morphological evidence. *Molecular Phylogenetics and Evolution*, 33, 259–279.
https://doi.org/10.1016/j.ympev.2004.06.001

Macpherson, E. & Baba, K. (2011) Chapter 2. Taxonomy of squat lobsters. *In*: Poore, G.C.B., Ahyong, S.T. & Taylor, J. (Eds.), *The biology of squat lobsters*. CSIRO Publishing, Melbourne, pp. 39–71. [also published as *Crustacean Issues. Vol. 20*. CRC Press, Boca Raton]

Macpherson, E. & Machordom, A. (2001) Phylogenetic relationships of species of *Raymunida* (Decapoda: Galatheidae) based on morphology and mitochondrial cytochrome oxidase sequences, with the recognition of four new species. *Journal of Crustacean Biology*, 21, 696–714.

https://doi.org/10.1163/20021975-99990168

Macpherson, E. & Machordom, A. (2005) Use of morphological and molecular data to identify three new sibling species of the genus *Munida* Leach, 1820 (Crustacea, Decapoda, Galatheidae) from New Caledonia. *Journal of Natural History*, 39, 819–834.
https://doi.org/10.1080/00222930400002473

Macpherson, E. & Robainas-Barcia, A. (2015) Species of the genus *Galathea* Fabricius, 1793 (Crustacea, Decapoda, Galatheidae) from the Indian and Pacific Oceans, with descriptions of 92 new species. *Zootaxa*, 3913 (1), 1–335.
https://doi.org/10.11646/zootaxa.3913.1.1

Macpherson, E., Rodríguez-Flores, P.C. & Machordom, A. (2017a) New sibling species and new occurrences of squat lobsters (Crustacea, Decapoda) from the western Indian Ocean. *European Journal of Taxonomy*, 343, 1–61.
https://doi.org/10.5852/ejt.2017.343

Macpherson, E., Beuck, L., Roder, C. & Voolstra, C.R. (2017b) A new species of squat lobster of the genus *Munida* (Galatheoidea, Munididae) from the Red Sea. *Crustaceana*, 90, 1005–1014.
https://doi.org/10.1163/15685403-00003584

Mathews, L.M., Schubart, C.D., Neigel, J.E. & Felder, D.L. (2002) Genetic, ecological, and behavioural divergence between two sibling snapping shrimp species (Crustacea: Decapoda: *Alpheus*). *Molecular Ecology*, 11, 1427–1437.
https://doi.org/10.1046/j.1365-294X.2002.01539.x

McCallum, A.W., Cabezas, P. & Andreakis, N. (2016) Deep-sea squat lobsters of the genus *Paramunida* Baba, 1988 (Crustacea: Decapoda: Munididae) from north-western Australia: new records and description of three new species. *Zootaxa*, 4173, 201–224.
http://doi.org/10.11646/zootaxa.4173.3.1

Milne Edwards, A. (1880) Reports on the results of dredging under the supervision of Alexander Agassiz, in the Gulf of Mexico and in the Caribbean Sea, etc. VIII. Études préliminaires sur les Crustacés. *Bulletin of the Museum of Comparative Zoology at Harvard College*, 8, 1–168, pls. 1, 2.

Milne Edwards, A. & Bouvier, E.L. (1894) Considérations générales sur la famille des Galathéidés. *Annales des Sciences Naturelles*, Zoologie, Series 7, 16, 191–327.

Milne Edwards, A. & Bouvier, E.L. (1897) Reports on the results of dredging, under the supervision of Alexander Agassiz, in the Gulf of Mexico (1877–78), in the Caribbean Sea (1878–79), and along the Atlantic coast of the United States (1880), by the U. S. Coast Survey steamer "Blake," Lieut.-Com. C.D. Sigsbee, U.S.N., and Commander J.R. Bartlett, U.S.N., commanding. XXXV: Description des Crustacés de la Famille des Galathéidés recueilli spendant l'expédition. *Memoirs of the Museum of Comparative Zoology at Harvard College*, 19, 5–141.

Milne Edwards, A. & Bouvier, E.L. (1900) Crustacés Décapodes. Première partie. Brachyoures et Anomoures. *Expéditions scientifiques du Travailleur et du Talisman*, 1880–1883, 1–396, 32 pls.

Miyake, S. & Baba, K. (1967) New and rare species of the family Galatheidae (Crustacea, Anomura) from the Sagami Bay in the collection of the Biological Laboratory, Imperial Household, Japan. *Journal of the Faculty of Agriculture, Kyushu University*, 14, 213–224.

Ortmann, A.E. (1898–1901) Crustacea (Zweite Hälfte: Malacostraca). *In:* Gerstaecker, A. (Ed.), *Die Klassen und Ordnungender Arthropoden wissenschaftlich dargestellt in Wort und Bild 5. Abtheilung 2*. C.F. Winter'sche Verlagshand-lung,Leipzig, pp. i–viii + 1–1319, pls. 1–128.

Palumbi, S.R., Martin, A.P., Romano, S., McMillan, W.O., Stice, L. & Grabowski, G. (1991) *The simple fool's guide to PCR*. Special Publishing Department of Zoology, University of Hawaii, Honolulu, 43 pp.

Poupin, J. (1996) *Atlas des crustacés marins profonds de Polynésie Française Récoltés du navire Marara (1986/1996)*. Service Mixte de Surveillance Radiologique et Biologique, Montlhéry, 59 pp.

Poupin, J. & Corbari, L. (2016) A preliminary assessment of the deep-sea Decapoda collected during the KARUBENTHOS 2015 Expedition to Guadeloupe Island. *Zootaxa*, 4190 (1), 1–107.
https://doi.org/10.11646/zootaxa.4190.1.1

Puillandre, N., Macpherson, E., Lambourdière, J., Cruaud, C., Boisselier-Dubayle, M.C. & Samadi, S. (2011) Barcoding type-specimens helps to reliably link species names to molecular taxonomic units in *Eumunida* Smith, 1883 (Decapoda, Eumunididae). *Invertebrate Systematics*, 25, 322–333.
https://doi.org/10.1071/IS11022

Richer de Forges, B., Chan, T.-Y., Corbari, L., Lemaitre, R., Macpherson, E., Ahyong, S.T. & Ng, P.K.L. (2013) The MUSORSTOM-TDSB deep-sea benthos exploration program (1976–2012): An overview of crustacean discoveries and new perspectives on deep-sea zoology and biogeography. *In*: Ahyong, S.T., Chan, T.-Y., Corbari, L. & Ng, P.K.L. (Eds.), Tropical Deep-Sea Benthos 27. *Mémoires du Muséum national d'Histoire naturelle*, 204, pp. 13–66.

Rodríguez-Flores, P.C., Machordom, A. & Macpherson, E. (2017) Three new species of squat lobsters of the genus *Fennerogalathea* Baba, 1988 (Decapoda: Galatheidae) from the Pacific Ocean. *Zootaxa*, 4276 (1), 46–60.
https://doi.org/10.11646/zootaxa.4276.1.2

Rowden, A.A., Schnabel, K.E., Schlacher, T.A., Macpherson, E., Ahyong, S.T. & Richer de Forges, B. (2010) Squat lobster assemblages on seamounts differ from some, but not all, deep-sea habitats of comparable depth. *Marine Ecology*, 31 (Supplement 1), 63–83.
https://doi.org/10.1111/j.1439-0485.2010.00374.x

Schnabel, K.E., Ahyong, S.T. & Maas, E.W. (2011) Galatheoidea are not monophyletic— molecular and morphological phylogeny of the squat lobsters (Decapoda: Anomura) with recognition of a new superfamily. *Molecular Phylogenetics and Evolution*, 58, 157–168.
https://doi.org/10.1016/j.ympev.2010.11.011

Tong, J.G., Chan, T.-Y. & Chu, K.H. (2000) A preliminary phylogenetic analysis of *Metapenaeopsis* (Decapoda: Penaeidae) based on mitochondrial DNA sequences of selected species from the Indo-West Pacific. *Journal of Crustacean Biology*, 20, 541–549.
https://doi.org/10.1163/20021975-99990070

Yaldwyn, J.C. & Webber, W.R. (2011) Annotated checklist of New Zealand Decapoda (Arthropoda: Crustacea). *Tuhinga*, 22, 171–272.

Whiteaves, J.F. (1874) On recent deep-sea dredging operations in the Gulf of St. Lawrence. *American Journal of Science*, Series 3, 7, 210–219.

Revision of the squat lobsters of the genus *Phylladiorhynchus* Baba, 1969 (Crustacea, Decapoda, Galatheidae) with the description of 41 new species

Paula C. Rodríguez-Flores[1,2*], Enrique Macpherson[1,3] & Annie Machordom[2.4]

[1] *Centre d'Estudis Avançats de Blanes (CEAB-CSIC), C. acc. Cala Sant Francesc 14 17300 Blanes, Girona, Spain*

[2] *Museo Nacional de Ciencias Naturales (MNCN-CSIC), José Gutiérrez Abascal, 2, 28006 Madrid, Spain*

[3]*macpherson@ceab.csic.es; https://orcid.org/0000-0003-4849-4532*

[4]*annie@mncn.csic.es; https://orcid.org/0000-0003-0341-0809*

*Corresponding author. paularodriguezflores@gmail.com; https://orcid.org/0000-0003-1555-9598

Abstract

The genus *Phylladiorhynchus* Baba, 1969 currently contains 11 recognized species, all occurring in the shallow waters and continental shelf of the Indian and Pacific oceans. Recent expeditions of these oceans have resulted in the collection of numerous new specimens in need of revision. We have revised this material using an integrative approach that analyses both morphological and molecular (COI and 16S) characters. We describe 41 new species and resurrect three old names: *P. integrus* (Benedict, 1902) and *P. lenzi* (Rathbun, 1907), previously synonymized with *P. pusillus* (Henderson, 1885), and *P. serrirostris* (Melin, 1939), previously synonymized with *P. integrirostris* (Dana, 1852). All species of the genus are described and illustrated. Some species are barely discernible on the basis of morphological characters but are highly divergent genetically. *Phylladiorhynchus* species are mainly distinguishable by the number of epigastric spines and lateral spines of the carapace, the shape and the armature of the rostrum, the number and pattern of the ridges on the carapace and abdomen, the shape of thoracic sternite 3 and the armature of the P2–4 dactyli. A dichotomous identification key to all species is provided.

Key words: Mitochondrial markers, diversity, taxonomy, systematics, Galatheoidea, Anomura, Decapoda, Indian Ocean, Pacific Ocean

Introduction

The genus *Phylladiorhynchus* was originally described by Baba (1969) to include some small species of the genus *Galathea* that have a dagger-shaped rostrum with well-developed supraocular spines, small lateral sub-apical spines and broad excavated orbits. In addition, males lack of the first pair of gonopods. Specifically, Baba (1969) included the species *Galathea serrirostris* Melin, 1939 and *Galathea ikedai* Miyake & Baba, 1965, both described from the Bonin Islands, Japan, and the type species of the genus, *Galathea pusilla* Henderson, 1885, from Twofold Bay, Australia. Since its original description, other species have been included in the genus: *P. caribensis* Mayo, 1972 was described from the Caribbean Sea and *P. antonbruuni* Tirmizi & Javed, 1980 and *P. bengalensis* Tirmizi & Javed, 1980, from the Indian Ocean (Mayo 1972; Tirmizi & Javed 1980). Also, Lewinsohn (1982), after revising material from the Red Sea, transferred *Galathea integrirostris* Dana, 1852 to *Phylladiorhynchus*.

In 1991, Baba revised *Phylladiorhynchus*. He considered *P. serrirostris* (Melin, 1939) as a junior synonym of *P. integrirostris* (Dana, 1852), and *Galathea integra* Benedict, 1902 as a junior synonym of *P. pusillus* (Henderson, 1885). He also placed *P. caribensis* and *P. antonbruuni* in different genera: *Anomoeomunida* Baba, 1993 and *Munida* Leach, 1820, respectively (Baba 1991, 1993). Following Baba's (1991) revision, Macpherson (2008) described *P. nudus* Macpherson, 2008 from the Dampier Archipelago in Western Australia and, in the "Catalogue of squat lobsters of the world" (Baba *et al.* 2008), the species *Galathea lenzi* Rathbun, 1907 from Chile and *G. integra* Benedict, 1902 from Japan were synonymized with *P. pusillus*. Schnabel & Ahyong (2019), in their revision of New Zealand and southeastern Australian species, redescribed the type species of the genus, *P. pusillus* (Henderson, 1885) (type locality: Twofold Bay, Australia), and *P. integrirostris*, for which the original type material from Hawaii was lost. These authors also described six new *Phylladiorhynchus* species, thereby increasing the number of recognized species in the genus to 11.

In recent decades, numerous expeditions to the littoral, continental shelf and slope of the Indian and Pacific oceans (from the Red Sea and Madagascar to French Polynesian and Chilean waters) have been carried out, many as part of the Tropical Deep-Sea Benthos program (Richer de Forges *et al.* 2013) or other worldwide programs (e.g. those led by Gustav Paulay at the Florida Museum of Natural History). As a result of this sampling effort, a considerable number of specimens belonging to *Phylladiorhynchus* are housed in several different museum collections. To fully assess the diversity of the genus, we studied this material using both morphological characters and molecular markers (cytochrome c oxidase subunit I, COI, and 16S rRNA). We describe 41 new species, revealing extraordinary morphological and molecular diversity within the genus, with its

now more than 50 species. We also analyzed the type material of *Galathea lenzi* from Chile and *G. integra* and *G. serrirostris* from Japan to demonstrate the validity of these species. Moreover, we show that some species, despite being separated by large genetic distances, are distinguishable by only a few subtle morphological characters.

Material and methods

Sampling

All of the specimens analyzed in this study (more than 2100) were previously collected from the Indian and Pacific oceans over the course of several different expeditions and biodiversity surveys (e.g. Richer de Forges *et al.* 2013). Specimens from shallow waters were collected by scuba diving using different procedures including dead coral brushing, vacuum cleaning, hand picking, or they were retrieved from previously deployed Autonomous Reef Monitoring Structures (ARMS). Specimens from the continental shelf and slope were collected by dredging and trawling or retrieved from previously deployed lumen lumen nets (tangle nets). We analyzed material from Chile, French Polynesia, Hawaii, American Samoa, Kiribati, Mariana Islands, Taiwan, Japan, Philippines, Indonesia, Papua New Guinea, Vanuatu, New Caledonia, Chesterfield Islands, Queensland, Western Australia, Chagos Archipelago, Red Sea, Reunion Island, Comores and Mayotte Islands, Madagascar and Walters Shoal.

The material examined is deposited in the following museums: Muséum national d'Histoire naturelle, Paris (MNHN); Western Australia Museum, Perth (WAM); Florida Museum of Natural History, Florida (UF), National Taiwan Ocean University, Keelung (NTOU), National Museum of Marine Biology and Aquarium, Pingtung (NMMBA); National Museum of Natural History, Washington, D.C. (USNM); National Institute of Water and Atmospheric Research (formerly New Zealand Oceanographic Institute), Wellington (NIWA); Oxford University Museum of Natural History, Oxford (OUMNH); Uppsala universitet Evolutionsmuseet, Uppsala [Museum of Evolution of Uppsala University, Zoological Collection (UPSZTY)].

Morphological examination

The general terminology employed for the morphological description of *Phylladiorhynchus* specific traits largely follows Baba *et al.* (2009, 2011), Macpherson & Baba (2011), Macpherson & Robainas-Barcia (2015) and Schnabel & Ahyong (2019). Measurements were taken following Schnabel & Ahyong (2019). The size of the carapace is indicated by the postorbital carapace length measured along the dorsal midline from the posterior margin of the orbit to the posterior margin of the carapace. Rostrum length is measured from the tip of the rostrum to between the lateral basal incisions; rostrum

breadth is measured as the distance between the left and the right lateral basal incisions. The ridges on the posterior branchial region are always counted along the lateral margins, excluding the mid-transverse ridge and the posterior-most ridge anterior to the posterior margin of the carapace. Different appendages were measured as follows: length of the eye peduncle along the lateral margin of the peduncle; width at the midlength of the peduncle; length of antennular article 1 at its midlength (excluding distal spines), and breadth at its widest portion; length of each pereiopod article along its extensor margin (excluding distal spine), and breadth at its widest portion. The ranges of meristic and morphological variations are included in the descriptions; holotype measurements are shown in brackets. Abbreviations: F = females, M = males, Mxp3 = third maxilliped, ov. = ovigerous, P1 = first pereiopod (cheliped), P2–4 = second to fourth pereiopods (first to third walking legs).

Specimens from some species were mounted on an aluminum stub and studied under a HITACHI TM300 Scanning Electron Microscope (SEM) with a previous metallic coating.

We identified four types of rostra (Fig. 1): (1) leaf-like, with an indistinct to distinct pair of sub-apical spines, breadth at medial rostral length more than half the breadth at the basis, lateral margins always convex; (2) triangular, usually without a pair of sub-apical spines, breadth at medial rostral length half or less than half the breadth at the basis, lateral margins always straight or slightly concave; (3) dagger-shaped, with or without a pair of sub-apical spines, breadth at medial rostral length equal to the breadth at the basis, lateral margins straight or slightly convex; (4) bottle-shaped, with a pair of small sub-apical spines, margins straight, proximally parallel, distally convex and convergent (triangular).

Molecular analysis

The molecular analyses were performed as previously described (Rodríguez-Flores *et al.* 2017, 2019a,b,c). Tissue was isolated from P1 to 5, depending on the availability of legs and specimen size. DNA extractions were performed using the DNeasy kit (Qiagen) following the manufacturer's protocol. Samples were first digested with proteinase in ATL buffer for 18–24 hours; RNase was also added. Partial sequences of the mitochondrial cytochrome c oxidase subunit I (COI) and 16S rRNA (16S) genes were amplified by polymerase chain reaction (PCR) using the following primers: 16SAR/16SBR (Palumbi *et al.* 1991) and 16S1471/16SR1472 (Crandall & Fitzpatrick 1996) for 16S, and LCO1490/HCOI2198 (Folmer *et al.* 1994) and COI-H (Machordom *et al.* 2003) for COI. When amplification with these primers was not possible due to DNA degradation, an alternative pair of primers, Uni-MinibarF1/UniMinibarR1, for a small

COI fragment (=mini-barcode) of 158 base pairs (bp) was used (Meusnier *et al.* 2008). PCR amplifications were carried out in a final volume of 25 μl that included distilled H$_2$O, 5 μl of 5× buffer solution with MgCl$_2$ (Bioline), 0.2 mM of each deoxyribonucleotide triphosphate (dNTP), 0.2 μM of forward and reverse primers, 2–5 U of MyTaq polymerase (Bioline) and 2–4 μl of DNA template (2–20 ng/μl). The following thermal cycling conditions were used: initial denaturation at 95 °C for 3 min, 35–40 cycles of denaturation at 95 °C for 45–60s, annealing at 42–45 °C for 1 min and extension at 72 °C for 45–60s, followed by a final extension step at 72 °C for 10 min. The amplified fragments were purified using ExoSAP-IT (Affymetrix) or by gel extraction from a 1.5% TA-buffered agarose gel, filtering PCR products by centrifugation at 13,000 rpm for 10 min. BigDye Terminator and an ABI 3730 genetic analyzer were used to sequence both strands. Sequencing services were provided by SECUGEN (Madrid, Spain) and MACROGEN (Madrid, Spain). Forward and reverse DNA sequences obtained for each specimen were checked and assembled using Sequencher 4.8 (Gene Code Corporation). The mitochondrial 16S matrix was aligned using MAFFT (Katoh *et al.* 2002), followed by manual correction in AliView (Larsson 2014). Uncorrected divergences (p) within and among species were calculated using MEGA 7.0.26 (Kumar *et al.* 2016). Sequenced specimens and GenBank accession numbers for each marker are presented in Table (Appendix).

Results

Overall, our results reveal the rich diversity of the genus *Phylladiorhynchus*, with its 55 species. We resurrect some old names currently considered as synonyms and describe and illustrate new taxa. Almost all of the taxonomic units are distinguishable based on constant clear and/or subtle morphological characters and are genetically different, with some species presenting unexpectedly large genetic distances. Interspecific genetic divergences ranged 7–36% and 2–27% for COI and 16S, respectively. Intraspecific distances ranged 0–4.7% for COI and 0–1.2% for 16S.

Systematic account

Family Galatheidae Samouelle, 1819

Genus *Phylladiorhynchus* Baba, 1969

Phylladiorhynchus Baba, 1969: 3.—Baba, 2005: 200.—Baba *et al.*, 2008: 175.—Baba *et al.*, 2009: 286.—Macpherson & Baba, 2011: 55.—Schnabel & Ahyong, 2019: 304.

Type species. *Galathea pusilla* Henderson, 1885, by original designation.

Diagnosis. (Modified after Macpherson & Baba 2011; Schnabel & Ahyong 2019) Carapace dorsally unarmed or with a few epigastric spines, rarely with parahepatic spines, with distinct transverse ridges; lateral margin spinose. Rostrum triangular, dagger-shaped, leaf-like or bottle-shaped, usually with well-developed supraocular basal and subapical spine on each side, margin usually minutely serrated. Lateral orbital spine always present. Thoracic sternite 3 with posterior margin widely or narrowly contiguous to sternite 4. Telson subdivision incomplete, conformed by ten plates. Eyes movable; cornea usually as wide as peduncle. Antennular article 1 with 3–5 distal spines (nearly always including double distolateral spine). Antennal article 1 with strong ventral distomesial process usually overreaching antennal article 4. Mxp3 ischium with distal spines, crista dentata with row of spines along entire margin; merus much shorter than ischium, with strong spines on flexor and extensor distal margins. G1 absent; G2 present. P1 spinose, fingers distally with row of spines along curved margin, tip excavated, spooned.
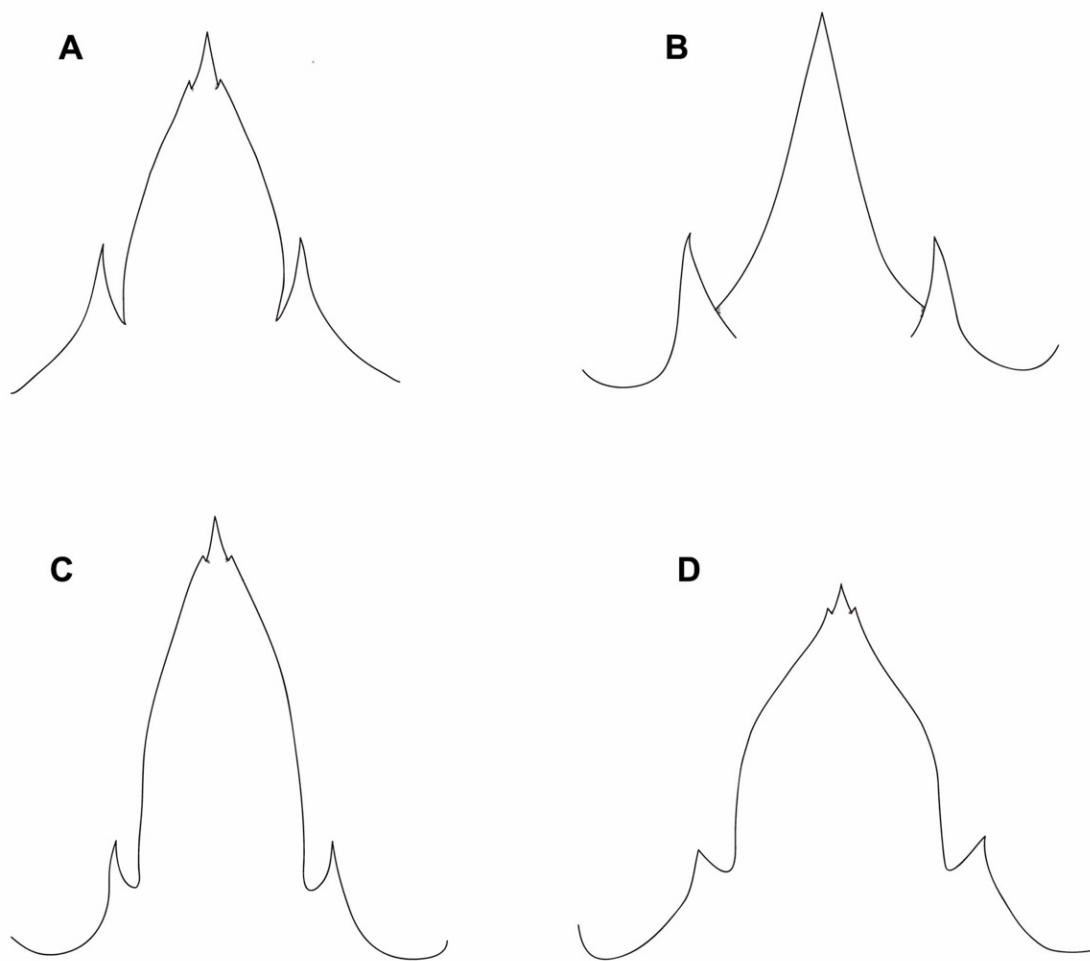
FIGURE 1. Types of rostra. A, leaf-like. B, triangular. C, dagger-shaped. D, bottle-shaped.

Key to species of the genus *Phylladiorhynchus*

1. Epigastric ridge of carapace unarmed **2**

—Epigastric ridge of carapace with spines **6**

2. Pterygostomian   flap   with   small   spine   on   upper
margin…………………………….......................*P. nudus* Macpherson, 2008

—Upper margin of pterygostomian flap unarmed.. **3**

3. Anterior branchial margin of carapace with 2 spines. Proximal half of rostrum
margin straight, distal half convex (bottle-shaped) .... *P. phlias* **n. sp.**

—Anterior branchial margin of carapace with 3 spines. Rostrum
margin slightly convex **4**

4. Anterior epigastric ridge distinct and medially interrupted. Thoracic
sternite 3 laterally projected .... *P. jeffkinchi* **n. sp.**

—Anterior epigastric ridge usually undistinct, or scale-like. Lateral
angles of thoracic sternite 3 not projected.. **5**

5. Colour brownish. Carapace ridges with scattered very long plumose
setae .... *P. marina* **n. sp.**

—Colour orange. Carapace ridges without long plumose setae *P. phanus* **n. sp**.

6. Protogastric region armed with parahepatic spines ... *P. heptacanthus* **n. sp.**

—Parahepatic spines on protogastric region absent **7**

7. Flexor margin of Mxp3 merus with 2–3 prominent spines **8**

—Flexor margin of Mxp3 merus with one prominent spine only................ **23**

8. Epigastric region with 2 spines.. *P. iphiclus* **n. sp.**

—Epigastric region with 3–5 spines... **9**

9. Epigastric region with 3 spines... **10**

—Epigastric region with 4–5 spines... **11**

10. Rostrum leaf-like, with minute or distinct pair of subapical spines, lateral margins convex. P2–4 propodi stout, 4–5 x as long as wide. Three anterior branchial spines. .... *P. hylas* **n. sp.**

— Rostrum triangular: without distinct pair of subapical spines, lateral margins straight. P2–4 propodi slender, 8–9 x as long as wide. Two anterior branchial spines .... *P. idas* **n. sp.**

11. Epigastric region with 4 spines **12**

— Epigastric region with 5 spines or with 4 spines and one median process or a scale with thick plumose setae.. **13**

12. Rostrum triangular, margins slightly concave. Thoracic sternite 4 widely contiguous to sternite 3.. *P. boucheti* **n. sp.**

— Rostrum dagger-like, margins slightly convex. Thoracic sternite 4 narrowly contiguous to sternite 3 .... *P. maestratii* **n. sp.**

13. Epigastric ridge with 4 spines and one median process or scale with thick plumose setae, rarely with 5 spines (see *P. butes*). **14**

—Epigastric ridge with 5 spines **15**

14. Antennal article 2 armed distally with well-developed mesial and lateral spines .... *P. butes* **n. sp.**

—Antennal article 2 unarmed, otherwise with small distomesial spine or granule... *P. cepheus* **n. sp.**

15. Rostrum leaf-like, (subapical spines always present, lateral margins convex). Anterior protogastric ridge medially interrupted, with one scale behind median epigastric spine................................... *P. eneus* **n. sp.**

—Rostrum triangular, (subapical spines absent or, if present, obsolescent, lateral margins straight or slightly concave). Anterior protogastric ridge not interrupted medially, without scale behind median epigastric spine. **16**

16. Anterior branchial margin with 2 spines **17**

— Anterior branchial margin with 3 spines... **18**

17. Anterior mesogastric ridge scale-like; anterior metagastric ridge not medially interrupted .... *P. punctatus* **n. sp.**

—Anterior mesogastric ridge not medially interrupted or with small medial gap; anterior metagastric ridge medially interrupted…………............ *P. kermadecensis* Schnabel & Ahyong, 2019

18. Anterior margin of thoracic sternite 3 nearly transverse with median and lateral projections .... *P. bengalensis* Tirmizi & Javed, 1980

— Anterior margin of thoracic sternite 3 moderately convex sometimes with feeble median excavation **19**

19. Anterior metagastric ridge not interrupted. Antennule article 1 with 4 distal spines (double distolateral spine absent*P. ikedai* (Miyake & Baba, 1965)

—Anterior metagastric ridge scale-like. Antennule article 1 with 5 distal spines (double distolateral spine present) **20**

20. Pleonal tergite 3 with anterior and posterior transverse ridges *P. acastus* **n. sp.**

—Pleonal tergite 3 without posterior transverse ridge................................ **21**

21. Anterior protogastric ridge usually medially interrupted ……………….....................................*P. erebus* Schnabel & Ahyong, 2019

—Anterior protogastric ridge always not medially interrupted.................... **22**

22. Anterior mesogastric ridge medially interrupted .... *P. argus* **n. sp.**

—Anterior mesogastric ridge not medially interrupted........... *P. paulae* **n. sp.**

23. Epigastric ridge with 5 spines, with median spine................................ **24**

—Epigastric ridge with 2–6 spines, without median spine **25**

24. Proximal half of extensor margin of P2–4 propodi armed with 1–4 well-developed spines. P2–4 propodi slender (6–7 x as long as wide)…... *P. koumac* **n. sp.**

— Extensor margin of P2–4 propodi unarmed, otherwise serrated. P2–4 propodi stout (4–5 x as long as wide).......................... *P. pulchrus* **n. sp.**

25. Epigastric region with 4 spines, lateral pair much smaller (sometimes granular) than mesial pair (in *P. pusillus* and related species often with 2 or 6 spines.. **26**

—Epigastric region with 2 spines **33**

26. Anterior branchial margin of carapace with 2 spines .... *P. pollux* **n. sp.**

— Anterior branchial margin of carapace with 3 spines; **27**

27. Anterior margin of thoracic sternite 3 convex, without median projection. Anterior metagastric ridge medially interrupted. Pleonal tergite 3 usually without posterior transverse ridge................................. **28**

— Anterior margin of thoracic sternite 3 biconcave, with obtuse median projection. Anterior metagastric ridge continuous, not medially interrupted. Pleonal tergite 3 with anterior and posterior transverse ridge **31**

28. Anterior mesogastric ridge medially interrupted.............. *P. porteri* **n. sp.**

— Anterior mesogastric ridge not medially interrupted. …........................ **29**

29. Antennular lateral-most spine very small to indistinct. Antennal article 3 armed distally with well-developed mesial and lateral spines... *P. lenzi* (Rathbun, 1907)

—Antennular lateralmost spine always distinct. Antennal article 3 armed distally with small mesial spine only **30**

30. Thoracic sternite 3 moderately produced anterolaterally .... *P. poeas* **n. sp.**

— Thoracic sternite 3 anterolateral margins with broad granule or square .... *P. pusillus* (Henderson, 1885)

31. Rostrum lateral margins straight … .... *P. nui* Schnabel & Ahyong, 2019

— Rostrum lateral margins convex. …... **32**

32. Antennular lateralmost spine always distinct. Antennal article 2 armed with a well-developed lateral spine, reaching or overreaching article3 .... *P. australis* Schnabel & Ahyong, 2019

— Antennular lateralmost spine very small to indistinct. Antennal article 2 unarmed, otherwise with a minute spine .... ……………………………...........…………...*P. integrus* (Benedict, 1902)

33. Anterior branchial margin with 2 spines... **34**

— Anterior branchial margin with 3 spines... **42**

34. Pleonal tergite 3 with anterior and posterior transverse ridge……………………………………………… *P. serrirostris* (Melin, 1939)

— Pleonal tergite 3 without posterior transverse ridge **35**

35. Hepatic margin with small spine between anterolateral and first branchial spines **36**

—Hepatic margin without small spine between anterolateral and first branchial spines **37**

36. Carapace with some scales between main ridges. Sternite 3 broad, more than 3 x as wide as long. Ocular peduncle narrower than cornea. .... *P. peneleos* **n. sp.**

—Carapace without scales between main ridges. Sternite 3 moderately broad, less than twice as wide as long. Ocular peduncle as wide as or wider than cornea.. *P. bahamut* **n. sp.**

37. Anterior metagastric ridge not medially interrupted. Rostrum without subapical spines or obsolescent **38**

—Anterior metagastric ridge medially interrupted or scale-like. Rostrum with subapical spines... **39**

38. Anterior margin of thoracic sternite 3 straight or slightly convex, produced anterolaterally. Antennal article 3 usually with distomesial spine. Colour basis of carapace and pleon whitish with reddish patches... *P. barbeae* **n. sp.**

— Anterior margin of thoracic sternite 3 medially projected or convex, anterolaterally rounded. Antennal article 3 unarmed. Base colour of carapace and pleon green or light orange............................. *P. pepei* **n. sp.**

39. Anterior metagastric ridge scale-like. Carapace ridges barely distinct with a few short setae .... *P. orpheus* **n. sp.**

—Anterior metagastric medially interrupted. Carapace ridges clearly distinct with dense short setae. **40**

40. Rostrum margin convex from the basis to the tip .... *P. lynceus* **n. sp.**

—Rostrum margin proximally straight **41**

41. Carapace ridges with a few or without thick iridescent setae*P. integrirostris* (Dana, 1852)

—Carapace ridges always with thick iridescent setae............. *P. priasus* **n. sp.**

42. P2–4 dactyli without sharp upright cuticular spines (dactylar spines) at bases of movable spines **43**

—P2–4 dactyli with sharp upright cuticular spines (dactylar spines) at bases of movable spines **50**

43. Pleonal tergite 3 with anterior and posterior transverse ridges............... **44**

—Pleonal tergite 3 without posterior transverse ridge................................ **47**

44. Subapical spines of rostrum well developed. Posterior transverse ridge of pleonal tergite 3 continuous **45**

—Subapical spines of rostrum minute. Posterior transverse ridge of pleonal tergite 3 medially interrupted or scale-like **46**

45. Anterior metagastric ridge medially not interrupted or interrupted. Anterior margin of thoracic sternite 3 medially projected. Large median scale in metagastric area .... *P. laureae* **n. sp.**

—Anterior metagastric ridge usually scale-like. Anterior margin of thoracic sternite 3 slightly convex. Small median scale in metagastric area... *P. gustavi* **n. sp.**

46. Thoracic sternite 3 quadrangular (less than twice as long as broad). Scale between epigastric spines with thick setae................. *P. tiphys* **n. sp.**

—Thoracic sternite 3 moderately broad (twice as long as broad). Scale between epigastric spines with thick setae absent................. *P. zetes* **n. sp.**

47. Rostrum without subapical spines or obsolescent. Anterior upper margin of pterygostomian flap usually serrated .... *P. medea* **n. sp.**

—Rostrum with small subapical spines. Anterior upper margin of pterygostomian flap usually smooth **48**

48. Antennal article 3 with distomesial and distolateral spines. *P. janiqueae* **n. sp.**

—Antennal article 3 with distomesial spine only. **49**

49. Rostrum with well-developed subapical spines (tridentiform). Thoracic sternite 3 quadrangular (less than twice wider than long) .... *P. talaus* **n. sp.**

—Rostrum with minute subapical spines. Thoracic sternite 3 moderately broad (twice as wide as long) .... *P. triginta* Schnabel & Ahyong, 2019

50. Pleonal terguites 2–4 with anterior and posterior ridges. Carapace always with secondary ridges. Rostrum dagger-like **51**

—Pleonal terguite 4 with anterior ridges only. Carapace rarely with secondary ridges. Rostrum leaf-like **54**

51. Spines of antennal article 2 clearly different, distomesial minute. P1 very slender (P1 male more than 3.5 x as long as carapace)……………………… *Phylladiorhynchus spinosus* Schnabel & Ahyong, 2019

—Spines of antennal article 2 subequal. P1 moderately slender or stout (P1 male about or less than 3.0 x as long as carapace)............................ **52**

52. Antennal article 3 usually armed with distinct distomesial spine. Carapace broader than long .... *P. asclepius* **n. sp.**

—Antennal article 3 unarmed or with small process. Carapace usually as long a broad or slightly longer than broad **53**

53. Carapace and pleonal ridges and ocular peduncles with numerousthick iridescent setae. Rostrum margin straight *P. euryalus* **n. sp.**

—Carapace and pleonal ridges and ocular peduncles with scattered thick iridescent setae. Rostrum margin nearly straight or slightly convex .... *P. lini* **n. sp.**

54. Anterior metagastric ridge medially or laterally interrupted ....
………………………...*P. amphion* **n. sp.**

—Anterior metagastric ridge not interrupted...................... *P. joannotae* **n. sp.**

Phylladiorhynchus acastus **n. sp.**

(Figs. 2, 11A, 54A)

Type material. *Holotype*. Chesterfield Islands. EBISCO Stn CP2507, 24°43'S, 159°43'E, 286 m, 7 October 2005: ov. F 2.4 mm (MNHN-IU-2014-13796).

Paratypes. Philippines. MUSORSTOM 1 Stn 18, 13°57'N, 120°17'E, 150–159 m, 21 March 1976: 1 ov. F 2.0 mm (MNHN-IU-2014-13867).

Papua New Guinea. KAVIENG Stn DW4412, 02º33'S, 150º40'E, 500–600 m, 27 August 2014: 1 M mm (MNHN-IU-2014-10017).

Vanuatu. MUSORSTOM 8 Stn CP1132, 15°38'S, 167°03'E, 161–182 m, 11 October 1994: 1 M 2.0 mm, 2 ov. F 2.0–2.1 mm (MNHN-IU-2016-424).—MUSORSTOM 8 Stn CP1133, 15°39'S, 167°03'E, 174–210 m, 11 October 1994: 1 M 2.9 mm, 1 ov. F 2.4 mm (MNHN-IU-2019-2700).

Chesterfield Islands. EBISCO Stn CP2493, 24°44'S, 159°43'E, 285–545 m, 6 October 2005: 1 ov. F 3.1 mm (MNHN-IU-2019-2692).—KANADEEP Stn CP4930, 25º08'S, 159º55'E, 300 m, 3 September 2017: 1 M 2.1 mm (MNHN-IU-2017-2521).—Stn CP4934, 25º04'S, 159º55'E, 290–300 m, 3–4 September 2017: 2 M 2.4–3.0 mm, 2 ov. F 2.2–2.9 mm (MNHN-IU-2017-2529).—Stn DW4940, 25°29'S, 159°49'E, 310–320 m, 4 September 2017: 1 M 2.6 mm, 1, F 2.1 mm (MNHN-IU-2017-2634).—Stn DW4943, 25º25'S, 159º51'E, 300–310 m, 4 September 2017: 3 M 2.4–2.9 mm (MNHN-IU-2017-2646).—Stn CP4953, 24º10'S, 159º41'E, 270–320 m, 5 September 2017: 1 M 1.9 mm, 1 broken (MNHN-IU-2019-2688).

New Caledonia. LIFOU Stn 1648, 20°54.1'S, 167°03.3'E, 150–200 m, 7 November 2000: 1 M 1.7 mm (MNHN- IU-2019-2676).

Etymology. From the name *Acastus*, an Argonaut, son of Pelias and Anaxibia (Phylomache). The name is considered a substantive in apposition.

Description. *Carapace:* as long as or slightly longer than broad; transverse ridges with dense short setae, and few scattered iridescent thick long setae. Gastric region flattened, with 4 transverse ridges: epigastric ridge indistinct, with 5 spines (1 median and
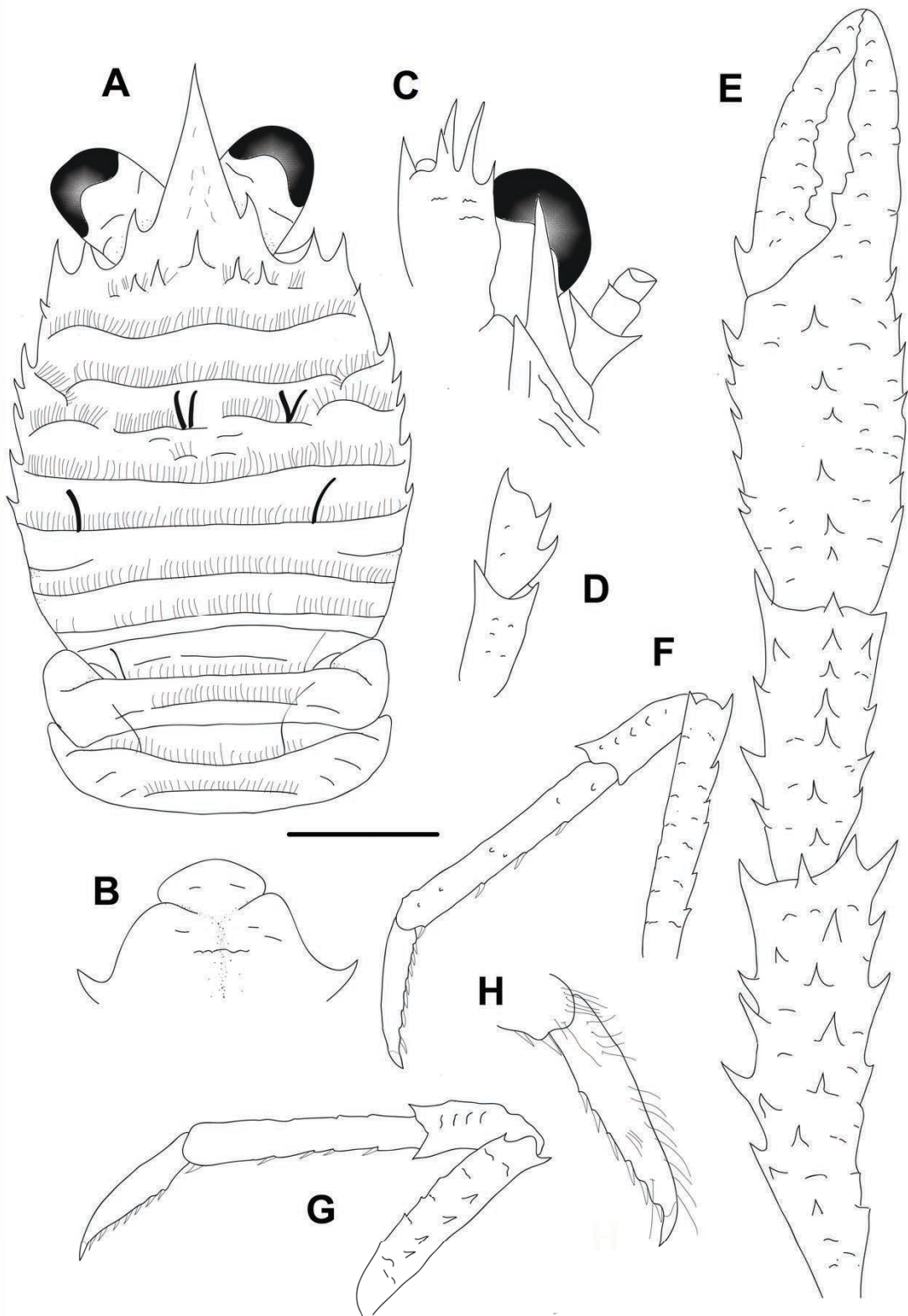
FIGURE 2. *Phylladiorhynchus acastus* **n. sp**., holotype ovigerous female, 2.4 mm (MNHN-IU-2014-13796): A, carapace and pleon, dorsal view. B, thoracic sternites 3 and 4. C, left cephalic region, showing antennular and antennal peduncles, ventral view. D, right Mxp3, lateral view. E, right P1, dorsal view. F, left P2, lateral view. G, left P4, lateral view. H, dactylus of left P2, lateral view. Scale bar: A, E, F, G = 1.0 mm; B–D, H = 0.6 mm.

2 pairs of spines laterally); anterior protogastric ridge not medially interrupted (interrupted only in the paratype MNHN-IU-2014-10017), nearly extending laterally to carapace margin; anterior mesogastric ridge not medially interrupted, laterally interrupted by anterior branch of cervical groove, and continuing uninterrupted to first branchial spine; anterior metagastric ridge scale-like, sometimes followed by short scattered scales on posterior metagastric region. Mid-transverse ridge not interrupted, slightly medially depressed, preceded by shallow or indistinct cervical groove, followed by 2 not interrupted, or minutely interrupted ridges, interspersed with 1 short lateral ridge and sometimes few, short scattered scales. Lateral margins slightly convex, with 7 spines: first anterolateral spine well-developed, reaching anteriorly to level of lateral orbital spine, second spine (hepatic) small, slightly dorsomesially from lateral margin, and followed by 5 branchial spines (3 anterior and 2 posterior). Rostrum triangular, horizontal, dorsally flattish or slightly concave, 1.8–[2.0] times as long as broad, length [0.5]–0.4 and breadth 0.2–[0.3] that of carapace; lateral margins smooth and straight, with well-developed supraocular basal spines, subapical spines absent. Pterygostomian flap ending in acute tooth, upper margin smooth.

Sternum: 1.1 as wide as long. Sternite 3 moderately broad, [2.1]2.0–3.0 times as wide as long, anterior margin convex, with or without median feeble excavation. Sternite 4 widely contiguous to sternite 3; surface not depressed in midline, smooth; greatest width [2.7]2.0–3.0 times that of sternite 3, [3.0]2.0–3.0 times as wide as long.

Pleon: Elevated ridges with short setae and a few scattered long setae. Tergites 2 and 3 with anterior and posterior transverse elevated ridges; tergite 4 with anterior transverse ridge; tergites 5–6 smooth.

Eye: Eye stalk length about [1.3]1.0–1.3 times broader than long, peduncle distally setose, not distinctly expanded proximally; maximum corneal diameter [1.0]1.0 × rostrum width*,* as wide as eyestalk.

Antennule: Article 1 1.3 times longer than wide, with 5 spines: distomesial spine well-developed; proximal lateral spine small, always present.

Antenna: Article 1 with prominent mesial process, distally falling well short of lateralmost antennular spine. Article 2 with distinct distal spines laterally and mesially. Article 3 often with small distomesial spine. Article 4 unarmed.

Mxp3: Ischium with distinct distal spines on flexor and extensor margins. Merus [0.6]0.4–0.5 × length of ischium, with well-developed distal spine on extensor margin and 2 strong spines on flexor margin.

P1: 3.5–3.6 (males), [2.7]–2.8 (females) times carapace length; subcylindrical, scales with dense short setae and long stiff setae; merus, carpus and palm with spines along mesial, dorsal and lateral surfaces, distal and mesial spines usually stronger than others. Merus [1.2]1.1–1.3 length of carapace, 1.7 times as long as carpus. Carpus [2.4]2.2–2.4 times as long as wide. Palm [1.1]1.0–1.1 × carpus length, [1.8]2.2–2.4 times as long as broad. Fingers subequal in length to palm; fixed finger unarmed; movable finger with well-developed basal spine.

P2–4: Slender, subcylindrical, moderately setose and spinose. Meri successively shorter posteriorly: P3 merus 0.7 times length of P2 merus, P4 merus 0.9 times length of P3 merus. P2 merus, 0.8–0.9 times carapace length, 5.5–6.0 times as long as broad, 1.1–1.4 times as long as P2 propodus; P3 merus 5.4–5.5 times as long as broad, 1.4 times as long as P3 propodus; P4 merus [4.9]–5.4 times as long as broad, 1.1–1.4 times as long as P4 propodus; extensor margin of P2 and P3 with row of spines, proximally diminishing, with prominent distal spine; P4 extensor margin irregular, with distal spine; flexor margins of P2–4 irregular, each with distal spine; P4 lateral surface with median row of 4 small spines, absent in P2–3. Carpi unarmed on extensor margin on P3–4, distal spine prominent on P2–3, minute on P4; row of small spines below extensor margin on lateral surface of P2–3, unarmed on P4; flexor margin unarmed. Propodi moderately slender, [4.8–5.4]5.0–6.0 times as long as broad; extensor margin irregular, unarmed or with 2–4 proximal spines; flexor margin with 2–4 slender movable spines in addition to distal pair. Dactyli [0.6]–0.7 × length of propodi, ending in incurved, strong, sharp spine; flexor margin with 6–7 movable spines.

Eggs: Ov. F carried approximately 5–12 eggs of 0.3–0.4 mm diameter.

Colour. Base colour of carapace orange, gastric region covered by purple and golden-yellow patches; granules golden-yellow and orange. Rostrum light orange. Pleonal tergites 1–4 light orange, with scales and granules orange or reddish; tergites 5–6 and telson whitish. P1 light orange, spines wittish, fingers with reddish strip, distal tips wittish. P2–4 light orange, spines along flexor margins whitish; distal portion of meri, carpi and propodi and proximal part of carpi wittish, propodi and dactyli with orange bands.

Genetic data. COI and 16S, Table 1.

Distribution. Philippines, Papua New Guinea, Vanuatu, Chesterfield Islands and New Caledonia, from 150 to 600 m.

Remarks. *Phylladiorhynchus acastus* belongs to the group of species that has 5 epigastric spines, the rostrum margins straight, the subapical spines of the rostrum absent,

3 spines on the anterior branchial margin, and the Mxp3 merus with two prominent spines along the flexor margin. *Phylladiorhynchus acastus* closely resembles to *P. argus*, from French Polynesia, New Caledonia and Chesterfield Islands, and *P. paulae*, from SW Indian Ocean (see the differences under the Remarks of *P. paulae*).

The specimen from Papua New Guinea has the anterior protogastric ridge of the carapace interrupted and a pattern of setae slightly different than specimens from the Phillipines, Vanuatu and New Caledonia. Since there is a single specimen from this population and we were not able to obtain molecular data, we decide to identify this specimen as species *P. acastus* until the collection of additional material from Papua New Guinea. Furthermore, the specimens fron Chesterfield Islands (KANADEEP, Stn CP4934, Stn DW4943) have the extensor margin of the P2–4 propodi armed with 2–4 proximal spines, whereas this margin is unarmed in the other species, suggesting that this character could be variable.

The genetic divergences between *P. acastus* and other species were always higher than 12% (COI) and 3% (16S), both minimum values respect to *P. paulae*. The mean intraspecific divergences were 0.15% for COI and 0% for 16S.

***Phylladiorhynchus amphion* n. sp.**

(Figs. 3, 11B-C)

Type material. *Holotype*. Western Australia. S end Ashmore Reef. Stn 134/K13, 12º17.76'S, 123º01.632'E, 12 m, 30 September 2013: 1 M 2.4 mm (WAM C55691).

Paratypes. Western Australia. W Point Ashmore. Stn 135/K13, 12º14.622'S, 122º14.622'E, no depth, 1 October 2013: 1 M 2.2 mm, 1 ov. F 2.4 mm (WAM C53888).— Vulcan Shoal Stn 146/K13, 12º47.958'S, 124º16.002'E, 19 m, 6 October 2013: 1 ov. F 2.2 mm (WAM C55694).—Eugene McDermont Shoal. Stn 147/K13, 13º04.614'S, 124º35.01'E, 22 m, 6 October 2013: 1 M 2.8 mm (WAM C55695).—Rowley Shoals, Clerke Reef. Stn 151/K14, 17º15.114'S, 119º21.54'E, 12–20 m, 2 October 2014: 1 M 2.4 mm, 1 F 2.1 mm (WAM C56280).—Stn 154/K14, 17º16.794'S, 119º22.596'E, no depth, 4 October 2014: 1 M 2.4 mm, 1 F 2.6 mm (WAM C53887).—Imperieuse Reef. Stn 157/K14-T2, 17º30.42'S, 118º57.948'E, 12–15 m, 5 October 2014: 1 M 1.8 mm, 2 ov. F 2.1–2.2 mm (WAM C53891).

Etymology. From the name *Amphion*, an Argonaut, son of Hyperasius and Hypso. The name is considered a substantive in apposition.
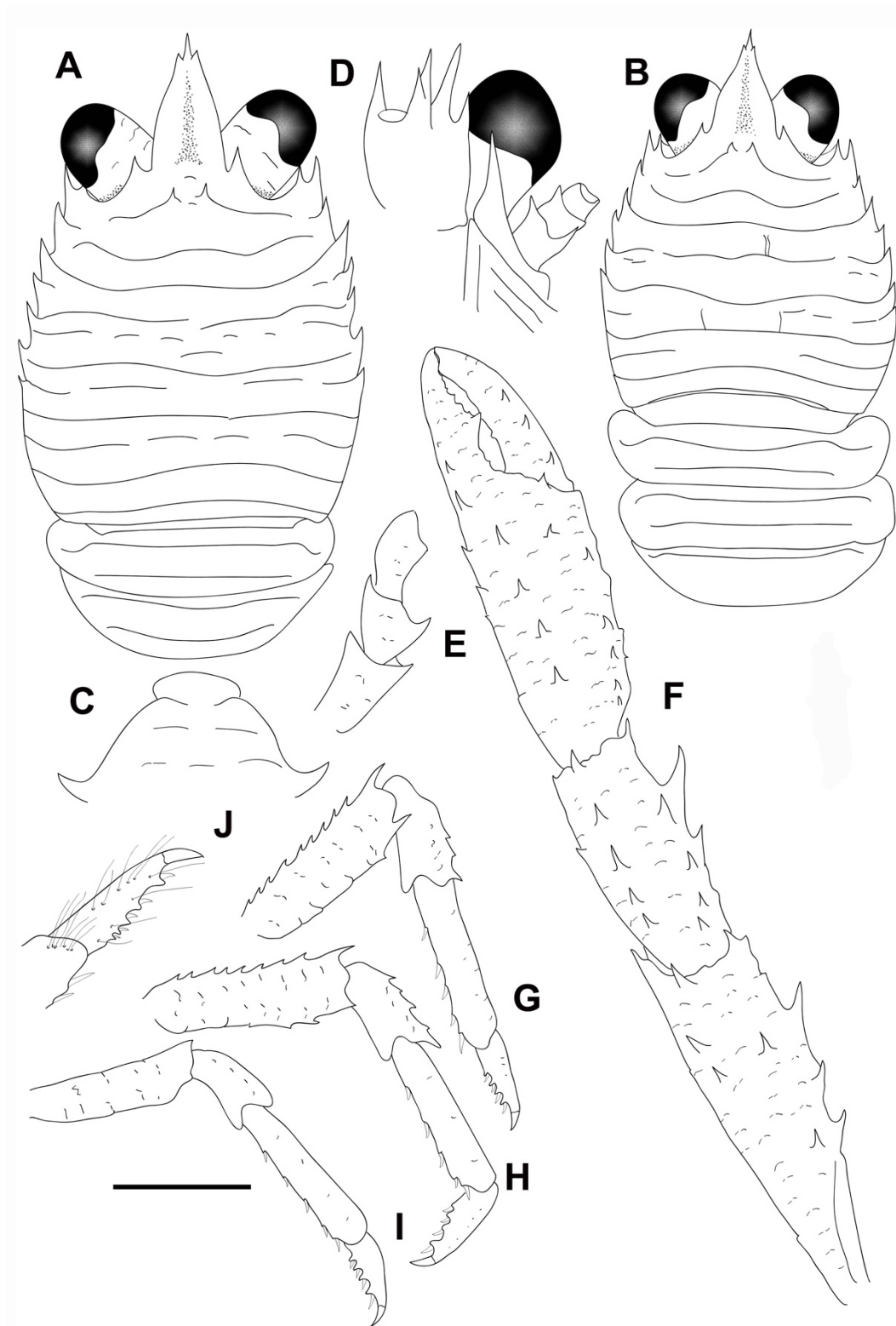
FIGURE 3. *Phylladiorhynchus amphion* **n. sp**., A, C-J, holotype male 2.4 mm (WAM C55691); B, paratype ovigerous female 2.1 mm (WAM C53891): A, B, carapace and pleon, dorsal view. C, thoracic sternites 3 and 4. D, left cephalic region, showing antennular and antennal peduncles, ventral view. E, right Mxp3, lateral view. F, left P1, dorsal view. G, right P2, lateral view. H, right P3, lateral view. I, right P4, lateral view. J, dactylus of right P2, lateral view. Scale bar: A, B, F-I = 1.0 mm; C–E, J = 0.6 mm.

Description. *Carapace:* as long as or slightly broader than long, sexually dimorphic (wider on females) 0.9–1.0 (males), [0.8]–0.9 (females) times as long as broad; transverse ridges with dense short setae and few scattered thick setae. Gastric region slightly convex with 4 transverse ridges: epigastric ridge distinct with 2 median spines and some lateral short scales, often followed by small scattered scales; anterior protogastric ridge not medially interrupted, nearly extending laterally to carapace margin, often followed by small scattered scales; anterior mesogastric ridge not medially interrupted, continuing to first branchial spine; anterior metagastric often medially interrupted, sometimes followed by short scattered scales on posterior metagastric region. Mid-transverse ridge not interrupted, slightly medially depressed, cervical groove indistinct, followed by 2 not interrupted or minutely interrupted ridges, interspersed with 2 short lateral ridges and sometimes few, short scattered scales. Lateral margins convex, with 6–7 distinct spines: first anterolateral spine well-developed, reaching anteriorly to level of lateral orbital spine, second spine (hepatic) well-developed, slightly dorsomesially from lateral margin, and followed by 4–5 branchial spines (3 anterior and 1–2 posterior). Rostrum leaf-like, horizontal, dorsally flattish or slightly concave, sexually dimorphic (shorter and wider in females) [1.6]–1.8 (males), 1.2–1.4 (females) times as long as broad, length [0.4]0.3–0.5 and breadth 0.2–[0.3] that of carapace; lateral margins smooth and convex, with well-developed supraocular basal spines and small subapical spines. Pterygostomian flap ending in blunt tooth, upper margin smooth.

Sternum: Slightly wider than long. Sternite 3 moderately broad, 2.3–[2.5] times as wide as long, anterior margin convex, anterolaterally rounded. Sternite 4 widely contiguous to sternite 3; anterolaterally smooth, surface depressed in midline, smooth; greatest width 2.4–[3.0] times that of sternite 3, 2.5–[3.0] times as wide as long.

Pleon: Elevated ridges with short setae and a few scattered long setae. Tergites 2–3 with anterior and posterior transverse elevated ridges; tergite 4 with anterior transverse ridge, posterior transverse ridge absent; tergites 5–6 smooth.

Eye: Eye stalk length about 0.9–[1.1] times broader than long, peduncle distally setose, not distinctly expanded proximally; cornea expanded distally, maximum corneal diameter 0.8–[0.9] × rostrum width*,* as wide as eyestalk.

Antennule: Article 1 slightly longer than wide, with 5 distal spines: distomesial spine well-developed; proximal lateral spine small, always present.

Antenna: Article 1 with prominent mesial process, distally falling well short of lateralmost antennular spine. Article 2 with well-developed distomesial and distolateral spines. Article 3 with distomesial spine. Article 4 unarmed.

Mxp3: Ischium with distinct distal spines on flexor and extensor margins. Merus 0.8[0.8] × length of ischium, with well-developed distal spine on extensor and flexor margins.

P1: 3.0–[3.2] (males), 2.0–2.2 (females) times carapace length; subcylindrical, spiny and with long stiff setae and dense thick iridescent and plumose setae; merus, carpus and palm with spines along mesial, dorsal and lateral surfaces, distal and mesial spines usually stronger than others. Merus 0.8–[1.2] length of carapace, [1.6]1.5–1.8 times as long as carpus. Carpus 1.7–[2.2] times as long as wide. Palm [1.1]–1.2 × carpus length, 1.4–[2.0] times as long as broad. Fingers [0.8]0.8 × palm length; fixed finger with 1–2 basal spines; movable finger with 3 spines.

P2–4: stout, setose and spinose. Meri successively shorter posteriorly: P3 merus 0.8–[0.9] times length of P2 merus, P4 merus [0.9]0.9 times length of P3 merus. P2 merus, [0.6]0.6 times carapace length, [3.0]–3.8 times as long as broad, 1.1–[1.2] times as long as P2 propodus; P3 merus 2.8–[3.2] times as long as broad, 1.0–[1.2] times as long as P3 propodus; P4 merus [3.5] times as long as broad, [1.1] times as long as P4 propodus; extensor margin of P2 and P3 with row of spines, proximally diminishing, with prominent distal spine; P4 extensor margin irregular, unarmed; flexor margin irregular, with distal spine on P2–3, absent or small on P4. Carpi with 2–4 spines on extensor margin on P2–3, unarmed on P4; distal spine prominent on P2–3, absent on P4; row of granules below extensor margin on lateral surface of P2–4; flexor margin unarmed. Propodi stout, [4.0–4.3]3.9–4.6 times as long as broad; extensor margin irregular; flexor margin with 3–4 slender movable spines in addition to distal pair. Dactyli [0.5–0.7]0.5–0.6 × length of propodi, ending in incurved, strong, sharp spine; flexor margin with dactylar spines at basis of 5–6 movable spines.

Eggs: Ov. F carried approximately 10–25 eggs of 0.3–0.5 mm diameter.

Colour. Unknown.

Genetic data. COI and 16S, Table 1.

Distribution. Western Australia, from 12 to 22 m.

Remarks. *Phylladiorhynchus amphion* belongs to the group of species having 2 epigastric spines, 1 hepatic spine, 3 spines on anterior branchial margin of the carapace and dactylar spines along the flexor margin of P2–4 dactyli. The closest relative is *P. joannotae* from French Polynesia, Guam Island, Papua New Guinea, Vanuatu and New Caledonia (see the differences under the Remarks of this species).

The mean intraspecific genetic divergences were 1.8% for COI and 1.2% for 16S.

***Phylladiorhynchus argus* n. sp.**

(Fig. 4, 11D)

Phylladiorhynchus ikedai.—Baba, 1991: 485 fig. 4a, b (in part, only material from MUSORSTORM 4, Stn 238 [MNHN Ga-2043], MUSORSTORM 6, Stn DW485 [MNHN Ga-2045] and CALSUB, Pl 16 [MNHN Ga-2046]).

Type material. *Holotype.* New Caledonia. EXBODI Stn DW3785, 22°15'S, 167°10'E, 386–387 m, 02 September 2011: M 2.5 mm (MNHN-IU-2011-7659).

Paratypes. New Caledonia. MUSORSTOM 4 Stn CP238, 22º13'S, 167º14'E, 500–510 m, 2 October 1985: 1 ov. F 3.5 mm (MNHN-IU-2014-23836 (Ga-2043)).—MUSORSTOM 6 Stn DW485, 21º23.48'S, 167º59.33'E, 380 m, 23 February 1989: 1 F 3.2 mm (MNHN-IU-2014-23835 (Ga-2045)).—CALSUB Pl 16, 20º37.8'S, 167º02.7'E, 500 m, 7 March 1989: 1 M 3.2 mm (MNHN-IU-2013-19941 (Ga-2046)).—KANACONO Stn DW4778, 23°03'S, 168°18'E, 170–248 m, 28 August 2016: 1 M 2.9 mm (MNHN-IU-2016-488).

Chesterfield Islands. KANADEEP Stn CP4985, 20º49'S, 160º57'E, 480–540 m, 10 September 2017: 1 M 3.0 mm (MNHN-IU-2017-3138).

French Polynesia. BENTHAUS Stn DW2006, 22°27'S, 151°19'W, 350–450 m, 24 November 2002: 1 M 3.4 mm (MNHN-IU-2014-13883).

Etymology. From the name *Argus*, an Argonaut, son of Phrixus; builder of the boat Argo. The name is considered a substantive in apposition.

Description. *Carapace:* As long as or slightly longer than broad; transverse ridges with dense short setae, and few scattered thick setae. Gastric region flattened with some transverse ridges: epigastric ridge indistinct, with 5 spines (1 median and 2 pairs of spines laterally); anterior protogastric ridge not medially interrupted, nearly extending laterally to carapace margin; anterior mesogastric ridge widely or minutely interrupted, laterally interrupted by anterior branch of cervical groove, continuing to first branchial spine; anterior metagastric ridge scale-like. Mid-transverse ridge not interrupted, medially depressed, preceded by distinct cervical groove, followed by 2 not interrupted or minutely interrupted ridges, interspersed with 1 short lateral ridge and few, short scattered scales. Lateral margins slightly convex, with 7 spines: first anterolateral spine well-developed, reaching end of lateral orbital spine, second spine (hepatic) small to well-developed, slightly dorsomesially from lateral margin, and followed by 5 branchial spines (3 anterior
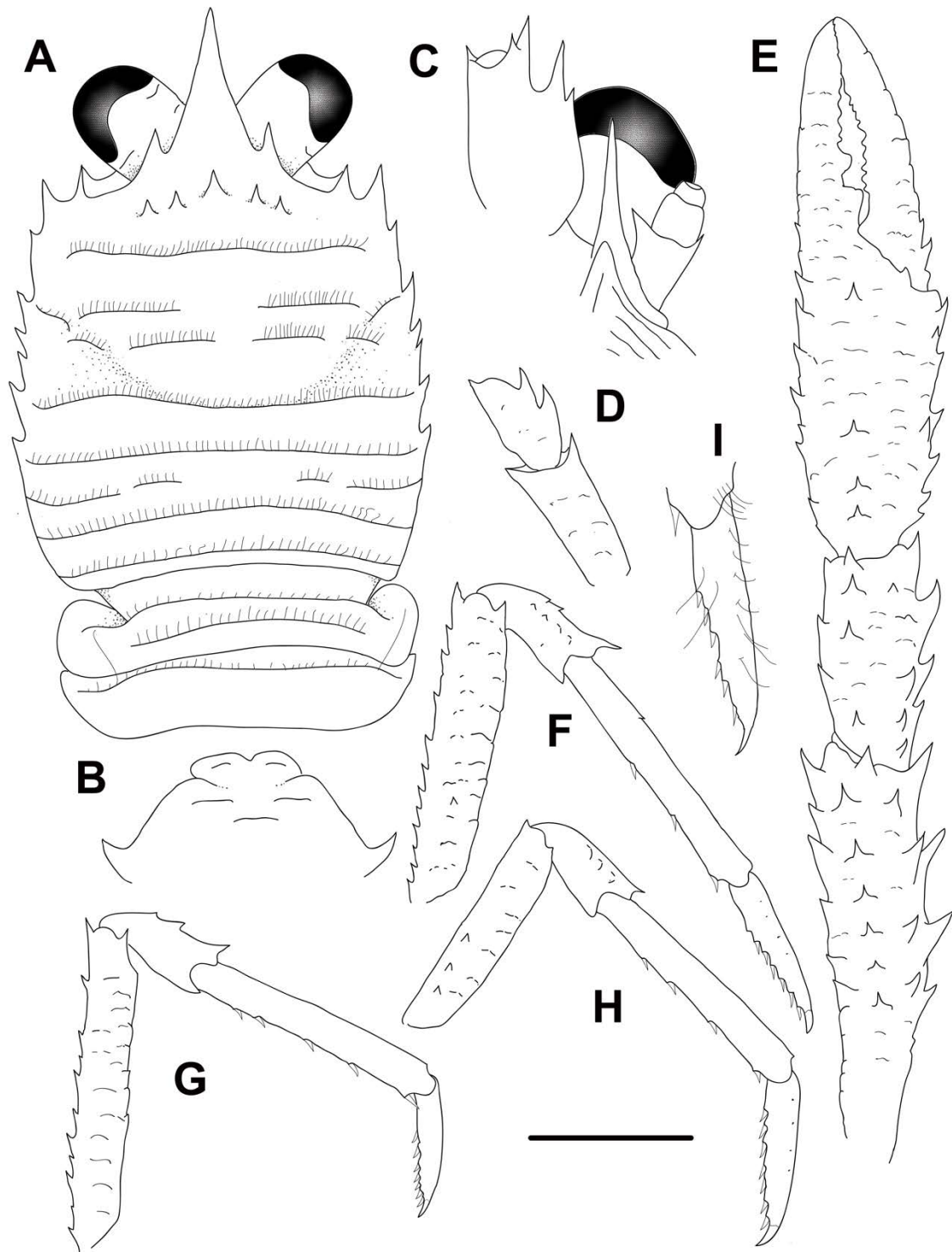
FIGURE 4. *Phylladiorhynchus argus* **n. sp**., holotype male 2.5 mm (MNHN-IU-2011-7659): A, carapace and pleon, dorsal view. B, thoracic sternites 3 and 4. C, left cephalic region, showing antennular and antennal peduncles, ventral view. D, right Mxp3, lateral view. E, left P1, dorsal view. F, right P2, lateral view. G, right P3, lateral view. H, right P4, lateral view. I, dactylus of right P2, lateral view. Scale bar: A, E-H = 1.0 mm; B–D, I = 0.6 mm.

well-developed subequal branchial spines and 2 well developed posterior branchial spines decreasing in size posteriorly). Rostrum triangular, horizontal, dorsally flattish or slightly concave, [1.5]1.2–1.6 times as long as broad, length [0.35]0.3–0.4 and breadth [0.25]0.2–0.3 that of carapace; lateral margins smooth and straight, with well-developed supraocular basal spines, subapical spines absent. Pterygostomian flap ending in blunt tooth, upper margin smooth.

Sternum: About as wide as long. Sternite 3 sharply broad, [4.0]–4.2 times as wide as long, anterior margin convex with a median deep notch flanked by 2 lobes. Sternite 4 widely contiguous to sternite 3; surface depressed in midline, smooth; greatest width [2.6]2.3–2.6 times that of sternite 3, [2.6]–2.8 times as wide as long.

Pleon: Transverse ridges with short setae and scattered few setae. Tergite 2 with anterior and posterior transverse elevated ridges; tergites 3 and 4 with anterior transverse ridge; tergites 5–6 smooth.

Eye: Eye stalk length about [1.2] times broader than long, peduncle distally setose, not distinctly expanded proximally; maximum corneal diameter [1.2] × rostrum width*,* as wide as eyestalk.

Antennule: Article 1 1.5 times longer than wide, with 5 spines: distomesial spine small; proximal lateral spine small, always present.

Antenna: Article 1 with prominent mesial process, distally falling well short of lateralmost antennular spine. Article 2 with distinct distal spines laterally and mesially. Articles 3 and 4 unarmed.

Mxp3: Ischium with distinct distal spines on flexor and extensor margins. Merus [0.6]0.6 × length of ischium, with well-developed distal spine on extensor margin and 2 strong spines on flexor margin.

P1: [3.1]3.5 (males), 2.8 (females) times carapace length; subcylindrical, spiny and with scattered long stiff setae and some few plumose setae; merus, carpus and palm with spines along mesial, dorsal and lateral surfaces, distal and mesial spines usually stronger than others. Merus [1.2]1.1–1.3 length of carapace, 1.7–[2.5] times as long as carpus. Carpus [2.0]–3.0 times as long as wide. Palm [1.4]1.1–1.5 × carpus length, [1.8]1.6–2.0 times as long as broad. Fingers 0.7–[1.0] × palm length; fixed finger unarmed; movable finger with well-developed basal spine .

P2–4: Slender, subcylindrical, moderately setose and spinose. Meri successively shorter posteriorly: P3 merus 0.7–[0.8]times length of P2 merus, P4 merus [0.7]–0.8 times

length of P3 merus. P2 merus, [0.8] or as long as carapace length, [5.5]–7.4 times as long as broad, [1.3]–1.6 times as long as P2 propodus; P3 merus [6.0]–6.2 times as long as broad, [1.3]–1.4 times as long as P3 propodus; P4 merus [4.5]–5.9 times as long as broad, [1.0]–1.3 times as long as P4 propodus; extensor margin of P2 and P3 with row of spines, proximally diminishing, with prominent distal spine; P4 extensor margin irregular with small distal spine; flexor margins of P2–4 irregular, each with distal spine; P4 lateral surface with median row of 3 small spines, absent in P2–3. Carpi with 3 or 4 spines on extensor margin on P2–3, unarmed on P4; distal spine prominent on P2–3, smaller on P4; row of small spines below extensor margin on lateral surface of P2–3, unarmed on P4; flexor margin unarmed. Propodi slender, [6.1–7.0]6.1–7.8 times as long as broad; extensor margin irregular, usually unarmed or armed with proximal spine on P2–3; flexor margin with 2–4 slender movable spines in addition to distal pair. Dactyli [0.6–0.7]0.6–0.7 × length of propodi, ending in incurved, strong, sharp spine; flexor margin with 7–8 movable spines.

Eggs: ov. F (MNHN-IU-2014-23836) 12 eggs of 0.3–0.4 mm diameter.

Colour. Unknown.

Genetic data. COI and 16S, Table 1.

Distribution. French Polynesia, New Caledonia and Chesterfield Islands from 170 to 610 m.

Remarks. *Phylladiorhynchus argus* belongs to the group of species that has 5 epigastric spines, the rostrum margin straight, the subapical spines of the rostrum absent, 3 spines on the anterior branchial margin, and the Mxp3 merus with two prominent spines along the flexor margin. *Phylladiorhynchus argus* closely resembles *P. acastus* from Philippines, Papua New Guinea, Vanuatu, Chesterfield Islands and New Caledonia, and *P. paulae*, from SW Indian Ocean (see the differences under the Remarks of *P. paulae*).

***Phylladiorhynchus asclepius* n. sp.**

(Figs. 5, 11E, 30G-I, Q, R)

Phylladiorhynchus integrirostris.—Macpherson, 2008: 293–294. (Dampier Archipelago, Western Australia).

Records requiring verification:

Phylladiorhynchus spinosus.—Schnabel & Ahyong, 2019: 335 (in part, only material from Western Australia).
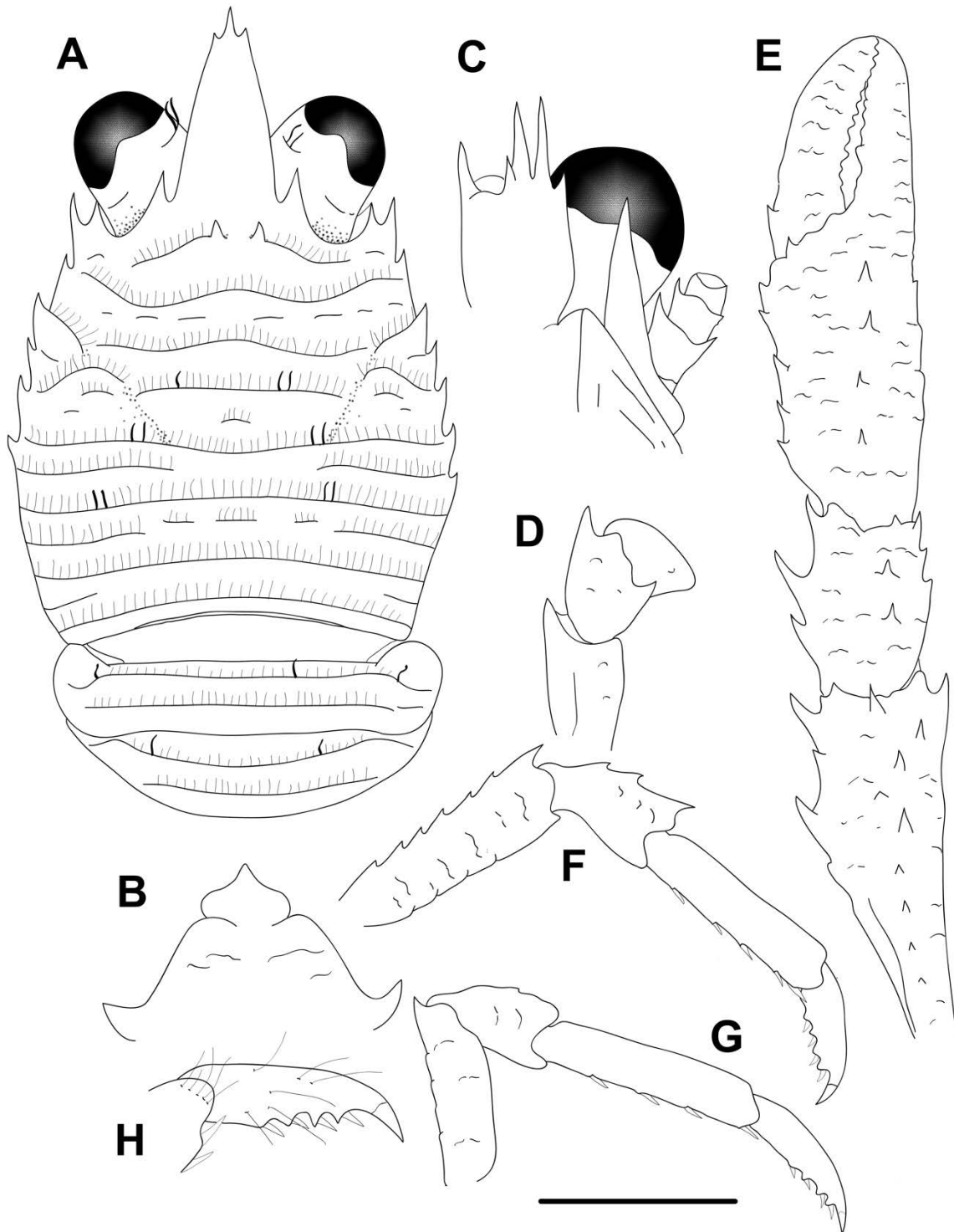
FIGURE 5. *Phylladiorhynchus asclepius* **n. sp**., holotype male 2.1 mm (UF22296): A, carapace and pleon, dorsal view. B, thoracic sternites 3 and 4. C, left cephalic region, showing antennular and antennal peduncles, ventral view. D, right Mxp3, lateral view. E, right P1, dorsal view. F, right P2, lateral view. G, right P4, lateral view. H, dactylus of right P2, lateral view. Scale bar: A, E-G = 1.0 mm; B–D, H = 0.6 mm.

Type material. Holotype. Western Australia. Ningaloo Reef. 22.6083ºS, 113.6249ºE, 10 m, 01 May 2009: M 2.1 mm (UF22296).

Paratypes. Western Australia. Dampier. Stn DA3/99/50 20º32.84'S, 116º26.73'E, 10–20 m, 31 August 1999: 1 M 2.4 mm, 2 ov. F 2.2–2.4 mm (WAM C27667).—Vulcan Shoal. Stn 146/K13, 12º47.958'S, 124º16.002'E, 19 m, 6 October 2013: 1 M 2.4 mm (WAM C55694-2).—Ningaloo Reef. 22.6083ºS, 113.6249ºE, 10 m, 1 May 2009: 1 ov. F 2.1 mm (UF22401).—22.681ºS, 113.6304ºE, 15 m, rubble, 20 May 2006: 1 M 2.4 mm (UF27886).—Norwegian Channel. 22.6006ºS, 113.6274ºE, 23 m (in rubble), 28 May 2006: 1 ov. F 2.1 mm (UF27601).

Etymology. From the name *Asclepius*, an Argonaut, son of Apollo and Coronis or Arsinoe. The name is considered a substantive in apposition.

Description. *Carapace:* Usually broader than long (0.8–[0.9] times as long as wide); transverse ridges with dense short setae and thick iridescent setae. Gastric region slightly convex with some transverse ridges: epigastric ridge distinct with 2 median spines and some lateral short scales, followed by small short scales on posterior epigastric region; anterior protogastric ridge not medially interrupted, nearly extending laterally to carapace margin, often followed by uninterrupted posterior protogastric ridge or short scales; anterior mesogastric ridge not medially interrupted, laterally interrupted by anterior branch of cervical groove, and continuing uninterrupted to first branchial spine; anterior metagastric ridge not medially interrupted, followed by posterior scale-like metagastric ridge. Mid-transverse ridge not interrupted, medially depressed, followed by shallow or indistinct cervical groove, followed by 2–3 not interrupted or minutely interrupted ridges, interspersed with 2 interrupted riges and some few short scales. Lateral margins convex, with 6 distinct spines: first anterolateral spine well-developed, reaching anteriorly to level of lateral orbital spine, second spine (hepatic) well-developed, slightly dorsomesially from lateral margin, and followed by 4 branchial spines (3 anterior and 1 posterior). Rostrum dagger-like, horizontal dorsally flattish or slighly concave [1.8]–2.0 times as long as broad, length [0.5]0.5 and breadth 0.2–[0.3] that of carapace; lateral margins smooth and straight or nearly straight, with well-developed supraocular basal spines and subapical spines. Pterygostomian flap with anterior spine, upper margin smooth.

Sternum: As wide as long. Sternite 3 moderately broad, [1.4]–2.1 times as wide as long, anterior margin convex, with a blunted median projection, anterolaterally rounded. Sternite 4 widely contiguous to sternite 3; anterolaterally smooth, surface depressed in midline, smooth; greatest width 2.6–[3.1] times that of sternite 3, [2.6]–3.3 times as wide as long.

Pleon: Elevated ridges with short setae and a few scattered long setae. Tergite 2–4 with anterior and posterior transverse elevated ridges; tergites 5–6 smooth.

Eye: Eye stalk length about 0.9–[1.1] times broader than long, peduncle distally setose, not distinctly expanded proximally, with few short transverse striae on lateral surfaces; cornea expanded distally, maximum corneal diameter [0.8]–1.0 × rostrum width, [0.8] as long as eyestalk.

Antennule: Article 1 longer than wide, with 5 distal spines: distomesial spine well-developed; proximal lateral spine small, always present.

Antenna: Article 1 with prominent mesial process, distally falling well short of lateralmost antennular spine. Article 2 with well-developed distomesial and distolateral spines. Article 3 with small to distinct spine. Article 4 unarmed.

Mxp3: Ischium with distinct distal spines on flexor and extensor margins. Merus [0.8]0.8 × length of ischium, with well-developed distal spine on extensor and flexor margins.

P1: [2.3]–2.7 (males), 2.0–2.1 (females) times carapace length; subcylindrical, spiny and with long stiff setae; merus, carpus and palm with spines along mesial, dorsal and lateral surfaces, distal and mesial spines usually stronger than others. Merus [0.8]–1.0 length of carapace, [2.0]–2.3 times as long as carpus. Carpus 1.2–[1.3] times as long as wide. Palm [1.3]1.3 × carpus length, [1.4]–1.5 times as long as broad. Fingers [0.9]–1.0× palm length; fixed finger with 0–1 basal spines; movable finger unarmed.

P2–4 (P3 lost in holotype): Setose and spinose. Meri successively shorter posteriorly: P3 merus 0.9 times length of P2 merus, P4 merus 0.8–0.9 times length of P3 merus. P2 merus, 0.6–[0.7] times carapace length, 3.3–3.8 times as long as broad, 1.1–1.2 times as long as P2 propodus; P3 merus 3.6–3.7 times as long as broad, 1.1–1.2 times as long as P3 propodus; P4 merus 3.7–4.0 times as long as broad, 1.0–1.1 times as long as P4 propodus; extensor margin of P2 and P3 with row of spines, proximally diminishing, with prominent distal spine; P4 extensor margin irregular, unarmed; flexor margin irregular, with distal spine on P2–3, absent or small on P4. Carpi with 2–4 small spines on extensor margin on P2–3, unarmed on P4; distal spine prominent on P2–3, absent on P4; row of granules below extensor margin on lateral surface of P2–4; flexor margin unarmed. Propodi stout, [4.0–4.5]3.8–4.0 times as long as broad; extensor margin irregular; flexor margin with 3–6 slender movable spines in addition to distal pair. Dactyli [0.6]0.6–0.7 × length of propodi, ending in incurved, strong, sharp spine; flexor margin with cuticular spines at basis of 5–6 movable spines.

Eggs: Ov. F carried approximately 8–15 eggs of 0.4–0.5 mm diameter.

Colour. Unknown.

Genetic data. COI and 16S, Table 1.

Distribution. Western Australia, from 10 to 23 m.

Remarks. *Phylladiorhynchus asclepius* belongs to the group of species having 2 epigastric spines, 1 hepatic spine, 3 spines on anterior branchial margin, rostrum dagger-like, (margin straights or nearly straight) and dactylar spines along the flexor margin of the P2–4 dactyli. This species complex includes the following species: *P. asclepius*, *P. euryalus*, from Australia **(**Queensland), New Caledonia and Chesterfield Islands, *P. lini,* and *P. spinosus* Schnabel & Ahyong, 2019. These species are morphologically very similar and genetically very distinct (see the differences under the Remarks of *P. spinosus*).

The mean intraspecific genetic divergences were 0.6% for COI and 0.2% for 16S.

Phylladiorhynchus australis Schnabel & Ahyong, 2019

(Fig. 11F)

Galathea pusilla.—Thomson, 1899: 193, pl. 21, fig. 7 (Wanganui, Cook Strait, Paterson Inlet, 14.6 m).—Chilton, 1906: 267. (Channel Islands, Auckland, 46 m).—Chilton, 1911: 303 (New Zealand, 64 m).—Borradaile, 1916: 92 (off Three Kings Islands and off North Cape, New Zealand, 183–128 m).—Hale, 1927: 80 (South Australia, 137 m).

Phylladiorhynchus pusillus.—Rowden *et al.*, 2010, tab. 3 (in part).

Phylladiorhynchus australis Schnabel & Ahyong, 2019: 304, figs. 2, 3, 15A (New Zealand and westward to southern Australia, 15–366 m).

Material examined. NIWA 76630, Stn. TAN1108/166, North Canterbury, 43.099–43.095°S, 173.446–173.444°E, 79 m, 26 May 2011: 4 M 4.4–5.2 mm, 1 ov. F 4.1 mm, 7F 4.0–4.8 mm. Donated to MNHN (MNHN-IU-2019-2596).

Genetic data. COI and 16S, Table 1.

Distribution. New Zealand continental shelf, from the Snares to the Three King Islands and northwards to Norfolk Island, and westward to southern Australia (New South Wales to South Australia), between 15 and 366 m (from Schnabel & Ahyong 2019).

Remarks. The species closely resembles *P. nui* Schnabel & Ahyong, 2019, from New Zealand and Eastern Australia and *P. integrus* (Benedict, 1902) from Japan to Chesterfield Islands (see the differences under the Remarks of *P. integrus*).

***Phylladiorhynchus bahamut* n. sp.**

(Figs. 6, 11G)

Phylladiorhynchus integrirostris.—Lewinsohn, 1982: 295, fig. 1 (Gulf of Aqaba, N Red
Sea).

Type material. *Holotype.* Saudi Arabia. Yanbu. Ras Majiz. Highly dissected reef, 38.2761º, 23.7725º, 4–8 m, 3 March 2014: 1 M 2.5 mm (UF40205).

Etymology. From *Bahamut*, a Persian sea monster supporting the structure that holds up the earth. The name is a substantive in apposition.

Description. *Carapace:* As long as or slightly longer than broad; transverse ridges with dense short setae and some scattered iridescent thick long setae. Gastric region slightly convex with 4 transverse ridges: epigastric ridge distinct with 2 median spines, short scales laterally; anterior protogastric ridge not medially interrupted, nearly extending laterally to carapace margin; anterior mesogastric ridge not medially interrupted, laterally continuing to first branchial spine; anterior metagastric ridge not medially interrupted, followed by median scale. Mid-transverse ridge not interrupted, medially depressed, cervical groove indistinct, followed by 2 not interrupted or minutely interrupted ridges, interspersed with 1 short lateral ridge and some few short scales. Lateral margins nearly straight or slightly convex, with 5 distinct spines: first anterolateral spine well-developed, reaching anteriorly to level of lateral orbital spine, second spine (hepatic) small, slightly dorsomesially from lateral margin, and followed by 3 branchial spines (2 anterior and 1 posterior). Rostrum leaf-like, horizontal, dorsally slightly concave, [1.4] times as long as broad, length [0.4] and breadth [0.2] that of carapace; lateral margins minutely serrated and convex, with well-developed supraocular basal spines, subapical spines absent. Pterygostomian flap ending in blunt tooth, upper margin smooth.

Sternum: As wide as long. Sternite 3 moderately broad, [1.7] times as wide as long, anterior margin serrated and convex, with a median projection. Sternite 4 widely contiguous to sternite 3; anterolaterally serrated, surface flattish, smooth; greatest width [3.2] times that of sternite 3, [2.9] times as wide as long.
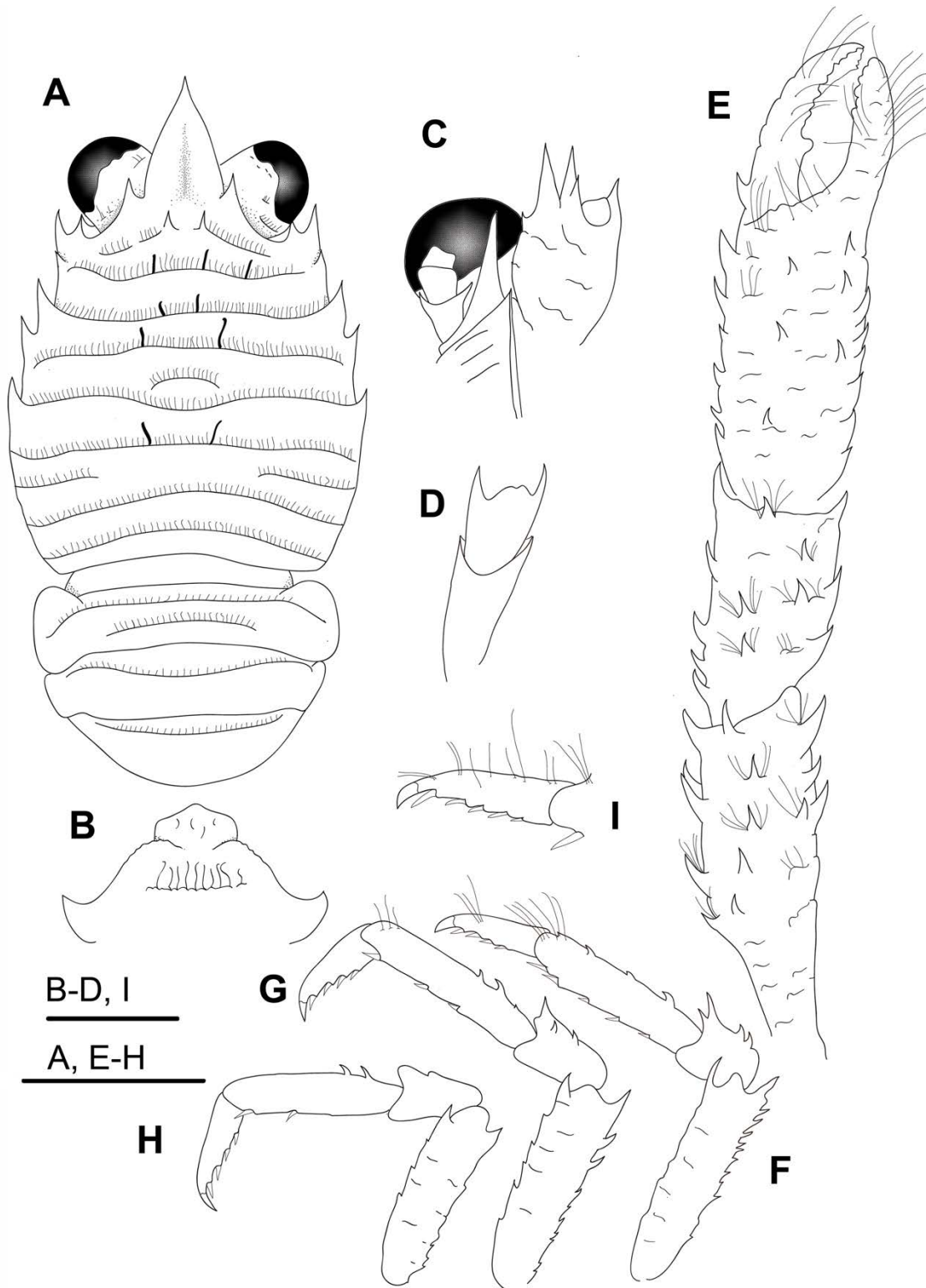
FIGURE 6. *Phylladiorhynchus bahamut* **n. sp**., holotype male 2.5 mm (UF40205): A, carapace and pleon, dorsal view. B, thoracic sternites 3 and 4. C, right cephalic region, showing antennular and antennal peduncles, ventral view. D, left Mxp3, lateral view. E, right P1, dorsal view. F, left P2, lateral view. G, left P3, lateral view. H, left P4, lateral view. I, dactylus of left P2, lateral view. Scale bars: 1.0 mm.

Pleon: Elevated ridges with short setae and a few scattered long setae. Tergite 2 with anterior and posterior transverse elevated ridges; tergites 3–4 with anterior transverse ridge only; tergites 5–6 smooth.

Eye: Eye stalk length about [1.1] times broader than long, peduncle distally setose, not distinctly expanded proximally; cornea expanded distally, maximum corneal diameter [1.1] × rostrum width*,* as wide as or wider than eyestalk.

Antennule: Article 1 slightly longer than wide, with 5 distal spines: distomesial spine well-developed; proximal lateral spine small, obsolescent.

Antenna: Article 1 with prominent mesial process, nearly reaching end of lateralmost antennular spine. Article 2 with well-developed distomesial and distolateral spines. Articles 3 and 4 unarmed.

Mxp3: Ischium with distinct distal spines on flexor and extensor margins. Merus [0.8] × length of ischium, with well-developed distal spine on extensor and flexor margins.

P1: [3.3] (male) times carapace length; subcylindrical, spiny and with long stiff setae, without plumose setae; merus, carpus and palm with spines along mesial, dorsal and lateral surfaces, distal and mesial spines usually stronger than others. Merus [1.1] length of carapace, [1.6] times as long as carpus. Carpus [1.8] times as long as wide. Palm [1.3] × carpus length, [2.1] times as long as broad. Fingers [0.7] × palm length; fixed finger with with small basal spine; movable finger unarmed.

P2–4: Slender, densely setose and spinose. Meri successively shorter posteriorly: P3 merus [0.9] times length of P2 merus; P4 merus [0.9] times length of P3 merus. P2 merus [4.7] times as long as broad, [1.3] times as long as P3 propodus; P3 merus [3.4] times as long as broad, [1.2] times as long as P3 propodus; P4 merus [3.6] times as long as broad, [1.1] times as long as P4 propodus; extensor margin of P3 with row of spines, proximally diminishing, with prominent distal spine; P4 extensor margin irregular, unarmed; flexor margin irregular, with distal spine on P3, distal spine absent in P4. Carpi with 1–3 spines on extensor margin on P3, unarmed on P4; distal spine prominent on P3, smaller on P4; granules below extensor margin on lateral surface of P3–4; flexor margin unarmed. Propodi stout, [4.5–4.6] times as long as broad; extensor margin irregular, armed with 2–4 spines on proximal half; flexor margin with 3–4 slender movable spines in addition to distal pair. Dactyli [0.6] × length of propodi, ending in incurved, strong, sharp spine; flexor margin with 4 movable spines.

Eggs: No data.

Colour. Unknown.

Genetic data. COI and 16S, Table 1.

Distribution. Red Sea, from 4 to 8 m.

Remarks. *Phylladiorhynchus bahamut* agrees with the species recorded and illustrated by Lewinsohn (1982) from the Gulf of Aqaba, who also pointed out that it might be a different species than *P. integrirostris. Phylladiorhynchus bahamut* belongs to the group of species having 2 median epigastric spines, the hepatic margin with a small spine and 2 spines on the anterior branchial margin. The closest species is *P. peneleos* (see the differences under the Remarks of this species).

***Phylladiorhynchus barbeae* n.sp.**

(Figs. 7, 11H, 54 B-C)

Type material. *Holotype.* Papua New Guinea. PAPUA NIUGINI Stn PR76 05°01.6'S, 145°47.9'E, 2–15 m, 21 November 2012: M 2.5 mm (MNHN- IU-2014-13813)

Paratypes. Papua New Guinea. PAPUA NIUGINI Stn PS07, 05°10.8'S, 145°49.8'E, 13 m, 8 November 2012: 1 ov. F 1.8 mm (MNHN-IU-2019-2670).—Stn PB13, 05°17.8'S, 145°46.9'E, 13 m, 12 November 2012: 1 M 2.3 mm, 1 F 2.4 mm (MNHN-IU-2019-2667).—Stn PB29, 05°18'S, 145°46.1'E, 17 m, 27 November 2012: 1 ov. F 1.6 mm (MNHN-IU-2019-2641).—Stn PB33, 05°09.1'S, 145°49.7'E, 30 m, 3 December 2012: 1 F 2.4 mm (MNHN-IU-2019-2668).—Stn PS08, 05°11.037'S, 145°48.431'E, 8 m, 30 December 2012: 1 M 1.4 mm (MNHN-IU-2014-13865).—Stn PB39, 05°15.9'S, 145°47.1'E, 18–27 m, 6 December 2012: 2 F 2.1–2.3 mm, 1 parasitized (MNHN-IU-2019-2638).—KAVIENG Stn KB16, 02°34.6'S, 150°46.3'E, 13–14 m, 7 June 2014: 1 M parasitized 1.8 mm (MNHN-IU2014-13619).—Stn KB20, 02°45.2'S, 150°41.7'E, 8 m, 9 June 2014: 1 ov. F 2.3 mm (MNHN-IU-2014-2311).

Vanuatu. SANTO Stn FB43, 15°28.4'S, 167°14.9'E, 19 m, 30 September 2006: 1 M 2.1 mm (MNHN-IU-2019-2642).—Stn FB68, 15°35.4'S, 166°59.7'E, 11 m, 11 October 2006: 1 M 2.5 mm (MNHN-IU-2014-13875).—Stn FB72, 15°36.1'S, 166°58.5'E, 16 m, 12 October 2006, 1 M 1.6 mm (MNHN-IU2014-13810).—Stn DB20, 15°30.5'S, 167°01.4'E, 20–25 m, 15 September 2006: 2 M 1.3–2.0 mm (MNHN- IU-2019-2630).—Stn ZR12, 15º36.7'S, 167º02.0'E, 2-30 m, 5 October 2006: 1 M 2.0 mm (MNHN-IU-2014-13808), 1 M 2.2 mm (MNHN-IU-2019-2643).

New Caledonia. Lagon Est. Stn 0607, 22°12.1'S, 167°02.5'E, 48–54 m, 5 August 1986: 1 ov. F 2.8 mm (MNHN-IU-2014-13740).—Touho. 20°36'36.27"S,
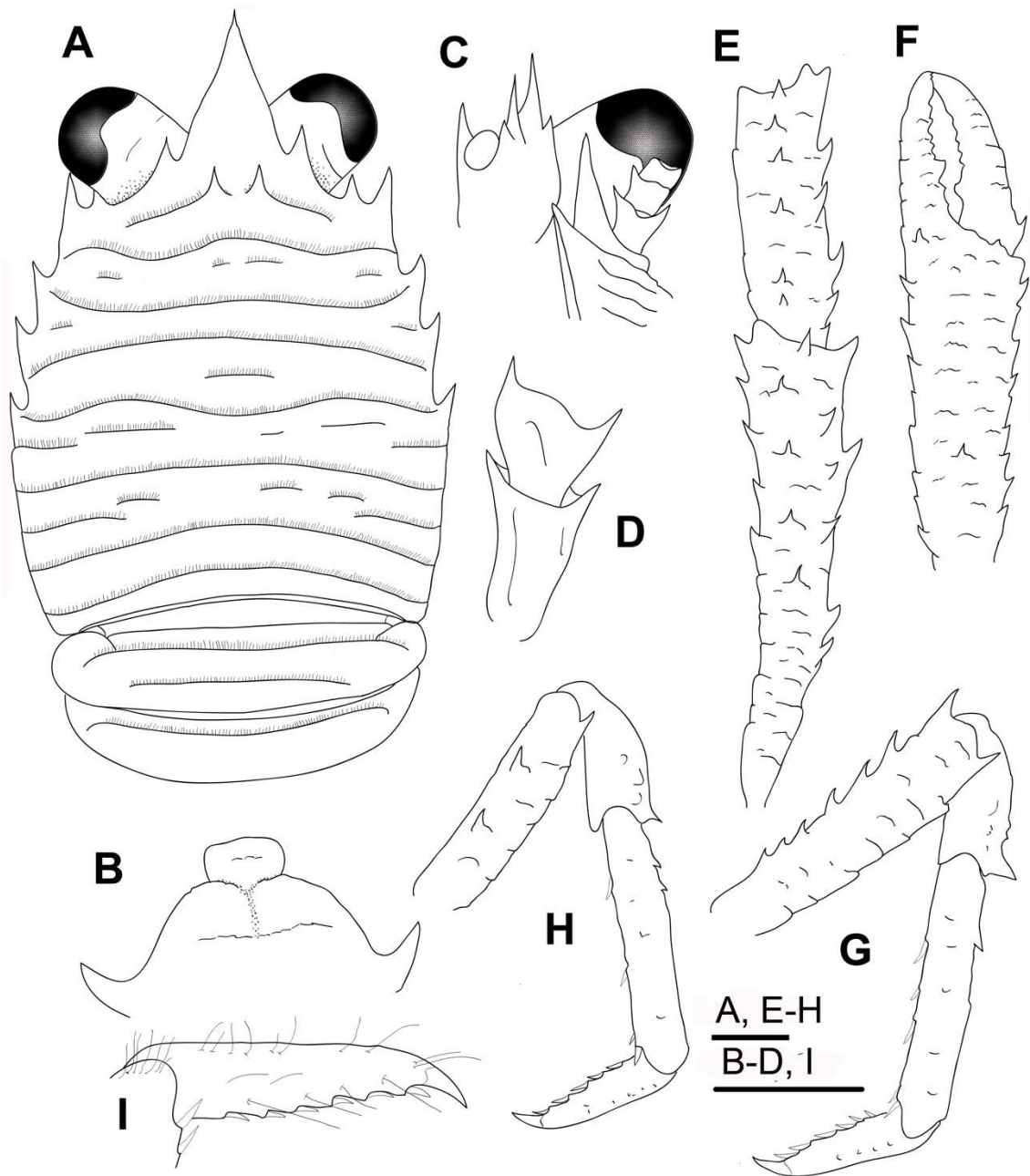
FIGURE 7. *Phylladiorhynchus barbeae* **n. sp**., A-D, G-I, holotype male 2.5 mm (MNHN-IU-2014-13813); E-F, paratype male 3.1 mm (MNHN-IU-13861): A, carapace and pleon, dorsal view. B, thoracic sternites 3 and 4. C, left cephalic region, showing antennular and antennal peduncles, ventral view. D, right Mxp3, lateral view. E, left P1, merus and carpus, dorsal view. F, left P1, propodus and dactylus, dorsal view right. G, right P2, lateral view. H, right P4, lateral view. I, dactylus of right P2, lateral view. Scale bar: A, E-H = 1.0 mm; B-D, I = 0.6 mm.

148

165°13'27.22"E, 5–7 m, September 1993: 1 M 3.1 mm, 1 ov. F 1.7 mm (MNHN-IU-2014-13861).

Etymology. Named after Any Barbé, mother of one of the authors, for her unremitting support.

Description. *Carapace:* as long as or slightly longer than broad; transverse ridges with dense short setae. Gastric region slightly convex, with 4 transverse ridges: epigastric ridge distinct with 2 median spines; anterior protogastric ridge not medially interrupted, nearly extending laterally to carapace margin, sometimes followed by a few short scales; anterior mesogastric ridge not medially interrupted, laterally continuing to first branchial spine, followed by some short lateral scales; anterior metagastric ridge not medially interrupted, followed by a short median scale. Mid-transverse ridge not interrupted, medially depressed, cervical groove indistinct, followed by 2–3 not interrupted or minutely interrupted ridges, interspersed with 2 short lateral ridge and sometimes few, short scattered scales. Lateral margins nearly straight or slightly convex, with 4 distinct spines: first anterolateral spine well-developed, reaching anteriorly to level of lateral orbital spine, hepatic margin unarmed; anterolateral spine followed by 3 branchial spines (2 anterior and 1 posterior). Rostrum leaf-like, horizontal, dorsally flattened, [1.2]1.1–1.5 times as long as broad, length [0.3]–0.4 and breadth [0.2]–0.3 that of carapace; lateral margins serrated and convex, with well-developed supraocular basal spines, subapical spines absent. Pterygostomian flap ending in blunt tooth, upper margin smooth.

Sternum: As wide as long. Sternite 3 moderately broad, [1.8]–2.0 times as wide as long, anterior margin serrated and slightly convex or straight. Sternite 4 widely contiguous to sternite 3; anterolaterally serrated, surface depressed in midline, smooth; greatest width 3.3–[3.4] times that of sternite 3, 2.5–[2.6] times as wide as long.

Pleon: Elevated ridges with short setae and a few scattered long setae. Tergite 2 with anterior and posterior transverse elevated ridges; tergites 3–4 with anterior transverse ridge; tergites 5–6 smooth.

Eye: Eye stalk length about 0.9–[1.0] times broader than long, peduncle distally setose, not distinctly expanded proximally; maximum corneal diameter [0.7]0.7 × rostrum width, as wide as eyestalk.

Antennule: Article 1 slightly longer than wide, with 5 distal spines: distomesial spine well-developed; proximal lateral spine small, always present.

Antenna: Article 1 with prominent mesial process, distally falling well short of lateralmost antennular spine. Article 2 with well-developed distomesial and distolateral spines. Article 3 often with distomesial spine. Article 4 unarmed.

Mxp3: Ischium with distinct distal spines on flexor and extensor margins; crista dentata with row of spines along entire margin. Merus [0.7]0.6–0.7 × length of ischium, with well-developed distal spine on extensor and flexor margins.

P1: Slender, 2.8–3.9 (males), 2.6–2.7 (females) times carapace length; subcylindrical, spiny and with long stiff setae and dense thick and plumose setae; merus, carpus and palm with spines along mesial, dorsal and lateral surfaces, distal and mesial spines usually stronger than others. Merus 0.9–1.4 length of carapace, 1.5–1.7 times as long as carpus. Carpus 3.0–3.4 times as long as wide. Palm 1.1 × carpus length, 2.9–3.0 times as long as broad. Fingers 0.6–0.7 × palm length; fixed finger unarmed; movable finger with a basal spine.

P2–4 (P3 lost in holotype): Slender, densely setose and spinose. Meri successively shorter posteriorly: P3 merus 0.6 times length of P2 merus, P4 merus 0.9 times length of P3 merus. P2 merus, [0.8]0.7 times carapace length, [4.0]3.9–4.2 times as long as broad, [1.0]1.1 times as long as P2 propodus; P3 merus 4.2 times as long as broad, 1–1.1 times as long as P3 propodus; P4 merus 4.2–4.7 [4.5] times as long as broad, [1.0]1.0–1.1 times as long as P4 propodus; extensor margin of P2 and P3 with row of spines, proximally diminishing, with prominent distal spine; P4 extensor margin irregular, unarmed; flexor margin irregular, with distal spine on P2–4, P4 lateral surface with median row of 2 spines. Carpi with 1–3 minute spines on extensor margin on P2–3, unarmed on P4; distal spine prominent on P2–3, smaller on P4; row of small granules below extensor margin on lateral surface of P2–4; flexor margin unarmed. Propodi slender, [5.5–6.5]5.2–7.2 times as long as broad; extensor margin irregular, armed with 1–4 spines on proximal half; flexor margin with 3–4 slender movable spines in addition to distal pair. Dactyli [0.6]0.6 × length of propodi, ending in incurved, strong, sharp spine; flexor margin with 5–6 movable spines.

Eggs: Ov. F carried approximately 10–20 eggs of 0.3–0.5 mm diameter.

Colour. Base colour of carapace and pleon whitish. Carapace and pleon covered by yellow-golden granules and reddish-brownish or orange patches and bands. Epigastric spines reddish-brownish and spines on carapace margin whitish. Rostrum and ocular peduncles with dense yellow granules, reddish-brownish or orange patches on peduncles and rostrum margins and tip. Pleonal tergites 2–4 with a median longitudinal reddish-brownish stripe. P1 whitish basally, covered by some reddish-brownish spots basally on

merus; carpus, palm light brown, spines reddish-brownish, fingers reddish-brownish. P2–4 light whitish, spines along flexor margins whitish; meri, propodi and dactyli with reddish-brownish stripes.

Genetic data. COI and 16S, Table 1.

Distribution. Papua New Guinea, Vanuatu, New Caledonia from 2 to 54 m.

Remarks. *Phylladiorhynchus barbeae* belongs to the group of species having 2 median epigastric spines, the hepatic margin unarmed and 2 spines on the anterior branchial margin. The closest species is *P. pepei* from Madagascar (see the differences under the Remarks of this species).

The mean intraspecific genetic divergences were 0.2% (COI) and 0% (16S).

Phylladiorhynchus bengalensis Tirmizi & Javed, 1980

Phylladiorhynchus bengalensis Tirmizi & Javed, 1980a: 258, fig. 2 (Andaman Sea, 77 m).—Tirmizi & Javed, 1993: 31, fig. 14 (redescription).—Baba, 2005: 304 (key, synonymies).—Baba *et al.*, 2008: 175 (compilation).—Schnabel & Ahyong, 2019: 304 (key).

Distribution. Only known from the type locality, Andaman Sea, at 77 m.

Remarks. The species is only known by the holotype male and it is characterized by the presence of 5 epigastric spines, 1 small hepatic spine, and 3 spines on the anterior branchial margin. The closest relative is *P. ikedai* (Miyake & Baba, 1965) from Bonin Islands, Japan. However, they can be easily differentiated by the shape of the thoracic sternite 3, with the anterior margin nearly transverse, and median and lateral projections, in *P. bengalensis,* whereas the sternite has the anterior margin convex, with feeble median excavation in *P. ikedai*.

***Phylladiorhynchus boucheti* n. sp.**

(Figs. 8, 11I)

Type material. *Holotype*. Chesterfield Islands. KANADEEP Stn DW4969, 21º00'S, 158º30'E, 500–750 m, 8 September 2017: M 2.6 mm (MNHN-IU-2017-3816)

Paratypes. Chesterfield Islands. KANADEEP Stn DW4969, 21º00'S, 158º30'E, 500–750 m, 8 September 2017: 1 M 3.0 mm (MNHN-IU-2019-2690).—Stn DW4993, 4º15'S, 166º58'E, 560–610 m, 13 September 2017: 1 ov. F 2.5 mm (MNHN-IU-2017-3830)
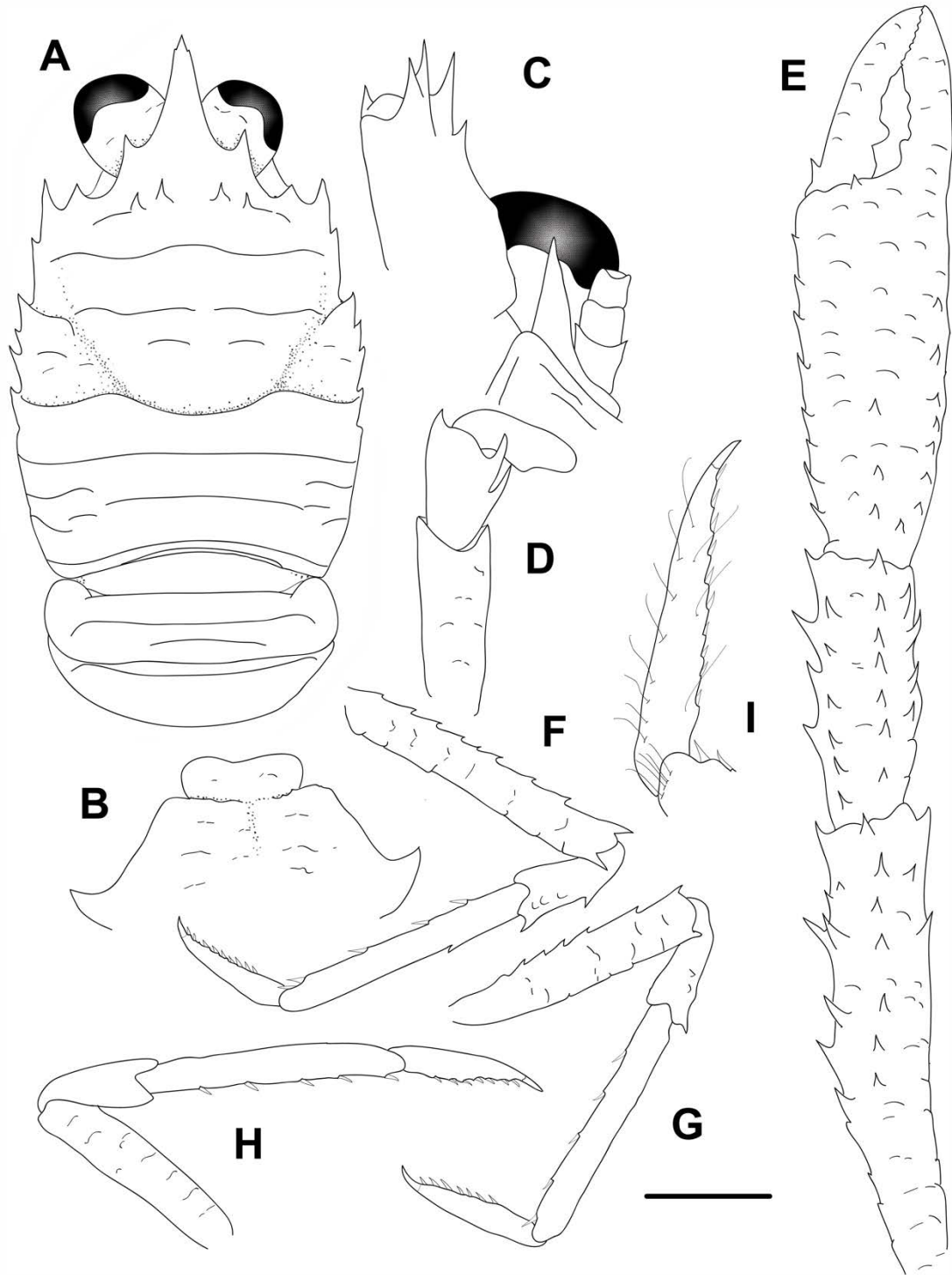
FIGURE 8. *Phylladiorhynchus boucheti* **n. sp**., holotype male 2.6 mm (MNHN-IU-2017-3816): A, carapace and pleon, dorsal view. B, thoracic sternites 3 and 4. C, left cephalic region, showing antennular and antennal peduncles, ventral view. D, left Mxp3, lateral view. E, right P1, dorsal view. F, right P2, lateral view. G, right P3, lateral view. H, right P4, lateral view. I, dactylus of right P2, lateral view. Scale bar: A, E-H = 1.0 mm; B–D, I = 0.6 mm.

Etymology. Named after Philippe Bouchet, head of conservation of the general mollusk collection of the Muséum national d'Histoire naturelle, Paris.

Description. *Carapace*: as long as or longer than broad ([1.0]–1.2 times as long as broad); transverse ridges with dense short setae, without long setae. Gastric region flattened, with 3 transverse ridges: epigastric ridge distinct with 4 spines; anterior protogastric ridge not medially interrupted, nearly extending laterally to carapace margin; anterior mesogastric ridge medially interrupted, laterally interrupted by cervical groove; anterior metagastric area with a few scales, otherwise absent. Mid-transverse ridge not interrupted, medially depressed, preceded by distinct cervical groove, followed by 2 not interrupted or minutely interrupted ridges, interspersed with 2 short lateral ridges and few, short scattered scales. Lateral margins straight or slightly convex, with 6–7 spines: first anterolateral spine well-developed, overreaching anteriorly level of lateral orbital spine, second spine (hepatic) well-developed, slightly dorsomesially from lateral margin, and followed by 4–5 branchial spines (3 anterior and 1–2 posterior). Rostrum subtriangular, horizontal, dorsally flattish or slightly concave, 0.8–[1.3] times as long as broad, length 0.2–[0.3] and breadth [0.3]0.3 that of carapace; lateral margins smooth and slightly concave, with well-developed supraocular basal spines, and minute subapical spines. Orbit sharply excavated. Pterygostomian flap ending in blunt tooth; upper margin smooth.

Sternum: As wide as long. Sternite 3 moderately broad, [3.5]–4.5 times as wide as long, anterior margin slightly concave, or straight, with median feeble excavation. Sternite 4 widely contiguous to sternite 3; surface depressed in midline, smooth; greatest width [3.0]3.0 times that of sternite 3, 2.7–[2.9] times as wide as long.

Pleon: Elevated ridges with a few scattered short setae. Tergite 2 with anterior and posterior transverse elevated ridges; tergites 3–4 with anterior transverse ridge; tergites 5–6 smooth.

Eye: Eye stalk length as broad as long, peduncle distally setose, not distinctly expanded proximally; maximum corneal diameter 1.0–[1.1] × rostrum width*,* as wide as eyestalk.

Antennule: Article 1 1.5 times longer than wide, with 5 distal spines: distomesial spine well-developed; proximal lateral spine small.

Antenna: Article 1 with prominent mesial process, distally clearly not reaching lateralmost antennular spine. Article 2 with minute distal spines laterally and mesially. Articles 3 and 4 unarmed.

Mxp3: Ischium with distinct distal spines on flexor and extensor margins. Merus [0.6]–0.7 × length of ischium, with well-developed distal spine on extensor margin and 2 strong spines on flexor margin.

P1: [3.9] times carapace length (male), 2.9 (female); subcylindrical, spiny and with scattered long stiff setae; merus, carpus and palm with spines along mesial, dorsal and lateral surfaces, mesial spines usually stronger than others. Merus 1.2–[1.6] length of carapace, [2.1]–2.3 times as long as carpus. Carpus [2.7]–3.5 times as long as wide. Palm 1.1–[1.3] × carpus length, [2.6]–2.7 times as long as broad. Fingers [0.6]–0.8 × palm length; fixed finger unarmed; movable finger with basal spine.

P2–4: Slender, subcylindrical, moderately setose and spinose. Meri successively shorter posteriorly: P3 merus 0.7–[0.8] times length of P2 merus, P4 merus 0.8–[0.9] times length of P3 merus. P2 merus, [0.9]0.9 times carapace length, [7.2]7.0–8.5 times as long as broad, [1.3]–1.4 times as long as P2 propodus; P3 merus [6.5]–9 times as long as broad, [1.1]–1.3 times as long as P3 propodus; P4 merus [5.4]5.0–7.1 times as long as broad, as long as P4 propodus; extensor margin of P2 and P3 with row of spines, proximally diminishing, with prominent distal spine; P4 extensor margin irregular, distal spine absent; flexor margins of P2–3 irregular, with distal spine, absent in P4. Carpi with 1–2 spines on extensor margin on P2–3, distal spine prominent, unarmed on P4; row of small spines below extensor margin on lateral surface of P2–3. Propodi slender, [5.5–7.0]7.1–9.0 times as long as broad; extensor margin irregular, usually armed with distinct spine on proximal half of P2; flexor margin with 4 slender movable spines in addition to distal pair. Dactyli [0.6]0.5–0.6 × length of propodi, ending in incurved, strong, sharp spine; flexor margin with 7–10 movable spines.

Eggs: Ov. F (MNHN-IU-2017-3830) carried 25 eggs of 0.3–0.5 mm diameter.

Colour. Unknown.

Genetic data. COI, Table 1.

Distribution. Chesterfield Islands, from 500 to 750 m.

Remarks. *Phylladiorhynchus boucheti* is characterized by the presence of a triangular rostrum, 4 epigastric spines, 3 spines on the anterior branchial margin of the carapace and Mxp3 merus with 2 spines on the flexor margin. *Phylladiorhynchus boucheti* closely resembles to *P. iphiclus* from French Polynesia and Vanuatu (see the differences under the Remarks of this species).

***Phylladiorhynchus butes* n. sp.**

(Figs. 9, 11J)

Phylladiorhynchus ikedai.—Baba, 1991, 485, fig. 4a (in part, only specimens from
MUSORSTOM 6, Stn CP401 [MNHN Ga-2044]).

Records requiring verification:

Phylladiorhynchus ikedai.—Baba, 2005: 200, 304 (Key Islands).

Type material. *Holotype.* Indonesia. KARUBAR Stn DW18, 05°18'S, 133°01'E, 205–
212 m, 24 October 1991: M 3.0 mm (MNHN-IU-2014-13803).

Paratypes. Indonesia. KARUBAR Stn DW18, 05°18'S, 133°01'E, 205–212 m, 25
October 1991: 1 F 2.7 mm (MNHN-IU-2019-2697).

New Caledonia. MUSORSTOM 6 Stn CP401, 20°42.15'S, 167°00.35'E, 270 m, 14
February 1989: 1 M 2.3 mm (MNHN-IU-2014-23834 (Ga-2044)).—EXBODI Stn
CP3829, 22°02'S, 167°05'E, 350–360 m, 8 September 2011: 1 ov. F 2.4 mm (MNHN-
IU-2019-2694).

Chesterfield Islands. EBISCO Stn DW2547, 21°06'S, 158°36'E, 356–438 m, 11
October 2005: 1 F 2.1 mm (MNHN-IU-2016-449).—KANADEEP Stn DW5025,
20º23'S, 158º40'E, 350–420 m, 21 September 2017: 1 M 2.6 mm (MNHN-IU-2017-
2754)**.**

French Polynesia. TARASOC Stn DW3503, 17°34'S, 149°18'W, 350 m, 25
October 2009: 2 ov. F 2.1–2.2 mm (MNHN-IU-2014-13735).

Etymology. From the name *Butes*, an Argonaut, son of Coronus. The name is
considered a substantive in apposition.

Description. *Carapace:* as long as or slightly longer than broad; transverse ridges
with dense short setae. Gastric region flattened with 4 transverse ridges: epigastric ridge
indistinct, with some few plumose setae, with 4–5 spines (1 median spine or one median
produced scale usually with thick plumose setae, and 2 pairs of spines laterally); anterior
protogastric ridge not medially interrupted, nearly extending laterally to carapace margin;
anterior mesogastric ridge not medially interrupted, or minutely interrupted, laterally
interrupted by anterior branch of cervical groove, continuing uninterrupted to first
branchial spine; anterior metagastric ridge scale-like. Mid-transverse ridge not
interrupted, preceded by shallow or undistinct cervical groove, followed by 2 not
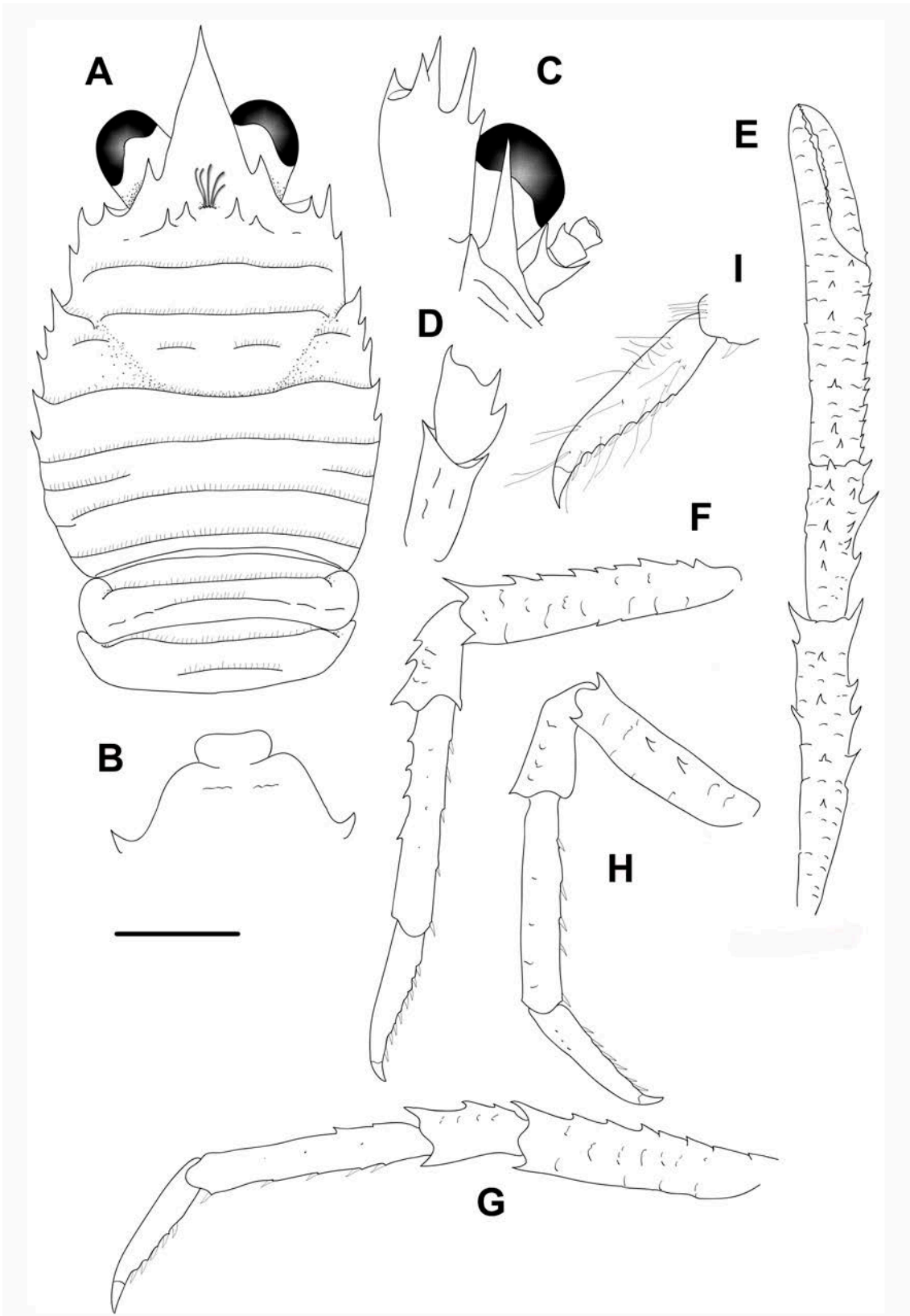
FIGURE 9. *Phylladiorhynchus butes* **n. sp**., A-D, F-I, holotype male 3.0 mm (MNHN-IU-2014-13803); E, paratype female 2.1 mm (MNHN-IU-2016-449): A, carapace and pleon, dorsal view. B, thoracic sternites 3 and 4. C, left cephalic region, showing antennular and antennal peduncles, ventral view. D, right Mxp3, lateral view. E, left P1, dorsal view. F, left P2, lateral view. G, left P3, lateral view. H, left P4, lateral view. I, dactylus of left P2, lateral view. Scale bar: A, E-H = 1.0 mm; B-D, I = 0.6 mm.

interrupted or minutely interrupted ridges, interspersed with 1–2 short lateral ridges and sometimes few, short scattered scales. Lateral margins slightly convex, with 7 spines: first anterolateral spine well-developed, reaching or exceeding level of lateral orbital spine, second spine (hepatic) small, slightly dorsomesially from lateral margin, and followed by 5 branchial spines (3 anterior and 2 posterior). Rostrum leaf-like, horizontal, dorsally flattish or slightly concave, [1.6]1.5–1.8 times as long as broad, length [0.4]–0.5 and breadth [0.3]0.3 that of carapace; lateral margins smooth and slightly convex, with well-developed supraocular basal spines, subapical spines minute or absent. Pterygostomian flap with anterior small spine; upper margin smooth.

Sternum: As wide as or slightly longer than wide. Sternite 3 quadrangular, 1.2–[1.7] times as wide as long, anterior margin straight or slightly convex, moderately produced anterolaterally. Sternite 4 widely contiguous to sternite 3; surface not depressed in midline, smooth; greatest width 2.4–[3.0] times that of sternite 3, 1.7–[2.2] times as wide as long.

Pleon: Elevated ridges with short setae and few scattered long setae. Tergite 2–3 with anterior and posterior transverse elevated ridges; tergite 4 with anterior transverse ridge; tergites 5–6 smooth.

Eye: Eye stalk length about [1.1] times broader than long, peduncle distally setose, not distinctly expanded proximally; maximum corneal diameter [1.1] × rostrum width, as wide as eyestalk.

Antennule: Article 1 1.3 times longer than wide, with 5 spines: distomesial spine well-developed; proximal lateral spine small, always present.

Antenna: Article 1 with prominent mesial process, nearly reaching end of lateralmost antennular spine. Article 2 with distinct distal spines laterally and mesially. Article 3 with small distomesial spine. Article 4 unarmed.

Mxp3: Ischium with distinct distal spines on flexor and extensor margins. Merus 0.5 × length of ischium with well-developed distal spine on extensor margin and 2 strong spines on flexor margin.

P1: 3.4–3.6 (males and females) times carapace length; slender, subcylindrical, spiny and with scattered long stiff setae; merus, carpus and palm with spines along mesial, dorsal and lateral surfaces, distal and mesial spines usually stronger than others. Merus 1.3–1.4 length of carapace, 1.9–2 times as long as carpus. Carpus 3.1–3.3 times as long as wide. Palm 1.3–1.4 × carpus length, 3.0–3.6 times as long as broad. Fingers unarmed, 0.7–0.8 × palm length.

P2–4: Slender, subcylindrical, moderately setose and spinose. Meri successively shorter posteriorly: P3 merus 0.8–[0.9] times length of P2 merus, P4 merus [0.8]–0.9 times length of P3 merus. P2 merus, [0.8]–0.9 times carapace length, [4.5]–5.5 times as long as broad, [1.3]1.2 times as long as P2 propodus; P3 merus [4.5]–5 times as long as broad, 1.1–[1.3] times as long as P3 propodus; P4 merus [4.0]–5.1 times as long as broad, [1.0]–1.2 times as long as P4 propodus; extensor margin of P2 and P3 with row of spines, proximally diminishing, with prominent distal spine; P4 extensor margin irregular, with small distal spine; flexor margins of P2–4 irregular, each with distal spine; P4 lateral surface with 1–2 small spines, absent in P2–3. Carpi with 3 or 4 spines on extensor margin on P2–3, unarmed on P4; distal spine prominent on P2–3, smaller on P4; row of small spines below extensor margin on lateral surface of P2–3, unarmed on P4; flexor margin unarmed. Propodi moderately slender, [5.5–6.0]6.0–7.5 times as long as broad; extensor margin irregular, usually armed with 2–4 small proximal spines on P2–3; flexor margin with 2–4 slender movable spines in addition to distal pair. Dactyli [0.6–0.7] 0.6–0.7 × length of propodi, ending in incurved, strong, sharp spine; flexor margin with 5–8 movable spines.

Eggs: Ov. F carried approximately 5–15 eggs of 0.4–0.6 mm diameter.

Colour. Unknown.

Genetic data. COI and 16S, Table 1.

Distribution. New Caledonia, Chesterfield Islands, Indonesia (Kei Islands), French Polynesia, from 205 to 438 m**.**

Remarks. *Phylladiorhynchus butes* belongs to the group of species having the epigastric ridge with 4 spines and often one median process or scale with thick plumose setae (rarely with 5 spines). *Phylladiorhynchus butes* resembles *P. cepheus*, from French Polynesia, and *P. maestrati*, from New Caledonia (see the differences under the Remarks of *P. maestratii*).

The mean intraspecific genetic divergences were 0.3% (COI) and 0.3% (16S).

***Phylladiorhynchus cepheus* n. sp.**

(Figs. 10, 11K)

Type material. *Holotype.* French Polynesia. BENTHAUS Stn DW2009, 22°32'S, 151°20'W, 320–450 m, 24 November 2002: ov. F 3.4 mm (MNHN-IU-2014-13860).
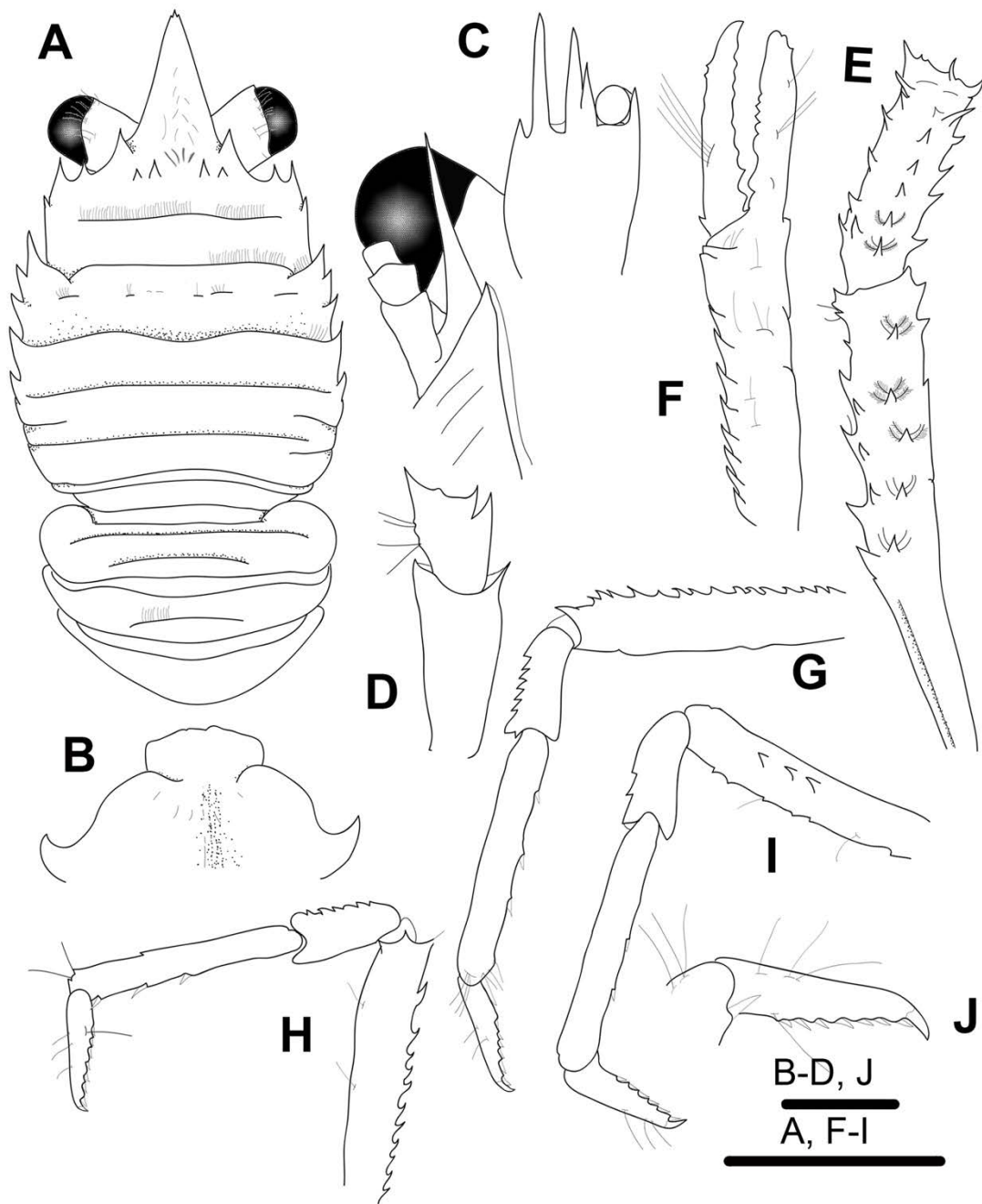
FIGURE 10. *Phylladiorhynchus cepheus* **n. sp**., A-D, G-I, holotype ovigerous female 3.4 mm (MNHN-IU-2014-13860): A, carapace and pleon, dorsal view. B, thoracic sternites 3 and 4. C, right cephalic region, showing antennular and antennal peduncles, ventral view. D, right Mxp3, lateral view. E, right P1, merus and carpus, dorsal view. F, right P1, propodus and dactylus, dorsal view right. G, left P2, lateral view. H, left P3, lateral view. I, left P4, lateral view. J, dactylus of right P2, lateral view. Scale bars: 1.0 mm.

Paratypes. French Polynesia. BENTHAUS Stn DW1945, 23°49'S, 147°42'W, 120–500 m, 17 November 2002: 1 M 2.4 mm (MNHN-IU-2014-13858).—Stn DW2006, 22°27'S, 151°19'W, 350–450 m, 24 November 2002: 1 M 2.7 mm, 1 ov. F 2.2 mm (MNHN-IU-2014-13882).—BENTHAUS Stn DW2009, 22°32'S, 151°20'W, 320–450 m, 24 November 2002: 1 ov. F 2.5 mm (MNHN-IU-2019-2686), 1 ov. F 3.1 (MNHN-IU-2014-13732).

Etymology. From the name *Cepheus*, an Argonaut, son of Coronus. The name is considered a substantive in apposition.

Description. *Carapace:* [1.1]–1.2 times as long as broad, transverse ridges with dense short setae. Gastric region flattened, with 3–4 transverse ridges: epigastric ridge indistinct, with a few plumose setae, and 4–5 spines (1 median spine or usually 1 median produced process or scale with thick setae, and 2 pairs of spines laterally); anterior protogastric ridge not medially interrupted; anterior mesogastric ridge not medially interrupted, laterally interrupted by cervical groove; anterior metagastric ridge scale-like, otherwise absent, with short scattered scales in anterior metagastric area . Mid-transverse ridge not interrupted, preceded by shallow or undistinct cervical groove, followed by 2 not interrupted or minutely interrupted ridges, interspersed with 1–2 short lateral ridges and few, short scattered scales. Lateral margins straight, with 7 spines: first anterolateral spine well-developed, reaching or exceeding level of lateral orbital spine, second spine (hepatic) small, slightly dorsomesially from lateral margin, and followed by 5 branchial spines (3 anterior and 2 posterior). Rostrum leaf-like, horizontal, dorsally flattish or slightly concave [1.5]–1.9 times as long as broad, length [0.4]0.4–0.5 and breadth [0.3]0.2–0.3 that of carapace; lateral margins smooth and slightly convex, with well-developed supraocular basal spines and minute subapical spines. Pterygostomian flap ending in blunt tooth; upper margin smooth.

Sternum: As wide as long. Sternite 3 moderately broad [2.3]2.0–2.5 times as wide as long, anterior margin convex. Sternite 4 widely contiguous to sternite 3; surface depressed in midline, smooth; greatest width [2.8]2.4–2.8 times that of sternite 3, [3.0]–3.0 times as wide as long.

Pleon: Elevated ridges with short setae. Tergite 2 with anterior and posterior transverse elevated ridges; tergites 3–4 with anterior transverse ridge; tergites 5–6 smooth.

Eye: Eye stalk length about [1.1]1.0–1.1 times broader than long, peduncle distally setose, not distinctly expanded proximally; maximum corneal diameter [0.8]–0.9 × rostrum width*,* as wide as eyestalk.

Antennule: Article 1.4 times longer than wide, with 5 distal spines: distomesial spine well-developed; proximal lateral spine small, always present.

Antenna: Article 1 with prominent mesial process, nearly reaching end of lateralmost antennular spine. Article 2 unarmed, sometimes with minute distolateral spine or granule. Articles 3 and 4 unarmed.

Mxp3: Ischium with distinct distal spines on flexor and extensor margins. Merus [0.6]0.5–0.6× length of ischium at midlength, extensor margin with well-developed distal spine, flexor margin with 2 strong spines.

P1: slender 4.5–5.0 times carapace length (males), [3.7]3.5–3.9 (females); subcylindrical, spiny and with scattered long stiff setae and dense plumose thick setae; merus, carpus and palm with spines along mesial, dorsal and lateral surfaces, mesial spines usually stronger than others. Merus [1.4]1.3–1.9 length of carapace, [2.1]–2.5 times as long as carpus. Carpus [3.3]2.4–3.3 times as long as wide. Palm [1.3]–1.4 × carpus length, [3.9]3.3–4.6 times as long as broad. Fingers [0.7]0.6–0.8 × palm length; fixed and movable fingers each with basal spine.

P2–4: Slender, subcylindrical, moderately setose and spinose. Meri successively shorter posteriorly: P3 merus [0.5]–0.6 times length of P2 merus, P4 merus 0.9–[1.0] times length of P3 merus. P2 merus, [0.8]–1.0 times carapace length, [5.4]–6.3 times as long as broad, [1.1]–1.3 times as long as P2 propodus; P3 merus [5.1]–5.3 times as long as broad, [1.2]1.2 times as long as P3 propodus; P4 merus 5.5–[5.9] times as long as broad, as long as P4 propodus; extensor margin of P2 and P3 with row of spines, proximally diminishing, with prominent distal spine; P4 extensor margin irregular, distal spine absent; flexor margins with distal spine in P2–3, absent in P4; P4 lateral surface with 3 small spines, absent in P2–3. Carpi with 8–9 small spines on extensor margin on P2–3 (serrated), with 2 small spines on P4; distal spine prominent on P2, smaller or absent in P3–4; flexor margin unarmed. Propodi slender, [7.5–8.0]7.8–8.0 times as long as broad; extensor margin irregular, usually unarmed; flexor margin with 2–3 slender movable spines in addition to distal pair. Dactyli [0.4–0.5]0.4–0.5 × length of propodi, ending in incurved, strong, sharp spine; flexor margin with 6–7 movable spines.

Eggs: Ov. F carried approximately 30–40 eggs of 0.3–0.4 mm diameter.

Colour. Unknown.

Genetic data. COI and 16S, Table 1.

Distribution. French Polynesia, from 230 to 500 m**.**

Remarks. *Phylladiorhynchus cepheus* belongs to the group that present the epigastric ridge with 4 spines and often one median process or scale with thick plumose setae (rarely with 5 spines), 3 spines on the anterior branchial margin of the carapace and the Mxp3 merus with two prominent spines along the flexor margin. *Phylladiorhynchus cepheus* closely resembles to *P. butes*, from New Caledonia, Chesterfield Islands, Indonesia and French Polynesia, and *P. maestratii*, from New Caledonia, (see the differences under the Remarks of *P. maestratii*).

Phylladiorhynchus eneus n. sp.

(Figs. 11L, 12)

Phylladiorhynchus ikedai.—Baba, 1991, 485 (in part only specimens from MUSORSTOM 4, Stn 151 [MNHN Ga-2042] and CALSUB, Pl 18 [MNHN Ga-2047]).

Records requiring verification:

Phylladiorhynchus ikedai.—Baba, 2005: 200, 304 (Kei Islands).

Type material. *Holotype.* Indonesia. KARUBAR Stn DW18, 05°18'S, 133°01'E, 205–212 m, 24 October 1991: M 3.0 mm (MNHN-IU-2014-13846).

Paratypes. Philippines. MUSORSTOM 2 Stn CP01, 14°00'N, 120°18'E, 188–198 m, 20 November 1980: 1 M 2.1 mm (MNHN-IU-2014-13801).

Indonesia. KARUBAR Stn DW18, 05°18'S, 133°01'E, 205–212 m, 24 October 1991: 1 F 2.8 mm (MNHN-IU-2016-497).—Stn DW50, 07°59'S, 133°02'E, 184–186 m, 30 October 1991: 1 F 1.7 mm (MNHN-IU-2014-13850).

Papua New Guinea. BIOPAPUA Stn DW3770, 05°34'S, 51°32'E, 220–294 m, 16 October 2010: 1 M 2.5 mm (MNHN-IU-2011-2157).

New Caledonia. MUSORSTOM 4 Stn DW151, 19º07'S, 163º22'E, 200 m, 14 September 1985: 1 M 2.2 mm (MNHN-IU-2014-23833 (Ga-2042)).—CALSUB Pl 18, 22º46'S, 167º20'E, 200–300 m, 29 March 1989: 1 M 2.3 mm (MNHN-IU-2014-23837 (Ga-2047)).—Lagon Nord. Stn DW1151, 19°01'S, 163°27'E, 270–280 m, 28 October 1989: 1 M 3.2 mm (MNHN-IU-2014-13798).—EXBODI Stn CP3833, 22°02'S, 167°04'E, 325–332 m, 8 September 2011: 1 M 2.4 mm (MNHN-IU-2019-2695).—KANACONO Stn CP4656, 22°40'S, 167°12'E, 219–244 m, 10 August 2016: 1 F 2.4 mm (MNHN-IU-2017-11637).—Stn CP4665, 22°52'S, 167°20'E, 535–563 m, 11 August 2016: 1 M 1.9 mm, 2 F 2.4–2.5 mm (MNHN- IU-2017-3954).
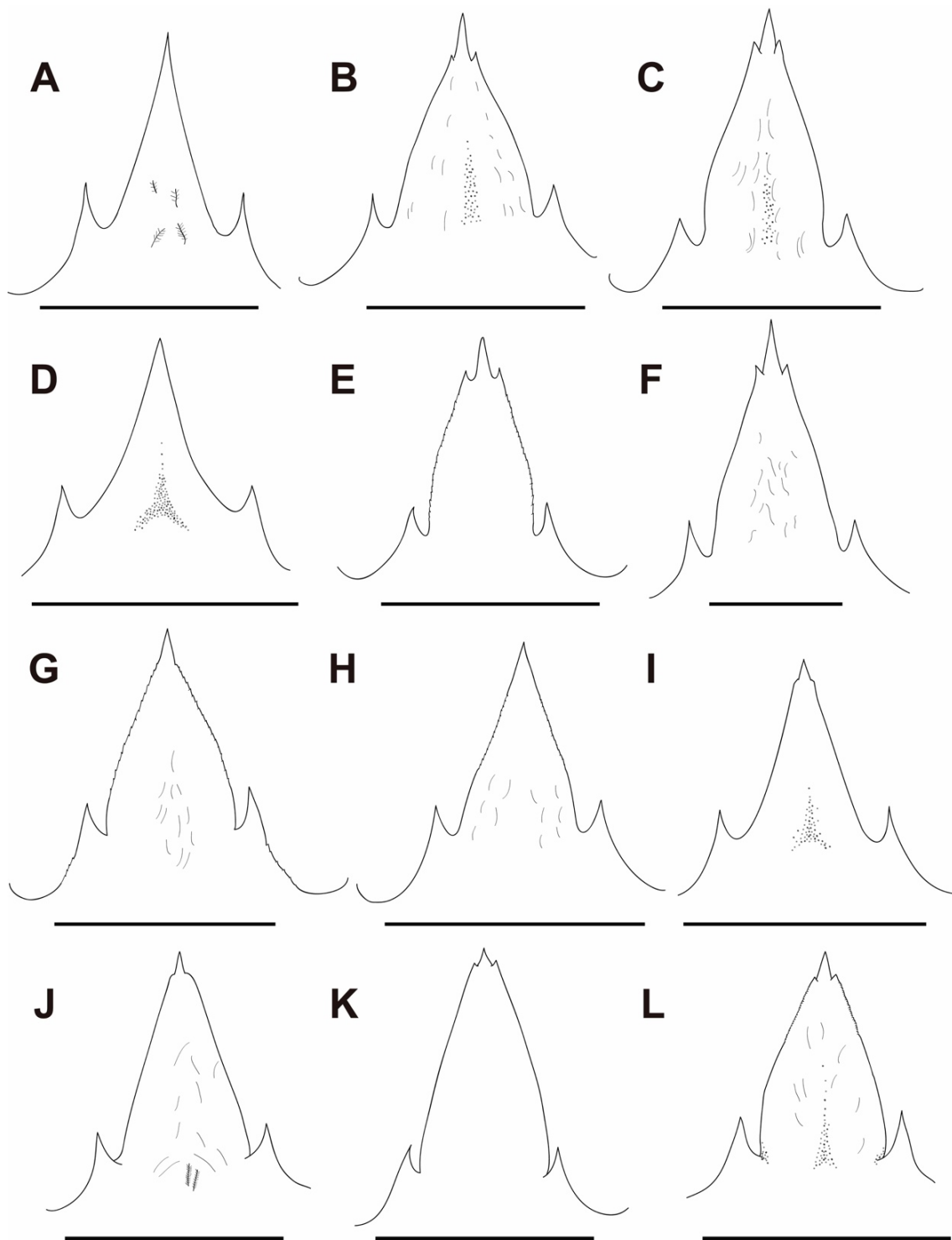
FIGURE 11. Rostrum, dorsal view. A, *Phylladiorhynchus acastus* **n. sp**., paratype male 2.6 mm (MNHN-IU-2017-2646). B, *P. amphion* **n. sp**., holotype male 2.4 mm (WAM C55691). C, *P. amphion* **n. sp**., paratype female 2.6 mm (WAM C53887). D, *P. argus* **n. sp**., paratype ovigerous female 3.5 mm (MNHN-IU-2014-23836). E, *P. asclepius* **n. sp**., paratype ovigerous female 2.1 mm (UF22401). F, *P. australis* Schnabel & Ahyong, 2019, female 4.0 mm (MNHN-IU-2019-2596). G, *P. bahamut* **n. sp**., holotype male 2.5 mm (UF40205). H, *P. barbeae* **n. sp**., paratype male 2.2 mm (MNHN-IU-2019-2643). I, *P. boucheti* **n. sp**., paratype ovigerous female 2.5 mm (MNHN-IU-2017-3830). J, *P. butes* **n. sp**., paratype female 2.1 mm (MNHN-IU-2016-449). K, *P. cepheus* **n. sp**., paratype male 2.4 mm (MNHN-IU-2014-13858). L, *P. eneus* **n. sp**., paratype male 2.1 mm (MNHN-IU-2014-13801). Scale bars = 1 mm.

163
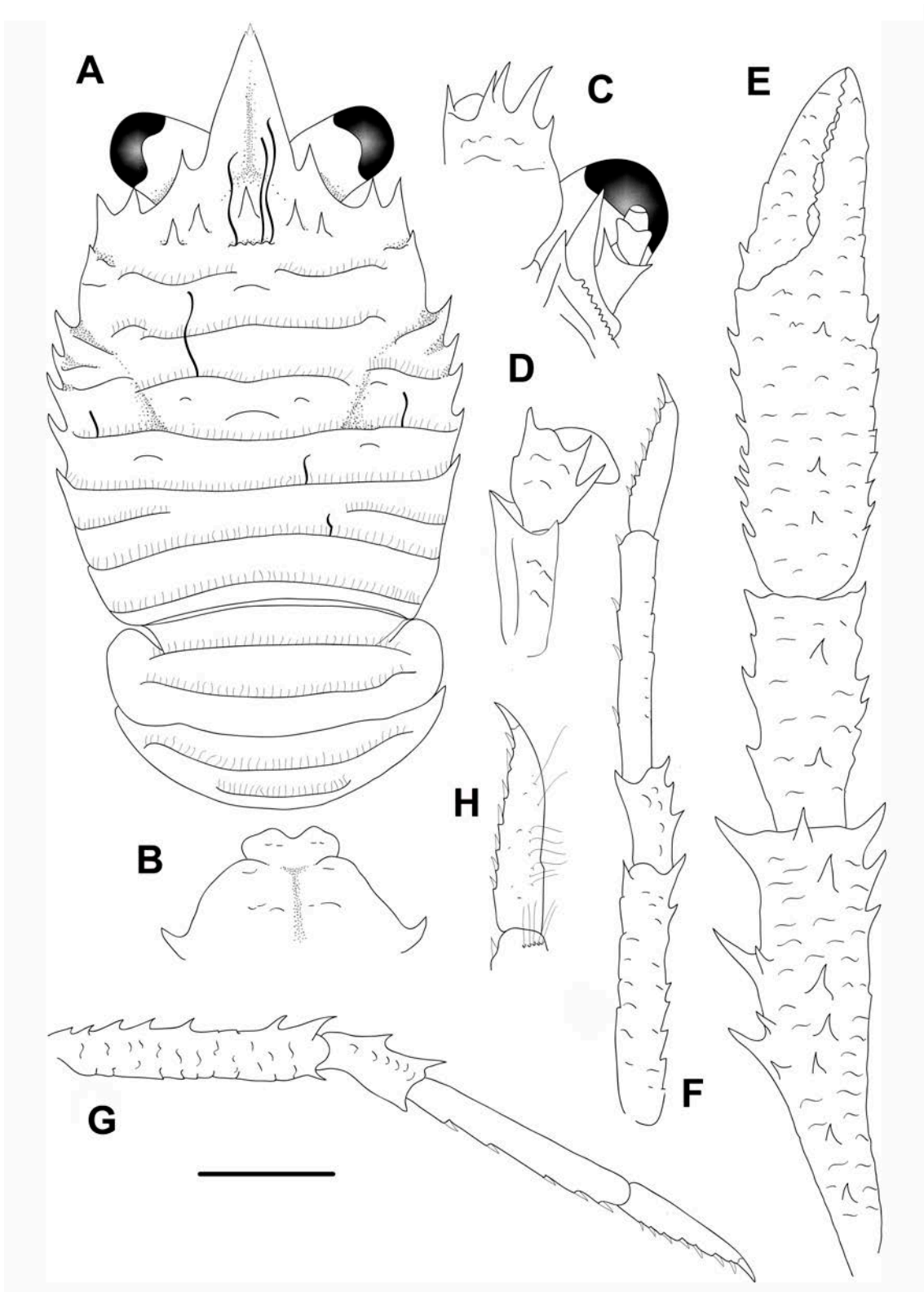
FIGURE 12. *Phylladiorhynchus eneus* **n. sp**., holotype male 3.0 mm (MNHN-IU-2014-13846): A, carapace and pleon, dorsal view. B, thoracic sternites 3 and 4. C, left cephalic region, showing antennular and antennal peduncles, ventral view. D, right Mxp3, lateral view. E, right P1, dorsal view. F, left P2, lateral view. G, right P3, lateral view. H, dactylus of left P2, lateral view. Scale bar: A, E-G = 1.0 mm; B–D, H = 0.6 mm.

Etymology. From the name *Eneus*, an Argonaut, son of Caeneus. The name is considered a substantive in apposition.

Description. *Carapace:* Moderately robust, 0.9–[1.0] times as long as broad; transverse ridges with dense short setae, and few scattered thick iridescent setae. Gastric region convex (uplifted dorsally) with some transverse ridges: epigastric ridge indistinct, with 5 spines (1 median and 2 pairs of spines laterally) followed by median scale behind epigastric ridge, often armed with very long thick plumose setae; anterior protogastric ridge medially interrupted, followed by 1 median scale in protogastric area; anterior mesogastric ridge not medially interrupted, laterally interrupted by anterior branch of cervical groove; anterior metagastric ridge not medially interrupted, and followed by a few scales on posterior metagastric region. Mid-transverse ridge medially depressed, not interrupted, preceded by distinct cervical groove, followed by 2 not interrupted or minutely interrupted ridges, interspersed with 1 short lateral ridge. Lateral margins clearly convex, with 7 spines: first anterolateral spine well-developed, reaching end of lateral orbital spine, second spine (hepatic) small, slightly dorsomesially from lateral margin, and followed by 5 branchial spines (3 anterior and 2 posterior). Rostrum leaf-like, horizontal, dorsally flattish or slightly concave, [1.3]–1.5 times as long as broad, length 0.3–[0.4] and breadth 0.2–[0.3] that of carapace; lateral margins serrated and convex, with well-developed supraocular basal spines, subapical spines minute or obsolescent. Pterygostomian flap ending in anterior spine, upper margin serrated.

Sternum: As wide as long or slightly wider than long. Sternite 3 moderately broad, [2.5]2–3 times as wide as long, anterior margin convex with a median deep notch. Sternite 4 widely contiguous to sternite 3; surface depressed in midline, smooth; greatest width [2.7]2.6–2.7 times that of sternite 3, [2.6]2.3–2.6 times as wide as long.

Pleon: Elevated ridges with short setae and a few scattered long setae. Tergites 2–3 with anterior and posterior transverse elevated ridges; tergite 4 with anterior transverse ridge; tergites 5–6 smooth.

Eye: Eye stalk length about 1.2–1.3 times broader than long, peduncle distally setose, not distinctly expanded proximally; maximum corneal diameter 0.75 × rostrum width, as wide as eyestalk.

Antennule: Article 1 slightly longer than wide, with 5 spines: distomesial spine small; proximal lateral spine small, always present.

Antenna: Article 1 with prominent mesial process, distally clearly not reaching lateralmost antennular spine. Article 2 with distinct distomesial and distolateral spines. Articles 3 and 4 unarmed.

Mxp3: Ischium with distinct distal spines on flexor and extensor margins. Merus 0.5–[0.6] × length of ischium, with well-developed distal spine on extensor margin and 2 strong spines on flexor margin.

P1: [3.1]3.0–3.3 (males), 2.8–2.9 (females) times carapace length; subcylindrical, spiny and with dense short setae and scattered long stiff setae; merus, carpus and palm with spines along mesial, dorsal and lateral surfaces, distal and mesial spines usually stronger than others. Merus [1.2]1.1–1.3 length of carapace, [2.0]–2.7 times as long as carpus. Carpus 1.8–[2.3] times as long as wide. Palm 1.2–[1.3]× carpus length, [2.2]–2.7 times as long as broad with parallel rows of spines running along lateral and mesial margin and scattered spines on dorsal and ventral surfaces. Fingers [0.75]0.7–0.9 × palm length fixed finger unarmed; movable finger with well-developed basal spine.

P2–4: Slender, subcylindrical, moderately setose and spinose. Meri successively shorter posteriorly: P3 merus [1.0]0.8–1.0 times length of P2 merus, P4 merus [lost in holotype]0.9 times length of P3 merus. P2 merus, [0.7]–0.8 times carapace length, 4.9–[5.0] times as long as broad, 1.1–[1.2] times as long as P2 propodus; P3 merus [6.0]–7.0 times as long as broad, [1.1]–1.3 times as long as P3 propodus; P4 merus 7.0 times as long as broad, as long as P4 propodus; extensor margin of P2 and P3 with row of spines, proximally diminishing, with prominent distal spine; P4 extensor margin irregular, with small distal spine; flexor margins of P2–4 irregular, each with distal spine; P4 lateral surface with median row of 4 small spines, absent in P2–3. Carpi with 2 or 3 spines on extensor margin on P2–3, unarmed on P4; distal spine prominent on P2–3, smaller on P4; row of small spines below extensor margin on lateral surface of P2–3, unarmed on P4; flexor margins of all P2–4 irregular, each with distal spine. Propodi slender, [7.5–8.5]7–10 times as long as broad; extensor margin irregular, usually unarmed; flexor margin with 3–4 slender movable spines in addition to distal pair. Dactyli [0.65–0.7]0.7–0.8 × length of propodi, ending in incurved, strong, sharp spine; flexor margin with 6–7 movable spines.

Eggs: No data.

Colour. Unknown.

Genetic data. COI, mini-barcode fragment (158 bp).

Distribution. Philippines, Indonesia, Papua New Guinea and New Caledonia, from 184 to 563 m.

Remarks. *Phylladiorhynchus eneus* belongs to the group of species having the epigastric ridge with 5 spines, 3 spines on the anterior branchial margin of the carapace

and the Mxp3 merus with 2 prominent spines along the flexor margin. This group contains the following species: *P. acastus* from the Philippines, Papua New Guinea, Vanuatu, Chesterfield Islands and New Caledonia, *P. argus*, from French Polynesia, New Caledonia and Chesterfield Islands, *P. paulae,* from SW Indian Ocean, and *P. erebus* Schnabel & Ahyong, 2019 from Norfolk and Kermadec Ridges. However, the new species can be distinguished from the other species of the group by the following characters:

-   One median scale behind the median epigastric spine in *P. eneus*, whereas this scale is absent in the other species.
-   The anterior protogastric ridge is medially interrupted or scale-like in *P. eneus*, whereas this ridge is not interrupted in the other species.
-   The P2–4 propodi are more slender (7–10 times longer than wide) in *P. eneus*, whereas these propodi are 4–7 times longer than wide in the other species.

The genetic divergences between *P. eneus* and other species were always higher than 18% (COI, based on the 158 bp mini-barcode). The two sequences of *P. eneus* from New Caledonia diverged 0.6%.

Phylladiorhynchus erebus Schnabel & Ahyong, 2019

Phylladiorhynchus erebus Schnabel & Ahyong, 2019: 311, figs. 4, 5.

Genetic data. COI, Table 1.

Distribution. New Zealand, Norfolk Ridge, at 378 m.

Remarks. This species is characterized by the presence of 5 epigastric spines, 3 spines on the anterior branchial margin and the anterior protogastric ridge usually medially interrupted. The species is closely related to *P. acastus* from the Philippines, Papua New Guinea, Vanuatu, Chesterfield Islands and New Caledonia, *P. argus*, from French Polynesia, New Caledonia and Chesterfield Islands, *P. paulae,* from SW Indian Ocean, and *P. eneus* from Indonesia to New Caledonia (see the differences under the Remarks of *P. eneus*).

Phylladiorhynchus euryalus n. sp.

(Figs. 13, 21A, 30A-C, M-N)

Phylladiorhynchus integrirostris.—Baba 1991: 486 (in part).
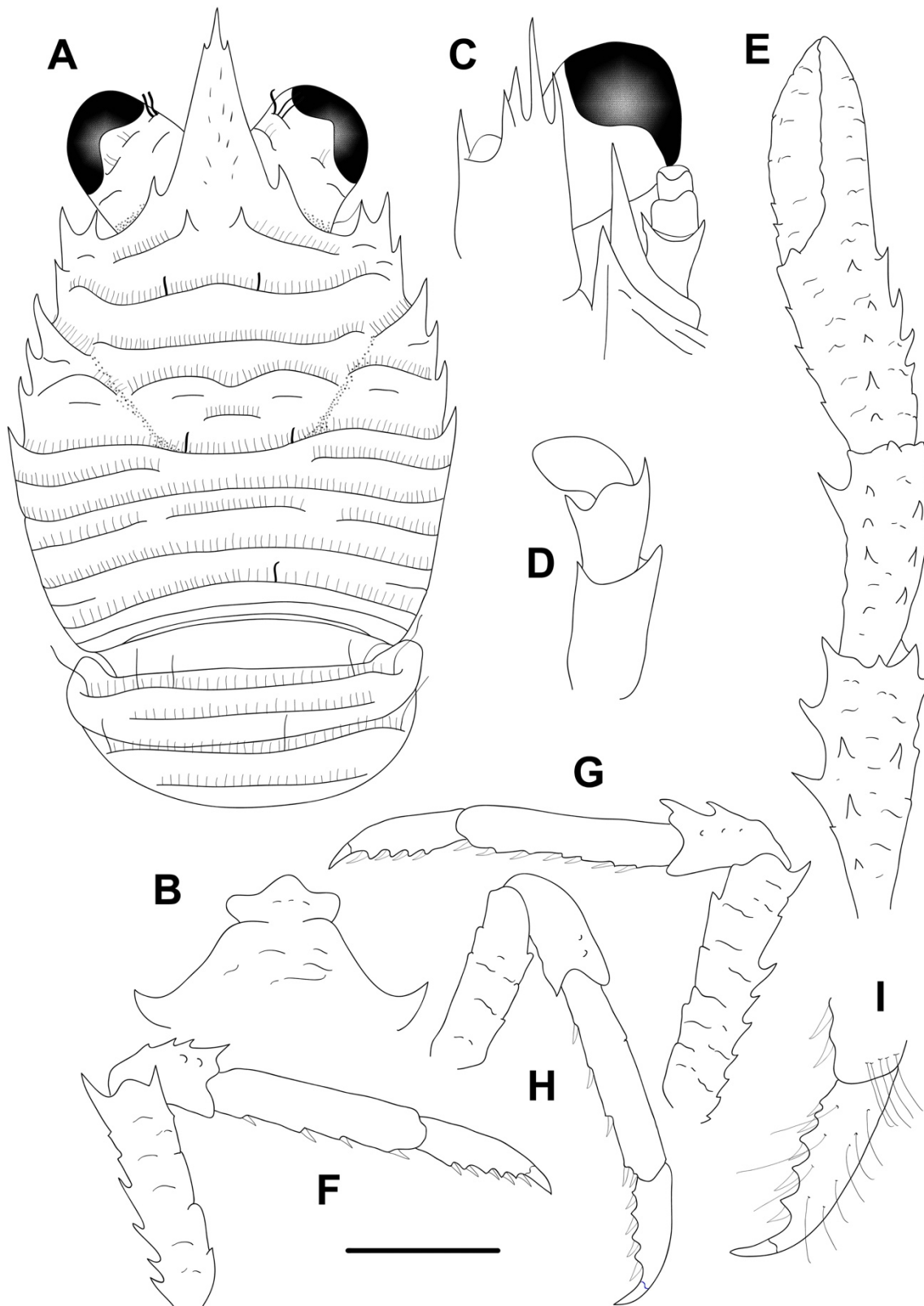
FIGURE 13. *Phylladiorhynchus euryalus* **n. sp**., holotype ovigerous female 2.8 mm (UF25255): A, carapace and pleon, dorsal view. B, thoracic sternites 3 and 4. C, left cephalic region, showing antennular and antennal peduncles, ventral view. D, left Mxp3, lateral view. E, right P1, dorsal view. F, right P2, lateral view. G, left P3, lateral view. H, right P4, lateral view. I, dactylus of right P2, lateral view. Scale bar: A, E-H = 1.0 mm; B–D, I = 0.6 mm.

Type material. *Holotype.* Australia. Queensland, Heron Is. 23.4733ºS, 151.9505ºE, no depth, 17 November 2006: ov. F 2.8 mm (UF25255).

Paratypes. Australia. Queensland, Heron Island. 23.4418ºS, 151.9004ºE, no depth, 16 November 2006: 1 M 1.8 mm (UF34732).—23.5545ºS, 152.0339ºE, no depth, 16 November 2006: 1 F 1.1 mm (UF26300).—23.4733ºS, 151.9505ºE, no depth, 17 November 2006: 1 F 1.8 mm (UF25213), 2 M 1.6–1.8 mm (UF25216), 1 ov. F 2.8 mm UF25255), 2 ov. F 2.1–2.3 mm (UF25215), 1 ov. F 2.7 mm (UF25222).

New Caledonia. Ouen Is. Prony Bay. Stn 101, 22º31.0'S, 166º35.9'E, 18 m, August 1984: 1 ov. F 2.8 mm (MNHN-IU-2019-2618).—Grand Recif Sud. Stn 297, 22º38.9'S, 116º45.6'E, 30 m, November 1984: 2 M 3.2–3.3 mm (MNHN-IU-2019-2612).—Stn 304, 22º39.8'S, 166º47.9'E, 27 m, November 1984: 1 M 3.2 mm, 2 ov. F 3.5–3.6 mm (MNHN-IU-2019-2617).—Stn 338, 22º44.7'S, 166º49.1'E, 32 m, November 1984: 1 M 3.2 mm (MNHN-IU-2019-2611).—Stn 291, 22º38.4'S 166º43.7'E, 31 m, November 1984: 1 M 2.7 mm (MNHN-IU-2019-2609).—Stn 296, 22º41'S, 166º44'E, 26 m, November 1984: 2 F 2.3–3.5 mm (MNHN-IU-2016-489).—Passe Sarcelle. 35–40 m, 1 ov. F 2.7 mm (MNHN-IU-2019-2610).—Lagon. Stn 336, 22º41.5'S, 166º51.4'E, 26 m, November 1984: 2 M 2.3–3.4 mm (MNHN-IU-2014-13911).—Recif Serrez. 7 m, 7 September 1992: 1 F 3.4 mm (MNHN-IU-2019-2615).—LIFOU Stn 1410, 20°56.7' S, 167°03.1' E, 2–4 m, 25 November 2000: 1 M 2.1 mm (MNHN-IU-2019-2604).

Chesterfield Islands. CORAIL 2 Stn DW101, 19°09'S 158°26,2'E, 37 m, 27 July 1988: 1 M 2.3 mm (MNHN-IU-2016-480 (Ga-2053)).—Stn CP23, 20°30.6'S, 161°03.6'E, 80–83 m, 22 July 1988: 2 ov. F 2.0–2.1 mm (MNHN-IU-2016-479 (Ga-2048)).—Stn CP24, 20°27.4'S, 161°04.7'E, 74–75 m, 22 July 1988: 1 ov. F 1.9 mm (MNHN-IU-2016-471 (Ga-2049)).—Stn DW33,19°25'S, 158°52,1'E, 52 m, 23 July 1988: 1 ov. F 2.1 mm (MNHN-IU-2016-478).

Etymology. From the name *Euryalus*, an Argonaut, son of Mecisteus. The name is considered a substantive in apposition.

Description. *Carapace:* As long as or slightly longer than broad; transverse ridges with dense short setae and thick iridescent setae. Gastric region slightly convex with some transverse ridges: epigastric ridge distinct with 2 median spines and some lateral short scales, followed by small short scales on posterior epigastric region; anterior protogastric ridge not medially interrupted, nearly extending laterally to carapace margin, often followed by uninterrupted posterior protogastric ridge or short scales; anterior mesogastric ridge not medially interrupted, laterally interrupted by anterior branch of cervical groove, and continuing uninterrupted to first branchial spine, often followed by

small scales; anterior metagastric ridge not medially interrupted, followed by posterior scale-like metagastric ridge. Mid-transverse ridge not interrupted, medially depressed, followed by shallow or indistinct cervical groove, followed by 2–3 not interrupted or minutely interrupted ridges, interspersed with 2 interrupted ridges and some few short scales. Lateral margins convex, with 6 distinct spines: first anterolateral spine well-developed, reaching anteriorly to level of lateral orbital spine, second spine (hepatic) well-developed, slightly dorsomesially from lateral margin, and followed by 4 branchial spines (3 anterior and 1 posterior). Rostrum dagger-like, horizontal dorsally flattish or slighly concave [1.5]–1.9 times as long as broad, length [0.4]–0.5 and breadth [0.3]0.3 that of carapace; lateral margins smooth and straight or nearly straight, with well-developed supraocular basal spines and subapical spines. Pterygostomian flap with anterior spine, upper margin smooth.

Sternum: As wide as long. Sternite 3 moderately broad, 2.2–[2.3] times as wide as long, anterior margin convex, with blunted median projection, anterolaterally rounded. Sternite 4 widely contiguous to sternite 3; anterolaterally smooth, surface depressed in midline, smooth; greatest width [2.7]–3.2 times that of sternite 3, [2.5]–4 times as wide as long.

Pleon: Elevated ridges with short setae and a few scattered long setae. Tergite 2–4 with anterior and posterior transverse elevated ridges; tergites 5–6 smooth.

Eye: Eye stalk length about 0.9–[1.1] times broader than long, peduncle distally setose, not distinctly expanded proximally, with few short transverse striae on lateral surfaces; cornea expanded distally, maximum corneal diameter 0.8–[0.9] × rostrum width, [0.8] as long as eyestalk.

Antennule: Article 1 longer than wide, with 5 distal spines: distomesial spine well-developed; proximal lateral spine prominent, reaching half-length of lateral spine, always present.

Antenna: Article 1 with prominent mesial process, distally falling well short of lateralmost antennular spine. Article 2 with well-developed distomesial and distolateral spines. Article 3 and 4 unarmed.

Mxp3: Ischium with distinct distal spines on flexor and extensor margins. Merus [1.1] × length of ischium, with well-developed distal spine on extensor and flexor margins.

P1: Moderately slender, 2.6–3.1 (males), 2.0–[2.2] (females) times carapace length; subcylindrical, spiny and with long stiff setae; merus, carpus and palm with spines along

mesial, dorsal and lateral surfaces, distal and mesial spines usually stronger than others. Merus [0.7]–1.3 length of carapace, [1.4]–1.6 times as long as carpus. Carpus 1.5–[2.2] times as long as wide. Palm [1.0]–1.1 × carpus length, [2.0]–2.1 times as long as broad. Fingers 0.9–[1.1.] × palm length; fixed finger with 0–1 basal spines; movable finger unarmed.

P2–4: Setose and spinose. Meri successively shorter posteriorly: P3 merus [0.8]–0.9 times length of P2 merus, P4 merus [0.8]–0.9 times length of P3 merus. P2 merus, 0.6–[0.7] times carapace length, 3.6–[4.3] times as long as broad, 1.1–[1.4] times as long as P2 propodus; P3 merus [3.6]–3.7 times as long as broad, 1.1–[1.4] times as long as P3 propodus; P4 merus 3.2–[3.6] times as long as broad, [1.1]1.1 times as long as P4 propodus; extensor margin of P2 and P3 with row of spines, proximally diminishing, with prominent distal spine; P4 extensor margin irregular, unarmed; flexor margin irregular, with distal spine on P2–3, absent or small on P4. Carpi with 2–4 small spines on extensor margin on P2–3, unarmed on P4; distal spine prominent on P2–3, absent on P4; row of granules below extensor margin on lateral surface of P2–4; flexor margin unarmed. Propodi stout, [3.0–4.0]3.6–4.0 times as long as broad; extensor margin irregular; flexor margin with 3–6 slender movable spines in addition to distal pair. Dactyli 0.6–[0.7] × length of propodi, ending in incurved, strong, sharp spine; flexor margin with cuticular spines at basis of 5–6 movable spines.

Eggs: Ov. F carried approximately 9–20 eggs of 0.5–0.6 mm diameter.

Colour. Unknown.

Genetic data. COI and 16S, Table 1.

Distribution. Australia, Queensland (Heron Islands), New Caledonia and Chesterfield Islands, from 2 to 83 m.

Remarks. *Phylladiorhynchus euryalus* belongs to the species-group having 2 epigastric spines, 1 hepatic spine, 3 spines on anterior branchial margin, rostrum dagger-like, (margin straight or nearly straight) and dactylar spines along the flexor margin of the P2–4 dactyli. This species complex includes the following species: *P. asclepius*, from Western Australia, *P. euryalus*, from Queensland, New Caledonia and Chesterfield Islands, *P. lini,* from Taiwan, and *P. spinosus* Schnabel & Ahyong, 2019, from New Zealand and New Caledonia. These species are morphologically very similar although genetically very distinct (see the differences under the Remarks of *P. spinosus*).

The mean intraspecific genetic divergences were 1.3% (COI) and 0.7% (16S).

***Phylladiorhynchus gustavi* n. sp.**

(Figs. 14, 21B, 27A-B, 54D)

Type material. *Holotype.* French Polynesia. Society Islands, Moorea Island, NE of Tareu Pass, 17.4836ºS, 149.8581ºW, 22 m, 24 July 2006: ov. F 2.2 (UF9766).

Paratypes. Cook Islands. Rarotonga Island, Matavera, 21.226ºS, 159.7293ºW, 9–24 m, 26 June 2006: 1 ov. F 2.0 mm (UF9232).

French Polynesia. Society Islands. Moorea Is. 17.506ºS, 149.759ºW, 15–22 m, 27 May 2006: 1 ov. F 1.8 mm (UF9471), 1 ov. F 2.0 (UF9603).—17.4836ºS, 149.8581ºW, 22 m, 24 July 2006: 1 M 1.7 (UF9756).—17.4768ºS, 149.8327ºW, 5 August 2006: 2 M 1.0–2.2 mm, 1 ov. F 2.1 mm (UF14832).—17.4764ºS, 149.8327ºW, 4–7 m, 10 November 2008: 1 M 2.3 mm (UF16338), 1 ov. F, 2.3 mm (UF16370), 1 M 2.4 mm, 1 ov. F 2.1 mm, 1 F 1.7 mm (UF18384),1 M 2.4 mm (UF16399).—Maharepa, 2 m, 11 October 2008: 1 ov. F 2.3 mm (UF15431).—on Pocillopora, June 2009: 1 M 2.0 mm (UF37850).—17.484ºS, 149.9264ºW, 19–20 m, 3 November 2009: 1 M 1.8 mm (UF23879).—17.4756ºS, 149.8425ºE, 13–17 m, 5 December 2009: 1 ov. F 2.2 mm (UF24183).—17.4764ºS, 149.8316ºW, 13 m, 31 January 2012: 4 M 1.4–2.1 mm, 9 ov. F 1.7–2.1 mm, 2 F 1.2–1.9 mm (UF33774).—17.4759ºS, 149.8419ºW, 13 m, 4 February 2012: 10 M 1.4–2.3 mm, 9 ov. F 1.6–2.3 mm, 1 F 1.9 mm (UF33968), 1 F 2.2 mm (UF33966), 1 M 2.0 mm (UF33967). Gambier Islands. Totegegie Airport, 23.0776ºS, 134.8884ºW, 22.5 m, 6 February 2013: 1 ov. F 2.3 mm (UF35486), 1 M 2.2 mm (UF35473), 1 F 1.8 mm (UF35479), 1 ov. F 2.5 mm (UF35481), 1 M 2.3 mm (UF35485).

French Polynesia. BENTHAUS Stn DW1926, 24°38.16'S, 146°00.82'W, 50–90 m, 13 November 2002: 1 M 2.2 mm, 1 ov. F 2.6 mm (MNHN- IU-2019-2592).

Etymology. The new species is named after our colleague Gustav Paulay from the Florida Museum of Natural History for his valuable contribution to marine research.

Description. *Carapace*: Slightly broader than long; transverse ridges with dense short setae and long and thick iridescent setae. Gastric region slightly convex with some transverse ridges: epigastric ridge distinct with 2 spines, short scales laterally; anterior protogastric ridge not medially interrupted, nearly extending laterally to carapace margin, sometimes followed by small scales; anterior mesogastric ridge not medially interrupted, laterally continuing to first branchial spine, sometimes followed by some short lateral scales; anterior metagastric ridge scale-like, often followed by some short small scale. Mid-transverse ridge not interrupted, medially depressed, cervical groove indistinct, followed by 2 not interrupted or minutely interrupted ridges, interspersed with 1 short
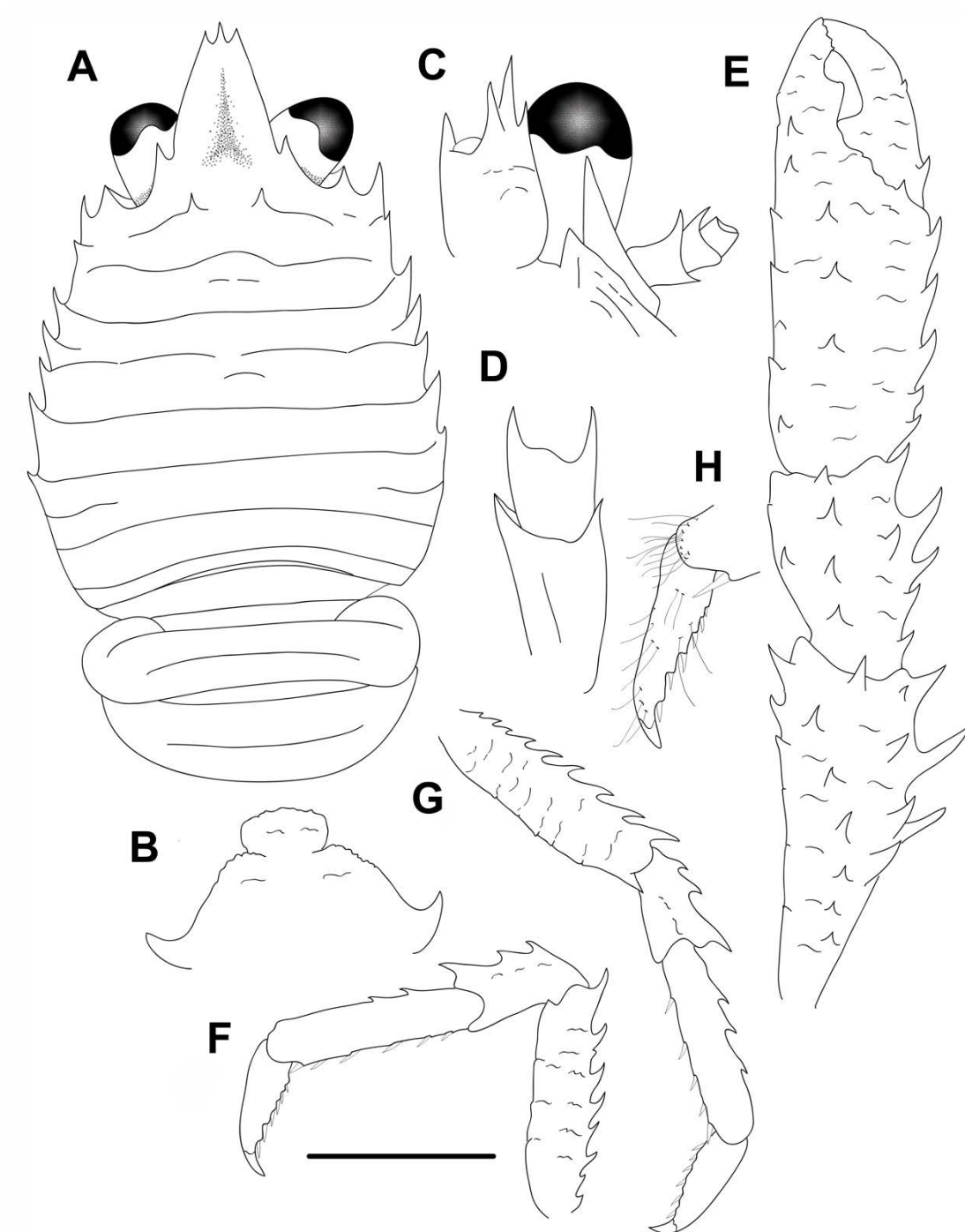
FIGURE 14. *Phylladiorhynchus gustavi* **n. sp**., holotype ovigerous female 2.2 mm (UF9766): A, carapace and pleon, dorsal view. B, thoracic sternites 3 and 4. C, left cephalic region, showing antennular and antennal peduncles, ventral view. D, right Mxp3, lateral view. E, left P1, dorsal view. F, left P2, lateral view. G, right P3, lateral view. H, dactylus of left P2, lateral view. Scale bar: A, E-G = 1.0 mm; B– D, H = 0.6 mm.

lateral ridge and some few short scales. Lateral margins slightly convex, with 6–7 distinct spines: first anterolateral spine well-developed, reaching anteriorly to level of lateral orbital spine, second spine (hepatic) small, slightly dorsomesially from lateral margin, and followed by 5 branchial spines (3 anterior and 1–2 posterior). Rostrum leaf-like, horizontal, dorsally concave, [1.1]–1.4 times as long as broad, length [0.3]–0.4 and breadth 0.2–[0.3] that of carapace; lateral margins serrated and strongly convex, with well-developed supraocular basal spines and small subapical spines (tridentiform). Pterygostomian flap ending in blunt tooth, upper margin smooth.

Sternum: As wide as long. Sternite 3 moderately broad, 1.8–[1.9] times as wide as long, anterior margin serrated and convex, anterolaterally rounded. Sternite 4 widely contiguous to sternite 3; anterolaterally serrated, surface depressed in midline, smooth; greatest width [3.3] times that of sternite 3, [2.5] times as wide as long.

Pleon: Elevated ridges with short setae and a few scattered long setae. Tergites 2–3 with anterior and posterior transverse elevated ridges; tergite 4 with anterior transverse ridge only; tergites 5–6 smooth.

Eye: Eye stalk length about 1.0–[1.1] times broader than long, peduncle distally setose, not distinctly expanded proximally; cornea expanded distally, maximum corneal diameter [0.6]–0.7 x × rostrum width, narrower than eyestalk, (0.8–0.9 maximum peduncle width).

Antennule: Article 1 slightly longer than wide, with 5 distal spines: distomesial spine well-developed; proximal lateral spine small, always present.

Antenna: Article 1 with prominent mesial process distally falling well short or overreaching lateralmost antennular spine. Article 2 with well-developed distomesial and distolateral spines. Article 3 with distomesial spine. Article 4 unarmed.

Mxp3: Ischium with distinct distal spines on flexor and extensor margins; crista dentata with row of spines along entire margin. Merus 0.7–[0.8] × length of ischium, with well-developed distal spine on extensor and flexor margins.

P1: [2.8]–3.0 (males), 1.9–2.0 (females) times carapace length; subcylindrical, spiny and with long stiff setae and iridescent setae; merus, carpus and palm with spines along mesial, dorsal and lateral surfaces, distal and mesial spines usually stronger than others. Merus 0.7–[1.0] length of carapace, [1.6]–1.9 times as long as carpus. Carpus [1.5]–1.7 times as long as wide. Palm [1.1]–1.2 × carpus length, [1.5]–1.6 times as long as broad. Fingers [0.8]0.8 × palm length fixed finger with 2 small basal spines, movable finger with basal spine or unarmed.

P2–4: Stout, setose, with iridiscent setae, and spinose. Meri successively shorter posteriorly: P3 merus [0.9]0.9 times length of P2 merus, P4 merus [0.8]–0.9 times length of P3 merus. P2 merus, [0.7]–0.9 times carapace length, 3.1–[3.4] times as long as broad, 1.1–[1.2] times as long as P2 propodus; P3 merus 3.4–[3.8] times as long as broad, 1.1–[1.2] times as long as P3 propodus; P4 merus 3.2 times as long as broad, 1.0–1.1 times as long as P4 propodus; extensor margin of P2 and P3 with row of spines, proximally diminishing, with prominent distal spine; P4 extensor margin irregular, unarmed; flexor margin irregular, with distal spine on P2–3, distal spine absent in P4. Carpi with 1–3 spines on extensor margin on P2–3, unarmed on P4; distal spine prominent on P2–3, smaller on P4; granules below extensor margin on lateral surface of P2–4; flexor margin unarmed. Propodi stout, [4.0]3.6–4.3 times as long as broad; extensor margin irregular, armed with 2–4 spines on proximal half; flexor margin with 3–6 slender movable spines in addition to distal pair. Dactyli [0.6]0.6–0.7 × length of propodi, ending in incurved, strong, sharp spine; flexor margin with 5–6 movable spines.

Eggs: Ov. F carried approximately 8–20 eggs of 0.4–0.6 mm diameter.

Colour. Base colour of carapace whitish or beige, gastric and cardiac region covered by yellow granules, two brownish patches behind mid-transverse ridge, epigastric spines brownish, marginal spines whitish, with some small brownish patches. Rostrum margin and orbit margins whitish, some yellow spots covering peduncles and rostrum basis, supraocular spines, tip and rostrum margin translucent. Pleonal tergites 1–4 beige, with dense whitish granules; anterior ridges of tergites 2–4 whitish, with brownish stripes. P1 whitish or beige with scattered brownish spots, spines whitish, tip of fingers light brown. P2–4 whitish, spines along flexor margins whitish or brown; meri whitish basally and meri with brownish bands, dactili brownish.

Genetic data. COI, Table 1.

Distribution. French Polynesia, Society Islands, between 2 and 90 m.

Remarks. *Phylladiorhynchus gustavi* belongs to the group of species having 2 epigastric spines, 1 hepatic spine and 3 spines on anterior branchial margin. The closest species is *P. laureae*, from from Japan, Mariana Islands, American Samoa, Papua New Guinea, Vanuatu and New Caledonia, (see the differences under the Remarks of this species).

The mean intraspecific genetic divergence in *P. gustavi* was 0.4% (COI).

Phylladiorhynchus heptacanthus n. sp.

(Figs. 15, 21C)

Type material. *Holotype*. Chesterfield Islands. KANADEEP Stn DW4960, 23º04'S, 159º28'E, 310 m, 6 September 2017: F 2.1 mm (MNHN-IU-2017-2534).

Paratypes. Chesterfield Islands. EBISCO no Stn number: 1 ov. F 1.8 mm (MNHN-IU-2014-13851). KANADEEP Stn DW4950, 24º05'S, 159º42'E, 330–500 m, 5 September 2017: 1 M 2.2 mm (MNHN-IU-2017-2515).—Stn CP4953, 24º10'S, 159º41'E, 270–320 m, 5 September 2017: 4 M 1.0–1.4 mm, 2 ov. F 1.6–1.8 mm, 6 F 1.4–1.8 mm (MNHN-IU-2017-3326).—Stn DW4961, 23º02'S, 159º28'E, 300–430 m, 6 September 2017: 1 F 2.2 mm (MNHN-IU-2017-2729).

New Caledonia. KANACONO Stn CP4673, 22°47'S, 167°27'E, 244–285 m, 13 August 2016: 1 ov. F 1.9 mm (MNHN-IU-2017-11724).

Etymology. From the Greek *hepta*, seven, and *akantha,* spine, in reference to the seven spines on the dorsal surface of the carapace.

Description. *Carapace:* Robust or massive, [0.8]0.8–0.9 times as long as broad; transverse ridges elevated, serrated, with few short setae, and few scattered long thick iridescent setae. Gastric region convex (uplifted dorsally) with transverse scale-like ridges: epigastric ridge indistinct, with 5 spines (1 median and and 2 pairs of spines laterally), followed by 1 scale behind median epigastric spine; anterior protogastric ridge undistinct or scale like, not continuing laterally to carapace margin, armed with 1 parahepatic spine on each side, behind lateralmost epigastric spines, posterior protogastric area scale-like; anterior mesogastric ridge undistinct with some few scales or scale-like, laterally continuing with some few scales, posterior mesogastric ridge scale-like; anterior metagastric ridge scale-like, followed by small scale(s) on posterior metagastric region. Mid-transverse ridge not interrupted, medially depressed, serrated laterally, preceded by distinct cervical groove, followed by 2 not interrupted or minutely interrupted ridges, interspersed with 1 short lateral ridge and some few scales. Lateral margins clearly convex, with 7 spines: first anterolateral spine well-developed, not reaching anteriorly end of strong lateral orbital spine, second spine (hepatic) well-developed, and followed by 5 branchial spines (3 anterior and 2 posterior). Rostrum leaf-like, dorsally sharply concave in anteroposterior midline, [1.1]1.0–3.0 times as long as broad, length [0.4]–0.4 and breadth [0.3]0.3 that of carapace; lateral margins serrated and convex, with small supraocular basal spines, subapical spines absent. Pterygostomian flap ending in anterior spine, upper margin smooth, with series of elevated ridges.
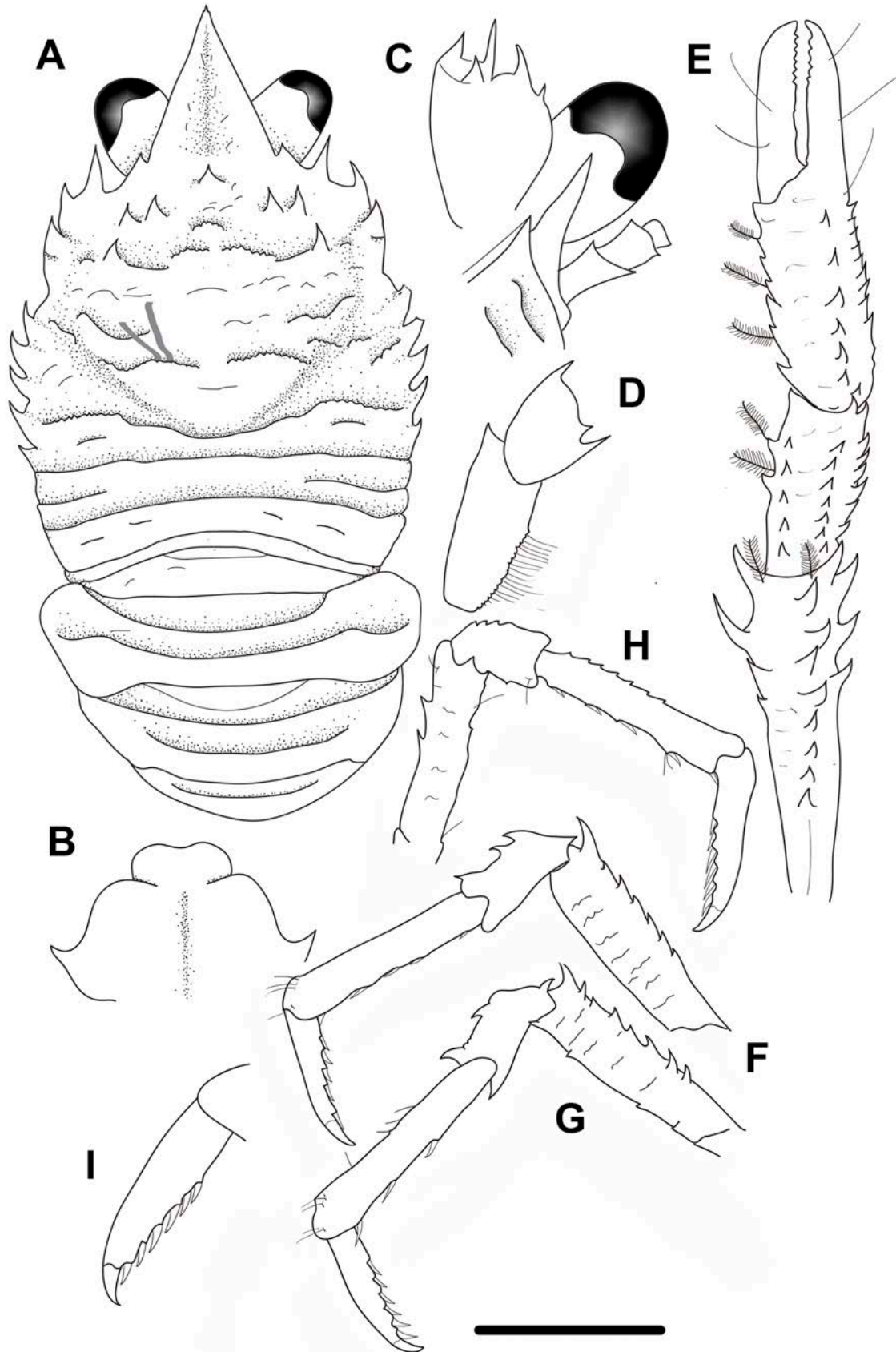
FIGURE 15. *Phylladiorhynchus heptacanthus* **n. sp**., holotype female 2.1 mm (MNHN-IU-2017-2534): A, carapace and pleon, dorsal view. B, thoracic sternites 3 and 4. C, left cephalic region, showing antennular and antennal peduncles, ventral view. D, right Mxp3, lateral view. E, right P1, dorsal view. F, left P2, lateral view. G, left P3, lateral view. H, right P4, lateral view. I, dactylus of left P2, lateral view. Scale bar: A, E-H = 1.0 mm; B–D, I = 0.6 mm.

Sternum: 0.9 times as long as wide. Sternite 3 moderately broad, [2.4]–2.6 times as wide as long, anterior margin straight, or slightly convex. Sternite 4 widely contiguous to sternite 3; surface depressed in midline, smooth; greatest width [2.7]–2.6 times that of sternite 3, [2.5]–2.5 times as wide as long.

Pleon: Elevated ridges uplifted dorsally, with a few scattered short setae. Tergites 2–3 with anterior and posterior transverse elevated ridges; tergite 4 with anterior transverse ridge; tergites 5–6 smooth.

Eye: Eye stalk length about [1.5]1.3–1.6 times broader than long, peduncle distally setose, not distinctly expanded proximally; maximum corneal diameter [0.5]–0.6 × rostrum width*,* narrower than eyestalk.

Antennule: Article 1 1.4 longer than wide, with 5 spines, distomesial spine well-developed, proximal lateral spine small.

Antenna: Article 1 with prominent mesial process, distally falling well short of lateralmost antennular spine. Article 2 with small distal spines laterally and mesially. Article 3 with minute or distinct distomesial and distolateral spines. Article 4 unarmed.

Mxp3: Ischium with distinct distal spines on flexor and extensor margins. Merus [0.5] × length of ischium at midlength, often with 1 distal spine on extensor margin and 2 spines on flexor margin.

P1: [2.2] (female) (lost in most specimens) times carapace length; subcylindrical, spiny and with scattered long stiff setae and scattered plumose setae; merus, carpus and palm with spines along mesial, dorsal and lateral surfaces, distal and mesial spines usually stronger than others. Merus as long as carapace. Carpus [1.9]–2.0 times as long as wide. Palm 1.2–[1.3] × carpus length, [2.3] times as long as broad. Fingers unarmed, [0.7]–0.8 × palm length.

P2–4: (lost in most specimens) Stout, subcylindrical, moderately setose and spinose. Meri successively shorter posteriorly: P3 merus [0.8] times length of P2 merus, P4 merus [0.8] times length of P3 merus. P2 merus, 0.6 times carapace length, 4.4 times as long as broad, [0.9] times as long as P2 propodus; P3 merus [5] times as long as broad, [1.2] times as long as P3 propodus; P4 merus [4.6] times as long as broad, [0.9] times as long as P4 propodus; extensor margin of P2–P3 with row of spines, proximally diminishing, with prominent distal spine; P4 extensor margin with 2 spines, distal spine absent; flexor margins of P2–4 irregular,with distal spine; P2–4 lateral surface with short striae. Carpi with 1–2 spines on extensor margin on P2–3, serrated on P4; distal spine prominent on P2–4; P2–4 flexor margins irregular, with distal spine. Propodi stout, [6.8]–

7.0 times as long as broad, extensor margin irregular, flexor margin with 2–3 slender movable spines in addition to distal pair. Dactyli 0.6–0.7 × length of propodi, ending in incurved, strong, sharp spine; flexor margin with 5–6 movable spines.

Eggs. Ov. F carried approximately 5–15 eggs of 0.5–0.6 mm diameter.

Colour. After some months in ethanol: light orange with reddish spots and patches remaining in carapace, rostrum and pleon.

Genetic data. COI, mini-barcode fragment (158 bp).

Distribution. New Caledonia and Chesterfield Islands, depth 244–500 m.

Remarks. *Phylladiorhynchus heptacanthus* belongs to the group of species having 5 epigastric spines, 3 spines on the anterior branchial margin and a leaf-like rostrum (margins clearly convex with subapical spines). The closest species is *P. eneus*, from Indonesia, Philippines, Papua New Guinea and New Caledonia. However, *P. heptacanthus* is easily distinguished from this species by the presence of parahepatic spines in *P. heptacanthu*s, being absent in *P. eneus*. Furthermore, the rostrum supraocular basal spines are small in *P. heptacanthu*s, whereas they are well-developed in *P. eneus*.

The COI divergence (mini-barcode fragment) between *P. eneus* and *P. heptacanthus* was 22%.

Phylladiorhynchus hylas n. sp.

(Figs. 16, 21D)

Records requiring verification:

Galathea pusilla.—Tirmizi, 1966: 175, figs 1A-C (Red Sea).

Type material. *Holotype.* Reunion Island. MD32 Stn CP43, 21º20.7'S, 55º26.9'E, 73–77 m, 18 August 1982: M 1.9 mm (MNHN-IU-2016-496).

Paratypes. Reunion Island. MD32 Stn CP43, 21º20.7'S, 55º26.9'E, 73–77 m, 18 August 1982: 1 M 1.7 mm, 1 ov. F 1.6 mm (MNHN-IU-2016-495).

Etymology. From the name *Hylas*, an Argonaut, son of Theiodamas and Menodice. The name is considered a substantive in apposition.

Description. *Carapace:* [0.9]0.9 times as long as broad; transverse ridges with some short setae, and few scattered iridescent thick long setae. Gastric region slightly
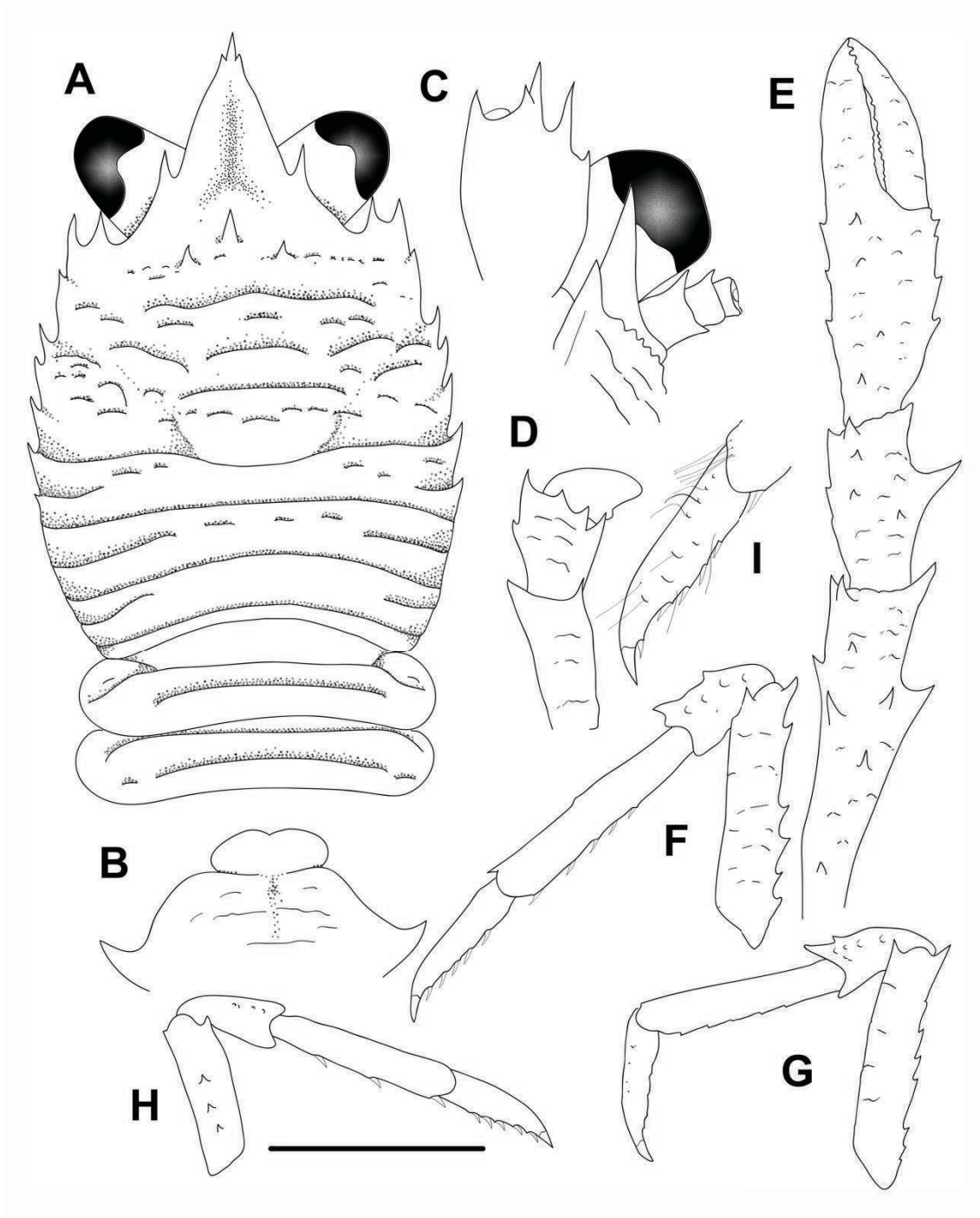
FIGURE 16. *Phylladiorhynchus hylas* **n. sp**., holotype male 1.9 mm (MNHN-IU-2016-496): A, carapace and pleon, dorsal view. B, thoracic sternites 3 and 4. C, left cephalic region, showing antennular and antennal peduncles, ventral view. D, right Mxp3, lateral view. E, left P1, dorsal view. F, left P2, lateral view. G, left P3, lateral view. H, right P4, lateral view. I, dactylus of left P2, lateral view. Scale bar: A, E-H = 1.0 mm; B–D, I = 0.6 mm.

convex with some transverse ridges: epigastric ridge indistinct, with 3 spines (1 median and 2 spines laterally) and some outer granules, continuing with some few scales; anterior protogastric ridge not medially interrupted, laterally interrupted with some few scales to carapace margin, posterior protogastric ridge scale-like; anterior mesogastric ridge scale-like, laterally interrupted by anterior branch of cervical groove, laterally continuing with some few scales, posterior mesogastric area with some few scales; anterior metagastric not medially interrupted, followed by small scales on posterior metagastric region. Mid-transverse ridge not interrupted, medially depressed, preceded by a shallow or indistinct cervical groove, followed by 2 not interrupted or minutely interrupted ridges, interspersed with 3 short lateral ridges. Lateral margins slighly convex, with 7 spines: first anterolateral spine well-developed, reaching end of lateral orbital spine, second spine (hepatic) minute, and followed by 5 branchial spines (3 anterior and 2 posterior). Rostrum leaf-like, horizontal, dorsally flattish, 1.1–[1.2] times as long as broad, length [0.4]0.4 and breadth [0.3]0.3 that of carapace; lateral margins serrated and convex, with well-developed supraocular spines, lateral margins of supraocular spines serrated, subapical spines distinct. Orbit sharply excavated. Pterygostomian flap ending in anterior spine, upper margin serrated.

Sternum: As wide as long. Sternite 3 moderately broad, 2.0–[2.6] times as wide as long, anterior margin convex, and with median feeble excavation. Sternite 4 widely contiguous to sternite 3; surface depressed in midline, smooth; greatest width 2.7–[2.9] times that of sternite 3, 2.3–[2.8] times as wide as long.

Pleon: Elevated ridges with a few scattered short setae. Tergites 2–3 with anterior and posterior transverse elevated ridges; tergite 4 with anterior transverse ridge only; tergites 5–6 smooth.

Eye: Eye stalk length about [1.1]1.1 times broader than long, peduncle distally setose, not distinctly expanded proximally; maximum corneal diameter [0.8] × rostrum width*,* as wide as eyestalk.

Antennule: Article 1 1.3 times longer than wide, with 5 spines: distomesial spine well-developed; proximal lateral spine minute.

Antenna: Article 1 with prominent mesial process, distally clearly not reaching lateralmost antennular spine. Article 2 with small distomesial and distolateral spines. Article 3 sometimes with small distomesial spine. Article 4 unarmed.

Mxp3: Ischium with distinct distal spines on flexor and extensor margins. Merus [0.7]–0.8 × length of ischium, with 1 median and 1 distal spine on extensor margin, 1 and 3 much larger spines on flexor margin.

P1: [2.3] (male) times carapace length; subcylindrical, spiny, with scattered long stiff setae and some few thick setae; merus, carpus and palm with spines along mesial, dorsal and lateral surfaces, distal and mesial spines usually stronger than others. Merus [0.9] length of carapace, [2.0] times as long as carpus. Carpus [2.1] times as long as wide. Palm [1.1] × carpus length, [1.9] times as long as broad. Fingers [0.9] x palm length; unarmed.

P2–4: Subcylindrical, moderately setose and spinose. Meri successively shorter posteriorly: P3 merus [0.8] times length of P2 merus, P4 merus [0.7] times length of P3 merus. P2 merus, [0.7]–0.8 times carapace length, [4.9]–5.7 times as long as broad, [1.2]1.4 times as long as P2 propodus; P3 merus [4.4] times as long as broad, [1.3] times as long as P3 propodus; P4 merus [3.3] times as long as broad, [1.0] times as long as P4 propodus; extensor margin of P2 and P3 with row of spines, proximally diminishing, with prominent distal spine; P4 extensor margin irregular, with small distal spine; flexor margins of P2–4 serrated, each with distal spine; P4 lateral surface with median row of 3 small spines. Carpi with 2 or 3 spines on extensor margin on P2–3, unarmed on P4; distal spine prominent on P2–3, smaller on P4; row of small spines below extensor margin on lateral surface of P2–3, unarmed on P4; flexor margins P2–4 irregular, each with distal spine. Propodi stout, [4.4–4.8]4.0–5.0 times as long as broad; extensor margin serrated, unarmed; flexor margin with 2–4 slender movable spines in addition to distal pair. Dactyli [0.7–0.8]0.7–0.8 × length of propodi, ending in incurved, strong, sharp spine; flexor margin with 5 movable spines.

Eggs. Ov. F (MNHN-IU-2016-495) carried 5 eggs of 0.3 mm diameter.

Colour. Unknown.

Genetic data. No data.

Distribution. Indian Ocean, Reunion Island, probably Red Sea, at 73–77 m.

Remarks. The specimens identified and illustrated by Tirmizi (1966) as *P. pusillus* are very similar to the new species, although they are different from *P. pusillus* (see also Lewinshon 1969; Schnabel & Ahyong 2019). Unfortunately, we have not examined this material and the status of these specimens should be identified in future studies. *Phylladiorhynchus hylas* has 3 spines on the epigastric ridge and closely resembles *P. koumac,* from New Caledonia, and *P. pulchrus,* from French Polynesia, Phillipines, and Vanuatu. However, they can be easily differentiated by the number of epigastric spines, 3 spines in *P. hylas* and 5 spines in the other species.

***Phylladiorhynchus idas* n. sp.**

(Fig. 17)

Type material. *Holotype.* French Polynesia. TARASOC Stn DW3393, 15°49.2'S, 148°16.8'W, 800 m, 7 October 2009: F 2.5 mm (MNHN-IU-2014-13842).

 Etymology. From the name *Idas*, an Argonaut, son of Aphareus and Arene. The name is considered a substantive in apposition.

 Description. *Carapace:* Slightly longer than broad; transverse ridges with short setae. Gastric region flattened, with 4 transverse ridges: epigastric ridge indistinct, with 3 spines (1 median and 2 lateral spines) and some outer granules; anterior protogastric ridge medially interrupted, nearly extending laterally to carapace margin; anterior mesogastric ridge medially interrupted, laterally interrupted by anterior branch of cervical groove; anterior metagastric ridge undistinct, with some few small scales in the anterior metagastric area. Mid-transverse ridge not interrupted, slightly medially depressed, preceded by shallow or indistinct cervical groove, followed by 2 not interrupted or minutely interrupted ridges, interspersed with 1 short lateral ridge. Lateral margins slightly convex, with 6 spines: first anterolateral spine well-developed, reaching end of lateral orbital spine, second spine (hepatic) minute but distinct, slightly dorsomesially from lateral margin, and followed by 4 branchial spines (2 anterior spines, first well-developed, followed by a second obsolescent to undistinct spine, and 2 posterior spines). Rostrum triangular, horizontal, dorsally flattish or slightly concave, [1.1] times as long as broad, length [0.3] and breadth [0.3] that of carapace; lateral margins smooth and slightly concave proximally, with well-developed supraocular spines, subapical spines absent. Pterygostomian flap ending in blunt tooth, upper margin smooth.

 Sternum: As wide as long. Sternite 3 broad, [3.0] times as wide as long, anterior margin convex, with a median feeble excavation, moderately produced anterolaterally. Sternite 4 widely contiguous to sternite 3; surface not depressed in midline, smooth; greatest width [2.5] times that of sternite 3, [2.8] times as wide as long.

 Pleon: Elevated ridges with short setae and with few scattered long setae. Tergite 2 with anterior and posterior transverse elevated ridges; tergites 3 and 4 with anterior transverse ridge; tergites 5–6 smooth.

 Eye: Eye stalk length about as broad as long, peduncle distally setose, not distinctly expanded proximally; maximum corneal diameter [1.4] × rostrum width*,* as wide as eyestalk.
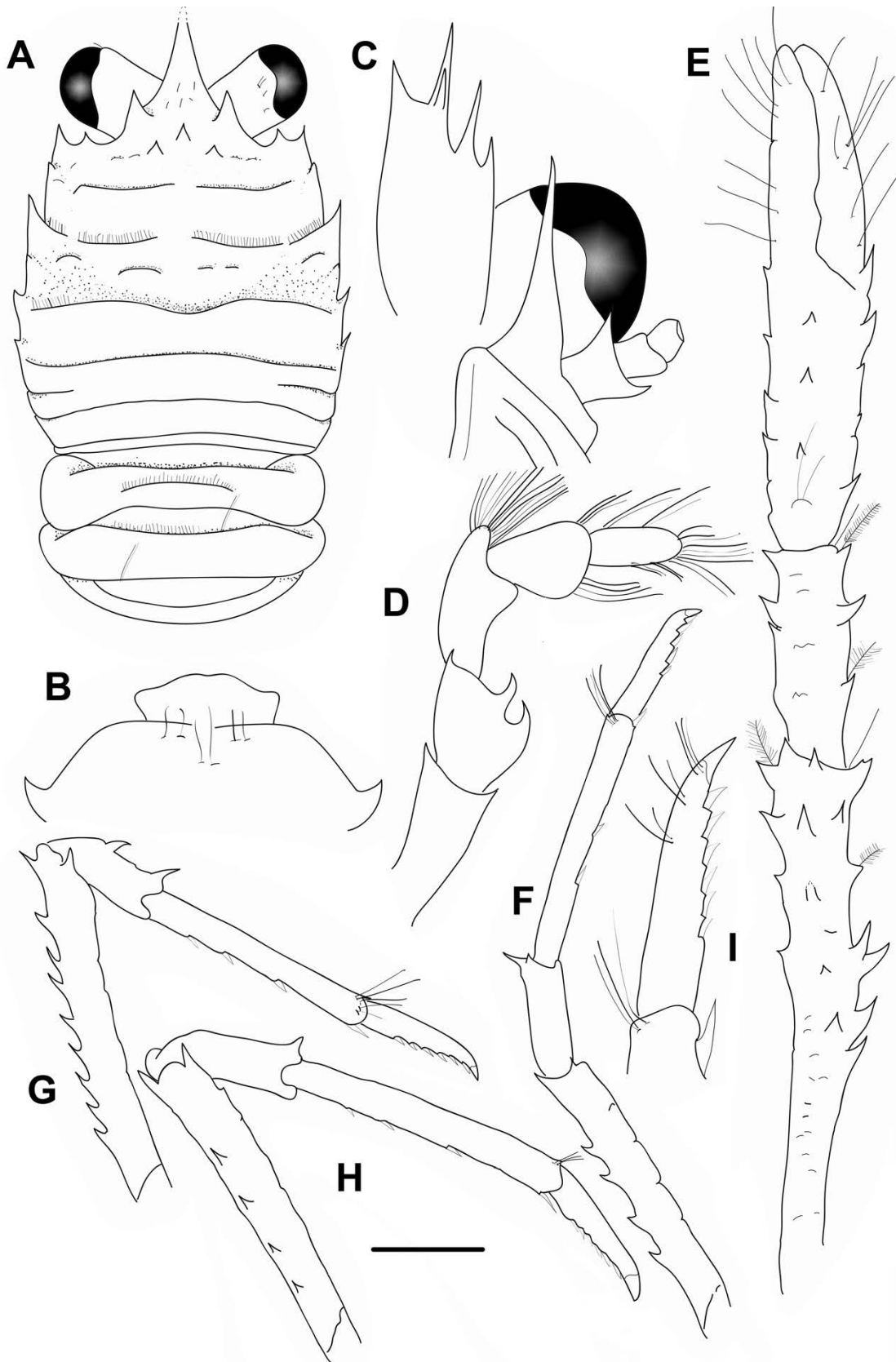
FIGURE 17. *Phylladiorhynchus idas* **n. sp**., holotype ovigerous female 2.5 mm (MNHN-IU-2014-13842): A, carapace and pleon, dorsal view. B, thoracic sternites 3 and 4. C, left cephalic region, showing antennular and antennal peduncles, ventral view. D, right Mxp3, lateral view. E, left P1, dorsal view. F, right P2, lateral view. G, right P3, lateral view. H, right P4, lateral view. I, dactylus of right P2, lateral view. Scale bar: A, E-H = 1.0 mm; B–D, I = 0.6 mm.

Antennule: Article 1 more than 1.5 times longer than wide, with 5 spines: distomesial spine well-developed; proximal lateral spine small.

Antenna: Article 1 with prominent mesial process, nearly reaching lateralmost antennular spine end. Article 2 with distinct distomesial and distolateral spines. Articles 3 and 4 unarmed.

Mxp3: Ischium with distinct distal spines on flexor and extensor margins. Merus [0.7] × length of ischium at middle length, with well-developed distal spine on extensor margin and 2 strong spines on flexor margin.

P1: [3.8] times carapace length; subcylindrical, spiny and with several plumose setae on merus, and carpus and long stiff setae on palm and fingers; merus, carpus and palm with spines along mesial, dorsal and lateral surfaces, distal and mesial spines usually stronger than others. Merus [1.5] length of carapace, [2.4] times as long as carpus. Carpus [3.2] times as long as wide. Palm [1.2] 1.2. × carpus length, [3.2] times as long as broad. Fingers subequal in length to palm; fixed finger unarmed; movable finger with well-developed basal spine.

P2–4: Slender, subcylindrical, moderately setose and spinose. Meri successively shorter posteriorly: P3 merus [0.6] times length of P2 merus, P4 merus [0.9] times length of P3 merus. P2 merus, as long as carapace length, [9.2] times as long as broad, [1.4] times as long as P2 propodus; P3 merus [8.3] times as long as broad, [1.2] times as long as P3 propodus; P4 merus [7] times as long as broad, [1.1] times as long as P4 propodus; extensor margin of P2 and P3 with row of spines, proximally diminishing, with prominent distal spine; P4 extensor margin irregular, with distal spine; flexor margins of P2–4 irregular, each with distal spine; P4 lateral surface with median row of 4 small spines, absent in others. Carpi armed on extensor margin with 1 spine on P2, unarmed on P3–4, distal spine prominent on P2–4. Propodi sharply slender, [10.0–10.1] times as long as broad; extensor margin irregular, usually unarmed; flexor margin with 2–4 slender movable spines in addition to distal pair. Dactyli [0.5] × length of propodus, ending in incurved, strong, sharp spine; flexor margin with 5–6 movable spines.

Eggs. No data.

Colour. Unknown.

Genetic data. No data.

Distribution. French Polynesia, 800 m.

     Remarks. *Phylladiorhynchus idas* resembles *P. kermadecensis* Schnabel & Ahyong, 2019, from New Zealand. However, both species can be distinguished by the following characters:

-     The carapace has 5 epigastric spines in *P. kermadecensis,* whereas there are 3 spines and a few granules in *P. idas*.
-     The anterior protogastric ridge is not medially interrupted or with a small median gap in *P. kermadecensis,* whereas, the anterior protogastric ridge is medially interrupted in *P. idas*.
-      The anterior metagastric ridge is medially interrupted in *P. kermadecensis* whereas this ridge is scale-like in *P. idas*.
-     Posterior branchial margin with one spine in *P. kermadecensis*, whereas there are 2 spines in *P. idas*.
-     The extensor margins of P2–3 propodi are usually armed with 2 proximal spines in *P. kermadecensis*, whereas these margins are usually unarmed in *P. idas*.
-     The flexor margin of the P2–4 dactili have 10–11 movable spines in *P. kermadecensis*, whereas there are 5–6 movable spines in *P. idas*.

Phylladiorhynchus ikedai (Miyake & Baba, 1965)

Galathea ikedai Miyake & Baba, 1965: 588, figs 3, 4 (near Muko-jima, Bonin Islands).

Phylladiorhynchus ikedai.—Baba, 1969: 5 (reexamination of type material).—Baba *et al*., 2008: 175 (compilation).

Not *Phylladiorhynchus ikedai*.—Baba, 1991: 485, figs 4a–b (= *P. argus* n. sp., *P. butes* n. sp., *P. eneus* n.sp., *P. maestratii* n. sp.).

Records requiring verification:

Phylladiorhynchus ikedai.—Baba, 1977: 252 (Maldives).—Baba, 2005: 200, 304 (Kei Islands, 245–300 m, Japan, Fukuoka, 110 m).—Dong & Li, 2013a: 1317, fig. 2 (South China Sea, 168 m).

     Distribution. Only known from the type locality, Bonin Islands, Japan.

     Remarks. The species is only known by the male holotype. The species is characterized by the presence of 5 epigastric spines, 1 hepatic spine, 3 anterior branchial spines, the anterior metagastric ridge not medially interrupted and the antennular article 1 with 4 spines only. The existence of some closely related species, e.g. *P. argus* n. sp., *P. butes* n.sp., *P. eneus* n.sp., suggests that some occurrences of *P. ikedai* should be confirmed. Unfortunately, we have not studied the specimens from Maldives (Baba

1977), Japan (Fukuoka) (Baba 2005) and South China Sea (Dong & Li 2013), recommending further revision to confirm their identity.

Phylladiorhynchus integrirostris (Dana, 1852)

(Figs. 21E, 37A-B)

Galathea integrirostris Dana, 1852: 482 (type locality: Kure Atoll, Hawaiian Islands) Dana, 1855: pl. 30, figs. 12a, 12b.

Phylladiorhynchus integrirostris.—Castro, 2011: 15 (list of Hawaii occurrences).—Baba *et al*., 2008: 175 (compilation, in part).—Schnabel & Ahyong, 2019: 316, Fig. 6 (selection of neotype).

Not *Phylladiorhynchus integrirostris*.—Lewinsohn, 1982: 295, fig. 1 (Gulf of Aqaba, N Red Sea) (= *P. bahamut* n. sp.).—Baba, 1991: Baba, 1991: 486 (in part), fig 4. (New Caledonia = *P. spinosus* Schnabel & Ahyong, 2019).—Ahyong, 2007: 42, fig. 21 (Lord Howe Rise, 72–82 m) (= *P. triginta* n. sp.).—Macpherson, 2008: 293 (Dampier Archipelago, W Australia, intertidal–24 m) (= *P. asclepius* n. sp.).

Records requiring verification:

Phylladiorhynchus integrirostris.—DiSalvo *et al*., 1988: 458 (Easter Island).—Baba, 1991: 485, 487, fig. 4c, d (in part) (only citations from Juan Fernández Islands, Easter Island, 0–160 m).—Tirmizi & Javed, 1993: 33, fig. 15 (Mozambique Channel, W of Durban, off Somali Republic, and Andaman Islands, 38–138 m).—Poupin, 2003: 25 (list, Easter Island).—Fujita, 2007: 78, figs 3, 4 (larvae).—Dong & Li, 2013a: 1317, fig. 3 (South China Sea, 6-11 m).—De los Ríos Escalante & Ibáñez Arancibia, 2016: 79 (Easter Island, list).—Retamal & Arana, 2016: 22 (Chilean oceanic islands, list).

Material examined. Hawaiian Islands. French Frigate Shoals. 27.765ºN, 166.169ºW, 32 m, 17 October 2006: 1 M 2.1 mm, 2 F 1.7–2.0 mm.—23.7695ºN, 166.2608ºW, 10 m, 21 0ctober 2006: 1 ov. F 2.4 mm.—Cory Pittman, October 2006: 1 ov. F 1.7 mm.—Stn FFS-1121, 23.63835ºN, 166.18005ºW, 12 m, 5 September 2013: 1 M 1.7 mm.—Stn FFS-1123, 23.63835ºN, 166.18005ºW, 12 m, 5 September 2013: 1 F 1.6 mm.—Stn FFS-288, 23.63835ºN, 166.18005ºW, 12 m, 5 September 2013: 1 M 1.9 mm, 1 F 1.5 mm.—Stn FFS-353, 23.63835ºN, 166.18005ºW, 12 m, 5 September 2013: 1 ov. F 1.9 mm.—Stn FFS-354, 23.63835ºN, 166.18005ºW, 12 m, 5 September 2013: 1 M 2.0 mm.—Stn FFS-438, 23.63835ºN, 166.18005ºW, 12 m, 5 September 2013: 2 M 1.2–1.6 mm, 1 ov. F 1.8 mm.—Stn FFS-440, 23.63835ºN, 166.18005ºW, 12 m, 05 September 2013: 1 M 1.4 mm.—Stn FFS-479, 23.62792ºN, 166.13538ºW, 10 m, 5 September 2013: 1 F 2.0 mm.—

Stn FFS-559, 23.62792ºN, 166.13538ºW, 10 m, 5 September 2013: 2 F 1.5–1.6 mm.—Stn FFS-692: 2 M 2.2–2.3 mm.—Stn FFS-693: 1 M 2.0 mm.—Stn FFS-735: 1 ov. F 2.3 mm.—Stn FFS-736: 2 F 1.4–1.9 mm.—Stn FFS-737: 1 ov. F 2.2 mm.—Stn FFS-788: 1 M 1.7 mm, 2 F 1.6–2.1 mm.—Stn FFS-789: (no station data) 1 specimen broken.—Stn FFS-821: 1 M 1.9 mm, 1 ov. F 2.1 mm, 2 F 1.7–2.0 mm.—Stn FFS-822: (no station data) 1 M broken.—Stn FFS-851: 1 ov. F 2.2 mm.—Stn FFS-882: 1 ov. F 2.3 mm.—Stn FFS-919: 2 M 1.4–2.2 mm, 2 ov. F 1.9–2.3 mm.—Hawaii Island. Stn HAW-1453, 0 m: 1 M 1.7 mm.—Stn HAW-443, 19.03821667ºN, 155.88255ºW, 15 m, 4 August 2013: 2 M 1.8–2.0 mm, 3 ov. F 1.7–2.0 mm, 3 F 1.6–1.7 mm.—Stn HAW-507, 19.03821667ºN, 155.88255ºW, 15 m, 4 August 2013: 7 M 1.6–2.3 mm, 1 ov. F 1.8 mm, 2 F 1.7–1.9 mm.—Stn HAW-509, 19.03821667ºN, 155.88255ºW, 15 m, 4 August 2013: 2 ov. F 2.2–2.4 mm, 2 F 1.4–1.5 mm.—Stn HAW-510, 19.03821667ºN, 155.88255ºW, 15 m, 4 August 2013: 1 ov. F 2.0 mm, 2 F 1.8–2.1 mm.—Stn HAW-593, 19.03821667ºN, 155.88255ºW, 15 m, 4 August 2013: 3 M 1.6–2.2 mm, 3 F 1.5–1.8 mm.—Stn HAW-595, 19.03821667ºN, 155.88255ºW, 15 m, 4 August 2013: 1 M 1.6 mm, 1 F 1.8 mm.—Stn HAW-596, 19.03821667ºN, 155.88255ºW, 15 m, 4 August 2013: 1 M 1.1 mm, 1 F 1.7 mm.—Stn HAW-692, 18.96859682ºN, 155.730732ºW, 15 m, 7 August 2013: 6 M 1.4–2.0 mm, 4 ov. F 1.2–1.8 mm, 5 F 1.0–1.9 mm.—Stn HAW-740, 18.96859682ºN, 155.730732ºW, 15 m, 7 August 2013: 1 M 2.0 mm, 1 F 1.4 mm.—Stn HAW-743, 18.96859682ºN, 155.730732ºW, 15 m, 7 August 2013: 2 M 1.2–2.1 mm, 2 ov. F 2.0–2.2 mm, 2 F 1.6–1.8 mm.—Stn HAW-803, 18.96859682ºN, 155.730732ºW, 15 m, 7 August 2013: 3 M 1.8–2.2 mm, 3 ov. F 1.8–2.1 mm, 2 F 1.7–1.8 mm.—Stn HAW-805, 18.96859682ºN, 155.730732ºW, 15 m, 7 August 2013: 1 F 1.4 mm.—Stn HAW-978, 18.96859682ºN, 155.730732ºW, 15 m, 7 August 2013: 1 M 1.9 mm.—Stn HAW-980, 19.03821667ºN, 155.88255ºW, 15 m, 4 August 2013: 3 M 1.8–2.1 mm, 2 ov. F 1.7–2.0 mm, 2 F 1.4–1.5 mm, 1 larvae.—Stn HAW-981, 19.03821667ºN, 155.88255ºW, 15 m, 4 August 2013: 1 F 1.2 mm. Kauai Island. Stn KAU-526, 22.16405324ºN, 159.298801ºW, 14 m, 13 August 2013: 2 M 1.6–2.1 mm, 1 F 2.3 mm.—Stn KAU-622, 22.16405324ºN, 159.298801ºW, 14 m, 13 August 2013: 1 M 1.8 mm.—Stn KAU-623, 22.16405324ºN, 159.298801ºW, 14 m, 13 August 2013: 2 M 1.2–2.0 mm, 2 ov. F 1.6–2.0 mm, 1 F 1.9 mm.—Stn KAU-625, 22.16405324ºN, 159.298801ºW, 14 m, 13 August 2013: 2 M 1.6–2.1 mm, 2 ov. F 1.9–2.0 mm.—Stn KAU-652, 22.16684307ºN, 159.6800101ºW, 13 m, 15 August 2013: 2 M 1.5–1.8 mm, 1 ov. F 1.9 mm.—Stn KAU-772, 22.16684307ºN, 159.6800101ºW, 13 m, 15 August 2013: 1 F 1.1 mm.—Stn KAU-774, 22.16684307ºN, 159.6800101ºW, 13 m, 15 August 2013: 1 M 1.9 mm, 3 F 1.1–1.9 mm.—Stn KAU-831, 21.8897599ºN, 159,6088704ºW, 12 m, 17 August 2013: 1 M 1.5 mm, 1 ov. F 1.2 mm, 2 F 1.6–1.8 mm, 1 postlarvae 1.0 mm.—Stn KAU-832, 21.8897599ºN, 159.6088704ºW, 12 m, 17 August 2013: 6 M 1.2–1.9 mm, 1 ov. F 1.9 mm.—Stn KAU-835, 21.8897599ºN, 159,6088704ºW, 12 m, 17 August 2013: 1 M 1.8 mm.—Stn KAU-922, 21.8897599ºN,

159.6088704ºW, 12 m, 17 August 2013: 5 M 1.6–1.9 mm, 1 ov. F 1.9 mm, 2 F 1.3–2.0 mm, 2 postlarvae 1.0 mm.—Stn KAU-923, 21.8897599ºN, 159.6088704ºW, 12 m, 17 August 2013: 1 M 1.8 mm, 1 ov. F 1.9 mm, 1 F 1.6 mm.—Stn KAU-924, 21.8897599ºN, 159.6088704ºW, 12 m, 17 August 2013: 1 M 1.4 mm.—Stn KAU-944, 21.8897599ºN, 159.6088704ºW, 12 m, 17 August 2013: 1 F 1.6 mm. Kure Atoll. Stn KUR-301, 28.416767ºN, 178.378433ºW, 14 m, 14 July 2013: 4 M 1.7–2.0 mm.—Stn KUR-301, 28.416767ºN, 178.378433ºW, 14 m, 14 July 2013: 1 ov. F 2.1 mm.—Stn KUR-348, 28.38230758ºN, 178.3244794ºW, 10 m, 14 July 2013: 12 M 1.2–2.4 mm, 3 ov. F 1.9–2.2 mm, 9 F 1.1–2.2 mm.—Stn KUR-476, 28.38230758ºN, 178.3244794ºW, 10 m, 14 July 2013: 6 M 1.5–2.3 mm, 3 ov. F 1.5–2.3 mm, 2 F 1.8–2.2 mm. Lisianski Island. Stn LIS-212, 26.07841509ºN, 173.9970114ºW, 15 m, 12 September 2013: 1 F 1.8 mm.—Stn LIS-213, 26.07841509ºN, 173.9970114ºW, 15 m, 12 September 2013: 1 M 1.7 mm.—Stn LIS-239, 25.94462ºN, 173.95361ºW, 15 m, 13 September 2013: 2 M 1.7–2.0 mm, 1 F 1.8 mm.—Stn LIS-260, 26.07841509ºN, 173.9970114ºW, 15 m, 12 September 2013: 1 M 1.8 mm, 1 ov. F 1.9 mm.—Stn LIS-301, 26.07841509ºN, 173.9970114ºW, 15 m, 12 September 2013: 1 ov. F 2.3 mm, 1 F 2.2 mm.—Stn LIS-302, 26.07841509ºN, 173.9970114ºW, 15 m, 12 September 2013: 1 M 1.7 mm, 2 ov. F 1.6–2.0 mm, 1 F 2.0 mm.—Stn LIS-326, 25.94462ºN, 173.95361ºW, 15 m, 13 September 2013: 3 M 1.8–2.3 mm, 1 ov. F 1.4 mm, 1 F 1.4 mm.—Stn LIS-336, 25.94462ºN, 173.95361ºW, 15 m, 13 September 2013: 2 M 1.3–1.8 mm, 1 F 1.4 mm.—Stn LIS-340, 25.94462ºN, 173.95361ºW, 15 m, 13 September 2013: 1 ov. F 2.1 mm, 1 F 2.2 mm. Maui Island. Airport Beach, Halimeda bed, 6–17 m, 15 March 2009: 1 M 1.9 mm (UF20156).—Stn MAI-196, 20.76226207ºN, 155.9797715ºW, 12 m, 9 August 2013: 1 M 2.2 mm.—Stn MAI-236, 20.76226207ºN, 155.9797715ºW, 12 m, 9 August 2013: 1 M 1.6 mm, 1 F 1.7 mm. Oahu Island. 21.289ºN, 157.865ºW, 9–12 m, 1 December 2008: 1 M 1.6 mm (UF15285), 1 ov. F 1.8 mm (UF15269), 1 ov. F 2.5 mm (UF15270).—Stn OAH-420, 21.41212947ºN, 157.7097973ºW, 15 m, 23 August 2013: 2 M 1.5–1.9 mm, 3 F 1.2-1.4 mm, 1 postlarvae 1.0 mm.—Stn OAH-448, 21.41212947ºN, 157.7097973ºW, 15 m, 23 August 2013: 1 F 1.8 mm.—Stn OAH-516, 21.41212947ºN, 157.7097973ºW, 15 m, 23 August 2013: 2 M 1.4–1.8 mm, 2 ov. F 2.0–2.2 mm, 2 F 1.8–2.0 mm.—Stn OAH-662: 2 M 1.8–2.2 mm, 1 F 1.4 mm.—Stn OAH-738: 1 M 2.2 mm, 1 F 1.4 mm.—Stn OAH-947: 1 M 1.7 mm. Pearl and Hermes Atoll. Stn PHR-1019, 27.785833ºN, 175.780283ºW, 14 m, 10 September 2013: 2 F 1.2–1.3 mm.—Stn PHR-1020, 27.785833ºN, 175.780283ºW, 14 m, 10 September 2013: 1 M 1.6 mm, 1 ov. F 1.4 mm, 1 F 1.2 mm.—Stn PHR-1036, 27.78543745ºN, 175.8235427ºW, 14 m, 10 September 2013: 2 ov. F 1.4–1.5 mm, 2 F 1.3–1.4 mm.—Stn PHR-1079, 27.78543745ºN, 175.8235427ºW, 14 m, 10 September 2013: 3 M 1.8–2.0 mm.—Stn PHR-1080, 27.78543745ºN, 175.8235427ºW, 14 m, 10 September 2013: 4 M 1.1–1.3 mm, 2 F 1.0–1.2 mm.—Stn PHR-1252, 27.785833ºN, 175.780283ºW, 14 m, 10 September 2013: 1 F 1.0 mm.—Stn PHR-754, 27.785833ºN,

175.780283ºW, 14 m, 10 September 2013: 2 F 1.4–1.5 mm.—Stn PHR-857, 27.753133ºN, 175.948767ºW, 15 m, 11 September 2013: 2 M 1.4 –1.9 mm, 1 F 1.5 mm.—Stn PHR-890, 27.785833ºN, 175.780283ºW, 14 m, 10 September 2013: 1 M 1.6 mm.—Stn PHR-892, 27.785833ºN, 175.780283ºW, 14 m, 10 September 2013: 4 M 1.6–1.8 mm, 5 F 1.3–1.6 mm.—Stn PHR-936, 27.78543745ºN, 175.8235427ºW, 14 m, 10 September 2013: 1 F 1.5 mm.—Stn PHR-937, 27.78543745ºN, 175.5958235427ºW, 14 m, 10 September 2013: 1 M 2.0 mm.—Stn PHR-938, 27.78543745ºN, 175.8235427ºW, 14 m, 10 September 2013: 4 M 1.1–1.8 mm, 1 ov. F 1.8 mm, 2 F 1.4–1.6 mm (UF).

Eggs: Ov. F carried approximately 10–25 eggs of 0.4–0.5 mm diameter.

Genetic data. COI and 16S, Table 1.

Distribution. Hawaiian Islands, between 0 and 32 m.

Remarks. The species was re-described by Schnabel & Ahyong (2019) and selecting a neotype. *Phylladiorhynchus integrirostris* belongs to the group of species having the epigastric ridge armed with 2 spines and the anterior branchial margin of the carapace armed with 2 spines only. The species is geographically restricted to the Hawaiian Islands (Schnabel & Ahyong 2019). However, *P. integrirostris* closely resembles *P. lynceus* from Chagos Archipelago, Kiribati and Samoa, and *P. priasus* from Northern Marianas Islands, Guam and Wake Islands. The 3 species are barely distinguishable morphologically although they are clearly different genetically (see the differences under the Remarks of *P. priasus*). Furthermore, these 3 species are also close to *P. orpheus* (see the differences under the Remarks of *P. orpheus*).

Phylladiorhynchus serrirostris (Melin, 1939), only known from Bonin Islands, has been also considered a synonym of *P. integrirostris*; however, both should be considered different and valid species (see the differences under the Remarks of *P. serrirostris*).

The mean intraspecific genetic divergences were 0.3% (COI) and 0.1% (16S).

Phylladiorhynchus integrus (Benedict, 1902)

(Figs. 18, 19, 21F)

Galathea integra Benedict, 1902: 248 (type locality: off Honshu, Japan [Ose Zaki, S. 55d, W. 2.25 M], 110–128 m [syntypes, USNM 26168]).—Balss, 1913: 7, fig. 4 (Japan, 110-180 m).—Yokoya, 1933: 55 (Japan, off Shiwoya, S of Inuboe-zaki, E coast of Aomori Pref., Sagami Bay, Suruga Bay, E of Omaezaki, N of Tanegashima, E of Kagoshima, N of Goto I. N of Noto, N of Oga W of Aomori Pref. W of Tsugaru
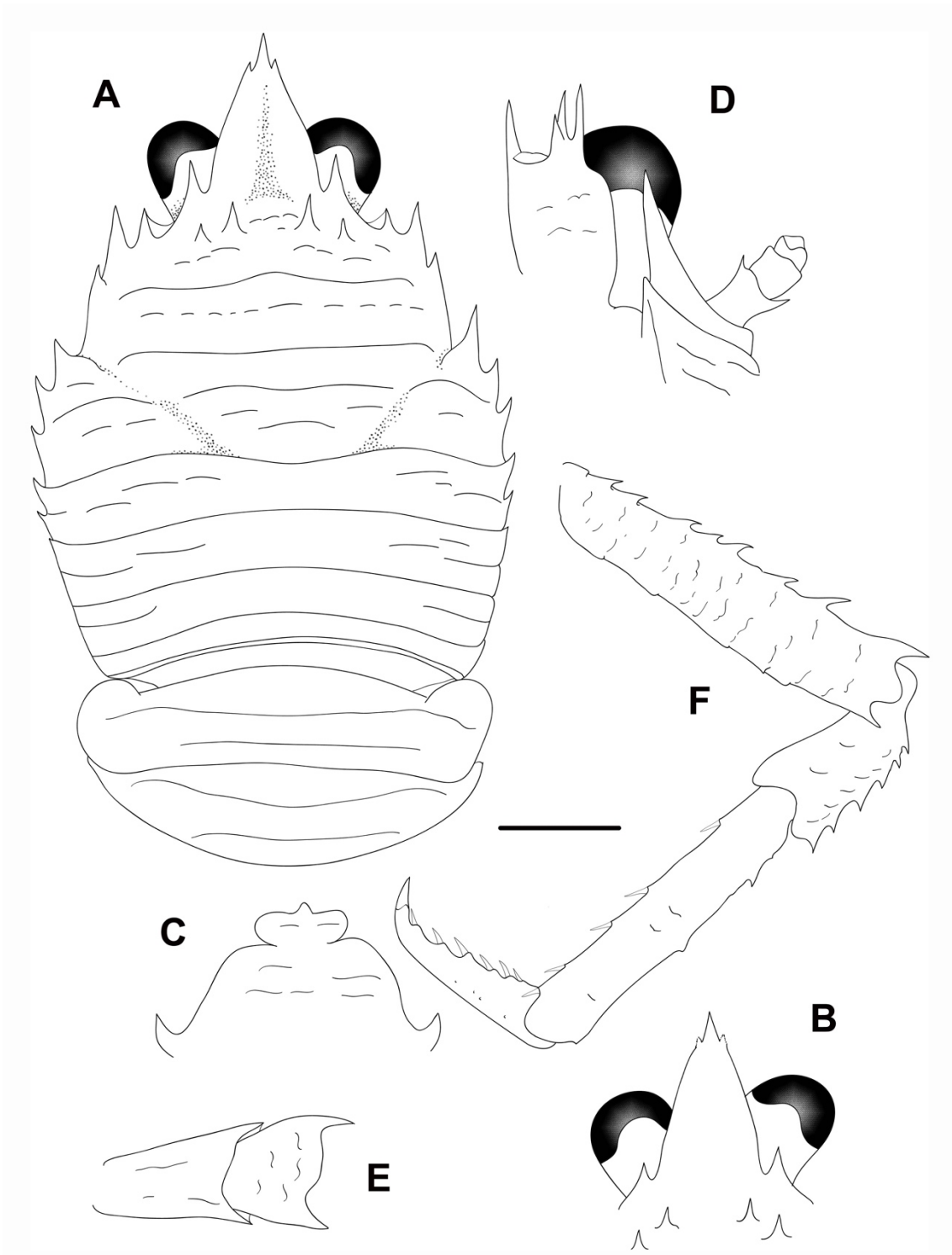
FIGURE 18. *Phylladiorhynchus integrus* (Benedict, 1902), A, C-F, lectotype ovigerous female 3.6 mm (USNM26188); B, paralectotype male 3.0 mm (USNM26168): A, carapace and pleon, dorsal view. B, rostrum, dorsal view. C, thoracic sternites 3 and 4. D, left cephalic region, showing antennular and antennal peduncles, ventral view. E, right Mxp3, lateral view. F, right P2, lateral view. Scale bar: A, E-H = 1.0 mm; B–D, I = 0.6 mm.
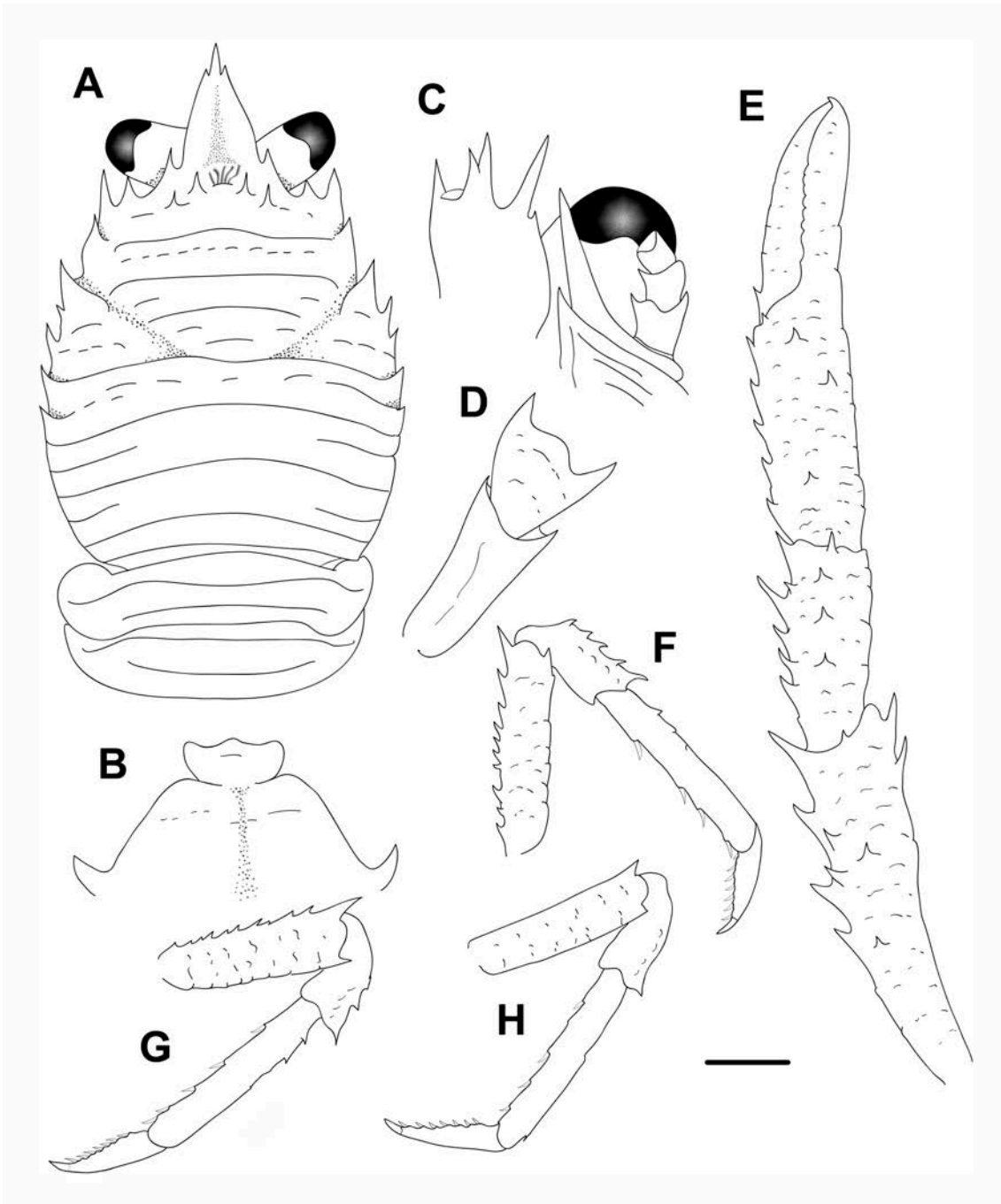
FIGURE 19. *Phylladiorhynchus integrus* (Benedict, 1902), female 4.8 mm (MNHN-IU-2014-13804): A, carapace and pleon, dorsal view. B, thoracic sternites 3 and 4. C, left cephalic region, showing antennular and antennal peduncles, ventral view. D, right Mxp3, lateral view. E, right P1, dorsal view. F, right P2, lateral view. G, right P3, lateral view. H, right P4, lateral view. Scale bar: A, E-H = 1.0 mm; B–D = 0.5 mm.

Strait, Tsugaru Strait, 71–307 m).—Makarov, 1938: 88, fig. 31 (no record).—Miyake, in Miyake & Nakazawa, 1947: 732, fig. 2117 (no record).

Records requiring verification:

Galathea integra.—Laurie, 1926: 135 (Providence, 106 m).

Phylladiorhynchus ikedai.—Baba, 2005: 200, 304.

Phylladiorhynchus pusillus.—Miyake, 1965: 635, fig. 1044 (no record).—Miyake & Baba, 1967: 234, fig. 6 (East China Sea, 102–196 m).—Baba *et al*., 2009: 287, fig. 263, 264 (Taiwan 115–1261m).—Lee *et al*., 2019: 730, figs. 3, 4 (South of Jeju Is., Korea, 150 m).

Type material. *Lectotype*. Japan. Honshu. [Ose Zaki, S. 55d, W. 2.25 M], 110–128 m, ov. F 3.6 mm **(**USNM 26168).

   Paralectotypes. Japan. Honshu. [Ose Zaki, S. 55d, W. 2.25 M], 110–128 m, 17 M 3.0–4.8 mm, 11 ov. F 2.8–3.7 mm **(**USNM 26168).

   Other material. Taiwan. Aodi, Taipei County. Stn CP58, 24°35.1'N, 122°05.8'E, 221–254 m, 4 August 2000: 3 M 2.7–3.2 mm, 1 ov. F 3.5 mm (NTOU).—Stn CP76, 24°56.54'N, 122°01.51'E, 115–170 m, 7 May 2001: 1 F 1.8 mm (NTOU).—Stn CP85, 24°00.55'N, 122°00.54'E, 255–390 m, 9 May 2001: 6 M 2.2–4.0 mm (NTOU).—Stn DW149, 22°18.5'N, 121°29.37'E, 258 m, 20 May 2002: 1 M 2.0 mm (NTOU).—Stn CP277, 24°23.57'N, 122°14.12'E, 1222–1261 m, 14 June 2005: 1 M 3.8 mm (NTOU).—Stn OCP287, 24°57.522'N, 122°5.303'E, 259–349 m, 8 August 2005: 11 M 2.1–2.6 mm, 1 ov. F 2.6 mm, 8 F 1.5–2.7 mm (NTOU).—Stn OCP288, 24°57.701'N, 122°5.346'E, 263–352 m, 8 August 2005: 27 M 1.1–4.2 mm, 2 ov. F 2.4– 2.6 mm, 13 F 2.1–3.0 mm (NTOU).—Stn OCP 293, 24°58.367'N, 122°5.289'E, 262–232 m, 8 August 2005: 28 M 1.5–3.4 mm, 3 ov. F 2.4–2.7 mm, 25 F 1.4–3.4 mm (NTOU).

   Indonesia. KARUBAR Stn CP05, 05°49'S, 132°18'E, 296–299 m, 22 October 1991: 1 F 3.1 mm (MNHN-IU-2016-9659).—Stn DW13, 05°26'S, 132°38'E, 417–425 m, 24 October 1991: 1 F 4.8 mm (MNHN-IU-2014-13804), 1 F broken (MNHN-IU-2014-13854).—Stn CP16, 05°17'S, 132°50'E, 315–349 m, 24 October 1991: 1 M 4.2 mm (MNHN-IU-2014-13852), 1 ov. F 3.5 mm (MNHN-IU-2016-426).—Stn CP25, 05°30'S, 132°52'E, 336–346 m, 26 October 1991: 1 F 2.9 mm (MNHN-IU-2014-13856).—Stn CP36, 06°05'S, 132°44'E, 210–268 m, 27 October 1991: 1 ov. F 3.2 mm (MNHN-IU-2014-13853).

Chesterfield Islands. EBISCO Stn DW2603, 19º37.761'S, 158º43.898'E, 568–570 m, 18 October 2005: 1 ov. F 4.1 mm (MNHN-IU-2014-13855).—Stn DW2603, 19º37.761'S, 158º43.898'E, 568–570 m, 18 October 2005: 1 ov. F 3.5 mm (MNHN-IU-2016-425).—KANADEEP Stn DW4975, 19º45'S, 158º35'E, 386–428 m, 9 September 2017: 1 ov. F, 3.3 mm (MNHN-IU-2017-2432).

Description. *Carapace:* as long as or slightly broader than long; transverse ridges with dense short setae and few scattered long thick iridescent setae. Gastric region slightly convex, with some transverse ridges: epigastric ridge distinct usually armed with 4 epigastric spines, inner pair longer, often a median scale with thick or plumose setae anterior to epigastric ridge; anterior protogastric ridge not medially interrupted, nearly extending laterally to carapace margin; anterior mesogastric ridge not medially interrupted, laterally interrupted by cervical groove, laterally continuing to first branchial spine; anterior metagastric ridge not medially interrupted, laterally interrupted; posterior epigastric, protogatric, mesogastric, and metagastric ridges scale-like. Mid-transverse ridge uninterrupted, medially slightly depressed, preceded by shallow or indistinct cervical groove, followed by 3 uninterrupted or minutely interrupted ridges, interspersed with 2 short lateral ridge and sometimes few, short scattered scales. Lateral margins slightly convex, with 7–8 spines: first anterolateral spine well-developed, reaching anteriorly to level of lateral orbital spine, second spine (hepatic) well-developed, slightly dorsomesially from lateral margin, and followed by 5–6 branchial spines (3 anterior and 2–3 posterior). Rostrum subtriangular, horizontal, dorsally flattish or slightly concave, [1.6]–1.9 times as long as broad, length [0.4]–0.5 and breadth 0.2–[0.3] that of carapace; lateral margins smooth and convex, with well-developed supraocular basal spines and small subapical spines. Pterygostomian flap ending in blunt tooth, upper margin smooth.

Sternum: As wide as long. Sternite 3 moderately broad, [2.0]–2.5 times as wide as long, anterior margin with obtuse median projection. Sternite 4 widely contiguous to sternite 3; surface depressed in midline, smooth; greatest width 2.5–[3.4] times that of sternite 3, 2.6–[2.8] times as wide as long.

Pleon: Elevated ridges with dense short setae and scattered long setae. Tergites 2–3 with anterior and posterior transverse elevated ridges; tergite 4 with anterior transverse ridge; tergites 5–6 smooth.

Eye: Eye stalk length about 0.9 times broader than long, peduncle distally setose, not distinctly expanded proximally, with few short transverse striae on lateral surfaces; maximum corneal diameter [1.2]1.2 × rostrum width, as wide as eyestalk, (0.95 times maximum peduncle width).

Antennule: Article 1 1.3 times longer than wide, with 4 well-developed distal spines: distomesial spine well-developed; proximal lateral spine usually absent, minute if present.

Antenna: Article 1 with prominent mesial process, distally falling short of lateral antennular spine. Article 2 with minute distomesial spine, distolateral spine larger than distomesial. Article 3 with minute or obsolescent distal mesial spine. Article 4 unarmed.

Mxp3: Ischium with distinct distal spines on flexor and extensor margins. Merus [0.6]–0.7 × length of ischium, with well-developed distal spine on extensor and flexor margins.

P1: 3.1(males), 2.9–3.3 (females) times carapace length; subcylindrical, spiny and with scattered long stiff setae; merus, carpus and palm with spines along mesial, dorsal and lateral surfaces, distal and mesial spines usually stronger than others. Merus 1.1–1.7 length of carapace, 2.1–3.2 times as long as carpus. Carpus 1.5–2.7 times as long as wide. Palm 1.2 × carpus length, 1.7–2.5 times as long as broad. Fingers 0.8–0.9 × palm length; fixed finger lateral margin unarmed; movable finger with small to well-developed basal spine.

P2–4 (P2 in lectotype only): Slender, subcylindrical, moderately setose and spinose. Meri successively shorter posteriorly: P3 merus 0.4–0.6 times length of P2 merus, P4 merus 0.8 times length of P3 merus. P2 merus, 0.6–0.7[0.9] times carapace length, [4.8]5.2–6.5 times as long as broad, [1.2]1.2–1.3 times as long as P2 propodus; P3 merus 4.8–6.3 times as long as broad, 1.1–1.2 times as long as P3 propodus; P4 merus 4.4 times as long as broad, as long as P4 propodus; extensor margin of P2 and P3 with row of spines, proximally diminishing, with prominent distal spine; P4 extensor margin irregular, distal spine present; flexor margin irregular, with distal spine on P2–3, absent in P4; P2–3 lateral surface unarmed. Carpi with 2–6 spines on extensor margin on P2–3, unarmed on P4; distal spine prominent on P2–3, smaller or absent on P4; row granules below extensor margin on lateral surface of P2–4; flexor margin unarmed. Propodi moderately slender, 5.0–6.4[6.0] times as long as broad; extensor margin irregular usually armed proximally with 3 small spines on P2–3; flexor margin with 3– slender movable spines in addition to distal pair. Dactyli [0.5]–0.6 × length of propodi, ending in incurved, strong, sharp spine; flexor margin with 6–8 movable spines.

Eggs. Ov. F carried approximately 30–50 eggs of 0.4–0.5 mm diameter.

Colour. Carapace and pleon translucent white or diffuse orange red; carapace lateral spines and rostral supraocular basal spines orange red. P1 diffuse orange-red. P2–4 with diffuse, clear orange-red bandings (after Baba *et al*. 2009).

Genetic data. COI and 16S, Table 1.

Distribution. Japan, Korea, Taiwan, Indonesia, Chesterfield Islands, from 110 to 1261 m.

Remarks. *Phylladiorhynchus integrus* was described as *Galathea integra,* by Benedict (1902) from specimens collected in Honshu, Japan. The species was posteriorly collected in other Japanese localities (as *G. integra*) and from Taiwan, Korea and Eastern China Sea (as *P. pusillus*) (see above). The examination of the type specimens of the species indicates that it belongs to a valid species, widely distributed along the western Pacific, and being differentiated from other species of *Phylladiorhynchus* by some constant morphological differences. *Phylladiorhynchus integrus* belongs to the group of the species having 4 spines on the epigastric ridge, 1 well-developed hepatic spine, the anterior metagastric ridge not medially interrupted, the anterior margin of the sternite 3 medially projected and a single spine on the flexor margin of Mxp3 merus. The species closely resembles *P. australis* Schnabel & Ahyong, 2019 and *P. nui* Schnabel & Ahyong, 2019 from Eastern Australia and New Zealand. However, the three species can be distinguished among them by the following characters:

- The rostrum lateral margin is straight in *P. nui,* whereas it is convex in *P. australis* and *P. integrus*.
- The lateral-most spine of the antennular article 1 is very small to indistinct in *P. nui* and *P. integrus,* whereas this spine is always distinct in *P. australis*.
- The antennal article 2 is armed with a well-developed distolateral spine, reaching or overreaching the end of article 3 in *P. australis*, whereas this spine is minute or obsolescent in *P. nui* and P. *integrus*.
- The P2–4 propodi are more slender in *P. nui* (6 times as long as broad) than in *P. australis* and *P. integrus* (5 times as long as broad).
- The flexor margin of the P2–4 dactyli has 9–11 movable spines in *P. nui,* having 6–9 spines in *P. australis* and *P. integrus*.

P. integrus diverged 12–13% (COI) and 5–6% (16S) from *P. nui* and *P. australis*, respectively.

***Phylladiorhynchus iphiclus* n. sp.**

(Figs. 20, 21G)

Type material. *Holotype.* French Polynesia. BENTHAUS Stn DW1894, 27°40.13'S, 144°21.51'W, 100 m, 8 November 2002: ov. F 2.3 mm (MNHN- IU-2019-2662).
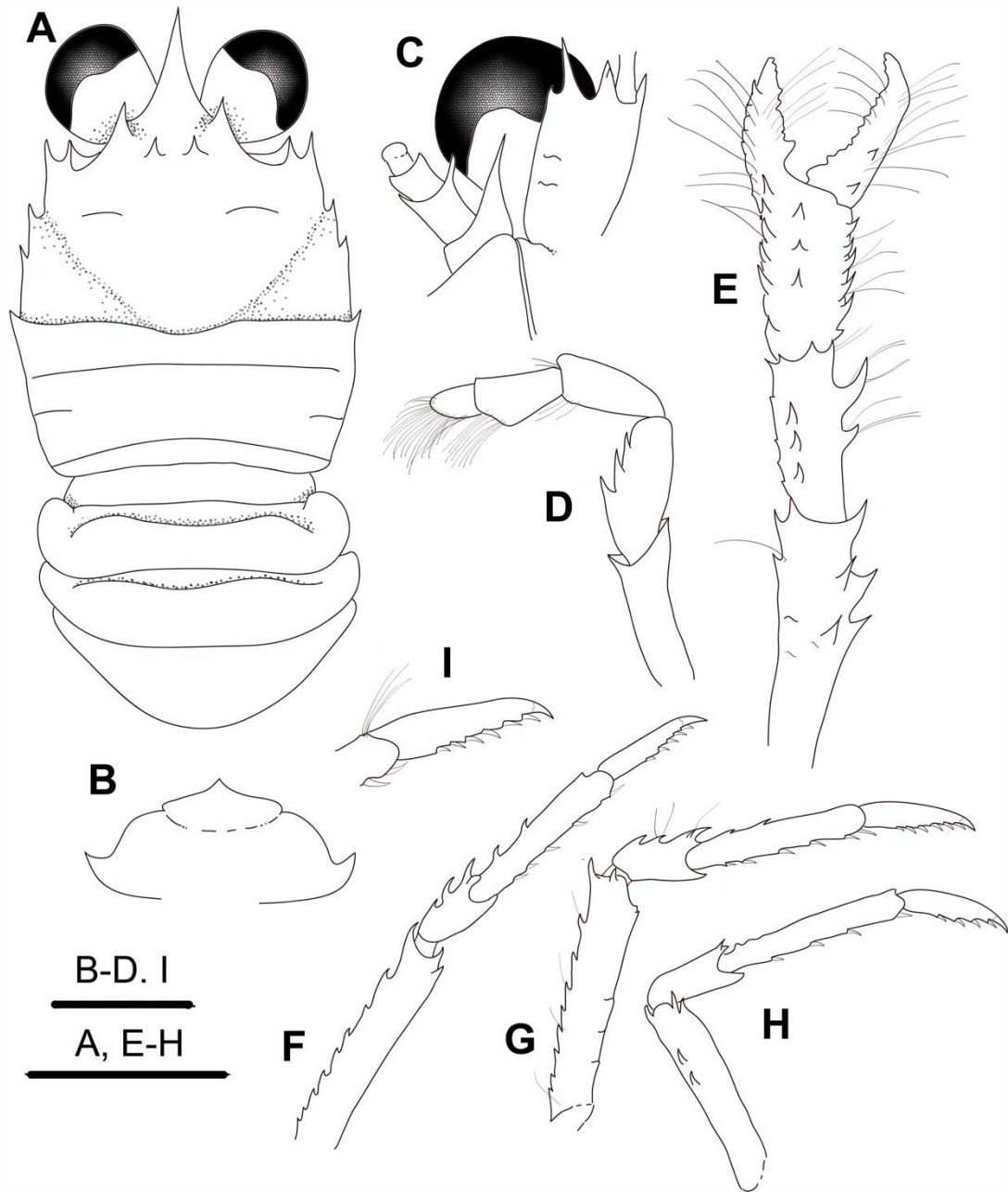
FIGURE 20. *Phylladiorhynchus iphiclus* **n. sp**., holotype ovigerous female 2.3 mm (MNHN-IU-2019-2662): A, carapace and pleon, dorsal view. B, thoracic sternites 3 and 4. C, right cephalic region, showing antennular and antennal peduncles, ventral view. D, left Mxp3, lateral view. E, left P1, dorsal view. F, right P2, lateral view. G, right P3, lateral view. H, right P4, lateral view. I, dactylus of right P2, lateral view. Scale bars: 1.0 mm.

Paratypes. Vanuatu. SANTO, no station: 1 M broken (MNHN-IU-2019-2651).

Etymology. From the name *Iphiclus*, an Argonaut, son of Phylacus and Clymene. The name is considered a substantive in apposition.

Description. *Carapace:* as long as broad; transverse ridges scattered and indistinct, without setae. Gastric region flattened and smooth, transverse ridges barely distinct: epigastric ridge indistinct, with 2 median spines; 2 lateral scales on anterior protogastric region. Mid-transverse ridge not interrupted, medially depressed, preceded by distinct cervical groove, followed by 1 not medially interrupted ridge and 1 short lateral ridge. Lateral margins slightly convex, with 4 spines: first anterolateral spine well-developed, reaching end of lateral orbital spine, hepatic margin unarmed; anterolateral spine followed by 3 branchial spines (2 anterior and 1 posterior spines). Rostrum triangular, horizontal, dorsally flattish or slightly concave, 1.2–[1.3] times as long as broad, length [0.3]0.3 and breadth [0.3]0.3 that of carapace; lateral margins smooth and straight, with well-developed supraocular spines, subapical spines absent. Pterygostomian flap ending in blunt tooth, upper margin smooth.

Sternum: As wide as long. Sternite 3 moderately broad, [2.2]–2.5 times as wide as long, anterior margin with obtuse median projection, anterolaterally rounded. Sternite 4 widely contiguous to sternite 3; surface depressed in midline, smooth; greatest width 2.1–[2.3] times that of sternite 3, 2.8–[3.2] times as wide as long.

Pleon: Transverse ridges with a few scattered short setae. Tergites 2–4 with anterior transverse ridge only; tergites 5–6 smooth.

Eye: Eye stalk as broad as long, peduncle not setose, not distinctly expanded proximally; cornea expanded distally, cornea expanded, maximum corneal diameter [1.3]1.3 × rostrum width, [1.2]–1.3 times maximum peduncle width.

Antennule: Article 1 1.3 times longer than wide, with 4 spines: distomesial spine small, distolateral spines with a blunt process or granule (no double distolateral spine); proximal lateral spine small, always present.

Antenna: Article 1 with prominent mesial process distally clearly not reaching lateralmost antennular spine. Article 2 with distinct distal spines laterally and mesially. Article 3 with distomesial spine. Article 4 unarmed.

Mxp3: Ischium with distinct distal spines on flexor and extensor margins. Merus [0.7] × length of ischium, extensor margin unarmed, flexor margin with 3 spines, decreasing in size distally.

P1: 2.8 male, [2.5] (female) times carapace length; subcylindrical, spiny and with scattered long stiff setae and some thick iridescent setae; merus, carpus and palm with spines along mesial, dorsal and lateral surfaces, distal and mesial spines usually stronger than others. Merus as long as carapace, 1.5–[1.7] times as long as carpus. Carpus 1.8–[2.5] times as long as wide. Palm 0.8–[0.9] × carpus length, [1.5]–1.6 times as long as broad. Fingers as long as palm length, fixed finger with distal spine on lateral margin; movable finger with 2 basal spines.

P2–4: Slender, subcylindrical, moderately setose and spinose. Meri successively shorter posteriorly: P3 merus 0.8–[0.9] times length of P2 merus, P4 merus [0.8]–0.9 times length of P3 merus. P2 merus, [0.8] or as long as carapace length, [5.2]–5.4 times as long as broad, 1.3–[1.5] times as long as P2 propodus; P3 merus 5–[5.3] times as long as broad, 1.1–[1.6] times as long as P3 propodus; P4 merus 4–[4.8] times as long as broad, 1.1–[1.2] times as long as P4 propodus; extensor margin of P2 and P3 with row of spines, proximally diminishing, with prominent distal spine; P4 extensor margin irregular but unarmed other than small distal spine; flexor margins of all legs irregular, with distal spine; P4 lateral surface with median row of 2 small spines, absent in others. Carpi with 2 spines on extensor margin on P2–3, unarmed on P4; distal spine prominent on P2–3, smaller on P4; flexor margin unarmed. Propodi slender, [5.0–5.5]5.6–7.0 times as long as broad; extensor margin irregular, usually armed with a 1–2 proximal spines on P2–4; flexor margin with 3–4 slender movable spines in addition to distal pair. Dactyli [0.7]0.6–0.7 × length of propodi, ending in incurved, strong, sharp spine; flexor margin with 5–6 movable spines.

Eggs: ov. F (MNHN- IU-2019-2662) carried 10 eggs of 0.4 mm diameter

Colour. Unknown.

Genetic data. No data.

Distribution. French Polynesia and Vanuatu, 100 m.

Remarks. *Phylladiorhynchus iphiclus* is easily distiguished from the other species by having the Mxp3 merus with 3 prominent spines along the flexor margin, the rostrum triangular and 2 spines on the epigastric ridge. *Phylladiorhynchus iphiclus* resembles to *P. boucheti*, from Chesterfield Islands, however, they can be distinguished by the following characters:

-       The epigastric ridge has 2 spines in *P. iphiclus*, whereas there are 4 spines in *P. boucheti*.

-       The gastric ridges are obsolescent or absent in *P. iphiclus*, whereas the protogastric and mesogastric ridges are distinct in *P. boucheti*.

-       The carapace anterior margin has 2 spines in *P. iphiclus*, whereas there are 3 spines in *P. boucheti*.

-       The flexor margin of Mxp3 merus is armed with 3 spines, whereas there are 2 spines in *P. boucheti*. Furthermore, the extensor margin is unarmed in *P. iphiclus*, having a distal spine in *P. boucheti*.

Phylladiorhynchus janiqueae n. sp.

(Figs. 21H, 22, 54E)

Records requiring verification:

Phylladiorhynchus serrirostris.—Tirmizi & Javed, 1980: 260, fig. 3 (Mozambique Channel, off South Africa, off Somalia, Andaman Sea).

Phylladiorhynchus integrirostris.—Tirmizi & Javed, 1993: 33, fig. 15 (Mozambique Channel, off South Africa, off Somalia, Andaman Sea).

Type material. *Holotype.* Madagascar. ATIMO VATAE Stn TB01, 24°59.8'S, 47°05.7'E, 22 m, 30 April 2010: M 2.3 mm (MNHN-IU-2014-13799).

Paratypes. SW Indian Ocean. MD08 Stn DC32, 33º50'S, 43º11'E, 40–43 m, 15 March 1976: 1 ov. F 3.0 mm (MNHN-IU-2016-467).—Stn CC31 St 6, 33°10'S, 43°52'E, 36–47 m, 15–16 March 1976: 1 M 2.5 mm, 1 ov. F 2.4 mm (MNHN-IU-2016-481).—Stn DC33, 33º50'S, 43º11'E, 25–30 m, 16 March 1976: 1 M 2.8 mm (MNHN-IU-2016-466).

Reunion Island. MD32 Stn CP43, 21º20.7'S, 55º26.9'E, 73–77 m, 18 August 1982: 5 M 1.5–2.3 mm, 5 ov. F 1.8–2.3 mm, 4 F 1.5–1.8 mm (MNHN-IU-2019-2696).

Madagascar. ATIMO VATAE Stn CP3511, 25°15.0'S, 47°14.5'E , 97–98 m, 29 April 2010: 1 F 2.0 mm (MNHN-IU-2010-2750).—Stn TB02, 25°01.3'S, 47°00.5'E, 18 m, 1 May 2010: 1 M 2.7 mm (MNHN-IU-2016-462).—Stn DW3530, 24°35.9'S, 47°32.1'E, 80–86 m, 2 May 2010: 1 M 2.5 mm (MNHN-IU-2016-485).—Stn CP3546, 25°22.7'S , 46°42.5'E, 84–85 m, 4 May 2010: 1 M 2.2 mm (MNHN-IU-2016-483), 1 M 1.7 mm (MNHN-IU-2014-13800).—Stn CP3579, 25°54.5'S, 45°33.2'E, 65–66 m, 9 May 2010: 1 M 2.1 mm (MNHN-IU-2016-464).—Stn DW3605, 25°54.5'S , 44°51.0'E, 56–57 m, 13 May 2010: 2 M 2.3–2.5 mm (MNHN-IU-2016-484).—Stn CP3624, 25°38.1'S, 45°57.0'E, 63–63 m, 15 May 2010: 1 M 1.8 mm (MNHN-IU-2016-482).
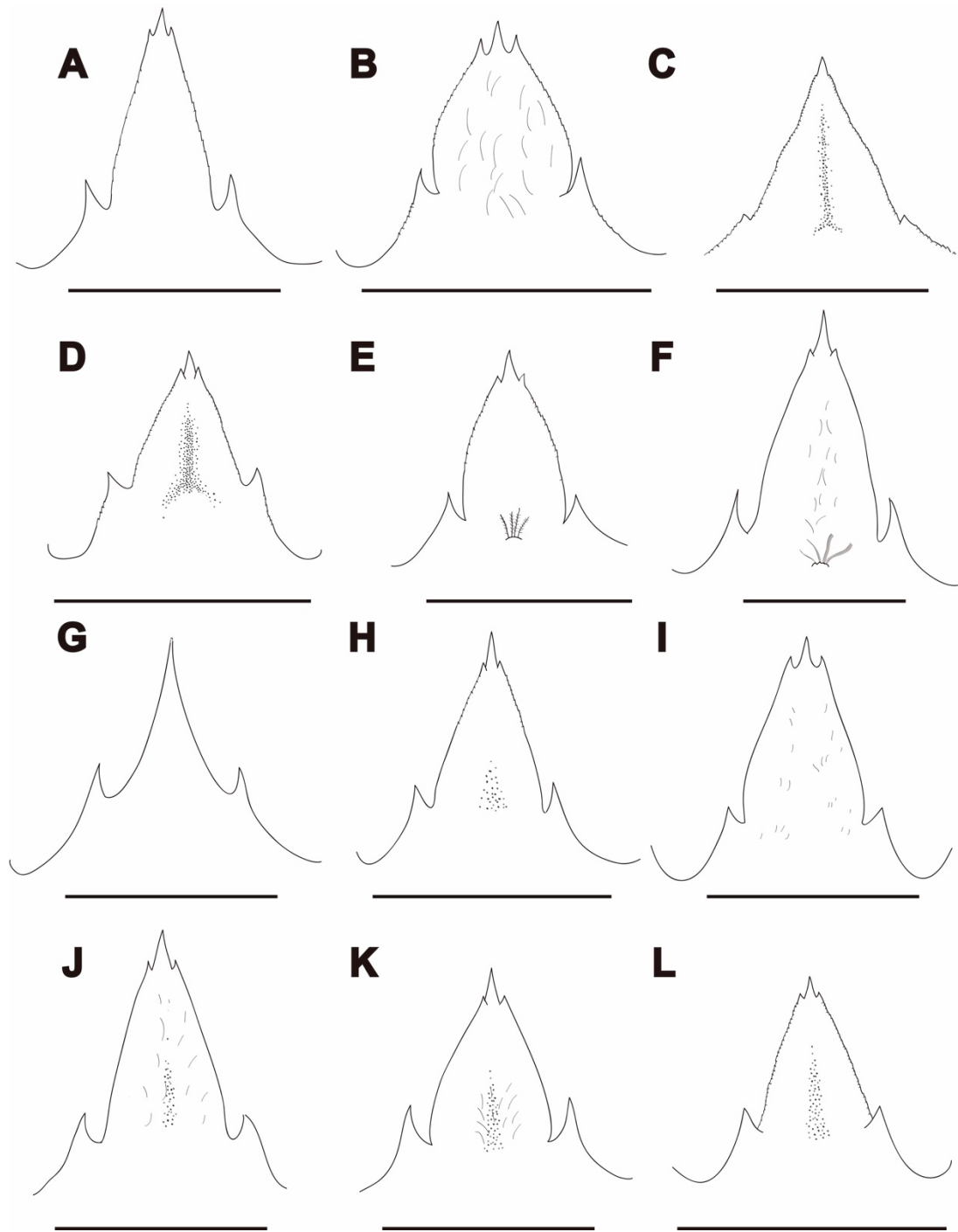
FIGURE 21. Rostrum, dorsal view. A, *Phylladiorhynchus euryalus* **n. sp.**, paratype male 1.8 mm (UF34732). B, *P. gustavi* **n. sp.**, paratype male 1.7 mm (UF9756). C, *P. heptacanthus* **n. sp**., holotype female 2.1 mm (MNHN-IU-2017-2534). D, *P. hylas* **n. sp.**, paratype female 1.6 mm (MNHN-IU-2016-495). E, *P. integrirostris* (Dana, 1852), male 1.6 mm (UF15285). F, *P. integrus* (Benedict, 1902), ovigerous female 3.2 mm (MNHN-IU-2014-13853). G, *P. iphiclus* **n. sp.**, holotype ovigerous female 2.3 mm (MNHN-IU-2019-2662). H, *P. janiqueae* **n. sp.**, paratype male 1.8 mm (MNHN-IU-2016-482). I, *P. jeffkinchi* **n. sp**., paratype male 2.7 mm (MNHN-IU-2014-13565). J, *P. joannotae* **n. sp.**, paratype male 2.1 mm (MNHN-IU-2014-20055). K, *P. joannotae* **n. sp.**, holotype ovigerous female 2.1 mm (MNHN-IU-2014-13805). L, *P. koumac* **n. sp.**, paratype male 1.5 mm (MNHN-IU-2014-20121). Scale bars:1 mm.
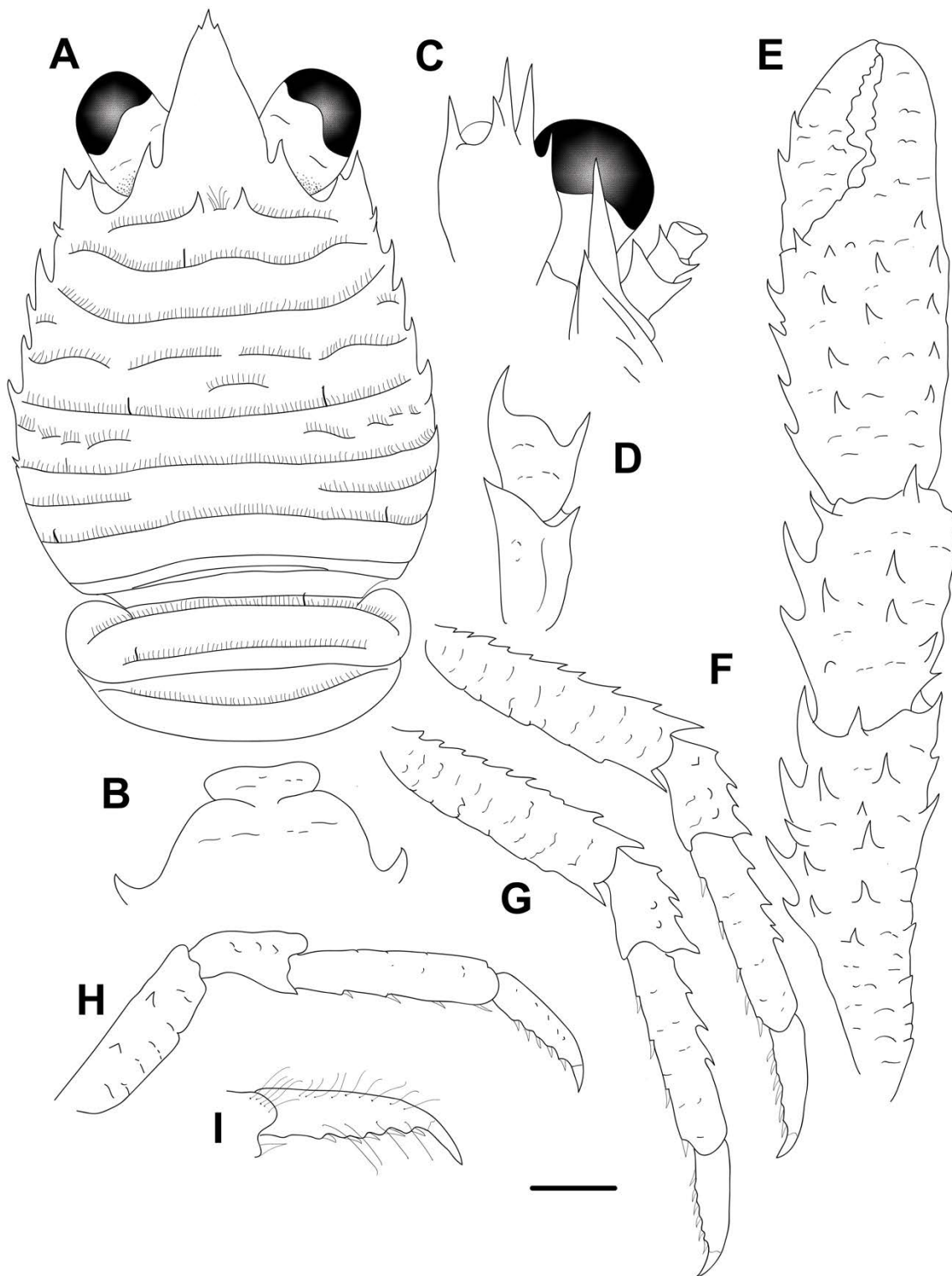
FIGURE 22. *Phylladiorhynchus janiqueae* **n. sp**., holotype male 2.3 mm (MNHN-IU-2014-13799): A, carapace and pleon, dorsal view. B, thoracic sternites 3 and 4. C, left cephalic region, showing antennular and antennal peduncles, ventral view. D, right Mxp3, lateral view. E, right P1, dorsal view. F, right P2, lateral view. G, right P3, lateral view. H, right P4, lateral view. I, dactylus of right P2, lateral view. Scale bar: A, E-H = 1.0 mm; B–D, I = 0.6 mm.

SW Indian Ocean. WALTER SHOALS Stn WS03, 33°12.2'S, 43°50.8'E, 40 m, 30 April 2017: 1 F 1.4 mm (MNHN-IU-2016-455), 7 M 1.4–2.1 mm, 8 F 1.4–2.2 mm, 4 postlarvae 1.0–1.1 mm (MNHN-IU-2016-459).—Stn WB05, 33°15.1'S, 43°54.5'E, 26–30 m, 1 May 2017: 4 M 1.5–1.8 mm, 8 F 1.2–2.2 mm, 3 postlarvae 1.0–1.1 mm (MNHN-IU-2016-456), 6 M 1.7–2.7 mm, 1 ov. F 2.5 mm, 4 F 1.4–1.6 mm (MNHN-IU-2016-458), 1 M 2.2 mm (MNHN-IU-2014-12606), 1 M 1.9 mm (MNHN-IU-2014-13841).—Stn WS06, 33°15.1'S, 43°54.5'E, 26 m, 1 May 2017: 1 M 1.9 mm, 2 F 1.2–1.3 mm (MNHN-IU-2017-3613).—Stn WS07, 33°15.4'S, 43°52.2'E, 30–33 m, 2 May 2017: 3 M 1.3–1.7 mm, 3 F 1.3–1.9 mm (MNHN-IU-2016-487).—Stn WS08, 33°13.7'S, 43°55.9'E, 30–33 m, 3 May 2017: 1 M 1.8 mm (MNHN-IU-2014-13840), 2 M 1.3–2.2 mm, 5 F 1.3–2.3 mm (MNHN-IU-2017-3333), 9 M 1.3–2.1 mm, 7 F 1.2–2.2 mm, 11 postlarvae 1.0–1.1 mm (MNHN-IU-2016-460).—Stn WB09, 33°13.8'S, 43°55.8'E, 27–30 m, 4 May 2017: 16 M 1.2–3.1 mm, 15 F 1.4–2.2 mm, 7 postlarvae 1.0–1.1 mm, (MNHN-IU-2014-13839), 1 postlarvae 1.0 mm (MNHN-IU-2016-457), 1 F 1.3 mm (MNHN-IU-2017-2960), 2 M 2.1–2.4 mm, 4 F 1.5–2.1 mm, 10 postlarvae, 0.9–1.0 mm (MNHN-IU-2017-3316).—Stn WB10, 33°09.1'S, 43°51.8'E, 30 m, 6 May 2017: 26 M 1.5–2.1 mm, 25 F 1.2–2.5 mm, 14 postlarvae 1.0–1.2 mm (MNHN-IU-2019-2689), 13 M 1.1–2.4 mm, 15 F 1.1–2.3 mm, 3, postlarvae 1.0–1.1 mm, (MNHN-IU-2017-3812), 1 M 2.4 mm (MNHN-IU-2014-12639), 2, postlarvae, 1 broken (MNHN-IU-2017-2990).

Etymology. The new species is named after Janique Etienne, Senior Officer in charge of High Seas projects with Fonds Français pour l'Environnement Mondial (FFEM), in recognition for her support to the Walters Shoals expedition.

Description. *Carapace:* [0.9]–1.1 times as long as broad; transverse ridges with dense short setae and few scattered long and thick iridescent setae. Gastric region with 4 transverse ridges: epigastric ridge distinct with 2 median spines; anterior protogastric ridge not medially interrupted, nearly extending laterally to carapace margin; anterior mesogastric ridge not medially interrupted, laterally continuing to first branchial spine; anterior metagastric ridge scale-like (rarely medially interrupted), sometimes followed by a short small scale. Mid-transverse ridge not interrupted, medially slightly depressed, cervical groove indistinct, followed by 2 not interrupted or minutely interrupted ridges, interspersed with 1 short lateral ridge and some few short scales. Lateral margins slightly convex, with 6–7 distinct spines: first anterolateral spine well-developed, reaching anteriorly to level of lateral orbital spine, second spine (hepatic) small, slightly dorsomesially from lateral margin, and followed by 4–5 branchial spines (3 anterior and 1–2 posterior). Rostrum leaf-like, horizontal, dorsally convex, [1.4]–1.6 times as long as broad, length [0.4]0.4 and breadth [0.3]0.3 that of carapace; lateral margins smooth or

minutely serrated and convex, with well-developed supraocular basal spines and small subapical spines. Pterygostomian flap ending in anterior spine, upper margin smooth.

Sternum: As wide as long. Sternite 3 moderately broad, 1.9–[3.0] times as wide as long, anterior margin slightly convex or straight. Sternite 4 widely contiguous to sternite 3; anterolaterally smooth, surface depressed in midline, smooth; greatest width 2.0–[2.5] times that of sternite 3, 2.7–[3.5] times as wide as long.

Pleon: Tergite 2 with anterior and posterior transverse elevated ridges, with short setae and a few scattered long setae; tergites 3–4 with anterior transverse ridge only; tergites 5–6 smooth.

Eye: Eye stalk length about [1.1]1.1 times broader than long, peduncle distally setose, not distinctly expanded proximally; cornea expanded distally, maximum corneal diameter [0.9]0.9 × rostrum width*,* as wide as eyestalk.

Antennule: Article 1 slightly longer than wide, with 5 distal spines: distomesial spine well-developed; proximal lateral spine small, always present.

Antenna: Article 1 with prominent mesial process distally falling well short of lateralmost antennular spine. Article 2 with well-developed distomesial and distolateral spines. Article 3 with distomesial spine and distolateral spines, otherwise only distomesial spine. Article 4 unarmed.

Mxp3: Ischium with distinct distal spines on flexor and extensor margins. Merus 0.6–[0.8]X × length of ischium, with well-developed distal spine on extensor and flexor margins.

P1: 2.0–[3.0] (males), 1.7–1.9 (females) times carapace length; subcylindrical, spiny and with dense long stiff setae; merus, carpus and palm with spines along mesial, dorsal and lateral surfaces, distal and mesial spines usually stronger than others. Merus 0.7–[1.1] length of carapace, 1.7–[1.8] times as long as carpus, . Carpus [1.5]–2 times as long as wide. Palm [1.1]1.1 × carpus length, [1.4]–1.7 times as long as broad. Fingers [0.9]0.8–1.0 × palm length; fixed finger with 2 small basal spines; movable finger with 1–2 basal spines or unarmed.

P2–4: stout, setose and spinose. Meri successively shorter posteriorly: P3 merus [0.9]–1.0 times length of P2 merus, P4 merus [0.8]–0.9 times length of P3 merus. P2 merus, 0.5–[0.7] times carapace length, 3.8–[4.0].times as long as broad, 1–[1.4] times as long as P2 propodus; P3 merus 3.2–[3.9] times as long as broad, 1.1–[1.3] times as long as P3 propodus; P4 merus [3.3]2.9–3.6 times as long as broad, 1.0–[1.1] times as long as

P4 propodus; extensor margin of P2 and P3 with row of spines, proximally diminishing, with prominent distal spine; P4 extensor margin irregular, unarmed; flexor margin irregular, with distal spine on P2–3, distal spine absent in P4, P4 lateral surface with median row of 2 small spines, absent in P2–3. Carpi with 1–3 spines on extensor margin on P2–3, unarmed on P4; distal spine prominent on P2–3, smaller on P4; granules below extensor margin on lateral surface of P2–4; flexor margin unarmed. Propodi stout, [4.3–4.6]3.7–4.4 times as long as broad; extensor margin irregular, armed with 2–4 spines on proximal half, otherwise unarmed; flexor margin with 3–4 slender movable spines in addition to distal pair. Dactyli [0.6–0.7]0.6–0.7 × length of propodi, ending in incurved, strong, sharp spine; flexor margin with 5–6 movable spines.

Eggs: Ov. F carried approximately 20–35 eggs of 0.4–0.5 mm diameter.

Colour. Base colour of carapace orange, gastric and cardiac region covered by reddish granules and spots, epigastric spines dark orange, marginal spines orange, first posterior branchial spine reddish. Rostrum and ocular peduncles orange, covered by reddish granules and spots, supraocular spines dark orange. Pleonal tergites 1–4 orange, densely with reddish granules, anterior ridges of tergites 2–4 with whitish stripes; tergites 5–6 and telson translucent. P1 light orange with scattered reddish spots, spines dark orange, tip of fingers whitish. P2–4 whitish or translucent, spines reddish or dark orange; meri, carpi, propodi and dactyli with orange bands.

Genetic data. COI and 16S, Table 1.

Distribution. South West Indian Ocean, Madagascar, Reunion Island and Walter Shoals, from 18 to 98 m.

Remarks. *Phylladiorhynchus janiqueae* belongs to the group of species having 2 epigastric spines, 1 hepatic spine, 3 spines on the anterior branchial margin and the pleonal tergite 3 with the anterior ridge only. This species fits with the illustrations from Tirmizi & Javed (1980, 1993) from the Indian Ocean, however we have not examined this material, therefore the identification of these specimens remains dubious. The new species is closely related with *P. medea* from French Polynesia and New Caledonia (see the differences under the Remarks of this species).

Phylladiorhynchus jeffkinchi **n. sp.**

(Figs. 21I, 23, 54F)

Type material. *Holotype.* Papua New Guinea. KAVIENG Stn KS31, 02°39.5'S, 150°37.7'E, 15 m, 12 June 2014: ov. F 2.4 mm (MNHN-IU-2014-13661).
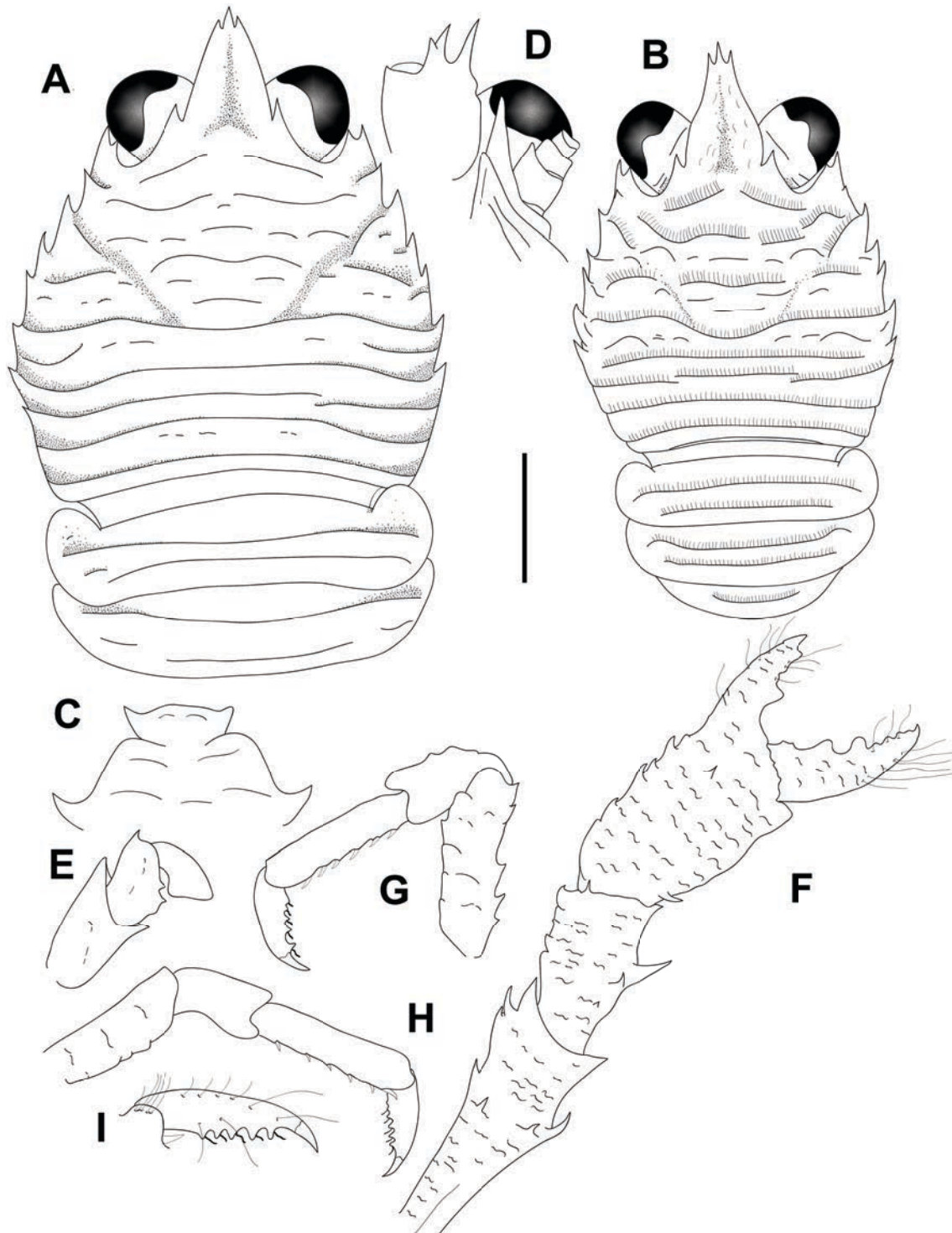
FIGURE 23. *Phylladiorhynchus jeffkinchi* **n. sp**., A-D, G-I, holotype ovigerous female 2.4 mm (MNHN-IU-2014-13661); B, F, paratype male 2.7 mm (IU-2014-13565): A, B, carapace and pleon, dorsal view. C, thoracic sternites 3 and 4. D, left cephalic region, showing antennular and antennal peduncles, ventral view. E, right Mxp3, lateral view. F, left P1, dorsal view. G, left P3, lateral view. H, right P4, lateral view. I, dactylus of right P4, lateral view. Scale bar: A, B, F-H = 1.0 mm; C–E, I = 0.6 mm.

Paratypes. Papua New Guinea. KAVIENG Stn KB06, 02º41.2'S, 150º41.2'E, 8 m, 4 June 2014: 1 F 2.0 mm (MNHN-IU-2014-13639).—Stn KS15, 02º41.2'S, 150°41.2'E, 3–5 m, 6 June 2014: 1 ov. F 2.2 mm (MNHN-IU-2014-2176).—Stn KS23, 02º40.8'S, 150º42.7'E, 4–7 m, 8 June 2014: 1 ov. F 1.8 mm (MNHN-IU-2014-13528), 3 M 1.1–1.5 mm, 1 ov. F 1.9 mm (MNHN-IU-2016-5835).—Stn KB18, 02º40.8'S, 150º42.7'E, 4–7 m, 8 June 2014: 1 M 2.0 mm (MNHN-IU-2014-13623).—Stn KD36, 02°35.1'S, 150°29'E, 8 m, 16 June 2014: 1 ov. F 2.2 mm (MNHN-IU-2014-13530).—Stn KS41, 02º36.6'S, 150º32.9'E, 2–7 m, 16 June 2014: 2 M 1.7–1.9 mm (MNHN-IU-2014-13647).—Stn KS43, 02º35.2'S, 150º29.1'E, 4–12 m, 16 June 2014: 8 M 1.2–1.7 mm, 3 ov. F 1.8–2.0 mm, 5 F 1.4–1.6 mm, 2 postlarvae 1.0 mm (MNHN-IU-2016-5851).—Stn KD78, 02°42.6'S, 150°43.4'E, 6–10 m, 26 June 2014, 1 M 2.7 mm (MNHN-IU-2014-13565).

Etymology. Named after Jeff Kinch, formerly Principal of Papua New Guinea National Fisheries Authority's, National Fisheries College in Kavieng.

Description. *Carapace:* Robust or massive, sexually dimorphic (wider on females), [0.9]0.9 (males), 0.8(females) times as long as broad; transverse ridges elevated, uplifted dorsally, densely covered with short setae, long and thick setae absent. Gastric region convex (uplifted) with some transverse ridges: epigastric ridge distinct, medially interrupted, unarmed; anterior protogastric ridge usually medially and laterally interrupted, with some few scales to carapace margin, often followed by some few short scales; anterior mesogastric ridge scale-like, laterally interrupted by anterior branch of cervical groove, continuing with some few scales, often followed by some few short scales; anterior metagastric ridge not medially interrupted, laterally interrupted, followed by scales on posterior metagastric region. Mid-transverse ridge not interrupted, cervical groove distinct, followed by 3 not interrupted or minutely interrupted ridges, interspersed with 1 laterally interrupted or scale-like ridge, and some few scattered scales. Lateral margins clearly convex, with 7–8 spines: first anterolateral spine well-developed, exceeding lateral orbital spine, second spine (hepatic) small, slightly dorsomesially from lateral margin, and followed by 5–6 branchial spines behind distinct anterior cervical groove (3 anterior and 1–2 posterior). Rostrum leaf-like, horizontal, dorsally flattish or slightly concave, [1.5]1.4–1.7 times as long as broad, length [0.4]0.4–0.5 and breadth [0.3]0.2–0.3 that of carapace; lateral margins smooth and convex, with well-developed basal supraocular and subapical spines. Pterygostomian flap ending in blunt tooth; upper margin unarmed.

Sternum: Sternite 3 moderately broad, [2.0]–2.5 times as wide as long, anterior margin convex, with anterolateral projections. Sternite 4 widely contiguous to sternite 3; surface flattened, smooth; greatest width [3.0]–3.0 times that of sternite 3, [2.5]–2.7 times as wide as long.

Pleon: Elevated ridges uplifted dorsally, with few short setae. Tergites 2–4 with anterior and posterior transverse elevated ridges; tergites 5–6 smooth.

Eye: Eye stalk length about [0.9]0.9 times broader than long, peduncle distally setose, not distinctly expanded proximally; maximum corneal diameter [1.0]1.0 × rostrum width*,* about as wide as eyestalk.

Antennule: Article 1 longer than wide, with 3 distal spines: distomesial spine absent, pair of distolateral spines present; proximal lateral spine absent. Short striae covering mesial surfaces.

Antenna: Article 1 with prominent mesial process distally clearly not reaching lateral antennular spine. Article 2 unarmed, sometimes with minute distomesial spine. Articles 3 and 4 unarmed.

Mxp3: Ischium with distinct distal spines on flexor and extensor margins. Merus [0.5]–0.6 × length of ischium, with 0–1 median small spine and well-developed distal spine on extensor margin and 2 spines on flexor margin.

P1: 2.6–2.7 times carapace length (male) [1.5]–1.6 (female); subcylindrical, moderately spiny and with scattered long stiff setae. Merus [0.6]0.5–0.9 length of carapace, [1.7]1.6–1.8 times as long as carpus, with few scattered spines, mesial spines strongest. Carpus [1.5]1.6–1.9 times as long as wide with few scattered spines, mesial most prominent. Palm [1.2]1.2–1.3 × carpus length, [1.4]1.3–3.0 times as long as broad with scattered small spines on dorsal and ventral surfaces, lateral and mesial margins irregular, with scattered small spines. Fingers unarmed, [0.9]0.7–0.9 × palm length.

P2–4: Moderately stout, setose and few spinose. Meri successively shorter posteriorly: P3 merus 0.7–0.9 times length of P2 merus, P4 merus 0.8–0.9 times length of P3 merus. P2 merus, 0.6 times carapace length, 3.8 times as long as broad, 1.1 times as long as P2 propodus; P3 merus 3.4–3.8 times as long as broad, 1.1–1.2 times as long as P3 propodus; P4 merus 1.2 times as long as broad, as long as P4 propodus; extensor margins of P2 and P3 with row of few small spines, proximally diminishing, with well-developed distal spine; P4 extensor margin irregular but unarmed; flexor margins irregular, with distal spine on P2–3, absent in P4. Carpi with 1–2 small spines on extensor margins on P2–3, unarmed on P4; distal spine prominent on P2–3, absent on P4; row of small spines below extensor margin on lateral surface of P2–3, unarmed on P4. Propodi stout, 3–4 times as long as broad; extensor margins irregular, usually unarmed; flexor margins with 3–5 slender movable spines in addition to distal pair. Dactyli 0.7–0.8 × length of propodi, ending in incurved, strong, sharp spine; flexor margins with 5–6 well-developed dactylar spines, each with 1 spinule.

Eggs: Ov. F carried approximately 8–20 eggs of 0.3–0.5 mm diameter.

Colour. Base colour of carapace green-brownish with some whitish and dark brown patches on gastric region, (epigastric, protogastric ridges and cervical groove), elevated ridges with whitish and brownish small spots, marginal spines whitish. Rostrum brownish; margin, tip and supraocular spines whitish with dark brown stripes diminishing proximally. Pleonal tergites 2–6 brownish, with medial whitish stripe, and lateral brownish and whitish stripes, ridges of tergites 2–4 whish a median brownish spot; uropods and telson whitish. P1 whitish-pale brown, with brownish bands distally on meri, carpi, and palm; spines whitish. P2–4 whitish; distal portion of meri, carpi and propodi darker, dactyli whitish-translucid.

Genetic data. COI and 16S, Table 1.

Distribution. Papua New Guinea, from 3 to 15 m.

Remarks. *Phylladiorhynchus jeffkinchi* belongs to the group of species characterized by having the epigastric ridge unarmed, the carapace and pleon ridges elevated, uplifted, and dactylar spines on the flexor margins of the dactyli. The new species resembles *P. phanus*, from Papua New Guinea and *P. marina*, from Vanuatu. However, *P. jeffkinchi* can be distinguished from these species on the basis of the following characters:

- The anterior epigastric ridge is always distinct and medially interrupted in *P. jeffkinchi*, whereas it is often indistinct or scale-like in *P. phanus* and *P. marina*.
- The anterior protogastric ridge is often medially interrupted in *P. jeffkinchi*, whereas it is not interrupted in *P. phanus* and *P. marina*.
- The carapace is densely covered by short setae in *P. jeffkinchi*, whereas these setae are shorter and less dense in *P. phanus* and *P. marina*.
- The anterior margin of the sternite 3 is convex and anterolaterally projected in *P. jeffkinchi*, whereas these anterolaterally projections are absent in *P. phanus* and *P. marina*.

The genetic divergences among *P. jeffkinchi, P. marina* and *P. phanus* were 7% (16S) and larger than 14% (COI).

***Phylladiorhynchus joannotae* n. sp.**

(Figs. 21K, 24, 54G-H)

Type material: *Holotype.* Vanuatu. SANTO Stn DB33, 15°34.7'S, 167°13.8'E, 14–25 m, 18 September 2006: 1 ov. F 2.1 mm (IU-2014-13805).
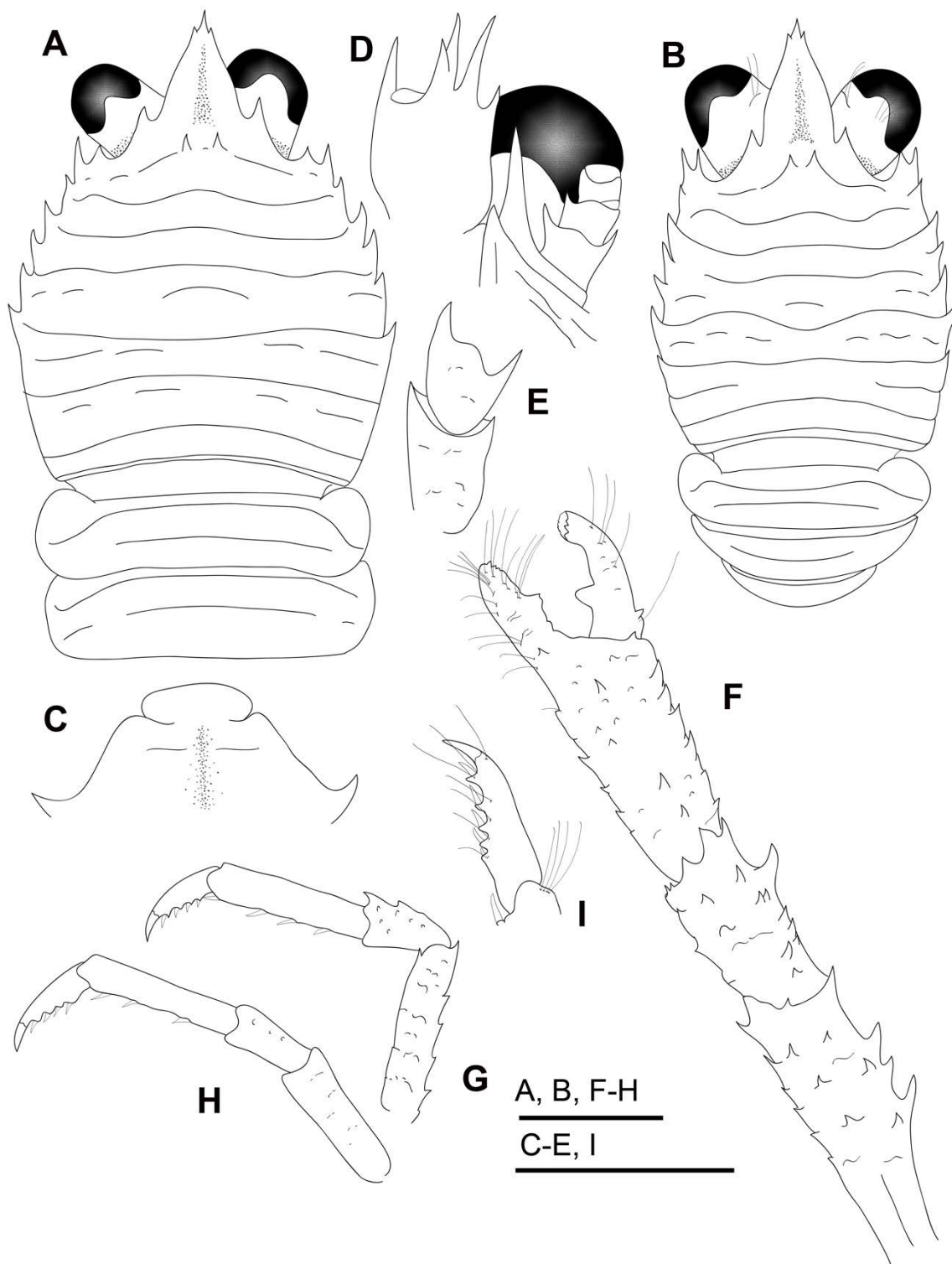
FIGURE 24. *Phylladiorhynchus joannotae* **n. sp**., A, C-E, H-I, holotype ovigerous female 2.1 mm (MNHN-IU-2014-13805); B, F, paratype male 2.1 mm (MNHN-IU-2014-20055): A, B, carapace and pleon, dorsal view. C, thoracic sternites 3 and 4. D, left cephalic region, showing antennular and antennal peduncles, ventral view. E, right Mxp3, lateral view. F, left P1, dorsal view. G, left P3, lateral view. H, left P4, lateral view. I, dactylus of left P3, lateral view. Scale bars = 1.0 mm.

Paratypes. American Samoa. Olosega Island. OLO-057, 14.18140174ºS, 169.6267462ºW, 14 m, 14 March 2015: 1 ov. F 2.0 mm.—OLO-211, 14.18140174ºS, 169.6267462ºW, 14 m, 14 March 2015: 1 M 2.2 mm.

French Polynesia. Society Islands, Moorea Island, Fore reef NE of Tareu Pass, outer reef slope, rubble, 17.4803ºS, 149.8539ºW, 35–37 m, 2 August 2006: 1 broken (UF10072).—17.4826ºS, 149.8962ºW, 14 October 2008: 1 ov. F 2.2 mm (UF15544).—17.5145ºS, 149.7616ºW, 22 m, 23 October 2008: 1 ov. F 1.8 mm (UF16051).—17.5303ºS, 149.7621ºW, 15–32 m, 27 October 2008: 1 ov. F 1.9 mm (UF16169).

Northern Mariana Islands. Saipan Island. Stn SAI-441, 15.09782849ºN, 145.7434357ºE, 17 m, 11 April 2014, 1 M 1.6 mm, 1 ov. F 2.0 mm (2014).—Stn SAI-477, 15.09782849ºN, 145.7434357ºE, 17 m, 11 April 2014: 1 M 2.0 mm (2014).—Stn SAI-584, 15.09782849ºN, 145.7434357ºE, 17 m, 11 April 2014: 1 M 2.0 mm (2014).—Pagan Island. Stn PAG-694, 18.0706862ºN, 145.7137933ºE, 37 m, 20 April 2014: 1 ov. F 2.2 mm, 1 F 1.9 mm (2014).—Stn PAG-809, 18.0706862ºN, 145.7137933ºE, 37 m, 20 April 2014: 1 M 1.4 mm (2014).

Marshall Islands. Wake Island. Stn WAK-115, 19.2917761ºN, 166.6072896ºE, 14 m, 17 March 2014: 1 F 1.7 mm (2014).

Vanuatu. SANTO Stn ZB9, 15°40.6'S, 167°05.1'E, 5–7 m, 02 October 2006: 1 ov. F 1.7 mm (MNHN-IU-2019-2627).—Stn DB86, 15°38.5'S, 167°15.1'E, 13 m, 04 October 2006: 1 ov. F 2.3 mm (MNHN-IU-2014-13809).—Stn DB1, 15°33.1'S, 167°17.8'E, 15–25 m, 10 September 2006: 1 M 1.8 mm (MNHN-IU-2019-2628).—Stn FB72, 15°36.1'S, 166°58.5'E, 16 m, 12 October 2006: 1 M 2.2 mm, 1 postlarvae (MNHN-IU-2014-13877).—Stn DB29, 15°38.9'S, 167°05.1'E, 15 m, 17 September 2006: 1 M 1.9 mm, 1 F 1.7 mm (MNHN-IU-2014-13869).—Stn ZB6, 15°36.8'S, 167°01.3'E, 30 m, 28 September 2006: 1 F 1.7 mm (MNHN-IU-2014-13871).

Chesterfield Islands, Ebisco, Stn DW2569, 20º23.777'S, 158º40.198'E, 50 m, 14 October 2005: 1 ov. F 1.7 mm (MNHN-IU-2014-13912).

New Caledonia. New Caledonia, Lagon Est, Stn 735, 22º05.1'S, 166º57.2'E, 15–34 m, August 1986: 1 M 2.5 mm (MNHN-IU-2019-2620).—Touho Dive, 7 September 1993: 1 M 1.7 mm, 2 ov. F 2.0–2.1 mm, 1 F 2.1 mm (MNHN-IU-2019-2614).—Touho, 6 September 1993: 2 M 1.5–1.6 mm, 2 F 1.7–1.8 mm (MNHN-IU-2016-498).—Exp. Mont. Komac, 12 m, 7 October 1993: 1 M parasitized 2.5 mm (MNHN-IU-2019-2634).—LIFOU Stn 1452, 20°54.6' S, 167°02.1' E, 2–25 m, 20 November 2000: 1 M 2.2 mm, 1 ov. F 2.0 mm (MNHN-IU-2019-2599).—Stn 1430, 24 November 2000: 1 ov. F 2.6 mm (MNHN-IU-2019-2622).—Stn 1455, 20°56.8'S, 167°02.7'E, 15–20 m, 25 November

2000: 1 M 2.0 mm, 2 ov. F 2.1–2.2 mm (IU-2019-2626).—KOUMAC Stn KB612, 20.6695ºS, 164.18941ºE, 13 m, 01 November 2019: 1 M 1.5 mm, 1 F parasitized 1.6 mm, 1 postlarvae 1.0 mm (MNHN-2019-2580) 1 broken (MNHN-IU-2014-3426).—Stn KB613, 20.6682ºS, 164.18962ºE, 15 m, 01 November 2019: 1 ov. F 1.5 mm (MNHN-IU-2019-1556), 1 M 1.3 mm, 5 ov. F 1.4–1.9 mm, 2 F 1.1–2.0 mm (MNHN-IU-2019-1573).—Stn KB615, 20.6943ºS, 164.24786ºE, 13 m, 02 November 2019: 1 ov. F 1.5 mm (MNHN-IU-2019-1560), 4 F 1.5–1.8 mm (MNHN-IU-2014-20198).—Stn KB619, 20.5135ºS, 164.03151ºE, 12 m, 03 November 2019: 2 M 1.8–1.9 mm (MNHN-IU-2019-1562), 1 F 1.8 mm (IU-2019-5518).—Stn KB622, 20.75144ºS, 164.23203ºE, 19 m, 04 November 2019: 2 M 1.4–1.5 mm, 2 F parasitized 1.5–1.6 mm (MNHN-IU-2019-1572).—Stn KB623, 20.7518ºS, 164.2340ºE, 12 m, 05 November 2019: 2 M 1.5–1.6 mm, 3 F 1.1–1.8 mm, 1 postlarvae 1.0 mm (MNHN-IU-2019-3418).—Stn KB624, 20.62347ºS, 164.14964ºE, 3 m, 05 November 2019: 1 M 1.3 mm (MNHN-IU-2019-3420), 1 M 1.4 mm (MNHN-IU-2019-3428).—Stn KB631, 20.52698ºS, 164.02615ºE, 3 m, 08 November 2019: 1 M 1.8 mm, 1 postlarvae 1.0 mm (MNHN-IU-2014-20079).—Stn KB633, 20.59318ºS, 164.25161ºE, 41 m, 10 November 2019: 2 M 1.0–1.2 mm, 3 ov. F 1.4–1.5 mm, 1 F 1.2 mm (MNHN-IU-2014-20048).—Stn KB636, 20.63948ºS, 164.18293ºE, 3 m, 10 November 2019: 1 F 1.9 mm (MNHN-IU-2014-20062), 1 M 1.8 mm, 1 ov. F 2.1 mm, 1 F parasitized 1.7 mm (MNHN-IU-2014-20064), 1 M 1.6 mm (MNHN-IU-2014-20066).—Stn KL39, 20.7511ºS, 164.23276ºE, 26 m, 10 November 2019: 4 M 1.4–1.8 mm, 4 F parasitized 1.5–1.8 mm (MNHN-IU-2014-20172), 1 F 1.3 mm (MNHN-IU-2014-20046), 1 M 2.1 mm, 2 ov. F 1.9–2.5 mm, 3 F 1.7–2.0 mm (MNHN-IU-2014-20055), 1 ov. F 2.3 mm (MNHN-IU-2014-20056).—Stn KL40, 20.75156ºS, 164.2343ºE, 52 m, 10 November 2019: 1 ov. F 2.2 mm (MNHN-IU-2014-20083).—Stn KL03, 20.67485ºS, 164.214266ºE, 50 m, 11 November 2019: 1 F 1.8 mm (MNHN-IU-2014-20069).—Stn KB638, 20.594533ºS, 164.10925ºE, 4 m, 13 November 2019: 1 M 2.0 mm, 1 ov. F 2.6 mm, 1 F parasitized 2.0 mm (MNHN-IU-2014-20119).—Stn KB639, 20.7511ºS, 164.23245ºE, 22 m, 13 November 2019: 1 ov. F 1.7 mm, 3 F 1.6–2.2 mm (MNHN-IU-2014-20196).—Stn KB640, 20.72511ºS, 164.26738ºE, 6 m, 13 November 2019: 1 M parasitized 2.0 mm (MNHN-IU-2014-20111), 2 M 1.5–2.0 mm, 1 ov. F 2.4 mm (MNHN-IU-2014-20112).—Stn KD558, 20.72775ºS, 164.26546ºE, 6 m, 13 November 2019: 1 F parasitized 1.9 mm (MNHN-IU-2014-20088).—Stn KB641, 20.7988ºS, 164.27253ºE, 36 m, 14 November 2019: 1 broken (MNHN-IU-2014-20102).—Stn KB643, 20.61416ºS, 164.13703ºE, 3 m, 14 November 2019: 2 M 1.4–2.5 mm, 6 ov. F 2.4–2.6 mm (MNHN-IU-2014-20096), 1 M 2.2 mm (MNHN-IU-2019-5320), 1 ov. F 2.1 mm (MNHN-IU-2019-5319).—Stn KB645, 20.67573ºS, 164.2171ºE, 16 m, 15 November 2019: 1 F 1.3 mm (MNHN-IU-2014-20115), 2 M 1.2–1.3 mm, 5 F 1.0–1.2 mm (MNHN-IU-2014-20125).—Stn KB646, 20.644983ºS, 164.24386ºE, 12 m, 15 November 2019: 1 F parasitized 2.1 mm (MNHN-IU-2014-20114), 1 M 1.7 mm, 1

postlarvae 0.9 mm (MNHN-IU-2014-20118).—Stn KB647, 20.664116ºS, 164.189983ºE, 38 m, 16 November 2019: 1 ov. F 1.6 mm, 3 F 1.0–1.9 mm (MNHN-IU-2014-20139).—Stn KL27, 20.7878ºS, 164.27191ºE, 102 m, 16 November 2019: 1 juv. 1.0 mm (MNHN-IU-2014-20129).—Stn KL37, 20.8319ºS, 164.27818ºE, 81 m, 16 November 2019: 1 M 1.1 mm (MNHN-IU-2014-20132).—Stn KB649, 20.80583ºS, 164.26916ºE, 42 m, 18 November 2019: 5 F 1.7–1.9 mm, 5 postlarvae 0.9–1.0 mm (MNHN-IU-2014-20154).—Stn KB651, 20.83145ºS, 164.280556ºE, 12 m, 18 November 2019: 1 postlarvae 1.1 mm (MNHN-IU-2014-20143), 1 F 1.0 mm (MNHN-IU-2014-20147).—Stn KB651, 20.83145ºS, 164.280556ºE, 12 m, 18 November 2019: 1 postlarvae 1.1 mm (MNHN-IU-2014-20148), 1 F 1.8 mm (MNHN-IU-2014-20144).—Stn KB654, 20.44587ºS, 163.97254ºE, 15 m, 19 November 2019: 7 F parasitized 1.1–2.1 mm (MNHN-IU-2014-20164).—Stn KB655, 20.68517ºS, 164.27078ºE, 6 m, 20 November 2019: 1 M 1.9 mm, 1 F parasitized 2.2 mm (MNHN-IU-2014-20193).—Stn KB659, 20.66049ºS, 164.26852ºE, 15 m, 21 November 2019: 1 M 1.9 mm (MNHN-IU-2014-20176).—Stn KB664, 20.66925ºS, 164.230805ºE, 3 m, 23 November 2019: 1 F parasitized 1.8 mm (MNHN-IU-2014-20184).—Stn ARMS 2B, November 2019: 1 M 1.7 mm (MNHN-IU-2014-20074).—Stn ARMS 8B, November 2019: 1 M 1.8 mm, 2 ov. F 2.2.–2.3 mm (MNHN-IU-2014-20162).

Etymology. The new species is named after Pascale Joannot, Head of the MNHN Expeditions programme, who has been instrumental in raising support for the Our Planet Reviewed New Caledonia expeditions.

Description. *Carapace:* as long as or slightly broader than long, sexually dimorphic (wider on females) 0.9–1.0 (males), [0.8]–0.9 (females); transverse ridges with dense short setae and few scattered thick and iridescent setae. Gastric region slightly convex with 4 transverse ridges: epigastric ridge distinct with 2 median spines and some lateral short scales, often followed by small scattered scales; anterior protogastric ridge not medially interrupted, nearly extending laterally to carapace margin, often followed by small scattered scales; anterior mesogastric ridge not medially interrupted, continuing to first branchial spine; anterior metagastric not medially interrupted, sometimes followed by short scattered scales on posterior metagastric region. Mid-transverse ridge not interrupted, medially slightly depressed, cervical groove indistinct, followed by 2 not interrupted or minutely interrupted ridges, interspersed with 2 short lateral ridges and some few short scales. Lateral margins convex, with 6 distinct spines: first anterolateral spine well-developed, reaching anteriorly to level of lateral orbital spine, second spine (hepatic) well-developed, slightly dorsomesially from lateral margin, and followed by 4–5 branchial spines (3 anterior and 1–2 posterior). Rostrum leaf-like, horizontal, dorsally flattish or slightly concave, sexually dimorphic (shorter and wider on females) 1.5–1.8

(males), [1.1]–1.6 times as long as broad, length [0.3]–0.4 and breadth 0.2–[0.3] that of carapace; lateral margins smooth and convex, with well-developed supraocular basal spines and small subapical spines. Pterygostomian flap ending in blunt tooth, upper margin smooth.

Sternum: Slightly wider than long. Sternite 3 broad, [2.8]–3.0 times as wide as long, anterior margin convex, anterolaterally rounded. Sternite 4 widely contiguous to sternite 3; anterolaterally serrated, surface depressed in midline, smooth; greatest width [2.9]–3.0 times that of sternite 3, 3.0–[3.5] times as wide as long.

Pleon: Elevated ridges with short setae and a few scattered long setae. Tergites 2–3 with anterior and posterior transverse elevated ridges; tergite 4 with anterior transverse ridge, posterior transverse ridge absent; tergites 5–6 smooth.

Eye: Eye stalk length about 0.9–[1.1] times broader than long, peduncle distally setose, not distinctly expanded proximally; cornea expanded distally, maximum corneal diameter [0.9] × rostrum width, as wide as eyestalk.

Antennule: Article 1 slightly longer than wide, with 5 distal spines: distomesial spine well-developed; proximal lateral spine small, always present.

Antenna: Article 1 with prominent mesial process, distally falling well short of lateralmost antennular spine. Article 2 with well-developed distomesial and distolateral spines. Article 3 with distomesial spine. Article 4 unarmed.

Mxp3: Ischium with distinct distal spines on flexor and extensor margins. Merus 0.8[0.8] × length of ischium, with well-developed distal spine on extensor and flexor margins.

P1: [3.3]3.0–3.5 (males), 1.8–2.2 (females) times carapace length; subcylindrical, spiny and with long stiff setae and dense thick iridescent and plumose setae; merus, carpus and palm with spines along mesial, dorsal and lateral surfaces, distal and mesial spines usually stronger than others. Merus 0.7–[1.2] length of carapace, [1.6]2.2 times as long as carpus. Carpus 1.5–[2.0] times as long as wide. Palm [1.2]–1.2 × carpus length, 1.9–[2.2] times as long as broad. Fingers [0.7]1.0 × palm length; fixed finger with 1–2 basal spines; movable finger with 3 spines.

P2–4: Setose and spinose. Meri successively shorter posteriorly: P3 merus 0.9 times length of P2 merus, P4 merus 0.8–0.9 times length of P3 merus. P2 merus, 0.5 times carapace length, 3.5–3.6 times as long as broad, 1.0–1.1 times as long as P2 propodus; P3 merus 3.0–4.3 times as long as broad, 1.1–1.3 times as long as P3 propodus; P4 merus

2.6–3.0 times as long as broad, 1.0 times as long as P4 propodus; extensor margin of P2 and P3 with row of spines, proximally diminishing, with prominent distal spine; P4 extensor margin irregular, unarmed; flexor margin irregular, with distal spine on P2–3, absent on P4. Carpi with 1–3 spines on extensor margin on P2–3, unarmed on P4; distal spine prominent on P2–3, absent on P4; granules below extensor margin on lateral surface of P2–4; flexor margin unarmed. Propodi stout, [4.0–5.0]3.7–4.8 times as long as broad; extensor margin irregular; flexor margin with 3 slender movable spines in addition to distal pair. Dactyli [0.6–0.7]0.6 × length of propodi, ending in incurved, strong, sharp spine; flexor margin with cuticular spines at basis of 5–6 movable spines.

Eggs: Ov. F carried approximately 20–25 eggs of 0.3 mm diameter.

Colour. Base colour of carapace whitish, covered by granules and brownish spots, gastric and cardiac region with a big reddish patch, often covering only the epigastric region. Rostrum and supraocular spines whitish. Pleonal tergites 2–4 whitish, covered by granules and brownish spots, anterior ridges of tergites 2–4 with brownish stripes and patches; tergites 5–6 and telson whitish-translucid. P1 whitish, spines dark brwon, meri, carpi, palm and finger covered by brownish bands and whitish spots. P2–4 whitish, meri, carpi and propodi covered by brownish bands, dactyli whitish.

Genetic data. COI and 16S, Table 1.

Distribution. French Polynesia, Vanuatu, Papua New Guinea, Guam Island, Northern Mariana Islands, American Samoa and New Caledonia, from 5 to 102 m.

Remarks. *Phylladiorhynchus joannotae* belongs to the group of species having 2 epigastric spines, 1 hepatic spine, 3 spines on the anterior branchial margin of the carapace and cuticular spines along the flexor margin of the P2-4 dactyli. The closest species is *P. amphion*, from Western Australia. However, these species can be distinguished in basis of the following characters:

- The metagastric ridge is usually interrupted in *P. amphion,* whereas it is not medially interrupted in *P. joannotae.*
- *P. joannotae* has iridescent setae in the carapace and pleon, whereas these setae are absent in *P. amphion.*

P. joannotae showed divergences of 9% (COI) and 6% (16S) with the closest relative (*P. amphion*).

Phylladiorhynchus kermadecensis Schnabel & Ahyong, 2019

Phylladiorhynchus kermadecensis Schnabel & Ahyong, 2019: 318, figs. 5, 7.

Distribution. New Zealand, Kermadec Islands, 195-287 m.

Remarks. As Schnabel & Ahyong (2019) pointed out, the species is characterized by the presence of 5 epigastric spines and 2 spines on the anterior branchial margin. The closest species is *P. punctatus*, from New Caledonia. Both species can be differentiated by the interrumptions in the gastric ridges (see the differences under the Remarks of this species).

Phylladiorhynchus koumac **n. sp.**

(Figs. 21L, 25, 54I)

Type material. *Holotype*. New Caledonia. KOUMAC Stn KB629, 20.59121ºS, 164.21503ºE, 10 m, 7 November 2019: F 1.6 mm (MNHN-IU-2019-3427).

Paratypes. New Caledonia. LIFOU Stn 1436, 20°55.5'S, 167°04.2'E, 10–20 m, 10 November 2000: 1 F 1.8 mm (MNHN-IU-2014-13847).

New Caledonia. KOUMAC Stn KL07, 20.64605ºS, 164.18498ºE, 82 m, 15 November 2019: 1 M 1.5 mm (MNHN-IU-2014-20121).—Stn KL22, 20.4459ºS, 163.97176ºE, 47 m, 19 November 2019: 1 F 1.4 mm (MNHN-IU-2014-20170) parasitized.—Stn KL25, 20.75421ºS, 164.22986ºE, 65 m, 10 November 2019: 1 F 1.8 mm (MNHN-IU-2014-20035).—Stn KL03, 20.67485ºS, 164.214266ºE, 50 m, 11 November 2019: 1 F 1.8 mm (MNHN-IU-2014-20069).

Etymology. Named after the expedition KOUMAC aimed to catalogue the marine biodiversity of the lagoons of Koumac, New Caledonia. The name is considered as a substantive in apposition.

Description. *Carapace:* Robust or massive, [0.9]–1.1 times as long as broad; transverse ridges elevated, serrated, with few short setae, and few scattered long thick iridescent setae. Gastric region convex (uplifted dorsally), with some transverse ridges: epigastric ridge indistinct, with 5 spines (1 median and 2 pairs of small spines laterally); anterior protogastric ridge not medially interrupted, laterally with some few scales, posterior protogastric region often with a few scales; anterior mesogastric ridge scale-like, laterally interrupted by anterior branch of cervical groove; anterior metagastric ridge scale-like, followed by some few scales on posterior metagastric area. Mid-transverse ridge not interrupted, medially depressed, preceded by distinct cervical groove, followed by 1–2 not interrupted or minutely interrupted ridges, interspersed with 2 short lateral ridges. Lateral margins clearly convex, with 7 spines: first anterolateral spine well-developed, reaching end of lateral orbital spine, second spine (hepatic) well-developed,
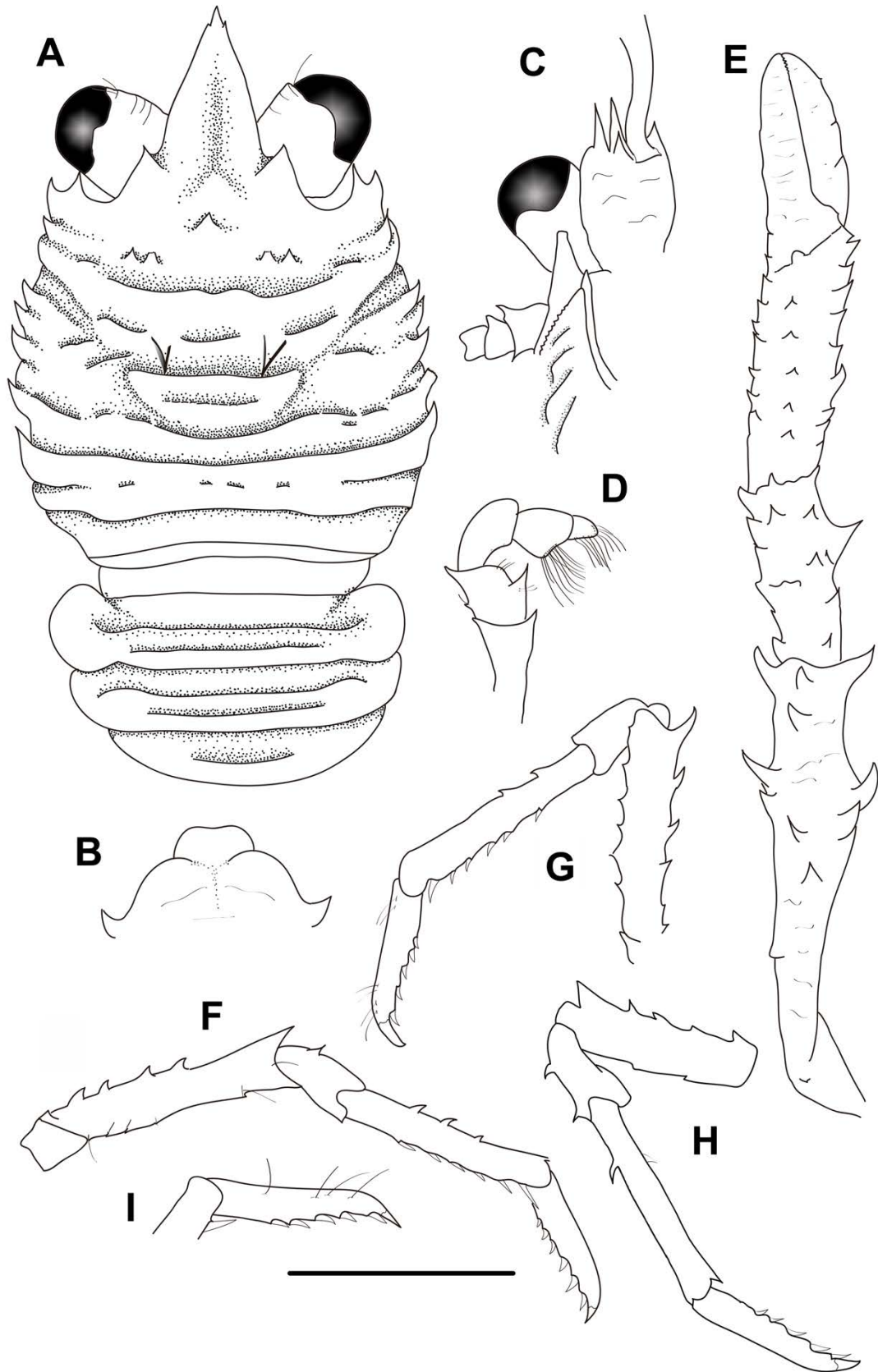
FIGURE 25. *Phylladiorhynchus koumac* **n. sp**., holotype female 1.6 mm (MNHN-IU-2019-3427): A, carapace and pleon, dorsal view. B, thoracic sternites 3 and 4. C, right cephalic region, showing antennular and antennal peduncles, ventral view. D, right Mxp3, lateral view. E, left P1, dorsal view. F, right P2, lateral view. G, left P3, lateral view. H, left P4, lateral view. I, dactylus of right P2, lateral view. Scale bar: A, E-H = 1.0 mm; B–D, I = 0.6 mm.

slightly dorsomesially from lateral margin, and followed by 5 branchial spines (3 anterior and 2 posterior). Rostrum leaf-like, horizontal, dorsally flattish or slightly concave, 1.3–[1.4] times as long as broad, length [0.4]0.4 and breadth 0.25–[0.3]that of carapace; lateral margins serrated and convex, with well-developed supraocular spines, subapical spines well-developed. Pterygostomian flap ending in blunt tooth, upper margin serrated, with series of elevated striae.

Sternum: As wide as or slightly wider than long, lateral margins of posterior half slightly divergent. Sternite 3 moderately broad, 2.5–[2.8] times as wide as long, anterior margin convex. Sternite 4 widely contiguous to sternite 3; surface flattened, smooth; greatest width 2.7–[2.9] times that of sternite 3, [2.6]2.6 times as wide as long.

Pleon: Elevated ridges uplifted dorsally, with a few scattered short setae. Tergites 2–3 with anterior and posterior transverse elevated ridges; tergite 4 with anterior transverse ridge; tergites 5–6 smooth.

Eye: Eye stalk length about [1.6]1.4–1.6 times broader than long, peduncle distally setose, not distinctly expanded proximally; maximum corneal diameter [1.1]–1.1 × rostrum width*,* as wide as eyestalk.

Antennule: Article 1 slightly longer than wide, with 4 spines: distomesial spine well-developed; proximal lateral spine absent. Short striae covering mesial surfaces.

Antenna: Article 1 with prominent mesial process distally clearly not reaching lateral antennular spine. Article 2 with small distal spines laterally and mesially. Articles 3 and 4 unarmed.

Mxp3: Ischium with distinct distal spines on flexor and extensor margins. Merus [0.6]0.6 × length of ischium at midlength, with 0–1 median and 1 well-developed distal spines on extensor margin and 1 strong spine on flexor margin.

P1: [2.5]2.5–3.0 (males), (lost in females) times carapace length, subcylindrical, spiny and with scattered long stiff setae; merus, carpus and palm with spines along mesial, dorsal and lateral surfaces, distal and mesial spines usually stronger than others. Merus [1.0]1.1 length of carapace, [2.1]–2.7 times as long as carpus. Carpus [2.2] times as long as wide. Palm [1.3]–1.4 × carpus length, [2.8]–2.1 times as long as broad. Fingers unarmed, [0.7]–0.8 × palm length.

P2–4 (lost in most specimens)*:* Stout, subcylindrical, moderately setose and spinose, with few scattered plumose setae. Meri successively shorter posteriorly: P3 merus [0.6] times length of P2 merus, P4 merus [0.9] times length of P3 merus; P2 merus,

[0.6] times carapace length, [5] times as long as broad, [1.1] times as long as P2 propodus; P3 merus [4.4] times as long as broad, [0.9] times as long as P3 propodus; P4 merus [3.3] times as long as broad, [0.8] times as long as P4 propodus; extensor margin of P2 and P3 with row of spines, proximally diminishing, with prominent distal spine; P4 extensor margin irregular, with small distal spine; flexor margins of P2–4 irregular, each with distal spine. Carpi with 2 or 3 spines on extensor margin on P2–3, unarmed on P4; distal spine prominent on P2–3, smaller on P4; row of small spines below extensor margin on lateral surface of P2–3, unarmed on P4; flexor margins with distal spine. Propodi moderately slender, 6–7 times as long as broad; extensor margin irregular, usually armed with 1–3 well-developed spines on P2–4; flexor margin with 2–5 slender movable spines in addition to distal pair. Dactyli 0.7–0.8 × length of propodi, ending in incurved, strong, sharp spine; flexor margin with 5–6 movable spines.

Eggs. No data.

Colour. Base colour of carapace grey, gastric region covered by a witthish median band on posterior half, whitish divergent bands on gastric regions and scattered patches; granules and spines brownish. Rostrum and supraocular basal spines covered by wittish lateral band, tip whitish. Pleonal tergites 1–4 grey, with scales and granules brownish with whitish median longitudinal band. P2–4 whitish, spines along flexor margins whitish; half portion of meri, carpi and propodi with brownish-grey bands.

Genetic data. COI and 16S, Table 1.

Distribution. New Caledonia, Koumac, between 10 and 82 m.

Remarks. *Phylladiorhynchus koumac* belongs to the species group that has 5 epigastric spines, 3 spines on the anterior branchial margin, gastric region strongly convex, the rostrum leaf-like (margins clearly convex and subapical spines present), and elevated ridges uplifted dorsally. The new species resembles closely to *P. pulchrus,* from French Polynesia, the Philippines, and Vanuatu (see the differences under the Remarks of this species).

***Phylladiorhynchus laureae* n. sp.**

(Figs. 26, 33A)

Type material. *Holotype.* New Caledonia. LIFOU Stn 1457 20°46.8' S, 167°02.75' E, 5–10 m, 27 November 2000: ov. F 2.4 mm (MNHN-IU-2014-13739).

Paratypes. Japan. Okinawa. Iriomote Is. Nakano Beach, 24.4323ºN, 123.7916ºE, 19 m, 9 July 2010: 1 M 2.0 mm (UF26910).
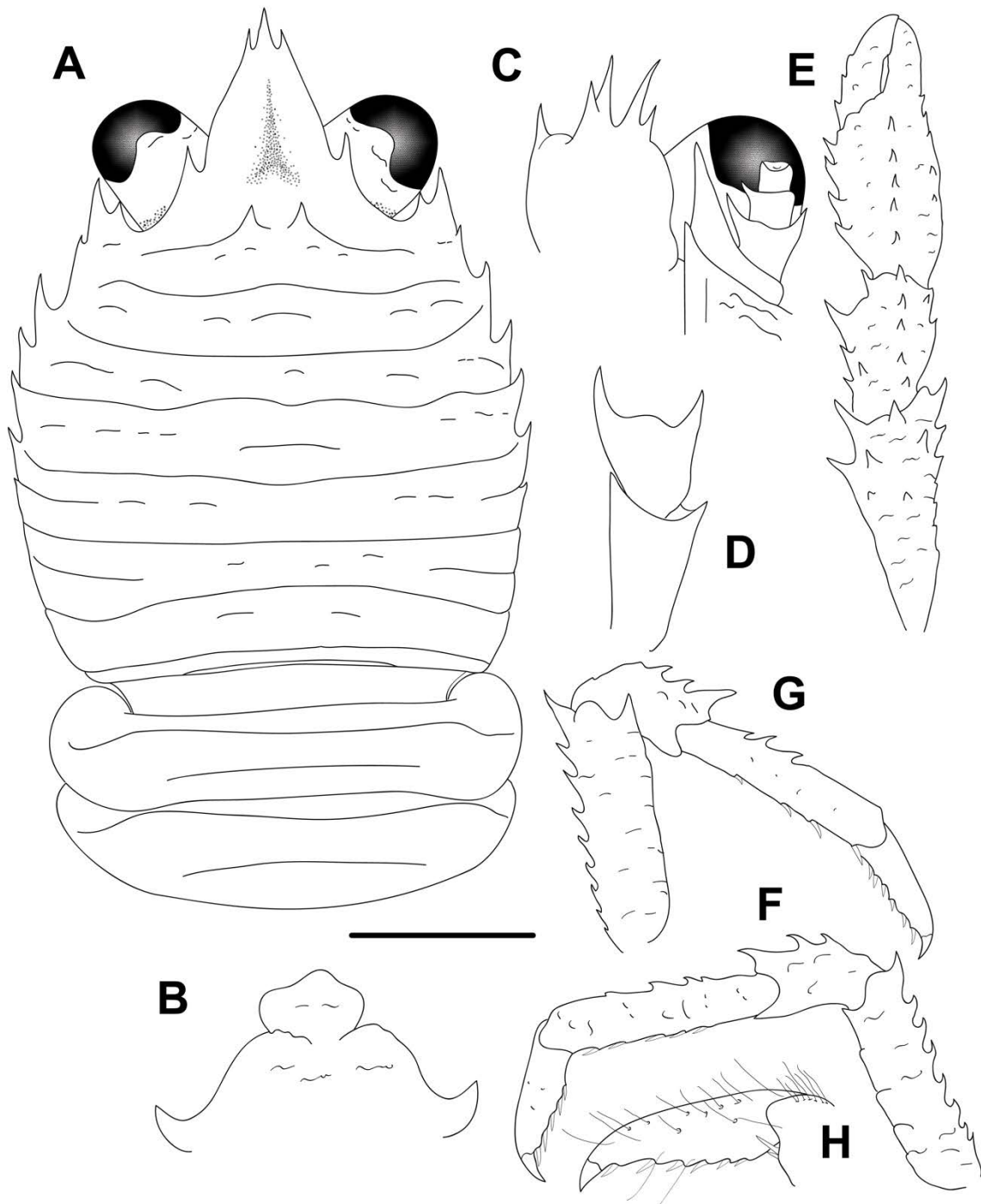
FIGURE 26. *Phylladiorhynchus laureae* **n. sp**., A-D, F-H, holotype ovigerous female 2.4 mm (MNHN-IU-2014-13739); E, paratype male 2.0 mm (MNHN-IU-2014-13645): A, carapace and pleon, dorsal view. B, thoracic sternites 3 and 4. C, left cephalic region, showing antennular and antennal peduncles, ventral view. D, right Mxp3, lateral view. E, right P1, dorsal view. F, left P2, lateral view. G, right P3, lateral view. H, dactylus of left P2, lateral view. Scale bar: A, F-G = 1.0 mm; B–E, H = 0.6 mm.
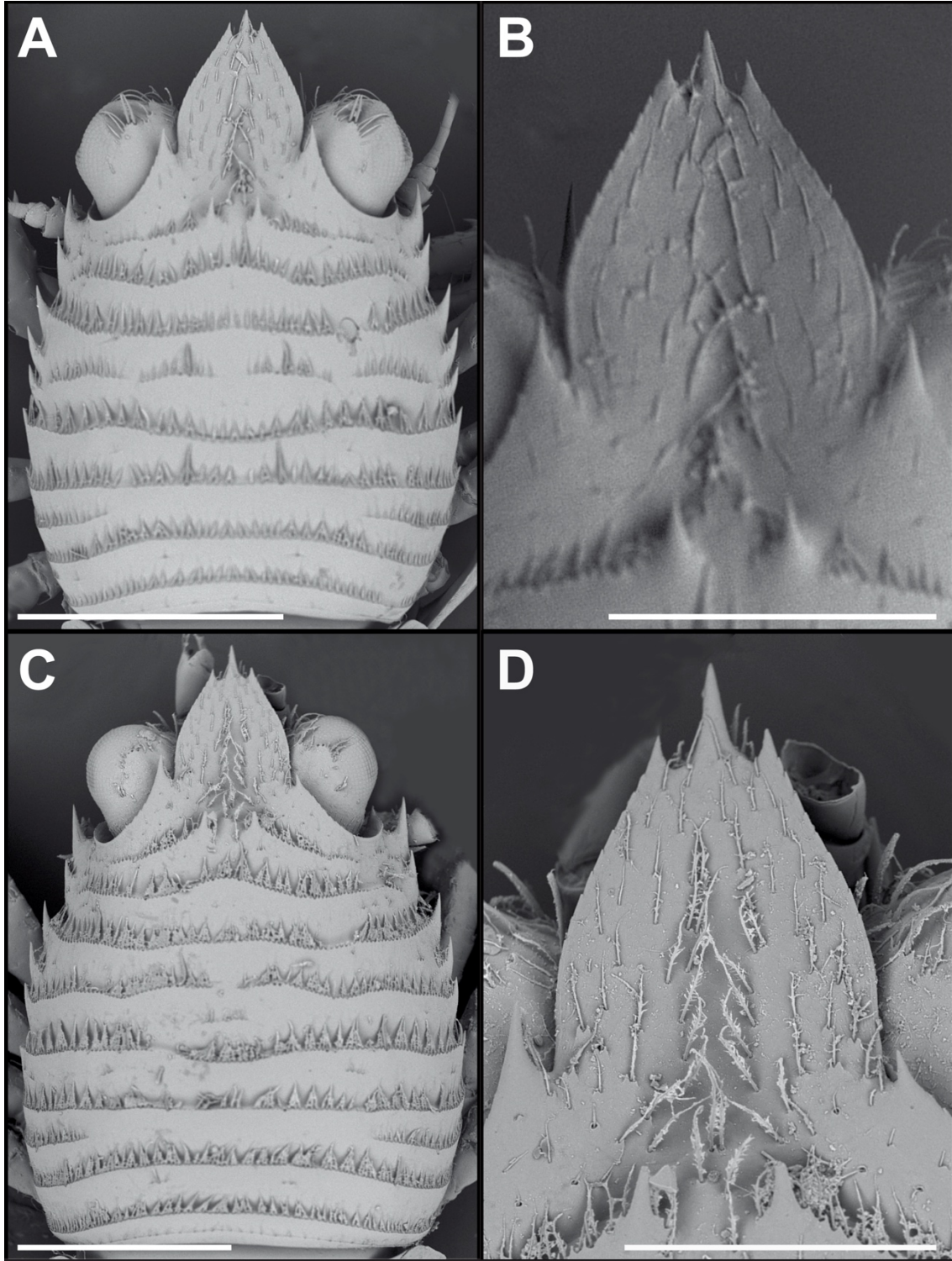
FIGURE 27. A-C, Carapace, dorsal view; B-D, rostrum, dorsal view. A-B, *Phylladiorhynchus gustavi* **n. sp.***,* paratype male 2.0 mm (UF33968). C-D, *Phylladiorhynchus laurae* **n. sp.**, paratype ovigerous female 2.0 mm (UF). Scale bars: A, C = 1 mm, B, D = 0.5 mm.

Papua New Guinea. KAVIENG Stn KS33, 02°38.2'S, 150°38.7'E, 8–10 m, 13 June 2014: 1 ov. F 2.8 mm (MNHN-IU-2014-13559), 1 M 2.0 mm (MNHN-IU-2014-13645).

Vanuatu. SANTO Stn DB1, 15°33.1'S, 167°17.8'E, 15–25 m, 10 September 2006: 1 M 2.0 mm, 1 ov. F 1.9 mm (MNHN-IU-2019-2629).—Stn DR21, 15°36.5'S, 167°01.4'E, 22–25 m, 15 September 2006: 1 F 1.3 mm (MNHN-IU-2014-13884).—Stn DB29, 15°38.9'S, 167°05.1'E, 15 m, 17 September 2006: 1 M 1.5 mm (MNHN-IU-2019-2624).—Stn DS49, 15°38.7'S, 167°05.2'E, 10–17 m, 21 September 2006: 1 M 2.4 mm (MNHN-IU-2019-2631).—Stn DB63,15°26.9'S, 167°15.8'E, 21 m, 25 September 2006: 2 ov. F 2.0–2.1 mm (MNHN-IU-2014-13872).—Stn DB65, 15°25.8'S, 167°13.0'E, 13 m, 26 September 2006: 2 M 2.0–2.2 mm, 4 ov. F 1.7–2.1 mm, 3 F 1.8–2.3 mm (MNHN-IU-2014-13870).—Stn DB69, 15°24.4'S, 167°13.0'E, 38 m, 27 September 2006: 1 M 2.0 mm (MNHN-IU-2029-2625).—Stn DB75, 15°22.9'S, 167°11.9'E, 20 m, 28 September 2006: 1 M 2.0 mm (MNHN-IU-2014-13885).—Stn FB43, 15°28.4'S, 167°14.9'E, 19 m, 30 September 2006: 1 M 2.0 mm, 2 ov. F 1.7–1.8 mm (MNHN-IU-2019-2590).—Stn FB64, 15°35.4'S, 166°59.2'E, intertidal, 10 October 2006: 1 M 3.0 mm (MNHN-IU-2014-13807).—no Stn number: 1 M 1.9 mm (MNHN-IU-2019-2623).

New Caledonia. Exp. Mont. Komac 12 m, 7 October 1993: 1 F 1.7 mm (IU-2019-2635).—LIFOU Stn 1435, 20°55.2' S, 167°00.7' E, 5–30 m, 8 November 2000: 1 ov. F 2.0 mm (MNHN-IU-2019-2608).—Stn 1430, 24 November 2000: 2 ov. F 2.2–2.4 mm (MNHN-IU-2019-2632).—Stn 1457, 20°46.8'S, 167°02.75'E, 5–10 m, 27 November 2000: 1 ov. F 2.4 mm (MNHN-IU-2014-13739).—KOUMAC Stn KB631, 20.52698ºS, 164.02615ºE, 3 m, 08 November 2019: 1 F parasitized 1.7 mm (MNHN-IU-2019-2581).—Stn KL39, 20.7511ºS, 164.23276ºE, 26 m, 10 November 2019: 2 F parasitized 1.8–2.0 mm (MNHN-IU-2019-2582), 1 F 1.8 mm (MNHN-IU-2014-20123).—Stn ARMS 9C: 1 ov. F 1.1 mm (MNHN-IU-2014-20145).—Stn KB659, 20.66049ºS, 164.26852ºE, 15 m, 21 November 2019: 1 M 2.3 mm (MNHN-IU-2014-20175)

Mariana Islands. Guam Island. Mid-western coast, at Orote northern tip, dead coral, 25 m, 20 June 2002: 2 M 1.1–1.7 mm, 1 ov. F 1.6 (UF3122).—Stn GUA-597, 13.57847ºN, 144.82831ºE, 11 m, 25 March 2014: 3 M 1.4–1.7 mm, 6 ov. F 1.5–2.4 mm (UF).—Stn GUA-645, 13.57847ºN, 144.82831ºE, 10 m, 25 March 2014: 1 ov. F 2.0 mm (UF).—Stn GUA-693, 13.57847ºN, 144.82831ºE, 11 m, 25 March 2014: 1 M 2.0 mm (UF).—Stn GUA-698, 13.57847ºN, 144.82831ºE, 11 m, 25 March 2014: 1 ov. F 1.8 mm (UF).—Stn GUA-880, 13.30553ºN, 144.65257ºE, 12 m, 27 March 2014: 1 ov. F 1.9 mm (UF).—Stn GUA-877, 13.30553ºN, 144.65257ºE, 12 m, 27 March 2014: 1 M 1.4 mm (UF).—Stn GUA-756, 13.30553ºN, 144.65257ºE, 12 m, 27 March 2014: 1 M 1.9 mm, 1 ov. F 2.0 mm, 1 F 2.1 mm (UF).—Stn GUA-805, 13.30553ºN, 144.65257ºE, 12 m, 27 March 2014: 2 ov. F 2.0–2.1 mm (UF).—Stn GUA-810, 13.30553ºN, 144.65257ºE, 12

m, 27 March 2014: 1 F parasitized, 2.0 mm (UF).—Stn GUA-878, 13.30553ºN, 144.65257ºE, 12 m, 27 March 2014: 1 M 1.8 mm (UF).—Stn GUA-947, 13.48871ºN, 144.87796ºE, 14 m, 28 March 2014: 1 M 1.8 mm (UF).—Stn GUA-1216, 13.44878ºN, 144.62596ºE, 14 m, 31 March 2014: 2 M 1.6–2.0 mm, 1 ov. F 1.9 mm (UF).—Stn GUA-1201, 13.44878ºN, 144.62596ºE, 14 m, 31 March 2014: 1 ov. F 1.5 mm (UF).—Stn GUA-1204, 13.44878ºN, 144.62596ºE, 14 m, 31 March 2014: 1 M 2.0 mm (UF).

Northern Mariana Islands. Saipan Island. Stn SAI-442, 15.09782849ºN, 145.7434357ºE, 17 m, 11 April 2014: 4 M 1.2–2.0 mm, 5 ov. F 1.7–2.1 mm (UF).—Stn SAI-543, 15.09782849ºN, 145.7434357ºE, 17 m, 11 April 2014: 4 M 1.1–1.9 mm, 2 ov. F 1.7–1.9 mm (UF).—Stn SAI-544, 15.09782849ºN, 145.7434357ºE, 17 m, 11 April 2014: 1 M 2.0 mm, 2 ov. F 2.1–2.3 mm (UF).—Stn SAI-641, 15.15620417ºN, 145.6899585ºE, 11 m, 17 April 2014: 4 M 1.2–2.1 mm, 8 ov. F 1.8–2.5 mm (UF).—Stn SAI-586, 15.09782849ºN, 145.7434357ºE, 17 m, 11 April 2014: 2 M 2.1–2.4 mm, 3 ov. F 1.5–2.1 mm (UF).—Stn SAI-437, 15.09782849ºN, 145.7434357ºE, 17 m, 11 April 2014: 3 M 1.9–2.3 mm, 1 ov. F 1.8 mm (UF).—Stn SAI-708, 15.15620417ºN, 145.6899585ºE, 11 m, 17 April 2014: 2 M 1.8–1.9 mm, 4 ov. F 1.8–2.0 mm, 1 F 1.2 mm (UF).—Stn SAI-756, 15.15620417ºN, 145.6899585ºE, 11 m, 17 April 2014: 3 ov. F 1.7–2.1 mm (UF).—Stn SAI-789, 15.15620417ºN, 145.6899585ºE, 11 m, 17 April 2014: 3 M 1.9–2.3 mm, 4 ov. F 1.7–2.2 mm, 1 F 1.2 mm (UF).—Stn SAI-878, 15.27406ºN, 145.79106ºE, 9 m, 18 April 2014: 1 F 1.8 mm (UF).—Stn SAI-889, 15.27406ºN, 145.79106ºE, 9 m, 18 April 2014: 11 M 1.5–2.3 mm, 8 ov. F 1.4–2.0 mm (UF).—Stn SAI-957, 15.27406ºN, 145.79106ºE, 9 m, 18 April 2014: 3 M 1.5–2.0 mm, 5 ov. F 1.6–2.2 mm, 1 F 1.8 mm (UF).—Stn SAI-786, NO DATA, 1 postlarvae.

American Samoa. Olosega Island. Stn OLO-186, 14.18140174ºS, 169.6267462ºW, 14 m, 14 March 2015: 1 ov. F 2.0 mm (UF).—Tutuila Island. Stn TUT-117, 14.36046ºS, 170.75024ºW, 17 m, 26 February 2015: 1 M 1.7 mm, 1 ov. F 1.9 mm (UF).—Stn TUT-374, 14.36613333ºS, 170.7628833ºW, 12 m, 5 March 2015: 1 M 1.9 mm, 1 ov. F 2.0 mm (UF).—Rose Atoll. Stn ROS-689, 14.55965ºS, 168.1601167ºW, 14 m, 18 March 2015: 1 M 1.9 mm (UF).

Etymology. Named after our colleague and host Laure Corbari, curator of the Crustacean Collection of the Muséum national d'Histoire naturelle, Paris.

Description. *Carapace:* Slightly broader than long; transverse ridges with dense short setae and long and thick iridescent setae. Gastric region slightly convex with 4 transverse ridges: epigastric ridge distinct with 2 median spines, often with short scales laterally; anterior protogastric ridge not medially interrupted, extending laterally to carapace margin, sometimes followed by small scales on posterior protogatric ridge;

anterior mesogastric ridge not medially interrupted, laterally continuing to first branchial spine, followed by some lateral scales; anterior metagastric ridge medially interrupted or not medially interrupted, followed always by one median scale and often other small scales in posterior metagastric region. Mid-transverse ridge not interrupted, medially depressed, cervical groove indistinct, followed by 2 not interrupted or minutely interrupted ridges, interspersed with 1–2 short lateral ridges and some few short scales. Lateral margins slightly convex, with 6–7 distinct spines: first anterolateral spine well-developed, exceeding level of lateral orbital spine, second spine (hepatic) small, slightly dorsomesially from lateral margin, and followed by 5 branchial spines (3 anterior and 1–2 posterior). Rostrum leaf-like, horizontal, dorsally concave, [1.1]–1.4 times as long as broad, length [0.3]–0.4 and breadth [0.3]0.3 that of carapace; lateral margins serrated and strongly convex, with well-developed supraocular basal spines and strong subapical spines (tridentiform). Pterygostomian flap ending in blunt tooth, upper margin smooth.

Sternum: As wide as long. Sternite 3 quadrangular, [1.5]1.0–1.8 times as wide as long, anterior margin serrated, with a median projection, anterolaterally rounded. Sternite 4 widely contiguous to sternite 3; anterolaterally serrated, surface depressed in midline, smooth; greatest width 2.6–[3.0] times that of sternite 3, [3.0]3.0 times as wide as long.

Pleon: Elevated ridges with short setae and a few scattered long setae. Tergites 2–3 with anterior and posterior transverse elevated ridges; tergite 4 with anterior transverse ridge only; tergites 5–6 smooth.

Eye: Eye stalk length about [1.1]–1.2 times broader than long, peduncle distally setose, not distinctly expanded proximally; cornea expanded distally, maximum corneal diameter 0.8–[0.9] × rostrum width*,* narrower than eyestalk, (0.8 times maximum peduncle width).

Antennule: Article 1 slightly longer than wide, with 5 distal spines: distomesial spine well-developed; proximal lateral spine small, always present.

Antenna: Article 1 with prominent mesial process, distally falling well short or overreaching lateralmost antennular spine. Article 2 with well-developed distomesial and distolateral spines. Article 3 with distomesial spine. Article 4 unarmed.

Mxp3: Ischium with distinct distal spines on flexor and extensor margins; crista dentata with row of spines along entire margin. Merus [0.8]0.8 × length of ischium, with well-developed distal spine on extensor and flexor margins.

P1: 2.3–3.1 (males), [1.4]–2.1 (females) times carapace length; subcylindrical, spiny and with long stiff setae and iridescent setae; merus, carpus and palm with spines

along mesial, dorsal and lateral surfaces, distal and mesial spines usually stronger than others. Merus [0.5]–0.9 length of carapace, 1.4–[1.6] times as long as carpus. Carpus [1.6]–2.3 times as long as wide. Palm [1.1]1.0–1.2 × carpus length, [1.7]1.6–2.2 times as long as broad. Fingers [0.7]–0.8 × palm length; fixed finger with small basal spine; movable finger unarmed.

P2–4 (P4 lost in the holotype): Stout, setose, with iridiscent setae, and spinose. Meri successively shorter posteriorly: P3 merus [0.9]–1.0 times length of P2 merus, P4 merus 0.8–0.9 times length of P3 merus. P2 merus, 0.5–[0.6] times carapace length, [3.2]–3.7 times as long as broad, [1.3]1.2–1.5 times as long as P2 propodus; P3 merus 2.5–[3.2] times as long as broad, [1.1]–1.4 times as long as P3 propodus; P4 merus 2.3–2.8 times as long as broad, 0.9–1.4 times as long as P4 propodus; extensor margin of P2 and P3 with row of spines, proximally diminishing, with prominent distal spine; P4 extensor margin irregular, unarmed; flexor margin irregular,with distal spine on P2–3, distal spine absent in P4. Carpi with 1–3 spines on extensor margin on P2–3, unarmed on P4; distal spine prominent on P2–3, smaller on P4; granules below extensor margin on lateral surface of P2–4; flexor margin unarmed. Propodi stout, [4.2–4.7]3.3–5 times as long as broad; extensor margin irregular, armed with 2–4 spines on proximal half; flexor margin with 3–6 slender movable spines in addition to distal pair. Dactyli [0.6]0.6–0.8 × length of propodi, ending in incurved, strong, sharp spine; flexor margin with 5–6 movable spines.

Eggs: Ov. F carried approximately 7–35 eggs of 0.3–0.5 mm diameter.

Colour. Base colour of carapace brownish or dark green. Carapace and Rostrum and Pleon, covered by granules and small dark brown spots, ridges brownish, spines on anterior branchial margin and epigastric spines covered by dark brown patches. Ocular peduncles covered by dark-brown granules, whittish and reddish spots, cornea reddish. Rostrum whittish. Pleon light orange, ridges with brownish-dark orange stripes. P1 whitish, spines brownish, merus, carpus, palm and fingers covered by dark brown spots. P2–4 light whitish, spines brownish; meri, propodi and dactyli covered by dark orange brownish stripes.

Genetic data. COI and 16S, Table 1.

Distribution. Japan, Papua New Guinea, Vanuatu, New Caledonia, Guam Island, Northern Mariana Islands and American Samoa. Intertidal to 38 m.

Remarks. *Phylladiorhynchus laureae* belongs to the group of species having 2 epigastric spines, 1 hepatic spine and 3 spines on anterior branchial margin. *Phylladiorhynchus laureae* closely resembles to *P. gustavi* from French Polynesia. Both

species are very similar morphologically, although very different genetically. Both species can be distinguished by the following subtle characters:

- The anterior metagastric ridge is often scale-like in *P. gustavi,* whereas it is usually medially interrupted in *P. laureae.*
- The metagastric ridge is followed by a large scale in *P. laureae*, whereas this scale is very small or absent in *P. gustavi.*
- The anterior margin of the sternite 3 is medially projected in *P. laureae*, whereas it is usually convex in *P. gustavi.*

The sequences of *P. laureae* (COI) were 8% divergent from *P. gustavi*. The mean intraspecific divergences in *P. laureae* were 1.8% for COI and 0.6% for 16S.

***Phylladiorhynchus lenzi* (Rathbun, 1907)**

(Fig. 28)

Galathea lenzi Rathbun, 1907: 49, pl. 3, fig. 1 (Corral, Chile).—Porter, 1916a: 96 (Corral, Chile).—Porter, 1916b: 112 (Corral, Chile).

Records requiring verification:

Galathea latirostris.—Lenz, 1902: 742 (Juan Fernandez Island) (not *Galathea latirostris* Dana, 1852)

Galathea lenzi.—Balss, 1922: 334 (Juan Fernandez island).—Haig, 1955: 31, fig. 6 (Juan Fernandez island).—Retamal, 1981: 22 (Corral to Concepcion, Chile).—Andrade, 1985: 111 (Juan Fernandez island).— Castila & Rozbaczylo, 1987: 183 (list, Juan Fernandez).—Poupin, 2003: 24 (list, Chile, Salas y Gomez islands).—Retamal, 2004: 60, fig. 10 (Chilean coast, Salas y Gomez, Juan Fernandez islands).

Phylladiorhynchus pusillus.—De los Ríos Escalante & Ibáñez Arancibia, 2016: 79 (Easter Island, list).—Mujica *et al.*, 2019: 775, figs. 1–5 (larval development, Easter Island).

Type material. *Lectotype.* Chile, Corral, Valdivia: ov. F 2.7 mm (USNM 32261).

Paralectotype. Chile, Corral, Valdivia: 1 ov. F 2.6 mm (USNM 32261).

Description. *Carapace:* Slightly wider than long. Gastric region slightly convex with 4 transverse ridges: epigastric ridge distinct with 2 median pairs of spines symmetrically distant of median area; anterior protogastric ridge not medially interrupted, nearly extending laterally to carapace margin; anterior mesogastric ridge not medially
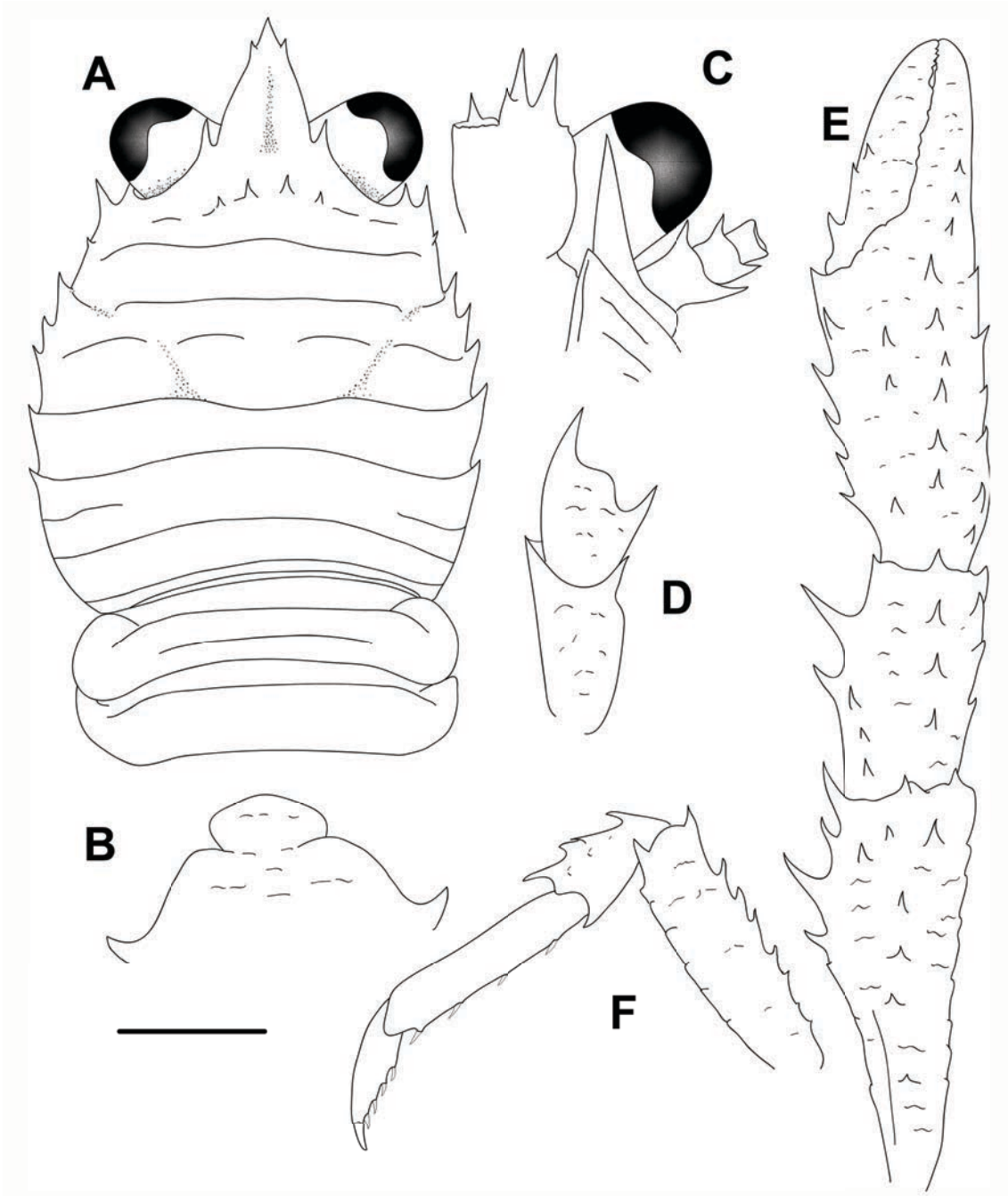
FIGURE 28. *Phylladiorhynchus lenzi* (Rathbun, 1907), lectotype ovigerous female 2.7 mm (USNM 32261): A, carapace and pleon, dorsal view. B, thoracic sternites 3 and 4. C, left cephalic region, showing antennular and antennal peduncles, ventral view. D, right Mxp3, lateral view. E, right P1, dorsal view. F, left P2, lateral view. Scale bar: A, E-F = 1.0 mm; B–D = 0.6 mm.

interrupted, laterally interrupted by cervical groove, laterally continuing uninterrupted to first branchial spine; anterior metagastric ridge scale-like. Mid-transverse ridge uninterrupted, preceded by shallow or undistinct cervical groove, followed by 2 uninterrupted or minutely interrupted ridges, interspersed with 1 short lateral ridge. Lateral margins convex, with 7 spines: first anterolateral spine well-developed, reaching anteriorly to level of lateral orbital spine, second spine (hepatic) small, slightly dorsomesially from lateral margin, and followed by 5 branchial spines behind distinct anterior cervical groove (3 anterior and 2 posterior). Rostrum subtriangular, horizontal, dorsally flattish or slightly concave, 1.3 times as long as broad, length 0.3 and breadth 0.2 that of carapace; lateral margins smooth and convex, with well-developed supraocular basal spines and small subapical spines. Pterygostomian flap ending in blunt tooth, upper margin smooth.

Sternum: As wide as long. Sternite 3 moderately broad, twice as wide as long, anterior margin convex, anterolaterally convex. Sternite 4 widely contiguous to sternite 3; surface depressed in midline, smooth; greatest width 3 times that of sternite 3, 3.2 times as wide as long.

Pleon: Tergite 2 with anterior and posterior transverse elevated ridges; tergites 3–4 with anterior transverse ridge only; tergites 5–6 smooth.

Eye: Eye stalk length about 1.2 times broader than long, peduncle distally setose, not distinctly expanded proximally; maximum corneal diameter 1.2 × rostrum width*,* as wide as eyestalk, (as wide as maximum peduncle width).

Antennule: Article 1 slightly longer than wide, with 4 well-developed distal spines: distomesial spine well-developed; proximal lateral spine absent, otherwise present as a granule.

Antenna: Article 1 with prominent mesial process distally falling well short of lateral antennular spine. Article 2 with well-developed distal spines laterally and mesially. Article 3 with well-developed distomesial and distolateral spines. Article 4 unarmed.

Mxp3: Ischium with distinct distal spines on flexor and extensor margins. Merus 0.7–0.8 × length of ischium, with well-developed distal spine on extensor margin and 1 much larger spine at flexor margin.

P1: 3 times carapace length; subcylindrical, spiny; merus, carpus and palm with spines along mesial, dorsal and lateral surfaces, distal and mesial spines usually stronger than others. Merus 1.1 length of carapace, 1.8 times as long as carpus. Carpus 1.8 times

as long as wide. Palm 1.2 × carpus length, 1.8 times as long as broad. Fingers 0.8 × palm length; some marginal spines along proximal half of movable and fixed fingers.

P2 (presumably, other walking legs lost)*:* Stout, moderately setose and spinose. Merus, 0.7 times carapace length, 3.7 times as long as broad, 1.5 times as long as propodus; extensor margin with row of spines, proximally diminishing, with prominent distal spine; flexor margin irregular, with distal spine; lateral surface with scales. Carpus with 3 spines on extensor margin on; row of small acute granules below extensor margin on lateral surface; flexor margin unarmed other than distal spine. Propodi stout, 3.8 times as long as broad; extensor margin irregular unarmed; flexor margin with 3 slender movable spines in addition to distal pair. Dactyli 0.6 × length of propodi, ending in incurved, strong, sharp spine; flexor margin with 4 movable spinules.

Colour. Unknown.

Genetic data. No data.

Distribution. Only known from Corral, Valdivia (Chile), unknown depth.

Remarks. *Phylladiorhynchus lenzi* was described by Rathbun (1907) from 4 specimens collected by C.E. Porter in waters of Corral, Valdivia Province (Chile), with a very short diagnosis and one photo. The species was posteriorly cited in other localities along the coast (e.g. Concepcion area), as well as in the oceanic islands (e.g. Juan Fernandez, Salas y Gomez) (see above). However, until now, no complete description of the species existed, avoiding a comparison among the specimens from different localities as well as with other species.

Furthermore, when examining specimens from different Chilean localities, e.g. Corral (type specimens) and Valparaiso (coll. Porter, 1899, deposited in the MNHN of Paris) we found that they belong to two different species (*P. lenzi* and *P. porteri*). Unfortunately, we failed in examining specimens from Chilean oceanic islands and the identity of the specimens of *Phylladiorhynchus* in these islands should be confirmed.

P. lenzi belongs to the group of species having usually 4 spines on the epigastric ridge, the anterior metagastric ridge scale-like, a very small hepatic spine, the anterior margin of the thoracic sternite 3 convex and one spine on the flexor margin of the Mxp3 merus. This group contains 4 species: *P. pusillus* from New Zealand and Australia*, P. lenzi*, from Chile*, P. porteri*, from Chile, *P. poeas* from French Polynesia.

   P. lenzi has been currently synonymized with *P. pusillus* (Henderson, 1885) (Baba *et al*. 2008; Schnabel & Ahyong 2019). However, *P. lenzi* can be distinguished from *P. pusillus* and *P. poeas* by subtle but constant differences:

-          The proximal lateral spine of the antennular article is always distinct in *P. pusillus*, whereas this spine is very small to indistinct in *P. lenzi* and *P. poeas*.

-          The antennal article 3 is armed with a small distomesial spine in *P. pusillus*, whereas this article has well-developed distomesial and distolateral spines in *P. lenzi* and *P. poeas*.

   P. lenzi is also close to *P. porteri* (see the differences under the Remarks of this species).

Phylladiorhynchus lini n. sp.

(Figs. 29, 30J-L, S-T, 33B, 55A, 56D-I)

Type material. *Holotype.* Taiwan. Kenting County, National museum of marine biology & aquarium, Houbihu, 21°56'10.9"N, 120°44'48.5"E, 7–10 m, 2 June 2019: F 2.2 mm (NMMBCD5596).

   Paratypes. Taiwan. Kenting County. Small fishing port S of Wanlitung. 21.9706ºN 120.7156ºE, 5–8 m, 30 June 2007: 1 ov. F 2.6 (UF11812).—Kenting County, National museum of marine biology & aquarium, Water outlet, 21°55'55.3"N, 120°44'41.6"E, 8–10 m, 23 May 2011: 1 M 3.4 mm (NMMBCD).—21°55'55.3"N, 120°44'41.6"E, 8–10 m, 24 May 2011: 1 ov. F 3.0 mm, 1 F 3.2 mm (NMMBCD).—21°55'23.4"N, 120°49'55.8"E, 7–10 m, 30 May 2011: 9 M 2.6–3.7 mm, 2 F 2.9–3.2 mm, 9 ov. F 1.7–3.1 mm (NMMBCD).—21°55'55.3"N, 120°44'41.6"E, 8–10 m, 25 July 2011: 2 M 3.0–3.1 mm, 1 ov. F 2.1 mm (NMMBCD).—21°55'55.3"N, 120°44'41.6"E, 8–10 m, 5 October 2011: 2 F 2.5–3.1 mm (NMMBCD).—21°55'55.3"N, 120°44'41.6"E, 8–10 m, 13 October 2011: 1 M 2.2 mm (NMMBCD).—21°55'55.3"N, 120°44'41.6"E, 8–10 m, 19 November 2011: 1 F 2.6 mm (NMMBCD).—21°55'55.3"N, 120°44'41.6"E, 8–10 m, 3 May 2012: 1 ov. F 3.0 mm (NMMBCD).—Houbihu, 21°56'10.9"N, 120°44'48.5"E, 7–10 m, 14 May 2012: 1 ov. F 2.9 mm (NMMBCD).—Houbihu, 21°56'10.9"N, 120°44'48.5"E, 7–10 m, 29 June 2013: 1 ov. F 2.5 mm (NMMBCD).—Hojie, 21°57'19.5"N, 120°42'42.5"E, 24–26 m, 26 February 2013: 1 ov. F 2.7 mm (NMMBCD).—Houbihu, 21°56'10.9"N, 120°44'48.5"E, 7–10 m, 2 June 2019: 1 M 1.7 mm, 1 ov. F 2.5 mm, 1 F 1.4 mm (MNHN- IU-2016-1490).
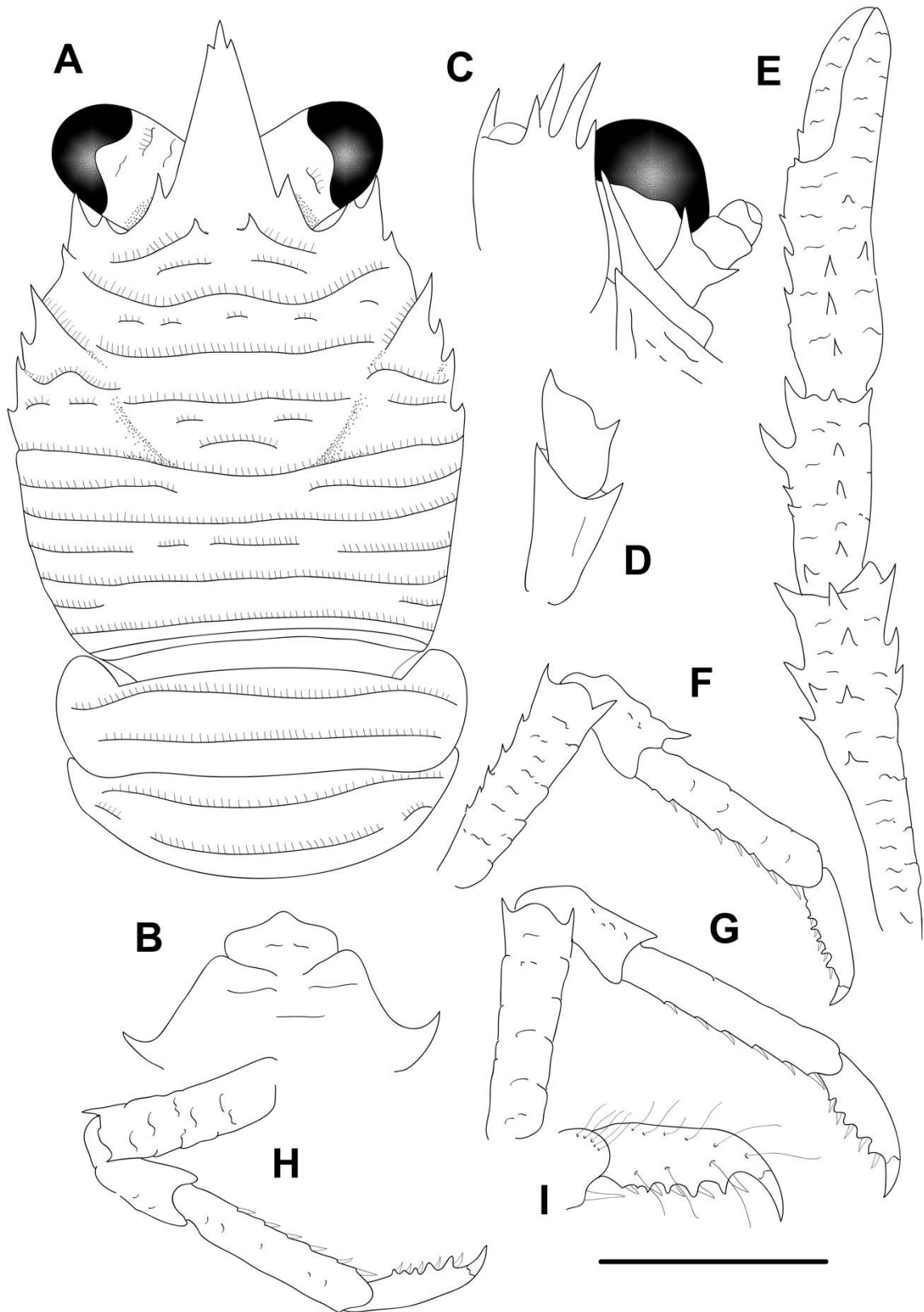
FIGURE 29. *Phylladiorhynchus lini* **n. sp**., holotype female 2.2 mm (NMMBCD5596): A, carapace and pleon, dorsal view. B, thoracic sternites 3 and 4. C, left cephalic region, showing antennular and antennal peduncles, ventral view. D, right Mxp3, lateral view. E, right P1, dorsal view. F, right P2, lateral view. G, right P3, lateral view. H, left P4, lateral view. I, dactylus of right P2, lateral view. Scale bar: A, E-H = 1.0 mm; B–D, I = 0.6 mm.

Etymology. The species is named after our colleague Chia-wei Lin, from the National museum of marine biology & aquarium, Pingtung, Taiwan, who collected most of the specimens.

Description. *Carapace:* As long as or slightly longer than broad; transverse ridges with dense short setae and some thick setae. Gastric region slightly convex with some transverse ridges: epigastric ridge distinct with 2 median spines and some lateral short scales, followed by small short scales on posterior epigastric region; anterior protogastric ridge not medially interrupted, nearly extending laterally to carapace margin, often followed by uninterrupted posterior protogastric ridge or short scales; anterior mesogastric ridge not medially interrupted, laterally interrupted by anterior branch of cervical groove, and continuing uninterrupted to first branchial spine; anterior metagastric ridge not medially interrupted, followed by posterior scale-like metagastric ridge. Mid-transverse ridge not interrupted, medially depressed, followed by shallow or indistinct cervical groove, followed by 2–3 not interrupted or minutely interrupted ridges, interspersed with 2 interrupted riges and some few short scales. Lateral margins slightly convex, with 6 distinct spines: first anterolateral spine well-developed, reaching anteriorly to level of lateral orbital spine, second spine (hepatic) well-developed, slightly dorsomesially from lateral margin, and followed by 4 branchial spines (3 anterior and 1 posterior). Rostrum dagger-like, horizontal dorsally flattish or slighly concave [1.5]–1.8 times as long as broad, length [0.4]–0.5 and breadth 0.2–[0.3] that of carapace; lateral margins smooth and straight or nearly straight, with well-developed supraocular basal spines and subapical spines. Pterygostomian flap with anterior spine, upper margin smooth.

Sternum: As wide as long. Sternite 3 moderately broad, [1.9]–2.3 times as wide as long, anterior margin convex, with a blunted median projection, anterolaterally rounded. Sternite 4 widely contiguous to sternite 3; anterolaterally smooth, surface depressed in midline, smooth; greatest width [2.5]–2.9 times that of sternite 3, 2.7–[3.5] times as wide as long.

Pleon: Elevated ridges with short setae and a few scattered long setae. Tergite 2–4 with anterior and posterior transverse elevated ridges; tergites 5–6 smooth.

Eye: Eye stalk length about 0.9–[1.1] times broader than long, peduncle distally setose, not distinctly expanded proximally, with few short transverse striae on lateral surfaces; cornea expanded distally, maximum corneal diameter [0.9]–1.0 × rostrum width*,* as wide as eyestalk.

Antennule: Article 1 longer than wide, with 5 distal spines: distomesial spine well-developed; proximal lateral spine small, always present.

Antenna: Article 1 with prominent mesial process, distally falling well short of lateralmost antennular spine. Article 2 with well-developed distomesial and distolateral spines. Article 3 and 4 unarmed.

Mxp3: Ischium with distinct distal spines on flexor and extensor margins. Merus [0.6]–0.7 × length of ischium, with well-developed distal spine on extensor and flexor margins.

P1: Slender, 3.0 (males), 2.0–[2.3] (females) times carapace length; subcylindrical, spiny and with long stiff setae; merus, carpus and palm with spines along mesial, dorsal and lateral surfaces, distal and mesial spines usually stronger than others. Merus 0.7–[0.9] length of carapace, 1.5–[1.8] times as long as carpus. Carpus [2.5]–3.1 times as long as wide. Palm [1.1]1.1 × carpus length, 2.3–[2.7] times as long as broad. Fingers [0.7]0.7× palm length; fixed finger with 0–1 basal spines; movable finger with 1 basal spine.

P2–4: setose and spinose. Meri successively shorter posteriorly: P3 merus [0.9]0.9 times length of P2 merus, P4 merus [0.8]–0.9 times length of P3 merus. P2 merus, 1.5–[1.8] times carapace length, [3.4]–4.4 times as long as broad, [1.1]1.1 times as long as P2 propodus; P3 merus [3.6]–3.7 times as long as broad, 1.0–[1.2] times as long as P3 propodus; P4 merus [3.2]–3.7 times as long as broad, 1.0–[1.1] times as long as P4 propodus; extensor margin of P2 and P3 with row of spines, proximally diminishing, with prominent distal spine; P4 extensor margin irregular, unarmed; flexor margin irregular, with distal spine on P2–3, absent or small on P4. Carpi with 2–4 small spines on extensor margin on P2–3, unarmed on P4; distal spine prominent on P2–3, absent on P4; row of granules below extensor margin on lateral surface of P2–4; flexor margin unarmed. Propodi stout, [4.0–5.0]4.3–5.0 times as long as broad; extensor margin irregular; flexor margin with 3–6 slender movable spines in addition to distal pair. Dactyli [0.6–0.7]0.5 × length of propodi, ending in incurved, strong, sharp spine; flexor margin with cuticular spines at basis of 5–6 movable spines.

Eggs: Ov. F carried approximately 4–15 eggs of 0.5 mm diameter.

Colour. Variable colour pattern. Base colour dark to light brown, sometimes orange. Rostrum whitish or brownish; anterior half of carapace margin sometimes with large whitish band; dorsal surface of carapace and pleon sometimes with large whitish spots. P1 usually with whitish bands. P2-4 with dusky and whitish bands.

Genetic data. COI and 16S, Table 1.

Distribution. Taiwan, Kenting, between 5 and 8 m.

Remarks. *Phylladiorhynchus lini* belongs to the group of species having 2 epigastric spines, 1 hepatic spine, 3 spines on the anterior branchial margin, rostrum dagger-like (margin straights or nearly straight) and dactylar spines along the flexor margin of the P2–4 dactyli. The new species is closely related to *P. spinosus* Schnabel & Ahyong, 2019, from New Zealand and Australia (see the differences under the Remarks of *P. spinosus*).

The mean intraspecific genetic divergences in *P. lini* were 0.6% (COI) and 0.2% (16S).
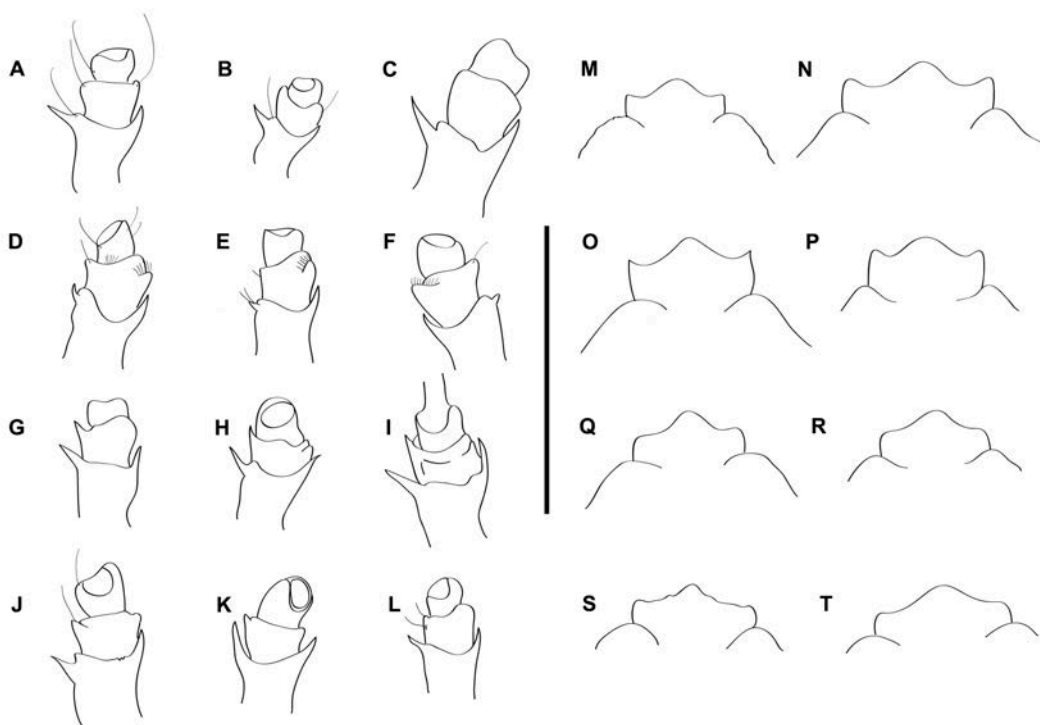
FIGURE 30. Variability in the armature of the antennal articles 2-4 (A-L) and in the shape of the thoracic sternite 3 (M-T). *P. euryalus* **n. sp.**: A, M, paratype male 1.8 mm (UF34732); B, paratype male 1.6 mm (UF25216); C, N, paratype female 3.5 mm (MNHN-IU-2016-489). *P. spinosus* Schnabel & Ahyong, 2019: D, O, male 2.7 mm (MNHN-IU-2016-491); E, paratype male 2.6 mm (MNHN-IU-2013-9439); F, P, paratype male 2.5 mm (MNHN-IU-2016-470). *P. asclepius* **n. sp.**: G, Q, paratype male 2.1 mm (UF22296); H, R, paratype ovigerous female 2.1 mm (UF27601); I, paratype male 2.4 mm (UF27886). *P. lini* **n. sp.**: J, S, paratype ovigerous female 2.6 mm (UF11812); K, T, paratype ovigerous female 2.5 mm (MNHN-IU-2016-490); L, paratype male 1.7 mm (MNHN-IU-2016-490). Scale bar: 1 mm.

Phylladiorhynchus lynceus **n. sp.**

(Figs. 31, 33C, 37E-F)

Type material. *Holotype.* Chagos Archipelago, Great Chagos Bank, Brothers Island. Stn CH0614 dead branching coral heads. Outer Reef Slope, 8–12 m, February 2012: ov. F 2.0 mm (MNHN-IU-2019-2593)
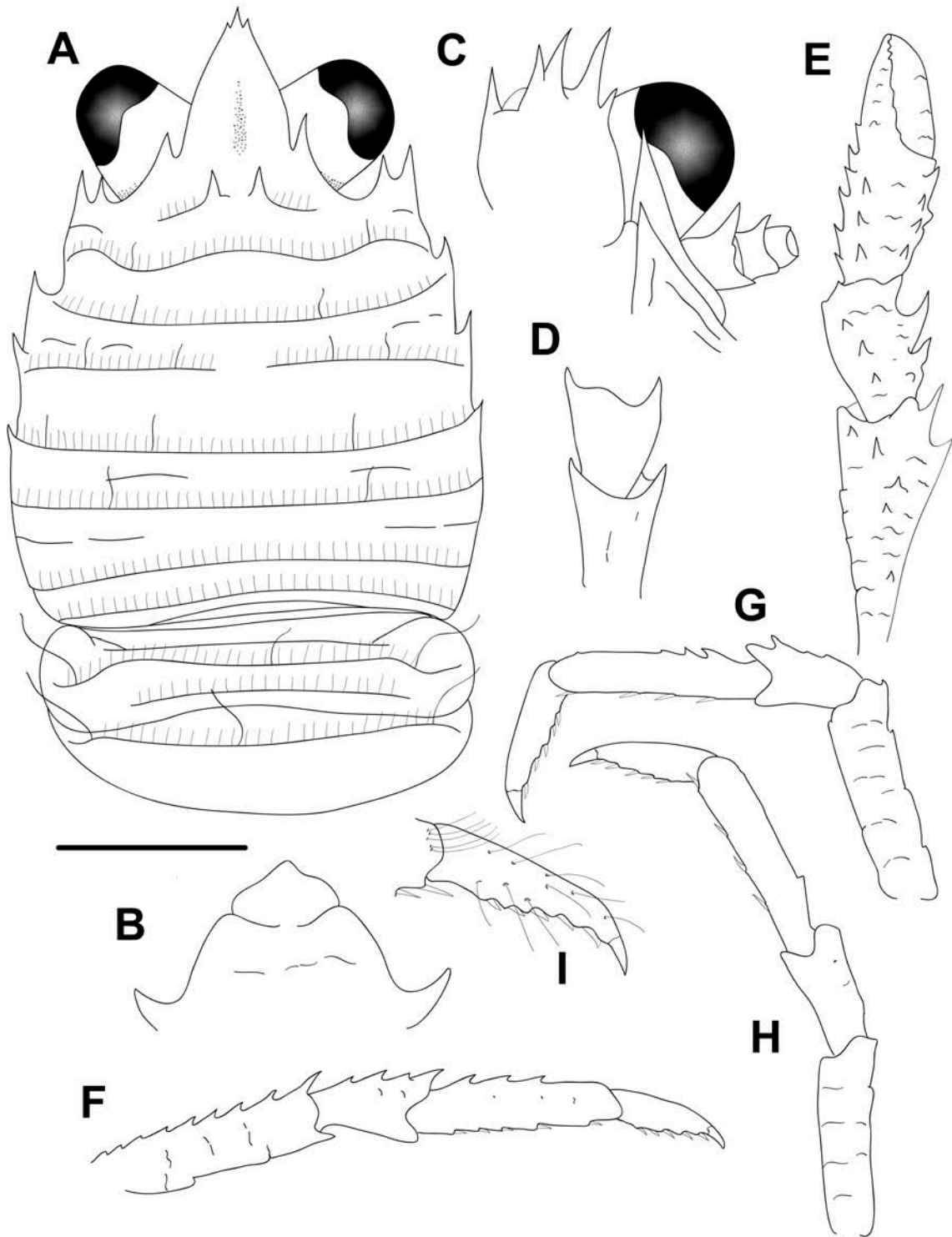
FIGURE 31. *Phylladiorhynchus lynceus* **n. sp**., holotype ovigerous female 2.0 mm (MNHN-IU-2019-2593): A, carapace and pleon, dorsal view. B, thoracic sternites 3 and 4. C, left cephalic region, showing antennular and antennal peduncles, ventral view. D, right Mxp3, lateral view. E, left P1, dorsal view. F, right P2, lateral view. G, right P3, lateral view. H, left P4, lateral view. I, dactylus of right P2, lateral view. Scale bar: A, E-H = 1.0 mm; B–D, I = 0.6 mm.

Paratypes. Chagos Archipelago, Great Chagos Bank, Eagle Island. Stn CH1364 dead branching coral heads. Outer Reef Slope, 8–12 m, February 2012: 1 ov. F 1.4 mm, 1 F 1.3 mm (MNHN-IU-2019-2594).—Stn CH0447, 1 M 1.7 mm (OUMNH.ZC.2014-09-064).—Stn CH0230, 1 M 1.2 mm (OUMNH.Zc.2014-09-065).

American Samoa. Olosega Island. Stn OLO-187, 14.18140174ºS, 169.6267462ºW, 14 m, 14 March 2015: 1 M 1.8 mm.—Stn OLO-094, 14.18140174ºS, 169.6267462ºW, 14 m, 14 March 2015: 1 ov. F 2.1 mm.—Rose Atoll. Stn ROS-610, 14.54895ºS, 168.13792ºW, 15 m, 17 March 2015: 8 M 1.4–2.1 mm, 8 ov. F1.5–2.3 mm.—Stn ROS-527, 14.54895ºS, 168.13792ºW, 15 m, 17 March 2015: 1 M 1.9 mm, 1 ov. F 1.8 mm.—Stn ROS-562, 14.54895ºS, 168.13792ºW, 15 m, 17 March 2015: 10 M 1.4–2.1 mm, 13 ov. F 1.4–2.1 mm, 2 F1.5–1.8 mm.—Ofu Island. Stn OFU-121, 14.17765914ºS, 169.649504ºW, 14 m, 21 March 2015: 1 ov. F 2.3 mm.—Stn OFU-168, 14.17765914ºS, 169.649504ºW, 14 m, 21 March 2015: 1 M 1.9 mm, 1 ov. F, 2.2 mm.—Stn OFU-280, 14.18628333ºS, 169.6599ºW, 14 m, 26 March 2015: 1 M 1.8 mm, 1 ov. F 1.9 mm.

Kiribati. Line Islands. 9.91ºS, 150.21ºW, 11 m, 8 November 2013: 1 M1.9 mm (UF41803).—Millenium island. 9.91ºS, 150.21ºW, 12 m, 5 November 2013: 1 M 1.8 mm 1 ov. F 1.3 mm (UF40895).—Phoenix islands, Orona island. 4.519ºS 172.227ºW, 12 m, 17 September 2015: 1 ov. F 1.7 mm (UF51296).—4.520ºS, 172.230ºW, 15 m, 18 September 2015: 1 M 1.5 mm (UF51370), 2 M 1.8–1.9 mm 1 ov. F 1.8 mm (UF51363).—Nikumaroro island.4.656ºS, 174.545ºW, 14 m, 23 September 2015: 1 ov. F 1.7 mm (UF51559).—4.694º S 174.490ºE, 7.5–9 m, 25 September 2015: 1 M 1.3 mm (UF51644).

Western Australia. Hibernia Reef. Stn 142/K13, 11º59.292'S, 123º21.154'E, no depth, 4 October 2013: 1 M 2.1 mm (WAM C55689).—Rowley Shoals. Mermaid Reef. Stn 178/K14-T1, 17º09.69'S, 119º38.826'E, 12–18 m, 13 October 2014: 1 ov. F 1.6 mm (WAM C53889).

Etymology. From the name *Lynceus*, an Argonaut, son of Aphareus and Arene. The name is considered a substantive in apposition.

Description. *Carapace:* As long as or slightly longer than broad; transverse ridges with dense short setae and few scattered long and thick setae. Gastric region slightly convex with 4 transverse ridges: epigastric ridge distinct with 2 spines (Samoa and Kiribati specimens often with 1 median produced scale usually with thick plumose setae before epigastric ridge), short scales laterally; anterior protogastric ridge not medially interrupted, nearly extending laterally to carapace margin; anterior mesogastric ridge not medially interrupted, laterally continuing to first branchial spine; sometimes followed by some short small scales; anterior metagastric ridge medially interrupted. Mid-transverse

ridge not interrupted, cervical groove indistinct, followed by 2 not interrupted or minutely interrupted ridges, interspersed with 1 short lateral ridge and sometimes few, short scattered scales. Lateral margins slightly convex, with 4 distinct spines: first anterolateral spine well-developed, reaching anteriorly to level of lateral orbital spine, hepatic margin unarmed; anterolateral spine followed by 3 branchial spines (2 anterior and 1 posterior spines). Rostrum leaf-like, horizontal, dorsally concave, [1.5]–1.6 times as long as broad, length [0.3]–0.4 and breadth 0.2–[0.3] that of carapace; lateral margins serrated and convex, with well-developed supraocular basal spines and small subapical spines. Pterygostomian flap ending in blunt tooth, upper margin smooth.

Sternum: As wide as long. Sternite 3 quadrangular, slightly wider than long ([1.5]1.5 times as wide as long), anterior margin with median blunted projection, lateral margins rounded. Sternite 4 widely contiguous to sternite 3; surface depressed in midline, smooth; greatest width 3.0[3.0] times that of sternite 3, [2.7]2.5–3.0 times as wide as long.

Pleon: Elevated ridges with short setae and a few scattered long setae. Tergite 2 with anterior and posterior transverse elevated ridges; tergites 3–4 with anterior transverse ridge; tergites 5–6 smooth.

Eye: Eye stalk length about 0.9–[1.0] times broader than long, peduncle distally setose, slightly expanded proximally; maximum corneal diameter 0.8–[0.9] × rostrum width*,* narrower than eyestalk, (0.8 times maximum peduncle width).

Antennule: Article 1 slightly longer than wide, with 5 distal spines: distomesial spine small; proximal lateral spine small, always present.

Antenna: Article 1 with prominent mesial process, distally falling well short of lateralmost antennular spine. Article 2 with well-developed distomesial and distolateral spines. Article 3 with distomesial spine. Article 4 unarmed.

Mxp3: Ischium with distinct distal spines on flexor and extensor margins. Merus 0.6–[0.8] × length of ischium, with distal spine on extensor and flexor margins.

P1: 1.7–2.0 (males), 2.0 (females) times carapace length; subcylindrical, spiny and with dense long stiff setae; merus, carpus and palm with spines along mesial, dorsal and lateral surfaces, distal and mesial spines usually stronger than others. Merus 0.7–0.8 length of carapace, 2–2.1 times as long as carpus. Carpus 1.2–1.3 times as long as wide. Palm 1.2–1.3 × carpus length, 1.5–1.7 times as long as broad. Fingers unarmed, 0.6–0.9 × palm length.

P2–4: Stout, setose and spinose. Meri successively shorter posteriorly: P3 merus 0.7–[0.8] times length of P2 merus, P4 merus [0.8]0.8 times length of P3 merus. P2 merus, 0.7–[0.8] times carapace length, [3.6]–3.8 times as long as broad, [1.2]–1.3 times as long as P2 propodus; P3 merus 3.7 times as long as broad, [1.0]–1.1 times as long as P3 propodus; P4 merus [2.8]2.7–3.2 times as long as broad, [1.0]–1.1 times as long as P4 propodus; extensor margin of P2 and P3 with row of spines, proximally diminishing, with prominent distal spine; P4 extensor margin irregular, unarmed; flexor margin irregular,with distal spine on P2–3, unarmed on P4. Carpi with 1–3 prominent spines on extensor margin on P2–3, unarmed on P4; distal spine prominent on P2–3, smaller on P4; row of small spines or granules below extensor margin on lateral surface of P2–3, unarmed on P4; flexor margin unarmed. Propodi stout, [3.8]3.3–4.3 times as long as broad; extensor margin irregular, armed with 1–3 spines on proximal half or unarmed; flexor margin with 3–4 slender movable spines in addition to distal pair. Dactyli 0.7–[0.8] × length of propodi, ending in incurved, strong, sharp spine; flexor margin with 4–6 movable spines.

Eggs: Ov. F carried approximately 5–25 eggs of 0.3–0.4 mm diameter.

Colour. Unknown.

Genetic data. COI and 16S, Table 1.

Distribution. Chagos Archipelago, Western Australia, Kiribati, American Samoa, between 7.5 and 18 m.

Remarks. *Phylladiorhynchus lynceus* belongs to the group of species with 2 epigastric spines and 2 spines on the anterobranquial margin. The closest species are: *P. integrirostris*, from Hawaii and *P. priasus* from the Mariana and Marshall Islands. The three species are barely distinguishable morphologically, although they are genetically very different (see the differences under the Remarks of *P. priasus*). Furthermore, these 3 species are also close to *P. orpheus* (see the differences under the Remarks of *P. orpheus*).

The intraspecific genetic divergences in *P. lynceus* ranged from 1 to 2.3% (COI) and 0% to 1% (16S).

Phylladiorhynchus maestratii n. sp.

(Fig. 32)

Phylladiorhynchus ikedai.—Baba, 1991, 485 (in part, only some specimens from CALSUB Pl 16).
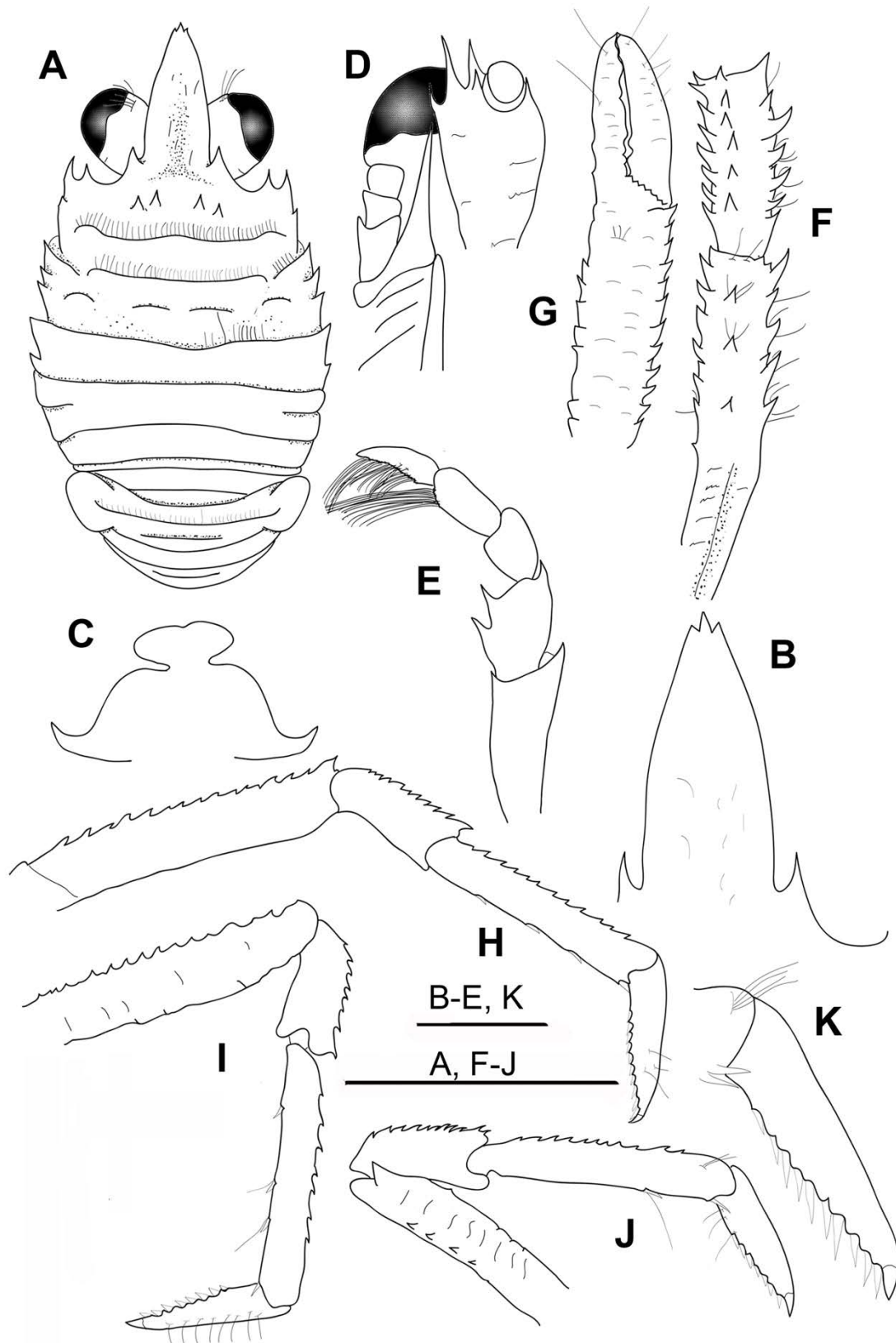
FIGURE 32. *Phylladiorhynchus maestratii* **n. sp**., A-E, holotype male 2.3 mm (MNHN-IU-2017-2736); F-J, paratype ovigerous female 3.1 mm (MNHN-IU-2017-11662): A, carapace and pleon, dorsal view. B, rostrum, dorsal view. C, thoracic sternites 3 and 4. D, right cephalic region, showing antennular and antennal peduncles, ventral view. E, left Mxp3, lateral view. F, left P1, merus and carpus, dorsal view. G, left P1, propodus and dactylus, dorsal view. H, right P2, lateral view. I, right P3, lateral view. J, right P4, lateral view. K, dactylus of right P2, lateral view. Scale bars: 1.0 mm.

Type material. *Holotype.* Chesterfield Islands. KANADEEP Stn DW4962, 23º02'S, 159º28'E, 315–1260 m, 6 September 2017: M 2.3 mm (MNHN-IU-2017-2736)

Paratypes. New Caledonia. CALSUB Pl 16, 20º37.8'S, 167º02.7'E, 500 m, 7 March 1989: 1 M broken (MNHN-IU-2013-19942), 1 M 1.8 mm (MNHN-IU-2013-19943).— KANACONO Stn CP4684, 22°24'S, 167°24'E, 493–694 m, 14 August 2016: 1 M 1.7 mm (MNHN-IU-2017-11683).—Stn DW4749, 23°38'S, 167°44'E, 440–457 m, 24 August 2016: 1 ov. F 3.1 mm (MNHN-IU-2017-11662).

Etymology. Named after Philippe Maestrati, curatorial assistant of the general mollusk collection of the Muséum national d'Histoire naturelle, Paris.

Description. *Carapace:* [1.2]1.1–1.2 times as long as broad; transverse ridges with dense short setae and scattered long setae. Gastric region flattened with 4 transverse ridges: epigastric ridge indistinct, with 4 spines (2 pairs of spines laterally, sometimes with median granule); anterior protogastric ridge not medially interrupted, nearly extending laterally to carapace margin; anterior mesogastric ridge not medially interrupted, or minutely interrupted, laterally interrupted by anterior branch of cervical groove; anterior metagastric ridge scale-like. Mid-transverse ridge not interrupted, preceded by shallow cervical groove, followed by 2 not interrupted or minutely interrupted ridges, interspersed with 1–2 short lateral ridges and few, short scattered scales. Lateral margins straight or slightly convex, with 7 spines: first anterolateral spine well-developed, reaching or slightly exceeding level of lateral orbital spine, second spine (hepatic) small, slightly dorsomesially from lateral margin, and followed by 5 branchial spines (3 anterior and 2 posterior). Rostrum dagger-like, horizontal, dorsally slightly or deeply concave, [2.1]2.0–2.1 times as long as broad, length [0.5]0.4–0.5 and breadth [0.3] 0.3 that of carapace; lateral margins smooth, convex, with well-developed supraocular spines, subapical spines distinct. Pterygostomian flap ending in blunt tooth, upper margin smooth.

Sternum: As wide as long. Sternite 3 moderately broad [2.3]2.0–2.3 times as wide as long anterior margin convex. Sternite 4 narrowly contiguous to sternite 3; surface depressed in midline, smooth; greatest width 3 times that of sternite 3, [3.0]2.5–3.0 times as wide as long.

Pleon: Elevated ridges with short setae and a few scattered long setae Tergite 2 with anterior and posterior transverse elevated ridges; tergites 3–4 with anterior transverse ridges only; tergites 5–6 smooth.

Eye: Eye stalk as broad as long, peduncle distally setose, not distinctly expanded proximally, maximum corneal diameter [1.0]0.9–1.0 × rostrum width, as wide as eyestalk.

Antennule: Article 1 1.3 times longer than wide, with 5 distal spines, distomesial spine well-developed; proximal lateral spine small.

Antenna: Article 1 with prominent mesial process distally clearly not reaching lateralmost antennular spine. Article 2 unarmed, sometimes with minute distolateral spine. Articles 3 and 4 unarmed.

Mxp3: Ischium with distinct distal spines on flexor and extensor margins. Merus half length of ischium, extensor margin with distal spine, flexor margin with 2 strong spines.

P1: [2.9] times carapace length (males), 2.8 (female), subcylindrical, spiny and with scattered long stiff setae and dense short thick setae; merus, carpus and palm with spines along mesial, dorsal and lateral surfaces, mesial spines usually stronger than others. Merus [1.1]1.1 length of carapace, [2.1]–2.3 times as long as carpus. Carpus [2.4]–2.5 times as long as wide. Palm [1.4]1.4 × carpus length, [2.9]–3.4 times as long as broad. Fingers unarmed, [0.7]0.7 × palm length.

P2–4 (lost in holotype): Slender, subcylindrical, moderately setose and spinose. Meri successively shorter posteriorly: P3 merus 0.7 times length of P2 merus, P4 merus 0.9 times length of P3 merus. P2 merus, 0.8 times carapace length, 9 times as long as broad, 1.3 times as long as P2 propodus; P3 merus 5 times as long as broad, 1.3 times as long as P3 propodus; P4 merus 4 times as long as broad, 1.2 times as long as P4 propodus; extensor margin of P2 and P3 with row of spines, proximally diminishing, with prominent distal spine; P4 extensor margin irregular, unarmedt; flexor margins of P2–4 irregular; P4 lateral surface with 4 small spines. Carpi extensor margin with 8–9 small spines on extensor margin on P2–3; distal spine prominent on P2, smaller or absent in P3–4; flexor margin unarmed. Propodi moderately slender, 6.3–7.0 times as long as broad; extensor margin irregular, usually serrated, with 7–10 small spines; flexor margins with 2–3 slender movable spines in addition to distal pair. Dactyli 0.5–0.6 × length of propodi, ending in incurved, strong, sharp spine; flexor margins with 8–10 movable spines.

Colour. Unknown.

Genetic data. COI and 16S, Table 1.

Distribution. New Caledonia, Chesterfield Islands, from 315 to 1260 m**.**

Remarks. *Phylladiorhynchus maestratii* belongs to the group of species having the epigastric ridge with 4 spines and often one median process or scale with thick plumose setae (rarely with 5 spines), 3 spines on the anterior branchial margin of the carapace and the Mxp3 merus with two prominent spines along the flexor margin. *Phylladiorhynchus maestratii* is close to *P. cepheus* from French Polynesia and *P. butes*, from New Caledonia, Chesterfield Islands, Indonesia and French Polynesia, however these species can be distinguished in basis of the following characters:

- The median epigastric process, spine or scale with thick setae is always present in *P. cepheus* and *P. butes*, whereas this process is absent or is present as a simple granule in *P. maestratii*.
- The rostrum is less than twice longer than wide in *P. cepheus* and *P. butes*, whereas it is more than twice longer than wide in *P. maestratii*.
- The sternite 4 is widely contiguous to sternite 3 in *P. cepheus* and *P. butes*, whereas it is narrowly contiguous in *P. maestratii*.
- The dactili flexor margins have 8–10 movable spines in *P. maestratii*, whereas these margins have 6–7 movable spines in *P. cepheus*.

The genetic divergences among these species were larger than 7% (COI) and 5% (16S).

Phylladiorhynchus marina n. sp.

 (Figs. 33D, 34, 55B)

Type material. *Holotype*. Vanuatu. SANTO Stn DB14, 15°30.9'S, 167°11'E, 10–14 m, 13 October 2006: ov. F 2.0 mm (MNHN-IU-2014-13887).

Paratypes. Vanuatu. SANTO Stn DS6 light, 15°30.9'S, 167°11.1'E, 8-15 m, 11 September 2006: 1 M 1.4 mm, 3 ov. F 1.7–1.8 mm (MNHN-IU-2014-13893).—Stn FR2, 15°33.3'S, 167°08.8'E, 1–25 m, 11 September 2006: 1 F 1.8 mm (MNHN-IU-2014-13889).—Stn DB16, 15°35.5'S, 167°15.8'E, 32–40 m, 14 September 2006: 1 M 1.5 mm (MNHN-IU-2014-13891).—Stn DB40, 15°29.8'S, 167°15.1'E, 5 m, 19 September 2006: 3 M 1.5–1.6 mm (MNHN-IU-2019-2646), 1 ov. F 1.5 mm (MNHN-IU-2016-453), 1 F 1.6 mm (MNHN-IU-2014-13862).—Stn DB46, 15°28.8'S, 167°15.2'E, 2–3 m, 20 September 2006: 1 F 1.7 mm (MNHN-IU-2019-2644).—Stn DB53, 15°28.8'S, 167°15.2'E, 5 m, 22 September 2006: 5 M 1.4–1.8 mm, 11 ov. F 1.2–1.8 mm, 5 F 1.3–2.1 mm (MNHN-IU-2019-2652), 8 M 1.2–1.5 mm, 3 ov. F 1.7–2.0 mm, 1 F 1.4 mm (MNHN-IU-2019-2645).—Stn AT42, 15°37.5'S, 167°02.3'E, 112-148 m, 28 September 2006: 1 M 1.4 mm (MNHN-IU-2014-13895).—Stn NS36, 15°31.7'S, 167°09.5'E, 2–3 m, 2 October 2006: 1 ov. F 1.5 mm (MNHN-IU-2014-13806).—Stn FB40, 15°22.9'S,
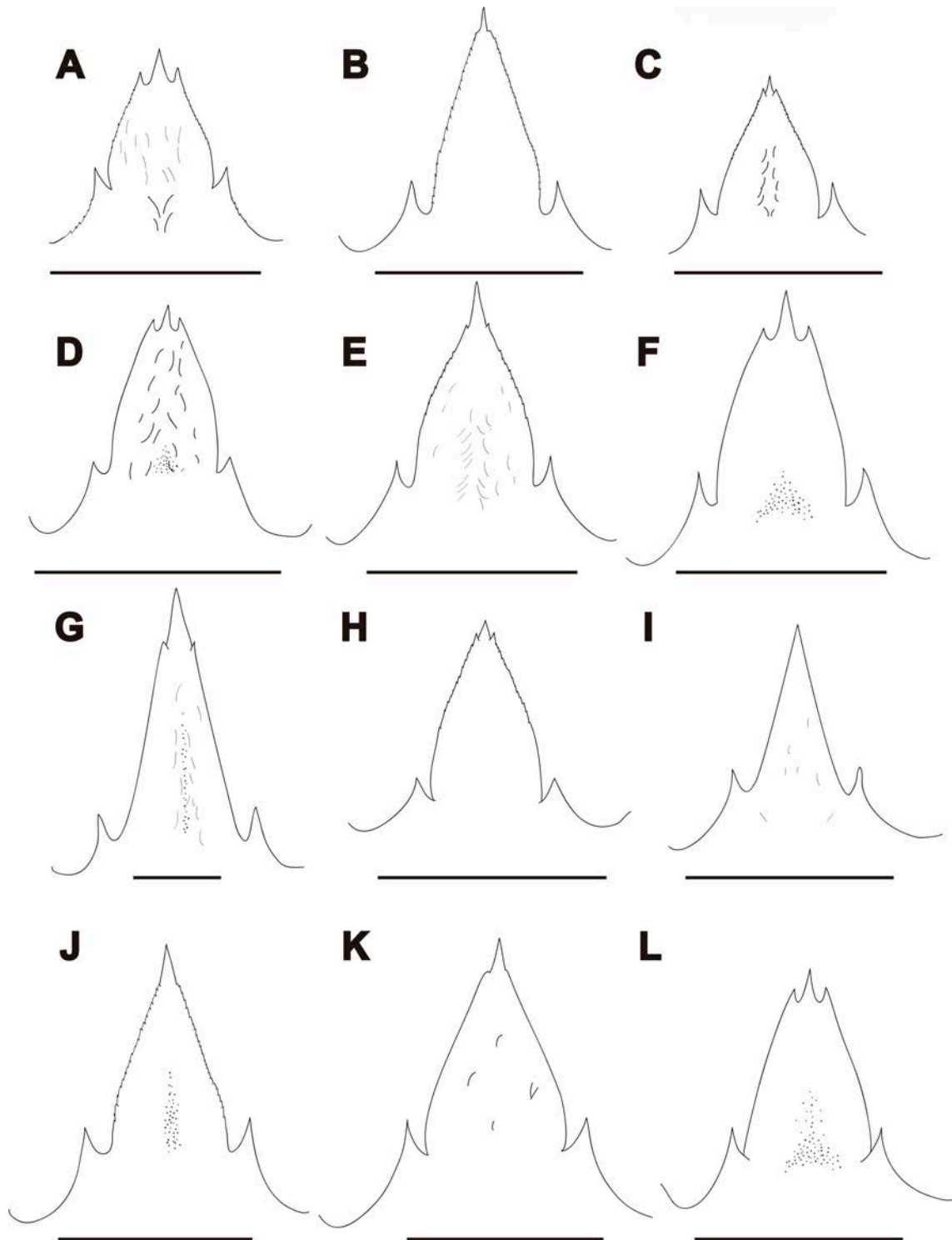
FIGURE 33. Rostrum, dorsal view. A, *Phylladiorhynchus laureae* **n. sp.**, paratype female 1.7 mm (MNHN-IU-2019-2635). B, *P. lini* **n. sp.**, holotype female 2.2 mm. C, *P. lynceus* **n. sp.**, holotype ovigerous female 2.0 mm (Chagos CH0614). D, *P. marina* **n. sp.**, paratype male 1.5 mm (MNHN-IU-2019-2653). E, *P. medea* **n. sp.**, holotype male 2.1 mm (MNHN-IU-2014-13795). F, *P. nudus* Macpherson, 2008, ovigerous female 2.4 mm (WAM C46587). G, *P. nui* Schnabel & Ahyong, 2019, male 6.5 mm (MNHN-IU-2019-2595). H, *P. orpheus* **n. sp.**, paratype male 1.9 mm (UF33962). I, *P. paulae* **n. sp.**, paratype male 2.3 mm (MNHN-IU-2019-2699). J, *P. penelos* **n. sp.**, paratype male 3.3 mm (UF1224). K, *P. pepei* **n. sp.**, holotype male 3,2 mm (MNHN-IU-2016-486). L, *P. phanus* **n. sp.**, paratype male 2.1 mm (MNHN-IU-2019-2687). Scale bars = 1 mm.
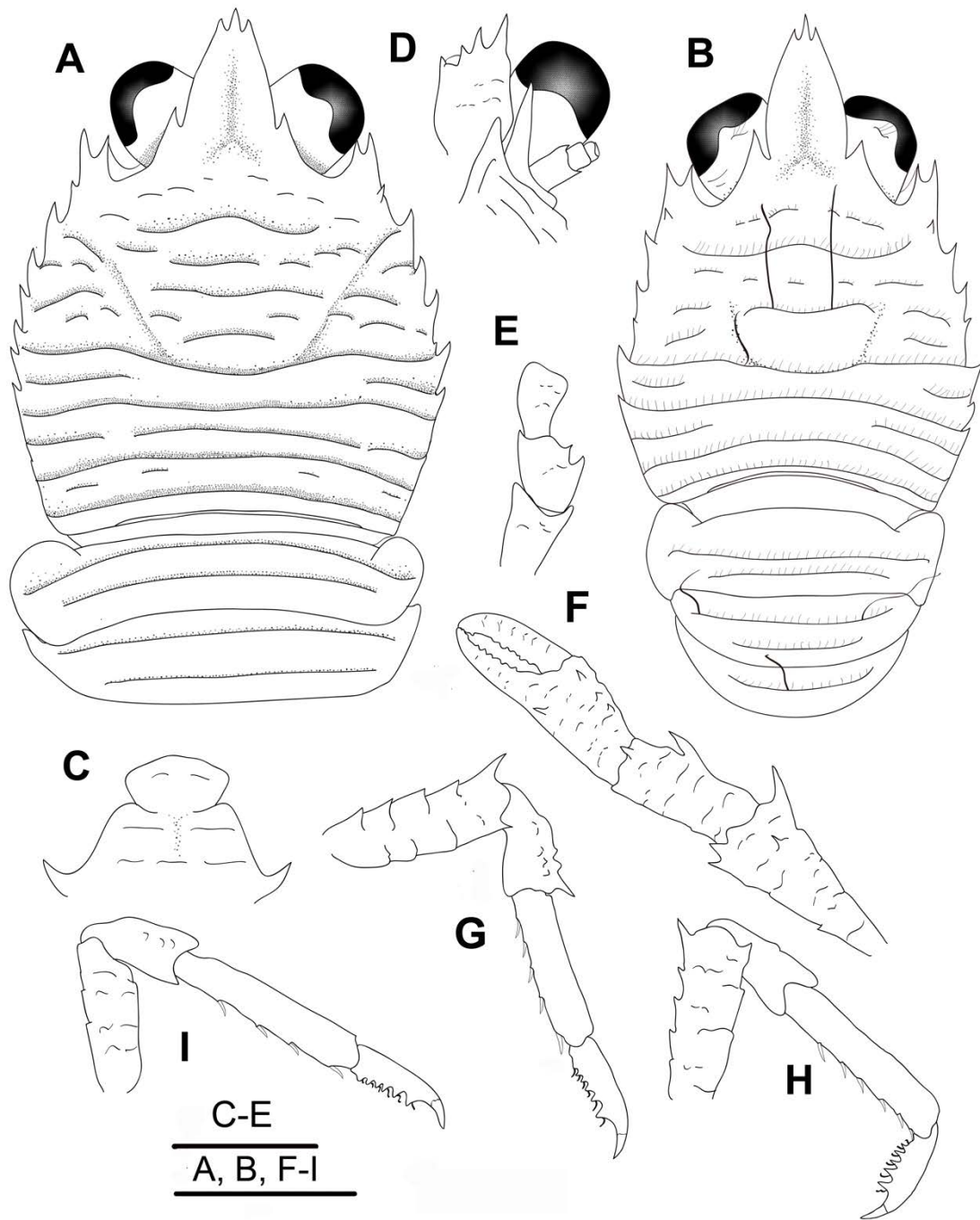
FIGURE 34. *Phylladiorhynchus marina* **n. sp**., A, C-I, holotype ovigerous female 2.0 mm (MNHN-IU-2014-13887); B, paratype male 1.5 mm (MNHN-IU-2019-2653): A, B, carapace and pleon, dorsal view. C, thoracic sternites 3 and 4. D, left cephalic region, showing antennular and antennal peduncles, ventral view. E, right Mxp3, lateral view. F, left P1, dorsal view. G, right P2, lateral view. H, right P3, lateral view. I, right P4, lateral view. Scale bars: A, B, F-I = 1.0 mm; C–E = 0.6 mm.

167°11.7'E, 9 m, 29 September 2006: 1 postlarvae 1.6 mm (MNHN-IU-2014-13876).—Stn DB83, 15°43.4'S, 167°15.0'E, 6 m, 3 October 2006: 1 M 1.4 mm (MNHN-IU-2014-13892).—Stn DS91, 15°33.7'S, 167°08.4'E, 7 m, 6 October 2006: 2 M 1.4–1.5 mm, 1 ov. F 2.3 mm (MNHN-IU-2014-13888).—Stn FB56, 15°35.2'S, 167°02.1'E, 3–18 m, 7 October 2006: 1 ov. F 1.6 mm (MNHN-IU-2014-13896).—Stn EP34, 15°33.3'S, 167°12.9'E, 40–60 m, 14 October 2006: 1 ov. F 1.5 mm (MNHN-IU-2019-2647).—Stn EP36, 15°33.3'S, 167°12.7'E, 20–60 m, 14 October 2006: 2 M 1.4–2.2 mm, 1 ov. F 1.9 mm (MNHN-IU-2019-2650), 4 M 1.4–1.8 mm, 3 ov. F 1.9–2.2 mm, 1 F 1.4 mm (MNHN-IU-2019-2649), 1 M 1.5 mm, 1 ov. F 2.0 mm, 4 F 1.6–2.3 mm (MNHN-IU-2019-2653).—Stn LD31, 15°34.3'S, 167°11.9'E, 1–3 m, 14 October 2006: 2 ov. F 2.4–2.6 mm (MNHN-IU-2014-13890).—Stn FB80, 15°33.1'S, 167°09.6'E, 2 m, 14 October 2006: 1 F 1.7 mm (MNHN-IU-2014-13894).—Stn LD35, 15°32.8'S, 167°11.6'E, 3–8 m, 16 October 2006: 2 M 1.4-2.3 mm, 3 ov. F 1.3–2.1 mm, 1 F 2.2 mm (MNHN-IU-2014-13897).—SE corner of Espiritu Santo Island (mixed illegible or confused labels) Sep/Oct 2006: 5 F 1.7–2.1 mm (MNHN-IU-2019-2648).

Etymology. Named in memorian of Marina Alcobendas, from the Spanish National Museum of Natural Sciences, evolutionary biologist and dear colleague. The name is considered as a substantive in apposition

Description. *Carapace:* Robust or massive, sexually dimorphic (wider on females), 0.9–[1.2] (males), 0.8–0.9 (females) times as long as broad; transverse ridges elevated, uplifted dorsally, with few short setae and scattered long thick plumose setae. Gastric region convex (uplifted) with some transverse ridges: epigastric ridge unarmed, scale-like, often undistinct; anterior protogastric ridge not medially interrupted, laterally interrupted with some few scales, often followed by some few short scales; anterior mesogastric ridge scale-like, laterally interrupted by anterior branch of cervical groove, continuing with some few scales, often followed by some few short scales; anterior metagastric ridge medially uninterrupted, followed by few scales on posterior metagastric region. Mid-transverse ridge not interrupted, cervical groove distinct, followed by 2 not interrupted or minutely interrupted ridges, interspersed with 1 laterally interrupted or scale-like ridge and 1–2 short lateral ridges. Lateral margins clearly convex, with 7–8 spines: first anterolateral spine well-developed, exceeding lateral orbital spine, second spine (hepatic) minute, often obsolescent in males, slightly dorsomesially from lateral margin, and followed by 5–6 branchial spines (3 anterior and 2–3 posterior). Rostrum leaf-like, horizontal, dorsally slightly or deeply concave, [1.5]1.6–1.9 times as long as broad, length [0.4]0.3–0.5 and breadth [0.2]–0.3 that of carapace; lateral margins minutely serrated and convex, with well-developed supraocular and subapical spines. Pterygostomian flap ending in blunt tooth; upper margin unarmed.

Sternum: Sternite 3 moderately broad, [1.8]–1.9 times as wide as long, anterior margin convex. Sternite 4 widely contiguous to sternite 3; surface flattened, smooth; greatest width [2.5]3.0–3.1 times that of sternite 3, 2–[2.1] times as wide as long.

Pleon: Elevated ridges uplifted dorsally, with few short setae. Tergites 2–4 with anterior and posterior transverse elevated ridges; tergites 5–6 smooth.

Eye: Eye stalk length about [1.0]1.0 times broader than long, peduncle distally setose, not distinctly expanded proximally; maximum corneal diameter 0.9[1.0] × rostrum width*,* as wide as eyestalk.

Antennule: Article 1 longer than wide, with 3–4 distal spines: distomesial spine small or obsolescent; proximal lateral spine absent. Short striae covering mesial surfaces.

Antenna: Article 1 with prominent mesial process, distally not reaching lateral antennular spine. Article 2 often with minute distal spines laterally and mesially. Articles 3 and 4 unarmed.

Mxp3: Ischium with distinct distal spines on flexor and extensor margins. Merus [0.6] × length of ischium, with 1 well-developed distal spine on extensor margin and 2 spines on flexor margin, proximal spine slightly larger than distal.

P1: 2.0 times carapace length (males), [1.3]–1.6 (females), subcylindrical, with scattered spines and long stiff setae; merus and carpus with spines along mesial, dorsal and lateral surfaces, distal and mesial spines usually stronger than others. Merus [0.5]0.5–1.0 length of carapace, [1.5]1.5–2.1 times as long as carpus. Carpus 1.5–1.9[2.0] times as long as wide. Palm [0.7]0.7–0.9 × carpus length, [1.4]1.2–1.5 times as long as broad with scattered small spines on dorsal and ventral surfaces, lateral and mesial margins irregular, with 1 small spine on distomesial margin. Fingers unarmed, [1.1]1.0–1.1× palm length*.*

P2–4: Moderately stout, setose and few spinose. Meri successively shorter posteriorly: P3 merus 0.8–[0.9] times length of P2 merus, P4 merus 0.7–[0.9] times length of P3 merus. P2 merus, [1.5]1.7–2.4 times carapace length, [4.0]–4.2 times as long as broad, [1.3]1.3 times as long as P2 propodus; P3 merus [3.5]–3.6 times as long as broad, [1.1]–1.2 times as long as P3 propodus; P4 merus [2.5]3.0–3.3 times as long as broad, as long as P4 propodus; extensor margins of P2 and P3 with row of few small spines, proximally diminishing in size, with well-developed distal spine; P4 extensor margin irregular but unarmed; flexor margins irregular, with distal spine on P2–3, absent in P4. Carpi with 1 spine on extensor margins of P2–3, unarmed on P4; distal spine prominent on P2–3, absent on P4; row of small spines below extensor margin on lateral surface of P2–3, unarmed on P4. Propodi stout, [4.5–5.0]4.4–4.5 times as long as broad; extensor

margins irregular, usually unarmed; flexor margins with 3–4 slender movable spines in addition to distal pair. Dactyli [0.8]0.8–0.9 × length of propodi, ending in incurved, strong, sharp spine; flexor margins with 5–6 well-developed dactylar spines, each with 1 spinule.

Eggs: Ov. F carried approximately 7–25 eggs of 0.3–0.4 mm diameter.

Colour. Base colour of carapace brownish, anterior region (from mid-transverse ridge) darker, with few pale-brown patches in gastric region, two symmetrical small dark brownish spots on epigastric and mid-transverse ridges. Rostrum brownish, with small dark brownish spots close to rostrum margin, tip and supraocular spines. Pleonal tergites 2–6 brownish, with white stripes medially and laterally, ridges of tergites 2–4 pale yellow with brownish-reddish small spots medially and brownish-reddish bands laterally; uropods and telson whitish-translucid. P1 pale brown, covered by small dark brownish spots, meri and carpi darker, brownish, palm and fingers spines whitish. P2–4 pale brown-whitish; propodi with two dark brown bands, dactyli whitish-translucid.

Genetic data. COI and 16S, Table 1.

Distribution. Vanuatu, between 4 and 15 m.

Remarks. *Phylladiorhynchus marina* belongs to the group of species having the epigastric ridge unarmed, the carapace and pleon ridges elevated, uplifted, and dactylar spines on the flexor margins of the dactyli. The new species is closely related to *P. phanus* from Papua New Guinea (see the differences under the Remarks of this species).

The mean intraspecific genetic divergences were 0.8% (COI) and 0.8% (16S).

***Phylladiorhynchus medea* n. sp.**

(Figs. 33E, 35, 55C)

Type material. *Holotype.* French Polynesia. Rapa. Stn 30, 27º38.2'S, 144º18.2'W, 16–20 m, 16/18 November 2002: M 2.2 mm (MNHN-IU-2016-493).

Paratypes. South China Sea. Macclesfield Bank. Stn 24, 15°26'30"N, 114°14'E, 24–63 m, May 1892: 1 ov. F 2.4 mm (MNHN-IU-2016-9639).

Chesterfield Islands. CORAIL 2 Stn CP25, 20°25'S, 161°05'E, 67–70 m, 22 July 1988: 1 M 1.6 mm (MNHN-IU-2016-472 (Ga-2050)).

New Caledonia. Lagon Nord. Stn DW1097, 19°51.7'S, 163°42.5'E, 33–34 m, 24 October 1989: 1 M 2.1 mm (MNHN-IU-2014-13795).—Touho. September 1993: 1 ov. F
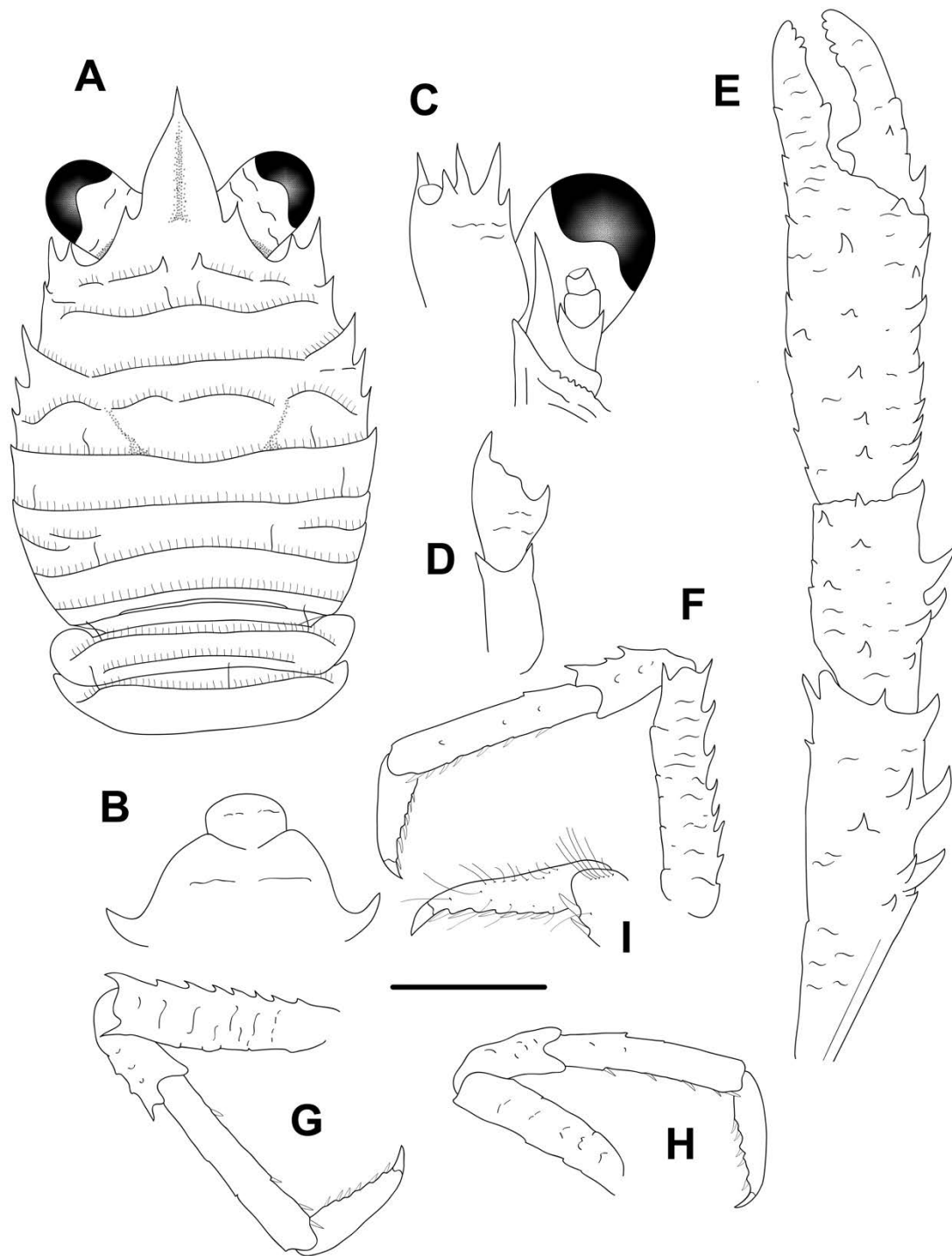
FIGURE 35. *Phylladiorhynchus medea* **n. sp**., A-D, F-I, holotype male 2.2 mm (MNHN-IU-2016-493): A, carapace and pleon, dorsal view. B, thoracic sternites 3 and 4. C, left cephalic region, showing antennular and antennal peduncles, ventral view. D, right Mxp3, lateral view. E, left P1, dorsal view. F, left P2, lateral view. G, left P3, lateral view. H, right P4, lateral view. I, dactylus of left P2, lateral view. Scale bar: A, E-H = 1.0 mm; B–D, I = 0.6 mm.

2.4 mm (MNHN-IU-2019-2616).—KOUMAC Stn KL25, 20.75421ºS, 164.22986ºE, 65 m, 10 November 2019: 1 M 1.4 mm (MNHN-IU-2014-20045).—Stn KL03, 20.67485ºS, 164.214266ºE, 50 m, 11 November 2019: 2 ov. F 2.0–2.3 mm (MNHN-IU-2014-20052), 1 F parasitized 1.9 mm (MNHN-IU-2014-20063).—Stn KB642, 20.7093ºS, 164.25715ºE, 28 m, 14 November 2019: 2 M 1.7–broken (MNHN-IU-2014-20109).—Stn KB647, 20.664116ºS, 164.189983ºE, 38 m, 16 November 2019: 2 M 1.5–2.0 mm (MNHN-IU-2014-20140).—Stn KL22, 20.4459ºS, 163.97176ºE, 47 m, 19 November 2019: 2 M 1.9–2.0 mm (MNHN-IU-2014-20158). 2 M 1.5–1.7 mm, 2 ov. F 1.9–2.0 mm, 3 postlarvae 0.9–1.0 mm (MNHN-IU-2014-20169).

French Polynesia. BENTHAUS Stn CP1918, 27°03'S, 146°04'W, 130–140 m, 12 November 2002: 3 M 2.5 mm, 5 ov. F 2.5–3.4 mm (MNHN-IU-2019-2591).—Stn CP1922, 27°04'S, 146°04'W, 150–163 m, 12 November 2002: 1 ov. F 2.1 mm (MNHN-IU-2019-2597).—Rapa. Stn 5, 27º05.6'S, 144º18.5'W, 8 m, 4 November 2002: 4 M 2.6–3.4 mm, 3 ov. F 2.5–3.6 mm, (MNHN-IU-2019-2587).—Stn 4, 27º34.3'S, 144º22.1'W, 18 m, 4 November 2002: 6 M 2.0–3.4 mm, 3 ov. F 2.6–3.0 mm, 3 F 1.5–2.0 mm (MNHN-IU-2019-2585).—Stn 4, 27º34.3'S, 144º22.1'W, 18 m, 4 November 2002: 1 M 2.0 mm, F 1.5–2.0 mm (MNHN-IU-2014-13908).—Stn 9, 27°37.3'S, 144°22.2'W, 3–24 m, 6 November 2002: 1 ov. F 2.2 mm (MNHN-IU-2014-13901).—Stn 9, 27°37.3'S, 144°22.2'W, 3–24 m, 6 November 2002: 1 M 2.2 mm (MNHN-IU-2014-13907).—Stn 10, 27°34.8'S, 144°22.8'W, 16–18 m, 7 November 2002: 1 ov. F 2.5 mm(MNHN-IU-2019-2584).—Stn 11, 27°37.2'S, 144°18.2'W, 2 m, 7 November 2002: 1 ov. F 2.2 mm (MNHN-IU-2019-2605).—Stn 14, 27°35.8'S, 144º13.6'W, 2 m, 8 November 2002: 1 M 2.1 mm, 1 ov. F 2.3 mm, (MNHN-IU-2019-2586).—Stn 16, 27°36.3'S, 144°184'W, 5 m, 8 November 2002: 1 ov. F 2.1 mm (MNHN-IU-2014-13906).—Stn 20, 27°35.4'S, 144°23.3'W, 5 m, 12 November 2002: 4 ov. F 2.2–2.8 mm (MNHN-IU-2019-2588).—Stn 25, 27º38.4'S, 144º18.9'W, 3 m, 13 November 2002: 1, ov. F, 1.8 mm, (MNHN-IU-2014-13902).—Stn 27, 27º38.7'S, 144º18.7'W, 6 m, 14 November 2002: 1 M 2.3 mm (MNHN-IU-2014-13910).—Stn 29, 27º34.3'S, 144º21.0'W, 2–4 m, 15 November 2002: 1 ov. F 2.2 mm, (MNHN-IU-2014-13903).—Stn 29, 27º34.3'S, 144º21.0'W, 2–4 m, 15 November 2002: 1 M 2.7 mm, 4 ov. F, 2.0–2.6 mm, (MNHN-IU-2019-2636).—Stn 30, 27º38.2'S, 144º18.2'W, 16–20 m, 16/18 November 2002: 1 M 2.2 mm, (MNHN-IU-2016-493), 6 M, 2.0–2.5 mm (MNHN-IU-2016-509), 1 M broken, (MNHN-IU-2016-494), 1 M 2.0 mm, 5 ov. F 2.1–2.7 mm (MNHN-IU-2014-13905).—Stn 32, 27º35.8'S, 144º23.0'W, 15–20 m, 18/23 November 2002: 4 M 2.0–2.5 mm, 8 ov. F 2.2–2.7 mm (MNHN-IU-2019-2603), 1 M 2.8 mm, 2 ov. F 1.8–2.1 mm, 1 F 2.0 mm (MNHN-IU-2016-1493).—Stn 33, 27º34.8'S, 144º20.8'W, 30 m, 19 November 2002: 4 M 2.0–3.0 mm, 2 ov. F 2.1–2.5 mm, 1 F 2.0 mm, (MNHN-IU-2019-2607).—Stn 36, 27º33.5'S ,

144°20.8'W, 27 m, 21 November 2002: 1 M, 2.5 mm, 4 ov. F 2.0–2.6 mm, (MNHN-IU-2019-2606).

Etymology. From the name *Medea*, daughter of Aeetes, joined the Argo when the Fleece was recovered. The name is considered a substantive in apposition.

Description. *Carapace:* as long as or slightly longer than broad; transverse ridges with dense short setae and some few scattered iridescent setae. Gastric region slightly convex with 4 transverse ridges: epigastric ridge distinct with 2 median spines and some lateral short scales, often followed by some short scales; anterior protogastric ridge not medially interrupted, extending laterally to carapace margin followed by some short scales; anterior mesogastric ridge not medially interrupted, laterally interrupted by cervical groove; anterior metagastric scale-like, often followed by some short scales. Mid-transverse ridge not interrupted, medially slightly depressed, cervical groove distinct, followed by 2 not interrupted or minutely interrupted ridges, interspersed with 1 short lateral ridge and some few short scales. Lateral margins nearly straight, with 6 distinct spines: first anterolateral spine well-developed, reaching anteriorly to level of lateral orbital spine, second spine (hepatic) small, slightly dorsomesially from lateral margin, and followed by 4 branchial spines (3 anterior and 1 posterior). Rostrum leaf-like, horizontal, dorsally convex, 1.3–[1.5] times as long as broad, length 0.3–[0.4] and breadth [0.2]–0.3 that of carapace; lateral margins serrated and convex, with well-developed basal supraocular spines, subapical spines absent or obsolescent. Pterygostomian flap with anterior spine, upper margin serrated.

Sternum: As wide as long. Sternite 3 moderately broad, [1.5]–2.9 times as wide as long, anterior margin convex, anterolaterally rounded. Sternite 4 widely contiguous to sternite 3; anterolaterally serrated, surface depressed in midline, smooth; greatest width 2.2–[3.5] times that of sternite 3, 2.3–[3.0] times as wide as long.

Pleon: Elevated ridges with short setae and a few scattered long setae. Tergite 2 with anterior and posterior transverse elevated ridges; tergites 3–4 with anterior transverse ridge; tergites 5–6 smooth.

Eye: Eye stalk length about 1.0–[1.1] times broader than long, peduncle distally setose, not distinctly expanded proximally, with few short transverse striae on lateral surfaces; cornea expanded distally, maximum corneal diameter 0.8–[0.9] × rostrum width, as wide as eyestalk.

Antennule: Article 1 slightly longer than wide, with 5 distal spines: distomesial spine well-developed; proximal lateral spine small, always present.

Antenna: Article 1 with prominent mesial process, distally not reaching lateralmost antennular spine. Article 2 with well-developed distomesial and distolateral spines. Article 3 and 4 unarmed.

Mxp3: Ischium with distinct distal spines on flexor and extensor margins. Merus 0.7–[0.8] × length of ischium, with well-developed distal spine on extensor and flexor margins.

P1(lost in holotype): 2.5–3.8 (males), 2.6 (females) times carapace length, subcylindrical, spiny and with long stiff setae; merus, carpus and pam with spines along mesial, dorsal and lateral surfaces, distal and mesial spines usually stronger than others. Merus 0.8 length of carapace, 2.2 times as long as carpus. Carpus 1.8 times as long as wide. Palm 1.6 × carpus length, 3.4 times as long as broad. Fingers 0.5 × palm length, fixed finger with 2 basal spines; movable finger with 1–2 basal spines.

P2–4: stout, setose and spinose. Meri successively shorter posteriorly: P3 merus [0.9]0.9 times length of P2 merus, P4 merus [0.8]–0.9 times length of P3 merus. P2 merus, 0.6–[0.7] times carapace length, [4.0]–4.5 times as long as broad, [1.2]–1.3 times as long as P2 propodus; P3 merus [3.5]–4.1 times as long as broad, 1.1–[1.2] times as long as P3 propodus; P4 merus 3.6–[3.7] times as long as broad, 0.9–[1.0] times as long as P4 propodus; extensor margin of P2 and P3 with row of spines, proximally diminishing, with prominent distal spine; P4 extensor margin irregular, unarmed; flexor margin irregular, with distal spine on P2–3, absent on P4. Carpi with 2 spines on extensor margin on P2–3, unarmed on P4; distal spine prominent on P2–3, absent on P4; granules below extensor margin on lateral surface of P2–4; flexor margin unarmed. Propodi moderately stout, [4.5–5.5]5.0–6.3 times as long as broad; extensor margin irregular; flexor margin with 3–6 slender movable spines in addition to distal pair. Dactyli [0.5–0.7]0.6–0.7 × length of propodi, ending in incurved, strong, sharp spine; flexor margin with 5–6 movable spines.

Eggs: Ov. F carried approximately 10–25 eggs of 0.3–0.4 mm diameter.

Colour. Base colour of carapace light orange-yellow. Carapace and Rostrum and Pleon, covered by granules and small dark orange spots, ridges and epigastric spines dark orange, third spine on anterior branchial margin covered by dark brown-reddish patch. Ocular peduncles oranges, covered by small dark-orange granules. Pleon light orange, ridges with brownish-dark orange stripes. P1 whitish, spines orange, merus, carpus, palm and fingers covered by whitish strips, distal tip finger orange. P2–4 light whitish-translucent, covered by whitish spots, spines dark-orange; meri, propodi and dactyli covered by dark orange stripes, dactyly distal part wittish to light orange.

Genetic data. COI and 16S, Table 1.

Distribution. South China Sea (Macclesfield Bank), New Caledonia and French Polynesia, between 15 and 163 m.

Remarks. *Phylladiorhynchus medea* belongs to the group of species having 2 epigastric spines, 1 hepatic spine, 3 spines on the anterior branchial margin and the pleonal tergite 3 with the anterior ridge only. The new species closely resembles *P. janiqueae*, however, both species can be distinguished by the following characters:

- The rostrum has small subapical spines in *P. janiqueae,* whereas these spines are absent or obsolescent in *P. medea*.
- The anterior upper margin of the pterygostomian flap is smooth in *P. janiqueae,* whereas this margin is usually serrated in *P. medea.*
- The antennal article 3 has a small distomesial spine in *P. janiqueae,* whereas this spine is absent in *P. medea.*

The new species is also close to *P. zetes* from the French Polynesia (see the differences under the Remarks of this species).

The genetic divergences between *P. medea* and *P. janiqueae* were 11% (COI) and 6% (16S). The mean intraspecific genetic divergences of *P. medea* were 0.6% (COI) and 0.3% (16S).

Phylladiorhynchus nudus Macpherson, 2008

(Fig. 33F)

 Phylladiorhynchus nudus Macpherson, 2008: 294, fig. 2 (Dampier Archipelago, W Australia, 2–5 m).—Baba *et al*., 2008: 176 (compilation).

Type material. *Paratype.* Western Australia. Dampier Archipelago. Stn DA3/99/61, 20º34.66'S, 116º39.72'E, 3–5 m, 14 September 1999: 1 M 2.7 mm (WAM C25991).

Other material. Western Australia. Montgomery Island. Stn 22/K09-adhoc, 15º56.659'S, 124º16.398'E, no depth, 22 October 2009: 1 ov. F 2.2 mm (WAM C44013).—Stn 24/K09-T2, 16º00.865'S, 124º10.386'E, no depth, in sponge, 23 October 2009: 2 M 1.2–1.9 mm (WAM C44014).—Stn 27/K09-Q3, 15º00'S, 124º00'E, no depth, 24 October 2009: 1 F 2.2 mm (WAM C44038).—Long Reef. Stn 50/K10-Q2, 13º54.927'S, 125º46.459'E, 2 m, 22 October 2010: 1 F 2.2 mm (WAM C46583).—Stn 50/K10-Q2, 13º54.927'S, 125º46.459'E, no depth, 22 October 2010: 1 M 2.3 mm, 1 ov. F 2.4 mm (WAM C46587).—Adele Island. Stn 07/K09-Q3, 15º29.474'S, 123º09.798'E, 0 m, 5 October 2009: 2 F 1.4–1.8 mm (WAM C44006).—Stn 11/K09-T1, 15º34.895'S,

123º09.792'E, 0–3.5 m, 17 October 2009: 1 ov. F 2.3 mm (WAM C44003).—Ningaloo Reef. 22.7473ºS, 113.0752ºE, 11 m, 1 May 2009: 1 M 2.5 mm (UF22848).

Eggs: Ov. F carried approximately 30–40 eggs of 0.4–0.5 mm diameter.

Colour. Unknown.

Genetic data. COI and 16S, Table 1.

Distribution. The species was described from the Dampier Archipelago (NW Australia) (Macpherson, 2008). The new records extend its distribution range along the Western Australia, between 0 and 11 m.

Remarks. *Phylladiorhynchus nudus* belongs to group of species having the epigastric ridge unarmed, the carapace and the pleon ridges elevated, uplifted, and dactylar spines on the flexor margin of the P2–4 dactyli. The group includes *P. marina, P. jeffkinchi, P.nuds* and *phanus*. However, *P. nudus* can be easily distinguished from the rest of the species of this group by the presence of a spine on the upper margin of the pterygostomiam flap, whereas this margin is unarmed in the other species.

The genetic divergences between *P. nudus* and other species were always higher than 14% for COI and 13% for 16S

***Phylladiorhynchus nui* Schnabel & Ahyong, 2019**

(Fig. 33G)

Phylladiorhynchus pusillus.—Haig, 1973: 282 (S of Cape Everard (Victoria), S and SW of Mt Cann (Victoria), and off St. Helens Point, Tasmania, 110–183 m).

Phylladiorhynchus cf. *pusillus.*—Ahyong, 2007: 42, fig. 20B, 22.

Phylladiorhynchus sp. 1.—Rowden *et al.*, 2010: tab. 3.

Phylladiorhynchus nui Schnabel & Ahyong, 2019: 320, figs. 3, 8, 9, 15B.

Material examined. NIWA 54279, Stn. TAN0905/119, Iceberg Seamount, 44.158–44.162°S, 174.555–174.552°W, 487–616 m, 28 Jun 2009: 11 M 5.0–9.0 mm, 18 F 4.1–8.2 mm, donated to MNHN (MNHN-IU-2019-2595).

Genetic data. COI and 16S, Table 1.

Distribution. SE Australia, Tasmania, New Zealand, between 46 and 1246 m (from Schnabel & Ahyong 2019).

Remarks. The species closely resembles *P. australis* Schnabel & Ahyong, 2019, from New Zealand and Southern Australia, and *P. integrus* (Benedict, 1902) from Japan to Chesterfield Islands (see the differences under the Remarks of *P. integrus*).

Phylladiorhynchus orpheus **n. sp.**

(Figs. 33H, 36, 55D)

Type material. *Holotype.* French Polynesia, Society Islands. Moorea Island. 17º4758ºS, 149.8322ºW, 20 m, 25 July 2006: ov. F 2.0 mm (UF9732).

Paratypes. French Polynesia. Marquesas Islands. PAKAIHI I TE MOANA Stn MQ2-GR-B, 8°56.231'S, 140°07.240'W, 20–23 m, January 2012: 1 M broken (MHNH-IU-2014-13730).

French Polynesia. Society Islands. Moorea Island. 17.5145ºS, 149.7616ºW, 20 m, 23 October 2008: 1 M 2.1 mm (UF36172).—17.4764ºS, 149.8316ºW, 13 m, 31 January 2012: 1 M 2.0 mm (UF33772), 1 M 2.7 mm (UF33773).—17.4759ºS, 149.8419ºW, 13 m, 3 February 2012: 1 F 1.9 mm (UF33866), 1 M 1.6 mm, 1 F 2.4 mm (UF33867), 1 ov. F 2.2 mm (UF33961), 4 M 1.1–1.9 mm, 6 ov. F 1.8–2.0 mm (UF33962).—17.4764ºS, 149.8316ºW, 13 m, 6 February 2012: 6 M 1.4–2.0 mm, 5 ov. F 1.6–2.0 mm, 1 F 2.2 mm (UF34088).—17.4785ºS, 149.8477ºW, 13 m, 7 February 2012: 1 M 2.0 mm, 4 ov. F1.6–2.3 mm, 1 F 1.7 mm (UF34158).—17.4785ºS, 149.8477ºW, 13 m, 8 February 2012: 1 ov. F 2.6 mm (UF34209).—BENTHAUS Stn DW1968, 23°23'S, 150°44'W, 100–120 m, 20 November 2002: 1 M 2.3 mm (MNHN-IU-2019-2633).

Northern Mariana Islands. Saipan Island. Stn SAI-435, 15.09782849ºN, 145.7434357ºE, 17m, 11 April 2014: 1 ov.F 2.0 mm (UF).—Stn SAI-640, 15.15620417ºN, 145.6899585ºE, 11 m, 17 April 2014: 4 M 1.3–2.0 mm, 1 F 2.3 mm (UF).—Stn SAI-788, 15.15620417ºN, 145.6899585ºE, 11 m, 17 April 2014: 1 M 1.4 mM 1 F 2.0 mm (UF).—Stn SAI-947, 15.27406ºN, 145.79106ºE, 9 m, 18 April 2014: 2 M 1.6–2.0 mm, 1 ov. F 1.8 mm (UF).—Pagan Island. Stn PAG-404, 18.10734ºN, 145.78587ºE, 11 m, 20 April 2014: 2 M 1.3–2.3 mm (UF).—Stn PAG-409, 18.10734ºN, 145.78587ºE, 11 m, 20 April 2014: 1 F 1.9 mm (UF).—Stn PAG-478, 18.10734ºN, 145.78587ºE, 11 m, 20 April 2014: 1 M 1.5 mm, 1 ov. F 2.0 mm (UF).—Stn PAG-695, 18.0706862ºN, 145.7137933ºE, 11 m, 20 April 2014: 1 M 2.0 mm, 1 ov. F 1.9 mm (UF).—Stn PAG-696, 18.0706862ºN, 145.7137933ºE, 11 m, 20 April 2014: 2 ov. F 2.1–2.4 mm (UF).—Stn PAG-1149, 18.0706862ºN, 145.7137933ºE, 11 m, 20 April 2014: 1 M 1.9 mm (UF).—Stn PAG-839, 18.11947952ºN, 145.7555622ºE, 12 m, 23 April 2014: 1 M 1.5 mm, 2 ov. F 1.6–1.8 mm (UF).—Stn PAG-898, 18.11947952ºN, 145.7555622ºE,
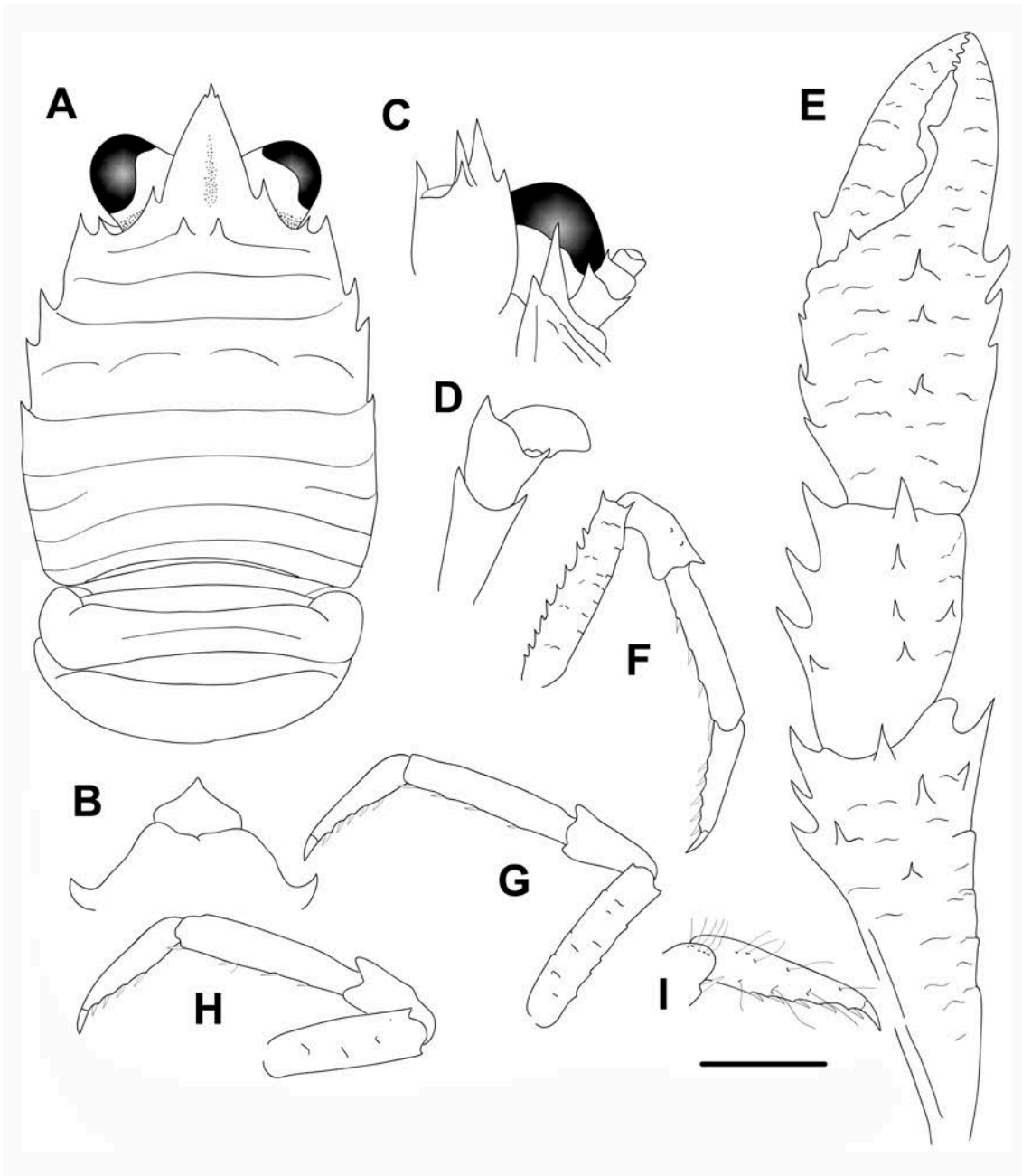
FIGURE 36. *Phylladiorhynchus orpheus* **n. sp**., holotype ovigerous female 2.0 mm (UF9732): A, carapace and pleon, dorsal view. B, thoracic sternites 3 and 4. C, left cephalic region, showing antennular and antennal peduncles, ventral view. D, right Mxp3, lateral view. E, right P1, dorsal view. F, right P2, lateral view. G, left P3, lateral view. H, left P4, lateral view. I, dactylus of right P2, lateral view. Scale bar: A, E-H = 1.0 mm; B–D, I = 0.6 mm.

12 m, 23 April 2014: 3 M 1.5–2.4 mm 2 ov. F 2.0–2.3 mm (UF).—Maug Islands. Stn MAU-475, 20.01416942ºN, 145.2342278ºE, 15 m, 03 May 2014: 1 M 1.6 mm (UF).

Mariana Islands. Guam Island. Stn GUA-645, 13.57847ºN, 144.82831ºE, 11 m, 25 March 2014: 1 M 1.3 mm, 1ov. F 1.8 mm (UF).—Stn GUA-688, 13.57847ºN, 144.82831ºE, 11 m, 25 March 2014: 1 ov. F 2.4 mm (UF).

American Samoa. Rose Atoll. Stn ROS-777, 14.52938333ºS, 168.1534833ºW, 10 m, 16 March 2015: 1 F 1.2 mm (UF).—Stn ROS-689, 14.55965ºS, 168.1601167ºW, 45 m, 18 March 2015: 1 M 1.2 mm (UF).—Tutuila Island. Stn TUT 138, 14.36046ºS,170.75024ºW, 17 m, 26 February 2015: 1 F 2.1 mm (UF).

Kiribati. Line islands, Millenium island. 9.91ºS, 150.21ºW, 12 m, 5 November 2013: 1 ov. F 2.0 mm, in dead Pocillopora (UF39269).—Jarvis Island. Stn JAR-653, 0.369001552ºS, 160.008115ºW, 16 m, 10 April 2015: 1 M 1.8 mm (UF).

Papua New Guinea. PAPUA NIUGINI Stn PB07, 05°10.8'S,145°49.8'E, 22 m, 30 December 2012: 1 M 2.0 mm (MNHN-IU-2013-397).—KAVIENG Stn KB28, 02º43.7'S,150º38.4'E, 15–26 m, 11 June 2014: 1 M 1.7 mm (MNHN-IU-2014-13657).

New Caledonia. LIFOU Stn 1429, 20°47.5' S, 167°07.1' E, 8–18 m, 24 November 2000: 2 ov. F 2.1–2.4 mm (MNHN-IU-2019-2601).

Etymology. From the name *Orpheus*, an Argonaut, son of Calliope and Oeagrus. The name is considered a substantive in apposition.

Description. *Carapace*: [1.1]1.1–1.2 longer than broad; transverse ridges with a few short setae. Gastric region flattened with 4 transverse ridges (usually barely distinct): epigastric ridge with 2 median spines; anterior protogastric ridge not medially interrupted, nearly extending laterally to carapace margin; anterior mesogastric ridge not medially interrupted, laterally continuing to first branchial spine, followed by some short lateral scales; anterior metagastric ridge scale-like, often followed by a short scale. Mid-transverse ridge not interrupted, medially depressed, preceded by cervical groove slightly distinct, followed by 2 not interrupted or minutely interrupted ridges, interspersed with 1 short lateral ridge and sometimes few, short scattered scales. Lateral margins straight or slightly convex, with 4 distinct spines: first anterolateral spine well-developed, reaching anteriorly to level of lateral orbital spine, hepatic margin unarmed; anterolateral spine followed by 3 branchial spines (2 anterior and 1 posterior). Rostrum leaf-like, horizontal, dorsally concave, [1.5]1.4–1.6 times as long as broad, length 03–[0.4] and breadth 0.2–[0.3] that of carapace; lateral margins serrated and convex, with well-developed

supraocular spines, and small subapical spines. Pterygostomian flap ending in acute tooth, upper margin smooth.

Sternum: As wide as long. Sternite 3 moderately broad, [1.8]–2.0 times as wide as long, anterior margin convex, with blunted median projection, lateral margins rounded. Sternite 4 widely contiguous to sternite 3; surface depressed in midline, smooth; greatest width [3.0] 3.0 times that of sternite 3, 2.6–[2.7] times as wide as long.

Pleon: Elevated ridges with a few scattered short setae. Tergite 2 with anterior and posterior transverse elevated ridges with short setae and a few scattered long setae; tergites 3–4 with anterior transverse ridge; tergites 5–6 smooth.

Eye: Eye stalk length about [1.0]–1.1 times broader than long, peduncle distally setose, slightly expanded proximally; maximum corneal diameter 0.8–[0.9] × rostrum width*,* as wide as eyestalk.

Antennule: Article 1 slightly longer than wide, with 5 distal spines: distomesial spine well-developed; proximal lateral spine small, always present.

Antenna: Article 1 with prominent mesial process distally not reaching lateralmost antennular spine. Article 2 with well-developed distomesial and distolateral spines. Article 3 with distomesial spine. Article 4 unarmed.

Mxp3: Ischium with distinct distal spines on flexor and extensor margins. Merus [0.7]0.7× length of ischium, with well-developed distal spine on extensor and flexor margins.

P1: 1.9–2.3 (males), 1.8–1.9 (females) times carapace length; subcylindrical, spiny and with dense long stiff setae; merus, carpus and palm with spines along mesial, dorsal and lateral surfaces, distal and mesial spines usually stronger than others. Merus 0.6–0.7 length of carapace, 1.3–1.9 times as long as carpus. Carpus 1.3–1.7 times as long as wide. Palm 1.1 × carpus length, 1.1–1.4 times as long as broad. Fingers [0.9]–1.1 × palm length; fixed finger unarmed; movable finger with basal spine.

P2–4: Stout, moderately setose and spinose. Meri successively shorter posteriorly: P3 merus 0.9 times length of P2 merus, P4 merus [0.8]–0.9 times length of P3 merus. P2 merus, [0.5]0.5–0.6 times carapace length, 4.6–[4.7] times as long as broad, [1.1]–1.2 times as long as P2 propodus; P3 merus [4.5]4.4–4.7 times as long as broad, [1.1]–1.3 times as long as P3 propodus; P4 merus [3.4]3.2–3.6 times as long as broad, [1.0]–1.1 times as long as P4 propodus; extensor margin of P2–3 with row of spines, proximally diminishing, with prominent distal spine; P4 extensor margin irregular, unarmed; flexor

margin irregular,with distal spine on P2–3, distal spine absent in P4. Carpi extensor margin unarmed on P2–4; distal spine prominent on P2–3, smaller on P4; extensor margin on lateral surface of P2–4 unarmed; flexor margin unarmed. Propodi stout, [4.7]4.5–5.0 times as long as broad; extensor margin unarmed; flexor margin with 3–4 slender movable spines in addition to distal pair. Dactyli [0.6]–0.8 × length of propodi, ending in incurved, strong, sharp spine; flexor margin with 4–5 movable spines.

Eggs: Ov. F carried approximately 5–20 eggs of 0.3–0.5 mm diameter.

Colour. Base colour of carapace and Pleon light orange-dark orange. Carapace and Pleon covered by granules and small dark orange spots and blue-purple patches and bands. Epigastric spines and spines on carapace margin blue-purple. Rostrum with a two blue-purple at basis and tip. Ocular peduncles oranges, covered by small granules and a basal blue-purple patch. P1 whitish, spines whitish, covered by small whitish granules, and brownish stripes distally on merus, carpus, basally on palm and fingers, distal tip finger whitish. P2–4 light whitish-translucent, covered by whitish spots, spines along flexor margins whitish; meri, propodi and dactyli with brownish transverse stripes.

Genetic data. COI and 16S, Table 1.

Distribution. Papua New Guinea, Northern Mariana Islands, Guam Island, American Samoa (Rose Atoll), Kiribati, New Caledonia and French Polynesia from 9 to 120 m.

Remarks. *Phylladiorhynchus orpheus* belongs to the group of species with 2 median epigastric spies, without hepatic spine and 2 spines on the anterior branchial margin. *Phylladiorhynchus orpheus* is closely related to *P. lynceus*, from Chagos, Western Australia, Kiribati and Samoa, *P. priasus*, from Mariana and Marshall Islands, and *P. integrirostris* from Hawaii. However, the new species can be easily distinguished from these species by the following differences:

- The rostrum margins are usually smooth in *P. orpheus,* whereas these margins are always serrated in the other species.
- The carapace ridges are flattened and often indistinct in *P. orpheus,* whereas these ridges are elevated and distinct in the other species.
- The metagastric ridge is scale-like in *P. orpheus,* whereas this ridge is medially interrupted in the other species.
- The extensor margins of P2–4 propodi are unarmed in *P. orpheus,* whereas these margins are armed with 1–3 proximal spines in the other species.

The specimens from Kiribati, Phoenix Islands, and from Papua New Guinea have a the thoracic sternite 3 with a different shape. Furthermore, they have a different colour pattern. A revision of additional material from both localities, including genetic data, will be necessary to clarify if these small differences are intraspecific variations.

The genetic divergences between *P. orpheus* and the other closely related species were very high: 19–22% (COI) and 13–16% (16S).
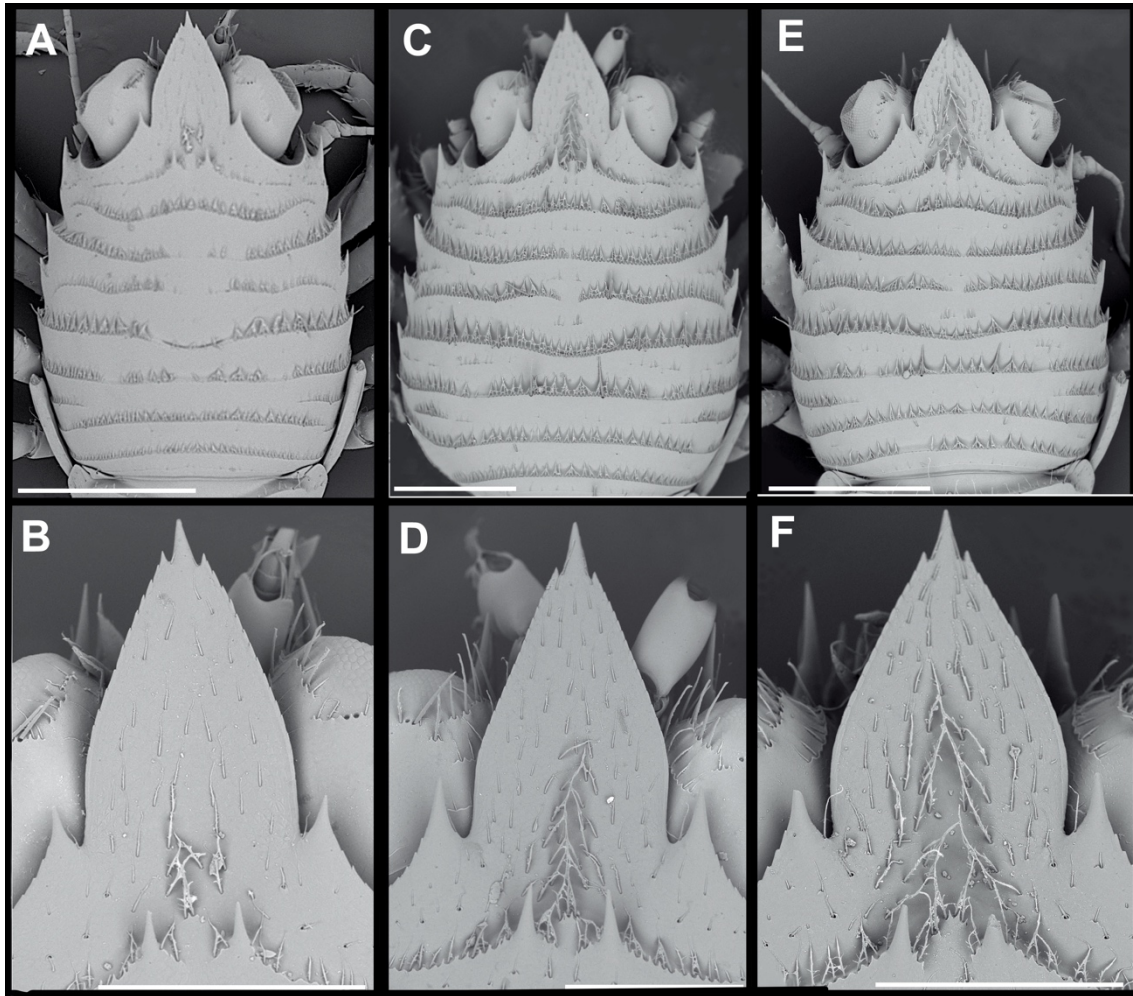
FIGURE 37. A, C, E, Carapace, dorsal view; B, D, F, rostrum, dorsal view. A-B, *Phylladiorhynchus integrirostris* (Dana, 1852), male 2.0 mm (KUR-301). C-D, *Phylladiorhynchus priasus* **n. sp.**, paratype male 2.0 mm (WAK-252). E-F, *Phylladiorhynchus lynceus* **n. sp.**, paratype male 1.8 mm (OFU-280). Scale bars: A, C, E = 1 mm; B, D, F = 0.5 mm.

Phylladiorhynchus paulae n. sp.

(Figs. 33P, 38, 55E)

Type material. *Holotype*. Mayotte and Comores Islands. BIOMAGLO Stn DW4800, 11°27'S, 47°19'E, 240–255 m, 24 January 2017: M 3.7 mm (MNHN-IU-2016-7002).
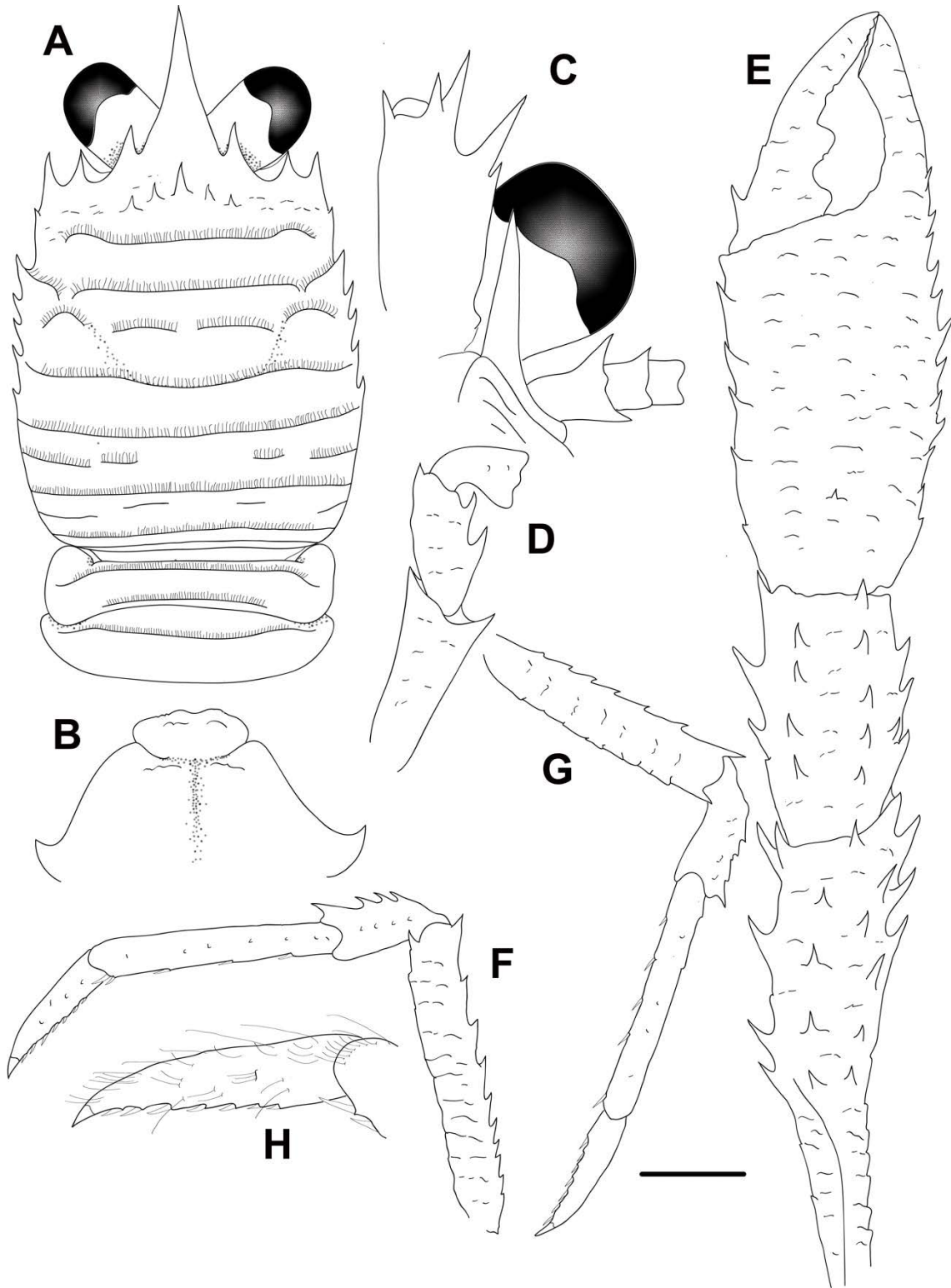
FIGURE 38. *Phylladiorhynchus paulae* **n. sp**., holotype male 3.7 mm (MNHN-IU-2016-7002): A, carapace and pleon, dorsal view. B, thoracic sternites 3 and 4. C, left cephalic region, showing antennular and antennal peduncles, ventral view. D, right Mxp3, lateral view. E, right P1, dorsal view. F, left P2, lateral view. G, right P3, lateral view. H, dactylus of left P2, lateral view. Scale bar: A, E-G = 1.0 mm; B–D, H = 0.5 mm.

Paratypes. Reunion Island. MD32 Stn DC2, 21º12.4'S, 55º49.4'E, 160–190 m, 12 August 1982: 1 M 2.7 mm (MNHN-IU-2019-2691).—Stn CP177, no data: 1 M 2.3 mm (MNHN-IU-2019-2699).

Mayotte and Comores Islands. BIOMAGLO Stn DW4800, 11°27'S, 47°19'E, 240–255 m, 24 January 2017: 1 F 3.3 mm (MNHN-IU-2016-7003).—Stn DW4838, 11°59'S, 43°31'E, 185–267 m, 29 January 2017: 1 ov. F 3.4 mm (MNHN-IU-2017-428).

Etymology. Named after our colleague Paula Martin Lefèvre, collection manager in the Muséum national d'Histoire naturelle, Paris.

Description. *Carapace:* as long as or slightly longer than broad; transverse ridges with some few short setae. Gastric region flattened with 4 transverse ridges: epigastric ridge indistinct, with 5 spines (1 median and 2 pairs of spines laterally); anterior protogastric ridge not medially interrupted or minutely medially interrupted, nearly extending laterally to carapace margin; anterior mesogastric ridge not medially interrupted, laterally interrupted by anterior branch of cervical groove, continuing to first branchial spine; anterior metagastric ridge scale-like. Mid-transverse ridge not interrupted, medially depressed, preceded by shallow to distinct cervical groove, followed by 2 not interrupted or minutely interrupted ridges, interspersed with 1–2 short lateral ridges and sometimes few, short scattered scales. Lateral margins slightly convex, with 7 spines: first anterolateral spine well-developed, reaching anteriorly to level of lateral orbital spine, second spine (hepatic) small, slightly dorsomesially from lateral margin, and followed by 5 branchial spines (3 anterior and 2 posterior). Rostrum triangular, horizontal, dorsally flattish or slightly concave, [1.2]–1.8 times as long as broad, length 0.3–[0.4] and breadth [0.3]0.2 that of carapace; lateral margins smooth and straight, with well-developed supraocular spines, subapical spines absent. Pterygostomian flap ending in blunt tooth, upper margin smooth.

Sternum: 1.2 as wide as long. Sternite 3 moderately broad, [2.3]2.0–3.0 times as wide as long, anterior margin straight or with a median feeble excavation, moderately produced anterolaterally. Sternite 4 widely contiguous to sternite 3; surface not depressed in midline, smooth; greatest width 2.0–[3.0] times that of sternite 3, [2.5]2.0–3.0 times as wide as long.

Pleon: Transverse elevated ridges with short setae. Tergite 2 with anterior and posterior transverse elevated ridges; tergites 3 and 4 with anterior transverse ridge; tergites 5–6 smooth.

Eye: Eye stalk length about [1.2]1.0–1.2 times broader than long, peduncle distally setose, not distinctly expanded proximally; maximum corneal diameter [1.0]1.0 × rostrum width*,* as wide as eyestalk.

Antennule: Article 1 1.5 times longer than wide, with 5 spines: distomesial spine small; proximal lateral spine small, always present.

Antenna: Article 1 with prominent mesial process, distally falling well short of lateralmost antennular spine. Article 2 with well-developed distal spines, distomesial larger than distolateral. Article 3 with often with a small to distinct distomesial spine. Article 4 unarmed.

Mxp3: Ischium with distinct distal spines on flexor and extensor margins. Merus [0.6]0.6 × length of ischium, with well-developed distal spine on extensor margin and 2 strong spines on flexor margin.

P1: 2.8–[3.5] (males), 2.8–3.0 (females) times carapace length; subcylindrical, spiny and with scattered long stiff setae; merus, carpus and palm with spines along mesial, dorsal and lateral surfaces, distal and mesial spines usually stronger than others. Merus 1.0–[1.3] length of carapace, [1.8]–2.5 times as long as carpus. Carpus [2.0]2.2–2.4 times as long as wide. Palm [1.1]–1.4 × carpus length, [1.5]–2 times as long as broad. Fingers [0.9]–1.0 times longer than palm; fixed finger unarmed or with basal spine; movable finger with well-developed basal spine.

P2–4: Slender, subcylindrical, moderately setose and spinose. Meri successively shorter posteriorly: P3 merus [0.7]–0.8 times length of P2 merus, P4 merus [0.8]–0.9 times length of P3 merus. P2 merus, [0.8]–0.9 times carapace length, 5.6–[6.0] times as long as broad, [1.4]1.4 times as long as P2 propodus; P3 merus [6.5]–7.1 times as long as broad, [1.2]–1.4 times as long as P3 propodus; P4 merus [5.0]–5.4 times as long as broad, [1.2]1.2 times as long as P4 propodus; extensor margin of P2 and P3 with row of spines, proximally diminishing, with prominent distal spine; P4 extensor margin irregular, withdistal spine; flexor margins of P2–4 irregular, each with distal spine; P4 lateral surface with median row 4 small spines, absent in others. Carpi with 3 or 4 spines on extensor margin on P2–3, unarmed on P4; distal spine prominent on P2–3, minute on P4; row of small spines below extensor margin on lateral surface of P2–3, unarmed on P4; flexor margin unarmed. Propodi slender, [7.2–7.3]7.0–7.5 times as long as broad; extensor margin irregular, usually unarmed; flexor margin with 3–4 movable spines in addition to distal pair. Dactyli [0.6]0.5–0.6 × length of propodi, ending in incurved, strong, sharp spine; flexor margin with [7–8]6–8 movable spines.

Eggs: Ov. F (MNHN-IU-2017-428) carried 18 eggs of 0.3–0.4 mm diameter.

Colour. Base colour of carapace light orange, gastric region covered by dark orange granules and golden-yellow spots. Rostrum and supraocular spines light orange. Pleonal tergites 1–4 light orange, with scales and granules orange and golden-yellow; tergites 5–6 and telson whitish. P1 orange, row of spines along lateral and mesial margins whitish and light orange, whitish strips on distal meri and carpi; fingers with a whitish strip, distal tips and proximal part orange. P2–4 light orange, proximal part of meri whitish, distal portion of meri, carpi and propodi and proximal part of carpi, propodi and dactyli with orange bands, distal half of dactyli whitish.

Genetic data. COI and 16S, Table 1.

Distribution. Mayotte and Comores Islands, Reunion Island, between 160 and 255 m.

Remarks. *Phylladiorhynchus paulae* belongs to the group of species that present 5 epigastric spines, the rostrum margin straight, the subapical spines of the rostrum absent, 3 spines on the anterior branchial margin, and the Mxp3 merus with two prominent spines along the flexor margin. *Phylladiorhynchus paulae* closely resembles to *P. acastus*, from the Philippines, Papua New Guinea, Vanuatu, Chesterfield Islands and New Caledonia, and *P. argus*, from French Polynesia, New Caledonia and Chesterfield Islands, however, they can be distinguished by the following characters:

-   The dorsal carapace ridges have scattered long thick iridescent setae in *P. acastus*, whereas these setae are absent in *P. paulae* and they are short in *P. argus*.
-   The anterior mesogastric ridge is medially interrupted in *P. argus*, whereas it is not medially interrupted in *P. acastus* and *P. paulae*.
-   The pleonal tergite 3 has 2 ridges (anterior and posterior) in *P. acastus*, whereas there is only one anterior ridge in *P. argus* and *P. paulae*.
-   The shape of the sternite 3 is sharply broad in *P. argus*, being more than 4 times as wide as long, whereas the sternite 3 is moderately broad in *P. acastus* and *P. paulae* (2–3 times as wide as long).
-   The antennal article 3 has a small to well-developed distomesial spine in *P. paulae* and *P. acastus*, whereas this article is unarmed in *P. argus*.

The genetic distances between these species were always quite large: *P. paulae* diverges 10–12% (COI) and 3–5% (16S) from *P. argus* and *P. acastus*. The mean intraspecific divergences were 0.6% for COI and 0% for 16S.

***Phylladiorhynchus peneleos* n. sp.**

(Figs. 39, 55F)

Type material. *Holotype.* French Polynesia. Rapa. Stn 28, 27°38.4'S, 144°20.6'W, 30 m, 15 November 2002: ov. F 2.8 mm (MNHN-IU-2014-13734).

Paratypes. French Polynesia. Society Islands, Moorea. Off E Opunohu pass, at Shark Feeding buoy, outer reef slope from within rubble, 17.4817ºS, 149.8558ºW, 17–18 m, 16 October 2008: 1 F 3.0 mm (UF15626).—Between Temae and Afarealtu. Outer reef slope, 17.5145ºS, 149.761ºW, 20 m, 23 October 2008: 1 ov. F 2.2 mm (UF36172), 1, ov. F, 2.4 mm, (UF16035), 1 M 2.0 mm (UF16078).—17.4759ºS, 149.8419ºW, 11 m, 30 January 2012: 1 ov. F 2.1 mm (UF34661).

Mariana Islands. Guam Island. Glass Breakwater. Near mouth of Apra harbour, among rocks, 3–6 m, 17 October 2001: 1 M 3.3 mm (UF1224).

New Caledonia. Exp. Mont. Komac, 12 m, 7 October 1993: 1 F 2.0 mm (MNHN-IU-2016-468).

Etymology. From the name *Peneleos*, an Argonaut, son of Hippalmus and Asterope. The name is considered a substantive in apposition**.**

Description. *Carapace:* As long as or slightly longer than broad; transverse ridges with dense short setae. Gastric region with 4 transverse ridges: epigastric ridge distinct, with 2 median spines (rarely with some outer small spine or granules), short scales laterally; anterior protogastric ridge not medially interrupted, nearly extending laterally to carapace margin, sometimes followed by a posterior protogatric ridge; anterior mesogastric ridge not medially interrupted, laterally continuing to first branchial spine, followed by some short lateral scales; anterior metagastric ridge not medially interrupted, followed by some short scales. Mid-transverse ridge not interrupted, medially depressed, cervical groove indistinct, followed by 2–3 not interrupted or minutely interrupted ridges, interspersed with 1 short lateral ridge and some few short scales. Lateral margins nearly straight or slightly convex, with 5 distinct spines: first anterolateral spine well-developed, reaching anteriorly to level of lateral orbital spine, second spine (hepatic) small, slightly dorsomesially from lateral margin, and followed by 3 branchial spines (2 anterior and 1 posterior). Rostrum leaf-like, horizontal, dorsally flattish, 1.6–[1.7] times as long as broad, length 0.3–[0.4] and breadth [0.2]0.2 that of carapace; lateral margins serrated and convex, with well-developed supraocular spines, subapical spines absent. Pterygostomian flap ending in blunt tooth, upper margin smooth.
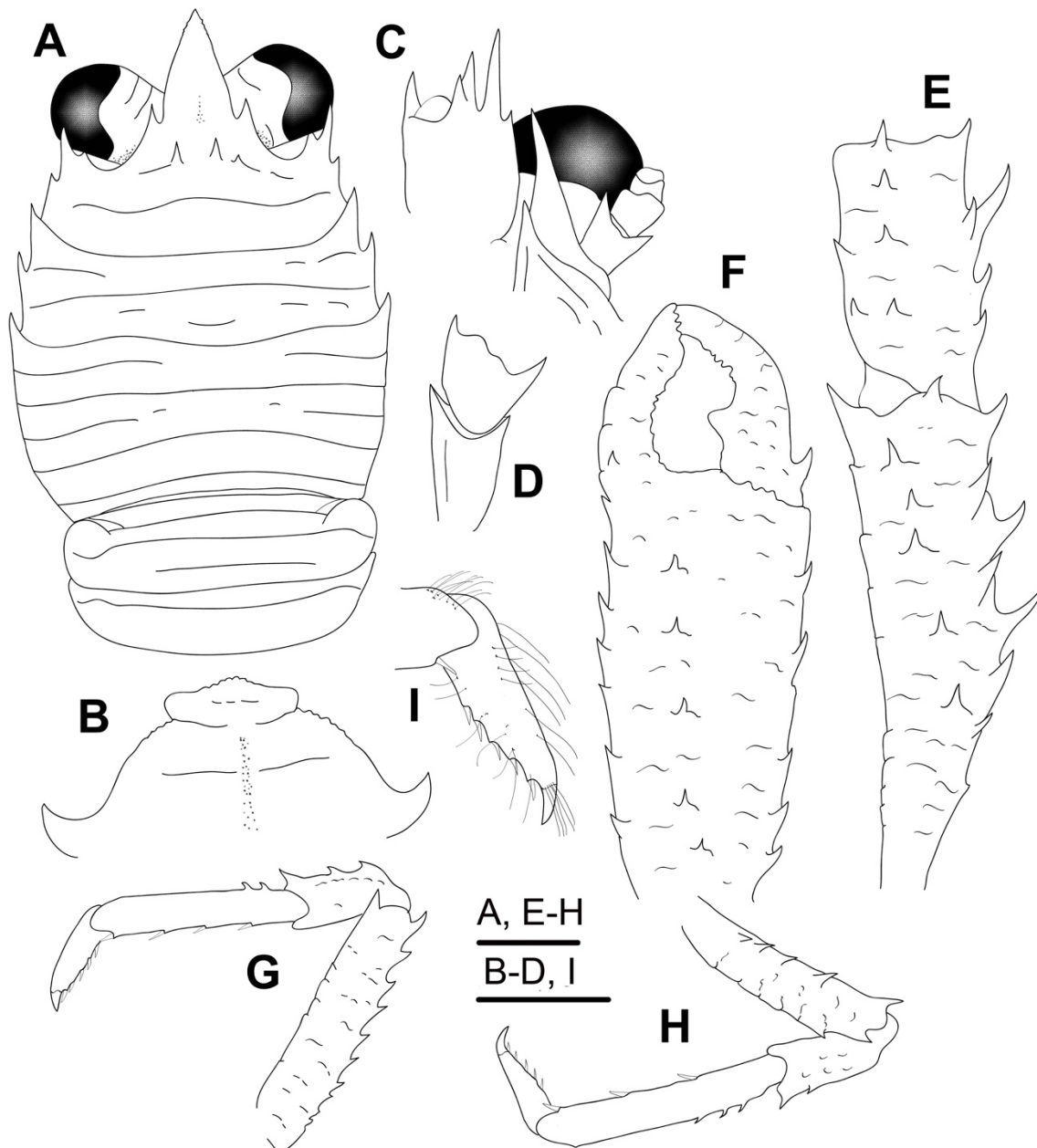
FIGURE 39. *Phylladiorhynchus peneleos* **n. sp**., A-D, G-I, holotype ovigerous female 2.8 mm (MNHN-IU-2014-13734); E-F, paratype male 3.3 mm (UF1224): A, carapace and pleon, dorsal view. B, thoracic sternites 3 and 4. C, left cephalic region, showing antennular and antennal peduncles, ventral view. D, right Mxp3, lateral view. E, left P1, merus and carpus, dorsal view. F, left P1, propodus and dactylus, dorsal view. G, left P2, lateral view. H, right P4, lateral view. I, dactylus of right P4, lateral view. Scale bars: 1.0 mm.

Sternum: As wide as long. Sternite 3 sharply broad, 3.4–[4.0] times as wide as long, anterior margin serrated and convex, with a median projection, produced anterolaterally. Sternite 4 widely contiguous to sternite 3; anterolaterally serrated, surface depressed in midline, smooth; greatest width 1.3–[1.4] times that of sternite 3, [3.1]–3.2 times as wide as long.

Pleon: Elevated ridges, with short setae and a few scattered long setae. Tergite 2 with anterior and posterior transverse; tergites 3–4 with anterior transverse ridge; tergites 5–6 smooth.

Eye: Eye stalk length about [0.7]–0.8 times broader than long, peduncle distally setose, not distinctly expanded proximally; cornea expanded distally, maximum corneal diameter [1.0]1.1 × rostrum width, 0.7–0.8 times maximum peduncle width.

Antennule: Article 1 slightly longer than wide, with 5 distal spines: distomesial spine well-developed; proximal lateral spine small, always present.

Antenna: Article 1 with prominent mesial process, nearly reaching end of proximal lateral antennular spine. Article 2 with well-developed distomesial and distolateral spines. Article 3 and 4 unarmed.

Mxp3: Ischium with distinct distal spines on flexor and extensor margins. Merus [0.7]0.6 × length of ischium, with well-developed distal spine on extensor and flexor margins.

P1: 2.8–3.8 (males), 2.3–2.4 (females) times carapace length; subcylindrical, spiny and with long stiff setae and dense thick iridescent and plumose setae; merus, carpus and palm with spines along mesial, dorsal and lateral surfaces, distal and mesial spines usually stronger than others. Merus 0.9–1.4 length of carapace. Carpus 1.7–1.9 times as long as wide. Palm 1.0–1.4 × carpus length, 2.0–2.5 times as long as broad. Fingers 0.6–1.0 × palm length; fixed finger with small basal spine; movable finger unarmed.

P2–4: Slender, densely setose and spinose. Meri successively shorter posteriorly: P3 merus 0.7–[0.8] times length of P2 merus, P4 merus [0.8]–0.9 times length of P3 merus. P2 merus, 0.7–[0.8] times carapace length, [4.0]–5.0 times as long as broad, [1.2] 1.3 times as long as P2 propodus; P3 merus 3.8–4 times as long as broad, [1.0]–1.1 times as long as P3 propodus; P4 merus 3.6–[3.6] times as long as broad, [1.0]–1.1 times as long as P4 propodus; extensor margin of P2 and P3 with row of spines, proximally diminishing, with prominent distal spine; P4 extensor margin irregular, unarmed; flexor margin irregular, with distal spine on P2–3, distal spine absent in P4. Carpi with 1–3 spines on extensor margin on P2–3, unarmed on P4; distal spine prominent on P2–3,

smaller on P4; granules below extensor margin on lateral surface of P2–4; flexor margin unarmed. Propodi moderately slender, [5.0–5.8]4.9–6.0 times as long as broad; extensor margin irregular, armed with 2–4 spines on proximal half; flexor margin with 3–4 slender movable spines in addition to distal pair. Dactyli [0.5–0.6]0.6 × length of propodi, ending in incurved, strong, sharp spine; flexor margin with 5–6 movable spines.

Eggs: Ov. F carried approximately 6–20 eggs of 0.3–0.4 mm diameter.

Colour. Base colour of carapace light orange, gastric and cardiac region covered by orange and whitish granules, epigastric spines dark orange, marginal spines whitish. Rostrum margin, supraocular spines and orbit margins dark orange, dark orange granules covering peduncles and rostrum. Pleonal tergites 1–4 light orange, with dark orange-brownish small spots, lateralmost darker; anterior ridges of tergites 2–4 dark orange-brownish. P1 light orange, spines dark orange, tip of fingers dark orange-reddish. P2–4 whitish, covered by small orange spots, spines along flexor margins orange; meri, propodi and dactyli with dark orange-brownish bands.

Genetic data. COI and 16S, Table 1.

Distribution. Guam Island, French Polynesia and New Caledonia, between 3 and 30 m.

Remarks. *Phylladiorhynchus peneleos* belongs to the group of species having 2 median epigastric spines, the hepatic margin armed with 1 spine, and 2 spines on the anterior branchial margin. The new species is morphologically close to *P. bahamut*, from the Red Sea. However, they can be distinguished by the following characters:

-       The gastric region has several secondary ridges in *P. peneleos,* whereas these ridges are absent in *P. bahamut*.
-       The carapace ridges have some iridescent thick setae in *P. bahamut,* whereas these setae are in *P. peneleos*.
-       The sternite 3 is broad, more than 3 times wider than long, in P. peneleos, whereas the sternite 3 is less than twice wider than long in *P. bahamut*.
-       The cornea is wider than the eyestalk in *P. peneleos,* whereas it is 0.7–0.8 times width of the eyestalk in *P. bahamut*.
-       The P1 have plumose setae in *P. peneleos,* whereas these setae are absent in *P. bahamut*.

The genetic divergences between *P. peneleos* and *P. bahamut* were very high 32% (COI) and 14% (16S). The mean intraspecific divergences were 0.15% for COI and 0% for 16S.

Phylladiorhynchus pepei n. sp.

(Figs. 33K, 40, 55G)

Type material. *Holotype.* Madagascar. ATIMO VATAE Stn TB02, 25°01.3'S, 47°00.5'E, 18 m, 1 May 2010: M 3.2 mm (MNHN-IU-2016-486).

Paratypes. Madagascar. ATIMO VATAE Stn TP02, 25°01.5'S, 47°01.4'E, 25–30 m, 29 April 2010: 1 ov. F 2.7 mm (MNHN-IU2010-2730).—Stn TB02-TB03, 25°01.3'S, 47°00.5'E, 18 m, 1 May 2010: 2 M 2.5–2.6 mm (MNHN-IU2016-463).—Stn TB02, 25°01.3'S, 47°00.5'E, 18 m, 1 May 2010: 1 ov. F 2.5 mm (MNHN-IU2016-461).—Stn TB03, 25°01.3'S, 47°00.5'E, 18 m, 1 May 2010: 2 ov. F 2.8–3.2 mm (MNHN-IU2016-465).—Stn TB05, 25°02.2'S, 47°00.4'E, 23 m, 1 May 2010: 2 ov. F 2.7–2.9 mm, 2 F 2.5–2.6 mm (MNHN-IU2010-2742).

Etymology. Named after Pepe Fernández, from the National Museum of Natural Sciences, Madrid, biologist especially interested in registering new species.

Description. *Carapace:* As long as or slightly longer than broad, transverse ridges with dense short setae and few scattered long and thick iridescent setae. Gastric region slightly convex with 4 transverse ridges: epigastric ridge distinct with 2 median spines, often followed by short scales; anterior protogastric ridge not medially interrupted, nearly extending laterally to carapace margin, often followed by protogastric ridge not interrupted (in large specimens) or scale-like; anterior mesogastric ridge not medially interrupted, laterally continuing to first branchial spine, followed by some short lateral scales; anterior metagastric ridge not medially interrupted, followed by short scales. Mid-transverse ridge not interrupted, medially depressed, preceeded by a shallow or indistinct cervical groove, followed by 2 not interrupted or minutely interrupted ridges, interspersed with 2 short lateral ridge and sometimes few, short scattered scales. Lateral margins slightly convex, with 4 distinct spines: first anterolateral spine well-developed, reaching anteriorly to level of lateral orbital spine, hepatic margin unarmed; anterolateral spine followed by 3 branchial spines (2 anterior and 1 posterior). Rostrum leaf-like, horizontal, dorsally flattened, 1.3–[1.5] times as long as broad, length 0.3–[0.4] and breadth [0.2]–0.3 that of carapace; lateral margins smooth and convex, with well-developed supraocular spines, subapical spines absent or obsolescent. Pterygostomian flap ending in acute tooth, upper margin smooth.

Sternum: As wide as long. Sternite 3 moderately broad, [1.8]1.5–2.0 times as wide as long, anterior margin convex, anterolaterally rounded. Sternite 4 widely contiguous to sternite 3, surface depressed in midline, smooth; greatest width [2.8]–3.0 times that of sternite 3, [2.8]–3.0 times as wide as long.
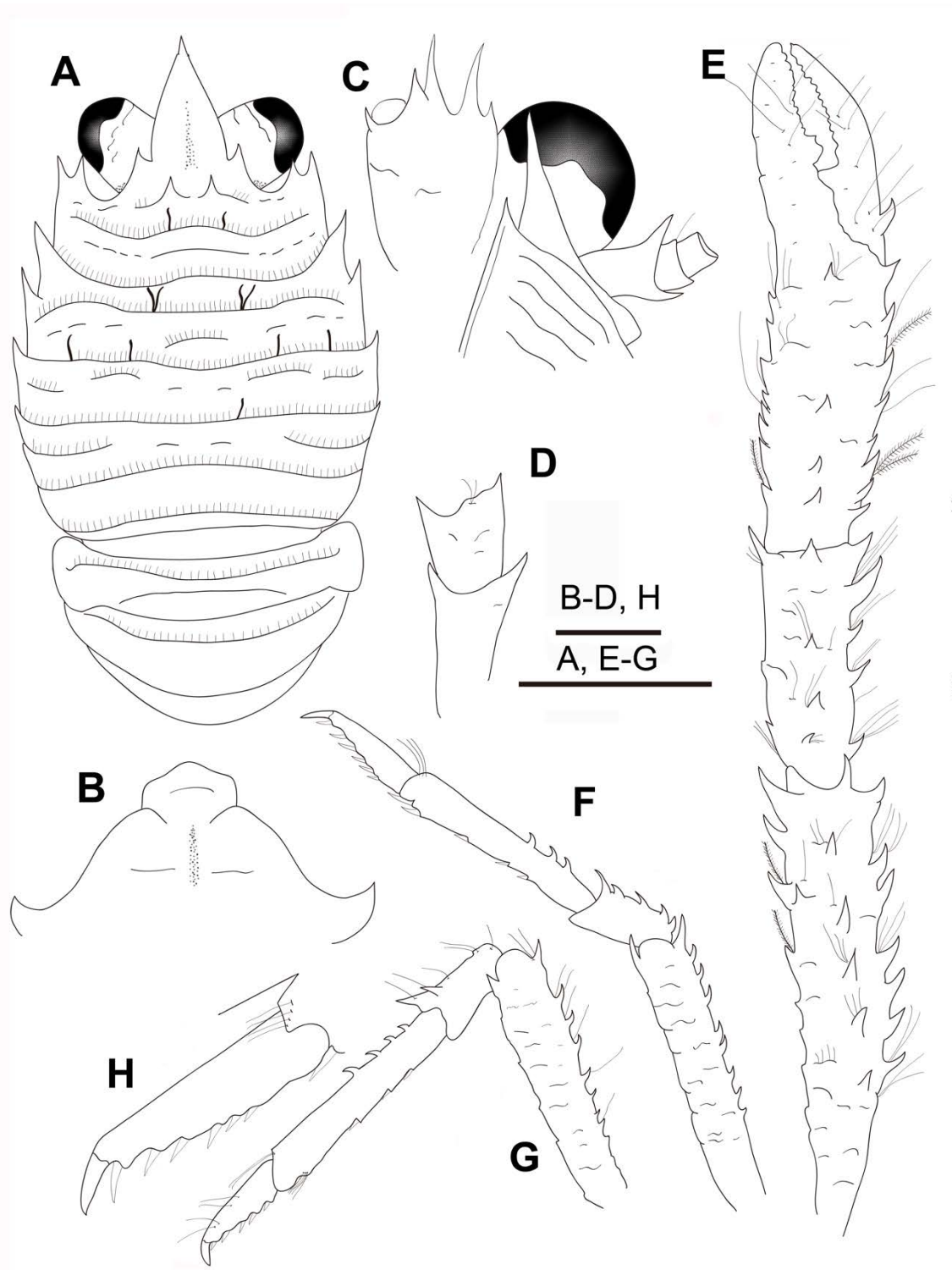
FIGURE 40. *Phylladiorhynchus pepei* **n. sp**., A-D, G-H, holotype male 3.2 mm (MNHN-IU-2016-486): A, carapace and pleon, dorsal view. B, thoracic sternites 3 and 4. C, left cephalic region, showing antennular and antennal peduncles, ventral view. D, right Mxp3, lateral view. E, left P1, dorsal view. F, left P2, lateral view. G, left P3, lateral view. H, dactylus of left P2, lateral view. Scale bars: 1.0 mm.

Pleon: Elevated ridges with short setae and a few scattered long setae. Tergite 2 with anterior and posterior transverse elevated ridges; tergites 3–4 with anterior transverse ridge; tergites 5–6 smooth.

Eye: Eye stalk length about [0.9]0.9 times broader than long, peduncle distally setose, not distinctly expanded proximally; maximum corneal diameter 0.7–[0.9] × rostrum width*,* as wide as eyestalk.

Antennule: Article 1 slightly longer than wide, with 5 distal spines: distomesial spine well-developed; proximal lateral spine small, always present.

Antenna: Article 1 with prominent mesial process nearly reaching end of lateralmost antennular spine. Article 2 with well-developed distomesial and distolateral spines. Article 3 and 4 unarmed.

Mxp3: Ischium with distinct distal spines on flexor and extensor margins. Merus [0.6]–0.6 × length of ischium, with well-developed distal spine on extensor and flexor margins.

P1: 2.9–[3.3] (males), 2.2–2.8 (females) times carapace length; subcylindrical, spiny and with long stiff setae and dense thick and plumose setae; merus, carpus and palm with spines along mesial, dorsal and lateral surfaces, distal and mesial spines usually stronger than others. Merus 1.1–[1.3] length of carapace, [1.9]1.6–2.2 times as long as carpus. Carpus [2.6]1.9–2.7 times as long as wide. Palm 0.9–[1.2] × carpus length, 1.5–[2.3] times as long as broad. Fingers [0.7]–1.0 × palm length; fixed finger unarmed; movable finger with a basal spine.

P2–4: Moderatley stout, densely setose and spinose. Meri successively shorter posteriorly: P3 merus [0.6]0.6 times length of P2 merus, P4 merus 0.8–0.9 times length of P3 merus. P2 merus, 1.8–[2.1] times carapace length, 3.8–[5.0] times as long as broad, [1.2]–1.4 times as long as P2 propodus; P3 merus [3.9]3.7–4.0 times as long as broad, 0.9–[1.1] times as long as P3 propodus; P4 merus 4 times as long as broad, as long as P4 propodus; extensor margin of P2 and P3 with row of spines, proximally diminishing, with prominent distal spine; P4 extensor margin irregular, unarmed; flexor margin irregular, with distal spine on P2–4, P4 lateral surface with median row of 2 spines. Carpi with 1–4 minute spines on extensor margin on P2–3, unarmed on P4; distal spine prominent on P2–3, smaller on P4; row of small spines below extensor margin on lateral surface of P2–3; flexor margin unarmed. Propodi moderately stout, [5.0–5.6]4.0–5.8 times as long as broad; extensor margin irregular, armed with 3 spines on proximal half; flexor margin with 3–4 slender movable spines in addition to distal pair. Dactyli [0.5–0.6]0.6–0.7 ×

length of propodi, ending in incurved, strong, sharp spine; flexor margin with 5–6 movable spines.

Eggs: Ov. F carried approximately 20–30 eggs of 0.3–0.6 mm diameter.

Colour. Base colour of carapace green-orange, gastric and cardiac region covered by orange patches, scattered yellow granules and few reddish small spots, epigastric spines dark orange-reddish, marginal spines whitish. Rostrum margin and orbit margins dark orange, dark orange spots covering peduncles and rostrum, supraocular spines and tip of rostrum darker orange-reddish. Pleonal tergites 1–4 green-orange, with dense dark orange-brownish granules; anterior ridges of tergites 2–4 dark orange-brownish, with some whitish stripes; tergites 5–6 and telson light green or light orange, granules scattered. P1 green, spines dark orange-reddish, tip of fingers dark orange-reddish. P2–4 light green-orange, spines along flexor margins dark orange-reddish; meri whitish basally, meri, propodi and dactyli with dark green-brownish bands.

Genetic data. COI and 16S, Table 1.

Distribution. Madagascar, between 18 and 30 m.

Remarks. *Phylladiorhynchus pepei* belongs to the group of species having 2 median epigastric spines, the hepatic margin unarmed and 2 spines on the anterior branchial margin. This species is easily characterized by the absence of subapical spines. The new species resembles closely to *P. barbeae*, from Papua New Guinea, Vanuatu, New Caledonia. However, both species can be distinguished in the basis of the following characters:

-       The anterior margin of the sternite 3 is straight or slightly convex, and produced anterolaterally in *P. barbeae*, whereas this margin is medially produced, and anterolaterally rounded in *P. pepei*.
-       The antennal article 3 is often armed with a distomesial spine in *P. barbeae*, whereas this article is unarmed in *P. pepei*.
-       The P2–4 propodi are slender in *P. barbeae* (5–7 times as long as wide), whereas they are stout (<5 times as long as wide) in *P. pepei*.
-       The colour pattern of the carapace and pleon are whitish, with reddish patches, in *P. barbeae*, whereas the colour pattern is green or light orange, with no reddish patches, in *P. pepei*.

The genetic divergences between *P. pepei* and *P. barbeae* were 7% (COI) and 3% (16S).

Phylladiorhynchus phanus n. sp.

 (Figs. 33L, 41, 55H)

Type material. *Holotype*. Papua New Guinea. PAPUA NIUGINI Stn PB12 05°11.8'S, 145°48.8'E, 7–15 m, 30 December 2012: M 1.6 mm (MNHN-IU-2014-13812).

    Paratypes. Papua New Guinea. PAPUA NIUGINI Stn PS02, 05°12.1'S, 145°49.3'E, 15–17 m, 6 November 2012: 2 F 1.1–1.4 mm (MNHN-IU-2019-2669).—Stn PD19, 05°05.4'S, 145°48.5'E, 3–10 m, 13 November 2012: 2 M 1.3–1.7 mm, 1 ov. F 1.8 mm (MNHN-IU-2019-2665).—Stn PD23, 05°06'S, 145°49.2'E, 3–7 m, 14 November 2012: 1 M 2.0 mm, 2 ov. F 1.8–2.2 mm (MNHN-IU-2014-13900).—Stn PD24, 05°05.3'S, 145°48.6'E, 3–6 m, 14 November 2012: 2 ov. F 2.0–2.2 mm, 2 F 1.4–2.0 mm (MNHN-IU-2016-450), 1 M 1.6 mm (MNHN-IU-2016-451).—Stn PD25, 05°05'S, 145°49.1'E, 3–5 m, 14 November 2012: 1 M postlarva 0.9 mm, 1 F 1.5 mm (MNHN-IU-2019-2654).—Stn PB19, 05°05.1'S, 145°48.6'E, 10 m, 16 November 2012: 3 M 1.0–1.5 mm (MNHN-IU-2019-2673).—Stn PR69, 05°01.6'S, 145°48.1'E, 2–15 m, 20 November 2012: 1 M 1.8 mm (MNHN-IU-2014-13811).—Stn PD56, 05°09.7'S, 145°48.3'E, 2–5 m, 29 November 2012: 1 ov. F 1.6 mm (MNHN-IU-2019-2658).—Stn PR129, 05°11.3'S, 145°49.5'E, 1–24 m, 29 November 2012: 1 ov. F 1.7 mm (MNHN-IU-2014-13899).—Stn PR142, 05°11.8'S, 145°49.2'E, 2–18 m, 30 November 2012: 1 M 1.2 mm, 1 F 1.3 mm (MNHN-IU-2013-7074).—Stn PD62, 05°09.8'S, 145°48.4'E, 1–3 m, 1 December 2012: 1 M 1.8–2.0 mm, 1 ov. F 1.8 mm (MNHN-IU-2014-13879) P79.—Stn PD79, 05°07'S, 145°48.5'E, 20 m, 10 December 2012: 1 M 1.5 mm, 1 ov. F 1.8 mm (MNHN-IU-2019-2671).—Stn PD31, 05°05.3'S, 145°48.1'E, 1–6 m, 12–13 December 2012: 1 M 1.8 mm (MNHN-IU-2014-13878).—Stn PD19, 05°05.4'S, 145°48.5'E, 3–10 m, 30 December 2012: 1 M 1.5 mm (MNHN-IU-2017-1343).—Stn PB15, 05°04.7'S, 145°48.9'E, 5 m, 30 December 2012: 2 ov. F 1.5–1.6 mm, 1 F 1.8 mm (MNHN-IU-2019-2659).—Stn PB08, 05°11'S, 145°48.4'E, 4–5 m, 30 December 2012: 1 ov. F 1.6 mm (MNHN-IU-2013-355), 1 M 1.4 mm, 6 ov. F 1.8–2.2 mm, 1 F 1.7 mm (MNHN-IU-2016-454), 1 M 2.1 mm, 3 ov. F 1.8-2.2 mm (MNHN-IU-2019-2687), 1 M 1.4 mm (MNHN-IU-2014-13898).—Stn PS31, 05°08.167'S, 145°49.417'E, 10–37 m, 30 December 2012: 1 M 1.3 mm (MNHN-IU-2013-861).—Stn PS15, 05°05.79'S, 145°48.194'E, 12 m, 30 December 2012: 1 M 1.7 mm, 1 ov. F 1.9 mm (MNHN-IU-2019-2672).—Stn PB37, 05°15.9'S, 145°47.1'E, 10 m, 30 December 2012: 1 ov. F 2.3 mm (MNHN-IU-2016-1483).—Stn PS08, 05°11.037'S, 145°48.431'E, 8 m, 30 December 2012: 1 M 1.4 mm, 1 ov. F 1.4 mm, 7 F 1.0–1.4 mm (MNHN-IU-2014-13864).—Stn PB19, 05°05.1'S, 145°48.6'E, 10 m, 30 December 2012: 2 M, 1.4–1.8 mm (MNHN-IU-2014-13880).—Stn PS23, 05°04.573'S, 145°49.209'E, 21 m, 30 December 2012: 1 M 1.7 mm (MNHN-IU-2019-2657).—Stn PB24, 04°59.1'S, 145°47.6'E, 1 m, 30 December 2012: 1 M 1.3 mm
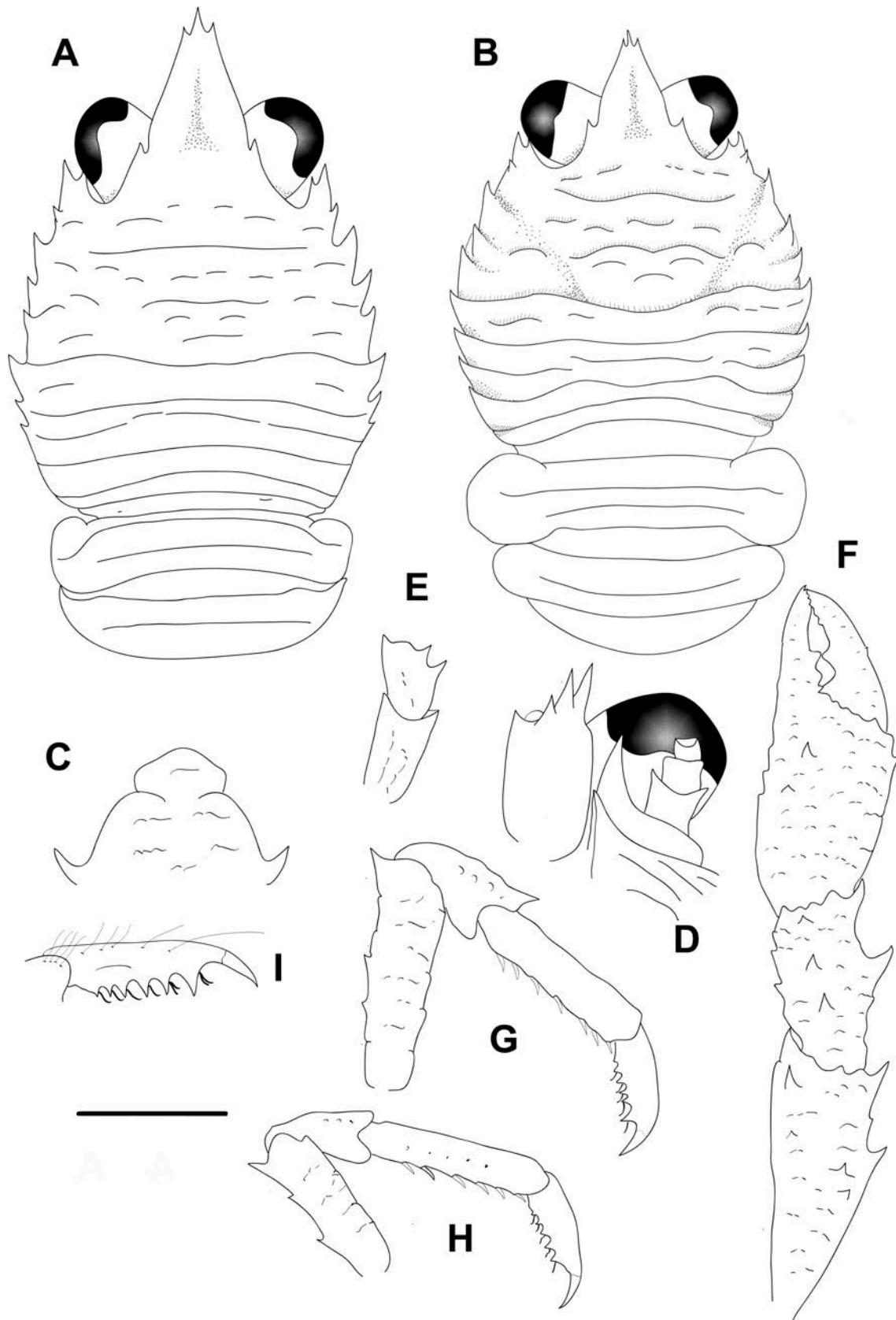
FIGURE 41. *Phylladiorhynchus phanus* **n. sp**., A, C-F, holotype male 1.6 mm (MNHN-IU-2014-13812); B, G-I, paratype ov female 2.0 mm (MNHN-IU-2016-450): A, B, carapace and pleon, dorsal view. C, thoracic sternites 3 and 4. D, left cephalic region, showing antennular and antennal peduncles, ventral view. E, right Mxp3, lateral view. F, left P1, dorsal view. G, right P2, lateral view. H, right P3, lateral view. I, right P2, lateral view. Scale bar: A, B, F-I = 1.0 mm; C–E = 0.6 mm.

(MNHN-IU-2019-2656).—Stn PB53, 05°08.1'S, 145°48.2'E, 3 m, 30 December 2012: 1 F 1.5 mm (MNHN-IU-2019-2655).—KAVIENG Stn KB54, 02º31.9'S, 150º27.5'E, 11 m, 20 June 2014: 1 ov. F 2.5 mm (MNHN- IU-2014-2893).

Etymology. From the name *Phanus*, an Argonaut, son of Dionysus and Ariadne. The name is considered a substantive in apposition.

Description. *Carapace:* Robust or massive, sexually dimorphic, (wider on females) 0.9–[1.0] (males), 0.7–0.9 (females) times as long as broad; transverse ridges elevated, uplifted dorsally, with short setae and scattered thick setae. Gastric region convex (uplifted) with some transverse ridges: epigastric ridge unarmed, scale-like, continuing laterally with few small scales, often indistinct; anterior protogastric ridge not medially interrupted, laterally interrupted with some few scales, often followed by some few short scales; anterior mesogastric ridge scale-like, laterally interrupted by anterior branch of cervical groove, continuing with some few scales, often followed by some few short scales; anterior metagastric ridge medially uninterrupted, laterally interrupted, followed by some few scales on posterior metagastric region. Mid-transverse ridge not interrupted, cervical groove distinct, followed by 2 not interrupted or minutely interrupted ridges, interspersed with 1 laterally interrupted or scale-like ridge and 1–2 short lateral ridges. Lateral margins clearly convex, with 7–8 spines: first anterolateral spine well-developed, exceeding lateral orbital spine, second spine (hepatic) minute, often obsolescent in males, slightly dorsomesially from lateral margin, and followed by 5–6 branchial spines behind distinct anterior cervical groove (3 anterior and 2–3 posterior). Rostrum leaf-like, horizontal, dorsally slightly or deeply concave, [1.5]1.6–1.9 times as long as broad, length 0.3–[0.5] and breadth 0.2–[0.3] that of carapace; lateral margins smooth and convex, with well-developed supraocular and subapical spines. Pterygostomian flap without anterior spine; surface unarmed.

Sternum: As wide as long or slightly wider than long, lateral margins of posterior half slightly divergent. Sternite 3 moderately broad, [1.9]–2.4 times as wide as long, anterior margin convex. Sternite 4 widely contiguous to sternite 3; surface flattened, smooth; greatest width [2.8]3.0–3.1 times that of sternite 3, 2.0–[2.3] times as wide as long.

Pleon: Elevated ridges uplifted dorsally, with few short setae. Tergites 2–4 with anterior and posterior transverse elevated ridges; tergites 5–6 smooth.

Eye: Eye stalk length about [1.0]1.0 times broader than long, peduncle distally setose, not distinctly expanded proximally, with few short transverse striae on lateral surfaces; maximum corneal diameter 0.9[1.0] × rostrum width, as wide as eyestalk.

Antennule: Article 1 longer than wide, with 3–4 distal spines: distomesial spine small or obsolescent; proximal lateral spine absent.

Antenna: Article 1 with prominent mesial process distally not reaching lateral antennular spine. Article 2 often with minute distal spines laterally and mesially. Articles 3 and 4 unarmed.

Mxp3: Ischium with distinct distal spines on flexor and extensor margin. Merus [0.6]0.6 × length of ischium, with 1 well-developed distal spine on extensor margin and 2 spines, subequal in size, on flexor margin.

P1: [2.4]2.0– 2.7 times carapace length (males), 1.3 (females), subcylindrical, with scattered spines and long stiff setae; merus and carpus with spines along mesial, dorsal and lateral surfaces, distal and mesial spines usually stronger than others. Merus [0.9]0.5–1.0 length of carapace, [1.6]1.5–2.1 times as long as carpus. Carpus 1.1–1.7 [1.9] times as long as wide. Palm [0.9]0.7–1 × carpus length, 1.1–1.2[1.4] times as long as broad with scattered small spines on dorsal and ventral surfaces, lateral and mesial margin irregular, with 1 small spine on distal mesial margin. Fingers unarmed, [0.9]0.9–1.3 × palm length.

P2–4 (P2–3 absent from holotype)*:* Moderately stout, setose and few spinose. Meri successively shorter posteriorly: P3 merus 0.9 times length of P2 merus, P4 merus 0.7–0.8 times length of P3 merus. P2 merus, 1.7–2.4 times carapace length, 3.8–4.0 times as long as broad, 1.2 times as long as P2 propodus; P3 merus 3.6–4.0 times as long as broad, 1.1–1.2 times as long as P3 propodus; P4 merus 2.7–2.8 times as long as broad, as long as P4 propodus; extensor margins of P2 and P3 with row of few small spines, proximally diminishing, with well-developed distal spine; P4 extensor margin irregular but unarmed, distal spine absent; flexor margins of all legs irregular, with distal spine on P2–3, distal spine absent in P4. Carpi with 1 spine on extensor margins on P2–3, unarmed on P4; distal spine prominent on P2–3, absent on P4; row of small spines below extensor margins on lateral surface of P2–3, unarmed on P4. Propodi stout, 4.0–5.0 times as long as broad; extensor margins irregular, usually unarmed; flexor margins with 5–6 slender movable spines in addition to distal pair. Dactyli 0.7–0.8 × length of propodi, ending in incurved, strong, sharp spine; flexor margins with 5–6 well-developed dactylar spines, each with 1 spinule.

Eggs: Ov. F carried approximately 8–30 eggs of 0.3–0.4 mm diameter.

Colour. Base colour of carapace orange-dark yellow, cervical groove and gastric and hepatic regions darker, with dark orange-reddish patches and small brownish parahepatic spots. Rostrum pale orange, with some small brownish spots distally, margin, tip and supraocular spines whitish. Pleonal tergites 2–6 dark orange, yellow medially,

lighter laterally, ridges of tergites 2–4 pale orange-yellow with brownish-reddish small spots medially and brownish-reddish bands laterally; uropods and telson whitish-translucid. P1 whitish-pale yellow, with dark orange-brownish bands distally on meri, carpi, and palm, spines whitish. P2–4 whitish-pale yellow; distal portion of meri, carpi and propodi and proximal part of meri dark orange, dactyli whitish-translucid.

Genetic data. COI and 16S, Table 1.

Distribution. Papua New Guinea, between 1 and 37 m.

Remarks. *Phylladiorhynchus phanus* belongs to the group of species having the epigastric ridge unarmed, the carapace and pleon ridges elevated, uplifted, and dactylar spines on the flexor margins of the P2-4 dactyli. The new species is closely related to *P. marina* from Vanuatu. Both species are highly similar, and very difficult to distinguish using morphological characters only, therefore they can be considered as cryptic species. Both species might be distinguished on the basis of their different coloration (color basis of the carapace orange in *P. phanus*, whereas the colour pattern is brownish in *P. marina*, see Figures 55B, 55H). Furthermore, there are some scattered long plumose setae on the carapace ridges of *P. marina*, whereas these setae are always absent in *P. phanus*. However, we cannot discard an overlap between these characters, since we ignore the variation of the colour pattern at population level. On the other hand, the setae can be missing in preserved specimens. Furthermore, *P. phanus* is also close to *P. phlias*, from Papua New Guinea (see the differences under the Remarks of this species).

The genetic divergences between *P. phanus* and *P. marina* were 13% (COI) and 4% (16S). The mean intraspecific genetic divergences of *P. phanus* were 0.7% (COI) and 0.1% (16S).

***Phylladiorhynchus phlias* n. sp.**

 (Figs. 42, 50A, 55I)

Type material. *Holotype*. Papua New Guinea. KAVIENG Stn KZ16, 02°34.7'S, 150°47.5'E, 1–2 m, 23 June 2014: ov. F 2.2 mm (MNHN-IU-2014-13535).

Paratypes. Papua New Guinea. PAPUA NIUGINI Stn PS09, 05°12.3'S, 145°48.8'E, 8–10 m, 9 November 2012: 1 M 1.2 mm, 1 ov. F 1.8 mm (MNHN-IU-2014-13886) P26.—Stn PD19, 05°05.4'S, 145°48.5'E, 10 m, 13 November 2012: 3 M 1.2–1.8 mm, 2 ov. F 1.5–1.7 mm, 2 F broken (MNHN-IU-2019-2674), 1 ov. F 1.3 mm (MNHN-IU-2013-703).—Stn PD24, 05°05.3'S, 145°48.6'E, 3–6 m, 14 November 2012: 2 ov. F 1.5–1.9 mm 2 F 1.9–2.0 mm (MNHN-IU-2019-2660), 1 M 1.4 mm (MNHN-IU-2016-
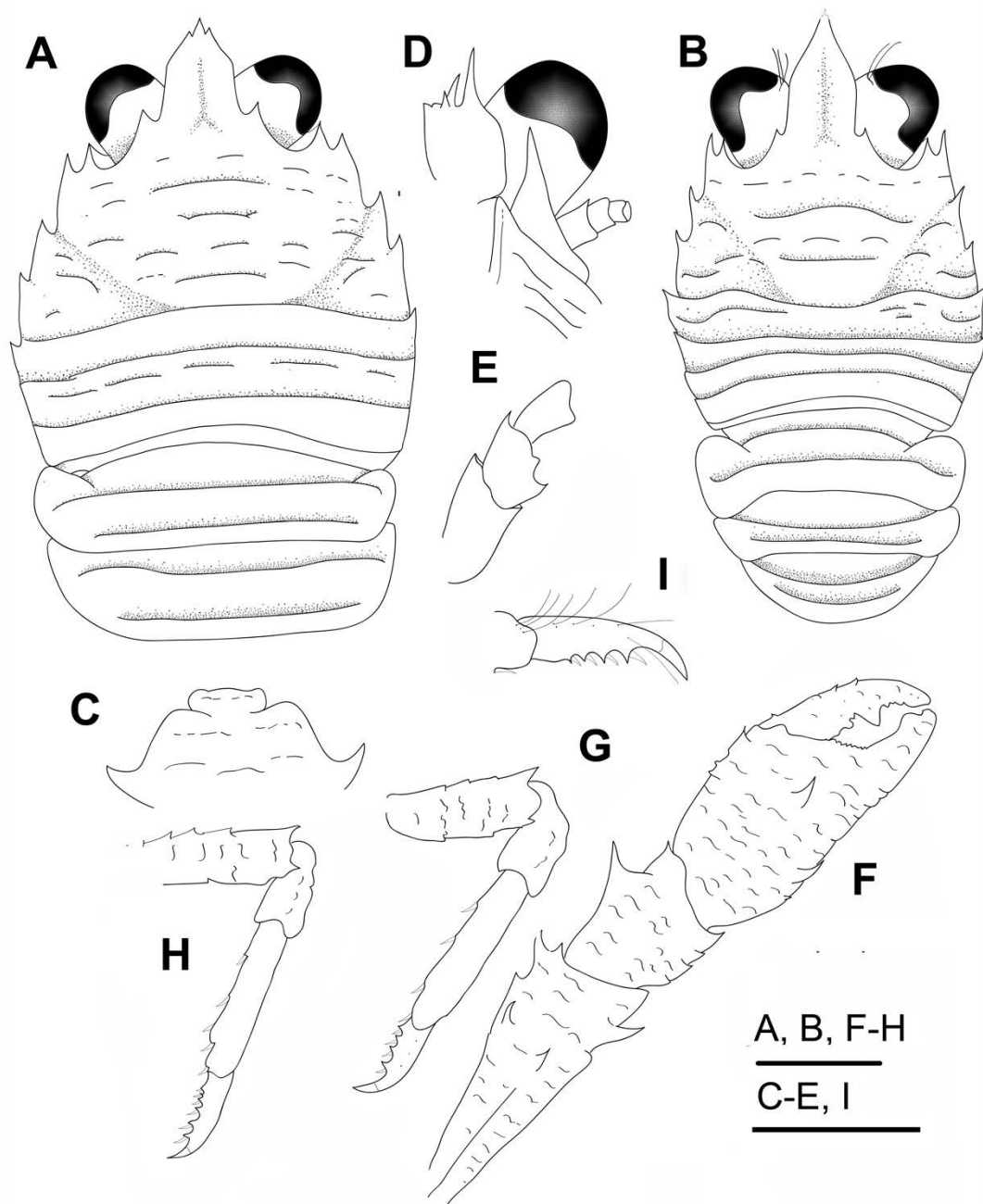
FIGURE 42. *Phylladiorhynchus phlias* **n. sp**., A, C-E, G-I, holotype ovigerous female 2.2 mm (MNHN-IU-2014-13535); B, F, paratype male 1.4 mm (MNHNIU-2014-13866): A, B, carapace and pleon, dorsal view. C, thoracic sternites 3 and 4. D, left cephalic region, showing antennular and antennal peduncles, ventral view. E, right Mxp3, lateral view. F, right P1, dorsal view. G, right P2, lateral view. H, right P3, lateral view. I, dactylus of right P2, lateral view. Scale bars: 1.0 mm.

452).—Stn PD65, 05°08.5'S, 145°48.5'E, 1–4 m, 1 December 2012: 1 M 1.3 mm (MNHN-IU-2014-139139).—Stn PB50, 05°04.7'S, 145°48.9'E, 3 m, 30 December 2012: 1 M 1.7 mm (MNHN-IU-2016-1492).—Stn PS12, 05°05.332'S, 145°48.569'E, 6 m, 30 December 2012: 1 M 1.4 mm, 2 ov. F 1.3–1.5 mm, 2 F 1.1–1.4 mm (MNHN-IU-2014-13866).—Stn PS13, 05°05.902'S, 145°49.261'E, 8 m, 30 December 2012: 7 M 1.1–1.4 mm, 3 ov. F 1.4–1.6 mm, 1 F 1.0 mm (MNHN-IU-2014-13881).—Stn PS18, 05°01.598'S, 145°48.059'E, 16 m, 30 December 2012: 1 ov. F 1.5 mm (MNHN-IU-2019-2666).—KAVIENG Stn KS07, 02°41.2'S, 150°41.2'E, 8 m, 4 June 2014: 1 F 1.4 mm (MNHN-IU-2016-5832).—Stn KD36, 02°35.1'S, 150°29'E, 8 m, 16 June 2014: 1 F 1.4 mm (MNHN-IU-2014-13695).

Etymology. From the name *Phlias*, an Argonaut, son of Dionysus and Ariadne. The name is considered a substantive in apposition.

Description. *Carapace:* Robust or massive, sexually dimorphic, (wider on females) 0.9–1.0 (males), [0.7]–0.8(females) times as long as broad; transverse ridges elevated, uplifted dorsally, with very few short setae. Gastric region convex (uplifted) with some transverse ridges: epigastric ridge indistinct, unarmed, with some few scales, anterior protogastric ridge not medially interrupted, laterally interrupted with some few scales to carapace margin, sometimes followed by a few some short scales; anterior mesogastric ridge scale-like, otherwise indistinct, laterally interrupted by anterior branch of cervical groove, laterally continuing with some few scales; often followed by short scales; anterior metagastric ridge scale-like, followed by some few scales on posterior metagastric region. Mid- transverse ridge not interrupted, preceded by shallow or indistinct cervical groove, followed by 2 not interrupted or minutely interrupted ridges, interspersed with 1 laterally interrupted or scale-like ridge and 1 short lateral ridge. Lateral margins clearly convex, with 4–5 spines: first anterolateral spine well-developed, reaching end of lateral orbital spine, hepatic spine absent, followed by 3–4 spines (2 anterior well-developed branchial spines subequal in size, second slightly dorsomesially from lateral margin, 1–2 posterior branchial spines very small). Rostrum bottle-shaped (proximally straight and distally convex), horizontal, dorsally flattish or slightly concave, [1.1]1.2–1.3 (females), 1.8 (males) times as long as broad, length [0.3]–0.5 and breadth [0.2]0.2 that of carapace; lateral margins finely serrated, with well-developed supraocular spines, subapical spines small. Pterygostomian flap ending in blunt tooth; upper margin smooth.

Sternum: As wide as long or slightly wider than long, lateral margins of posterior half slightly divergent. Sternite 3 moderately broad, [2.6]1.7–2.7 times as wide as long, anterior margin straight or slightly convex. Sternite 4 widely contiguous to and wider

than sternite 3; surface flattened, smooth; greatest width 3.3–[3.4] times that of sternite 3, 2.4–[2.5] times as wide as long.

Pleon: Elevated ridges uplifted dorsally, with few short setae. Tergites 2–3 with anterior and posterior transverse elevated ridges; tergite 4 with anterior transverse ridge only; tergites 5–6 smooth.

Eye: Eye stalk length about [0.9] 0.9 times broader than long, peduncle distally setose, not distinctly expanded proximally; maximum corneal diameter [0.9]0.9 × rostrum width*,* as wide as eyestalk.

Antennule: Article 1 slightly longer than wide, with 3–4 distal spines: distomesial spine minute or absent; proximal lateral spine absent.

Antenna: Article 1 with prominent mesial process distally not reaching lateral antennular spine. Article 2 unarmed, sometimes with minute distomesial spine. Articles 3 and 4 unarmed.

Mxp3: Ischium with distinct distal spines on flexor and extensor margins. Merus [0.4]0.4 × length of ischium, with 0–1 median small spine and well-developed distal spine on extensor margin and 2 not larger spines, subequal in size, on flexor margin.

P1 (lost in holotype): 2.2–2.3 times carapace length (males), 1.4 (females); subcylindrical, with scattered spines and long stiff setae, with some thick short setae; merus, carpus and palm with spines along mesial, dorsal and lateral surfaces, distal and mesial spines usually stronger than others. Merus 0.5–0.8 length of carapace, 1.7–2 times as long as carpus. Carpus 1.3–1.7 times as long as wide. Palm 0.8–1.0 × carpus length, 1.2–1.3 times as long as broad irregular and unarmed in all the surfaces, otherwise a small spine on basal mesial margin. Fingers unarmed, 1.0–1.3 × palm length.

P2–4 (lost in most specimens)*:* Stout, moderately setose and few spinose. Meri successively shorter posteriorly: P3 merus 0.9 times length of P2 merus, P4 merus []0.7–0.9 times length of P3 merus. P2 merus, 0.4–0.5 times carapace length, 3.2 times as long as broad, 1.2–1.3 times as long as P2 propodus; P3 merus 3.2–3.5 times as long as broad, 1.0–1.2 times as long as P3 propodus; P4 merus 2.8–3.2 times as long as broad, as long as P4 propodus; extensor margins of P2–3 irregular, unarmed, with small distal spine; P4 extensor margin irregular, unarmed, distal spine absent; flexor margins of all legs irregular, with distal spine on P2–3, distal spine absent in P4. Carpi extensor margins irregular or granulated, unarmed on P2–4. Propodi stout, 3.5–4.5 times as long as broad; extensor margins irregular, usually unarmed; flexor margins with 2–4 slender movable spines in addition to distal pair. Dactyli 0.7–0.9 × length of propodi, ending in incurved,

strong, sharp spine; flexor margin with 4–6 well-developed dactylar spines, each with movable spinule.

Eggs: Ov. F carried approximately 5–15 eggs of 0.4–0.5 mm diameter.

Colour. Base colour of carapace whitish- pale yellow, cardiac region with by two symmetrical small brownish spots. Rostrum and supraocular spines whitish- pale yellow. Pleonal tergites 2–4 whitish-pale yellow laterally and whitish-translucid medially, anterior ridges of tergites 2–4 whitish-pale yellow with brownish small spots; tergites 5–6 and telson whitish-translucid. P1 whitish-pale yellow, spines whitish. P2–4 whitish-pale yellow, with translucid bands; distal portion of meri, carpi and propodi and proximal part of meri whitish pale yellow, dactyli translucid.

Genetic data. COI and 16S, Table 1.

Distribution. Papua New Guinea, between 1 and 10 m.

Remarks. *Phylladiorhynchus phlias* belongs to the group of species characterized by having the epigastric ridge unarmed, the carapace and pleon ridges elevated, uplifted, and dactylar spines on the flexor margins of the P2-4 dactyli. The closest species are *P. phanus*, from Papua New Guinea, and *P. marina*, from Vanuatu, however these species can be distinguished on the basis of the following morphological characters:

-        The rostrum is bottle-shaped in *P. phlias*, whereas it is leaf-like in the other species.
-        The hepatic spine is absent in *P. phlias*, whereas it is present in *P. phanus* and *P. marina*.
-        The anterior branchial margin has 2 branchial spines in *P. phlias*, whereas this margin has 3 spines in in the other species.

The genetic divergences between *P. phlias*, and these species were larger than 15% (COI) and 12% (16S).

Phylladiorhynchus poeas **n. sp.**

(Figs. 43, 50B, 56A)

Type material. *Holotype.* French Polynesia. BENTHAUS Stn DW1866, 28°59'S, 140°14.85'W, 50–100 m, 4 November 2002: M 2.8 mm (IU-2014-13736).

Paratypes. French Polynesia. BENTHAUS Stn DW1866, 28°59'S, 140°14.85'W, 50–120 m, 4 November 2002: 5 M 2.2–3.5 mm, 5; ov. F 2.1–3.4 mm 2 F 3.0–3.4 mm, 1
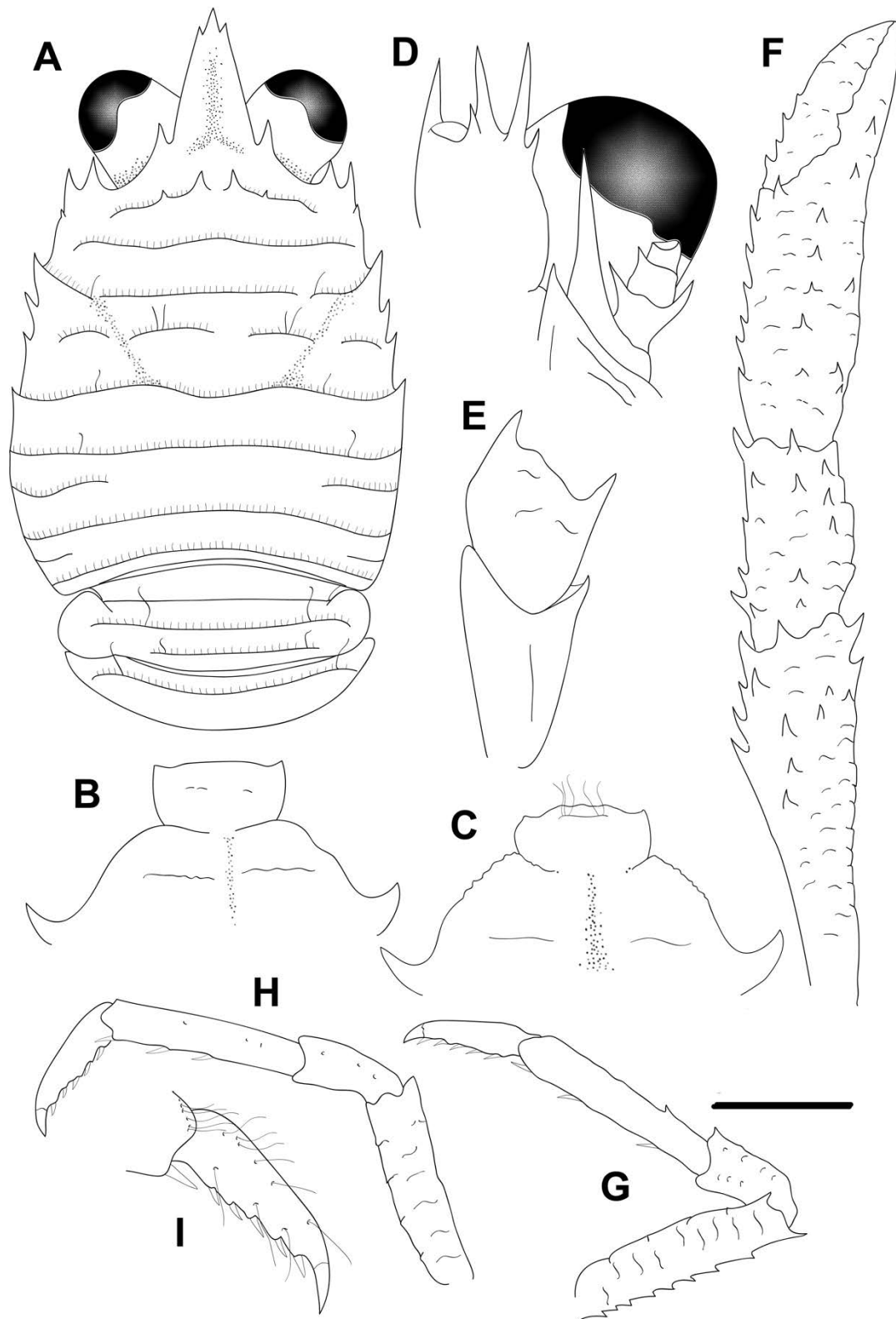
FIGURE 43. *Phylladiorhynchus poeas* **n. sp**., holotype male 2.8 mm (MNHN-IU-2014-13736); C: paratype male 3.3 mm (MNHN-IU-2016-9658): A, carapace and pleon, dorsal view. B, C, thoracic sternites 3 and 4. D, left cephalic region, showing antennular and antennal peduncles, ventral view. E, right Mxp3, lateral view. F, right P1, dorsal view. G left P2, lateral view. H, left P4, lateral view. I, dactylus of right P2, lateral view. Scale bar: A, F-H = 1.0 mm; B–D, I = 0.5 mm.

M 3.4 mm (MNHN-IU-2016-9658), 1 M 2.5 mm (MNHN-IU-2014-13859).—Stn DW1867, 28°59'S, 140°14'W, 127–170 m, 4 November 2002: 2 M 2.0–2.2 mm (MNHN-IU-2019-2681).—Stn DW1876, 28°59'S, 140°15'W, 150–160 m, 4 November 2002: 2 M 2.1–2.8 mm (MNHN-IU-2019-2693).—Stn DW1877, 28°59'S, 140°15'W, 59–150 m, 4 November 2002: 1 M 2.8 mm (MNHN-IU-2014-13904), 8 M 2.3–3.7 mm, 5 ov. F 2.5–3.4 mm, 3 F 2.5–2.8 mm (MNHN-IU-2014-13738), 1 M 3.6 mm (MNHN-IU-2014-13731), 9 M 1.7–4.0 mm, 8 F 2.0-3.1 mm (MNHN-IU-2019-2677), 1 M 3.4 mm, 1 ov. F 2.8 mm (MNHN-IU-2016-9634).—Stn DW1880, 27°54.8'S, 143°29.45'W, 90–94 m, 6 November 2002: 2 M 2.0-2.3 mm, 4 ov. F 1.8–2.8 mm (MNHN-IU-2019-2682), 3 M 2.1–2.8 mm, 1 ov. F 2.0 mm (MNHN-IU-2014-13857).—Stn DW1881, 27°55'S, 143°29'W, 112-121 m, 6 November 2002: 1 M 2.2 mm (MNHN-IU-2019-2684), 1 ov. F 2.6 mm (MNHN-IU-2019-2680).—Stn DW1894, 27°40.13'S, 144°21.51'W, 100 m, 8 November 2002: 2 M 1.8-2.2 mm (MNHN-IU-2019-2664), 1 ov. F 2.4 mm (MNHN-IU-2019-2661).—Stn DW1898, 27°34'S, 144°27'W, 580–820 m, 8 November 2002: 1 M 3.3 mm (MNHN-IU-2014-13737).—Stn CP1908, 27°25'S, 144°01'W, 100–118 m, 9 November 2002: 3 M 2.3–3.4 mm, 1 ov. F 2.5 mm, 2 F 2.0–2.2 mm (MNHN-IU-2019-2683).—Stn CP1918, 27°03'S, 146°04'W, 130–140 m, 12 November 2002: 1 M 2.3 mm (MNHN-IU-2019-2685).—Stn DW1936, 24°39.7'S, 145°57.09'W, 80-100 m, 14 November 2002: 1 ov. F 2.0 mm (MNHN-IU-2019-2663).—Stn DW1939, 23°49.67'S, 147°41.62'W, 100 m, 15 November 2002: 1 M 2.0 mm (MNHN-IU-2019-2679).—Stn DW2013, 22°38.57'S, 152°49.73'W, 80–93 m, 25 November 2002: 1 M 2.3 mm (MNHN-IU-2019-2678).

Etymology. From the name *Poeas*, an Argonaut, son of Thaumacus and father of Philoctetes. The name is considered a substantive in apposition.

Description. *Carapace:* as long as or slightly longer than broad; transverse ridges with dense short setae and few scattered long and thick setae. Gastric region slightly convex with 4 transverse ridges: epigastric ridge distinct with 1, 2 or 3 (if specimen is massive) pairs of spines in transverse row, innermost pair always the largest, outer pairs (when present), smaller, sometimes indicated by granules; anterior protogastric ridge non interrupted medially, nearly extending laterally to carapace margin; anterior mesogastric ridge not medially interrupted, laterally interrupted by cervical groove, laterally continuing to first branchial spine; anterior metagastric ridge scale-like,. Mid-transverse ridge uninterrupted, preceded by distinct cervical groove, followed by 2 uninterrupted or minutely interrupted ridges, interspersed with 1 short lateral ridge. Lateral margins convex, with 6–7 spines: first anterolateral spine well-developed, reaching anteriorly to level of lateral orbital spine, second spine (hepatic) small to obsolescent, slightly dorsomesially from lateral margin, and followed by 4–5 branchial spines behind distinct

anterior cervical groove (3 anterior and 1–2 posterior). Rostrum subtriangular, horizontal, dorsally flattish or slightly concave, [1.6]–1.8 times as long as broad, length [0.4]–0.5 and breadth [0.2]–0.3 that of carapace; lateral margins serrated and convex, with well-developed supraocular basal spines and small subapical spines. Pterygostomian flap with anterior spine; upper margin smooth.

Sternum: As wide as long. Sternite 3 moderately broad, 1.5–[2.2] times as wide as long, anterior margin convex, often serrated, moderately produced anterolaterally. Sternite 4 widely contiguous to sternite 3; surface depressed in midline, smooth; greatest width 2.7–[2.8] times that of sternite 3, 2.4–[2.7] times as wide as long.

Pleon: Elevated ridges with short setae and a few scattered long setae. Tergite 2 with anterior and posterior transverse elevated ridges; tergites 3–4 with anterior transverse ridge only; tergites 5–6 smooth.

Eye: Eye stalk length about [0.8]0.8 times broader than long, peduncle distally setose, not distinctly expanded proximally; maximum corneal diameter [0.9]0.9 × rostrum width*,* as wide as eyestalk.

Antennule: Article 1 slightly longer than wide, with 5 distal spines: distomesial spine well-developed; proximal lateral spine small, always present.

Antenna: Article 1 with prominent mesial process, distally falling well short of lateralmost antennular spine. Article 2 with well-developed distomesial and distolateral spines. Article 3 with distomesial spine. Article 4 unarmed.

Mxp3: Ischium with distinct distal spines on flexor and extensor margins. Merus [0.6]–0.7 × length of ischium, with well-developed distal spine on extensor and flexor margins.

P1 (lost in holotype): 2.8–3.1 (males), 2.4–2.5(females) times carapace length; subcylindrical, spiny and with dense long stiff setae; merus, carpus and palm with spines along mesial, dorsal and lateral surfaces, distal and mesial spines usually stronger than others. Merus 1.0–1.1 length of carapace, 1.7–1.9 times as long as carpus. Carpus 1.4–1.8 times as long as wide. Palm 1.2–1.3 × carpus length, 1.8–2.4 times as long as broad. Fingers 0.7–0.8 × palm length; fixed finger with several proximal spines; movable finger with 1 well-developed basal spine and several small spines or granules on dorsal surface.

P2–4: Densely setose and spinose. Meri successively shorter posteriorly: P3 merus 0.8 times length of P2 merus, P4 merus 0.9–1.0 times length of P3 merus. P2 merus, [0.6]0.6 times carapace length, [4.0]–4.4 times as long as broad, [1.2]–1.6 times as long

as P2 propodus; P3 merus 3.6–4 times as long as broad, 1.3–1.4 times as long as P3 propodus; P4 merus 2.7–[3.8] times as long as broad, [1.1]–1.2 times as long as P4 propodus; extensor margin of P2 and P3 with row of spines, proximally diminishing, with prominent distal spine; P4 extensor margin irregular, unarmed; flexor margin irregular, with distal spine on P2–3, distal spine absent in P4. Carpi with 0–2 prominent spines on extensor margin on P2–3, unarmed on P4; distal spine prominent on P2–3, smaller on P4; row of small spines below extensor margin on lateral surface of P2–3, unarmed on P4; flexor margin unarmed. Propodi moderately stout, [5.0–5.5]4.5–6.0 times as long as broad; extensor margin irregular, armed with 1–4 distinct well-developed spines; flexor margin with 3-4 slender movable spines in addition to distal pair. Dactyli [0.6]0.6–0.8 × length of propodi, ending in incurved, strong, sharp spine; flexor margin with 4–6 movable spines.

Eggs: Ov. F carried approximately 10–30 eggs of 0.3 mm diameter.

Colour. Base colour of carapace light orange to dark orange; carapace, rostrum, supraocular spines and ocular peduncles covered by orange spots, epigastric spines and ridges darker. Pleonal tergites 1–4 light orange, darker on lateral margins and ridges; anterior ridges with few wittish spots. P1 dark orange, covered by light orange setae. P2–4 light orange, darker on extensor and flexor margins.

Genetic data. COI and 16S, Table 1.

Distribution. French Polynesia, almost all specimens were found between 50 and 160 m. A single specimen was found in a station of 580–820 m depth (MNHN-IU-2014-13737) that we consider as an anomaly.

Remarks. The new species is morphologically undistinguishable from *P. pusillus* from Australia, Tasmania and New Zealand and they can be considered as cryptic species. However, genetically they are very different for mitochondrial genes. Schnabel & Ahyong (2019) revised the type material and numerous topotypic specimens of *P. pusillus* and found that one of the diagnostic characters of the species (4 spines on the epigastric ridge) showed a certain variability. After examination of a huge quantity of material from Australia, Tasmania and New Zealand, Schnabel & Ahyong (2019) reported a variation in the number and size of the epigastric spines, from 1 to 3 pairs of epigastric spines, with the lateralmost being granules in small specimens. The new species from French Polynesia has a similar variation in this character, with specimens having 2 to 6 spines and/or granules, recommending caution when using this character for species delimitation. Unfortunately, we don't know the colour pattern of *P. pusillus* to compare with the colouration of the new species. Therefore, future studies will confirm the

existence of additional differences to separate morphologically both species. A subtle character useful to distinguish both species might be the thoracic sternite 3 moderately produced anterolaterally in *P. poeas*; whereas with broad granule or square in *P. pusillus* (Schnabel & Ahyong 2019).

The genetic divergences between *P. poeas* and *P. pusillus* were 8% (COI) and 2% (16S). No intraspecific divergences were observed in both genes.

Phylladiorhynchus pollux n. sp.

(Figs. 44, 50C)

Type material. *Holotype.* New Caledonia. LIFOU Stn 1451, 20°47.3'S, 167°06.8'E, 10–21 m, 19 November 2000: ov. F 3.5 mm (MNHN- IU-2014-13797)

Paratypes. New Caledonia, Recif Mbere, 22º19.9'S, 166º13.2'E, 10 m, 5 May 1993: 1 M 3.8 mm (MNHN-IU-2019-2698).

Etymology. From the name *Pollux*, an Argonaut, son of Zeus and Leda. The name is considered a substantive in apposition.

Description. *Carapace:* As long as or slightly longer than broad; transverse ridges with dense short setae, and few scattered short and thick setae. Gastric region slightly convex, with some transverse ridges: epigastric ridge armed with 4 epigastric spines; anterior protogastric ridge not medially interrupted, nearly extending laterally to carapace margin, followed by a posterior protogastric ridge not medially interrupted; anterior mesogastric ridge not medially interrupted, laterally continuing to first branchial spine, posterior mesogastric ridge absent, otherwise scale like; anterior metagastric ridge not medially interrupted, laterally continuing to second branchial spine, followed by posterior median metagastric scale; secondary scales can be present between ridges. Mid-transverse ridge not interrupted, medially depressed, preceded by distinct cervical groove, followed by 2 uninterrupted or minutely interrupted ridge, interspersed with 2 scale-like ridges. Lateral margins slightly convex, with 5 spines: first anterolateral spine well-developed, overreaching level of lateral orbital spine, second spine (hepatic) well-developed, slightly dorsomesial from lateral margin, and followed by 3 branchial spines (2 anterior and 1 posterior). Rostrum subtriangular, horizontal, dorsally flattish, narrow [1.7]1.8–1.9 times as long as broad, length [0.4]0.4 and breadth [0.2]0.2 that of carapace; lateral margins smooth and convex, with well-developed supraocular basal supraocular spines, subapical spines minutes. Pterygostomian flap ending in blunt tooth, upper margin irregular.
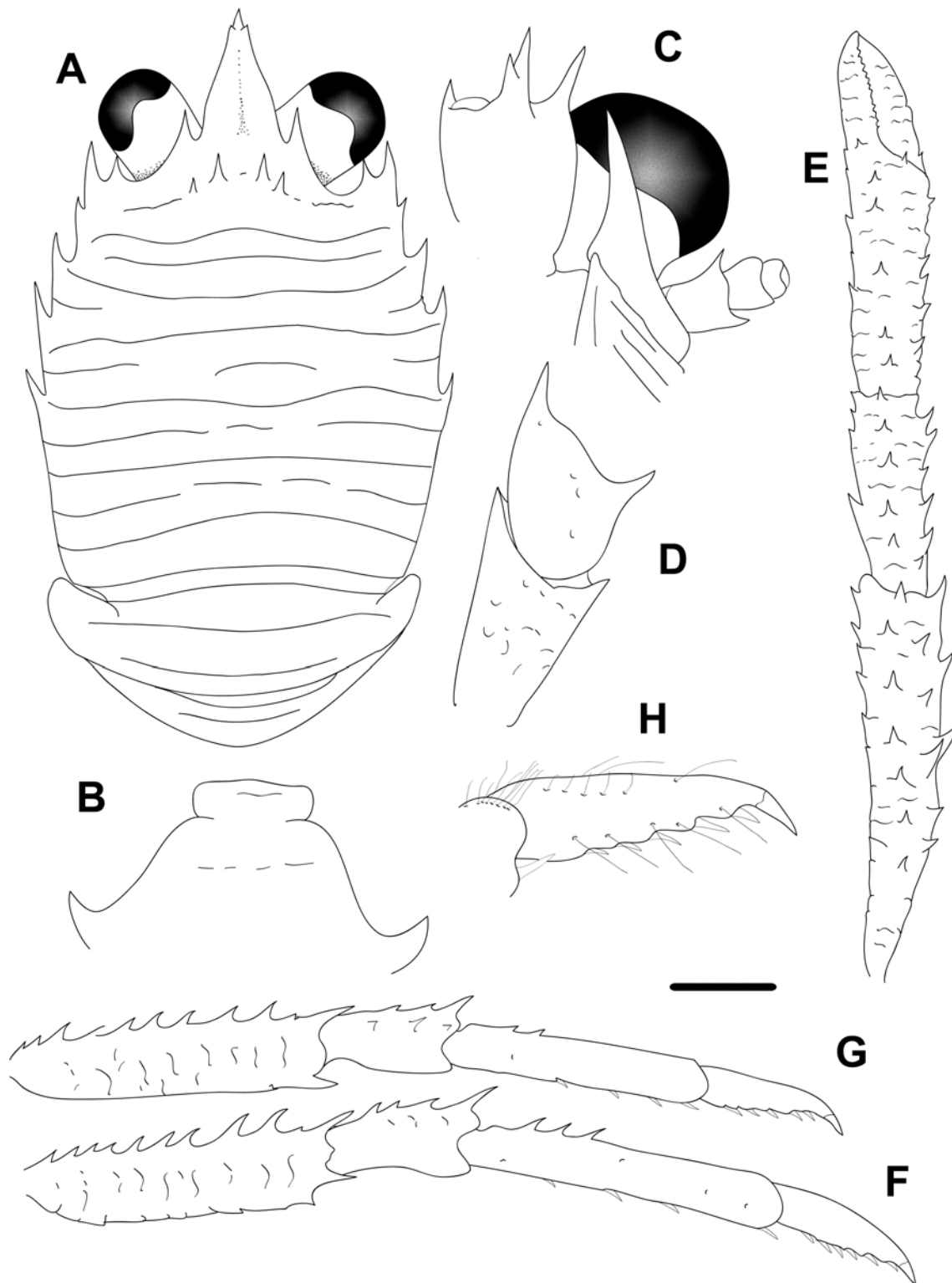
FIGURE 44. *Phylladiorhynchus pollux* **n. sp**., A-D, F-H, holotype ovigerous female 3.5 mm (MNHN-IU-2014-13797); E, paratype male 3.8 mm (MNHN-IU-2019-2698): A, carapace and pleon, dorsal view. B, thoracic sternites 3 and 4. C, left cephalic region, showing antennular and antennal peduncles, ventral view. D, right Mxp3, lateral view. E, left P1, dorsal view. F, right P2, lateral view. G, right P3, lateral view. H, dactylus of right P2, lateral view. Scale bar: A, E-G = 1.0 mm; B–D, H = 0.5 mm.

Sternum: As wide as long. Sternite 3 moderately broad, 2.0–[3.0] times as wide as long, anterior margin straight. Sternite 4 widely contiguous to sternite 3; surface depressed in midline, smooth; greatest width [3.5]–4.6 times that of sternite 3, 2.6–[2.7] times as wide as long.

Pleon: Elevated ridges with with short setae and a few scattered thick setae. Tergite 2–3 with anterior and posterior transverse elevated ridges; tergite 4 with anterior transverse ridge; tergites 5–6 smooth.

Eye: Eye stalk length about 0.9–[1.0] times broader than long, peduncle distally setose, not distinctly expanded proximally; maximum corneal diameter [1.1]–1.2 × rostrum width, as wide as eyestalk.

Antennule: Article 1 slightly longer than wide, with 4–5 well-developed distal spines: distomesial spine well-developed; proximal lateral spine absent or minute.

Antenna: Article 1 with prominent mesial process, distally falling well short of lateral antennular spine. Article 2 with small distomesial and distolateral spines. Articles 3 and 4 unarmed.

Mxp3: Ischium with distinct distal spines on flexor and extensor margins. Merus and ischium subequal in size, with well-developed distal spine on extensor and flexor margins.

P1: 3.4 (male) [2.1] (female) times carapace length; subcylindrical, spiny and densely covered with plumose setae and scattered long stiff setae; merus, carpus and palm with spines along mesial, dorsal and lateral surfaces, distal and mesial spines usually stronger than others. Merus 1.2–1.3 length of carapace, twice as long as carpus. Carpus twice as long as wide. Palm 1.3 × carpus length, 2.8 times as long as broad. Fingers 0.7 × palm length; fixed finger unarmed; movable finger with small basal spine.

P2–3 (P4 lost in both specimens): Moderately stout, subcylindrical, highly setose and spinose, densely cover by plumose setae: P3 merus 0.6–[0.9] times length of P2 merus. P2 merus, [0.8]0.8 times carapace length, 4.4–[4.7] times as long as broad, 1.2–[1.4] times as long as P2 propodus; P3 merus [4.3]–4.6 times as long as broad, [1.1]–1.2 times as long as P3 propodus; extensor margin of P2 and P3 with row of spines, proximally diminishing, with prominent distal spine; flexor margin irregular,with distal spine on P2–3. Carpi with 3–4 spines on extensor margin on P2–3; distal spine prominent; row of small spines below extensor margin on lateral surface of P2–3; flexor margin unarmed or with small distal spine. Propodi moderately stout, 5.0–5.5 [5.6–6.5] times long as broad; extensor margin irregular, armed proximally with 2–4 small spines on P2–

3; flexor margin with 3–4 slender movable spines in addition to distal pair. Dactyli [0.5-0.6]0.5–0.6 × length of propodi, ending in incurved, strong, sharp spine; flexor margin with 5–6 movable spines.

Eggs. No data. The holotype carried one egg of 0.5 mm diameter.

Colour. Unknown.

Genetic data. COI and 16S, Table 1.

Distribution. New Caledonia, between 10 and 21 m.

Remarks. *Phylladiorhynchus pollux* belongs to the group of species having 4 epigastric spines and Mxp3 merus with one prominent spine along the flexor margin. The group of species includes *P. australis* Schnabel & Ahyong, 2019, from New Zealand and Southern Australia, *P. integrus* (Benedict, 1902) from Japan to Chesterfield Islands*, P. lenzi*, from Chile, *P. nui,* from SE Australia, Tasmania, New Zealand, *P. poeas*, from French Polynesia, *P. porteri*, from Chile, and *P. pusillus*, from SW Pacific. However, the new species is easily distinguished from these species by the number of spines on the anterior branchial margin: 2 spines in *P. pollux* and 3 spines in the other species. Furthermore, the posterior protogastric ridge is not medially interrupted in *P. pollux*, being absent or scale-like in the other species.

The sequences of *P. pollux* were more than 22% (COI) and 11% (16S) divergent from all other species.

Phylladiorhynchus porteri **n. sp.**

(Figs. 45, 50D)

Type material. *Holotype.* Chile, Valparaiso, Coll. Porter, 1899: M 2.7 mm (MNHN-IU-2019-2598 (Ga-763)).

Paratypes. Chile, Valparaiso, Coll. Porter, 1899: 3 M 2.0–2.7 mm, 4 ov. F 2.4–2.8 mm (MNHN-IU-2014-23831 (Ga-763)).

Etymology. Named after C.E. Porter, chilean naturalist, who collected the specimens.

Description. *Carapace*: As long as broad; transverse ridges with dense short setae, and few scattered long thick setae. Gastric region slightly convex with 4 transverse ridges: epigastric ridge distinct with 2 or 3 (if specimen is massive) pairs of spines in transverse row, innermost pair always the largest, outer pair(s) prominent, smaller or absent,
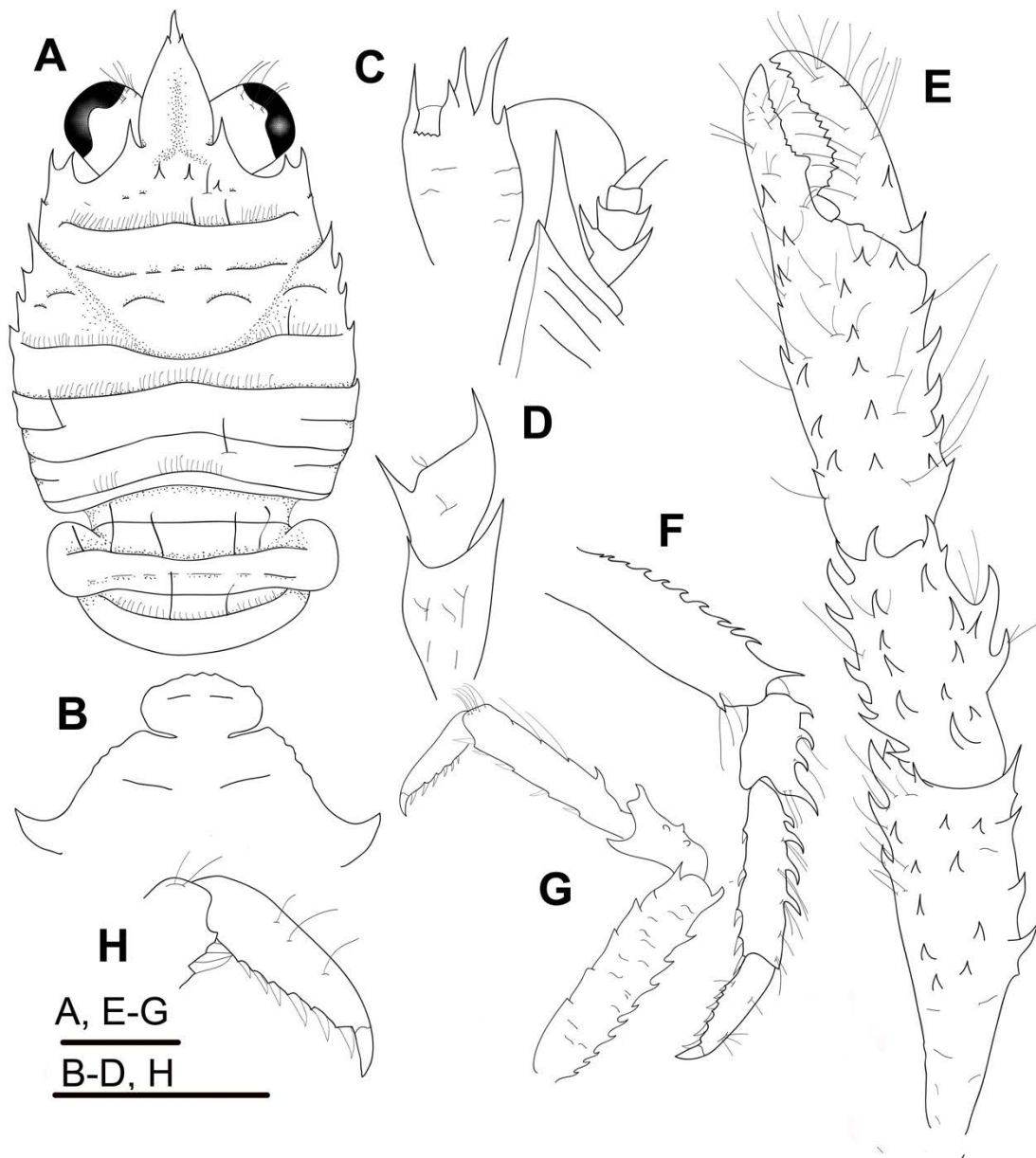
FIGURE 45. *Phylladiorhynchus porteri* **n. sp**., A-D, F-H, holotype male 2.7 mm (MNHN IU-2019-2598 (Ga-763)), G, paratype male 2.0 mm (MNHN- IU-2014-23831): A, carapace and pleon, dorsal view. B, thoracic sternites 3 and 4. C, left cephalic region, showing antennular and antennal peduncles, ventral view. D, left Mxp3, lateral view. E, left P1, dorsal view. F, right P2, lateral view. G, attached leg, presumably left P3, lateral view. H, dactylus of right P2, lateral view. Scale bars: 1.0 mm.

sometimes indicated by granules; anterior protogastric ridge medially uninterrupted, nearly extending laterally to carapace margin; anterior mesogastric ridge medially interrupted, with several median scales, laterally interrupted by cervical groove, laterally continuing uninterrupted to first branchial spine; anterior metagastric ridge scale-like. Mid-transverse ridge uninterrupted, preceded by distinct cervical groove, followed by 2 uninterrupted or minutely interrupted ridges, interspersed with 1 short lateral ridge. Lateral margins convex, with 7 spines: first anterolateral spine well-developed, reaching anteriorly to level of lateral orbital spine, second spine (hepatic) small to obsolescent, slightly dorsomesially from lateral margin, and followed by 5 branchial spines behind distinct anterior cervical groove (3 anterior and 2 posterior). Rostrum subtriangular, lanceolate, horizontal, dorsally flattish or slightly concave, [1.8]1.4–1.8 times as long as broad, length [0.4]–0.4 and breadth [0.2]–0.3 that of carapace; lateral margins smooth and convex, with well-developed supraocular basal spines and small subapical spines. Pterygostomian flap ending in blunt tooth; upper margin unarmed.

Sternum: As wide as long. Sternite 3 moderately broad, 1.8–2.0[2.0] times as wide as long, anterior margin convex. Sternite 4 widely contiguous to sternite 3; surface depressed in midline, smooth; greatest width [2.9]–3 times that of sternite 3, 2–3[3] times as wide as long.

Pleon: Elevated ridges with short setae and a few scattered long setae. Tergite 2 with anterior and posterior transverse elevated ridges; tergites 3–4 with anterior transverse ridge only; tergites 5–6 smooth.

Eye: Eye stalk length about [0.9]–1.0 times broader than long, peduncle distally setose, not distinctly expanded proximally, with few short transverse striae on lateral surfaces; maximum corneal diameter 0.7–[0.8] × rostrum width, as wide as eyestalk, (0.9 times maximum peduncle width).

Antennule: Article 1 slightly longer than wide, with 5 distal spines: distomesial spine well-developed; proximal lateral spine small, always present. Short striae covering mesial surfaces.

Antenna: Article 1 with prominent mesial process, distally falling well short of lateralmost antennular spine. Article 2 with well-developed distal spines laterally and mesially. Article 3 with distomesial and distolateral spines. Article 4 unarmed.

Mxp3: Ischium with distinct distal spines on flexor and extensor margins; crista dentata with row of spines along entire margin. Merus 0.6– [0.7] × length of ischium, with well-developed distal spine on extensor margin and one much larger spine on flexor margin.

P1(only in males): [3.0] times carapace length (male), subcylindrical, spiny and with dense long stiff setae; merus, carpus and palm with spines along mesial, dorsal and lateral surfaces, distal and mesial spines usually stronger than others. Merus 1.4 length of carapace, [1.6]–2.3 times as long as carpus. Carpus 1.5–[1.7] times as long as wide. Palm [1.2]–1.4 × carpus length, 1.8–1.9 [1.9] times as long as broad. Fingers [0.8]0.8 × palm length; movable and fixed fingers with several proximal marginal spines.

P2–4: (attached legs only) Stout, densely setose and spinose. Meri successively shorter posteriorly: P3 merus 0.6 times length of P2 merus, P4 merus 0.8 times length of P3 merus. P2 merus, [0.8]0.8 times carapace length, 2.7– [3.6] times as long as broad, 1.3–1.6 [1.6] times as long as P2 propodus; P3 merus 4 twice as long as broad, 1.3 times as long as P3 propodus; P4 merus 3.6 times as long as broad, 1.2 times as long as P4 propodus; extensor margin of P2 and P3 with row of spines, proximally diminishing, with prominent distal spine; P4 extensor margin irregularunarmed; flexor margins irregular, with distal spine on P2–3, distal spine absent in P4. Carpi with prominent spines on extensor margin on P2–3, unarmed on 4; distal spine prominent on P2–3, smaller on P4; row of small spines below extensor margin on lateral surface of P2–3, unarmed on P4; flexor margin unarmed. Propodi stout, [3.5]3.3–4.3 times as long as broad; extensor margin irregular usually armed with 1–4 well-developed spines; flexor margin with 4 slender movable spines in addition to distal pair. Dactyli [0.78]0.6–0.8 × length of propodi, ending in incurved, strong, sharp spine; flexor margin with 4–6 movable spines

Colour. Unknown.

Genetic data. No data.

Distribution. Chile, Valparaíso, unknown depth.

Remarks. *Phylladiorhynchus porteri* belongs to the group of species having usually 4 spines on the epigastric ridge, the anterior metagastric ridge scale-like, a very small hepatic spine, the anterior margin of the thoracic sternite 3 convex and one spine on the flexor margin of the Mxp3 merus. *Phylladiorhynchus porteri* is closely related to *P. lenzi* (Rathbun, 1907), from Chile. However, they can be easily distinguished by the following aspects:

- The rostrum is more lanceolate in *P. porteri* than in *P. lenzi*.
- The anterior mesogastric ridge is medially interrupted, with some few medial scales in *P. porteri*, whereas this ridge is uninterrupted in *P. lenzi*.
- The distomesial and the proximal lateral spines of the antennular article 1 are small or minute in *P. lenzi*, whereas these spines are well developed in *P. porteri*.

-        The spines on the P2-4 meri are stronger in *P. porteri* than in *P. lenzi*. Furthermore, the extensor margin of the propodi have well developed spines in *P. porteri*, being unarmed in *P. lenzi*.

Phylladiorhynchus priasus n. sp.

(Figs. 37 C-D, 46, 50E)

Type material. *Holotype.* Mariana Islands. Maug Islands. Stn MAU-385, 20.02973294ºN, 145.2084746ºE, 17 m, 04 May 2014: M 2.2 mm (UFXXXX).

Paratypes: Northern Mariana Islands. Maug Islands. Stn MAU-302, 20.01416942ºN, 145.2342278ºE, 15 m, 03 May 2014: 4 M 1.4–1.8 mm, 3 ov. F 1.6–1.9 mm, 1 F 1.7 mm (UF).—Stn MAU-303, 20.01416942ºN, 145.2342278ºE, 15, 03 May 2014: 4 M 1.4–2.3 mm (UF).—Stn MAU-304, 20.01416942ºN, 145.2342278ºE, 15 m, 3 May 2014: 2 M 1.8–2.1 mm, 5 ov. F 1.8–2.2 mm (UF).—Stn MAU-305, 20.01416942ºN, 145.2342278ºE, 15 m, 3 May 2014:1 M 1.6 mm, 2 ov. F 1.8–2.1 mm (UF).—Stn MAU-354, 20.01416942ºN, 145.2342278ºE, 15 m, 3 May 2014: 1 M 1.4 mm, 4 ov. F 2.0–2.3 mm (UF).—Stn MAU-355, 20.01416942ºN, 145.2342278ºE, 15 m, 3 May 2014: 1 M 2.4 mm, 1 ov. F 2.0 mm, 1 M 2.1 mm (UF).—Stn MAU-357, 20.01416942ºN, 145.2342278ºE, 15 m, 3 May 2014: 8 M 1.3–2.2 mm, 11 ov. F 1.5–2.3 mm, 6 F 1.4–1.9 mm (UF).—Stn MAU-476, 20.01416942ºN, 145.2342278ºE, 15 m, 3 May 2014: 1 F 1.9 mm (UF).—Stn MAU-478, 20.01416942ºN, 145.2342278ºE, 15 m, 3 May 2014: 2 M 1.4–1.9 mm, 1 F 1.5 mm (UF).—Stn MAU-479 20.01416942ºN, 145.2342278ºE, 15 m, 3 May 2014: 1 M 1.8 mm 3 ov. F 1.8–2.4 mm (UF).—Stn MAU-383, 20.02973294ºN, 145.2084746ºE, 17 m, 4 May 2014: 4 M 1.4–1.9 mm, 4 ov. F 1.6–2.1 mm (UF).—Stn MAU-384, 20.02973294ºN, 145.2084746ºE, 17 m, 04 May 2014: 1 M 2.1 mm, 4 ov. F 2.0–2.4 mm (UF).—Stn MAU-385, 20.02973294ºN, 145.2084746ºE, 17 m, 04 May 2014: 4 M 2.1–2.8 mm, 5 ov. F 2.0–2.1 mm, 1 F 1.9 mm (UF)

Northern Mariana Islands. Pagan Island. Stn PAG-407, 18.10734ºN, 145.78587ºE, 11 m, 20 April 2014: 1 M 1.3 mm, 2 ov. F 2.0–2.1 mm (UF).—Stn PAG-480, 18.10734ºN, 145.78587ºE, 11 m, 20 April 2014: 1 ov. F 2.0 mm (UF).—Stn PAG-483 18.10734ºN, 145.78587ºE, 11 m, 20 April 2014: 7 M 1.4 –2.4 mm, 3 ov. F 2.2–2.5 mm (UF).—Stn PAG-565, 18.10734ºN, 145.78587ºE, 11 m, 20 April 2014: 1 ov. F 2.2 mm (UF).—Stn PAG-566, 18.10734ºN, 145.78587ºE, 11 m, 20 April 2014: 2 M 1.8–2.3 mm, 1 ov. F 2.3 mm, 1 F 1.6 mm (UF).—Stn PAG-567, 18.10734ºN, 145.78587ºE, 11 m, 20 April 2014: 2 M 2.3–2.8 mm (UF).—Stn PAG-568, 18.10734ºN, 145.78587ºE, 11 m, 20 April 2014: 3 M 1.3–1.5 mm (UF).—Stn PAG-571, 18.10734ºN, 145.78587ºE, 11 m, 20 April 2014: 1 F 1.8 mm (UF).—Stn PAG-573 18.10734ºN, 145.78587ºE, 11 m, 20 April 2014: 2 M
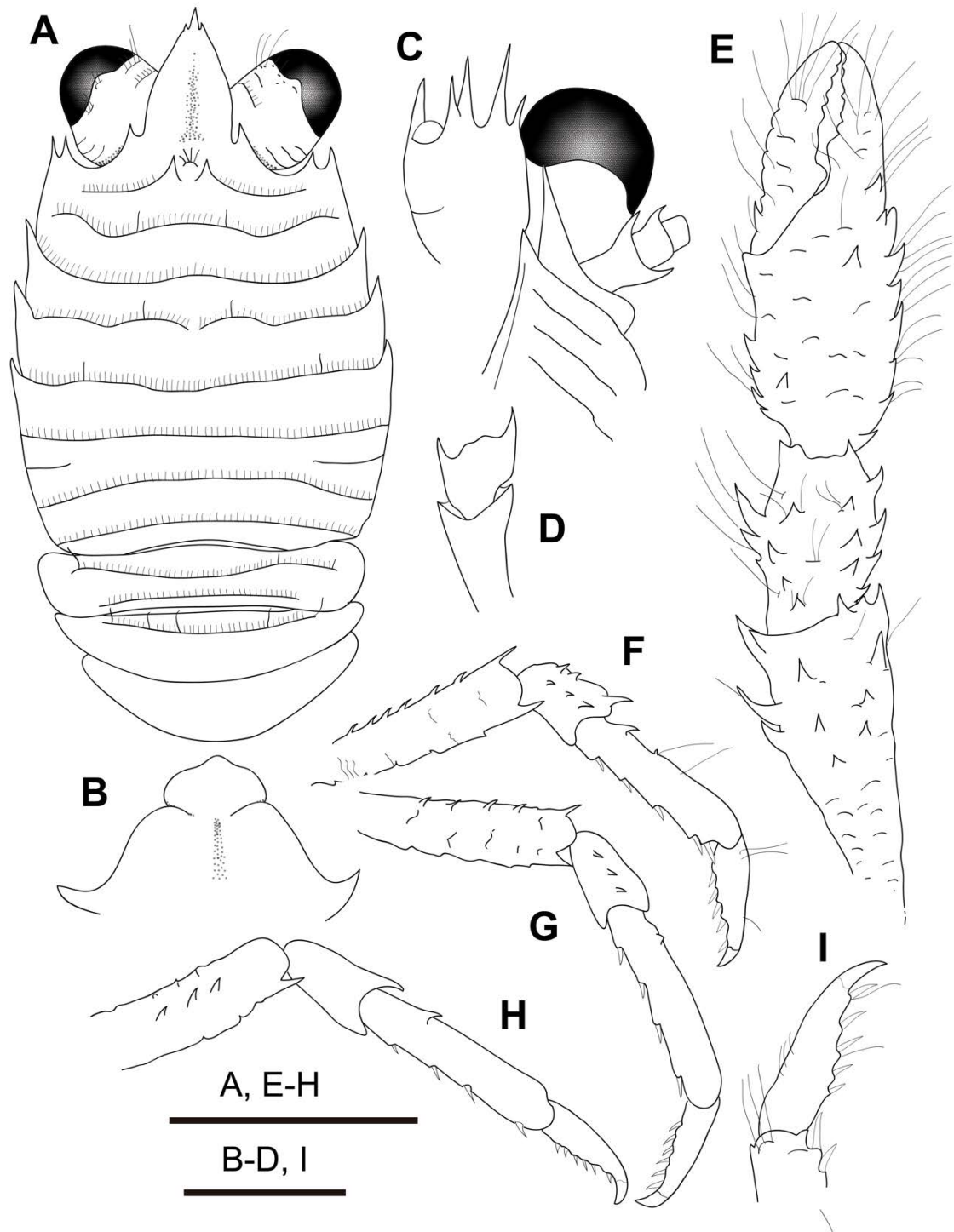
FIGURE 46. *Phylladiorhynchus priasus* **n. sp**., A-D, G-H, holotype male 2.2 mm (MAU-385, UFXXXX); A, carapace and pleon, dorsal view. B, thoracic sternites 3 and 4. C, left cephalic region, showing antennular and antennal peduncles, ventral view. D, left Mxp3, lateral view. E, right P1, dorsal view. F, right P2, lateral view. G, right P3, lateral view. H, right P4, lateral view. I, dactylus of right P2, lateral view. Scale bars: 1.0 mm.

1.8–1.9 mm (UF).—Stn PAG-603, 18.10734ºN, 145.78587ºE, 11 m, 20 April 2014:1 ov. F 2.1 mm (UF).—Stn PAG-694, 18.0706862ºN, 145.7137933ºE, 11 m, 20 April 2014: 1 M 1.4 mm, 1 ov. F 2.1 mm (UF).—Stn PAG-697, 18.0706862ºN, 145.7137933ºE, 11m, 20 April 2014: 1 M 1.8 mm, 1 ov. F 1.9 mm (UF).—Stn PAG-762, 18.0706862ºN, 145.7137933ºE, 11m, 20 April 2014: 1 M 1.7 mm, 1 ov. F 2.0 mm (UF).—Stn PAG-809, 18.0706862ºN, 145.7137933ºE, 11 m, 20 April 2014: 2 M 1.4–1.6 mm, 1 F 1.5 mm (UF).—Stn PAG-810, 18.0706862ºN, 145.7137933ºE, 11 m, 20 April 2014: 1 ov. F 1.8 mm (UF).—Stn PAG-840, 18.11947952ºN, 145.7555622ºE, 12 m, 23 April 2014: 2 M 2.0–2.3 mm (UF).—Stn PAG-841 18.11947952ºN, 145.7555622ºE, 12 m, 23 April 2014: 1 M 2.0 mm, 1 ov. F 2.1 mm (UF).—Stn PAG-865, 18.11947952ºN, 145.7555622ºE, 12 m, 23 April 2014: 1 ov. F 1.8 mm (UF).—Stn PAG-896, 18.11947952ºN, 145.7555622ºE, 12 m, 23 April 2014: 2 M 1.8–1.9 mm, 1 ov. F 2.0 mm, 1 F 1.8 mm (UF).—Stn PAG-900, 18.11947952ºN, 145.7555622ºE, 12 m, 23 April 2014: 1 M 1.8 mm (UF).—Stn PAG-957, 18.11947952ºN, 145.7555622ºE, 12 m, 23 April 2014: 1 M 2.0 mm, 1 ov. F 1.7 mm, 2 F 1.6–2.0 mm (UF).

Mariana Islands. Guam Island. 13.5167ºN, 144.8ºE, 10–25 m, 27 June 2003: 1 ov. F 1.6 mm (UF4173) (UF).—Stn GUA-601, 13.57847ºN, 144.82831ºE, 11 m, 25 March 2014: 1 F 2.1 mm (UF).—Stn GUA-645, 13.57847ºN, 144.82831ºE, 11 m, 25 March 2014: 2 M1.6–2.0 mm (UF).—Stn GUA-695, 13.57847ºN, 144.82831ºE, 11 m, 25 March 2014: 1 ov. F 1.9 mm (UF).—Stn GUA-877, 13.30553ºN, 144.65257ºE, 12 m, 27 March 2014: 1 M 1.5 mm (UF).

Marshall Islands. Wake Island. 19º17.259'N, 166º36.782'E, 11.5–13.5 m, 18 November 2005: 1ov. F 2.0 mm (UF8548).—no position, 15–21 m, 24 March 2009: 1ov. F1.8 mm (UF36081).—Stn WAK-083, 19.2917761ºN, 166.6072896ºE, 14 m, 17 March 2014: 1 ov. F2.2 mm (UF).—Stn WAK-084, 19.2917761ºN, 166.6072896ºE, 14 m, 17 March 2014: 5 M 1.6–2.2 mm, 4 ov. F 1.8–2.2 mm (UF).—Stn WAK-084, 19.2917761ºN, 166.6072896ºE, 14 m, 17 March 2014: 1 M 2.3 mm (UF).—Stn WAK-114, 19.2917761ºN, 166.6072896ºE, 14 m, 17 March 2014: 1 M 2.2 mm (UF).—Stn WAK-117, 19.2917761ºN, 166.6072896ºE, 14 m, 17 March 2014: 1 ov. F 1.7 mm (UF).—Stn WAK-118, 19.2917761ºN, 166.6072896ºE, 14 m, 17 March 2014: 15 M 1.5–2.0 mm, 6 ov. F 1.8–2.1 mm (UF).—Stn WAK-152, 19.31627096ºN, 166.5983406ºE, 12 m, 16 March 2014: 5 M 1.9–2.3 mm, 4 ov. F 1.8–2.1 mm, 5 F1.9–2.3 mm (UF).—Stn WAK-189, 19.27067533ºN, 166.6516393ºE, 14 m, 19 March 2014: 3 ov. F 2.0–2.5 mm, 1 F 2.0 mm (UF).—Stn WAK-218, 19.27067533ºN, 166.6516393ºE, 14 m, 19 March 2014: 2 M 1.9–2.2 mm (UF).—Stn WAK-219, 19.27067533ºN, 166.6516393ºE, 14 m, 19 March 2014: 3 M 2.5–2.6 mm (UF).—Stn WAK-220, 19.27067533ºN, 166.6516393ºE, 14 m, 19 March 2014: 1 ov. F 2.0 mm (UF).—Stn WAK-221,

19.27067533ºN, 166.6516393ºE, 14 m, 19 March 2014: 1 M 1.9 mm, 2 ov. F 1.9–2.0 mm (UF).—Stn WAK-222, 19.27067533ºN, 166.6516393ºE, 14 m, 19 March 2014: 5 M 1.4–2.2 mm, 8 ov. F 1.7–2.3 mm (UF).—Stn WAK-252, 19.27067533ºN, 166.6516393ºE, 14 m, 19 March 2014: 16 M 1.3–2.3 mm, 21 ov. F 1.6–2.5 mm (UF).—Stn WAK-256, 19.27067533ºN, 166.6516393ºE, 14 m, 19 March 2014: 2 M 2.0–2.1 mm, 2 ov. F 1.8–2.1 mm, 1 F 1.7 mm (UF).—Stn WAK-280, 19.27067533ºN, 166.6516393ºE, 14 m, 19 March 2014: 6 M 1.6–2.3 mm, 9 ov. F 1.5–2.2 mm, 1 F 1.7 mm (UF).

Etymology. From the name *Priasus*, an Argonaut, son of Caeneus and Phocus. The name is considered a substantive in apposition.

Description. *Carapace:* Slightly longer than broad; transverse ridges with dense short setae and few scattered long and thick iridescent setae. Gastric region with 4 transverse ridges: epigastric ridge distinct with 2 median spines, usually 1 median produced scale usually with thick plumose setae before epigastric ridge; anterior protogastric ridge not medially interrupted, nearly extending laterally to carapace margin; anterior mesogastric ridge not medially interrupted, laterally continuing to first branchial spine, sometimes followed by some short small scales; anterior metagastric ridge medially interrupted. Mid-transverse ridge not interrupted, cervical groove indistinct, followed by 2 not interrupted or minutely interrupted ridges, interspersed with 1 short lateral ridge and sometimes few, short scattered scales. Lateral margins slightly convex, with 4 distinct spines: first anterolateral spine well-developed, reaching anteriorly to level of lateral orbital spine, hepatic margin unarmed; anterolateral spine followed by 3 branchial spines (2 anterior and 1 posterior). Rostrum bottle-shaped, horizontal, dorsally concave, [1.1]–1.4 times as long as broad, length [0.3]–0.4 and breadth 0.25–[0.3] that of carapace; lateral margins serrated, straight proximally and distally slightly convex, with well-developed supraocular basal spines and small subapical spines. Pterygostomian flap ending in blunt tooth, upper margin smooth.

Sternum: As wide as long. Sternite 3 quadrangular, slightly wider than long ([1.5]1.5 times as wide as long), anterior margin with a median blunted projection, lateral margins rounded. Sternite 4 widely contiguous to sternite 3; surface depressed in midline, smooth; greatest width [2.9]–3.3 times that of sternite 3, 2.1–[2.9] times as wide as long.

Pleon: Elevated ridges with short setae and a few scattered long setae. Tergite 2 with anterior and posterior transverse elevated ridges; tergites 3–4 with anterior transverse ridge; tergites 5–6 smooth.

Eye: Eye stalk length about [0.9] times broader than long, peduncle distally setose, slightly expanded proximally; maximum corneal diameter [0.6]–0.7 × rostrum width, as narrower than eyestalk, (0.8–0.9 times maximum peduncle width).

Antennule: Article 1 slightly longer than wide, with 5 distal spines: distomesial spine well-developed; proximal lateral spine small, always present.

Antenna: Article 1 with prominent mesial process distally falling well short of lateralmost antennular spine. Article 2 with well-developed distomesial and distolateral spines. Article 3 with distomesial spine. Article 4 unarmed.

Mxp3: Ischium with distinct distal spines on flexor and extensor margins. Merus [0.7]0.6–0.8 × length of ischium, with well-developed distal spine on extensor and flexor margins.

P1: [2.2]–2.9 (males), 1.8–2.1 (females) times carapace length; subcylindrical, spiny and with dense long stiff setae; merus, carpus and palm with spines along mesial, dorsal and lateral surfaces, mesial spines usually stronger than others. Merus [0.8]–0.9 length of carapace, [2.2]1.8–2.3 times as long as carpus. Carpus [1.3]1.1–1.4 times as long as wide. Palm [1.2]–1.4 × carpus length, [1.3]–1.7 times as long as broad. Fingers 0.6–[1] × palm length; fixed finger with 1–2 basal spines; movable finger with 1 basal spine.

P2–4: Stout, setose and spinose. Meri successively shorter posteriorly: P3 merus [0.7]0.7 times length of P2 merus, P4 merus [0.9]0.8–0.9 times length of P3 merus. P2 merus, 1.6–[1.7] times carapace length, 3.8–[5.0] times as long as broad, 1.2–[1.4] times as long as P2 propodus; P3 merus 3.8–[4.2] times as long as broad, [1.1]–1.4 times as long as P3 propodus; P4 merus 3.3–[3.4] times as long as broad, 1.0–[1.1] times as long as P4 propodus; extensor margin of P2 and P3 with row of spines, proximally diminishing, with prominent distal spine; P4 extensor margin irregular, unarmed; flexor margin irregular,with distal spine on P2–3, distal spine absent in P4, P4 lateral surface with row of 2–4 spines. Carpi with 1–3 prominent spines on extensor margin on P2–3, unarmed on P4; distal spine prominent on P2–3, smaller on P4; row of small spines or granules below extensor margin on lateral surface of P2–3, unarmed on P4; flexor margin unarmed. Propodi stout, [4.0–5.0]3.7–5.6 times as long as broad; extensor margins irregular, armed with 1–3 spines on proximal half or unarmed; flexor margins with 3–4 slender movable spines in addition to distal pair. Dactyli [0.5–0.7] 0.5–0.8 × length of propodi, ending in incurved, strong, sharp spine; flexor margin with 5–6 movable spines.

Eggs: Ov. F carried approximately 10–35 eggs of 0.3–0.5 mm diameter.

Colour. Unknown.

Genetic data. COI and 16S, Table 1.

Distribution. Mariana Islands, Guam Island, Marshall Islands, Wake Island, between 10 and 25 m.

Remarks. *Phylladiorhynchus priasus* belongs to the group of species with 2 epigastric spines, hepatic margin unarmed and 2 spines on the anterobranquial margin. The closest species are *P. integrirostris,* from Hawaii, and *P. lynceus,* from Chagos, Western Australia, Kiribati and Samoa. The 3 species are barely distinguishable morphologicaly although they are clearly different genetically. However, these species can be distigushed among them by the following subtle traits:

- *Phylladiorhynchus priasus* and *P. integrirostris* usually have a median produced scale, behind epigastric ridge, usually with thick setae [not in the neotype neither in the material examined by Schnabel & Ahyong (2019)]. However, this scale is always absent in all specimens examined of *P. lynceus*.
- The rostrum is proximally straight (bottle-shaped) in *P. priasus* and *P. integrirostris,* whereas it is convex (leaf-like) in *P. lynceus*.
- The carapace has numerous thick iridescent setae in *P. lynceus* and *P. priasus*, whereas these setae are usually absent in *P. integrirostris*.

The genetic divergences between *P. priasus* and *P. lynceus* were 7% (COI) and 2% (16S). These divergences were larger between *P. priasus* and *P. integrirostris*, 23% (COI) and 12% (16S).

P. priasus is also close to *P. orpheus* (see the differences under the Remarks of *P. orpheus*).

The mean intraspecific genetic divergences were 0.4% (COI) and 0.1% (16S).

Phylladiorhynchus pulchrus **n. sp.**

(Figs. 47, 50F)

Type material. *Holotype*. French Polynesia. MUSORSTOM 9 Stn CP1156, 07°59'S, 140°43.7'W, 80 m, 23 August 1997: M 1.6 mm (MNHN-IU-2014-13849).

Paratypes Philippines. MUSORSTOM 3 Stn DR117, 12°31'N, 120°39'E, 92–97 m, 3 June 1985: 1 M 1.4–1.8 mm, 2 ov. F 1.8–2.0 mm (MNHN-IU-2014-13848), 1 M 1.4 mm (MNHN-IU-2017-1342).
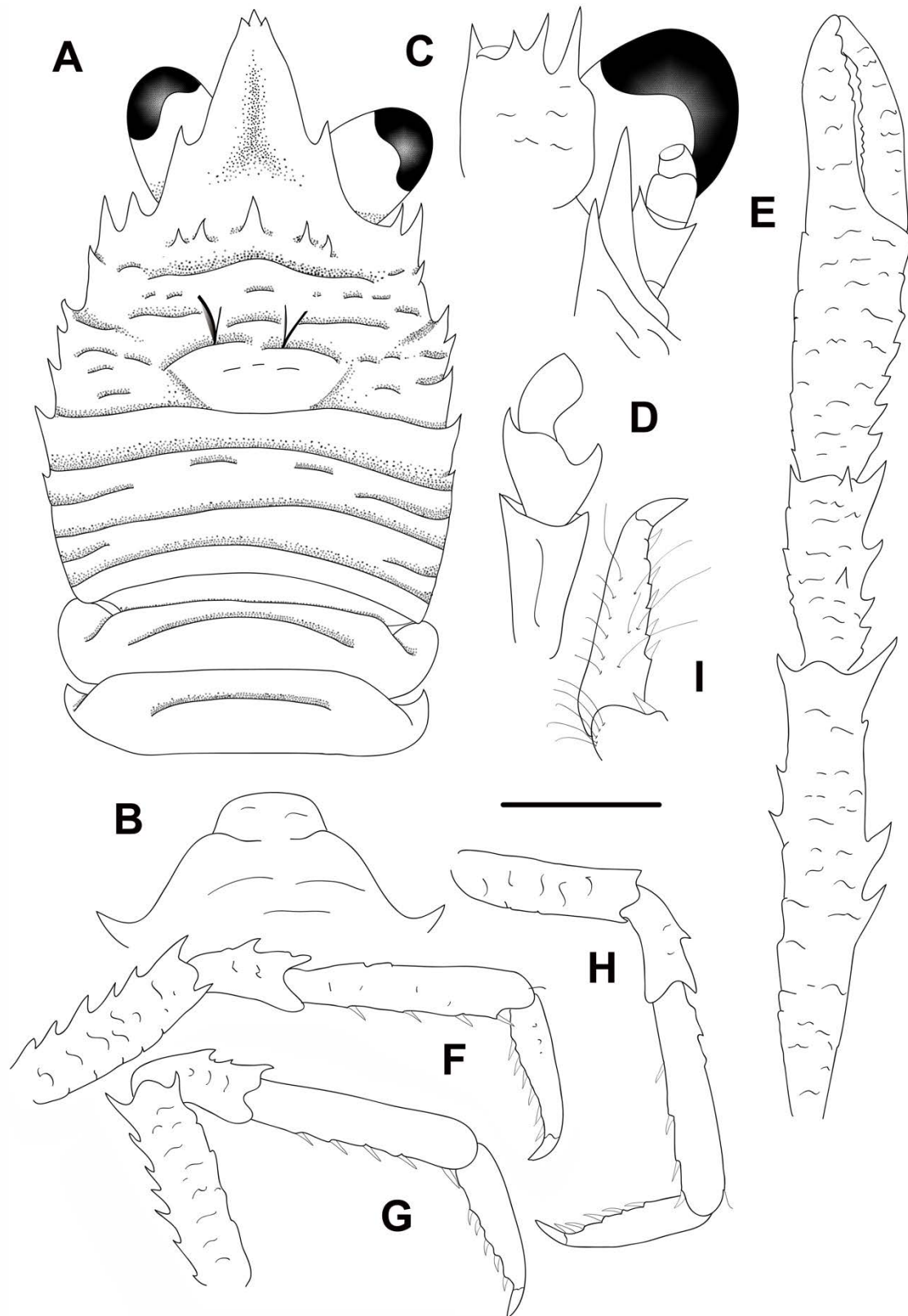
FIGURE 47. *Phylladiorhynchus pulchrus* **n. sp**., A-D, F-I, holotype male 1.6 mm (MNHN-IU-2014-13849); E, paratype male 1.5 mm (MNHN-IU-2014-13868): A, carapace and pleon, dorsal view. B, thoracic sternites 3 and 4. C, left cephalic region, showing antennular and antennal peduncles, ventral view. D, right Mxp3, lateral view. E, left P1, dorsal view. F, right P2, lateral view. G, right P3, lateral view. H, right P4, lateral view. I, dactylus of right P2, lateral view. Scale bar: A, E-H = 1.0 mm; B–D, I = 0.6 mm.

Vanuatu. SANTO Stn DS103, 15°34.1'S, 167°16'E, 10–80 m, 14 October 2006: 1 M 1.5 mm (MNHN-IU-2014-13868).

French Polynesia. MUSORSTOM 9 Stn CP1239, 09°42.2'S, 139°03.6'W, 89–95 m, 31 August 1997: 1 ov. F 2.0 mm (MNHN-IU-2014-13733).—no station: 1 M 1.8 mm (MNHN-IU-2019-2675).

Etymology. From the latin *pulcher*, beautiful, in reference to the beauty of this species.

Description. *Carapace:* Robust or massive, [0.9]0.9–1.1 times as long as broad; transverse ridges elevated, serrated, with few short setae, and few scattered long thick iridescent setae. Gastric region convex (uplifted dorsally) with some transverse ridges: epigastric ridge indistinct, with 5 spines (1 median and 2 pairs of spines laterally); anterior protogastric ridge not medially interrupted, laterally interrupted with some few scales to carapace margin, posterior protogastric ridge scale-like; anterior mesogastric ridge scale-like, laterally interrupted by anterior branch of cervical groove, laterally continuing with some few scales; anterior metagastric ridge scale-like, followed by some few scales on posterior metagastric area. Mid- transverse ridge not interrupted, medially depressed, preceded by cervical groove, followed by 1–2 not interrupted or minutely interrupted ridges, interspersed with 2 short lateral ridges. Lateral margins clearly convex, with 7 spines: first anterolateral spine well-developed, reaching end of lateral orbital spine, second spine (hepatic) well-developed, slightly dorsomesially from lateral margin, and followed by 5 branchial spines (3 anterior and, 2 posterior). Rostrum leaf-like, horizontal, dorsally flattish or slightly concave, [1.1]1.5–1.6 times as long as broad, length [0.4]0.4 and breadth [0.3]0.25–0.3 that of carapace; lateral margins serrated and convex, with well-developed supraocular spines, subapical spines well-developed. Pterygostomian flap ending in anterior spine, upper margin smooth or serrated, with series of elevated striae.

Sternum: As wide as long or slightly wider than long, lateral margins of posterior half slightly divergent. Sternite 3 broad, [2.2]–2.5 times as wide as long, anterior margin convex. Sternite 4 widely contiguous to sternite 3; surface flattened, smooth; greatest width [2.9]2.7–2.9 times that of sternite 3, [2.9]2.6–2.9 times as wide as long.

Pleon: Elevated ridges uplifted dorsally, with a few scattered short setae. Tergites 2–3 with anterior and posterior transverse elevated ridges; tergite 4 with anterior transverse ridge; tergites 5–6 smooth.

Eye: Eye stalk length about [1.3] times broader than long, peduncle distally setose, not distinctly expanded proximally; maximum corneal diameter [0.7] × rostrum width, as wide as eyestalk.

Antennule: Article 1 slightly longer than wide, with 4 distal spines: distomesial spine well-developed; proximal lateral spine absent.

Antenna: Article 1 with prominent mesial process distally not reaching lateral antennular spine. Article 2 with small distal spines laterally and mesially. Articles 3 and 4 unarmed.

Mxp3: Ischium with distinct distal spines on flexor and extensor margins. Merus [0.5]0.5–0.6 × length of ischium at midlength, with 0–1 median small spine and and 1 well-developed distal spines on extensor margin and 1 strong spine on flexor margin.

P1 (lost in holotype): 2.5–3.0 (males) times carapace length; subcylindrical, spiny and with scattered long stiff setae; merus, carpus and palm with spines along mesial, dorsal and lateral surfaces, distal and mesial spines usually stronger than others. Merus1.1 length of carapace, 2.5–2.7 times as long as carpus. Carpus 1.8–2.4 times as long as wide. Palm 1.3–1.6 × carpus length, 2.1–2.5 times as long as broad. Fingers unarmed, 0.8 × palm length.

P2–4 (lost in most specimens): Subcylindrical, moderately setose and spinose, with few scattered plumose setae. Meri successively shorter posteriorly: P3 merus [0.8]0.8 times length of P2 merus, P4 merus [0.8]–0.9 times length of P3 merus; P2 merus, [0.6]0.8 times carapace length, [3.5]–4.7 times as long as broad, [1.0]–1.4 times as long as P2 propodus; P3 merus [4.0]4.2–5.5 times as long as broad, [1.1]–1.3 times as long as P3 propodus; P4 merus [4.1]–5.2 times as long as broad, [0.9]–1.1 times as long as P4 propodus; extensor margin of P2 and P3 with row of spines, proximally diminishing, with prominent distal spine; P4 extensor margin irregular, unarmed other than small distal spine otherwise serrated on proximal half; flexor margins of all legs irregular, with distal spine. Carpi with 2 or 3 spines on extensor margin on P2–3, unarmed on P4; distal spine prominent on P2–3, smaller on P4; row of small spines below extensor margin on lateral surface of P2–3, unarmed on P4; flexor margins of P2–4 irregular, each with distal spine. Propodi stout, [4.2–5.2]4–5 times as long as broad; extensor margin irregular, unarmed or with minute proximal spines; flexor margin with 3–4 slender movable spines in addition to distal pair. Dactyli [0.7]–0.8 × length of propodi, ending in incurved, strong, sharp spine; flexor margin with 5–6 movable spines.

Eggs. Ov. F carried approximately 5–10 eggs of 0.3 mm diameter.

Colour. Unknown.

Genetic data. COI and 16S, Table 1.

Distribution. French Polynesia, Philippines and Vanuatu, from 10 to 97 m.

Remarks. *Phylladiorhynchus pulchrus* belongs to the group of species having 5 epigastric spines, 3 spines on the anterior branchial margin, gastric region strongly convex, the rostrum leaf-like (margins clearly convex and subapical spines present), and carapace ridges uplifted dorsally. The new species is closely related to *P. koumac* from New Caledonia and they can be distinguished by subtle differences:

- The proximal half of the extensor margin of the P2–4 propodi has well-developed spines in *P. koumac*, whereas these spines are obsolescent or absent in *P. pulchrus*.
- The P2–4 propodi are slender (6–7 times as long as wide) in *P. koumac*, whereas they are stout (4–5 times as long as wide) in *P. pulchrus*.

The sequences of *P. pulchrus* were 11% (COI) and 10% (16S) divergent from *P. koumac*.

***Phylladiorhynchus punctatus* n. sp.**

(Figs. 48, 50G, 56B)

Type material. *Holotype*. New Caledonia. LIFOU Stn 1648, 20°54.1'S, 167°03.3'E, 150–200 m, 7 November 2000: ov. F 2.8 mm (MNHN-IU-2014-13844).

Paratypes. New Caledonia. LIFOU Stn 1647, 20°42.45'S, 167°08.0'E, 150–200 m, 6 November 2000: 1 M 3.2 mm (MNHN-IU-2014-13845).—Stn 1648, 20°54.1'S, 167°03.3'E, 150–200 m, 7 November 2000: 1 F 1.8 mm (MNHN-IU-2014-13843).

New Caledonia. KOUMAC Stn KL17, 20.55685ºS, 164.0732667ºE, 92 m, 14 November 2019: 1 M 1.7 mm (MNHN-IU-2014-20101).

Etymology. From the Latin *punctum*, spot, in reference of the red spots covering the pleonal tergites of this species.

Description. *Carapace:* As long as broad, transverse ridges with few short setae. Gastric region flattened, with 4 transverse ridges: epigastric ridge indistinct, with 5 spines (1 median and 2 pairs of spines laterally); anterior protogastric ridge not medially interrupted, laterally interrupted with some few scales; anterior mesogastric ridge scale-like (with 1 to 3 scales), laterally interrupted by anterior branch of cervical groove,
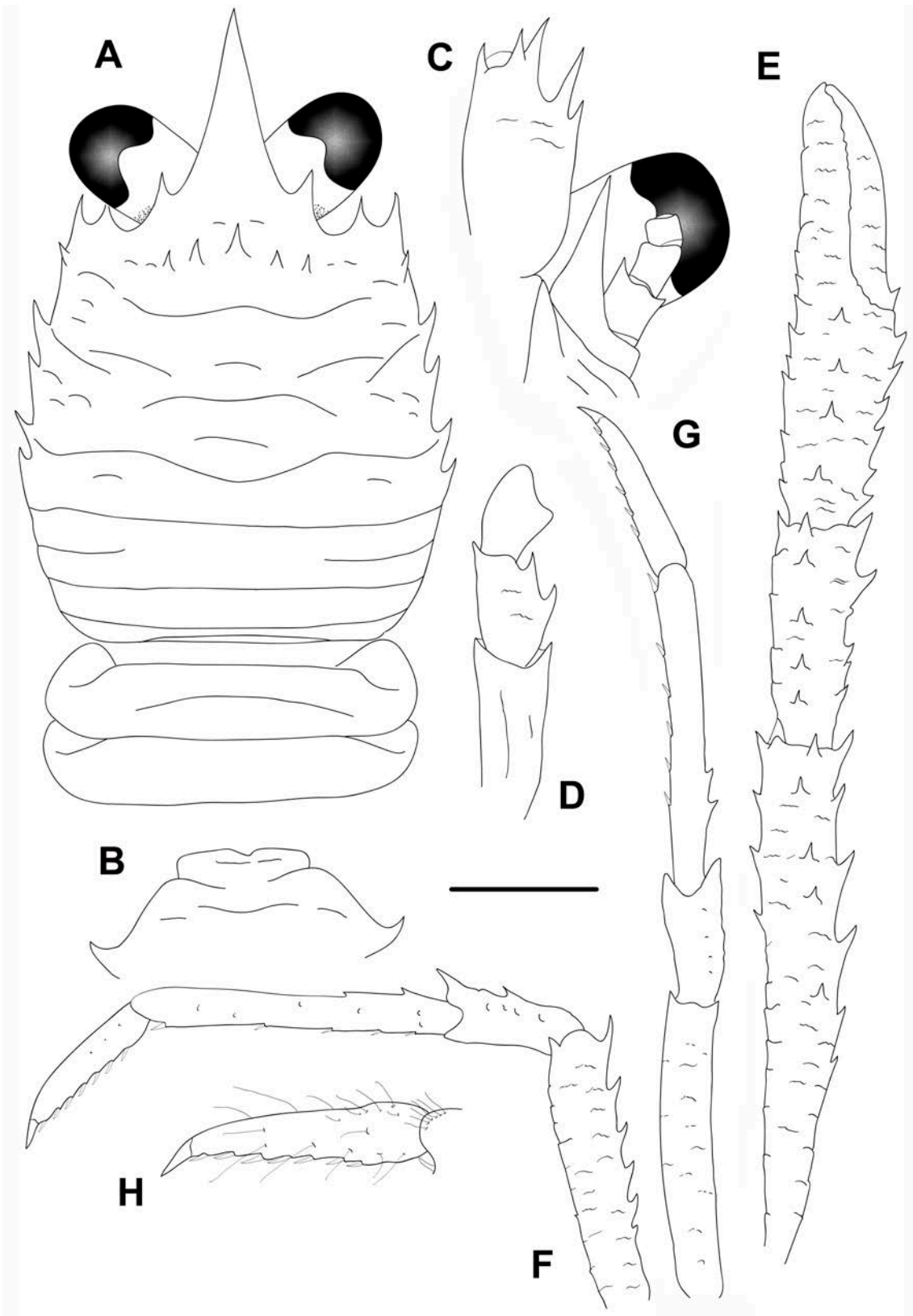
FIGURE 48. *Phylladiorhynchus punctatus* **n. sp**., holotype ovigerous female 2.8 mm (MNHN-IU-2014-13844); E, paratype male 3.2 mm (MNHN-IU-2014-13845): A, carapace and pleon, dorsal view. B, thoracic sternites 3 and 4. C, left cephalic region, showing antennular and antennal peduncles, ventral view. D, right Mxp3, lateral view. E, left P1, dorsal view. F, left P2, lateral view. G, left P3, lateral view. H, dactylus of right P2, lateral view. Scale bar: A, F-G = 1.0 mm; E = 1.3 mm; B–D, H = 0.6 mm.

laterally continuing uninterrupted to first branchial spine; anterior metagastric ridge scale-like and followed by some few scales on posterior metagastric area. Mid-transverse ridge not interrupted, medially depressed, preceded by a distinct cervical groove, followed by 2 not interrupted or minutely interrupted ridges, interspersed with 1 short lateral ridge and few short, scattered scales. Lateral margins straight or slightly convex, with 6 spines: first anterolateral spine well-developed, reaching end of lateral orbital spine, second spine (hepatic) well-developed, slightly dorsomesially from lateral margin, and followed by 4 branchial spines (2 anterior and 2 posterior). Rostrum triangular, horizontal, dorsally flattish or slightly concave, 1.4–[1.6] times as long as broad, length [0.4]0.4 and breadth [0.3]0.3 that of carapace; lateral margins smooth and straight, with well-developed supraocular spines, subapical spines absent. Pterygostomian flap ending in small spine, upper margin smooth.

Sternum: As wide as long. Sternite 3 sharply broad, [3.4]3.3–4.0 times as wide as long, anterior margin straight or moderately convex, with a median deep notch, moderately produced anterolaterally. Sternite 4 widely contiguous to sternite 3; surface depressed in midline, smooth; greatest width [2.4]1.5–1.7 times that of sternite 3, [3.3]–4.2 times as wide as long.

Pleon: Elevated ridges with short setae and with few scattered long setae. Tergite 2 with anterior and posterior transverse elevated ridges; tergites 3–4 with anterior transverse ridge; tergites 5–6 smooth.

Eye: Eye stalk length about 1.3 times broader than long, peduncle distally setose, not distinctly expanded proximally; maximum corneal diameter 1.0 × rostrum width, as wide as eyestalk.

Antennule: Article 1 1.3 times longer than wide, with 5 spines: distomesial spine small; proximal lateral spine well developed, always present.

Antenna: Article 1 with prominent mesial process, distally not reaching lateralmost antennular spine. Article 2 with small distomesial and distolateral spines. Articles 3 and 4 unarmed.

Mxp3: Ischium with distinct distal spines on flexor and extensor margins; crista dentata with row of spines along entire margin. Merus [0.5]0.5 × length of ischium, with well-developed distal spine on extensor margin and 2 strong spines on flexor margin.

P1 (lost in holotype and in males): 3.5 (females) times carapace length; subcylindrical, spiny and with scattered long stiff setae; merus, carpus and palm with spines along mesial, dorsal and lateral surfaces, distal and mesial spines usually stronger

than others. Merus 1.4 length of carapace, 2–2.5 times as long as carpus. Carpus 2.5–2.9 times as long as wide. Palm 1.1× carpus length, 2.2–3.5 times as long as broad. Fingers subequal in length to palm; fixed finger unarmed; movable finger with well-developed basal spine.

P2–4: Slender, subcylindrical, moderately setose and spinose. Meri successively shorter posteriorly: P3 merus [1.0]0.9–1.0 times length of P2 merus, P4 merus [0.9]0.9 times length of P3 merus. P2 merus, [0.7]0.8 times carapace length, [6.0]–8.0 times as long as broad, [1.0]1.3 times as long as P2 propodus; P3 merus [6.0]7.0 times as long as broad, [1.0]1.0 times as long as P3 propodus; P4 merus [5.5]4.5 times as long as broad, as long as P4 propodus; extensor margin of P2 and P3 with row of spines, proximally diminishing, with prominent distal spine; P4 extensor margin irregular, with small distal spine; flexor margins of P2–4 irregular, each with distal spine; P4 lateral surface with median row of 3 small spines, absent in P2–3. Carpi with 3 or 4 spines on extensor margin on P2–3, unarmed on P4; distal spine prominent on P2–3, smaller on P4; row of small spines below extensor margin on lateral surface of P2–3, unarmed on P4; flexor margins on P2-4 with distal spine. Propodi slender, 7.0–[9.0] times as long as broad; extensor margin usually armed with 1–2 small spines on proximal half of P2–4; flexor margin with 4 slender movable spines in addition to distal pair. Dactyli [0.6]–0.7 × length of propodi, ending in incurved, strong, sharp spine; flexor margin with 6–7 movable spines.

Colour. Base colour of carapace light orange; carapace, rostrum, supraocular spines and ocular peduncles covered by orange and golden-yellow spots, epigastric spines orange. Pleonal tergites 1–4 light orange, darker on lateral margins; tergites 3–4 each with two symmetrical vertical witthish stripes and 2 reddish spots. P2–4 witish, meri, carpi, propodi and dactyli covered with reddish bands, distal half of dactyli whitish.

Genetic data. COI and 16S, Table 1.

Distribution. New Caledonia and Chesterfield Islands, from 92 to 200 m**.**

Remarks. *Phylladiorhynchus punctatus* belongs to the group of species having 5 epigastric spines, 2 spines on the anterior branchial margin and the Mxp3 merus with 2 prominent spines along the flexor margin. *Phylladiorhynchus punctatus* resembles *P. kermadecensis* Schnabel & Ahyong, 2019 from New Zealand, however they can be distinguished by the following characters:

-       The rostrum margins are slightly concave in *P. kermadecensis,* whereas these margins are straight in *P. punctatus*.
-       The anterior mesogastric ridge is scale-like in *P. punctatus*, whereas this ridge is not medially interrupted in *P. kermadecensis*.

-        The anterior metagastric ridge is not medially interrupted in *P. punctatus*, whereas it is medially interrupted in *P. kermadecensis*.

The sequences of *P. punctatus* were 17% (COI) and 7% (16S) divergent from *P. kermadecensis*.

Phylladiorhynchus pusillus (Henderson, 1885)

(from Schnabel & Ahyong 2019)

Galathea pusilla Henderson, 1885: 407 (Twofold Bay, Australia, 275 m).—Henderson, 1888: 121, pl. 12, figs. 1, 1a, 1b (Twofold Bay, Australia, 275 m).—Whitelegge, 1900: 185 (off Bondi, New South Wales, 91 m).—Grant & McCulloch, 1906: 49, pl. 4, figs. 5, 5a (part, Port Phillip Heads, Victoria).

Phylladiorhynchus pusillus.—Davie, 2002: 66.—Poore, 2004: 238, fig. 66b (compilation, key).—Poore *et al.*, 2008: 22 (SW Australia, 95–439 m) (part).—Baba *et al.*, 2008: 176 (compilation, in part).—Rowden *et al.*, 2010, tab. 3 (in part).—Schnabel & Ahyong, 2019: 329, figs. 10-12 (selection of lectotype, southeastern, southern and western Australia and northern New Zealand, between 10 and 274 m).

Not *Galathea pusilla*.—Thomson, 1899: 193, pl. 21, fig. 7 (Whanganui, Cook Strait, Paterson Inlet, 14.6 m) (= *P. australis* Schnabel & Ahyong, 2019).—Chilton, 1906: 267 (Channel Islands, Auckland, 46 m) (= *P. australis* Schnabel & Ahyong, 2019).—Grant & McCulloch, 1906: 49 (part, Mast Head Island specimen = *P. spinosus* Schnabel & Ahyong, 2019).—Chilton, 1911: 303 (New Zealand) (= *P. australis* Schnabel & Ahyong, 2019).—Borradaile, 1916: 92 (off Three Kings Islands and off North Cape, 183–128 m) (= *P. australis* Schnabel & Ahyong, 2019).—Hale, 1927: 80 (South Australia, 75 fathoms) (= *P. australis* Schnabel & Ahyong, 2019).

Not *Phylladiorhynchus pusillus*.—Miyake & Baba, 1967: 234, fig. 6 (East China Sea, 102–196 m) (different species, undetermined).—Haig, 1973: 282 (S of Cape Everard (Victoria), S and SW of Mt Cann (Victoria) and off St. Helens Point, Tasmania, 110–183 m) (= *P. nui* Schnabel & Ahyong, 2019).—Baba, 1991: 486–487, fig. 4e, f (different species, undetermined).—Baba *et al.*, 2009: 287–289, figs. 263, 264 (different species, undetermined).—Lee *et al.*, 2019: 730, figs. 3, 4 (different species, undetermined).

Not *Phylladiorhynchus cf. pusillus*.—Ahyong, 2007: 42, fig. 20B, 22. (= *P. nui* Schnabel & Ahyong, 2019).

Records requiring verification:

Galathea pusilla.—Guiler, 1952: 36 (D'Entrecasteaux Channel, Tasmania).—Miyake, 1965: 635, fig. 1044 (no record).—Tirmizi, 1966: 175, fig. 1.—Zarenkov, 1968: 177, fig. 22 (Victoria, Australia, 110 m).—Lewinsohn, 1969: 116 (no record).

Phylladiorhynchus pusillus.—Baba, 1969: 4 (Sagami Bay, 200–300 m).—Baba, 2005: 201, 305 (key, synonymies, Kei Islands and Japan (Sagami Bay and W of Nagasaki), 146–549 m).

Genetic data. COI and 16S, Table 1.

Distribution. After the complete redescription by Schnabel & Ahyong (2019), the species is found along the southeastern, southern and western Australia and northern New Zealand, between 10 and 274 m.

Remarks. Schnabel & Ahyong (2019) provided a complete description of the species, with a comparison with other species. As these authors pointed out, *P. pusillus* shows a certain variability in the number of epigastric spines, recommending caution in the use of this character. The species is very close to *P. poeas*, from French Polynesia (see the differences under the Remarks of *P. poeas*).

Phylladiorhynchus serrirostris (Melin, 1939)

(Figs. 49, 50H)

Galathea serrirostris Melin, 1939: 72: figs 43–47 (type locality: Port Lloyd, Tokinoura, Hatsume, E of Chichijima (Bonin Islands), shallow to 128 m).—Miyake & Baba, 1965: 590, figs 5, 6 (Bonin Islands).

Records requiring verification:

Galathea serrirostris.—Miyake & Baba, 1966a: 67, fig. 8 (Amami-oshima, Ryukyu Islands, Japan, intertidal).

Phylladiorhynchus serrirostris.—Baba, 1969: 4 (W of Tanegashima, S Kyushu, Japan, 35–40 m).—Baba, 1977: 251 (Ternate, 2–4 m).—Baba, 1979: 644 (Marsegu Island, subtidal).—Tirmizi & Javed, 1980: 260, fig. 3 (Mozambique Channel, off South Africa, off Somalia Republic, and Andaman Sea, 38–138 m).—Baba, 1989: 61 (Palau Islands, subtidal).—Peyrot-Clausade, 1989: 112 (Tuamotu Archipelago, 5–
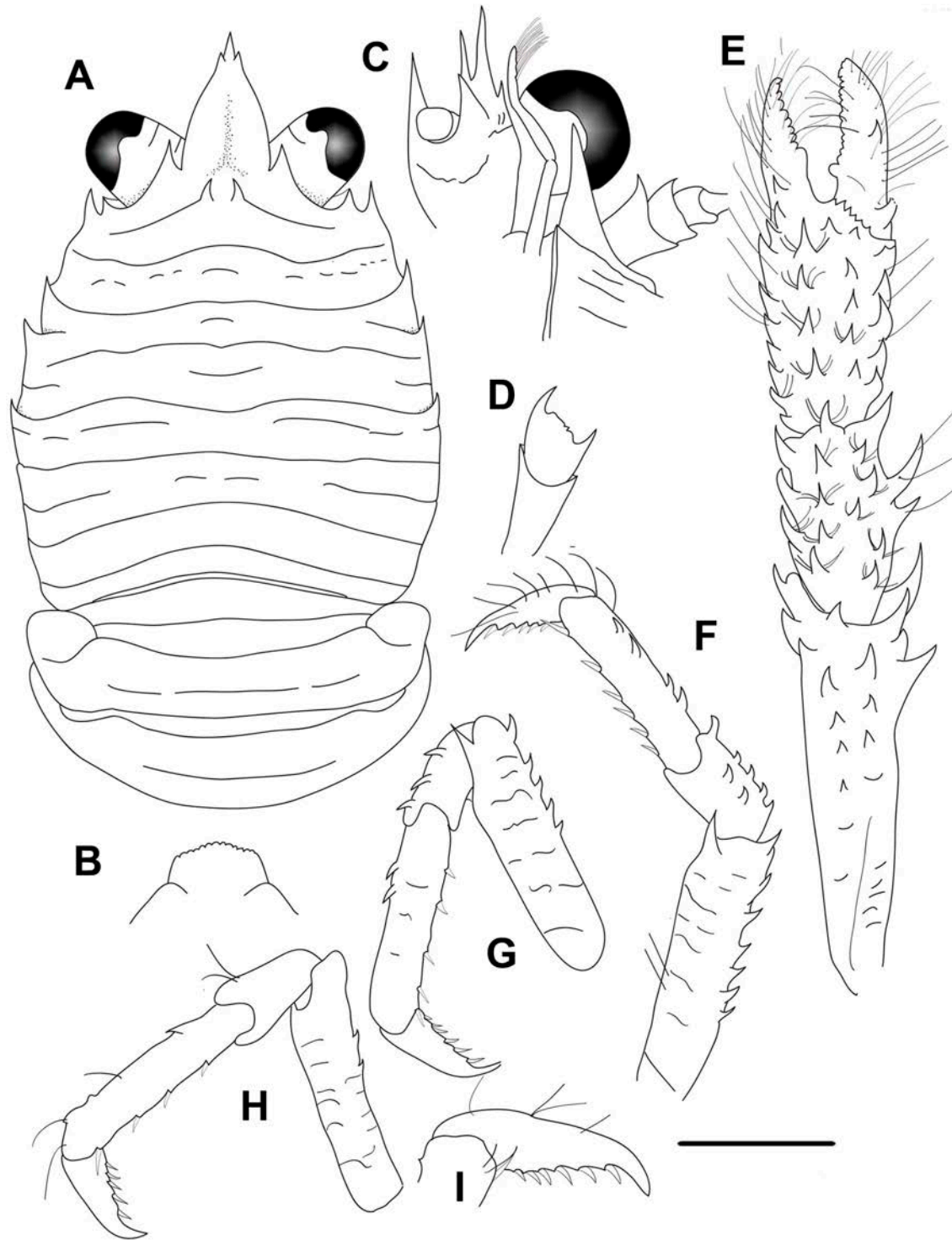
FIGURE 49. *Phylladiorhynchus serrirostris* (Melin, 1939), lectotype ovigerous female 2.9 mm (UPSZTY 183822): A, carapace and pleon, dorsal view. B, thoracic sternites 3 and 4. C, left cephalic region, showing antennular and antennal peduncles, ventral view. D, right Mxp3, lateral view. E, left P1, dorsal view. F, left P2, lateral view. G, left P3, lateral view. H, left P4, lateral view. I, dactylus of right P2, lateral view. Scale bar: A, E-H = 1.0 mm; B–D, I = 0.6 mm.

30 m).—Baba, 1990: 969 (Madagascar, 60 m).—Poupin, 1996a: 20 (compilation of French Polynesia records).

Type material. *Lectoype.* Dr. Sixten Bocks Japan exp. 1914. Bonin Islands (Ogasawara), Port Loyd. 23/7. Djup: dykare. Botten: korall. Det. G. Melin.: ov. F 2.9 mm (UPSZTY 183822)

Paralectotypes. Dr. Sixten Bocks Japan exp. 1914. Bonin Islands (Ogasawara), Port Loyd. 23/7. Djup: dykare. Botten: korall. Det. G. Melin: 12 M 1.9–3.0 mm, 11 ov. F 2.1–3.0 mm, 1 F parasitized 1.9 mm, 1 broken (UPSZTY 2531)

Description. *Carapace:* As long as or slightly longer than broad; transverse ridges with dense short setae and few scattered long and thick setae. Gastric region slightly convex with some transverse ridges: epigastric ridge distinct with 2 median spines, often followed by few short scales; anterior protogastric ridge not medially interrupted, nearly extending laterally to carapace margin, followed by a posterior protogastric scale-like ridge; anterior mesogastric ridge not medially interrupted, often followed by some scales on posterior mesogastric area; anterior metagastric ridge minutely medially interrupted, followed by a short median scale. Mid-transverse ridge not interrupted, cervical groove indistinct, followed by 2–3 not interrupted or minutely interrupted ridges, interspersed with 1–2 interrupted ridges. Lateral margins slightly convex, with 4 distinct spines: first anterolateral spine well-developed, reaching anteriorly to level of lateral orbital spine, hepatic margin unarmed; anterolateral spine followed by 3 branchial spines (2 anterior and 1 posterior). Rostrum leaf-like, horizontal, dorsally concave, [1.4]1.2–1.7 times as long as broad, length [0.3]–0.4 and breadth [0.2]–0.3 that of carapace; lateral margins serrated and slightly convex, with well-developed supraocular basal spines and small subapical spines. Pterygostomian flap ending in acute tooth, upper margin serrated.

Sternum: As wide as long. Sternite 3 moderately broad, [2.0]–2.1 times as wide as long, anterior margin serrated and convex, slightly produced anterolaterally. Sternite 4 widely contiguous to sternite 3; anterolaterally serrated, surface depressed in midline, smooth; greatest width 2–[3] times that of sternite 3, [2.7] times as wide as long.

Pleon: Elevated ridges with short setae and a few scattered long setae. Tergite 2–3 with anterior and posterior transverse elevated ridges; tergite 4 with anterior transverse ridge only; tergites 5–6 smooth.

Eye: Eye stalk length about [0.8]–0.9 times broader than long, peduncle distally setose, not distinctly expanded proximally; maximum corneal diameter [0.6] × rostrum width, as wide as eyestalk.

Antennule: Article 1 slightly longer than wide, with 5 distal spines: distomesial spine well-developed;

proximal lateral spine small, always present.

Antenna: Article 1 with prominent mesial process, distally falling well short lateralmost antennular spine. Article 2 with well-developed distomesial and distolateral spines. Article 3 with distomesial spine. Article 4 unarmed.

Mxp3: Ischium with distinct distal spines on flexor and extensor margins. Merus [0.6]–0.7 × length of ischium, with well-developed distal spine on extensor and flexor margins.

P1: 2.4–3 (males), [2.4]–3.0 (females) times carapace length; subcylindrical, densely spiny and densely with long stiff setae; merus, carpus and palm with several rows of spines along mesial, dorsal and lateral surfaces, distal and mesial spines usually stronger than others. Merus 0.6–[0.9] length of carapace, 1.6–[2.0] times as long as carpus. Carpus 1.4–[1.6] times as long as wide. Palm [1.1]–1.4 × carpus length, 1.4–[1.6] times as long as broad. Fingers [0.8]–0.9 × palm length fixed finger with 2 basal spines; movable finger with 2 basal spines.

P2–4: Stout, setose and spinose. Meri successively shorter posteriorly: P3 merus [0.7]0.7 times length of P2 merus, P4 merus [0.8]0.8 times length of P3 merus. P2 merus, 0.4–[0.6] times carapace length, [4.2]3.5–4.5 times as long as broad, [1.2]0.9–1.3 times as long as P2 propodus; P3 merus [3.1]–4 times as long as broad, [1.2–]0.9–1.3 times as long as P3 propodus; P4 merus [3.8] times as long as broad, [0.9] times as long as P4 propodus; extensor margin of P2 and P3 with row of spines, proximally diminishing, with prominent distal spine; P4 extensor margin irregular, with 1–2 spines, ; flexor margin irregular, with distal spine on P2–4; P4 lateral surface with 2–3 spines. Carpi with 2–4 well-developed spines on extensor margin on P2–3, unarmed on P4; distal spine prominent on P2–3, smaller on P4; flexor margin unarmed. Propodi stout, [4–5]3.6–5 times as long as broad; extensor margin irregular, armed with 1–4 spines on P2–P4; flexor margin with 3–4 slender movable spines in addition to distal pair. Dactyli [0.5–0.6]0.5–0.8 × length of propodi, ending in incurved, strong, sharp spine; flexor margin with 4–6 movable spines.

Eggs: Ov. F carried approximately 10–50 eggs of 0.2–0.4 mm diameter.

Colour. Unknown.

Genetic data. No data.

Distribution. Japan: Bonin Islands, Ryukyu Islands, intertidal to 128 m

Remarks. *Phylladiorhynchus serrirostris* was described as *Galathea serrirostris* by Melin (1939), from specimens collected in Bonin Islands, Japan. Tirmizi (1966) considered *G. serrirostris* identical to *G. pusilla*, however, Miyake & Baba (1965, 1967) considered *G. pusilla* and *G. serrirostris* as close, but not identical species. After, Baba (1991) included *P. serrirostris* as a junior synonym of *P. integrirostris*. The study of the type material of *P. serrirostris,* and its comparison with the numerous specimens of *P. integrirostris* suggests that they can be considered as different species. Therefore, we have considered *P. serrirostris* as a valid species. The 2 species belong to the group of species having 2 epigastric spines, hepatic margin unarmed and 2 spines on the anterior branchial margin. *Phylladiorhynchus serrirostris* is easily differentiable from *P. integrirostris* by the following characters:

-       The anterior metagastric ridge is not medially interrupted in *P. serrirostris,* whereas it is medially interrupted in *P. integrirostris.*
-       The posterior gastric ridges (posterior protogastric, mesogastric and metagastric) are usually present in *P. serrirostris,* whereas they are absent in *P. integrirostris.*
-       The pleonal tergite 3 has 2 ridges (anterior and posterior) in *P. serrirostris,* whereas there is only the anterior ridge in *P. integrirostris.*
-       The P1 are densely spinose in *P. serrirostris*, whereas they are scarcely spinose in *P. integrirostris.*

Phylladiorhynchus spinosus **Schnabel & Ahyong, 2019**

(Figs. 30D-F, O-P, 50I)

Phylladiorhynchus spinosus Schnabel & Ahyong, 2019: 338, figs 13–14.

Phylladiorhynchus integrirostris.—Baba, 1991: 486 (in part), fig 4.

Material examined. New Caledonia CHALCAL 1 Stn DC26, 19°10.7'S,158°35'E, 48 m, 18 July 1984: 1 M 2.6 mm (MNHN-IU-2013-9439 (Ga-2055)).—Stn DC55, 21°23.9'S, 158°59.6'E, 55 m, 25 July 1984: 1 M 2.9 mm (MNHN-IU-2016-473 (Ga-2056)).—Ouen Is. Prony Bay. Stn 121, 22º28'S, 166º43.1'E, 12 m, August 1984: 1 ov. F 3.7 mm (MNHN-IU-2019-2613).—Stn 242, 22º22'S, 167º02.2'E, 25 m, October 1984: 1 M 3.4 mm (MNHN-IU-2019-2619).—Lagon Est. Stn 713, 21º22.6'S, 166º00.7'E, 34–35 m, 11 August 1986: 1 M 3.3 mm (MNHN-IU-2016-492), 1 M 2.7 mm (MNHN-IU-2016-491).—Stn 782, 21º06.1'S, 165º36.7'E, 30 m January 1987: 1 M 2.7 mm (MNHN-IU-2019-2621).

The genetic divergences between *P. spinosus* and other closely related species were around 8% (COI) and 6-7% (16S).

The subtle morphological differences among specimens of *P. spinosus* from different localities were mentioned by Schnabel & Ahyong (2019). Unfortunately, we have not examined the type specimens of *P. spinosus,* however, we suggest that this species is probably restricted to Queensland, Norfolk Ridge and Norfolk Islands area. Their material from Western Australia could be similar to *P. asclepius*, although it should be confirmed in the future.

Phylladiorhynchus talaus n. sp.

(Figs. 50J, 51)

Type material. *Holotype.* Western Australia. Montilivet Island Stn 117/K12, 14º17.3'S, 125º13.534'E, 0–11 m, 25 October 2012: 1 ov. F 1.9 mm (WAM C51399).

Paratypes. Indonesia. Rumphius Exp. II. 1975, NE coast Marsegu Is., on coral. 18 January 1975: 1 M 2.7 mm (MNHN-IU-2014-23832 (Ga-1154)).

Papua New Guinea. PAPUA NIUGINI Stn PB39, 05°15,9'S, 145°47,1'E, 18–27 m, 6 December 2012: 1 M 2.1 mm (MNHN-IU-2019-2637).—KAVIENG Stn KB36, 02º38.8'S, 150º38.4'E, 3–8 m, 13 June 2014: 1 M 2.3 mm, 1 F 2.2 mm (MNHN-IU-2014-13664).—Stn KB58, 02º34.1'S, 150º37.5'E, 12 m, 22 June 2014: 1 F 2.5 mm (MNHN-IU-2016-5858).—Stn KB60, 02º32.5'S, 150º35.3'E, 20 m, 23 June 2014: 1 F 1.8 mm (MNHN-IU-2016-476).

Western Australia. Adele Island Stn 01/K09-adhoc, 15º31.406'S, 123º12.318'E, 0–20 m, 13 October 2009: 1 ov. F 2.4 mm (WAM C43997).—Stn 02/K09-adhoc, 15º31.152'S, 123º11.742'E, 0–14 m, 14 October 2009: 1 ov. F 1.8 mm (WAM C43826).—Ningaloo Reef. 22.7581ºS, 113.6491ºE, 13 m, 1 May 2009. 1 F 1.8 mm (UF217029).—22.6083ºS 113.6249ºE 10 m 1 May 2009 1 M 2.1 mm (UF22293).

Etymology. From the name *Talaus*, an Argonaut, son of Bias and Pero. The name is considered a substantive in apposition.

Description. *Carapace:* As long as or slightly longer than broad; transverse ridges with dense short setae and few scattered long and thick iridescent setae. Gastric region slightly convex with 4 transverse ridges: epigastric ridge distinct with 2 median spines and some lateral short scales; anterior protogastric ridge not medially interrupted, nearly extending laterally to carapace margin; anterior mesogastric ridge not medially interrupted, laterally continuing to first branchial spine; anterior metagastric scale-like or
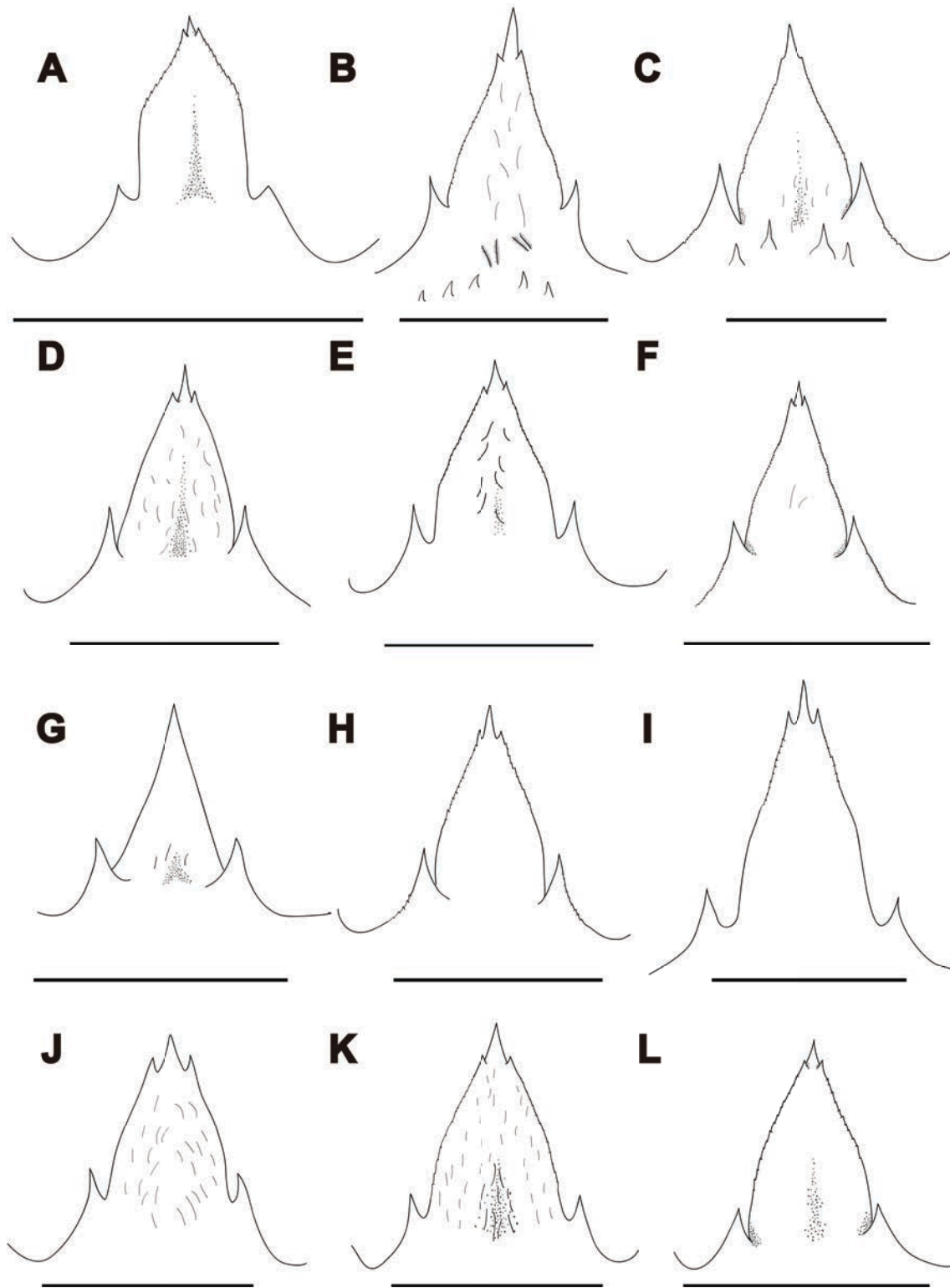
FIGURE 50. Rostrum, dorsal view. A, *Phylladiorhynchus phlias* **n. sp**., paratype male 1.4 mm (MNHN-IU-2014-1388). B, *P. poeas* **n. sp**., paratype male 3.3 mm (MNHN-IU-2014-13737). C, *P. pollux* **n. sp**., holotype ovigerous female 3.5 mm (MNHN-IU-2014-13797). D, *P. porteri* **n. sp**., paratype female 2.4 mm (MNHN-IU-2014-23831). E, *P. priasus* **n. sp**., paratype ovigerous female 2.1 mm (MAU-385). F, *P. pulchrus* **n. sp**., paratype male 1.8 mm (MNHN-IU-2019-2675). G, *P. punctatus* **n. sp**., paratype male 1.7 mm (MNHN-IU-2019-20101). H, *P. serrirostris* (Melin, 1939), paralectotype male 2.3 mm (UPSTY2531). I, *P. spinosus* Schnabel & Ahyong, 2019, male 3.3 mm (MNHN-IU-2016-492). J, *P. talaus* **n. sp**., paratype ovigerous female 2.4 mm (WAM C43997). K, *P. tiphys* **n. sp**., holotype male 2.4 mm (MNHN-IU-2014-13794). L, *P. zetes* **n. sp**., holotype male 2.1 mm (UF30059). Scale bars: 1 mm.

313
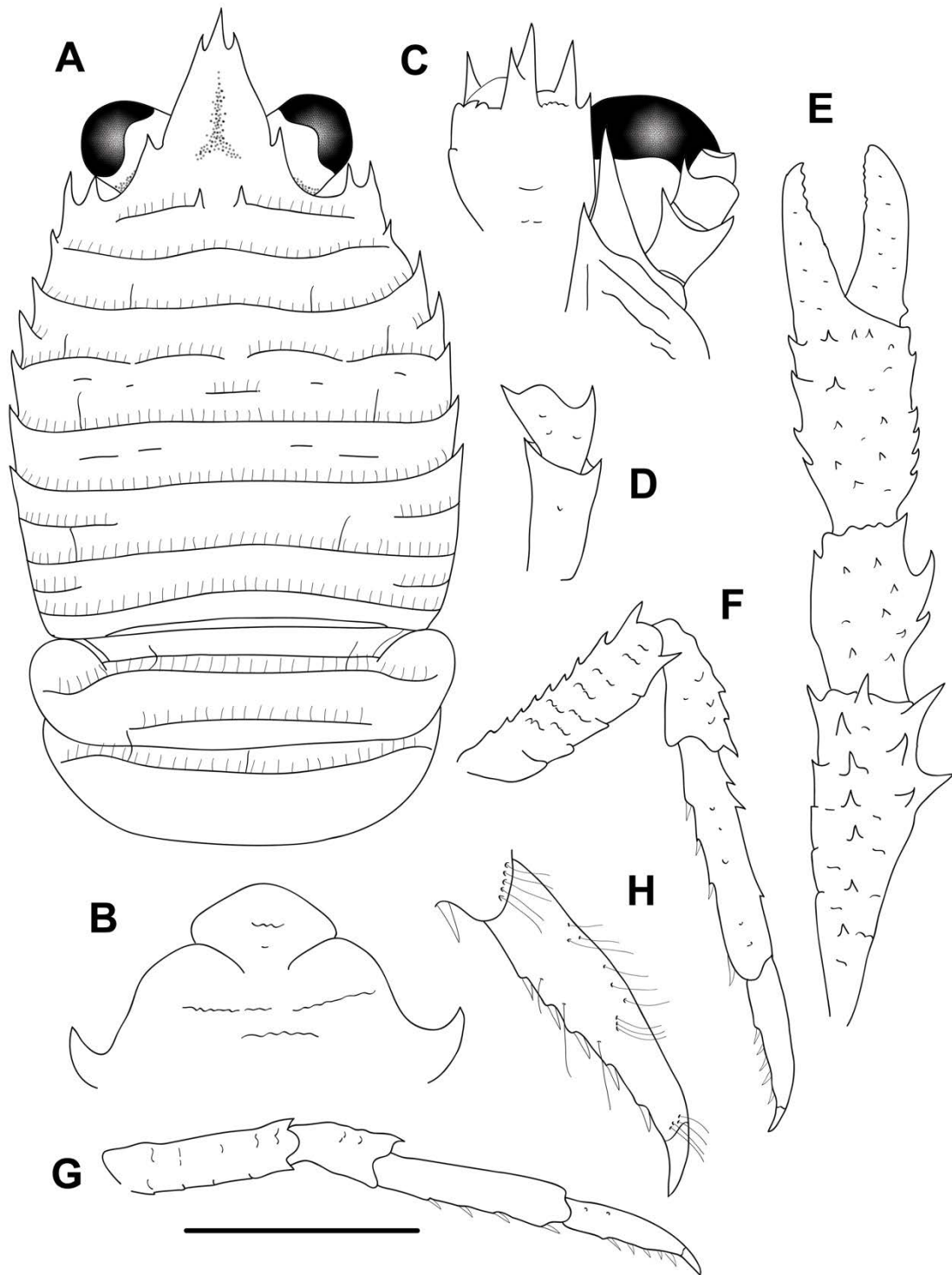
FIGURE 51. *Phylladiorhynchus talaus* **n. sp**., holotype ovigerous female 1.9 mm (WAM C51399); E, paratype female 2.2 mm (MNHN-IU-2014-13664): A, carapace and pleon, dorsal view. B, thoracic sternites 3 and 4. C, left cephalic region, showing antennular and antennal peduncles, ventral view. D, right Mxp3, lateral view. E, left P1, dorsal view. F, right P2, lateral view. G, right P4, lateral view. H, dactylus of right P2, lateral view. Scale bar: A, E-G = 1.0 mm; B–D, H = 0.6 mm.

medially and laterally minutely interrupted, sometimes followed by short scales. Mid-transverse ridge not interrupted, medially slightly depressed, cervical groove indistinct, followed by 2 not interrupted or minutely interrupted ridges, interspersed with 2 short lateral ridges and some few short scales. Lateral margins convex slightly convex, with 7 distinct spines: first anterolateral spine well-developed, reaching anteriorly to level of lateral orbital spine, second spine (hepatic) small, slightly dorsomesially from lateral margin, and followed by 5 branchial spines (3 anterior and 2 posterior). Rostrum leaf-like, horizontal, dorsally convex, [1.2]–1.3 times as long as broad, length [0.3]–0.4 and breadth [0.3]0.3 that of carapace; lateral margins smooth or minutely serrated and convex, with well-developed supraocular basal spines and small subapical spines (tridentiform). Pterygostomian flap with anterior spine, upper margin smooth.

Sternum: As wide as long. Sternite 3 quadrangular, 1.5–[1.7] times as wide as long, anterior margin convex, anterolaterally rounded. Sternite 4 widely contiguous to sternite 3; anterolaterally serrated, surface depressed in midline, smooth; greatest width [2.5]–3.3 times that of sternite 3, 3.3–[3.5] times as wide as long.

Pleon: Elevated ridges with short setae and a few scattered long setae. Tergite 2 with anterior and posterior transverse elevated ridges; tergite 3–4 with anterior transverse ridge, posterior transverse ridge absent; tergites 5–6 smooth.

Eye: Eye stalk length about 0.9–[1.1] times broader than long, peduncle distally setose, not distinctly expanded proximally; cornea expanded distally, maximum corneal diameter [1.1]–1.2 × rostrum width*,* as wide as eyestalk.

Antennule: Article 1 slightly longer than wide, with 5 distal spines: distomesial spine well-developed; proximal lateral spine small, always present.

Antenna: Article 1 with prominent mesial process, distally falling short or overreaching lateral antennular spine. Article 2 with well-developed distomesial and distolateral spines. Articles 3 with small distomesial spine. Article 4 unarmed.

Mxp3: Ischium with distinct distal spines on flexor and extensor margins. Merus 0.7–[0.8]× length of ischium, with well-developed distal spine on extensor and flexor margins.

P1: 2.3 (males), [2.0]–2.5 (females) times carapace length; subcylindrical, spiny and with long stiff setae; merus, carpus and palm with spines along mesial, dorsal and lateral surfaces, distal and mesial spines usually stronger than others. Merus [0.8]0.6–0.9 length of carapace, [1.9]1.6–2.1 times as long as carpus. Carpus [1.6]1.5–1.9 times as

long as wide. Palm [1.1]–1.3 × carpus length, [1.5]–2.3 times as long as broad. Fingers unarmed, 0.7–[1.1] × palm length.

P2–4 (P3 lost in holotype): Setose and spinose. Meri successively shorter posteriorly: P3 merus 0.8–0.9 times length of P2 merus, P4 merus 0.7–0.9 times length of P3 merus. P2 merus, [0.5]–0.6 times carapace length, [3.5]–4.5 times as long as broad, [1.1]–1.3 times as long as P2 propodus; P3 merus 3.5–4.0 times as long as broad, 0.9 times as long as P3 propodus; P4 merus 3.0–[3.3] times as long as broad, 0.9–[1.1] times as long as P4 propodus; extensor margin of P2 and P3 with row of spines, proximally diminishing, with prominent distal spine; P4 extensor margin irregular, unarmed; flexor margin irregular, with distal spine on P2–4. Carpi with 4 spines on extensor margin on P2–3, unarmed on P4; distal spine prominent on P2–3, absent on P4; granules below extensor margin on lateral surface of P2–4; flexor margin unarmed. Propodi stout, [4.3–4.7]5.0–5.8 times as long as broad; extensor margin irregular, armed with 3 spines; flexor margin with 3–4 slender movable spines in addition to distal pair. Dactyli [0.7–0.8]0.6 × length of propodi, ending in incurved, strong, sharp spine; flexor margin with 5–6 movable spines.

Eggs: Ov. F carried approximately 15–40 eggs of 0.4–0.5 mm diameter.

Colour. Unknown.

Genetic data. COI and 16S, Table 1.

Distribution. Indonesia, Marsegu Island (Seram Island), Papua New Guinea, and Western Australia, from 0 to 27 m.

Remarks. *Phylladiorhynchus talaus* belongs to the group of species having 2 epigastric spines, 1 hepatic spine and 3 spines on anterior branchial margin. The closest species is *P. triginta* Schnabel & Ahyong, 2019 from Tasman Sea and Norfolk Island, but they are easily differentiated by several characters (see the differences under the Remarks of this species).

The mean intraspecific genetic divergences were 2.3% (COI) and 0.2% (16S).

Phylladiorhynchus tiphys **n. sp.**

(Figs. 50K, 52)

Type material. *Holotype.* New Caledonia. SURPRISES Stn DW1395, 18°17.6'S, 163°01.9'E, 34–36 m, 13 May 1999: M 2.4 mm (MNHN-IU-2014-13794).
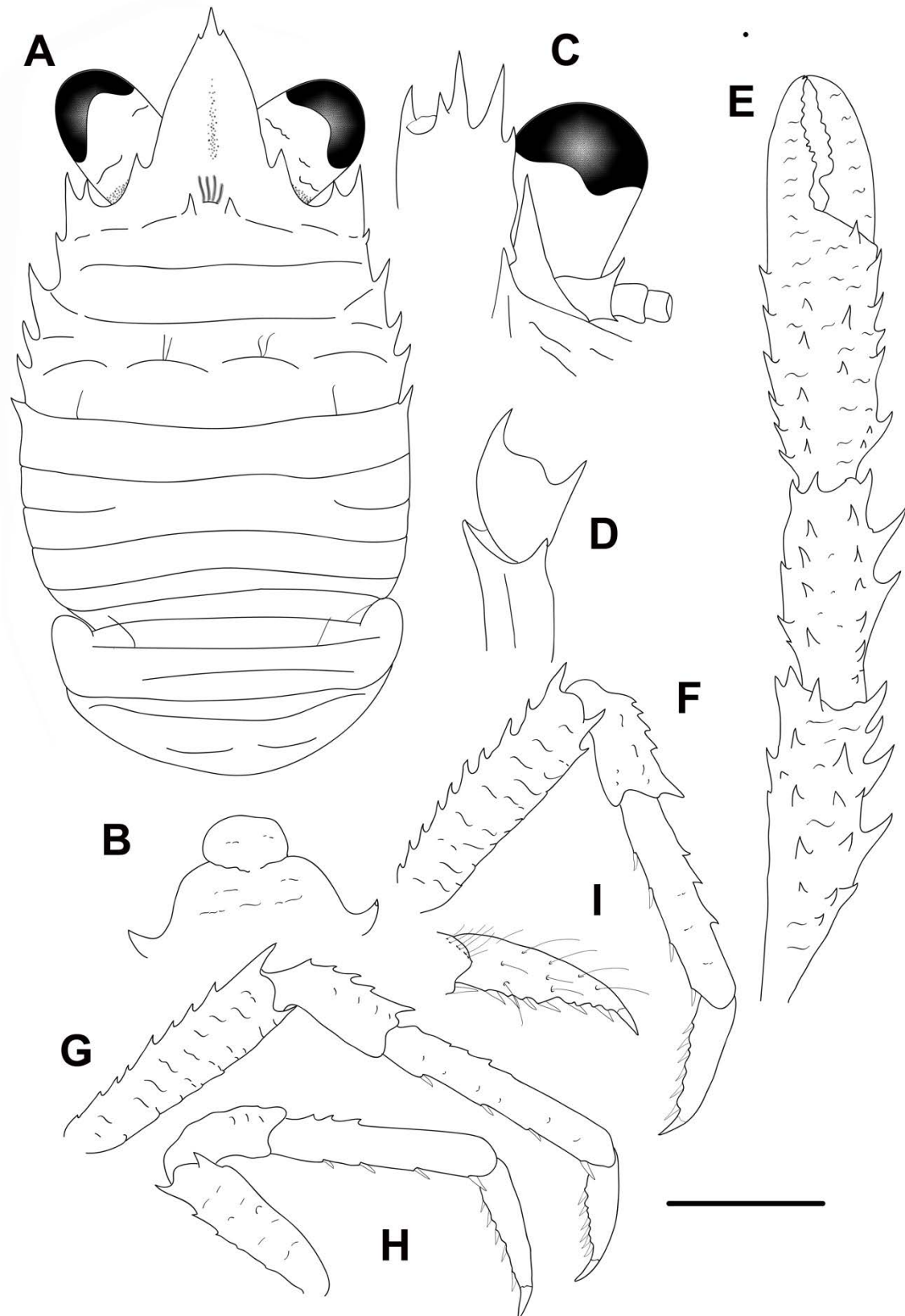
FIGURE 52. *Phylladiorhynchus tiphys* **n. sp**., holotype male 2.4 mm (MNHN-IU-2014-13794): A, carapace and pleon, dorsal view. B, thoracic sternites 3 and 4. C, left cephalic region, showing antennular and antennal peduncles, ventral view. D, right Mxp3, lateral view. E, left P1, dorsal view. F, right P2, lateral view. G, right P3, lateral view. H, right P4, lateral view. I, dactylus of right P2, lateral view. Scale bar: A, E-H = 1.0 mm; B–D, I = 0.6 mm.

Paratypes. New Caledonia. CHALCAL 2 Stn DW80, 23°27'S, 168°02'E, 80–160 m, 31 October 1986: 2 M 2.4–2.9 mm, 1 ov. F 2.1 mm (MNHN-IU-2016-477).

Etymology. From the name *Tiphys*, an Argonaut, son of Hagnias. The name is considered a substantive in apposition.

Description. *Carapace:* As long as or slightly longer than broad; transverse ridges with dense short setae and few scattered long and thick iridescent setae. Gastric region slightly convex with 4 transverse ridges: epigastric ridge distinct with 2 median spines, scale between spines with thick setae, short scales laterally; anterior protogastric ridge not medially interrupted, nearly extending laterally to carapace margin; anterior mesogastric ridge not medially interrupted, laterally continuing to first branchial spine; anterior metagastric ridge scale-like. Mid-transverse ridge not interrupted, medially slightly depressed, preceded by a shallor or indistinct cervical groove, followed by 2 not interrupted or minutely interrupted ridges, interspersed with 1 short lateral ridge and some few short scales. Lateral margins straight or slightly convex, with 6 distinct spines: first anterolateral spine well-developed, reaching anteriorly to level of lateral orbital spine, second spine (hepatic) small, slightly dorsomesially from lateral margin, and followed by 4 branchial spines (3 anterior and 1 posterior). Rostrum leaf-like, horizontal, dorsally convex, [1.2]–1.7 times as long as broad, length [0.4]0.4 and breadth [0.3]0.3 that of carapace; lateral margins minutely serrated and convex, with well-developed supraocular basal spines and small subapical spines. Pterygostomian flap with anterior spine, upper margin smooth.

Sternum: As wide as long. Sternite 3 moderately broad, 1.2–[1.5] times as wide as long, anterior margin convex, anterolaterally projected. Sternite 4 widely contiguous to sternite 3; anterolaterally smooth, surface depressed in midline, smooth; greatest width [3.0]–3.5 times that of sternite 3, 2.5–3.0 times as wide as long.

Pleon: Elevated ridges with short setae and a few scattered long setae. Tergite 2 with anterior and posterior transverse elevated ridges; tergite 3 with anterior transverse ridge, posterior transverse ridge interrupted; tergite 4 with anterior transverse ridge; tergites 5–6 smooth.

Eye: Eye stalk length about [1.1] times broader than long, peduncle distally setose, not distinctly expanded proximally, with few short transverse striae on lateral surfaces; cornea expanded distally, maximum corneal diameter [0.6] × rostrum width, as wide as eyestalk.

Antennule: Article 1 slightly longer than wide, with 5 distal spines: distomesial spine well-developed; proximal lateral spine small, always present.

Antenna: Article 1 with prominent mesial process distally not reaching lateralmost antennular spine. Article 2 with well-developed distomesial and distolateral spines. Articles 3 and 4 unarmed.

Mxp3: Ischium with distinct distal spines on flexor and extensor margins. Merus [0.8] × length of ischium, with well-developed distal spine on extensor and flexor margins.

P1: [2.4]–3.0 (males), 2.3 (females) times carapace length; subcylindrical, spiny and with long stiff setae; merus, carpus and palm with spines along mesial, dorsal and lateral surfaces, distal and mesial spines usually stronger than others. Merus [0.8]–0.9 length of carapace, [1.3]–2 times as long as carpus. Carpus 2.0–[2.5] times as long as wide. Palm [1.1]–1.2 × carpus length, 2.0–[2.2] times as long as broad. Fingers unarmed, [0.7]–0.8 × palm length.

P2–4: Stout, setose and spinose. Meri successively shorter posteriorly: P3 merus [0.9] times length of P2 merus, P4 merus [0.7] times length of P3 merus. P2 merus, [0.7] times carapace length, [3.5]–4.7 times as long as broad, [1.2]1.2 times as long as P2 propodus; P3 merus [3.9] times as long as broad, [1.1] times as long as P3 propodus; P4 merus [3.2]–3.5 times as long as broad, [0.9]0.9 times as long as P4 propodus; extensor margin of P2 and P3 with row of spines, proximally diminishing, with prominent distal spine; P4 extensor margin irregular, with some spines; flexor margin irregular, with distal spine on P2–4. Carpi with 4 spines on extensor margin on P2–3, unarmed on P4; distal spine prominent on P2–3, absent on P4; granules below extensor margin on lateral surface of P2–4; flexor margin unarmed. Propodi stout, [4.5–5.5]5.5–6.0 times as long as broad; extensor margin irregular, armed with 3 spines; flexor margin with 3–4 slender movable spines in addition to distal pair. Dactyli [0.6–0.7]0.5–0.7 × length of propodi, ending in incurved, strong, sharp spine; flexor margin with 5–6 movable spines.

Eggs: Ov. F (MNHN-IU-2016-477) carried 17 eggs of 0.3 mm diameter.

Colour. Unknown.

Genetic data. COI and 16S, Table 1.

Distribution. New Caledonia, between 34 and 160 m.

Remarks. *Phylladiorhynchus tiphys* belongs to the group of species having 2 epigastric spines, 1 hepatic spine, and 3 spines on the anterior branchial margin. *Phylladiorhynchus tiphys* closely resembles to *P. zetes* from the French Polynesia (see the differences under the Remarks of this species).

Phylladiorhynchus triginta Schnabel & Ahyong, 2019

Phylladiorhynchus triginta Schnabel & Ahyong, 2019: 339, figs. 12, 14.

Phylladiorhynchus integrirostris.—Ahyong, 2007: 42, fig. 21.

Genetic data. COI, Table 1.

Distribution. Tasman Sea, Lord Howe Island, Middleton Reef and Norfolk Island at 10–84 m (Schnabel & Ahyong 2019).

Remarks. The species belongs to the group of species with 2 epigastric spines, hepatic margin armed with 1 small spine and 3 spines along the anterior branchial margin. The closest relative is *P. talaus*, from Indonesia, Papua New Guinea, and Western Australia. The two species can be differentiated by the following characters:

- The rostrum has well-developed subapical spines in *P. talaus*, whereas these spines are minute in *P. triginta*.

- The thoracic sternite 3 is quadrangular (less than twice wider than long) in *P. talaus*, whereas this sternite is moderately broad (twice as wide as long) in *P. triginta*.

The genetic divergence between *P. triginta* and *P. talaus* is very high, 27% (COI).

Phylladiorhynchus zetes n. sp.

(Figs. 50L, 53, 56C)

Type material. *Holotype.* French Polynesia. Marquesas Islands. Nuku Hiva . Ohotea Point, W side of Taiohae bay, 08.9309ºS, 140.0978ºW, 36 m, 28 November 2012 : M parasitized 2.1 mm (UF30059).

Paratypes: French Polynesia. Marquesas Islands. PAKAIHI I TE MOANA Stn MQ2-GR-B, 08°56.231'S, 140°07.240'W, 20–23 m, 7 January 2012: 4 M 1.2–1.6 mm, 1 ov. F 2.3 mm, 3 F 1.2–1.7 mm (MNHN-IU-2019-2639).—Stn MQ11-GRS, 10°00.845'S, 139°07.345'W, 6–12 m, 15 January 2012: 1 F 1.7 mm (MNHN- IU-2019-2602).—Stn MQ15-GR-B, 10°28.31'S, 138°40.68'W, 0–28 m, 17 June 2012: 2 M 2.0–2.2 mm (MNHN-IU-2019-2593).—Stn MQ19-B, 9°45.672'S, 138°50.695'W, 10–25 m, 21 January 2012: 2 M 1.8–2.3 mm (MNHN-IU-2019-2600).—Stn MQ27-GR-B, 08°40.690'S, 140°37.233'W, 5–22 m, 25 January 2012: 1 M 1.5 mm (MNHN-IU-2019-2589).
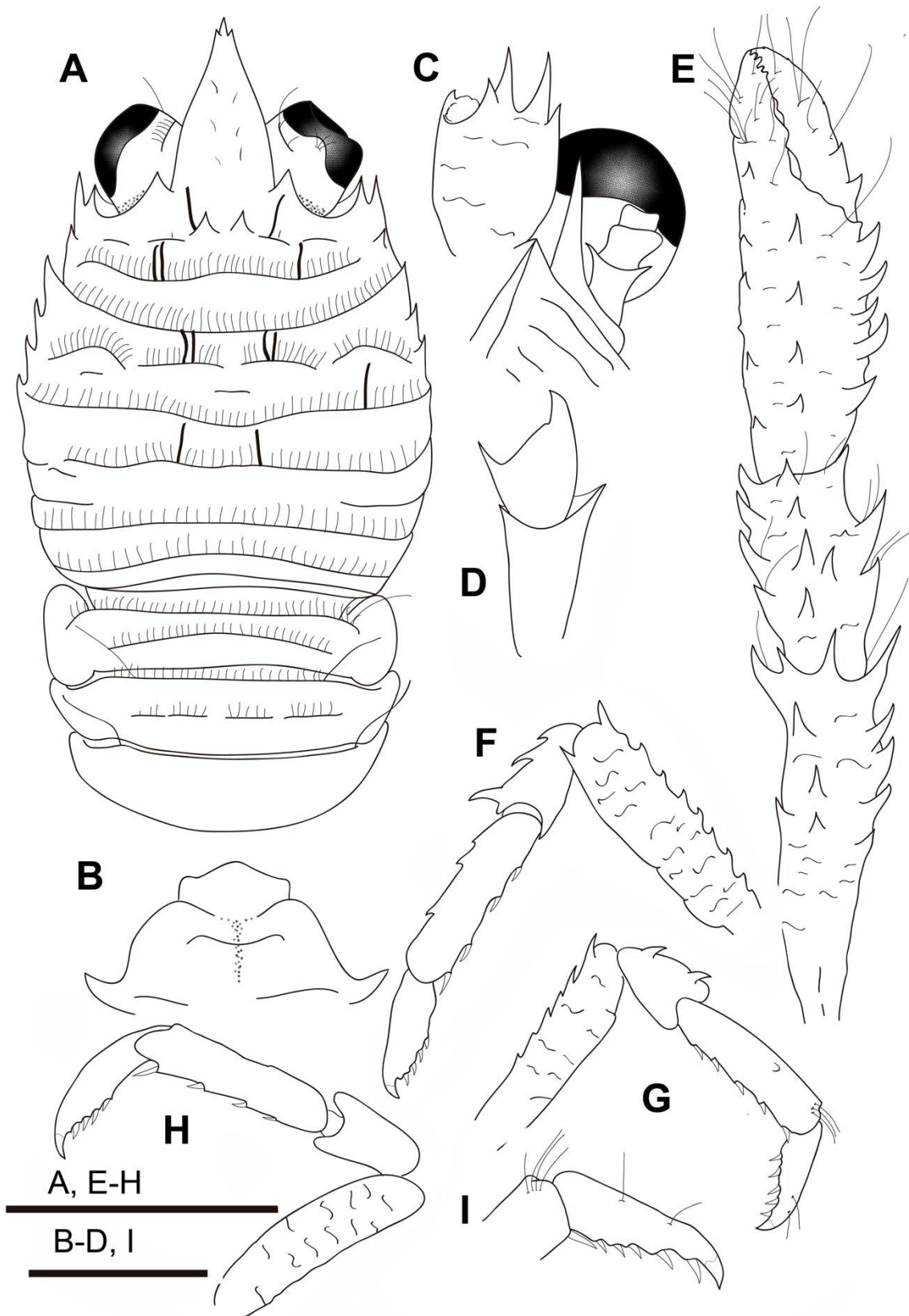
FIGURE 53. *Phylladiorhynchus zetes* **n. sp**., A-D, G-H, holotype male 2.1 mm (UF30059): A, carapace and pleon, dorsal view. B, thoracic sternites 3 and 4. C, left cephalic region, showing antennular and antennal peduncles, ventral view. D, left Mxp3, lateral view. E, left P1, dorsal view. F, left P2, lateral view. G, right P3, lateral view. H, left P4, lateral view. I, dactylus of right P3, lateral view. Scale bars: 1.0 mm.

French Polynesia. BENTHAUS Stn DW1926, 24°38.16'S, 146°00.82'W, 50–90 m 13 November 2002: 1 F parasitized 2.4 mm (MNHN-IU-2014-13873).—Society Islands. Moorea Islands. 17.5044ºS, 149.7584ºW, 65–66 m, 26 January 2012: 1 M 1.5 mm (UF33537).—17.5044ºS, 149.7584ºW, 65–66 m, 26 January 2012: ov. F 1.4 mm (UF33536).—17.5526ºS, 149.7735ºW, 57 m, 27 January 2012: 1 M 1.5 mm (UF33636).

French Polynesia. Marquesas Islands. MUSORSTOM 9 Stn DW1203, 9°52.7'S, 139°02.2'W, 60 m, 28 August 1997: 1 M 1.8 mm (MNHN-IU-2014-13874).—Stn CP1264, 9°21.3'S, 140°07.7'W, 53–57 m, 03 September 1997: 1 M 2.6 mm (MNHN-IU-2019-2640).

Etymology. From the name *Zetes*, an Argonaut, son of Boreas and Oreithyia. The name is considered a substantive in apposition.

Description. *Carapace*: As long as or slightly wider than long; transverse ridges with dense short setae and few long and thick iridescent setae. Gastric region slightly convex with 4 transverse ridges: epigastric ridge indistinct with 2 median spines and some, and several lateral short scales; anterior protogastric ridge not medially interrupted, nearly extending laterally to carapace margin; anterior mesogastric ridge not medially interrupted, laterally continuing to first branchial spine; anterior metagastric scale-like, often followed by a small scale. Mid-transverse ridge not interrupted, medially slightly depressed, preceeded by shallow or indistinct cervical groove, followed by 2 not interrupted or laterally interrupted ridges, interspersed with 1 short lateral ridge and some few short scales. Lateral margins straight or slightly convex, with 6 distinct spines: first anterolateral spine well-developed, reaching anteriorly to level of lateral orbital spine, second spine (hepatic) small, slightly dorsomesial from lateral margin, and followed by 4 branchial spines (3 anterior and 1 posterior). Rostrum leaf-like, horizontal, dorsally convex, 1.3–[1.5] times as long as broad, length [0.4]0.4 and breadth [0.3]0.3 that of carapace; lateral margins minutely serrated and convex, with well-developed supraocular basal spines and subapical spines small. Pterygostomian flap with anterior spine, upper margin smooth.

Sternum: As wide as long. Sternite 3 moderately broad, 1.9–[2.0] times as wide as long, anterior margin convex. Sternite 4 widely contiguous to sternite 3; anterolaterally smooth, surface depressed in midline, smooth; greatest width 2.5–[2.7] times that of sternite 3, [2.7]–2.8 times as wide as long.

Pleon: Elevated ridges with short setae and a few scattered long setae. Tergite 2 with anterior and posterior transverse elevated ridges; tergite 3 with anterior transverse

ridge, posterior transverse ridge interrupted; tergite 4 with anterior transverse ridge; tergites 5–6 smooth.

Eye: Eye stalk length about [1.1] times broader than long, peduncle distally setose, not distinctly expanded proximally, with few short transverse striae on lateral surfaces; cornea expanded distally, maximum corneal diameter 0.7–[1.0] × rostrum width*,* as wide as eyestalk.

Antennule: Article 1 slightly longer than wide, with 5 distal spines: distomesial spine well-developed; proximal lateral spine small, always present.

Antenna: Article 1 with prominent mesial process. Article 2 with well-developed distomesial and distolateral spines. Articles 3 and 4 unarmed.

Mxp3: Ischium with distinct distal spines on flexor and extensor margins. Merus 0.6–[0.8]× length of ischium, with well-developed distal spine on extensor and flexor margins.

P1: [2.6]–3.0 (males), 2.3–2.4 (females) times carapace length; subcylindrical, spiny and with long stiff setae; merus, carpus and palm with spines along mesial, dorsal and lateral surfaces, distal and mesial spines stronger than others. Merus 0.8–[1.0] length of carapace, 1.6–[2.0] times as long as carpus. Carpus [1.7]–2.5 times as long as wide. Palm 1.0–[1.2] × carpus length, [1.8]1.8 times as long as broad. Fingers 0.7–[0.8] × palm length fixed finger with 2 basal spines; movable finger with 1–2 basal spines.

P2–4: Stout, setose and spinose. Meri successively shorter posteriorly: P3 merus 0.9–[0.9] times length of P2 merus, P4 merus 0.8–[0.9] times length of P3 merus. P2 merus, 0.6–[0.7] times carapace length, 3.0–[3.5] times as long as broad, 1.1–[1.4] times as long as P2 propodus; P3 merus 3.6–[3.7] times as long as broad, 1.0–[1.3] times as long as P3 propodus; P4 merus 3.5–[3.8] times as long as broad, 0.9–[1.2] times as long as P4 propodus; extensor margin of P2 and P3 with row of spines, proximally diminishing, with prominent distal spine; P4 extensor margin irregular, unarmed; flexor margin irregular, with distal spine on P2–4. Carpi with 1–2 spines on extensor margin on P2–3, unarmed on P4; distal spine prominent on P2–3, absent on P4; granules below extensor margin on lateral surface of P2–4; flexor margin unarmed. Propodi stout, [3.5–3.7]3.1–3.9 times as long as broad; extensor margin irregular, armed with 0–3 spines; flexor margin with 3–4 slender movable spines in addition to distal pair. Dactyli [0.7]0.6 × length of propodi, ending in incurved, strong, sharp spine; flexor margin with 5–6 movable spines.

Eggs: Ov. F carried approximately 12–20 eggs of 0.2–0.3 mm diameter.

Colour. Base colour of carapace and Pleon light orange. Carapace, Rostrum, and Pleon covered by granules and small orange spots and wittish patches and bands. Ocular peduncles oranges, covered by small granules. P1 whitish, spines orange, palm and fingers orange, distal tip finger darker. P2–4 light whitish-translucent, covered by whitish spots, spines dark-orange; meri, propodi and dactyli distal part wittish to light orange.

Genetic data. COI and 16S, Table 1.

Distribution. French Polynesia, 20 to 23 m.

Remarks. *Phylladiorhynchus zetes* belongs to the group of species having 2 epigastric spines, 1 hepatic spine, 3 spines on the anterior branchial margin and the pleonal tergite 3 with the posterior ridge interrupted. *Phylladiorhynchus zetes* closely resembles *P. tiphys* from New Caledonia. and they can be distinguished by the following characters:

-   One scale with thick setae between the epigastric spines in *P. tiphys,* whereas this scale is absent in *P. zetes*.

-   The thoracic sternite 3 is quadrangular (less than twice as long as wide) in *P. tiphys,* whereas this sternite is moderately broad (more than twice as long as broad) in *P. zetes*.

-   The P2–4 propodi are usually stout in *P. zetes* (3.1–3.9 times as long as broad), whereas they are more slender in *P. tiphys* (3.5–4.5 as long as broad).

Phylladiorhynchus zetes is also highly similar to *P. medea*, also found in French Polynesia and New Caledonia. Both species can be distinguished by the following characters:

-   The rostrum has small or minute subapical spines in *P. zetes*, whereas these spines are obsolescent in *P. medea.*

-   The pleonal tergite 3 has a posterior ridge in *P. zetes,* whereas this ridge is absent in *P. medea*.

-   The P2–4 propodi are usually stout in *P. zetes* (3.1–3.9 times as long as broad), whereas they are more slender in *P. medea* (3.5–4.5 as long as broad).

The genetic divergences among *P. zetes*, *P. tiphys* and *P. medea* ranged between 7–11% (COI) and 3–6% (16S). The mean intraspecific genetic divergences of *P. zetes* were 0.2% (COI) and 0% (16S).

Conclusions

The results of this revision confirm the existence of 55 species belonging to the genus *Phylladiorhynchus*, 41 of which are newly described. We also confirm the validity of the species *P. integrus* (Benedict, 1902) and *P. lenzi* (Rathbun, 1907), currently considered synonyms of *P. pusillus* (Henderson, 1885), and of *P. serrirostris* (Melin, 1939), a synonym of *P. integrirostris* (Dana, 1852) (Baba *et al.* 2008; Schnabel & Ahyong 2019). Our results validate the traditional morphological characters previously used to distinguish *Phylladiorhynchus* species, e.g., the number of epigastric spines and the shape of thoracic sternite 3 (Baba 1969; Tirmizi & Javed 1980; Baba 1991; Macpherson 2008). In agreement with the results of Schnabel & Ahyong (2019), we also found some other distinctive characters that can be used to diagnose *Phylladiorhynchus* species, e.g., the shape and number of ridges on the carapace and pleon, the number of spines along the lateral margins of the carapace and the shape of the rostrum. Some groups of species, characterized by their conservative morphology, are barely distinguishable on the basis of morphological characters, despite presenting high genetic divergences. Such conservation made it difficult to delimit and define some closely related species within groups, for instance, the group comprising *P. lynceus, P. integrirostris* and *P. priasus* or *P. asclepius*, *P. euryalus*, *P. lini* and *P. spinosus*. We also observed intraspecific variability in the number of epigastric spines (e.g. in *P. poeas* and *P. porteri*), as was previously observed in *P. pusillus* (Schnabel & Ahyong, 2019). Furthermore, we observed sexual dimorphism in rostrum shape in some species (e.g., *P. amphion*), making the delimitation of these taxa difficult.

The molecular divergences obtained for *Phylladiorhynchus* species were similar overall but high compared with those observed for other squat lobster species (Cabezas *et al.* 2010; Macpherson & Robainas-Barcia 2015; Rodríguez-Flores *et al.* 2019a, 2019b; Macpherson *et al.* 2020). Most species pairs showed a divergence greater than 20% for COI and 10% for 16S (see Table 1), with very low intraspecific variability. Some values represent unexpectedly high levels of genetic divergence (up to 27% for 16S and 36% for COI), exceeding mean divergences reported for other galatheoid species (and even genera) (Machordom & Macpherson 2004; Cabezas *et al.* 2011; Macpherson & Robainas-Barcia 2013; Rodríguez-Flores *et al.* 2019c), suggesting the existence of different genera.
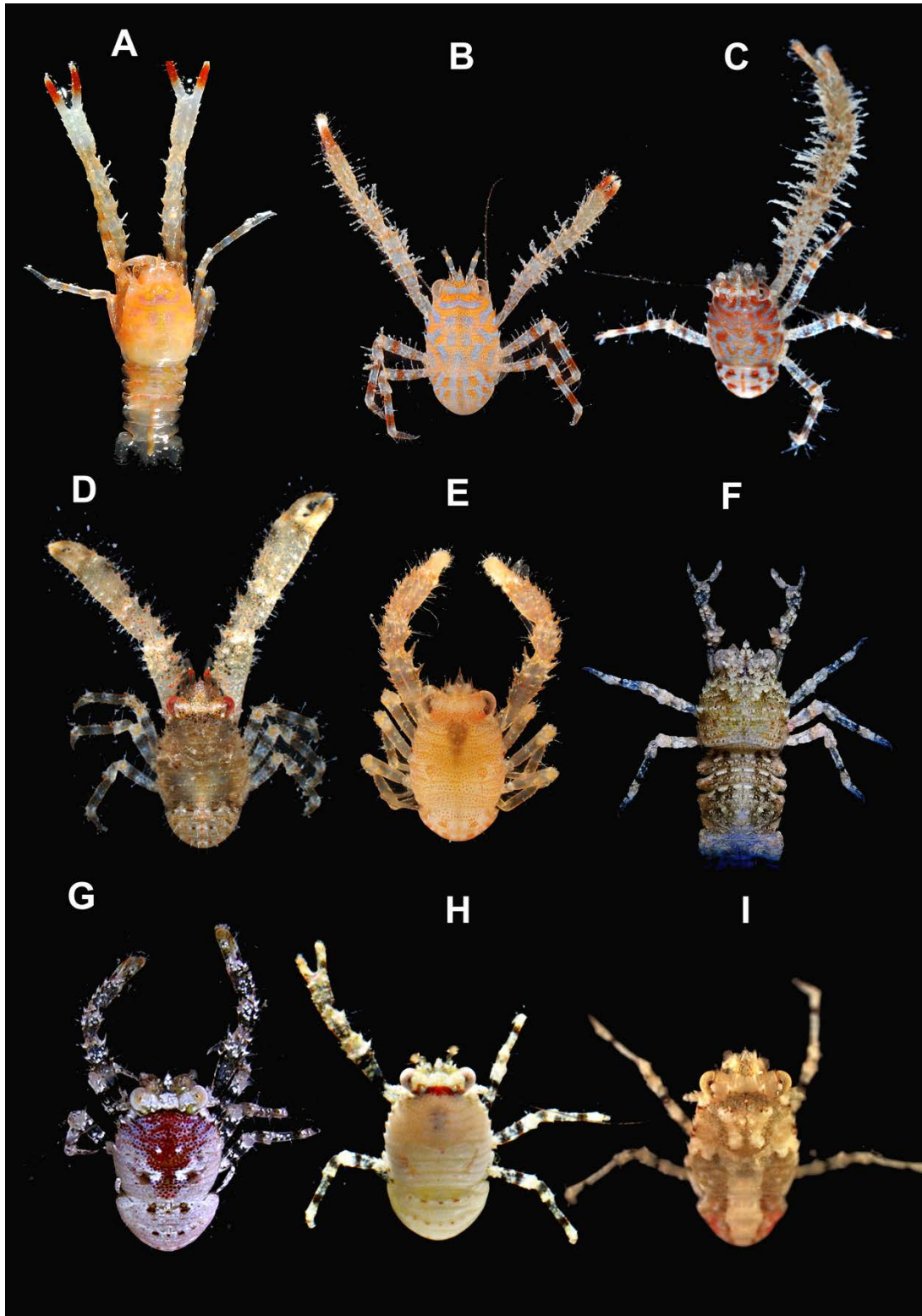
FIGURE 54. Colour in life, dorsal view. A. *Phylladiorhynchus acastus* **n. sp**. Papua New Guinea, male 2.5 mm (MNHN-IU-2014-10017). B, *Phylladiorhynhus barbeae* **n. sp.** Papua New Guinea, paratype male 1.6 mm (MNHN-IU-2014-13810). C, *Phylladiorhynhus barbeae* **n. sp.** Papua New Guinea, male 2.5 mm (MNHN-IU-2014-13813). D, *Phylladiorhynchus gustavi* **n. sp.** French Polynesia, male 2.3 mm (UF16338). E, *Phylladiorhynchus janiqueae* **n. sp**. Walter shoals, male 1.8 mm (MNHN-IU-2014-13840). F, *Phylladiorhynchus jeffkinchi* **n. sp**. Papua New Guinea, ovigerous female 2.2 mm (MNHN-IU-2014-2176). G, *Phylladiorhynchus joannotae* **n. sp.** French Polynesia, ovigerous female 2.2 mm (UF15544). H, *Phylladiorhynchus joannotae* **n. sp.** New Caledonia, female 1.0 mm (MNHN-IU-2014-20147). I, *Phylladiorhynchus koumac* **n. sp.** New Caledonia, male 1.5 mm (MNHN-IU-2014-20121).
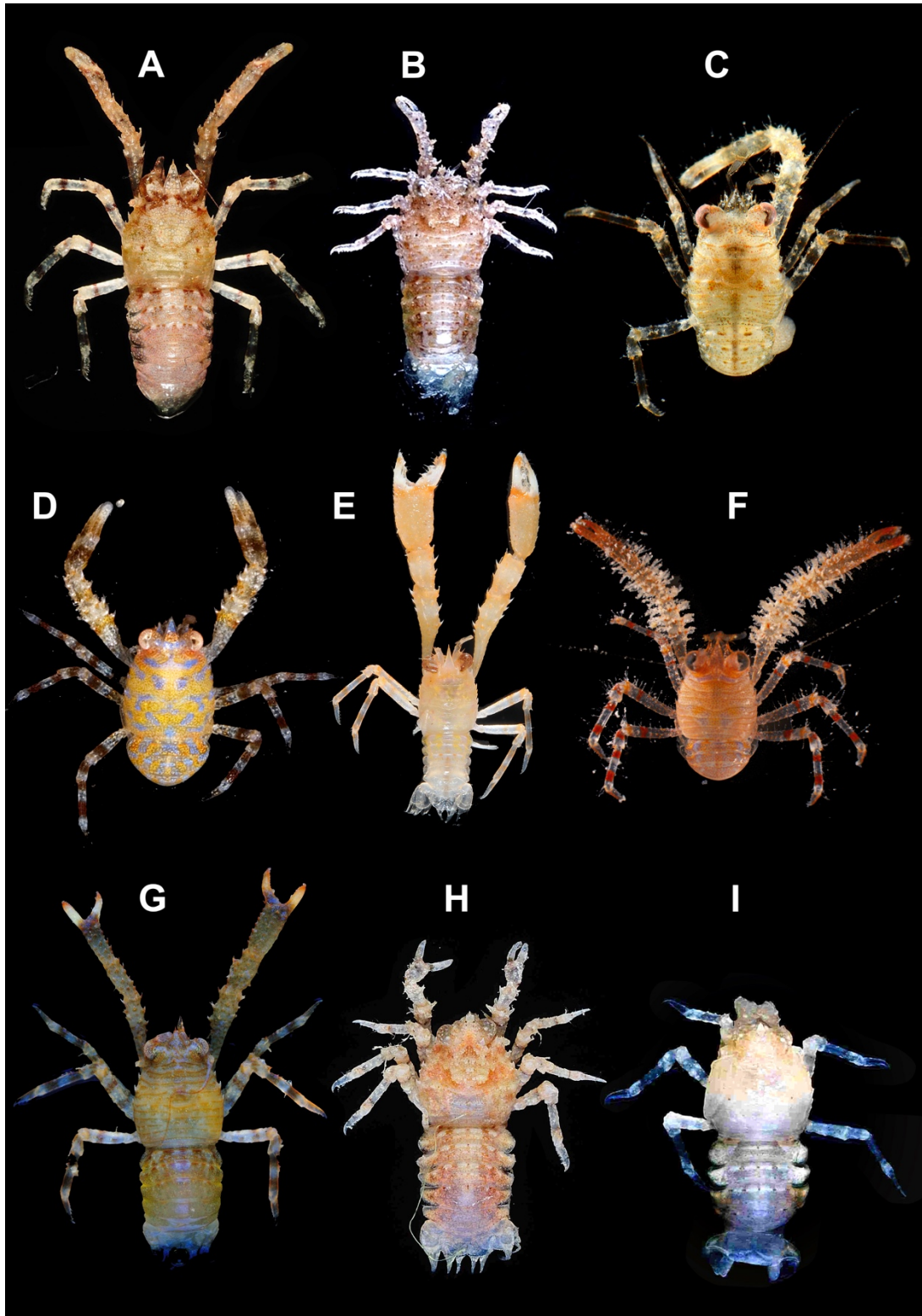
FIGURE 55. Colour in life, dorsal view. A, *Phylladiorhynchus lini* **n. sp**. Taiwan, holotype female 2.2 mm (NMMBCD5596). B, *Phylladiorhynchus marina* **n. sp**. Vanuatu, ovigerous female 2.0 mm (MNHN-IU-2014-13887). C, *Phylladiorhynchus medea* **n. sp.** New Caledonia, female 1.9 mm (MNHN-IU-2014-20063). D, *Phylladiorhynchus orpheus* **n. sp.** French Polynesia, ovigerous female 2.0 mm (UF9732). E, *Phylladiorhynchus paulae* n. sp. îles de Mayotte. des Glorieuses et des Comores, female 3.3 mm (MNHN-IU-2016-7003). F, *Phylladiorhynchus peneleos* n. sp. French Polynesia, male 2.0 mm (UF16078). G, *Phylladiorhynhus pepei* **n. sp.** Madagascar, male 3.2 mm (MNHN-IU-2016-486). H, *Phylladiorhynchus phanus* **n. sp.** Papua New Guinea, ovigerous female 2.5 mm (MNHN-IU-2014-2893). I. *Phylladiorhynchus phlias* **n. sp.** Papua New Guinea, ovigerous female 1.3 mm (MNHN-IU-2013-703).
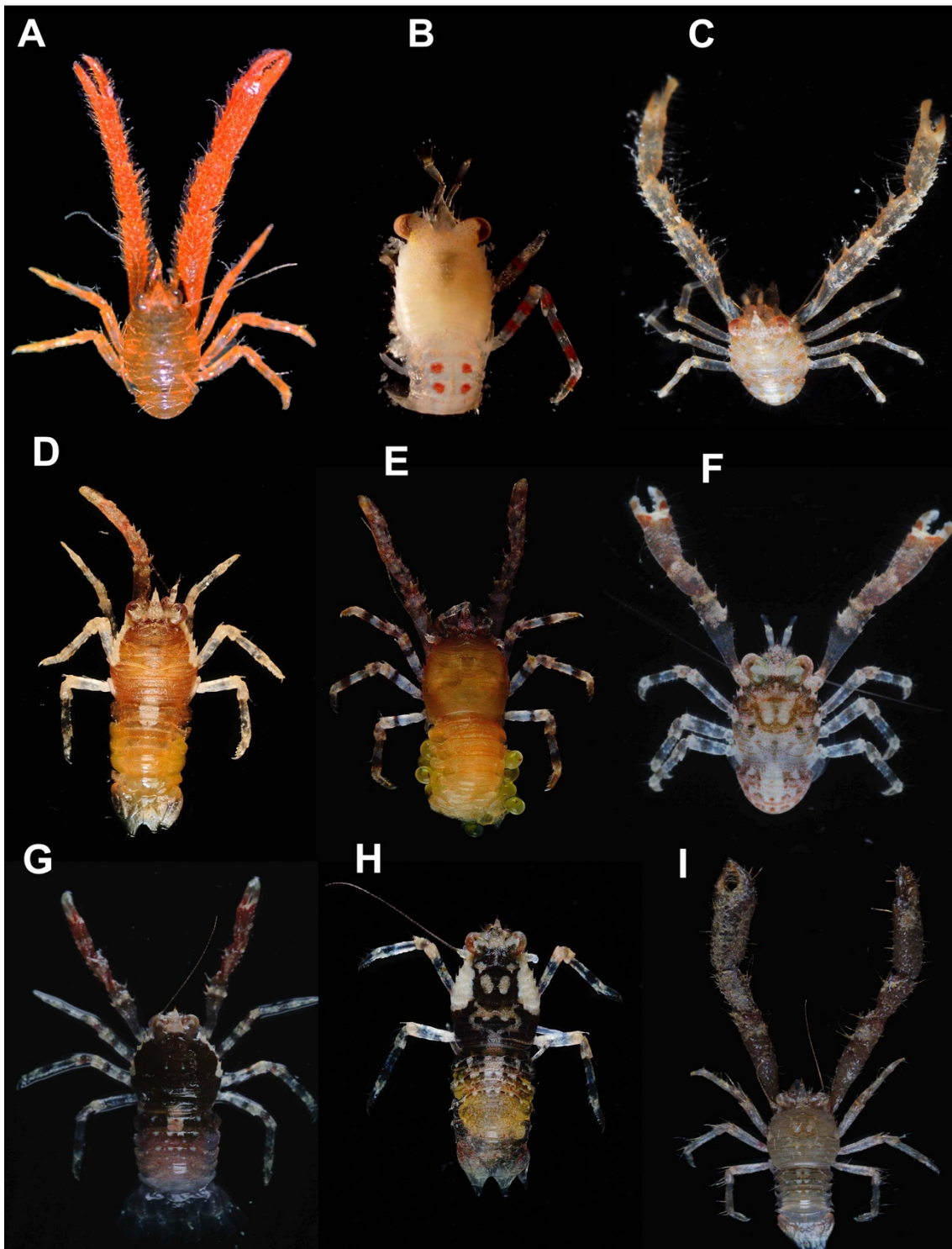
FIGURE 56. Colour in life, dorsal view. A, *Phylladiorhynchus poeas* **n. sp.** French Polynesia, male 2.5 mm (MNHN-IU-2014-13859). B, *Phylladiorhynchus punctatus* **n. sp.** New Caledonia, male 1.7 mm (MNHN-IU-2014-20101). C, *Phylladiorhynchus zetes* **n. sp.**, French Polynesia, ovigerous female 1.5 mm (UF33536). Colour variability. *Phylladiorhynchus lini* **n. sp**. Taiwan. D, paratype ovigerous female 2.5 mm (MNHN-IU-2016-1490). E, paratype ovigerous female 2.7 mm. F, paratype male 2.2 mm. G, paratype ovigerous female 3.0 mm. H, paratype ovigerous female 2.5 mm. I, paratype male 3.0 mm.

The lowest interspecific genetic divergences observed were 2% for 16S and 7% for COI, which were observed for species pairs differentiated from each other by several subtle but constant morphological characters. However, we were not able to find any clear or subtle morphological traits to distinguish the sister species *P. pusillus* and *P. poeas* (genetic divergence: 2% for 16S and 8% for COI). As these two species present a disjunct distribution, in Australia-New Zealand and French Polynesia, respectively, we consider them as different species (vicariant cryptic species).

Our revision illustrates the utility of combining a large sampling effort with morphological and molecular data in order to describe the real and rich diversity of *Phylladiorhynchus*. However, it also reveals that additional sampling effort is needed for some geographic areas, for instance in the Indian Ocean, Indonesia and SE Pacific Ocean, in order to improve our knowledge of this interesting and diverse genus.

(UPNG).

References

Ahyong, S. T. (2007) Decapod Crustacea collected by the NORFANZ expedition: Galatheidae and Polychelidae. *Zootaxa,* 1593, 1–54.

Andrade, H. (1985) Crustáceos decápodos marinos del Archipiélago de Juan Fernandez. *In:* Arana, P. (Ed.) *Investigaciones marinas en el Archipiélago de Juan Fernandez.Chile*. Universidad Católica de Valparaíso, Valparaíso, pp. 109–116.

Baba, K. (1969) Four new genera with their representatives and six new species of the Galatheidae in the collection of the Zoological Laboratory, Kyushu University, with redefinition of the genus Galathea. *Ohmu*, 2, 1–32.

Baba, K. (1977) Biological results of the Snellius Expedition XXVIII. The galatheid Crustacea of the Snellius Expedition. *Zoologische Mededelingen, Leiden*, 50, 243–259.

Baba, K. (1979) Expédition Rumphius II (1975) Crustacés parasites, commensaux, etc. (Th. Monod et R. Sèrene, éd.) VII. Galatheid crustaceans (Decapoda, Anomura). *Bulletin du Muséum national d'Histoire naturelle, Paris (4e série) Section A*, 1, 643–657.

Baba, K. (1989) Anomuran crustaceans obtained by dredging from Oshima Strait, Amami-Oshima of the Ryukyu Islands. *Memoirs of the National Science Museum, Tokyo*, 22, 127–134.

Baba, K. (1990) Chirostylid and galatheid crustaceans of Madagascar (Decapoda, Anomura). *Bulletin du Muséum national d'Histoire naturelle, Paris (4e série) Section A*, 11, 921–975.

Baba, K. (1991) Crustacea Decapoda: *Alainius* gen. nov., *Leiogalathea* Baba, 1969, and *Phylladiorhynchus* Baba, 1969 (Galatheidae) from New Caledonia. *In*: Crosnier, A. (ed.), Résultats des Campagnes MUSORSTOM, volume 9. *Mémoires du Muséum national d'Histoire naturelle, Paris* (A), 152, 479–491.

Baba, K. (1993) *Anomoeomunida*, a new genus proposed for *Phylladiorhynchus caribensis* Mayo, 1972 (Crustacea: Decapoda: Galatheidae). *Proceedings of the Biological Society of Washington,* 106, 102–105.

Baba, K. (2005) Deep-sea chirostylid and galatheid crustaceans (Decapoda: Anomura) from the Indo-West Pacific, with a list of species. *Galathea Reports*, 20, 1–317

Baba, K., Macpherson, E., Poore, G.C.B., Ahyong, S.T., Bermudez, A., Cabezas, P., Lin, C.W., Nizinski, M., Rodrigues, C. & Schnabel, K. E. (2008) Catalogue of squat lobsters of the world (Crustacea: Decapoda: Anomura-families Chirostylidae, Galatheidae and Kiwaidae). *Zootaxa*, 1905, 1–220.

Baba, K., Macpherson, E., Lin, C.-W. & Chan, T.-Y. (2009) *Crustacean fauna of Taiwan: squat lobsters (Chirostylidae and Galatheidae)*. Keelung: National Taiwan Ocean University, 312 pp.

Baba, K., Ahyong, S. T. & Macpherson, E. (2011) Morphology of marine squat lobsters. *In*: G. C. B. Poore, S. T. Ahyong & J. Taylor (Eds), T*he biology of squat lobsters*. CRC Press, Boca Raton, USA, pp. 1–38.

Balss, H. (1913) Neue Galatheiden aus der Ausbeute der deutschen Tiefsee-Expedition. 'Valdivia'. *Zoologischer Anzeiger*, 41, 221–226.

Balss, H. (1922) Decapoden von Juan Fernandez. *In:* Skottsberg, C. (Ed.) *The Natural History of Juan Fernandez and Easter Island. Zoology*, Uppsala, pp. 329–340.

Benedict, J.E. (1902) Description of a new genus and forty six new species of crustaceans of the family Galatheidae with a list of the known marine species. *Proceedings of the Biological Society of Washington*, 26, 243–334.

Borradaile, L.A. (1916) Crustacea. Part 1. - Decapoda. *British Antarctic (Terra Nova) Expedition, 1910. Natural History Reports Zoology*, 3, 75-110, figs. 111–116.

Cabezas, P., Macpherson, E., & Machordom, A. (2010) Taxonomic revision of the genus *Paramunida* Baba, 1988 (Crustacea: Decapoda: Galatheidae): a morphological and molecular approach. *Zootaxa*, 2712, 1–60.

Cabezas, P., Lin, C.W., & Chan, T.Y. (2011) Two new species of the deep-sea squat lobster genus *Munida* Leach, 1820 (Crustacea: Decapoda: Munididae) from Taiwan: morphological and molecular evidence. *Zootaxa*, 3036, 26–38.

Castilla, J. C. & Rozbaczylo, N. (1987) Invertebrados marinos de Isla de Pascua y Sala y Gómez. Islas oceánicas chilenas: conocimiento científico y necesidades de investigación. *In:* Castilla JC (ed). *Islas Oceánicas Chilenas: Conocimiento científicos y necesidades de investigaciones.* Ediciones Univ Católica de Chile, Santiago, pp 191–215

Castro, P. (2011) Catalog of the anomuran and brachyuran crabs (Crustacea: Decapoda: Anomura, Brachyura) of the Hawaiian Islands. *Zootaxa,* 2947, 1-154.

Chilton, C. (1906) Report of some Crustacea dredged off the coast of Auckland. *Transactions and proceedings of the New Zealand Institute,* 38, 265–269.

Chilton, C. (1911) Crustacea. Scientific Results New Zealand Governm. Trawling Expedition 1907. *Records of the Canterbury Museum*, 1, 285–312.

Crandall, K.A. & Fitzpatrick Jr, J.F. (1996). Crayfish molecular systematics: using a combination of procedures to estimate phylogeny. *Systematic Biology*, 45, 1–26.

Dana, J.D. (1852) Crustacea. Part I. *United States Exploring Expedition, during the years 1838, 1839, 1840, 1841, 1842, under the command of Charles Wilkes, U.S.N.*, 13, 1–685, with a folio atlas of 96 pls (published 1885).

Davie, P.J.F. (2002) *Crustacea: Malacostraca: Eucarida (Part 2): Decapoda – Anomura, Brachyura*. CSIRO Publishing, Melbourne, xiv + 641 pp.

De los Ríos Escalante, P. & Ibáñez Arancibia, E. (2016) A checklist of marine crustaceans known from Easter Island. *Crustaceana*, 89, 63–84.

DiSalvo, L.H., Randall, J.E. & Cea, A. (1988) Ecological Reconnaissance of the Easter Island Sublittoral Marine-Environment. *National Geographic Research*, 4(4), 451–473.

Dong, C. & Li, X. Z. (2013) Galatheid squat lobster species from Chinese waters. *Chinese Journal of Oceanology and Limnology,* 31, 1315–1321.

Folmer, O., Black, M., Hoeh, W., Lutz, R. & Vrijenhoek, R. (1994) DNA primers for amplification of mitochondrial cytochrome c oxidase subunit I from diverse metazoan invertebrates. *Molecular Marine Biology and Biotechnology*, 3(5), 294–9.

Fujita, Y. (2007) First zoeas of two shallow-water galatheids, *Lauriea gardineri* (Laurie, 1926) and *Phylladiorhynchus integrirostris* (Dana, 1853) (Crustacea; Decapoda; Anomura; Galatheidae). *Proceedings of the Biological Society of Washington*, 120, 74–85.

Grant, F.E. & McCulloch, A.R. (1906) On a collection of Crustacea from the Port Curtis district, Queensland. *Proceedings of the Linnean Society of New South Wales*, 1906, 2–53, pls 1–4.

Guiler, E.R. (1952) A list of the Crustacea of Tasmania. *Records of the Queen Victoria Museum, Launceston,* 3(3), 15–44.

Haig, J. (1955) Reports of the Lund University Chile Expedition 1948–49. 20. The Crustacea Anomura of Chile. *Lunds Universtitets Arsskrift N.F. Avd.*, 2, 51, 1–68.

Haig, J. (1973) Galatheidea (Crustacea, Decapoda, Anomura) collected by the F.I.S. Endeavour. *Records of the Australian Museum*, 28, 269–289

Hale, H.M. (1927) *The Crustaceans of South Australia. Part I.* Adelaide: Government Printer.

Henderson, J.R. (1885) Diagnoses of new species of Galatheidae collected during the "Challenger" expedition. *Annals and Magazine of Natural History, series V,* 16, 407–421.

Henderson, J.R. (1888) Report on the Anomura collected by H.M.S. *Challenger* during the years 1873–76. *Report on the Scientific Results of the Voyage of H.M.S. Challenger during the years 1873–76. Zoology*, 27, 1–221, 21 pls.

Katoh, K., Misawa, K., Kuma, K.I. & Miyata, T. (2002) MAFFT: a novel method for rapid multiple sequence alignment based on fast Fourier transform. *Nucleic Acids Research*, 30 (14), 3059–3066.

Kumar, S., Stecher, G. & Tamura, K. (2016) MEGA7: molecular evolutionary genetics analysis version 7.0 for bigger datasets. *Molecular Biology and Evolution*, 33 (7), 1870–1874.

Larsson, A. (2014) AliView: a fast and lightweight alignment viewer and editor for large data sets. *Bioinformatics,* 30 (22), 3276–3278. http://dx.doi.org/10.1093/bioinformatics/btu531

Laurie, R.D. (1926) Reports of the Percy Sladen Trust Expedition to the Indian Ocean in 1905, under the leadership of Mr. J. Stanley Gardiner, M.A. Vol. 8, No. VI. - Anomura collected by Mr. J. Stanley Gardiner in the western Indian Ocean in H.M.S. Sealark. *Transactions of the Linnean Society of London, Series 2 Zoology,* 19, 121–167, pl. 128, 129.

Leach, W.E. (1820) Galatéadées. *In: Dictionnaire des Sciences Naturelles*. F. G. Levreault, Paris, pp. 49–56.

Lee, S.-H., Lee, S.-K., Kim, S.H. & Kim, W. (2019) First records of two squat lobsters (Decapoda, Galatheidae) from Korea. *Crustaceana*, 92, 725–737.

Lenz, H. (1902) Die Crustaceen der Sammlung Plate (Decapoda und Stomatopoda). *Zoologische Jahrbücher. Abteilung für Systematik*, 5, 731–772, pl. 23.

Lewinsohn, C. (1969) Die Anomuren des Roten Meeres (Crustacea Decapoda: Paguridea, Galatheidea, Hippidea). *Zoologische Verhandelingen, Leiden*, 104, 1–213, pls 1–2.

Lewinsohn, C. (1982) *Phylladiorhynchus integrirostris* (Dana) und *Lauriea gardineri* (Laurie) (Decapoda, Anomura) aus dem nordlichen Roten Meer. *Crustaceana*, 42, 295–301.

Machordom, A. & Macpherson, E. (2004) Rapid radiation and cryptic speciation in squat lobsters of the genus *Munida* (Crustacea, Decapoda) and related genera in the South West Pacific: molecular and morphological evidence. *Molecular Phylogenetics and Evolution*, 33, 259–279.

Machordom, A., Araujo, R., Erpenbeck, D. & Ramos, M. Á. (2003) Phylogeography and conservation genetics of endangered European Margaritiferidae (Bivalvia: Unionoidea). *Biological Journal of the Linnean Society*, 78, 235–252.

Macpherson, E. (2008) Some new records of shallow-water galatheid crustaceans (Anomura: Galatheidae) from the Dampier Archipelago, Western Australia. *Records of the Western Australian Museum Supplement*, 72, 289–297.

Macpherson, E. & Baba, K. (2011) Taxonomy of squat lobsters. In: G. C. B. Poore, S. T. Ahyong & J. Taylor (Eds), *The biology of squat lobsters*. CRC Press, Boca Raton, USA, 39–71 pp.

Macpherson, E. & Robainas-Barcia, A. (2013) A new genus and some new species of the genus Lauriea Baba, 1971 (Crustacea, Decapoda, Galatheidae) from the Pacific and Indian Oceans, using molecular and morphological characters. *Zootaxa*, 3599, 136–160.

Macpherson, E. & Robainas-Barcia, A. (2015) Species of the genus Galathea Fabricius, 1793 (Crustacea, Decapoda, Galatheidae) from the Indian and Pacific Oceans, with descriptions of 92 new species. *Zootaxa*, 3913, 1–335.

Macpherson, E., Rodríguez-Flores P.C. & Machordom, A. (2020) Squat lobsters of the families Munididae and Munidopsidae from Papua New Guinea. In: Ahyong ST, Chan T-Y, Corbari L (Eds) Tropical Deep-Sea Benthos 31, Papua New Guinea. Muséum national d'Histoire naturelle, Paris: 11-120 (*Mémoires du Muséum national d'Histoire naturelle,* 213). ISBN: 978-2-85653-913-2.

Makarov, V.V. (1938) Anomura. Rakoobraznyey, Vol. 10, No. 3. In: Shtakel'berg, A.A. (ed.), *Fauna SSSR, (new series)* 16, x + 324 pp., 5 pls. Academii Nauk SSSR,

Moscow (English translation, 1962: Crustacea, Anomura. Jerusalem: Israel Program for Scientific Translation. 278 pp.)

Mayo, B. (1972) Three new species of the family Galatheidae (Crustacea, Anomura) from the western Atlantic. *Bulletin of Marine Science*, 22, 522–535.

Melin, G. (1939) Paguriden und Galatheiden von Prof. Dr. Sixten Bocks Expedition nach den Bonin-Inseln 1914. *Kungliga Svenska Vetenskapsakademiens Handlingar*, 18, 1–119.

Meusnier, I., Singer, G.A.C., Landry, J.-F., Hickey, D.A., Hebert, P.D.N. & Hajibabaei, M. (2008) A universal DNA mini-barcode for biodiversity analysis. *BioMed Central Genomics*, 9, 214.

Miyake, S. (1965) Crustacea, Anomura. *In:* Okada, Y.K. & Uchida, T. (Eds.) *New illustrated encyclopedia of the fauna of Japan*, Tokyo, pp. 630–652.

Miyake, S. & Baba, K. (1965) Some galatheids obtained from the Bonin Islands (Crustacea, Anomura). *Journal of the Faculty of Agriculture, Kyushu University,* 13, 585–593.

Miyake, S. & Baba, K. (1966) Descriptions of galatheids collected from coral reefs of the Ryukyu Islands (Crustacea, Anomura) *Journal of the Faculty of Agriculture, Kyushu University*, 14, 57–79

Miyake, S. & Baba, K. (1967) Galatheids of the East China Sea (Chirostylidae and Galatheidae, Decapoda, Crustacea) *Journal of the Faculty of Agriculture, Kyushu University*, 14, 225–246.

Miyake, S. & Nakazawa, K. (1947) Crustacea, Anomura. *In:* Uchida, S. (Ed.) *Illustrated encyclopedia of the fauna of Japan (exclusive of insects) Revised edition.* Hokuryukan, Tokyo, pp. 731–750, figs 2115–2171.

Mujica, A., González-Cornejo, F., Meerhoff, E. & Yannicelli, B. (2019) Larval development of Phylladiorhynchus pusillus (Henderson, 1885) (Decapoda, Anomura, Galatheidae). *Latin American Journal of Aquatic Research*, 47, 774–783.

Palumbi, S., Martin, A., Romano, S., Mcmillian, W. O., Stice, L. & Grabowski, G. (1991) Simple fool's guide to PCR. University of Hawaii, Honolulu. 45 pp.

Peyrot-Clausade, M. (1989) Crab cryptofauna (Brachyura and Anomura) of Tikehau, Tuamotu Archipelago, French Polynesia. *Coral Reefs*, 8, 109–117.

Poore, G.C.B. (2004) *Marine decapod Crustacea of southern Australia. A guide to identification (with chapter on Stomatopoda by Shane Ahyong)*. Melbourne: CSIRO Publishing, 574 pp.

Poore, G.C.B., McCallum, A. & Taylor, A.C. (2008) Decapod Crustacea of the continental margin of southwestern adn central Western Australia: preliminary identifications of 524 species from FRV *Southern Surveyor* voyage SS10-2005. *Museum Victoria Science Report*, 11, 1–106.

Porter, C.E. (1916a) Materiales para la fauna carcinologica de Chile. XII. – Sobre los Galatheidae del Museo Nacional. *Revista Chilena de Historia Natural*, 20, 111–117.

Porter, C.E. (1916b) Los crustaceos decapodos Chilenos del Museo Nacional (estudios criticos) III. – La fam. Galatheidae. *Boletin Museo Nacional de Historia Natural, Chile*, 9, 95–100.

Poupin, J. (1996) Crustacea Decapoda of French Polynesia (Astacidea, Palinuridea, Anomura, Brachyura). *Atoll Research Bulletin*, 442, 1–114.

Poupin, J. (2003) Crustacea Decapoda and Stomapoda of Easter Island and surrounding areas. A documented checklist with historical overview and biogeographic comments. *Atoll Research Bulletin*, 500, 1–50

Rathbun, M.J. (1907) South American Crustacea. *Revista Chilena de Historia Natural,* 11, 45–50, fig. 41, pls. 42, 43.

Retamal, M.A. (1981) Catálogo ilustrado de los crustáceos decápodos de Chile. *Gayana Zoología*, 44, 1–110.

Retamal, M.A. (2004) Decápodos de las islas oceánicas chilenas: Pascua y Salas y Gómez. *Ciencia y Tecnología del Mar*, 27, 55–68.

Retamal, M.A. & Arana, P.M. (2016) Record of stomatopods and decapods, including descriptions of the species of commercial interest from the submarine rises and surrounding waters of the Chilean oceanic islands (southeastern Pacific Ocean). *Latin American Journal of Aquatic Research*, 44, 16–33.

Richer de Forges, B., Chan, T.Y., Corbari, L., Lemaitre, R., Macpherson, E., Ahyong, S.T. & Ng, P.K.L. (2013) The MUSORSTOM-TDSB deep-sea benthos exploration program (1976-2012): An overview of crustacean discoveries and new perspectives on deep-sea zoology and biogeography. In Ahyong S. T., Chan T.-Y., Corbari L. & Ng P. K. L. (eds), Tropical Deep-Sea Benthos 27. *Mémoires du Muséum national d'Histoire naturelle,* 204, 13–66.

Rodríguez-Flores, P.C., Machordom, A. & Macpherson, E. (2017) Three new species of squat lobsters of the genus *Fennerogalathea* Baba, 1988 (Decapoda: Galatheidae) from the Pacific Ocean. *Zootaxa,* 4276, 46–60.

Rodríguez-Flores, P.C., Macpherson, E., Buckley, D. & Machordom, A. (2019a) High morphological similarity coupled with high genetic differentiation in new sympatric species of coral-reef squat lobsters (Crustacea, Decapoda, Galatheidae). *Zoological Journal of the Linnean Society,* 185, 984–1017.

Rodríguez-Flores, P.C., Macpherson, E. & Machordom, A. (2019b) Revision of the squat lobsters of the genus *Leiogalathea* Baba, 1969 (Crustacea, Decapoda, Munidopsidae) with the description of 15 new species. *Zootaxa,* 4560, 201–256.

Rodríguez-Flores, P.C., Machordom, A., Abelló, P., Cuesta, J.A. & Macpherson, E. (2019c). Species delimitation and multi-locus species tree solve an old taxonomic problem for European squat lobsters of the genus Munida Leach, 1820. *Marine Biodiversity*, 49, 1751–1773.

Rowden, A.A., Schnabel, K.E., Schlacher, T.A., Macpherson, E., Ahyong, S.T. & Richer de Forges, B. (2010) Squat lobster assemblages on seamounts differ from some, but not all, deep-sea habitats of comparable depth. *Marine Ecology*, 31, 63–83.

Samouelle, G. (1819) *The entomologists' useful compendium; or an introduction to the knowledge of British Insects, comprising the best means of obtaining and preserving them, and a description of the apparatus generally used; together with the genera of Linné, and modern methods of arranging the Classes Crustacea, Myriapoda, spiders, mites and insects, from their affinities and structure, according to the views of Dr. Leach. Also an explanation of the terms used in entomology; a calendar of the times of appearance and usual situations of near 3,000 species of British Insects; with instructions for collecting and fitting up objects for the microscope*. London: Thomas Boys.

Schnabel, K.E. & Ahyong, S.T. (2019) The squat lobster genus *Phylladiorhynchus* Baba, 1969 in New Zealand and eastern Australia, with description of six new species. *Zootaxa*, 4688, 301–347

Thomson, G.M. (1899) A revision of the Crustacea Anomura of New Zealand. *Transactions of the Royal Society of New Zealand, Zoology*, 31, 169–197.

Tirmizi, N.M. (1966) Crustacea: Galatheidae. *The John Murray Expedition 1933–34. Scientific Reports*, 11, 167–234.

Tirmizi, N.M. & Javed, W. (1980) Two new species and one new record of *Phylladiorhynchus* Baba from the Indian Ocean (Decapoda, Galatheidae) *Crustaceana*, 39, 255–262.

Tirmizi, N.M. & Javed, W. (1993) *Indian Ocean galatheids (Crustacea: Anomura)* Marine Reference Collection and Resource Centre, University of Karachi: Karachi. 147 pp

Whitelegge, T. (1900) Crustacea Part 1. Scientific results of the trawling expedition of H.M.C.S. Thetis, off the coast of New South Wales, in February and March, 1898. *Australian Museum Memoir,* 4, 133–199, pls 132–135

Yokoya, Y. (1936) Some rare and new species of decapod crustaceans found in the vicinity of the Misaki Marine Biological Station. *Japanese Journal of Zoology*, 7, 129–146.

Zarenkov, N.A. (1968) Crustacea Decapoda collected in the Antarctic and Antiboreal regions by the Soviet Antarctic Expedition. *Issledovaniya Fauny Morei, SSSR*, 6, 153–199 (In Russian.

TABLE 1. Uncorrected pairwise genetic distances (%) for the analyzed markers. Under diagonal are represented the divergences among COI sequences, up to the diagonal are represented the 16S distances.

Species	1	2	3	4	5	6	7	8	9	10	11	12	13	14	15	16	17	18	19	20	21	22	23	24	25	26	27	28	29	30	31	32	33	34	35	36	37	38	39	40	41	42	43	44	45
1 P. acastus		16	6	19	14	21	21	na	9	9	na	18	na	18	14	16	15	17	7	17	18	17	20	9	15	17	15	13	20	3	19	21	15	18	18	19	19	18	8	18	19	18	16	na	16
2 P. amphion	16		15	19	15	21	21	na	13	13	na	19	na	18	14	16	17	16	16	20	19	17	19	13	18	20	18	15	22	15	19	22	17	21	18	19	18	23	14	19	19	18	16	na	19
3 P. argus	13	16		18	14	20	19	na	13	13	na	18	na	19	14	16	17	16	7	17	17	17	20	10	15	20	15	14	22	5	18	20	15	18	18	21	18	20	8	19	18	17	19	na	17
4 P. asclepius	17	16	16		20	22	22	na	18	18	na	7	na	24	20	19	20	20	19	21	19	5	22	19	19	22	16	20	26	18	22	23	18	21	19	22	21	24	19	19	7	20	19	na	20
5 P. australis	17	19	18	16		28	21	na	13	13	na	18	na	20	6	18	17	16	13	19	18	18	21	13	17	20	15	3	21	12	19	21	17	18	19	21	21	21	13	17	20	19	18	na	18
6 P. bahamut	29	26	27	26	28		4	na	19	20	na	22	na	20	22	17	22	20	20	22	16	22	20	19	22	17	19	3	21	20	14	3	22	23	15	14	15	23	18	14	22	16	16	na	16
7 P. barbeae	29	28	28	26	28	9		na	19	19	na	23	na	20	22	17	23	21	20	23	15	21	20	19	22	17	20	21	22	19	13	3	22	23	14	14	21	24	18	14	22	16	16	na	16
8 P. boucheti	16	17	14	15	18	28	28		na	4	na	17	na	16	13	14	15	15	8	17	15	16	17	5	15	17	15	13	18	8	17	20	14	17	16	17	16	18	6	15	18	16	15	na	15
9 P. butes	15	15	14	13	15	27	27	11		na	na	17	na	17	14	15	15	15	9	16	16	16	18	5	17	17	15	14	19	8	18	20	16	18	17	17	18	18	7	17	18	15	16	na	16
10 P. cepheus	17	18	17	15	17	28	28	12	10		na	17	na	16	13	15	15	14	8	17	16	16	17	5	15	17	15	13	18	6	17	20	14	17	16	17	16	18	6	15	18	16	15	na	15
11 P. erebus	15	15	14	15	13	27	27	11	na	na		na	na	23	18	19	19	20	18	22	20	6	22	18	18	21	15	20	25	17	22	23	16	22	20	21	21	24	17	19	8	19	19	na	19
12 P. euryalus	18	17	17	8	17	27	28	11	16	14	16		na	25	20	17	20	20	18	20	19	23	17	16	20	18	21	19	13	18	17	21	21	23	18	21	20	22	17	18	24	18	19	na	18
13 P. gustavi	24	25	25	22	24	30	30	17	21	17	22	24		na	na	na	na	na	na	na	na	na	na	na	na	na	na	na	na	na	na	na	na	na	na	na	na	na	na	na	na	na	na	na	na
14 P. integrirostris	26	22	23	23	26	32	33	23	24	25	24	25	27		20	17	18	18	18	17	18	17	13	16	20	18	21	19	13	18	17	21	16	19	18	16	12	22	17	18	24	18	19	na	18
15 P. integrus	19	20	17	18	13	26	27	19	19	19	19	20	27	25		19	16	14	13	18	18	18	20	12	17	20	15	5	21	12	20	22	17	20	19	22	20	20	13	18	19	20	19	na	19
16 P. janiqueae	20	20	22	18	21	26	26	20	16	19	17	20	21	26	23		19	18	16	17	12	19	18	16	19	6	18	19	18	15	14	17	18	17	8	16	18	20	14	7	19	13	5	na	4
17 P. jeffkinchi	18	18	20	17	18	29	30	15	14	17	16	18	24	25	21	20		18	16	22	18	19	21	16	7	20	13	17	22	15	21	23	7	21	19	22	21	24	16	18	20	20	19	na	19
18 P. joannotae	17	9	16	13	17	26	26	16	14	14	15	15	21	26	21	20	16		16	19	19	18	20	15	17	19	16	15	21	16	19	21	17	21	17	19	19	22	14	19	19	18	17	na	18
19 P. kermadecensis	15	18	15	16	20	31	30	16	na	17	17	21	27	26	26	18	19	20		17	20	17	19	19	20	18	16	13	20	11	19	20	20	18	15	20	19	7	18	19	19	18	17	na	17
20 P. koumac	20	19	18	18	21	31	32	19	18	19	20	20	24	26	22	19	20	19	22		20	21	22	16	22	19	21	19	23	17	20	23	21	23	19	22	21	10	15	10	22	19	18	na	18
21 P. laureae	23	23	25	22	24	30	29	22	21	21	21	24	8	28	28	23	25	22	26	25		19	19	16	19	14	18	18	20	16	14	16	19	17	10	15	18	22	16	10	18	10	11	na	12
22 P. lini	19	18	19	8	16	27	27	17	16	16	16	10	21	24	20	19	18	16	21	19	20		22	17	17	20	15	18	24	16	20	22	15	20	19	21	21	23	16	18	6	19	18	na	19
23 P. lynceus	23	22	22	17	21	30	30	21	21	22	20	20	26	23	24	21	20	21	25	24	23	19		17	20	20	21	21	16	20	19	21	21	22	19	21	21	22	17	17	23	18	18	na	19
24 P. maestratii	17	16	14	14	15	29	29	13	7	10	13	16	22	24	20	17	16	14	17	18	26	19	20		17	17	16	13	18	8	16	20	16	19	17	18	17	17	6	17	20	16	16	na	16
25 P. marina	21	20	21	20	22	31	31	20	20	20	20	21	26	26	26	21	22	19	21	20	25	20	23	18		20	14	17	23	16	21	22	4	12	19	20	20	22	16	20	18	20	19	na	19
26 P. medea	23	21	22	22	22	28	29	23	18	21	21	22	24	26	26	11	22	20	23	26	24	22	24	18	24		19	21	19	17	17	16	13	14	18	19	20	23	16	10	21	13	6	na	6
27 P. nudus	19	16	18	18	14	26	26	17	13	16	15	15	22	23	18	18	16	17	26	20	23	15	19	19	24	22		16	22	17	19	21	17	18	17	19	20	21	13	18	20	19	18	na	19
28 P. nui	17	19	18	16	8	25	28	17	15	16	16	17	25	26	23	19	22	14	20	20	21	17	21	15	20	22	15		20	11	19	21	17	18	19	21	20	21	13	18	20	19	18	na	19
29 P. orpheus	23	21	21	18	21	27	29	22	21	22	21	19	26	22	24	18	23	20	24	22	26	20	16	21	24	23	20	21		20	20	23	22	24	20	22	15	23	19	19	27	20	20	na	20
30 P. paulae	12	17	10	16	16	29	29	15	13	15	14	18	25	24	19	15	15	16	15	19	24	19	20	14	19	22	16	17	23		18	20	15	17	16	17	19	18	7	15	18	16	15	na	16
31 P. peneleos	32	32	31	31	31	32	33	31	30	30	31	33	31	35	32	32	31	32	32	32	32	32	31	32	33	31	30	31	34	18		14	21	21	13	11	19	21	13	21	22	13	14	na	15
32 P. pepei	31	30	30	28	30	8	7	29	29	29	29	29	31	36	29	28	31	29	32	31	32	28	29	29	32	23	29	28	31	31	35		31	23	15	14	22	24	14	14	22	17	17	na	16
33 P. phanus	21	19	20	17	19	29	29	19	18	19	18	18	25	23	21	21	14	18	22	20	21	19	23	17	13	16	16	19	22	20	32	31		18	18	20	21	22	14	18	17	20	19	na	18
34 P. phlias	19	18	18	14	15	30	30	18	16	18	17	17	22	24	18	18	16	17	20	20	23	17	20	16	18	18	15	14	20	17	33	30	15		18	18	22	23	15	19	21	20	18	na	18
35 P. poeas	27	25	25	23	24	27	28	24	22	23	24	26	27	29	27	25	26	25	26	28	28	24	25	24	29	22	23	25	26	25	28	28	26	27		14	19	23	15	2	19	11	9	na	8
36 P. pollux	27	25	25	24	24	28	28	25	23	23	25	25	27	29	25	26	26	25	26	28	28	25	27	24	28	22	23	25	26	22	31	29	21	22	24		20	22	17	15	21	15	18	na	17
37 P. priasus	23	22	22	18	20	31	31	21	20	20	20	23	26	23	24	23	23	21	25	25	27	20	26	20	23	23	19	19	20	22	35	31	23	20	26	27		21	17	13	22	18	19	na	19
38 P. pulchrus	22	21	21	23	23	32	32	22	21	21	22	23	26	28	23	24	23	21	23	11	22	22	26	21	23	27	21	21	24	22	33	29	18	19	26	24	24		15	18	24	22	22	na	21
39 P. punctattus	16	16	13	16	17	29	29	13	13	14	14	17	23	25	19	20	17	14	17	20	22	18	21	14	19	22	14	14	21	14	35	33	27	18	25	25	22	21		15	18	15	14	na	14
40 P. pusillus	25	24	24	23	25	26	26	25	22	23	25	25	23	28	26	20	27	26	28	27	27	22	25	24	28	20	23	25	26	25	29	31	18	17	24	24	25	31	24		19	11	8	na	8
41 P. spinosus	17	17	18	8	15	23	25	16	15	15	14	10	23	24	20	19	17	15	21	20	22	8	20	15	20	20	13	15	19	18	32	28	18	17	25	25	28	27	17	24		19	19	na	20
42 P. talaus	26	25	25	23	24	28	28	26	23	25	25	25	23	28	28	23	26	24	25	28	29	24	28	24	29	22	22	24	28	25	32	32	28	26	24	26	28	27	24	25	24		12	na	12
43 P. tiphys	21	19	20	20	22	26	26	20	16	19	18	19	18	26	23	25	22	22	22	26	29	21	23	17	22	11	18	20	23	21	30	28	20	20	25	23	24	23	18	24	19	22		na	7
44 P. triginta	21	20	20	19	21	30	30	21	19	18	19	19	18	25	26	24	21	19	22	22	30	23	24	22	23	23	21	21	23	23	31	32	21	20	25	26	24	24	18	25	20	27	22		22
45 P. zetes	22	19	21	18	21	25	27	21	17	20	18	19	20	25	23	10	21	17	21	24	23	19	22	18	23	11	19	21	23	21	31	28	21	21	20	25	22	26	20	21	24	24	7	22	

Appendix. Material employed for DNA sequencing including voucher codes, DNA codes, species id, cruise, geographic area and GenBank accession numbers.

Voucher code	DNA code	Species	Cruise	Geographic area	COI	16S
MNHN-IU-2014-13796	G517	*P. acastus* **n. sp.**	EBISCO	Chesterfield Islands	XXXXX	XXXXX
MNHN-IU-2017-2634	P55	*P. acastus* **n. sp.**	KANADEEP	New Caledonia	XXXXX	XXXXX
WAM C56280	G658	*P. amphion* **n. sp.**		Western Australia	XXXXX	XXXXX
WAM C55691	P5	*P. amphion* **n. sp.**		Western Australia	XXXXX	XXXXX
MNHN-IU-2011-7659	P14	*P. argus* **n. sp.**	EXBODI	New Caledonia	XXXXX	XXXXX
UF22401	G584	*P. asclepius* **n. sp.**		Western Australia	XXXXX	XXXXX
UF27601	P6	*P. asclepius* **n. sp.**		Western Australia	XXXXX	
UF27886	G751	*P. asclepius* **n. sp.**		Western Australia.		XXXXX
NIWA 92587	KS99	*P. australis* Schnabel & Ahyong, 2019		New Zealand	XXXXX	
NIWA 108588	KS100	*P. australis* Schnabel & Ahyong, 2019		New Zealand	XXXXX	XXXXX
NIWA 56530	KS101	*P. australis* Schnabel & Ahyong, 2019		New Zealand	XXXXX	XXXXX
NIWA 122226	KS102	*P. australis* Schnabel & Ahyong, 2019		New Zealand	XXXXX	
NIWA 57421	KS103	*P. australis* Schnabel & Ahyong, 2019		New Zealand	XXXXX	XXXXX
UF40205	P82	*P. bahamut* **n. sp.**		Red Sea	XXXXX	XXXXX
MNHN-IU-2014-13740	G514	*P. barbeae* **n. sp.**	Lagon Est	New Caledonia	XXXXX	XXXXX
MNHN-IU-2014-13808	G529	*P. barbeae* **n. sp.**	SANTO	Vanuatu	XXXXX	XXXXX
MNHN-IU-2014-13810	G531	*P. barbeae* **n. sp.**	SANTO	Vanuatu	XXXXX	XXXXX
MNHN-IU-2014-13813	G535	*P. barbeae* **n. sp.**	PAPUA NIUGINI	Papua New Guinea	XXXXX	XXXXX
MNHN-IU-2017-3816	P56	*P. boucheti* **n. sp.**	KANADEEP	New Caledonia	XXXXX	
MNHN-IU-2014-13735	G509	*P. butes* **n. sp.**	TARASOC	French Polynesia	XXXXX	XXXXX
MNHN-IU-2014-13803	G524	*P. butes* **n. sp.**	KARUBAR	Indonesia	XXXXX	XXXXX
MNHN-IU-2016-449	P17	*P. butes* **n. sp.**	EBISCO	Chesterfield Islands	XXXXX	XXXXX
MNHN-IU-2014-13860	P70	*P. cepheus* **n. sp.**	BENTHAUS	French Polynesia	XXXXX	XXXXX
MNHN-IU-2019-2695	P69	*P. eneus* **n. sp.**	EXBODI	New Caledonia	XXXXX	

MNHN-IU-2017-3954	G676	*P. eneus* **n. sp.**	KANACONO	New Caledonia	XXXXX	
NIWA 123247	KS91	*P. erebus* Schnabel & Ahyong, 2019		New Zealand	XXXXX	
UF25216	G536	*P. euryalus* **n. sp.**		Queensland, Australia	XXXXX	XXXXX
UF34732	G537	*P. euryalus* **n. sp.**		Queensland, Australia	XXXXX	XXXXX
MNHN-IU-2014-13911	G598	*P. euryalus* **n. sp.**	Lagon Est	New Caledonia	XXXXX	XXXXX
UF252555	P7	P. euryalus n. sP.		Queensland, Australia	XXXXX	
MNHN-IU-2016-489	P29	P. euryalus n. sP.	Grand Recif Sud	New Caledonia	XXXXX	XXXXX
MNHN-IU-2019-2615	P30	P. euryalus n. sP.	Recif Serrez	New Caledonia	XXXXX	
UF35486	P4	*P. gustavi* **n. sp.**		French Polynesia	XXXXX	
UF33774	G581	*P. gustavi* **n. sp.**		French Polynesia	XXXXX	
MNHN-IU-2017-11724	G756	*P. heptacanthus* **n. sp.**	KANACONO	New Caledonia	XXXXX	
UF20156	G570	*P. integrirostris* (Dana 1852)		Hawaii	XXXXX	XXXXX
FFS 354	G688	*P. integrirostris* (Dana 1852)		Hawaii		XXXXX
FFS 353	G690	*P. integrirostris* (Dana 1852)		Hawaii	XXXXX	XXXXX
FFS 882	G691	*P. integrirostris* (Dana 1852)		Hawaii	XXXXX	
FFS 735	G692	*P. integrirostris* (Dana 1852)		Hawaii	XXXXX	
HAW 740	G693	*P. integrirostris* (Dana 1852)		Hawaii	XXXXX	XXXXX
PHR 754	G694	*P. integrirostris* (Dana 1852)		Hawaii		XXXXX
PHR 937	G696	*P. integrirostris* (Dana 1852)		Hawaii		XXXXX
KUR-301	G699	*P. integrirostris* (Dana 1852)		Hawaii	XXXXX	XXXXX
OAH-947	G702	*P. integrirostris* (Dana 1852)		Hawaii	XXXXX	XXXXX
MAI-236	G703	*P. integrirostris* (Dana 1852)		Hawaii	XXXXX	
MAI-196	G704	*P. integrirostris* (Dana 1852)		Hawaii	XXXXX	XXXXX
UF15285	G746	*P. integrirostris* (Dana 1852)		Hawaii		XXXXX
UF15270	G747	*P. integrirostris* (Dana 1852)		Hawaii	XXXXX	
MNHN-IU-2016-425	P34	*P. integrus* (Benedict, 1902)	EBISCO	Chesterfield Islands	XXXXX	
MNHN-IU-2016-426	P35	*P. integrus* (Benedict, 1902)	KARUBAR	Indonesia	XXXXX	XXXXX

NTOU	P48	*P. integrus* (Benedict, 1902)		Taiwan	XXXXX	
MNHN-IU-2014-13804	G525	*P. integrus* (Benedict, 1902)	KARUBAR	Indonesia	XXXXX	XXXXX
MNHN-IU-2014-13799	G520	*P. janiqueae* **n. sp.**	ATIMO VATAE	Madagascar	XXXXX	XXXXX
MNHN-IU-2014-13800	G521	*P. janiqueae* **n. sp.**	ATIMO VATAE	Madagascar	XXXXX	XXXXX
MNHN-IU-2014-13840	G496	*P. janiqueae* **n. sp.**	WALTER SHOALS	SW Indian	XXXXX	XXXXX
MNHN-IU-2014-13841	G497	*P. janiqueae* **n. sp.**	WALTER SHOALS	SW Indian	XXXXX	XXXXX
MNHN-IU-2014-13565	G501	*P. jeffkinchi* **n. sp.**	KAVIENG	Papua New Guinea	XXXXX	XXXXX
MNHN-IU-2014-13661	G503	*P. jeffkinchi* **n. sp.**	KAVIENG	Papua New Guinea	XXXXX	XXXXX
MNHN-IU-2014-2176	G740	*P. jeffkinchi* **n. sp.**	KAVIENG	Papua New Guinea	XXXXX	XXXXX
MNHN-IU-2014-13805	G526	*P. joannotae* **n. sp.**	SANTO	Vanuatu	XXXXX	XXXXX
MNHN-IU-2014-13809	G530	*P. joannotae* **n. sp.**	SANTO	Vanuatu	XXXXX	XXXXX
UF16051	G577	*P. joannotae* **n. sp.**		French Polynesia	XXXXX	XXXXX
UF16169	G580	*P. joannotae* **n. sp.**		French Polynesia	XXXXX	XXXXX
MNHN-IU-IU-2019-2599	G591	*P. joannotae* **n. sp.**	LIFOU	New Caledonia	XXXXX	XXXXX
MNHN-IU-2014-20143	G661	*P. joannotae* **n. sp.**	KOUMAC	New Caledonia	XXXXX	XXXXX
MNHN-IU-2019-5518	G663	*P. joannotae* **n. sp.**	KOUMAC	New Caledonia	XXXXX	XXXXX
MNHN-IU-2014-20148	G664	*P. joannotae* **n. sp.**	KOUMAC	New Caledonia	XXXXX	XXXXX
MNHN-IU-2014-20056	G669	*P. joannotae* **n. sp.**	KOUMAC	New Caledonia	XXXXX	XXXXX
MNHN-IU-2014-20198	G670	*P. joannotae* **n. sp.**	KOUMAC	New Caledonia	XXXXX	XXXXX
MNHN-IU-2014-3426	G671	*P. joannotae* **n. sp.**	KOUMAC	New Caledonia	XXXXX	XXXXX
MNHN-IU-2014-20066	G673	*P. joannotae* **n. sp.**	KOUMAC	New Caledonia	XXXXX	XXXXX
NIWA 118955	KS93	*P. kermadecensis* Schnabel & Ahyong, 2019		New Zealand	XXXXX	XXXXX
MNHN-IU-2014-20035	G662	*P. koumac* **n. sp.**	KOUMAC	New Caledonia	XXXXX	XXXXX
MNHN-IU-2014-20121	G666	*P. koumac* **n. sp.**	KOUMAC	New Caledonia	XXXXX	XXXXX
MNHN-IU-2014-20170	G667	*P. koumac* **n. sp.**	KOUMAC	New Caledonia	XXXXX	XXXXX
MNHN-IU-2019-3427	G668	*P. koumac* **n. sp.**	KOUMAC	New Caledonia	XXXXX	XXXXX
MNHN-IU-2014-13645	G502	*P. laureae* **n. sp.**	KAVIENG	Papua New Guinea	XXXXX	XXXXX

MNHN-IU-2014-13739	G513	*P. laureae* **n. sp.**	LIFOU	New Caledonia	XXXXX	XXXXX
MNHN-IU-2014-13807	G528	*P. laureae* **n. sp.**	SANTO	Vanuatu	XXXXX	XXXXX
UF26910	G578	*P. laureae* **n. sp.**		Japan	XXXXX	XXXXX
NMMBA	P51	*P. lini* **n. sp.**		Taiwan	XXXXX	XXXXX
MNHN-IU-2016-1490	P52	*P. lini* **n. sp.**		Taiwan	XXXXX	XXXXX
MNHN-IU-2019-2593	G532	*P. lynceus* **n. sp.**	Great Chagos Bank - Brothers Island	Chagos	XXXXX	XXXXX
OFU-168	G731	*P. lynceus* **n. sp.**		American Samoa		XXXXX
OLO-187	G732	*P. lynceus* **n. sp.**		American Samoa	XXXXX	XXXXX
ROS-527	G734	*P. lynceus* **n. sp.**		American Samoa		XXXXX
UF51644	G742	*P. lynceus* **n. sp.**		Kiribati		XXXXX
UF51370	G743	*P. lynceus* **n. sp.**		Kiribati	XXXXX	XXXXX
UF51559	G744	*P. lynceus* **n. sp.**		Kiribati	XXXXX	XXXXX
MNHN-IU-2017-11662	G680	*P. maestratii* **n. sp.**	KANACONO	New Caledonia	XXXXX	XXXXX
MNHN-IU-2014-13806	G527	*P. marina* **n. sp.**	SANTO	Vanuatu	XXXXX	
MNHN-IU-2014-13897	G587	*P. marina* **n. sp.**	SANTO	Vanuatu	XXXXX	XXXXX
MNHN-IU-2014-13897	P74	*P. marina* **n. sp.**	SANTO	Vanuatu	XXXXX	
MNHN-IU-2019-2650	G588	*P. marina* **n. sp.**	SANTO	Vanuatu	XXXXX	XXXXX
MNHN-IU-2014-13795	G516	*P. medea* **n. sp.**	LAGON NORD	New Caledonia	XXXXX	XXXXX
MNHN-IU-2019-2636	G757	*P. medea* **n. sp.**	RAPA	French Polynesia	MINIBAR OK	
MNHN-IU-2016-1493	G811	*P. medea* **n. sp.**	RAPA	French Polynesia	XXXXX	XXXXX
MNHN-IU-2016-1493	G816	*P. medea* **n. sp.**	RAPA	French Polynesia		XXXXX
MNHN-IU-2019-2605	G817	*P. medea* **n. sp.**	RAPA	French Polynesia	XXXXX	XXXXX
MNHN-IU-2016-494	G596	*P. medea* **n. sp.**	RAPA	French Polynesia	XXXXX	XXXXX
MNHN-IU-2016-493	G597	*P. medea* **n. sp.**	RAPA	French Polynesia	XXXXX	XXXXX
WAM C46583	G656	*P. nudus* Macpherson, 2008		Western Australia	XXXXX	XXXXX
WAM C44003	G657	*P. nudus* Macpherson, 2009		Western Australia		XXXXX
NIWA 42691	KS86	*P. nui* Schnabel & Ahyong, 2019		New Zealand	XXXXX	XXXXX
NIWA 33658	KS87	*P. nui* Schnabel & Ahyong, 2019		New Zealand	XXXXX	XXXXX

NIWA 33657	KS88	*P. nui* Schnabel & Ahyong, 2019		New Zealand	XXXXX	XXXXX
NIWA 42692	KS89	*P. nui* Schnabel & Ahyong, 2019		New Zealand	XXXXX	
NIWA 24566	KS90	*P. nui* Schnabel & Ahyong, 2019		New Zealand	XXXXX	XXXXX
NIWA 33723	KS104	*P. nui* Schnabel & Ahyong, 2019		New Zealand	XXXXX	XXXXX
UF33962	G569	*P. orpheus* **n. sp.**		French Polynesia	XXXXX	XXXXX
UF33867	P23	*P. orpheus* **n. sp.**		French Polynesia	XXXXX	
UF33961	P24	*P. orpheus* **n. sp.**		French Polynesia	XXXXX	
PAG-898	P63	*P. orpheus* **n. sp.**		Mariana Islands	XXXXX	
UF34088	G582	*P. orpheus* n. sp.		French Polynesia	XXXXX	
MNHN-IU-2016-7002	G494	*P. paulae* **n. sp.**	BIOMAGLO	Îles de Mayotte. des Glorieuses et des Comores	XXXXX	XXXXX
MNHN-IU-2016-7003	G495	*P. paulae* **n. sp.**	BIOMAGLO	Îles de Mayotte. des Glorieuses et des Comores	XXXXX	XXXXX
MNHN-IU-2014-13734	G508	*P. peneleos* **n. sp.**	RAPA	French Polynesia	XXXXX	XXXXX
UF16035	G575	*P. peneleos* **n. sp.**		French Polynesia	XXXXX	XXXXX
UF16078	G576	*P. peneleos* **n. sp.**		French Polynesia	XXXXX	XXXXX
UF16078	P22	*P. peneleos* **n. sp.**		French Polynesia	XXXXX	XXXXX
UF15626	P20	*P. peneleos* **n. sp.**		French Polynesia		XXXXX
UF36172	P41	*P. peneleos* **n. sp.**		French Polynesia		XXXXX
MNHN-IU-2016-486	G683	*P. pepei* **n. sp.**	ATIMO VATAE	Madagascar		XXXXX
MNHN-IU-2016-465	G748	*P. pepei* **n. sp.**	ATIMO VATAE	Madagascar	XXXXX	XXXXX
MNHN-IU-2014-13811	G533	*P. phanus* **n. sp.**	PAPUA NIUGINI	Papua New Guinea	XXXXX	XXXXX
MNHN-IU-2014-13812	G534	*P. phanus* **n. sp.**	PAPUA NIUGINI	Papua New Guinea	XXXXX	XXXXX
MNHN-IU-2016-451	G585	*P. phanus* **n. sp.**	PAPUA NIUGINI	Papua New Guinea	XXXXX	XXXXX
MNHN-IU-2017-1343	G601	*P. phanus* **n. sp.**	PAPUA NIUGINI	Papua New Guinea	XXXXX	XXXXX
MNHN-IU-2016-452	G586	*P. phlias* **n. sp.**	PAPUA NIUGINI	Papua New Guinea	XXXXX	XXXXX
MNHN-IU-2016-452	P75	*P. phlias* **n. sp.**	PAPUA NIUGINI	Papua New Guinea	XXXXX	

MNHN-IU-2014-13736	G510	*P. poeas* **n. sp.**	BENTHAUS	French Polynesia	XXXXX	XXXXX
MNHN-IU-2019-2685	G589	*P. poeas* **n. sp.**	BENTHAUS	French Polynesia	XXXXX	XXXXX
MNHN-IU-2014-13731	G590	*P. poeas* **n. sp.**	BENTHAUS	French Polynesia	XXXXX	XXXXX
MNHN-IU-2016-9658	P38	*P. poeas* **n. sp.**	BENTHAUS	French Polynesia	XXXXX	XXXXX
MNHN-IU-2019_2698	P40	*P. pollux* **n. sp.**	Recif Mbere	New Caledonia	XXXXX	XXXXX
MAU-385	P62	*P. priasus* **n. sp.**		Mariana Islands	XXXXX	
MAU-355	G705	*P. priasus* **n. sp.**		Mariana Islands		XXXXX
MAU-383	G708	*P. priasus* **n. sp.**		Mariana Islands	XXXXX	XXXXX
MAU-305	G709	*P. priasus* **n. sp.**		Mariana Islands	XXXXX	XXXXX
PAG-900	G710	*P. priasus* **n. sp.**		Mariana Islands	XXXXX	
PAG-810	G715	*P. priasus* **n. sp.**		Mariana Islands	XXXXX	
PAG-478	G717	*P. priasus* **n. sp.**		Mariana Islands	XXXXX	
PAG-409	G718	*P. priasus* **n. sp.**		Mariana Islands	XXXXX	
GUAM-601	G721	*P. priasus* **n. sp.**		Guam	XXXXX	XXXXX
GUAM-645	G722	*P. priasus* **n. sp.**		Guam	XXXXX	XXXXX
WAK-218	G726	*P. priasus* **n. sp.**		Wake Island	XXXXX	XXXXX
WAK-221	G727	*P. priasus* **n. sp.**		Wake Island	XXXXX	
WAK-084	G729	*P. priasus* **n. sp.**		Wake Island		XXXXX
MNHN-IU-2019-2675	G592	*P. pulchrus* **n. sp.**	MUSORSTOM 9	French Polynesia	XXXXX	XXXXX
MNHN-IU-2014-20101	G665	*P. punctatus* **n. sp.**	KOUMAC	New Caledonia	XXXXX	XXXXX
NIWA57503	KS92	*P. pusillus* (Henderson, 1885)		Australia	XXXXX	XXXXX
NIWA135602	KS94	*P. pusillus* (Henderson, 1885)		Australia	XXXXX	XXXXX
NIWA 135601	KS95	*P. pusillus* (Henderson, 1885)		Australia	XXXXX	XXXXX
MNHN-IU-2016-492	G599	*P. spinosus* Schnabel & Ahyong, 2019	Lagon Est	New Caledonia	XXXXX	XXXXX
MNHN-IU-2014-13664	G500	*P. talaus* **n. sp.**	KAVIENG	Papua New Guinea	XXXXX	XXXXX
WAM C51399	G660	P. talaus n. sP.		Western Australia	XXXXX	XXXXX
MNHN-IU-2014-13794	G515	*P. tiphys* **n. sp.**	SURPRISES	New Caledonia	XXXXX	XXXXX
NIWA 28066	KS85	*P. triginta* Schnabel & Ahyong, 2019		Australia	XXXXX	

UF30059	P18	*P. zetes* **n. sp.**		French Polynesia	XXXXX	XXXXX
MNHN-IU-2019-2639	G754	*P. zetes* **n. sp.**		French Polynesia	XXXXX	
UF33536	G813	*P. zetes* **n. sp.**		French Polynesia		XXXXX

SENCKENBERG

ORIGINAL PAPER

Species delimitation and multi-locus species tree solve an old taxonomic problem for European squat lobsters of the genus *Munida* Leach, 1820

Paula C. Rodríguez-Flores [1,2] · Annie Machordom [1] · Pere Abelló [3] · Jose A. Cuesta [4] · Enrique Macpherson [2]

Abstract

The taxonomy of *Munida* Leach, 1820 from the north-eastern Atlantic and Mediterranean Sea was studied using a comparative analysis of morphological characters and molecular markers (mitochondrial and nuclear). Generalized Mixed Yule Coalescence and the Poisson tree process models were used to delimit two groups of closely related species associated with uncertain nomenclature and taxonomic status: (1) *Munida intermedia* A. Milne Edwards & Bouvier, 1899, *M. rugosa* (Fabricius, 1775), *M. sarsi* Huus, 1935 and *M. tenuimana* Sars, 1872 and (2) *M. rutllanti* Zariquiey-Álvarez, 1952 and *M. speciosa* von Martens, 1878. We found that *M. tenuimana* is restricted to northern Atlantic waters (north of approx. 48° N), while Mediterranean and Bay of Biscay specimens previously assigned to this taxon actually belong to a different species, indicating that the name *Munida perarmata* A. Milne Edwards & Bouvier, 1894 should be resurrected. Furthermore, *M. rutllanti* is shown to be a junior synonym of *M. speciosa*, a species that has thus far only been reported along western Africa. In addition, three species are re-described and a key to European *Munida* is provided. The validity of the morphological characters used to distinguish the different species is discussed. Phylogenetic analyses revealed three independent lineages with unsolved relationships among them, including high genetic distances for some species. These findings indicate highly divergent lineages of the European *Munida* and several events of colonization along the eastern Atlantic.

Abbreviations

Mxp3	Third maxilliped
P1	First pereiopod (cheliped)
P2–4	Second to fourth pereiopods (first to third walking legs)
M	Males
F	Females
ov	Ovigerous

Communicated by S. De Grave

✉ Paula C. Rodríguez-Flores
paulacrf@mncn.csic.es

1 Museo Nacional de Ciencias Naturales (MNCN-CSIC), C/ José Gutiérrez Abascal, 2, 28006 Madrid, Spain

2 Centre d'Estudis Avançats de Blanes (CEAB-CSIC), Carrer Accés Cala Sant Francesc, 14, 17300 Blanes, Girona, Spain

3 Institut de Ciències del Mar (ICM-CSIC), Passeig Marítim de la Barceloneta, 37-49, E-08003 Barcelona, Spain

4 Instituto de Ciencias Marinas de Andalucía (ICMAN-CSIC), Avda. República Saharaui, 2, 11519 Puerto Real, Cádiz, Spain

Introduction

The squat lobsters of the family Munididae Ahyong, Baba, Macpherson & Poore, 2010, comprise 20 genera and more than 400 species (Ahyong et al. 2010). *Munida* Leach, 1820, with more than 250 described species, is the most speciose and widely distributed genus of the family (Leach 1820; Baba et al. 2008; Macpherson and Baba 2011). In the north-eastern Atlantic and Mediterranean Sea, the genus *Munida* is

Ⓢ Springer

represented by eight species. Five of these including *M. curvimana* A. Milne Edwards & Bouvier, 1894, *M. intermedia* A. Milne Edwards & Bouvier, 1899, *M. rugosa* (Fabricius, 1775), *M. rutllanti* Zariquiey-Álvarez, 1952 and *M. tenuimana* G.O. Sars, 1872, are all found on the continental shelf and slope of both basins. The remaining three however, *M. microphthalma* A. Milne Edwards, 1880, *M. sanctipauli* Henderson, 1885 and *M. sarsi* Huus, 1935, are only found in Atlantic waters (Fabricius 1775; Sars 1872; A. Milne Edwards 1880; Henderson 1885; A. Milne Edwards and Bouvier 1894, 1899; Huus 1935; Zariquiey-Álvarez 1952; Udekem d'Acoz d'Udekem d'Acoz 1999; Ingle and Christiansen 2004; García-Raso et al. 2018). Although these eight species are often collected as by-catch of demersal fisheries throughout the study area (Muñoz et al. 2012), their biology is still poorly known. This particularly relates to their larval stages, which remain undescribed for most of these species (González-Gordillo et al. 2001; Landeira et al. 2017).

These north-eastern Atlantic and Mediterranean *Munida* species have been included in several taxonomic revisions due to their numerous nomenclatural uncertainties. Two comprehensive revisions summarized the current status of the genus in the north-eastern Atlantic: Zariquiey-Álvarez (1952) and Rice and Saint Laurent (1986). However, as d'Udekem d'Acoz (1999) pointed out, some species still present a dubious or controversial taxonomic status. In addition, few molecular studies of the genus have been reported. Thus far, only *M. rugosa* and *M. sarsi* have been studied genetically at the population level (Bailie 2009).

The most controversial species is *M. tenuimana*, known in Europe from Norway (type locality) to the Mediterranean Sea (Rice and Saint Laurent 1986) and reported along the Atlantic coast of Canada (Squires 1970). However, several authors (e.g., Bouvier 1922; Zariquiey-Álvarez 1952; d'Udekem d'Acoz 1999) considered that the specimens from the Mediterranean Sea and Atlantic coasts of the Iberian Peninsula northwards to the Bay of Biscay belong to a different species: *M. perarmata*. This species was originally described by A. Milne Edwards and Bouvier (1894) from two specimens, one collected in Marseille (French Mediterranean) and the other in the Bay of Biscay (eastern Atlantic). The differences between *M. tenuimana* and *M. perarmata* were based on the presence or absence of cardiac spines on the carapace and the number of short striae on the sternites. These characters, after an examination of numerous specimens from both basins, were considered by Rice and Saint Laurent (1986) as variable and thus could not be used reliably to differentiate the species. Therefore, *M. perarmata* has since been considered a junior synonym of *M. tenuimana*.

Among the other European *Munida*, the morphological differences are clear and numerous characters provide enough evidence to distinguish all of these species. However, *M. rutllanti*, described by Zariquiey-Álvarez (1952) from

specimens collected in the Alboran Sea (western Mediterranean), is morphologically close to *M. speciosa* Von Martens, 1878 a common species found along western Africa (Miyake and Baba 1970; Macpherson 1983, 1991). These two species can be distinguished only by the number of spines along the flexor margin of the merus of the third maxilliped and the presence of tubercles on the third abdominal somite (Miyake and Baba 1970). The species was later reported from the Mediterranean Sea, Portugal, the Cantabrian Sea (d'Udekem d'Acoz 1999; Baba et al. 2008) and Mauritania (Muñoz et al. 2012; Matos-Pita and de Ramil 2014). *Munida rutllanti* is also morphologically close to *M. iris* A. Milne Edwards, 1880 from the western Atlantic (Baba et al. 2008; de Melo-Filho 2006). In fact, *M. rutllanti* was originally described by Zariquiey-Álvarez (1952) as a subspecies of *M. iris* (*M. iris rutllanti*) but was subsequently considered an independent species (García-Raso 1996; d'Udekem d'Acoz 1999).

In this study, the hypotheses about these, and related, taxa are tested to resolve their controversial taxonomic status and clarify their phylogenetic relationships. To do this, we sequenced and analyzed five gene fragments (nuclear and mitochondrial) from most European species of *Munida* from eastern Atlantic and Mediterranean waters including *M. curvimana, M. intermedia, M. rugosa, M. rutllanti, M. sarsi*, and *M. tenuimana*. We also included *M. speciosa* from western Africa, *M. microphthalma* from north-eastern and western Atlantic and *M. iris* from French Guiana and the Caribbean Sea. Specifically, this study evaluates the ability of the molecular characters to inform on the taxonomy of squat lobsters and perform species delimitation analyses with the genetic data, comparing different approaches based on coalescence or phylogenetics. We also validate species through morphological examinations and perform phylogenetic analyses to elucidate relationships among these closely related species commonly found in the north-eastern Atlantic. To conclude, a brief diagnosis and figures of the controversial species and a key to the north-eastern Atlantic *Munida* are provided.

Material and methods

Sampling and morphological examination

The specimens examined were obtained from the collections of the Muséum national d'Histoire naturelle (MNHN), Paris (France); Institute of Marine Sciences (ICM), Barcelona (Spain); Senckenberg Museum (SMF), Frankfurt (Germany) and the Spanish Institute of Oceanography (IEO), Cadiz (Spain). Additional samples were collected through trawl survey epibenthic hauls during several cruises along the eastern Atlantic and Mediterranean coasts over the continental shelf
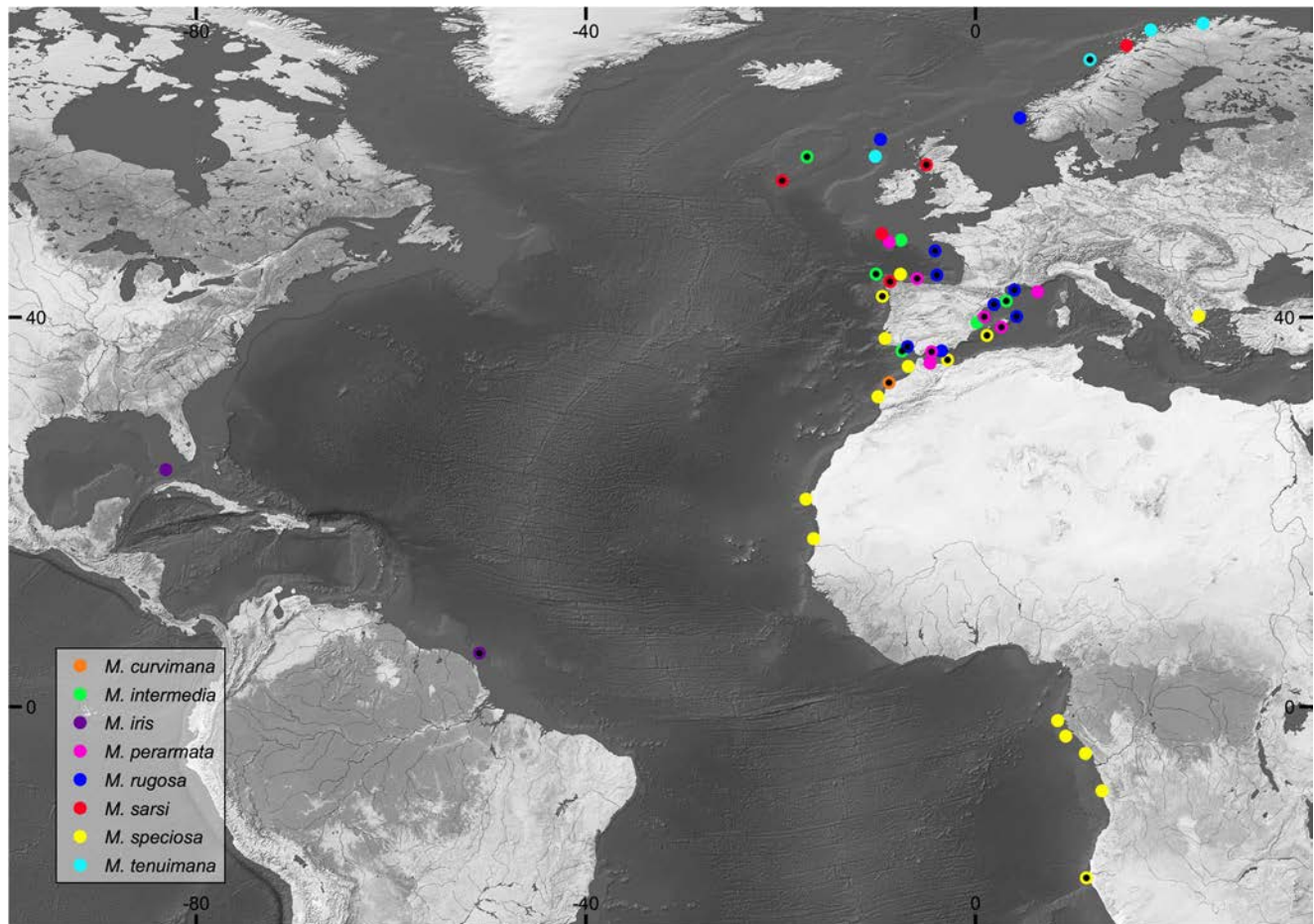
Fig. 1 Map showing the localities of the material examined and sequenced (black dots) of the *Munida* species included in the study (excluding *M. microphthalma*). Specimens originally identified as *M. rutllanti* have been incorporated under the species name *M. speciosa*. Specimens originally identified as *M. tenuimana* from the Mediterranean Sea and Bay of Biscay appear as *M. perarmata* (see text for details and synonyms). Close samplings are included in a single dot for clarity. The shapefile was obtained from the Flanders Marine Institute (2018)

and slope (e.g., ARSA, DEMERSALES, MEDITS). Figure 1 shows a map indicating the sampling localities of the specimens (and species) analyzed in this study. Geographic coordinates are listed in the material examined of each species, in the material sequencing and in the Supplementary Material. The map was built using QGIS Geographic Information System v 3.4.1 (QGIS Development Team 2018).

The general terminology employed for morphological descriptions largely followed Baba et al. (2009, 2011). The size of the carapace was determined by the postorbital carapace length measured along the dorsal midline from the posterior margin of the orbit to the posterior margin of the carapace. The ridges on the posterior branchial region were always counted along the lateral margins, excluding the mid-transverse ridge and the posterior-most ridge anterior to the posterior margin of the carapace. The length of the ocular peduncle was measured along its lateral margin; the width was measured at the mid-length of the ocular peduncle and the orbit. The length of each pereiopod article was measured along its extensor margin (excluding distal spine), and the breadth was measured at its widest portion.

The synonymies of the different species used in this study were restricted to names used in the original descriptions and those used posteriorly to Baba et al. (2008).

DNA extraction, amplification, and sequencing

Tissue samples were taken from the pereiopods (or occasionally from the pleopods) and digested in 180 μl of ATL buffer with 20 μl of proteinase K for 18–24 h. DNA was extracted using the DNeasy Blood and Tissue Kit (Qiagen) following the manufacturer's protocol. Prior to extraction, samples were treated with RNase A 100 mg/ml for 4 min. Fragments were sequenced from two mitochondrial genes [cytochrome c oxidase subunit I (COI) and 16S RNA (16S)] and three nuclear genes [18S RNA (18S), Histone H3 (H3) and phosphoenolpyruvate carboxykinase (PEPCK)]. Table 1 lists the primer pairs used in this study. Each PCR contained 2 μl of template DNA, 0.2 mM of each deoxyribonucleotide triphosphate (dNTP), 0.2 μM of each forward and reverse primer, 1–2 U of MyTaq

Table 1 Set of primers used in this study

Gene	Primer name	Sequence 5'to 3'	Reference
COI	COI L2198	GGTCAACAAATCATAAAGATATTGG	Folmer et al. 1994
COI	COI H	TCAGGGTGACCAAAAAATCA	Machordom et al. 2003
COI	tenuiCOIFwint	GGAGCCTGAGCMGGWATAGTAGG	This study
COI	tenuiCOIRev1int	GTGTTGATAYAAAATAGGGTCTC	This study
COI	tenuiCOIRev2int	ATAAAGGTATTCGATCTAAGGT	This study
16S rDNA	16S ar	CGCCTGTTTATCAAAAACAT	Palumbi et al. 1991
16S rDNA	16S br	CCGGTCTGAACTCAGATCACGT	Palumbi et al. 1991
16S rDNA	16S L am	YGMCTGTTTADCAAAAACAT	Lydeard et al. 1996
16S rDNA	16S H am	CCKKTYTGAACTCARMTCAYGT	Lydeard et al. 1996
H3	H3-F	ATGGCTCGTACCAAGCAGACVGC	Colgan et al. 1998
H3	H3-R	ATATCCTTRGGCATRATRGTGAC	Colgan et al. 1998
18S rDNA	18S A	AACCTGGTTGATCCTGCCAGT	Medlin et al. 1988
18S rDNA	18S L	CCAACTACGAGCTTTT	Apakupakul et al. 1999
18S rDNA	18S C	CGGTAATTCCAGCTC	Apakupakul et al. 1999
18S rDNA	18S Y	CAGACAAATCGCTCC	Apakupakul et al. 1999
18S rDNA	18S O	AAGGGCACCACCAG	Medlin et al. 1988
18S rDNA	18S B	TGATCCTTCCGCAGGTTCACCT	Apakupakul et al. 1999
18S rDNA	18S 1F	TACCTGGTTGATCCTGCCAGTAG	Whiting 2002
18S rDNA	18S 2b.9	TATCTGATCGCCTTCGAACCTCT	Whiting 2002
PEPCK	F2	GCAAGACCAACCTGGCCATG ATGAC	Tsang et al. 2008
PEPCK	R3	CGGGYCTCCATGCTSAGCCARTG	Tsang et al. 2008

Polymerase (Bioline), 5 μl of 5x buffer with MgCl$_2$ and sterilized H$_2$O to a final volume of 25 μl. The gene fragments were amplified under the following conditions: an initial denaturation at 95 °C for 3 min followed by 40 cycles of denaturation at 95 °C for 45–60 s, annealing at 42–55 °C for 45–60 s, and extension at 72 °C for 45–60 s, followed by a final extension at 72 °C for 10 min.

The amplified fragments were purified using ExoSAP-IT (Affymetrix) and, when double bands were present, using β-agarase (BioLabs) following the manufacturer's instructions. After purification, both strands were sequenced at SECUGEN (Madrid). Sequences obtained for each specimen were checked and assembled using Sequencher 4.8 (Gene Code Corporation). Multiple sequence alignments of the ribosomal fragments (16S and 18S) were performed using MAFFT (Katoh et al. 2002) with a posterior manual correction in the alignment editor Se-Al (http://tree.bio.ed.ac.uk/software/seal/). The putative presence of pseudogenes was checked by translating the open reading frame of the protein-encoding genes (COI, H3 and PEPCK) and checking for stop codons and congruence in the alignment (e.g., presence of indels).

The analyzed specimens are listed in Table 2. New sequences were deposited in GenBank. In our analyses, we also included the following sequences of Atlantic specimens of *Munida* available in GenBank: JN564843-8; KX022412, KX022442, KX022458, KX022467-8; MF490055, MF490159; JQ306225-30; and KT209144 (Matzen da Silva et al. 2011; García-Merchán et al. 2012; Raupach et al. 2015; Coykendall et al. 2017; Mantelatto et al. 2018).

Species delimitation, phylogenetic analyses, and species tree estimation

Species boundaries were first analyzed on the basis of genetic distances. To compare different pair of species, uncorrected divergences (p) within and between species were calculated with PAUP (Swofford 2002). The averages of the genetic distances were calculated and represented as percentages.

Different approaches were used for species delimitation, phylogenetic inference and species tree estimation. Here, species delimitation was first analyzed using single-locus data (mitochondrial dataset: COI + 16S) and the Generalized Mixed Yule Coalescent model in a Bayesian framework (bGMYC) (Pons et al. 2006; Reid and Carstens 2012), which works with ultrametric trees to delimit the number of species by detecting a threshold in the branching pattern that can be attributed to speciation. Then the Bayesian implementation of

the Poisson tree process model (bPTP) (Zhang et al. 2013) was run to compare the number of species delimited by each model. The PTP model works with non-ultrametric trees to calculate the number of species in terms of the number of substitutions, which indicates branch length. After the delimitation analyses, a Bayesian inference (BI) approach was used to obtain a phylogenetic tree and applied a method of coalescent-based species tree estimation using the concatenated matrix comprised of mitochondrial and nuclear genes. In all analyses, *Leiogalathea* sp. Rodríguez-Flores et al. (2019a) (Munidopsidae) was chosen as the outgroup (MK140849, MK140886). This species was chosen because relationships within Munididae are not yet established and the closest relative to *Munida* is currently unknown.

In order to run a bGMYC analysis, an ultrametric tree is first needed. To generate this tree, BEAUTi v1.8.4 and BEAST v1.8.4 (Drummond et al. 2012) was implemented. Firstly, the best partition scheme and evolutionary model that fit the data was obtained with PartitionFinder v1.1.0 (Lanfear et al. 2012), relying on the Bayesian information criterion (BIC). As the dataset includes some closely related species, the prior Extended Bayesian Skyline Plot (Heled and Drummond 2008) was selected, which is used to infer past population dynamics based on the coalescent model. The uncorrelated relaxed clock (without fossil calibrations) was chosen, which allows for different substitution rates among branches (Drummond et al. 2006), and a mean rate fixed to 1 for 16S. For the mean rate of COI, a uniform distribution was used with the lower and upper values as 0 and 1, respectively, to allow the rate to be estimated based on 16S. The Markov chains Monte Carlo (MCMC) were run for 5×10^6 generations sampling every 5×10^2 generations with 25% of the samples as burn-in. The bGMYC analysis was first run with the resulting maximum clade credibility (MCC) tree and then with 100 randomly selected trees from the 7500 post-burn-in trees in the bGMYC1.0.2 package (Reid and Carstens 2012) in R 3.3.2 (R Core Team 2016). In both cases, the following uniform priors were used: Yule process rate change (0–5), coalescence process rate change (0–1.5), and threshold parameter or number of taxa (1–16). Then, a scale for these parameters (1, 1, 0.2) was fixed and the results were plotted to check for convergence.

For the bPTP analyses, a Bayesian inference (BI) and a maximum likelihood (ML) tree were used as inputs for comparison. The rooted BI phylogenetic tree was obtained using MrBayes v3.2.1 (Ronquist and Huelsenbeck 2003). Posterior probabilities (pP) were estimated by running MCMC for 5×10^6 generations, sampling trees and parameters every 500 generations and discarding 25% of the generations as burn-in. PhyML v3.1 (Guindon and Gascuel 2003) was used to obtain the ML phylogenetic tree. This program works with a model of evolution for all concatenated data; therefore, jModelTest 2.1.5 (Guindon and Gascuel 2003; Darriba et al. 2012) was used following the BIC to calculate the best substitution model for the combined mitochondrial dataset. For the bPTP analyses, the Exelixis Lab species

delimitation web server was used (https://species.h-its.org). Default values were used for the priors: the number of MCMC generations was 10^5, as recommended for small trees built from less than 50 taxa, thinning was set to 100 and burn-in to 25% of the initial samples. Convergence of the parameters was checked after the run.

To explore potential conflicts between different loci (e.g., incongruence of the information of each gene) in the species validation based on mitochondrial matrices, both phylogenetic and species tree relationships with concatenated mitochondrial and nuclear matrices were established. To test the monophyly of putative taxa, a BI analysis was conducted using MrBayes v3.1.2 running MCMC for 5×10^6 generations, sampling trees and parameters every 500 generations and discarding 25% of the generations as burn-in. Species Tree Ancestral Reconstruction was performed with *BEAST (Heled and Drummond 2010) implemented in BEAST v1.8.4, considering the species previously delimited though the single-locus methods. This method calculates a species tree from multiple loci and several specimens per species. *BEAST was run considering the best partition model that fit our concatenated data as determined by PartitionFinder v1.1.0. We chose an uncorrelated lognormal clock, a Yule process prior for the species tree and uniform priors (initial value 1, upper value 10, lower value 0) for COI and nuclear genes rates, which were estimated from the 16S rate (fixed value = 1). The marginal likelihood of two species tree hypotheses (considering 9 or 10 species, see results of species delimitation analyses for details) was estimated with a stepping stone and path sampling analyses in *BEAST. The most probable species tree was selected by a Bayesian factor test in the mtraceR package in R (Pacioni et al. 2015) according to the marginal likelihood obtained for each species tree hypothesis. This package calculates the log Bayes factors of all the models of interest and compares them against the model with the highest marginal likelihood (the reference model). The models were then ranked according to the logBF and their probability estimated. All BEAST analyses were run in the CIPRES Science Gateway v.3.1 (Miller et al. 2010). After running these analyses, the effective sample size (ESS) of each parameter was visualized in Tracer v1.7 (Rambaut et al. 2018). The results were synthesized and annotated on a MCC tree generated in Tree Annotator v1.8.4 (Drummond and Rambaut 2007) after 25% of the trees were discarded as burn-in. The resulting MCC trees from each analysis were visualized and edited in FigTree v1.4.3 (Rambaut 2012).

Results

Sequence traits and phylogenetic relationships among the Atlantic *Munida* lineages

After alignment, the sequence data used for analyses consisted of 4009 characters: 657 bp (COI), 529 bp (16S), 1903 bp (18S),

Table 2 Material used for DNA analyses of *Munida* species including taxonomy, coordinates, depth, geographic area, voucher codes, and GenBank accession numbers. Hyphens (−) represent no data

| Species	Species id. (after this study)	COI	16S	18S	H3	PEPCK	Geographic area	Latitude	Longitude	Depth (m)	Voucher
M. curvimana	*M. curvimana*	MK138911	MK141709	MK157305	MK157347	MK157389	NW Africa	34° 15' N	07° 49' W	210	IEO-CD-CCLME11/709
M. curvimana	*M. curvimana*	MK138912	MK141710	MK157306	MK157348	MK157390	NW Africa	34° 15' N	07° 49' W	210	IEO-CD-CCLME11/710
M. intermedia	*M. intermedia*	MK138913	MK141711	MK157307	MK157349	MK157391	NW Mediterranean	41° 34' N	02° 33' E	250	ICMD002514
M. intermedia	*M. intermedia*	MK138914	MK141712	MK157308	MK157350	MK157392	NW Mediterranean	41° 34' N	02° 33' E	250	ICMD002515
M. intermedia	*M. intermedia*	MK138915	MK141713	MK157309	MK157351	MK157393	NW Spain	42° 44' N	09° 16' W	560	ICMD002516
M. intermedia	*M. intermedia*	MK138916	MK141714	MK157310	MK157352	MK157394	NW Spain	42° 44' N	09° 16' W	560	ICMD002517
M. intermedia	*M. intermedia*	MK138917	−	MK157311	MK157353	MK157395	NW Mediterranean	41° 34' N	02° 33' E	250	ICMD002518
M. intermedia	*M. intermedia*	MK138918	MK141715	MK157312	MK157354	MK157396	NW Mediterranean	41° 34' N	02° 33' E	250	ICMD002519
M. intermedia	*M. intermedia*	MK138919	−	−	MK157355	−	SW Spain	36° 29' N	07° 12' W	579	ICMD002520
M. intermedia	*M. intermedia*	MK138920	MK141716	MK157313	MK157356	MK157397	SW Spain	36° 29' N	06° 47' W	277	ICMD002521
M. intermedia	*M. intermedia*	MK138921	MK141717	MK157314	MK157357	MK157398	SW Spain	36° 47'N	07° 17' W	487	ICMD002522
M. intermedia	*M. intermedia*	MK138922	−	MK157315	MK157358	−	NE Atlantic	56° 30' N	17° 18' W	629	ICMD002523
M. iris	*M. iris*	MK138923	MK141718	MK157316	MK157359	MK157399	W Central Atlantic	05° 30' N	50° 56' W	224–225	MNHN-IU-2016-9640
M. iris	*M. iris*	MK138924	MK141719	MK157317	MK157360	MK157400	W Central Atlantic	06° 44' N	52° 30' W	303–307	MNHN-IU-2013-2568
M. microphthalma	*M. microphthalma*	MK138925	MK141720	MK157318	MK157361	MK157401	SW Atlantic	24° 26' S	42° 44' W	1220	ICMD002524
M. tenuimana	*M. perarmata*	MK138926	MK141721	MK157319	MK157362	MK157402	W Mediterranean	38° 58' N	02° 39' E	738	ICMD002525
M. tenuimana	*M. perarmata*	MK138927	MK141722	MK157320	MK157363	MK157403	W Mediterranean	38° 58' N	02° 39' E	738	ICMD002526
M. tenuimana	*M. perarmata*	MK138928	MK141723	MK157321	MK157364	MK157404	W Mediterranean	38° 48' N	00° 49' E	696	ICMD002527
M. tenuimana	*M. perarmata*	MK138929	MK141724	MK157322	MK157365	MK157405	W Mediterranean	39° 13' N	01° 27' E	539	ICMD002528
M. tenuimana	*M. perarmata*	MK138930	MK141725	MK157323	MK157366	MK157406	SW Mediterranean	36° 17' N	04° 45' W	758	ICMD002529
M. tenuimana	*M. perarmata*	MK138931	MK141726	MK157324	MK157367	MK157407	NW Spain.	43° 54' N	05° 03' W	835	ICMD002530
M. rugosa	*M. rugosa*	MK138932	MK141727	MK157325	MK157368	−	SW Mediterranean	36° 37' N	04° 20' W	122	ICMD002531
M. rugosa	*M. rugosa*	MK138933	MK141728	MK157326	MK157369	MK157408	NW Mediterranean	40° 25' N	00° 59' E	130	ICMD002532
M. rugosa	*M. rugosa*	MK138934	MK141729	MK157327	MK157370	MK157409	W Mediterranean	39° 50' N	04° 22' E	72	ICMD002533
M. rugosa	*M. rugosa*	MK138935	MK141730	MK157328	MK157371	MK157410	NE Atlantic	47° 35' N	04° 12' W	100	ICMD002534
M. rugosa	*M. rugosa*	MK138936	MK141731	MK157329	MK157372	MK157411	NW Spain.	44° 42' N	05° 06' W	102	ICMD002535
M. rugosa	*M. rugosa*	MK138937	MK141732	MK157330	MK157373	MK157412	SW Spain	36° 29' N	06° 47' W	277	ICMD002536
M. rutllanti	*M. speciosa*	MK138938	MK141733	MK157331	−	MK157413	NW Spain.	42° 30' N	09° 24' W	251	ICMD002537
M. rutllanti	*M. speciosa*	MK138939	MK141734	MK157332	MK157374	MK157414	SW Mediterranean	36° 43' N	02° 17' W	244	ICMD002538
M. rutllanti	*M. speciosa*	MK138940	MK141735	MK157333	MK157375	MK157415	SW Mediterranean	36° 32' N	04° 26' W	133	ICMD002539
M. rutllanti	*M. speciosa*	MK138941	MK141736	MK157334	MK157376	MK157416	W Mediterranean	39° 12' N	01° 35' E	318	ICMD002540
M. rutllanti	*M. speciosa*	MK138942	−	−	−	−	NW Mediterranean	42° 15' N	03° 21' E	510	ICMD002546
M. rutllanti	*M. speciosa*	MK138943	−	MK157335	MK157377	−	SW Mediterranean	36° 31' N	04° 23' W	245	ICMD002541
M. rutllanti	*M. speciosa*	MK138944	MK141737	MK157336	MK157378	−	W Mediterranean	38° 48' N	00° 49' E	696	ICMD002542
M. sarsi	*M. sarsi*	MK138945	MK141738	MK157337	MK157379	MK157417	NW Spain	42° 44' N	09° 16' W	560	ICMD002543

Table 2 (continued)

Species	Species id. (after this study)	COI	16S	18S	H3	PEPCK	Geographic area	Latitude	Longitude	Depth (m)	Voucher
M. sarsi	*M. sarsi*	MK138946	MK141739	MK157338	MK157380	–	NW Spain	42° 44' N	09° 16' W	560	ICMD002544
M. sarsi	*M. sarsi*	MK138947	MK141740	MK157339	MK157381	MK157418	NE Atlantic	57° 41' N	09° 07' W	485	ICMD002545
M. sarsi	*M. sarsi*	MK138948	MK141741	MK157340	MK157382	MK157419	NW Spain	42° 44' N	09° 16' W	560	ICMD002547
M. sarsi	*M. sarsi*	MK138949	MK141742	MK157341	MK157383	MK157420	NW Spain	42° 44' N	09° 16' W	560	ICMD002548
M. sarsi	*M. sarsi*	MK138950	MK141743	MK157342	–	–	NE Atlantic	56° 30' N	17° 18' W	674	ICMD002549
M. speciosa	*M. speciosa*	MK138951	MK141744	–	–	–	SW Africa	17° 37' S	11° 23' E	270	ICMD002550
M. speciosa	*M. speciosa*	MK138952	MK141745	MK157343	MK157384	–	SW Africa	19° 25' S	11° 36' E	336–340	ICMD002551
M. speciosa	*M. speciosa*	MK138953	MK141746	–	MK157385	–	SW Africa	19° 04' S	11° 38' E	295	ICMD002552
M. speciosa	*M. speciosa*	MK138954	MK141747	MK157344	MK157386	–	SW Africa	17° 37' S	11° 23' E	270	ICMD002553
M. tenuimana	*M. tenuimana*	MK138955	MK141748	MK157345	MK157387	–	NE Atlantic	68° 00' N	15° 17' E	630	ICMD002554
M. tenuimana	*M. tenuimana*	MK138956	MK141749	MK157346	MK157388	MK157421	NE Atlantic	68° 02' N	15° 15' E	513	ICMD002555

328 bp (H3), and 592 bp (PEPCK) for the individuals analyzed (42 in the mitochondrial matrix; 39 in the concatenated matrix). Additionally, for the genetic distance analyses, individual gene matrices was generated, which included sequences available in GenBank using the COI, 16S, 18S, H3 and PEPCK sequences of 61, 47, 42, 41, and 33 specimens, respectively (Table 2). The substitution models that best fit our data, under the BIC, were GTR + G for the concatenated mitochondrial dataset, TVMef + I + G for 18S and TrN + G for both H3 and PEPCK.

The phylogenetic analyses of the mitochondrial and concatenated matrices revealed that the analyzed taxa (terminal lineages = species) resolved as monophyletic and well-supported groups, with Bayesian posterior probabilities (pP) > 0.95 and non-parametric bootstrap supports for the Maximum likelihood (ML) > 70 (Figs. 2 and 3). The following clades were recovered: *M. curvimana*, *M. intermedia*, *M. microphthalma*, *M. rugosa*, *M. rutllanti* + *M. speciosa*, *M. sarsi*, *M. tenuimana* from the Mediterranean Sea and Bay of Biscay and *M. tenuimana* from off the coast of Norway. These lineages were found to be strictly monophyletic; therefore, we herein consider *M. tenuimana* specimens from the Mediterranean Sea and Bay of Biscay as *M. perarmata*. We also consider *M. rutllanti* specimens as *M. speciosa*. The only exception was *M. iris*, which remained as a differentiated clade (pP = 0.99) within the *M. speciosa* lineage in the phylogeny derived from the concatenated dataset (Fig. 3). However, the mitochondrial gene analyses recovered the species as sister groups (pP = 1; no support for the ML) (Fig. 2). According to the phylogenetic analyses of the concatenated matrix, species of *Munida* from the eastern Atlantic are separated into three well-differentiated lineages with unsolved relationships among them. The first lineage was comprised of the abyssal species *M. microphthalma* from the eastern and western Atlantic; the second of the species of European *Munida* sensu stricto (*Munida curvimana*, *M. intermedia*, *M. perarmata*, *M. rugosa*, *M. sarsi*, and *M. tenuimana* from off the coast of Norway) and the third of *M. rutllanti* = *M. speciosa* (with no differentiation) from the eastern Atlantic and *M. iris* from the western Atlantic. These three lineages together formed a polytomy, and thus the relationship among them could not be resolved. The clade constituted by the strictly European *Munida* was composed of closely related species, but their basal relationships remained unsupported. All analyses highly supported the sister group relationship between *M. intermedia* and *M. rugosa*. The sister group relationship between *M. sarsi* and *M. perarmata* was moderately supported in the BI analyses (pP = 0.94 and 0.93 for mitochondrial and concatenated analyses, respectively). These two clades (*M. intermedia* + *M. rugosa* and *M. sarsi* + *M. perarmata*) resolved as sister groups in the BI analysis of the mitochondrial dataset with high support (pP = 0.98); however, this relationship was unsupported in the analyses of the concatenated dataset. *Munida curvimana* resolved as the sister group of these clades with high support in all analyses (pP = 1). Interestingly, no phylogeographic structure was detected for the species

Fig. 2 Bayesian consensus tree based on the analysis of the concatenated mitochondrial dataset (COI + 16S). Values at nodes represent ML boostrap support and Bayesian posterior probabilities, respectively. Results of the species delimitation analyses are also indicated by the colored bars: bPTP with ML tree in red, bPTP with Bayesian tree in green, bGMYC with $P = 0.5$ in gray and bGMYC with $P = 0.05$ in blue. Branch tips are labeled according to the morphospecies
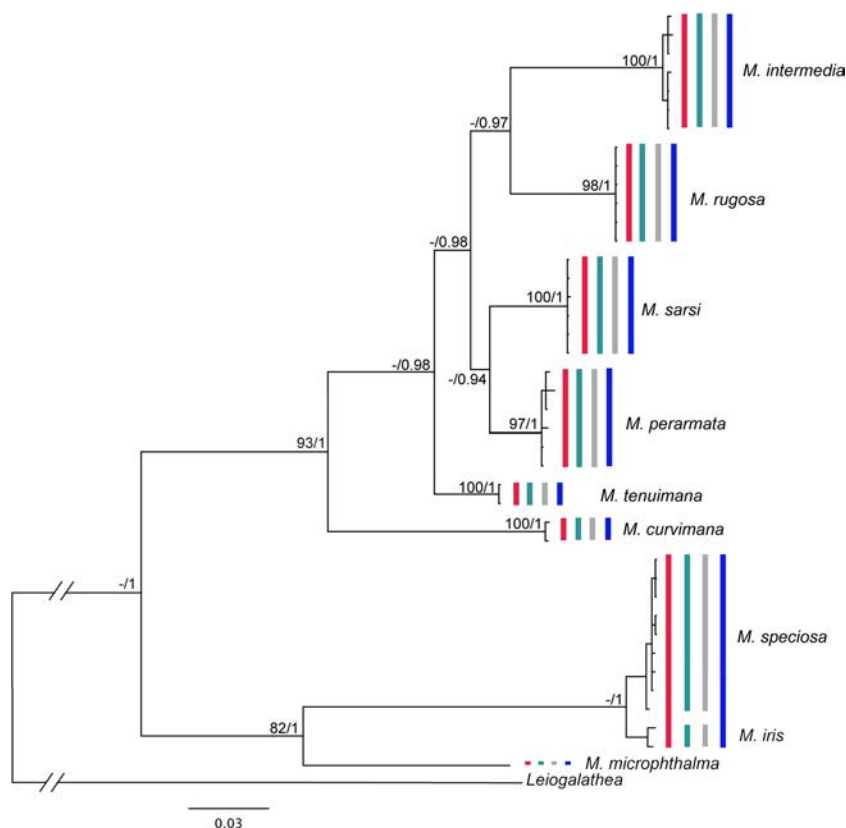
found in both the Mediterranean and the Atlantic (i.e., *M. intermedia*, *M. rugosa*, and *M. perarmata*) (Figs. 2 and 3).

## Genetic distances among lineages of European *Munida*

Genetic variability, as determined by genetic divergences, supported the phylogenetic results. Genetic distances of up to 0.1% for all markers analyzed were observed between *M. speciosa* specimens from the north-eastern Atlantic (initially identified as *M. rutllanti*) and those from western Africa. *Munida tenuimana* sensu stricto from off the coast of Norway and *M. tenuimana* from the Mediterranean Sea and Bay of Biscay (considered here as *M. perarmata*) showed relatively high genetic distances (e.g., 6.0% for COI and 2% for 16S). Although not observed for COI, the intraspecific distance of *M. iris* for 16S (0.3%) was the same as the lowest interspecific distance observed for this species (with *M. speciosa*). Generally, the divergences observed among the analyzed species ranged extensively for the mitochondrial markers, and in some cases, were unexpectedly high (distances ranged from 2.7 to 17.9% for COI and 0.4 to 13.2% for 16S) (Table 3). Some relatively high genetic distances were found for the nuclear marker 18S (ranging from 0.9 to 11.6%). This marker helped to differentiate species, excluding *M. iris* from *M. speciosa* (which showed a distance of only 0.1%). The H3 gene fragment could only distinguish the species group comprised of *M. curvimana*, *M. intermedia*, *M. rugosa*, *M. perarmata*, *M. sarsi*, and

M. tenuimana (i.e., species with very few genetic differences among them in this marker, from 0.0 to 0.6%) from *M. micropthalma* and *M. speciosa*, with divergences ranging from 1.9 to 2.9% (Table 4). The most closely related species are *M. intermedia*, *M. rugosa*, *M. perarmata*, *M. sarsi*, and *M. tenuimana*. This species group presented high genetic distances with respect to the other species for COI, 16S and 18S (ranging from 13.6 to 17.9%, 9.0 to 13.2%, and 5.9 to 8.5%, respectively). Intraspecific genetic distances were lower than expected and varied up to 0.9%, 0.3%, and 0.5% for COI, 16S, and 18S, respectively (Tables 3 and 4). The largest intraspecific genetic distance observed was in *M. iris* (COI 0.9%) when comparing our sequences from French Guiana to those available in GenBank, which correspond to material from the Gulf of Mexico (Tables 2 and 3).

Species delimitation and species tree estimation

The two approaches used to delimit species, bPTP and bGMYC, showed similar results (Fig. 2) and consistently recovered the following species: *M. curvimana*, *M. intermedia*, *M. micropthalma*, *M. perarmata*, *M. rugosa*, *M. speciosa*, *M. sarsi*, and *M. tenuimana*. Although the bPTP analyses using the Bayesian tree resulted in a highly supported partition with nine inferred species, the most supported one was built of eight species using the ML tree. In the bGMYC analysis, two probability thresholds were considered: the mean of the analyses ($P = 0.5$: 9 species) and the more restrictive analysis ($P =$

Springer
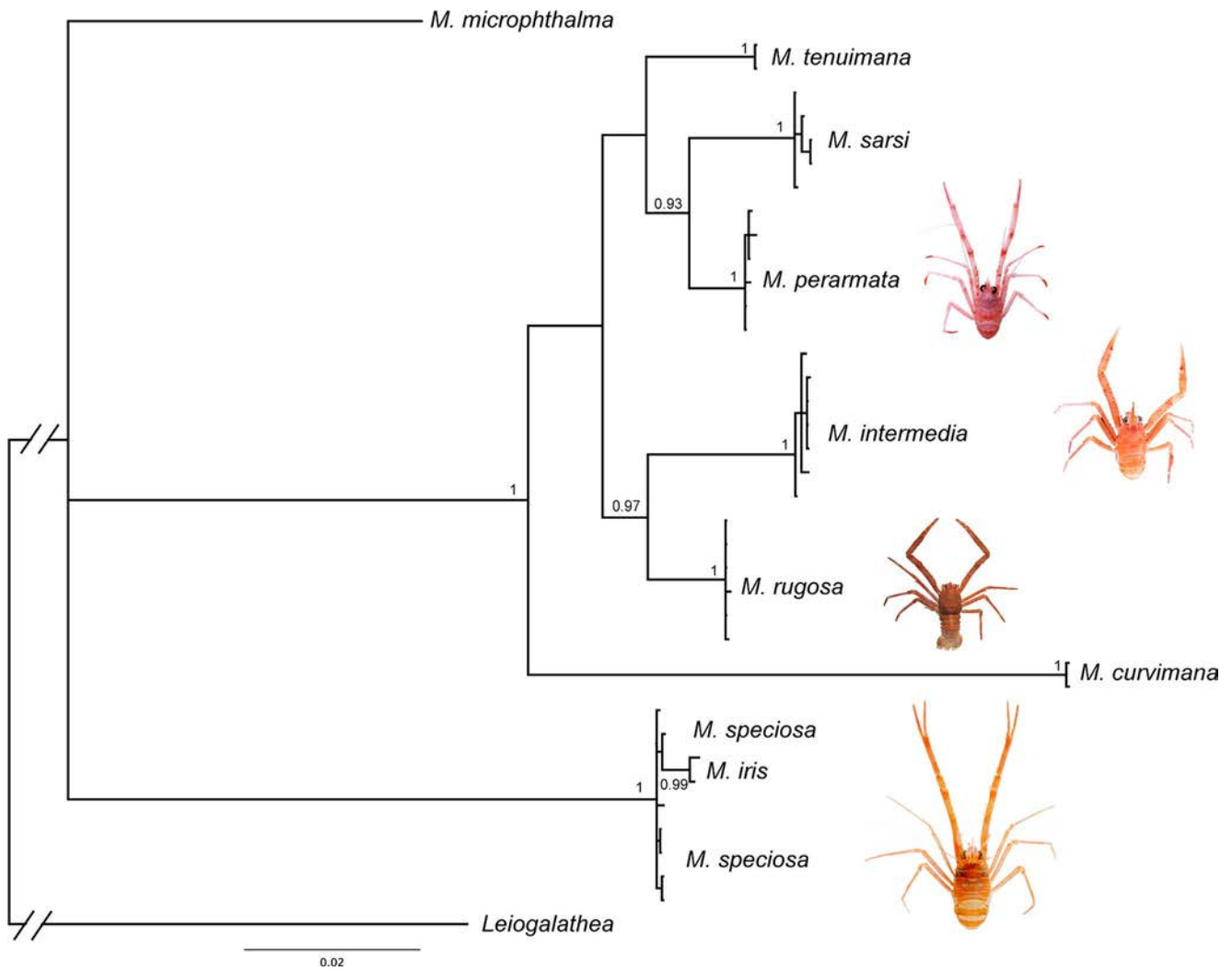
Fig. 3 Bayesian consensus tree based on the analysis of the concatenated dataset (COI + 16S + 18S + H3 + PEPCK). Values at nodes represent Bayesian posterior probabilities. Branch tips are labeled according to the morphospecies

Table 3 Average of the uncorrected pairwise genetic distances between *Munida* species as percentages for COI and 16S. Divergence values are shown for COI below the diagonal and for 16S above the diagonal. Genetic intraspecific distances for COI and 16S, respectively, are marked in italics in the diagonal. Hyphens (−) represent no data

	M. curvimana	*M. intermedia*	*M. iris*	*M. microphthalma*	*M. perarmata*	*M. rugosa*	*M. sanctipauli*	*M. sarsi*	*M. speciosa*	*M. tenuimana*
M. curvimana	*0.0, 0.3*	7.6	15.8	13.2	5.3	7.6	–	6.4	15.7	5.9
M. intermedia	13.1	*0.6, 0.0*	12.7	9.3	3.2	2.0	–	3.5	12.5	2.5
M. iris	14.9	16.7	*0.9, 0.3*	8.4	12.9	11.9	–	12.9	0.3	13.2
M. microphthalma	13.1	16.5	15.0	*0.2, 0.0*	10.0	9.0	–	10.5	8.3	9.3
M. perarmata	11.5	8.7	14.4	13.6	*0.1, 0.3*	2.7	–	2.2	12.7	2.0
M. rugosa	13.2	10.0	16.5	14.8	7.3	*0.0, 0.0*	–	3.0	11.8	2.3
M. sanctipauli	14.2	17.0	13.5	11.3	14.9	17.0	*0.5, −*	–	–	–
M. sarsi	12.0	11.4	16.3	15.1	6.5	10.2	16.0	*0.0, 0.0*	12.8	2.8
M. speciosa	15.6	17.9	2.7	14.9	14.9	17.7	13.2	16.2	*0.1, 0.0*	13.0
M. tenuimana	11.0	8.9	15.6	13.8	6.0	9.5	15.0	8.0	16.2	*0.0, 0.0*

Table 4 Average of the uncorrected pairwise genetic distances between *Munida* species as percentages for H3 and 18S. Divergence values are shown for H3 below the diagonal and for 18S above the diagonal. Genetic intraspecific distances for H3 and 18S, respectively, are marked in italics in the diagonal. Hyphens (−) represent no data

	M. curvimana	M. intermedia	M. iris	M. microphthalma	M. perarmata	M. rugosa	M. sarsi	M. speciosa	M. tenuimana
M. curvimana	*0.0, 0.0*	6.0	8.5	8.4	6.2	6.0	6.3	11.6	8.1
M. intermedia	0.3	*0.0, 0.5*	6.2	5.3	1.0	0.7	1.7	6.8	1.8
M. iris	1.6	1.9	*0.0, 0.1*	5.9	6.4	6.1	6.8	0.1	6.7
M. microphthalma	2.5	2.2	2.9	*−, −*	5.4	5.1	5.9	7.5	6.7
M. perarmata	0.6	0.3	1.6	2.5	*0.0, 0.5*	0.9	1.1	7.8	1.7
M. rugosa	0.3	0.0	1.9	2.2	0.3	*0.0, 0.02*	1.4	7.1	1.5
M. sarsi	0.3	0.0	1.9	2.2	0.3	0.0	*0.0, 0.1*	8.5	2.1
M. speciosa	1.6	1.9	0.0	2.9	1.6	1.9	1.9	*0.0, 0.0*	6.7
M. tenuimana	0.3	0.0	1.9	2.2	0.3	0.0	0.0	1.9	*0.0, −*

0.05: 8 species). By doing so, over-splitting the samples and/or inferred species was avoided when the less restrictive analysis was considered (*P* = 0.95: 14 species). As for *M. iris*, and its relationship with *M. speciosa*, both the bPTP with ML tree and the bGMYC (*P* = 0.05) analyses considered the clade as a single species. In contrast, the bPTP with the Bayesian tree and the bGMYC (*P* = 0.5) analyses split the clade into two distinct species, *M. iris* and *M. speciosa* (Fig. 2).

The species tree resulting from the *BEAST analysis revealed topological incongruences compared with the phylogenetic tree obtained by Bayesian analyses of the mitochondrial and concatenated data. The main incongruence was found in the European *Munida* sensu stricto clade with the inclusion of *M. curvimana* within the *rugosa-intermedia* group (species tree not shown). According to the results of the Bayes factor test, the most likely species tree resulted when (1) *M. iris* and *M. speciosa* were considered independent taxa rather than when (2) *M. iris* was considered as part of the lineage *speciosa*: log marginal likelihood under stepping stone model (1) = − 11,420 and (2) = − 11,423.03, logBF (1) = 0 and (2) = − 6.06; *p* (1) = 0.998 and (2) = 0.002.

Species validation and taxonomic status of the European *Munida*

Morphological analyses of 321 *Munida* specimens from the western Atlantic revealed 9 well-differentiated morphotypes that can be easily assigned to each species. Furthermore, the molecular results showed that the historically controversial species *M. intermedia*, *M. rugosa*, *M. sarsi*, and *M. tenuimana* sensu stricto (only Atlantic populations) were considered as species in the species delimitation analyses, reciprocally monophyletic in the phylogenetic analyses and presented consistent differences in all characters analyzed (see results above). Therefore, they are considered as valid

taxonomic units. *Munida speciosa* and *M. rutllanti* showed similar values of both intraspecific and interspecific genetic distances and did not resolve as reciprocally monophyletic for any of the loci analyzed. In fact, none of our results supported two differentiated species. Hence, *M. rutllanti* should be considered as a junior synonym of *M. speciosa* (see below for the variability of their morphological characters). Additionally, *M. iris* from the western Atlantic seems to be the closest relative of *M. speciosa*. Both species present low genetic distances, and the species hypotheses tested through species delimitation methods were not fully congruent. However, due to subtle but constant morphological differences and the large geographic distances that separate their distribution areas, both *M. iris* and *M. speciosa* are considered here as valid species.

The specimens of *M. tenuimana* from the Mediterranean Sea to the Bay of Biscay showed clear morphological and molecular differences from those collected from the northeastern Atlantic near Norway and Ireland. These groups should be considered as different species (Figs. 2 and 3). Consequently, the name *Munida perarmata* should be resurrected for the specimens collected from the Mediterranean Sea to the Bay of Biscay (see below for the morphological differences between species).

Morphological characterization and systematic account

Below, a brief diagnosis is provided, avoiding non-distinctive morphological characters, of the three controversial species: *M. perarmata, M. speciosa*, and *M. tenuimana*. More extensive descriptions can be found in previous studies (see e.g., d'Udekem d'Acoz 1999; Baba et al. 2008 and references therein).

Key to species of the genus *Munida* from European waters

1. Lateral parts of posterior thoracic sternites with granules……………………………………………………*M. sanctipauli*
— Lateral parts of posterior thoracic sternites without granules ……………………………………………………**2**

2. Eyes small, cornea barely wider than eyestalk. Maximum corneal diameter about 1/4 length of anterior border of carapace between external orbital spines ……………………………………………………………………………**3**
— Eyes large, cornea dilated. Maximum corneal diameter equal to or greater than 1/4 length of anterior border of carapace between external orbital spines………………………………………………………………………………………**4**

3. Abdominal somites 2 and 3 with spines on anterior ridge……………………………………………………*M. rugosa*
— Abdominal somites unarmed or with spines on anterior ridge of somite 2…………………………*M. microphthalma*

4. P1 fingers more than 3 times length of palm. Abdominal somites only with spines on anterior ridge of somite 2……………………………………………………………………………………………………*M. curvimana*
— P1 fingers as long as or slightly longer than palm. Abdominal somites at least with spines along anterior ridge of somites 2 and 3 (rarely absent on somite 3). ………………………………………………………………………………………**5**

5. Antennal article 1 mesially expanded to epistomic ridge…………………………………………………*M. speciosa*
— Antennal article 1 not mesially expanded to epistomic ridge……………………………………………………**6**

6. Extensor margin of merus of Mxp3 with distal spine. Abdominal somite 4 with or without spines……………………………………………………………………………………………………*M. intermedia*
— Extensor margin of merus of Mxp3 unarmed. Abdominal somite 4 almost always with at least one pair of spines……**7**

7. Numerous spinules on hepatic and anterior branchial regions of carapace………………………………………*M. sarsi*
— A single spinule on hepatic region, anterior branchial region unarmed……………………………………………**8**

8. Carapace usually with cardiac spines. 9–10 ridges in cardiac region and 10–12 interrupted or scale-like transverse ridges in each branchial region. Abdominal somites 2–3 each with 6–7 additional transverse ridges on tergite other than anterior ridge……………………………………………………………………………………………*M. perarmata*
— Carapace unarmed in cardiac region. 6–7 ridges in cardiac region and 6–8 interrupted or scale-like transverse ridges in each branchial region. Abdominal somites 2–3 each with 2–4 additional transverse ridges on tergite other than anterior ridge………………………………………………………………………………………*M. tenuimana*

Munida perarmata A. Milne Edwards & Bouvier, 1894

Fig. 4

Munida perarmata A. Milne Edwards & Bouvier, 1894: 257, 325.

Munida tenuimana Baba et al. 2008: 125 (in part, only citations from the Mediterranean Sea to the Bay of Biscay). — Cartes et al. 2014: 168.

Material examined. Type material. *Lectotype*. Female 9.8 mm, MNHN-IU-2014-10968, Mediterranean Sea, Marseille, Travailleur, Stn 1, 43° 02' N, 05°19' E, 555 m, 4 July 1881.

Paralectotype. Female broken, MNHN-IU-2014-10969, Atlantic Ocean, Bay of Biscay, Travailleur, Stn 2, 43° 36' N, 01° 55' W, 1019 m, 17 July 1880.

Other material.

Atlantic Ocean

Celtic Sea. Jean Charcot. Stn 16, 47° 39.8' N, 08° 05.3' W, 900–1120 m, 5 December 1968: 1 M 12.0 mm (MNHN-Ga1040). — Stn CP26, 47° 26.5' N, 06° 30.2' W, 550–600 m, 7 December 1968: 1 M 8.4 mm, 1 ov. F 9.8 mm (MNHN-Ga978). — PROCELT 1. Stn K233, 47° 42' N,

08° 02' W, 919–1085 m, 26 June 1984: 1 M 20.4 mm (MNHN-Ga1541).

Bay of Biscay. NORATLANTE. Stn P128 (B20), 47° 41' N, 08° 06' W, 1174 m, 1 November 1969: 1 M 15.7 mm, 1 F 7.3 mm (MNHN-Ga1048). — BIOGAS 1. Stn CM01, 47° 44' N, 08° 51' W, 1010 m, 4 August 1972: 3 M 16.3–23.0 mm, 4 F 14.0–15.5 mm (ICMD002556). — Stn DS04, 47°42.9'N, 08°03.5'W, 1100 m, 1 August 1972: 2 M 14.7–17.5 mm, 4 F 10.0–12.1 mm (ICMD002557).

Cantabric Sea. DEMERSALES 2014, Stn 102, 43° 54' N, 05° 03' W, 835 m, 12 August 2014: 1 M 6.6 mm, 1 ov. F 11.2 mm (IEO-CD-ST/1605, ICMD002530).

NW Spain. THALASSA 1968. Stn U818, 42° 42.3' N, 09° 35.6' W, 840–880 m, 20 October 1968: 2 M 14.4–19.2 mm (MNHN-Ga977).

Western Mediterranean Sea. 42° 15' N, 03° 10' E, no depth, January 1957: 1 M 18.0 mm, 1 F 18.8 mm (ICMD 1250/1998). — Mallorca Channel. Stn B21, 38° 57' N, 02° 10' E, 1000 m, 18 June 1958: 1 F 8.0 mm (MNHN-Ga973). — 300–400 m, July 1958: 2 F 18.3–20.8 mm (MNHN-Ga974, Ga1041). — MARCA 4, Stn P2, 40° 40' 23.9" N, 01° 55' 36.1" E, 1612–1635 m, 19 September 1983: 1 M 15.5 mm, 1 F 14.4 mm

(ICMD002558). — Stn P3, 40° 41' N, 2° 21' E, 1777–1815 m, 20 September 1983: 2 M 15.2–18.3 mm, 2 F 19.0–20.0 mm (ICMD 94/1996). — Stn P4, 40° 26' 35.9" N, 02° 09' 54.0" E 1824–1871 m, 20 September 1983: 2 F 14.4–16.5 mm (ICMD002559). — Stn P5, 40° 13' 54.1" N, 02° 29' 24.0" E, 1743–1770 m, 21 September 1983: 1 M 19.4 mm, 2 F 14.9–17.3 mm (ICMD002560). — Stn P6, 40° 15' 00.0" N, 02° 43' 18.1" E, 1751–1778 m, 21 September 1983: 1 M 16.3 mm, 2 F 15.0–18.2 mm (ICMD002561). — Stn P9, 40° 23' 35.9" N, 03° 05' 42.0" E, 1678–1695 m, 25 September 1983: 2 M 8.7–15.5 mm, 2 F 17.5–18.3 mm (ICMD002562). — Stn P10, 40° 14' 12.1" N, 03° 07' 54.1" E, 1632–1660 m, 23 September 1983: 1 M 10.2 mm, 1 F 19.1 mm (ICMD002563). — Stn P13, 39° 59' 53.9" N, 02° 30' 47.9" E, 1479–1523 m, 25 September 1983: 1 M 16.2 mm, 1 F 13.0 mm (ICMD002564). — Stn P16, 40° 55' 48.0" N, 02° 06' 29.9" E, 1127–1179 m, 28 September 1983: 1 M 17.5 mm, 1 F 18.3 mm (ICMD002565). — POLYMEDE 2, Stn CM19, 36° 39.90' N, 02° 34.20' W, 225 m, 1 April 1972: 4 M 18.0–20.5 mm, 1 ov. F 18.2 mm, 1 M 15.4 mm (MNHN-Ga987). — Stn CM08, 35° 17.2' N, 4° 40' W, 281 m, 8 May 1972: 1 M 22.0 mm (ICMD002566). — OBSERVADORES-PTORRES, 36° 17' N, 04° 45' W, 758 m, 20 March 2008: 1 M 15.5 mm (ICMD002529). — MEDITS2009, Stn M09L079, 39° 13' N, 01° 27' E, 539 m 28 April 2009: 1 F 14.5 mm (ICMD002528). —IDEADOS2010. Stn ID210 Pati9, 38° 58' N, 02° 39' E, 738 m, 20 July 2010: 2 M 17.2–18.0 mm (ICMD002525, ICMD002526). — MEDITS2011. Stn M11L070, 38° 48' N, 00° 49' E, 696 m, 25 May 2011: 1 F 16.6 mm (ICMD002527).

Diagnosis

Carapace: Gastric region with 2 epigastric spines behind supraocular spines and 9–12 transverse ridges behind these spines, most of these ridges interrupted or scale-like; one small parahepatic on each side, with row of 2–3 protogastric spines between them; 1–2 mesogastric spines behind each parahepatic spine; 2 median metagastric spines. Anterior branchial with scale-like ridges and 1–2 branchial dorsal spine. Cardiac region with 9–10 ridges after cervical groove; anterior half usually with two transverse rows of 3 spines, and 1–2 additional unpaired spines on posterior half; these spines can be absent in a few Atlantic specimens. Each posterior branchial region with 1–2 postcervical spines and a few scattered small spines on posterior half; 10–12 interrupted or scale-like transverse ridges. Posterior margin preceded by elevated ridge with 6–7 spines.

Sternum: 0.7 times longer than wide, maximum width at sternite 7. Surface of thoracic sternites with numerous short striae on sternites 3–5; distal margin of sternite 4 transverse, broadly contiguous to sternite 3.

Abdomen: Anterior ridge of somites 2–4 with 6, 4 and 4 spines, respectively; posterior ridge of somites 2–3 sometimes with 1–2 median spines. Somites 2–3 each with 6–7 additional transverse ridges on tergite other than anterior ridge.

Eyes: Ocular peduncles as long as broad, maximum corneal diameter 0.3 distance between bases of antero-lateral spines.

Antennule: Article 1 with 2 well-developed distal spines, distomesial spine clearly longer than distolateral; two lateral spines, distal much longer than proximal and not exceeding distolateral spine.

Antenna: Article 1 with short distomesial spine (absent in a few specimens) not reaching distal margin of article 2. Article 2 with distomesial spine clearly shorter than distolateral spine, distolateral not reaching end of article 3. Article 3 with strong distomesial spine, barely exceeding antennal peduncle. Article 4 with short distolateral spine.

Mxp3: Merus shorter than ischium; flexor margin with strong median spine; extensor margin unarmed or with minute distal spine.

P1: Palm 4.7–6.0 times longer than broad, with 4 rows of spines along mesial, dorsal, lateral and ventral sides. Fingers slightly longer than palm, each with small distal spine; movable finger with additional proximal spine.

P2–4: Long and slender, with numerous plumose and non-iridiscent setae along extensor margin of articles. P2 2.8–3.0 times carapace length. Meri shorter posteriorly (P3 merus 0.9 length of P2 merus, P4 merus 0.7–0.8 length of P3 merus). Dactyli slender, length 0.5 that of propodi; flexor margin with 16–19 movable spinules, distal fourth unarmed, with a thin spinule at base of unguis; P2 dactylus 7.5–8.5 times longer than wide.

Remarks

Intraspecific genetic variability within *M. perarmata* was low (0.1%, 0.3%, and 0.5% for COI, 16S and 18S, respectively) for the analyzed specimens from the Mediterranean and the Atlantic basins (see more under the Remarks of *M. tenuimana*).

Distribution

The Mediterranean Sea and the eastern Atlantic Ocean from the Gulf of Cadiz to the Bay of Biscay and the Celtic Sea, between 300 and 1899 m.
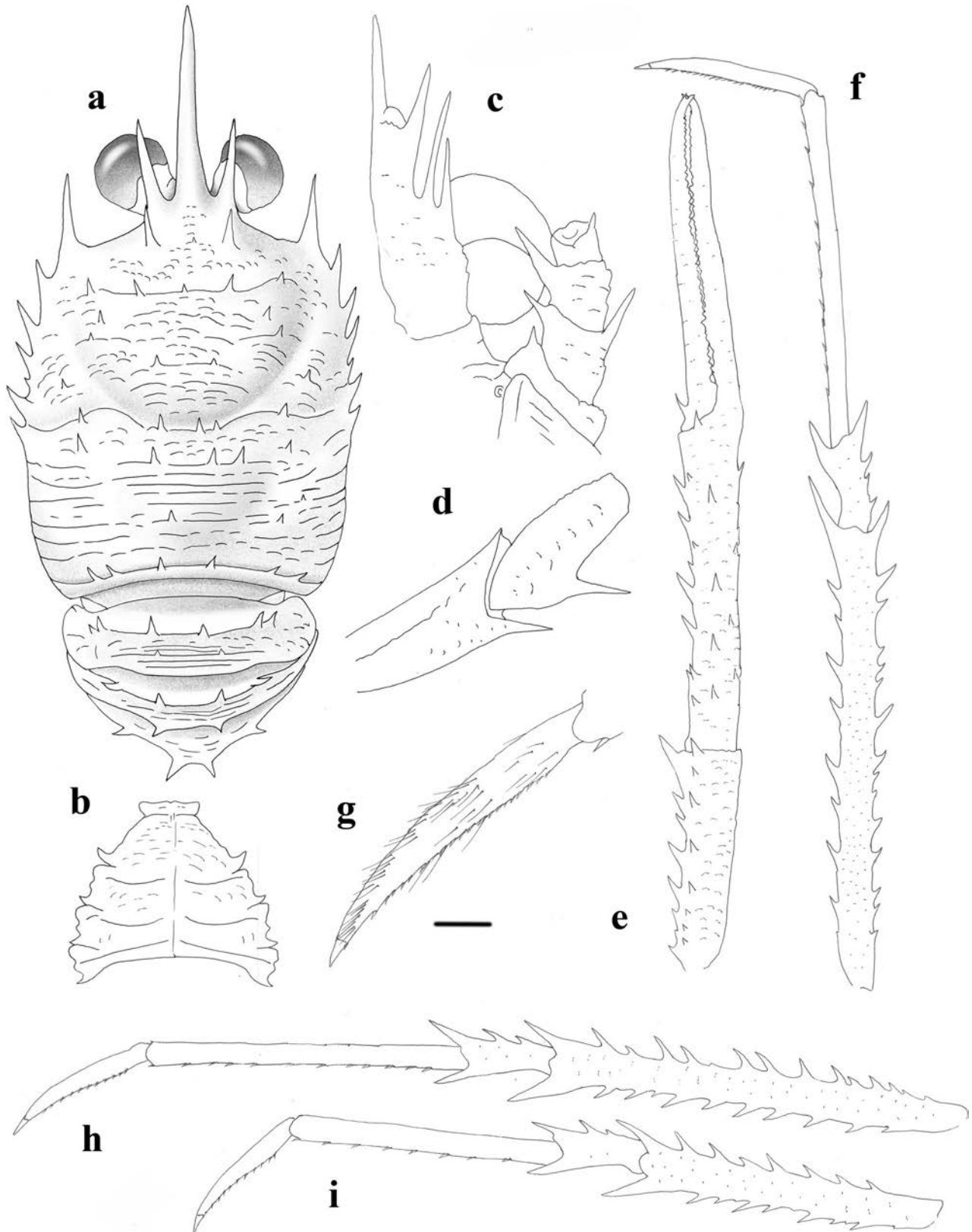
Fig. 4 *Munida perarmata* A. Milne Edwards and Bouvier, 1894. NW Mediterranean. Cruise MARCA 4, Stn P4, female, 16.5 mm (ICMD002559). **a** Carapace and abdomen, dorsal view; **b** Sternum; **c** Cephalic region showing antennular and antennal peduncles, ventral view; **d** Right Mxp3, lateral view; **e** Right P1, carpus to dactylus, dorsal view; **f** Left P2, lateral view; **g** Dactylus of left P2, lateral view; **h** Left P3, lateral view; **i** Left P4, lateral view. Scales: **a**, **b**, **e**, **f**, **h**, **i** = 2.0 mm; **c**, **d**, **g** = 1.0 mm

Munida speciosa von Martens, 1878

Fig. 5

Munida speciosa von Martens, 1878: 133. — Baba et al. 2008: 122. — Muñoz et al. 2012: 480. — Matos-Pita and de Ramil 2014: 421.
Munida iris ssp. rutllanti Zariquiey-Álvarez, 1952: 28–29.
Munida rutllanti Baba et al. 2008: 119.
Munida iris A. Milne Edwards and Bouvier 1900: 285 (not *Munida iris* A. Milne Edwards, 1880).

Material examined

European Atlantic coasts

NW Spain. Galicia. DEMERSALES 04, 42° 30.35' N, 09° 24.48' W, 696 m, July 2004: 1 M 14.6 mm (ICMD002537, ICMD002542).

Portugal. Stn M19-259 AT 129, 37° 38' N, 09° 5.6' W, 260–302 m, 18 March 1970: 1 F 12.6 mm (SMF-5929).

Gulf of Cadiz. ARSA 2013–02, Stn L7, 20 February 2013: 2 M 10.5–11.4 mm, 4 F 11.4–11.7 mm (ICMD002568).

Western Mediterranean Sea. Melilla (collected by fishing vessels, between 1946 and 1950, no depth): 5 M 19.2–20.6 mm, 5 F 16.0–20.0 mm (type material of *M. rutllanti*) (ICMZ 1219 to 1222/1998; ICMZ 1271 to1274/1998). — no data: 1 F 20.2 mm (MNHN-IU-2014-12,271). — 42° 15' N, 03° 21' E, 510 m, no date: 1 M 14.4 mm (ICMD002546). — Gulf of Valencia, no depth, June 1992: 17 M 12.9–17.8 mm, 1 ov. F 12.8 mm, 6 F 14.4–16.7 mm (MNHN-Ga2394). — POLYMEDE 2, Stn CM19, no data: 4 M 18.0–20.5 mm, 1 ov. F 18.2 mm, 1 M 15.4 mm (MNHN-Ga987). — OBSERVADORES-PTORRES, 36° 31' N, 04° 23' W, 245 m, 20 March 2008: 1 F 14.3 mm (ICMD002541). — MEDITS2009, Stn M09L003, 36° 32' N, 04° 26' W, 133 m, 8 April 2009: 1 F 13.0 mm (ICMD002539). — Stn M09L078, 39° 12' N, 01° 35' E, 318 m, 8 April 2009: 1 M 12.5 mm (ICMD002540). — MEDITS2011, Stn M11L027, 36° 43' N, 02° 17' W, 244 m, 12 May 2011: 1 M 15.7 mm (ICMD002538). — Alicante. 38° 10' 16.7" N, 0° 09' 04.0" E, 118 m, 16 May 2014: 3 M 12.5–18.0 mm (ICMD000476-77).

Eastern Mediterranean Sea. Greece. Thermaikos Gulf, 2 December 1971: 1 M 10.5 mm (SMF-7454).

Western Africa.

Morocco. Stn M9c-085a AT020, 33° 10.5' N, 09° 17.5' W, 170–345 m, 20 June 1967: 1 M 12.3 mm, 4 F 11.0–14.2 mm (SMF-5928). — Stn M44-235 BSN17, 21° 20.7' N, 17° 24.5' W, 80–100 m, 25 February 1975: 2 M 9.5–11.4 mm (SMF-39218). — Stn M44-236 BSN18, 21° 19.7' N, 17° 29.7' W, 257–265 m, 26 February 1975: 1 F 11.5 mm (SMF-39229). — Stn M44–244 BSN20, 21° 20.1' N, 17° 29.2' W, 216–221 m,

27 February 1977: 3 M 11.6–13.5 mm, 6 F 12.0–13.4 mm (SMF-39230).

Mauritania. Stn M44-132 BSN04, 17° 4' N, 16° 48.1' W, 400 m, 10 February 1977: 1 M 12.3 mm (SMF-39215). — Stn M44-135 BSN04, 17° 5.8' N, 16° 46.2' W, 291–306 m, 12 February 1977: 2 M 10.0–12.4 mm, 2 F 11.3–12.6 mm (SMF-39216). — Stn M44-194 BSN09, 17° 6' N, 16° 45.4' W, 187–198 m, 17 February 1977: 2 F 11.5–13.4 mm (SMF-39227). — Stn M44-208 BSN11, 17° 6.1' N, 16° 44.9' W, 198–200 m, 19 February 1977: 1 M 12.5 mm (SMF-39228).

Guinea Bissau. Stn 112, 11° 30' N, 17° 21' W, 162–210 m, 21 January 1985: 2 F 17.4–20.0 mm (ICMD002569). — Stn 214, 11° 31' N, 17° 20' W, 78–122 m, 8 February 1985: 1 M 5.7 mm, 1 F 4.4 mm (ICMD002570).

Gulf of Guinea. Stn 17, 400 m, 6 April 1964: 1 M 9.8 mm, 2 F 14.4–14.5 mm (MNHN-IU-2014-12268). — Stn 199, 01° 26.4' S, 08° 26' E, 400 m, 3 September 1963: 2 F 11.5–11.8 mm (SMF-31903).

Gabon. St Geronimo, 03° 02' S, 09° 16' E, 346 m, 6 September 1963: 1 F 10.0 mm (MNHN-Ga831).

Congo. Pointe Noire, 400 m, 13 January 1964: 1 F 17.2 mm (MNHN-IU-2014-12,269). — 04° 49' S, 11° 17' E, 300–600 m, 30 October 1969: 2 M 14.3–15.2 mm, 1 F 21.0 mm (MNHN- Ga1051). — 05° 04' S, 11° 24' E, 300–308 m, 21 September 1967: 1 M 16.5 mm (MNHN-IU-2014-12270).

Angola. 08° 40' S, 12° 59' E, 204 m, 21 May 1989: 3 M 12.2–13.6 mm, 5 F 10.4–13.1 mm (SMF-39243). — no depth, May 2000: 1 M 19.5 mm, 2 F 21.4–22.2 mm (ICMD002571). — ZAIANKO-BIOL2. Stn PL 36-CP 9, 07° 22.57' S, 11° 33.02' E, 350 m, 25 August 2000: 1 M 12.4 mm (ICMD002572).

Namibia. BENGUELA 2. Stn P45, 19° 25' S, 11° 36' E, 336–340 m, 25 August 1980: 4 M 9.2–12.0 mm, 8 F 10.1–13.5 mm (ICMD002573, ICMD002551). — Stn P48, 19° 04' S, 11° 38' E, 295 m, 26 August 1980: 1 M 10.5 mm, 2 ov. F 13.0–13.5 mm (ICMD002583, ICMD002552). — Stn P70, 17° 37' S, 11° 23' E, 265–275 m, 15 September 1980: 2 M 9.8–11.7 mm, 4 F 10.5–13.0 mm (ICMD002574, ICMD002550, ICMD002553).

Diagnosis

Carapace: Gastric region with 3–4 pairs of epigastric spines, largest pair behind supraocular spines; 1–2 parahepatic spines on each side. Anterior branchial region with 1–2 spines on each side, cardiac regions unarmed. Posterior branchial region with 1–2 postcervical spines on each side and 10–12 transverse ridges after cervical groove and before posterior ridge.

Sternum: 0.8 times longer than wide, maximum width at sternite 7. Surface of thoracic sternites with some short striae
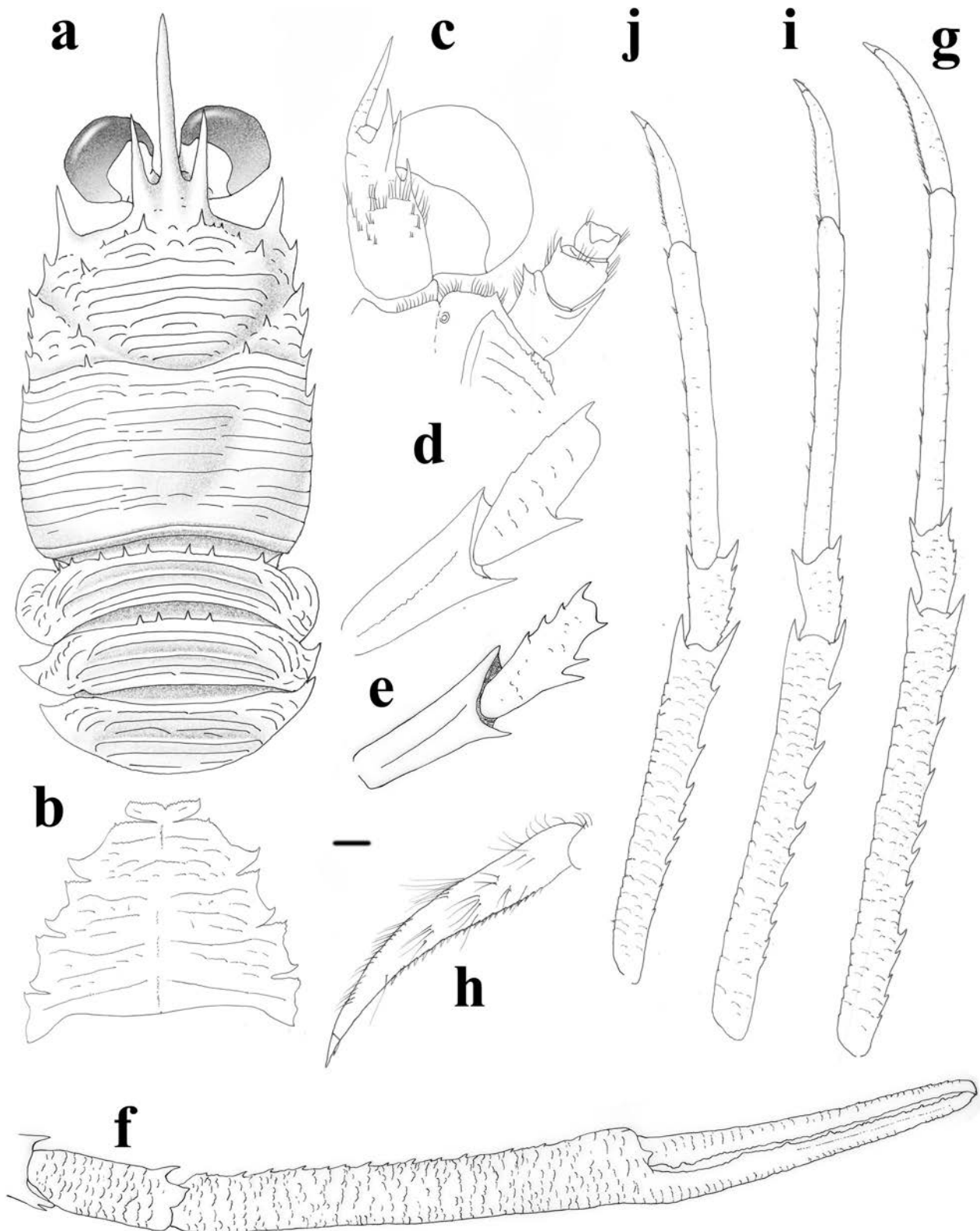
Fig. 5 *Munida speciosa* Von Martens, 1878. a–d, f–j NW Guinea Bissau, Stn 112, female 20.0 mm (ICMD002569); e *M. speciosa*, lectotype of *M. rutllanti* Zariquey-Alvarez, 1952, male, 19.4 mm, Melilla, SW Mediterranean (ICMZ 1219); a Carapace and abdomen, dorsal view; b Sternum. c Cephalic region showing antennular and antennal peduncles, ventral view; d, e Right Mxp3, lateral view; f Right P1, carpus to dactylus, dorsal view; g Left P2, lateral view; h Dactylus of left P2, lateral view; i Left P3, lateral view; j Left P4, lateral view. Scales: a, f, g, i, j = 2.0 mm; b, c, d, e, h = 1.0 mm

on sternites 3–6; distal margin of sternite 4 transverse, with minute spines/granules, broadly contiguous to sternite 3.

Abdomen: Anterior ridge of somites 2–3 with 2–8 and 0–4 spines, respectively. Somites 2–5 each with 4–5 transverse ridges on tergite behind anterior ridge.

Eyes: Ocular peduncles as long as broad, maximum corneal diameter 0.4–0.5 distance between bases of anterolateral spines.

Antennule: Article 1 with 2 well-developed distal spines, distomesial spine clearly longer than distolateral; two lateral spines, distal longer than proximal and not exceeding distolateral spine.

Antenna: Article 1 with short distomesial spine not reaching distal margin of article 2, mesially expanded to epistomic ridge, reaching level of lateral margin of antennular peduncle. Article 2 with distomesial spine shorter than distolateral spine, distolateral not reaching end of article 3. Article 3 with short distomesial spines, not exceeding antennal peduncle.

Mxp3: Merus shorter than ischium; flexor margin with strong median spine and 0–3 additional spines along distal half; extensor margin with 3–4 spines, distal most longer than others. Carpus unarmed.

P1: Palm 6.0–7.0 times longer than broad, with row of small ventromesial spines. Fingers 0.7–1.0 times longer than palm, each with small distal spine; movable finger with additional proximal spine.

P2–4: Long and slender, squamate, with numerous plumose and iridescent setae along extensor margin of articles. P2 3.0–3.5 times carapace length. Meri shorter posteriorly (P3 merus 0.8–0.9 length of P2 merus, P4 merus 0.8–0.9 length of P3 merus). Dactyli slender, length 0.5–0.6 that of propodi; flexor margin with 15–29 movable spinules, distal third unarmed, with thin spinule at base of unguis; P2 dactylus 8 times longer than wide.

Remarks

Munida speciosa was originally described by von Martens (1878) from specimens collected in Guinea Bissau. It belongs to the group of species with five spines along the branchial margin of the carapace, spines along the anterior ridge of abdominal somites 2–3 (rarely absent on somite 3), dilated corneae, antennal article 1 mesially expanded to the epistomic ridge and the extensor margin of the Mxp3 merus with a distal spine. The closest species are *M. iris* A. Milne Edwards, 1894 from the western Atlantic and *M. rutllanti* Zariquiey-Álvarez, 1952, described as *M. iris* ssp. *rutllanti* from specimens collected in the south-western Mediterranean.

Munida speciosa and *M. rutllanti* have been compared by different authors (e.g., Miyake and Baba 1970). The two species were differentiated by the number of spines along the flexor margin of the Mxp3 merus (3 spines in *M. rutllanti*

and 1 spine in *M. speciosa*) and the dorsal series of tubercles on abdominal tergite 3 (Miyake and Baba 1970). Specimens assigned to each species on the basis of morphology have been collected from northwest Africa (Matos-Pita and de Ramil 2014). However, following the examination of numerous specimens (see above), it was observed that these characters are variable and thus not useful to differentiate species. Furthermore, the molecular data showed that there are no genetic differences among specimens from the different localities. Therefore, *M. rutllanti* must be considered as a junior synonym of *M. speciosa*.

Munida iris is also closely related to *M. speciosa*, and some authors have considered them as a single species (e.g., A. Milne Edwards and Bouvier 1900; Melo-Filho de Melo-Filho 2006). However, the molecular and morphological comparisons of specimens [*M. iris*: French Guyanne, Stn 4394, 224–225 m: 1 F 8.0 mm (MNHN-IU-2016-9640); Stn 4373, 303–307 m: 1 ov. F 30.7 mm (MNHN-IU-2013-2568); Florida, 256–360 m: 1 F 18.5 mm (ICM-CSIC Zariquiey Collection: ICMZ1247/1998)] distinguish two species that can be differentiated by subtle but constant morphological characters. These differences were also pointed out by Zariquiey-Álvarez (1952): (1) abdominal somites 2–3 each have 6–7 ridges, other than the anterior ridge, in *M. iris*, whereas there are only 4–5 ridges in *M. speciosa*. Furthermore, the spines on abdominal somite 3 are always absent in *M. iris*, whereas they are usually present in *M. speciosa*. The genetic differences between *M. speciosa* and *M. iris* are 2.7% for COI, 0.3% for 16S, and 0.1% for 18S. The intraspecific genetic distances of *M. speciosa* from the Atlantic and Mediterranean basins and West Africa were relatively low: 0.3% for COI, 0.1% for 16S and no genetic distance for 18S.

Distribution

From the NW coasts of Spain to northern Namibia and the Mediterranean Sea, between 40 and 1303 m.

Munida tenuimana G.O. Sars, 1872

Fig. 6

Munida tenuimana Sars, 1872: 257. — Baba et al. 2008: 125 (in part, only citations from NW Ireland to Norway, Iceland, Davis Strait to Newfoundland).

Material examined. Type material *Neotype*: Male 13.8 mm, MNHN-IU-2016-9641, Norway, PROSPEC 1, Stn 726, 69° 33.4' N, 18° 00' E, 387 m, 27 September 2002.

Other material. Norway. Stn 922, 58° 16' N, 05° 48' 15″ E, 343 m, 6 July 1898: 1 F 13.3 mm (MNHN-Ga979). — Hjerundfijord, 432 m, 5 July 1906: 1 M 15.0 mm (MNHN-Ga1047). —Korsfjorden, 70° 14' N, 23° 22' E, no depth, no
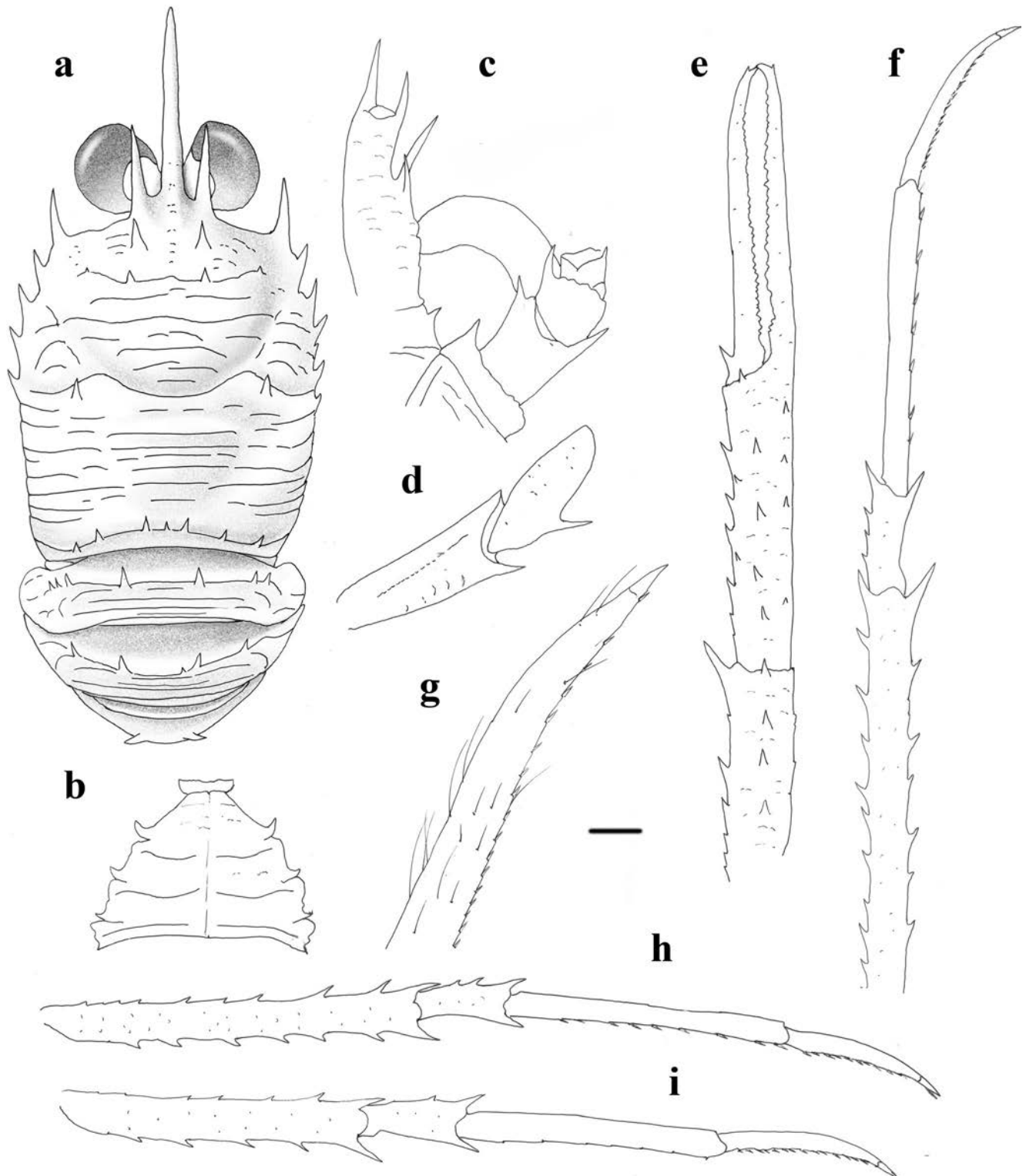
Fig. 6 *Munida tenuimana* G.O. Sars, 1872. Norway, Cruise PROSPEC 1, Stn 726, male, 13.8 mm, neotype (MNHN-IU-2016-9641). **a** Carapace and abdomen, dorsal view; **b** Sternum; **c** Cephalic region showing antennular and antennal peduncles, ventral view; **d** Right Mxp3, lateral view; **e** Right P1, carpus to dactylus, dorsal view; **f** Right P2, lateral view; **g** Dactylus of right P2, lateral view; **h** Right P3, lateral view; **i** Right P4, lateral view. Scales: **a, b, e, f, h, i** = 2.0 mm; **c, d, g** = 1.0 mm

date: 1 F 9.7 mm (ICMD002575). — Vestfjorden, 68° 02.11' N, 15° 15.65' E, 513 m, no date: 1 M 12.0 mm (ICMD002555). — Okssundet, 68° 01.58' N, 15° 15.39' E, 499 m, no date: 1 M 10.5 mm (ICMD002577). —

LOPHELIA. Stn 711, 68° 00.4' N, 15° 17.8' E, 630 m, 25 September 2002: 2 M 10.5–22.4 mm (ICMD002578, ICMD002554). — PROSPEC 1. Stn 726, 69° 33.4' N, 18° 00' E, 387 m, 27 September 2002: 3 M 8.8–13.2 mm, 1 ov. F 13.3 mm (MNHN-IU-2016-9642).

NW Ireland. PROSPEC 1. Stn CPH04, 56° 32.53' N, 10° 17.03' W, 1185 m, 8 July 1996: 3 M 7.4–10.8 mm, 1 ov. F 14.8 mm, 2 F 6.7–7.4 mm (ICMD002580). — Stn CPH08, 55° 17.83' N, 10° 09.84' W, 1170–1184 m, 12 July 1996: 3 M 15.2–18.6 mm, 3 ov. F 17.0–17.8 mm, 1 F 14.7 mm (ICMD002581). — Stn CPH09, 55° 21.34' N, 10° 04.95' W, 990–1004 m, 12 July 1996: 3 ov. F 19.5–21.0 mm, 1 F 11.8 mm (ICMD002582).

Diagnosis

Carapace: Gastric region with 2 epigastric spines behind supraocular spines and 7–8 transverse ridges behind these spines, usually not scale-like; one small parahepatic on each side, with 2 median protogastric spines between them. Anterior branchial region unarmed. Cardiac region unarmed, with 6–7 ridges after cervical groove. Posterior branchial region with 1 postcervical spine on each side and 6–8 transverse ridges counted along the lateral margin, exclusive of the mid-transverse ridge and the posterior-most ridge. Posterior margin preceded by elevated ridge with 5–7 spines.

Sternum: 0.7 times longer than wide, maximum width at sternite 7. Surface of thoracic sternites smooth or with a few short striae on sternites 3–5; distal margin of sternite 4 transverse, broadly contiguous to sternite 3.

Abdomen: Anterior ridge of somites 2–4 with 6–7, 4–5 and 2 spines, respectively. Somites 2–3 each with 2–4 additional transverse ridges on tergite other than anterior ridge.

Eyes: Ocular peduncles as long as broad, maximum corneal diameter 0.3 distance between bases of anterolateral spines.

Antennule: Article 1 with 2 well-developed distal spines, distomesial spine clearly longer than distolateral; two lateral spines, distal much longer than proximal and not exceeding distolateral spine.

Antenna: Article 1 with short distomesial spine not reaching distal margin of article 2. Article 2 with distomesial spine clearly shorter than distolateral spine, distolateral not reaching end of article 3. Article 3 with well-developed distomesial spine, barely exceeding antennal peduncle. Article 4 with minute distolateral spine.

Mxp3: Merus shorter than ischium; flexor margin with strong median spine; extensor margin unarmed.

P1: Palm 3.4–4.0 times longer than broad, with 4 rows of spines along mesial, dorsal, lateral and ventral sides. Fingers 1.2–1.4 times longer than palm, each with small distal spine; movable finger with additional proximal spine.

P2–4: Long and slender, with numerous plumose and non-iridescent setae along extensor margin of articles. P2 2.5–3.0

times carapace length. Meri shorter posteriorly (P3 merus 0.9 length of P2 merus, P4 merus 0.6–0.8 length of P3 merus). Dactyli slender, length 0.5–0.7 that of propodi; flexor margin with 13–17 movable spinules, distal fifth unarmed, with thin spinule at base of unguis; P2 dactylus 8 times longer than wide.

Remarks

Munida tenuimana and *M. perarmata* were considered as different species by Zariquiey-Álvarez (1952) in his revision of the European species of *Munida*. The two species were distinguished by the presence of cardiac spines and numerous short striae on the sternites in *M. perarmata*, which were absent and much less numerous, respectively, in *M. tenuimana*. He concluded that *M. perarmata* was restricted to the Mediterranean and *M. tenuimana* to the Atlantic. After this revision, some authors, e.g., Forest (1965), Zariquiey-Álvarez (1968) and Stevcic (1990), considered *M. tenuimana* and *M. perarmata* to be distinct species. However, the revision of Rice and Saint Laurent (Rice and de Saint Laurent 1986) included numerous specimens of these European species from Norway (type locality of *M. tenuimana*) to the Mediterranean Sea (type locality of *M. perarmata*). They concluded that, although these characters could distinguish specimens from the Atlantic and Mediterranean basins, the differences were "not sufficiently consistent to warrant the recognition of even sub-specific status". However, d'Udekem d'Acoz (d'Udekem d'Acoz 1999), following a personal communication by A. Koukouras, suggested that the species should be considered different, although they did not discuss which differences warranted this suggestion.

The morphological examination and molecular analyses of specimens from the Atlantic Ocean and the Mediterranean Sea confirm the occurrence of two differentiated species, and that the morphological differences indicated by Zariquiey-Álvarez (1952) are valid. However, their occurrence is not directly related to their geographic distribution to either the Atlantic Ocean or Mediterranean Sea. Rather, the results presented here indicate that *M. tenuimana* is restricted to the northern Atlantic Ocean from Davis Strait, Iceland and Norway to Northern Ireland, while *M. perarmata* is distributed from the Celtic Sea and Bay of Biscay in the Atlantic Ocean to the Mediterranean Sea (Fig. 1).

As Zariquiey-Álvarez (1952) pointed out, the two species can be distinguished by the presence of spines on the cardiac region and numerous short piliferous striae on the sternal plastron in *M. perarmata*, which are absent and much less numerous, respectively, in *M. tenuimana*. The presence of cardiac spines is nearly constant in all examined specimens, although the number of spines on the carapace is sometimes lower (or absent in a few specimens) in the Atlantic specimens. The most constant character to

differentiate the two species is the number of secondary ridges on the carapace and abdomen. *Munida perarmata* has numerous scale-like ridges among the main ridges, which are clearly less numerous in *M. tenuimana*. For instance, *M. perarmata* has 9–10 ridges in the cardiac region and 10–12 interrupted or scale-like transverse ridges in each branchial region, and abdominal somites 2–3 each have 6–7 additional transverse ridges on the tergite other than the anterior ridge. In contrast, *M. tenuimana* has 6–7 ridges in the cardiac region and 6–8 transverse ridges in each branchial region, and abdominal somites 2–3 each have 2–4 additional transverse ridges on the tergite other than the anterior ridge.

In order to fix the taxonomic position of this species, we propose here the selection of a neotype, since the type material of Sars (1872) is lost. The genetic distances between *M. tenuimana* and *M. perarmata* were 6.0% for COI, 2.0% for 16S, and 1.7% for 18S (Tables 3 and 4).

Distribution

The North Atlantic Ocean from Davis Strait to Newfoundland, Iceland, Norway, the western coast of Sweden, Barents Sea, Faroe Islands and north of Ireland, between 115 and 1455 m.

Discussion

The concordance of the morphological and molecular analyses presented here resolves a longstanding taxonomic debate related to the European species of the genus *Munida*. The nomenclatural and taxonomic controversy concerning the species *M. intermedia*, *M. rugosa*, *M. sarsi*, and *M. tenuimana* was partially addressed through several revisions (Zariquiey-Álvarez 1952, 1968; Rice and de Saint Laurent 1986; d'Udekem d'Acoz 1999); however, the status of *M. tenuimana* remained dubious. The use of variable characters to define species (Rice and de Saint Laurent 1986), instead of confirmed apomorphies with phylogenetic value, was the main cause of confusion. Given this context, material from several geographic areas have been re-examined and the identifications of several specimens have been revised as a result. We also used several methods to delimit species including those based on genetic distances (Hebert et al. 2003), phylogenetic trees (Pons et al. 2006; Zhang et al. 2013), multispecies coalescence (i.e., species trees) (Reid and Carstens 2012) and morphological consistencies for each inferred species. The results of these methods were largely congruent and provided similar information to support the delimited taxa and their relationships. However, the delimitation of one pair of species, *M. iris* and *M. speciosa*, remains dubious.

Molecular tools have proven to be very useful to identify diagnostic traits and to resolve taxonomic issues at several levels, especially in closely related species (e.g., see cases of cryptic species in squat lobster in: Machordom and Macpherson 2004; Cabezas et al. 2011; Rodríguez-Flores et al. 2019b). More precisely, when the most conservative criterion is adopted, and certain morphological variability is discarded due to inconsistencies in the diagnosis of a particular species, molecular data can help test whether that variability truly arose as a product of speciation (e.g., Flot et al. 2011). For example, Rice and Saint Laurent (Rice and de Saint Laurent 1986) considered that the morphological differences between *M. perarmata* and *M. tenuimana* are not sufficiently consistent to consider them as distinct species. However, the molecular analyses of the present study all indicated that these two are indeed distinct species. Therefore, the consistent differences we observed in the number of ridges/striae in the carapace and the abdomen reflect species-specific characters. Such characters have phylogenetic value, and moreover, they have already been shown to be able to delimit other closely related species of the genus, for instance within the *M. compressa* Baba, 1988 (*M. compressa* + *M. cornuta* Macpherson, 1994 + *M. rubridigitalis* Baba, 1994) or *M. curvirostris* Henderson, 1885 (*M. compacta* Macpherson, 1997 + *M. curvirostris* + *M. rhodonia* Macpherson, 1994) species groups from the Pacific Ocean (Baba 1988, 1994; Macpherson 1994, 1997; Machordom and Macpherson 2004). Alternatively, molecular tools can help identify which morphological characters are homoplastic or highly variable within a species likely due to rapid and local adaptation (e.g., adaptive morphological diversification) instead of speciation processes (Brower 1994). For instance, *M. speciosa* and *M. rutllanti* represent a case of dimorphic species with some phenotypic variability. *Munida rutllanti* and *M. speciosa* use to be differentiated by the number of spines along the flexor margin of the third maxilliped (Miyake and Baba 1970; Matos-Pita and de Ramil 2014), but this trait was shown to be variable and is therefore not useful to differentiate the species.

However, the resolution offered by molecular phylogenetic data to set species boundaries can be limited in particular cases (Leavitt et al. 2016). Mitochondrial DNA (mtDNA) has been primarily used to differentiate individuals at the species level (i.e., DNA barcoding) and to set species boundaries in crustaceans and many other invertebrate groups (Hebert et al. 2003; Lefébure et al. 2006; Araujo et al. 2018). In crustaceans, a commonly cited threshold to delimit species has been around 3% genetic divergence or 0.16 substitutions/site for COI (Lefébure et al. 2006; Muñoz et al. 2013). Nevertheless, interspecific divergences in squat lobsters are usually greater than 6% for COI, including species of *Munida* (Machordom and Macpherson 2004; Cabezas et al. 2011). One of the arguments to use mtDNA to delimit species is that the difference between in inter- and intraspecific genetic distances typically shows a

clear barcoding gap (Hebert et al. 2003). According to this argument, *M. iris* should not be considered a valid taxon, or, alternatively, the sequence data could be insufficient to differentiate this species from *M. speciosa*. Speciation is measured using genetic sequences in terms of time based on the patterns of nucleotide substitutions, which occur at certain rates (e.g., Nei 1987). What happens when speciation cannot be detected because not enough time has passed to accumulate mutations in the molecular markers? In these cases, sequence data may not be informative to distinguish lineages that are otherwise phenotypically, ecologically and/or biogeographically well characterized. *Munida iris* and *M. speciosa* may represent a good example: although not distinguishable by molecular means, they have morphological traits (e.g., the pattern of striation in the carapace and abdomen) with phylogenetic value (Machordom and Macpherson 2004) that differentiate them. Additionally, these species are distributed along distinct geographic areas. *Munida iris* is distributed in the western Atlantic, e.g., French Guiana, Florida, Gulf of Mexico and Brazil (de Melo-Filho 2006; Coykendall et al. 2017), whereas *M. speciosa* is distributed along the eastern Atlantic from the NW Iberian Peninsula to Namibia (Neves 1977; Macpherson 1983) with no overlap in their known distributions. For these reasons, they are considered here as valid species and seem to constitute lineages in an early stage of speciation. As most species delimitation approaches are based on mtDNA, the potential capacity of nuclear markers, which can accurately determine sequence similarity, degree of isolation and gene flow, to set thresholds has been less explored. (Petit and Excoffier 2009). Recently, a fragment of the nuclear gene 28S BF/BR (Palero et al. 2009) was used to delimit some squat lobster species (Puillandre et al. 2011; Rodríguez-Flores et al. 2019b) and here we have tested the usefulness of a large fragment of the 18S gene, a potential marker for species delimitation that should be further explored. The setting of species boundaries should rely on the congruence of several approaches (based on morphology, geography, genetic and/or ecology) and not only on genetics (Will and Rubinoff 2004; Carstens et al. 2013).

Munida is the most diverse genus of squat lobsters worldwide (Baba et al. 2008). The extreme homoplasy and the general trend to be morphologically conservative not only make morphological studies very difficult but also have led to the detection of several cryptic species (Macpherson and Machordom 2005), with many more expected to be discovered. The phylogenetic results of the present study could not reconstruct the deep relationships within *Munida* from the eastern Atlantic reported in previous phylogenetic reconstructions (Machordom and Macpherson 2004; Cabezas et al. 2011); however, even in these studies, the deepest relationships remained unresolved. Resolving the phylogenetic relationships within *Munida* may be more confounded by evidence from previous phylogenetic reconstructions that suggests the genus

may actually be comprised of multiple genera. For instance, Bracken-Grissom et al. (2013) showed that the genus is poly- or paraphyletic when analyzed with closely related species of the family Galatheidae. Machordom and Macpherson (2004) and Cabezas et al. (2008) both demonstrated high support for the splitting of the genus *Munida* into different genera (see Baba et al. 2008 and references therein). A similar pattern has been observed in the squat lobsters of the superfamily Chirostyloidea (Bracken-Grissom et al. 2013). Here, extremely large differences were found between species belonging to different groups of Atlantic *Munida* as represented by either genetic distances (e.g., *M. rugosa* – *M. speciosa*: mean = 17.7% for COI and 11.8% for 16S) or highly divergent lineages (see Table 3 and Fig. 3). Intergeneric values cited for related squat lobsters range from 16 to 21% for COI and 11.1 to 19.1% for 16S (see e.g., Macpherson and Machordom 2001 and Cabezas et al. 2008). Therefore, results presented here indicate that the different European species assigned to *Munida* may belong to several distinct genera. Our findings are consistent with those of Cabezas et al. (2011), who also reported high genetic distances among the species of the genus that reached or surpassed intergeneric distances and suggested the putative existence of several independent genera within *Munida* sensu *lato*. These lineages independently could have colonized the north-eastern Atlantic several times; however, a more comprehensive analysis including more taxa would be required to test this hypothesis. An extensive examination of *Munida* specimens from the different oceans, and of species of other Munididae genera, would help to establish the overall systematics of the genus and to unravel its evolutionary history.

Compliance with ethical standards

Conflict of interest The authors declare that they have no conflict of interest.

References

Ahyong ST, Baba K, Macpherson E, Poore GCB (2010) A new classification of the Galatheoidea (Crustacea: Decapoda: Anomura). Zootaxa 2676:57–68

Apakupakul K, Siddall ME, Burreson EM (1999) Higher level relationships of leeches (Annelida: Clitellata: Euhirudinea) based on morphology and gene sequences. Mol Phylogenet Evol 12(3):350–359

Araujo R, Buckley D, Nagel KO, García-Jiménez R, Machordom A (2018) Species boundaries, geographic distribution and evolutionary history of the Western Palaearctic freshwater mussels *Unio* (Bivalvia: Unionidae). Zool J Linnean Soc 182(2):275–299

Baba K (1988) Chirostylid and galatheid crustaceans (Decapoda: Anomura) of the "Albatross" Philippine expedition, 1907-1910. Res Crustac, Spec Number 2:1–203

Baba K (1994) Deep-sea galatheid crustaceans (Anomura: Galatheidae) collected by the 'Cidaris I' expedition off Central Queensland, Australia. Mem Queensl Mus 35:1–21

Baba K, Macpherson E, Poore GCB, Ahyong ST, Bermudez A, Cabezas P, Lin CW, Nizinski M, Rodrigues C, Schnabel KE (2008) Catalogue of squat lobsters of the world (Crustacea: Decapoda: Anomura - families Chirostylidae, Galatheidae and Kiwaidae). Zootaxa 1905:1–220

Baba K, Macpherson E, Lin CW, Chan TY (2009) Crustacean Fauna of Taiwan squat lobsters (Chirostylidae and Galatheidae). National Taiwan Ocean University, Keelung

Baba K, Ahyong ST, Macpherson E (2011) Chapter 1 morphology of the marine squat lobsters. In: Poore GCB, Ahyong ST, Taylor J (eds) The biology of squat lobsters. CSIRO Publishing: Melbourne and CRC Press, Boca Raton, pp 1–37

Bailie DA (2009) Phylogeny, population genetics and mating strategies of the squat lobster species *Munida rugosa* and *Munida sarsi* (Crustacea, Decapoda, Galatheidae). Dissertation, University of Belfast

Bouvier EL (1922) Observations complémentaires sur les crustacés décapodes (Abstraction faite des Carides) provenant des Campagnes de SAS le Prince de Monaco. Résultats des Campagnes Scientifiques accomplies sur son Yacht par Albert Ier Prince Souverain de Monaco 62:1-106, pls 1–6

Bracken-Grissom HD, Cannon ME, Cabezas P, Feldmann RM, Schweitzer CE, Ahyong ST, Felder LD, Lemaitre R, Crandall KA (2013) A comprehensive and integrative reconstruction of evolutionary history for Anomura (Crustacea: Decapoda). BMC Evol Biol 13(1):128

Brower AV (1994) Rapid morphological radiation and convergence among races of the butterfly *Heliconius erato* inferred from patterns of mitochondrial DNA evolution. Proc Natl Acad Sci U S A 91(14): 6491–6495

Cabezas P, Macpherson E, Machordom A (2008) A new genus of squat lobster (Decapoda: Anomura: Galatheidae) from the South West

Pacific and Indian Ocean inferred from morphological and molecular evidence. J Crustac Biol 28(1):68–75

Cabezas P, Macpherson E, Machordom A (2011) *Allogalathea* (Decapoda: Galatheidae): a monospecific genus of squat lobsters? Zool J Linnean Soc 156:465–493

Carstens BC, Pelletier TA, Reid NM, Satler JD (2013) How to fail at species delimitation. Mol Ecol 22 (17):4369–4383

Cartes JE, Papiol V, Frutos I, Macpherson E, González-Pola C, Punzón A, Valeiras X, Serrano A (2014) Distribution and biogeographic trends of decapod assemblages from Galicia Bank (NE Atlantic) at depths between 700 and 1800 m, with connexions to regional water masses. Deep Sea Res Part II Top Stud Oceanogr 106:165–178

Colgan DJ, McLauchlan A, Wilson GDF, Livingston SP, Edgecombe GD, Macaranas J, Cassis G, Gray MR (1998) Histone H3 and U2 snRNA DNA sequences and arthropod molecular evolution. Aust J Zool 46(5):419–437

Coykendall DK, Nizinski MS, Morrison CL (2017) A phylogenetic perspective on diversity of Galatheoidea (*Munida*, *Munidopsis*) from cold-water coral and cold seep communities in the western North Atlantic. Deep Sea Res Part II Top Stud Oceanogr 137:258–272

Darriba D, Taboada GL, Doallo R, Posada D (2012) jModelTest 2: more models, new heuristics and parallel computing. Nat Methods 9(8): 772

QGIS Development Team (2018). QGIS geographic information system. Open Source Geospatial Foundation Project. http://qgis.osgeo.org

Drummond AJ, Rambaut A (2007) BEAST: Bayesian evolutionary analysis by sampling trees. BMC Evol Biol 7(1):214

Drummond AJ, Ho SY, Phillips MJ, Rambaut A (2006) Relaxed phylogenetics and dating with confidence. PLoS Biol 4(5):e88

Drummond AJ, Suchard MA, Xie D, Rambaut A (2012) Bayesian phylogenetics with BEAUti and the BEAST 17. Mol Biol Evol 29(8): 1969–1973

d'Udekem d'Acoz C (1999) Inventaire et distribution des crustacés décapodes de l'Atlantique nord-oriental, de la Méditerranée et des eaux continentales adjacentes au nord de 25°N. Patrimoines Naturels (MNHN/SPN) 40:1–383

Fabricius JC (1775) Systema Entomologiae, sistens Insectorum classes, ordines, genera, species, adjectis Sysnonymis, Locis, Descriptionibus, Observationibus. Kortii, Flensburgi et Lipsiae, 832 pp

Flanders Marine Institute (2018) Maritime boundaries geodatabase: maritime boundaries and exclusive economic zones (200NM), version 10. **Available online at** http://www.marineregions.org/ https://doi.org/10.14284/312

Flot JF, Blanchot J, Charpy L, Cruaud C, Licuanan WY, Nakano Y, Payri C, Tillier S (2011) Incongruence between morphotypes and genetically delimited species in the coral genus *Stylophora*: phenotypic plasticity, morphological convergence, morphological stasis or interspecific hybridization? BMC Ecol 11(1):22

Folmer O, Black M, Hoeh W, Lutz R, Vrijenhoek R (1994) DNA primers for amplification of mitochondrial cytochrome c oxidase subunit I from diverse metazoan invertebrates. Mol Mar Biol Biotechnol 3: 294–299

Forest J (1965) Campagnes du "Professeur Lacaze-Duthiers" aux Baléares: juin 1953 et août 1954. Crustacés décapodes. Vie Milieu 16:325–413

García-Merchán VH, Robainas-Barcia A, Abelló P, Macpherson E, Palero F, García-Rodríguez M, García-Rodríguez M, Gil de Sola L, Pascual M (2012) Phylogeographic patterns of decapod crustaceans at the Atlantic–Mediterranean transition. Mol Phylogenet Evol 62(2):664–672

García-Raso JE (1996) Crustacea Decapoda (excl Sergestidae) from Ibero-Moroccan waters results of Balgim-84 expedition. Bull Mar Sci 58(3):730–752

García-Raso JE, Cuesta JA, Abelló P, Macpherson E (2018) Updating changes in the Iberian decapod crustacean fauna (excluding crabs) after 50 years. Sci Mar 82(4):207–229

González-Gordillo JI, Santos AD, Rodríguez A (2001) Checklist and annotated bibliography of decapod crustacean larvae from the Southwestern European coast (Gibraltar Strait area). Sci Mar 65(4):275–305

Guindon S, Gascuel O (2003) A simple, fast, and accurate algorithm to estimate large phylogenies by maximum likelihood. Syst Biol 52(5): 696–704

Hebert PD, Ratnasingham S, de Waard JR (2003) Barcoding animal life: cytochrome c oxidase subunit 1 divergences among closely related species. Proc R Soc Lond B Biol Sci 270(Suppl 1):S96–S99

Heled J, Drummond AJ (2008) Bayesian inference of population size history from multiple loci. BMC Evol Biol 8(1):289

Heled J, Drummond AJ (2010) Bayesian inference of species trees from multilocus data. Mol Biol Evol 27(3):570–580

Henderson JR (1885) Diagnoses of new species of Galatheidae collected during the "Challenger" expedition. Ann Mag Nat Hist (ser 5) 16: 407–421

Huus J (1935) Zur morphologischsystematischen und biologischen Kenntniss der nordischen *Munida* Larven (Crustacea-Decapoda). Bergens Museum Ärbok 8:1-29 4 pls

Ingle RW, Christiansen ME (2004) Lobsters, mud shrimps and anomuran crabs. Keys and notes for the identification of species. Field Studies Council for Linnaean Society of London Estuarine and Coastal Sciences Assocation, Shrewbury, 271 pp

Katoh K, Misawa K, Kuma KI, Miyata T (2002) MAFFT: a novel method for rapid multiple sequence alignment based on fast Fourier transform. Nucleic Acids Res 30(14):3059–3066

Landeira JM, Brochier T, Mason E, Lozano-Soldevilla F, Hernández-León S, Barton ED (2017) Transport pathways of decapod larvae under intense mesoscale activity in the Canary-African coastal transition zone: implications for population connectivity. Sci Mar 81(3): 299–315

Lanfear R, Calcott B, Ho SY, Guindon S (2012) PartitionFinder: combined selection of partitioning schemes and substitution models for phylogenetic analyses. Mol Biol Evol 29(6):1695–1701

Leach WE (1820) Galatéadées. In: Dictionnaire des Sciences Naturelles. F. G. Levreault, Paris 49–56 pp.

Leavitt SD, Divakar PK, Crespo A, Lumbsch HT (2016) A matter of time—understanding the limits of the power of molecular data for delimiting species boundaries. Herzogia 29(2):479–492

Lefébure T, Douady CJ, Gouy M, Gibert J (2006) Relationship between morphological taxonomy and molecular divergence within Crustacea: proposal of a molecular threshold to help species delimitation. Mol Phylogenet Evol 40(2):435–447

Lydeard C, Mulvey M, Davis GM (1996) Molecular systematics and evolution of reproductive traits of north American freshwater unionacean mussels (Mollusca: Bivalvia) as inferred from 16S rRNA gene sequences. Philos Trans R Soc Lond Ser B Biol Sci 351(1347):1593–1603

Machordom A, Macpherson E (2004) Rapid radiation and cryptic speciation in squat lobsters of the genus *Munida* (Crustacea, Decapoda) and related genera in the South West Pacific: molecular and morphological evidence. Mol Phylogenet Evol 33(2):259–279

Machordom A, Araujo R, Erpenbeck D, Ramos MÁ (2003) Phylogeography and conservation genetics of endangered European Margaritiferidae (Bivalvia: Unionoidea). Biol J Linn Soc 78:235–252

Macpherson E (1983) Crustáceos decápodos capturados en las costas de Namibia. Resultados Exped cient 11:3–80

Macpherson E (1991) Biogeography and community structure of the decapod crustacean fauna off Namibia (Southeast Atlantic). J Crustac Biol 11:401–415

Macpherson E (1994) Crustacea Decapoda: studies on the genus *Munida* Leach, 1820 (Galatheidae) in New Caledonia and adjacent waters with descriptions of 56 new species. Résult camp Musorstom 12: 421–569

Macpherson E (1997) Crustacea Decapoda: species of the genera *Agononida* Baba & de Saint Laurent, 1996 and *Munida* Leach, 1820 (Galatheidae) from the KARUBAR Cruise. In: Crosnier, A. et al. (Ed.) Résultats des Campagnes MUSORSTOM 16. Campagne Franco-Indonésienne KARUBAR. Mém Mus natl d'Hist nat. Série A, Zoologie 172:597–612

Macpherson E, Baba K (2011) Chapter 2 taxonomy of squat lobsters. In: Poore GCB, Ahyong ST, Taylor J (eds) The biology of squat lobsters. CSIRO Publishing: Melbourne and CRC Press, Boca Raton, pp 39–71

Macpherson E, Machordom A (2001) Phylogenetic relationships of species of *Raymunida* (Decapoda: Galatheidae) based on morphology and mitochondrial cytochrome oxidase sequences, with the recognition of four new species. J Crustac Biol 21(3):696–714

Macpherson E, Machordom A (2005) Use of morphological and molecular data to identify three new sibling species of the genus *Munida* Leach, 1820 (Crustacea, Decapoda, Galatheidae) from New Caledonia. J Nat Hist 39(11):819–834

Mantelatto FL, Terossi M, Negri M, Buranelli RC, Robles R, Magalhães Tamburus AF, Rossi N, Miyazaki MJ (2018) DNA sequence database as a tool to identify decapod crustaceans on the São Paulo coastline. Mitochondrial DNA A DNA Mapp Seq Anal 29(5): 805–815

Matos-Pita SS, de Ramil F (2014) Squat lobsters (Crustacea: Anomura) from Mauritanian waters (West Africa) with the description of a new species of *Munidopsis*. Zootaxa 3765:418–434

Matzen da Silva J, Creer S, Antonina DS, Costa AC, Cunha MR, Costa FO, Carvalho GR (2011) Systematic and evolutionary insights derived from mtDNA COI barcode diversity in the Decapoda (Crustacea: Malacostraca). PLoS One 6:1–15

Medlin L, Elwood HJ, Stickel S, Sogin ML (1988) The characterization of enzymatically amplified eukaryotic 16S-like rRNA-coding regions. Gene 71(2):491–499

de Melo-Filho GAS (2006) Reports on the results of the NOc "Prof W Besnard" expeditions to the southern coast of Brazil under the Revizee Program: Chirostylidae and Galatheidae (Crustacea: Decapoda: Anomura). Zootaxa 1238:1–22

Miller MA, Pfeiffer W, Schwartz T (2010) Creating the CIPRES science gateway for inference of large phylogenetic trees. In: Proceedings of the Gateway Computing Environments Workshop (GCE) New Orleans pp 1-8

Milne Edwards A (1880) Reports on the results of dredging under the supervision of Alexander Agassiz, in the Gulf ofMexico and in the Caribbean Sea, etc. VIII. Études préliminaires sur les Crustacés. Bull Mus Comp Zool 8:1-168 pls 1, 2

Milne Edwards A, Bouvier EL (1894) Considerations génerales sur la famille des Galatheides. Ann Sci Nat, Zool (ser 7) 16:191–327

Milne Edwards A, Bouvier EL (1899) Crustacés décapodes provenant des campagnes de l'Hirondelle (supplément) et de la Princesse-Alice (1891–1897). Résult Camp scient Prince Souverain Monaco 13:1–106

Milne Edwards A, Bouvier EL (1900) Crustacés décapodes Première partie Brachyures et Anomoures. In: Milne-Edwards, A (Ed) Expéditions scientifiques du Travailleur et du Talisman pendant les années 1880, 1881, 1882, 1883 Masson Paris pp 1-396, 32 pls

Miyake S, Baba K (1970) The Crustacea Galatheidae from the tropical-subtropical region of West Africa, with a list of the known species. Atlantide Report 11:61–97

Muñoz I, Garcia-Isarch E, Sobrino I, Burgos C, Funny R, Gonzalez-Porto M (2012) Distribution, abundance and assemblages of decapod crustaceans in waters off Guinea-Bisau (north-west Africa). J Mar Biol Assoc UK 92:475–494

Muñoz J, Amat F, Green AJ, Figuerola J, Gómez A (2013) Bird migratory flyways influence the phylogeography of the invasive brine shrimp *Artemia franciscana* in its native American range. PeerJ 1:e200

Nei M (1987) Molecular evolutionary genetics. Press, Columbia University

Neves AM (1977) Crustáceos decápodes marinhos de Portugal continental existentes no Museu Bocage III Anomura. Arq Mus Bocage Nova Ser 2(27):1–6

Pacioni C, Hunt H, Allentoft ME, Vaughan TG, Wayne AF, Baynes A, Haouchar D, Dortch J, Bunce M (2015) Genetic diversity loss in a biodiversity hotspot: ancient DNA quantifies genetic decline and former connectivity in a critically endangered marsupial. Mol Ecol 24(3):5813–5828

Palero F, Crandall KA, Abelló P, Macpherson E, Pascual M (2009) Phylogenetic relationships between spiny, slipper and coral lobsters (Crustacea, Decapoda, Achelata). Mol Phylogenet Evol 50(1):152–162

Palumbi SR, Martin AP, Romano S, McMillan WO, Stice L, Grabowski G (1991) The simple fool's guide to PCR. Special Publishing Department of Zoology, University of Hawaii, Honolulu

Petit RJ, Excoffier L (2009) Gene flow and species delimitation. Trends Ecol Evol 24(7):386–393

Pons J, Barraclough TG, Gomez-Zurita J, Cardoso A, Duran DP, Hazell S, Kamoun S, Sumlin WD, Vogler AP (2006) Sequence-based species delimitation for the DNA taxonomy of undescribed insects. Syst Biol 55(4):595–609

Puillandre N, Macpherson E, Lambourdière J, Cruaud C, Boisselier-Dubayle MC, Samadi S (2011) Barcoding type specimens helps to identify synonyms and an unnamed new species in *Eumunida* Smith, 1883 (Decapoda: Eumunididae). Invertebr Syst 25(4):322–333

R core team (2016) R: a language and environment for statistical computing Vienna, Austria: R Foundation for Statistical Computing

Rambaut A (2012) Figtree v 1.4.0. http://tree.bio.ed.ac.uk/software/figtree/

Rambaut A, Drummond AJ, Xie D, Baele G, Suchard MA (2018) Posterior summarisation in Bayesian phylogenetics using Tracer 1.7. Systematic Biology 67(5):901–904. https://doi.org/10.1093/sysbio/syy032

Raupach MJ, Barco A, Steinke D, Beermann J et al (2015) The application of DNA barcodes for the identification of marine crustaceans from the North Sea and adjacent regions. PLoS One 10(9):e0139421

Reid NM, Carstens BC (2012) Phylogenetic estimation error can decrease the accuracy of species delimitation: a Bayesian implementation of the general mixed yule-coalescent model. BMC Evol Biol 12(1):196

Rice AL, de Saint Laurent M (1986) The nomenclature and diagnostic characters of four north-eastern Atlantic species of the genus *Munida* Leach: *Munida rugosa* (Fabricius), *M tenuimana* GO Sars, *M intermedia* A Milne Edwards and Bouvier, and *M sarsi* Huss (Crustacea, Decapoda, Galatheidae). J Nat Hist 20:143–163

Rodríguez-Flores PC, Macpherson E, Machordom (2019a) Revision of the squat lobsters of the genus *Leiogalathea* Baba, 1969 (Crustacea, Decapoda, Munidopsidae) with the description of 15 new species. Zootaxa 4560(2):201–256

Rodríguez-Flores PC, Macpherson E, Buckley D, Machordom A (2019b) High morphological similarity coupled with high genetic differentiation in new sympatric species of coral-reef squat lobsters (Crustacea, Decapoda, Galatheidae). Zool J Linnean Soc. https://doi.org/10.1093/zoolinnean/zly074

Ronquist F, Huelsenbeck JP (2003) MrBayes 3: Bayesian phylogenetic inference under mixed models. Bioinformatics 19(12):1572–1574

Sars GO (1872) Underígelser over Hardengerfjordens Fauna I Crustacea. Forh i Vidensk-Selskapet in Krist 1871:245–286

Squires HJ (1970) Decapod Crustacea of the Atlantic coast of Canada. Can Bull Fish Aquat Sci 221:1–532

Stevcic Z (1990) Check-list of the Adriatic decapod Crustacea. Acta Adriat 31:183–274

Swofford DL (2002) PAUP*: phylogenetic analysis using parsimony (* and other methods). Sunderland, MA

Tsang LM, Ma KY, Ahyong ST, Chan TY, Chu KH (2008) Phylogeny of Decapoda using two nuclear protein-coding genes: origin and evolution of the Reptantia. Mol Phylogenet Evol 48(1):359–368

Von Martens E (1878) Einige Crustaceen und Mollusken, welche das zoologische Museum in letzter Zeit erhalten. Sberi Ges naturf Freunde zu Berl 1878:131–135

Whiting MF (2002) Mecoptera is paraphyletic: multiple genes and phylogeny of Mecoptera and Siphonaptera. Zool Scr 31(1):93–104

Will KW, Rubinoff D (2004) Myth of the molecule: DNA barcodes for species cannot replace morphology for identification and classification. Cladistics 20(1):47–55

Zariquiey-Álvarez R (1952) Estudio de las especies europeas del gen *Munida* Leach 1818. Eos Rev Esp Entom 28:143–231

Zariquiey-Álvarez R (1968) Crustáceos decápodos Ibéricos. Invest Pesq (Spain) 32: i–xv,1-510

Zhang J, Kapli P, Pavlidis P, Stamatakis A (2013) A general species delimitation method with applications to phylogenetic placements. Bioinformatics 29(22):2869–2876

Supplementary Material: Table S1. Examined material of *Munida*.

Col./Voucher Code	Species	Area	Cruise	Station	Latitude	Longitude	Depth (m)	Date	N	Sex	Size (mm)	N	Sex	Size (mm)	N	Sex	Size (mm)
ICMD002523	*M. intermedia*	NE Atlantic	M61	Stn GKG-25	56°30'N	17°18'W	629	11 June 2004	1	F	8.0						
ICMD002583	*M. intermedia*	NE Atlantic	BIOGAS 1	Stn CW01	47°55'N	07°40'W	280	4 August 1972	3	F	12.7-18.6						
ICMD002520	*M. intermedia*	SW Spain	ARSA 2010-11	Stn L29	36° 29'N	07°12'W	579	15 November 2010	1	F	9.7						
ICMD002584	*M. intermedia*	SW Spain	ARSA 2010-11	Stn L31	36° 27'N	07°04'W	559	26 February 2013	1	F	9.8						
ICMD002585	*M. intermedia*	SW Spain	ARSA 2013-02	Stn L39	36°44'N	07°13'W	490	27 February 2013	2	M	8.2-11.3						
ICMD002586	*M. intermedia*	SW Spain	ARSA 2013-02	Stn L34	36°42'N	06°57'W	265	26 February 2013	1	M	19.4						
ICMD002587	*M. intermedia*	SW Spain	ARSA 2013-02	Stn L30	36°28'N	07°00'W	441	25 February 2013	1	M	14.5	1	ov. F	10.5			
ICMD002588	*M. intermedia*	SW Spain	ARSA 2013-02	Stn L7	36°17'N	06°39'W	268	20 February 2013	5	M	15.4-19.7	2	ov. F	15.6-16.0			
ICMD002589	*M. intermedia*	SW Spain	ARSA 2013-02	Stn L40	36°39'N	07°14'W	538	27 February 2013	2	M	13.4-13.8	1	ov. F	12.7			
ICMD002521	*M. intermedia*	SW Spain	ARSA 2013-02	Stn L42	36° 29'N	06°47'W	277	28 February 2013	1	ov. F	14.0						
ICMD002522	*M. intermedia*	SW Spain	ARSA 2013-02	Stn L38	36° 47'N	07°17'W	487	27 February 2013	1	M	12.3	1	ov. F	13.3	1	F	12.4
ICMD002590	*M. intermedia*	SW Spain	ARSA 2013-02	Stn L42	36°29'N	06°47'W	430	27 February 2013	1	ov. F	14.4						
ICMD002522	*M. intermedia*	SW Spain	ARSA 2013-02	Stn L38	36° 47'N	07°17'W	487	27 February 2013	1	M	12.0	1	ov. F	13.6	1	F	12.6
ICMD002514/ICMD002518	*M. intermedia*	NW Mediterranean	Commercial Trawl		41°34'N	02°33'E	250	July 2001	1	M	12.3						
ICMD002515/ICMD002519	*M. intermedia*	NW Mediterranean	Commercial Trawl		41°34'N	02°33'E	250	July 2002	1	ov. F	13.8						
ICMD002591	*M. intermedia*	NW Mediterranean	PROMARES	Stn A7	39°36'N	03°28'E	900	13 July 2011	1	F	7.2						

ICMD	Species	Region	Survey/Gear	Station	Latitude	Longitude	Depth	Date	N	Sex	Size	N	Sex	Size
ICMD002519	M. intermedia	NW Mediterranean	Commercial Trawl		41º34'N	02º33'E	450	July 2001	2	M	17.8-21.2	2	F	15.6-21.6
ICMD002516	M. intermedia	NW Spain	Demersales 09	Stn L139	42º44'N	09º16'W	560	24 July 2009	1	M	22.4	1	F	20.2
ICMD002517	M. intermedia	NW Spain	Demersales 10	Stn L140	42º44'N	09º16'W	560	25 July 2009	1	F	19.5			
ICMD002519	M. intermedia	NW Spain	Demersales 09	Stn L139	42º44'N	09º16'W	560	24 July 2009	1	F	19.0			
ICMD002592	M. intermedia	W Mediterranean	MEDITS2012	Stn L086	39º27'N	00º09'E	581	20 May 2012	1	F	8.5			
ICMD002593	M. rugosa	NE Atlantic	Commercial Trawl		60º28'N	03º28'E	95	June 2001	1	M	15.4			
ICMD002594	M. rugosa	NE Atlantic	Commercial Trawl		60º28'N	03º28'E	95	June 2001	1	F	17.0			
ICMD002595	M. rugosa	NE Atlantic	Charcot	Stn 9	47º35'N	04º12'W	100	13 June 1969	3	M	13.8-17.1	1	F	15.5
ICMD002596	M. rugosa	NW Spain	Demersales 14	Stn L124	44º46'N	06º06'W	107	14 August 2014	1	F	19.5			
ICMD002597	M. rugosa	NW Spain	ICTIO 82	Stn 17	44º42'N	09º17'W	120	12 July 1982	1	M	22.3			
ICMD002535	M. rugosa	NW Spain	Demersales 14	Stn 82	44º42'N	05º06'W	102	6 August 2014	1	F	27.3			
ICMD002598	M. rugosa	NW France	Commercial Trawl		47º35'N	04º12'W	100	13 June 1969	1	M	18.3			
ICMD002534	M. rugosa	NW France	Commercial Trawl		47º35'N	04º12'W	100	13 June 1969	1	F	21.4			
ICMD002599	M. rugosa	SW Spain	ARSA 2013-02	Stn L42	36º29'N	06º47'W	277	27 February 2013	1	ov. F	19.0			
ICMD002536	M. rugosa	SW Spain	ARSA 2013-02	Stn L42	36º29'N	06º47'W	277	27 February 2013	1	ov. F	19.3			
ICMD002532	M. rugosa	NW Mediterranean	Commercial Trawl		40º25'N	00º59'E	130	June 2004	1	M	20 0			
ICMD002600	M. rugosa	NW Mediterranean	Commercial Trawl		39º52'N	04º05'E	100	July 1955	1	M	27.0			
ICMD002601	M. rugosa	NW Mediterranean	Commercial Trawl		39º52'N	04º05'E	100	July 1955	1	F	25.4			
ICMD002533	M. rugosa	NW Mediterranean	MAO-BENTOS_2014	Stn P28	39º50'N	04º23'E	72	28 January 2014	1	M	22.3			

ICMD002531	*M. rugosa*	SW Mediterranean	MEDITS2012	Stn 12	36°37'N	04°20'W	122	22 May 2012	1	F	22.6			
ICMD002604	*M. rugosa*	NE Atlantic	Commercial Trawl		W Scotland	no position	no depth	June 2001	1	F	17.9			
ICMD002605	*M. rugosa*	NE Atlantic	Commercial Trawl		W Scotland	no position	no depth	June 2002	1	M	32.0			
ICMD002549	*M. sarsi*	NE Atlantic	M61	Stn GKG-27	56°30'N	17°18'W	674	11 June2004	1	F	10.2			
ICMD002606	*M. sarsi*	W France	BIOGAS 1	Stn DS02	47°56'N	07°40'W	400	1 August 1972	13	M	12.0-21.6	16	F	7.1-18.4
ICMD002607	*M. sarsi*	W France	BIOGAS 1	Stn CW01	47°55'N	07°40'W	280	4 August 1972	3	M	19.5-21.2			
ICMD002608	*M. sarsi*	NE Atlantic	LOPHELIA	Stn 713	67°57'N	15°31'E	404	25 September 2002	2	M	12.3-12.6			
ICMD002609	*M. sarsi*	NE Atlantic	Commercial Trawl		67°57'N	15°31'E	404	25 September 2002	2	F	11.3-12.9			
ICMD002543/ ICMD002548	*M. sarsi*	NW Spain	Demersales 09	Stn L139	42°44'N	09°16'W	560	24 July 2009	1	M	20.0			
ICMD002544/ ICMD002549	*M. sarsi*	NW Spain	Demersales 09	Stn L139	42°44'N	09°16'W	560	24 July 2009	1	F	10.6			
ICMD002545	*M. sarsi*	NE Atlantic	Commercial Trawl	W Scotland	57°41'N	09°07'W	485	June 2002	1	M	23.5			

CAPÍTULO II
RELACIONES FILOGENÉTICAS EN
GALATHEOIDEA

CAPÍTULO II

RELACIONES FILOGENÉTICAS EN GALATHEOIDEA

Artículos incluidos:

Palero F, **Rodríguez-Flores PC**, Cabezas P, Machordom A, Macpherson E, & Corbari L. 2019. Evolution of squat lobsters (Crustacea, Galatheoidea): mitogenomic data suggest an early divergent Porcellanidae. *Hydrobiologia,* 833(1), 173–184

Rodríguez-Flores PC, Macpherson E, Baba K, Ahyong ST, Chan T-Y, Lin C-W, & Machordom A. Moving forward by moving back: integrative systematics supports revival of old, and creation of new genera in the composite taxon, *Munidopsis* Whiteaves, 1874. *The Crustacean Society Mid-Year Meeting* 2019, Hong Kong, May 2019 (**manuscrito en preparación**)

Rodríguez-Flores PC, Macpherson E, Buckley D, & Machordom A. 2019. High morphological similarity coupled with high genetic differentiation in new sympatric species of coral-reef squat lobsters (Crustacea: Decapoda: Galatheidae). *Zoological Journal of the Linnean Society,* 185: 984–1017

PRIMARY RESEARCH PAPER

Evolution of squat lobsters (Crustacea, Galatheoidea): mitogenomic data suggest an early divergent Porcellanidae

Ferran Palero · **Paula C. Rodríguez-Flores** · **Patricia Cabezas** ·
Annie Machordom · **Enrique Macpherson** · **Laure Corbari**

Abstract Squat lobsters constitute an exceptional group to address evolutionary studies in marine species because of their high diversity at multiple taxonomic levels. The families included within Galatheoidea are characterized by morphological, molecular, and ecological differences. Previous phylogenetic reconstructions have considered either Galatheidae, Porcellanidae, or even Munidopsidae as the most derived family within Galatheoidea, but evolutionary relationships within the superfamily have not been fully resolved yet. In order to test previous phylogenetic hypotheses on the relative placement of Porcellanidae within the Galatheoidea, and further characterize mitochondrial gene order in Munidopsidae, the first complete mitochondrial genomic sequence of a Galatheidae squat lobster (*Galathea aegyptiaca*) and the partial mitogenome of *Munidopsis polymorpha* are reported here. These new sequences complement previous studies to include all extant families and provide further evidence on the importance of mitochondrial gene rearrangements in Galatheoidea. Implications of the new phylogenetic

F. Palero (✉)
Department of Invertebrate Zoology and Hydrobiology,
Faculty of Biology and Environmental Protection,
University of Lodz, ul. Banacha 12/16, 90-237 Łódź,
Poland
e-mail: fpalero@ceab.csic.es

F. Palero · P. C. Rodríguez-Flores · E. Macpherson
Centre d'Estudis Avançats de Blanes (CEAB-CSIC),
Carrer d'Accés a la Cala Sant Francesc 14, 17300 Blanes,
Spain
e-mail: paulacrf@mncn.csic.es

E. Macpherson
e-mail: macpherson@ceab.csic.es

P. C. Rodríguez-Flores · P. Cabezas · A. Machordom
Museo Nacional de Ciencias Naturales (MNCN-CSIC),
José Gutiérrez Abascal, 2, 28006 Madrid, Spain
e-mail: pcabezaspadilla@gmail.com

A. Machordom
e-mail: annie@mncn.csic.es

L. Corbari
Institut de Systématique, Évolution, Biodiversité (ISYEB
UMR 7205), Muséum national d'Histoire naturelle,
CNRS, Sorbonne Université, EPHE, 57 rue Cuvier, CP
51, 75005 Paris, France
e-mail: corbari@mnhn.fr

🍃 Springer

data on the evolution of carcinization within Anomura are also discussed.

Introduction

Squat lobsters constitute an exceptional group to address evolutionary studies because of their high diversity at multiple taxonomic levels (Baba et al., 2008). They are found in nearly all latitudes and marine habitats, from deep sea to shallow-water ecosystems (Schnabel et al., 2011). Squat lobsters constitute a significant part of the deep-sea fauna, living in close association with other marine organisms like feather stars, sponges, or corals (Baba et al., 2008; Baeza, 2011). According to recent taxonomic studies, squat lobsters are paraphyletic and include members from two well-defined superfamilies (Chirostyloidea and Galatheoidea) (Schnabel et al., 2011; Bracken-Grissom et al., 2013). Chirostyloidea comprise Eumunididae, Sternostylidae, Chirostylidae, and Kiwaidae, the last three families being originally included in the Galatheoidea superfamily (Martin & Davis, 2001; Macpherson et al., 2005; Ahyong et al., 2011; Baba et al., 2018). The members of Galatheoidea sensu stricto (Ahyong et al., 2010) are characterized by having a tail fan (telson and uropods) that is bent (not folded) against the preceding somite (Zariquiey Alvarez, 1968; Macpherson & Baba, 2011), by having a telson subdivided into plates, and a 4-articulate antennal peduncle (Ahyong et al., 2010). Galatheoidea currently contains four families: Galatheidae Samouelle, 1819, Munididae Ahyong et al., 2010, Munidopsidae Ortmann, 1898, and Porcellanidae Haworth, 1825 (Ahyong et al., 2010). Galatheidae and Porcellanidae are mainly found in shallow waters, Munididae are widely distributed along continental shelves, and Munidopsidae mostly includes deep-sea species from below 1,000 m (Ahyong et al., 2010; Schnabel et al., 2011).

Evolutionary relationships within the Galatheoidea superfamily have not been fully resolved yet. The four families present a high diversity in their external morphology, which renders cladistic analyses inconsistent. For instance, the porcelain crabs

(Porcellanidae) are the only galatheoids with a crab-like body form. They have the entire pleon folded under the cephalothorax, and their carapace is usually broader than long (Ahyong et al., 2010; Keiler et al., 2015). Munididae present a spiniform rostrum, in most cases flanked with two supraorbital spines; Galatheidae have a triangular or subtriangular rostrum, broad at its base; and almost all Munidopsidae have reduced eyes and lack of body pigmentation. The placement of Porcellanidae within Galatheoidea is strongly supported in previous phylogenetic analyses based on morphology and molecular data (Schnabel et al., 2011; Bracken-Grissom et al., 2013), but relationships between Porcellanidae and other Galatheoidea families remain unclear. Milne-Edwards & Bouvier (1894) first suggested *Galathea* to represent the ancestor of the group, with Porcellanidae being an early offshoot and *Munida* originating the Munidopsidae lineage. Three alternative hypotheses have been proposed regarding the placement of porcellanids within Galatheoidea: (1) Galatheidae and Porcellanidae are sister groups (Martin & Abele, 1986; McLaughlin et al., 2007; Ahyong et al., 2009; Schnabel et al., 2011), (2) Porcellanidae as the sister group of a clade formed by Munididae and Galatheidae (Bracken-Grissom et al., 2013), or (3) Porcellanidae as the earliest branching within Galatheoidea (Morrison et al., 2002; Tsang et al., 2011; Roterman et al., 2018; Tan et al., 2018). Several phylogenetic reconstructions consider Munidopsidae as the sister group of the remaining Galatheoidea (Bracken et al., 2009; Schnabel et al., 2011), which implies that Porcellanidae must have acquired the crab-like form after diverging from Munididae to Galatheidae (see Fig. 3.3 in Ahyong et al., 2011). Nevertheless, a recent study on the phylogeny of Kiwaidae (Chirostyloidea) including both mitochondrial and nuclear genes suggests an earlier branching of Porcellanidae (Roterman et al., 2018).

The recent development of high-throughput sequencing has significantly reduced the amount of effort needed to obtain sequencing data from mitochondrial genomes (Boore, 1999). The fractions of the genomes that show high copy numbers, including mitochondrial DNA, can be retrieved using a relatively shallow sequencing approach (Roehrdanz et al., 2014). Furthermore, mitochondrial phylogenetics can present some advantages over nuclear-based phylogenies as gene content is highly conserved,

mitochondrial proteins present a greater grade of orthology, and mtDNA provides additional characters like reorganization of the genome. Mitogenomic-based phylogenies have allowed a better understanding of deep phylogenetic relationships and character evolution reconstructions in many invertebrates (Podsiadlowski et al., 2009; Bernt et al., 2013; Osca et al., 2014). A recent study has addressed phylogenetic relationships within the Anomura using mitochondrial sequences and gene order rearrangements (Tan et al., 2018). Galatheoidea mitogenomes apparently show a complex gene rearrangement scenario, including transpositions, deletions, duplications, and tandem duplications with random loss. This study included no data on Galatheidae though, and the only representative of Munidopsidae (*Shinkaia crosnieri* Baba & Williams, 1998) presented a highly divergent mitochondrial gene order with the loss of several transfer RNA genes.

In order to test previous phylogenetic hypotheses on the relative placement of Porcellanidae within the Galatheoidea and further characterize gene order in Munidopsidae, the first complete mitochondrial genomic sequence of a Galatheidae squat lobster (*Galathea aegyptiaca* Paul'son, 1875) and the partial mitogenome of *Munidopsis polymorpha* Koelbel, 1892 are reported here. These new sequences complement previous studies to include all extant families and provide further evidence on the importance of mitochondrial gene rearrangements in Galatheoidea. Implications of the new phylogenetic data on the evolution of carcinization within Anomura are also discussed.

Materials and methods

A different approach was carried out for obtaining mitogenomic data in *Munidopsis polymorpha* and *Galathea aegyptiaca*. Approximately 30 specimens of *M. polymorpha*, a decapod endemic to an anchialine cave system of the Corona lava tube in Lanzarote (Canary Islands), were captured using hand nets and preserved in absolute ethanol. Total DNA was extracted from tissue samples using the magnetic Charge Switch gDNA Micro Tissue Kit (Invitrogen) and DNA from a single specimen was used for long PCR amplification with the Z Taq (Takara, Otsu, Japan) polymerase approach (Yamauchi et al., 2002).

Amplified fragments were purified by ethanol precipitation prior to sequencing both strands using the same PCR primers and Big Dye Terminator (Applied Biosystems). Sequences were run in an ABI 3730 Genetic Analyzer (Applied Biosystems). The starting material for *Galathea aegyptiaca* was one male specimen collected from the Red Sea (18.0731 N, 40.8859 E) and kept at the Florida Museum of Natural History collections (Catalogue Number: UF 36010). Total genomic DNA was extracted from a single pereiopod using the QIAamp DNA mini Kit (QIA-GEN Inc) and sent out for library construction and sequencing to the Get-PlaGe core facilities of GenoToul (Toulouse, France). The library was built using the Illumina TruSeq Nano DNA Library Prep Kit (Illumina) and sequenced on the high-speed sequencer Illumina HiSeq 3,000 in 2 × 150 pb paired-ends. Paired-end reads of the of *G. aegyptiaca* genomic library were subjected to quality inspection using the FastQC software (Andrews, 2010), and the Velvet de novo assembler (Zerbino & Birney, 2008) was used to obtain contigs (long continuous sequences) out of the short-reads by building a k-mer graph. A local database including every crustacean mitochondrial genome available in GenBank was used to screen the contigs collection after sequence assembly by running a BLAST search. The complete mitochondrial genome of *Galathea aegyptiaca* was thus identified within a single contig of 16 kb.

Gene annotation, alignment, and model selection

The mitochondrial genome annotation server (MITOS) pipeline was used to compute a consistent de novo annotation of the mitogenomic sequences. MITOS is a fully automated pipeline for the annotation of metazoan mitochondrial genomes that combines BLAST searches with previously annotated protein sequences, thereby avoiding the need for a built-in database of specifically curated protein models. Both tRNAs and rRNAs are annotated using specific covariance models for each of the structured RNAs. The complete mitogenomes from Galatheoidea (*Munida gregaria*: NC_030255.1; *M. isos*: MF457406.1; *Neopetrolisthes maculatus*: NC_020024.1; *Petrolisthes haswelli*: NC_025572.1; and *Shinkaia crosnieri*: NC_011013.1) and two Chirostyloidea outgroups (*Gastroptychus investigatoris*:

KY352237.1 and *Kiwa tyleri*: NC_034927.1) were obtained from GenBank (Yang & Yang, 2008; Shen et al., 2013; Lee et al., 2016; Tan et al., 2016, 2018; Zhang et al., 2017a), annotated de novo also using the MITOS pipeline and used for further phylogenetic analyses. Amino acid sequences for each protein-coding gene were aligned separately using MAFFT and then we concatenated alignments for all genes. To improve reliability, conserved (ungapped) blocks of sequences were extracted from the concatenated amino acid alignment by using Gblocks server with default settings (Castresana, 2000; Talavera & Castresana, 2007). The best-fit substitution model was tested with ProtTest v.2.4 (Abascal et al., 2005), which showed mtArt to be the most likely substitution model for every protein-coding alignment.

Phylogenetic inference and hypotheses testing

Maximum likelihood (ML) phylogenetic tree reconstruction was applied using the program PhyML v.3.0 (Guindon et al., 2010). The MtArt model of protein sequence evolution was used with an estimated proportion of invariable sites and a Gamma distribution of rates across four classes. Nodal support was assessed using 500 bootstrap replicates, due to computational constraints imposed by the size of our dataset. Aligned and concatenated protein-coding sequences were also used to estimate phylogenetic relationships with the Bayesian inference (BI) approach implemented in the software BEAST v.2.4.7 (Drummond et al., 2012). A rooted phylogeny was estimated with BEAST, applying an uncorrelated lognormal relaxed clock, Yule model as a tree prior, and Gamma site heterogeneity model with four site categories and mtREV substitution model. Four independent Markov chains were run in BEAST for 10 million generations, sampling every 1000th generation. Tracer v.1.4.1 (Drummond & Rambaut, 2007) was used to summarize the Markov chains and visually inspect the trace plots (all showed good mixing and convergence). The effective sample sizes (ESS) for the runs were above 200 for most parameters reported in Tracer. The maximum clade credibility (MCC) tree was obtained from the posterior tree distributions using TreeAnnotator v.1.4.8 (from the BEAST package).

Besides the unconstrained search, BEAST runs were carried out using the same conditions but including several constrained searches in order to test the main hypotheses of the evolution of Galatheoidea lobsters: (1) Galatheidae and Porcellanidae as sister groups, (2) Porcellanidae as the sister group of a clade formed by Munididae and Galatheidae, and (3) Porcellanidae as the earliest branching within Galatheoidea. The Bayes factor approach was used to compare the different models, evaluating the hypothesis (H_0) that our constrained and unconstrained BI topologies explain the data equally well, versus the alternative hypothesis (H_1) that constrained BI searches provide a poorer explanation of the data. The Bayes factor was calculated as twice the difference in the harmonic mean of log-likelihood scores between alternative hypotheses (Brandley et al., 2005) and these values were compared to the framework provided by Kass & Raftery (1995), where < 0 is evidence against H_1, 0–2 provides no evidence for H_1, 2–6 is positive support for H_1, 6–10 is strong support for H_1, and > 10 is very strong support for H_1 (Kass & Raftery, 1995; Palero et al., 2009).

Results

Mitochondrial genomes

The complete mitochondrial genome sequence of *Galathea aegyptiaca* is 16,051 bp long and, as with most metazoan mitogenomes, it encodes 13 protein-coding genes, 22 transfer RNA (tRNA), and 2 ribosomal RNA (rRNA) genes (Table 1; Fig. 1). These genes are variously oriented between the two strands of the mitogenome, the light strand (or L-strand) contains the ribosomal genes (12S and 16S rDNA), 8 tRNA genes and 4 protein-coding genes (nad1, nad4, nad4 l, and nad5), and the heavy strand (or H-strand) contains the remaining genes.

Only a partial mitochondrial genome sequence (15,725 bp) was obtained for *Munidopsis polymorpha*, including every gene except trnA, trnE, trnQ, and trnS1 and incomplete sequences for genes nad3, nad6, and cytb (see *Gene order* section). Despite being incomplete, the newly obtained data on mitochondrial gene order (MGO) for *M. polymorpha* have important implications for mitogenome evolution in squat lobsters. GC content in *G. aegyptiaca* (26.7%) was similar to that observed in other Galatheoidea (*S. crosnieri*: 27.1%; *M. gregaria*: 25.1%) or

Table 1 Gene content of the mitochondrial genome of *Galathea aegyptiaca* and the partial mitogenome of *Munidopsis polymorpha*

Feature	Type	*Galathea aegyptiaca*		*Munidopsis polymorpha*	
		Start	End	Start	End
Cytochrome c oxidase subunit I (Cox1)	CDS	6	1,515	1,256	2,770
tRNA-Leu (L2)	tRNA	1,534	1,599	2,790	2,856
Cytochrome c oxidase subunit II (Cox2)	CDS	1,606	2,278	2,865	3,533
tRNA-Lys (K)	tRNA	2,291	2,357	3,553	3,618
tRNA-Ile (I)	tRNA	2,361	2,428	13,338	13,407
tRNA-Met (M)	tRNA	2,431	2,497	3,729	3,797
tRNA-Ala (A)	tRNA	2,505	2,571	–	–
NADH dehydrogenase subunit 2 (nad2)	CDS	2,614	3,550	3,915	4,790
tRNA-Asp (D)	tRNA	3,603	3,669	4,905	4,971
ATP synthase F0 subunit 8 (Atp8)	CDS	3,669	3,825	4,972	5,127
ATP synthase F0 subunit 6 (Atp6)	CDS	3,821	4,487	5,124	5,789
Cytochrome c oxidase subunit III (Cox3)	CDS	4,495	5,281	5,798	6,586
tRNA-Ser (S1)	tRNA	5,316	5,382	–	–
tRNA-Glu (E)	tRNA	5,384	5,451	–	–
tRNA-Phe (F)	tRNA	6,223	6,287	11,186	11,250
NADH dehydrogenase subunit 5 (nad5)	CDS	6,294	7,959	11,273	12,953
tRNA-His (H)	tRNA	8,102	8,171	12,980	13,044
tRNA-His (H)	tRNA	–	–	13,958	14,022
NADH dehydrogenase subunit 4 (nad4)	CDS	8,184	9,366	14,036	15,238
NADH dehydrogenase subunit 4L (nad4L)	CDS	9,506	9,779	15,358	15,633
tRNA-Thr (T)	tRNA	9,808	9,876	15,660	15,725
NADH dehydrogenase subunit 6 (nad6)	CDS	9,897	10,401	13,613	13,930
Cytochrome b (cytb)	CDS	10,412	11,549	4	594
tRNA-Ser (S2)	tRNA	11,547	11,615	593	659
tRNA-Pro (P)	tRNA	11,625	11,691	7,215	7,285
NADH dehydrogenase subunit 1 (nad1)	CDS	11,729	12,632	7,331	8,218
tRNA-Leu (L1)	tRNA	12,655	12,722	8,270	8,339
Large subunit (16S rRNA)	rRNA	12,678	14,038	8,295	9,662
tRNA-Val (V)	tRNA	14,042	14,113	9,675	9,742
Small subunit (12S rRNA)	rRNA	14,112	14,929	9,741	10,569
tRNA-Trp (W)	tRNA	15,193	15,262	1,025	1,092
tRNA-Gly (G)	tRNA	15,269	15,336	3,618	3,682
NADH dehydrogenase subunit 3 (nad3)	CDS	15,345	15,681	6,609	6,676
tRNA-Arg (R)	tRNA	15,695	15,759	6,690	6,745
tRNA-Asn (N)	tRNA	15,759	15,826	–	–
tRNA-Gln (Q)	tRNA	15,839	15,906	1,122	1,188
tRNA-Cys (C)	tRNA	15,915	15,983	1,189	1,254
tRNA-Tyr (Y)	tRNA	15,982	16,049	–	–

The minus sign (−) indicates whenever a particular gene was not detected

Chirostyloidea (*G. investigatoris*: 28.3%), but guanine content was low (A = 35.5; C = 16.2; G = 10.5; T = 37.8). The relative frequency of different amino acids in protein-coding regions of *G. aegyptiaca* or *M.*
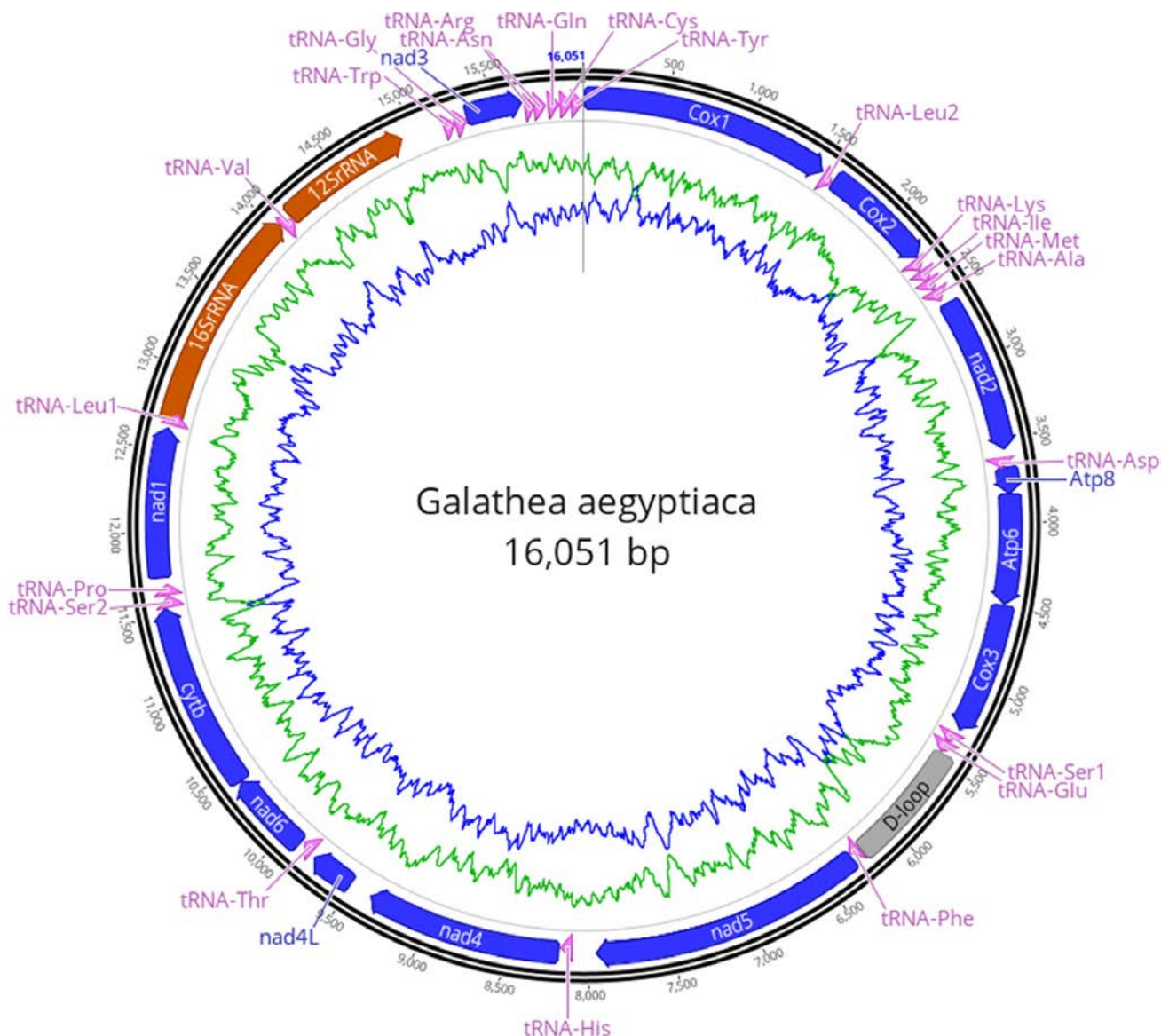
Fig. 1 Complete mitochondrial genome of *Galathea aegyptiaca* Paul'son, 1875 (Florida Museum of Natural History collections catalogue number: UF 36010). Protein-coding genes (Blue), ribosomal (Orange), and transfer RNA (Rose) genes are presented using the Abbreviations shown in Table 1. The inner graph indicates the AT (green) and GC (blue) content along the genome using a 100 bp sliding window

polymorpha mitogenomes was variable, but the most frequent were in both cases hydrophobic amino acids like Leucine (13.7 and 15%), Phenylalanine (9.9 and 10.9%), or Isoleucine (9.4% and 8.3%). The most frequent polar amino acid was Serine (10.8% and 12.7%), followed by Glycine (5.7%) in *G. aegyptiaca,* or Asparagine (5.1%) in *M. polymorpha*. A strong codon preference was observed in both polar and non-polar amino acids for both taxa (Table 2).

Phylogenetic analyses and hypotheses testing

After sequence alignment and trimming, the final dataset of 13 protein-coding genes included a total of 3,477 amino acid positions. The model considered to describe the substitution pattern the best was the mtArt + G+I model according to both the BIC score (62521.96) and AICc value (62395.71). Non-uniformity of evolutionary rates among sites was modeled by using a discrete Gamma distribution ($G = 0.57$) and by assuming that a fraction of sites are

Table 2 Codon usage for the protein-coding genes in the mitochondrial genome of *Galathea aegyptiaca* and the partial mitogenome of *Munidopsis polymorpha*

Amino acid	Code	*Galathea aegyptiaca*	*Munidopsis polymorpha*
Alanine	A	GCA (31.6%), GCC (15.5%), GCG (5.7%), **GCT** (47.1%)	GCA (34.4%), GCC (9.0%), GCG (0.8%), **GCT** (55.7%)
Cysteine	C	TGC (23.4%), **TGT** (76.6%)	TGC (18.5%), **TGT** (81.5%)
Aspartic acid	D	GAC (16.9%), **GAT** (83.1%)	GAC (15.2%), **GAT** (84.8%)
Glutamic acid	E	**GAA** (78.3%), GAG (21.7%)	**GAA** (74.6%), GAG (25.4%)
Phenylalanine	F	TTC (17.7%), **TTT** (82.3%)	TTC (15.7%), **TTT** (84.3%)
Glycine	G	**GGA** (46.9%), GGT (35.5%), GGC (4.3%), GGG (13.3%)	**GGA** (43.1%), GGT (30.6%), GGC (9.0%), GGG (17.4%)
Histidine	H	CAC (18.8%), **CAT** (81.3%)	CAC (12.2%), **CAT** (87.8%)
Isoleucine	I	ATC (10.6%), **ATT** (89.4%)	ATC (11.6%), **ATT** (88.4%)
Lysine	K	**AAA** (78.0%), AAG (22.0%)	**AAA** (85.4%), AAG (14.6%)
Leucine	L	CTA (11.8%), CTC (2.4%), CTG (1.4%), CTT (18.7%), **TTA** (59.3%), TTG (6.5%)	CTA (7.3%), CTC (3.1%), CTG (0.0%), CTT (17.2%), **TTA** (65.3%), TTG (7.1%)
Methionine	M	**ATA** (83.2%), ATG (16.8%)	**ATA** (87.2%), ATG (12.8%)
Asparagine	N	AAC (16.5%), **AAT** (83.5%)	AAC (19.4%), **AAT** (80.6%)
Proline	P	CCA (29.9%), CCC (12.7%), CCG (6.0%), **CCT** (51.5%)	CCA (17.9%), CCC (10.7%), CCG (1.2%), **CCT** (70.2%)
Glutamine	Q	**CAA** (91.9%), CAG (8.1%)	**CAA** (88.9%), CAG (11.1%)
Arginine	R	**CGA** (62.1%), CGC (3.4%), CGG (3.4%), CGT (31.0%)	**CGA** (41.7%), CGC (13.9%), CGG (16.7%), CGT (27.8%)
Serine	S	AGA (21.6%), AGC (5.0%), AGG (9.8%), AGT (7.0%), TCA (22.3%), TCC (6.8%), TCG (3.3%), **TCT** (24.3%)	AGA (26.0%), AGC (6.8%), AGG (6.0%), AGT (7.0%), TCA (15.1%), TCC (7.5%), TCG (1.6%), **TCT** (30.1%)
Threonine	T	**ACA** (43.2%), ACC (12.0%), ACG (1.6%), **ACT** (43.2%)	**ACA** (31.6%), ACC (7.0%), ACG (5.3%), **ACT** (56.1%)
Valine	V	GTA (40.2%), GTC (3.1%), GTG (9.8%), **GTT** (46.9%)	GTA (42.9%), GTC (2.4%), GTG (9.5%), **GTT** (45.2%)
Tryptophan	W	**TGA** (86.9%), TGG (13.1%)	**TGA** (62.8%), TGG (37.2%)
Tyrosine	Y	TAC (17.0%), **TAT** (83.0%)	TAC (22.8%), **TAT** (77.2%)
Stop codons	*	**TAA** (63.6%), TAG (36.4%)	**TAA** (69.7%), TAG (30.3%)

The most frequently used triplet for each amino acid is highlighted in bold

evolutionarily invariable (I = 21.8%). The tree with the highest log likelihood is shown in Fig. 2. All representatives of the Galatheoidea formed a well-supported monophyletic clade. Most importantly, Galatheidae appeared as sister of the Munididae lineage, with high support in both ML and Bayesian analyses. Munidopsidae emerged as the sister lineage of the clade constituted by Galatheidae and Munididae, the three families uniting the Galatheoidea with typical squat lobster morphology. This grouping also appeared highly supported for all analyses, supporting the placement of Porcellanidae as the sister lineage of the rest of Galatheoidea families. Bayes factors were computed in order to test the statistical support for previously established hypotheses. Both hypotheses grouping Galatheidae and Porcellanidae as sister groups (lnL = − 30142.95 ± 2.66), and the Porcellanidae as the sister group of a clade formed by Munididae and Galatheidae (lnL = − 30113.10 ± 3.11) showed much lower mean log-likelihood values than the topology including Porcellanidae as the earliest branching within Galatheoidea (lnL = − 30077.76 ± 4.70). Accordingly, the Bayes factor provided very strong support (BF > 10) for a monophyletic clade Munidopsidae/Munididae/Galatheidae when compared both against a topology grouping
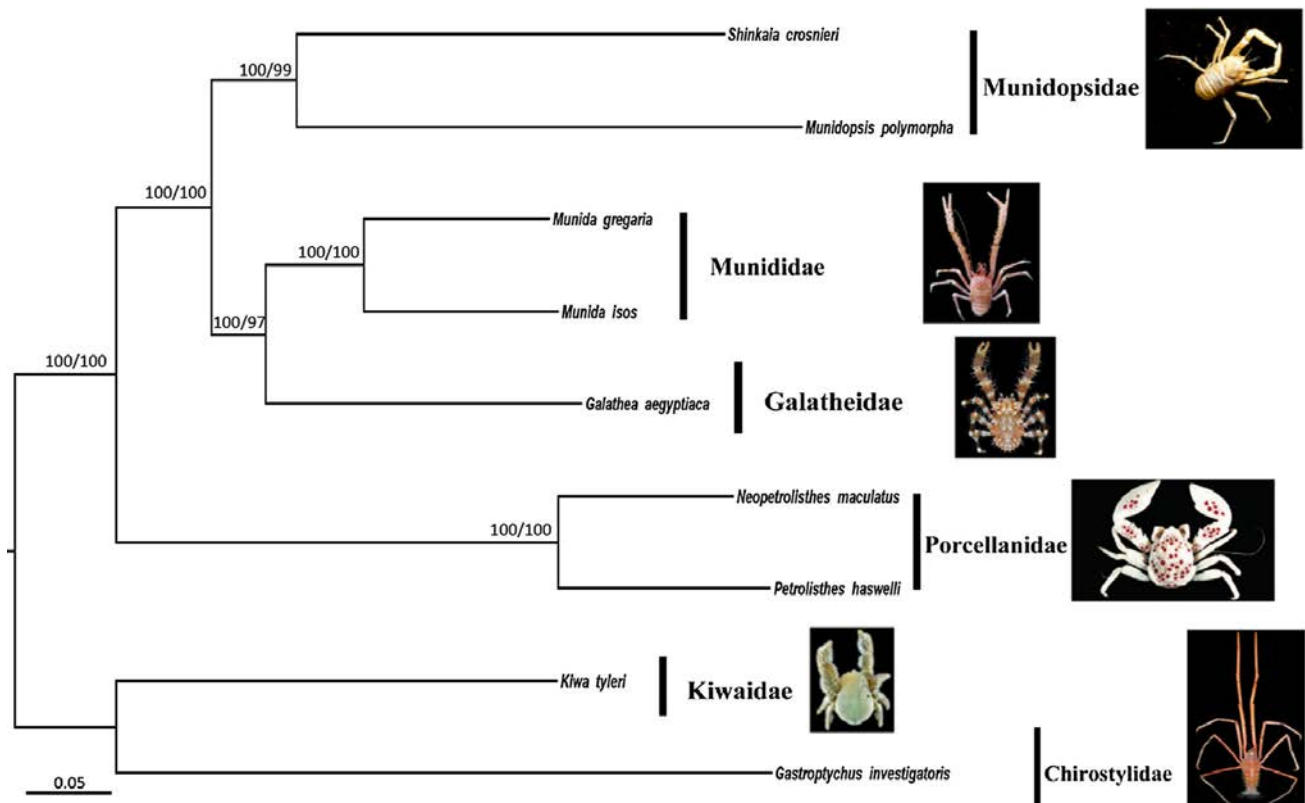
Fig. 2 Phylogenetic consensus tree showing the relationship between the different families of Galatheoidea. Bootstrap branch support for ML analysis (before slash) and Bayesian posterior probabilities (after slash) are indicated above a cut-off value of 70 and 95, respectively. The photographs included correspond to representative species of each family and were obtained from the MNHN crustacean database (https://science.mnhn.fr/institution/mnhn/collection/iu/list)

Porcellanidae/Galatheidae (BF = 65.17) or Porcellanidae/Munididae/Galatheidae (BF = 35.32).
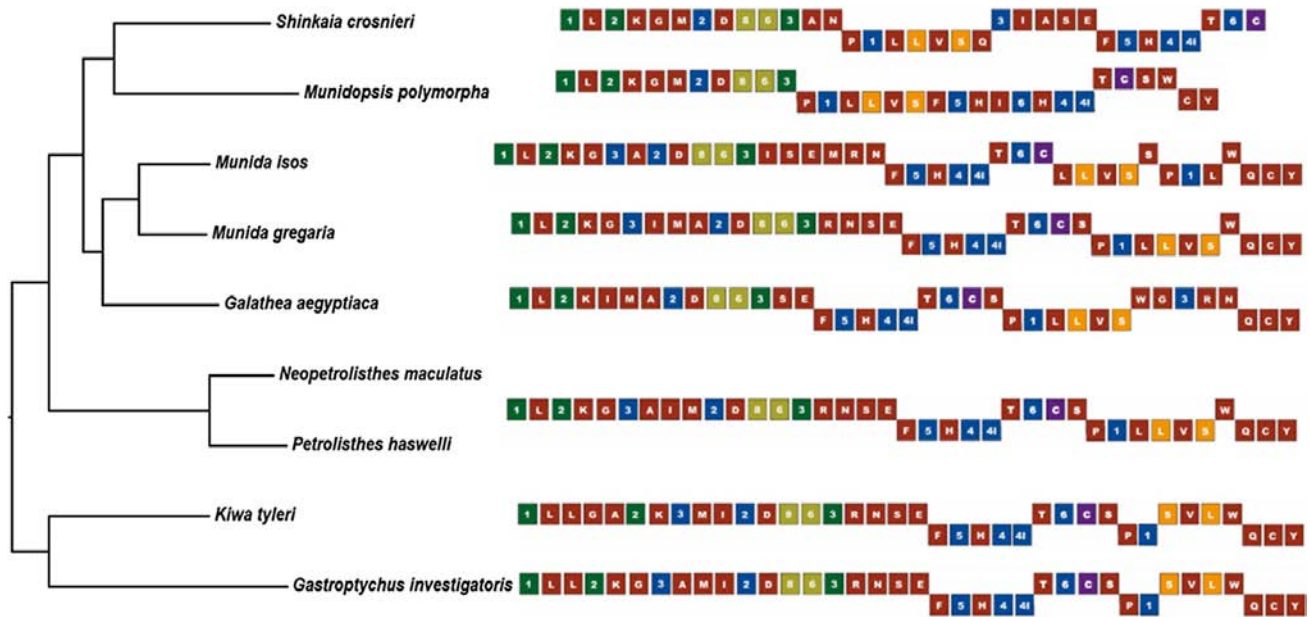
Gene order

Mitochondrial gene order (MGO) is typically considered to be highly conserved, with changes in position observed only for tRNAs in most cases. However, the mitogenomes of both *G. aegyptiaca* and *M. polymorpha* show MGOs not previously described in other Anomura (Fig. 3). The mitogenome gene order of *G. aegyptiaca* is closest to that of *Munida gregaria*, which provides further support for the close relationship between both families. The simplest gene rearrangement scenario for the *Galathea* MGO implies a transposition of tRNA-Gly (G) and nad3, together with tRNA-Arg (R) and tRNA-Asn (N), in between the genes encoding for tRNA-Trp (W) and tRNA-Gln (Q). The unique shift of the tRNA-Gly, nad3, tRNA-Arg, and tRNA-Asn genes in *G. aegyptiaca* might be secondary because it differs from that found in

munidids (*M. gregaria*) and porcellanids. Although the mitochondrial genome sequence of *M. polymorpha* is still incomplete, the closest MGO corresponded to that of *S. crosnieri*, as expected given the phylogenetic results. Both Munidopsidae taxa presented an identical gene-cluster spanning from Cox1 to Cox3. Nevertheless, *M. polymorpha* presents a unique configuration, where all protein-coding genes of the light strand are grouped in a single gene-cluster together with the ribosomal genes. Our results also show that several of those tRNA missing in *Shinkaia* are still present in *Munidopsis*, suggesting that the deletion of several genes must have occurred within the Munidopsidae (Fig. 3).

Discussion

The first full mitogenome of a galatheid squat lobster (*Galathea aegyptiaca*) and the partial mitogenome of a second Munidopsidae (*Munidopsis polymorpha*) are

Fig. 3 Visualization of the mitochondrial gene order after de novo annotation of the genomes. Genes located on the plus strand are drawn in the upper part and genes annotated on the minus strand are shown in the lower region. A single pattern is shown in porcellanids because both species present the same mitochondrial gene arrangement

reported here. This is the first study focusing on the relationships among Galatheoidea sensu Ahyong et al. (2010) and using mitogenomic data with representation of every family currently recognized. Members of Galatheidae have been poorly represented in previous molecular phylogenetic studies because most systematic research has been focused on elucidating higher-level relationships (Ahyong et al., 2009; Schnabel et al., 2011; Bracken-Grissom et al., 2013). The new phylogenetic and MGO results provide further evidence supporting the monophyly of Galatheoidea sensu Ahyong et al. (2010) and a monophyletic Galatheidae and Munididae clade. The support for a clade containing the Galatheidae and Porcellanidae found in previous studies relied on using ribosomal gene sequences (16S, 18S, and partial 28S rDNA) (Schnabel et al., 2011). However, there are no unambiguous morphological changes supporting the grouping of Galatheidae + Porcellanidae, although both families share the presence of a broad rostrum (Ahyong et al., 2010). The addition of markers in a later study resulted in Porcellanidae forming a monophyletic clade together with Munididae and Galatheidae (Bracken-Grissom et al., 2013), but this might be due to taxon sampling because as many species of porcellanids were included as for the other galatheoids combined. The results obtained here are in agreement

with those recently presented by Roterman et al. (2018) using both mitochondrial and nuclear markers.

Although current consensus seems to acknowledge a close relationship between Galatheidae and Porcellanidae (Ahyong et al., 2009; Schnabel et al., 2011), morphological characters have been insufficient to fully resolve internal relationships within Galatheoidea, even with the inclusion of adult morphology, sperm, and larval characters (Schnabel et al., 2011). The progressive 'carcinization' of porcellanids, which includes an overall change of carapace shape and reduction of the abdomen, has obscured the relationships with other anomurans. Porcellanidae constitutes in fact the sister lineage of a clade including all Galatheoidea with a squat lobster form (i.e., Munidopsidae, Munididae, and Galatheidae). The early splitting of Porcellanidae observed in the present study is in good agreement with morphological data. Characters that differentiate porcelain crabs from the squat lobsters include the shape of their third maxilliped, which is operculiform and without an epipod in Porcellanidae and pediform with epipod in Galatheidae, Munididae, and Munidopsidae. Also, the antennal peduncle has a different point of insertion in Porcellanidae than in other Galatheoidea, being laterally or posteriorly inserted instead of anterolaterally (Macpherson & Baba, 2011).

🖄 Springer

According to our results, Munidopsidae constitutes the earliest Galatheoidea lineage with a squat lobster form and can be differentiated from Galatheidae to Munididae by the lack of a flagellum on the exopod of the first maxilliped and the absence of striae on the dorsal surface of the carapace (Ahyong et al., 2010). The partial mitogenome sequence of *Munidopsis polymorpha* confirms earlier suggestions that Munidopsidae mitochondria might have been subject to an increased number of gene rearrangements (Yang & Yang, 2008; Tan et al., 2018). Protein-coding genes are usually present in both heavy and light chains of the mitochondrial genome, but they appear to be grouped in a single cluster in *M. polymorpha*. The abilities of deep-sea animals, like munidopsid squat lobsters, to tolerate extreme pressure and temperature conditions are due to pervasive adaptations at the biochemical level (Somero, 1992; Childress, 1995). For example, mitogenomes of some Alvinocarididae shrimp present conserved sequence blocks with non-canonical open reading frames which may be involved in adjusting mitochondrial energy metabolism to adapt to the hydrothermal environment (Sun et al., 2018). Recent transcriptomic data uncovered strong codon and amino acid usage biases in deep-sea polynoid worms, with preference for more positively charged amino acids (i.e., histidine and arginine) and less negatively charged amino acids (i.e., aspartic acid and glutamic acid) (Zhang et al., 2017b). Analyzing more Galatheoidea taxa from shallow and deep waters, particularly within the Munidopsidae, could help to infer the sequence of gene rearrangements and elucidating whether they are associated with environmental factors. The genus *Leiogalathea*, transferred to Munidopsidae after recent molecular analyses (Ahyong et al., 2009; Schnabel et al., 2011), is an ideal candidate for further studies, since it retains certain intermediate features between Munidopsidae and Galatheidae (Baba, 1969).

Morphological stasis and extreme convergence are commonly found among squat lobsters, which results in species complexes and cryptic taxa (Machordom & Macpherson, 2004; Cabezas et al., 2012; Palero et al., 2017), and renders morphological systematics particularly challenging. *Munida* and related genera were included within the Galatheidae for a long time (Baba et al., 2008) and Munididae was only recently established based on the trispinous or trifid frontal margin of the carapace and the ecological affinities

shared by most genera, usually occurring at outer shelf or slope depths (Ahyong et al., 2010). Members from both Galatheidae and Munididae families present eyes with a well-developed cornea, the antennal peduncle directed anteriorly or anterolaterally, a flagellum on the first maxilliped, and transverse striae or tubercles usually covering the carapace (Ahyong et al., 2010; Macpherson & Baba, 2011). Moreover, recent molecular studies suggest that Munididae could be paraphyletic (Bracken-Grissom et al., 2013) and the morphological character employed to define the family might constitute an evolutionary convergence without phylogenetic value. A taxonomic revision including more taxa and molecular markers, in addition to further studies on gene order evolution, is desirable to test the reciprocal monophyly of Munididae and Galatheidae. The phylogenetic analyses carried out here show that protein-coding mitochondrial genes are informative at the supra-family level. The reduction in sequencing costs presents an excellent opportunity to obtain mitogenomic data and increase our understanding on the evolution of this group of squat lobsters.

References

Abascal, F., R. Zardoya & D. Posada, 2005. ProtTest: selection of best-fit models of protein evolution. Bioinformatics 21: 2104–2105.

Ahyong, S. T., K. Baba, E. Macpherson & G. C. B. Poore, 2010. A new classification of the Galatheoidea (Crustacea: Decapoda: Anomura). Zootaxa 68: 57–68.

Ahyong, S. T., K. E. Schnabel & E. W. Maas, 2009. Anomuran phylogeny: new insights from molecular data. In Martin, J. W., K. A. Crandall & D. L. Felder (eds), Decapod Crustacean Phylogenetics. CRC Press, Boca Raton: 399–414.

Ahyong, S. T., K. E. Schnabel & E. Macpherson, 2011. Phylogeny and fossil record of marine squat lobsters. In Poore, G., S. Ahyong & J. Taylor (eds), The Biology of Squat Lobsters. CSIRO Publishing, Melbourne: 73–104.

Andrews S., 2010. FastQC: a quality control tool for high throughput sequence data. Babraham Bioinformatics.

Baba, K., E. Macpherson, G. C. B. Poore, S. T. Ahyong, A. Bermudez, P. Cabezas, C.-W. C. W. Lin, M. Nizinski, C. Rodrigues & K. E. Schnabel, 2008. Catalogue of squat lobsters of the world (Crustacea: Decapoda: Anomura—Families Chirostylidae, Galatheidae and Kiwaidae). Zootaxa 1905: 1–220.

Baba, K., S. T. Ahyong & K. E. Schnabel, 2018. Rediagnosis of the squat lobster genus Gastroptychus Caullery, 1896, with a new genus Sternostylus and a new family Sternostylidae (Crustacea: Decapoda: Anomura: Chirostyloidea). Zootaxa 4524: 77–86.

Baeza, J., 2011. Squat lobsters as symbionts and in chemo-autotrophic environments. In Poore, G., S. Ahyong & J. Taylor (eds), The Biology of Squat Lobsters. CSIRO Publishing, Melbourne: 249–270.

Bernt, M., A. Braband, B. Schierwater & P. F. Stadler, 2013. Genetic aspects of mitochondrial genome evolution. Molecular Phylogenetics and Evolution 69: 328–338.

Boore, J. L., 1999. Animal mitochondrial genomes. Nucleic Acids Research 27: 1767–1780.

Bracken-Grissom, H. D., M. E. Cannon, P. Cabezas, R. M. Feldmann, C. E. Schweitzer, S. T. Ahyong, D. L. Felder, R. Lemaitre & K. A. Crandall, 2013. A comprehensive and integrative reconstruction of evolutionary history for Anomura (Crustacea: Decapoda). BMC Evolutionary Biology 13: 128.

Bracken, H. D., A. Toon, D. L. Felder, J. W. Martin, M. Finley, J. Rasmussen, F. Palero & K. A. Crandall, 2009. The decapod tree of life: compiling the data and moving toward a consensus of decapod evolution. Arthropod Systematics and Phylogeny 67: 99–116.

Brandley, M. C., A. Schmitz & T. W. Reeder, 2005. Partitioned Bayesian analyses, partition choice, and the phylogenetic relationships of scincid lizards. Systematic Biology 54: 373–390.

Cabezas, P., I. Sanmartín, G. Paulay, E. Macpherson & A. Machordom, 2012. Deep under the sea: unraveling the evolutionary history of the deep-sea squat lobster Paramunida (Decapoda, Munididae). Evolution 66: 1878–1896.

Castresana, J., 2000. Selection of conserved blocks from multiple alignments for their use in phylogenetic analysis. Molecular Biology and Evolution 17: 540–552.

Childress, J. J., 1995. Are there physiological and biochemical adaptations of metabolism in deep-sea animals? Trends in Ecology & Evolution 10: 30–36.

Drummond, A. J. & A. Rambaut, 2007. BEAST: bayesian evolutionary analysis by sampling trees. BMC Evolutionary Biology 7: 214.

Drummond, A. J., M. A. Suchard, D. Xie & A. Rambaut, 2012. Bayesian phylogenetics with BEAUti and the BEAST 1.7. Molecular Biology and Evolution 29: 1969–1973.

Guindon, S., J. F. Dufayard, V. Lefort, M. Anisimova, W. Hordijk & O. Gascuel, 2010. New algorithms and methods to estimate maximum-likelihood phylogenies: assessing the performance of PhyML 3.0. Systematic Biology 59: 307–321.

Kass, E. R. & E. A. Raftery, 1995. Bayes factors. Journal of the American Statistical Association 90: 773–795.

Keiler, J., S. Richter & C. S. Wirkner, 2015. Evolutionary morphology of the organ systems in squat lobsters and porcelain crabs (Crustacea: Decapoda: Anomala): an insight into carcinization. Journal of Morphology 276: 1–21.

Lee, C. W., J. H. Song, G. S. Min & S. Kim, 2016. The complete mitochondrial genome of squat lobster, Munida gregaria (Anomura, Galatheoidea, Munididae). Mitochondrial DNA Part B: Resources 1: 204–206.

Machordom, A. & E. Macpherson, 2004. Rapid radiation and cryptic speciation in squat lobsters of the genus Munida (Crustacea, Decapoda) and related genera in the South West Pacific: molecular and morphological evidence. Molecular Phylogenetics and Evolution 33: 259–279.

Macpherson, E. & K. Baba, 2011. Taxonomy of squat lobsters. In Poore, G., S. T. Ahyong & J. Taylor (eds), The Biology of Squat Lobsters. CSIRO Publishing, Melbourne: 40–73.

Macpherson, E., W. Jones & M. Segonzac, 2005. A new squat lobster family of Galatheoidea (Crustacea, Decapoda, Anomura) from the hydrothermal vents of the Pacific-Antarctic Ridge. Zoosystema 27: 709–723.

Martin, J. W. & L. G. Abele, 1986. Phylogenetic realtionships of the genus Aegla (Decapoda: Anomura: Aeglidae), whith comments on anomuran phylogeny. Journal of Crustacean Biology 6: 576–616.

Martin, J. W. & G. E. Davis, 2001. An updated classification of the recent crustacea. Natural History Museum of Los Angeles County, Science Series 39: 1–124.

McLaughlin, P. A., R. Lemaitre & U. Sorhannus, 2007. Hermit crab phylogeny: a reappraisal and its "fall-out". Journal of Crustacean Biology 27: 97–115.

Milne-Edwards, A. & E. L. Bouvier, 1894. Considerations génerales sur la famille des Galathéidés. Annales des Sciences Naturelles, Zoologie 16: 191–327.

Morrison, C. L., A. W. Harvey, S. Lavery, K. Tieu, Y. Huang & C. W. Cunningham, 2002. Mitochondrial gene rearrangements confirm the parallel evolution of the crab—like form. Proceedings of the Royal Society of London, Part B 269: 345–350.

Osca, D., I. Irisarri, C. Todt, C. Grande & R. Zardoya, 2014. The complete mitochondrial genome of Scutopus ventrolineatus (Mollusca: Chaetodermomorpha) supports the Aculifera hypothesis. BMC Evolutionary Biology 14: 1–10.

Palero, F., K. A. Crandall, P. Abelló, E. Macpherson & M. Pascual, 2009. Phylogenetic relationships between spiny, slipper and coral lobsters (Crustacea, Decapoda, Achelata). Molecular Phylogenetics and Evolution 50: 152–162.

Palero, F., A. Robainas-Barcia, L. Corbari & E. Macpherson, 2017. Phylogeny and evolution of shallow-water squat lobsters (Decapoda, Galatheoidea) from the Indo-Pacific. Zoologica Scripta 46: 584–595.

Podsiadlowski, L., A. Braband, T. H. Struck, J. von Döhren & T. Bartolomaeus, 2009. Phylogeny and mitochondrial gene order variation in Lophotrochozoa in the light of new mitogenomic data from Nemertea. BMC Genomics 10: 1–14.

Springer

Roehrdanz, R., S. L. Cameron, M. Toutges & S. S. Wichmann, 2014. The complete mitochondrial genome of the tarnished plant bug, *Lygus lineolaris* (Heteroptera: Miridae). Mitochondrial DNA 1736: 1–2.

Roterman, C. N., W. K. Lee, X. Liu, R. Lin, X. Li & Y. J. Won, 2018. A new yeti crab phylogeny: vent origins with indications of regional extinction in the East Pacific. PLoS ONE 13: e0194696.

Schnabel, K. E., S. T. Ahyong & E. W. Maas, 2011. Galatheoidea are not monophyletic—molecular and morphological phylogeny of the squat lobsters (Decapoda: Anomura) with recognition of a new superfamily. Molecular Phylogenetics and Evolution 58: 157–168.

Shen, H., A. Braband & G. Scholtz, 2013. Mitogenomic analysis of decapod crustacean phylogeny corroborates traditional views on their relationships. Molecular Phylogenetics and Evolution 66: 776–789.

Somero, G. N., 1992. Biochemical ecology of deep-sea animals. Experientia 48: 537–543.

Sun, S., M. Hui, M. Wang & Z. Sha, 2018. The complete mitochondrial genome of the alvinocaridid shrimp *Shinkaicaris leurokolos* (Decapoda, Caridea): insight into the mitochondrial genetic basis of deep-sea hydrothermal vent adaptation in the shrimp. Comparative Biochemistry and Physiology - Part D: Genomics and Proteomics 25: 42–52.

Talavera, G. & J. Castresana, 2007. Improvement of phylogenies after removing divergent and ambiguously aligned blocks from protein sequence alignments. Systematic Biology 56: 564–577.

Tan, M. H., H. M. Gan, Y. P. Lee & C. M. Austin, 2016. The complete mitogenome of the porcelain crab *Petrolisthes haswelli* Miers, 1884 (Crustacea: Decapoda: Anomura). Mitochondrial DNA Part A: DNA mapping, sequencing, and analysis 27: 3983–3984.

Tan, M. H., H. M. Gan, Y. P. Lee, S. Linton, F. Grandjean, M. L. Bartholomei-Santos, A. D. Miller & C. M. Austin, 2018. ORDER within the chaos: insights into phylogenetic relationships within the Anomura (Crustacea: Decapoda) from mitochondrial sequences and gene order rearrangements. Molecular Phylogenetics and Evolution 127: 320–331.

Tsang, L. M., T. Y. Chan, S. T. Ahyong & K. H. Chu, 2011. Hermit to king, or hermit to all: multiple transitions to crab-like forms from hermit crab ancestors. Systematic Biology 60: 616–629.

Yamauchi, M., M. Miya & M. Nishida, 2002. Complete mitochondrial DNA sequence of the Japanese spiny lobster, *Panulirus japonicus* (Crustacea: Decapoda). Gene 295: 89–96.

Yang, J. S. & W. J. Yang, 2008. The complete mitochondrial genome sequence of the hydrothermal vent galatheid crab *Shinkaia crosnieri* (Crustacea: Decapoda: Anomura): a novel arrangement and incomplete tRNA suite. BMC Genomics 9: 1–13.

Zariquiey Álvarez, R., 1968. Crustáceos Decápodos Ibéricos. Investigación Pesquera, Barcelona.

Zerbino, D. R. & E. Birney, 2008. Velvet: algorithms for de novo short read assembly using de Bruijn graphs. Genome Research 18: 821–829.

Zhang, D., Y. Zhou, H. Cheng & C. Wang, 2017a. The complete mitochondrial genome of a yeti crab *Kiwa tyleri* Thatje, 2015 (Crustacea: Decapod: Anomura: Kiwaidae) from deep-sea hydrothermal vent. Mitochondrial DNA Part B 2: 141–142.

Zhang, Y., J. Sun, C. Chen, H. K. Watanabe, D. Feng, Y. Zhang, J. M. Y. Chiu, P. Y. Qian & J. W. Qiu, 2017b. Adaptation and evolution of deep-sea scale worms (Annelida: Polynoidae): insights from transcriptome comparison with a shallow-water species. Scientific Reports 7: 46205.

Moving forward by moving back: integrative systematics supports revival of old, and creation of new genera in the composite deep-sea taxon, *Munidopsis* Whiteaves, 1874

P. C. Rodríguez-Flores[1,2], E. Macpherson[1], K. Baba[3], S. T. Ahyong[4, 5] T.-Y Chan[6], C-W Lin[7] & A. Machordom[2]

[1] Centre d'Estudis Avançats de Blanes (CEAB-CSIC), C. acc. Cala Sant Francesc 14 17300 Blanes, Girona, Spain.
[2] Museo Nacional de Ciencias Naturales (MNCN-CSIC), José Gutiérrez Abascal, 2, 28006 Madrid, Spain.
[3] Kumamoto University, Faculty of Education, 2-40-1 Kurokami, Kumamoto 860-8555, Japan
[4] Australian Museum Research Institute, Australian Museum, 1 William Street, Sydney NSW 2010, Australia.
[5] School of Biological, Earth & Environmental Sciences, University of New South Wales NSW 2052, Australia.
[6] Institute of Marine Biology and Center of Excellence for the Oceans, National Taiwan Ocean University, Keelung 20224, Taiwan, R.O.C.
[7] National museum of marine biology & aquarium No. 2, Houwan Road, Checheng Township, Pingtung County, Taiwan, 944

ABSTRACT

Squat lobsters of the genus *Munidopsis* are exceptionally diverse (>260 species) and distributed worldwide. Although predominantly occurring on the outer slope, they also live in numerous other habitats, including anchialine caves and hydrothermal vent areas, at depths ranging from the surface of the sea to more than 5000 m. *Munidopsis* is highly diverse morphologically, with multiple genera or subgenera currently in its synonymy. Previous molecular studies indicate that the generic classification does not reflect the phylogeny of the genus, rendering the genus para-or polyphyletic and suggesting that some clades correspond to formerly recognized genera or subgenera. The present study, analyzing 75 species and four genes (COI, 16S, 28S and PEPCK), recovers the currently accepted genera, *Munidopsis* and *Galacantha*, as paraphyletic, together with around 20 clades with strong genetic divergences, commensurate with other squat lobster genera. Moreover, these clades can be morphologically diagnosable. Therefore, we advocate the restoration of the old genera and subgenera (*Anoplonotus*, *Bathyankrystes*, *Elasmonotus*, *Galathodes*, *Galathopsis*, *Orophorhynchus*), and recognition of new genera for several of the clades delineated herein. We identify the key morphological features diagnostic of the major clades and relate these characters to current taxonomy and classification. Finally, we discuss the morphological character evolution in a context of the timing and evolutionary history of Munidopsidae.

INTRODUCTION

The squat lobsters of the genus *Munidopsis* Whiteaves, 1874 are commonly found living on the continental slope, usually deeper than 500 m, and on the abyssal plain > 2000 m (Baba 2005; Baba et al. 2008, 2009). They are characterized by the loss of pigmentation and the eyes reduction and they are extremely diverse morphologically (Mayo 1974, Ayhong et al. 2011) (Fig. 1). The genus was established in 1874 by Whiteaves to include a new species (*M. curvirostra* Whiteaves, 1874) collected in the Gulf of St. Lawrence (NW Atlantic Ocean).
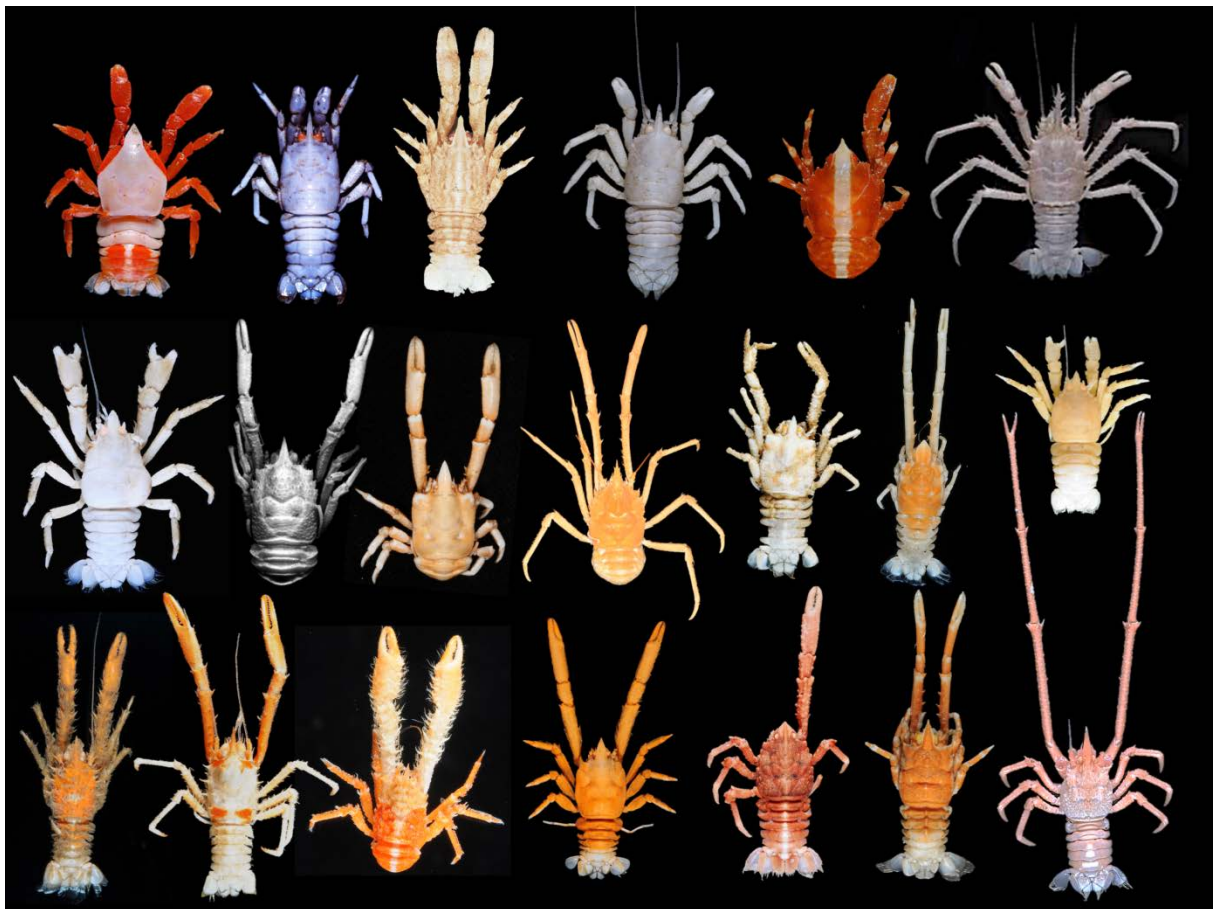
Figure 1. Morphological diversity of genus *Munidopsis*. Pictures credits: L. Corbari, T-Y. Chan.

The taxonomic status of the species belonging to this genus has received a remarkable improvement after the studies published in the last decades, demonstrating the existence of more than 250 species (e.g. Baba 1988, 2005, Ahyong & Poore 2004, Macpherson & Segonzac 2005, Osawa et al. 2006, 2008, Schnabel & Bruce 2006, Macpherson 2007, Jones & Macpherson 2007, Lin et al. 2007, Lin et al. 2013, Macpherson et al. 2016, Rodríguez-Flores et al. 2018, 2019a). However, the genus has a very old and complex taxonomic history, not yet resolved.

The high diversity of this genus was mentioned by A. Milne-Edwards (1880) in his preliminary report on the crustaceans collected by the "Blake" during the trawling expedition into the Caribbean Sea and Gulf of Mexico. This author described briefly four new genera to include 22 new species: *Galacantha* (2 species), *Galathodes* (10), *Elasmonotus* (4), and *Orophorhynchus* (6). Posteriorly, Smith (1883) described a new genus *Anoplonotus* to include a new species (*A. politus* Smith, 1883).

The study of the Anomura collected by the "Challenger" Expedition from around the world was published in a preliminary report (Henderson 1885). This author synonymized the genus *Galathodes* with *Munidopsis* and created a new subgenus *Galathopsis* for species intermediate between *Munidopsis* and *Elasmonotus*. In the final report of the expedition (Henderson 1888), the genus *Orophorhynchus* was synonymized with *Munidopsis* and *Galathopsis* and *Anoplonotus* were suppressed as synonyms of *Elasmonotus*. The genus *Galacantha* was maintained.

Faxon (1893), in his preliminary report of the eastern Pacific species, included *Galathodes, Orophorhynchus, Elasmonotus* and *Anoplonotus* in *Munidopsis*, but treated *Galacantha* separately. The final report of the "Albatross" was published by Faxon (1895) including the complete description and illustration of 18 new species. He placed the four genera of A. Milne-Edwards into the genus *Munidopsis*. However, Alcock (1901) agreed with Faxon that *Elasmonotus, Galathodes* and *Orophorhynchus* could not be separated into well-defined genera, distinct from *Munidopsis*. Furthermore, he considered all of them as subgenera of *Munidopsis* and created a new subgenus: *Bathyankyristes*. During these years, Ortmann (1892) described two new species from Japan: *Galacantha camelus* Ortmann, 1892 and *Munidopsis taurulus* Ortmann, 1892. Benedict (1902), in his important work on the galatheids, compiled a world list of species, with synonymies, remarks and distributions, and described 14 new species of *Munidopsis*. He included *Galathodes, Orophorhynchus* and *Elasmonotus* in *Munidopsis* (101 species), and maintained *Galacantha* (7 species) as a separate genus.

Finally, Chace (1939, 1942) working on the galatheids from the western Atlantic Ocean, discussed the problems encountered in subdividing the large genus into different genera or subgenera. He agreed in the existence of different groups, although the presence of intermediate species between them recommend the recognition of only one genus *Munidopsis*. More recently, after a large revision of specimens of *Munidopsis* from deep-waters of the Indian and Pacific Oceans, the genus *Galacantha* was reestablished based on having a set of constant characters (Macpherson 2007).

This complex taxonomic history led to the hypothesis that *Munidopsis* is a composite taxon, including multiple genera with independent evolutionary histories and trends. Integrating molecular phylogenetics with morphological data to determine taxon delimitations is the logical next step. Ahyong et al. (2011a) proposed a phylogenetic tree based on mitochondrial COI and

16S characters and around forty Munidopsidae taxa, suggesting that *Munidopsis* is para- or polyphyletic, indicating monophyly for some of the morphologically-recognized old groups, and recommending a broader study of Munidopsidae including more characters, more taxa and considering the fossil records. Thus, the current Family Munidopsidae classification includes the genera *Leiogalathea* Baba 1969, with 18 species lacking the general habitus of Munidopsidae (Rodríguez-Flores et al. 2019a), *Galacantha* with 11 species, characterized by the presence of a row of prominent spines in the midline of the carapace and the abdominal somites (Macpherson 2007), *Munidopsis* (> 260 species), and the monotypic genus *Shinkaia* Baba & Williams, 1998 exclusively found in hydrothermal vents.

A key stone to gain a better understanding of the taxonomy and evolution of this fascinating deep-sea squat lobsters will be to define congruent lineages sharing evolutionary histories and trends. This will reflect a more realistic picture of the diversification of the group. Therefore, our aim for this work is answering two taxonomic and phylogenetic questions: (1) to confirm that the genus *Munidopsis* is a complex of multiple genera with independent evolutionary histories, and (2) to approach how many of them can be morphologically and genetically delimited. For this purpose, we are reconstructing comprehensively the phylogenetic relationships of the species of the genus *Munidopsis,* including the most complete data set to date.

METHODOLOGY

The examined and sequenced material belong to biological collections of the Muséum national d'Histoire naturelle in Paris (MNHN), the National Taiwan Ocean University in Keelung (NTOU) and the Australian Museum in Sidney (AM). More than 300 specimens were studied. The specimens have been analyzed morphologically, rendering a matrix which includes 35 discrete morphological characters concerning telson, carapace and rostrum, peduncles and cornea, walking legs and chelipeds.

The methodology implemented to DNA extraction, amplification and sequencing follows recent studies (e.g., Cabezas et al. 2012, Rodríguez-Flores et al. 2017, 2019b). We have analyzed four molecular markers for this work, two mitochondrial (COI, 16S) and two nuclear markers (28S, PEPCK) for a first selection of 75 species including 139 specimens. Details of primers for these markers can be found in Rodríguez-Flores et al. (2019b).

The DNA sequences were revised using Sequencher v.4.8 (Gene Codes Corporation). Ribosomal gene sequences were aligned using MAFFT (Katoh et al. 2002), with a posterior manual correction in AliView (Larsson 2014). The matrix was built with all concatenated genes in PAUP v.4.0a (Swofford 2002) and included in the end a total of 2906 molecular characters for 139 specimens of 75 Munidopsidae species. Some phylogenetic analyses were conducted: Bayesian Inference (BI) and divergence time estimation of species clusters using a molecular

clock, with fossil calibration and molecular substitution rates obtained from decapods and related squat lobsters (Bracken-Grissom et al. 2013, Cabezas et al. 2012, Rodríguez-Flores et al. 2019c). We used other squat lobster no munidopsids as outgroups (Galatheidae Samouelle, 1819 and Munididae Ahyong, Baba, Macpherson & Poore, 2010).

To estimate the posterior probabilities in BI, two parallel runs of four Metropolis-coupled Markov chains Monte Carlo (MC3) were run for 10^7 generations, sampling every 1000 generations, in MrBayes v.3.2.1 (Ronquist & Huelsenbeck 2003).

Divergence time estimation was carried out in BEAST v2.5.1 (Bouckaert et al. 2014). An uncorrelated relaxed log normal clock model was implemented with values drawn from a distribution with a mean of 0.002 and a standard deviation of 0.1 for the 16S clock rate [obtained from Cabezas et al. (2012) and Rodríguez-Flores et al. (2019c)]. A birth–death model was used for the tree prior. Normal distributions were chosen as temporal priors for the calibration point (mean = 140, stdv = 20, offset = 1). This point was the node of all Munidopsidae genera excluding *Leiogalathea* (Bracken-Grissom et al. 2013, Rodríguez-Flores et al. 2019c): Munidopsinae. The Markov Chains Monte Carlo (MCMC) was run for 5×10^8 generations per run, and parameters were logged every 5×10^4 generations.

RESULTS AND DISCUSSION

According to our results (Figs. 2 and 3) the family Munidopsidae is strongly supported as monophyletic, as already shown by previous phylogenetic approaches (e.g., Ahyong et al. 2009, Schnabel et al. 2011, Ahyong et al. 2011, Bracken-Grissom et al. 2013). Munidopsidae is morphologically diagnosable by having the reduced or absent flagellum on maxilliped 1, which constitutes the chief synapomorphy, reduced eyes, usually the lack of pigmentation, and the common presence of tuberculate or squamate carapace instead of striate (Ahyong et al. 2010, 2011).

The present study, analyzing about a third of the *Munidopsis* species, with mitochondrial and nuclear partial genes, and morphological characters, recovers the currently accepted genera, *Munidopsis* Whiteaves, 1874 and *Galacantha* A. Milne Edwards, 1880, as non-monophyletic. These results again agree with previous phylogenetic reconstructions (Ahyong et al. 2009, 2011). The polyphyly of *Munidopsis* respect to *Galacantha* and *Shinkaia* Baba & Williams, 1998, led to reconsider all the proposed taxonomy for Munidopsidae. The uniqueness of *Shinkaia* and *Galacantha* from *Munidopsis* species, makes pointless to consider all the species as one single genus (*Munidopsis*) without breaking the compactness usually required to define a genus level taxa (diagnosis).

Moreover, tree topology (Fig. 2) recovered more than 20 highly divergent lineages with high Bayesian supports [posterior probability (pP) >0.95], although showing some unclear deep

phylogenetic relationships. Some of the highly supported clades correspond to previously recognized genera or subgenera (A. Milne-Edwards 1880, Smith 1883, Henderson 1885, Alcock 1901) and other would correspond to new genera.

We have followed specific criteria to delimit the existence of different genera: (1) a shared long independent evolutionary history, establishing monophyletic lineages conformed by their common ancestor and all their descendants, that consequently would share evolutionary trends; (2) the presence of synapomorphies in each lineage, as a particular combination of morphological characters, that consistently differ from other lineages. Likewise, such synapomorphies could be also ecological, related to the habitat (for instance lineages restricted to abyssal depths, or lineages restricted to hydrothermal vents); and (3) the existence of a congruence in the biogeographic patterns. These principles are largely extended in integrative taxonomy (Dayrat 2005).

Therefore, the recovered genus-level lineages are well supported also by a combination of morphological characters that are not shared by species from different lineages. We have restituted the previously synonymized genera names, when pertinent, and numbered the rest of them from 1 to 17 (Fig. 2). All of these genera can be differentiated by constant morphological characters (see Appendix). For instance, the Genus 1 [containing *M. abbreviata* (A. Milne Edwards, 1880) and *M. dentifalx* Osawa et al., 2007] is characterized by having a triangular rostrum, the second to fourth abdominal somites with a median spine and 10 telson plates; the genus *Anoplonotus* Smith, 1883, is characterized by having dactyli of walking legs unarmed and chelipeds at least twice of carapace length (Smith 1883, Ahyong et al. 2011a); the genus *Bathyankyristes* Alcock & Anderson, 1894, is characterized by having subchelate walking legs. The Genus 11 is characterized by having a distally trifid rostrum, dorsal surface of the carapace smooth, abdominal somites 2–3 with a median spine and 10 telson plates. The genus *Galathodes* A. Milne Edwards, 1880, is characterized by the abdomen spineless, the rostrum spiniform and tridentate and 7–8 telson plates. This genus would include several species, such as *Munidopsis serricornis* (Lovén, 1852) or *M. treis* Ahyong & Poore, 2004 (Ahyong et al. 2011a) being particularly diverse in comparison with others.

Interestingly, *Shinkaia cronieri* Baba & Williams, 1998, appeared clustered with *Munidopsis lentigo* Williams & Van Dover, 1983. Both lineages contain species exclusively linked to hydrothermal vents. They share the presence of a pad of setae in the chelipeds with an unknown function.

Munidopsis sensu stricto must be re-defined and it would be constituted by a few species with mainly an Atlantic distribution (e.g. *M. chuni* Balss, 1913 and *M. bispinata* Miyake & Baba, 1970), although there is at least one Indo-Pacific species, e.g. *M. scobina*. *Munidopsis* is characterized by having a styliform or acutely triangular rostrum and the presence of some median spines along the carapace and abdominal somites.
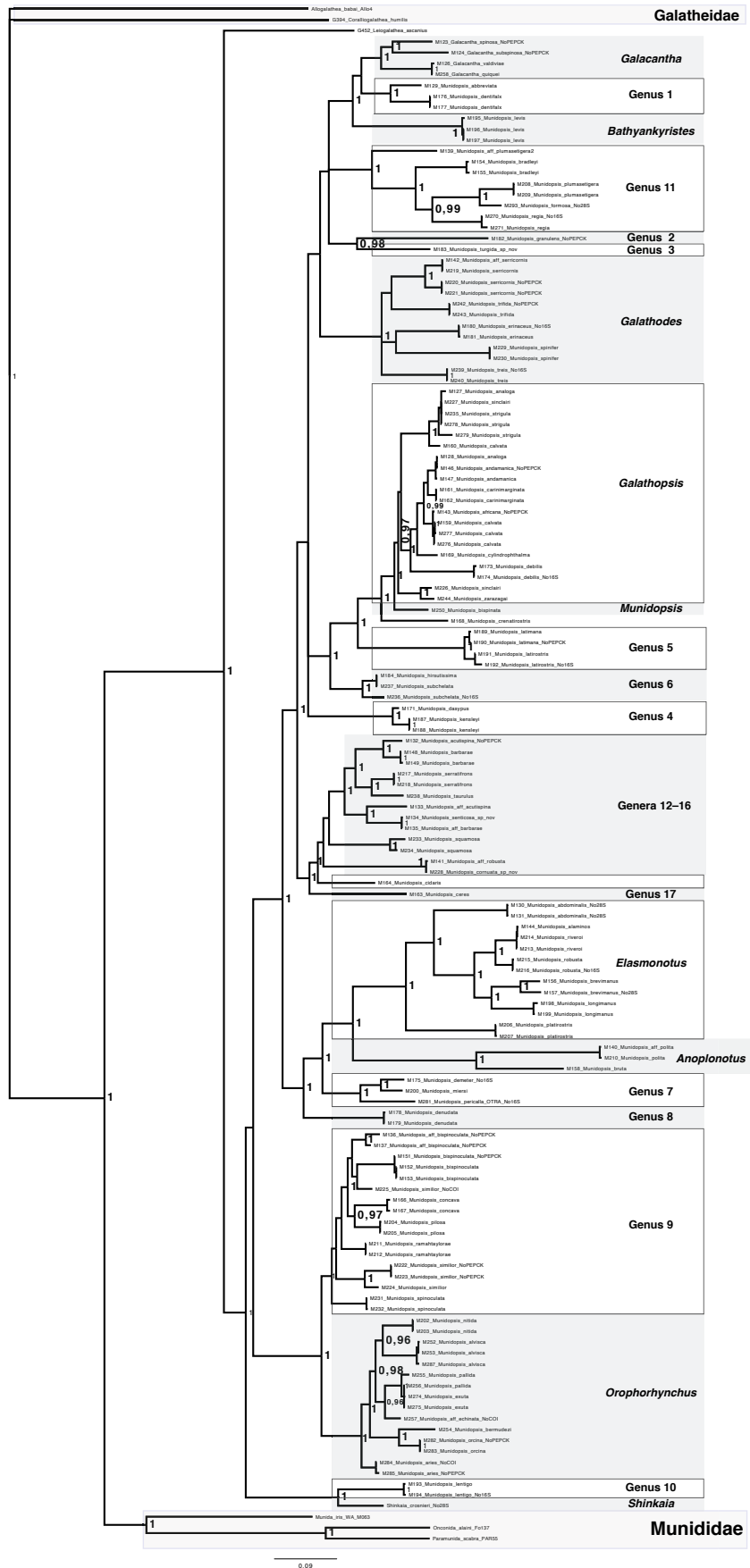
Figure 2. Phylogenetic tree based on concatenated nuclear and mitochondrial data (COI, 16S, 28S and PEPCK). Numbers above branches indicate Bayesian posterior probability (pP). Values of pP lower than 0.85 are not shown. Delimited genera are indicated with boxes.
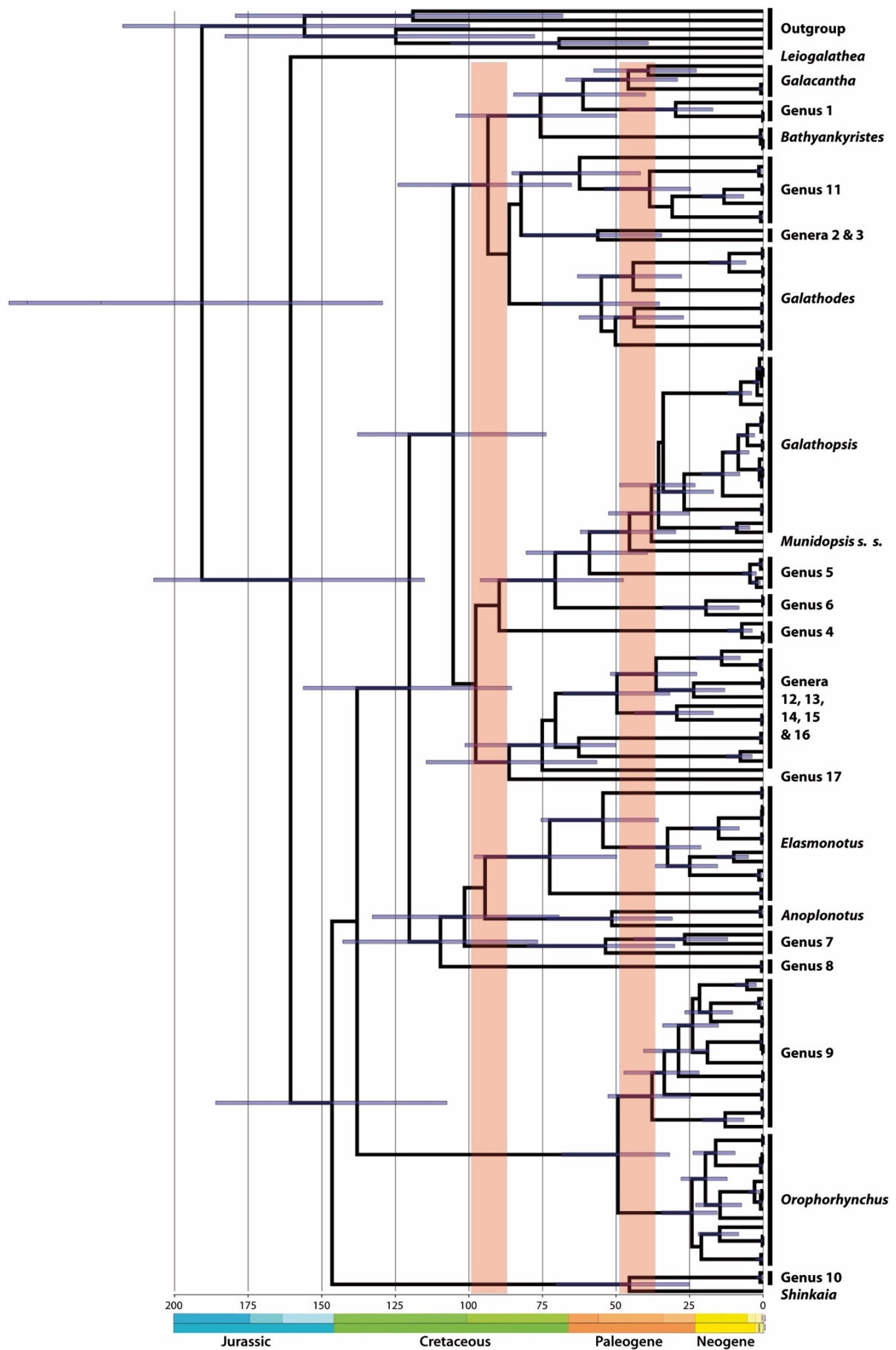
Figure 3. Chronogram showing 95% High Posterior Density credibility intervals for well supported recovered nodes (pP >0.9). Red areas indicate periods of intense cladogenesis. Delimited genera are indicated at branch tips.

Furthermore, *Orophorhynchus* A. Milne Edwards, 1880, is maybe the most remarkable group, since it includes the deepest, abyssal species: *Munidopsis petalorhyncha* Baba, 2005*, M. thieli* Türkay, 1975 or *M. parfaiti* (Filhol, 1885) appear at depths of more than 5000 meters; and on the other hand, the larger species [*M. aries* (A. Milne Edwards, 1880)] (Baba 2005, Baba et al. 2008). There are species in the *Orophorhynchus* group having similar morphology and yet vicariant distribution: for instance, *M. albatrossae* W.E. Pequegnat & L.H. Pequegnat, 1973 from the Pacific and *M. aries* from the Atlantic. In the other hand there are cosmopolitan species distributed worldwide, for instance, *M. antonii* (Filhol, 1884), *M. bairdii* (Smith, 1884) or *M. nitida* (A. Milne Edwards, 1880) among others. Our results (Figs. 1 and 2) together with previous studies (Jones & Macpherson 2007, Dong et al. 2019) revealed low genetic distances within this group, which might indicate recent speciation or slow evolutionary rates, and even cosmopolitan distribution for some species. Cosmopolitan distributions are frequently described for species living at abyssal depths (Rex et al. 1993, Schornikov 2005, McClain & Hardy 2010), supported by the inclusion of molecular characters in some cases. But cryptic species complexes or several species previously identified as a single morphospecies have also been identified (McClain & Hardy 2010). Thus, to answer whether there are cosmopolitan species in *Orophorhynchus* or represent species complexes, we should include more robust data.

According to our reconstructed chronogram the origin of Munidopsidae was placed in the Late Jurassic (Fig. 3), which is slightly younger respect to the appearance of first Munidopsidae fossil (*Paleomunidopsis* Van Straelen, 1925) in the Middle Jurassic. However, the first major radiation of the group, according to the emergence of many taxa in the fossil record, was placed in the Tithonian, Late Jurassic (Robins et al. 2013, 2015). Two main events of cladogenesis can be observed in our reconstruction, the most ancient placed in the Cretaceous and a more recent in the Paleogene, constituting the origin of the diversification of the defined genus-level lineages. All the recovered genus-level clades constituted ancient lineages with a common ancestor estimated with a minimum age between 50 to 40 million years old (Fig. 3); therefore, most of them have had a long independent evolutionary history.

Shinkaia + *M. lentigo* (Shinkainae) were the first offshoot within Munidopsinae (excluding *Leiogalathea* Baba, 1969). *Orophorhynchus* and Genus 9 species-group also constituted early-branching lineages, splitting from the rest of munidopsids during the Early Cretaceous. The ancestor of Shinkainae was estimated around 48 million years old. Therefore, the existence 40 million years ago of an extinct species of *Shinkaia* with morphology and habitat highly similar to the extant species (Schweitzer & Feldmann 2008) supports our estimated age. The sister genera *Orophorhynchus* and the Genus 9 species group had a split estimated at about 50 million years. Both lineages share a deeper bathymetric pattern, but are clearly distinguishable morphologically. They are characterized by the presence of ocular spines, but placed mesially (in the inner lateral side) in *Orophorhynchus* or medially in the Genus 9, and by the different length of the chelipeds.

A lot of fossil taxa are belonging to the family Munidopsidae (e.g., Ahyong et al. 2010, Ahyong et al. 2011b, Robins et al. 2013) and some of them can tentatively be assigned to some of the groups here defined. For instance, *Munidopsis canadiensis* Garassino, De Angeli & Ross 2015 can be morphologically assigned to the genus *Orophorhynchus* supporting our estimate Paleogene age. However, other fossils would require a deeper morphological study in order to assign them to the different groups, as the case of *M. palmuelleri* Hyžný, Gašparič, Robins & Schlögl 2014 or *M. lieskovensis* Hyžný & Schlögl, 2011 from the Tethys in the Miocene.

CONCLUSIONS

The polyphyly of *Munidopsis* was confirmed as well as the existence of more than 20 highly divergent and morphologically congruent lineages. Therefore, the former genus *Munidopsis* includes at least 20 genera. Some of these clades unequivocally correspond to previously recognized taxa, e.g. *Elasmonotus, Galathopsis, Galathodes, Orophorhynchus,* among others, while others likely represent new genera. The recovered genus-level clades are ancient lineages: the majority of these genera diversified in average 40–50 million years ago, which would imply independent and different evolutionary history and trends. *Munidopsis sensu* stricto contains a few species, mostly from the Atlantic Ocean. *Munidopsis lentigo* belongs to the subfamily Shinkainae; this taxon constitutes the earliest–branching lineage within Munidopsidae.

ACKNOWLEDGMENTS

REFERENCES

Ahyong, S. T., & Poore, G. C. (2004). Deep-water Galatheidae (Crustacea: Decapoda: Anomura) from southern and eastern Australia. Zootaxa, 472(1), 1–76.

Ahyong, S. T., Andreakis, N., & Taylor, J. (2011a). Mitochondrial phylogeny of the deep-sea squat lobsters, Munidopsidae (Galatheoidea). *Zoologischer Anzeiger-A Journal of Comparative Zoology*, 250(4), 367–377.

Ahyong, S. T., Baba, K., Macpherson, E., & Poore, G. C. (2010). A new classification of the Galatheoidea (Crustacea: Decapoda: Anomura). *Zootaxa*, 2676(1), 57–68.

Ahyong, S. T., Schnabel, K. E., & Maas, E. W. (2009). Anomuran phylogeny: new insights from molecular data. Decapod crustacean phylogenetics, 18, 16.

Ahyong, S. T., Schnabel, K. E., Macpherson, E. (2011b) Phylogeny and fossil record of marine squat lobsters. In: Poore, G. C. B., Ahyong, S. & Taylor, J. (eds.). *The Biology of Squat Lobsters.* Museum Victoria: CSIRO Publishing, 73–104.

Alcock, A. (1901). *A descriptive catalogue of the Indian deep-sea Crustacea Decapoda Macrura and Anaomala, in the Indian Museum*. Indian Museum, Calcuta, 290 pp.

Baba, K. (1969). Four new genera with their representatives and six new species of the Galatheidae in the collection of the Zoological Laboratory, Kyushu University, with redefinition of the genus *Galathea*. *Ohmu*, 2, 1–32.

Baba, K. (1988) Chirostylid and galatheid crustaceans (Decapoda: Anomura) of the „Albatross" Philippine Expedition, 1907–1910. *Researches on Crustacea, Special Number*, 2, 1–203.

Baba, K. (2005). Deep-sea chirostylid and galatheid crustaceans (Decapoda: Anomura) from the Indo-Pacific, with a list of species. *Galathea Report*, 20, 1–317.

Baba, K. & Williams, A. B. (1998). New Galatheoidea (Crustacea, Decapoda, Anomura) from hydrothermal systems in the West Pacific Ocean: Bismarck Archipelago and Okinawa Trough. *Zoosystema*, 20 (2), 143–156.

Baba, K., Macpherson, E., Lin, C. W., & Chan, T. Y. (2009). Crustacean Fauna of Taiwan. Squat Lobsters (Chirostylidae and Galatheidae). National Taiwan Ocean University, Keelung City, 312 pp.

Baba, K., Macpherson, E., Poore, G. C., Ahyong, S. T., Bermudez, A., Cabezas, P., Lin, C.-W., Nizinski, M., Rodrigues C., & Schnabel, K. E. (2008). Catalogue of squat lobsters of the world (Crustacea: Decapoda: Anomura—families Chirostylidae, Galatheidae and Kiwaidae). *Zootaxa*, 1905, 1–220.

Balss, H. (1913). Neue Galatheiden aus der Ausbeute der deutschen Tiefsee-Expedition 'Valdivia'. *Zoologischer Anzeiger*, 41, 221-226.

Benedict, J.E. (1902) Description of a new genus and forty six new species of crustaceans of the family Galatheidae with a list of the known marine species. Proceedings of the Biological Society of Washington, 26, 243–334.

Benedict, J.E. (1902) Description of a new genus and forty six new species of crustaceans of the family Galatheidae with a list of the known marine species. *Proceedings of the Biological Society of Washington*, 26, 243–334.

Bouckaert, R., Heled, J., Kühnert, D., Vaughan, T., Wu, C. H., Xie, D., ... & Drummond, A. J. (2014). BEAST 2: a software platform for Bayesian evolutionary analysis. *PLoS Comput Biol*, *10*(4), e1003537.

Bracken-Grissom, H. D., Cannon, M. E., Cabezas, P., Feldmann, R. M., Schweitzer, C. E., Ahyong, S. T., ... & Crandall, K. A. (2013). A comprehensive and integrative reconstruction of evolutionary history for Anomura (Crustacea: Decapoda). *BMC Evolutionary Biology*, *13*(1), 128.

Cabezas, P., Sanmartín, I., Paulay, G., Macpherson, E., & Machordom, A. (2012). Deep under the sea: unraveling the evolutionary history of the deep-sea squat lobster *Paramunida* (Decapoda, Munididae). *Evolution*, 66 (6), 1878–1896.

Chace, F.A. (1939) Reports on the scientific results of the first Atlantis Expedition to the West Indies, etc. Preliminary descriptions of one new genus and seventeen new species of decapod and stomatopod Crustacea. *Memorias de la Sociedad Cubana de Historia Natural*, 13, 31–54.

Chace, F.A. (1942). The Anomura Crustacea. I. Galatheidea. Reports of the scientific results of the Atlantis Expeditions to the West Indies, under the joint auspices of the University of Havana and Harvard University. *Torreia*, 11, 1–10.

Dayrat, B. (2005). Towards integrative taxonomy. *Biological Journal of the Linnean Society*, *85*(3), 407–417.

Dong, D., Xu, P., Li, X. Z., & Wang, C. (2019). *Munidopsis* species (Crustacea: Decapoda: Munidopsidae) from carcass falls in Weijia Guyot, West Pacific, with recognition of a new species based on integrative taxonomy. *PeerJ*, 7, e8089.

Faxon, W. (1893) Reports on the dredging operations off the west coast of Central America to the Galapagos, to the west coast of Mexico, and in the Gulf of California, in charge of Alexander Agassiz, carried on by the U.S. Fish Commission Steamer „Albatross", during 1891 ... VI. Preliminary descriptions of new species of Crustacea. Bulletin of the Museum of Comparative Zoology at Harvard College, 24, 149–220.

Faxon, W. (1895) XV. The stalk-eyed Crustacea. In: Reports on an exploration off the west coasts of Mexico, Central and South America, and off the Galapagos Islands, in charge of Alexander Agassiz, by the U.S. Fish Commission Steamer „Albatross" during 1891, Lieut.-Commander Z.L. Tanner, U.S.N., commanding. Memoirs of the Museum of Comparative Zoology at Harvard College, 18, 1–230.

Filhol, H. (1884) Explorations sous-marines. Voyage du Talisman. La Nature, Paris, 12, 119–122, 134–138, 147–151, 161–164, 182–186, 198–202, 230–234, 278–282, 326–330, 391–394.

Filhol, H. (1885) La vie au fond des mers. Les explorations sous-marines et les voyages du Travailleur et du Talisman. Masson, Paris, 303 pp

Henderson, J.R. (1885). Diagnoses of new species of Galatheidae collected during the "Challenger" expedition. *Annals and Magazine of Natural History* (ser. 5), 16, 407–421.

Hyžný, M., & Schloegl, J. (2011). An early Miocene deep-water decapod crustacean faunule from the Vienna Basin (Western Carpathians, Slovakia). *Palaeontology*, 54(2), 323–349.

Hyžný, M., Gašparič, R., Robins, C. M., & Schlögl, J. (2014). Miocene squat lobsters (Decapoda, Anomura, Galatheoidea) of the Central Paratethys–a review, with description of a new species of *Munidopsis. Scripta Geologica*, 147, 241.

Jones, W. J. & Macpherson, E. (2007). Molecular phylogeny of the East Pacific squat lobsters of the genus *Munidopsis* (Decapoda: Galatheidae) with the descriptions of seven new species. *Journal of Crustacean Biology*, 27(3), 477–501.

Katoh, K., Misawa, K., Kuma, K. I., & Miyata, T. (2002). MAFFT: a novel method for rapid multiple sequence alignment based on fast Fourier transform. *Nucleic acids research, 30*(14), 3059–3066.

Koelbel, C. (1892). Beitraege zur Kenntnis der Crustaceen der Canarischen Inseln.

Larsson, A. (2014). AliView: a fast and lightweight alignment viewer and editor for large datasets. *Bioinformatics*, *30*(22), 3276–3278.

Lin, C. W., Osawa, M., & Chan, T. Y. (2007). A new *Munidopsis* (Crustacea: Decapoda: Galatheidae) associated with gorgonian corals from the deep waters off Taiwan. *Proceedings of the Biological Society of Washington*, 120 (2), 167–175.

Lin, C. W., Tsuchida, S., Lin, S., Berndt, C., & Chan, T. Y. (2013). *Munidopsis lauensis* Baba & de Saint Laurent, 1992 (Decapoda, Anomura, Munidopsidae), a newly recorded squat lobster from a cold seep in Taiwan. *Zootaxa*, 3737(1), 92–96.

Lovén, S. (1852) De svenska arterna af slägtet Galathea. Ofversigt af Konglige Vetenskaps-Akademiens Förhandlingar, 9, 20–23.

Macpherson, E. (2007). Species of the genus *Munidopsis* Whiteaves, 1784 from the Indian and Pacific oceans and reestablishment of the genus *Galacantha* A. Milne-Edwards, 1880 (Crustacea, Decapoda, Galatheidae). *Zootaxa*, 1417, 1–135.

Macpherson, E., & Segonzac, M. (2005). Species of the genus *Munidopsis* (Crustacea, Decapoda, Galatheidae) from the deep Atlantic Ocean, including cold-seep and hydrothermal vent areas. *Zootaxa*, 1095 (3), 1–60.

Macpherson, E., Beuck, L., & Freiwald, A. (2016). Some species of *Munidopsis* from the Gulf of Mexico, Florida Straits and Caribbean Sea (Decapoda: Munidopsidae), with the description of two new species. *Zootaxa*, 4137 (3), 405–416.

Mayo, B. S. (1974). *The Systematics and Distribution of the Deep-sea Genus Munidopsis (crustacea Galatheidae) in the Western Atlantic Ocean*. Doctoral dissertation, Miami, University of Miami; 342pp.

McClain, C. R., & Hardy, S. M. (2010). The dynamics of biogeographic ranges in the deep sea. *Proceedings of the Royal Society B: Biological Sciences*, 277(1700), 3533–3546.

Milne Edwards, A. (1880). Reports on the results of dredging under the supervision of Alexander Agassiz, in the Gulf of Mexico and in the Caribbean Sea, etc. VIII. Études préliminaires sur les Crustacés. *Bulletin of the Museum of Comparative Zoology at Harvard College*, 8, 1–168.

Miyake, S.; Baba, K. (1970). The Crustacea Galatheidae from the tropical-subtropical region of West Africa, with a list of the known species. *Atlantide Report*, 11, 61-97.

Nyborg, T. G., Garassino, A., De Angeli, A., & Ross, R. L. (2015). A new squat lobster (Crustacea, Anomura, Munidopsidae) from the Middle-Late Eocene of British Columbia (Canada). *Neues Jahrbuch für Geologie und Paläontologie, Abhandlungen*, *275*(3), 357–361.

Ortmann, A. E. (1892). Die Decapoden-Krebse des Strassburger Museum, mit beson derer Berücksichtigung der von Herrn Dr. Doederlein bei Japan und bei den Liu-Kiu-Inseln gesammelten und zur Zeit im Strassburger Museum aufbe wahrten Formen.IV. Die Abtheilungen Galatheidea und Paguridea. Zoologisher Jahrbüchern. Abtheilung für Systematik, Geographie und Biologie der Thiere. 6: 241–326

Osawa, M., Lin, C. W., & Chan, T. Y. (2006). *Munidopsis* (Decapoda: Anomura: Galatheidae) from the abyssal depths of Taiwan, with description of one new species. *Journal of Crustacean Biology*, 26(3), 420–428.

Osawa, M., Lin, C. W., & Chan, T. Y. (2008). Species of *Galacantha* and *Munidopsis* (Crustacea: Decapoda: Anomura: Galatheidae) from the deep-waters off Taiwan, with the description of two new species. *Scientia Marina*, 72 (1), 37–57.

Osawa, M.; Lin, C.-W.; Chan, T.-Y. (2007). A new deep-sea squat lobster of the genus Munidopsis Whiteaves, 1874 (Crustacea: Decapoda: Anomura: Galatheidae) collected by the Panglao 2005 expedition to the Philippines. Raffles Bulletin of Zoology. Suppl. 16: 15-20

Pequegnat, W.E.; Pequegnat, L.H. (1973). *Munidopsis albatrossae*, a new species of deep-sea Galatheidae (Decapoda, Anomura) from the eastern Pacific Ocean. *Crustaceana*, 24(2), 163–168.

Rex, M. A., Stuart, C. T., Hessler, R. R., Allen, J. A., Sanders, H. L., & Wilson, G. D. (1993). Global-scale latitudinal patterns of species diversity in the deep-sea benthos. *Nature*, 365(6447), 636.

Robins, C. M., Feldmann, R. M., & Schweitzer, C. E. (2013). Nine new genera and 24 new species of the Munidopsidae (Decapoda: Anomura: Galatheoidea) from the Jurassic Ernstbrunn Limestone of Austria, and notes on fossil munidopsid classification. *Annalen des Naturhistorischen Museums in Wien. Serie A für Mineralogie und Petrographie, Geologie und Paläontologie, Anthropologie und Prähistorie*, 167–251.

Robins, C. M., Fraaije, R. H., Klompmaker, A. A., Van Bakel, B. W., & Jagt, J. W. (2015). New material and redescription of *Gastrosacus wetzleri* von Meyer, 1851 (Decapoda, Anomura, Galatheoidea) from the Late Jurassic of southern Germany. *Neues Jahrbuch für Geologie und Paläontologie-Abhandlungen*, 275 (1), 83–91.

Rodríguez-Flores, P. C., Macpherson, E., & Machordom, A. (2018). Three new species of squat lobsters of the genus *Munidopsis* Whiteaves, 1874, from Guadeloupe Island, Caribbean Sea (Crustacea, Decapoda, Munidopsidae). *Zootaxa*, 4422 (4), 569–580.

Rodríguez-Flores, P. C., Macpherson, E., & Machordom, A. (2019a). Revision of the squat lobsters of the genus *Leiogalathea* Baba, 1969 (Crustacea, Decapoda, Munidopsidae) with the description of 15 new species. *Zootaxa*, 4560 (2), 201–256.

Rodríguez-Flores, P. C., Machordom, A., Abelló, P., Cuesta, J. A., & Macpherson, E. (2019b). Species delimitation and multi-locus species tree solve an old taxonomic problem for European squat lobsters of the genus Munida Leach, 1820. *Marine Biodiversity, 49*(4), 1751–1773.

Rodríguez-Flores, P. C., Macpherson, E., Buckley, D., & Machordom, A. (2019c). High morphological similarity coupled with high genetic differentiation in new sympatric species of coral-reef squat lobsters (Crustacea: Decapoda: Galatheidae). *Zoological Journal of the Linnean Society, 185*(4), 984–1017.

Rodríguez-Flores, P.C., Machordom, A. & Macpherson E. (2017) Three new species of squat lobsters of the genus *Fennerogalathea* Baba, 1988 (Decapoda: Galatheidae) from the Pacific Ocean. *Zootaxa, 4276*, 46–60.

Ronquist, F., & Huelsenbeck, J. P. (2003). MrBayes 3: Bayesian phylogenetic inference under mixed models. Bioinformatics, 19(12), 1572-1574.

Schnabel, K. E., & Bruce, N. L. (2006). New records of Munidopsis (Crustacea: Anomura: Galatheidae) from New Zealand with description of two new species from a seamount and underwater canyon. *Zootaxa, 1172*(1), 49–67.

Schnabel, K. E., Cabezas, P., McCallum, A., Macpherson, E., Ahyong, S. T., & Baba, K. (2011). Worldwide distribution patterns of squat lobsters. In: Poore, G. C. B., Ahyong, S. & Taylor, J. (eds.). *The Biology of Squat Lobsters*. Museum Victoria: CSIRO Publishing, 149–182.

Schornikov, E. I. (2005). The question of cosmopolitanism in the deep-sea ostracod fauna: the example of the genus *Pedicythere*. *Hydrobiologia*, 538(1-3), 193–215.

Schweitzer, C. E., & Feldmann, R. M. (2008). New Eocene hydrocarbon seep decapod crustacean (Anomura: Galatheidae: Shinkainae) and its paleobiology. *Journal of Paleontology*, 82(5), 1021–1029.

Smith, S.I. (1883). Preliminary report on the Brachyura and Anomura dredged in deep water off the south coast of New England by the United States Fish Commission in 1880, 1881, and 1882. *Proceedings of the United States National Museum*, 6, 1–57.

Smith, S.I. (1884). Report on the decapod Crustacea of the Albatross dredgings off the east coast of the United States in 1883. In: *Report of the Commissioner for 1882. Part X. United States Commission of Fish and Fisheries*, Washington D.C., pp. 345-426; Pls. 1-10.

Swofford, D. L. (2002). PAUP: phylogenetic analysis using parsimony, version 4.0 b10.

Türkay, M. (1975) Decapoda Reptantia aus den Iberischen Tiefseebecken Auswertung der Fahrten 3 (1966) und 15 (1968) von F.S. „Meteor". "Meteor" Forschungs-Ergebnisse, Reihe D, 20, 66–70.

Van Straelen, V. (1925). Contribution à l'étude des crustacés décapodes de la Période Jurassique. *Mémoires de l'Académie Royale de Belgique,* (Science). *Pt. 4, ser. 2,* 7, 1–462, pls 1310.

Whiteaves, J. F. (1874). On recent deep Sea dredging operations in the Gulf of St. Lawrence. *American Journal of Science and Arts*, ser. 3, 7, 210–218.

Williams, A. B.; Van Dover, C. L. (1983). A new species of *Munidopsis* from submarine thermal vents of the east Pacific Rise at 21°N (Anomura: Galatheidae). *Proceedings of the Biological Society of Washington*, 96, 481–488.

APPENDIX: Morphological characterization of genera.

Genus 1

(e.g. *Munidopsis abbreviata, M. dentifalx*)

Carapace slightly longer than broad; dorsal surface smooth, unarmed, sometimes with small epigastric processes. Rostrum triangular, sometimes with small distal spines. Frontal margin slightly oblique, without delimited orbit, antennal spine absent. Lateral margins subparallel, anterolateral spine present, followed by several spines.

Sternum as long as wide, maximum width at sternites 6 and 7; sternite 3 moderately broad, twice wider than long, width about one–third that of sternite 4.

Abdominal somites 2–4 with median spine; telson with 10–12 plates. Eyes movable, without eye–spines, cornea globular, clearly shorter than remaining eyestalk. P1 longer than carapace, P2 not reaching or exceeding P1; P2–4 long and slender, P2 merus 5–6 times longer than wide and 0.6–0.7 carapace length; dactyli moderately curved; flexor margin with teeth decreasing in size proximally, each with slender corneous spine. Epipods on P1–3.

Genus 2

(e.g. *Munidopsis granulens*)

Carapace slightly longer than broad; dorsal surface densely granulated, with 2 epigastric protuberances. Rostrum spade–shaped, constricted between eyes. Frontal margin slightly oblique behind ocular peduncle, transverse between antenna and anterolateral angle. Lateral margins unarmed, subparallel, anterolateral corner rounded.

Sternum 1.2 times longer than wide, maximum width at sternites 6 to 7; sternite 3 moderately broad, twice wider than long, width about half that of sternite 4.

Abdomen unarmed; telson with 8 plates. Eyes small, fused to rostrum, without eye–spines, cornea globular, granulate overgrowths covering posteromesial part of corneae dorsally and ventrally. P1 longer than carapace, P2 not reaching end of P1; P2–4 stout, P2 merus 3 times longer than wide and 0.4 carapace length, dactyli moderately curved; flexor margin with teeth decreasing in size proximally, each with slender corneous spine. Epipods on P1–3.

Genus 3

(e.g. *Munidopsis turgida*)

Carapace slightly longer than broad; dorsal surface granulated; two thick epigastric processes; regions well delineated by deep furrows including distinct posterior cervical grooves. Rostrum

spade–shaped, lateral margins concave in proximal half between eyes. Frontal margin transverse behind ocular peduncle, then transverse toward anterolateral angle of carapace. Lateral margins straight and subparallel, unarmed, anterolateral corner rounded.

Sternum as long as broad, maximum width at sternites 6 and 7; sternite 3 moderately broad, 2.5 times wider than long, width about half that of sternite 4.

Abdomen unarmed, somites 2–4 each with elevated transverse ridge, each with 3 low processes; telson with 8 plates. Eyes with ocular peduncle fused to granular overgrowths covering mesial part of cornea. P1 longer than carapace, P2 not reaching or exceeding P1; P2–4 stout, P2 merus 3 times longer than wide and 0.8 carapace length; dactyli moderately curved; flexor margin with teeth decreasing in size proximally, each with slender corneous spine. Epipods on P1.

Genus 4

(e.g. *Munidopsis dasypus, M. kensleyi*)

Carapace longer than broad; dorsal surface smooth; without epigastric spines. Rostrum spiniform. Frontal margin slightly oblique behind ocular peduncle. Lateral margins subparallel unarmed or a few spines, anterolateral corner with spine.

Sternum 1.5 times longer than wide, maximum width at sternites 4 to 6; sternite 3 moderately broad, twice wider than long, width 0.4 times that of sternite 4.

Abdomen unarmed; telson with 8–9 plates. Eyes movable, long and slender, without eye–spines, cornea globular clearly smaller than remaining eyestalk. P1 longer than carapace, P2 not reaching or exceeding P1; P2–4 moderately stout, P2 merus 4 times longer than wide and 0.6 carapace length; dactyli moderately curved; flexor margin with teeth decreasing in size proximally, each with slender corneous spine. Epipods on P1.

Genus 5

(e.g. *Munidopsis latimana*)

Carapace slightly longer than broad; dorsal surface smooth, unarmed. Rostrum flat, broadly triangular, lateral borders unarmed. Frontal margin with delimited orbit and strong antennal spine. Lateral margins with anterolateral spine followed by 4–8 small but sharp spines on branchial region.

Sternum as long as wide, maximum width at sternites 6 and 7; sternite 3 moderately broad, three times wider than long, width about one–third that of sternite 4.

Abdomen unarmed; telson with 12 plates. Eyes movable, without eye–spines, cornea globular. P1 longer than carapace, P2 not reaching end of P1; P2–4 moderately stout, P2 merus 3 times longer than wide and 0.6 carapace length; dactyli moderately curved; flexor margin with teeth decreasing in size proximally, each with slender corneous spine. Epipods absent from pereiopods.

Genus 6

(e.g. *Munidopsis hirsutissima, M. subchaelata*).

Carapace quadrangular, dorsal surface without spines, moderately rugose; lateral margins straight. Rostrum triangular, short, lateral margins unarmed. Frontal margin slightly oblique, without delimited orbit, antennal spine sometimes present. Lateral margins slightly convex, anterolateral spine small followed by some small spines.

Sternum 1.3 times longer than wide, maximum width at sternites 4 to 6; sternite 3 moderately broad, twice wider than long, width about one–fourth that of sternite 4.

Abdomen unarmed; telson with 12 plates. Eyes movable, eye–spine present; cornea ventral in position, hardly visible in dorsal view. P1 longer than carapace, P2 not reaching or exceeding P1; P2–4 moderately stout, P2 merus 3 times longer than wide and 0.6 carapace length; dactyli moderately curved; flexor margin with teeth decreasing in size proximally, each with slender corneous spine. Epipods absent from pereiopods.

Genus 7

(e.g. *Munidopsis miersii*)

Carapace granulated, longer than broad; cervical groove distinct, regions well defined; gastric region with pair of large rounded epigastric processes. Rostrum broadly triangular, unarmed. Frontal margin concavely oblique behind ocular peduncle, leading to produced process behind antennal peduncle, then concavely transverse toward produced anterolateral corner of carapace. Lateral margins granulated, unarmed, except anterolateral spine.

Sternum as long as wide, maximum width at sternites 6 and 7; Sternite 3 moderately broad, 2.5 times wider than long, width about half that of sternite 4.

Abdomen unarmed; telson with 7 plates. Eyes movable, without eye–spine; cornea subglobular, as long as remaining eyestalk. P1 longer than carapace, P2 not reaching or exceeding P1; P2–4 moderately stout, P2 merus 3 times longer than wide and 0.5 carapace length; dactyli moderately curved; flexor margin with teeth decreasing in size proximally, each with slender corneous spine. Epipods absent from pereiopods.

Genus 8

(e.g. *Munidopsis denudata*)

Carapace slightly longer than broad; dorsal surface smooth, unarmed. Rostrum broadly triangular, unarmed. Frontal margin transverse, without antennal spine. Lateral margins unarmed, subparallel, anterolateral corner rounded.

Sternum as long as wide, maximum width at sternite 7; sternite 3 moderately broad, 3 times wider than long, width about half that of sternite 4.

Abdomen unarmed; telson with 7 plates. Eyes movable, without eye–spines, cornea globular, small, longer than remaining eyestalk. P1 longer than carapace, P2 not reaching or exceeding P1; P2–4 moderately stout, extensor margin of meri to propodi crested dactyli moderately curved; P2 merus 2.5 times longer than wide and 0.6 carapace length; flexor margin with teeth decreasing in size proximally, each with slender corneous spine. Epipods absent from pereiopods.

Genus 9

(e.g. *Munidopsis bispinoculata, M. concava, M. pilosa, M. ramahtaylorae, M. similior, M. spinoculata*).

Carapace slightly longer than broad; dorsal surface smooth. Rostrum narrowly triangular or lanceolate, sometimes concave in proximal third. Frontal margin slightly oblique with antennal spine. Lateral margins somewhat convex, anterolateral corner with small spine, sometimes followed by a few small spines.

Sternum as long as wide, maximum width at sternite 7; sternite 3 moderately broad, width about one fourth that of sternite 4; sternite 4 with some spines on anterior margin.

Abdomen unarmed; telson with 8 plates. Eyes fused to carapace, cornea well developed, main eye–spine on median part of cornea, continuous or not with eyestalk. P1 slightly longer than carapace, P2 reaching or exceeding P1; P2–4 stout, P2 merus 2.5–3.0 times as long as wide and 0.5–0.6 carapace length; dactyli moderately curved; flexor margin with teeth decreasing in size proximally, each with slender corneous spine. Epipods absent from pereiopods.

Genus 10

(e.g. *Munidopsis lentigo*)

Carapace longer than broad; dorsal surface smooth. Rostrum triangular. Frontal margin slightly oblique behind ocular peduncle, with antennal spine. Lateral subparallel, with anterolateral spine, followed by some spines.

Sternum 1.3 times longer than wide, maximum width at sternite 7; sternite 3 moderately broad, twice wider than long, width about half that of sternite 4.

Abdomen unarmed; telson with 9 plates. Eyes fixed, with strong flat median spine, cornea globular, small. P1 longer than carapace; chela with lenticular–shaped spot on ventral surface; P2 not reaching or exceeding P1; P2–4 stout, P2 merus 3.5 times as long as wide and 0.7 carapace length; dactyli moderately curved; flexor margin with teeth decreasing in size proximally, each with slender corneous spine. Epipods absent from pereiopods.

Genus 11

(e.g. *Munidopsis bradleyi, M. dudugera, M. plumasetigera, M. regia*)

Carapace slightly longer than broad; dorsal surface smooth, with two epigastric spines and often with some additional spines on gastric and cardiac regions. Rostrum trifid distally. Frontal margin oblique behind ocular peduncle, leading to antennal (outer orbital) spine. Lateral margins weakly convex and subparallel; anterolateral spine well developed, followed by some spines.

Sternum as long as wide, maximum width at sternites 6 to 7; sternite 3 moderately broad, 3 times wider than long, width about one–third that of sternite 4.

Abdomen with median spines on somites 2 and 3; telson with 10 plates. Eyes movable, cornea subglobular, unarmed, as wide as eyestalk. P1 longer than carapace, P2 not reaching or exceeding P1; P2–4 moderately slender, P2 merus 6 times longer than wide and 0.8 carapace length; dactyli moderately curved; flexor margin with teeth decreasing in size proximally, each with slender corneous spine. Epipods on P1 or absent from pereiopods.

Genera 12, 13, 14

(e.g. *Munidopsis acutispina, M. barbarae, M. senticosa, M. serratifrons, M. taurulus*)

Carapace as long as broad; dorsal surface covered with small spines. Rostrum trifid distally. Frontal margin concave behind ocular peduncle, leading to strong antennal (outer orbital) spine. Lateral margins weakly convex and subparallel; anterolateral spine well developed, followed by some spines.

Sternum as long as wide, maximum width at sternite 7; sternite 3 moderately broad, 4 times wider than long, width about one–fourth that of sternite 4.

Abdomen unarmed; telson with 7 plates. Eyes movable, cornea subglobular, with small median spine projecting from upper surface. P1 longer than carapace, P2 not reaching end of P1; P2–4 slender, P2 merus 5 times longer than wide and 0.8 carapace length; dactyli moderately curved; flexor margin with teeth decreasing in size proximally, each with slender corneous spine. Epipods absent from pereiopods.

Genus 15

(e.g. *Munidopsis squamosa*)

Carapace slightly longer than broad; dorsal surface heavily sculptured, with numerous tuberosities. Rostrum small, triangular. Frontal margin with 2 granulate projections lateral to rostrum between eyes, without antennal (outer orbital) spine. Lateral margins weakly convex and subparallel; anterolateral angle and lateral margins granulate, without spines.

Sternum as long as wide, maximum width at sternite 7; sternite 3 moderately broad, twice wider than long, width about half that of sternite 4.

Abdomen unarmed, somites smooth; telson with 8 plates. Eyes fused to carapace, cornea subglobular, mesial surface with large granulate projection. P1 longer than carapace, P2 not reaching end of P1; P2–4 stout, P2 merus 2.7 times longer than wide and 0.5 carapace length; dactyli moderately curved; flexor margin with teeth decreasing in size proximally, each with slender corneous spine. Epipods on P1–3.

Genus 16

(e.g. *Munidopsis corniculata*)

Carapace slightly longer than broad; dorsal surface smooth, with two epigastric spines and large median spine on gastric and cardiac regions. Rostrum narrowly triangular. Frontal margin transverse; antennal spine near anterolateral spine Lateral margins weakly convex and subparallel; anterolateral spine well developed, followed by several small spines.

Sternum as long as broad, maximum width at sternite 7. Sternite 3 moderately broad, 2.5 times wider than long, width about one–third that of sternite 4.

Abdomen with somites 2 4 each with elevated transverse ridge and one median thick spine; telson with 8 plates. Ocular peduncle fused; cornea subglobular, unarmed. P1 longer than carapace, P2 not reaching or exceeding P1; P2–4 moderately slender, P2 merus 3 times longer

than wide, 0.9 carapace length; dactyli moderately curved; flexor margin with teeth decreasing in size proximally, each with slender corneous spine. Epipods absent from pereiopods.

Genus 17

(e.g. *Munidopsis ceres*)

Carapace as long as broad; dorsal surface covered with tubercles and nearly devoid of setae; pair of large epigastric processes. Rostrum broad, apex blunt, lateral margins strongly concave in proximal half. Frontal margin concavely transverse behind ocular peduncle, leading to slightly produced process behind antennal peduncle. Lateral margins weakly convex and subparallel; anterolateral corner produced into a large spine followed by several large acute processes.

Sternum as long as wide, maximum width at sternite 7; sternite 3 moderately broad, about 3 times wider than long, width about one–third that of sternite 4.

Abdomen unarmed, with numerous small protuberances; telson with 8 plates. Eyes with ocular peduncle fixed, without eye–spine; surface with small protuberances; semicircular cornea cupped within broad–base eyestalk, broader than third antennal segment. P1 longer than carapace, P2 not reaching or exceeding P1; P2–4 stout, P2 merus longer than wide and 0.5 carapace length; dactyli moderately curved; flexor margin with teeth decreasing in size proximally, each with slender corneous spine. Epipods on P1–3.

***Anoplonotus* Smith, 1883**

Type species: *A. politus* Smith, 1883

Carapace as long as wide, dorsal surface smooth, granulate or tuberculate, without acute spines, with or without epigastric processes; areas distinct; gastric and cardiac region separated by deep depression; frontal margin without antennal spine; lateral margins unarmed. Rostrum triangular, narrow, not acute at tip, less than one–third carapace length.

Sternum 0.75 times longer than wide, maximum width at sternites 6 and 7; sternite 3 short and wide, width about half that of sternite 4.

Abdomen spineless; telson with 8 plates. Eyes small, movable, unarmed, cornea small, globular. Antennular article 1 swollen laterally. Basal part of each Mxp 3 separated by an appreciable gap. P1 long and slender, at least twice carapace length, longer than P2. P2–4 spineless, P2 merus 6 times longer than wide and 0.9 carapace length; dactyli curved, with flexor margin smooth, unarmed. Epipods absent from all pereiopods.

Bathyankyristes **Alcock & Anderson, 1894**

Potential type species: *B. levis* Alcock & Anderson, 1894

Carapace slightly longer than broad, dorsal surface smooth, slightly convex, without epigastric spines or processes; lateral margins subparallel, with several spines, areas distinct; frontal margin with slightly delimited orbit, transverse, without antennal spine. Rostrum narrowly triangular, acute at tip, less than one–half carapace length.

Sternum as long as wide, maximum width at sternite 7; sternite 3 short, at lower level than other sternites, 3 times longer than wide, width about one–third that of sternite 4.

Abdomen spineless; telson with 8 plates. Eyes small, movable, unarmed, cornea small, globular. Antennular article 1 swollen laterally. Basal part of each Mxp 3 not separated by an appreciable gap. P1 long and slender, at least twice carapace length, longer than P2. P2–4 propodi expanded distally, to form a subchela with the flexed dactylus; P2 merus 5.8 times longer than wide and 0.8 carapace length. Epipods absent from all pereiopods.

Elasmonotus **A. Milne Edwards, 1880**

Potential type species: *E. longimanus* A. Milne Edwards, 1880

Carapace longer than broad, dorsal surface smooth, granulate or minutely tuberculate, without acute spines slightly convex, with or without epigastric processes; lateral margins subparallel, unarmed, areas barely distinct, transverse grooves not distinct; frontal margin with delimited orbit, transverse, with/without antennal spine. Rostrum broadly triangular, not acute at tip, less than one–third carapace length.

Sternum 1.3 times longer than wide, maximum width at sternites 4 to 6; sternite 3 short and wide, width about half that of sternite 4.

Abdomen spineless, sometimes medially projected or with median spines; telson with 8–10 plates. Eyes small, movable, unarmed, cornea small, globular or slightly elongate. Antennular article 1 swollen laterally. Basal part of each Mxp 3 not separated by an appreciable gap. P1 long and slender, at least twice carapace length, longer than P2. P2 merus 3.4 times longer than wide and 0.5 carapace length; P2–4 dactyli curved, flexor margin with row of teeth and corneous spinules. Epipods absent from all pereiopods.

Galathodes **A. Milne Edwards, 1880**

Potential type species: *G. erinaceus* A. Milne Edwards, 1880

Carapace narrow, longer than wide; anterolateral angle spiniform. Rostrum spiniform, tridentate. Frontal margin without delimited orbit, antennal spine present; lateral margins slightly convex, subparallel, with anterolateral spine and followed with or without spines.

Sternum as long as wide, maximum width at sternites 6 and 7; sternite 3 half as long as wide, width about one–third that of sternite 4.

Abdomen spineless, sometimes medially projected or with spines; telson with 7–8 plates. Antennulae small, article 1 inflated. Eyes small, movable, corneae less wide than peduncle. P1 longer than P2. P2–4 dactyli with strong teeth along flexor margin; P2 merus 5–8 times longer than wide and 0.8 carapace length. Outer margin of endopodite of the uropods denticulated, or presenting spinulation. Sexual setae along lateral margins of telson well developed.

Galathopsis Henderson, 1885

Potential type species: *G. debilis* Henderson, 1885

Carapace slightly longer than broad; dorsal surface smooth. Rostrum triangular. Frontal margin slightly oblique behind ocular peduncle. Lateral margins unarmed, subparallel, anterolateral corner rounded or with small spine.

Sternum 1.67 times longer than wide, maximum width at sternites 4 to 6; sternite 3 moderately broad, twice wider than long, width about one–third that of sternite 4.

Abdomen unarmed; telson with 12 plates. Eyes movable, without eye–spines, cornea globular or longer than remaining eyestalk. P1 longer than carapace, P2 not reaching or exceeding P1; P2–4 stout, P2 merus 2.8 times longer than wide and 0.6 carapace length; dactyli moderately curved; flexor margin with teeth decreasing in size proximally, each with slender corneous spine. Epipods absent from pereiopods.

Munidopsis

Type species: *M. curvirostra* Whiteaves, 1874

Carapace slightly longer than broad; dorsal surface smooth, with pair of epigastric spines and some additional spines on gastric and cardiac regions. Rostrum styliform or acutely triangular, laterally unarmed. Frontal margin slightly without antennal spine. Lateral margins subparallel, with anterolateral spines, sometimes followed with several small spines.

Sternum slightly longer than wide, maximum width at sternite 7; sternite 3 moderately broad, 3 times wider than long, width about one–third that of sternite 4.

Abdomen with somites 2–3 (sometimes 4) armed with median spines; telson with 12 plates. Eyes movable, without eye–spines, cornea globular. P1 longer than carapace, P2 not reaching end of P1; P2–4 moderately slender, P2 merus 5.5–6.0 times longer than wide and 0.7–0.8 carapace length; dactyli moderately curved; flexor margin with teeth decreasing in size proximally, each with slender corneous spine. Epipods absent from pereiopods.

Orophorhynchus A. Milne Edwards, 1880

Potential type species: *O. aries* A. Milne Edwards, 1880

Carapace slightly longer than broad; dorsal surface usually smooth, with minute granules or scales, and sometimes with pair of epigastric spines. Rostrum triangular. Frontal margin slightly oblique, with or without antennal spine. Lateral margins subparallel, with anterolateral spine, followed with several spines.

Sternum as long as wide, maximum width at sternite 7; sternite 3 moderately broad, 3 times wider than long, width about one–third that of sternite 4.

Abdomen unarmed; telson with 8 plates. Eyes with very small corneae, fixed, sometimes below rostrum and with mesial eye–spine. P1 short and stout, shorter than P2. P2–4 stout, P2 merus 3.6 times longer than wide and 0.7 carapace length; dactyli moderately curved; flexor margin with teeth decreasing in size proximally, each with slender corneous spine. Epipods on P1 or absent from pereiopods.

Original Article

High morphological similarity coupled with high genetic differentiation in new sympatric species of coral-reef squat lobsters (Crustacea: Decapoda: Galatheidae)

PAULA C. RODRÍGUEZ-FLORES[1,2*], ENRIQUE MACPHERSON[2], DAVID BUCKLEY[1,2] AND ANNIE MACHORDOM[1]

[1]*Museo Nacional de Ciencias Naturales (MNCN-CSIC), José Gutiérrez Abascal 2, 28006 Madrid, Spain*
[2]*Centre d'Estudis Avançats de Blanes (CEAB-CSIC), C. d'Accés Cala Sant Francesc 14, 17300 Blanes, Spain*

The genus *Coralliogalathea* of the family Galatheidae is easily differentiated from other genera in the family by its small size, the presence of three to four small lateral teeth on the rostrum and the lack of the first pair of gonopods in males. The genus currently consists of only a single species, *Coralliogalathea humilis*, which lives in close association with corals in the Indian and Pacific Oceans. Using material collected across its distribution, we analysed both morphological characters and molecular markers (*COI*, 16S, 28S and 18S) to investigate cryptic species diversity, phylogenetic relationships within the genus, and the phylogenetic position of *Coralliogalathea* within the family Galatheidae. Our results support the validity of the two species previously synonymized with *C. humilis* and three new sympatric species found in Espiritu Santo, Vanuatu. Although these species are distinguishable only by subtle morphological characters, they are highly dissimilar genetically and constitute relatively deep divergent lineages. Furthermore, phylogenetic analyses of Galatheoidea resolved *Coralliogalathea* as an ancient genus within the superfamily that most probably diversified during the Eocene.

ADDITIONAL KEYWORDS: *Coralliogalathea* – molecular data – morphology – new species – squat lobsters.

INTRODUCTION

Revealing cryptic diversity is crucial to document global patterns of species richness and to understand the processes generating them (Hebert *et al.*, 2004; Bickford *et al.*, 2007). Cryptic species are defined by being (almost) indistinguishable morphologically (Bickford *et al.*, 2007). The use of molecular methods to analyse biodiversity has greatly increased the number of described cryptic species by providing a starting point for more detailed morphological comparisons (Lefébure *et al.*, 2006; Puillandre *et al.*, 2011).

Squat lobsters are an exceptionally diverse group of anomuran decapods (Baba *et al.*, 2008), in which high incidences of cryptic species are found (Macpherson & Machordom, 2005; Cabezas *et al.*, 2009). Although present in all the oceans and at all latitudes except in the high Antarctic, the highest level of taxonomic richness is found in the western-central Pacific Ocean (Baba *et al.*, 2008; Ahyong *et al.*, 2010), specifically in the Coral Sea and the Indo-Malay-Philippine archipelago (Schnabel *et al.*, 2011b; Cabezas *et al.*, 2012; Palero *et al.*, 2017). Much attention has been given recently to the taxonomy of squat lobsters (Schnabel *et al.*, 2011a), with numerous new species being described every year (e.*g*. Macpherson & Robainas-Barcia, 2015; McCallum *et al.*, 2016; Macpherson *et al.*, 2017; Rodríguez-Flores *et al.*, 2017, 2018). More than 1000 species of

squat lobsters are included in two superfamilies: Galatheoidea Samouelle, 1819 and Chirostyloidea Ortmann, 1892 (*sensu* Ahyong *et al.*, 2010). Molecular phylogenetic analyses have identified a large number of cryptic lineages, indicating an underestimation of the real diversity of the group, particularly for some Galatheoidea taxa with wide distributions that were previously considered monospecific or that included only a few species (Cabezas *et al.*, 2011; Macpherson & Robainas-Barcia, 2013; Rodríguez-Flores *et al.*, 2017). Furthermore, evolutionary studies of squat lobsters have revealed some decoupling of molecular and morphological variation in the group. Morphological stasis has been observed in several genera, including *Agononida*, *Allogalathea*, *Munida*, *Paramunida* and *Uroptychus* (see Machordom & Macpherson 2004; Cabezas *et al.*, 2009, 2011, 2012; Poore & Andreakis, 2011, 2012, 2014; Macpherson & Robainas-Barcia, 2013, 2015). In these cases, very low levels of morphological variation were linked to high genetic divergence among species. Therefore, to gain a better understanding of cryptic diversity in squat lobsters, morphological and molecular approaches are both required.

The squat lobster genus *Coralliogalathea* Baba & Javed, 1974 belongs to the family Galatheidae (*sensu* Ahyong *et al.*, 2010) and currently contains only one species, *Coralliogalathea humilis* (Nobili, 1905), which was originally described as *Galathea humilis* from specimens collected in Djibouti in the Gulf of Aden. The genus is easily differentiated from other taxa in the family by the following characters: a carapace with dorsal setiferous transverse striae and a lateral row of spines, a poorly defined cardiac region, a flattish triangular rostrum that is broad at its base and has three small lateral teeth, unarmed abdominal somites and the absence of the first pair of gonopods in males with the presence of the second pair (Baba *et al.*, 2009; Macpherson & Baba, 2011). Nobili (1906a) described a closely related species, *Galathea megalochira* Nobili, 1906, from Tuamotu Archipelago, French Polynesia. Later, Miyake (1953) described a third species, *Galathea tridentirostris*, from the Ryukyu Islands, Japan, as having a flattish rostrum and three small lateral teeth. Baba & Javed (1974) transferred these three species to a new genus, *Coralliogalathea*, and retained *C. humilis* as the only valid species, with a wide geographical distribution. A complete list of citations and synonymies for *C. humilis* is provided by Baba *et al.* (2008).

Several lines of evidence suggest, however, that *Coralliogalathea* could represent a complex of species. First, the genus has a wide distribution throughout several biogeographical areas in the Indo-West Pacific. *Coralliogalathea humilis*, a shallow-water species that usually inhabits coral reefs up to 30 m deep, has been reported from the eastern coast of Africa to French Polynesia and from Japan to Australia (Baba *et al.*, 2008; Dong & Li, 2010). Second, although considered monospecific, Baba & Javed (1974) observed some morphological variants within *Coralliogalathea*. Third, its habitat is linked to particular scleractinian coral species, suggesting that it might have a potentially restricted and fragmented distribution pattern that, if coupled with isolation, could lead to speciation. The taxonomic and evolutionary scenario for this genus, therefore, might be much more complex than previously thought. To explore this hypothesis, we assessed patterns of diversity within *Coralliogalathea* and identified the underlying processes that are likely to have generated such diversity. We first identified taxonomic units (species) using an integrative approach that combines morphological and molecular data. We then examined the phylogenetic relationships of the identified *Coralliogalathea* species and of this genus with other Galatheoidea genera. Finally, we estimated the divergence times of *Coralliogalathea* species and compared them with those of other squat lobster genera. Taken together, our analyses have provided insight into the geographical distribution and evolutionary history of *Coralliogalathea*.

We performed a morphological analysis on previously collected *Coralliogalathea* specimens (e.g. Richer de Forges *et al.*, 2013; Macpherson & Robainas-Barcia, 2015), together with the type material of *C. humilis* and *Galathea megalochira*. Unfortunately, the type material of the synonymized *G. tridentirostris* has been lost; therefore, we examined topotypic material from the Ryukyu Islands. An integrative approach that combines morphological and molecular data is considered more informative for species identification. Therefore, two mitochondrial markers, cytochrome *c* oxidase subunit I (*COI*) and 16S rRNA (16S), plus two nuclear markers, 28S rRNA (28S) and 18S rRNA (18S), were also analysed. These markers have been used previously to elucidate the systematic relationships and the existence of cryptic species of squat lobsters (Machordom & Macpherson, 2004; Cabezas *et al.*, 2011, 2012; Poore & Andreakis, 2012, 2014; Macpherson & Robainas-Barcia, 2013, 2015; Palero *et al.*, 2017; Rodríguez-Flores *et al.*, 2017).

MATERIAL AND METHODS

SAMPLING AND IDENTIFICATION

We carried out a morphological examination of > 150 specimens that were collected between 1976 and 2013 from the Indian and Pacific Oceans, mostly from Madagascar, the Red Sea, the Mariana Islands, Australia, Papua New Guinea, Vanuatu, New Caledonia and French Polynesia (see Richer de

Table 1. Material sequenced, including voucher codes, sampling localities, depths, expedition and available loci for each sample (X). GenBank accesion numbers: MK049280-MK049347

Species	Code	DNA Code	Locality	Depth (m)	Cruise	16S	*COI*	28S	18S
Coralliogalathea humilis	UF37403	G373	Saudi Arabia	7–8			X		
Coralliogalathea humilis	UF38080	G394	Saudi Arabia	7–8		X	X	X	
Coralliogalathea humilis	UF37156	G395	Saudi Arabia	1–2		X	X	X	X
Coralliogalathea joae **sp. nov.**	MNHN-IU-2013-17343	G392	Vanuatu	15–20	SANTO		X		
Coralliogalathea joae **sp. nov.**	MNHN-IU-2013-17346	G393	Vanuatu	6–43	SANTO	X	X		
Coralliogalathea joae **sp. nov.**	MNHN-IU-2013-17355	G399	Vanuatu	11	SANTO	X	X		
Coralliogalathea joae **sp. nov.**	MNHN-IU-2013-17352	G400	Vanuatu	5	SANTO	X	X		
Coralliogalathea joae **sp. nov.**	MNHN-IU-2014–2383	G426	Papua New Guinea	9–15	KAVIENG lagoon	X	X	X	
Coralliogalathea joae **sp. nov.**	MNHN-IU-2014-13592	G430	Papua New Guinea	15–17	KAVIENG lagoon	X	X	X	
Coralliogalathea megalochira	UF15778	G356	French Polynesia	1–2				X	
Coralliogalathea megalochira	UF15806	G357	French Polynesia	0		X	X	X	X
Coralliogalathea megalochira	UF16016	G396	French Polynesia	1–13		X	X	X	
Coralliogalathea megalochira	UF29148	G397	French Polynesia	0.5–2		X	X	X	X
Coralliogalathea minuta **sp. nov.**	MNHN-IU-2013-17329	G347	New Caledonia				X		
Coralliogalathea minuta **sp. nov.**	MNHN-IU-2013-17330	G348	New Caledonia	10		X	X		
Coralliogalathea minuta **sp. nov.**	MNHN-IU-2013-17380	G388	Lifou	Subtidal	LIFOU		X		
Coralliogalathea minuta **sp. nov.**	MNHN-IU-2013-17379	G389	Lifou	Subtidal	LIFOU	X	X	X	
Coralliogalathea minuta **sp. nov.**	MNHN-IU-2013-17378	G401	Lifou	Subtidal	LIFOU		X		
Coralliogalathea minuta **sp. nov.**	MNHN-IU-2013-17377	G402	Lifou	Subtidal	LIFOU		X		
Coralliogalathea minuta **sp. nov.**	MNHN-IU-2013-17369	G404	Vanuatu	2–4	SANTO	X	X	X	
Coralliogalathea parva **sp. nov.**	MNHN-IU-2013-17326	G349	Vanuatu	2	SANTO	X		X	
Coralliogalathea parva **sp. nov.**	MNHN-IU-2013-17383	G390	Vanuatu	5	SANTO	X	X	X	
Coralliogalathea parva **sp. nov.**	MNHN-IU-2013-17382	G391	Vanuatu	2–3	SANTO		X	X	
Coralliogalathea parva **sp. nov.**	UF26641	G398	Mariana Islands	0–4		X		X	
Coralliogalathea parva **sp. nov.**	MNHN-IU-2013-17386	G403	Vanuatu	15–20	SANTO	X		X	
Coralliogalathea tridentirostris	UF43051	G437	Philippines	3–6		X	X	X	X

Forges *et al.*, 2013; and http://musorstom.mnhn.fr/). The material is stored in several museums, including the Muséum national d'Histoire naturelle (MNHN) in Paris (France), the Senckenberg Museum (SMF) in Frankfurt (Germany), the Florida Museum of Natural History at the University of Florida (UF) in Gainesville (FL, USA) and the Zoological Laboratory at Kyushu University (ZLKU) in Fukuoka (Japan).

For the most part, we adopted the general terminology used by Baba *et al.* (2009, 2011) for morphological descriptions. The size of the carapace was determined by measuring the postorbital carapace length along the dorsal midline from the posterior margin of the orbit to the posterior margin of the carapace. Rostrum length was measured from the tip of the rostrum to between the lateral basal incisions; rostrum breadth was measured as the distance between the left and right lateral basal incisions. The ridges on the posterior branchial region, excluding the mid-transverse ridge and the posterior-most ridge anterior to the posterior margin of the carapace, were always counted along the lateral margins. Antennular and antennal segment length was measured along the lateral margins excluding distal spines; the width was measured at the midlength of each segment. The length of each pereiopod article was measured along its extensor margin (excluding distal spine), and the breadth was measured at its widest portion.

Abbreviations: **coll.**, collected; **F**, females; **G1**, first gonopod; **G2**, second gonopod; **juv.**, juvenile; **M**, males; **Mxp3**, third maxilliped; **ov.**, ovigerous; **P1**, first pereiopod (cheliped); **P2–4**, second to fourth pereiopods (first to third walking legs); and **Stn**, station.

DNA EXTRACTION, AMPLIFICATION AND SEQUENCING

In total, 26 specimens preserved in ethanol were used for molecular analyses (Table 1). DNA was extracted from one or two pereiopods per sample, depending on specimen size, using the Qiagen DNeasy Blood and Tissue Kit, following the manufacturer's instructions (Qiagen), including the RNAse step. Before DNA extraction, tissues were digested overnight with 180 μL of ATL buffer and 20 μL of proteinase K. Partial sequences for two mitochondrial and two nuclear genes were amplified for molecular analyses. The barcoding region of the protein-encoding gene *COI* (Folmer region) was amplified using primers LCO1490 (Folmer *et al.*, 1994) and COI-H (Machordom *et al.*, 2003). If these primers failed to amplify a product, the degenerated primers COI jgL and jgH (Geller *et al.*, 2013) were used. Ribosomal mitochondrial 16S and nuclear 28S and 18S fragments were amplified with the following primer pairs: 16SAR/BR (Palumbi *et al.*, 1991) or 16S-1471/16S-1472 (Crandall & Fitzpatrick, 1996), 28S BF/BR (Palero *et al.*, 2009) and 18S 1f/b2.9 (Whiting, 2002), respectively. Despite

multiple attempts, we could not amplify some of the gene fragments from several samples.

Polymerase chain reaction (PCR) amplifications were performed in a total volume of 25 μL consisting of 5 μL of 5× buffer solution with $MgCl_2$ (Bioline) and 0.2 mM of each deoxyribonucleotide triphosphate (dNTP), 0.2 μM of forward and reverse primers, 2–5 U of MyTaq polymerase (Bioline), 2–5 μL of DNA template (2–20 ng/μL) and distilled H_2O. The following thermal cycling conditions were used: an initial denaturation at 95 °C for 3 min, followed by 40 cycles of denaturation at 95 °C for 45–60 s, annealing at 42–50 °C for 1 min and extension at 72 °C for 45–60 s, plus a final extension at 72 °C for 10 min.

Amplified DNA products were purified using ExoSAP-IT (Affymetrix) or β-agarase (BioLabs) when multiple bands were observed on the agarose gels. Sequencing of both strands was performed by Secugen (Madrid) using BigDye Terminator and an ABI 3730 genetic analyser. New sequences were deposited in GenBank (Table 1).

SEQUENCE ALIGNMENT, MOLECULAR DIVERGENCES AND PHYLOGENETIC ANALYSES

The DNA sequences for each specimen and each gene region were trimmed and assembled using Sequencher v.4.8 (Gene Codes Corporation). Ribosomal gene sequences were aligned using MAFFT (Katoh *et al.*, 2002), followed by manual correction in the Se-Al alignment editor (http://tree.bio.ed.ac.uk/software/seal/). To check for pseudogenes, *COI* sequences were translated to look for stop codons using ExPASy (http://web.expasy.org/translate). We also calculated the number of non-synonymous substitutions per non-synonymous site (K_a), the number of synonymous substitutions per synonymous site (K_s) and the ratio K_a/K_s using DnaSP v.6 (Rozas *et al.*, 2017). To compare molecular divergences among species and specimens, uncorrected divergences (p) were calculated for each gene fragment (*COI*, 16S and 28S) in PAUP v.4.0a (build 156; Swofford, 2002).

Gene sampling was not homogeneous. Therefore, to avoid missing data and to use the best and most complete information available to address the different phylogenetic questions, three different datasets were analysed (Appendix 1). Phylogenetic relationships among identified *Coralliogalathea* species were determined with the concatenated matrix of *COI*, 16S and 28S gene fragments (referred to as matrix I). The mitochondrial and nuclear datasets were first analysed separately to test for congruence. *Galathea bolivari* Zariquiey Álvarez, 1950 and *Fennerogalathea ensifera* Rodríguez-Flores *et al.*, 2017 were selected as Galatheidae outgroups. To test the monophyly of *Coralliogalathea* and to explore its

phylogenetic relationship within Galatheoidea, we used a concatenated dataset composed of all four gene fragments (matrix II). Several Galatheoidea representatives used in previous phylogenetic studies were also included (see Appendix 2; Schnabel *et al.*, 2011a; Bracken-Grissom *et al.*, 2013), and *Calcinus laevimanus* (Randall, 1840) was chosen as an outgroup following phylogenetic hypotheses proposed for Anomura (Bracken-Grissom *et al.*, 2013). For divergence time estimations, we used the mitochondrial matrix (matrix III) because it included more *Coralliogalathea* individuals and covered more geographical locations. Several Galatheoidea genera used in previous studies were also included in this dataset to provide a relative time framework (Appendices 1 and 2; Cabezas *et al.*, 2012; Bracken-Grissom *et al.*, 2013; Davis *et al.*, 2016; Palero *et al.*, 2017).

Bayesian inference (BI), maximum likelihood (ML) and maximum parsimony (MP) methods were used to infer the phylogenetic relationships among *Coralliogalathea* species (using matrix I) and the phylogenetic position of the genus within Galatheoidea (using matrix II). In matrix II, the lengths of the 28S marker varied among taxa because some of the sequences obtained from GenBank were of different regions of the gene and hardly overlapped in the alignment. Therefore, we performed two different analyses (one with 28S and one without) to test for congruence. To estimate the posterior probabilities in BI, two parallel runs of four Metropolis-coupled Markov chains Monte Carlo (MC^3) were run for 10^7 generations, sampling every 1000 generations, in MrBayes v.3.2.1 (Ronquist & Huelsenbeck, 2003). Of the initial trees, 25% were discarded as burn-in. Convergence among chains was checked in Tracer v.1.5 (http://tree.bio.ed.ac.uk/software/tracer/) after first confirming that the standard deviation of split frequencies for each chain was < 0.01. The ML tree was obtained with PHYML v.3.1 (Guindon & Gascuel, 2003) using the best substitution model for the combined data estimated with jModelTest v.2.1.5 (Guindon & Gascuel, 2003; Darriba *et al.*, 2012) under the Bayesian information criterion (BIC). The MP analyses were implemented in PAUP* v.4.0a through a heuristic search with a tree bisection and reconnection (TBR) swapping algorithm with reconnection limit = 8, ten random stepwise additions and treating gaps as a new state ('fifth base'). Non-parametric bootstrap analyses for ML and MP were conducted with 1000 pseudoreplicates.

DIVERGENCE TIME ESTIMATION

Estimation of divergence times (using matrix III) was carried out in BEAST v.1.8.4 (Drummond *et al.*, 2012). We first calculated the best partition scheme fitting the data with PartitionFinder v.1.1.0 (Lanfear *et al.*, 2012), resulting in four partitions (16S and the three codon positions of *COI*) and the models specified in Appendix 1. We then ran and compared two analyses in BEAST. We compared two relaxed clock models to check for their influence on the time estimates and substitution rates retreived: a relaxed uncorrelated lognormal clock model, which allows different rates of evolution on each branch of the tree (Drummond *et al.*, 2006), and a random local clock model, which is more precise for abrupt and sustained rate shifts of rate evolution along clades of the tree (Crisp *et al.*, 2014). We estimated the marginal likelihood of each clock model with a stepping stone and path sampling analysis in BEAST and selected the best model with a Bayesian factor test in mtraceR in R (Pacioni *et al.*, 2015). The mtracerR routine estimates the log Bayes factors (logBF) of all the models of interest and compares them against the model with the highest marginal likekihood (the reference model). The models were then ranked according to their logBF (values of −2 or less indicate support for the reference model, and values of −6 or less indicate strong support) and their probability estimated.

For these analyses, we selected a birth–death tree prior and designated multiple calibration points. The time to the most recent common ancestor (TMRCA) of Galatheoidea was specified using the age of the oldest known Galatheoidea fossil, *Palaeomunidopsis moutieri* Van Straelen, 1925, from the Bathonian (Middle Jurassic) (Robins *et al.*, 2013). We also assigned time priors to several nodes taking into account dating analyses from published data, such as the TMRCA of Munidopsidae and Porcellanidae, and the TMRCA of the genus *Paramunida* (Cabezas *et al.*, 2012; Bracken-Grissom *et al.*, 2013; Davis *et al.*, 2016). We specified these priors following the criteria of Ho & Phillips (2009), who highly recommend using lognormal distributions to describe the probability density of temporal priors from palaeontological data. Finally, we used uninformative priors for the substitution rates (gamma distribution with an initial value of 0.01, a shape of 0.1 and a scale of 2.0). The Markov chains Monte Carlo (MCMC) were run for 9×10^8 generations per run, and all parameters were logged every 9×10^4 generations. The effective sample size (ESSs) of each parameter and the appropriate burn-in were determined in Tracer v.1.5. The results were synthesized and annotated in a maximum clade credibility (MCC) tree generated in Tree Annotator v.1.8.4 (Drummond & Rambaut, 2007) after 25% of the trees were discarded as burn-in. The resulting MCC trees from each analysis were visualized and edited in FigTree v.1.4.3 (Rambaut, 2012).

RESULTS

The morphological and molecular analyses of 158 and 26 *Coralliogalathea* specimens, respectively, from several

localities across the Indo-Pacific region have revealed six independent evolutionary lineages within this genus that are differentiated by subtle morphological characters and very high genetic divergence. Moreover, six distinct morphotypes could be identified from the low but consistent morphological variation observed among lineages; therefore, they were treated as species under the evolutionary species concept (see Discussion). Besides *C. humilis*, *C. megalochira* and *C. tridentirostris*, the two species previously synonymized with *C. humilis*, and three new species, *Coralliogalathea joae*, *Coralliogalathea minuta* and *Coralliogalathea parva* are herein considered valid species names.

SPECIES BOUNDARIES

COI and 16S fragments were successfully sequenced for 23 and 19 of the specimens, respectively (Table 1). Based on the resulting mitochondrial phylogeny, nuclear 18S and 28S fragments were then amplified and sequenced from selected representatives of each lineage to complement the mitochondrial dataset. However, 18S sequences were obtained for only three of the species; thus, this dataset was not used to set the species boundaries. The nuclear and mitochondrial datasets had similar phylogenetic signals when analysed separately; therefore, phylogenetic analyses of the *Coralliogalathea* species were performed using a concatenated matrix of these three genes (matrix I). This data matrix was composed of 12 specimens of *Coralliogalathea* and one specimen each of the Galatheidae species *F. ensifera* and *G. bolivari* as outgroups. The combined alignment was composed of 2144 characters, of which 1153 were constant, 436 were parsimony uninformative and 555 were parsimony informative. The alignment of only the mitochondrial fragments consisted of 1184 characters, of which 774 were constant, 107 were parsimony uninformative and 303 were parsimony informative. The 28S alignment contained a total of 960 characters, of which 379 were constant, 329 were parsimony uninformative and 252 were parsimony informative.

Translated *COI* sequences did not have indels or stop codons, indicating the absence of pseudogenes, and the K_a/K_s rates among the *Coralliogalathea* species ranged from 0.0154 to 0.0412. We observed two to nine nonsynonymous substitutions and 25–60 synonymous substitutions among the different *Coralliogalathea* species.

A high level of genetic divergence among analysed species was observed, with distances ranging from 6.7 to 15.1% for *COI* and from 2.4 to 15.7% for 16S. Intraspecific genetic distances varied from 0.3 to 1.3% and from 0.2 to 0.6% for *COI* and 16S, respectively (Table 2). Relatively high genetic distances for 28S (ranging from 5.8 to 7.9%) helped to discriminate

Table 2. Genetic distances (averages of the uncorrected p-distances) between species of *Coralliogalathea*, expressed as percentages

	Coralliogalathea humilis	*Coralliogalathea joae* **sp. nov.**	*Coralliogalathea megalochira*	*Coralliogalathea minuta* **sp. nov.**	*Coralliogalathea parva* **sp. nov.**	*Coralliogalathea tridentirostris*
Coralliogalathea humilis	**0.3, 0.2**	8.8	9.8	2.4	10.1	12.2
Coralliogalathea joae **sp. nov.**	13.5	**1.1, 0.2**	12.5	9.1	13.6	14.3
Coralliogalathea megalochira	13.4	13.6	**0.9, 0.2**	9.0	2.4	14.3
Coralliogalathea minuta **sp. nov.**	9.2	14.1	13.9	**0.5, 0.3**	10.0	12.0
Coralliogalathea parva **sp. nov.**	13.1	13.0	6.7	13.6	**1.3, 0.6**	15.7
Coralliogalathea tridentirostris	14.1	14.7	15.0	14.0	15.1	–

Numbers on the diagonal in bold indicate intraspecific distances for *COI* and 16S, respectively. Molecular divergences for *COI* sequences are indicated beneath the diagonal; numbers above the diagonal show distances for 16S.

some species, even after excluding gapped characters. However, low divergence for 28S was observed between *C. megalochira* and *C. parva* (0.4%) and between *C. humilis* and *C. minuta* (0.3%), similar to their mitochondrial divergences (Tables 2 and 3). Therefore, these two pairs represent the most closely related species in *Coralliogalathea*.

Consistent species-level differences were found in the morphological characters of the analysed species of *Coralliogalathea*, including the presence/absence of an additional spine on the rostrum margin, the shape/morphology of the rostrum, the shape (in terms of length/width) of the merus on pereiopods 2–4, the presence/absence of a ridge on abdominal somite 4 and the shape of the carapace in terms of length/width (see in the Description of each species).

PHYLOGENETIC RELATIONSHIPS AMONG
CORALLIOGALATHEA SPECIES

Our results revealed that *Coralliogalathea* is monophyletic and strongly supported. Trees obtained from the three different analyses (BI, ML and MP) had the same topology (Fig. 1). The partition analyses identified the following models of substitution for each codon of *COI* and each gene of matrix I: *COI1*, HKY+G; *COI2*, TrN+I; *COI3*, F81; 16S, K81uf+G; and 28S, TrNef+G. The most likely model for the concatenated dataset of all genes was TIM1+I+G (Appendix 1).

Each *Coralliogalathea* species appeared as a well-supported monophyletic taxon (posterior probability = 1, except for *C. megalochira*, and bootstrap supports 86–100). *Coralliogalathea megalochira* + *C. parva* grouped together with high support, as did the clade formed by *C. humilis* + *C. minuta*. Although phylogenetic analyses showed these two clades as sister groups, this relationship was not highly supported. These two groups formed a well-supported clade with *C. tridentirostris*, but the relationships among the three lineages remain unclear (Fig. 1). All of the analyses supported *C. joae* as the sister group to all other *Coralliogalathea* species. This species has an additional spine on the margin of the rostrum, a character that distinguishes it from the other species.

The topology of the 28S gene tree from matrix I (not shown) was very similar to the mitochondrial tree, although the species pairs *C. megalochira*–*C. parva* and *C. humilis*–*C. minuta* were not as well resolved.

Remarkably, the greatest genetic distances were found between pairs or groups of species that live in sympatry (*sensu* Rivas, 1964), specifically *C. joae*, *C. minuta* and *C. parva* from Espiritu Santo, Vanuatu (Table 2). The lowest genetic distances were observed between allopatric species with disjunct distributions (*sensu* Rivas, 1964); for instance, between *C. megalochira* from French Polynesia and *C. parva* from

Table 3. Genetic distances for the 28S (averages of uncorrected p-distances) between species of *Coralliogalathea*, expressed as percentages

	Coralliogalathea humilis	*Coralliogalathea joae* **sp. nov.**	*Coralliogalathea megalochira*	*Coralliogalathea minuta* **sp. nov.**	*Coralliogalathea parva* **sp. nov.**	*Coralliogalathea tridentirostris*
Coralliogalathea humilis	**0**					
Coralliogalathea joae **sp. nov.**	7.4	**0.6**				
Coralliogalathea megalochira	5.7	7.1	**0**			
Coralliogalathea minuta **sp. nov.**	0.3	7.5	5.5	**0.2**		
Coralliogalathea parva **sp. nov.**	6.1	7.5	0.4	5.8	**0.4**	
Coralliogalathea tridentirostris	7.6	7.6	6.9	7.9	7.2	–

Numbers in bold indicate intraspecific distances.
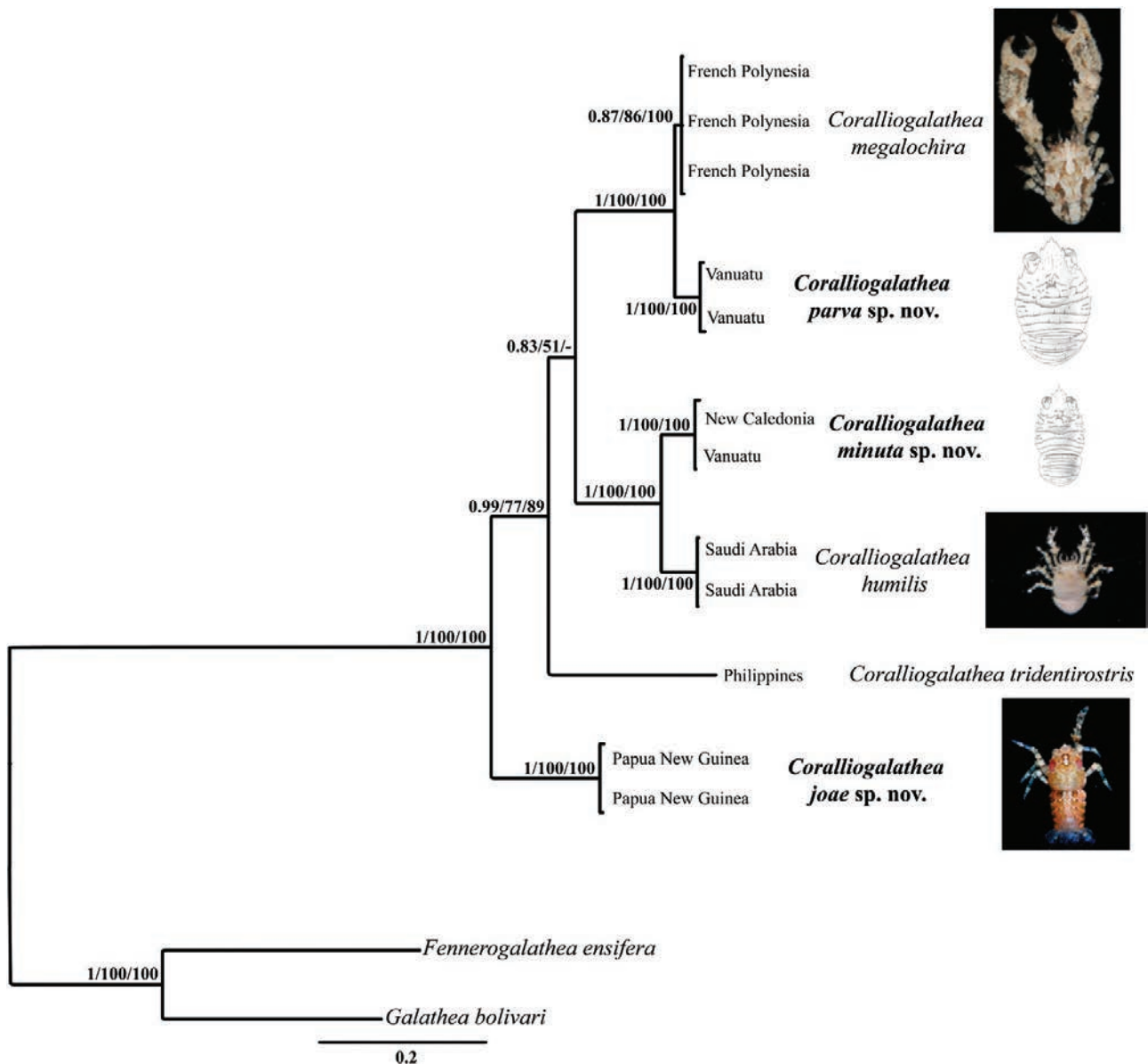
Figure 1. Phylogeny of *Coralliogalathea* species based on concatenated *COI*, 16S and 28S sequences and Bayesian inference (BI), maximum likelihood (ML) and maximum parsimony (MP) approaches. The tree was rooted with *Galathea bolivari* and *Fennerogalathea ensifera*. Numbers above branches indicate Bayesian posterior probabilities (BPPs) for BI analyses and the bootstrap branch supports for ML and MP analyses, respectively. Tip branch labels indicate the localities of the specimens of the different *Coralliogalathea* species.

Vanuatu (Coral Sea) and *C. humilis* from Djibouti (Gulf of Aden) and *C. minuta* from Vanuatu (Coral Sea) (Tables 2 and 3; Fig. 1).

PHYLOGENETIC PLACEMENT OF *CORALLIOGALATHEA*

The phylogenetic relationships of *Coralliogalathea* within Galatheoidea were inferred using a concatenated dataset of *COI*, 16S, 28S and 18S (matrix II: 23 taxa and 4438 characters, or 2380 characters when 28S sequences were excluded). Substitution models are summarized in Appendix 1. The genus *Coralliogalathea* is included in the family Galatheidae with high posterior probability and boostrap supports (Fig. 2), and as the sister lineage of a clade composed of three closely related Galatheidae genera, *Allogalathea* + *Fennerogalathea* + *Galathea*. The branch length of *Coralliogalathea* was relatively long compared with those of the other analysed genera.
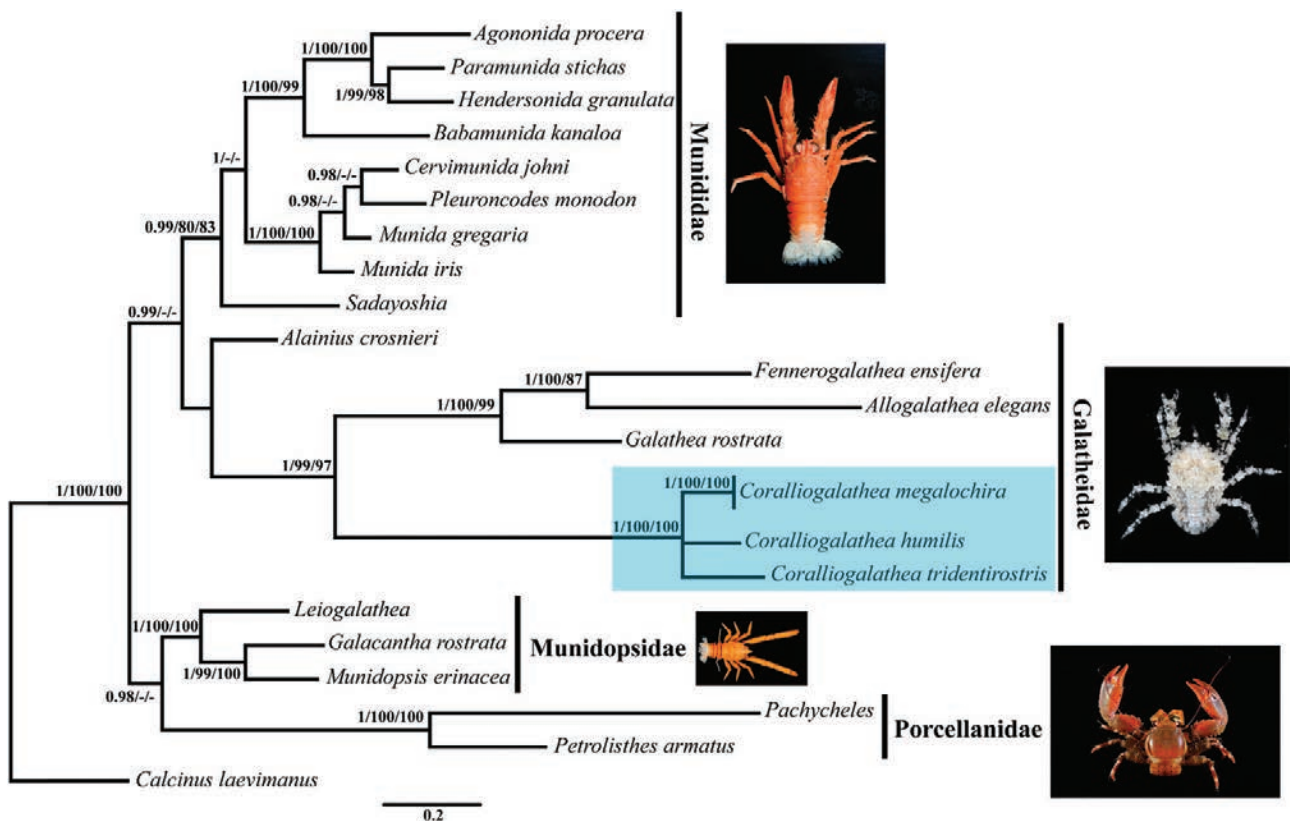
Figure 2. Bayesian phylogeny based on molecular concatenated data (*COI*, 16S, 28S and 18S) of Galatheoidea, including some *Coralliogalathea* species. Numbers above branches indicate Bayesian posterior probabilities (BPPs) and bootstrap branch supports for maximum likelihood (ML) and maximum parsimony (MP) analyses, respectively.

Alainius crosnieri clustered with the clade that included *Coralliogalathea* + (*Allogalathea* + *Fennerogalathea* + *Galathea*), suggesting that it is the most divergent lineage among the Galatheidae genera; however, this relationship was not supported.

Although it did not modify the basic topology of the tree, the addition of the 28S sequences to the matrix, which were originally included to explore the phylogenetic position of *Coralliogalathea*, was problematic owing to the lack of a fully overlapping alignment. The addition of 28S lowered the support of *Alainius* as sister genus to the other Galatheidae genera, although posterior probabilities and boostrap supports were similar for the other recovered clades. Our results support the family Galatheidae as the sister group of the family Munididae. However, the inclusion of more representatives of both families is needed to support this relationship more robustly.

DIVERGENCE TIME ESTIMATION

The matrix for dating analyses (matrix III) included 44 taxa, 16 of which were *Coralliogalathea* specimens,

and 1198 characters. Four partitions were considered: the first, second and third codon position in *COI* (GTR+I+G, F81+I and HKY+G, respectively) and 16S (TVM+I+G). According to the results of the Bayes factor test, the uncorrelated lognormal relaxed clock model was preferred over the random local clock model (log marginal likelihood −13 562.551 and −13 588.689, respectively; logBF = −52.276; p = 1). The resulting MCC tree showed a topology similar to the one recovered in the phylogenetic analyses (Fig. 2), although almost all of the depicted basal relationships were not supported (Fig. 3). Time estimations for unresolved nodes (posterior probability < 0.9) were not considered (Fig. 3). According to our estimations, *Coralliogalathea* emerged earlier than most of the squat lobster genera of Galatheoidea analysed [most recent common ancestor (MRCA) of *Coralliogalathea*, 48 Mya; with a 95% Highest Posterior Density interval (HPD$_{95}$) of 32–68 Mya], well before the emergence of the related genera *Lauriea* (MRCA, 19 Mya; HPD$_{95}$ = 11–30 Mya), *Paramunida* + *Hendersonida* (MRCA, 32 Mya; HPD$_{95}$ = 29–35 Mya) and *Raymunida* (MRCA, 24 Mya; HPD$_{95}$ = 11–43 Mya). *Sadayoshia* (MRCA, 60 Mya;
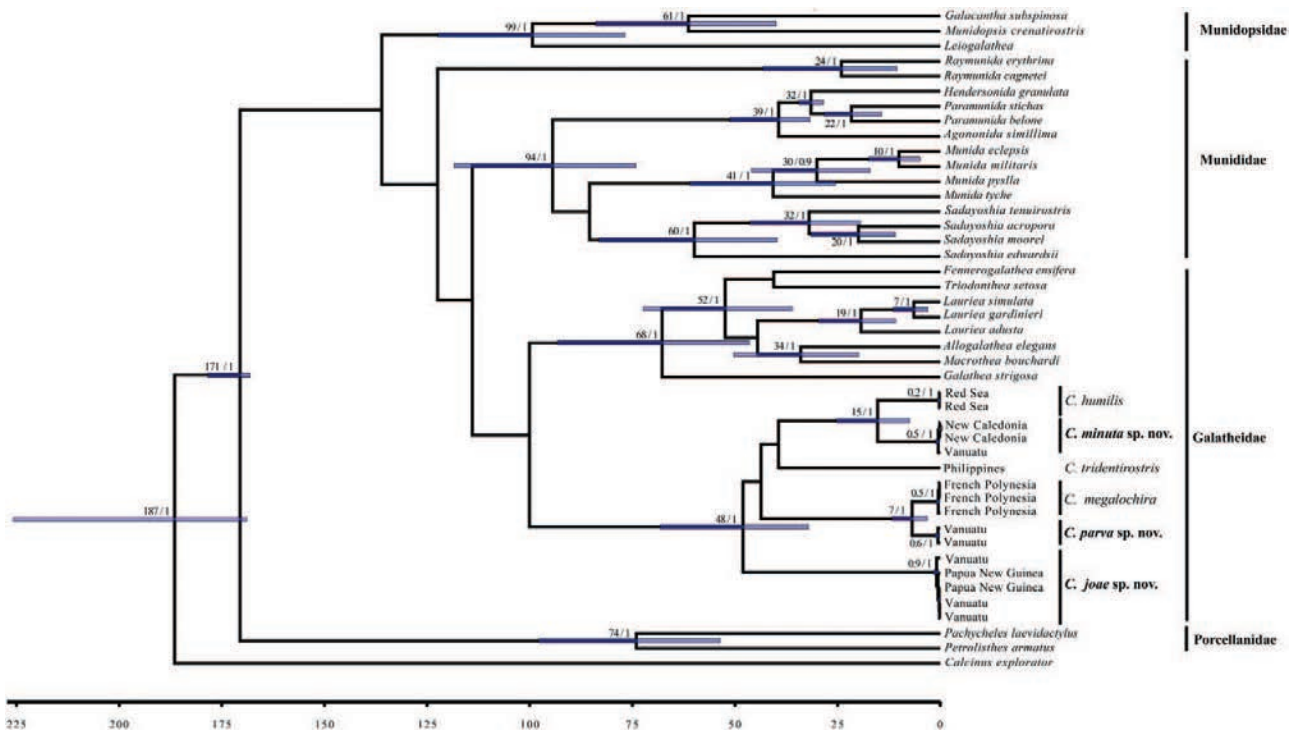
Figure 3. Calibrated phylogenetic tree based on the mitochondrial genes *COI* and 16S of the *Coralliogalathea* species and related genera of Galatheoidea. Numbers above branches indicate time to most recent common ancestor (TMRCA) estimation (median dates) and posterior probabilities. Tip branch labels for *Coralliogalathea* species indicate the localities of the specimens.

HPD$_{95}$ = 40–83 Mya) seems to have emerged before the diversification of *Coralliogalathea*. Although cladogenesis events that originated *Coralliogalathea* lineages were not well supported, our analyses revealed highly divergent mitochondrial lineages with deep relationships. Our estimations supported the dating of two diversification events that followed the emergence of the genus *Coralliogalathea*. The clade formed of the sister species *C. humilis* + *C. minuta* appeared during the Miocene (MRCA, 15 Mya; HPD$_{95}$ = 8–25 Mya), followed by the lineage composed of *C. megalochira* + *C. parva* in a more recent event (MRCA, 7 Mya; HPD$_{95}$ = 3–12 Mya). Interestingly, diversification of *Coralliogalathea* began before that of some distinct Galatheidae genera (e.g. MRCA *Macrothea*–*Allogalathea*: 34 Mya; HPD$_{95}$ = 20–50 Mya).

SYSTEMATIC ACCOUNT

FAMILY GALATHEIDAE SAMOUELLE, 1819

GENUS *CORALLIOGALATHEA* BABA & JAVED, 1974

Coralliogalathea Baba & Javed, 1974: 61 [gender: feminine]. – Baba, 2005: 67 [key]. – Baba *et al.*, 2008: 59 [synonymies]. – Macpherson & Baba, 2011: 53.

Type species: Galathea humilis Nobili, 1905, by monotypy.

Diagnosis: Carapace dorsally unarmed with transverse striae, laterally with row of spines. Transverse ridges with numerous short fine setae and some thick plumose setae. Cardiac region poorly defined. Rostrum flattish triangular, broad at base, with three or four small lateral teeth. Abdominal somites unarmed. Telson subdivision incomplete. Sternite 3 anteriorly produced. Eyestalks short; cornea somewhat dilated and well pigmented. Antennular article 1 globular, with three distal spines, distodorsal, distolateral and distomesial. Article 1 of antennal peduncle with well-developed distomesial spine; articles 2–3 unarmed. Mxp3 ischium triangular in cross-section; merus shorter than ischium, armed with spines on flexor margin. P1 relatively short and spinose, with some finely setiferous scales, with scattered long, thick, non-plumose setae. P2–4 moderately short, with row of spines on extensor crests of meri and carpi; flexor margin of dactylus with row of distinct diminishing teeth, each bearing stiff corneous seta, ultimate tooth usually prominent, epipods absent on pereiopods. G1 absent; G2 present.

KEY TO SPECIES OF THE GENUS *CORALLIOGALATHEA* IN THE INDIAN AND PACIFIC OCEANS

1. Rostrum with four lateral teeth .... ***C. joae* sp. nov.**
   Rostrum with three lateral teeth 2
2. Rostrum clearly wider (measured between proximal spines) than long (measured between proximal spines and tip of rostrum) .... *C. tridentirostris* (Miyake, 1953)
   Rostrum as long as or longer than wide 3
3. Fourth abdominal somite smooth, without transverse stria behind anterior ridge, at most minute setose scales. Third sternite wider than long. Metagastric ridge usually uninterrupted … *C. humilis* (Nobili, 1905)
   Fourth abdominal somite with transverse stria behind anterior ridge. Third sternite longer than, or as long as, wide. Metagastric ridge usually medially interrupted 4
4. Rostrum lanceolate. Carapace slightly shorter than wide or as long as wide .... ***C. minuta* sp. nov.**
   Rostrum spatulate. Carapace clearly wider (≥ 1.2 times) than long 5
5. Lateral margin of rostrum between proximal and median spines clearly convex. P2–3 propodi 5.0–6.5 times as long as broad .... ***C. parva* sp. nov.**
   Lateral margin of rostrum between proximal and median spines straight. P2–3 propodi 4.0–4.5 times as long as broad .... *C. megalochira* (Nobili, 1906)

CORALLIOGALATHEA HUMILIS (NOBILI, 1905)

(FIGS 4, 5A, B)

Galathea humilis Nobili, 1905: 397. – Nobili, 1906a: 124, pl. 8, fig. 4. – Doflein & Balss, 1913: 169 [list]. – Lewinsohn, 1969: 117, fig. 22.

Coralliogalathea humilis (Nobili, 1905): Baba & Javed, 1974: 62. – Tirmizi & Javed, 1993: 37, fig. 16.

Material examined
Syntypes: Red Sea. Djibouti, H. Coutiere, collected, 1897: three M, 1.9–2.0 mm, two ov. F, 2.1–2.3 mm (MNHN-IU-2013-17324).

Red Sea. Saudi Arabia. Farasan Banks, Dolphen Lagoon, 19.0053°N, 40.1482°E, 1–7 m, 4 March 2013: one ov. F, 2.0 mm (UF36151). – Farasan Banks, Marca Is., 18.2206°N, 41°3244°E, 5–15 m, 6 March 2013: one ov. F, 2.1 mm (UF36158). – Farasan Is., Zahrat Durakah, 16.8359°N, 42.3063°E, 2–6 m, 11 March 2013: one M, 1.6 mm (UF37026). – Al Lith, 20.1672°N, 40.2233°E, 1–2 m, 21 March 2013: one ov. F, 2.1 mm (UF37156). – off Thuwai, Abu Shosha Reef, 22.2044°N, 39.047°E, 7–8 m, 23 March 2013: three M, 1.4–1.6 mm (UF37403). – Jaz'air, 27.6384°N, 35.3062°E, 10 m, 27 September 2013: one ov. F, 2.7 mm, one F, 1.3 mm (UF36439). – Gulf of Aqaba, 28.4039°N, 34.7407°E, 7–8 m, 29 September 2013: one M, 1.4 mm (UF38080). – 28.1846°N, 34.6381°E, 3–10 m, 1 October 2013: one M, 1.2 mm (UF38193). – Shi'b Al Khamsa, 38.6163°N, 22.7489°E, 8 m, 6 March 2014: one M, 1.7 mm (UF40269). – Wajh Barrier, 25.407°N, 36.690°E, 5–7 m, 30 January 2016: one ov. F, 1.9 mm (UF42374). – Wajh Barrier, 25.407°N, 36.690°E, 5–7 m, 30 January 2016: one ov. F, 2.3 mm (UF42390).

Madagascar. Tulear, coll. Thomassin. Stn 489: one ov. F, 2.5 mm (MNHN-IU-2013-17320). – Stn 498, one M, 2.2 mm (MNHN-IU-2013-17322). – Stn 617, one M, 1.8 mm (MNHN-IU-2013-17309). – Stn 678, one juv., 1.0 mm (MNHN-IU-2013-17310). – Stn 761, two M, 1.7–1.8 mm, one F, 1.6 mm, one juv., 1.0 mm (MNHN-IU-2013-17312). – Stn 762, one juv., 1.0 mm (MNHN-IU-2013-17316). – Stn 775, one M, 1.8 mm, one F, 1.6 mm (MNHN-IU-2013-17313). – Stn 844B, two M, 1.5–1.9 mm, five F, 1.5–2.4 mm (MNHN-IU-2013-17319). – Stn 896, nine M, 1.2–2.2 mm, five ov. F, 2.2–2.6 mm, two F, 1.9–2.1 mm (MNHN-IU-2013-17311). – Stn 902A, two M, 1.8–1.9 mm, one ov. F, 1.9 mm, one F, 1.7 mm (MNHN-IU-2013-17318). – Stn 1635, one ov. F, 2.0 mm, one juv., 1.0 mm (MNHN-IU-2013-17315).

Other material: Red Sea. Djibouti. Moucha Is., Maskali Bank, 11.6992°N, 43.1432°E, 7–17 m, 27 September 2012: two M, 1.3–2.0 mm, one ov. F, 1.6 mm (UF33346).

Red Sea. Jubal, Gulf of Suez, Routh reef, Col. Dolfus, 29 December, 1928: one F, 1.1 mm (MNHN-IU-2013-17321).

Red Sea. Sudan. Stn SAN46, Al Bahr al Ahmar. Sanganeb, 9 m, 25 March 1991: one ov. F, 2.6 mm (SMF). – Stn SAN12, Al Bahr al Ahmar. Sanganeb, S-Jetty, E-Side, 2 m, 4 April 1991: six M, 1.6–2.0 mm, three ov. F, 1.6–2.4 mm, four F, 1.6–1.8 mm (SMF). – Stn SAN3, Al Bahr al Ahmar. Sanganeb, N-Jetty, E-side, 1 m, 5 April 1991: seven M, 1.7–2.4 mm, four ov. F, 1.8–2.3 mm, five F, 1.6–1.8 mm (SMF). – Stn SAN2, Al Bahr al Ahmar, Sanganeb, S-Jetty, W-side, 1 m, in *Stylophora*, 6 April 1991: four M, 1.5–2.0 mm, three ov. F, 1.8–2.0 mm, two F, 1.5–1.6 mm (SMF). – Stn SAN8, Al Bahr al Ahmar. Sanganeb, S-Jetty, W-side, 1 m, 6 April 1991: four M, 1.5–2.0 mm, seven ov. F, 1.6–2.3 mm, two F, 2.0–2.1 mm (SMF). – Stn SAN13, Al Bahr al Ahmar. Sanganeb, N-Jetty, reef-plateau, 1 m, 8 April 1991: three M, 1.7–2.0 mm, four ov. F, 2.1–2.5 mm, one F, 1.6 mm (SMF). – Stn SAN25, Al Bahr al Ahmar. Sanganeb, 11 m, 8 April 1991: one
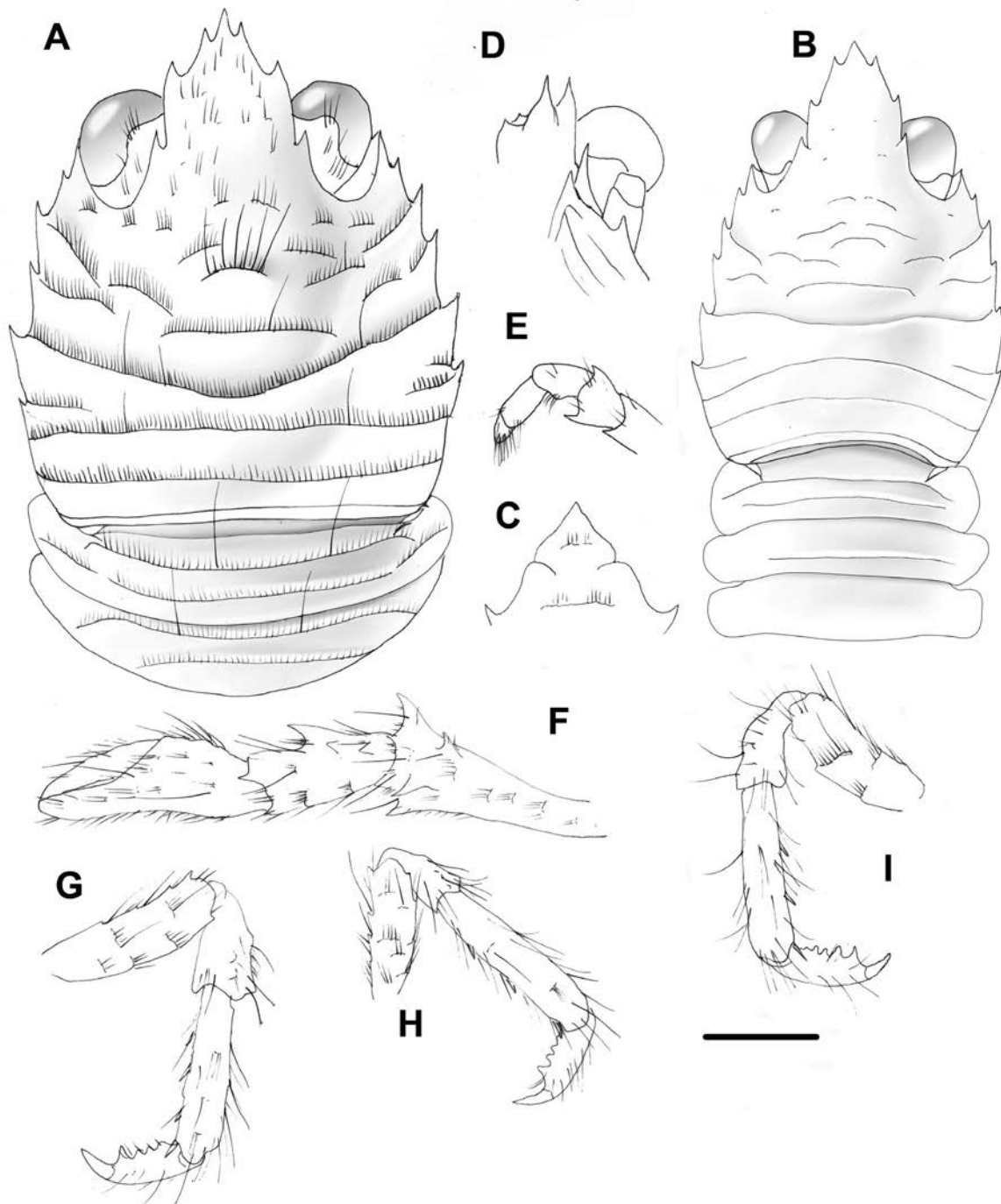
Figure 4. *Coralliogalathea humilis* (Nobili, 1905), A, C–I, ovigerous female, 1.6 mm, Red Sea, Djibouti (UF33346). B, syntype, male 1.9 mm, Red Sea, Djibouti (MNHN-IU-2013-17324). A, B, carapace and abdomen, dorsal view. C, thoracic sternites 3 and 4. D, left part of cephalothorax, ventral view, showing antennular and antennal peduncles, and anterior part of pterygostomian flap. E, right Mxp3, lateral view; F, left P1, dorsal view. G, right P2, lateral view. H, right P3, lateral view. I, left P4, lateral view. Scale bar: 0.5 mm.

M, 2.2 mm (SMF). – Stn SAN28, Al Bahr al Ahmar, 9 April 1991: one ov. F, 2.1 mm (SMF). – Stn SAN45, Al Bahr al Ahmar, 15 April 1991: three M, 2.2–2.5 mm, one ov. F, 2.5 mm, one F, 2.6 mm (SMF). – Stn SAN167, Al Bahr al Ahmar. Port Sudan, Wingate Reef, 7 m, in living *Pocillopora* sp., 19 September 1992: one ov. F, 2.8 mm
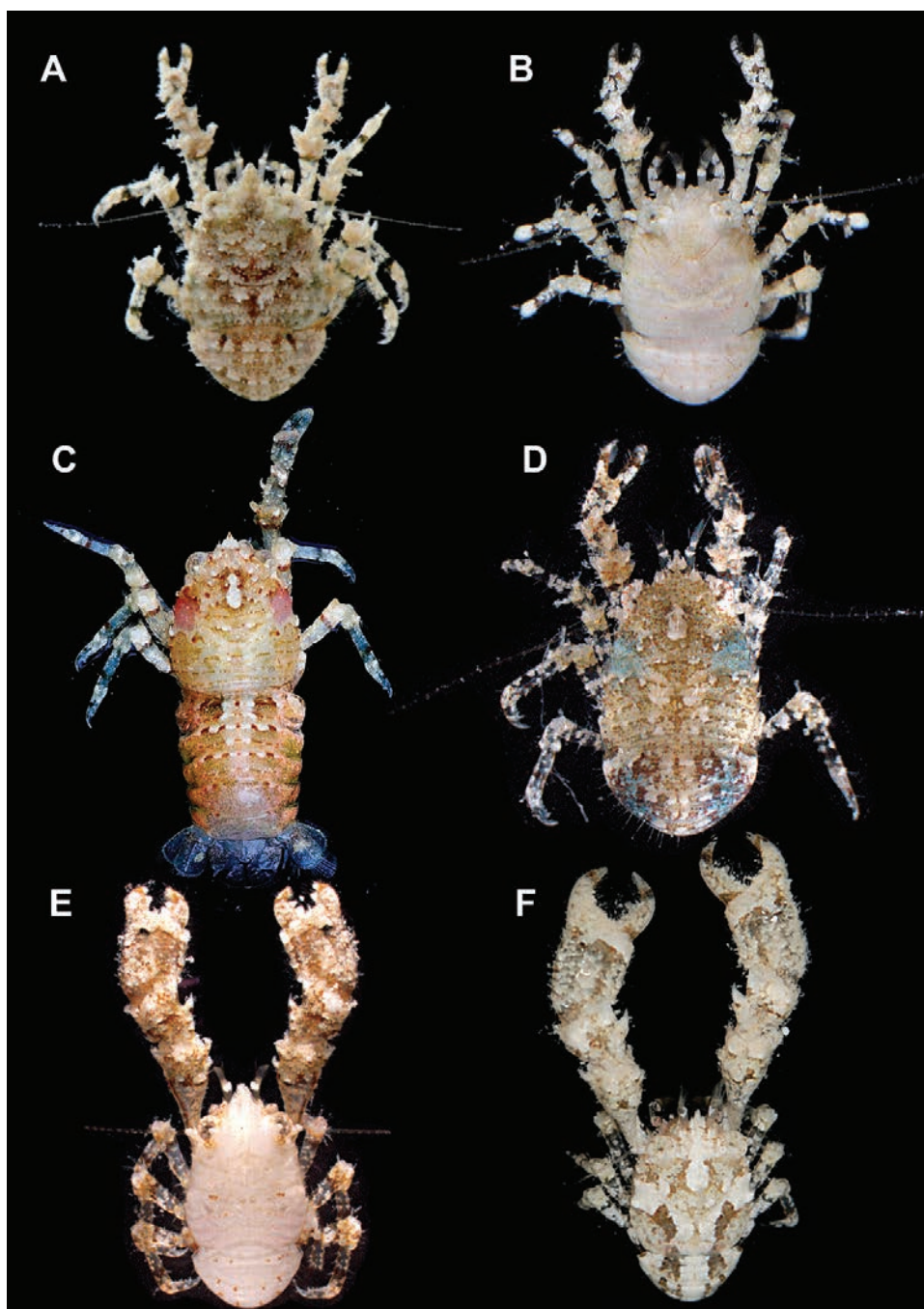
Figure 5. A, *Coralliogalathea humilis* (Nobili, 1905), Saudi Arabia, ovigerous female, 2.1 mm, UF37156. B, *Coralliogalathea humilis* (Nobili, 1905) Saudi Arabia, ovigerous female, 2.0 mm, UF36158. C, ***Coralliogalathea joae* sp. nov.**, Papua New Guinea, ovigerous female, 2.3 mm, MNHN-IU-2014-2383. D, *Coralliogalathea megalochira* (Nobili, 1906), French Polynesia, ovigerous female, 1.3 mm, UF15764. E, *Coralliogalathea megalochira* (Nobili, 1906), French Polynesia, male, 2.1 mm, UF15806. F, *Coralliogalathea megalochira* (Nobili, 1906), French Polynesia, male, 1.5 mm, UF23930.

(SMF). – Stn SAN115, Al Bahr al Ahmar. Sanganeb, 1 m, 26 September 1992: five M, 2.1–2.5 mm, two ov. F, 2.4–2.5 mm, two F, 2.1–2.2 mm (SMF). – Stn SAN117, Al Bahr al Ahmar. Sanganeb, S-Jetty, 14 m, 27 September 1992: two F, 2.0–2.1 mm (SMF). – Stn SAN127, Al Bahr al Ahmar, 29 September 1992: one M, 2.0 mm, one ov. F, 2.1 mm (SMF). – Stn SAN125, Al Bahr al Ahmar. Sanganeb, 14 m, 30 September 1992: one ov. F, 2.1 mm (SMF). – Stn SAN129, Al Bahr al Ahmar. Sanganeb, N-Jetty, 1 m, 1 October 1992: one M, 2.2 mm (SMF).

– Stn SAN148, Al Bahr al Ahmar. Sanganeb, 22 m, 3 October 1992: one M, 2.0 mm, one ov. F, 1.8 mm (SMF). – Stn SAN106, Al Bahr al Ahmar. Sanganeb, 6–10 m, 3 October 1993: one ov. F, 2.2 mm (SMF). – Rabigh, Stn SAN1, coast guard, 7 April 2011: one M, 2.4 mm (SMF).

Red Sea. Jeddah, 21.88483°N, 38.9727°E, 0.5 m, 17 April 2011: four M, 1.5–2.0 mm, one ov. F, 1.6 mm (SMF).

Madagascar. Tulear, coll. Thomassin, Stn 1666, two ov. F, 1.8–2.1 mm (MNHN-IU-2013-17317). – No Stn number: one juv., 1.0 mm (MNHN-IU-2013-17323), one ov. F, 2.0 mm (MNHN-IU-2013-17314).

Description
Carapace: 1.1–1.3 times broader than long; cervical groove distinct, laterally bifurcated; most ridges on gastric region interrupted, with some scattered scale-like ridges; one scale-like epigastric ridge; two protogastric ridges, anterior ridge medially interrupted, posterior ridge short, arcuate, slightly prominent, with thick plumose setae; one mesogastric ridge, medially interrupted, not extending to anteriormost marginal branchial spines; one metagastric ridge, not medially interrupted and not extending to anterior branchial ridges. Anterior branchial region with distinct ridges. Mid-transverse ridge usually uninterrupted, preceded by shallow cervical groove, followed by three transverse ridges, two of them uninterrupted. Lateral margins slightly convex medially, with five or six spines: one spine in front of and four or five spines behind anterior cervical groove; first spine anterolateral, small, at level of orbit, located at midlength between outer orbital spine and anteriormost spine of branchial margin; two spines on anterior branchial margin, and two or three spines on posterior branchial margin; third spine, when present, very small. Strong outer orbital spine. Rostrum spatulate, horizontal, slightly longer than broad, length 0.4 and breadth 0.3 that of carapace; dorsal surface nearly horizontal in lateral view, concave at base; lateral margin with three incised sharp teeth; margin between proximal and median spines straight.

Pterygostomian flap rugose, with one distinct spine on upper margin near linea anomurica, with sparse short setae, anterior margin bluntly angular.

Sternum: Nearly as long as broad; lateral extremities gently divergent posteriorly. Third sternite triangular, 1.2 times wider than long.

Abdomen: Somites 2–3 each with uninterrupted transverse ridge on tergite behind anterior ridge; somite 4 smooth or with minute setose scales on tergite; somites 5 and 6 smooth, posteromedian margin of somite 6 straight.

Eyes: Ocular peduncles as long as broad, maximal corneal diameter 0.7 of rostrum width.

Antennule: Article 1 with two well-developed distodorsal and distolateral mucronated spines, distodorsal larger; one small distomesial spine and one minute distomesial spine on dorsal side. Ultimate article without a tuft of fine setae on distodorsal margin.

Antenna: Article 1 with strong distomesial spine barely reaching distal margin of article 2.

Mxp3: Ischium with spine on flexor distal margin; crista dentata with eight to ten denticles. Merus as long as ischium; flexor margin with one strong spine; extensor margin with one distal spine. Carpus unarmed.

P1: Males 2.1–3.6 and females 1.6–2.1 times carapace length. Merus 0.7–0.8 length of carapace, 1.5–1.7 times as long as carpus, with some dorsomesial and a few ventromesial spines. Carpus 1.0–1.5 length of palm, 1.7–2.5 times as long as broad; dorsal surface with small spines; mesial row of spines, median spine strong. Palm 1.3–1.4 times as long as broad, unarmed. Fingers unarmed, 0.9–1.3 length of palm, each finger distally with two rows of teeth, spooned.

P2–4: With setose striae and some long plumose setae. P2 1.8 times carapace length. Meri successively shorter posteriorly (P3 merus 0.8 length of P2 merus, P4 merus 0.9 length of P3 merus); P2 merus 0.5 carapace length, 3.2 times as long as broad, as long as P2 propodus; P3 merus 3.0 times as long as broad, as long as P3 propodus; P4 merus 2.7 times as long as broad, 0.9 length of P4 propodus. Extensor margins of meri with row of three or four proximally diminishing spines on P2–3, unarmed on P4; flexor margins distally ending in small spine followed proximally by several eminences; lateral sides unarmed. Carpi with no or one distal spine on extensor margin; lateral surface with several acute granules sub-paralleling extensor margin on P2–4; flexor distal margin with small spine. P2–4 propodi 4.0–5.8 times as long as broad; extensor margin unarmed; flexor margin with three or four slender, movable spines on P2–4. Dactyli distally ending in well-curved strong spine, length 0.6–0.7 that of propodi.

Coloration: Base colour of carapace, abdomen and pereiopods light brown. Anterior half of abdomen sometimes with brown median longitudinal stripe. Most distal portion of pereiopod articles darker.

Remarks
Coralliogalathea humilis is easily distinguished from *C. tridentirostris* (Miyake, 1953) from Japan by the shape of the rostrum, which is clearly wider (measured between the proximal spines) than long (measured between proximal spines and the tip of rostrum) in *C. tridentirostris*; in *C. humilis*, the rostrum is as long as, or longer than, it is wide.

Furthermore, *C. humilis* can be differentiated from *C. megalochira*, *C. minuta* and *C. parva* by its absence

of a transverse stria in the fourth abdominal somite, a third sternite that is wider than long and a metagastric ridge of the carapace that is usually uninterrupted. In the other three species, the fourth abdominal somite has a transverse stria behind the anterior ridge, the third sternite is longer than, or as long as, it is wide, and the metagastric ridge of the carapace is usually medially interrupted.

Based on molecular analyses, the most closely related species to *C. humilis* is *C. minuta*, with divergence values of 9.2% for *COI* and 2.4% for 16S. The greatest divergence observed was between *C. humilis* and *C. tridentirostris* (14.1 and 12.2% for *COI* and 16S, respectively). Average intraspecific distances in *C. humilis* were 0.3 and 0.2% for *COI* and 16S, respectively (Table 2).

Distribution

Red Sea, Madagascar, from 0.5 to 17 m, on stones and dead and living corals (*Stylophora* sp., *Acropora* sp., *Seriatopora* sp. and *Pocillopora* sp.).

<div align="center">

CORRALLIOGALATHEA JOAE **SP. NOV.**

(FIGS 5C, 6)

</div>

urn:lsid:zoobank.org:act:9E36D411-7E7A-4990-A34C-158CCE102059

Material examined

Holotype: Vanuatu. SANTO cruise, Stn EP36, 15.555°S, 167.045°E, 20–60 m, 15 October 2006: ov. F, 2.4 mm (MNHN-IU-2013-17344).

Paratypes: Madagascar. Tulear, coll. Tomassin, Stn 896: one ov. F, 2.4 mm (MNHN-IU-2013-17331).

Papua New Guinea. Papua Niugini, Stn PR48, 05.12°S, 145.8233°E, no depth, 17 November 2012: one ov., F 2.4 mm (MNHN-IU-2013-17361). – Stn PB11, 05.20833°S, 145.81833°E, 13 m, 30 December 2012: one ov. F, 2.3 mm (MNHN-IU-2013-367). – Stn PB31, 05.1567°S, 145.8333°E, 31 m, 30 December 2012: one ov. F, 1.5 mm (MNHN-IU-2013-17347). – Stn PS23, 05.0762166°S, 145.82015°E, 21 m, 30 December 2012: three M, 1.2–1.6 mm, two ov. F, 1.5–1.7 mm (MNHN-IU-2013-17360).

KAVIENG lagoon cruise, Stn KB04, 02.55°S, 150.7667°E, 15–17 m, 3 June 2014, one M, 1.5 mm, one F, 1.4 mm (MNHN-IU-2014-13694-13592). – Stn KB26, 02.7333°S, 150.7167°E, 9–15 m, 10 June 2014, one ov. F, 2.3 mm (MNHN-IU-2014-2383).

Vanuatu. SANTO cruise, Stn ED16, 15.5883°S, 167.1233°E, 5–7 m, 17 September 2006: one M, 1.5 mm (MNHN-IU-2013-17358). – Stn DB40, 15.4967°S, 167.2517°E, 5 m, 19 September 2006: two M, 1.7–2.0 mm, one ov. F, 1.8 mm (MNHN-IU-2013-17342). – Stn DB53,

15.48°S, 167.2533°E, 5 m, 22 September 2006: two ov. F, 1.8–2.1 mm (MNHN-IU-2013-17352, 17353). – Stn DB58, 15.41°S, 167.2383°E, 6–43 m, 23 September 2006: one M, 1.6 mm (MNHN-IU-2013-17346). Stn ZB20, 15.6017°S, 167.09°E, 15–20 m, 10 October 2006: one ov. F, 1.5 mm (MNHN-IU-2013-17343). – Stn FB68, 15.59°S, 166.995°E, 11 m, 11 October 2006: one ov. F, 1.9 mm (MNHN-IU-2013-17355).

Western Australia. Ningaloo Reef, 22.6083°S, 113.6249°E, 15 m, 2009: one M, 2.0 mm (UF23446).

Other material: KAVIENG lagoon cruise, Stn KB06, 02.6833°S, 150.6833°E, 8 m, 4 June 2014: one F, 1.5 mm (MNHN-IU-2014-13638). – Stn KB16, 02.5666°S, 150.7667°E, 13–14 m, 7 June 2014, one ov. F, 1.9 mm, one F, 1.4 mm (MNHN-IU-2014-13617-13512). – Stn KD11, 02.6666°S, 50.7°E, 15 m, 8 June 2014, one ov. F, 2.0 mm (MNHN-IU-2014-13642). – Stn KB22, 02.75°S, 150.7167°E, 8–24 m, 10 June 2014, one ov. F, 1.6 mm (MNHN-IU-2014–2333). – Stn KD23, 02.65°S, 150.6°E, 5–10 m, 12 June 2014, two M, 1.6–1.8 mm (MNHN-IU-2014-13582). – Stn KS41, 02.6°S, 150.5333°E, 2–7 m, 16 June 2014, one M, 1.8 mm (MNHN-IU-2014-13648). – Stn KB74, 02.75°S, 150.7333°E, 20 m, 27 June 2014, one M, 2.0 mm (MNHN-IU-2014-13581).

Vanuatu. SANTO cruise, Stn DB65, 15.43°S, 167.2167°E, 13 m, 26 September 2006: one M, 1.6 mm, five ov. F, 1.2–1.4 mm (MNHN-IU-2013-17348). – Stn DB80, 15.6183°S, 167.125°E, 18 m, 2 October 2006: two M, 1.6–1.8 mm, two ov. F, 1.6–1.7 mm (MNHN-IU-2013-17356). – Stn NS36, 15.5283°S, 167.1583°E, 2–3 m, 2 October 2006: one M, 1.8 mm, three ov. F, 1.3–1.7 mm (MNHN-IU-2013-17357). – Stn DB86, 15.6416°S, 167.2517°E, 13 m, 4 October 2006: one F, 1.5 mm (MNHN-IU-2013-17351). – Stn EP32, 15.61°S, 167.0333°E, 100 m, 14 October 2006: one ov. F, 2.0 mm (MNHN-IU-2013-17349). – Stn FS96, 15.5516°S, 167.16°E, 35 m, 14 October 2006: one M, 1.3 mm, one ov. F, 1.6 mm (MNHN-IU-2013-17354). – Stn FB80, 15.5516°S, 167.16°E, 2 m, 14 October 2006: three M, 1.5–2.0 mm, four ov. F, 1.8–2.2 mm (MNHN-IU-2013-17327). – Stn FS82, 15.5383°S, 167.29°E, 8–20 m, 15 October 2006: two M, 1.5–1.8 mm, one ov. F, 2.0 mm, one F, 1.5 mm (MNHN-IU-2013-17350). – Stn EP36, 15.555°S, 167.2116°E, 20–60 m, 15 October 2006: two ov. F, 2.1–2.4 mm (MNHN-IU-2013-17359). – Stn EP39, 15.5616°S, 167.275°E, 75–80 m, 17 October 2006: one ov. F, 1.8 mm (MNHN-IU-2013-17345).

Eastern Australia. Queensland, Lizard Island, 14.3902°S, 145.2737°E, 10–12 m, 9 February 2009: one ov. F, 2.6 mm (UF16689). – 14.6504°S, 145.4621°E, no depth, 20 February 2009: one ov. F, 2.1 mm (UF18286).
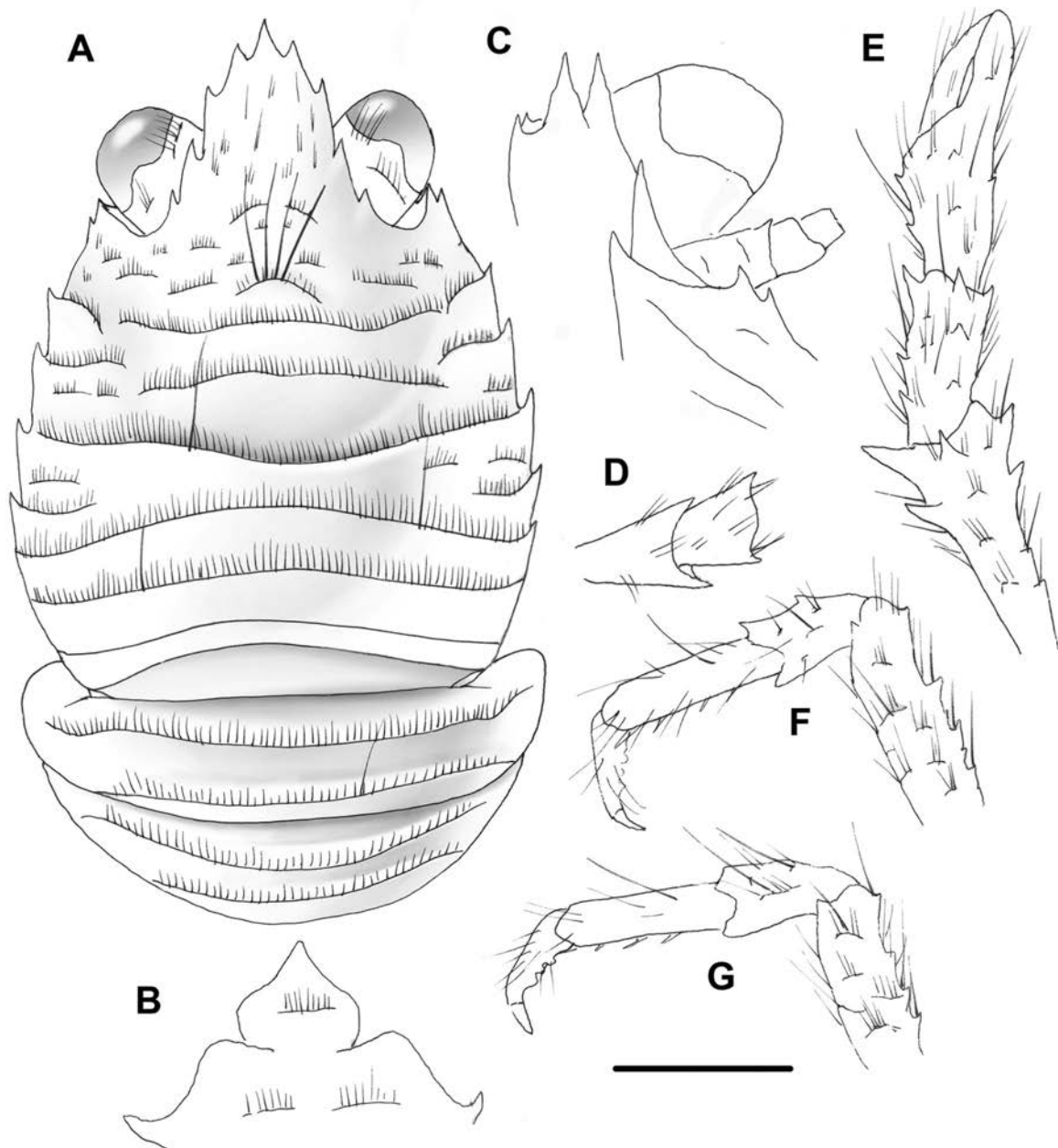
Figure 6. *Coralliogalathea joae* **sp. nov.**, Vanuatu, holotype, ovigerous female, 2.4 mm (MNHN-IU-2013-17344). A, carapace and abdomen, dorsal view. B, thoracic sternites 3 and 4. C, left part of cephalothorax, ventral view, showing antennular and antennal peduncles, and anterior part of pterygostomian flap. D, right Mxp3, lateral view. E, right P1, dorsal view. F, left P3, lateral view. G, left P3, lateral view. Scale bar: 1 mm in A, E–G; 1.6 mm in B–D.

Etymology
Named after Jo Taylor for her contributions to squat lobster systematics.

Description
Carapace: 1.0–1.2 times broader than long; cervical groove distinct, laterally bifurcated; one medially interrupted or scale-like epigastric ridge; two protogastric ridges, anterior ridge medially interrupted or scale like, posterior ridge short, arcuate, clearly prominent, with thick plumose setae; one mesogastric ridge, uninterrupted, not extending to anteriormost marginal branchial spines; one metagastric ridge, uninterrupted and not extending to anterior branchial ridges. Anterior branchial region with distinct ridges. Mid-transverse

ridge usually uninterrupted, preceded by shallow cervical groove, followed by three transverse ridges, two of them uninterrupted. Lateral margins slightly convex medially, with six spines: one spine in front of and five spines behind anterior cervical groove; first spine anterolateral, small, clearly before level of orbit, located near outer orbital spine; two spines on anterior branchial margin, and three spines on posterior branchial margin, last spine small. Strong outer orbital spine. Rostrum spatulate, horizontal, as long as or slightly longer than broad, length 0.4 and breadth 0.3–0.4 that of carapace; dorsal surface nearly horizontal or slightly concave in lateral view; lateral margin with four incised sharp teeth, basal pair of spines smaller than others.

Pterygostomian flap rugose, with one or two distinct spines on upper margin near linea anomurica, with sparse short setae, anterior margin bluntly angular.

Sternum: Nearly as long as broad; lateral extremities gently divergent posteriorly. Third sternite triangular, 1.0–1.3 times wider than long.

Abdomen: Somites 2–4 each with uninterrupted transverse stria behind anterior ridge; somites 5 and 6 smooth, posteromedian margin of somite 6 straight.

Eyes: Ocular peduncles as long as broad, maximal corneal diameter 0.7 of rostrum width.

Antennule: Article 1 with two well-developed distodorsal and distolateral mucronated spines, distodorsal larger; distomesial spine small; one minute distomesial spine on dorsal side. Ultimate article without a tuft of fine setae on distodorsal margin.

Antenna: Article 1 with strong distomesial spine barely reaching distal margin of article 2.

Mxp3: Ischium with minute spine on flexor distal margin; crista dentata with nine or ten denticles. Merus as long as ischium; flexor margin with one strong spine; extensor margin with one distal spine. Carpus unarmed.

P1: Males 2.3–3.8 and females 1.7–2.1 times carapace length. Merus 0.6–0.7 length of carapace, 1.3–1.6 times as long as carpus, with some dorsomesial and a few ventromesial spines. Carpus 1.0–1.5 length of palm, 1.5–2.5 times as long as broad; dorsal surface with small spines; mesial row with two or three well-developed spines. Palm 1.0–1.3 times as long as broad, with a few small spines along lateral and mesial margins. Fingers unarmed, 1.0–1.3 length of palm, each finger distally with four or five teeth, and spooned.

P2–4: Moderately short, with setose striae and some long plumose setae. P2 1.5–1.7 times carapace length. Meri successively shorter posteriorly (P3 merus 0.8–0.9 length of P2 merus, P4 merus 0.7–0.9 length of

P3 merus); P2 merus 0.5–0.6 carapace length, 3.0–3.5 times as long as broad, 1.2 length of P2 propodus; P3 merus 3.0 times as long as broad, 1.2 length of P3 propodus; P4 merus 2.7–3.0 times as long as broad, 0.9–1.2 length of P4 propodus. Extensor margins of meri with row of four to six proximally diminishing spines on P2–3, unarmed on P4; flexor margins distally ending in small spine followed proximally by several eminences; lateral sides unarmed. Carpi with no to three spines on extensor margin; lateral surface with several spines or acute granules sub-paralleling extensor margin on P2–4; flexor distal margin unarmed. P2–4 propodi 3.8–4.8 times as long as broad; extensor margin unarmed; flexor margin with three or four slender, movable spines on P2–4. Dactyli distally ending in well-curved strong spine, length 0.6–0.7 that of propodi.

Remarks
Coralliogalathea joae is easily distinguished from the other species of the genus by the number of lateral teeth on the rostrum; four in *C. joae* and three in the other species.

Coralliogalathea joae is genetically very distinct from the rest of the species. Genetic divergences with the other species ranged from 13.0 to 14.7% for *COI* and from 8.8 to 14.3% for 16S. Average intraspecific distances were 1.1 and 0.2% for *COI* and 16S, respectively (Table 2).

Distribution
Madagascar, Western and Eastern Australia, Papua New Guinea, Vanuatu, 2–100 m, in corals (e.g. *Pocillopora* sp.).

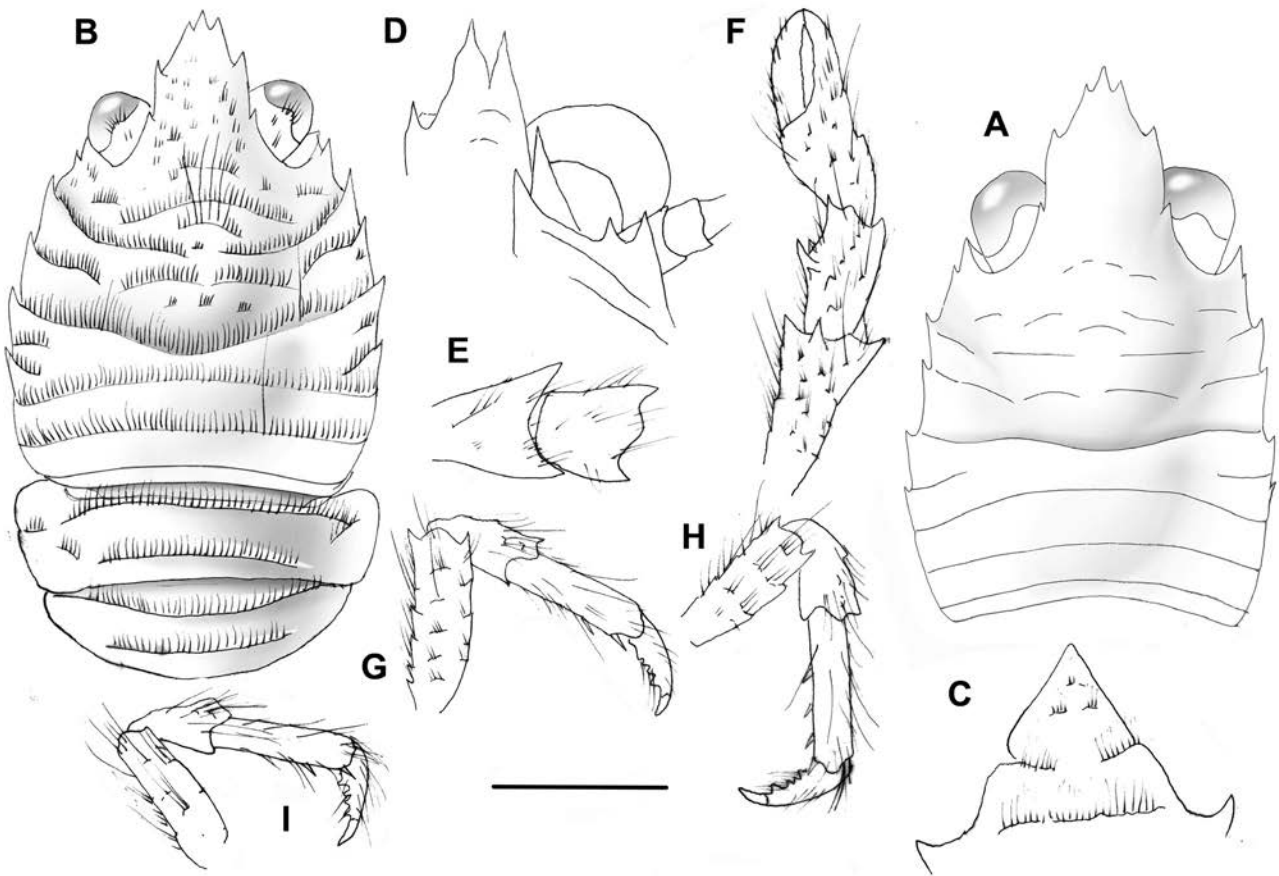### *CORALLIOGALATHEA MEGALOCHIRA* (NOBILI, 1906) **COMB. NOV.**
(FIGS 5D–F, 7)

Galathea megalochira Nobili, 1906b: 260. – Nobili, 1907: 376, pl. 1, figs 12, 12a, 12b. – Doflein & Balss, 1913: 169 [list].

Coralliogalathea humilis. – Peyrot-Clausade, 1989: 112. – Poupin, 1996: 19. – Baba *et al.*, 2008: 59 [in part].

Material examined
Holotype: French Polynesia. Tuamotu Archipelago, Ohura Lagoon, G. Seurat, 1905 coll.: M, 1.8 mm (MNHN-IU-2013-17319).

Paratypes: French Polynesia. Fakarava Atoll, Havaiki Pearl farm, atoll lagoon, on pearl baskets and ropes, 16.0723°S, 145.6238°W, 15 m, 6 June 2006: one M, 2.2 mm (UF9600). – Gambier, Terevai, 23.1517°S, 135.0554°W, 0.5–9 m, 8 February 2013: one M, 1.3 mm (UF35495). – Gambier, Stn B3, 22 November 1965: one ov. F, 2.1 mm (MNHN-IU-2013-17341).

Figure 7. *Coralliogalathea megalochira* (Nobili, 1906), A, male, holotype, 1.8 mm, French Polynesia, Tuamotu Archipelago, (MNHN-IU-2013-17319). B–I, ovigerous female, 1.9 mm, French Polynesia, Society Archipelago, Moorea (UF23698). A, B, carapace and abdomen, dorsal view. C, thoracic sternites 3 and 4. D, left part of cephalothorax, ventral view, showing antennular and antennal peduncles, and anterior part of pterygostomian flap. E, right Mxp3, lateral view. F, right P1, dorsal view. G, right P2, lateral view. H, right P3, lateral view. I, right P4, lateral view. Scale bar: 1 mm in A, B, F–I; 2 mm in C–E.

French Polynesia. Society Archipelago, Moorea, 17.4775°S, 149.8412°W, 1–2 m, 18 October 2008: one M, 1.5 mm, one ov., F 1.6 mm (UF15764, UF15778). – 17.5493°S, 149.784°W, 0 m, 19 October 2008: two M, 2.0–2.1 mm, one ov. F, 2.2 mm (UF15802, UF15806). – 17.5493°S, 149.784°W, 0 m, 19 October 2008: two ov. F, 2.0 mm (UF15782). – 17.4902°S, 149.826°W, 1–13 m, 22 October 2008: one M, 1.6 mm (UF16016). – 17.4893°S, 149.8258°W, 1–1.5 m, 24 October 2009: one ov. F, 1.9 mm (UF23698). – 17.4827°S, 149.83°W, 2–3 m, 8 November 2009: one M, 1.5 mm (UF23930). – 17.4824°S, 149.824°W, 1 m, 1 November 2010: one M, 1.1 mm, one ov. F, 1.6 mm, one F, 1.4 mm (UF28957). 17.5101°S, 149.8513°W, 0.5–2 m, 19 November 2010: one M, 2.2 mm (UF29148).

French Polynesia. Austral Archipelago, Stn 5, 27.0933°S, 144.30833°W, 8 m, 4 November 2002: three M, 1.6–2.0 mm, one F, 1.5 mm (MNHN-IU-2013-17338). – Stn 14, 27.5967°S, 44.2267°W, 2 m, 8 November 2002: one M, 1.8 mm, one ov. F, 2.2 mm (MNHN-IU-2013-17339).

Other material: French Polynesia. Society Archipelago, Moorea, 17.4908°S, 149.8255°W, 12–14 m, 23 January 2012: one M, 1.8 mm (UF33386). – 17.4908°S, 149.8255°W, 12–14 m, 23 January 2012: one ov. F, 2.1 mm (UF33385). – 17.4908°S, 149.8255°W, 15 m, 23 January 2012: one M, 1.7 mm (UF33411). – 17.4908°S, 149.8255°W, 1–11 m, 24 January 2012: two M, 1.7–1.9 mm, three ov. F, 1.7–2.3 mm (UF33425). – 17.48°S, 149.84°W, 0–2 m, 6 February 2012: one M, 1.8 mm (UF34077). – 17.48°S, 149.84°W, 0–2 m, 6 February 2012: one M, 1.7 mm (UF34078).

French Polynesia. Rarapai Island, Stn 17, 27.5767°S, 144.3783°W, 9 m, 10 November 2002: one M, 1.6 mm (MNHN-IU-2013-17336). – Stn 21, 27.57°S, 144.3433°W, 5 m, 12 November 2002: three M, 1.3–1.5 mm, four ov. F, 1.4–1.6 mm, two

F, 1.3–1.5 mm (MNHN-IU-2013-17337). – Stn 29, 27.5717°S, 144.35°W, 2–4 m, 15 November 2002: one M, 2.1 mm, two ov. F, 2.0–2.4 mm, one F, 2.0 mm (MNHN-IU-2013-17340). – Stn 38, 27.6233°S, 144.3067°W, 2 m, 22 November 2002: one ov. F, 2.0 mm (MNHN-IU-2013-17335).

Description
Carapace: 1.2–1.3 times broader than long; dorsally unarmed; cervical groove distinct, laterally bifurcated; most ridges on gastric region interrupted, with some scattered scale-like ridges; one scale-like epigastric ridge; two protogastric ridges, anterior ridge medially interrupted, posterior ridge short, arcuate, slightly prominent, with thick, long plumose setae; one mesogastric ridge, medially interrupted, not extending to anteriormost marginal branchial spines; one metagastric ridge, medially interrupted and not extending to anterior branchial ridges. Anterior branchial region with distinct ridges. Mid-transverse ridge uninterrupted, preceded by shallow cervical groove, followed by three transverse ridges, two of them uninterrupted. Lateral margins slightly convex medially, with five spines: one spine in front of and four spines behind anterior cervical groove; first spine anterolateral, small, at level of orbit, located at midlength between outer orbital spine and anteriormost spine of branchial margin; two spines on anterior branchial margin, and two spines on posterior branchial margin. Strong outer orbital spine. Rostrum spatulate, as long as broad, length 0.4 and breadth 0.3 that of carapace; dorsal surface slightly concave at base; lateral margin with three incised sharp teeth; margin between proximal and median spines straight.

Pterygostomian flap rugose, with one or two distinct spines on upper margin near linea anomurica, with sparse short setae, anterior margin bluntly angular.

Sternum: Nearly as long as broad; lateral extremities gently divergent posteriorly. Third sternite triangular, as wide as long.

Abdomen: Somites 2–4 each with an uninterrupted transverse ridge behind anterior ridge on tergite, ridge on somite 4 sometimes medially interrupted or scale like; somites 5 and 6 smooth, posteromedian margin of somite 6 straight.

Eyes: Ocular peduncles as long as broad, maximal corneal diameter 0.7 of rostrum width.

Antennule: Article 1 with two well-developed distodorsal and distolateral mucronated spines, distodorsal larger; distomesial spine minute. Ultimate article without a tuft of fine setae on distodorsal margin.

Antenna: Article 1 with strong distomesial spine barely reaching distal margin of article 3. Articles 2–3 unarmed.

Mxp3: Ischium with spine on flexor distal margin; crista dentata with nine to 11 denticles. Merus as long as ischium; flexor margin with one strong spine; extensor margin with one distal spine. Carpus unarmed.

P1: Males 2.4–2.9 and females 1.4–2.0 times carapace length. Merus 0.5 (females) or 0.9–1.0 (males) length of carapace, 1.3–1.6 times as long as carpus, with some dorsomesial and a few ventromesial spines. Carpus 1.4–1.8 length of palm, 1.2–1.5 times as long as broad; dorsal surface with small spines; mesial row of spines, median spine strong. Palm 1.1–1.4 times as long as broad, a few small spines along lateral and mesial margins. Fingers unarmed, 1.3–1.5 length of palm, each finger distally with two rows of teeth, spooned.

P2–4: With setose striae and some long plumose setae. P2 1.6–1.8 times carapace length. Meri successively shorter posteriorly (P3 merus 0.8 length of P2 merus, P4 merus 0.9–1.0 length of P3 merus); P2 merus 0.5–0.6 carapace length, 3.2 times as long as broad, 1.0–1.2 length of P2 propodus; P3 merus 3.0–3.2 times as long as broad, 1.0–1.3 length of P3 propodus; P4 merus 3.0 times as long as broad, 0.9–1.2 length of P4 propodus. Extensor margins of meri with row of three or four proximally diminishing spines on P2–3, unarmed on P4; flexor margins distally unarmed or ending in a minute spine followed proximally by several eminences; lateral sides unarmed. Carpi with zero to two spines on extensor margin; lateral surface with several acute granules or spines sub-paralleling extensor margin on P2–4; flexor distal margin with minute spine. P2–4 propodi 4.0–4.5 times as long as broad; extensor margin unarmed; flexor margin with three or four slender movable spines on P2–4. Dactyli distally ending in well-curved strong spine, length 0.6–0.7 that of propodi.

Coloration: Base colour of carapace, abdomen and pereiopods light brown. Numerous dark brown spots of different sizes on carapace and abdomen. Anterior half of abdomen sometimes with brown median longitudinal stripe. Most distal portion of pereiopod articles darker.

Remarks
Coralliogalathea megalochira is closely related to *C. parva* from Vanuatu, Papua New Guinea and the Mariana Islands. The following aspects can distinguish both species. The lateral margin of the rostrum between proximal and median teeth is

clearly convex in *C. parva*; this margin is straight in *C. megalochira*. The walking legs are more slender in *C. parva* than in *C. megalochira*. The P2–3 propodi are 5.0–6.5 times as long as broad in *C. parva*, whereas they are 4.0–4.5 times as long as broad in *C. megalochira*.

The observed genetic divergence between *C. megalochira* and *C. parva* was 6.7% for *COI* and 2.4% for 16S (Table 2).

Distribution
French Polynesia (Austral, Tuamotu and Society Archipelagos), 0–13 m.

CORALLIOGALATHEA MINUTA SP. NOV.
(FIGS 8, 9)

urn:lsid:zoobank.org:act:AA5397D5-56FF-4DC8-8F27-F5D4ED82ECAA

Material examined
Holotype: New Caledonia, Touho Island, 20.7833°S, 165.2167°E, September 1993: M, 2.6 mm (MNHN-IU-2013-17329).

Paratypes: New Caledonia. Lifou Island, LIFOU cruise, Stn 1475, 20.93°S, 167.3166°E, subtidal, 11 November 2000: ten M, 1.5–3.2 mm, six ov. F, 1.6–2.4 mm, one F, 2.1 mm (MNHN-IU-2013-17377-17381). – Stn 1406, 20.78°S, 167.1283°E, intertidal, 18 November 2000: one M, 1.6 mm, six ov. F, 1.5–1.9 mm (MNHN-IU-2013-17367). – Stn 1426, 20.765°S, 167.1033°E, 4–7 m, 20 November 2000: one ov. F, 1.9 mm, one F, 2.0 mm (MNHN-IU-2013-17366). – Stn 1467, 20.7766°S, 167.09°E, 90 m, 20 November 2000: two ov. F, 2.3–2.4 mm (MNHN-IU-2013-17363). – Stn 1418, 20.7816°S, 167.1316°E, 1–5 m, 21 November 2000: one M, 1.7 mm, two ov. F, 1.6–1.8 mm (MNHN-IU-2013-17368). – Stn 1421, 20.8733°S, 167.1416°E, 4 m, 26 November 2000: one ov. F, 1.8 mm (MNHN-IU-2013-17365).

New Caledonia, Touho Island. 20.7833°S, 165.2167°E, 10 m, 7 September 1993: two M, 1.6–2.0 mm, two ov. F, 2.1–2.2 mm (MNHN-IU-2013-17364), one M, 1.8 mm (MNHN-IU-2013-17330). Vanuatu. SANTO cruise, Stn LD10, 15.3633°S 167.19°E, 2–4 m, 29 September 2006: one ov. F, 2.0 mm (MNHN-IU-2013-17369).

Other material: New Caledonia, Touho Island, Stn LF4, 20.7025°S, 167.165°E, 8 m, 28 November 1995: one M, 2.1 mm (MNHN-IU-2013-17362).

Vanuatu. SANTO cruise, Stn EP10, 15.6333°S, 167.2267°E, 45–101 m, 15 September 2006: one M, 1.3 mm, one F, 2.0 mm (MNHN-IU-2013-17376). – Stn DB40, 15.4966°S, 167.2516°E, 5 m, 19 September 2006: two M, 1.5–1.7 mm, four ov. F, 1.6–1.8 mm (MNHN-IU-2013-17374). – Stn DB83, 15.7233°S,
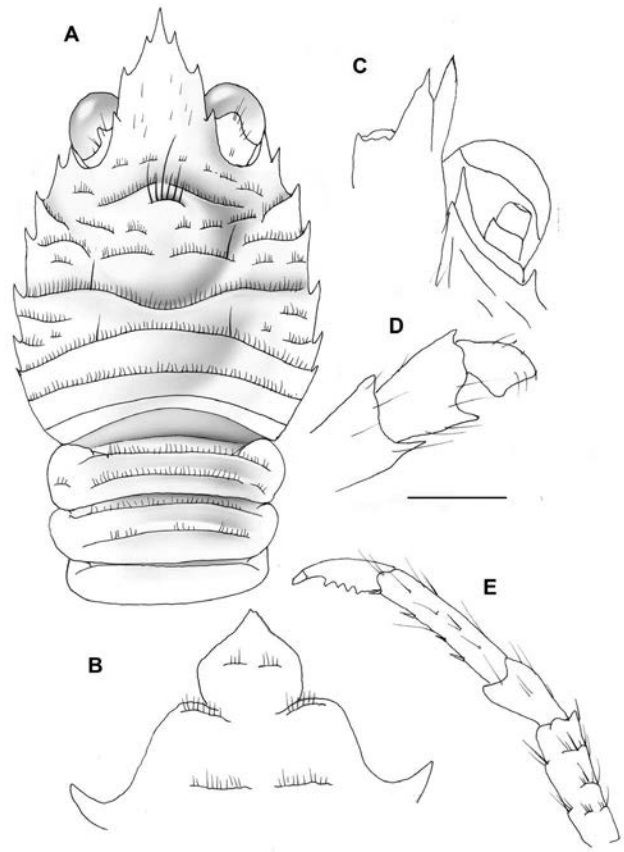
Figure 8. *Coralliogalathea minuta* **sp. nov.**, New Caledonia, Touho Island, male, holotype, 2.6 mm (MNHN-IU-2013-17329). A, carapace and abdomen, dorsal view. B, thoracic sternites 3 and 4. C, left part of cephalothorax, ventral view, showing antennular and antennal peduncles, and anterior part of pterygostomian flap. D, right Mxp3, lateral view. E, left P4, lateral view. Scale bar: 1 mm in A, E; 2 mm in B–D.

167.25°E, 6 m, 3 October 2006: two M, 1.2–1.6 mm, ten ov. F, 1.7–1.9 mm (MNHN-IU-2013-17370). – Stn ZR12, 15.6117°S, 167.0333°E, 2–30 m, 5 October 2006: two M, 1.8–2.1 mm, one ov. F, 1.9 mm (MNHN-IU-2013-17375). – Stn FS51, 15.7116°S, 167.2516°E, 2–3 m, 5 October 2006: two M, 1.8–1.9 mm (MNHN-IU-2013-17373). – Stn LD25, 15.5416°S, 167.175°E, 3–4 m, 7 October 2006: one ov. F, 1.8 mm (MNHN-IU-2013-17371). – Stn EP36, 15.5517°S, 167.2067°E, 20–60 m, 15 October 2006: one ov. F, 1.8 mm (MNHN-IU-2013-17372).

Etymology
From the Latin *minutus*, meaning small, in reference to the size of the species.

Description
Carapace: 1.0–1.1 times broader than long; cervical groove barely distinct; most ridges on gastric region interrupted or scale like; one scale-like epigastric
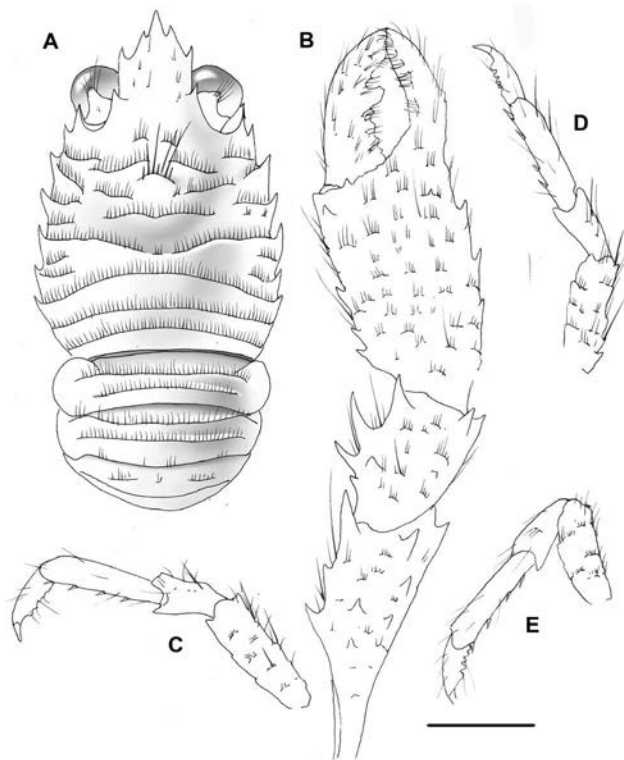
Figure 9. *Coralliogalathea minuta* **sp. nov.**, New Caledonia. Lifou Island, paratype, male, 2.1 mm (MNHN-IU-2013-17379). A, carapace and abdomen, dorsal view. B, right P1, dorsal view. C, left P2, lateral view. D, left P3, lateral view. E, left P4, lateral view. Scale bar: 1 mm.

ridge; two scale-like protogastric ridges, posterior ridge short, arcuate, with thick plumose setae; one mesogastric ridge, medially interrupted or scale like, not extending to anteriormost marginal branchial spines; one metagastric ridge, medially interrupted and not extending to anterior branchial ridges. Anterior branchial region with distinct ridges. Mid-transverse ridge usually uninterrupted, preceded by shallow cervical groove, followed by three transverse ridges, two of them uninterrupted. Lateral margins slightly convex medially, with five or six spines: one spine in front of and four or five spines behind anterior cervical groove; first spine anterolateral, small, at level of or slightly behind orbit, located at midlength between outer orbital spine and anteriormost spine of branchial margin; two spines on anterior branchial margin, and two or three spines on posterior branchial margin. Strong outer orbital spine. Rostrum lanceolate, slightly longer than broad, length 0.3 and breadth 0.3 that of carapace; dorsal surface concave at base; lateral margin with three incised sharp teeth, margin between proximal and median spines straight.

Pterygostomian flap rugose, with one distinct spine on upper margin near linea anomurica, with sparse short setae, anterior margin bluntly angular.

Sternum: Nearly as long as broad; lateral extremities gently divergent posteriorly. Third sternite triangular, as wide as long.

Abdomen: Somites 2–3 each with two uninterrupted transverse ridges on tergite, anterior ridge slightly more elevated than posterior ridge; somite 4 with posterior ridge scale like; somites 5 and 6 smooth, posteromedian margin of somite 6 straight.

Eyes: Ocular peduncles as long as broad, maximal corneal diameter 0.7 of rostrum width.

Antennule: Article 1 with two well-developed distodorsal and distolateral mucronated spines, distodorsal larger, with small mesial spine at base; distomesial spine small. Ultimate article without a tuft of fine setae on distodorsal margin.

Antenna: Article 1 with strong distomesial spine barely reaching distal margin of article 3.

Mxp3: Ischium with minute spine on flexor distal margin. Merus as long as ischium; flexor margin with one strong spine; extensor margin with one distal spine. Carpus unarmed.

P1: Males 3.0–3.8 and females 1.7–2.5 times carapace length. Merus 0.9–1.0 length of carapace, 1.8 times as long as carpus, with some dorsomesial and a few ventromesial spines. Carpus 0.7 length of palm, 1.4 times as long as broad; dorsal surface with small spines or acute granules; mesial row of strong spines, with one or two ventral spines. Palm 1.4 times as long as broad, a few acute granules along lateral and mesial margins. Fingers unarmed, 0.8 length of palm, each finger distally with two rows of teeth, spooned.

P2–4: With setose striae and some long plumose setae. P2 1.6 times carapace length. Meri successively shorter posteriorly (P3 merus 0.9 length of P2 merus, P4 merus 0.9 length of P3 merus); P2 merus 0.5–0.6 carapace length, 3.3 times as long as broad, 1.3 length of P2 propodus; P3 merus 3.2 times as long as broad, 1.3 length of P3 propodus; P4 merus 3.0 times as long as broad, 1.0–1.2 length of P4 propodus. Extensor margins of meri with row of three to five proximally diminishing small spines on P2–3, unarmed on P4; flexor margins distally ending in small spine followed proximally by several eminences; lateral sides unarmed. Carpi unarmed on extensor margin; lateral surface with several acute granules sub-paralleling extensor margin on P2–4; flexor distal margin unarmed. P2–4 propodi 4.0–4.8 times as long as broad; extensor margin

unarmed; flexor margin with four slender movable spines on P2–4. Dactyli distally ending in well-curved strong spine, length 0.6 that of propodi.

Remarks
Coralliogalathea minuta is morphologically related to *C. parva* from Vanuatu, Papua New Guinea and the Mariana Islands and *C. megalochira* from French Polynesia. *Coralliogalathea minuta* is easily distinguished from the other species by the shapes of the rostrum and the carapace. The rostrum is lanceolate in *C. minuta* and spatulate in the other species, and the carapace is slightly shorter than, or as long as, it is wide in *C. minuta*, whereas it is clearly wider (≥ 1.2 times) than long in the other species.

Genetic divergences between *C. minuta* and its most similar species were, with *C. parva*, 13.6 and 10% for *COI* and 16S, respectively, and with *C. megalochira*, 13.9 and 9% for *COI* and 16S, respectively (Table 2). The genetic distance between *C. minuta* and *C. humilis* was the lowest observed among *Coralliogalathea* species (see above).

Distribution
New Caledonia, Vanuatu, subtidal to 101 m.

CORALLIOGALATHEA PARVA **SP. NOV.**
(FIG. 10)

urn:lsid:zoobank.org:act:3D1A8B9E-538B-4450-AB1B-CC20F46B9BE8

Material examined
*Holotype:* Vanuatu. Stn FB80, 15.5516°S, 167.16°E, 2 m, 14 October 2006: M, 2.1 mm (MNHN-IU-2013-17328).

Paratypes: Mariana Islands, Guam Island. Pago Bay, reef flat to crest channel, under rocks, 0–2 m, 2003: one ov. F, 2.1 mm (UF4229). – Cabras, 13.4649°N, 144.6872°E, 0–4 m, 20 June 2010: one M, 2.7 mm (UF26641).

Papua New Guinea, Bismark Archipelago, Tungelo Island, Mascot Channel, reef flat adjacent to channel, sand and seagrass, 2.655°S, 150.46°E, 1–2 m, 2 July 2003: one ov. F, 1.7 mm (UF4837).

KAVIENG lagoon cruise, Stn KS21, 02.5667°S, 150.7667°E, 4 m, 7 June 2014: one ov. F, 1.6 mm (MNHN-IU-2014-13507). – Stn KB30, 02.7333°S, 150.65°E, 8–15 m, 11 June 2014: two M, 1.5–2 mm, (MNHN-IU-2014-13693-13636). – Stn KB36, 02.6333°S, 150.6333°E, 3–8 m, 13 June 2014: one M, 1.7 mm, one F, 1.5 mm (MNHN-IU-2014-13690-13665). – Stn KS41, 02.6°S, 150.5333°E, 2–7 m, 16 June 2014: one ov. F, 1.9 mm (MNHN-IU-2014-13692).

Vanuatu. SANTO cruise, Stn DB40, 15.4967°S, 167.2517°E, 5 m, 19 September 2006: three M, 1.2 mm, six ov. F, 1.3–1.8 mm, one F, 1.3 mm
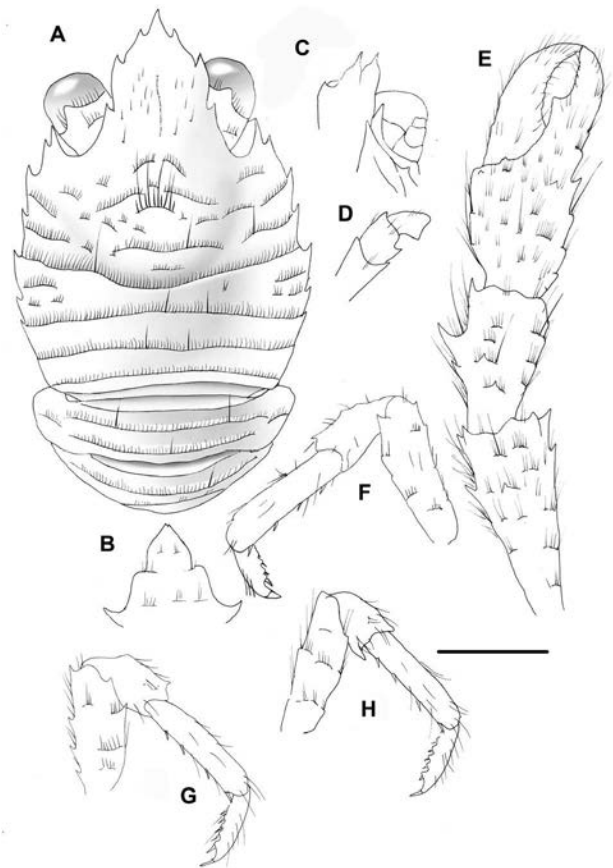
Figure 10. *Coralliogalathea parva* sp. nov., Vanuatu, male, holotype, 2.1 mm (MNHN-IU-2013-17328). A, carapace and abdomen, dorsal view. B, thoracic sternites 3 and 4. C, left part of cephalothorax, ventral view, showing antennular and antennal peduncles, and anterior part of pterygostomian flap. D, right Mxp3, lateral view. E, right P1, dorsal view. F, left P2, lateral view. G, right P3, lateral view. H, right P4, lateral view. Scale bar: 1 mm.

(MNHN-IU-2013-17383). Stn FB61, 15.5733°S, 167.21°E, 2–3 m, 7 October 2006: one M, 1.6 mm (MNHN-IU-2013-17382). – Stn ZB20, 15.6016°S, 167.09°E, 15–20 m, 10 October 2006: one ov. F, 1.6 mm (MNHN-IU-2013-17386). – Stn FB80, 15.5516°S, 167.16°E, 2 m, 14 October 2006: three M, 1.5–2.0 mm, four ov. F, 1.8–2.2 mm (MNHN-IU-2013-17326).

Other material: Vanuatu. SANTO cruise, Stn DB12, 15.61°S, 167.1683°E, 10–18 m, 13 September 2006: one ov. F, 1.4 mm (MNHN-IU-2013-17387). – Stn EP10, 15.6333°S, 167.2266°E, 45–101 m, 15 September 2006: one M, 1.3 mm, one F, 2.0 mm (MNHN) – Stn DB53, 15.48°S, 167.2533°E, 5 m, 22 September 2006: five M, 1.4–1.7 mm, four ov. F, 1.5–1.8 mm (MNHN-IU-2013-17385). – Stn DB67, 15.3816°S, 167.2183°E, 7 m, 26 September 2006: one M, 1.6 mm (MNHN-IU-2013-17392). – Stn DB71, 15.36°S, 167.2083°E, 7 m, 27 September 2006:

one M, 1.7 mm, two ov. F, 1.6–1.8 mm, one F, 1.4 mm (MNHN-IU-2013-17390). – Stn NS36, 15.5283°S, 167.1583°E, 2–3 m, 2 October 2006: one M, 1.8 mm (MNHN-IU-2013-17389). – Stn DB83, 15.7233°S, 167.25°E, 6 m, 3 October 2006: three M, 1.2–1.6 mm, ten ov. F, 1.7–1.9 mm (MNHN). – Stn FB52, 15.7116°S, 167.2516°E, 7 m, 5 October 2006: six M, 1.4–1.6 mm; eight ov. F, 1.3–1.6 mm (MNHN-IU-2013-17388). – Stn FB92, 15.56°S, 167.2766°E, 2–4 m, 14 October 2006: one M, 1.7 mm, two ov. F, 1.6–1.8 mm (MNHN-IU-2013-17393). – Stn FS79, 15.5516°S, 167.16°E, 2 m, 14 October 2006: one M, 1.4 mm, one F, 1.4 mm (MNHN-IU-2013-17391). – Stn FB80, 15.5516°S, 167.16°E, 2 m, 14 October 2006: 11 M, 1.3–2.4 mm, 13 ov. F, 1.6–2.3 mm (MNHN-IU-2013-17384). – Stn LD35, 15.5466°S, 167.1933°E, 3–8 m, 16 October 2006: one M, 1.3 mm (MNHN-IU-2013-17394).

Etymology
From the Latin *parvus*, meaning little, in reference to the small size of the species.

Description
Carapace: 1.2–1.3 times broader than long; cervical groove barely distinct; most ridges on gastric region interrupted or scale-like; one scale-like epigastric ridge; two scale-like protogastric ridges 1.2–1.3 times broader than long, posterior ridge short, arcuate, with thick plumose setae; one mesogastric ridge, medially interrupted or scale like, not extending to anteriormost marginal branchial spines; one metagastric ridge, uninterrupted and not extending to anterior branchial ridges. Anterior branchial region with distinct ridges. Mid-transverse ridge usually uninterrupted, preceded by shallow cervical groove, followed by three transverse ridges, two of them uninterrupted. Lateral margins slightly convex medially, with five or six spines: one spine in front of and four or five spines behind anterior cervical groove; first spine anterolateral, small, at level of orbit, located at midlength between outer orbital spine and anteriormost spine of branchial margin; two spines on anterior branchial margin, and two or three spines on posterior branchial margin. Strong outer orbital spine; infraorbital margin with two strong spines. Rostrum spatulate, slightly longer than broad, length 0.4 and breadth 0.3 that of carapace; dorsal surface concave at base; lateral margin with three incised sharp teeth, margin between proximal and median spine clearly convex.

Pterygostomian flap rugose, with one distinct spine on upper margin near linea anomurica, with sparse short setae, anterior margin bluntly angular.

Sternum: Nearly as long as broad; lateral extremities gently divergent posteriorly. Third sternite triangular, longer than wide.

Abdomen: Somites 2–3 each with two uninterrupted transverse ridges on tergite, anterior ridge slightly more elevated than posterior ridge; somite 4 smooth or with posterior scale-like ridge; somites 5 and 6 smooth, posteromedian margin of somite 6 straight.

Eyes: Ocular peduncles as long as broad, maximal corneal diameter 0.7 of rostrum width.

Antennule: Article 1 with two well-developed distodorsal and distolateral mucronated spines, distodorsal larger. Ultimate article without a tuft of fine setae on distodorsal margin.

Antenna: Article 1 with strong distomesial spine barely reaching distal margin of article 3.

Mxp3: Ischium with minute spine on flexor distal margin. Merus as long as ischium; flexor margin with one strong spine; extensor margin with one distal spine. Carpus unarmed.

P1: Males 2.7–3.1 and females 1.8–1.9 times carapace length. Merus 0.8–0.9 length of carapace, 1.5 times as long as carpus, with some dorsomesial and a few ventromesial spines. Carpus 1.0–1.2 length of palm, 1.7–1.8 times as long as broad; dorsal surface with small spines or acute granules; mesial row of spines, median and distal spines strong. Palm 1.2 times as long as broad, a few acute granules along lateral and mesial margins. Fingers unarmed, 1.2 length of palm, each finger distally with two rows of teeth, spooned.

P2–4: With setose striae and some long plumose setae. P2 1.7 times carapace length. Meri successively shorter posteriorly (P3 merus 0.9 length of P2 merus; P4 merus 0.9–1.0 length of P3 merus); P2 merus 0.6 carapace length, 3.0 times as long as broad, 1.0–1.1 length of P2 propodus; P3 merus 2.5 times as long as broad, 1.1–1.2 length of P3 propodus; P4 merus 2.7 times as long as broad, 1.1–1.3 length of P4 propodus. Extensor margins of meri with row of three or four proximally diminishing small spines on P2–3, unarmed on P4; flexor margins distally ending in small spine followed proximally by several eminences; lateral sides unarmed. Carpi unarmed or with one or two minute spines on extensor margin; lateral surface with several acute granules sub-paralleling extensor margin on P2–4; flexor distal margin unarmed. P2–4 propodi 5.0–6.5 times as long as broad; extensor margin unarmed; flexor margin with four slender, movable spines on P2–4. Dactyli distally ending in well-curved strong spine, length 0.6 that of propodi.

Remarks
Coralliogalathea parva is closely related to *C. megalochira* from French Polynesia (see the differences under the Remarks for *C. megalochira*).

These species also presented the lowest genetic divergence among the species of *Coralliogalathea* (6.7% for *COI* and 2.4% for 16S). Average mean intraspecific distances were 1.3 and 0.6% for *COI* and 16S, respectively (Table 2).

Distribution

Mariana Islands, Papua New Guinea, Vanuatu, under rocks, sand and seagrass, 0–20 m.

CORALLIOGALATHEA TRIDENTIROSTRIS (MIYAKE, 1953) **COMB. NOV.**
(FIG. 11)

Galathea tridentirostris Miyake, 1953: 202, figs 3, 4.
Coralliogalathea humilis. – Baba & Javed, 1974: 62, fig. 1 [in part].

Dubious identification

Coralliogalathea humilis. – Baba, 1977: 250. – Baba, 1982: 61. – Takada *et al.*, 2009: 42. – Dong & Li, 2010: 34, figs 4, 5.

Material examined

Japan. Kabira, Ishigaki-jima, Ryukyu Islands, 17 February 1968 (coll. Nakasone): one ov. F, 1.4 mm (ZLKU 14528). – 21 February 1970 (coll. Keiji Baba): one M, 1.5 mm (MNHN-IU-2013-17395).

Philippines, Oriental Mindoro province. Puerto Galera, western corner of San Antonio Island, 13.523°N, 120.9473°E, 3–6 m, 7 April 2015: one F, 1 mm (UF43051).

Description

Carapace: 1.2–1.3 times broader than long; cervical groove distinct, laterally bifurcated; most ridges on gastric region interrupted or scale like; one scale-like
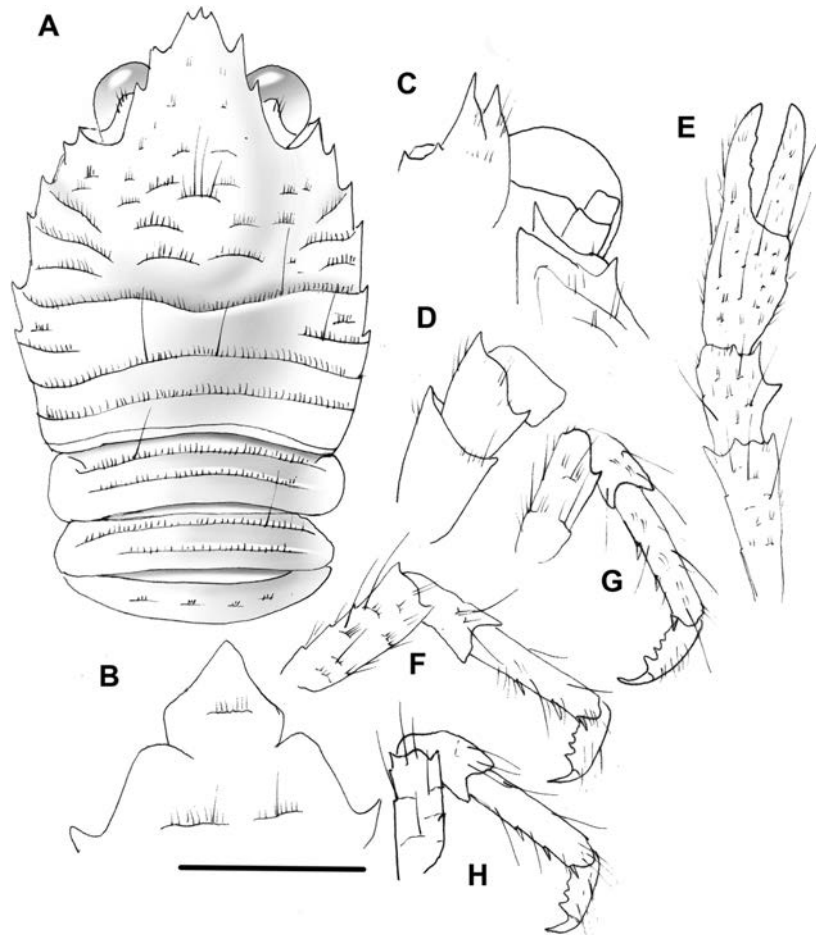
Figure 11. *Coralliogalathea tridentirostris* (Miyake, 1953), Japan, Ishigaki-jima, Ryukyu Islands, male, 1.5 mm (MNHN-IU-2013-17395). A, carapace and abdomen, dorsal view. B, thoracic sternites 3 and 4. C, left part of cephalothorax, ventral view, showing antennular and antennal peduncles, and anterior part of pterygostomian flap. D, right Mxp3, lateral view. E, left P1, dorsal view. F, right P2, lateral view. G, right P3, lateral view. H, right P4, lateral view. Scale bar: 1 mm in A, E–H; 2 mm in B–D.

epigastric ridge; two scale-like protogastric ridges, posterior ridge short, arcuate, with thick plumose setae; one mesogastric ridge, medially interrupted or scale like, not extending to anteriormost marginal branchial spines; one metagastric ridge, medially interrupted and not extending to anterior branchial ridges. Anterior branchial region with distinct ridges. Mid-transverse ridge usually uninterrupted, preceded by shallow cervical groove, followed by three transverse ridges, two of them uninterrupted. Lateral margins slightly convex medially, with five spines: one spine in front of and four spines behind anterior cervical groove; first spine anterolateral, small, at level of or slightly behind orbit, located at midlength between outer orbital spine and anteriormost spine of branchial margin, with small spine ventral to and between first and second; two spines on anterior branchial margin, and two spines on posterior branchial margin. Strong outer orbital spine; infraorbital margin with two strong spines. Rostrum spatulate, clearly wider than long, length 0.4 and breadth 0.3 that of carapace; dorsal surface concave at base; lateral margin with three incised sharp teeth, margin between proximal and median spines straight.

Pterygostomian flap rugose, with one distinct spine on upper margin near linea anomurica, with sparse short setae, anterior margin bluntly angular.

Sternum: Nearly as long as broad; lateral extremities gently divergent posteriorly. Third sternite triangular, as wide as long.

Abdomen: Somites 2–3 each with two uninterrupted transverse ridges on tergite, anterior ridge slightly more elevated than posterior ridge; somite 4 with posterior ridge scale like; somites 5 and 6 smooth, posteromedian margin of somite 6 straight.

Eyes: Ocular peduncles as long as broad, maximal corneal diameter 0.7 of rostrum width.

Antennule: Article 1 with two well-developed distodorsal and distolateral mucronated spines, distodorsal larger. Ultimate article without a tuft of fine setae on distodorsal margin.

Antenna: Article 1 with strong distomesial spine barely reaching distal margin of article 3.

Mxp3: Ischium with minute spine on flexor distal margin. Merus as long as ischium; flexor margin with one strong spine; extensor margin with one distal spine. Carpus unarmed.

P1: Female 2.2 times carapace length. Merus 0.5–0.6 length of carapace, 1.9 times as long as carpus, with some dorsomesial and a few ventromesial spines.

Carpus 1.0–1.1 length of palm, 1.7 times as long as broad; dorsal surface with small spines or acute granules; mesial row of spines, median spine strong. Palm 1.4 times as long as broad, with a few acute granules along lateral and mesial margins. Fingers unarmed, 1.2 length of palm, each finger distally with two rows of teeth, spooned.

P2–4: With setose striae and some long plumose setae. P2 1.6 times carapace length. Meri successively shorter posteriorly (P3 merus 0.9 length of P2 merus; P4 merus 0.9 length of P3 merus); P2 merus 0.5–0.6 carapace length, 3.5 times as long as broad, 1.0–1.2 length of P2 propodus; P3 merus 3.7 times as long as broad, 1.1–1.3 length of P3 propodus; P4 merus 3.5 times as long as broad, 1.0–1.2 length of P4 propodus. Extensor margins of meri with row of three or four proximally diminishing small spines on P2–3, unarmed on P4; flexor margins distally ending in small spine followed proximally by several eminences; lateral sides unarmed. Carpi unarmed on extensor margin; lateral surface with several acute granules sub-paralleling extensor margin on P2–4; flexor distal margin unarmed. P2–4 propodi 3.6–4.2 times as long as broad; extensor margin unarmed; flexor margin with three or four slender, movable spines on P2–4. Dactyli distally ending in well-curved strong spine, length 0.6 that of propodi.

Remarks
Coralliogalathea tridentirostris was first described by Miyake (1953) based on numerous specimens collected in Ishigaki-jima, Ryukyu Islands. Unfortunately, this material appears to be lost. We used new topotypic material (originally preserved in formalin) and material from Oriental Mindoro province (Phillipines) to redescribe the species. The material used for sequencing was collected from the Philippines and morphologically corresponds to the same species. The specimens examined have a different rostrum shape that is clearly wider than it is long; in the other species, the rostrum is as long as, or longer than, it is wide. *Coralliogalathea tridentirostris* also had higher genetic distances with respect to the other species, ranging from 14.1 to 15.1% for *COI* and from 12.2 to 15.5% for 16S (Table 2). However, additional molecular analyses of more specimens are needed to confirm the status of the species.

Distribution
Japan, Kabira, Ishigaki-jima, Ryukyu Islands; South China, Jinqing Island; Philippines, Oriental Mindoro province, subtidal. Specimens from the Ryukyu Islands were collected from coral rubble, mainly *Acropora* sp. (Takada *et al.*, 2009) and the basal portion of some species of *Seriatopora* (Baba & Javed, 1974).

DISCUSSION

SPECIES BOUNDARIES

The use of molecular techniques to analyse biodiversity has greatly increased the number of newly recognized taxa and, in taxonomic studies, has revealed a source of previously unnoticed variability in what are known as cryptic species (Hebert *et al.*, 2004; Bickford *et al.*, 2007; Puillandre *et al.*, 2011; Lajus *et al.*, 2015), constituting a powerful tool to establish species boundaries (Lefébure *et al.*, 2006). In squat lobsters, for instance, some genera are recognized as monospecific, whereas others consist of species complexes that contain more diversity than initially hypothesized (e.g. Cabezas *et al.*, 2011; Poore & Andreakis, 2011, 2012, 2014; Rodríguez-Flores *et al.*, 2017). In the case of *Coralliogalathea*, phylogenetic analyses have revealed six ancient lineages that are genetically well defined and reciprocally monophyletic. These six lineages correspond to six subtly different morphotypes. Therefore, we consider these lineages as independent species under the evolutionary species concept (Wiley, 1978): they each have their own identity, share a common ancestor and possess unique evolutionary fates. Notably, in the case of *C. joae*, its wide distributional range (from Madagascar to Vanuatu) suggests the possibility of hidden biodiversity. Sequencing of more material is needed to gain a better understanding of its taxonomic status.

Divergences between *Coralliogalathea* species are, in general, comparable with those observed for other squat lobster species (e.g. Machordom & Macpherson, 2004; Macpherson & Machordom, 2005; Cabezas *et al.*, 2009, 2012); however, in some cases, higher divergences are observed, even more than those observed between other Galatheoidea species. Reported *COI* divergences (as uncorrected p-distances) for species in the Galatheidae family range from 5 to 16%. The synonymous substitutions and nonsynonymous values observed for *Coralliogalathea* were similar to those seen among congeneric crustaceans such as copepods (Bucklin *et al.*, 1999) and consistent with rates observed in comparisons of functional genes. Divergence values for 16S are usually lower than those for *COI* by a third to a half (Cabezas *et al.*, 2011; Macpherson & Robainas-Barcia, 2013, 2015) owing to the faster molecular evolution of the protein-encoding *COI* gene (Hebert *et al.*, 2003). However, an extreme case of slowdown in the substitution rate of 16S was recently reported between species of *Fennerogalathea* (Rodríguez-Flores *et al.*, 2017). In the case of *Coralliogalathea*, the 16S sequences showed high levels of divergence. For instance, divergences between *C. joae* and the other species exceed the average divergence

for 16S observed between other Galatheidae species (Cabezas *et al.*, 2011; Macpherson & Robainas-Barcia, 2013, 2015). Molecular divergences between some *Coralliogalathea* species even exceed those observed between different genera within the Galatheidae family (e.g. *Lauriea–Macrothea–Triodonthea*; see Macpherson & Robainas-Barcia, 2013). Heterogeneity in divergence values has been reported for some species of the family Munididae; in these cases, it was hypothesized to be a consequence of different radiation events that modified patterns of diversification (Machordom & Macpherson, 2004; Cabezas *et al.*, 2009).

The mitochondrial markers *COI* and 16S are commonly used to help set molecular thresholds at lower taxonomic levels and, more specifically, to delimit species (Lefébure *et al.*, 2006). Although nuclear ribosomal markers are considered most informative at higher taxonomic levels, in our case and as was seen for some *Eumunida* species (Puillandre *et al.*, 2011), the 28S marker was also able to distinguish some of the *Coralliogalathea* species. This marker has been used to infer deeper phylogenetic relationships of squat lobsters (Cabezas *et al.*, 2012), but its efficacy in species delimitation has not yet been tested.

MORPHOLOGICAL DIFFERENTIATION

Previous studies have highlighted patterns of extreme morphological conservatism and morphological convergence in squat lobsters (Machordom & Macpherson, 2004; Baba, 2005; Jones & Macpherson, 2007; Cabezas *et al.*, 2009; Puillandre *et al.*, 2011; Poore & Andreakis, 2012, 2014). Genetically divergent morphotypes that are under some degree of morphological stasis are frequent among some Munididae species (Machordom & Macpherson, 2004; Cabezas *et al.*, 2009). Macpherson & Robainas-Barcia (2015) also documented the existence of several cryptic species in their revision of the Indo-Pacific species of the genus *Galathea*. The reported increase of cryptic diversity in squat lobsters is likely to be attributable, in part, to the following factors: (1) the difficulty of finding diagnostic characters as a consequence of the morphological stasis of the group; (2) the lack of detailed taxonomic work for some understudied genera; and (3) incomplete sampling (Machordom & Macpherson, 2004; Cabezas *et al.*, 2012; Lajus *et al.*, 2015).

In the present study, we attempted to address cryptic diversity within *Coralliogalathea* using both molecular and morphological approaches. We found subtle differences among morphological characters in the described *Coralliogalathea* species, particularly in the rostrum, carapace, pereiopods, third sternite and abdominal

segment ridges. The shape and relative length of the rostrum have proved to be useful characters for species differentiation in related squat lobsters (e.g. *Allogalathea*; Cabezas *et al.*, 2011; *Fennerogalathea*; Rodríguez-Flores *et al.*, 2017). The relative length and width of the pereiopod merus has also been a valuable character to discriminate between species of *Galathea* and *Allogalathea* (Cabezas *et al.*, 2011; Macpherson & Robainas-Barcia, 2015). Other variable characters observed between *Coralliogalathea* species include differences in the pattern of the metagastric ridge on the carapace, which is medially uninterrupted in *C. humilis* and usually interrupted in the other species. However, these types of morphological characters are not discrete; variation among species is very subtle and may overlap and, in most cases, the variations lack phylogenetic value (Machordom & Macpherson, 2004), although this might differ across different taxa. However, *C. joae* might represent an exception, because it is the most morphologically differentiated species within the genus, and it can be distinguished from the others by the presence of an additional spine on the margin of the rostrum.

Morphological stasis can be a consequence of recent speciation events, in which phenotypic changes do not keep pace with rapid genetic divergences (Crivellaro *et al.*, 2018). In contrast, morphological conservatism within species can result from maintained selection to a specific environment (Estes & Arnold, 2007). In squat lobsters, morphological stasis seems to be an inherent evolutionary feature of the group. This stasis is likely to be associated with genetic or developmental constraints rather than as a consequence of adaptations to a particular environment, because it has been observed in both shallow-water and deep-sea taxa, including those associated with chemosynthetic environments (Baba *et al.*, 2008; Cabezas *et al.*, 2012; Palero *et al.*, 2017).

In some instances, coloration patterns can be used to distinguish different squat lobster species (Macpherson & Machordom, 2001; Poore & Andreakis, 2012, 2014; Macpherson & Robainas-Barcia, 2013). However, colour can vary greatly within populations (Cabezas *et al.*, 2011). In *Coralliogalathea*, we observed intraspecific coloration variability (Fig. 5), which is likely to be associated with being coral cryptofauna (Peyrot-Clausade, 1989; Takada *et al.*, 2009). An environmental influence over colour patterns is common in other crustacean symbionts of macroinvertebrates (Zmarzly, 1990). Hence, as a coral symbiont, the colour pattern of *Coralliogalathea* might depend on local adaptations to the surrounding environment, e.g. using it as a disguise to blend in with the coral colonies (Enochs, 2012). With respect to sexual dimorphism in *Coralliogalathea*, we observed that the size of male

chelipeds is much larger (~1.3–1.8 times) than those of females (see Fig. 5). However, as Baba *et al.* (2011) pointed out, most squat lobsters show clear P1 differences between males and females.

MOLECULAR SYSTEMATICS OF *CORALLIOGALATHEA*

The taxonomy of squat lobsters was reorganized after recent phylogenetic studies (Ahyong *et al.*, 2009, 2010; Schnabel & Ahyong, 2010; Schnabel *et al.*, 2011a; Bracken-Grissom *et al.*, 2013). However, Galatheidae genera *sensu* Ahyong *et al.* (2010) have, thus far, been poorly represented in molecular phylogenies of Galatheoidea, because only a few genera have been analysed. Moreover, very few studies of the phylogenetic relationships of squat lobsters have been reported in the time since Bracken-Grissom *et al.* (2013) published their phylogeny of Anomura based on molecular and morphological data. Recent phylogenetic reconstructions have primarily focused on exploring the evolutionary history of and solving relationships among species at the genus level (McCallum *et al.*, 2016; Palero *et al.*, 2017). *Coralliogalathea* is currently classified as a genus of Galatheidae (Ahyong *et al.*, 2010; Macpherson & Baba, 2011). A triangular- or subtriangular-shaped rostrum that is broad at the base and the absence of supraorbital spines are synapomorphies shared with other Galatheidae genera (Macpherson & Baba, 2011). Our molecular results support both the inclusion of *Coralliogalathea* within Galatheidae and a clade composed of *Galathea*, *Allogalathea* and *Fennerogalathea*. Taken together, these findings suggest that the morphological characters defining this family have phylogenetic value (Ahyong *et al.*, 2010; Macpherson & Baba, 2011).

However, on the basis of morphology, the most closely related genus to *Coralliogalathea* may be *Phylladiorhynchus* (genus currently under revision), a hypothesis supported by the absence of the first pair of gonopods (G1) in males of both genera (Tirmizi & Javed, 1980; Macpherson & Baba, 2011). Although some *Galathea* species also lack the first pair of gonopods, the majority of species have it (Macpherson & Robainas-Barcia, 2015). Morphological and molecular revision of these and other Galatheidae genera will help to elucidate the sister group of *Coralliogalathea*.

Coralliogalathea appears to be a deeply divergent lineage within Galatheidae. The length of the branch leading to the *Coralliogalathea* lineage is much longer than those of branches leading to other Galatheoidea genera (Fig. 2). Heterogeneity in branch lengths could indicate that the diversification of the genus occurred while the extinction rate was high (Machordom & Macpherson, 2004). Alternatively, the rate of molecular evolution in *Coralliogalathea* lineages might have

changed drastically during their evolutionary history compared with other taxa. If this were the case, a pattern of rapid molecular substitution could have caused branch length heterogeneity. Accelerated rates of substitution among different lineages is commonly observed in crustaceans (Lefébure *et al.*, 2006; Crivellaro *et al.*, 2018) and in other invertebrate taxa (Moussalli & Herbert, 2016; Coppard & Lessios, 2017). Curiously, long branches are associated with lineages composed mainly of shallow-water taxa (Galatheidae) rather than deep-sea taxa (Munidopsidae and Munididae), suggesting decelerated evolution of deep-sea squat lobsters (see Fig. 2). We tested for the presence of potential rate shifts in clades along the phylogenetic tree by comparing the adequacy of two different molecular clocks (uncorrelated and random local) for our dataset. Although not conclusive, the results indicated a heterogeneous distribution of changes in rate shifts along the tree (uncorrelated clock), which did not appear to be related to any special characteristics of the taxa (e.g. shallow-water squat lobsters). Nevertheless, *Coralliogalathea* might have experienced accelerated evolutionary rates as a result of the cryptofauna lifestyle. A proper and explicit comparative study would be needed to analyse patterns of substitution across genetic markers and among species and their relationship to diversification trends in squat lobsters.

Divergence time estimation and evolutionary history of *Coralliogalathea*

The origin of diversification of some galatheoid squat lobsters was estimated to be during the Middle or Late Miocene, e.g. for *Munida* and *Allogalathea*, or early Oligocene for *Paramunida* (Machordom & Macpherson, 2004; Cabezas et al., 2011, 2012). However, we estimated that lineages within *Coralliogalathea* began to diversify much earlier, probably during the Eocene, compared with the other Galatheoidea mitochondrial lineages analysed. Our test did not support that abrupt and sustained rate shifts of molecular rate evolution occurred in *Coralliogalathea* in comparison with other Galatheoidea genera. Therefore, the genus is likely to represent an early divergent lineage within the superfamily. Comparisons of the estimated emergence of the lineages within *Coralliogalathea* with that of other Galatheiodea genera (Fig. 3) show, for instance, that the diversification events giving rise to *Raymunida*, *Paramunida* and *Lauriea* occurred later than the origin of diversification of *Coralliogalathea*. Even the TMRCA of *Macrothea* and *Allogalathea* occurred later than some of the *Coralliogalathea* species. However, Palero *et al.* (2017) reported older estimations for the diversification of the genera *Lauriea* and *Sadayoshia*

compared with our study. Differences in datasets and calibration methods probably account for the disparity. Furthermore, according to recent studies showing large differences in rates among clades, assuming a universal rate of substitution for mitochondrial DNA may lead to erroneous estimations (e.g. Coppard & Lessios, 2017). Therefore, in the present study, we used multiple calibrations based on fossil estimations, and previously reported diversification time estimations for several Galatheoidea genera (Cabezas *et al.*, 2012; Bracken-Grissom *et al.*, 2013; Davis *et al.*, 2016). Nevertheless, given the differences between our estimations and those of previous studies (Bracken-Grissom *et al.*, 2013, Davis *et al.*, 2016; Palero *et al.*, 2017), and the possibility that positions could be saturated by multiple substitutions in our mitochondrial DNA genealogy (Goldman, 1998), we have interpreted our results cautiously.

According to Rivas (1964), species are considered sympatric if they are related and have shared or overlapping distributions without the need to occupy the same macrohabitat. *Coralliogalathea* represents a very singular case because three of the taxa (*C. parva*, *C. minuta* and *C. joae*), displaying very subtle morphological variations, coexist in the same area (Vanuatu, Santo). Possible evolutionary scenarios that might explain the sympatric distribution of these species include the following: (1) recent colonization resulting from the expansion of a distribution area; and (2) local adaptations (specific adaptations to differences in environmental conditions) that led to sympatric speciation. Secondary contact can be accompanied by hybridization and interbreeding between evolutionary units when speciation is an incomplete or a very recent process. Congruence between our mitochondrial and nuclear phylogenetic reconstructions implies that gene flow between the *Coralliogalathea* lineages does not occur. Mitonuclear discordance would, otherwise, have been observed (e.g. Perea *et al.*, 2016). Thus, reproductive isolation between *C. joae*, *C. minuta* and *C. parva* seems to be complete. In contrast, if these sympatric species had arisen by ecological speciation, we would expect them to form a monophyletic group, which is not the case. Therefore, a more likely scenario is secondary contact as a consequence of the expansion of the distribution area of *Coralliogalathea* species following the allopatric evolution of evolutionary units. Alternatively, a very old sympatric speciation event could have occurred accompanied by multiple extinctions that resulted in ancient lineages that do not display sister group relationships or direct ancestry. More detailed sampling is necessary to discriminate between these hypotheses.

In contrast to the sympatric species in Vanuatu, the sister species *C. humilis* and *C. minuta* occur in

disparate geographical areas. Based on the biogeographical areas (Spalding *et al.*, 2007; Schnabel *et al.*, 2011b), *C. humilis* occurs in the western Indo-Pacific (Madagascar and the Red Sea) and *C. minuta* in the central Indo-Pacific (tropical southwest Pacific). These species are likely to have originated as a consequence of an allopatric speciation event that, according to our estimations, occurred during the Early Miocene. The sister species *C. megalochira* and *C. parva* also have an allopatric distribution: *C. megalochira* occurs in the eastern Indo-Pacific (southeast Polynesia) and *C. parva* in the central Indo-Pacific (eastern Coral Triangle and the tropical southwest Pacific). The speciation event leading to these two species occurred more recently, probably during the Upper Miocene. These findings are consistent with proposed diversification events in other squat lobsters during the Middle or Upper Miocene (Machordom & Macpherson, 2004; Cabezas *et al.*, 2011). High tectonic activity during this period and the appearance of new available habitats might have accounted for the rapid diversification of shallow-water taxa in the central Indo-Pacific (Williams & Duda, 2008). Furthermore, a correlation between diversification rates and global cooling and warming has recently been discovered among anomuran decapods, which indicated increased speciation in *Munida* during cooler temperatures (Davis *et al.*, 2016).

The central Indo-Pacific is a well-recognized area of diversification of squat lobsters (Machordom & Macpherson 2004; Macpherson *et al.*, 2010; Schnabel *et al.*, 2011b; Cabezas *et al.*, 2012) and constitutes a biodiversity hotspot for shallow-water marine taxa (Bowen *et al.*, 2013). Indeed, the first appearance of shallow-water squat lobsters (e.g. *Lauriea* and *Sadayoshia*) occurred in the tropical southwest Pacific (Cabezas *et al.*, 2011; Palero *et al.*, 2017). *Coralliogalathea* species appear to have the same pattern, particularly considering that the taxonomic richness of this genus is highest in this area. In contrast, deep-sea squat lobsters follow a different pattern of species diversity (Macpherson *et al.*, 2010). The influence of environmental heterogeneity and biotic factors on the biogeographical patterns of squat lobsters still needs to be determined in more detail. In order to address this and other hypotheses related to the biogeography and diversification of squat lobsters, an increase in sampling of more localities is essential.

ACKNOWLEDGEMENTS

REFERENCES

Ahyong ST, Baba K, Macpherson E, Poore GCB. 2010. A new classification of the Galatheoidea (Crustacea: Decapoda: Anomura). *Zootaxa* **2676:** 57–68.

Ahyong ST, Schnabel KE, Maas EW. 2009. Anomuran phylogeny: new insights from molecular data. In: Martin JW, Crandall KA, Felder DL, eds. *Crustacean issues, decapod crustacean phylogenetics*, *Vol.* **18**. Boca Raton: CRC Press, 399–414.

Baba K. 1977. Biological results of the Snellius Expedition XXVIII. The galatheid Crustacea of the Snellius Expedition. *Zoologische Mededelingen, Leiden* **50:** 243–259.

Baba K. 1982. Galatheids and pagurids of the Palau Islands (Crustacea: Anomura). *Proceedings of the Japanese Society of Systematic Zoology* **23:** 56–70.

Baba K. 2005. Deep-sea chirostylid and galatheid crustaceans (Decapoda: Anomura) from the Indo-West Pacific, with a list of species. *Galathea Reports* **20:** 1–317.

Baba K, Ahyong ST, Macpherson E. 2011. Morphology of the marine squat lobsters. In: Poore GCB, Ahyong ST, Taylor J, eds. *The biology of squat lobsters*. Melbourne: CSIRO Publishing and Boca Raton: CRC Press, 1–37.

Baba K, Javed W. 1974. *Coralliogalathea*, a new genus of Galatheidae (Crustacea, Anomura), with further notes on its type-species. *Annotationes Zoologicae Japonenses* **47:** 61–64.

Baba K, Macpherson E, Lin CW, Chan TY. 2009. *Crustacean fauna of Taiwan. Squat lobsters (Chirostylidae and Galatheidae)*. Keelung: National Taiwan Ocean University.

Baba K, Macpherson E, Poore GCB, Ahyong ST, Bermudez A, Cabezas P, Lin CW, Nizinski M, Rodrigues C, Schnabel KE. 2008. Catalogue of squat lobsters of the world (Crustacea: Decapoda: Anomura – families Chirostylidae, Galatheidae and Kiwaidae). *Zootaxa* **1905:** 1–220.

Bickford D, Lohman DJ, Sodhi NS, Ng PK, Meier R, Winker K, Ingram KK, Das I. 2007. Cryptic species as a window on diversity and conservation. *Trends in Ecology & Evolution* **22:** 148–155.

Bowen BW, Rocha LA, Toonen RJ, Karl SA; ToBo Laboratory. 2013. The origins of tropical marine biodiversity. *Trends in Ecology & Evolution* **28:** 359–366.

Bracken-Grissom HD, Cannon ME, Cabezas P, Feldmann RM, Schweitzer CE, Ahyong ST, Felder DL, Lemaitre R, Crandall KA. 2013. A comprehensive and integrative reconstruction of evolutionary history for Anomura (Crustacea: Decapoda). *BMC Evolutionary Biology* **13:** 128.

Bucklin A, Guarnieri M, Hill RS, Bentley AM, Kaartvedt S. 1999. Taxonomic and systematic assessment of planktonic copepods using mitochondrial COI sequence variation and competitive, species-specific PCR. *Hydrobiologia* **401:** 239–254.

Cabezas P, Macpherson E, Machordom A. 2009. Morphological and molecular description of new species of squat lobster (Crustacea: Decapoda: Galatheidae) from the Solomon and Fiji Islands (South-West Pacific). *Zoological Journal of the Linnean Society* **156:** 465–493.

Cabezas P, Macpherson E, Machordom A. 2011. *Allogalathea* (Decapoda: Galatheidae): a monospecific genus of squat lobster? *Zoological Journal of the Linnean Society* **162:** 245–270.

Cabezas P, Sanmartín I, Paulay G, Macpherson E, Machordom A. 2012. Deep under the sea: unraveling the evolutionary history of the deep-sea squat lobster *Paramunida* (Decapoda, Munididae). *Evolution* **66:** 1878–1896.

Coppard SE, Lessios HA. 2017. Phylogeography of the sand dollar genus *Encope*: implications regarding the Central American Isthmus and rates of molecular evolution. *Scientific Reports* **7:** 11520.

Crandall KA, Fitzpatrick JF. 1996. Crayfish molecular systematics: using a combination of procedures to estimate phylogeny. *Systematic Biology* **45:** 1–26.

Crisp MD, Hardy NB, Cook LG. 2014. Clock model makes a large difference to age estimates of long-stemmed clades with no internal calibration: a test using Australian grasstrees. *BMC Evolutionary Biology* **14:** 263.

Crivellaro MS, Zimmermann BL, Bartholomei-Santos ML, Crandall KA, Pérez-Losada M, Bond-Buckup G, Santos S. 2018. Looks can be deceiving: species delimitation reveals hidden diversity in the freshwater crab *Aegla longirostri* (Decapoda: Anomura). *Zoological Journal of the Linnean Society* **182:** 24–37.

Darriba D, Taboada GL, Doallo R, Posada D. 2012. jModelTest 2: more models, new heuristics and parallel computing. *Nature Methods* **9:** 772.

Davis KE, Hill J, Astrop TI, Wills MA. 2016. Global cooling as a driver of diversification in a major marine clade. *Nature Communications* **7:** 13003.

Doflein F, Balss H. 1913. Die Galatheiden der Deutschen Tiefsee-Expedition. *Wissenschaftliche Ergebnisse der Deutschen Tiefsee-Expedition auf dem Dampfer "Valdivia" 1898–1899* **20:** 125–184.

Dong C, Li XZ. 2010. First records of six galatheid species (Crustacea: Decapoda: Anomura) from Chinese waters. *Zootaxa* **2343:** 31–44.

Drummond AJ, Ho SY, Phillips MJ, Rambaut A. 2006. Relaxed phylogenetics and dating with confidence. *PLoS Biology* **4:** e88.

Drummond AJ, Rambaut A. 2007. BEAST: Bayesian evolutionary analysis by sampling trees. *BMC Evolutionary Biology* **7:** 214.

Drummond AJ, Suchard MA, Xie D, Rambaut A. 2012. Bayesian phylogenetics with BEAUti and the BEAST 1.7. *Molecular Biology and Evolution* **29:** 1969–1973.

Enochs IC. 2012. Motile cryptofauna associated with live and dead coral substrates: implications for coral mortality and framework erosion. *Marine Biology* **159:** 709–722.

Estes S, Arnold SJ. 2007. Resolving the paradox of stasis: models with stabilizing selection explain evolutionary divergence on all timescales. *The American Naturalist* **169:** 227–244.

Folmer O, Black M, Hoeh W, Lutz R, Vrijenhoek R. 1994. DNA primers for amplification of mitochondrial cytochrome *c* oxidase subunit I from diverse metazoan invertebrates. *Molecular Marine Biology and Biotechnology* **3:** 294–299.

Geller J, Meyer C, Parker M, Hawk H. 2013. Redesign of PCR primers for mitochondrial cytochrome *c* oxidase subunit I for marine invertebrates and application in all-taxa biotic surveys. *Molecular Ecology Resources* **13:** 851–861.

Goldman N. 1998. Phylogenetic information and experimental design in molecular systematics. *Proceedings of the Royal Society B: Biological Sciences* **265:** 1779–1786.

Guindon S, Gascuel O. 2003. A simple, fast, and accurate algorithm to estimate large phylogenies by maximum likelihood. *Systematic Biology* **52:** 696–704.

Hebert PD, Cywinska A, Ball SL. 2003. Biological identifications through DNA barcodes. *Proceedings of the Royal Society B: Biological Sciences* **270:** 313–321.

Hebert PD, Penton EH, Burns JM, Janzen DH, Hallwachs W. 2004. Ten species in one: DNA barcoding reveals cryptic species in the neotropical skipper butterfly *Astraptes fulgerator*. *Proceedings of the National Academy of Sciences of the United States of America* **101:** 14812–14817.

Ho SY, Phillips MJ. 2009. Accounting for calibration uncertainty in phylogenetic estimation of evolutionary divergence times. *Systematic Biology* **58:** 367–380.

Jones WJ, Macpherson E. 2007. Molecular phylogeny of the East Pacific squat lobsters of the genus *Munidopsis* (Decapoda: Galatheidae) with the descriptions of seven new species. *Journal of Crustacean Biology* **27:** 698–698.

Katoh K, Misawa K, Kuma K, Miyata T. 2002. MAFFT: a novel method for rapid multiple sequence alignment based on fast Fourier transform. *Nucleic Acids Research* **30:** 3059–3066.

Lajus D, Sukhikh N, Alekseev V. 2015. Cryptic or pseudocryptic: can morphological methods inform copepod taxonomy? An analysis of publications and a case study of the *Eurytemora affinis* species complex. *Ecology and Evolution* **5:** 2374–2385.

Lanfear R, Calcott B, Ho SY, Guindon S. 2012. PartitionFinder: combined selection of partitioning schemes and substitution models for phylogenetic analyses. *Molecular Biology and Evolution* **29:** 1695–1701.

Lefébure T, Douady CJ, Gouy M, Gibert J. 2006. Relationship between morphological taxonomy and molecular divergence within Crustacea: proposal of a molecular threshold to help species delimitation. *Molecular Phylogenetics and Evolution* **40:** 435–447.

Lewinsohn C. 1969. Die Anomuren des Roten Meeres (Crustacea Decapoda: Paguridea, Galatheidea, Hippidea). *Zoologische Verhandelingen Uitgegeven Door Het Rijksmuseum Van Natuurlijke Historie Te Leiden* **104:** 1–213.

Machordom A, Araujo R, Erpenbeck D, Ramos MÁ. 2003. Phylogeography and conservation genetics of endangered European Margaritiferidae (Bivalvia: Unionoidea). *Biological Journal of the Linnean Society* **78:** 235–252.

Machordom A, Macpherson E. 2004. Rapid radiation and cryptic speciation in galatheid crabs of the genus *Munida* (Crustacea, Decapoda) and related genera in the South West Pacific: molecular and morphological evidence. *Molecular Phylogenetics and Evolution* **33:** 259–279.

Macpherson E, Baba K. 2011. Taxonomy of squat lobsters. In: Poore GCB, Ahyong ST, Taylor J, eds. *The biology of squat lobsters*. Melbourne: CSIRO Publishing and Boca Raton: CRC Press, 39–71.

Macpherson E, de Forges BR, Schnabel KE, Samadi S, Boisselier MC, Garcia-Rubies A. 2010. Biogeography of the deep-sea galatheid squat lobsters of the Pacific Ocean. *Deep Sea Research Part I: Oceanographic Research Papers* **57:** 228–238.

Macpherson E, Machordom A. 2001. Phylogenetic relationships of species of *Raymunida* (Decapoda: Galatheidae) based on morphology and mitochondrial cytochrome oxidase sequences, with the recognition of four new species. *Journal of Crustacean Biology* **21:** 696–714.

Macpherson E, Machordom A. 2005. Use of morphological and molecular data to identify three new sibling species of the genus *Munida* Leach, 1820 (Crustacea, Decapoda, Galatheidae) from New Caledonia. *Journal of Natural History* **39:** 819–834.

Macpherson E, Robainas-Barcia A. 2013. A new genus and some new species of the genus *Lauriea* Baba, 1971 (Crustacea, Decapoda, Galatheidae) from the Pacific and Indian Oceans, using molecular and morphological characters. *Zootaxa* **3599:** 136–160.

Macpherson E, Robainas-Barcia A. 2015. Species of the genus *Galathea* Fabricius, 1793 (Crustacea, Decapoda, Galatheidae) from the Indian and Pacific Oceans, with descriptions of 92 new species. *Zootaxa* **3913:** 1–335.

Macpherson E, Rodríguez-Flores PC, Machordom A. 2017. New sibling species and new occurrences of squat lobsters (Crustacea, Decapoda) from the western Indian Ocean. *European Journal of Taxonomy* **343:** 1–61.

McCallum AW, Cabezas P, Andreakis N. 2016. Deep-sea squat lobsters of the genus *Paramunida* Baba, 1988 (Crustacea: Decapoda: Munididae) from north-western Australia: new records and description of three new species. *Zootaxa* **4173:** 201–224.

Miyake S. 1953. On three new species of *Galathea* from the Western Pacific. *Journal of the Faculty of Agriculture* **10:** 199–208.

Moussalli A, Herbert DG. 2016. Deep molecular divergence and exceptional morphological stasis in dwarf cannibal snails *Nata sensu lato* Watson, 1934 (Rhytididae) of southern Africa. *Molecular Phylogenetics and Evolution* **95:** 100–115.

Nobili G. 1905. Diagnoses préliminaires de 34 espèces et variétes nouvelles et de 2 genres nouveaux de Décapodes de la Mer Rouge. *Bulletin du Muséum National d'Histoire Naturelle, Paris* **11:** 393–411.

Nobili G. 1906a. Faune carcinologique de la Mer Rouge. Décapodes et Stomatopodes. *Annales des Sciences Naturelles* **4:** 1–347.

Nobili G. 1906b. Diagnoses préliminaires de Crustacés, Décapodes et Isopodes nouveaux recueillis par M. le Dr G. Seurat aux îles Toumotou. *Bulletin du Muséum National d'Histoire Naturelle, Paris* **5:** 256–270.

Nobili G. 1907. Ricerche sui Crostacei della Polinesia. Decapodi, Stomatopodi, Anisopodi e Isopodi. *Memorie della Reale Accademia della Scienze di Torino Serie 2* **57:** 351–430.

Pacioni C, Hunt H, Allentoft ME, Vaughan TG, Wayne AF, Baynes A, Haouchar D, Dortch J, Bunce M. 2015. Genetic diversity loss in a biodiversity hotspot: ancient DNA quantifies genetic decline and former connectivity in a critically endangered marsupial. *Molecular Ecology* **24:** 5813–5828.

Palero F, Crandall KA, Abelló P, Macpherson E, Pascual M. 2009. Phylogenetic relationships between spiny, slipper and coral lobsters (Crustacea, Decapoda, Achelata). *Molecular Phylogenetics and Evolution* **50:** 152–162.

Palero F, Robainas-Barcia A, Corbari L, Macpherson E. 2017. Phylogeny and evolution of shallow-water squat lobsters (Decapoda, Galatheoidea) from the Indo-Pacific. *Zoologica Scripta* **46:** 584–595.

Palumbi SR, Martin AP, Romano S, McMillan WO, Stice L, Grabowski G. 1991. *The simple fool's guide to PCR*. Honolulu: Special Publishing Department of Zoology, University of Hawaii.

Perea S, Vukić J, Šanda R, Doadrio I. 2016. Ancient mitochondrial capture as factor promoting mitonuclear discordance in freshwater fishes: a case study in the genus *Squalius* (Actinopterygii, Cyprinidae) in Greece. *PloS One* **11:** e0166292.

Peyrot-Clausade M. 1989. Crab cryptofauna (Brachyura and Anomura) of Tikehau, Tuamotu Archipelago, French Polynesia. *Coral Reefs* **8:** 109–117.

Poore GC, Andreakis N. 2011. Morphological, molecular and biogeographic evidence support two new species

in the *Uroptychus naso* complex (Crustacea: Decapoda: Chirostylidae). *Molecular Phylogenetics and Evolution* **60:** 152–169.

Poore GCB, Andreakis N. 2012. The *Agononida incerta* species complex unravelled (Crustacea: Decapoda: Anomura: Munididae). *Zootaxa* **3492:** 1–29.

Poore GC, Andreakis N. 2014. More species of the *Agononida incerta* complex revealed by molecules and morphology (Crustacea: Decapoda: Anomura: Munididae). *Zootaxa* **3860:** 201–225.

Poupin J. 1996. Crustacea decapoda of French Polynesia (Astacidea, Palinuridea, Anomura, Brachyura). *Atoll Research Bulletin* **442:** 1–114.

Puillandre N, Macpherson E, Lambourdière J, Cruaud C, Boisselier-Dubayle MC, Samadi S. 2011. Barcoding type specimens helps to identify synonyms and an unnamed new species in *Eumunida* Smith, 1883 (Decapoda: Eumunididae). *Invertebrate Systematics* **25:** 322–333.

Rambaut A. 2012. *FigTree v1.4.* Available at: http://tree.bio.ed.ac.uk/software/figtree/

Richer de Forges B, Chan TY, Corbari L, Lemaitre R, Macpherson E, Ahyong ST, Ng PKL. 2013. The MUSORSTOM-TDSB deep-sea benthos exploration program (1976–2012): an overview of crustacean discoveries and new perspectives on deep-sea zoology and biogeography. In: Ahyong ST, Chan T-Y, Corbari L, Ng PKL, eds. *Tropical Deep-Sea Benthos 27. Mémoires du Muséum National d'Histoire Naturelle* **204:** 13–66.

Rivas LR. 1964. A reinterpretation of the concepts "Sympatric" and "Allopatric" with proposal of the additional terms "Syntopic" and "Allotopic". *Systematic Zoology* **13:** 42–43.

Robins CM, Feldmann RM, Schweitzer CE. 2013. Nine new genera and 24 new species of the Munidopsidae (Decapoda: Anomura: Galatheoidea) from the Jurassic Ernstbrunn Limestone of Austria, and notes on fossil munidopsid classification. *Annalen des Naturhistorischen Museums in Wien* **A115:** 167–251.

Rodríguez-Flores PC, Machordom A, Macpherson E. 2017. Three new species of squat lobsters of the genus *Fennerogalathea* Baba, 1988 (Decapoda: Galatheidae) from the Pacific Ocean. *Zootaxa* **4276:** 46–60.

Rodríguez-Flores PC, Macpherson E, Machordom A. 2018. Three new species of squat lobsters of the genus *Munidopsis* Whiteaves, 1874, from Guadeloupe Island, Caribbean Sea (Crustacea, Decapoda, Munidopsidae). *Zootaxa* **4422:** 569–580.

Ronquist F, Huelsenbeck JP. 2003. MrBayes 3: Bayesian phylogenetic inference under mixed models. *Bioinformatics* **19:** 1572–1574.

Rozas J, Ferrer-Mata A, Sánchez-DelBarrio JC, Guirao-Rico S, Librado P, Ramos-Onsins SE, Sánchez-Gracia A. 2017. DnaSP 6: DNA sequence polymorphism analysis of large data sets. *Molecular Biology and Evolution* **34:** 3299–3302.

Schnabel KE, Ahyong ST. 2010. A new classification of the Chirostyloidea (Crustacea: Decapoda: Anomura). *Zootaxa* **2687:** 56–64.

Schnabel KE, Ahyong ST, Maas EW. 2011a. Galatheoidea are not monophyletic – molecular and morphological phylogeny of the squat lobsters (Decapoda: Anomura) with recognition of a new superfamily. *Molecular Phylogenetics and Evolution* **58:** 157–168.

Schnabel KE, Cabezas P, McCallum A, Macpherson E, Ahyong ST, Baba K. 2011b. Worldwide distribution patterns of squat lobsters. In: Poore GCB, Ahyong ST, Taylor J, eds. *The biology of squat lobsters*. Melbourne: CSIRO Publishing and Boca Raton: CRC Press, 149–182.

Spalding MD, Fox HE, Allen GR, Davidson N, Ferdaña ZA, Finlayson MAX, Halpern BS, Jorge MA, Lombana AL, Lourie SA, Martin KD. 2007. Marine ecoregions of the world: a bioregionalization of coastal and shelf areas. *BioScience* **57:** 573–583.

Swofford DL. 2002. *PAUP*: phylogeny analysis using parsimony (*and other methods). Version 4.0b10*. Sunderland: Sinauer Associates.

Takada Y, Abe O, Shibuno T. 2009. Population structure of two galatheid species (*Galathea mauritiana* and *Coralliogalathea humilis*) inhabiting interstices of coral rubble. *Crustacean Research* **38:** 42–54.

Tirmizi NM, Javed W. 1980. Two new species and one new record of *Phylladiorhynchus* Baba from the Indian Ocean (Decapoda, Galatheidae). *Crustaceana* **39:** 255–262.

Tirmizi NM, Javed W. 1993. *Indian Ocean galatheids (Crustacea: Anomura)*. Karachi: Marine Reference Collection and Resource Centre, University of Karachi.

Whiting MF. 2002. Mecoptera is paraphyletic: multiple genes and phylogeny of Mecoptera and Siphonaptera. *Zoologica Scripta* **31:** 93–104.

Wiley EO. 1978. The evolutionary species concept reconsidered. *Systematic Zoology* **27:** 17–26.

Williams ST, Duda TF Jr. 2008. Did tectonic activity stimulate Oligo–Miocene speciation in the Indo-West Pacific? *Evolution* **62:** 1618–1634.

Zmarzly DL. 1990. Adaptive coloration of pontoniine shrimps (Crustacea: Decapoda: Caridea). In Wicksten MK, ed. *Adaptive coloration in invertebrates: proceedings of a symposium*. College Station: Texas A&M University, Sea Grant College Program, 69–75.

**Appendix 1. Summary of the matrices, methods and substitution models used in the molecular analyses**

Dataset	Purpose	Loci	Characters	Number of taxa (ingroup)	Number of taxa (ougroup)	Partitions	Models of substitution		Analyses	Molecular clock model
							Partition data	Concatenated data		
Matrix I	*Coralliogalathea* phylogenetic relationships	*COI*, 16S, 28S	2144	10	2	*COI1, COI2, COI3*, 16S, 28S	HKY+G, TrN+I, F81, K81uf+G, TrNef+G	TIM1+I+G	BI, ML, MP	–
Matrix II	Phylogenetic placement of	*COI*, 16S, 18S	2380	4	19	–	–	012034+I+G+F	BI, ML, MP	–
	Coralliogalathea within Galatheoidea	*COI*, 16S, 18S, 28S	4438	4	19	–	–	012030+G+F	BI, ML, MP	–
Matrix III	Divergence time estimation	*COI*, 16S	1198	16	28	*COI1, COI2, COI3*, 16S	HKY+G, TrN+G, F81+I, K81uf+G	–	DTE	RLC UCLN

BI, Bayesian inference; DTE, divergence time estimation; ML, maximum likelihood; MP, maximum parsimony; RLC, random local clock; UCLN, uncorrelated lognormal clock.

Appendix 2. Species used in the phylogenetic reconstruction of Galatheoidea and in the dating analyses and GenBank accession numbers of the gene sequences

Taxonomy	*COI*	16S	28S	18S
Galatheidae				
Alainius crosnieri	AY351048	HQ380263	HQ380275	HQ380287
Allogalathea elegans	GU392176	GU392151	MK049341	MK049342
Fennerogalathea ensifera	KY230479	KY230489	MK049340	MK049343
Galathea rostrata	KP203785	KF182523	KF182664	KF182504
Galathea strigosa	MK049302	MK049304		
Lauriea adusta	KC133450	KC133508		
Lauriea gardinieri	KC133420	KC133475		
Lauriea simulata	KC133427	KC133483		
Macrothea bouchardi	KX929544	KX929635		
Triodonthea setosa	KC133431	KC133487		
Munididae				
Agononida procera	AY350917	EU821540	EU821573	EU821556
Agononida simillima	MK049303	MK049305		
Babamunida kanaloa	FJ858728	FJ858729	HQ380281	HQ380294
Cervimunida johni	AY351054	EU821546	EU821580	EU821563
Hendersonida granulata	AY351031	GU814684	GU814796	GU814748
Munida gregaria	KU728454	AY050075	AY596099	AF439382
Munida iris	KX022438	KF182521	KF182622	KF182491
Munida eclepsis	AY350952	AY351120		
Munida militaris	AY350975	AY351143		
Munida psylla	AY350992	AY351159		
Munida tyche	AY351016	AY351185		
Paramunida belone	GU814936	GU814731		
Paramunida stichas	AY351042	GU814658	GU814811	GU814763
Pleuroncodes monodon	AY351062	EU821545	EU821579	EU821562
Raymunida cagnetei	AF283869	AY351222		
Raymunida erythrina	AF283883	AY351233		
Sadayoshia acropora	KX929552	KX929646		
Sadayoshia edwardsii	KX929620	KX929654		
Sadayoshia moorei	KX929603	KX929693		
Sadayoshia tenuirostris	KX929580	KX929689		
Sadayoshia sp.			EU821581	EU821564
Munidopsidae				
Galacantha rostrata	JN166755	HQ380261	EU821576	EU821559
Galacantha subspinosa	JN166760	JN166749		
Leiogalathea	AY351055	AY351252	EU821574	EU821557
Munidopsis crenatirostris	JN166781	JN166738		
Munidopsis erinacea	JN166767	KF182524	KF182621	KF182479
Porcellanidae				
Pachycheles	KC858117	JF900725	AY596098	KF182502
Petrolisthes armatus	KY857510	KY857225	AF435989	AF436009
Outgroup				
Calcinus explorator	FJ620320	FJ620222		
Calcinus laevimanus	FJ620270	FJ620175	KF182632	KF182471
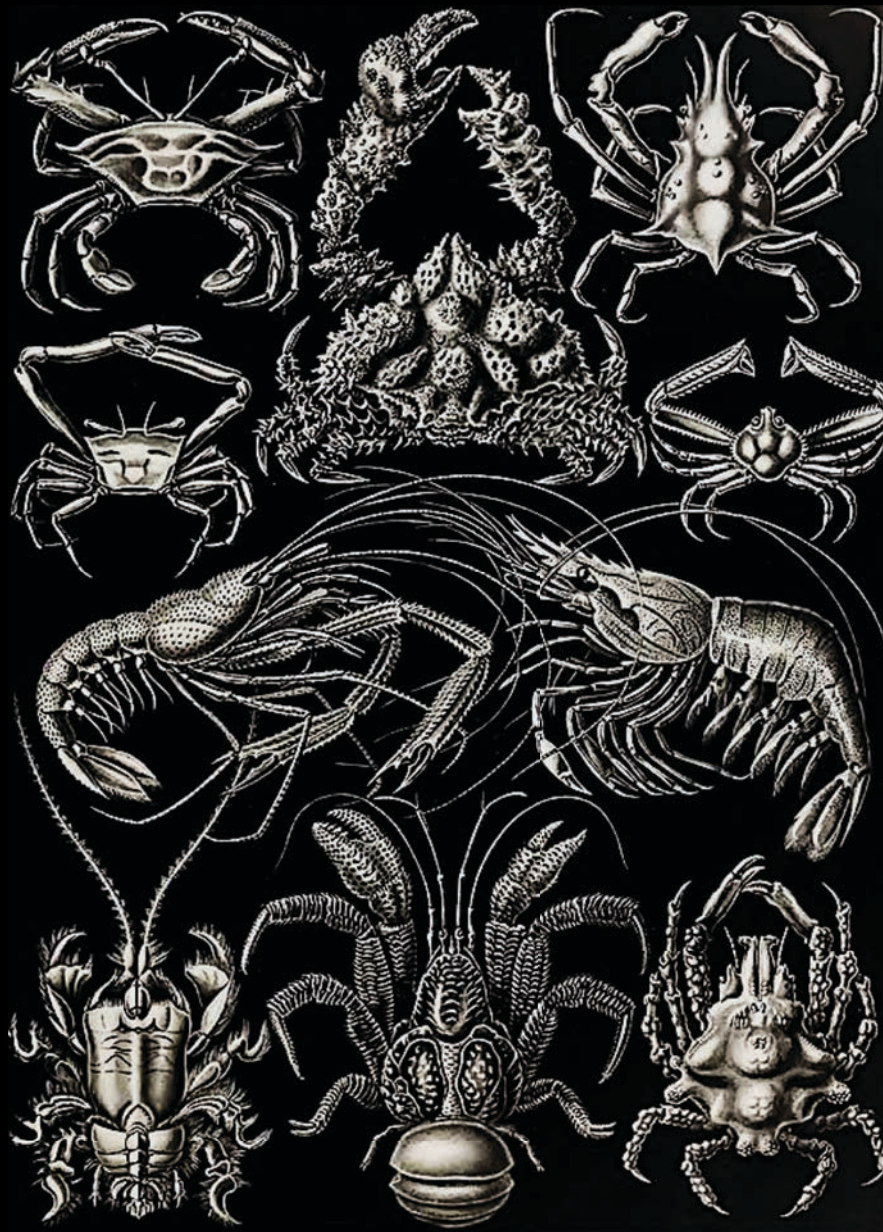
Capítulo III
Biogeografía y patrones evolutivos

Capítulo III

Biogeografía y patrones evolutivos

Artículos incluidos:

Rodríguez-Flores PC, Buckley D, Macpherson E, Corbari L, & Machordom A. 2020. Deep-sea squat lobster biogeography (Munidopsidae: *Leiogalathea*) unveils Tethyan vicariance and evolutionary patterns shared by shallow-water relatives. *Zoologica Scripta*, 49(3), 340–356.

Rodríguez-Flores PC, Macpherson E, Schnabel K, Ahyong ST, Corbari L & Machordom A. Phylogenetic relationships and evolutionary patterns of *Phylladiorhynchus* Baba, 1969 (Crustacea, Decapoda, Galatheidae). *The Crustacean Society Mid-Year Meeting* 2019, Hong Kong, May 2019 (**manuscrito en preparación**).

Deep-sea squat lobster biogeography (Munidopsidae: *Leiogalathea*) unveils Tethyan vicariance and evolutionary patterns shared by shallow-water relatives

Paula C. Rodríguez-Flores[1,2] 🔟 | David Buckley[3,4] 🔟 | Enrique Macpherson[2] 🔟 |
Laure Corbari[5] 🔟 | Annie Machordom[1] 🔟

[1]Museo Nacional de Ciencias Naturales (MNCN-CSIC), Madrid, Spain

[2]Centre d'Estudis Avançats de Blanes (CEAB-CSIC), Blanes, Spain

[3]Departamento de Biología (Genética), Facultad de Biología, Universidad Autónoma de Madrid, Madrid, Spain

[4]Centro de Investigación en Biodiversidad y Cambio Global (CIBC-UAM), Facultad de Biología, Universidad Autónoma de Madrid, Madrid, Spain

[5]Institut de Systématique Évolution Biodiversité (ISYEB, UMR 7205), Muséum national d'Histoire naturelle, CNRS, Sorbonne Université, EPHE, Paris, France

Correspondence
Paula C. Rodríguez-Flores, Museo Nacional de Ciencias Naturales (MNCN-CSIC), José Gutiérrez Abascal, 2, 28006 Madrid, Spain.
Email: paulacrf@mncn.csic.es

Abstract

The ecology, abundance and diversity of galatheoid squat lobsters make them an ideal group to study deep-sea diversification processes. Here, we reconstructed the evolutionary and biogeographic history of *Leiogalathea*, a genus of circum-tropical deep-sea squat lobsters, in order to compare patterns and processes that have affected shallow-water and deep-sea squat lobster species. We first built a multilocus phylogeny and a calibrated species tree with a relaxed clock using StarBEAST2 to reconstruct evolutionary relationships and divergence times among *Leiogalathea* species. We used BioGeoBEARS and a DEC model, implemented in RevBayes, to reconstruct ancestral distribution ranges and the biogeographic history of the genus. Our results showed that *Leiogalathea* is monophyletic and comprises four main lineages; morphological homogeneity is common within and between clades, except in one; the reconstructed ancestral range of the genus is in the Atlantic and Indian oceans (Tethys). They also revealed the divergence of the Atlantic species around 25 million years ago (Ma), intense cladogenesis 15–25 Ma and low levels of speciation over the last 5 million years (Myr). The four *Leiogalathea* lineages showed similar patterns of speciation: allopatric speciation followed by range expansion and subsequent stasis. *Leiogalathea* started diversifying during the Oligocene, likely in the Tethyan. The Atlantic lineage then split from its Indo-Pacific sister group due to vicariance driven by closure of the Tethys Seaway. The Atlantic lineage is less speciose compared with the Indo-Pacific lineages, with the Tropical Southwestern Pacific being the current centre of diversity. *Leiogalathea* diversification coincided with cladogenetic peaks in shallow-water genera, indicating that historical biogeographic events similarly shaped the diversification and distribution of both deep-sea and shallow-water squat lobsters.

KEYWORDS
allopatric speciation, comparative diversification, deep-sea speciation, Galatheoidea, historical patterns, morphological stasis

1 | INTRODUCTION

Contemporary species distributions result from evolutionary forces driving the diversification of organisms, along with their own intrinsic evolutionary dynamics, and the paleogeographic and environmental history of the occupied areas. Nowadays, we can use broad-scale, time-framed phylogenies to study the historical processes that shaped patterns of current biodiversity. Despite this, knowledge of the evolutionary pathways and historical biogeography of marine invertebrates, particularly those in the deep-sea benthos (below ~200 m of depth), is still sparse (McClain & Hardy, 2010).

The deep sea is characterized by high species diversity and a complex seascape comprised of patchy habitats such as canyons, seamounts, trenches and chemosynthetic systems (Levin et al., 2001; McClain & Hardy, 2010). However, vast portions of the ocean floor remain unexplored, making it extremely difficult to characterize true levels of diversity and to determine the geographic ranges of deep-sea taxa (Rex, Stuart, & Coyne, 2000). Also, collecting this fauna is challenging and costly and sometimes results in taxonomically and geographically biased samples (Eilertsen & Malaquias, 2015; Raupach, Mayer, Malyutina, & Wägele, 2009). This bias has led to taxonomic problems, apart from those related to cryptic speciation and/or phenotypic plasticity that have been revealed by molecular phylogenies (Vrijenhoek, 2009). Phylogenies of deep-sea taxa have been mostly used to resolve evolutionary relationships, analyse global patterns of deep-sea diversity or determine colonization time frames (e.g. Lins, Ho, Wilson, & Lo, 2012; Osborn, 2009; Raupach et al., 2009; Sha & Wang, 2018), but biogeographic reconstructions of widely distributed deep-sea genera are scarce (e.g. Cabezas, Sanmartín, Paulay, Macpherson, & Machordom, 2012; Herrera, Watanabe, & Shank, 2015; Roterman, Copley, Linse, Tyler, & Rogers, 2013; Roterman et al., 2018). Therefore, studying the evolutionary history of deep-sea taxa at the genus level remains a difficult task.

The factors influencing diversification in shallow-waters, such as temperature or sea-level fluctuations, may be less important in deep-sea diversification processes (Eilertsen & Malaquias, 2015). Rather, speciation of deep-sea taxa is more likely to be driven by conditions more strongly linked to the geomorphology, bathymetry, oxygen levels or food supply, and the physiological adaptations and dispersal capacities of organisms living in such environments (Williams et al., 2013). Nevertheless, some related deep-sea (bathyal depths, 1,000–4,000 m) and shallow-water organisms such as corals (Cairns, 2007) or squat lobsters (Macpherson et al., 2010; Schnabel et al., 2011) have the same geographic centres of diversity. Historical events (e.g. convergence of tectonic plates, barrier formation, climate and ocean current changes) may similarly affect diversification processes of both coastal and deep-sea organisms (Cabezas et al., 2012; Williams et al., 2013). However, only a few comparative studies have been conducted showing how historical events might have affected deep-sea and shallow-water diversification in closely related taxa (e.g. Eilertsen & Malaquias, 2015; O'Hara, Hugall, Woolley, Bribiesca-Contreras, & Bax, 2019).

Since the Eocene [~50 million years ago (Ma) to present], circum-tropical marine realms have been dramatically affected by geological history and paleoclimatic events. The Central Indo-Pacific (CIP) region, which includes the Coral Triangle (CT), currently constitutes the major marine biodiversity centre in the world, with a latitudinal and longitudinal species gradient (Briggs, 1999; Hoeksema, 2007; Veron et al., 2009). Historically, however, in the first half of the Cenozoic, the global centre of marine biodiversity was located in the western Tethys Sea (Vermeij, 2001) and the CIP harboured much less species diversity (Briggs, 1999). The Tethyan tropical peak of diversity was displaced eastwardly over time to its current location in the CT (Renema et al., 2008). The closure of the Tethyan Seaway during the so-called Terminal Tethyan Event (TTE) during the Early to Middle Miocene (14–18 Ma) drove isolation, allopatric fragmentation and diversification of local faunas (Hou & Li, 2018; Liu, Li, Ugolini, Momtazi, & Hou, 2018; Malaquias & Reid, 2009). More recently, the complete uplifting of the Isthmus of Panama (IOP) during the Pliocene has interrupted connectivity between the Atlantic and the Indo-Pacific oceans through the Central American Seaway (~3 Ma) (O'Dea et al., 2016). Tropical organism exchange between Atlantic and Pacific oceans through the western Indian Ocean was already in decline after the TTE and IOP; however, this break was further intensified by the Pliocene establishment of a cold-water barrier (Benguela upwelling system) in the southernmost part of Africa that is rarely crossed by tropical taxa (Macpherson, 1991; Rocha et al., 2005). These historical processes have been invoked to explain the biogeography and the current distribution patterns of shallow-water organisms (Briggs & Bowen, 2012, 2013; Cowman & Bellwood, 2013a), and they are often used in biogeographic hypotheses for deep-sea taxa. However, direct comparisons of related deep-sea and shallow-water taxa are needed to identify the historical biogeographic processes affecting deep-sea vs. shallow-water organisms.

Squat lobsters (Crustacea, Decapoda, Galatheoidea) represent an ideal group to approach this topic. They are extremely diverse in terms of species richness and ecological adaptations and occupy a vast plethora of marine environments, from coasts to depths of more than 5,000 m. Taxonomic interest in squat lobsters over the last two to three decades (e.g. Baba et al., 2008) has led to a dramatic increase in the number of recognized species (Macpherson & Robainas-Barcia, 2015; Rodríguez-Flores, Macpherson, & Machordom, 2019a). However, we are far from

knowing the true level of diversity of many genera in this group, including *Leiogalathea* spp., which comprises deep-sea species commonly found on continental shelves, seamounts and outer slopes (Baba et al., 2008). The genus belongs to the deep-sea family Munidopsidae and is distributed worldwide from continental shelf to bathyal depths (163–1,480 m), mostly in tropical latitudes of all major oceans, with the highest latitude records in New Zealand in the South and Japan and northwest Africa in the North (Figure 1a). *Leiogalathea* is characterized by extreme morphological conservatism (cryptic species), high incidence of endemic species (described from one single archipelago) together with some broadly distributed species in the Indo-Pacific region and comparatively poor diversity in the Atlantic Ocean (16 vs. 2 species) (Rodríguez-Flores, Macpherson, & Machordom, 2019a). The patterns of diversity and distribution of the Atlantic taxa raise questions about the origin and
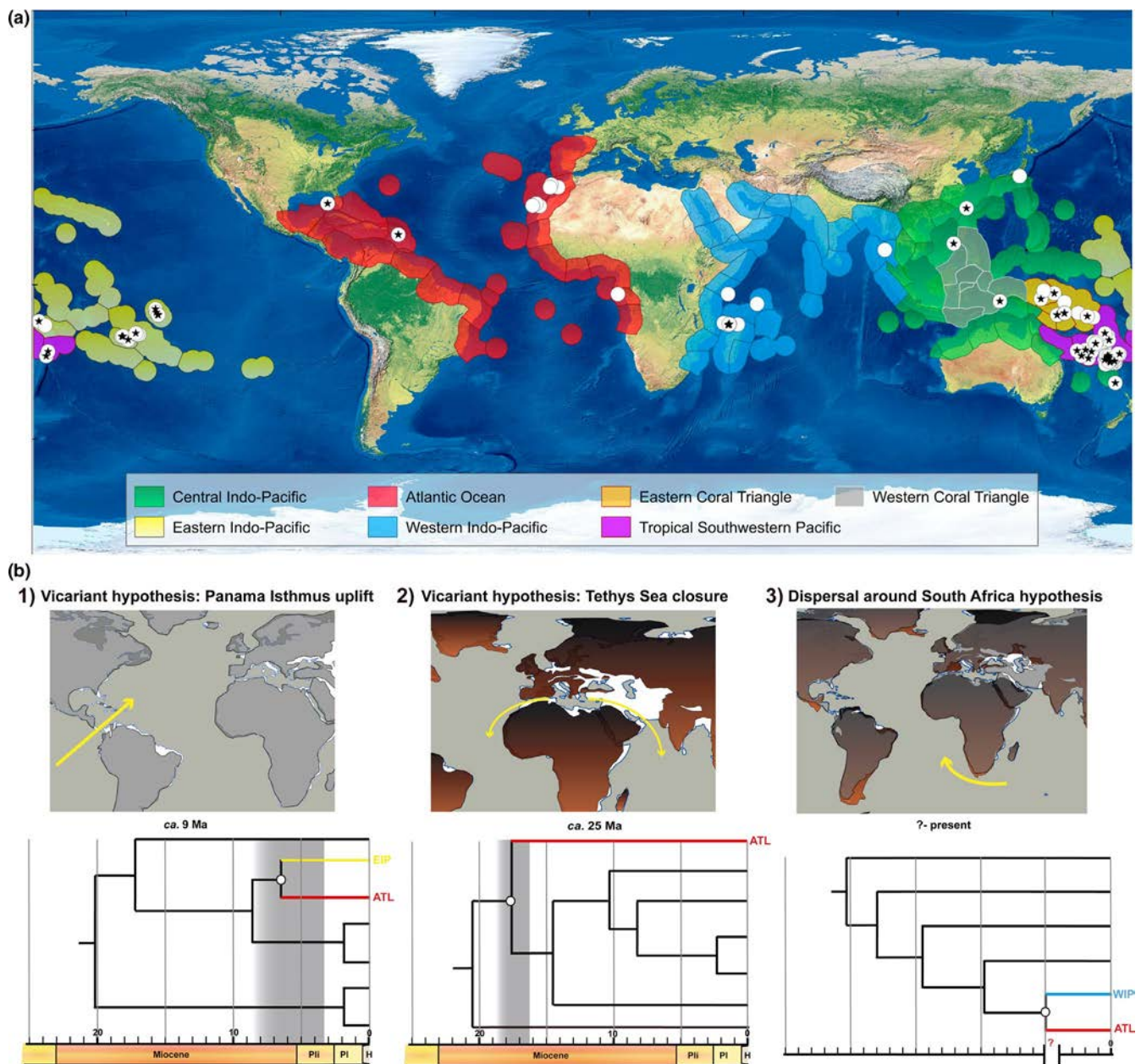
FIGURE 1 (a) Map showing the distribution of *Leiogalathea* within the different biogeographic areas. White dots indicate localities, and black stars indicate those localities from which material was sequenced. (b) Biogeographic scenarios to explain *Leiogalathea* species colonization of the Atlantic by vicariance or, alternatively, by dispersal: (1) vicariance driven by the rise of the Central American Isthmus, (2) vicariance driven by the Tethys Seaway closure and (3) dispersal around southern Africa from the western Indian Ocean. ATL: Atlantic, EIP: Eastern Indo-Pacific, WIP: Western Indo-Pacific. Marine Ecoregions of the World (MEOW) (Spalding et al., 2007) data were obtained from http://marineregions.org/wileyonlinelibrary.com]. Paleoshorelines are based on Heine, Yeo, and Müller (2015). Shapefiles were obtained from https://www.naturalearthdata.comwileyonlinelibrary.com]. Maps were created with Qgis v 3.6.2 (https://qgis.org/en/site/wileyonlinelibrary.com]) [Colour figure can be viewed at wileyonlinelibrary.com]

evolution of these lineages. Briggs and Bowen (2013) explained the origin of the current Atlantic fauna on the basis of different biogeographic scenarios. We consider the same scenarios here to account for the current distribution of *Leiogalathea*: (a) vicariance driven by the rise of the Central American Isthmus, which would have promoted cladogenesis between Atlantic and Eastern Indo-Pacific (EIP) lineages, and the closing of deep-water passages 9.2 Ma (O'Dea et al., 2016); (b) vicariance driven by closure of the Tethys Seaway leading to cladogenesis between Atlantic and Indo-Pacific lineages during the Early to Middle Miocene, around the TTE (14–18 Ma). Estimating the timing of cladogenesis between the Atlantic *Leiogalathea* and the other lineages would lead to reject and accept one of these vicariant hypotheses; however, (c) if vicariance is rejected, the default hypothesis of colonization by dispersal can be proposed (Crisp, Trewick, & Cook, 2011). *Leiogalathea* species could have colonized the Atlantic Ocean via dispersal around southern Africa from the western Indian Ocean. In this case, it would be difficult to establish an accurate temporal framework, although it would likely have happened before the cooling trend of the Benguela upwelling system (Pliocene) (Figure 1b).

Phylogenetic reconstructions in a temporal-spatial framework of related shallow-water (*Lauriea*, *Sadayoshia*, and *Coralliogalathea*) and deep-sea (*Paramunida*) squat lobsters have been published in recent years (Cabezas et al., 2012; Palero, Robainas-Barcia, Corbari, & Macpherson, 2017; Rodríguez-Flores, Macpherson, Buckley, & Machordom, 2019b). According to these studies, the Tropical Southwestern Pacific and the CT are the regions with highest species richness, and the Oligocene–Miocene transition was a period with extremely high cladogenetic rates. However, in order to better compare diversification processes in related shallow-water vs. deep-sea squat lobsters, studies of more deep-sea taxa are needed, making *Leiogalathea* a great model system.

Here, we reconstruct the evolutionary and biogeographic history of the deep-sea squat lobster genus *Leiogalathea*. Our aims are to (a) determine the phylogenetic relationships within the group and the timing and patterns of speciation, (b) analyse its ancestral distribution to consider alternative hypotheses on the Atlantic Ocean colonization and to discuss drivers of current patterns of species distribution (historical biogeography), and (c) contrast patterns and historical processes affecting shallow-water vs. deep-sea squat lobster genera.

2 | MATERIAL AND METHODS

2.1 | Sampling, bathymetry, geography and morphological examination

Specimens were collected by trawling and dredging in the Atlantic, Indian and Pacific oceans during several deep-sea cruises, most of which were organized by the Muséum national d'Histoire naturelle (MNHN) through the Tropical Deep Sea Benthos programme (Bouchet, Héros, Lozouet, & Maestrati, 2008; Poupin & Corbari, 2016; Richer de Forges et al., 2013). The sampling depths ranged from 163 to 1,500 m. Sampling areas included off the coast of Florida in the Gulf of Mexico and Guadeloupe Island in the Caribbean Sea; the northwestern coast of Africa in the eastern Atlantic; Mayotte and Glorieuses Islands and the Seychelles in the western Indian Ocean; Kai and Tanimbar islands in Indonesia; the Solomon Islands, Papua New Guinea in the Solomon Sea and New Ireland Island in the Bismarck Sea; the Solomon Islands, the Vanuatu archipelago, New Caledonia and Chesterfield Islands in the Coral Sea; Wallis and Futuna, Tonga Island, the Marquesas Islands and French Polynesia in the EIP (Figure 1). We also analysed sequences from a specimen from New Zealand. We conducted a morphological analysis of 436 specimens from approximately 120 localities. Of these, 70 were selected for molecular analyses, but some of them failed to amplify or sequence. The specimens are deposited in the scientific collections of the MNHN, Paris, the Forschungsinstitut und Natur-Museum Senckenberg, Frankfurt (SMF) and the National Institute of Water & Atmospheric Research, Wellington (NIWA).

Morphological characterization was performed as previously described (Rodríguez-Flores, Macpherson, & Machordom, 2019a). The evolutionary trends of some characters were also studied by mapping them on the species tree using Mesquite 3.40 (build 877) (Maddison & Maddison, 2018). Analysed characters included, among others, the armature of the carapace and rostrum and the shape of the walking legs (pereiopods), both of which are useful to distinguish groups of species (see Figure S1).

2.2 | DNA extraction, amplification and sequencing

Muscle tissue digestion, DNA extraction, amplification and sequencing were performed as previously described (Rodríguez-Flores, Macpherson, Buckley, et al., 2019b; Rodríguez-Flores, Macpherson, & Machordom, 2019a). Partial sequences of five genes, two mitochondrial (coding and ribosomal) and three nuclear (one coding and two ribosomal), were amplified for molecular analyses: the barcoding region of cytochrome c oxidase subunit I (COI), the mitochondrial large subunit ribosomal RNA (16S), the coding region of Histone 3 (H3) and fragments of two ribosomal nuclear genes (28S and 18S) (for the list of primers used in this study, see Table S1). As multiple copies of the 28S fragment were detected, we cloned the fragment using the pGEM-T Vector System (Promega). Sequencing of both strands of each fragment was performed by Secugen (Madrid) using BigDye Terminator and an ABI 3,730 genetic analyzer. New sequences were deposited in GenBank (Table S2).

2.3 | Sequence alignment and phylogenetic analyses

All DNA sequences were revised and assembled using Sequencher v4.8 (Gene Codes Corporation). Ribosomal gene sequences were first aligned automatically using MAFFT (Katoh, Misawa, Kuma, & Miyata, 2002) then manually corrected in the Se-Al alignment editor (http://tree.bio.ed.ac.uk/software/seal/). To detect whether pseudogenes were present, COI sequences were translated with the invertebrate mitochondrial genetic code to look for internal stop codons using ExPASy (https://web.expasy.org/translate/).

Phylogenetic relationships were inferred through Bayesian inference (BI), maximum likelihood (ML) and maximum parsimony (MP) methods. In the BI approach, two parallel runs of four Metropolis-Coupled Markov Chains Monte Carlo (MC^3) were run for 10^7 generations in MrBayes v3.2.1 (Ronquist & Huelsenbeck, 2003), sampling every 1,000 generations and using a mixed model to average among substitution models to obtain the posterior probabilities. The first 25% of the initial trees were discarded as burn-in. The analyses were run combining mitochondrial and nuclear markers in two partitions and with the full concatenated data set. The ML tree was built with phyML v3.1 (Guindon & Gascuel, 2003) after obtaining the best substitution model estimated for the concatenated data sets (mitochondrial and global data) using the program jModelTest 2.1.5 (Darriba, Taboada, Doallo, & Posada, 2012) following the Bayesian information criterion (BIC). The MP analyses were implemented in PAUP* v4.0a, applying a full heuristic search with a tree-bisection reconnection (TBR) branch swapping algorithm with reconnection limit = 8, ten random stepwise additions, and gaps treated as a new state ('fifth base'). Non-parametric bootstrap analyses for ML and MP were conducted with 1,000 pseudo replicates.

2.4 | Species tree and divergence time estimation

To explore conflicts between different loci (e.g. incongruence of the information of each gene), we built a species tree with mitochondrial and nuclear matrices using StarBEAST2 (Heled & Drummond, 2010) and compared the resulting tree with those of the individual genes.

There are no known *Leiogalathea* fossils to calibrate a molecular clock. Therefore, we calibrated the analysis with secondary calibration points derived from previous broadscale phylogenetic studies. According to Rodríguez-Flores, Macpherson, Buckley, et al. (2019b), who used fossil calibration and ages obtained from several other works, the divergence of *Leiogalathea* from its Munidopsidae relatives took place 74–120 Ma (average of 99 Ma), and the age of the most recent common ancestor (MRCA) of the outgroups used in

the present study (*Munidopsis crenatirostris* and *Galacantha subspinosa*, Munidopsidae) was 61 Ma (40–85 Ma).

Divergence time estimation was carried out in BEAST v2.5.1 (Bouckaert et al., 2014). This program uses relaxed clock models and allows for missing data and flexibility of model parameters. Before estimating divergence times, we first estimated the best partition scheme fitting the data with PartitionFinder v1.1.0 (Lanfear, Calcott, Ho, & Guindon, 2012) in order to determine which partitions following the same substitution pattern can be linked in the species tree and divergence estimation.

We selected an 'analytical population size integration' for the population model as there was no need to estimate exact population sizes for each species. A 'beastmodeltest' selecting 'TransitionTransversionSplit' was chosen for the site model to average among substitution models while estimating the posterior probability of the parameters (Bouckaert & Drummond, 2017). An uncorrelated relaxed log normal clock model was implemented with values drawn from a distribution with a mean of 0.002 and a standard deviation of 0.1 for the 16S clock rate. These rates were based on previously reported mitochondrial DNA rates of substitution for related crustaceans (Cabezas et al., 2012). Mean substitution rates were estimated for each gene, for which we assigned non-informative priors for the substitution rates (gamma distribution setting values for alpha and beta parameters as 0.01 and 100, respectively). We also used a birth–death model for the tree prior. Normal distributions were chosen as temporal priors for the calibration points (mean = 100, stdv = 10 for the root of the tree; and mean = 60, stdv = 10 for the MRCA of the outgroup *Galacantha subspinosa* and *Munidopsis crenatirostris*). The Markov Chains Monte Carlo (MCMC) was run for 5×10^8 generations per run, and parameters were logged every 5×10^4 generations. BEAST analyses were run in the CIPRES Science Gateway v.3.1 (Miller, Pfeiffer, & Schwartz, 2010).

Convergence of the chains (trace and effective sample sizes, ESSs) was assessed in Tracer v1.7. The results were summarized and annotated in a Maximum Clade Credibility (MCC) tree generated with Tree Annotator v2.5.1 (Rambaut & Drummond, 2014) after discarding the first 25% of the trees as burn-in. The resulting MCC trees from each analysis were edited in FigTree v1.4.3 (Rambaut, 2014).

2.5 | Ancestral range estimation

Biogeographic areas were defined following the 'Marine Ecoregions of the World' (MEOW) global classification system (Spalding et al., 2007), which uses patterns of mapped marine biodiversity to delimit realms, provinces and ecoregions. This system was previously used to reconstruct the biogeographic history of related shallow-water squat lobsters

(e.g. Palero et al., 2017; Schnabel et al., 2011). Our samples covered four realms: Tropical Atlantic, Western Indo-Pacific, Central Indo-Pacific and Eastern Indo-Pacific. We delimited six areas within these realms to consider geographic patterns of diversity in *Leiogalathea* (see Figure 1): (A) Atlantic, (N) Tropical Southwestern Pacific, (P) Eastern Coral Triangle, (I) Western Coral Triangle, (F) Eastern Indo-Pacific and (W) Western Indian Ocean (modified from Spalding et al., 2007). The New Zealand specimen of *L. ascanius* was genetically identical to those from New Caledonia and was included in the tropical southwestern Pacific region (Figure 2).

Historical biogeographic analyses were performed in the R package BioGeoBEARS (Matzke, 2013), which permits biogeographic model comparison, and then in RevBayes (Höhna et al., 2016) to reconstruct the geographic ancestral states and the evolution of geographic ranges. We first selected the best fit model for our data in BioGeoBEARS, which includes and compares the following models: Dispersal–Extinction–Cladogenesis (DEC) (Ree & Smith, 2008), Dispersal–Vicariance Analysis (DIVALIKE), BayArea (the range evolution model) and the Bayesian Binary Model of RASP (Yu, Harris, Blair, & He, 2015). We also allowed founder-event speciation processes (+J) to be integrated into all models. We then reconstructed the history of geographic ranges in a Bayesian framework using RevBayes, which also estimates migration rates (range expansion), extirpation rates (range contraction) and the probability of allopatry vs. sympatry according to the data.

In order to test the vicariant events, we ran an epoch DEC model in RevBayes, following the results from the model selection test in BioGeoBEARS (see below). We specified a time matrix with three epochs: 35–32 Ma, age of the MRCA of the ingroup; 16–14 Ma to represent the Terminal Tethyan Event; and the Present. We assigned three connectivity matrices to these epochs to represent paleo-connectivity among areas. Specifically, we coded the matrices to represent the disconnection and unlikely presence of *Leiogalathea* species in French Polynesia (F) at the root of the tree and the current disconnection of Atlantic and Indo-Pacific areas. A distance matrix between areas was generated to scale dispersal rates and probabilities. This was not an absolute distance matrix; rather, we coded relative distances between areas as adjacent (1), separated (100) and very far away (1,000). We constrained ancestral ranges to have a maximum of four areas to minimize the number of potential ancestral states. None of the current species is present in more than three discrete biogeographic areas. Four independent analyses for 25,000 generations were run. We visually and statistically checked for convergence and proper mixing of the MCMC analyses in Tracer v1.7 and the R package Bonsai (https://github.com/mikeryanmay/bonsai), respectively. Results from the four analyses were combined to generate the final biogeographic reconstructions, which were visualized and edited with RevGadgets in R. All scripts are provided in Supporting Information (S3).

3 | RESULTS

Most (85%) of the 18 *Leiogalathea* species described to date were included in our phylogenetic analyses (Table S2). *Leiogalathea laevirostris*, *L. imperialis* and *L. aeneas* samples were excluded as they were preserved in formalin. Our results (Figures 2–4, Figure S1) show the potential existence of one undescribed species (*Leiogalathea* sp. in the phylogenetic tree), which would increase the number of known species to 19. The complete alignment of the five partial genes consisted of 3,748 characters: 658 base pairs (bp) for COI; 533 bp for 16S; 331 bp for H3; 902 bp for 28S; and 1,324 bp for 18S. In most cases, phylogenetic analyses based on the mitochondrial and the concatenated matrices recovered congruent topologies, although lower clade supports were observed in the mitochondrial phylogeny (Figure 2).

3.1 | Phylogenetic analyses and morphological character evolution

The genus *Leiogalathea* was recovered as a monophyletic clade in all analyses [posterior probability (pp):1; bootstrap supports (bs): 100] (Figure 2). *Leiogalathea* species were grouped in four main lineages that, in most cases, presented different combinations of morphological synapomorphies (following the morphological characterization by Rodríguez-Flores, Macpherson, & Machordom, 2019a) but lacked a clear geographic structure. The two morphotypes mapped on the phylogeny (presence/absence of one spine on the hepatic margin of the carapace) were congruent among lineages except *L. ascanius*, which appeared morphologically convergent with clade III (Figure 2, Figure S1). The first lineage (clade I) consisted of four species: *L. juturna* from Taiwan and Indonesia; *L. paris* from French Polynesia, Wallis and Futuna, New Caledonia and Papua New Guinea; *L. priam* from Papua New Guinea; and *L. camilla* from New Caledonia. This lineage is remarkably conserved in terms of morphology (Figure S1). The morphotype of these species is characterized by the absence of a hepatic spine, stout pereiopods, an armed spinose rostrum, and a relatively small size (Rodríguez-Flores, Macpherson, & Machordom, 2019a). Relationships among clade I species were not clearly resolved in the mitochondrial phylogeny (Figure 2a); however, the sister group relationship between *L. camilla* and the rest of the species was highly supported in the combined phylogeny (Figure 2b). The sister group relationship between *L. priam* and the clade *L. juturna + L. paris* was also highly supported in the combined phylogeny (Figure 2b). The clade *L. juturna + L. paris* was well supported in both phylogenies. The morphology of the species also supports the phylogenetic distinction of *L. camilla* from
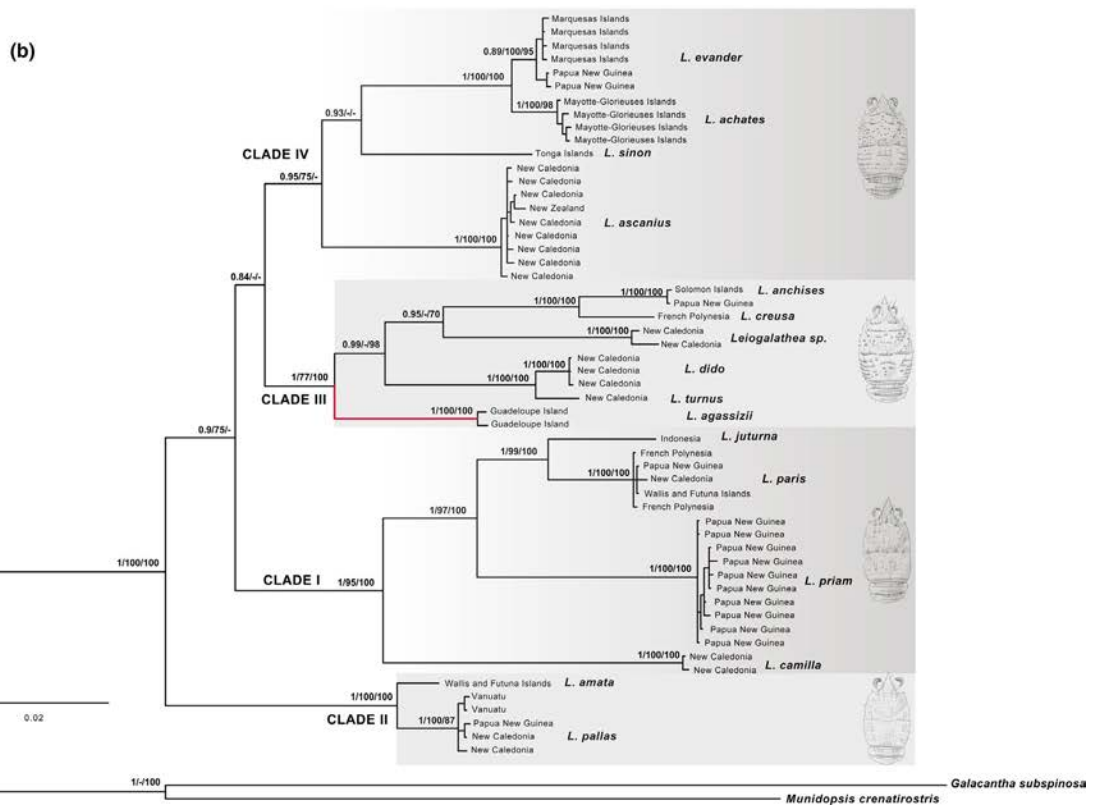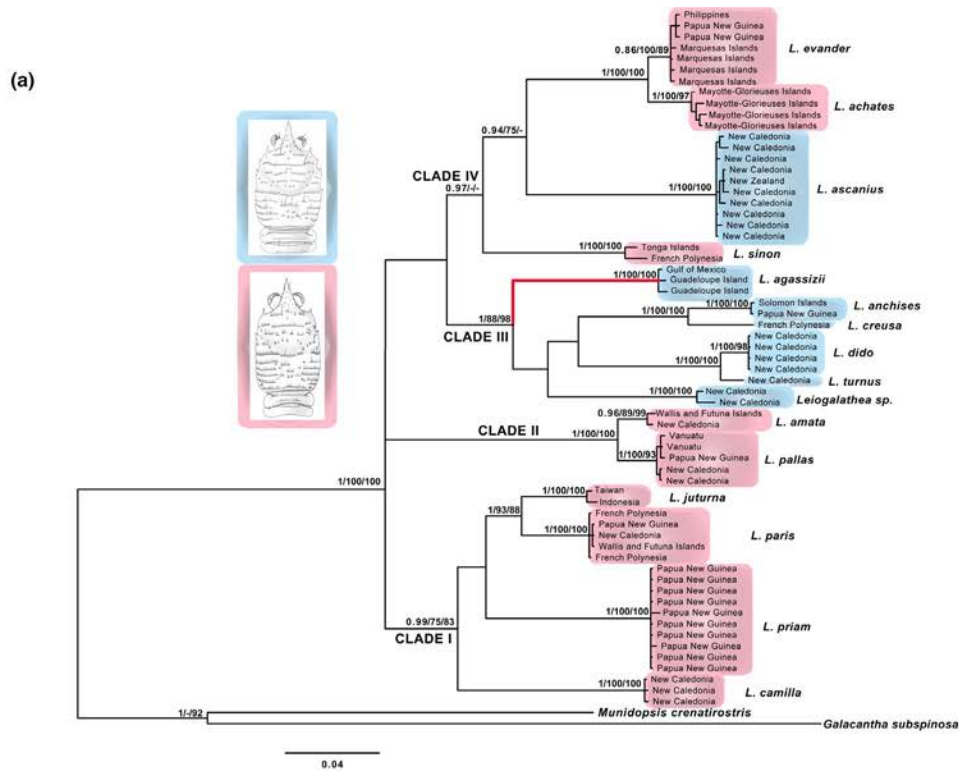
FIGURE 2 Phylogenetic tree based on (a) concatenated mitochondrial data and (b) concatenated nuclear plus mitochondrial data. The geographic location of each specimen is provided at the tips. The morphotypes of the main clades (I, II, III and IV) based on the spinulation of the hepatic margin of the carapace (blue spinose, pink unarmed) are also shown. The red branch indicates the Atlantic species, and, in b, the typical morphotype of each major clade is represented by an illustration of the carapace. Numbers above branches indicate posterior probability and bootstrap support values for the MP and ML analyses, respectively. Hyphens (−) indicate mean node unsupported in the corresponding analysis (Bayesian posterior probability lower than 0.85, MP and ML bootstrap support lower than 70) [Colour figure can be viewed at wileyonlinelibrary.com]
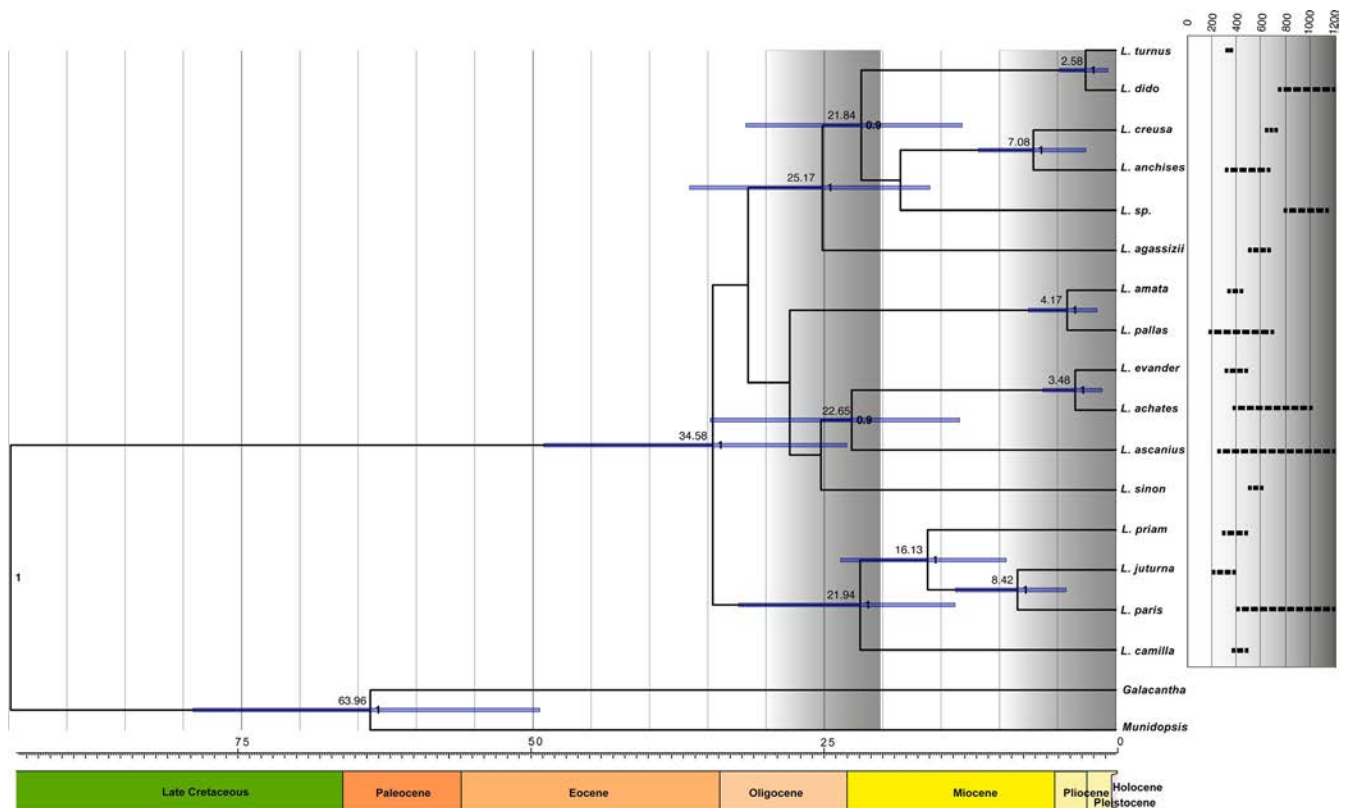
FIGURE 3 *Leiogalathea* maximum clade credibility (MCC) tree inferred by StarBEAST2, showing 95% HPD credibility intervals for each well supported recovered node. Numbers above branches represent average lineage divergence times; numbers in nodes represent posterior probabilities (higher than 0.9). Grey areas indicate periods of intense cladogenesis in the evolutionary history of *Leiogalathea*. Geological time chart was obtained with TimeScale Creator v7.3 (http://www.tscreator.orgwileyonlinelibrary.com]). Depth distribution for each *Leiogalathea* species is indicated at the tip of the branches [Colour figure can be viewed at wileyonlinelibrary.com]

the other clade I species: this species exhibits well-developed spines in the armature of the rostrum whereas the others (*L. priam, L. juturna,* and *L. paris*) do not (Figure S1) (Rodríguez-Flores, Macpherson, & Machordom, 2019a).

The second lineage (clade II) comprised two species: *L. amata* from New Caledonia and Wallis and Futuna and *L. pallas* from Vanuatu, New Caledonia and Papua New Guinea (Figure 2). The two species are quite different morphologically. *Leiogalathea amata* is a small species that is densely covered by setae, whereas *L. pallas* is a conspicuous spinose species that has a carapace and abdomen sparsely covered by setae (Rodríguez-Flores, Macpherson, & Machordom, 2019a). However, the clade is morphologically defined by having a smooth rostrum and an unarmed hepatic margin of the carapace (Figure S1).

In clade III, the Atlantic species *L. agassizii* was united with a group comprised of *L. anchises*, *L. creusa*, *L. dido* and *L. turnus* (Figure 2). Two pairs of sister species were recovered: *L. anchises + L. creusa* from Papua New Guinea and Polynesia, respectively, and *L. dido + L. turnus*, both from New Caledonia. These pairs were also related to a new species (*Leiogalathea* sp.)

from New Caledonia. However, the relationship among them and with respect to the Atlantic taxon was unresolved in the mitochondrial tree (Figure 2a). In the combined tree, the new species was recovered as sister species of *L. anchises + L. creusa* (Figure 2b). The morphology of clade III species is also very conserved: they are conspicuous, have a rostrum margin that is armed with several spines (5–7) and a carapace with 6–7 spines, including the hepatic spine (Figure 2a, Figure S1) (Rodríguez-Flores, Macpherson, & Machordom, 2019a).

The fourth lineage (clade IV) was only supported in the BI analyses and included diverse morphotypes. The sister species *L. evander* and *L. achates* from the Central Pacific–Polynesia and the West Indian Ocean, respectively, clustered with *L. ascanius* from New Caledonia and New Zealand (Figure 2a). *Leiogalathea sinon* from Polynesia was sister species to this group in the mitochondrial tree and to *L. evander + L. achates* in the combined tree; however, neither relationship was fully supported in all of the analyses. Clade IV species, except *L. ascanius*, lack a spine on the hepatic margin of the carapace (Figure 2a, Figure S1) (Rodríguez-Flores, Macpherson, & Machordom, 2019a), indicating morphological convergence of this trait with respect to clade I species.

3.2 | Species tree, divergence time estimation, rates of evolution and bathymetric ranges

The topology obtained from the StarBEAST analyses was congruent with the combined nuclear and mitochondrial phylogenetic tree and recovered the same main lineages and relationships (pp > 0.95; only clade IV had a pp < 0.95) (Figure 3). Nodes that were not well resolved were not considered for the time estimates. The MRCA of the genus was estimated around 35 Ma [highest 95% posterior density interval (HPD$_{95\%}$) 23–49 Ma] and those of the main clades around 20–25 Ma (Figure 3). For instance, the first lineage branching off in clade III was the Atlantic species *L. agassizii* around 25 Ma (HPD$_{95\%}$ 16–36 Ma). As shown in Figure 3, the Oligocene/Miocene boundary was an active period of diversification for the group, although within-clade diversification occurred mainly during the Miocene/Pliocene. Only one cladogenetic event definitively occurred during the Plio/Pleistocenic (diversification of *L. turnus*/*L. dido*).

The following average substitution rates were estimated for each gene: 5.6×10^{-3} (COI), 2×10^{-3} (16S), 3×10^{-3} (28S), 5.5×10^{-4} (18S) and 1.1×10^{-4} (H3).

A general overlap in the species depth distribution was observed (Figure 3) with wide bathymetric ranges, most of them appearing at 600–800 m, only a few records below 1,000 m (*L. ascanius* and *L. paris*) and only two species mainly restricted below this depth (*L. dido* and *Leiogalathea* sp).

3.3 | Geographic distribution and ancestral area reconstruction

According to the BioGeoBEARS analysis, the best fit model for our data was DEC with no founder event speciation (+J). The biogeographic reconstruction following an epoch DEC model in RevBayes is shown in Figure 4. The analysis considered three areas with moderate probability for the root (pp = 0.4): Atlantic Ocean, Western Indo-Pacific and Western Coral Triangle, all located in the westernmost part of the distribution (Figure 1). The reconstructed ancestral range for clade III was the Atlantic Ocean + Western Indo-Pacific (pp = 0.4), and an ancestor in the Atlantic was recovered for *L. agassizii* with a high probability (pp = 0.8). Clade IV started diversifying in the Western Indo-Pacific (pp = 0.8), with each of the lineages undergoing a range change that included migration towards the Central Indo-Pacific; only *L. achates* would remain in the clade ancestral range. According to the reconstruction, clade I originated in the Eastern Coral Triangle then migrated eastwards to the Eastern Indo-Pacific and westwards to the Western Coral Triangle. Clade II originated in the Tropical Southwestern Pacific during the Pliocene but subsequently underwent a range expansion

towards the Eastern Coral Triangle. Speciation processes in *Leiogalathea* were predominantly by allopatry (pp = 0.6) than sympatry (pp = 0.4). A high rate of extirpation (local extinction in part of the ancestral range) was also observed [0.98/Myr (million years), HPD$_{95\%}$ 0.22–1.97]. Migration rates (migration events/Myr) ranged from 0.03 to 0.53 (HPD$_{95\%}$, mean: 0.12). Range stasis was observed in the lineage leading to *L. dido* and *L. turnus*, and in *Leiogalathea* sp. and *L. camilla*, while range expansion was detected in the rest of the lineages.

4 | DISCUSSION

4.1 | *Leiogalathea* speciation patterns

Molecular studies of deep-sea fauna are crucial to unravel the taxonomic incongruences, such as those related to previously described morphospecies, that were obscuring evolutionary patterns in deep-sea taxa (Cabezas et al., 2012; Vrijenhoek, 2009). These studies have also indicated how diversity has been greatly underestimated in these taxa (Ritchie, Jamieson, & Piertney, 2015). *Leiogalathea* is a clear example: only two species were recognized (Baba et al., 2008) until a recent revision of the genus showed the existence of 18 species (Rodríguez-Flores, Macpherson, & Machordom, 2019a). Our results show, in general, that the genus is monophyletic, presents a high level of morphological convergence or homoplasy, having thus few morphological traits of phylogenetic value, exhibits overlap among most species depth ranges and contains pairs of sister species that show allopatric and sympatric speciation patterns (in a biogeographic sense). Speciation in the same geographic area occurred at least once in each major lineage of *Leiogalathea*. Interestingly, sympatric vs. allopatric speciation events in *Leiogalathea* have generated highly distinct species in terms of morphology. Divergence of the morphologically well-differentiated sister species *L. dido* and *L. turnus*, which have overlapping distributions around New Caledonia, constitutes the most recent speciation event within the genus. Differential niche occupation may explain the speciation: *L. turnus* has a bathymetric range of 333–375 m, whereas most of *L. dido* specimens have been recorded below 1,000 m and exhibit a conspicuous reduction in the ocular orbit (Figure 3, Figure S1.5; Rodríguez-Flores, Macpherson, & Machordom, 2019a). In this case, bathymetry might have driven/affected speciation in the absence of geographic isolation, as has been shown in hadal amphipods (Ritchie et al., 2015). On the other hand, the older speciation events seem to have been due to allopatry/vicariance and occurred without conspicuous morphological changes. For example, the sibling species *L. juturna* and *L. paris*, which are exceptionally similar and can only be differentiated by inconspicuous diagnostic characters
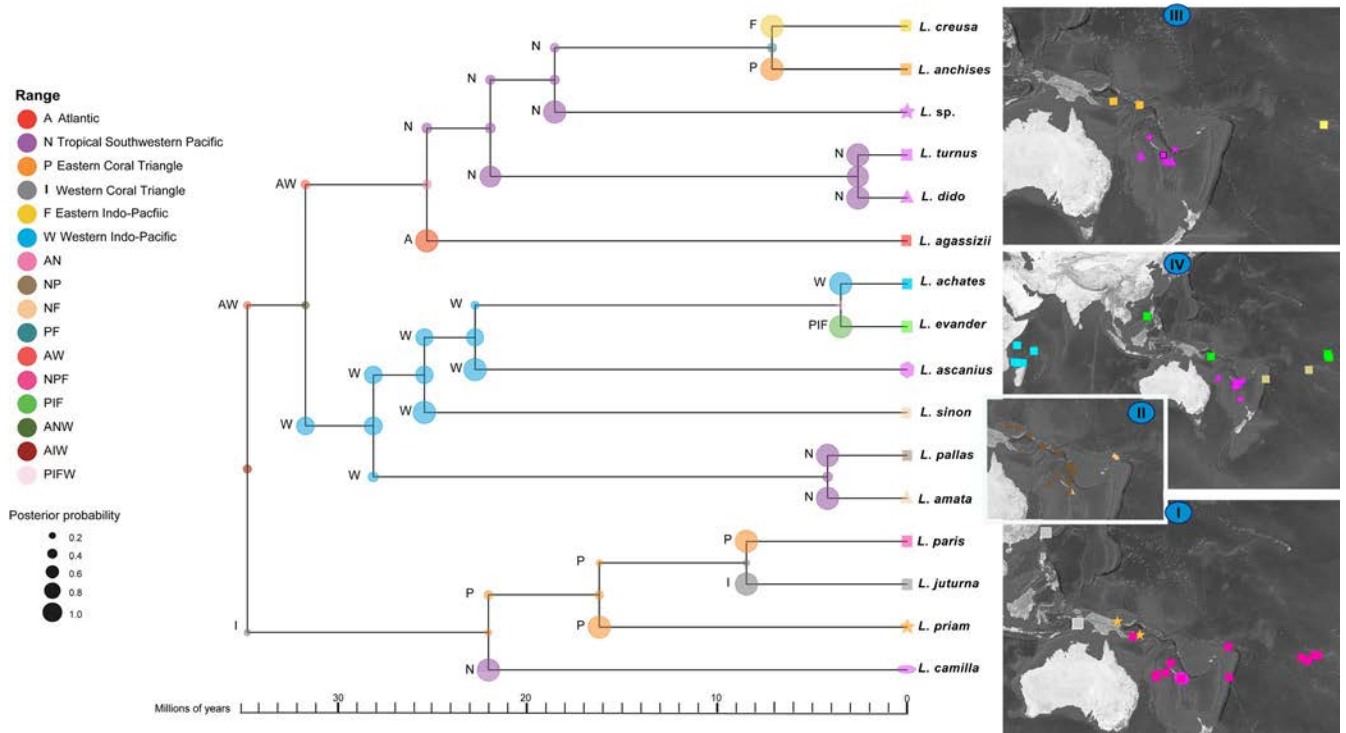
FIGURE 4 Range area reconstruction based on a Bayesian Dispersal–Extinction–Cladogenesis (DEC) reconstruction of the spatio-temporal evolution of *Leiogalathea* spp. using the MCC tree obtained in StarBEAST2. The biogeographic areas and the posterior probabilities of the biogeographic scenarios are also represented in the figure. Coloured shapes at the branch tips indicate contemporary distributions of the taxa. Maps illustrate geographic distribution of clades I, II, III (excluding the Atlantic *L. agassizii*) and IV [Colour figure can be viewed at wileyonlinelibrary.com]

(Rodríguez-Flores, Macpherson, & Machordom, 2019a), diverged and migrated towards the Western Coral Triangle in a comparatively ancient process compared with the morphologically distinctive species *L. dido* and *L. turnus* (8.4 vs. 2.6 Ma) (see Figure 4), occupy also a vicariant vertical distribution (Figure 3). Increased phenotypic differences related to sympatric speciation are not an uncommon phenomenon and are likely related to divergence in ecological traits (such as differences in microhabitat exploitation) and assortative mating phenomena (e.g. Moritz et al., 2018; Puritz et al., 2012). There are also several examples of cryptic species presenting allopatric distributions (e.g. Vrijenhoek, 2009). Ecological speciation processes, including those involving explosive radiations, have been shown to be generally faster than those due to vicariance (for instance, in *Drosophila*: 200,000 years vs. 2.7 Ma), and cases of rapid speciation have been detected in marine animals (sea stars, snails and fishes) (Bowen, Rocha, Toonen, & Karl, 2013). Genetic drift is hypothesized to lead to sexual isolation slower than isolation mediated by selective pressures, which could have a clear effect in just a few generations (Hendry, Wenburg, Bentzen, Volk, & Quinn, 2000; Puritz et al., 2012). Quantifying morphological change through time between sister species would help to determine whether speciation mode (allopatric vs.

sympatric) is correlated with morphological evolution in *Leiogalathea*.

Finally, in the case of the sister species *L. achates* and *L. evander*, we identified speciation involving dispersal. The known distribution ranges of the two species are restricted (localized) and separated from each other by more than 8,000 km (straight line distance) (SW Indian Ocean and Papua New Guinea/French Polynesia, respectively). A relatively recent long-term dispersal event between the western Indian Ocean and the CIP might explain this pattern. Vicariant sister species separated by thousands of kilometres have been also reported in *Coralliogalathea* (*C. humilis* vs. *C. minuta*) (Rodríguez-Flores, Macpherson, Buckley, et al., 2019b). As in related galatheid species, for instance *Lauriea punctata, Sadayoshia edwarsii* or *Allogalathea babai* (Baba et al., 2008; Palero et al., 2017), some *Leiogalathea* species exhibit a wide geographic distribution. Although not known for this genus, other related squat lobster species have free-swimming planktonic larvae (Baba, Fujita, Wehrtmann, & Scholtz, 2011) that might occasionally drift with the ocean currents, making long-distance dispersal events followed by establishment conceivable. Long-distance drifting is evidenced by genetic uniformity across immense geographic distances, which has been observed in many marine organisms including algae, mollusks, isopods and amphipods (Gillespie

et al., 2012). Indeed, widely distributed *Leiogalathea* species (e.g. *L. paris*) exhibited genetic homogeneity among very distant populations (see Figure 2).

4.2 | Historical biogeography

Our results indicate that the MRCA of *Leiogalathea* likely lived during the Late Eocene to Early Oligocene. The reconstructed ancestral range was located in the westernmost part of the genus current distribution (Atlantic and western Indian Ocean) and dated to the Late Eocene (Figures 3 and 4), both of which suggest a geographic origin in the Tethys realm. The Atlantic lineage currently includes only two species (*L. agassizii* and *L. aeneas*) and is characterized by a poor cladogenetic history compared with the Indo-Pacific lineages, which consist of more than 16 species (Rodríguez-Flores, Macpherson, & Machordom, 2019a).

The hypotheses for the origin of the Atlantic *Leiogalathea* were proposed as: (a) IOP vicariance, (b) TTE vicariance and (c) colonization from Indo-Pacific lineages surrounding southern Africa (Figure 1).

If the vicariance was driven by the IOP as suggested by the first vicariant hypothesis, Eastern Pacific and Western Atlantic would share lineages with a divergence estimated around the rise of the Isthmus (Cowman & Bellwood, 2013b). The genus is supposedly currently missing in the Eastern Pacific; therefore, if this particular biogeographic scenario happened, current Eastern Indo-Pacific lineages would be closely related to the Atlantic species, not observed in our results. Moreover, the estimated divergence between Atlantic and Pacific lineages, at the end of the Oligocene, largely precedes the closure of the Panamanian Isthmus.

On the other hand, a scenario of Atlantic colonization via dispersal from southmost tip of Africa (third hypothesis) requires a sister relationship among Indian and Atlantic lineages (Lessios & Robertson, 2013; Rocha et al., 2005). However, this relationship was not observed either.

In the second biogeographic hypothesis, ancient relict Tethyan lineages should be detected, with an early to middle Miocene age (14–20 Ma) (Hou & Li, 2018; Liu et al., 2018). The reconstruction results are in line with the second hypothesis (see Figure 1b): colonization of the Atlantic following a vicariant event caused by the Tethys closure. The Tethyan origin hypothesis is supported by the richness and abundance of related squat lobster fossils in the west Tethys during the second half of the Mesozoic and Early Cenozoic (e.g. Robins, Feldmann, & Schweitzer, 2013; Robins & Klompmaker, 2019). According to our divergence time estimates, divergence of the Atlantic lineage (25 Ma) slightly predates the Terminal Tethyan Event (TTE) (12–18 Ma), though the age of this episode overlaps with our estimated range of divergence (16–36 Ma). Vicariant patterns between

Atlantic and Indo-Pacific lineages have been extensively studied in shallow-water taxa, with divergence estimations ranging from 12 to 36 Ma and associated with vicariance driven by the TTE scenario (e.g. Cowman & Bellwood, 2013b; Liu et al., 2018; Thacker, 2015). However, there are several instances of other taxa with lineage divergences predating the TTE, some as far back as the Cenozoic to the early Eocene (e.g. Malaquias & Reid, 2009; Uribe, Williams, Templado, Buge, & Zardoya, 2017). The global cooling that characterized the end of the Eocene likely promoted extinction and diversification in some of these instances (Harzhauser et al., 2007). However, these estimates can also be explained by tectonic events previous to the Tethys closure (from the Eocene to the Miocene) (Hou & Li, 2018), lineage extinction (and/or incomplete sampling) and calibration inaccuracy (Malaquias & Reid, 2009). In the case of *Leiogalathea*, the most probable explanation of the time estimate is that deep-sea organisms might have been affected earlier by closure of the Tethys Seaway than their shallow-water counterparts (Eilertsen & Malaquias, 2015) due to the progressive disappearance of deep-water passages. In the Tethyan vicariance scenario, the level of genetic connectivity/isolation would vary depending on depth ranges on both sides of the barrier; therefore, the TTE might have affected bathyal marine organisms earlier than intertidal and shallow-water organisms (Liu et al., 2018). Comparisons of divergence times between sister species of related deep-sea and shallow-water taxa distributed at both sides of a biogeographic barrier remain to be examined in detail to test this hypothesis.

Other squat lobsters have a distribution pattern similar to *Leiogalathea* in the Atlantic. For instance, very few *Agononida, Galathea* or *Eumunida* species are found in the Atlantic compared with the CIP (Baba et al., 2008; Macpherson & Robainas-Barcia, 2015). Indeed, global diversity of squat lobsters is quite poor in the Atlantic compared with the CIP (Macpherson et al., 2010; Schnabel et al., 2011), an area that has clearly been acting as a centre of diversification over the last 20 Myr. Conversely, the Atlantic is considered an independent and isolated region in terms of species diversity (Cowman & Bellwood, 2013a; Macpherson, 1991; Rocha et al., 2005). The poor cladogenetic history of *Leiogalathea* and related squat lobsters in the Atlantic might be a result of a high rate of extinction and poor lineage replenishment from the Indo-Pacific due to a history of isolation generated by the formation of new barriers and the establishment of the South African (Benguela) cold-water current (Briggs & Bowen, 2013; Cowman & Bellwood, 2013a). A high rate of extinction in the Atlantic has already been demonstrated for fishes, echinoderms, bryozoans and plants (Antonelli & Sanmartín, 2011; Cowman & Bellwood, 2011; Di Martino, Jackson, Taylor, & Johnson, 2018). In addition, at the Eocene–Oligocene boundary, the deep sea underwent

a dramatic turnover in fauna (Whatley & Coles, 1991), which might have been related to environmental changes associated with this progressive isolation.

Our analyses of colonization patterns for the whole genus *Leiogalathea* suggest that the most likely path of dispersal from the Tethys was migration eastwards to the CIP, which is consistent with the pattern observed for some shallow-water taxa (Renema et al., 2008). Most *Leiogalathea* lineages were established in the CIP during the Pliocene after Miocene cladogenetic events, although the MRCA of clade I was already in the Eastern Coral Triangle by the Early Miocene (20 Ma). High diversity of coral reef fauna was already well established by the Late Miocene (Briggs, 1999). Consistent with this, our analyses showed an increase in diversity of *Leiogalathea* lineages at this time and in this place. Thus, the CIP and, within it, the Tropical Southwestern Pacific might have initially acted as a centre of accumulation (Bowen et al., 2013; Cowman & Bellwood, 2013a), after they had expanded their range. The CIP area then might have acted progressively as a centre of origin, promoting cladogenesis and rapid speciation (Williams & Duda, 2008; Williams et al., 2013). These hypotheses have been widely proposed and tested to explain the distribution patterns of coral reef and intertidal fauna in the CT (Bowen et al., 2013; Gaither et al., 2011). However, comparisons of diversification and biogeographic patterns with deep-sea taxa, such as *Leiogalathea* and other squat lobsters, were, until now, not possible.

4.3 | Comparisons of diversification and biogeographic patterns between shallow-water and deep-sea taxa

As observed in Galatheoidea and Chirostyloidea (Macpherson et al., 2010; Schnabel et al., 2011), *Leiogalathea* also has its centre of diversity in the Tropical Southwestern Pacific (nine species) with the number of species decreasing with distance, for instance, in the Eastern Coral Triangle and Eastern Indo-Pacific (Polynesia) (five species). A lower species richness is observed in all the other areas. Nine *Leiogalathea* species are found in New Caledonia, some of which have only been found in this area (e.g. *L. camilla*, *L. dido*, and *L. turnus*). Samadi, Bottan, Macpherson, Forges, and Boisselier (2006) argued that this region is highly productive, which would lead to an accumulation of squat lobster species instead of being a centre of speciation. Therefore, it is likely that these species have a broader distribution range.

Time-calibrated molecular phylogenies at the species level reflect the complex biogeographic history of the marine circum-tropical belt as far back as the Mesozoic. Our findings indicate that a major period of cladogenesis in *Leiogalathea* occurred 25–15 Ma (Late Oligocene to Early Miocene). Major diversification of coral reef fauna in the CIP is thought to have occurred approximately 25–20 Ma during the Paleogene–Neogene

transition (Palero et al., 2017; Rodríguez-Flores, Macpherson, Buckley, et al., 2019b; Williams & Duda, 2008) when the most important Cenozoic plate boundaries were reorganized (Hall, 2002). Intense diversification was also occurring in deep-sea taxa during this period (Cabezas et al., 2012; Eilertsen & Malaquias, 2015). Comparison of the timing of cladogenetic events and lineage diversity among *Leiogalathea* and other squat lobster genera (i.e. *Coralliogalathea*, *Lauriea*, *Paramunida* and *Sadayoshia*) revealed general evolutionary speciation trends affecting these tropical marine organisms (Figure 5). These genera are excellent candidates to compare evolutionary trends between shallow-water and deep-sea organisms because they present (a) overlapping geographic distributions, (b) comparable species diversity and (c) are phylogenetically related but (d) differ in their bathymetric ranges (depth distribution mostly above of 200 m in *Coralliogalathea*, *Lauriea* and *Sadayoshia*, and below 200 m in *Paramunida* and *Leiogalathea*; see Figure 5). The MRCA of these genera dates to the Middle to Late Eocene, a period characterized by anoxic events in the deep sea (McClain & Hardy, 2010) and progressive global cooling (Harzhauser et al., 2007), which seems to have had a key role in the evolution of the Anomura (Davis, Hill, Astrop, & Wills, 2017).

During the Oligocene to Miocene transition, high tectonic activity and climate and ocean current changes could have promoted speciation in both shallow-water and deep-sea squat lobsters (Cabezas et al., 2012). Consistent with this, increased cladogenesis during this period is observed in both groups (Figure 5). With the exception of the deep-sea genus *Paramunida*, diversification stasis was observed around the Middle Miocene for all genera. Hence, other processes such as lineage extinction and local adaptation might have unequally affected these taxa. Furthermore, the shallow-water genera *Coralliogalathea*, *Lauriea* and *Sadayoshia*, all of which are associated with coral reefs, show an absence of cladogenesis for the last 5 Myr (Palero et al., 2017; Rodríguez-Flores, Macpherson, Buckley, et al., 2019b). In this sense, Pliocene extinctions have had a relatively limited effect on shallow-water taxa in the tropical Indo-Pacific compared with the Atlantic (Malaquias & Reid, 2009; Palero et al., 2017; Vermeij, 2001; Williams & Duda, 2008). However, in the deep-sea genera *Paramunida* (Cabezas et al., 2012) and *Leiogalathea*, speciation, likely associated with the progressive cooling of the deep-sea bottom (Davis et al., 2017), appears to have been promoted during the Pliocene, as has been observed in other deep-sea invertebrates [e.g. deep-sea barnacles (Herrera et al., 2015) or yeti crabs (Roterman et al., 2018)]. Moreover, geographic isolation due to drastic changes in sea level (for instance, after the climatic changes in the Late Pleistocene) could have had a greater impact on reef fauna (Gaither et al., 2011) than on deep-sea fauna, in which processes related to water chemistry, temperature, nutrients and dispersal method might have been more influential for speciation (Ritchie et al., 2015). For instance, differences in dissolved oxygen
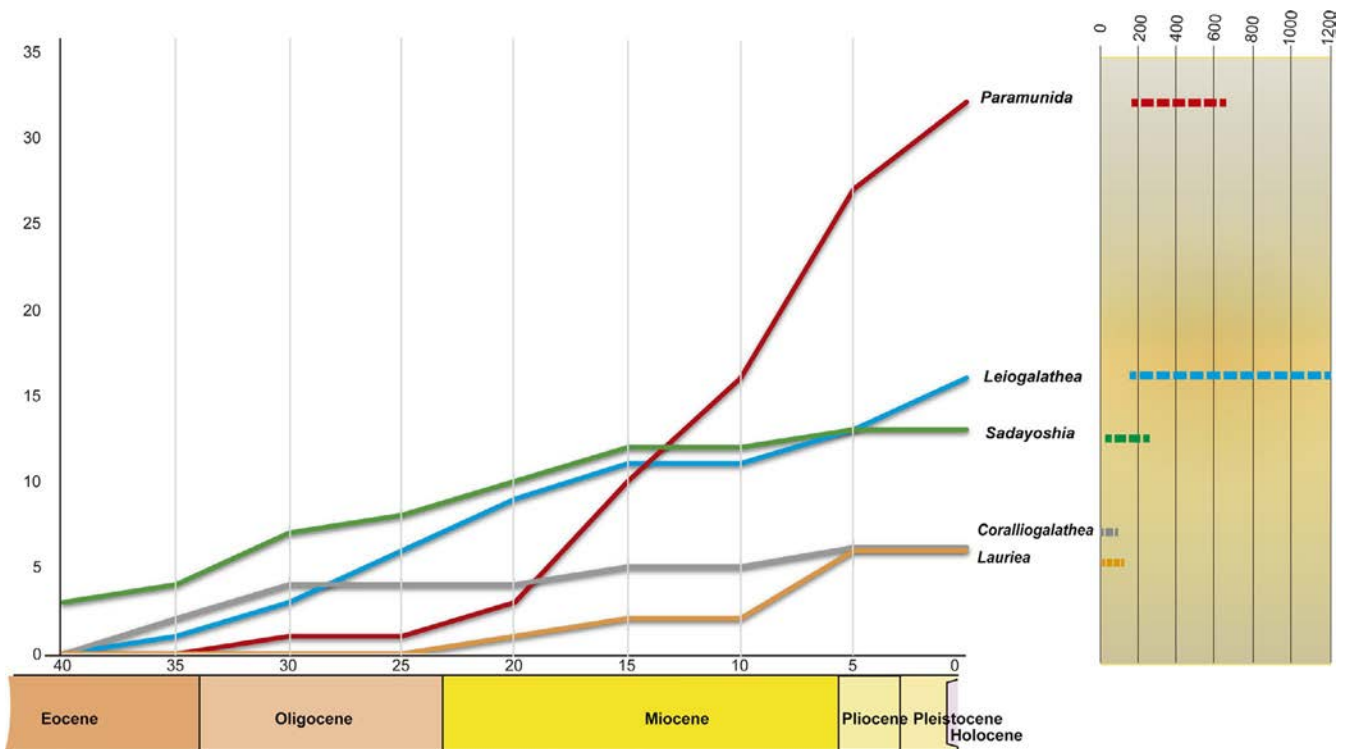
FIGURE 5 Graph showing evolutionary speciation trends in squat lobsters of the superfamily Galatheoidea: number of reconstructed lineages, estimated in increments of 5 Ma, for *Leiogalathea* and other galatheoid squat lobsters from shallow-waters (*Coralliogalathea*, *Lauriea*, *Sadayoshia*) and the deep sea (*Paramunida*) that overlap in their distribution (data for trend analysis compiled from this study and those of Rodríguez-Flores, Macpherson, Buckley, et al., 2019b, after re-treatment of the data from Cabezas et al., 2012 and Palero et al., 2017). Depth distribution for each squat lobster genus is indicated on the right of the graph [Colour figure can be viewed at wileyonlinelibrary.com]

levels seem to affect the composition and the vertical distribution of squat lobsters in the Gulf of California (Hendrickx & Serrano, 2014). Therefore, hypoxic and anoxic zones might have acted as vertical barriers, generating isolation and ultimately speciation. In line with this hypothesis, branch lengths in a previously published phylogenetic reconstruction seem to be different among shallow- and deep-water squat lobsters (Rodríguez-Flores, Macpherson, Buckley, et al., 2019b). Diverse coalescence times or distinct rates of evolution in deep-sea vs. shallow-water taxa may account for these differences since barriers to gene flow, dispersal pathways and selective pressures are highly dissimilar in both environments (McClain & Hardy, 2010). Comprehensive studies of how bathymetry affects evolutionary rates are still needed to establish which of these hypotheses are best supported.

Given the distribution overlap of these genera, the fact that their major centres of diversification coincide may not be surprising; however, there are slight geographic differences. For instance, only *Leiogalathea* presents extant Atlantic species, although there is one fossil species of *Sadayoshia* from coral reefs in the Western Tethys (Late Eocene; Müller & Collins, 1991), which might support also a Tethyan ancestral area for the genus, as in other squat lobsters (Ahyong, Schnabel, & Macpherson, 2011). For *Leiogalathea*, the Tropical Southwestern

Pacific, specifically New Caledonia, constitutes its major current centre of diversity, similar to the shallow-water genera *Lauriea* and *Sadayoshia* (Palero et al., 2017). *Coralliogalathea*, on the other hand, seems to have its main centre of diversity in the Eastern Coral Triangle (Rodríguez-Flores, Macpherson, Buckley, et al., 2019b), and *Paramunida* in the region that includes Fiji, Tonga, Vanuatu, and Wallis and Futuna Islands (Cabezas et al., 2012). However, the distribution range of *Paramunida* is restricted to shelves and slopes between 200 and 700 m around islands and continents in the CIP and the EIP (Cabezas et al., 2012). Furthermore, whereas generally *Paramunida* species appears narrowly distributed, the rest of the genera present widely distributed species, often with extensive bathymetric ranges [e.g. *Leiogalathea ascanius* (Figure 3) or *Sadayoshia lipkei* (Macpherson & Baba, 2012)]. Therefore, there are likely limitations to dispersal for *Paramunida* that could act as a promoter of rapid speciation (Cabezas et al., 2012). We conclude that the historical biogeography of squat lobster species and species-dependent factors such as local adaptation and dispersal capacities are the major drivers of current distribution patterns. However, the deep sea is, to a certain degree, dynamically associated with the same processes affecting the surface (Levin et al., 2001) and, therefore, deep-sea and

shallow-water squat lobsters are also similarly affected by the same historical processes.

Extinction and geographic persistence of lineages must be considered more accurately in this kind of inferences (Crisp et al., 2011). As such, we must consider the limitations of our interpretation of the results: (a) the lack of a fossil record for *Leiogalathea* limits the accuracy of the molecular clock calibration and hinders the inference of more accurate speciation/extinction rates; (b) sampling is biased towards the New Caledonia (or SW Pacific) region (Bouchet et al., 2008; Richer de Forges et al., 2013) (though other squat lobster genera such as *Paramunida* and *Coralliogalathea* show different diversification centres despite greater sampling of this area; Cabezas et al., 2012, Rodríguez-Flores, Macpherson, Buckley, et al., 2019b); and (c) we cannot discard other factors that could affect our biogeographic reconstructions including extinction of lineages from the Eastern Pacific (or from the Western Indo-Pacific), incomplete geographic sampling, or the existence of undescribed species from this and other under-sampled areas (see Baba, 2018; Baba & Wicksten, 2019; Rodríguez-Flores, Macpherson, & Machordom, 2019a). The historical biogeography of most deep-sea invertebrates is still a conundrum. However, the reconstruction we have presented here was based on the most comprehensive taxonomic and geographic sampling performed to date of any circum-tropical, deep-sea invertebrate, and thus, is expected to serve as an invaluable baseline study for future research.

ORCID

Paula C. Rodríguez-Flores 🆔 https://orcid.org/0000-0003-1555-9598
David Buckley 🆔 https://orcid.org/0000-0002-6514-2208
Enrique Macpherson 🆔 https://orcid.org/0000-0003-4849-4532
Laure Corbari 🆔 https://orcid.org/0000-0002-3323-6162
Annie Machordom 🆔 http://orcid.org/0000-0003-0341-0809

REFERENCES

Ahyong, S. T., Schnabel, K., & Macpherson, E. (2011) Phylogeny and fossil record of the marine squat lobsters. In G. C. B. Poore, S. T. Ahyong, & J. Taylor (Eds.), *Crustacean Issues. The biology of squat lobsters, 2011* (pp. 73–104). Melbourne, Vic.: CSIRO Publishing, Boca Raton: CRC Press.

Antonelli, A., & Sanmartín, I. (2011). Why are there so many plant species in the Neotropics? *Taxon*, *60*(2), 403–414. https://doi.org/10.1002/tax.602010

Baba, K. (2018). Chirostylidae of the Western and Central Pacific: *Uroptychus* and a new genus (Crustacea: Decapoda: Anomura). In *Tropical deep-sea benthos*. Vol. 30 (pp. 1–612), Paris: Mémoires du Muséum National d'Histoire Naturelle. 212.

Baba, K., Fujita, Y., Wehrtmann, I. S., & Scholtz, G. (2011). Developmental biology of squat lobsters. In G. C. B. Poore, S. T. Ahyong, & J. Taylor (Eds.), *Crustacean issues. The biology of squat lobsters, 2011* (pp. 105–149). Melbourne, Vic.: CSIRO Publishing, and Boca Raton, FL: CRC Press.

Baba, K., Macpherson, E., Poore, G. C. B., Ahyong, S. T., Bermudez, A., Cabezas, P., … Schnabel, K. E. (2008). Catalogue of squat lobsters of the world (Crustacea: Decapoda: Anomura—families Chirostylidae, Galatheidae and Kiwaidae). *Zootaxa*, *1905*, 1–220. https://doi.org/10.11646/zootaxa.1905.1.1

Baba, K., & Wicksten, M. K. (2019). Chirostyloidean squat lobsters (Crustacea: Decapoda: Anomura) from the Galapagos Islands. *Zootaxa*, *4564*(2), 391–421. https://doi.org/10.11646/zootaxa.4564.2.5

Bouchet, P., Héros, V., Lozouet, P., & Maestrati, P. (2008). A quarter-century of deep-sea malacological exploration in the South and

West Pacific: Where do we stand? How far to go. In V. Héros, R. H. Cowie, & P. Bouchet (Eds.), *Tropical deep-sea benthos 25*, Vol *196* (9–40), Paris: Muséum national d'Histoire naturelle.

Bouckaert, R. R., & Drummond, A. J. (2017). bModelTest: Bayesian phylogenetic site model averaging and model comparison. *BMC Evolutionary Biology*, *17*, 42. https://doi.org/10.1186/s12862-017-0890-6

Bouckaert, R., Heled, J., Kühnert, D., Vaughan, T., Wu, C.-H., Xie, D., … Drummond, A. J. (2014). BEAST 2: A software platform for Bayesian evolutionary analysis. *PLoS Computational Biology*, *10*(4), e1003537. https://doi.org/10.1371/journal.pcbi.1003537

Bowen, B. W., Rocha, L. A., Toonen, R. J., & Karl, S. A. (2013). The origins of tropical marine biodiversity. *Trends in Ecology & Evolution*, *28*(6), 359–366. https://doi.org/10.1016/j.tree.2013.01.018

Briggs, J. C. (1999). Coincident biogeographic patterns: Indo-west Pacific Ocean. *Evolution*, *53*(2), 326–335. https://doi.org/10.1111/j.1558-5646.1999.tb03769.x

Briggs, J. C., & Bowen, B. W. (2012). A realignment of marine biogeographic provinces with particular reference to fish distributions. *Journal of Biogeography*, *39*(1), 12–30. https://doi.org/10.1111/j.1365-2699.2011.02613.x

Briggs, J. C., & Bowen, B. W. (2013). Marine shelf habitat: Biogeography and evolution. *Journal of Biogeography*, *40*(6), 1023–1035. https://doi.org/10.1111/jbi.12082

Cabezas, P., Sanmartín, I., Paulay, G., Macpherson, E., & Machordom, A. (2012). Deep under the sea: Unraveling the evolutionary history of the deep-sea squat lobster *Paramunida* (Decapoda, Munididae). *Evolution*, *66*, 1878–1896. https://doi.org/10.1111/j.1558-5646.2011.01560.x

Cairns, S. D. (2007). Deep-water corals: An overview with special reference to diversity and distribution of deep-water scleractinian corals. *Bulletin of Marine Science*, *81*(3), 311–322.

Cowman, P. F., & Bellwood, D. R. (2011). Coral reefs as drivers of cladogenesis: Expanding coral reefs, cryptic extinction events, and the development of biodiversity hotspots. *Journal of Evolutionary Biology*, *24*(12), 2543–2562. https://doi.org/10.1111/j.1420-9101.2011.02391.x

Cowman, P. F., & Bellwood, D. R. (2013a). The historical biogeography of coral reef fishes: Global patterns of origination and dispersal. *Journal of Biogeography*, *40*(2), 209–224. https://doi.org/10.1111/jbi.12003

Cowman, P. F., & Bellwood, D. R. (2013b). Vicariance across major marine biogeographic barriers: Temporal concordance and the relative intensity of hard versus soft barriers. *Proceedings of the Royal Society B: Biological Sciences*, *280*, 20131541. https://doi.org/10.1098/rspb.2013.1541

Crisp, M. D., Trewick, S. A., & Cook, L. G. (2011). Hypothesis testing in biogeography. *Trends in Ecology & Evolution*, *26*(2), 66–72. https://doi.org/10.1016/j.tree.2010.11.005

Darriba, D., Taboada, G. L., Doallo, R., & Posada, D. (2012). jModelTest 2: More models, new heuristics and parallel computing. *Nature Methods*, *9*(8), 772. https://doi.org/10.1038/nmeth.2109

Davis, K. E., Hill, J., Astrop, T. I., & Wills, M. A. (2017). Global cooling as a driver of diversification in a major marine clade. *Nature Communications*, *7*, 13003. https://doi.org/10.1038/ncomms13003

Di Martino, E., Jackson, J. B., Taylor, P. D., & Johnson, K. G. (2018). Differences in extinction rates drove modern biogeographic patterns of tropical marine biodiversity. *Science. Advances*, *4*(4), eaaq1508. https://doi.org/10.1126/sciadv.aaq1508

Eilertsen, M. H., & Malaquias, M. A. E. (2015). Speciation in the dark: Diversification and biogeography of the deep-sea gastropod genus *Scaphander* in the Atlantic Ocean. *Journal of Biogeography*, *42*(5), 843–855. https://doi.org/10.1111/jbi.12471

Gaither, M. R., Bowen, B. W., Bordenave, T. R., Rocha, L. A., Newman, S. J., Gomez, J. A., … Craig, M. T. (2011). Phylogeography of the reef fish *Cephalopholisargus* (Epinephelidae) indicates Pleistocene isolation across the Indo-Pacific Barrier with contemporary overlap in the Coral Triangle. *BMC Evolutionary Biology*, *11*, 189. https://doi.org/10.1186/1471-2148-11-189

Gillespie, R. G., Baldwin, B. G., Waters, J. M., Fraser, C. I., Nikula, R., & Roderick, G. K. (2012). Long-distance dispersal: A framework for hypothesis testing. *Trends in Ecology & Evolution*, *27*(1), 47–56. https://doi.org/10.1016/j.tree.2011.08.009

Guindon, S., & Gascuel, O. (2003). A simple, fast, and accurate algorithm to estimate large phylogenies by maximum likelihood. *Systematic Biology*, *52*(5), 696–704. https://doi.org/10.1080/10635150390235520

Hall, R. (2002). Cenozoic geological and plate tectonic evolution of SE Asia and the SW Pacific: Computer-based reconstructions, model and animations. *Journal of Asian Earth Sciences*, *20*(4), 353–431. https://doi.org/10.1016/S1367-9120(01)00069-4

Harzhauser, M., Kroh, A., Mandic, O., Piller, W. E., Göhlich, U., Reuter, M., & Berning, B. (2007). Biogeographic responses to geodynamics: A key study all around the Oligo-Miocene Tethyan Seaway. *Zoologischer Anzeiger-A Journal of Comparative Zoology*, *246*(4), 241–256. https://doi.org/10.1016/j.jcz.2007.05.001

Heine, C., Yeo, L. G., & Müller, R. D. (2015). Evaluating global paleoshoreline models for the Cretaceous and Cenozoic. *Australian Journal of Earth Sciences*, *62*(3), 275–287. https://doi.org/10.1080/08120099.2015.1018321

Heled, J., & Drummond, A. J. (2010). Bayesian inference of species trees from multilocus data. *Molecular Biology and Evolution*, *27*(3), 570–580. https://doi.org/10.1093/molbev/msp274

Hendrickx, M., & Serrano, D. (2014). Effects of the oxygen minimum zone on squat lobster distributions in the Gulf of California, Mexico. *Central European Journal of Biology*, *9*(1), 92–103. https://doi.org/10.2478/s11535-013-0165-6

Hendry, A. P., Wenburg, J. K., Bentzen, P., Volk, E. C., & Quinn, T. P. (2000). Rapid evolution of reproductive isolation in the wild: Evidence from introduced salmon. *Science*, *290*(5491), 516–518.

Herrera, S., Watanabe, H., & Shank, T. M. (2015). Evolutionary and biogeographical patterns of barnacles from deep-sea hydrothermal vents. *Molecular Ecology*, *24*(3), 673–689. https://doi.org/10.1111/mec.13054

Hoeksema, B. (2007). Delineation of the Indo-Malayan centre of maximum marine biodiversity: The Coral Triangle. In W. Renema (Ed.), *Biogeography, time, and place: Distributions, barriers, and islands* (pp. 117–178). Dordrecht, The Netherlands: Springer.

Höhna, S., Landis, M. J., Heath, T. A., Boussau, B., Lartillot, N., Moore, B. R., … Ronquist, F. (2016). RevBayes: Bayesian phylogenetic inference using graphical models and an interactive model-specification language. *Systematic Biology*, *65*(4), 726–736. https://doi.org/10.1093/sysbio/syw021

Hou, Z., & Li, S. (2018). Tethyan changes shaped aquatic diversification. *Biological Reviews*, *93*(2), 874–896. https://doi.org/10.1111/brv.12376

Katoh, K., Misawa, K., Kuma, K. I., & Miyata, T. (2002). MAFFT: A novel method for rapid multiple sequence alignment based on fast Fourier transform. *Nucleic Acids Research*, *30*(14), 3059–3066. https://doi.org/10.1093/nar/gkf436

Lanfear, R., Calcott, B., Ho, S. Y., & Guindon, S. (2012). PartitionFinder: Combined selection of partitioning schemes and substitution models for phylogenetic analyses. *Molecular Biology and Evolution*, *29*(6), 1695–1701. https://doi.org/10.1093/molbev/mss020

Lessios, H. A., & Robertson, D. R. (2013). Speciation on a round planet: Phylogeography of the goatfish genus *Mulloidichthys*. *Journal of Biogeography*, *40*(12), 2373–2384. https://doi.org/10.1111/jbi.12176

Levin, L. A., Etter, R. J., Rex, M. A., Gooday, A. J., Smith, C. R., Pineda, J., … Pawson, D. (2001). Environmental influences on regional deep-sea species diversity. *Annual Review of Ecology and Systematics*, *32*(1), 51–93. https://doi.org/10.1146/annurev.ecolsys.32.081501.114002

Lins, L. S., Ho, S. Y., Wilson, G. D., & Lo, N. (2012). Evidence for Permo-Triassic colonization of the deep sea by isopods. *Biology Letters*, *8*(6), 979–982. https://doi.org/10.1098/rsbl.2012.0774

Liu, H., Li, S., Ugolini, A., Momtazi, F., & Hou, Z. (2018). Tethyan closure drove tropical marine biodiversity: Vicariant diversification of intertidal crustaceans. *Journal of Biogeography*, *45*(4), 941–951. https://doi.org/10.1111/jbi.13183

Macpherson, E. (1991). Biogeography and community structure of the decapod crustacean fauna off Namibia (Southeast Atlantic). *Journal of Crustacean Biology*, *11*(3), 401–415. https://doi.org/10.2307/1548466

Macpherson, E., & Baba, K. (2012). The squat lobsters of the genus *Sadayoshia* Baba, 1969 (Crustacea: Decapoda: Anomura: Munididae): New records including six new species from the Pacific Ocean. *Zootaxa*, *3589*, 30–48. https://doi.org/10.11646/zootaxa.3589.1.2

Macpherson, E., de Forges, B. R., Schnabel, K., Samadi, S., Boisselier, M. C., & Garcia-Rubies, A. (2010). Biogeography of the deep-sea galatheid squat lobsters of the Pacific Ocean. *Deep Sea Research Part I: Oceanographic Research Papers*, *57*(2), 228–238. https://doi.org/10.1016/j.dsr.2009.11.002

Macpherson, E., & Robainas-Barcia, A. (2015). Species of the genus *Galathea* Fabricius, 1793 (Crustacea, Decapoda, Galatheidae) from the Indian and Pacific Oceans, with descriptions of 92 new species. *Zootaxa*, *3913*(1), 1–335. https://doi.org/10.11646/zootaxa.3913.1.1

Maddison, W. P., & Maddison, D. R. (2018). *Mesquite: a modular system for evolutionary analysis*. Version 3.40. Retrieved from http://www.mesquiteproject.org

Malaquias, M. A. E., & Reid, D. G. (2009). Tethyan vicariance, relictualism and speciation: Evidence from a global molecular phylogeny of the opisthobranch genus *Bulla*. *Journal of Biogeography*, *36*(9), 1760–1777. https://doi.org/10.1111/j.1365-2699.2009.02118.x

Matzke, N. J. (2013). *BioGeoBEARS: BioGeography with Bayesian (and likelihood) evolutionary analysis in R Scripts, CRAN: The Comprehensive R ArchiveNet-work*, Berkeley, CA. Retrieved from https://cran.r-project.org/src/contrib/Archive/BioGeoBEARS/

McClain, C. R., & Hardy, S. M. (2010). The dynamics of biogeographic ranges in the deep sea. *Proceedings of the Royal Society B: Biological Sciences*, *277*(1700), 3533–3546. https://doi.org/10.1098/rspb.2010.1057

Miller, M. A., Pfeiffer, W., & Schwartz, T. (2010). Creating the CIPRES Science Gateway for inference of large phylogenetic trees. Proceedings of the Gateway Computing Environments Workshop (GCE), New Orleans, LA, 14 November 2010,1 (2010), pp. 1–8.

Moritz, C. C., Pratt, R. C., Bank, S., Bourke, G., Bragg, J. G., Doughty, P., … Tedeschi, L. G. (2018). Cryptic lineage diversity, body size divergence, and sympatry in a species complex of Australian lizards (*Gehyra*). *Evolution*, *72*(1), 54–66. https://doi.org/10.1111/evo.13380

Müller, P., & Collins, J. S. H. (1991). Late Eocene coral-associated decapods (Crustacea) from Hungary. *Contributions to Tertiary and Quaternary Geology*, *28*(2–3), 47–92.

O'Dea, A., Lessios, H. A., Coates, A. G., Eytan, R. I., Restrepo-Moreno, S. A., Cione, A. L., … Jackson, J. B. C. (2016). Formation of the Isthmus of Panama. *Science Advances*, *2*(8), e1600883. https://doi.org/10.1126/sciadv.1600883

O'Hara, T. D., Hugall, A. F., Woolley, S. N., Bribiesca-Contreras, G., & Bax, N. J. (2019). Contrasting processes drive ophiuroid phylodiversity across shallow and deep seafloors. *Nature*, *565*(7741), 636. https://doi.org/10.1038/s41586-019-0886-z

Osborn, K. J. (2009). Relationships within the Munnopsidae (Crustacea, Isopoda, Asellota) based on three genes. *Zoologica Scripta*, *38*(6), 617–635. https://doi.org/10.1111/j.1463-6409.2009.00394.x

Palero, F., Robainas-Barcia, A., Corbari, L., & Macpherson, E. (2017). Phylogeny and evolution of shallow-water squat lobsters (Decapoda, Galatheoidea) from the Indo-Pacific. *Zoologica Scripta*, *46*(5), 584–595. https://doi.org/10.1111/zsc.12230

Poupin, J., & Corbari, L. (2016). A preliminary assessment of the deep-sea Decapoda collected during the KARUBENTHOS 2015 Expedition to Guadeloupe Island. *Zootaxa*, *4190*(1), 1–107. https://doi.org/10.11646/zootaxa.4190.1.1

Puritz, J. B., Keever, C. C., Addison, J. A., Byrne, M., Hart, M. W., Grosberg, R. K., & Toonen, R. J. (2012). Extraordinarily rapid life-history divergence between *Cryptasterina* sea star species. *Proceedings of the Royal Society B: Biological Sciences*, *279*(1744), 3914–3922. https://doi.org/10.1098/rspb.2012.1343

Rambaut, A. (2014) FigTree v1.4.2. Retrieved from http://tree.bio.ed.ac.uk/software/figtree/

Rambaut, A., & Drummond, A. J. (2014). TreeAnnotator v2. 1.2. Edinburgh: University of Edinburgh, Institute of Evolutionary Biology.

Raupach, M. J., Mayer, C., Malyutina, M., & Wägele, J. W. (2009). Multiple origins of deep-sea *Asellota* (Crustacea: Isopoda) from shallow waters revealed by molecular data. *Proceedings of the Royal Society B: Biological Sciences*, *276*, 799–808. https://doi.org/10.1098/rspb.2008.1063

Ree, R. H., & Smith, S. A. (2008). Maximum likelihood inference of geographic range evolution by dispersal, local extinction, and cladogenesis. *Systematic Biology*, *57*(1), 4–14. https://doi.org/10.1080/10635150701883881

Renema, W., Bellwood, D. R., Braga, J. C., Bromfield, K., Hall, R., Johnson, K. G., … Pandolfi, J. M. (2008). Hopping hotspots: Global shifts in marine biodiversity. *Science*, *321*(5889), 654–657. https://doi.org/10.1126/science.1155674

Rex, M. A., Stuart, C. T., & Coyne, G. (2000). Latitudinal gradients of species richness in the deep-sea benthos of the North Atlantic. *Proceedings of the National Academy of Sciences of the United States of America*, *97*(8), 4082–4085. https://doi.org/10.1073/pnas.050589497

Richer de Forges, B., Chan, T. Y., Corbari, L., Lemaitre, R., Macpherson, E., Ahyong, S. T., & Ng, P. K. (2013). The MUSORSTOM-TDSB deep-sea benthos exploration programme (1976–2012): An overview of crustacean discoveries and new perspectives on deep-sea zoology and biogeography. In: S. T. Ahyong, T.-Y. Chan, L. Corbari, & P. K. L. Ng (Eds.), *Tropical Deep-Sea Benthos*, Vol. *27*. Paris: Mémoires du Muséum national d'Histoire naturelle *204*, 13–66.

Ritchie, H., Jamieson, A. J., & Piertney, S. B. (2015). Phylogenetic relationships among hadal amphipods of the Superfamily

Lysianassoidea: Implications for taxonomy and biogeography. *Deep Sea Research Part I: Oceanographic Research Papers*, *105*, 119–131. https://doi.org/10.1016/j.dsr.2015.08.014

Robins, C. M., Feldmann, R. M., & Schweitzer, C. E. (2013). Nine new genera and 24 new species of the Munidopsidae (Decapoda: Anomura: Galatheoidea) from the Jurassic Ernstbrunn Limestone of Austria, and notes on fossil munidopsid classification. *Annalen Des Naturhistorischen Museums in Wien, Serie A*, *115*, 167–251.

Robins, C. M., & Klompmaker, A. A. (2019). Extreme diversity and parasitism of Late Jurassic squat lobsters (Decapoda: Galatheoidea) and the oldest records of porcellanids and galatheids. *Zoological Journal of the Linnean Society*, *187*(4), 1131–1154. https://doi.org/10.1093/zoolinnean/zlz067

Rocha, L. A., Robertson, D. R., Rocha, C. R., Van Tassell, J. L., Craig, M. T., & Bowen, B. W. (2005). Recent invasion of the tropical Atlantic by an Indo-Pacific coral reef fish. *Molecular Ecology*, *14*(13), 3921–3928. https://doi.org/10.1111/j.1365-294X.2005.02698.x

Rodríguez-Flores, P. C., Macpherson, E., Buckley, D., & Machordom, A. (2019b). High morphological similarity coupled with high genetic differentiation in new sympatric species of coral-reef squat lobsters (Crustacea: Decapoda: Galatheidae). *Zoological Journal of the Linnean Society*, *185*(4), 984–1017. https://doi.org/10.1093/zoolinnean/zly074

Rodríguez-Flores, P. C., Macpherson, E., & Machordom, A. (2019a). Revision of the squat lobsters of the genus *Leiogalathea* Baba, 1969 (Crustacea, Decapoda, Munidopsidae) with the description of 15 new species. *Zootaxa*, *4560*(2), 201–256. https://doi.org/10.11646/zootaxa.4560.2.1

Ronquist, F., & Huelsenbeck, J. P. (2003). MrBayes 3: Bayesian phylogenetic inference under mixed models. *Bioinformatics*, *19*(12), 1572–1574. https://doi.org/10.1093/bioinformatics/btg180

Roterman, C. N., Copley, J. T., Linse, K. T., Tyler, P. A., & Rogers, A. D. (2013). The biogeography of the yeti crabs (Kiwaidae) with notes on the phylogeny of the Chirostyloidea (Decapoda: Anomura). *Proceedings of the Royal Society B: Biological Sciences*, *280*(1764), 20130718. https://doi.org/10.1098/rspb.2013.0718

Roterman, C. N., Lee, W. K., Liu, X., Lin, R., Li, X., & Won, Y. J. (2018). A new yeti crab phylogeny: Vent origins with indications of regional extinction in the East Pacific. *PLoS ONE*, *13*(3), e0194696. https://doi.org/10.1371/journal.pone.0194696

Samadi, S., Bottan, L., Macpherson, E., De Forges, B. R., & Boisselier, M. C. (2006). Seamount endemism questioned by the geographic distribution and population genetic structure of marine invertebrates. *Marine Biology*, *149*(6), 1463–1475. https://doi.org/10.1007/s00227-006-0306-4

Schnabel, K. E., Cabezas, P., McCallum, A., Macpherson, E., Ahyong, S. T., & Baba, K. (2011). World-wide distribution patterns of squat lobsters. In G. C. B. Poore, S. T. Ahyong, & J. Taylor (Eds.), *The biology of squat lobsters* (pp. 149–182). Melbourne, Vic.: CSIRO Publishing, Boca Raton: CRC Press.

Spalding, M. D., Fox, H. E., Allen, G. R., Davidson, N., Ferdaña, Z. A., Finlayson, M., … Robertson, J. (2007). Marine Ecoregions of the World: A Bioregionalization of Coastal and Shelf areas. *BioScience*, *57*(7), 573–583. https://doi.org/10.1641/B570707

Sun, S., Sha, Z., & Wang, Y. (2018). Phylogenetic position of Alvinocarididae (Crustacea: Decapoda: Caridea): New insights into the origin and evolutionary history of the hydrothermal vent alvinocarid shrimps. *Deep Sea Research Part I: Oceanographic Research Papers*, *141*, 93–105. https://doi.org/10.1016/j.dsr.2018.10.001

Thacker, C. E. (2015). Biogeography of goby lineages (Gobiiformes: Gobioidei): Origin, invasions and extinction throughout the Cenozoic. *Journal of Biogeography*, *42*(9), 1615–1625. https://doi.org/10.1111/jbi.12545

Uribe, J. E., Williams, S. T., Templado, J., Buge, B., & Zardoya, R. (2017). Phylogenetic relationships of Mediterranean and North-East Atlantic Cantharidinae and notes on Stomatellinae (Vetigastropoda: Trochidae). *Molecular Phylogenetics and Evolution*, *107*, 64–79. https://doi.org/10.1016/j.ympev.2016.10.009

Vermeij, G. J. (2001). Community assembly in the sea: geological history of the living shore biota. In M. D. Bertness, S. D. Gaines & M. E. Hay (Eds.), *Marine community ecology* (pp. 39–60). Sunderland, MA: Sinauer Associates.

Veron, J. E., Devantier, L. M., Turak, E., Green, A. L., Kininmonth, S., Stafford-Smith, M., & Peterson, N. (2009). Delineating the coral triangle. *Galaxea, Journal of Coral Reef Studies*, *11*(2), 91–100. https://doi.org/10.3755/galaxea.11.91

Vrijenhoek, R. C. (2009). Cryptic species, phenotypic plasticity, and complex life histories: Assessing deep-sea faunal diversity with molecular markers. *Deep Sea Research Part II: Topical Studies in Oceanography*, *56*(19–20), 1713–1723. https://doi.org/10.1016/j.dsr2.2009.05.016

Whatley, R. C., & Coles, G. P. (1991). Global change and the biostratigraphy of North Atlantic Cainozoic deep water Ostracoda. *Journal of Micropalaeontology*, *9*(2), 119–132. https://doi.org/10.1144/jm.9.2.119

Williams, S. T., & Duda, T. F. Jr (2008). Did tectonic activity stimulate Oligo-Miocene speciation in the Indo-West Pacific? *Evolution*, *62*(7), 1618–1634. https://doi.org/10.1111/j.1558-5646.2008.00399.x

Williams, S. T., Smith, L. M., Herbert, D. G., Marshall, B. A., Warén, A., Kiel, S., … Kano, Y. (2013). Cenozoic climate change and diversification on the continental shelf and slope: Evolution of gastropod diversity in the family Solariellidae (Trochoidea). *Ecology and Evolution*, *3*(4), 887–917. https://doi.org/10.1002/ece3.513

Yu, Y., Harris, A. J., Blair, C., & He, X. (2015). RASP (Reconstruct Ancestral State in Phylogenies): A tool for historical biogeography. *Molecular Phylogenetics and Evolution*, *87*, 46–49. https://doi.org/10.1016/j.ympev.2015.03.008

SUPPORTING INFORMATION

Additional supporting information may be found online in the Supporting Information section.

Supporting information S1. Morphological characters traced on the species tree with Mesquite v 3.40. Detailly information about measures and more informative morphological characters is provided in Rodríguez-Flores et al., (2019a).

1. Hepatic margin of the carapace unarmed or armed with a spine.

Parsimony reconstruction
Presence/absence hepatic spine

0
1
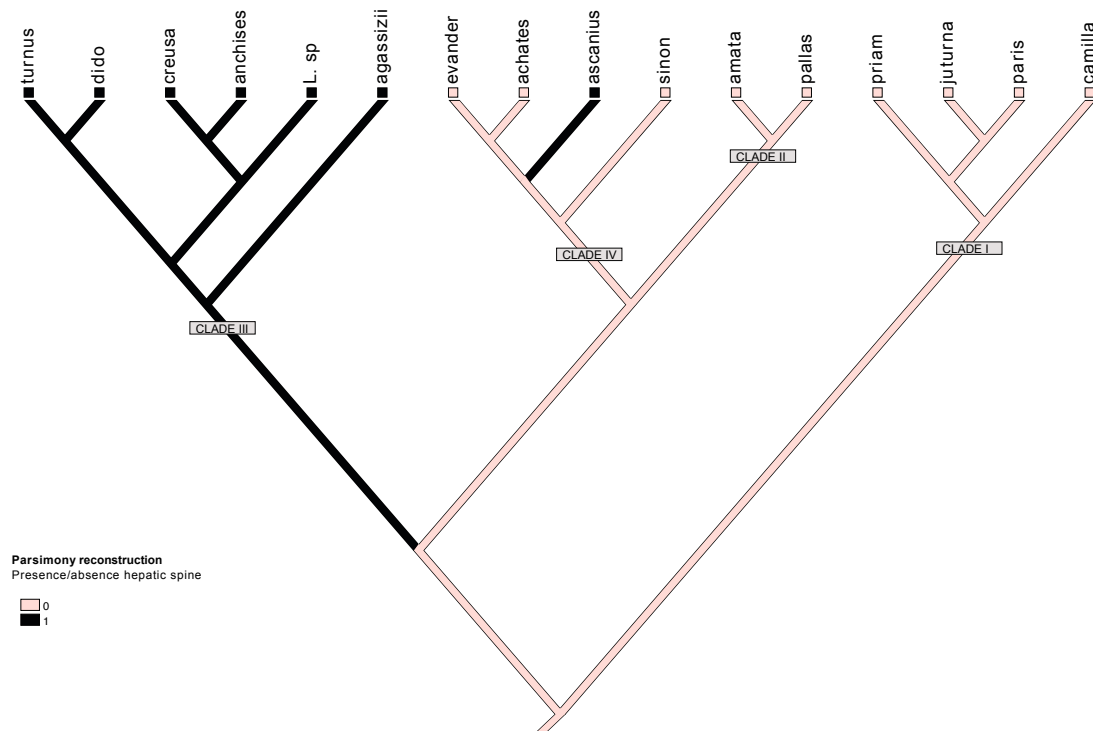
2. Spines on the rostrum margin (minutes, well-developed or rostrum unarmed).

Parsimony reconstruction
Spines on rostrum

rostrum unarmed
minute spines
well-developed spines

3. Number of spines on the carapace margin.

Parsimony reconstruction
Spines on carapace margin

- 1–2 spines
- 3–4 spines
- 5–7 spines
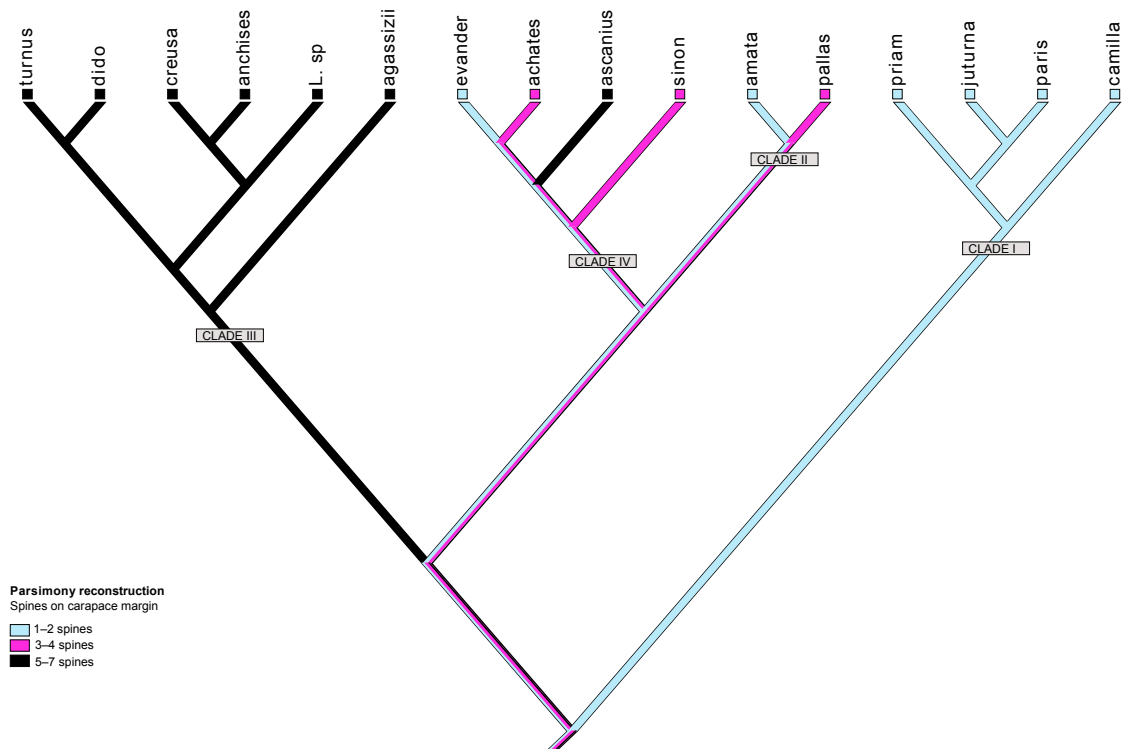
4. Maximum number of spines on flexor margin of walking leg dactyli

Parsimony reconstruction
Maximum number of teeth on dactyli flexor margin

- 6
- 7
- 8
- 9
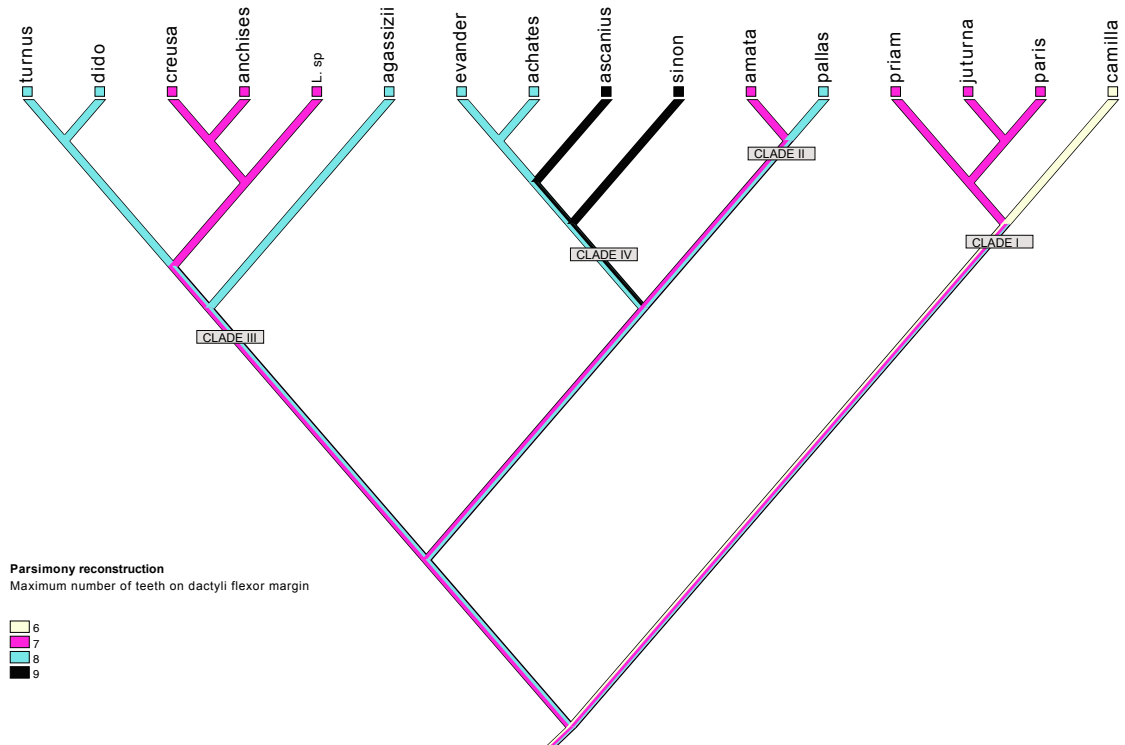
5. Eye reduction: Cornea narrower than ocular peduncle.

Parsimony reconstruction
Eye reduction

- 0
- 1
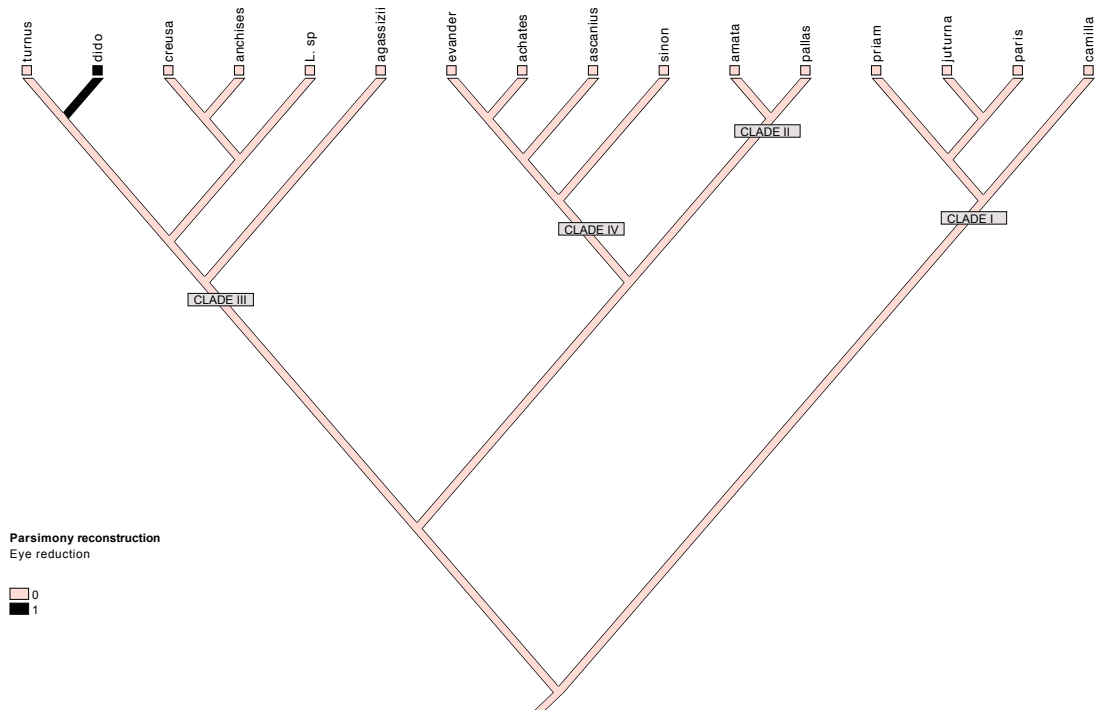
6. Shape of walking legs propodi: Stout (P2 propodi less than 6 times as long as broad) or slender (P2 propodus more than 8 times as long as broad).

Parsimony
Propodi of walking legs shape

- Stout
- Slender

Supporting information
Table S1.

Set of Primers used for this study including sequence 5–3', Primer name, gene fragment, reference and specificity of the Primer.

Seq 5'-3'	Name	Gene	Reference	Taxonomy
GGTCAACAAATCATAAAGAYATYGG	dgLCO1490	COI	Meyer 2003	Decapoda
TAAACTTCAGGGTGACCAAARAAYCA	dgHCO2198	COI	Meyer 2003	Decapoda
GGTCAACAAATCATAAAGATATTGG	COI L2198	COI	Folmer et al. 1994	Universal
TCAGGGTGACCAAAAAATCA	COI H	COI	Machordom et al. 2003	Universal
TITCIACIAAYCAYAARGAYATTGG	jgLCO1490	COI	Geller et al. 2013	Marine invertebrates
TAIACYTCIGGRTGICCRAARAAYCA	jgHCO2198	COI	Geller et al. 2013	Marine invertebrates
GAGCTCCAGATATAGCATTCC	COI-f	COI	van Syoc, 1995	Barnacles
AGTATAAGCGTCTGGGTAGTC	COI-r	COI	van Syoc, 1995	Barnacles
CCTGTTTANCAAAAACAT	16S 1471	16S	Crandall &Fitzpatrick 1996	Crayfish
AGATAGAAACCAACCTGG	16S 1472	16S	Crandall &Fitzpatrick 1996	Crayfish
CGCCTGTTTATCAAAAACAT	16S ar	16S	Palumbi et al. 1991	Universal
CCGGTCTGAACTCAGATCACGT	16S br	16S	Palumbi et al. 1991	Universal
CGACTGTTTAACAAAAACAT	16S-L-mar	16S	Lydeard et al., 1996	Fresh-water mussels
CCGTTCTGAACTCAGCTCATGT	16S-H-mar	16S	Lydeard et al., 1996	Fresh-water mussels
TACCTGGTTGATCCTGCCAGTAG	18S 1F	18S	Whiting (2002)	Insecta
TATCTGATCGCCTTCGAACCTCT	18S 2b.9	18S	Whiting (2002)	Insecta
AACCTGGTTGATCCTGCCAGT	18S A	18S	Apakupakul et al. (1999)	Leeches
CCAACTACGAGCTTTT	18S L	18S	Apakupakul et al. (1999)	Leeches
CGGTAATTCCAGCTC	18SrDNA-C	18S	Apakupakul et al. 1999	Leeches
CAGACAAATCGCTCC	18SrDNA-Y	18S	Apakupakul et al. 1999	Leeches
ATGGCTCGTACCAAGCAGACVGC	H3-F	H3	Colgan 1998	Arthropoda
ATATCCTTRGGCATRATRGTGAC	H3-R	H3	Colgan 1998	Arthropoda
CGGGCCAAGGAGTCCAACATGTG	28S BF	28S	Palero et al. (2009)	Crustacea
CCCACAGCGCCAGTTCTGCTTACC	28S BR	28S	Palero et al. (2009)	Crustacea
CTTCTTTAAGATTAATAATTCG	leioCOIfwint	COI	This study	Galatheoidea
GATGYTGATAAAGAATWGGATC	leioCOIRvint	COI	This study	Galatheoidea

Apakupakul K, Siddall ME, Burreson EM (1999) Higher level relationships of leeches (Annelida: Clitellata: Euhirudinea) based on morphology and gene sequences. Molecular Phylogenetics and Evolution, 12(3), 350–359.

Colgan DJ, McLauchlan A, Wilson GDF, Livingston SP, Edgecombe GD, Macaranas J, Cassis G, Gray MR (1998) Histone H3 and U2 snRNA DNA sequences and arthropod molecular evolution. Australian Journal of Zoology, 46(5), 419–437.

Crandall KA, Fitzpatrick Jr JF (1996) Crayfish molecular systematics: using a combination of procedures to estimate phylogeny. Systematic Biology, 45(1), 1–26.

Folmer O, Black M, Hoeh W, Lutz R, Vrijenhoek R (1994) DNA primers for amplification of mitochondrial cytochrome c oxidase subunit I from diverse metazoan invertebrates. Molecular Marine Biology and Biotechnology, 3, 294–299.

Geller J, Meyer C, Parker M, Hawk H (2013) Redesign of PCR primers for mitochondrial cytochrome c oxidase subunit I for marine invertebrates and application in all-taxa biotic surveys. Molecular Ecology Resources, 13(5), 851–861.

Lydeard C, Mulvey M, Davis GM (1996) Molecular systematics and evolution of reproductive traits of North American freshwater unionacean mussels (Mollusca: Bivalvia) as inferred from 16S rRNA gene sequences. Philosophical Transactions of the Royal Society of London. Series B: Biological Sciences, 351(1347), 1593–1603.

Machordom A, Araujo R, Erpenbeck D, Ramos MÁ (2003). Phylogeography and conservation genetics of endangered European Margaritiferidae (Bivalvia: Unionoidea). Biological Journal of the Linnean Society, 78(2), 235–252.

Meyer CP (2003) Molecular systematics of cowries (Gastropoda: Cypraeidae) and diversification patterns in the tropics. Biological Journal of the Linnean Society, 79, 401–459.

Palero F, Crandall KA, Abelló P, Macpherson E, Pascual M (2009) Phylogenetic relationships between spiny, slipper and coral lobsters (Crustacea, Decapoda, Achelata). Molecular Phylogenetics and Evolution, 50(1), 152–162.

Palumbi S (1991) Simple fool's guide to PCR.

Van Syoc R J (1995) Barnacle mitochondrial DNA: determining genetic relationships among species of Pollicipes. Crustacean Issues, 10, 269–296.

Whiting MF (2002) Mecoptera is paraphyletic: multiple genes and phylogeny of Mecoptera and Siphonaptera. Zoologica Scripta, 31(1), 93–104.

Supporting information
Table S2

Voucher Code	DNA CODE	Taxonomy	CRUISE	Geographic area	Station	Latitude	Longitude	Depth m	Date	Size mm	COI	16S	H3	28S	18S
MNHN-IU-2016-7125	G487	Leiogalathea achates	BIOMAGLO	Channel of Mozambique	DW4853	13°00'S	44°56'E	665–669 m	3/2/17	3.6	MK140857	MK140893	MN839863	MN839912	MN839955
MNHN-IU-2016-3203	G488	Leiogalathea achates	BIOMAGLO	Channel of Mozambique	DW4864	12°56'S	45°15'E	455–487 m	7/2/17	5.8	MK140858	MK140894	MN839864	MN839913	MN839956
MNHN-IU-2016-3206	G489	Leiogalathea achates	BIOMAGLO	Channel of Mozambique	DW4874	12°42'S	45°19'E	706–887 m	9/2/17	6.1	MN839784		MN839865	MN839914	MN839957
MNHN-IU-2016-8834	G490	Leiogalathea achates	BIOMAGLO	Channel of Mozambique	DW4873	12°42'S	45°22'E	795–1033 m	8/2/17	7	MN839785		MN839866	MN839915	
MNHN-IU-2016-3207	G491	Leiogalathea achates	BIOMAGLO	Channel of Mozambique	DW4873	12°42'S	45°22'E	795–1033 m	8/2/17	7.2	MK140859	MK140895	MN839867	MN839916	MN839958
SMF51247	G415	Leiogalathea agassizii	Caribbean Sea	Caribbean Sea	Station, 163 34-1	26°20.177N	84°45.564W	519 m	27/2/12	6.9	MK140828	MK140862			
MNHN-IU-2013-18858	G465	Leiogalathea agassizii	KARUBENTHOS 2	Caribbean Sea	Stn DW4510	16°15'N	61°51'W	660–690 m	7/6/15	6.7	MK140854	MK140890	MN839859	MN839908	MN839952
MNHN-IU-2013-18894	G466	Leiogalathea agassizii	KARUBENTHOS 2	Caribbean Sea	Stn DW4511	16°14'N	61°52'W	660–630 m	8/6/15	4.1	MK140855	MK140891	MN839860	MN839909	MN839953
MNHN-IU-2014-13779	G420/G567	Leiogalathea amata	MUSORSTOM 7	Wallis & Futuna	Stn DW807	11°48.7'S	178°18.0' W	440 m	27/11/93	3.6	MK140833	MK140867	MN839839		
MNHN-IU-2014-13780	G424	Leiogalathea amata	BATHUS 3	New Caledonia	Stn DW556	23°40' S	167°59' E	420–438 m	19/5/92	5.2		MK140871			
MNHN-IU-2014-13786	G418	Leiogalathea anchises	SALOMON 1	Solomon Islands	Stn CP1833	10°12'S	161°19'E	367–533 m	30/4/14	6.4	MK140831	MK140865	MN839837		MN839938
MNHN-IU-2015-350	G435	Leiogalathea anchises	MADEEP	Papua New Guinea	Stn DW4292	09°14'S	153°52'E	530–530 m	5/10/01	7.4	MK140839	MK140874	MN839844		MN839943
MNHN-IU-2013-17425	G425	Leiogalathea ascanius	NORFOLK 2	New Caledonia	Stn DW2027	23°26.34'S	167°51.38E	465–650 m	21/10/03	8.3	MK140837	MK140872	MN839842	MN839894	MN839941
MNHN-IU-2014-13706	G443	Leiogalathea ascanius	BATHUS 3	New Caledonia	Stn DW778	24°43' S	170°07' E	750–760 m	24/11/93	3.2		MK140878			
MNHN-IU-2014-13725	G451	Leiogalathea ascanius	HALIPRO 2	New Caledonia	Stn BT45	23°42'S	167°43'E	469–860 m	15/11/96	4.7	MK140848	MK140884	MN839851		MN839948
MNHN-IU-2014-13772	G452	Leiogalathea ascanius	EXBODI	New Caledonia	Stn CP3893	22°24'S	171°47'E	786–814 m	19/9/11	7.1	MK140849	MK140885	MN839852	MN839902	
MNHN-IU-2014-13743	G538	Leiogalathea ascanius	NORFOLK 2	New Caledonia	Stn DW2046	23°43.87'S	168°01.03'E	333–375 m	23/10/03	5.8	MN839786	MN839813	MN839868	MN839917	MN839959
MNHN-IU-2014-13757	G539	Leiogalathea ascanius	NORFOLK 2	New Caledonia	Stn DW2056	24°40'S	168°39'E	573–600 m	25/10/03	4.3	MN839787	MN839814	MN839869	MN839918	
MNHN-IU-2014-13755	G544	Leiogalathea ascanius	NORFOLK 2	New Caledonia	Stn DW2053	23°39.64'S	168°15.60'E	670–708 m	24/10/03	6.6	MN839792	MN839819	MN839874	MN839923	MN839964
MNHN-IU-2017-3627	G559	Leiogalathea ascanius	KANADEEP	New Caledonia	Stn CP4963	21°21'S	158°00'E	1000–978 m	7/9/17	4.5	MN839800	MN839827	MN839882	MN839931	MN839972
MNHN-IU-2017-3970	G560	Leiogalathea ascanius	KANACONO	New Caledonia	Stn DR4771	23°03'S	168°20'E	900–220 m	28/8/16	2.3	MN839801	MN839828	MN839883	MN839932	MN839973
NIWA9024	KS15 NIWA	Leiogalathea ascanius	TAN0413,	New Zealand	-	37°18'42.64''S	177° 7'16.31''E	725–550 m	-	-	MN839807	MN839834			
MNHN-IU-2014-13728	G444	Leiogalathea camilla	BATHUS 3	New Caledonia	Stn DW817	23°42' S	168°15' E	405–410 m	29/11/93	3.1	MK140843	MK140879			
MNHN-IU-2014-13788	G454	Leiogalathea camilla	NORFOLK 1	New Caledonia	Stn DW1704	23°47'S	168°17'E	420–400 m	25/6/01	3.0	MK140850	MK140886	MN839853		
MNHN-IU-2017-3949	G561	Leiogalathea camilla	KANACONO	New Caledonia	Stn DW4783	22°56'S	167°48'E	385–395 m	29/8/16	2.8	MN839802	MN839829	MN839884	MN839933	MN839974

470

Catalogue	Code	Species	Expedition	Country	Station	Latitude	Longitude	Depth	Date						
MNHN-IU-2014-13716	G441	Leiogalathea creusa	TARASOC	French Polynesia	Stn CP3376	15°41'S	146°54'W	646–737 m	4/10/09	5.0	MK140842		MN839841	MN839893	
MNHN-IU-2013-17431	G422	Leiogalathea dido	HALIPRO 2	New Caledonia	Stn BT55	25°04'S	168°44'E	1098–1480 m	17/11/96	9.8	MK140835	MK140869			
MNHN-IU-2013-17430	G423	Leiogalathea dido	HALIPRO 2	New Caledonia	Stn BT55	25°04'S	168°44'E	1098–1480 m	17/11/96	6.0	MK140836	MK140870	MN839854	MN839903	MN839949
MNHN-IU-2014-13783	G455	Leiogalathea dido	EBISCO	New Caledonia	Stn DW2488	23°50'S	161°42'E	996–932 m	5/10/05	4.6	MN839781	MN839808	MN839875	MN839924	MN839965
MNHN-IU-2014-13745	G545	Leiogalathea dido	NORFOLK 2	New Caledonia	Stn DW2055	23°39.23'S	168°16.43'E	900–950 m	24/10/03	5.0	MN839793	MN839820			
NTOU 170	170	Leiogalathea evander		Phillippines					-	-	MK140826	MK140860			
MNHN-IU-2013-17429	G417	Leiogalathea evander	MUSORSTOM 9	Marquesas Islands	Stn DR1255	9°38.5'S	139°48.4'W	416–440	2/9/97	4.0	MK140830	MK140864	MN839836	MN839890	MN839937
MNHN-IU-2015-820	G457	Leiogalathea evander	MADEEP	Papua New Guinea	Stn DW4288	09°12'S	153°54'E	504 m	30/4/14	3.9	MK140851	MK140887	MN839855	MN839904	MN839950
MNHN-IU-2013-17422	G540	Leiogalathea evander	MUSORSTOM 9	Marquesas Is, Polynesia	Stn CP1306	8°55.2'S	140°14.8'W	283–448 m	24/10/03	3.7	MN839788	MN839815	MN839870	MN839919	MN839960
MNHN-IU-2013-17420	G541	Leiogalathea evander	MUSORSTOM 9	Marquesas Is, Polynesia	Stn DR1253	9°47.9'S	139°38.1'W	360–405 m	2/9/97	4.8	MN839789	MN839816	MN839871	MN839920	MN839961
MNHN-IU-2016-5797	G553	Leiogalathea evander	MADEEP	Papua New Guinea	Stn DW4285	09°11'S	153°55'E	380–411 m	41759	3.7	MN839798	MN839825	MN839880	MN839929	MN839970
MNHN-IU-2013-17421	G481	Leiogalathea evander	MUSORSTOM 9	Marquesas Islands	Stn CP1282	7°51.7'S	140°30.6'W	416–460 m	2/9/97	4.9	MK140856	MK140892	MN839861	MN839910	
NTOU 65	65	Leiogalathea juturna		Taiwan					-	-	MK140827	MK140861			
MNHN-IU-2013-17404	G416	Leiogalathea juturna	KARUBAR	Indonesia	Stn DW18	05°18'S	133°01'E	205–212	24/10/91	4.2	MK140829	MK140863	MN839835	MN839889	MN839936
MNHN-IU-2014-13764	G447	Leiogalathea pallas	MUSORSTOM 8	Vanuatu	Stn DW1015	17°54'S	168°22'E	420–375 m	27/9/94	4.7	MK140845	MK140881	MN839848	MN839900	
MNHN-IU-2014-13775	G448	Leiogalathea pallas	SANTO	Vanuatu	Stn AT10	15°41'S	167°01'E	509–659 m	17/9/06	8.3	MK140846	MK140882	MN839849		
MNHN-IU-2014-13395	G458	Leiogalathea pallas	KAVIENG 2014	Papua New Guinea	Stn DW4470	02°45'S	150°37'E	163–358 m	3/9/14	6.0	MK140852	MK140888	MN839856	MN839905	MN839951
MNHN-IU-2014-13785	G459	Leiogalathea pallas	EBISCO	New Caledonia	Stn DW2629	21°06'S	160°46'E	569–583 m	21/10/05	6.9	MK140853	MK140889	MN839857	MN839906	
MNHN-IU-2017-2485	G563	Leiogalathea pallas	KANADEEP	New Caledonia	Stn DW4989	24°15'S	166°58'E	420–600 m	13/9/17	6.9	MN839804	MN839831	MN839886	MN839935	MN839976
MNHN-IU-2014-13720	G419	Leiogalathea paris	TARASOC	French Polynesia	Stn DW3484	17°47'S	149°23'W	300–650 m	23/10/09	5.2	MK140832	MK140866	MN839838	MN839891	MN839939
MNHN-IU-2015-296	G434	Leiogalathea paris	MADEEP	Papua New Guinea	Stn DW4314	09°48'S	151°33'E	278–420 m	3/5/14	2.0	MK140838	MK140873	MN839843	MN839895	MN839942
MNHN-IU-2011-4471	G450	Leiogalathea paris	TARASOC	French Polynesia	Stn DW3441	16°43'S	151°26'W	350–360 m	16/10/09	4.1	MK140847	MK140883	MN839850	MN839901	MN839947
MNHN-IU-2014-13714	G485	Leiogalathea paris	BORDAU 2	Tonga	Stn DW1616	23°04.22'S	175°54.09'W	664–781 m	17/6/00	4.5		MN839811			
MNHN-IU-2017-3834	G558	Leiogalathea paris	KANADEEP	New Caledonia	DW4962	23°02'S	159°28'E	315–1260 m	6/9/17	2.6	MN839799	MN839826	MN839881	MN839930	MN839971
MNHN-IU-2017-3535	G562	Leiogalathea paris	KANADEEP	New Caledonia	DW4921	21°39'S	162°42'E	800–800 m	1/9/17	2.7	MN839803	MN839830	MN839885	MN839934	MN839975
MNHN-IU-2014-13697	G436	Leiogalathea priam	MADEEP	Papua New Guinea	Stn DW4287	09°12'S	153°56'E	340–375 m	30/4/14	5.1	MK140840	MK140875	MN839845	MN839897	MN839944
MNHN-IU-2014-13696	G440	Leiogalathea priam	MADEEP	Papua New Guinea	Stn DW4314	09°48'S	151°33'E	278–420 m	3/5/14	3.1	MK140841	MK140876	MN839846	MN839898	MN839945

MNHN-IU voucher	Code	Species	Expedition	Country	Station	Latitude	Longitude	Depth	Date						
MNHN-IU-2014-13793	G460		PAPUA NIUGINI	Papua New Guinea	Stn DW3973	04°34'S	146°17'E	411–430 m	5/12/12	3.1	MN839782	MN839809	MN839858	MN839907	
MNHN-IU-2015-212	G542	Leiogalathea priam	MADEEP	Papua New Guinea	Stn DW4285	09°11'S	153°55'E	380–411 m	30/4/14	5.2	MN839790	MN839817	MN839872	MN839921	MN839962
MNHN-IU-2014-18573	G543	Leiogalathea priam	MADEEP	Papua New Guinea	Stn DW4286	09°12'S	153°55'E	306–365 m	30/4/14	4.8	MN839791	MN839818	MN839873	MN839922	MN839963
MNHN-IU-2014-13792	G549	Leiogalathea priam	MADEEP	Papua New Guinea	Stn DW4288	09°12'S	153°54'E	504 m	30/4/14	4.8	MN839794	MN839821	MN839876	MN839925	MN839966
MNHN-IU-2016-5797	G550	Leiogalathea priam	MADEEP	Papua New Guinea	Stn DW4285	09°11'S	153°55'E	380–411 m	30/4/14	3.7	MN839795	MN839822	MN839877	MN839926	MN839967
MNHN-IU-2014-9706	G551	Leiogalathea priam	MADEEP	Papua New Guinea	Stn DW4285	09°11'S	153°55'E	380–411 m	30/4/14	5.6	MN839796	MN839823	MN839878	MN839927	MN839968
MNHN-IU-2014-18341	G552	Leiogalathea priam	MADEEP	Papua New Guinea	Stn DW4286	09°12'S	153°55'E	306–365 m	30/4/14	5.1	MN839797	MN839824	MN839879	MN839928	MN839969
MNHN-IU-2016-522	G482	Leiogalathea priam	MADEEP	Papua New Guinea	Stn DW4288	09°12'S	153°54'E	504 m	30/4/14	5.1	MN839783	MN839810	MN839862	MN839911	MN839954
MNHN-IU-2014-13711	G421	Leiogalathea sinon	BORDAU 2	Tonga	Stn CP1539	21°37'S	175°19'W	558–586 m	5/6/00	8.3	MK140834	MK140868	MN839840	MN839892	MN839940
MNHN-IU-2014-13719	G442	Leiogalathea sinon	TARASOC	French Polynesia	Stn DW3435	16°41'S	151°02'W	500–612 m	15/10/09	3.2		MK140877			
MNHN-IU-2017-2395	G565	Leiogalathea sp	EXBODI	New Caledonia	Stn DW3945	19°04'S	164°01'E	983–1130	28/9/11	5.4	MN839806	MN839833	MN839888		
MNHN-IU-2011-6220	G564	Leiogalathea sp	EXBODI	New Caledonia	Stn DW3877	22°17'S	171°18'E	785 m	17/9/11	5.6	MN839805	MN839832	MN839887		
MNHN-IU-2014-13744	G445	Leiogalathea turnus	NORFOLK 2	New Caledonia	Stn DW2046	23°43.87'S	168°01.03'E	333–375 m	23/10/03	8.0	MK140844	MK140880	MN839847	MN839899	MN839946

Phylogenetic relationships and evolutionary patterns of *Phylladiorhynchus* Baba, 1969 (Crustacea, Decapoda, Galatheidae)

P. C. Rodríguez-Flores[1,2], E. Macpherson[1], K. Schnabel[3], S. T. Ahyong[.4,5], L. Corbari[6] & A. Machordom[2]

[1] Centre d'Estudis Avançats de Blanes (CEAB-CSIC), C. acc. Cala Sant Francesc 14 17300 Blanes, Girona, Spain.
[2] Museo Nacional de Ciencias Naturales (MNCN-CSIC), José Gutiérrez Abascal, 2, 28006 Madrid, Spain.
[3] Marine Biodiversity & Biosecurity, National Institute of Water & Atmospheric Research, Private Bag 14901 Kilbirnie, Wellington, New Zealand.
[4] Australian Museum Research Institute, Australian Museum, 1 William Street, Sydney NSW 2010, Australia
[5] School of Biological, Earth & Environmental Sciences, University of New South Wales NSW 2052, Australia
[6] Institut de Systématique, Évolution, Biodiversité (ISYEB UMR 7205), Muséum national d'Histoire naturelle, CNRS, Sorbonne Université, EPHE, 57 rue Cuvier, CP 51, 75005 Paris, France

ABSTRACT

The exceptional hidden diversity included in *Phylladiorhynchus* and its wide bathymetric and geographic range make it an interesting group to thoroughly study its evolutionary history. Here we have analysed 31 species of the genus (56% of total) and 3 molecular markers (COI, 16S and H3) as a preliminary approach to establish their phylogenetic relationships, the phylogenetic value of the morphological characters and the influence of the bathymetry in their evolutionary patterns. The genus is recovered as monophyletic and it is the sister group of the genus *Coralliogalathea*. All the analysed species are well supported lineages and appeared structured in ten different clades with high Bayesian posterior probability. Each clade is characterized by certain biogeographic patterns, a combination of morphological characters and all are genetically very differentiated from each other. However, most morphological characters useful to delimit species have no phylogenetic value. The ancestor of the genus most likely lived in shallow-water environments. The colonization of the deep-sea has taken place independently at least twice in the evolutionary history of *Phylladiorhynchus*. Moreover, phylogenetic signal of the environment (in terms of depth) was statistically significant, highlighting the importance of the bathymetry in the evolutionary history of *Phylladiorhynchus*.

INTRODUCTION

The squat lobsters of genus *Phylladiorhynchus* Baba, 1969 (family Galatheidae) form a group of species characterized by a small body size and usually a dagger-shaped or leaf-like rostrum. The genus has been proposed as the most closely related genus to *Coralliogalathea* Baba & Javed, 1974, a hypothesis supported by the absence of the first pair of male gonopods (G1) in both genera (Tirmizi & Javed 1980, Macpherson & Baba 2011, Rodríguez-Flores et al. 2019a). Until recently, the genus *Phylladiorhynchus* included five small Indo-Pacific species mainly differentiated on the basis of the number of spines on the epigastric ridge (Baba 1991). *Phylladiorhynchus bengalensis* Tirmizi & Javed, 1980 (5 spines) was found only in the Andaman Sea, and *P. nudus* Macpherson, 2008 from off Western Australia (epigastric ridge unarmed). The other three species, *P. ikedai* (Miyake & Baba, 1965) (5 epigastric spines), *P. integrirostris* (Dana, 1852) (2 epigastric spines) and *P. pusillus* (Henderson, 1885) (4 epigastric spines), were considered widely distributed in the Indo-Pacific. However, Schnabel & Ahyong (2019) and Rodríguez-Flores et al. (submitted) have revealed the existence of species complexes and an exceptional high diversity in this group, which currently reach 55 species supported by molecular and morphological data; although surely more species are pending to be discovered.
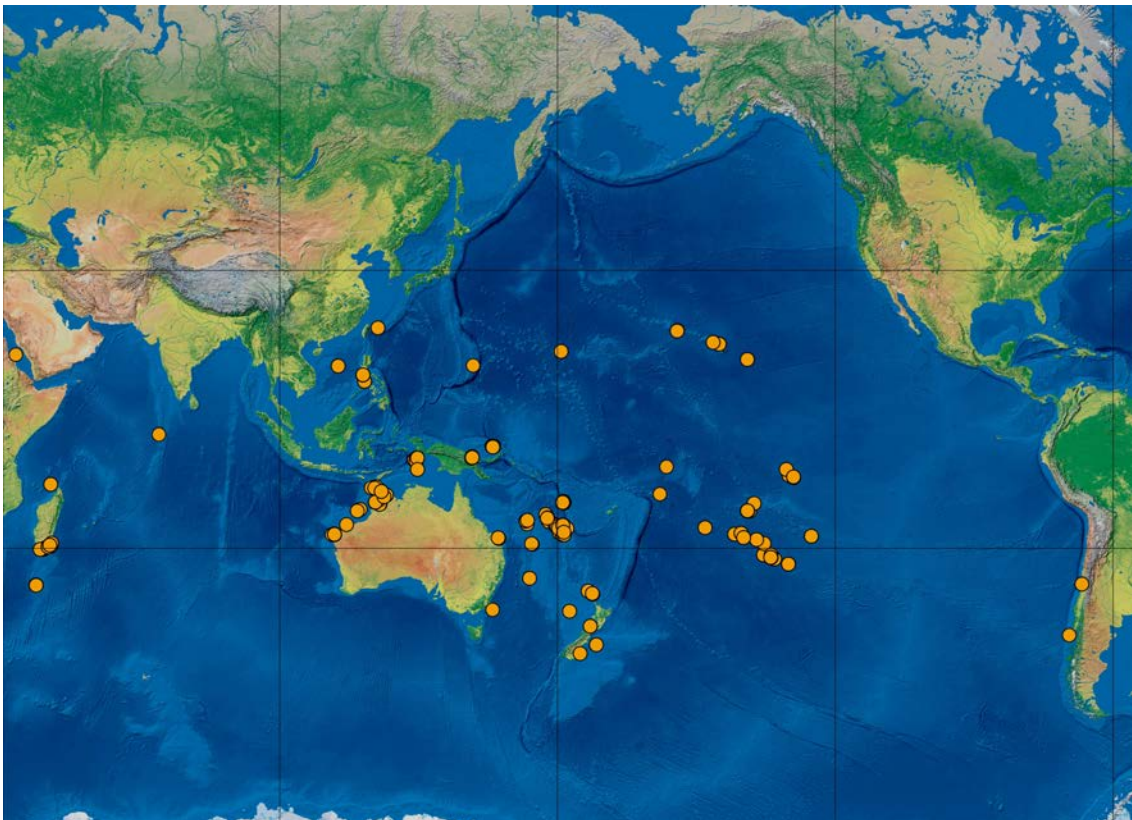
Figure 1. Map showing the sampling localities of *Phylladiorhynchus* along the distribution range of the genus (Indian and Pacific oceans).

The genus is distributed along the Indian and Pacific oceans, from the Red Sea to the Chilean coasts, mostly in tropical latitudes (Fig. 1) (Rathbun 1907, Tirmizi 1966, Baba et al. 2008). The highest latitude records are located in New Zealand in the South, and Korea and Japan in the North. The bathymetric range of the genus goes from intertidal to more than 1000 m (Baba et al. 2008, 2009, Dong & Li 2013, Lee et al. 2019, Schnabel & Ahyong 2019, Rodríguez-Flores et al. submitted) although the majority of species are found in coral reefs. This high diversity comprises cryptic species, or species barely distinguishable using morphological character only, as well as species presenting short genetic distances yet morphologically very different (Rodríguez-Flores et al. submitted). The genus also includes high regional diversity and endemism (for instance several species described from one single archipelago or restricted to a particular geographic area), and also some broadly distributed species along the Indo-Pacific waters (Schnabel & Ahyong 2019, Rodríguez-Flores et al. submitted).

The exceptional and unexpected diversity included in *Phylladiorhynchus* and its wide bathymetric and geographic ranges make it an interesting group to thoroughly study the evolutionary patterns that emerge from previous revisions including morphology and genetic data (Schnabel & Ahyong 2019, Rodríguez-Flores et al. submitted).

The objectives of this work are (1) to establish the relationships of the *Phylladiorhynchus* species in a Galatheoidea phylogenetic framework; (2) to discuss the phylogenetic value of the different distinctive traits (morphological, environmental and geographical) and particularly the main character traditionally used to define species (number of epigastric spines); and (3) to reconstruct the phylogenetic signal of the bathymetry by mapping this continuous trait on the tree, to determine the patterns of colonization of shallow *vs*. deep-sea (more than 200 m) using phylogenetic methods of trait evolution.

MATERIAL AND METHODS

The examined material is detailed in Rodríguez-Flores et al. (submitted), chapter I of the present dissertation. After the examination of this material (~ 2000 specimens), 280 specimens were selected for genetic analyses from the Indian and Pacific oceans (Fig. 1). However, we only were able to obtain molecular data from around 170 specimens, with an extraction success about 65%, that were used for species delimitation (Rodríguez-Flores et al. submitted). The methodology implemented to DNA extraction, amplification and sequencing follows previous studies (Rodríguez-

Flores et al. 2019a, b, 2020). Moreover, we had problems during the amplification and sequencing too, therefore we were not able to obtain genetic data for all the studied species. However, a more complete dataset is currently being processed. For the aims of this work we have analysed 67 specimens corresponding to 31 species of *Phylladiorhynchus* (56% of the known diversity) and the following molecular markers: mitochondrial (COI + 16S) and nuclear (H3). For laboratory methods see Rodríguez-Flores et al. (2019a).

The DNA sequences were revised using Sequencher v.4.8 (Gene Codes Corporation). Ribosomal gene sequences were aligned using MAFFT (Katoh et al. 2002), with a posterior manual correction in AliView (Larsson 2014). The matrix was built with all concatenated genes in PAUP v.4.0a (build 156; Swofford 2002) and included a total of 1557 molecular characters.

The conducted phylogenetic analyses were the following: Bayesian Inference (BI) and Bayesian estimation by sampling trees using coalescence to obtain an ultrametric tree that would serve as input for further phylogenetic comparative methods. We included in the analyses data from other squat lobster (families Galatheidae, Munidopsidae and Munididae) to test the monophyly. A porcellanid crab (*Pachycheles laevidactylus*, Porcellanidae, Galatheoidea), was employed as outgroup, for being the most closely related group of galatheoid squat lobsters (Palero et al. 2019).

To estimate the phylogenetic relationships and posterior probabilities in BI, two parallel runs of four Metropolis-coupled Markov chains Monte Carlo (MC3) were run for 10^7 generations, sampling every 1000 generations, in MrBayes v.3.2.1 (Ronquist & Huelsenbeck 2003).

The ultrametric tree was obtained with BEAST v2.5.1 (Bouckaert et al. 2014). An uncorrelated relaxed log normal clock model was implemented with values ranging from 5×10^{-4} to 0.01, implying a normal distribution with a mean = 0.002 and a standard deviation = 0.1 for the 16S clock rate [rate obtained from Cabezas et al. (2012) and Rodríguez-Flores et al. (2019b)]. A birth–death model was used for the tree prior. MCMC were run with a chain length = 5×10^8, sampling each 50000 generations. Convergence of chains and parameters were checked with Tracer 1.7 (Rambaut et al. 2018)

The mapping of the continuous trait evolution for the character "depth" (the maximum depth of the trawl where the sequenced specimens were collected, coded in meters) was performed using the R package *phytools* and the plotting function contMap (Revell 2012) with a previous tree pruning to remove the outgroups.

We measured the phylogenetic signal of the character depth with the R package *picante* to calculate *K* statistics, *p*-value and plot the phylogenetic signal (Blomberg et al. 2003, Kembel et al. 2010). The *K* statistic measures the phylogenetic signal after comparing the observed signal in a trait with the signal under a Brownian motion model character evolution on a tree (considering both topology and branch lengths) (Blomberg et al. 2003).

These analyses would constitute a first approach to study colonization patterns between deep-sea vs. shallow species and the effect of bathymetry in the evolution of the group, previous to tackle a broader study.

RESULTS AND DISCUSSION

Our results revealed the genus *Phylladiorhynchus* as monophyletic and *Coralliogalathea* as its sister group, although the generally accepted relationships among Galatheoidea families (Schnabel et al. 2011, Palero et al. 2019, Rodríguez-Flores et al. 2019a) were not recovered (Fig. 2), most likely due to an incomplete taxon sampling and the low number of characters used. Bayesian posterior probabilities (pP) are generally high for both deep and recent nodes. A total of 31 highly supported molecular lineages were recovered, which correspond to *Phylladiorhynchus* species with large phylogenetic distances, as seen in tree branch lengths (Fig. 2). The genetic distances among some of these species reached up to 36% and 27% for COI and 16S respectively. These values largely surpass those observed between other squat lobster genera (e.g., Machordom & Macpherson 2004, Cabezas et al. 2008, Macpherson & Robainas-Barcia 2013, Schnabel & Ahyong 2019, Rodríguez-Flores et al. submitted), suggesting that *Phylladiorhynchus* can be constituted by more than one genus. However, the degree of the morphological variation among some groups is poor, therefore failing to comply with the existence of consistent synapomorphies. This pattern could be a consequence of the acceleration of the molecular evolution rate, although to test this hypothesis we must include more genes and analyse a proxy of molecular evolution (e.g., transition over transversion, the ratio of non- synonymous over synonymous substitution rates or the CG-content along the lineages). On the other hand, some groups are rather distinctive or cohesive to consider them as genus-level lineages, although a more complete representation of the family Galatheidae would be needed to establish a robust phylogenetic framework in order to solve this taxonomic question.
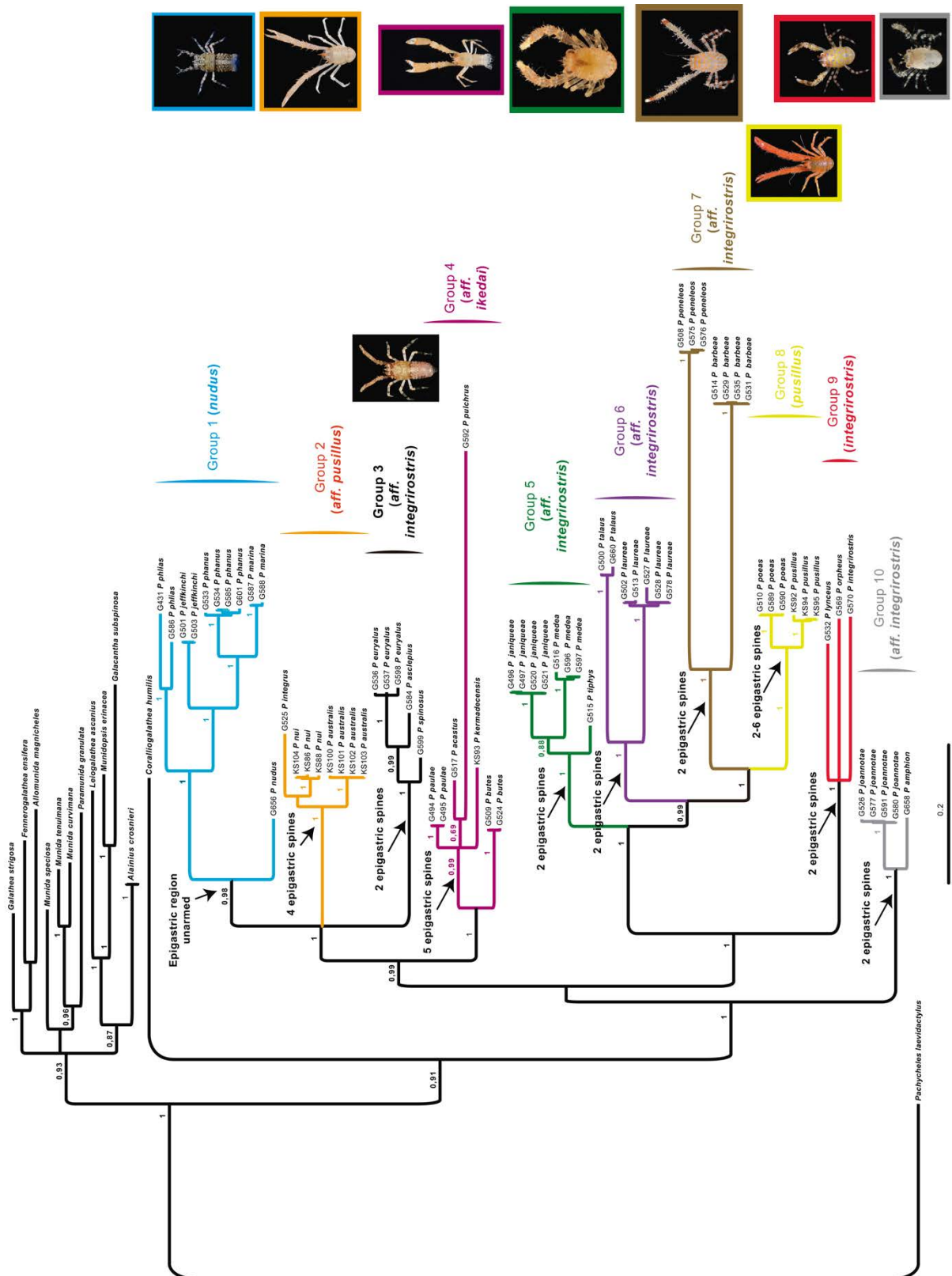
Figure 2. Phylogenetic tree based on concatenated genetic markers (COI, 16S and H3) obtained with BI. Numbers above branches indicate Bayesian posterior probability (pP). Values of pP lower than 0.85 are not shown. Arrows indicate the number of spines on the epigastric ridge. Species groups are indicated and illustrated at the branch tips. Credit images: L. Corbari, K. Schnabel, B. Richer de Forges, G. Paulay, T-Y. Chan and Z. Duris.

The analyzed species appeared structured in 10 different clades (Groups 1–10) supported with pP >0.95 (Fig. 1):

1. Group 1 includes *P. nudus* from Western Australia (Macpherson 2008) and related species from Papua New Guinea and Vanuatu, all of them characterized by having the epigastric ridge unarmed, a robust carapace and dactylar spines.

2. Group 2 is integrated by *P. integrus* (Benedict, 1902), a former synonym of *P. pusillus*, and two species restricted to New Zealand and southeastern Australia (Schnabel & Ahyong 2019); all these species present 4 spines in the epigastric ridge and the sternite 3 with anterior margin biconcave; *P. integrus* is widely distributed from Indonesia to New Caledonia.

3. Group 3, including species from Australia, New Zealand and New Caledonia (Schnabel & Ahyong 2019, Rodríguez-Flores et al. submitted), is characterized by having 2 epigastric spines, dactylar spines and a dagger-like rostrum.

4. Group 4 comprises the species with morphology close to *P. ikedai,* with the epigastric ridge armed with 5 epigastric spines (Miyake & Baba 1965) and usually a triangular rostrum; they are distributed from Madagascar to French Polynesia (Rodríguez-Flores et al. submitted).

5. Group 5 includes some cryptic species distributed from the SW Indian to French Polynesia having an extreme conservative morphology: 2 epigastric spines, a minute hepatic spine and leaf-like rostrum (Rodríguez-Flores et al. submitted).

6. Group 6 includes species widely distributed in the southwestern Indo-Pacific, characterized by having a tridentiform rostrum, with well-developed subapical spines and 2 epigastric spines (Rodríguez-Flores et al. submitted).

7. Group 7 is integrated by species with 2 epigastric spines and leaf-like rostrum, having also a very conservative morphology, yet a very high phylogenetic distance. The group distribution ranges from the Northern Mariana Islands to French Polynesia (Rodríguez-Flores et al. submitted).

8. Group 8 comprises two species, and includes *P. pusillus* (the type species of the genus) typically characterized by the presence of 4 spines in the epigastric ridge (Henderson 1885, Baba 1969, Baba 1991). However, in this species it seems that an allometric variation in this character exists (from 2 to 6 spines), recommending caution in the use of this character in the whole group (Poore 2004, Schnabel & Ahyong 2019, Rodríguez-Flores et al. submitted).

9. Group 9 comprises *P. integrirostris* and related species, characterized also by a conserved morphology (2 epigastric spines and 2 anterior spines on the branchial margin), high genetic distances, and disjunct distribution from Chagos (Indian Ocean) to French Polynesia and Hawaii (Dana 1852, Schnabel & Ahyong 2019, Rodríguez-Flores et al. submitted).

10. Group 10 is constituted by two sibling species, one restricted to Western Australia, and another widely distributed in the Indo-Pacific (from the Northern Mariana Islands to French Polynesia). These species have 2 epigastric spines and dactylar spines (Rodríguez-Flores et al. submitted).
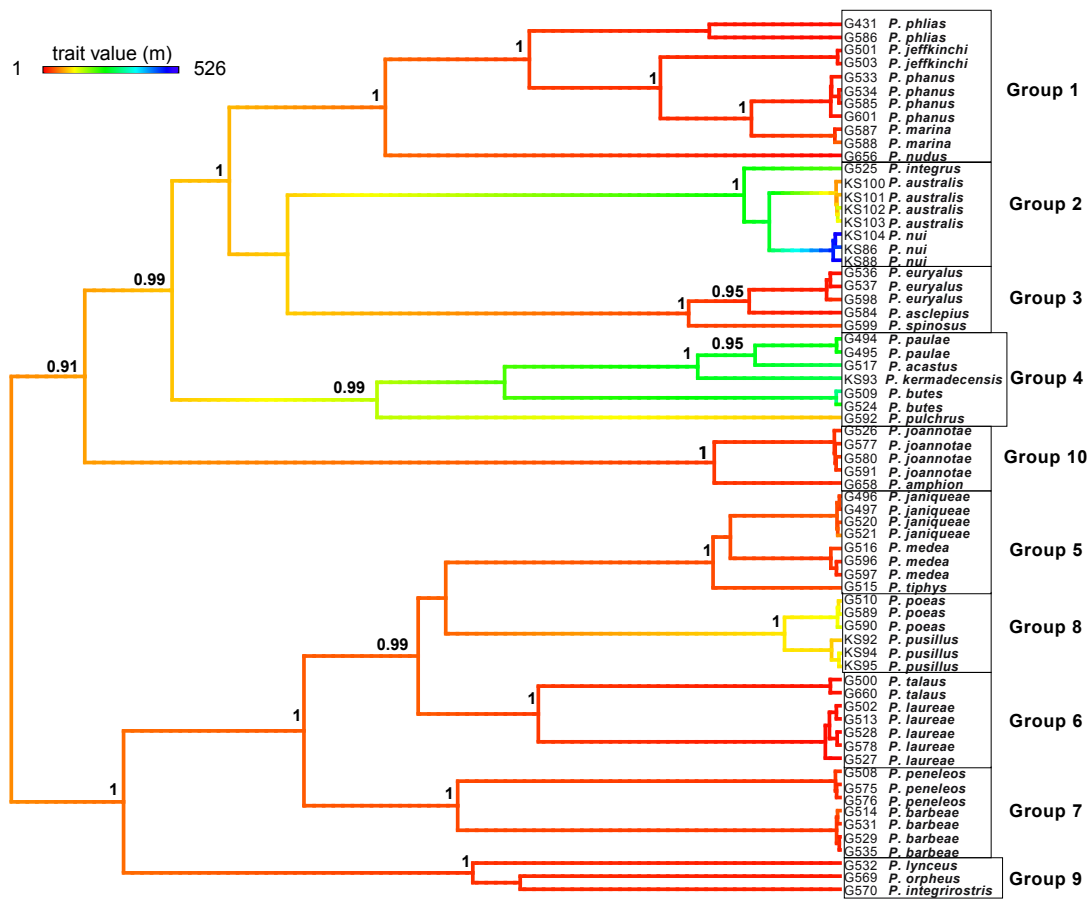
Figure 3. Phylogenetic hypothesis obtained from BEAST of the concatenated genes (COI, 16S and H3) after pruning outgroups and continuous trait mapping on the tree for the character "depth". Legend indicate the range of the continuous character. Numbers above branches indicate Bayesian posterior probability (pP). Values of pP lower than 0.85 are not shown. Species groups are indicated at the branch tips.

Groups 1–4 are clustered together and groups 5–9 as well (pP 0.99–1) and most internal phylogenetic relationships among these groups were well supported. On the other hand, tree topology did not support the number of epigastric spines as a valid synapomorphic character, since the character states 2 and 4 epigastric spines appear in several set of species across main lineages. Therefore, the presence and number of epigastric spines seems to be convergent (homoplasy), without phylogenetic value. The same case applies for most morphological characters used to discriminate species, e.g., rostrum shape, branchial marginal spines and even dactylar spines. The latter, also present in several *Galathea* species (Macpherson & Robainas-Barcia 2015) seems to be related to the way of life, holding tight to corals or sponges. A more detailed study of character evolution in *Phylladiorhynchus* would help to determine synapomorphic and autapomorphic traits in each lineage.

Although most *Phylladiorhynchus* species are recorded from reefs, there are several species living in the continental shelves and even in bathyal depths, e.g., *P. nui*, *P. integra* and most species from the *ikedai*-group (group 4) (Baba et al. 2009, Lee et al. 2019). This led to question if there is a single origin or multiple events of habitat occupation from a deep-water ancestor or alternatively from a shallow-water ancestor. The obtained results of our continuous trait mapping on the tree (Fig. 3) suggest that squat lobsters *Phylladiorhynchus* originated in a shallower environment and colonized deeper waters after diversification. This inference is congruent with the extant taxonomic diversity in coral reefs and shallow environments (Rodríguez-Flores et al. submitted). However, this explanatory hypothesis needs to be tested with alternative models including a more complete taxonomic sampling. Moreover, radiation towards deeper environments have independently occurred at least twice: (1) in the group 2, reaching the deepest records for *Phylladiorhynchus* (*P. nui* and *P. integra* down to >1200 m (Baba et al. 2009, Schnabel et al. 2019), and (2) in the group 4 (*ikedai*-group) (Figs. 3 and 4). The latter group is characterized by a greater diversity (about 15 species, although only 5 species have been analyzed), living along the continental shelf and slope (Rodríguez-Flores et al. submitted). Lastly, the group constituted by the sibling species *P. poeas* and *P. pusillus* seems to have preferences for shelf habitats, usually appearing below 50 meters and rarely surpassing 300 meters depth (Henderson 1888, Whitelegge 1900, Schnabel & Ahyong 2019, Rodríguez-Flores et al. submitted).

According to Kembel et al. (2010) phylogenetic signal is a quantitative measure of the degree to which phylogeny predicts the ecological similarity of species. For the bathymetry in *Phylladiorhynchus* species we obtained a K value = 1, which means some degree of phylogenetic signal or conservatism ($K \sim 0$, random or convergent pattern of evolution; $K > 1$, strong phylogenetic signal and conservatism of traits) (Blomberg et al.

2003). We also obtained a PIC.variance.P (*p*-value of observed vs. random variance of phylogenetic independent contrasts) = 0.001, which means the bathymetry has non-random phylogenetic signal in the phylogeny of *Phylladiorhynchus* (Fig. 4). The results highlight a particular relation of the phylogeny with the habitat, in which lineages would be characterized by their bathymetric ranges (Fig. 3 and 4). This might indicate a role of deep-sea colonization in the evolutionary history of *Phylladiorhynchus*. Moreover, bathymetry can act as factor of speciation, since many taxa present specific patterns of diversity at given depths (Schnabel et al. 2011b). Indeed, depth gradients have been considered important in shaping communities and may, ultimately, contribute to genetic differentiation between populations (Carlon & Budd 2002, McClain & Hardy 2010). It has even been suggested that bathymetry could act as a speciation driver in related groups of squat lobster (Schnabel et al. 2011b, Rodríguez-Flores et al. 2020).
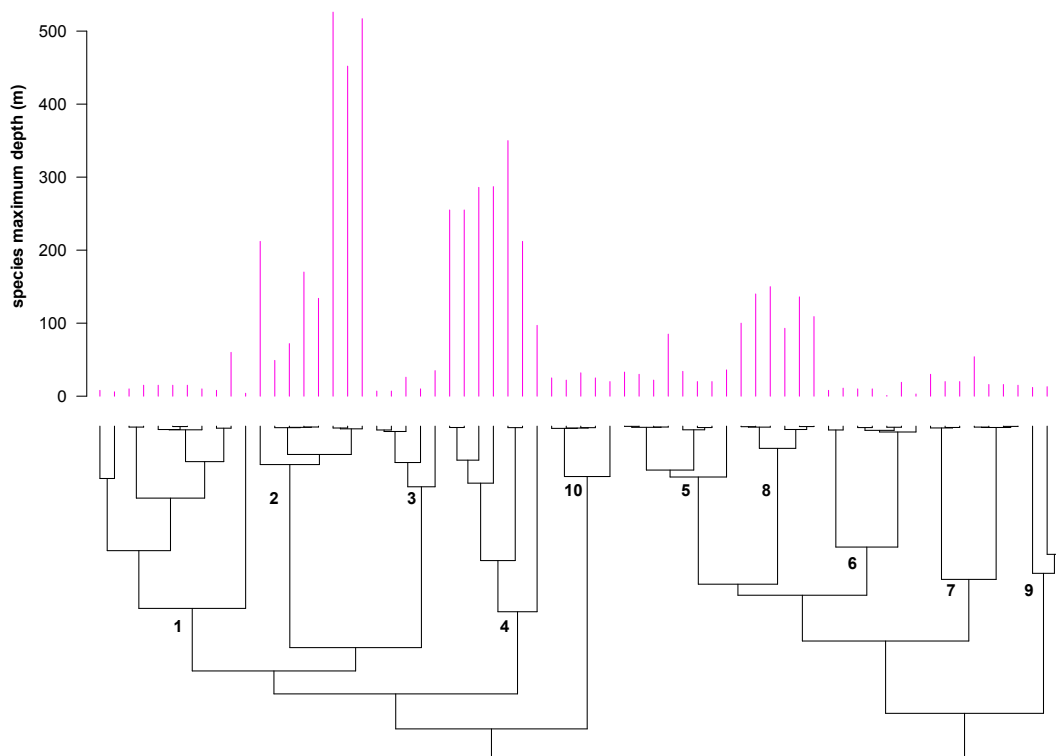
Figure 4. Graph showing the distribution bathymetric patterns in the tree and their phylogenetic signal. The axis indicates the maximum species depth (in meters) and the tree correspond to the phylogenetic hypothesis obtained from BEAST for the concatenated genes (COI, 16S and H3) after pruning outgroups. Species groups are indicated at the nodes.

Our results suggest that bathymetry could have been playing an important role in the diversification dynamics of *Phylladiorhynchus*, however this hypothesis needs to be properly tested.

ACKNOWLEDGMENTS

REFERENCES

Baba, K. (1969) Four new genera with their representatives and six new species of the Galatheidae in the collection of the Zoological Laboratory, Kyushu University, with redefinition of the genus *Galathea*. *Ohmu*, 2, 1–32.

Baba, K. (1991) Crustacea Decapoda: *Alainius* gen. nov., *Leiogalathea* Baba, 1969, and *Phylladiorhynchus* Baba, 1969 (Galatheidae) from New Caledonia. In: Crosnier, A. (Ed.) *Résultats des Campagnes MUSORSTOM 9. Mémoires du Muséum national d'Histoire naturelle. Série A, Zoologie,* 152, 479–491.

Baba, K. & Javed, W. (1974) *Coralliogalathea*, a new genus of Galatheidae (Crustacea, Anomura), with further notes on its type-species. *Annotationes Zoologicae Japonenses*, 47, 61–64.

Baba, K., Macpherson, E., Lin, C.-W. & Chan, T.-Y. (2009) *Crustacean fauna of Taiwan: squat lobsters (Chirostylidae and Galatheidae)*. Keelung: National Taiwan Ocean University, 312 pp.

Baba, K., Macpherson, E., Poore, G.C.B., Ahyong, S.T., Bermudez, A., Cabezas, P., Lin, C.-W., Nizinski, M., Rodrigues, C. & Schnabel, K.E. (2008) Catalogue of squat lobsters of the world (Crustacea: Decapoda: Anomura-families Chirostylidae, Galatheidae and Kiwaidae). *Zootaxa*, 1905 (1), 1–220.

Benedict, J. E. (1902) Description of a new genus and forty six new species of crustaceans of the family Galatheidae with a list of the known marine species. *Proceedings of the Biological Society of Washington*, 26, 243–334.

Blomberg, S. P., Garland Jr, T. & Ives, A. R. (2003) Testing for phylogenetic signal in comparative data: behavioral traits are more labile. *Evolution*, 57 (4), 717–745.

Bouckaert, R., Heled, J., Kühnert, D., Vaughan, T., Wu, C. H., Xie, D., Suchard, ;. A., Rambaut, A. & Drummond, A. J. (2014) BEAST 2: a software platform for Bayesian evolutionary analysis. *PLoS Computational Biology*, 10 (4), e1003537.

Cabezas, P., Macpherson, E. & Machordom, A. (2008) A new genus of squat lobster (Decapoda: Anomura: Galatheidae) from the South West Pacific and Indian Ocean inferred from morphological and molecular evidence. *Journal of Crustacean Biology*, 28 (1), 68–75.

Cabezas, P., Sanmartín, I., Paulay, G., Macpherson, E. & Machordom, A. (2012) Deep under the sea: unraveling the evolutionary history of the deep-sea squat lobster *Paramunida* (Decapoda, Munididae). *Evolution*, 66, 1878–1896.

Carlon, D. B., & Budd, A. F. (2002). Incipient speciation across a depth gradient in a scleractinian coral?. *Evolution*, *56*(11), 2227–2242.

Dana, J.D. (1852) Crustacea. Part I. *United States Exploring Expedition, during the years 1838, 1839, 1840, 1841, 1842, under the command of Charles Wilkes, U.S.N.*, 13, 1–685.

Dong, C., & Li, X. (2013). Galatheid squat lobster species from Chinese waters. *Chinese Journal of Oceanology and Limnology*, 31 (6), 1315–1321.

Henderson, J.R. (1885) Diagnoses of new species of Galatheidae collected during the "Challenger" expedition. *Annals and Magazine of Natural History, Series 5*, 16, 407–421.

Henderson, J.R. (1888) Report on the Anomura collected by H.M.S. Challenger during the years 1873-76. Report on the Scientific Results of the Voyage of H.M.S. Challenger during the years 1873–76. *Zoology*, 27, 1–221.

Javed, W. & Tirmizi, N. M. (1980) Two new species and one new record of *Phylladiorhynchus* Baba from the Indian Ocean (Decapoda, Galatheidae). *Crustaceana*, 39 (3), 255–262.

Katoh, K., Misawa, K., Kuma, K. & Miyata, T. (2002) MAFFT: a novel method for rapid multiple sequence alignment based on fast Fourier transform. *Nucleic Acids Research*, 30, 3059–3066.

Kembel, S. W., Cowan, P. D., Helmus, M. R., Cornwell, W. K., Morlon, H., Ackerly, D. D., Blomberg, S. P. & Webb, C. O. (2010) Picante: R tools for integrating phylogenies and ecology. *Bioinformatics*, 26 (11), 1463–1464.

Larsson, A. (2014) AliView: a fast and lightweight alignment viewer and editor for large datasets. *Bioinformatics*, 30 (22), 3276–3278.

Lee, S.-H., Lee, S.-K., Kim, S.H. & Kim, W. (2019) First records of two squat lobsters (Decapoda, Galatheidae) from Korea. *Crustaceana*, 92, 725–737.

Machordom, A. & Macpherson, E. (2004) Rapid radiation and cryptic speciation in squat lobsters of the genus *Munida* (Crustacea, Decapoda) and related genera in the South West Pacific: molecular and morphological evidence. *Molecular Phylogenetics and Evolution*, 33 (2), 259–-279.

Macpherson, E. (2008). Some new records of shallow-water galatheid crustaceans (Anomura: Galatheidae) from the Dampier Archipelago, Western Australia. *Records of the Western Australian Museum Supplement*, 72, 289–297.

Macpherson, E., & Baba, K. (2011). Taxonomy of squat lobsters. In: Poore, G. C. B., Ahyong, S. & Taylor, J. (eds.). *The Biology of Squat Lobsters*. Melbourne: CSIRO Publishing and Boca Raton: CRC Press, 39–71.

Macpherson, E. & Robainas-Barcia, A. (2013) A new genus and some new species of the genus *Lauriea* Baba, 1971 (Crustacea, Decapoda, Galatheidae) from the Pacific and Indian Oceans, using molecular and morphological characters. *Zootaxa*, 3599 (2), 136–160.

Macpherson, E. & Robainas-Barcia, A. (2015) Species of the genus *Galathea* Fabricius, 1793 (Crustacea, Decapoda, Galatheidae) from the Indian and Pacific Oceans, with descriptions of 92 new species. *Zootaxa*, 3913 (1), 1–335.

McClain, C. R., & Hardy, S. M. (2010). The dynamics of biogeographic ranges in the deep sea. Proceedings of the Royal Society B: Biological Sciences, 277(1700), 3533–3546.

Miyake, S. & Baba, K. (1965) Some galatheids obtained from the Bonin Islands (Crustacea, Anomura). *Journal of the Faculty of Agriculture, Kyushu University*, 13, 585–593.

Palero, F., Rodríguez-Flores, P. C., Cabezas, P., Machordom, A., Macpherson, E. & Corbari, L. (2019) Evolution of squat lobsters (Crustacea, Galatheoidea): mitogenomic data suggest an early divergent Porcellanidae. *Hydrobiologia*, 833 (1), 173–184.

Poore, G.C.B. (2004) *Marine decapod Crustacea of southern Australia. A guide to identification*. CSIRO Publishing, Melbourne, 574 pp.

Rambaut, A., Drummond, A. J., Xie, D., Baele, G. & Suchard, M. A. (2018) Posterior summarization in Bayesian phylogenetics using Tracer 1.7. *Systematic biology*, 67 (5), 901–904.

Rathbun, M. J. (1907) South American Crustacea. *Revista Chileana de Historia Natural*, 11, 45–50.

Revell, L. J. (2012) Phytools: an R package for phylogenetic comparative biology (and other things). *Methods in Ecology and Evolution*, 3 (2), 217–223.

Rodríguez-Flores, P. C., Macpherson, E., Buckley, D. & Machordom, A. (2019a) High morphological similarity coupled with high genetic differentiation in new sympatric species of coral-reef squat lobsters (Crustacea: Decapoda: Galatheidae). *Zoological Journal of the Linnean Society*, 185 (4), 984–1017.

Rodríguez-Flores, P. C., Machordom, A., Abelló, P., Cuesta, J. A. & Macpherson, E. (2019b) Species delimitation and multi-locus species tree solve an old taxonomic problem for European squat lobsters of the genus *Munida* Leach, 1820. *Marine Biodiversity*, 49 (4), 1751-1773.

Rodríguez-Flores, P. C Macpherson E, & Machordom A. Revision of the squat lobsters of the genus *Phylladiorhynchus* Baba, 1969 (Crustacea, Decapoda, Galatheidae) with the description of 41 new species (submitted to *Zootaxa*)

Rodríguez-Flores, P. C., Buckley, D., Macpherson, E., Corbari, L. & Machordom, A. (2020) Deep-sea squat lobster biogeography (Munidopsidae: *Leiogalathea*) unveils Tethyan vicariance and evolutionary patterns shared by shallow-water relatives. *Zoologica Scripta*, 49 (3), 340–356

Ronquist, F. & Huelsenbeck, J. P. (2003) MrBayes 3: Bayesian phylogenetic inference under mixed models. *Bioinformatics*, 19, 1572–1574.

Schnabel, K. E., Ahyong, S. T. & Maas, E. W. (2011a) Galatheoidea are not monophyletic–molecular and morphological phylogeny of the squat lobsters (Decapoda: Anomura) with recognition of a new superfamily. *Molecular phylogenetics and Evolution*, 58 (2), 157–168.

Schnabel, K. E., Cabezas, P., McCallum, A., Macpherson, E., Ahyong, S. T., & Baba, K. (2011). Worldwide distribution patterns of squat lobsters. In: Poore, G. C. B., Ahyong, S. & Taylor, J. (eds.). *The Biology of Squat Lobsters*. Melbourne: CSIRO Publishing and Boca Raton: CRC Press, 149-182.

Schnabel, K. E., & Ahyong, S. T. (2019). The squat lobster genus *Phylladiorhynchus* Baba, 1969 in New Zealand and eastern Australia, with description of six new species. *Zootaxa*, 4688 (3), 301–347.

Swofford, D. L.)2002) *PAUP*: phylogeny analysis using parsimony (*and other methods)*. Version 4.0b10. Sunderland: Sinauer Associates.

Tirmizi, N.M. (1966) Crustacea: Galatheidae. The John Murray Expedition 1933–34. *Scientific Reports*, 11, 167–234, figs. 161–140.

Whitelegge, T. (1900) Crustacea Part 1. Scientific results of the trawling expedition of H.M.C.S. Thetis, off the coast of New South Wales, in February and March, 1898. *Australian Museum, Sydney, Memoir*, 4, 133–199.

How Many Species Inhabit the Earth?

The sad truth is that no one knows. The answer is relevant to efforts to conserve biological diversity and could illuminate crucial questions about evolution and management of the environment

by Robert M. May

DISCUSIÓN GENERAL

La presente memoria recoge el estudio taxonómico de distintos grupos de Galatheoidea, en concreto de las de las familias Galatheidae, Munidopsidae y Munididae. Este estudio se ha realizado en un marco filogenético y evolutivo. Afortunadamente, se partía de un invaluable conocimiento previo gracias a los trabajos de Baba, Macpherson, Ahyong y Schnabel, entre otros (e.g. Baba et al. 2008, Poore et al. 2011 y referencias indicadas allí). Esta enorme labor de investigación anterior a la presente tesis doctoral ha permitido establecer un marco de trabajo y plantearnos ciertos retos o problemas pendientes de resolver para entender mejor los patrones observables en galateidos. De este modo, se ha incluido el mayor número de evidencias morfológicas, genéticas y geográficas, para inferir la historia evolutiva del grupo, lo que ha llevado al planteamiento de nuevas hipótesis explicativas; aunque, en general durante el desarrollo de esta tesis, han surgido más preguntas que respuestas.

Gracias al acceso a colecciones biológicas de referencia obtenidas en numerosas expediciones, se ha realizado el estudio de más de 300 especímenes de *Coralliogalathea*, 430 especímenes del género *Leiogalathea*, más de 100 especímenes del género *Munida* de aguas atlánticas y mediterráneas, 35 especímenes del género *Fennerogalathea*, alrededor de 300 especímenes del género *Munidopsis* y más de 2100 especímenes del género *Phylladiorhynchus*. Esto alcanza un valor total de unos 3300 especímenes examinados. Este esfuerzo, integrando el estudio morfológico con análisis moleculares, ha resultado en los descubrimientos taxonómicos detallados en esta memoria: descripción 65 nuevas especies, resurrección de varios antiguos taxones incluidos en sinonimia, planteamiento de nuevas hipótesis filogenéticas y la propuesta preliminar de 20 géneros nuevos.

1. Un alegato a favor de la Taxonomía

Saber cuántas especies existen, cómo identificarlas y dónde se encuentran es una medida directa de cuánto conocemos sobre la vida en nuestro planeta (May 1992, Mora et al. 2011, Appeltans et al. 2012). Sin embargo, el conocimiento de la diversidad real del planeta Tierra después de dos siglos y medio de investigación en sistemática es incompleto (Wilson 1985, 2002).

En los océanos las estimas de diversidad real son más inexactas que en el medio terrestre, probablemente porque ciertos ambientes marinos son bastante inaccesibles, difíciles de muestrear y requieren un esfuerzo considerable de medios humanos y económicos (Raupach et al. 2009, McClain y Hardy 2010). De acuerdo a las estimas de Appeltans et al. (2012), entre uno y dos tercios de la biodiversidad marina está por describir, principalmente en lo que respecta a invertebrados marinos.

A este conocimiento incompleto de lo que habita en nuestros océanos, se le suma el problema actual de crisis de diversidad (Wilson 1985), también llamada sexta extinción (Kolbert 2014). Varios millones de poblaciones y entre 3000 y 30.000 especies se extinguen anualmente (Pimm et al. 1995, Hughes et al. 1997). Se calcula, además, que entre el 20% y el 25% de las especies de nuestro planeta se encuentran amenazadas (Mora et al. 2011).

Desafortunadamente, cada vez hay menos taxónomos capaces de identificar y describir formalmente las especies (ver, por ejemplo, el caso extremo de Canadá en Packer et al. 2009 en el que predicen una desaparición total de taxónomos de insectos en menos de dos décadas). También el esfuerzo taxonómico es desigual, ya que existen grupos populares muy bien estudiados (por ejemplo, mamíferos, pájaros y reptiles), pero también grupos que han recibido un esfuerzo taxonómico menor y claramente insuficiente (ej. anfípodos, isópodos, tanaidáceos u oligoquetos) (Appeltans et al. 2012). A pesar de su papel fundamental, la taxonomía se encuentra entre las disciplinas científicas peor financiadas y con menos reconocimiento (Wilson 2003, 2004). Actualmente se forma a muy poca gente en taxonomía y hay una escasa posibilidad de promoción o de progreso en la carrera científica para los taxónomos. Esto se debe en parte a que el factor impacto de las revistas de taxonomía (la forma desafortunada de juzgar la calidad científica en muchas instituciones), suele ser bajo. Hay que añadir que muchas de las revistas con más impacto en el campo de la Zoología no aceptan descripciones formales. Por si esto fuera poco, en el año de presentación de esta memoria (2020) la revista líder en taxonomía (*Zootaxa* con 24.722 nuevos taxones) fue eliminada del JCR por sobrepasar el número permitido de autocitas. Afortunadamente esta decisión fue revisada y corregida, pero ejemplariza lo castigada que se encuentra nuestra disciplina. Sin embargo, se ha comentado que el factor de impacto (normalmente medido en función del número de citas únicamente en los dos años inmediatamente posteriores a la publicación) debería ser irrelevante para juzgar la repercusión del trabajo taxonómico pues, a pesar de su mayor o menor cantidad de citas, los artículos de taxonomía se siguen citando a largo plazo y su valor no es medible a través de un valor de impacto en un determinado momento (Krell 2002). Además, las autorías de las especies no son incluidas en la bibliografía y, por tanto, no consideradas como citas.

Centrándonos en el estudio de la diversidad marina y en los ambientes del grupo de estudio, existen hábitats en el océano particularmente sensibles a las alteraciones. Por ejemplo, los arrecifes de coral (Halpern et al. 2008), con consecuencias directas sobre las comunidades que albergan y las especies que permanecen por descubrir (Brown 1997, Appeltans et al. 2012). Por otro lado, el océano profundo no se ha explorado en su totalidad (Raupach et al. 2009, McClain y Hardy 2010). Este ecosistema además contiene

una gran riqueza de recursos para su explotación, como por ejemplo petróleo, gases y recursos minerales, como los nódulos polimetálicos. Estos recursos son muy codiciados, lo que ha dado lugar a propuestas de explotación masiva (Cordes y Levin 2018). Lamentablemente, se desconocen los efectos que esta explotación masiva puede tener sobre la diversidad escondida en dichos hábitats. Pero lo que sí se sabe es que el ritmo de estudio y descripción de la diversidad de nuestro planeta no sigue el ritmo de su desaparición irreversible.

2. Diversidad y delimitación de especies en Galatheoidea

La curva acumulativa de descripción de nuevas especies de Galatheoidea seguía una forma más o menos lineal desde el siglo XIX hasta finales del siglo XX (WoRMS http://www.marinespecies.org/aphia.php?p=stats). Desde finales del siglo pasado, la curva de acumulación de nuevas especies crece de manera exponencial, describiéndose cada año, como ya se ha mencionado, una media de una docena de especies. Esto se debe, además de a la enorme diversidad de especies, al gran esfuerzo taxonómico realizado en las últimas décadas (por ejemplo: Baba 1988, 2005, Macpherson 2007). El empleo de caracteres moleculares también impulsó este incremento en el ritmo de descripción de especies, pues ha permitido establecer límites en complejos de especies, constituidos por especies crípticas que eran considerados como una única especie (por ejemplo; Cabezas et al. 2011, Macpherson y Robainas-Barcia 2013).

En esta tesis doctoral, la revisión del género *Fennerogalathea* reveló la existencia de tres especies además de las dos conocidas (*F. chacei* y *F. chirostyloides*). La revisión del género *Coralliogalathea*, considerado hasta su revisión como un taxón monoespecífico, dio como resultado la descripción de tres nuevas especies y la recuperación de dos especies incluidas dentro de la sinonimia de la especie *C. humilis*. La revisión de *Leiogalathea* resultó en la adición de 15 especies nuevas a las dos conocidas (*L. laevirostris* y *L. agassizi*) y recuperó a *L. imperialis* del listado de sinonimias de *L. laevirostris*. Esta tarea de revisión taxonómica de géneros con relativamente pocas especies ha culminado con la revisión de *Phylladiorhynchus*, en la que se describen 41 especies nuevas para la ciencia y se resucitan tres sinónimos (dos de *P. pusillus* y uno de *P. integrirostris*). Además, se describieron tres especies nuevas del género *Munidopsis* de la plataforma continental caribeña y se realizaron reorganizaciones taxonómicas de las especies de *Munida* de las costas europeas, recuperando *M. perarmata* de la sinonimia de *M. tenuimana* y llegando a la conclusión de que *M. rutllanti* y *M. speciosa* constituían la misma especie.

Varios trabajos realizados en paralelo a los recopilados en esta tesis han dado como fruto la compilación de nuevos registros y descripciones de nuevas especies procedentes

de diferentes áreas geográficas. La revisión e identificación de material de campañas en Madagascar, Papúa Nueva Guinea e India han dado lugar a la descripción de 24 especies de los géneros *Munida*, *Munidopsis*, *Paramunida* y *Crosnierita* (Macpherson et al. 2017, 2020a, 2020b), incluyendo la segunda especie conocida para el género considerado como monotípico *Hendersonida* (Rodríguez-Flores et al. 2020).

Además, durante el periodo que abarca la realización de esta tesis, otros autores han descrito nuevos taxones del grupo. Por ejemplo, nuevas especies de *Munida* (Macpherson et al. 2017, Komai 2017, Liu et al. 2020) y *Munidopsis* (Dong et al. 2019, Marin et al 2020), además de 5 especies de *Phylladiorynchus* de Nueva Zelanda y Australia (Schnabel y Ahyong 2019).

Todos estos trabajos han incrementado la diversidad de Galatheoidea en más de 90 especies nuevas para la ciencia en el periodo 2017–2020, lo que refleja lo mucho que queda aún por aprender sobre la diversidad global de este grupo y que el estudio taxonómico es un paso esencial para poder realizar inferencias sobre la diversidad biológica, la historia evolutiva o biogeográfica de los organismos.

2.1 Caracteres morfológicos y su empleo en la delimitación especies

Previamente se ha mencionado que la identificación taxonómica del grupo de estudio está basada principalmente en caracteres morfológicos externos del caparazón, rostro, pleon, esternitos torácicos, quelípedos, pereiópodos, maxilípedos y las estructuras de la antena y anténula (Macpherson y Baba 2011). En las familias Galatheidae, Munididae y Munidopsidae los caracteres morfológicos útiles en la identificación y diagnosis de especies dependen de las particularidades morfológicas del grupo de estudio. Los taxones abordados en esta tesis son linajes clasificados a nivel de género y acumulan cierta variabilidad morfológica propia de cada uno de ellos, de tal manera que los caracteres discriminantes que permiten caracterizar especies de unos géneros no son útiles para otros. Por ejemplo, el patrón de estriación de caparazón resulta inútil para distinguir especies de *Fennerogalathea* debido a que carece de estrías, teniendo en su lugar espinas, mientras que en *Galathea*, *Coralliogalathea* o *Phylladiorhynchus* es uno de los caracteres diagnósticos.

Familia Galatheidae

Las especies de *Fennerogalathea* se caracterizan por tener un tamaño medio (entre 4 y 7 mm) y una diferenciación morfológica interespecífica muy baja. Los caracteres taxonómicos empleados para distinguir especies fueron la forma relativa del rostro, la relación de su longitud y su anchura y la comparación de la longitud del rostro respecto

a la longitud del pedúnculo ocular, además de la presencia de espinas en el margen anterior del caparazón y el tamaño proporcional de las espinas marginales del caparazón.

Al igual que en el caso anterior, las especies de *Coralliogalathea* se caracterizaron por presentar una pobre diferenciación morfológica entre especies. Además, son especies muy pequeñas, generalmente con caparazones de menos de 2 mm de longitud. Al igual que en *Fennerogalathea,* la forma de relativa del rostro fue útil y constante como carácter taxonómico. También lo fue la forma del margen del rostro (recto o curvo), así como el número de espinas de dicho margen. Otros caracteres menos conspicuos, empleados para distinguir especies, fueron la forma relativa del caparazón, la estriación del caparazón y del pleon y la forma relativa de los propodios de las patas marchadoras, medida como la longitud respecto a la anchura.

En *Phylladiorhynchus* se encontró una variabilidad morfológica mayor que en los grupos anteriores debido a la existencia de grupos de especies muy diferentes entre sí. La mayoría de las especies de este género también tienen un tamaño pequeño, entre 1 y 3 mm, aunque en particular el grupo de especies *integrus-australis-nui* presentó rangos de tamaño mayores que el resto de especies, alcanzando tallas de 7 mm. Los caracteres útiles para distinguir grupos de especies en *Phylladiorhynchus* fueron el número de espinas epigástricas, la forma del rostro, que presentó cierta disparidad entre grupos (triangular, en forma de hoja, en forma de botella, en forma de daga), el número de espinas en el margen flexor del Mxp3 y la presencia de espinas cuticulares en el margen flexor del dáctilo. Para distinguir especies dentro de tales grupos, los caracteres empleados fueron menos conspicuos: patrón de estriación del caparazón y del abdomen, patrón de sedas (iridiscentes, plumosas), forma relativa de los P2–4 y la forma relativa del rostro (relación altura con anchura). Es destacable que en algunas especies de *Phylladiorhynchus* se observó un marcado dimorfismo sexual en la forma/tamaño del caparazón y del rostro, siendo las hembras más grandes y robustas que los machos. Este dimorfismo difiere del observado en otros grupos de galateidos, en los que los machos se diferencian de las hembras por un mayor tamaño corporal y del quelípedo, sobre todo en especies de aguas someras. Estas diferencias en el dimorfismo entre *Phylladiorhynchus* y otros galateidos, sugieren diferentes procesos evolutivos implicados en la aparición del mismo. Por un lado, se ha sugerido que el tamaño mayor de los machos puede estar implicado en estrategias de apareamiento, en las que los machos buscarían activamente a las hembras y a menudo las defenderían (Thiel y Lovrich 2011). De esta forma, el dimorfismo podría deberse a procesos de selección sexual. Sin embargo, en el caso de las especies *Phylladiorhynchus* el dimorfismo puede estar relacionado con el tamaño de la puesta y algún tipo de cuidado parental por parte de las hembras (Thiel 2003).

La ausencia o escasez de caracteres discretos hace recurrir a menudo a caracteres continuos o morfométricos. Así, existe una gran cantidad de caracteres continuos que se han empleado para diferenciar especies de la familia Galatheidae (por ejemplo, la forma de los propodios), lo que a menudo da lugar a la posibilidad de solapamiento entre los valores obtenidos para distintas especies. Esto hace que con frecuencia sea difícil la caracterización morfológica en ausencia de datos moleculares. Otro tipo de caracteres continuos, como la longitud relativa de los pedúnculos oculares, se han usado para diferenciar y delimitar las especies de *Lauriea* (Macpherson y Robainas-Barcia 2013), género que también presenta una variabilidad morfológica muy limitada.

La forma y la longitud relativa del rostro o la longitud relativa y la anchura del pereiópodo también ha sido valiosos caracteres para discriminar especies de *Galathea* y *Allogalathea* (Cabezas et al. 2011, Macpherson y Robainas-Barcia 2015). Además, en *Galathea,* como en *Phylladiorhynchus,* se pueden distinguir especies en función del patrón de estriación del caparazón (Macpherson y Robainas-Barcia, 2015). A la luz de estas evidencias se podría inferir que la familia Galatheidae se caracteriza por presentar especies con muy baja diferenciación morfológica, y que los caracteres útiles para distinguir especies suelen coincidir en distintos grupos.

Familia Munididae

Las especies de *Munida* de las costas europeas son especies de tamaño grande (hasta 20 mm) que se distinguen bien en base a los tamaños de la córnea y de los dedos del P1, en la presencia de espinas en los somitos abdominales 2 y 3, en la presencia de espinas cardiacas y en la forma relativa de los P2–4. Curiosamente, algunas de estas especies, como *Munida tenuimana* y *M. speciosa*, presentan variabilidad intraespecífica en el número de espinas en la región cardiaca, en las espinas del cuarto somito pleonal, en el patrón de espinulación en el margen flexor del Mxp3, así como en la tuberculación del tercer somito pleonal (Miyake y Baba 1970, Rice y Saint Laurent 1986). Esta gran variabilidad morfológica intraespecífica dio lugar a una larga confusión taxonómica (Rice y Saint Laurent 1986), resuelta en esta tesis gracias a la ayuda de caracteres moleculares. También se conoce la existencia de otras especies del género con cierto grado de diferencias morfológicas intraespecíficas (Macpherson et al. 2020a, b). Además, las distancias genéticas entre algunas especies encontradas en el Atlántico (por ejemplo *M. speciosa* y *M. intermedia*) para genes muy conservados (18S) fueron muy elevadas, de lo que se hablará más adelante (Fig. 7). Por contra, otras muchas especies del género *Munida* y otros géneros de la familia Munididae destacan por ser morfológicamente muy similares entre sí y distinguibles únicamente por caracteres sutiles (Machordom y Macpherson 2004, Cabezas et al. 2010, Poore y Andreakis 2012, 2014). De modo que, en este sentido, la elevada diferenciación observada entre las especies de *Munida* del Atlántico oriental

podría ser una consecuencia de la existencia de géneros distintos que están por definir (Cabezas et al. 2011, Rodríguez-Flores et al. 2020).
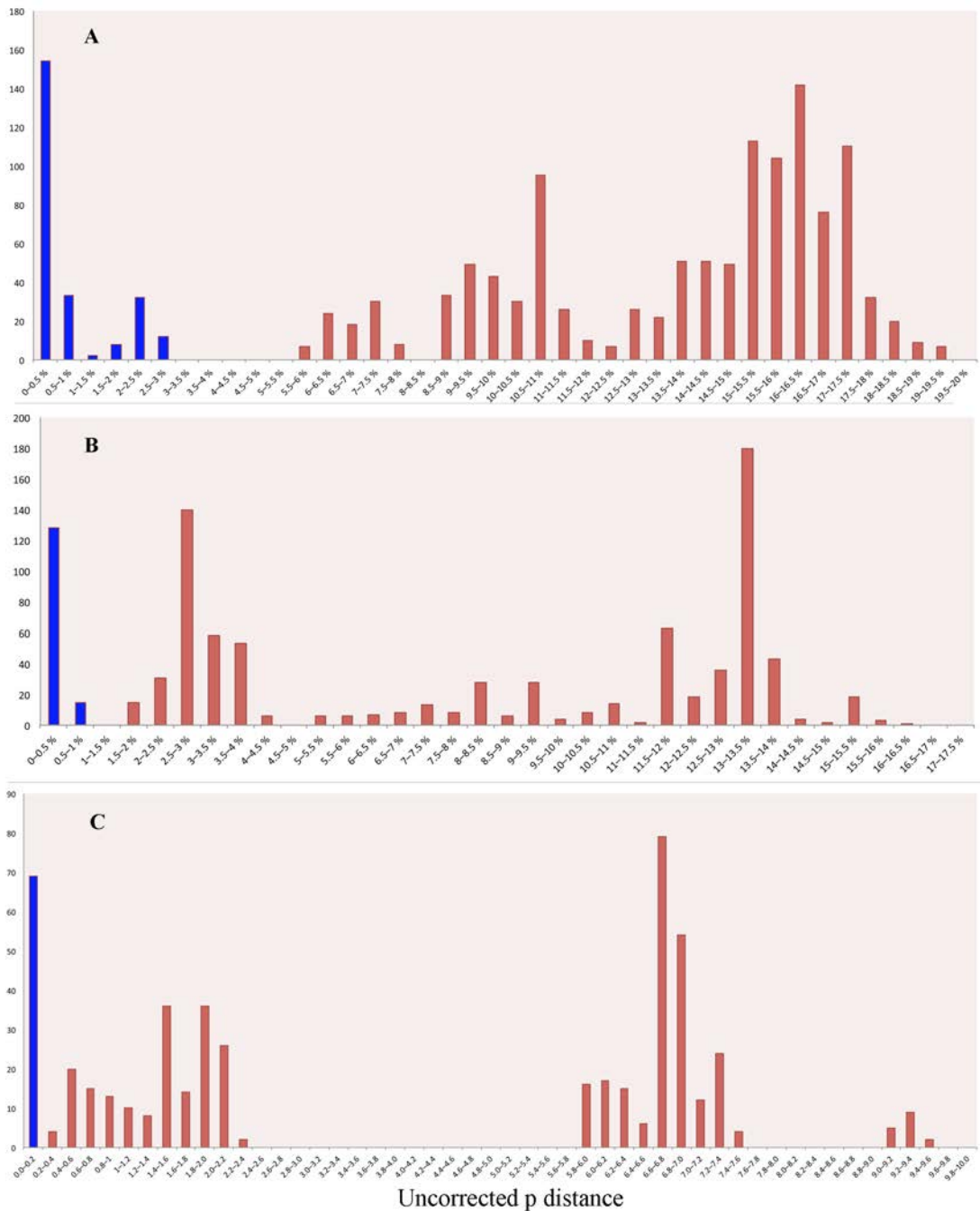
Figura 7. Representación de la frecuencia de las distancias genéticas respeto al valor de las distancias en *Munida* A. COI, B. 16S, C. 18S. Rojo= distancias interespecíficas, azul = distancias intraespecíficas.

Familia Munidopsidae

Las especies del género *Munidopsis* incluyen una enorme diversidad morfológica que, como se ha mencionado en el capítulo II de esta memoria, se debe a que *Munidopsis* constituye un taxón compuesto por linajes muy divergentes entre sí (Ahyong et al. 2011b). Por lo tanto, para describir el grado de diferenciación morfológica mostrada entre

especies, es necesario definir primero los grupos de especies o géneros que realmente existen.

El género *Leiogalathea* fue inicialmente incluido dentro de Galatheidae por presentar una morfología o *habitus* externo muy similar a otros géneros de la familia (Baba 1969): rostro triangular y ancho en la base, ojos desarrollados, caparazón con estrías y pigmentación. Sin embargo, las filogenias moleculares demostraron que *Leiogalathea* está más emparentado con los géneros *Galacantha* y *Munidopsis* que con otros grupos de Galatheidae, por lo que el género fue transferido a Munidopsidae (Ahyong et al. 2009, 2011b, Schnabel et al. 2011b, Macpherson y Baba 2011). Paradójicamente, las especies de *Leiogalathea* exhiben un patrón de diversificación morfológica muy bajo, como ocurre en los géneros de Galatheidae. Son especies de tamaño medio, de unos 4–5 mm, y se diferencian por caracteres muy sutiles del caparazón, número de espinas marginales, en la forma del rostro y la presencia de espínulas pequeñas en el rostro, en la forma de los propodios P2–4 y en el patrón de sedas del caparazón y quelípedos. Cabe destacar que se encontraron especies hermanas crípticas y especies hermanas muy variables morfológicamente. Se ha propuesto que este fenómeno puede ser el resultado de la respuesta adaptativa a distintos factores, lo que se comentará más adelante.

2.2 ¿El color importa?

Los galateidos pueden exhibir coloraciones muy llamativas y vistosas y que pueden ser utilizadas para diferenciar taxones. Lamentablemente no se tienen datos para muchas de las especies, pues el color se pierde poco tiempo después de la fijación en etanol. Sin embargo, algunas especies de *Phylladiorhynchus* se distinguen únicamente por presentar variaciones en el patrón de coloración, como ya se había observado en otros galateidos. Por ejemplo, en los géneros *Raymunida, Allogalathea, Galathea, Agononida, Sadayoshia* y *Lauriea* se encontraron patrones de coloración que ayudaron a la delimitación de algunas especies (Macpherson y Machordom 2000, 2001, Cabezas et al. 2011, Poore y Andreakis, 2012, 2014, Macpherson y Robainas-Barcia 2013, 2015). En los grupos aquí estudiados, también se han encontrado algunas especies que se distinguen en su patrón de coloración, como es el caso de *Phylladiorhynchus barbeae* y *P. pepei*. Sin embargo, existen taxones que presentan una variabilidad intraespecífica elevada en los patrones de coloración, o incluso patrones convergentes, siendo en este caso el color ineficaz para distinguir especies. Es el caso de las especies de *Coralliogalathea* y de algunas especies de *Phylladiorhynchus* (por ejemplo, *P. lini*). Esta variabilidad intraespecífica podría explicarse por diferentes estrategias de cripsis, debido a asociación cercana a distintas especies de corales en arrecifes.

En resumen, el color puede ser útil para diferenciar especies en algunos casos, como se ha observado en otras muchas especies de crustáceos (Poupin y Malay 2009, Felder et al. 2019, Kerkhove et al. 2019), mientras que en otros presenta variabilidad intraespecífica y no se puede asignar un patrón a cada especie (Titus et al. 2018). El color depende, en muchos casos, de adaptaciones locales al entorno circundante, de la selección direccional, de forma que sea útil para enviar señales intraespecíficas, señales de advertencia o como un camuflaje para confundirse con el entorno (Caro 2018). Por tanto, hay que ser cauto a la hora de delimitar especies usando sus patrones de coloración.

2.3 El uso de caracteres moleculares para la delimitación de especies

Tanto si la variabilidad morfológica es alta a nivel intraespecífico, como si es escasa para caracterizaciones interespecíficas, las herramientas moleculares constituyen un apoyo idóneo para delimitar especies (Knowlton 2000, Mathews et al. 2008).

Todas las revisiones taxonómicas de esta tesis se han apoyado, cuando estaban disponibles, en los datos de los marcadores moleculares citocromo c oxidasa subunidad I (COI) y 16S rDNA. Estos marcadores se han utilizado previamente para delimitar especies de galateidos (Machordom y Macpherson 2004, Baba 2005, Jones y Macpherson 2007, Cabezas et al. 2008, 2010, 2012, Baba et al. 2008, Macpherson y Baba 2010, Macpherson y Robainas-Barcia 2013, 2015), por lo que se cuenta con una gran cantidad de datos para hacer comparaciones entre distintos grupos y resultan un gran complemento a los datos morfológicos.

Los rangos de divergencia para distancias genéticas sin corregir variaron en función del grupo:

- *Coralliogalathea* presentó unos rangos interespecíficos desde 6.7% al 15.1% para el COI y de 2.4% al 15.7% para el 16S y distancias máximas intraespecíficas de 1.3% y 0.6% para el COI y el 16S respectivamente.
- *Fennerogalathea* presentó rangos para el COI desde 7.2% a 10% y desde 0.7% al 1.6% para el 16S, con distancias máximas intraespecíficas de 0.6% y 0.2% para el COI y 16S respectivamente.
- *Phylladiorhynchus* presentó divergencias entre especies de entre 7–36% y 2–27% para el COI y el 16S respectivamente, con una distancia máxima entre individuos de la misma especie de 4.7% para el COI y 1.2% para el 16S.
- Las especies de *Munida* del Atlántico analizadas presentaron distancias genéticas entre 2.7–17.9% para el COI y 0.4–13.2% para el 16S, con unas divergencias intraespecíficas de 0.9% y 0.3% para COI y 16S respectivamente.

- Las especies de *Leiogalathea* divergieron de 3.5% a 16.0% para el COI y entre 0.3% y 8.9% para el 16S y una distancia intraespecífica máxima de 0.9% y 0.5% para el COI y el 16S respectivamente.
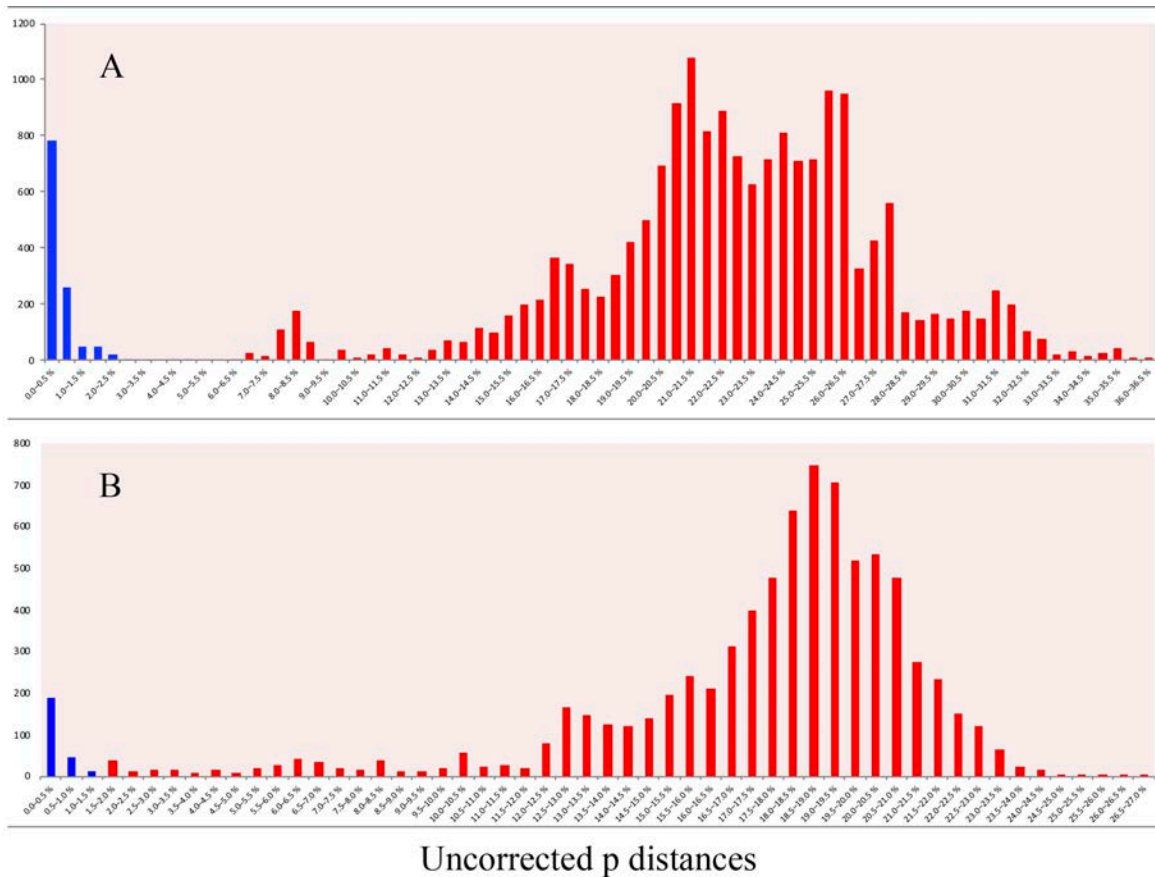
Los rangos interespecíficos obtenidos en los grupos aquí revisados son similares a los obtenidos en trabajos previos para las familias estudiadas en cuanto a distancias sin corregir (no se han comparado distancias patrísticas o distancias obtenidas aplicando modelos de substitución de otros estudios):

En Galatheidae se obtuvieron los siguientes valores: *Allogalathea* 10.94–15.53% (COI), 8.40–12.06% (16S); *Lauriea*: 5.2–10.6% (COI), 0.7–3.7% (16S); *Galathea*: 7.2%–24.6% (COI), 1.8–18.5% (16S) (Cabezas et al. 2011, Macpherson y Robainas-Barcia 2013, 2015).

Munididae: *Raymunida* 7.6%–13.2 % (COI); *Paramunida* 1.73%-11.47% (COI), 1.2%–8.7% (16S); *Agononida* 8.70–17.88% (COI) y 3.40–13.10% (16S); y para algunos grupos de *Munida* del Indo-Pacífico 10.3–12.9 (COI), 3.4–4.4% (16S) (Machordom y Macpherson 2000, Macpherson y Machordom 2001, Cabezas et al. 2009, 2012) llegando a valores de más del 17% para distintos grupos de especies del Atlántico y el Indo-Pacífico (Coykendall et al. 2017).

Munidopsidae: *Munidopsis* presenta una media de 9% para el COI y rangos de 2.7 a 15.9% (Jones y Macpherson 2007). Otros estudios indican distancias muy bajas entre especies para el COI, de 1.4–1.8% (Dong et al. 2019), mientras que también se reportan distancias mayores del 20% entre distintos grupos de especies (Coykendall et al. 2017). Aunque en general la variabilidad intraespecífica suele ser baja en Munidopsidae, se ha registrado que poblaciones de *Shinkaia* de surgencias frías divergen genéticamente en 2.1–3.8% de las de chimeneas hidrotermales para el marcador COI (Yang et al. 2016).

Como se puede observar en los datos obtenidos para esta tesis, la distancia mínima interespecífica nunca se solapó con la distancia máxima intraespecífica para el marcador COI. En pocos casos se solaparon valores intraespecíficos con interespecíficos en el marcador 16S. El 16S tiene una tasa de substitución más lenta, que puede ser entre dos y tres veces más lenta que la tasa de sustitución del COI en función del grupo de estudio (Vences et al. 2005, Lefébure et al. 2006, Dhar et al. 2016) y por ello se ha desaconsejado su uso para delimitar especies de crustáceos (Lefébure et al. 2006). En este sentido, en *Fennerogalathea* se encontró una extrema deceleración, siendo las distancias genéticas del 16S 7 veces menores que las del COI.

Figura 8. Representación de la frecuencia de las distancias genéticas respeto al valor de las distancias en *Phylladiorhynchus* A. COI, B. 16S. Rojo= distancias interespecíficas, azul = distancias intraespecíficas.

Los rangos obtenidos en esta tesis para el marcador universal COI (conocido como «código de barras»), encajan con los propuestos como límite para la delimitación de especies de crustáceos, en algunos casos sobrepasando los límites que considera Lefébure et al. (2006) para taxones supraespecíficos. Esto se debe a que algunos de los grupos estudiados (*Munida*, *Munidopsis* y *Phylladiorhynchus*) están constituidos por linajes evolutivos muy antiguos e independientes, probablemente supraespecíficos, que todavía están por definir.

Sin embargo, hay que tener cautela a la hora de delimitar taxones en función a un valor de porcentaje de divergencia. Por ejemplo, el famoso «barcoding gap» (separación que existe entre las distancias intraespecíficas y las interespecíficas para el marcador COI) puede desaparecer cuando el muestreo taxonómico es muy amplio (Meyer y Paulay 2005, Wiemers et al. 2007). En nuestro caso, si representásemos los valores obtenidos de *Coralliogalathea*, *Fennerogalathea*, *Phylladiorhynchus*, *Munida* y *Leiogalathea*, existiría un claro solapamiento entre valores intraespecíficos e interespecíficos. Por ejemplo, la distancia intraespecífica entre poblaciones de *Phylladiorhynchus integrus* alcanza un valor máximo de 4.7%, mientras que la distancia mínima entre especies de *Leiogalathea* es de 3.5% para este marcador. Sin embargo, estos valores no se solapan

cuando se estudian linajes evolutivos independientes por separado (ver Fig. 7 y 8). Una posible hipótesis a comprobar para explicar estos valores sería que la tasa de mutación no es constante entre diferentes linajes (Thomas et al. 2006, Nabholz et al. 2008, 2009, Shafir et al. 2020).

Es por eso por lo que para delimitar especies (así como taxones a niveles supraespecíficos) resulta fútil usar un porcentaje sin más evidencias, además de ser conceptualmente erróneo (Moritz y Cicero 2004, Will y Rubinoff 2004, Puillandre et al. 2012). Por otra parte, el uso único de ADN mitocondrial para delimitar especies puede enmascarar diferentes procesos, como por ejemplo la presencia de pseudogenes (transferencia de copias de DNA al núcleo) o la introgresión o hibridación entre diferentes linajes (contacto secundario), que se ponen de manifiesto al estudiar las relaciones con genes nucleares, y los fenómenos de especiación reciente o especiaciones rápidas con la separación incompleta de linajes (Moritz y Cicero 2004). Este último caso se ha visto repetido en nuestro grupo de estudio, como la especiación reciente de *M. iris* y *M. speciosa,* especies que viven en el Atlántico occidental y en el oriental, respectivamente y son morfológicamente distintas, pero con una baja diferenciación genética. También se observan fenómenos de especiación reciente en *Munidopsis,* en concreto entre especies del grupo *Orophorhynchus*, y en *Leiogalathea.*

Por tanto, para delimitar especies, aquí definidas como linajes (ancestro y sus descendientes) que comparten una identidad particular y una trayectoria y destino común, se requiere un criterio de reciprocidad monofilética usando distintos marcadores sumados a todas las evidencias morfológicas y geográficas posibles (Padial et al. 2010, Hillis et al. 2019).

3. Relaciones filogenéticas en Galatheoidea

El estatus taxonómico de las especies descritas en esta memoria se ha respaldado con datos morfológicos, moleculares y geográficos. Sin embargo, resolver las relaciones filogenéticas entre linajes basales o desvelar las relaciones supraespecíficas supone un reto en el estudio de Galatheoidea. Esto se debe, entre otras razones, a la baja resolución de los caracteres empleados que se reflejan en bajos apoyos estadísiticos a esos niveles (Machordom y Macpherson, 2004, Cabezas et al. 2009, 2011, 2012, Bracken-Grissom et al. 2013).

3.1 Relaciones entre familias

Previamente se ha comentado que la superfamilia Galatheoidea incluye además de las familias Galatheidae, Munididae, y Muniodopsidae (con anatomía externa similar a langosta) a la familia Porcellanidae, que presenta una morfología convergente de

cangrejo. Las relaciones filogenéticas entre estas familias no estaban claras, pues se habían propuesto, como se mencionó en la Introducción, varias hipótesis que partían de diferentes conjuntos de datos y muestreos taxonómicos incompletos (Martin y Abele 1986, Morrison et al. 2002, Pérez-Losada et al. 2002, Ahyong y O'Meally 2004, Porter et al. 2005, McLaughlin et al. 2007, Ahyong et al. 2009, Bracken-Grissom et al. 2009, 2013, Chu et al. 2009, Schnabel et al. 2011b). El consenso hasta el momento apoyaba las relaciones de Galatheidae + Porcellanidae, Munididae como grupo hermano de este clado y Munidopsidae como grupo externo (Ahyong et al. 2010).

En esta tesis se comprobó la hipótesis más aceptada con el análisis de mitogenomas de representantes de todas las familias conocidas de Galatheoidea. Nuestra reconstrucción no apoyó la hipótesis de consenso, sino una separación basal de Porcellanidae, que constituiría el grupo hermano del resto de familias, de las que Munidopsidae sería la rama externa. Estas relaciones las habían propuesto por primera vez A. Milne-Edwards y Bouvier en 1894, al establecer relaciones fenéticas en base a la similitud de la anatomía externa. La topología obtenida también se había recuperado en el trabajo de Roterman et al. (2018) enfocado en el estudio de las relaciones de los Kiwaidae «yeti crab», reuniendo evidencias tanto de genes mitocondriales como nucleares e incorporando datos fósiles.

Durante el estudio de *Coralliogalathea* incluido en esta tesis, se propusieron dos marcos filogenéticos para Galatheoidea con distintos marcadores y enfoques. Por un lado, un filograma que incluyó los genes COI, 16S, 28S y 18S; y por otro lado un cronograma con los genes COI y 16S, ambos incluyendo el muestreo taxonómico más amplio hasta el momento de la familia Galatheidae. El cronograma obtenido mediante análisis de coalescencia recuperó la misma topología que la obtenida con los mitogenomas (Porcellanidae como grupo externo del resto de familias de Galatheoidea). Ello sugiere un papel importante no solo del incremento de caracteres, sino también del muestreo taxonómico. Sin embargo, otros estudios con enfoque mitogenómico o filogenómico no han podido corroborar esta hipótesis al tener un muestreo taxonómico incompleto de familias, con foco en relaciones profundas de Anomura o de Decapoda (Tan et al. 2018, Wolfe et al. 2019).

Esta nueva propuesta de relaciones en Galatheoidea tiene implicaciones evolutivas respecto a la adquisición de la forma de cangrejo. Si considerásemos a Galatheidae como grupo hermano de Porcellanidae, la carcinización tendría lugar más recientemente (TMRCA = 172.8 My, Bracken-Grissom et al. 2013) y constituiría una reversión al carácter ancestral (forma de cangrejo, Bracken-Grissom et al. 2013) dentro del clado Galatheoidea. Sin embargo, la hipótesis que aquí se presenta, propone que la carcinización tuvo lugar antes y que la forma de langosta constituye una novedad

evolutiva (sinapomorfía de las familias Galatheidae, Munididae y Munidopsidae). En un marco temporal, esta separación de Porcellanidae habría tenido lugar antes que en la anterior hipótesis. En este caso, Roterman et al. (2018) recuperan un MRCA de Galatheoidea de unos 180 My. En el marco filogenético aportado para Galatheoidea durante el estudio del género *Coralliogalathea* se obtuvo un MRCA de 171 My para esta separación. Estas edades son algo anteriores a la aparición de los primeros fósiles de Porcellanidae, que aparecen por primera vez en el Jurásico Superior (161.2–145.5 My) (Schweitzer y Feldmann 2010). Estas diferencias pueden deberse a las calibraciones del reloj molecular o a la discontinuidad del registro fósil.

Como corolario, hay que remarcar que el muestreo taxonómico tiene consecuencias importantes en los resultados de los análisis filogenéticos, implicando cambios en la topología, en los apoyos y en la validez de los clados (Hillis 1998). El incremento en los análisis del número de caracteres, de taxones, o de ambos mejora la exactitud de la reconstrucción, teniendo un impacto primordial en la topología de los árboles (Graybeal 1998). Esto es consistente con reconstrucciones tanto de taxones actuales como en estudios paleontológicos, ya que al añadir más taxones se reduce el error en la inferencia filogenética mejorando de este modo la eficacia en la reconstrucción (Gauthier et al 1988, Donoghue et al. 1989, Huelsenbeck et al 1991, Pollock et al. 2002). En este caso, Galatheoidea presenta varias familias extintas (Robins et al. 2016) que también deberían ser consideradas para un estudio completo de las relaciones del grupo, máxime si se pretende estimar tiempos de divergencia para averiguar cuándo tuvieron lugar eventos relevantes en la historia evolutiva del grupo.

3.2 Relaciones supra-específicas

La definición de taxones a niveles supraespecíficos puede resultar algo menos objetiva que la delimitación de especies, pues toda la variabilidad incluida en un grupo puede solaparse con otro. Para delimitar estos grupos se siguen criterios evolutivos: linajes que comparten un ancestro común y todos sus descendientes y que comparten una serie de características diagnósticas o sinapomorfías, además de cierta diferenciación morfológica que no rompa la diagnosis. En este sentido es necesario resaltar el gran esfuerzo prevuio de delimitación de los géneros estudiados en esta tesis, *Coralliogalathea*, *Fennerogalathea*, *Leiogalathea* y *Phylladiorhynchus* (Baba 1969, 1988, 1991, Baba y Javed 1974), definidos originalmente en ausencia de datos moleculares. Estos géneros han resultado monofiléticos con el máximo apoyo para diferentes aproximaciones filogenéticas (BI, MP, ML). Los géneros más diversos, sin embargo, *Galathea, Munida* y *Munidopsis* (Baba et al. 2008, Macpherson y Baba 2011) requieren de un análisis más exhaustivo incluyendo todas las evidencias que se puedan reunir para considerar si son grupos naturales o polifiléticos.

En esta Tesis se ha comprobado la hipótesis de si el género *Munidopsis* es un grupo polifilético, como sugerían estudios previos con un muestreo taxonómico limitado (Ahyong et al., 2009, Schnabel et al. 2011b, Ahyong et al. 2011b), con el conjunto de datos más completo hasta la fecha en caracteres moleculares, morfológicos y muestreo taxonómico. El género, después de *Munida,* es el taxón más diverso del grupo, ya que actualmente engloba más de 260 especies. Como se ha comentado antes, es un grupo que se encuentra principalmente en el océano profundo a partir de los 200 m hasta más de 5000 m y se caracteriza por una elevada disparidad morfológica (Ahyong et al. 2011b), de tal forma que a lo largo de la historia se reconocieron varios grupos nada fáciles de delimitar debido a su diversificación morfológica, incluyendo ésta un alto grado de solapamiento entre grupos (A. Milne-Edwards 1880, Smith,1883, Henderson 1885, Chace 1939, 1942, Macpherson 2007). Los resultados de los datos moleculares evidenciaron más de 20 linajes dentro del género, caracterizados por una combinación de caracteres morfológicos y por sus patrones biogeográficos y batimétricos. Se ve necesario recuperar algunos de los géneros propuestos por antiguos investigadores, como es el caso de *Anoplonotus, Bathyankyristes*, *Elasmonotus*, *Galathopsis*, *Galathodes* y *Orophorhynchus*. Se encontraron como caracteres útiles para delimitar grupos morfológicos el número de placas del telson, que puede ser de 7 hasta 12 y que se mantiene constante en grupos monofiléticos, así como la presencia de espinas oculares y su posición (mesial o central), la ornamentación del margen flexor de los dáctilos, la forma del rostro (tridentado o triangular), la modificación de los propodios para formar subquelas y, en general, la ornamentación del caparazón. Junto con el análisis molecular de 75 especies para cuatro genes, para este trabajo se han estudiado morfológicamente más de 100 taxones de *Munidopsis* en una matriz unos 35 caracteres morfológicos, que sirvieron de apoyo para delimitar los grupos.

El hecho de delimitar taxones a nivel de género es un paso inicial clave para comprender la historia evolutiva de dichos linajes, para estudiar su tasa de especiación y extinción, su historia biogeográfica y su evolución morfológica. Esta cuestión se está actualmente abordando en múltiples grupos de crustáceos mediante una perspectiva integradora de moléculas, morfología, fósiles y distribuciones geográficas (Shih et al. 2016, Poore et al. 2019) incluyendo, entre los galateidos, el estudio del género compuesto *Munida* (en preparación).

4. Patrones evolutivos

Previamente se ha mencionado el reto que supone el estudio de la historia evolutiva de Galatheoidea, que incluye el estudio de la evolución morfológica, la historia biogeográfica y las tendencias de diversificación.

4.1 Patrones de especiación

Los caracteres empleados para distinguir especies presentan un alto grado de homoplasia, la mayor parte de ellos aparecen y desaparecen indistintamente en linajes independientes sin presentar señal filogenética alguna. Un ejemplo para ilustrar este patrón lo apreciamos en *Phylladiorhynchus*, ya que al mapear el carácter de 2 o 4 espinas epigástricas, nos encontramos que aparece en linajes de distintos clados. Este patrón de elevado grado de homoplasia (o convergencia morfológica) es característico del grupo (Machordom y Macpherson 2004, Cabezas et al. 2009, 2012).

La diferenciación morfológica entre las especies estudiadas de Galatheidae es particularmente baja, por lo que los géneros aquí estudiados se consideraban como taxones monoespecíficos (como *Coralliogalathea*) o con pocas especies (como *Fennerogalathea* o *Phylladiorhynchus*). Este patrón se reproduce en *Leiogalathea* (familia Munidopsidae). Resulta muy interesante el caso de *Leiogalathea*, pues nuestros datos indican que los patrones de variabilidad morfológica siguen tendencias similares a los observables para los géneros de Galatheidae estudiados. Esto podría deberse a convergencias de ambos linajes no solo en la anatomía externa sino también en las restricciones evolutivas sobre el cambio morfológico, que aparecen en toda la familia Galatheidae y, además, en *Leiogalathea* (Munidopsidae).

Volviendo a la Figura 5 de la Introducción (confrontación del cambio morfológico y el cambio genético en el tiempo), vemos que la mayoría de la variabilidad encontrada entre las especies analizadas de *Fennerogalathea* y *Coralliogalathea* se situarían en el gráfico por debajo de la recta. La recta ascendente implica correlación directa entre la divergencia genética y el cambio morfológico en el tiempo, fenómeno que no se da en *Fennerogalathea* ni en *Coralliogalathea*. Por ejemplo, las especies más recientes de *Coralliogalathea* presentan un TMRCA de 7 My y se diferencian en muy pocos caracteres, sugiriendo que la variación morfológica en dicho tiempo ha sido mínima. En *Leiogalathea,* la mayoría de las especies presentaron una baja diferenciación morfológica con alta diferenciación molecular e incluso especies pseudocrípticas, a pesar de ser especies con un origen de diversificación antiguo. Este patrón se conoce como estasis morfológica, entendida como una morfología conservada sin apenas cambios durante largos periodos de tiempo (Estes y Arnold 2007, Davis et al. 2014), en contraste con un incremento de la diferenciación genética en el mismo periodo (Eldrege et al. 2005, Struck et al. 2018, Fišer et al. 2018).

Las especies crípticas (Bickford 2007, Vrijenhoek 2009) pueden generarse como consecuencia de fenómenos de estasis (Gould & Eldredge 1977), en los que la morfología se conserva a través del tiempo a pesar del cambio en el entorno (Wake et al. 1983). Un

buen ejemplo de estasis morfológica lo constituye el género monoespecífico *Shinkaia* (Munidopsidae), ya que existen evidencias fósiles (*S. katapsyxis*) de que la morfología externa se ha conservado durante 40 My (Schweitzer y Feldmann 2008). Cabe destacar que el linaje Shinkainae es la rama de derivación más temprana en Munidopsinae (excluyendo *Leiogalathea*), por lo que este linaje puede tener restricciones y tendencias evolutivas distintas al resto de Munidopsidae. Un entorno altamente restringido prolongado durante mucho tiempo [por ejemplo, en *Shinkaia* hábitats quimiosintéticos del océano profundo desde el Eoceno (Schweitzer y Feldmann 2008)] puede ser el motor de la estasis morfológica en un linaje y la convergencia de caracteres entre distintos linajes (Lefébure et al. 2006, Struck et al. 2018).

En el caso de algunas especies de *Munidopsis*, y en particular de las especies abisales del grupo *Orophorhynchus* (Munidopsidae), ya se ha comentado que ocurre lo contrario: una elevada diversidad fenotípica en contraposición con una baja diferenciación genética (Tavares y Campinho 1998, Baba 2005, Samadi et al. 2006, Jones y Macpherson 2007, Macpherson 2011, Thaler et al. 2014, Dong et al. 2019). Por lo tanto, este caso se situaría en el otro extremo del gráfico. Se pueden plantear dos hipótesis para explicar este suceso: (1) es posible que dichos linajes de *Munidopsis* hayan diversificado mediante una radiación rápida explosiva (adaptativa o no adaptativa), fenómeno común en galateidos (Machordom y Macpherson 2004, Cabezas et al. 2012); o (2) las especies abisales tienen la tasa de substitución molecular más lenta, reflejándose en un menor cambio genético.

Por su parte, la gran diversida encontrada en *Phylladiorhynchus* se estructuró en más de 10 linajes independientes. La diferenciación morfológica entre grupos fue elevada, ya que se encontraron en torno a 50 caracteres para diferenciar especies. Sin embargo, los cambios morfológicos entre especies del mismo linaje fueron, en general, bajos, a excepción del linaje *ikedai* (especies de rostro triangular y en general de 3 a 5 espinas epigástricas). Es interesante remarcar que este linaje, típico de profundidades mayores a 200 m, engloba en conjunto la mayor diversidad morfológica encontrada para el género. Además, se encontraron pares de especies con poca diferenciación genética y morfológica, lo que supondría fenómenos de especiación reciente, en los que no se ha dado el tiempo necesario para la diferenciación morfológica y se encuentran en la zona gris de especiación (Roux et al. 2016, Struck et al. 2018). Este es el caso, por ejemplo, de *P. poeas* y *P. pusillus*. En este sentido, estas especies pueden haber sufrido una especiación alopátrica (Briggs 1999), ya que su distribución se restringe a áreas geográficas distantes (Australia y Polinesia). Otro fenómeno de especiación reciente por vicarianza observado en los galateidos fue el de *Munida iris vs. M. speciosa* de las costas atlánticas occidental y oriental, respectivamente. En *Coralliogalathea* no se han

observado fenómenos de especiación reciente, aunque sí distribuciones disjuntas y posibles eventos de vicarianza antiguos (de edades superiores a los 7 My) entre pares de especies del Mar Rojo *vs*. Vanuatu-Papúa Nueva Guinea y Vanuatu- Papúa Nueva Guinea *vs*. Polinesia.

En *Leiogalathea* cabe destacar que se encontraron ejemplos de pares de especies en los que el cambio morfológico fue mayor que la divergencia genética (*L. dido* y *L. turnus*). En este caso se observaron diferencias en la velocidad de los procesos de especiación, mucho más lentos en los procesos alopátricos que en los casos posibles de especiación simpátrica (entendida como especiación dentro de una misma área). Además, estos procesos también reflejan diferencias en el grado de diferenciación morfológica. Por ejemplo, *L. paris* y *L. juturna* presentan distribuciones alopátricas, se estima que divergieron hace 8 My, y sin embargo no presentan diferencias en los caracteres que utilizamos para la delimitación de especies (número de espinas en caparazón y rostro y misma forma del rostro). En las especies *L. dido* y *L. turnus*, ambas de Nueva Caledonia, se estima un tiempo de divergencia menor de 3 My, pero existen variaciones en los caracteres mencionados y otros adicionales entre este par de especies. En este caso podría haber ocurrido una especialización de nicho, ya que *L. dido* solo aparece por debajo del umbral de 1000 metros de profundidad. Este fenómeno de especialización ecológica se repite en algunas especies de *Phylladiorhynchus*, lo que se comentará más adelante.

4.2 Patrones biogeográficos

La distribución geográfica de *Coralliogalathea*, *Leiogalathea*, *Fennerogalathea* y *Phylladiorhynchus* presenta áreas solapantes y siguen un patrón de diversidad muy similar al observado en estudios previos de puntos calientes de diversidad marina (Briggs 1999, Myers et al. 2000, Bowen et al. 2013, Cowman y Bellwood 2013). La mayoría de estos trabajos se han realizado estudiando fauna marina de arrecife. Los pocos estudios de centros de diversidad en el océano profundo demuestran que el punto caliente de diversidad es similar al de la fauna somera (Cairns 2007, Schnabel et al. 2011a). Los centros de diversidad de los géneros estudiados a este respecto (Galatheidae y Munidopsidae), en general se solapan con los centros de diversidad obtenidos de estudios previos (Macpherson et al. 2010, Schnabel et al. 2011a, Cabezas et al. 2012) aunque presentan diferencias locales. En el área del Indo-Pacífico suroeste, Nueva Caledonia constituye el principal centro actual de diversidad para *Leiogalathea* y *Phylladiorhynchus*, similar a lo observado para los géneros de arrecife *Lauriea* y *Sadayoshia* (Palero et al. 2017). *Coralliogalathea*, por otro lado, parece tener su principal centro de diversidad en el área oriental del Triángulo de Coral. No obstante, puede existir un sesgo en esta elevada diversidad debido al mayor esfuerzo de muestreo efectuado en Nueva Caledonia y áreas adyacentes (Macpherson et al. 2010).

Es destacable la gran diversidad encontrada a nivel local (Cabezas et al. 2012, Schnabel y Ahyong 2019). Lo que se creía que eran especies de amplia distribución, han resultado ser complejos de especies con rangos de distribución más reducidos o incluso endémicas de un único archipiélago. Sin embargo, para poder discutir esto en profundidad se necesita un muestreo más amplio, pues existen zonas aun por explorar en las que la diversidad de especies de galateidos podría estar subestimada, por ejemplo, Indonesia, Filipinas, costas del océano Índico, etc., (Macpherson et al. 2020b). No obstante, algunas especies de *Phylladiorhynchus* y *Leiogalathea* presentan amplias distribuciones en el Indo-Pacífico, con distintos grados de heterogeneidad genética. Por ejemplo, *P. lynceus* se distribuye desde Chagos hasta Samoa (1.7% de distancia intraspecífica media para COI) o *L. paris* desde Papúa Nueva Guinea hasta la Polinesia presentando cierta homogeneidad genética. En este caso, las estrategias de reproducción pueden estar influyendo en estos patrones geográficos.

Se ha comentado que los galateidos presentan estrategias diferentes de tamaño y número de huevos, además del distinto número y duración de estados larvarios (Baba et al. 2011a). Ello puede influir en la capacidad de dispersión larvaria. Teóricamente, las especies de las familias Munididae y Galatheidae tienen larvas planctotróficas y de larga duración (Fujita et al. 2001, 2003, Fujita 2007, Baba et al. 2011a). Sin embargo, la limitada distribución geográfica de algunas especies podría indicar un cierto auto-reclutamiento o retención local de larvas, lo cual implicaría escasa capacidad de dispersión. Lamentablemente se tienen pocos datos de la biología larvaria en la mayoría de las especies, por lo que no se pueden hacer muchas inferencias a partir de las escasas evidencias existentes.

En *Coralliogalathea* y en en *Phylladiorhynchus* cabe señalar que se han encontrado especies crípticas muy antiguas coexistiendo en simpatría (*sensu* Rivas 1964). Esto puede deberse a un aumento del área de distribución original, es decir, las especies crípticas pudieron generarse por cladogénesis vicariante y ampliaron su rango de distribución hasta solaparse posteriormente (contacto secundario). Se ha visto que este es el proceso más común que explica la coincidencia de especies crípticas en el espacio, dado que los procesos de especiación ecológica pueden impedir la coexistencia a largo plazo (Bernardi et al. 2005, Westram et al. 2011, Vodă et al. 2015). Se necesitarían incluir más poblaciones a lo largo de la distribución geográfica de dichas especies a poder aceptar o rechazar esta hipótesis.

A diferencia de *Coralliogalathea*, *Fennerogalathea* y *Phylladiorhynchus*, cuyas distribuciones geográficas se restringen al Indo-Pacífico, dos especies de *Leiogalathea* habitan en el océano Atlántico. Durante el estudio de la historia biogeográfica de *Leiogalathea* comprobamos diferentes hipótesis de colonización del Atlántico, teniendo

en cuenta diferentes eventos biogeográficos, como el cierre del Tetis, el cierre del istmo de Panamá y eventos de larga dispersión. Nuestros análisis reconstruyeron un origen de diversificación en el Tetis para el género durante la transición Eoceno-Oligoceno y una compleja historia biogeográfica para *Leiogalathea*. Este origen biogeográfico de *Leiogalathea* en el Tetis coincide con la aparición de múltiples taxones de galateidos durante esa época y en la misma área (Beschin et al. 2016). Adicionalmente, el análisis de los patrones de colonización de *Leiogalathea* indicaron que su presencia en el Atlántico se debería un proceso de vicarianza por el cierre del Tetis. Posteriormente, la migración hacia el Este explicaría su llegada al punto de máxima diversidad actual en el Indo-Pacífico. Este patrón de colonización desde el Tetis hacia el Este es consistente con el patrón observado para otros taxones (Renema et al. 2008). La mayoría de los linajes de *Leiogalathea* se establecieron en su centro de diversidad actual durante el Plioceno, después de varios eventos de cladogénesis durante el Mioceno. Se observan patrones repetitivos en los diferentes linajes de la filogenia, como eventos de cambios de área geográfica, estasis y especiación tanto alopátrica como simpátrica (entendiéndose en el sentido de especiación en la misma área geográfica).

Paralelamente, la alta diversidad de la fauna de los arrecifes de coral en este punto caliente de diversidad mundial ya se había establecido para el Mioceno tardío (Briggs 1999). Al parecer, el Pacífico Suroccidental Tropical (*sensu* Spalding et al. 2007) actuó inicialmente como un centro de acumulación de especies para *Leiogalathea* mientras expandían su rango de distribución (Cowman y Bellwood 2013, Bowen et al. 2013). Posteriormente, el área podría haber actuado progresivamente como un centro de diversificación, promoviendo la cladogénesis y la rápida especiación.

Estas hipótesis han sido ampliamente propuestas y probadas para explicar los patrones de distribución de los arrecifes de coral y la fauna asociada en el punto caliente de diversidad marina del Indo-Pacífico (Gaither et al. 2011; Bowen et al. 2013). Además, se ha postulado que el movimiento de placas tectónicas, muy activo en esta área (Hall, 2002), ha influido en la distribución geográfica de la diversidad de distintos grupos (Williams y Duda, 2008, Cabezas et al. 2012, Williams et al. 2013).

4.3 Tendencias de diversificación

La comparación de los eventos de cladogénesis datados y la diversidad de linajes entre *Leiogalathea* y otros géneros (es decir, *Coralliogalathea*, *Lauriea*, *Paramunida* y *Sadayoshia*) (Palero et al. 2017) reveló tendencias evolutivas generales que afectan a estos organismos marinos tropicales (ver Fig. 9 LTT plot para *Coralliogalathea* y *Leiogalathea*). Por ejemplo, los géneros parecen coincidir en su tempo de diversificación, situado en el Eoceno y entorno a 40 My, a excepción de *Sadayoshia*, que es algo más

reciente. Durante la transición del Oligoceno al Mioceno, se observó un aumento de la cladogénesis para los grupos mencionados, con una diversificación alta o por encima de lo considerado como una diversificación constante en el tiempo (Fig. 9). A excepción de *Paramunida*, probablemente debido a un fenómeno de cladogénesis explosiva (Cabezas et al. 2012), se observó estasis en la diversificación alrededor del Mioceno Medio para todos los géneros. Por lo tanto, otros procesos como la extinción de linajes y la adaptación local podrían haber afectado de manera desigual a estos taxones. Además, los géneros de aguas someras *Coralliogalathea*, *Lauriea* y *Sadayoshia*, todos ellos asociados con arrecifes de coral, muestran una ausencia de cladogénesis durante los últimos 5 Myr (Palero et al, 2017). Sin embargo, en los géneros de aguas profundas *Paramunida* (Cabezas et al. 2012) y *Leiogalathea*, la especiación, probablemente asociada con el enfriamiento progresivo del fondo de aguas profundas (McClain y Hardy 2010, Davis et al. 2016), parece haberse promovido durante el Plioceno. Cladogénesis pliocénica también se ha observado en otros invertebrados de aguas profundas [por ejemplo, en otros cirrípedos abisales (Herrera et al. 2015) o en crustáceos decápodos de la familia Kiwaidae (Roterman et al., 2018)]. Las evidencias apuntan a que la diversificación podría ser mayor en galateidos de profundidad. Por consiguiente, pueden estar afectando distintos factores a los procesos de especiación en el océano profundo y en arrecifes de coral. Por ejemplo, los cambios en el nivel del mar durante las glaciaciones del Pleistoceno podrían afectar drásticamente a la fauna de arrecifes, mientras que factores relacionados con el cambio de temperatura y distribución diferencial de nutrientes en el océano profundo condicionarían en mayor medida a la fauna de profundidad (Gaither et al. 2011, Ritchie et al. 2015, Hendrickx y Serrano 2014).
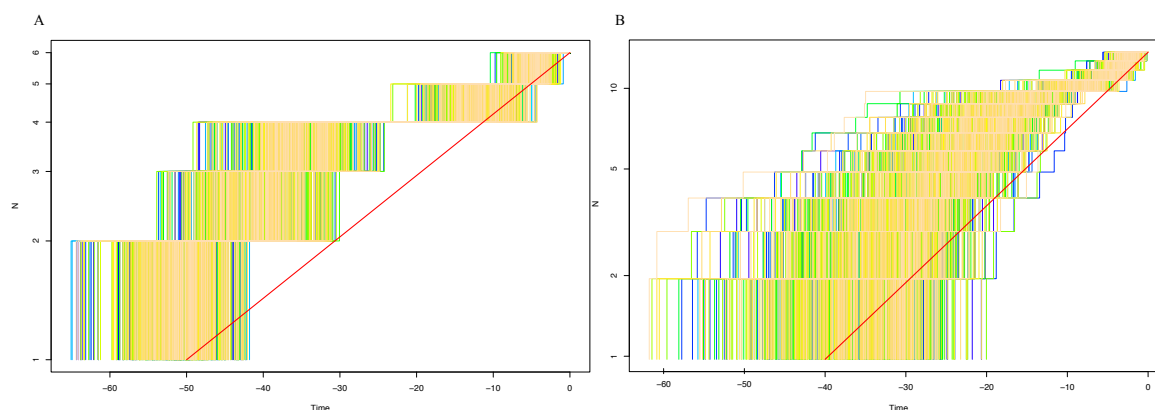
Figura 9. Gráficos LLT mostrando la diversificación de linajes (N) a través del tiempo (My) y respecto a una diversificación constante en el tiempo (recta roja). A = *Coralliogalathea* y B = *Leiogalathea*.

Como ya se ha comentado, los galateidos muestran una distribución batimétrica diferencial entre distintos linajes (Galatheidae, Munididae, Munidopsidae) (Schnabel et al. 2011a, Ahyong et al. 2010, Macpherson et al. 2010), aunque a niveles generales su

pico de máxima diversidad se encuentra en la plataforma continental (Schnabel et al. 2011a). Estos rangos particulares de distribución vertical en cada linaje pueden indicar que existen distintos procesos selectivos en la diversificación de estos organismos.

En la literatura se han planteado dos hipótesis alternativas para estudiar la diversidad en el océano profundo y su origen. La hipótesis tradicional y más aceptada propuso que la fauna marina bentónica se originó en ambientes marinos poco profundos y diversificó hacia aguas más profundas (Strugnell et al. 2008). Esta hipótesis se ha demostrado como válida para muchos animales marinos, incluyendo crustáceos (Wilson 1999, Raupach et al. 2009, Lorion et al. 2013, Yang et al. 2015, Cheng et al. 2018). Una hipótesis alternativa sugiere la vía evolutiva opuesta (desde ambientes profundos a los ambientes más someros), que también se ha demostrado en algunos grupos de organismos marinos, como los corales estilásteridos (Lindner et al. 2008).

En este sentido, *Phylladiorhynchus* constituye un grupo idóneo para comprobar estas hipótesis, pues presenta tanto grupos de especies que viven en arrecife de coral como especies típicas de plataforma, con una profundidad máxima de unos 1000 m. Nuestros resultados en relación a la evolución de ocupación de hábitat del género *Phylladiorhynchus* también ilustran un origen en aguas someras y un patrón de colonización hacia el océano profundo. Además, esta colonización parece que se ha dado de forma independiente en dos linajes de *Phylladiorhynchus*. Si se realizasen análisis más exhaustivos, incluyendo un muestreo taxonómico mayor y una mayor cantidad de caracteres (Rodríguez-Flores et al. en progreso) se podrían matizar estos resultados. Esto se debe a que existen más representantes de plataforma y talud que no se han añadido al estudio y que podrían completar la reconstrucción de la historia del grupo.

Por otro lado, las inferencias de las tendencias de diversificación de galateidos deben realizarse dentro de un marco analítico más complejo, en el que se estudie la tasa de diversificación neta resultante de las tasas de especiación y extinción y el efecto de la batimetría sobre estas, además de comprobación de distintos modelos incluyendo un muestreo taxonómico más completo. La resolución de los nodos y la longitud de las ramas depende directamente del número de taxones y de la cantidad y calidad de caracteres. Además, el estudio de los procesos de diversificación exclusivamente a partir de taxones actuales en ausencia de datos fósiles puede conducir a malinterpretaciones, incluso a la imposibilidad de recuperar tasas reales de diversificación, siempre teniendo en cuenta que la explicación de una determinada reconstrucción filogenética en el tiempo puede estar relacionada con infinitos escenarios de especiación y extinción equiprobables (Rabosky 2010, Louca y Pennell 2020).

En todo caso, es posible utilizar fuentes de datos independientes (no solo las propias secuencias), además de extraer una tasa de especiación que puede ser comparada entre linajes, o en diferentes momentos, y que podría ser útil para comprender los procesos que dieron lugar a las especies que están vivas hoy, incluso si no proporciona información sobre especies extintas (Pagel 2020). Si además integrásemos la valiosa información de la diversidad fósil (2 familias extintas, más de 25 géneros y cerca de 100 especies de galateidos, Ahyong et al. 2011a, Robins et al. 2013, 2016), la inferencia de los procesos evolutivos subyacentes a la diversificación de galateidos (tanto en el tiempo como en el espacio) sería mucho más exacta.

5. Perspectivas futuras

Para un mejor conocimiento de la riqueza de especies y comprensión de su historia evolutiva es necesario continuar describiendo especies e incrementando nuestro conocimiento de la diversidad de Galatheoidea. El objetivo debe ser convertir la curva exponencial de acumulación de especies en asintótica horizontal.

También se debe incrementar el muestreo taxonómico y de caracteres para completar no solo el estudio de *Munidopsis*, sino de *Galathea* y *Munida* con objeto de resolver relaciones filogenéticas, así como la existencia de más linajes independientes y su historia biogeográfica.

Es necesario añadir más estudios sobre filogeografía y biogeografía de otros linajes, de modo que se pueda entender mejor la historia evolutiva del grupo: predominancia de complejos de especies o especies cosmopolitas, origen biogeográfico, patrones de dispersión y especiación.

Con objeto de investigar el efecto de la batimetría en las tasas de especiación y/o en las tasas de evolución molecular se requiere una aproximación filogenómica, métodos de determinación de tasas de cambio molecular y el mayor muestreo taxonómico posible.

Para comprobar las hipótesis de cambio morfológico *vs.* cambio genético en los distintos grupos, se necesita cuantificar la variación morfológica mediante herramientas como la morfometría geométrica. Además, en este y en todos los casos anteriores los muestreos taxonómicos deberían de considerar los taxones fósiles, pues el grupo presenta un rico registro que no se ha integrado en profundidad en los estudios evolutivos de Galatheoidea. Como decía Gould, los árboles evolutivos que adornan nuestros libros de texto solo tienen datos en las puntas y en los nodos, el resto es inferencia, por razonable que sea, no la evidencia de los fósiles (Gould 1977).

CONCLUSIONES

De los estudios abordados en esta memoria, se pueden extraer las siguientes conclusiones:

1. La revisión de los géneros *Coralliogalathea*, *Fennerogalathea* y *Phylladiorhynchus* (Galatheidae), *Leiogalathea* y *Munidopsis* (Munidopsidae), y *Munida* del Atlántico (Munididae), utilizando una taxonomía integradora molecular-morfológica, ha dado lugar a la descripción de 65 nuevas especies y la recuperación de siete sinónimos.

2. La mayoría de los géneros estudiados de la familia Galatheidae se caracterizan por presentar especies con muy baja variabilidad morfológica. El género *Phylladiorhynchus*, sin embargo, presenta una diversidad morfológica amplia. Esto puede deberse a la presencia de linajes supraespecíficos independientes dentro del género

3. Los caracteres útiles para distinguir especies de Galatheidae suelen ser continuos y coinciden en distintos géneros: forma del rostro, estriación del caparazón, patrón de sedas sobre el caparazón y abdomen y forma de los propodios.

4. Las especies del género *Leiogalathea* siguen un patrón de variabilidad morfológica más similar a Galatheidae que a sus congéneres de la familia Munidopsidae.

5. Las especies de *Munida* del Atlántico, por el contrario, son variables morfológicamente a nivel intraespecífico. La existencia de linajes moleculares altamente divergentes e independientes en el Atlántico apoya la hipótesis de polifilia en *Munida*.

6. Los caracteres moleculares de marcadores mitocondriales son útiles para delimitar especies en conjunción con otras evidencias (marcadores nucleares, morfología, distribución geográfica). El rango de valores de las distancias genéticas para estos marcadores varía en función del grupo de estudio.

7. El análisis de mitogenomas da lugar a una topología en la que Porcellanidae se recupera como grupo externo de Galatheoidea. Esta nueva hipótesis filogenética es congruente con la anatomía externa de las distintas familias e implica que la carcinización es basal y la adquisición de forma de langosta es una apomorfía.

8. El género *Munidopsis* es polifilético y está compuesto por más de 20 linajes a nivel de género, diferenciados a nivel genético, morfológico, batimétrico y ecológico. Entre otros caracteres, el número de placas del telson, la presencia y posición de espinas oculares y el tipo de rostro son sinapomorfías morfológicas que definen dichos linajes.

9. El origen biogeográfico de *Leiogalathea* se sitúa en el Tetis durante el Oligoceno Tardío. Su presencia en el Atlántico se debe un proceso de vicarianza por el cierre del

Tetis. Posteriormente se dio una migración y diversificación hacia el Este, hasta su llegada al punto de máxima diversidad actual en el Indo-Pacífico.

10. El hábitat ancestral de *Phylladiorhynchus* está en aguas someras, colonizando posteriormente los hábitats más profundos. Esta colonización se produce de forma independiente en dos linajes de *Phylladiorhynchus*.

11. Existen coincidencias en los eventos de diversificación y patrones de diversidad geográfica en géneros del talud (*Leiogalathea, Paramunida*) y de arrecifes de coral (*Coralliogalathea, Sadayoshia*). Ello indica una historia biogeográfica común en los galateidos de los oceános Indico y Pacífico.

12. El esfuerzo taxonómico realizado a lo largo de estos años ha permitido inferir todos estos procesos evolutivos, destacando el papel de la taxonomía como parte esencial en el estudio de la evolución de la biodiversidad.

BIBLIOGRAFÍA

Adams, A. & White, A. (1848) Crustacea. In: Adams, A. (ed.), *The Zoology of the voyage of the HMS "Samarang" under the command of Captain Sir Edward Belcher, C.B., F.R.A.S., F.G.S., during the years 1843-1846*. London: Benham and Leeve, 1–66.

Ahyong, S. T. (2007) Decapod Crustacea collected by the NORFANZ Expedition: Galatheidae and Polychelidae. *Zootaxa*, 1593, 1–54.

Ahyong, S. T. & O'Meally, D. (2004) Phylogeny of the Decapoda Reptantia: resolution using three molecular loci and morphology. *The Raffles Bulletin of Zoology*, 52 (2), 673–693.

Ahyong, S. T., Andreakis, N. & Taylor, J. (2011b) Mitochondrial phylogeny of the deep-sea squat lobsters, Munidopsidae (Galatheoidea). *Zoologischer Anzeiger*, 250 (4), 367–377.

Ahyong, S. T., Baba, K., Macpherson, E. & Poore, G. C. (2010) A new classification of the Galatheoidea (Crustacea: Decapoda: Anomura). *Zootaxa*, 2676 (1), 57–68.

Ahyong, S. T., Schnabel, K. E. & Maas, E. W. (2009) Anomuran phylogeny: new insights from molecular data. In: Martin, J. W., Crandall, K. A. & Felder, D. L. (eds.), *Decapod Crustacean Phylogenetics. Crustacean Issues*, 18, 399–416.

Ahyong, S. T., Schnabel, K. E. & Macpherson, E. (2011a) Phylogeny and fossil record of marine squat lobsters. In: Poore, G. C. B., Ahyong, S. & Taylor, J. (eds.), *The Biology of Squat Lobsters.* Melbourne: CSIRO Publishing and Boca Raton: CRC Press, 73–104.

Appeltans, W., Ahyong, S. T., Anderson, G., Angel, M. V., Artois, T., Bailly, N., ... & Costello, M. J. (2012) The magnitude of global marine species diversity. *Current Biology*, 22 (23), 2189–2202.

Baba, K. (1969) Four new genera with their representatives and six new species of the Galatheidae in the collection of the Zoological Laboratory, Kyushu University, with redefinition of the genus *Galathea*. OHMU, 2, 1–32.

Baba, K. (1971) *Lauriea*, a new genus proposed for *Galathea gardineri* Laurie (Crustacea, Anomura, Galatheidae). *Memoirs of the Faculty of Education, Kumamoto University, Section 1 (Natural Science)*, 19, 51–53

Baba, K. (1988) Chirostylid and galatheid crustaceans (Decapoda: Anomura) of the "Albatross" Philippine Expedition, 1907–1910. *Researches on Crustacea, Special Number*, 2, 1–203.

Baba, K. (1991) Crustacea Decapoda: *Alainius* gen. nov., *Leiogalathea* Baba, 1969, and *Phylladiorhynchus* Baba, 1969 (Galatheidae) from New Caledonia. In: Crosnier, A. (Ed.) *Résultats des Campagnes MUSORSTOM 9. Mémoires du Muséum national d'Histoire naturelle. Série A, Zoologie,* 152, 479–491.

Baba, K. (1993) *Anomoeomunida*, a new genus proposed for *Phylladiorhynchus caribensis* Mayo, 1972 (Crustacea: Decapoda: Galatheidae). *Proceedings of the Biological Society of Washington*, 106, 102–105.

Baba, K. (1994) *Lauriea siagiani*, a new galatheid (Decapoda: Anomura: Galatheidae) from Bali, Indonesia. *Crustacean Research*, 23, 40-45.

Baba, K. (2005) Deep-sea chirostylid and galatheid crustaceans (Decapoda: Anomura) from the Indo-Pacific, with a list of species. *Galathea Report*, 20, 1–317.

Baba, K. (2008) *Torbenella*, a replacement name for *Torbenia* Baba, 2005 (Decapoda, Galatheidae) preoccupied by *Torbenia* Libert, 2000 (Insecta, Lepidoptera, Lycaenidae). *Crustaceana*, 81, 1021–1022.

Baba, K. & de Saint Laurent, M. (1996) Crustacea Decapoda: Revision of the genus *Bathymunida* Balss, 1914, and description of six new related genera (Galatheidae). In: Crosnier, A. (ed.), Résultats des Campagnes MUSORSTOM, volume 15. *Mémoires du Muséum National d'Histoire Naturelle, Paris*, 168, 433–502.

Baba, K. & Javed, W. (1974) *Coralliogalathea*, a new genus of Galatheidae (Crustacea, Anomura), with further notes on its type-species. *Annotationes Zoologicae Japonenses*, 47, 61–64.

Baba, K. & Poore, G. C. (2002). *Munidopsis* (Decapoda, Anomura) from south-eastern Australia. *Crustaceana*, 75 (3), 231–252.

BIBLIOGRAFÍA

Baba, K. & Wicksten, M. K. (1997) *Janetogalathea*, a new genus of squat lobster, with redescription of its type species *Galathea californiensis* Benedict, 1902 (Anomura: Galatheidae). *Crustacean Research*, 26, 38–46.

Baba, K. & Williams, A. B. (1998) New Galatheoidea (Crustacea, Decapoda, Anomura) from hydrothermal systems in the West Pacific Ocean Bismarck Archipelago and Okinawa Trough. *Zoosystema*, 20, 143–156.

Baba, K., Ahyong, S. T. & Macpherson, E. (2011b). Morphology of marine squat lobsters. In: Poore, G. C. B., Ahyong, S. & Taylor, J. (eds.), *The Biology of Squat Lobsters.* Melbourne: CSIRO Publishing and Boca Raton: CRC Press, 1-39.

Baba, K., Fujita, Y., Wehrtmann, I. S. & Scholtz, G. (2011a). Developmental biology of squat lobsters. In: Poore, G. C. B., Ahyong, S. & Taylor, J. (eds.), *The Biology of Squat Lobsters.* Melbourne: CSIRO Publishing and Boca Raton: CRC Press, 105-149.

Baba, K., Macpherson, E., Lin, C.-W. & Chan, T.-Y. (2009*) Crustacean Fauna of Taiwan: Squat Lobsters (Chirostylidae and Galatheidae).* Keelung: National Taiwan Ocean University.

Baba, K., Macpherson, E., Poore, G. C., Ahyong, S. T., Bermudez, A., Cabezas, P., Lin, C-W., Nizinski, M., Rodriguez, C. & Schnabel, K. E. (2008) Catalogue of squat lobsters of the world (Crustacea: Decapoda: Anomura families Chirostylidae, Galatheidae and Kiwaidae). *Zootaxa*, 1905 (1), 1–220.

Baeza, J. A. (2011). Squat lobsters as symbionts and in chemo-autotrophic environments. In: Poore, G. C. B., Ahyong, S. & Taylor, J. (eds.), *The Biology of Squat Lobsters.* Melbourne: CSIRO Publishing and Boca Raton: CRC Press, 249-270.

Balss, H. (1914) Ueber einige interessante Decapoden der "Pola'-Expeditionen in das Rote Meer. *Sitzungsberichte der Mathematisch-Naturwissenschaftlichen Klasse der Kaiserlichen Akademie der Wissenschaften in Wein*, 1914, 133–139.

Benedict, J. E. (1902) Description of a new genus and forty six new species of crustaceans of the family Galatheidae with a list of the known marine species. *Proceedings of the Biological Society of Washington*, 26, 243–334

Bernardi, G. (2005). Phylogeography and demography of sympatric sister surfperch species, Embiotoca jacksoni and E. lateralis along the California coast: historical versus ecological factors. Evolution, 59(2), 386–394.

Beschin, C., Busulini, A., Tessier, G. & Zorzin R. (2016) I crostacei associati a coralli nell'Eocene inferiore dell'area di Bolca (Verona e Vicenza, Italia nordorientale). *Memorie del Museo Civico di Storia Naturale di Verona, 2. Serie, Sezione Scienze della Terra*, 9, 1–189.

Bickford, D., Lohman, D. J., Sodhi, N. S., Ng, P. K., Meier, R., Winker, K.,... & Das, I. (2007). Cryptic species as a window on diversity and conservation. *Trends in ecology & evolution*, 22(3), 148–155.

Bouchet, P., Héros, V., Lozouet, P. & Maestrati, P. (2008) A quarter-century of deep-sea malacological exploration in the South and West Pacific: Where do we stand? How far to go. *Tropical deep-sea Benthos*, 25, 9–40.

Bouvier, E.-L. (1914). Sur la faune carcinologique de l'ile Maurice. Comptes Rendus Hebdomadaires de séances de l'Académie des Sciences. 159, 698–704

Bowen, B. W., Rocha, L. A., Toonen, R. J. & Karl, S. A. (2013). The origins of tropical marine biodiversity. *Trends in Ecology & Evolution*, 28(6), 359–366.

Boyd, C. M. (1960) The larval stages of *Pleuroncodes planipes* Stimpson (Crustacea, Decapoda, Galatheidae). *The Biological Bulletin*, 118 (1), 17–30.

Boyd, C. M. & Johnson, M. W. (1963) Variations in the larval stages of a decapod crustacean, *Pleuroncodes planipes* Stimpson (Galatheidae). *The Biological Bulletin*, 124 (2), 141–152.

Bracken-Grissom, H. D., Cannon, M. E., Cabezas, P., Feldmann, R. M., Schweitzer, C. E., Ahyong, S. T., Felder, D. L., Lemaitre, R. & Crandall, K. A. (2013) A comprehensive and integrative reconstruction of evolutionary history for Anomura (Crustacea: Decapoda). *BMC Evolutionary Biology*, 13 (1), 128.

Bracken-Grissom, H. D., Toon, A., Felder, D. L., Martin, J. W., Finley, M., Rasmussen, J., Palero, F. & Crandall, K. A. (2009) The decapod tree of life: compiling the data and

moving toward a consensus of decapod evolution. *Arthropod Systematics & Phylogeny*, 67 (1), 99–116.

Briggs, John C. "Modes of speciation: marine Indo-west Pacific." Bulletin of Marine Science 65.3 (1999): 645–656.

Brown, B. E. "Coral bleaching: causes and consequences." Coral reefs 16.1 (1997): S129–S138.

Cabezas, P. & Macpherson, E. (2014) A new species of *Paramunida* Baba, 1988 from the Central Pacific Ocean and a new genus to accommodate *P. granulata* (Henderson, 1885). *ZooKeys*, 425, 15–32.

Cabezas, P., Lin, C. W. & Chan, T. Y. (2011) Two new species of the deep-sea squat lobster genus *Munida* Leach, 1820 (Crustacea: Decapoda: Munididae) from Taiwan: morphological and molecular evidence. *Zootaxa*, 3036 (1), 26–38.

Cabezas, P., Macpherson, E. & Machordom, A. (2008) A new genus of squat lobster (Decapoda: Anomura: Galatheidae) from the South West Pacific and Indian Ocean inferred from morphological and molecular evidence. *Journal of Crustacean Biology*, 28 (1), 68–75.

Cabezas, P., Macpherson, E. & Machordom, A. (2009) Morphological and molecular Descriptionon of new species of squat lobster (Crustacea: Decapoda: Galatheidae) from the Solomon and Fiji Islands (South-West Pacific). *Zoological Journal of the Linnean Society*, 156 (3), 465–493.

Cabezas, P., Macpherson, E. & Machordom, A. (2010) Taxonomic revision of the genus *Paramunida* Baba, 1988 (Crustacea: Decapoda: Galatheidae): a morphological and molecular approach. *Zootaxa*, 2712 (1), 1–60.

Cabezas, P., Macpherson, E. & Machordom, A. (2011) *Allogalathea* (Decapoda: Galatheidae): a monospecific genus of squat lobster? *Zoological Journal of the Linnean Society*, 162 (2), 245–270.

Cabezas, P., Sanmartín, I., Paulay, G., Macpherson, E. & Machordom, A. (2012) Deep under the sea: unraveling the evolutionary history of the deep-sea squat lobster *Paramunida* (Decapoda, Munididae). *Evolution*, 66 (6), 1878–1896.

Cairns, S. D. (2007) Deep-water corals: an overview with special reference to diversity and distribution of deep-water scleractinian corals. *Bulletin of marine Science*, 81 (3), 311–322.

Caro, T. (2018) The functional significance of coloration in crabs. Biological Journal of the Linnean Society, 124 (1), 1–10.

Casadío, S., De Angeli, A., Feldmann, R. M., Garassino, A., Hetler, J. L., Parras, A. & Schweitzer, C. E. (2004) New decapod crustaceans (Thalassinidea, Galatheoidea, Brachyura) from the middle Oligocene of Patagonia, Argentina. *Annals of Carnegie Museum*, 73, 85–107.

Chace, F. A. (1939) Reports on the scientific results of the first Atlantis Expedition to the West Indies, etc. Preliminary descriptions of one new genus and seventeen new species of decapod and stomatopod Crustacea. *Memorias de la Sociedad Cubana de Historia Natural*, 13, 31–54.

Chace, F. A. (1942) The Anomura Crustacea. I. Galatheidea. Reports of the scientific results of the Atlantis Expeditions to the West Indies, under the joint auspices of the University of Havana and Havard University. *Torreia*, 11, 1–106.

Cheng, J., Chan, T. Y., Zhang, N., Sun, S. & Sha, Z. L. (2018) Mitochondrial phylogenomics reveals insights into taxonomy and evolution of Penaeoidea (Crustacea: Decapoda). *Zoologica Scripta*, 47 (5), 582–594.

Chu, K. H., Tsang, L. M., Ma, K. Y., Chan, T. Y. & Ng, P. K. L. (2009) Decapod phylogeny: what can protein-coding genes tell us?." In: Martin, J. W., Crandall, K. A. & Felder, D. L. (eds.), *Decapod Crustacean Phylogenetics*. *Crustacean Issues*, 18, 101–112.

Coleman, C. O. (2015) Taxonomy in times of the taxonomic impediment–examples from the community of experts on amphipod crustaceans. *Journal of Crustacean Biology*, 35 (6), 729–740.

Cordes, E. E. & Levin, L. A. (2018) Exploration before exploitation. *Science*, 359 (6377), 719.

Cowman, P. F. & Bellwood, D. R. (2013) Vicariance across major marine biogeographic

barriers: temporal concordance and the relative intensity of hard versus soft barriers. *Proceedings of the Royal Society B: Biological Sciences*, 280 (1768), 20131541.

Coykendall, D. K., Nizinski, M. S. & Morrison, C. L. (2017) A phylogenetic perspective on diversity of Galatheoidea (*Munida*, *Munidopsis*) from cold-water coral and cold seep communities in the western North Atlantic Ocean. *Deep Sea Research Part II: Topical Studies in Oceanography*, 137, 258–272.

Creasey, S., Rogers, A., Tyler, P., Gage, J. & Jollivet, D. (2000) Genetic and morphometric comparisons of squat lobster, *Munidopsis scobina* (Decapoda: Anomura: Galatheidae) populations, with notes on the phylogeny of the genus Munidopsis. *Deep Sea Research Part II: Topical Studies in Oceanography*, 47 (1-2), 87–118.

Croizat, L. (1964) *Space, time, form: The biological synthesis*. Caracas, Venezuela: Published by the author.

Cubelio, S. S., Tsuchida, S. & Watanabe, S. (2007) Vent associated *Munidopsis* (Decapoda: Anomura: Galatheidae) from Brothers Seamount, Kermadec arc, southwest Pacific, with description of one new species. *Journal of Crustacean Biology*, 27 (3), 513–519.

Dana, J. D. (1852) Conspectus crustaceorum, etc., Conspectus of the Crustacea of the Exploring Expedition under Capt. Wilkes, USN, including the Paguridea, continued, the Megalopidea, and the Macroura. Paguridea, continued, and subtribe Megalopidea. *Proceedings of the Academy of Natural Sciences*, 6, 6–28.

Davis, C. C., Schaefer, H., Xi, Z., Baum, D. A., Donoghue, M. J. & Harmon, L. J. (2014) Long-term morphological stasis maintained by a plant–pollinator mutualism. *Proceedings of the National Academy of Sciences*, 111 (16), 5914–5919.

Davis, K. E., Hill, J., Astrop, T. I. & Wills, M. A. (2016) Global cooling as a driver of diversification in a major marine clade. *Nature Communications*, 7 (1), 1–8.

Dayrat, B. (2005) Towards integrative taxonomy. *Biological Journal of the Linnean Society*, 85 (3), 407–415.

De Angeli, A., Garassino, A. & Ceccon, L. (2010) New report of the coral-associated decapods from the "Formazione di Castelgomberto" (early Oligocene) (Vicenza, NE Italy). *Atti della Società italiana di Scienze naturali e del Museo civico di Storia naturale in Milano*, 151 (2), 145–177.

De Queiroz, K. (1998) The general lineage concept of species, species criteria, and the process of speciation: a conceptual unification and terminological recommendations. In: Howard, D. J. & Berlocher, S. H. (eds.), *Endless forms species and speciation*. Oxford: Oxford University Press, 57–75.

De Queiroz, K. (2005) Ernst Mayr and the modern concept of species. *Proceedings of the National Academy of Sciences*, 102 (Suppl. 1), 6600–6607.

De Queiroz, K. (2007) Species concepts and species delimitation. *Systematic Biology*, 56 (6), 879–886.

Dhar, B., Ghose, A., Kundu, S., Malvika, S., Devi, N. N., Choudhury, A., ... & Ghosh, S. K. (2016) DNA barcoding: molecular positioning of living fossils (horseshoe crab). In: Trivedi, S., Ansari, A. A., Ghosh, S. K. & Rehman, H. (eds.), *DNA Barcoding in Marine Perspectives*. Cham: Springer, 181-199.

Dobzhansky, T. (1973) Nothing in biology makes sense except in the light of evolution. *The American Biology Teacher*, 35 (3), 125–129.

Dong, D. & Li, X. (2015) Galatheid and chirostylid crustaceans (Decapoda: Anomura) from a cold seep environment in the northeastern South China Sea. *Zootaxa*, 4057, 91–105.

Dong, D., Xu, P., Li, X. Z. & Wang, C. (2019) *Munidopsis* species (Crustacea: Decapoda: Munidopsidae) from carcass falls in Weijia Guyot, West Pacific, with recognition of a new species based on integrative taxonomy. *PeerJ*, 7, e8089.

Donoghue, M. J., Doyle, J. A., Gauthier, J., Kluge, A. G. & Rowe, T. (1989) The importance of fossils in phylogeny reconstruction. *Annual review of Ecology and Systematics*, 20 (1), 431–460.

Eldredge, N., Thompson, J. N., Brakefield, P. M., Gavrilets, S., Jablonski, D., Jackson, J. B.,... & Miller III, W. (2005). The dynamics of evolutionary stasis. *Paleobiology*, 31 (2_Suppl), 133–145.

BIBLIOGRAFÍA

Estes, S. & Arnold, S. J. (2007) Resolving the paradox of stasis: models with stabilizing selection explain evolutionary divergence on all timescales. *The American Naturalist*, 169 (2), 227–244.

Fabricius, J. C. (1793) *Entomologia systematica emendata et aucta. Secundum classes, ordines, genera, species adjectis synonimis, locis, observationibus, descriptionibus. Tom. II.* Copenhagen: C.G. Proft, fil.

Felder, D. L., Lemaitre, R. & Craig, C. (2019) Two new species of the *Phimochirus holthuisi* complex from the Gulf of Mexico, supported by morphology, color, and genetics (Crustacea: Anomura: Paguridae). *Zootaxa*, 4683 (4), 531–551.

Feldmann, R. M., & Schweitzer, C. E. (2006). Paleobiogeography of southern hemisphere decapod Crustacea. Journal of Paleontology, 80(1), 83-103.

Feldmann, R. M., Schweitzer, C. E. & Boessenecker, R. W. (2015). A New Squat Lobster (Decapoda: Anomura: Galatheoidea) from the Pliocene Purisima Formation, California. *Annals of Carnegie Museum*, 83 (2), 85–93.

Feldmann, R. M., Tshudy, D. M. & Thomson, M. R. (1993) Late cretaceous and paleocene decapod crustaceans from James Ross Basin, Antarctic Peninsula. *The Paleontological Society Memoir*, 28, 1–41.

Filhol, H. (1884). Explorations sous-marines. Voyage du ”Talisman”. *La Nature*, 12: 119394.

Fišer, C., Robinson, C. T. & Malard, F. (2018) Cryptic species as a window into the paradigm shift of the species concept. *Molecular Ecology*, 27 (3), 613–635.

Fitzhugh, K. (2006) The abduction of phylogenetic hypotheses. *Zootaxa*, 1145 (1), 1–110.

Fitzhugh, K. (2009) Species as explanatory hypotheses: refinements and implications. *Acta Biotheoretica*, 57 (1-2), 201–248.

Freudenstein, J. V., Broe, M. B., Folk, R. A. & Sinn, B. T. (2017) Biodiversity and the species concept—lineages are not enough. *Systematic Biology*, 66 (4), 644–656.

Fujita, Y. & Baba, K. (1999) Two galatheid associates of crinoids from the Ryukyu Islands (Decapoda: Anomura: Galatheidae), with their ecological notes. *Crustacean Research*, 28, 112–124.

Fujita, Y. (2007) First zoea of two shallow-water galatheids, *Lauriea gardineri* (Laurie, 1926) and *Phylladiorhynchus integrirostris* (Dana, 1853) (Crustacea: Decapoda: Anomura: Galatheidae). *Proceedings of the Biological Society of Washington*, 120 (1), 74–85.

Fujita, Y., Baba, K. & Shokita, S. (2001) Larval development of *Galathea inflata* Potts, 1925 (Decapoda: Anomura: Galatheidae) described from laboratory-reared material. *Crustacean Research*, 30, 111–132.

Fujita, Y., Baba, K. & Shokita, S. (2003) Larval development of *Galathea amboinensis* (Decapoda: Anomura: Galatheidae) under laboratory conditions. *Crustacean Research*, 32: 79–97.

Gaither, M. R., Bowen, B. W., Bordenave, T. R., Rocha, L. A., Newman, S. J., Gomez, J. A.,... & Craig, M. T. (2011) Phylogeography of the reef fish *Cephalopholis argus* (Epinephelidae) indicates Pleistocene isolation across the Indo-Pacific Barrier with contemporary overlap in the Coral Triangle. *BMC evolutionary biology*, 11(1), 189.

Gatt, M. & De Angeli, A. (2010). A new coral-associated decapod assemblage from the Upper Miocene (Messinian) Upper Coralline Limestone of Malta (Central Mediterranean). *Palaeontology*, 53(6), 1315–1348.

Gauthier, J., Kluge, A. G. & Rowe, T. (1988) Amniote phylogeny and the importance of fossils. *Cladistics*, 4(2), 105–209.

Goffredi, S. K., Jones, W. J., Erhlich, H., Springer, A. & Vrijenhoek, R. C. (2008) Epibiotic bacteria associated with the recently discovered Yeti crab, *Kiwa hirsuta. Environmental Microbiology*, 10 (10), 2623–2634.

Gore, R. H. (1979) Larval development of *Galathea rostrata* under laboratory conditions, with a discussion of larval development in the Galatheidae (Crustacea Anomura). *Fishery Bulletin*, 76, 781–806.

Gould, S. J. (1977). Evolution's Erratic Pace. *Natural History*, 86(5), 12–16.

Gould, S. J. (1990) *Wonderful life: the Burgess Shale and the nature of history*. New York: WW Norton & Company.

Gould, S. J. & Eldredge, N. (1977) Punctuated equilibria: the tempo and mode of evolution reconsidered. *Paleobiology*, 115–151.

Graybeal, A. (1998) Is it better to add taxa or characters to a difficult phylogenetic problem?. *Systematic biology*, 47(1), 9–17.

Halpern, B. S., Walbridge, S., Selkoe, K. A., Kappel, C. V., Micheli, F., D'Agrosa, C.,... & Fujita, R. (2008) A global map of human impact on marine ecosystems. *Science*, 319 (5865), 948–952.

Haworth, A. H. (1825) A new binary arrangement of the macrurous Crustacea. *Philosophical Magazine and Journal*, 65 (323), 183–184.

Hebert, P. D., Cywinska, A., Ball, S. L. & Dewaard, J. R. (2003) Biological identifications through DNA barcodes. *Proceedings of the Royal Society of London. Series B: Biological Sciences*, 270 (1512), 313–321.

Henderson, J. R. (1885) Diagnoses of new species of Galatheidae collected during the "Challenger" expedition. Annals and Magazine of Natural History (ser. 5), 16, 407–421.Hennig, W. (1966) *Phylogenetic systematics*. Urbana, IL.: University of Illinois Press.

Hennig, W. (1966) *Phylogenetic Systematics*. Urbana: Univ. Illinois Press.

Heros, V., Cowie, R. H. & Bouchet, P. (eds.) (2008) Tropical Deep-Sea Benthos. *Mémoires du Muséum national d'Histoire naturelle*, 196, 1–788.

Herrera, S., Watanabe, H. & Shank, T. M. (2015) Evolutionary and biogeographical patterns of barnacles from deep-sea hydrothermal vents. *Molecular Ecology*, 24 (3), 673–689.

Hillis, D. M. (1998) Taxonomic sampling, phylogenetic accuracy, and investigator bias. *Systematic Biology*, 47 (1), 3–8.

Hillis, D. M. (2019) Species delimitation in herpetology. *Journal of Herpetology*, 53 (1), 3–12.

Hoyoux, C., Zbinden, M., Samadi, S., Gaill, F. & Compère, P. (2009) Wood-based diet and gut microflora of a galatheid crab associated with Pacific deep-sea wood falls. *Marine Biology*, 156 (12), 2421–2439.

Hoyoux, C., Zbinden, M., Samadi, S., Gaill, F. & Compère, P. (2012) Diet and gut microorganisms of Munidopsis squat lobsters associated with natural woods and mesh-enclosed substrates in the deep South Pacific. *Marine Biology Research*, 8 (1), 28–47.

Huelsenbeck, J. P. (1991) When are fossils better than extant taxa in phylogenetic analysis? *Systematic Biology*, 40 (4), 458–469.

Hughes, J. B., Daily, G. C. & Ehrlich, P. R. (1997) Population diversity: its extent and extinction. *Science*, 278 (5338), 689–692.

Hyžný, M. & Schlögl, J. (2011) An early Miocene deep-water decapod crustacean faunule from the Vienna Basin (Western Carpathians, Slovakia). *Palaeontology*, 54 (2), 323–349.

Hyžný, M., Gašparič, R., Robins, C. M. & Schlögl, J. (2014). Miocene squat lobsters (Decapoda, Anomura, Galatheoidea) of the Central Paratethys–a review, with description of a new species of *Munidopsis*. *Scripta Geologica*, 147, 241–267.

Jones, W. J. & Macpherson, E. (2007) Molecular phylogeny of the east pacific squat lobsters of the genus *Munidopsis* (Decapoda: Galatheidae) with the descriptions of seven new species (vol 27, pg 477, 2007). *Journal of Crustacean Biology*, 27 (4), 698–698.

Karasawa, H. (1993) Cenozoic decapod Crustacea from southwest Japan. *Bulletin of the Mizunami Fossil Museum*, 20, 1–92.

Karasawa, H. (2000) Coral-associated decapod Crustacea from the Pliocene Daito Limestone Formation and Pleistocene Ryukyu Group, Ryukyu Islands, Japan. *Bulletin of the Mizunami Fossil Museum*, 27, 167–189.

Kerkhove, T. R., Boyen, J., De Backer, A., Mol, J. H., Volckaert, F. A., Leliaert, F. & De Troch, M. (2019) Multilocus data reveal cryptic species in the Atlantic seabob shrimp *Xiphopenaeus kroyeri* (Crustacea: Decapoda). *Biological Journal of the Linnean Society*, 127 (4), 847–862.

Kilgour, M. J. & Shirley, T. C. (2014) Reproductive biology of galatheoid and chirostyloid (Crustacea: Decapoda) squat lobsters from the Gulf of Mexico. *Zootaxa*, 3754, 381–419.

Kirschner, M. & Gerhart, J. (1998) Evolvability. *Proceedings of the National Academy of Sciences*, 95 (15), 8420–8427.

Klompmaker, A. A., Feldmann, R. M., Robins, C. M. & Schweitzer, C. E. (2012). Peak

diversity of Cretaceous galatheoids (Crustacea, Decapoda) from northern Spain. *Cretaceous Research*, 36, 125–145.

Knowlton, N. (2000) Molecular genetic analyses of species boundaries in the sea. *Hydrobiologia*, 420, 73–90.

Koelbel, C. (1892) Beitraege zur Kenntnis der Crustaceen der Canarischen Inseln. *Annalen des Naturhistorischen Museums in Wien*, 7, 105–116.

Kolbert, E. (2014) *The sixth extinction: An unnatural history*. New York: Henry Holt and Co.

Komai, T. (2017) A new squat lobster species of the genus *Munida* (Decapoda, Anomura, Munididae) from the deep-sea off the Ryukyu Islands, Japan. *Crustaceana,* 90 (7–10), 969–979.

Krell, F. T. (2002) Why impact factors don't work for taxonomy. *Nature*, 415 (6875), 957–957.

Lamarck, J. (1815). *Histoire naturelle des animaux sans vertèbres. I.* Paris: Verdiere.

Leach, W.E. (1820) Galatéadées. In: *Dictionnaire des Sciences Naturelles*. Paris: F. G. Levreault, 49–56.

Lefébure, T., Douady, C. J., Gouy, M. & Gibert, J. (2006) Relationship between morphological taxonomy and molecular divergence within Crustacea: proposal of a molecular threshold to help species delimitation. *Molecular phylogenetics and evolution*, 40 (2), 435–447.

Lin, C. W., Osawa, M. & Chan, T. Y. (2007) A new *Munidopsis* (Crustacea: Decapoda: Galatheidae) associated with gorgonian corals from the deep waters off Taiwan. *Proceedings of the Biological Society of Washington*, 120 (2), 167–174.

Lindner, A., Cairns, S. D. & Cunningham, C. W. (2008) From offshore to onshore: multiple origins of shallow-water corals from deep-sea ancestors. *PLoS One*, 3 (6), e2429.

Linnaeus, C. (1761). *Fauna Suecica sistens Animalia Sueciae Regni: Distributa per Classes, Ordines, Genera, Species, cum Differentiis Specierum, Synonymis Auctorum, Nominibus Incolarum, Locis Natalium, Descriptionibus insectorum*. Stockhom: Editio altera, auctior. Stockholmiae.

Lipton, P. (1991) Contrastive explanation and causal triangulation. *Philosophy of Science*, 58 (4), 687–697.

Liu, X., Li, X. & Lin, R. (2020) A new squat lobster species of the genus *Munida* Leach, 1820 (Crustacea: Anomura: Galatheoidea: Munididae) from hydrothermal vents on the Eastern Pacific Rise. *Zootaxa*, 4743 (1),131–136.

Lorion, J., Kiel, S., Faure, B., Kawato, M., Ho, S. Y., Marshall, B.,... & Fujiwara, Y. (2013) Adaptive radiation of chemosymbiotic deep-sea mussels. *Proceedings of the Royal Society B: Biological Sciences*, 280 (1770), 20131243.

Louca, S. & Pennell, M. W. (2020) Extant timetrees are consistent with a myriad of diversification histories. *Nature*, 580 (7804), 502–505.

Lovén, S. (1852) De svenska arterna af slägtet Galathea. *Ofversigt af Konglige Vetenskaps-Akademiens Förhandlingar*, 9, 20–23

Lovrich, G. A. & Thiel, M. (2011). Ecology, physiology, feeding and trophic role of squat lobsters. In: Poore, G. C. B., Ahyong, S. & Taylor, J. (eds.), *The Biology of Squat Lobsters*. Melbourne: CSIRO Publishing and Boca Raton: CRC Press, 183-222.

Machordom, A. & Macpherson, E. (2004) Rapid radiation and cryptic speciation in squat lobsters of the genus *Munida* (Crustacea, Decapoda) and related genera in the South West Pacific: molecular and morphological evidence. *Molecular Phylogenetics and Evolution*, 33 (2), 259–279.

MacLeay, W. S. (1838) On the Brachyurous Decapod Crustacea. Brought from the Cape by Dr. Smith. In: Smith, A. (ed.), *Illustrations of the Zoology of South Africa; consisting chiefly of Figures and Descriptions of the Objects of Natural History Collected during an Expedition into the Interior of South Africa, in the Years 1834, 1835, and 1836; fitted out by "The Cape of Good Hope Association for Exploring Central Africa"*. London: Published under the Authority of the Lords Commissioners of Her Majesty's Treasury, 53–71.

Macpherson, E. (1998) A new genus of Galatheidae (Crustacea, Anomura) from the western Pacific Ocean. *Zoosystema*, 20, 351–355.

Macpherson, E. (2006). Galatheidae (Crustacea, Decapoda) from the Austral Islands, Central Pacific. in: Richer de Forges, B. et al. (Ed.) Tropical Deep-Sea Benthos 24. *Mémoires du Muséum national d'Histoire naturelle* (1993) 193, 285–333.

Macpherson, E. (2007) Species of the genus *Munidopsis* Whiteaves, 1784 from the Indian and Pacific oceans and reestablishment of the genus *Galacantha* A. Milne-Edwards, 1880 (Crustacea, Decapoda, Galatheidae). *Zootaxa*, 1417, 1–135.

Macpherson, E. (2011) A new squat lobster of the genus *Munidopsis* (Crustacea: Decapoda: Munidopsidae) from the Mediterranean Sea. *Scientia Marina*, 75 (3), 525–532.

Macpherson, E. & Baba, K. (2010) Revision of the genus *Sadayoshia* (Anomura, Galatheidae), with description of four new species. In: Fransen, C.H.J.M., De Grave, S., & Ng P.K.L. (eds.), *Studies on Malacostraca: Lipke Bijdeley Holthuis Memorial Volume. Crustaceana Monographs*. 14: 415–452.

Macpherson, E. & Baba, K. (2011). Taxonomy of squat lobsters. In: Poore, G. C. B., Ahyong, S. & Taylor, J. (eds.), *The Biology of Squat Lobsters*. Melbourne: CSIRO Publishing and Boca Raton: CRC Press, 149–182.

Macpherson, E. & Baba, K. (2012) The squat lobsters of the genus Sadayoshia Baba, 1969 (Crustacea: Decapoda: Anomura: Munididae): new records including six new species from the Pacific Ocean. Zootaxa, 3589(1), 30–48.

Macpherson, E. & Cleva, R. (2010) Shallow-water squat lobsters (Crustacea, Decapoda, Galatheidae) from Mayotte (Comoros Island), La Réunion and Madagascar, with the description of a new genus and two new species." *Zootaxa,* 2612: 57–68.

Macpherson, E. & Machordom, A. (2000) *Raymunida*, new genus (Decapoda: Anomura: Galatheidae) from the Indian and Pacific oceans. *Journal of Crustacean Biology*, 20 (5), 253–258.

Macpherson, E. & Machordom, A. (2001) Phylogenetic relationships of species of *Raymunida* (Decapoda: Galatheidae) based on morphology and mitochondrial cytochrome oxidase sequences, with the recognition of four new species. *Journal of Crustacean Biology*, 21 (3), 696–714.

Macpherson, E. & Machordom, A. (2005) Description of three sibling new species of the genus *Munida* Leach, 1820 (Decapoda, Galatheidae) from New Caledonia using morphological and molecular data. *Journal of Natural History*, 39, 819–834.

Macpherson, E. & Robainas-Barcia, A. (2013) A new genus and some new species of the genus *Lauriea* Baba, 1971 (Crustacea, Decapoda, Galatheidae) from the Pacific and Indian Oceans, using molecular and morphological characters. *Zootaxa*, 3599 (2), 136–160.

Macpherson, E. & Robainas-Barcia, A. (2015) Species of the genus *Galathea* Fabricius, 1793 (Crustacea, Decapoda, Galatheidae) from the Indian and Pacific Oceans, with descriptions of 92 new species. *Zootaxa*, 3913 (1), 1–335.

Macpherson, E. & Segonzac, M. (2005) Species of the genus *Munidopsis* (Crustacea, Decapoda, Galatheidae) from the deep Atlantic Ocean, including cold-seep and hydrothermal vent areas. *Zootaxa*, 1095, 1–60.

Macpherson, E., Beuck, L. & Freiwald, A. (2016) Some species of *Munidopsis* from the Gulf of Mexico, Florida Straits and Caribbean Sea (Decapoda: Munidopsidae), with the description of two new species. *Zootaxa*, 4137 (3), 405–416.

Macpherson, E., Chan, T. Y., Kumar, A. B. & Rodríguez-Flores, P. C. (2020b) On some squat lobsters from India (Decapoda, Anomura, Munididae), with description of a new species of *Paramunida* Baba, 1988. *ZooKeys*, *965*, 17.

Macpherson, E., de Forges, B. R., Schnabel, K., Samadi, S., Boisselier, M. C. & Garcia-Rubies, A. (2010) Biogeography of the deep-sea galatheid squat lobsters of the Pacific Ocean. *Deep Sea Research Part I: Oceanographic Research Papers*, 57 (2), 228–238.

Macpherson, E., Jones, W. & Segonzac, M. (2005) A new squat lobster family of Galatheoidea (Crustacea, Decapoda, Anomura) from the hydrothermal vents of the Pacific-Antarctic Ridge. *Zoosystema*, 27 (4), 709–723.

Macpherson, E., Rodríguez-Flores, P. C. & Machordom, A. (2020a) Squat lobsters of the families Munididae and Munidopsidae from Papua New Guinea. In: Corbari, L., Ahyong, S. T. & Chan, T-Y. (eds), *Deep-sea crustaceans from Papua New Guinea*. Tropical Deep-

Sea Benthos 31. *Mémoires du Muséum National d'Histoire Naturelle*, 121, 11–120.

Malay, M. C. M. D. & Paulay, G. (2010) Peripatric speciation drives diversification and distributional pattern of reef hermit crabs (Decapoda: Diogenidae: *Calcinus*). *Evolution*, 64 (3), 634–662.

Margalef, R. (1968) *Perspectives in ecological theory*. Chicago: University of Chicago Press

Marin, I. (2020) Northern unicorns of the depths: diversity of the genus *Munidopsis* Whiteaves, 1874 (Decapoda: Anomura: Munidopsidae) in the northwestern Pacific Ocean, with descriptions of three new species along the Russian coast. *Progress in Oceanography*, 183, 102263.

Martin, J. W. & Abele, L. G. (1986) Phylogenetic relationships of the genus *Aegla* (Decapoda: Anomura: Aeglidae), with comments on anomuran phylogeny. *Journal of Crustacean Biology*, 6 (3), 576–612.

Martin, J. W. & Davis, G.E. (2001) An updated classification of the recent Crustacea. *Natural History Museum of Los Angeles County, Science Series*, 39, 1–124.

Mathews, L. M. & Warren, A. H. (2008) A new crayfish of the genus *Orconectes* Cope, 1872 from southern New England (Crustacea: Decapoda: Cambariidae). *Proceedings of the Biological Society of Washington*, 121 (3), 374–381.

May, R. M. (1992) How many species inhabit the earth?. *Scientific American*, 267 (4), 42–49.

Mayden, R. L. (1997) A hierarchy of species concepts: the denouement in the saga of the species problem. In: Claridge, M. F., Dawah, H. A. & Wilson, M. R. (eds.), *Species: The units of diversity*. London: Chapman & Hall, 381–423.

Mayo, B. S. (1974). *The Systematics and Distribution of the Deep-sea Genus Munidopsis (crustacea Galatheidae) in the Western Atlantic Ocean*. Doctoral dissertation, Miami, University of Miami.

McCallum, A. W., Cabezas, P. & Andreakis, N. (2016) Deep-sea squat lobsters of the genus *Paramunida* Baba, 1988 (Crustacea: Decapoda: Munididae) from north-western Australia: new records and description of three new species. *Zootaxa*, 4173 (3), 201–224.

McClain, C. R. & Hardy, S. M. (2010) The dynamics of biogeographic ranges in the deep sea. *Proceedings of the Royal Society B: Biological Sciences*, 277 (1700), 3533–3546.

McLaughlin, P. A., Lemaitre, R. & Sorhannus, U. (2007) Hermit crab phylogeny: a reappraisal and its "fall-out". *Journal of Crustacean Biology*, 27 (1), 97–115.

Meier, R. (2008) DNA sequences in taxonomy: opportunities and challenges. In: Wheeler, Q. D. (ed.), *The New Taxonomy*. Boca Raton, Fl.: CRC Press, Taylor and Francis Group, 95–127.

Meyer, C. P. & Paulay, G. (2005) DNA barcoding: error rates based on comprehensive sampling. *PLoS Biology*, 3 (12), e422.

Milne Edwards, A. (1880) Reports on the results of dredging under the supervision of Alexander Agassiz, in the Gulf of Mexico and in the Caribbean Sea, etc. VIII. Études préliminaires sur les Crustacés. *Bulletin of the Museum of Comparative Zoology at Harvard College*, 8, 1–168.

Milne-Edwards, A. & Bouvier, E. L. (1894) Considerations génerales sur la famille de Galathéides. *Annales des Sciences Naturelles, Zoologie*, 16, 191–327.

Milne-Edwards, A. & Bouvier, E. L. (1899) Crustacés décapodes provenant des campagnes de l'Hirondelle (supplément) et de la Princesse-Alice (1891–1897). *Résultats des Campagnes Scientifiques accomplis sur son Yacht par Albert Ier Prince Souverain de Monaco*. 13, 1–106.

Milne-Edwards, A. & Bouvier, E. L. (1900) Crustacés décapodes. Première partie. Brachyures et Anomoures. In: Milne-Edwards, A. (ed.), *Expéditions scientifiques du Travailleur et du Talisman pendant les années 1880, 1881, 1882, 1883*. Paris: Masson, 1–396.

Miyake, S. & Baba, K. (1970) The Crustacea Galatheidae from the Tropical-subtropical Region of West Africa: With a List of the Known Species. *Atlantide Report*, 11, 61–97.

Mora, C., Tittensor, D. P., Adl, S., Simpson, A. G. & Worm, B. (2011) How many species are there on Earth and in the ocean?. *PLoS Biol*, *9* (8), e1001127.

Moritz, C. & Cicero, C. (2004) DNA barcoding: promise and pitfalls. *PLoS Biol*ogy, 2 (10), e354.

Morrison, C. L., Harvey, A. W., Lavery, S., Tieu, K., Huang, Y. & Cunningham, C. W. (2002) Mitochondrial gene rearrangements confirm the parallel evolution of the crab-like form. *Proceedings of the Royal Society of London. Series B: Biological Sciences*, 269, 345–350.

Müller, P. & Collins, J. S. H. (1991) Late Eocene coral-associated decapods (Crustacea) from Hungary. *Mededelingen van de Werkgroep voor Tertiaire en Kwartaire Geologie*, 28 (2/3), 47–92.

Myers, N., Mittermeier, R. A., Mittermeier, C. G., Da Fonseca, G. A. & Kent, J. (2000) Biodiversity hotspots for conservation priorities. *Nature*, 403 (6772), 853–858.

Nabholz, B., Glémin, S. & Galtier, N. (2008) Strong variations of mitochondrial mutation rate across mammals—the longevity hypothesis. *Molecular Biology and Evolution*, 25 (1), 120–130.

Nabholz, B., Glémin, S. & Galtier, N. (2009) The erratic mitochondrial clock: variations of mutation rate, not population size, affect mtDNA diversity across birds and mammals. *BMC evolutionary biology*, 9 (1), 54.

Nakamura, M., Chen, C. & Mitarai, S. (2015) Insights into life-history traits of *Munidopsis* spp.(Anomura: Munidopsidae) from hydrothermal vent fields in the Okinawa Trough, in comparison with the existing data. *Deep Sea Research Part I: Oceanographic Research Papers*, 100, 48–53.

Niiniluoto, I. (1999) Defending abduction. *Philosophy of Science*, 66, S436–S451.

Nyborg, T. & Garassino, A. (2015) New fossil squat lobsters (Crustacea: Anomura: Munididae) from the Eastern Pacific. *Palaeodiversity*, 8, 95–101.

Ortmann, A. E. (1892) Die Decapoden-Krebse des Strassburger Museum, mit beson derer Berücksichtigung der von Herrn Dr. Doederlein bei Japan und bei den Liu-Kiu-Inseln gesammelten und zur Zeit im Strassburger Museum aufbe wahrten Formen.IV. Die Abtheilungen Galatheidea und Paguridea. *Zoologisher Jahrbüchern. Abtheilung für Systematik, Geographie und Biologie der Thiere*, 6, 241–326.

Ortmann, A.E. (1898–1901) Crustacea (Zweite Hälfte: Malacostraca). In: Gerstaecker, A. (ed.), *Die Klassen und Ordnungender Arthropoden wissenschaftlich dargestellt in Wort und Bild* 5. Abtheilung 2. Leipzig: C.F. Wintersche Verlagshandlung.

Packer, L., Grixti, J. C., Roughley, R. E. & Hanner, R. (2009) The status of taxonomy in Canada and the impact of DNA barcoding. *Canadian Journal of Zoology*, 87 (12), 1097–1110.

Padial, J. M., Miralles, A., De la Riva, I. & Vences, M. (2010) The integrative future of taxonomy. *Frontiers in Zoology*, 7, 1–14.

Pagel, M. (2020) Evolutionary trees can't reveal speciation and extinction rate. *Nature*, 580 (7804), 461–462.

Palero, F., Robainas-Barcia, A., Corbari, L. & Macpherson, E. (2017) Phylogeny and evolution of shallow-water squat lobsters (Decapoda, Galatheoidea) from the Indo-Pacific. *Zoologica Scripta*, 46 (5), 584–595.

Pante, E., Puillandre, N., Viricel, A., Arnaud-Haond, S., Aurelle, D., Castelin, M., Chenuil, A., Destombe, C., Forcioli, D., Valero, M., Viard, F. & Samadi, S. (2015) Species are hypotheses: avoid connectivity assessments based on pillars of sand. *Molecular Ecology*, 24 (3), 525–544.

Pearson, D. L., Hamilton, A. L. & Erwin, T. L. (2011) Recovery plan for the endangered taxonomy profession. *BioScience*, 61 (1), 58–63.

Pérez-Losada, M., Jara, C. G., Bond-Buckup, G., Porter, M. L. & Crandall, K. A. (2002) Phylogenetic position of the freshwater anomuran family Aeglidae. *Journal of Crustacean Biology*, 22 (3), 670–676.

Pimm, S. L., Russell, G. J., Gittleman, J. L. & Brooks, T. M. (1995) The future of biodiversity. *Science*, 269 (5222), 347–350.

Pollock, D. D., Zwickl, D. J., McGuire, J. A. & Hillis, D. M. (2002) Increased taxon sampling is advantageous for phylogenetic inference. *Systematic biology*, 51 (4), 664–671.

Poore, G. C. & Andreakis, N. (2012) The *Agonida incerta* species complex unravelled (Crustacea: Decapoda: Anomura: Munididae). *Zootaxa*, 3492 (1), 1–29.

Poore, G. C. & Andreakis, N. (2014) More species of the *Agononida incerta* complex revealed

by molecules and morphology (Crustacea: Decapoda: Anomura: Munididae). *Zootaxa*, 3860 (3), 201–225.

Poore, G. C., Ahyong, S. T., & Taylor, J. (eds.) (2011). *The biology of squat lobsters*. Melbourne: CSIRO Publishing and Boca Raton: CRC Press.

Poore, G. C., Dworschak, P. C., Robles, R., Mantelatto, F. L. & Felder, D. L. (2019) A new classification of Callianassidae and related families (Crustacea: Decapoda: Axiidea) derived from a molecular phylogeny with morphological support. *Memoirs of Museum Victoria*, 78, 73–146.

Porter, M. L., Pérez-Losada, M. & Crandall, K. A. (2005) Model-based multi-locus estimation of decapod phylogeny and divergence times. *Molecular Phylogenetics and Evolution*, 37 (2), 355–369.

Potts, F.A. (1915). The fauna associated with the crinoids of a tropical coral reef: with especial reference to its colour variations. Papers from the Tortugas Laboratory of the Carnegie Institute of Washington. 8, 71–96, plate 1.

Poupin, J. & Malay, M. C. (2009) Identification of a *Ciliopagurus strigatus* (Herbst, 1804) species-complex, with description of a new species from French Polynesia (Crustacea, Decapoda, Anomura, Diogenidae). *Zoosystema*, 31 (2), 209–232.

Puillandre, N., Lambert, A., Brouillet, S. & Achaz, G. (2012) ABGD, Automatic Barcode Gap Discovery for primary species delimitation. *Molecular ecology*, 21(8), 1864–1877.

Rabosky, D. L. (2010) Extinction rates should not be estimated from molecular phylogenies. *Evolution*, 64 (6), 1816–1824.

Reimann, A., Richter, S. & Scholtz, G. (2011) Phylogeny of the Anomala (Crustacea, Decapoda, Reptantia) based on the ossicles of the foregut. *Zoologischer Anzeiger*, 250 (4), 316–342.

Renema, W., Bellwood, D. R., Braga, J. C., Bromfield, K., Hall, R., Johnson, K. G., Lunt, P., Meyer, C. P., McMonagle, L. B., Morley, R. J., O'Dea, A., Todd, J. A., Wesselingh, F. P., Wilson, M. E. J. & Pandolfi, J. M. (2008) Hopping hotspots: global shifts in marine biodiversity. *Science*, 321 (5889), 654–657.

Rice, A. L. & de Saint Laurent, M. (1986) The nomenclature and diagnostic characters of four north-eastern Atlantic species of the genus *Munida* Leach: *M. rugosa* (Fabricius), *M. tenuimana* G. O. Sars, *M. intermedia* A. Milne Edwards and Bouvier, and *M. sarsi* Huus (Crustacea, Decapoda, Galatheidae). *Journal of Natural History*, 20 (1), 143–163.

Richer de Forges, B., Chan, T. Y., Corbari, L., Lemaitre, R., Macpherson, E., Ahyong, S. T. & Ng, P. K. L. (2013) The MUSORSTOM-TDSB deep-sea benthos exploration program (1976-2012): An overview of crustacean discoveries and new perspectives on deep-sea zoology and biogeography. In Ahyong S. T., Chan T.-Y., Corbari L. & Ng P. K. L. (eds), *Tropical Deep-Sea Benthos* 27. *Mémoires du Muséum national d'Histoire naturelle,* 204, 13–66

Rivas, L. R. (1964) A reinterpretation or the concepts "Sympatric" and "Allopatric" with proposal or the additional terms "Syntopic" and "Allotopic". *Systematic Zoology*, 13 (1), 42–43.

Robins, C. M. (2012) *Systematics and phylogeny of the fossil Galatheoidea (Anomura, Decapoda): uncovering their evolutionary path*. Doctoral dissertation, Kent State University.

Robins, C. M., Feldmann, R. M. & Schweitzer, C. E. (2013) Nine new genera and 24 new species of the Munidopsidae (Decapoda: Anomura: Galatheoidea) from the Jurassic Ernstbrunn Limestone of Austria, and notes on fossil munidopsid classification. *Annalen des Naturhistorischen Museums in Wien. Serie A für Mineralogie und Petrographie, Geologie und Paläontologie, Anthropologie und Prähistorie*, 115, 167–251.

Robins, C. M., Feldmann, R. M., Schweitzer, C. E. & Bonde, A. (2016) New families Paragalatheidae and Catillogalatheidae (Decapoda: Anomura: Galatheoidea) from the Mesozoic, restriction of the genus *Paragalathea*, and establishment of 6 new genera and 20 new species. *Annalen des Naturhistorischen Museums in Wien. Serie A für Mineralogie und Petrographie, Geologie und Paläontologie, Anthropologie und Prähistorie*, 118, 65–131.

Rodríguez-Flores, P. C., Macpherson, E. & Machordom, A. (2020) A new species of squat lobster of the genus *Hendersonida* (Crustacea, Decapoda, Munididae) from Papua New Guinea. *ZooKeys*, 935, 25.

Roterman, C. N., Lee, W. K., Liu, X., Lin, R., Li, X. & Won, Y. J. (2018) A new yeti crab phylogeny: vent origins with indications of regional extinction in the East Pacific. *PloS one*, 13 (3), e0194696.

Roux, C., Fraisse, C., Romiguier, J., Anciaux, Y., Galtier, N. & Bierne, N. (2016) Shedding light on the grey zone of speciation along a continuum of genomic divergence. *PLoS biology*, *14*(12), e2000234.

Rowden, A. A., Schnabel, K. E., Schlacher, T. A., Macpherson, E., Ahyong, S. T. & Richer de Forges, B. (2010) Squat lobster assemblages on seamounts differ from some, but not all, deep-sea habitats of comparable depth. *Marine Ecology*, 31, 63–83.

Sahling, H., Galkin, S.V., Salyuk, A., Greinert, J., Foerstel, H., Piepenburg, D. & Suess, E. (2003) Depth-related structure and ecological significance of cold-seep communities - a case study from the Sea of Okhotsk. *Deep Sea Research Part I: Oceanographic Research Papers*, 50, 1391–1409.

Samadi, S., Bottan, L., Macpherson, E., De Forges, B. R. & Boisselier, M. C. (2006) Seamount endemism questioned by the geographic distribution and population genetic structure of marine invertebrates. *Marine Biology*, 149 (6), 1463–1475.

Samouelle, G. (1819) *The Entomologist's useful compendium, or An introduction to the knowledge of British insects*. London: Thomas Boys.

Schnabel, K. E. & Ahyong, S. T. (2010) A new classification of the Chirostyloidea (Crustacea: Decapoda: Anomura). *Zootaxa*, 2687 (1), 56–64.

Schnabel, K. E., Ahyong, S. T. & Maas, E. W. (2011b) Galatheoidea are not monophyletic– molecular and morphological phylogeny of the squat lobsters (Decapoda: Anomura) with recognition of a new superfamily. *Molecular phylogenetics and Evolution*, 58(2), 157–168.

Schnabel, K. E., Cabezas, P., McCallum, A., Macpherson, E., Ahyong, S. T. & Baba, K. (2011a) Worldwide distribution patterns of squat lobsters. In: Poore, G. C. B., Ahyong, S. & Taylor, J. (eds.), *The Biology of Squat Lobsters*. Melbourne: CSIRO Publishing and Boca Raton: CRC Press, 149–182.

Schweitzer, C. E. & Feldmann, R. M. (2000) First notice of the Chirostylidae (Decapoda) in the fossil record and new Tertiary Galatheidae (Decapoda) from the Americas. *Bulletin of the Mizunami fossil Museum*, 27, 147–165.

Schweitzer, C. E. & Feldmann, R. M. (2008) New Eocene hydrocarbon seep decapod crustacean (Anomura: Galatheidae: Shinkaiinae) and its paleobiology. *Journal of Paleontology*, 82(5), 1021–1029.

Schweitzer, C. E. & Feldmann, R. M. (2010) Earliest known Porcellanidae (Decapoda: Anomura: Galatheoidea) (Jurassic:Tithonian). *Neues Jahrbuch für Geologie und Paläontologie-Abhandlungen*, 258 (2), 243–248.

Shafir, A., Azouri, D., Goldberg, E. E. & Mayrose, I. (2020) Heterogeneity in the rate of molecular sequence evolution substantially impacts the accuracy of detecting shifts in diversification rates. *Evolution*, 74, 1620–1639.

Shih, H. T., Ng, P. K., Davie, P. J., Schubart, C. D., Türkay, M., Naderloo, R.,... & Liu, M. Y. (2016) Systematics of the family Ocypodidae Rafinesque, 1815 (Crustacea: Brachyura), based on phylogenetic relationships, with a reorganization of subfamily rankings and a review of the taxonomic status of *Uca* Leach, 1814, sensu lato and its subgenera. *Raffles Bulletin of Zoology*, 64, 139–175.

Simpson, G. G. (1951) The species concept. *Evolution*, 5, 285–298.

Simpson, G. G. (1961) *Principles of animal taxonomy*. New York, NY: Columbia University Press.

Small, E. (1989) Systematics of biological systematics (or, taxonomy of taxonomy). *Taxon*, 38 (3), 335–356.

Smith, S.I. (1883) Preliminary report on the Brachyura and Anomura dredged in deep water off the south coast of New England by the United States Fish Commission in 1880, 1881, and 1882. *Proceedings of the United States National Museum*, 6, 1–57.

Spalding, M. D., Fox, H. E., Allen, G. R., Davidson, N., Ferdaña, Z. A., Finlayson, M. A. X.,... & Martin, K. D. (2007) Marine ecoregions of the world: a bioregionalization of coastal and shelf areas. *BioScience*, 57 (7), 573–583.

Stimpson, W. (1860) Notes on North American Crustacea, in the Museum of the Smithsonian Institution, No. II. *Annals of the Lyceum of Natural History of New York*, 7, 177–246, pls 2, 5.

Struck, T. H., Feder, J. L., Bendiksby, M., Birkeland, S., Cerca, J., Gusarov, V. I.,... & Stedje, B. (2018) Finding evolutionary processes hidden in cryptic species. *Trends in Ecology & Evolution*, 33 (3), 153–163.

Strugnell, J. M., Rogers, A. D., Prodöhl, P. A., Collins, M. A. & Allcock, A. L. (2008) The thermohaline expressway: the Southern Ocean as a centre of origin for deep-sea octopuses. *Cladistics*, 24 (6), 853–860.

Tan, M. H., Gan, H. M., Lee, Y. P., Linton, S., Grandjean, F., Bartholomei-Santos, M. L.,... & Austin, C. M. (2018) ORDER within the chaos: Insights into phylogenetic relationships within the Anomura (Crustacea: Decapoda) from mitochondrial sequences and gene order rearrangements. *Molecular phylogenetics and evolution*, *127*, 320–331.

Tavares, M. & Campinho, P. (1998) Three new records of deep-sea squat lobsters of the genus *Munidopsis* Whiteaves from the southwestern Atlantic Ocean (Decapoda: Galatheidae). *Crustacean research*, 27, 88-100.

Thaler, A. D., Plouviez, S., Saleu, W., Alei, F., Jacobson, A., Boyle, E. A., Schultz, T. F., Carlsson, J. & Van Dover, C. L. (2014) Comparative population structure of two deep-sea hydrothermal-vent-associated decapods (*Chorocaris* sp. 2 and *Munidopsis lauensis*) from southwestern Pacific back-arc basins. *PLoS One*, 9 (7), e101345.

Thiel, M (2003) Extended parental care in crustaceans–an update. *Revista Chilena de Historia Natural*, *76*(2), 205–218.

Thiel, M. & Lovrich, G. A. (2011) Agonistic behaviour and reproductive biology of squat lobsters. In: Poore, G. C. B., Ahyong, S. & Taylor, J. (eds.), *The Biology of Squat Lobsters.* Melbourne: CSIRO Publishing and Boca Raton: CRC Press, 223-247.

Thomas, J. A., Welch, J. J., Woolfit, M. & Bromham, L. (2006) There is no universal molecular clock for invertebrates, but rate variation does not scale with body size. *Proceedings of the National Academy of Sciences*, 103 (19), 7366–7371.

Tirmizi, N.M. & Javed, W. (1980). Nanogalathea raymondi, a new genus and species of Galatheidae (Decapoda, Anomura) from the Bay of Bengal. *Crustaceana*, 38, 127–130.

Titus, B. M., Daly, M., Hamilton, N., Berumen, M. L. & Baeza, J. A. (2018) Global species delimitation and phylogeography of the circumtropical 'sexy shrimp' *Thor amboinensis* reveals a cryptic species complex and secondary contact in the Indo-West Pacific. *Journal of Biogeography*, *45* (6), 1275–1287.

Tsang, L. M., Chan, T. Y., Ahyong, S. T. & Chu, K. H. (2011) Hermit to king, or hermit to all: multiple transitions to crab-like forms from hermit crab ancestors. *Systematic Biology*, 60 (5), 616–629.

Tsuchida, S., Fujiwara, Y. & Fujikura, K. (2003). Distribution and population structure of the galatheid crab Shinkaia crosnieri (Decapoda: Anomura: Galatheidae) in the southern Okinawa Trough. *Japanese Journal of Benthology*, 58, 84–88.

Valdecasas, A. G., Williams, D. & Wheeler, Q.D. (2008) "Integrative taxonomy" then and now: A response to Dayrat (2005). *Biological Journal of the Linnean Society*, 93 (1), 211–216.

Van Dover, C. L. & Williams A. B. (1991) Egg size in squat lobsters (Galatheoidea): constraint and freedom. In: Wenner, A. & Kuris, A. (eds.), *Crustacean egg production. Crustacean Issues*, 7, 143–156.

Van Dover, C. L., Factor, J. R., Williams, A. B. & Berg Jr, C. J. (1985) Reproductive patterns of decapod crustaceans from hydrothermal vents. *Bulletin of the Biological Society of Washington*, 6, 223–227.

Van Straelen, V. (1924) Contribution à l'étude des crustacés décapodes de la période jurassique.

Memoires de l'Académie Royale de Belgique, Classe des Sciences, Deuxième sér, 7, 1–462.

Vences, M., Thomas, M., Bonett, R. M. & Vieites, D. R. (2005) Deciphering amphibian diversity through DNA barcoding: chances and challenges. *Philosophical Transactions of the Royal Society B: Biological Sciences*, 360 (1462), 1859–1868.

Vodă, R., Dapporto, L., Dincă, V. & Vila, R. (2015) Why do cryptic species tend not to co-occur? A case study on two cryptic pairs of butterflies. *PloS one*, 10 (2), e0117802.

Vrijenhoek, R. C. (2009). Cryptic species, phenotypic plasticity, and complex life histories: assessing deep-sea faunal diversity with molecular markers. *Deep Sea Research Part II: Topical Studies in Oceanography*, 56 (19-20), 1713–1723.

Wake, D. B., Roth, G. & Wake, M. H. (1983) On the problem of stasis in organismal evolution. *Journal of theoretical Biology*, 101 (2), 211–224.

Wei, T., Li, M., Wu, C., Yan, X. Y., Fan, Y., Di, Z. & Wu, J. (2013) Do scientists trace hot topics? *Scientific Reports*, 3, 2207.

Wenner, L. E. (1982) Notes on the distribution and biology of Galatheidae and Chirostylidae (Decapoda: Anomura) from the Middle Atlantic Bight. *Journal of Crustacean Biology*, 2 (3), 360–377.

Westram, A. M., Jokela, J., Baumgartner, C. & Keller, I. (2011) Spatial distribution of cryptic species diversity in European freshwater amphipods (*Gammarus fossarum*) as revealed by pyrosequencing. *PloS one*, 6 (8), e23879.

Wheeler, Q. D. (2008) Introductory: toward the new taxonomy. In: Wheeler, Q. D. (ed.), *The New Taxonomy*. Systematics Association Special Volume Series 76. Boca Raton, Fl.: CRC Press, 1.

Whiteaves, J. F. (1874) On recent deep-sea dredging operations in the Gulf of St. Lawrence. *American Journal of Science*, Series 3, 7, 210–219.

Wiemers, M. & Fiedler, K. (2007) Does the DNA barcoding gap exist?–a case study in blue butterflies (Lepidoptera: Lycaenidae). *Frontiers in zoology*, 4 (1), 8.

Wiley, E. O. (1981) *Phylogenetics: the theory and practice of phylogenetic systematics*. New York: John Wiley & Sons.

Will, K. W. & Rubinoff, D. (2004) Myth of the molecule: DNA barcodes for species cannot replace morphology for identification and classification. *Cladistics*, 20 (1), 47–55.

Williams, S. T. & Duda Jr, T. F. (2008) Did Tectonic activity stimulate Oligo–Miocene speciation in the Indo-West Pacific?. Evolution: *International Journal of Organic Evolution*, 62 (7), 1618–1634.

Williams, S. T., Smith, L. M., Herbert, D. G., Marshall, B. A., Warén, A., Kiel, S.,... & Kano, Y. (2013) Cenozoic climate change and diversification on the continental shelf and slope: evolution of gastropod diversity in the family Solariellidae (Trochoidea). *Ecology and evolution*, 3 (4), 887–917.

Wilson, E. O. (1985) The biological diversity crisis. *BioScience*, 35 (11), 700–706.

Wilson, E. O. (2003) The encyclopedia of life. *Trends in Ecology & Evolution*, 18 (2), 77–80.

Wilson, E. O. (2004) Taxonomy as a fundamental discipline. *Philosophical Transactions of the Royal Society of London. Series B: Biological Sciences*, 359 (1444), 739–739.

Wilson, G. (1999) Some of the deep-sea fauna is ancient. *Crustaceana*, *72* (8), 101

Wolfe, J. M., Breinholt, J. W., Crandall, K. A., Lemmon, A. R., Lemmon, E. M., Timm, L. E.,... & Bracken-Grissom, H. D. (2019) A phylogenomic framework, evolutionary timeline and genomic resources for comparative studies of decapod crustaceans. *Proceedings of the Royal Society B*, 286 (1901), 20190079.

Yang, C. H., Sha, Z., Chan, T. Y., & Liu, R. (2015). Molecular phylogeny of the deep-sea penaeid shrimp genus *Parapenaeus* (Crustacea: Decapoda: Dendrobranchiata). *Zoologica Scripta*, 44 (3), 312–323.

Yang, C. H., Tsuchida, S., Fujikura, K., Fujiwara, Y., Kawato, M. & Chan, T. Y. (2016) Connectivity of the squat lobsters *Shinkaia crosnieri* (Crustacea: Decapoda: Galatheidae) between cold seep and hydrothermal vent habitats. *Bulletin of Marine Science*, 92 (1), 17–31.

APÉNDICE

OTRAS PUBLICACIONES

Artículos incluidos:

Macpherson E, **Rodríguez-Flores PC**, & Machordom A. 2017. New sibling species and new occurrences of squat lobsters (Crustacea, Decapoda) from the western Indian Ocean. *European Journal of Taxonomy*, 343, 1–61. https:// doi.org/10.5852/ejt.2017.343

Rodríguez Flores PC, Macpherson E, & Machordom A. 2020. A new species of squat lobster of the genus *Hendersonida* (Crustacea, Decapoda, Munididae) from Papua New Guinea. *Zookeys*, 935, 25–35. https://doi.org/10.3897/zookeys.935.51931

Macpherson E, Chan TY, Kumar AB, & **Rodríguez-Flores PC**. 2020. On some squat lobsters from India (Decapoda, Anomura, Munididae), with description of a new species of *Paramunida* Baba, 1988. *ZooKeys*, 965, 17–36. https://doi.org/10.3897/zookeys.965.55213

Macpherson E, **Rodríguez-Flores PC**, & Machordom A. 2020. New occurrences of squat lobsters of the genus *Eumunida* Smith, 1883 (Decapoda, Eumunididae) in New Caledonia, Solomon Islands and Papua-New Guinea, with the description of a new species. *Zootaxa*, 4786, 485–496. http://dx.doi.org/10.11646/zootaxa.4786.4.2.

Macpherson E, **Rodríguez-Flores PC**, & Machordom A. 2020. Squat lobsters of the families Munididae and Munidopsidae from Papua New Guinea. In: Ahyong ST, Chan T-Y, Corbari L (Eds) *Tropical Deep-Sea Benthos 31, Papua New Guinea*. Muséum national d'Histoire naturelle, Paris: 11-120 (*Mémoires du Muséum national d'Histoire naturelle*, 213). ISBN: 978-2-85653-913-2

M o n o g r a p h

urn:lsid:zoobank.org:pub:55D64626-2438-40E1-9D76-C3D5BDF2A38F

New sibling species and new occurrences of squat lobsters (Crustacea, Decapoda) from the western Indian Ocean

Enrique MACPHERSON [1,*], Paula C. RODRÍGUEZ-FLORES [2] & Annie MACHORDOM [3]

[1] Centre d'Estudis Avançats de Blanes (CEAB-CSIC),
C. acc. Cala Sant Francesc, 14, 17300 Blanes, Girona, Spain.
[2,3] Museo Nacional de Ciencias Naturales (MNCN-CSIC),
José Gutiérrez Abascal, 2, 28006 Madrid, Spain.

[*] Corresponding author: macpherson@ceab.csic.es
[2] Email: paularodriguezflores@gmail.com
[3] Email: annie@mncn.csic.es

[1] urn:lsid:zoobank.org:author:D0C9DD3A-7268-4357-81AC-B1C1D19899AB
[2] urn:lsid:zoobank.org:author:5069B10F-7957-447A-8B97-B5CC02C9B118
[3] urn:lsid:zoobank.org:author:9D83D93C-9324-4E04-905C-D22FE012A097

Abstract. Numerous specimens of squat lobsters belonging to the families Munididae, Munidopsidae and Eumunididae were collected during several cruises along the eastern coasts of Africa. The study of these specimens revealed the presence of 10 new species (one *Eumunida* Smith, 1883, eight *Munida* Leach, 1820 and one *Munidopsis* Whiteaves, 1874). We describe and illustrate these new species, providing some new data on occurrences and colour patterns for previously described taxa. We have also included molecular data from two mitochondrial markers (16S rRNA and COI) to support the taxonomic status of different species. Some deep-sea species show a clear increase in their geographic range distribution. Finally, a key to known species of the genus *Munida* from the western and central Indian Ocean is also presented.

Keywords. Eumunididae, Munididae, Munidopsidae, COI, 16S.

Introduction

The western Indian Ocean is considered one of the "hot spots" in marine biodiversity of the world (Myers *et al*. 2000). Numerous authors, from the Red Sea to South Africa and Madagascar, have studied the crustacean decapods of the area demonstrating the existence of a very rich fauna (Barnard 1950; Crosnier 1978; Ng & Kumar 2015), with a high proportion of endemic species (Spiridonov & Apel 2007; DiBattista *et al*. 2016). Among these decapods, the squat lobsters (Chirostyloidea and Galatheoidea) are

1

RESEARCH ARTICLE

A new species of squat lobster of the genus *Hendersonida* (Crustacea, Decapoda, Munididae) from Papua New Guinea

Paula C. Rodríguez-Flores[1,2], Enrique Macpherson[1], Annie Machordom[2]

1 *Centre d'Estudis Avançats de Blanes (CEAB-CSIC), C. acc. Cala Sant Francesc 14 17300 Blanes, Girona, Spain* **2** *Museo Nacional de Ciencias Naturales (MNCN-CSIC), José Gutiérrez Abascal, 2, 28006 Madrid, Spain*

Corresponding author: Paula C. Rodríguez-Flores (paularodriguezflores@gmail.com)

Citation: Rodríguez-Flores PC, Macpherson E, Machordom A (2020) A new species of squat lobster of the genus *Hendersonida* (Crustacea, Decapoda, Munididae) from Papua New Guinea. ZooKeys 935: 25–35. https://doi.org/10.3897/zookeys.935.51931

Abstract

Hendersonida parvirostris **sp. nov.** is described from Papua New Guinea. The new species can be distinguished from the only other species of the genus, *H. granulata* (Henderson, 1885), by the fewer spines on the dorsal carapace surface, the shape of the rostrum and supraocular spines, the antennal peduncles, and the length of the walking legs. Pairwise genetic distances estimated using the 16S rRNA and COI DNA gene fragments indicated high levels of sequence divergence between the new species and *H. granulata*. Phylogenetic analyses, however, recovered both species as sister species, supporting monophyly of the genus.

Keywords

Introduction

Squat lobsters of the family Munididae Ahyong, Baba, Macpherson & Poore, 2010 are recognised by the trispinose or trilobate front, usually composed of a slender rostrum flanked by supraorbital spines (Ahyong et al. 2010; Macpherson and Baba 2011). The family is one of the most diverse of the anomuran decapods, containing 21 genera and

RESEARCH ARTICLE

On some squat lobsters from India (Decapoda, Anomura, Munididae), with description of a new species of *Paramunida* Baba, 1988

Enrique Macpherson[1], Tin-Yam Chan[2], Appukuttannair Biju Kumar[3],
Paula C. Rodríguez-Flores[1]

1 *Centre d'Estudis Avançats de Blanes (CEAB-CSIC), C. acc. Cala Sant Francesc 14 17300 Blanes, Girona, Spain* **2** *Institute of Marine Biology and Center of Excellence for the Oceans, National Taiwan Ocean University, Keelung 20224, Taiwan, ROC* **3** *Department of Aquatic Biology and Fisheries, University of Kerala, Thiruvananthapuram 695581, Kerala, India*

Corresponding author: Tin-Yam Chan (tychan@ntou.edu.tw)

Abstract

Squat lobster specimens belonging to the family Munididae were recently collected along the southwestern coast of the mainland of India and in the Andaman Islands. The specimens belong to two known species, *Agononida prolixa* (Alcock, 1894) and *Munida compacta* Macpherson, 1997, and a new species, *Paramunida bineeshi* **sp. nov.**. We here redescribe *A. prolixa* and describe and figure the new species. *Munida compacta* is newly recorded from India, and we figure the live coloration. In addition, molecular and phylogenetic analyses of two mitochondrial markers (16S rRNA and COI) revealed the phylogenetic relationships of *M. compacta* and *P. bineeshi* **sp. nov.** with their most closely related congeners. The genetic similarity among the individuals of *M. compacta* from different locations is also addressed.

Keywords

Article

ZOOTAXA

New occurrences of squat lobsters of the genus *Eumunida* Smith, 1883 (Decapoda, Eumunididae) in New Caledonia, the Solomon Islands and Papua-New Guinea, with the description of a new species

ENRIQUE MACPHERSON[1]*, PAULA C. RODRÍGUEZ-FLORES[1,2,3] & ANNIE MACHORDOM[2,4]
[1]Centre d'Estudis Avançats de Blanes (CEAB-CSIC), C. acc. Cala Sant Francesc 14 17300 Blanes, Girona, Spain
[2]Museo Nacional de Ciencias Naturales (MNCN-CSIC), José Gutiérrez Abascal, 2, 28006 Madrid, Spain
[3] paulacrf@mncn.csic.es; https://orcid.org/0000-0003-1555-9598
[4] annie@mncn.csic.es; https://orcid.org/0000-0003-0341-0809
*Corresponding author. macpherson@ceab.csic.es; https://orcid.org/0000-0003-4849-4532

Abstract

Examination of numerous specimens of squat lobsters of the genus *Eumunida* Smith, 1883 collected by French cruises along the coasts of New Caledonia, the Solomon Islands and Papua-New Guinea revealed the presence of six species, including a new species. The collection data of all of these species are recorded. The new species, *E. turbulenta* **n. sp.**, is described and illustrated from New Caledonia and Chesterfield Islands.

Key words: Crustacea, Anomura, Chirostyloidea, morphology, West Pacific

Introduction

The genus *Eumunida* Smith, 1883 contains 33 species, four in the Atlantic Ocean (Baba *et al*. 2008; Tavares & Lima 2019), 28 in the Indo-West Pacific (Baba *et al*. 2008; Baba & Lin 2008; Komai & Tsuchida 2014; Macpherson *et al*. 2017; Komai *et al*. 2019; Osawa & Higashiji 2019) and one in the eastern Pacific (Baba & Wicksten 2019). All the species are common on the continental shelf and slope, usually associated with scleractinian and gorgonian corals (Quattrini *et al*. 2012; Ross *et al*. 2015). The number of species is higher in the southwestern Pacific than in other regions (Schnabel *et al*. 2011), the area around New Caledonia being one of the richest zones, with nine species. Previous studies have also explored the genetic relationships among *Eumunida* species, detecting cryptic/sister species synonymizing some morphology based species (Puillandre *et al*. 2011).

During the last decades, numerous expeditions have been carried out in waters around New Caledonia, the Chesterfield Islands, the Solomon Islands and Papua-New Guinea (e.g., Richer de Forges *et al*. 2013). Detailed study on the collected material revealed the presence of six species of *Eumunida*, new records for *E. pacifica* Gordon, 1930 and *E. smithii* Henderson, 1885 in the Solomon islands and Papua-New Guinea, and one undescribed species in New Caledonia and the Chesterfield Islands. The new species was previously reported as *E.* aff. *annulosa*, based on DNA sequence data (Puillandre *et al*. 2011).

Sampling and identification

Specimens were collected using beam trawls (CP), otter trawls for fish (CH) or Waren dredges (DW) on deep-sea cruises along the southwestern Pacific: 1986 (Norfolk ridge, New Caledonia, CHACAL 2), 1992 (New Caledonia, BERYX 11), 1993 (Loyalty Islands ridge and New Caledonia, SMIB 8, BATHUS 2, BATHUS 3), 1994 (New Caledonia, HALIPRO 1), 1995 (New Caledonia, SMIB 10), 1996 (Norfolk ridge, New Caledonia, HALIPRO 2), 2001 (Norfolk ridge, New Caledonia, NORFOLK 1), 2001 (Solomon Sea, Solomon Island, SALOMON 1), 2005 (Chesterfield Islands, New Caledonia, EBISCO), 2008 (New Caledonia, TERRASSES), 2010 (Bismarck Sea and

485

Squat lobsters of the families Munididae and Munidopsidae from Papua New Guinea

Enrique **Macpherson** [1], Paula C. **Rodríguez-Flores** [1] [2] & Annie **Machordom** [2]

[1] Centro de Estudios Avanzados de Blanes (CEAB-CSIC), Carrer Accès Cala Sant Francesc 14 17300 Blanes, Girona, Spain
macpherson@ceab.csic.es

[2] Museo Nacional de Ciencias Naturales (MNCN-CSIC), José Gutiérrez Abascal, 2, 28006 Madrid, Spain
paulacrf@mncn.csic.es, annie@mncn.csic.es

ABSTRACT

More than 5000 specimens of squat lobsters belonging to the families Munididae and Munidopsidae were collected during four cruises along the coasts of Papua New Guinea. The study of these specimens revealed the presence of 13 new species (one *Babamunida*, one *Crosnierita*, eight *Munida*, one *Paramunida* and two *Munidopsis*). Overall, 109 species of Munididae and 37 of Munidopsidae are recognized. We include the records of all species, describing and illustrating the new species. Furthermore, we provide some new data on the colour patterns for some species. We have also included molecular data from two mitochondrial markers (16S rRNA and COI) to support the taxonomic status of different new species.

RÉSUMÉ

Galathées des familles Munididae et Munidopsidae de Papouasie-Nouvelle-Guinée.

Plus de 5000 spécimens de Galathées appartenant aux familles Munididae et Munidopsidae ont été collectés lors de quatre campagnes océanographiques le long des côtes de la Papouasie-Nouvelle-Guinée. L'étude de ce matériel a révélé la présence de 13 nouvelles espèces (une appartenant au genre *Bathymunida*, une du genre *Crosnierita*, 8 espèces nouvelle pour le genre *Munida*, une nouvelle espèce de *Paramunida* et deux pour le genre *Munidopsis*). Un total de 109 espèces de Munididae et 37 de la famille des Munidopsidae sont présentées dans cette étude. De nouvelles données sur les patrons de couleurs de certaines espèces sont également décrites. Nous avons également inclus des données moléculaires issues de deux marqueurs mitochondriaux (16S rRNA et COI) afin de contribuer au statut taxonomique des différentes nouvelles espèces.